

**2018 14TH INTERNATIONAL SCIENTIFIC-
TECHNICAL CONFERENCE ON ACTUAL
PROBLEMS OF ELECTRONIC INSTRUMENT
ENGINEERING (APEIE) – 44894
PROCEEDINGS**

APEIE – 2018

**ТРУДЫ XIV МЕЖДУНАРОДНОЙ НАУЧНО-
ТЕХНИЧЕСКОЙ КОНФЕРЕНЦИИ
АКТУАЛЬНЫЕ ПРОБЛЕМЫ
ЭЛЕКТРОННОГО ПРИБОРОСТРОЕНИЯ**

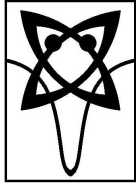
АПЭП – 2018

Sponsors:

Novosibirsk State Technical University

Спонсоры:

Новосибирский государственный технический университет



**2018 14TH INTERNATIONAL SCIENTIFIC-
TECHNICAL CONFERENCE ON ACTUAL
PROBLEMS OF ELECTRONIC INSTRUMENT
ENGINEERING (APEIE) PROCEEDINGS**

| | |
|----------------------|--------------------------|
| IEEE Catalog Number: | CFP18471-PRT |
| ISBN: | 978-1-5386-7053-8 |
| ISBN: | 978-5-7782-3614-1 |
| | Volume 1, Part 6:-475 c. |
| ISBN: | 978-5-7782-3615-8 |

Information about proceedings placed in <http://apeie.conf.nstu.ru/apeie2018/>

ISBN: 978-1-5386-7053-8 © IEEE, 2018

ISBN: 978-5-7782-3615-8 (Volume 1) © Novosibirsk State Technical University, 2018

ISBN: 978-5-7782-3614-1

**2018 14TH INTERNATIONAL SCIENTIFIC-
TECHNICAL CONFERENCE ON ACTUAL
PROBLEMS OF ELECTRONIC INSTRUMENT
ENGINEERING (APEIE) – 44894
PROCEEDINGS**

APEIE – 2018

**In 8 Volumes
Volume 1
Part 6**

Novosibirsk, October 2-6, 2018

**ТРУДЫ XIV МЕЖДУНАРОДНОЙ НАУЧНО-
ТЕХНИЧЕСКОЙ КОНФЕРЕНЦИИ
АКТУАЛЬНЫЕ ПРОБЛЕМЫ
ЭЛЕКТРОННОГО ПРИБОРОСТРОЕНИЯ**

АПЭП – 2018

**В 8 томах
Том 1
Часть 6**

Новосибирск, 2-6 октября, 2018

ORGANIZERS

ОРГАНИЗАТОРЫ КОНФЕРЕНЦИИ

| | |
|---|--|
|  | <p style="text-align: center;">Novosibirsk State Technical University</p> <p style="text-align: center;">Новосибирский государственный технический университет</p> |
|  | <p style="text-align: center;">Institute of Electrical and Electronics Engineers</p> <p style="text-align: center;">Американский институт инженеров электротехники и электроники</p> |
|  | <p style="text-align: center;">ФГУП “Сибирский государственный НИИ метрологии”</p> |
|  | <p style="text-align: center;">Academy of Medical-Technical Sciences of Russian Federation Siberian Branch</p> <p style="text-align: center;">Академия медико-технических наук Российской Федерации СО</p> |
|  | <p style="text-align: center;">АО “НИИ измерительных приборов – Новосибирский завод имени Коминтерна” (АО “НПО НИИИП-НЗиК”)</p> |
|  | <p style="text-align: center;">Siberian State University of Telecommunications and Information Sciences</p> <p style="text-align: center;">Сибирский государственный университет телекоммуникаций и информатики</p> |

INTERNATIONAL PROGRAMME COMMITTEE МЕЖДУНАРОДНЫЙ ПРОГРАММНЫЙ КОМИТЕТ

Chairman:

Dr. A.A. Bataev, NSTU Rector, Dr.Sci., Prof.,
Novosibirsk, Russia.

Председатель:

Батаев А.А, д.т.н., проф., ректор НГТУ.

Vice-Chairman:

Dr. Yu.A. Palchun, Dr.Sci., Prof. of
SIBSUTIS, Novosibirsk, Russia.

Заместитель председателя:

Пальчун Ю.А., д.т.н., проф., СИБГУТИ.

Members:

Dr. Ye. V. Il'ichev – Dr. Sci., Prof., Germany,
Roth H. – Dr. Sci., Prof., Germany,
Dr. D. Vinnikov – Dr. Sci., Prof., Estonia,
Dr. M. Kazmierkowski – Dr.Sci., Prof.,
Poland,
Dr. R. Strzelezki – Dr.Sci., Prof. Poland,
Dr. S.N. Bagaev – RAS academician, Dr.Sci.,
Novosibirsk, Russia,
Dr. M.B. Shtark – RMAS academician,
Dr.Sci., Novosibirsk, Russia,
Dr. V.V. Nekrasov – NSTU Vice Rector for
International Relations, Cand.Sci.,
Novosibirsk, Russia,
Dr. N.L. Novikov – Dr. Sci., Prof., Moscow,
Russia
Dr. V.A. Maistrenko – Dr.Sci., Prof., Omsk,
Russia,
Dr. N.D. Malyutin – Dr.Sci., Prof., Tomsk,
Russia,
Dr. A.B. Markhasin – Dr.Sci., Prof.,
Novosibirsk, Russia,
Dr. G.I. Peredelsky – Dr.Sci, Prof., Kursk,
Russia,
Dr. A.S. Rodionov – Dr. Sci., Head of R8
IEEE Siberian section, Novosibirsk, Russia
Dr. A.N. Sychev – Dr.Sci., Prof., Tomsk,
Russia,
Dr. G.Ya. Shaidurov – Dr.Sci., Prof.,
Krasnoyarsk, Russia.

Члены комитета:

Ильичев Е.В. – д.ф.-м.н., проф., Германия,
Рот Х. – д.т.н., проф., Германия,
Винников Д. – д.т.н., проф., Эстония,
Казмиерковский М. – д.т.н., проф., Польша,
Стржеleckи Р. – д.т.н., проф., Польша,
Багаев С.Н. – д.ф.-м.н., академик РАН,
Новосибирск,
Штарк М.Б. – д.б.н., академик РАН,
Новосибирск,
Некрасов В.В. – к.т.н., доц., проректор по
международным связям НГТУ
Новиков Н.Л. – д.т.н., проф., МЭИ,
Майстренко В.А. – д.т.н., проф., Омск,
Малютин Н.Д. – д.т.н., проф., ТУСУР,
Мархасин А.Б. – д.т.н., проф., СибГУТИ,
Передельский Г.И. – д.т.н., проф., КГТУ,
Родионов А.С. – д.т.н., ст.н.с., председатель
Сибирской секции R8 IEEE
Сычев А.Н. – д.т.н., проф., ТУСУР,
Шайдуров Г.Я. – д.т.н., проф., СФУ.

NATIONAL ORGANIZING COMMITTEE НАЦИОНАЛЬНЫЙ КОМИТЕТ

Chairpersons:

Dr. A.G. Vostretsov – NSTU Vice-Rector for research, Dr.Sci., Prof., Novosibirsk, Russia,
Dr. L.I. Lisitsyna – Dr.Sci., Prof., NSTU, Novosibirsk, Russia,
Dr. V.A. Khrustalev – Dean of REF, Dr.Sci., Prof., NSTU, Novosibirsk, Russia.

Vice-Chairmen:

Dr. V.K. Makukha – Dr.Sci., Prof., NSTU, Novosibirsk, Russia,
Dr. S.A. Kharitonov – Dr.Sci., Prof., NSTU, Novosibirsk, Russia,
Dr. G.V. Shuvalov – Cand.Sci, FSUI "SRIM", Novosibirsk, Russia.

Secretaries:

Dr. Yu.V. Morozov – Cand.Sci., Assoc.Prof., NSTU, Novosibirsk.
A.A. Blokhin – Assistant, NSTU, Novosibirsk,
R.S. Molchanov – M.S. Deg. student, NSTU, Novosibirsk.

Members:

Dr. S.V. Brovanov – NSTU Vice-Rector for teaching process, Dr.Sci., Prof., Novosibirsk,
Dr. I.A. Bakhovtsev – Cand.Sci., Assoc.Prof., NSTU, Novosibirsk,
Dr. B.K. Bogomolov – Cand.Sci., Assoc.Prof., NSTU, Novosibirsk
Dr. V.N. Vasyukov – Dr.Sci., Prof., NSTU, Novosibirsk,
Dr. A.V. Gavrilov – Cand. Sci., Assoc. Prof., NSTU, Novosibirsk
Dr. N.I. Gorlov – Dr.Sci., Prof., SIBSUTIS, Novosibirsk,
Dr. V.A. Gridchin – Dr.Sci., Prof., NSTU, Novosibirsk,

Председатели:

Вострецов А.Г.– д.т.н., проф., проректор по научной работе, НГТУ,
Лисицына Л.И.– д.т.н., проф., НГТУ,
Хрусталеv В.А. – д.т.н., проф., декан факультета РЭФ, НГТУ.

Заместители председателей:

Макуха В.К. – д.т.н., проф., НГТУ,
Харитонов С.А. – д.т.н., проф., НГТУ,
Шуvalov Г.В. – к.т.н., директор ФГУП “СНИИМ”.

Секретари:

Морозов Ю.В. – к.т.н., доц., НГТУ.
Блохин А.А – ассистент, НГТУ,
Молчанов Р.С. – магистрант, НГТУ.

Члены комитета:

Брованов С.В. – д.т.н., проф., проректор по учебной работе НГТУ,
Баховцев И.А. – к.т.н., доц., НГТУ,
Богомолов Б.К. – к.ф-м.н., доцент, НГТУ.
Васюков В.Н. – д.т.н., проф., НГТУ,
Гаврилов А.В. – к.т.н., доц., НГТУ,
Горлов Н.И. – д.т.н., проф., СибГУТИ,
Гриджин В.А. – д.т.н., проф., НГТУ,

N.A. Dvurechenskaya – SIBSUTIS Director of Scientific and Innovation Activity Center, Novosibirsk

Dr. G.N. Devyatkov – Dr.Sci., Prof., NSTU, Novosibirsk,

Dr. E.V. Dragunova – Cand.Sci., Assoc.Prof., NSTU, Novosibirsk,

Dr. V.A. Zhmud – Dr. Sci., Assoc. Prof., NSTU,

Mr. P.V. Zabolotniy – Gen.-Dir. JSC “SPO SRIMD-NFn.a.C”, Novosibirsk,

Dr. G.S. Zinoviev – Dr.Sci., Prof., NSTU, Novosibirsk,

Dr. D.E. Zakrevsky - Dr.Sci., Prof., NSTU, IPS SB RAS

Dr. A.V. Kiselev Dr.Sci., Prof., NSTU, Novosibirsk,

Dr. B.Yu. Lemeshko – Dr.Sci., Prof., NSTU, Novosibirsk,

Dr. A.V. Morozov – Cand.Sci., NSTU, Novosibirsk,

Dr. I.L. Reva – Cand. Sci., Assoc. Prof., NSTU, Novosibirsk

Dr. V.P. Razinkin – Dr.Sci., Prof., NSTU, Novosibirsk,

Dr. M.A. Stepanov – Cand.Sci., Assoc.Prof., NSTU, Novosibirsk,

Dr. A.A. Spektor – Dr.Sci., Prof., NSTU, Novosibirsk,

Dr. S.V. Sputai – Cand.Sci., Assoc.Prof., NSTU, Novosibirsk,

Dr. D.M. Toporkov – Cand. Sci., Assoc. Prof., NSTU, Novosibirsk,

Dr. G.V. Troshina – Cand. Sci., Assoc. Prof., NSTU, Novosibirsk,

Dr. P.E. Troyan – Dr.Sci., Prof., TUSUR, Tomsk,

Dr. V.A. Trushin – Cand. Sci., Assoc. Prof., NSTU, Novosibirsk,

Dr. M.V. Khairullina – Dr.Sci., Prof., NSTU, Novosibirsk,

Mr. A.A. Shevchenko – Director of LLC “Experimental Devices”,

Dr. A.F. Shevchenko – Dr. Sci., Prof., NSTU, Novosibirsk,

Dr. M.S. Shushnov – Cand. Sci., Assoc. Prof., SIBSUTIS, Novosibirsk,

Dr. A.N. Yakovlev – Cand.Sci., Prof., NSTU, Novosibirsk.

Двуреченская Н.А. – директор Центра научно-инновационной деятельности, СибГУТИ,

Девятков Г.Н. – д.т.н., проф., НГТУ,

Драгунова Е.В. – к.э.н., доц., НГТУ,

Жмудь В.А. - д.т.н., доц., НГТУ,

Заболотный П.В. – ген.дир.АО “НПО НИИИП-НЗиК”,

Зиновьев Г.С. – д.т.н., проф., НГТУ,

Закревский Д.Е. – д.т.н., проф., НГТУ, ИФП СО РАН

Киселев А.В. – д.т.н., проф., НГТУ,

Лемешко Б.Ю. – д.т.н., проф., НГТУ,

Морозов А.В. – к.т.н., НГТУ,

Рева И.Л. – к.т.н., доц., НГТУ,

Разинкин В.П. – д.т.н., проф., НГТУ,

Степанов М.А. – к.т.н., доц., НГТУ,

Спектор А.А. – д.т.н., проф., НГТУ,

Спутай С.В. – к.т.н., доц., НГТУ,

Топорков Д.М. – к.т.н., доц., НГТУ,

Трошина Г.В. – к.т.н., доц., НГТУ,

Троян П.Е. – д.т.н., проф., ТУСУР,

Трушин В.А. – к.т.н., доц., НГТУ,

Хайруллина М.В. – д.э.н., проф., НГТУ,

Шевченко А.А. – ген. директор ООО “Опытные приборы”,

Шевченко А.Ф. – д.т.н., проф., НГТУ,

Шушнов М.С. - к.т.н., доц., СибГУТИ,

Яковлев А.Н. – к.т.н., проф., НГТУ.

CONTENTS OF THE CONFERENCE PROCEEDINGS BY VOLUMES

| | |
|----------|---|
| Volume 1 | Papers in English. |
| Volume 2 | Section 1. Electron-Physical Section (Solid-State, Vacuum and Plasma Electronics: Physical Processes, Technologies (including nanotechnologies and nanomaterials), Equipment, Devices. |
| Volume 3 | Section 2. Metrology and Metrological Instrumentation. Section 3. Measuring Units, Devices and Systems. Information Protection. Section 4. Laboratory Equipment. |
| Volume 4 | Section 6. Radio Engineering (Image and Signal Processing and Modeling; Radio-Engineering Devices and Systems). Section 7. Telecommunications. Section 8. Design and Technology of Radio-Engineering Devices. Section 9. Radiolocation, Radioelectronic Complexes and Systems. |
| Volume 5 | Section 5. Lasers and Their Application. Medical Electronic Instrumentation. |
| Volume 6 | Section 10. Mathematical Simulation. Section 11. Computer Engineering. Information Systems and Technologies. |
| Volume 7 | Section 12. Power Electronics and Mechatronics. Section 13. Power Engineering, Electrical Engineering, Electromechanics. Section 14. Control Systems and Automatic Devices. |
| Volume 8 | Section 15. Economic Aspects of High Technology Industries Development. |

СОДЕРЖАНИЕ ТРУДОВ КОНФЕРЕНЦИИ ПО ТОМАМ

| | |
|-------|---|
| Том 1 | Труды на английском языке. |
| Том 2 | Секция 1. Электронно-физическая секция (твёрдотельная, вакуумная и плазменная электроника: физические процессы, технологии, (включая нанотехнологии и наноматериалы), оборудование, приборы). |
| Том 3 | Секция 2. Метрология и метрологическое обеспечение. Секция 3. Измерительные приборы, устройства и системы. Защита информации. Секция 4. Лабораторное оборудование. |
| Том 4 | Секция 6. Радиотехника (обработка и моделирование сигналов и изображений; радиотехнические устройства и системы). Секция 7. Телекоммуникации. Секция 8. Конструирование и технология радиоэлектронных средств. Секция 9. Радиолокация, радиоэлектронные комплексы и системы. |
| Том 5 | Секция 5. Лазеры и их применение. Медицинская электроника. |
| Том 6 | Секция 10. Математическое моделирование. Секция 11. Вычислительная техника. Информационные системы и технологии. |
| Том 7 | Секция 12. Силовая электроника и мехатроника. Секция 13. Электроэнергетика, электротехника, электромеханика. Секция 14. Устройства автоматики и системы управления. |
| Том 8 | Секция 15. Экономические аспекты развития высокотехнологичных отраслей. |

Volume 1
Part 6

Papers in English

Том 1
Часть 6

Труды на английском языке

Sections

**Power Electronics and Mechatronics
Control Systems and Automatic Devices
Economic Aspects of High Technology Industries
Development**

Секции

**Силовая электроника и мехатроника
Устройства автоматики и системы управления
Экономические аспекты развития
высокотехнологичных отраслей**

Analytical Research of Electromagnetic Processes in Direct Current Starter-Generator System «Synchronous Generator with Combined Excitation – Active Rectifier» (Generation Mode)

Sergey A. Kharitonov¹, *Member*, IEEE, Andrey S. Kharitonov¹, Dmitry L. Kaluzhskij¹, Svetlana V. Vorobyeva²

¹Novosibirsk State Technical University, Novosibirsk, Russia

²Siberian State University of Telecommunication and computer sciences, Novosibirsk, Russia

Abstract – The electromagnetic processes in the system with synchronous generator with the combined excitation for the parametric control of the excitation current are considered. Proposed three scenarios for the design of such system and control methods of flux linkage of winding of excitation. The possible modes of operation of the system are identified. The comparison of three scenarios of system design is carried out.

Index Terms – Active rectifier, synchronous generator.

I. INTRODUCTION

IN DIRECT CURRENT starter-generator systems for aircraft, where the source of electrical energy is a synchronous generator with a combined excitation driven by turbine engine or turboprop aircraft engine, can be applied a semiconductor converter based on an active rectifier. The Fig. 1 shows a functional scheme of such system, where are: SG – synchronous generator with combined excitation, WE – winding of excitation of the SG, AR – active rectifier based on a voltage inverter with sinusoidal pulse width modulation (SPWM), C_F , R_L – output filter capacitor and equivalent load resistance, i , u – phase current and voltage of SG, I_f – current of excitation of the SG, ω – cyclic frequency of the SG voltage, U_L – output voltage of the system.

Further, such a system will be called – direct current power generation system (DCPGS). This system has the following advantages:

- the shape of current of the SG is close to the sinusoidal;
- the role of the longitudinal element of the power filter is performed by the SG reactants;
- the circuit has the ability to increase the voltage compared to usual three-phase rectifier;
- due to the possibility of changing the direction of the power flow, the system can be a mode of electric starter start of the primary engine;
- in the presence of high-frequency SPWM significantly reduces the value of the capacitor of the output filter C_F ;

–the ability to adjust the voltage of the SG with excitation winding allows reducing significantly the flows reactive power between the SG and the semiconductor converter when changing the speed of rotation of the shaft.

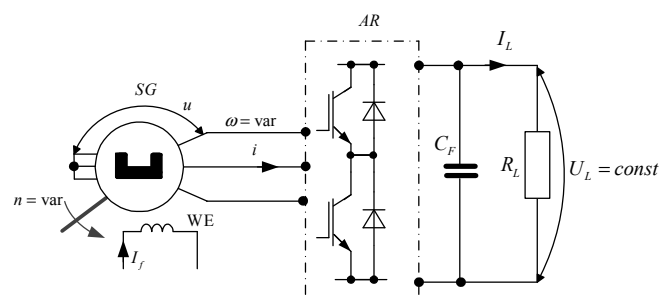


Fig. 1. Functional scheme of the DCPGS.

This system is analysed for the first time.

II. PROBLEM DEFINITION

The variable frequency and magnitude of the internal electromotive force (EMF) of the SG significantly affect the operating modes the AR and DCPGS as a whole [1,2].

The paper presents the results of an evaluation in static mode of the magnitude of currents and voltages in the system, as well as some energy parameters, provided that the constancy of the average value of the output voltage U_L , when the frequency ω and a value of load of DCPGS change.

In the system under consideration, it is necessary to separate the functions of voltage regulation on the load between the SG and the AR, as well as to determine the control methods, both in static and dynamic modes.

A system in which the SG is controlled parametrically is considered in advance, and the excitation current is formed according to a certain method in the frequency function (ω) of the SG voltage. Voltage stabilization at the load is provided by the AR.

III. PRINCIPLE OF OPERATION OF DCPGS. OPERATING MODES

In general, in such system, the stabilization of the load voltage is possible due to the regulation of the value of EMF of the SG by means of the winding of excitation, as well as the regulation of the SG voltage by means of AR by changing the value of the reactive current component of the SG.

The following considerations should be taken into account when determining how to stabilize and regulate the load voltage. Regulation of the SG winding of excitation has a low speed, but does not require large energy costs. The regulation using AR is much faster, but it is associated with overflows of significant reactive power [1,2]. In this regard, it is preferable to parry relatively slow perturbations on the rotation speed of the shaft and significant changes in the load current in the steady-state modes to assign to the control of winding of excitation. Dynamic (fast) disturbances of the load at low exposure times should be parried with the help of the AR regulators.

between E_{0nom} and E_Σ . Then, E_0 - EMF of the SG, produced by the permanent magnets.

It should be noted, that the character of the dependence $\Psi_f(\omega)$ is shown rather conditionally, it can be different and will be analyzed further.

In the first scenario (Fig. 2a) some average frequency value ω_0 is selected, at which Ψ_0 and E_{0nom} are determined, based on provision of the SG rated load at zero flux linkage Ψ_f . In this case, flux linkage Ψ_f to ensure of the load voltage at $\omega = \text{var}$ must be alternating, so in mode «I» flux linkages Ψ_0 и Ψ_f must match on sign, in mode «II» their signs should be opposite.

In the second scenario (Fig. 2b) flux linkage Ψ_0 and EMF E_{0nom} for the nominal load mode are selected when $\omega = \omega_{min}$. In this case flux linkage Ψ_f in order to stabilize U_L at changing of ω should always be opposite

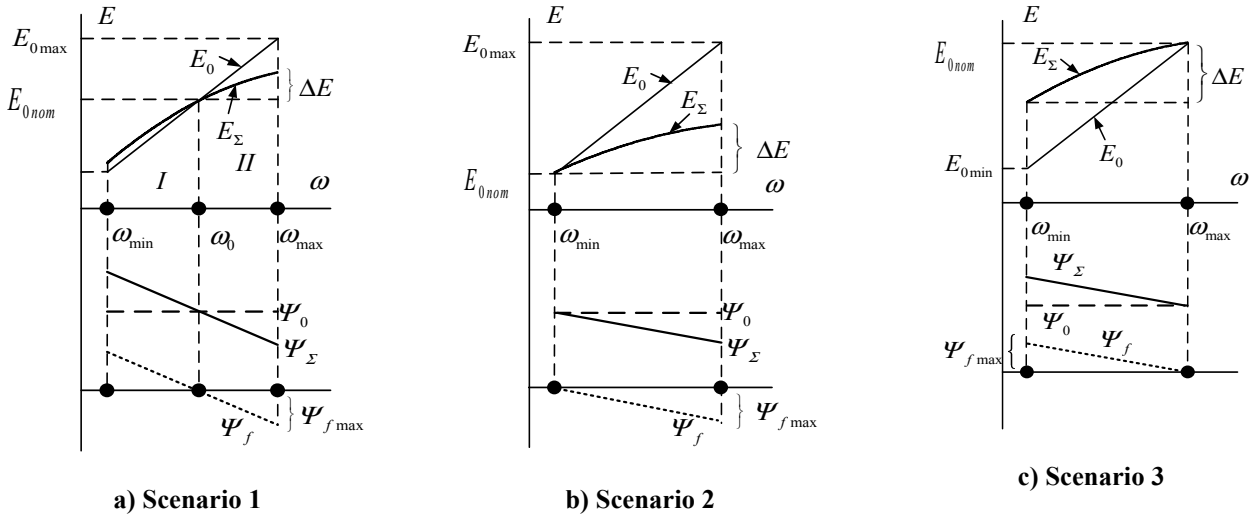


Fig. 2 Three scenarios for the design parameters and method of control DCPGS.

In the system under consideration, there three scenarios for designing parameters and ways to control DCPGS, they are easy to identify with the help of Fig. 2, where the character of the main adjustable parameters of the SG is qualitatively shown. Where: E, ω - the effective value of the idle EMF of the SG and its cyclic frequency, E_{0nom} - idle EMF of the SG, chosen from the condition of providing the nominal mode of load, E_{0min}, E_{0max} - minimum and maximum values of EMF of the SG, produced by the flux linkage from permanent magnets, ω_{min} и ω_{max} - minimum and maximum values of cyclic frequency of the SG, Ψ_0, Ψ_f - flux linkages, produced by the permanent magnets and winding of excitation, number of turns of the phase winding, $\Psi_\Sigma = \Psi_0 + \Psi_f$ - the total flux linkage, E_Σ - idle EMF of the SG, produced by the flux linkage Ψ_Σ , ΔE - difference

sign with respect to the flux linkage Ψ_0 and increase in magnitude with increasing frequency ω .

In the third scenario (Fig. 2c), flux linkage Ψ_0 and EMF E_{0nom} for the nominal load mode are selected when $\omega = \omega_{max}$. Obviously, in this case, to achieve the goal of stabilization U_L at changing of frequency ω , flux linkage Ψ_f must be one sign with Ψ_0 and increase with decreasing frequency ω .

IV. THEORY

A. Basic Assumption. Mathematical Description of the System

The analysis of electromagnetic processes in the system was carried out under the following assumptions:

- the static mode of DCPGS is considered;

- the magnetic system of the SG is unsaturated and linear;
- the SG has no damping circuits, its longitudinal and transverse inductances are approximately equal, that is $L_d \approx L_q = L$ (in fact, an implicit-pole SG is considered);
- EMF of the SG change according to the sinusoidal shape;
- active losses in the SG and AR are negligible.
- frequency of SPWM is significantly higher the frequency of voltage of the SG, currents and voltages in the SG circuit are analyzed by the main harmonics;
- the average value of the output voltage U_L is maintained constant due to the AR regulators, the stabilization is carried out mainly due to the change of phase of the control signal of AR while maintaining the constancy of its amplitude.

Taking into account the accepted assumptions, and also taking into account, that the AR is a symmetrical load, using the symbolic method of calculation of electric circuits of alternating current, the output circuit of the SG can be represented as a circuit shown on the Fig. 3. Where are:

$\dot{U}, \dot{E}, \dot{I}$ - complex values, herewith U, E, I - their effective values $j = \sqrt{-1}$, $\|\dot{E}\| = E = \omega \cdot \Psi_\Sigma = \omega \cdot (\Psi_0 + \Psi_f)$ - idle EMF of the SG, $\Psi_0 = \text{const}$ - flux linkage, produced by the permanent magnets $\|\dot{I}_G\| = I, L \approx (L_d + L_q)/2$ - current and equivalent total inductance of the SG, AR as a dependent voltage source the value of $\|\dot{U}_{AR}\| = U_{AR} = k_u \cdot M \cdot U_L$, in this case, it is equal to the voltage of the SG U , M - the depth of modulation of the AR, $k_u = \begin{cases} 1/2\sqrt{2} & \text{SPWM;} \\ 1/\sqrt{6} & \text{SVPWM;} \end{cases}$ coefficient depending on the type of PWM.

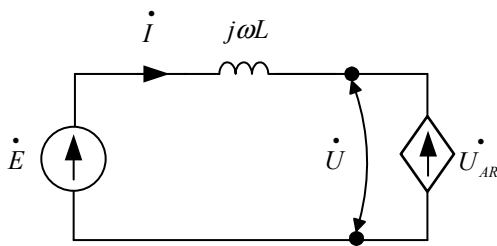


Fig. 3. Equivalent circuit of the output circuit of the SG.

The vector diagram of the output circuit of the SG for the first harmonic currents and voltages is given on the Fig. 4. Here is I_a, I_r - active and reactive components of the SG current.

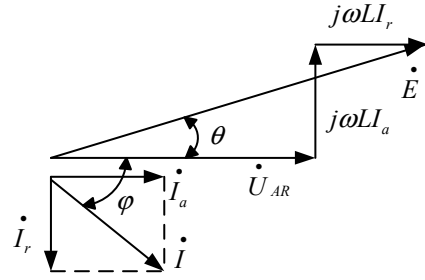


Fig. 4. Vector diagram of the output circuit of the SG.

From the vector diagram should:

$$(E)^2 = (U_{AR} + \omega L \cdot I_r)^2 + (\omega L \cdot I_a)^2; \quad (1)$$

$$\tan \theta = \frac{\omega L \cdot I_a}{E}.$$

The active component of the SG current can be determined from the balance of active power. Taking into account the assumption made, we believe, that the active power (P) consumed from the SG is equal load power (P_L)

$$P_L = P; P_L = U_L \cdot I_L; P = 3U_{AR}I_a = 3k_u \cdot M \cdot U_L \cdot I_a. \quad (2)$$

From the expression (2) we obtain

$$I_a = I_L / 3k_u \cdot M. \quad (3)$$

Considering the expression (3), and also the expression for the input voltage of AR (U_{AR}), the expression (1) is written as follows

$$\omega^2 \cdot (\Psi_0 + \Psi_f)^2 = \left(k_u M \cdot U_L + \omega L \cdot \frac{I_L}{3k_u \cdot M} \right)^2 + \left(\omega L \cdot \frac{I_L}{3k_u \cdot M} \right)^2. \quad (4)$$

For the generality of the results we use the relative units, which we denote, for example - U^* . As the basic values, we take the nominal values of the load voltage and current: $U_b = U_{Lnom}, I_b = I_{Lnom}$, as well as nominal load resistance $Z_b = R_{Lnom}$ and nominal power of the load $S_b = P_{Lnom} = U_{Lnom} I_{Lnom}$, as a base frequency value, we take the cyclic frequency of the voltage of the SG, on which the flux linkage Ψ_0 is determined, based on the mode of current overload in the absence of flux linkage of the excitation winding ($\Psi_f = 0$). For the first, second and third scenarios these will be frequencies, respectively $\omega_0, \omega_{min}, \omega_{max}$.

Taking into account relative units the expression (4) can be rewrite as follows

$$(I_{kz}^*)^2 \cdot \left(1 + \frac{\Psi_f}{\Psi_0} \right)^2 = \left(\frac{k_u M}{\omega^* X^*} + I_r^* \right)^2 + \left(\frac{I_L^*}{3k_u \cdot M} \right)^2, \quad (5)$$

where $I_{kz}^* = \Psi_0 / L I_{Lnom}$, $X^* = \omega_b L / R_{Lnom}$. Where I_{kz}^* - SG short-circuit current.

The total current, power factor and total power of the SG are determined by the following expression

$$I^* = \sqrt{(I_r^*)^2 + (I_a^*)^2}, \cos \varphi = \frac{I_a^*}{I^*}, \quad (6)$$

$$S^* = 3I^* \cdot U_{AR}^* = 3k_u M \cdot I^*.$$

B. Quantitative Assessment of Electrical Parameters of the DCPGS

Currents and voltages in the system depend on chosen design scenario and the control method.

When determining the parameters of the system, we will consider the minimum or maximum frequency (ω_{\min} , ω_{\max}) to be set, in addition to the nominal parameters of the load, minimum short-circuit current value (I_{kz}), maximum load current ($I_{L\max} = k_{over} \cdot I_{Lnom}$) in overload mode of the DCPGS (k_{over} - overload factor), when the quality of the generated voltage requirements according to GOST R 54073-2010 (Russian State Standard). As a result of the study, estimates of the following values will be obtained for three design scenarios:

- the value of idle EMF of the SG in different work modes;
- the flux linkages, produced by the permanent magnets and excitation winding;
- the value of the equivalent inductance of the SG;
- the full power and the power factor of the SG;
- the currents and voltages of the AR.

The proposed scenarios can be implemented using different laws of variation of flux linkage Ψ_f from the frequency ω in frequency range $\omega_{\min} \div \omega_{\max}$. The paper adopted, that the flux linkage of the excitation winding changes linearly (that corresponds to Fig. 2a). In this case the character of the change of flux linkage and EMF in the different scenarios will vary the selection of the base frequency ω_b , exactly: $\omega_b \in \{\omega_{\min}, \omega_{\max}\}$ - for the first scenario, $\omega_b = \omega_{\min}$ и $\omega_b = \omega_{\max}$ for the second and third scenarios. Then:

$$\Psi_f = \frac{-\Psi_{f\max}}{\omega_{\max} - \omega_b} (\omega - \omega_b). \quad (7)$$

As a result idle EMF of the SG will be change as follows

$$E(\omega) = \omega \cdot \left(\Psi_0 - \frac{\Psi_{f\max}}{\omega_{\max} - \omega_b} (\omega - \omega_b) \right). \quad (8)$$

Based on the definition of these scenarios, the value of the flux linkage Ψ_0 selected at $\omega = \omega_b$, $\cos \varphi = 1$, and also when $I_L = k_{over} I_{Lnom}$, where usually $k_{over} = 1.5 \div 2$. Taking into account these considerations and expression (4) we obtain

$$\omega_b \cdot \Psi_0 = E_{0nom} = \sqrt{(k_u M \cdot U_L)^2 + \left(X_b \cdot \frac{k_{over} I_{Lnom}}{3k_u \cdot M} \right)^2}, \quad (9)$$

$$X_b = \omega_b L.$$

As a rule, in aircraft supply systems, the required value of the short-circuit current in the load is set to ensure selective shutdown of branches with short-circuit. In short-circuit mode, the AR operates as a three-phase bridge unmanaged rectifier. The value of the short-circuit current at its output is determined according to expression [3]

$$I_{Lkz} = 3\sqrt{2}E(\omega)/\pi\omega L = 1,35 \cdot I_{kz},$$

Where I_{kz} - short-circuit current of the SG, I_{Lkz} - short-circuit current of the load.

We assume that in the short-circuit mode in the load, the excitation current of the SG is equal to zero, then the required value of the short-circuit current of the DCPGS output should be provided only by the flux linkage Ψ_0 . In this case:

$$I_{kz0} = E_{0nom} / X_0 = \Psi_0 / L. \quad (10)$$

where I_{kz0} - short-circuit current of the SG at flux linkage Ψ_0 , produced by the permanents magnets only.

In the presence of the excitation current short-circuit current of the SG will be determined by the following expression

$$I_{kz}(\omega) = E(\omega) / \omega L. \quad (11)$$

Substituting (10) into expression (9) and solving it relative to get E_{0nom} we obtain

$$E_{0nom} = \omega_b \cdot \Psi_0 = \frac{k_u M \cdot U_L}{\sqrt{1 - (k_{over} I_{Lnom} / 3k_u \cdot M \cdot I_{kz0})^2}}. \quad (12)$$

Thus, expressions (10) and (12) allow defining unambiguously Ψ_0 and L of the SG under specified load parameters, and also with the required short-circuit current I_{kz} .

The value of the flux linkage $\Psi_{f\max}$ of excitation winding determine at frequency $\omega = \omega_b$ from the condition

$$E(\omega_{\max}) = E_{0nom} + \Delta E, \quad (13)$$

Here the value ΔE should be set at the design stage.

Then

$$\Psi_{f\max} = \left[(\omega_{\max} / \omega_b - 1) \cdot E_{0nom} - \Delta E \right] / \omega_{\max}. \quad (14a)$$

$$\Psi_{f\max} = \left[(1 - \omega_{\min} / \omega_b) \cdot E_{0nom} - \Delta E \right] / \omega_{\min}. \quad (14b)$$

Expression (14a) is for first and second scenarios, and expression (14b) is for third scenario.

In this case if set $\Delta E = 0$, it means $E(\omega_{\max}) = E_{0nom}$ for the first and second scenarios, and $E(\omega_{\min}) = E_{0nom}$ for the third scenario, then the required value $\Psi_{f\max}$ will be determined as

$$\Psi_{f\max} = \frac{\omega_{\max} - \omega_b}{\omega_{\max}} \cdot \Psi_0 \text{ - first and second scenarios;}$$

$$\Psi_{f \max} = \frac{\omega_b - \omega_{\min}}{\omega_{\min}} \cdot \Psi_0 - \text{third scenarios.}$$

Consider the character of the changes of the SG currents depending on the operating modes.

From expressions (1) and (11) we obtain in relative units the following expression

$$\left[I_{kz}^*(\omega^*) \right]^2 = \left(k_u M / \omega^* X_b^* + I_r^* \right)^2 + \left(I_a^* \right)^2, \quad (15)$$

where

$$I_{kz}^*(\omega^*) = E^*(\omega^*) / \omega^* X_b^*, \quad k_u M / \omega^* X_b^* = U_{AR}^* / \omega^* X_b^*.$$

Expression (15) is an equation of circle in coordinates (I_a^*, I_r^*) with radius $R = I_{kz}^*(\omega^*)$ and center point O' with coordinates $(0, -k_u M / \omega^* X_b^*)$ [4].

In the polar coordinate system, this equation will reflect the dependence of the SG current absolute value I^* on the shift angle (φ) between the voltage and the current of the SG. The expression representing this dependence is as follows

$$I^*(\varphi) = -\frac{U_{AR}^*}{\omega^* X_0^*} \cdot \sin \varphi \pm \sqrt{\left[\frac{E^*(\omega^*)}{\omega^* X_0^*} \right]^2 - \left(\frac{U_{AR}^*}{\omega^* X_0^*} \cdot \cos \varphi \right)^2}. \quad (16)$$

For Fig. 5 shows in polar coordinates the graph of $I^*(\varphi)$, here is vector length, connecting point «0» with each point of the hodograph (16), is equal to the SG current (I^*). The projection of current vector on the direction, it is suitable in polar coordinates an angle equal to zero will be equal to the active component of the SG current I_a^* . The current projection in the orthogonal direction is equal to the reactive component of the SG current I_r^* . As follows from the

expression (16) and Fig. 5 each current value I_a^* , so and I_r^* , can match two current values I_r^* .

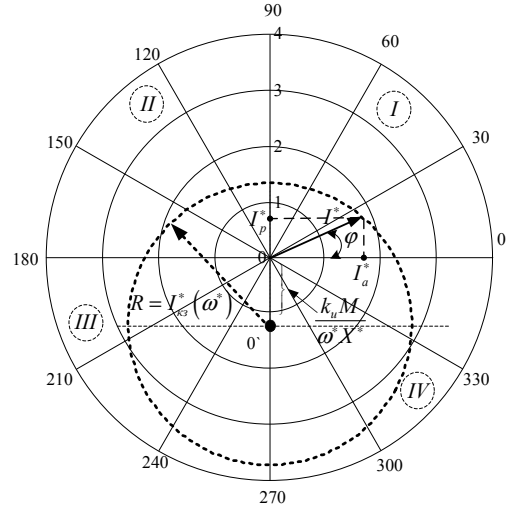


Fig. 5. Hodograph of the SG current and its orthogonal components.

As shown in [5] this value of the active current and power in the load can be realized at a large of the SG voltage and a relatively small current, as well as at high current and low voltage of the SG. This existence of a mode is determined by the relation between E^* and U_{AR}^* .

It should be noted, that this graph is valid for all modes of the system, exactly, for generation mode (quadrants I and IV) and motor mode electric starter start (quadrants II and III).

Let us consider in detail the possible states of the system in these modes. To do this select on the hodograph (16) characteristic points and for the study of these states will use vector diagram.

The Fig. 6 shows hodograph, built according to the expression (16) and it reflects the important points for the study of the state of the system: a,b,c,d,e,f, and the coordinates are defined for each point.

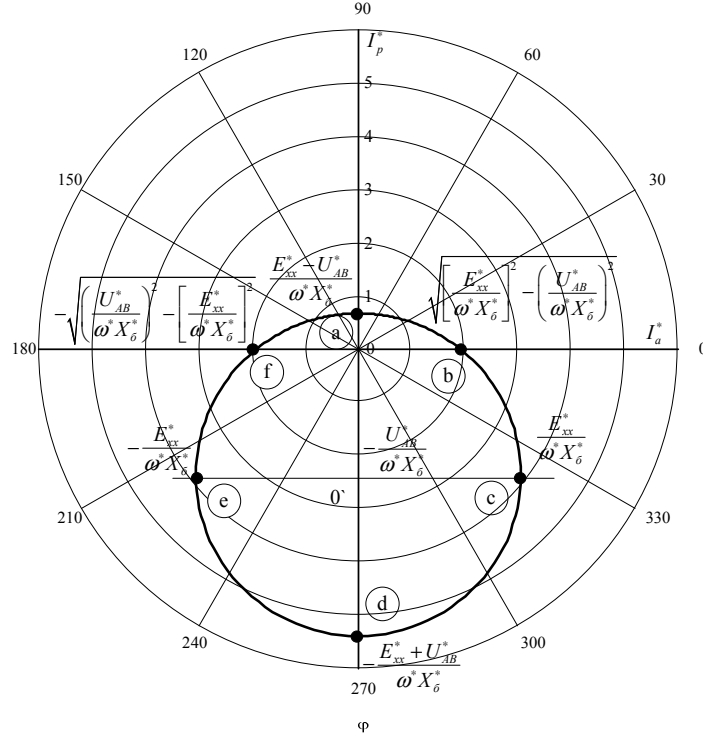


Fig. 6. Hodograph of the SG current with the characteristic points.

Two characteristic points «a» and «d» correspond to the transition from the generation mode to the motor mode and back. In these points, the active component of the current is zero ($I_a^* = 0$). Reactive component of the current I_r^* different from zero and is determined by the ratio E^* and U_{AR}^* as well as the magnitude of the reactance ωL .

Points «f» and «b» characterized the state of the system, in which there is a change of the sign of the shift angle (φ) between the voltage and the current of the SG, at the same time, this angle is zero at the points themselves ($I_p^* = 0$). The active component of the current at these points is determined by the expression

$$I_a^* = \sqrt{(E^*)^2 - (U_{AR}^*)^2} / \omega X_b^*. \quad (17)$$

At the same time in the sector «f-a-b» shift angle $\varphi < 0$ (inductive character), in the sector «b-c-d-e-f» - $\varphi > 0$ (capacitive character).

In the points «c» and «e» active component of the current I_a^* reaches the maximum possible value for this system and its value is

$$I_a^* = E^* / \omega X_b^*, \quad (18)$$

At the same time the reactive component of the current is different from zero and is

$$I_r^* = U_{AR}^* / \omega X_b^*. \quad (19)$$

VI. CONCLUSION

When designing of the DCPGS under different scenarios, the current load of the AR transistors will not be the same, although, the current value I_{kz0} , corresponding to the zero value of the excitation current, is the same in all scenarios. In transient modes, the short-circuit current can reach significantly large values. This is because, the excitation current will be reduced to zero during the finite time. And as follows from the calculations the maximum value of the short-circuit current ($I_{kz \max}^*$) can be in a system designed according to scenario 3 ($I_{kz \max}^* (\omega_{\min}^*) \approx 6$), the minimum value of this current will be in the system corresponding to scenario 2 ($I_{kz \max}^* (\omega_{\min}^*) \approx k_{over} \div 3$).

With respect to the voltage at which the transistors of the AR should be selected, the following can be noted. As we can see from Fig. 2 the maximum voltage applied to transistors is typical for the scenario 2, and minimum voltage is typical for the scenario 3. And in this case, the maximum value of the voltage will be determined by the values $\omega_{\max} \Psi_0$.

Thus, from the methodological point of view, in the system designed according to scenario 1, the installed power of transistors will be minimal, if it is estimated as the product of the maximum current, which will flow through it, and the maximum value of voltage that can be applied to it.

Let's compare the main parameters of the SG in different design scenarios. In this case, we take for certainty,

that $\Delta E^* \rightarrow 0$, ω_{\max} , E_{0nom} are the same in all scenarios and introduce the value of the frequency range $D = \omega_{\max} / \omega_{\min}$.

In the Table I for the scenarios considered, flux linkages Ψ_0 is given, expressed as a function of D и E_{0nom} / ω_{\max} (column 2), as well as the maximum value of the flux linkage ($\Psi_{f \max}$), which is produced by the excitation winding, related to the flux linkage (Ψ_0) produced by the permanent magnets $\Psi_{f \max}^* = \Psi_{f \max} / \Psi_0$ (column 3). Taking into account, that the flux linkage Ψ_0 , under accepted conditions of comparison, the minimum in scenario 3, with the aim of a comparison of the values of this flux linkage and $\Psi_{f \max}$ in different scenarios in columns 4 and 5 show the relationship

of these flux linkages to the flux linkage in the scenario 3: $\Psi_0 / (E_{0nom} / \omega_{\max})$ и $\Psi_{f \max} / (E_{0nom} / \omega_{\max})$ respectively.

As can be seen from the Table I, the maximum flux linkage from permanent magnets is typical for scenario 2, and minimum is typical for scenario 3. In this case, the flux linkage produced by the excitation winding has a maximum value in scenarios 2 and 3. If we assume that in the specified conditions of comparison, the installed power of the SG is to some extent proportional to the total flux linkage $\Psi_{f \max} + \Psi_0$, then theoretically in case of scenario 1 the SG will have less installed power.

Thus, from the comparison of DCPGS design scenarios, it follows that from the point of view of the installed power of AR and SG is preferred scenario 1.

TABLE 1
THE MAIN THEORETICAL RESULTS DEPENDING ON THE SCENARIO OF THE DCPGS DESIGN

| Scenario number | Ψ_0 | $\Psi_{f \max}^* = \Psi_{f \max} / \Psi_0$ | $\Psi_0 / (E_{0nom} / \omega_{\max})$ $E_{0nom} = const$ | $\Psi_{f \max} / (E_{0nom} / \omega_{\max})$ $E_{0nom} = const$ |
|-----------------|--|---|---|--|
| 1 | $\Psi_0 = E_{0nom} / \omega_0 =$ $= \frac{E_{0nom}}{\omega_{\max}} \cdot \left(\frac{2}{1+1/D} \right)_{D=2}$ $= 1.33 \cdot E_{0nom} / \omega_{\max}$ | $\Psi_{f \max}^* = \frac{\omega_{\max} - \omega_0}{\omega_{\max}} =$ $= \frac{1}{2} (1 - 1/D)_{D=2} =$ $= 0.25$ | 1.33 | $\frac{2}{3} (1 - 1/D)_{D=2} =$ $= 0.33$ |
| 2 | $\Psi_0 = E_{0nom} / \omega_{\min} =$ $= \frac{E_{0nom}}{\omega_{\max}} \cdot D_{D=2} =$ $= 2 \cdot E_{0nom} / \omega_{\max}$ | $\Psi_{f \max}^* = \frac{\omega_{\max} - \omega_{\min}}{\omega_{\max}} =$ $= (1 - 1/D)_{D=2} = 0.5$ | 2 | $2(1 - 1/D)_{D=2} = 1$ |
| 3 | $\Psi_0 = E_{0nom} / \omega_{\max}$ | $\Psi_{f \max}^* = \frac{\omega_{\max} - \omega_{\min}}{\omega_{\min}} =$ $= (D - 1)_{D=2} = 1$ | 1 | $(D - 1)_{D=2} = 1$ |

From the above we can conclude.

- Three scenarios of DCPGS design based on a synchronous generator with combined excitation and an active rectifier with high frequency SPWM are proposed and analyzed.
- It is shown that the parametric control of the excitation current of a synchronous generator with a combined excitation as part of the DCPGS according to the proposed law proportional to the voltage frequency of the generator allows to obtain the maximum energy efficiency of the system in terms of minimizing the flows of reactive power

between the generator and the active rectifier, which is characterized by a close to one value of the power factor SG.

- In modes other than the nominal, significant flows of reactive power between the generator and the active rectifier remain, but their level is lower than in similar modes in a system with an unregulated magnetoelectric generator.
- It is revealed that the scenario 1 design of the DCPGS with the orientation of the choice of the nominal regime at the midpoint of the frequency range of the voltage SG is preferable, since in this case theoretically the installed

capacity of SG and AR is less in comparison with scenarios 2 and 3.

- Parametric control of the excitation current of a synchronous generator with combined excitation does not realize all the possible advantages of this method of constructing of the DCPGS, but has the simplicity of building a control system and can be used as an additional control channel in a combined control system.



Svetlana V. Vorobyeva. She is Candidate of engineering sciences, associate professor and head of the department «Radiotechnical systems» at the Siberian state university of telecommunications and computer sciences. Her research interests include the noise immunity of digital communication channels, Systems digital radio.
E-mail: svetlana_v@ngs.ru

REFERENCES

- [1] Kharitonov S.A. Electromagnetic processes in electric power generation systems for autonomous objects: monograph / S.A. Kharitonov – Novosibirsk: NSTU, 2011. – 536 p.
- [2] Kharitonov S.A. An Analytical Analysis of a Wind Power Generation System Included Synchronous Generator with Permanent Magnets, active rectifier and Voltage Source Inverter. Wind Power. // Editor by S.V. Mueen, 2010 Intech, First published June 2010, Printed in India, p. 558
- [3] Razmadze S.M. Converter circuits and systems. - M.: HS, 1967, P. 527.
- [4] Com G. Com T. Mathematics handbook (for science officers and engineers). - M. – the Science, 1974. - 832 p.
- [5] Kharitonov S.A. Some energy relations of generation of electric energy “variable speed-constant frequency ” on the bases of synchronous generators with excitation from permanent magnets and voltage inverters. Technical electrodynamics. Thematic issue. Power electronics and energy efficiency. Part 3. Kiev, 2006, p.51-58.



Sergey A. Kharitonov received doctor of sciences in Electrical Engineering from Novosibirsk State Technical University, Novosibirsk (NSTU), and Ph. D work called as “ELECTRIC ENERGY GENERATING SYSTEM FOR WIND ENERGETICS AND INDEPENDENT MOBILE OBJECTS (Analysis and synthesis). He is currently Professor and Head Department of Electronics and Electrical Engineering in the NSTU. His research interests include different application field of industrial electronics.
E-mail: kharit1@yandex.ru



Andrey S. Kharitonov is Lead engineer, Institute of Power Electronics, Novosibirsk State Technical University, NSTU. His research interests are currently focused on control motor drive based on PMSM, systems of generating electrical energy based on synchronous generator, starter generator based on synchronous generator with permanent magnets for aircrafts.
E-mail: andrekh@yandex.ru



Dmitry L. Kaluzhskij, doct. of tech. sc., professor of department “Electronics and Electrical Engineering”, NSTU graduated from Novosibirsk Institute of Electrical Engineering (NIEE) in 1980. He works in NSTU (NIEE) from 1980. His area of scientific research is gearless electric motors and their control systems. Prof. Kaluzhskij has more than 40 papers.
E-mail: verp307@mail.ru

Reactive Power Compensators Based on Simple AC Voltage Regulators

Gennady S. Zinoviev, *Member, IEEE*, Aleksey V. Udovichenko, *Member, IEEE*
Novosibirsk State Technical University, Novosibirsk, Russia

Abstract – A new applying of AC voltage regulators with commutated capacitors is proposed. This allowed obtaining two versions of reactive power compensators. An analysis of such regulators using a direct calculation method is given, and the dependences of the output reactive power from the modulation depth are obtained. The quality of the generated capacitive current is estimated by its harmonic coefficient (THD). Comparison of compensators in terms of installed power of reactive elements and power loss in semiconductor elements is given.

Index Terms – Compensator, reactive power, harmonic ratio.

I. INTRODUCTION

SPEED REGULATED AC/DC current electric drives, Induction furnaces, welding installations and other devices for electrotechnologies consume a rapidly varying reactive power from the supply grid. This leads to a deterioration of the grid voltage quality, which adversely effects on the consumers themselves and also causes additional losses of electricity in the grid. In Russia, these losses reach 100 billion kWh and more (about 10% of the consumed electricity) and significantly exceed the values achieved in the nineties (about 80 billion kWh) with a comparable magnitude of the total electricity consumption of Russia [1]. A large part of these losses is occupied by losses caused by the presence of reactive power. In large regions, the amount of energy loss from reactive power transmission is estimated by ten and more billion kWh * hr / yr. Such significant indicators are caused by low $\cos\phi$ of industrial loads about the order from 0.7 to 0.85. It should be noted that with a power factor of 0.7, the energy losses are doubled. The growth of these losses leads to a decrease in the overall capacity of the electric grid and as a consequence to a decrease in new consumers. Also, low $\cos\phi$ can cause deterioration in the quality of electricity. Solving the problem of reducing losses is possible with the help of reactive power compensators. With these devices, it is rational to generate reactive power directly at connecting nodes of the electrical consumers.

First proposals on the use of autonomous voltage inverters in the reactive cell mode to compensate of any inactive power were made by us [2], there were proposals also abroad [3]. But these solutions, despite the high quality, have not yet received wide practical application because of their high unit cost. Therefore, the task of developing sufficiently effective but significantly simpler reactive power compensators is actual. The solution of this problem was achieved due to the implementation of reactive power compensators not on the

basis of a reactive inverter cell, but on the basis of a reactive cell of an AC voltage regulator [4-6].

II. SMALL VALVES THREE-PHASE COMPENSATORS OF REACTIVE POWER

Fig. 1 shows schemes of reactive power compensators based on AC voltage regulators with commutated capacitors with the 3 (Fig. 1a) and 6 (Fig. 1b) capacitors. Depending on the application method, where it is required to compensate the reactive power in a larger range, a variant with 6 capacitors is chosen.

It is necessary to provide a current to the grid that is lead of the grid voltage by 90° to compensate the reactive power of the grid. By regulating the duty cycle of the control pulse of the transistors $T1$ and $T2$, it is possible to regulate the capacitive current, and as a consequence of the reactive power. In Fig. 2 a diagram of the input current and voltage is presented.

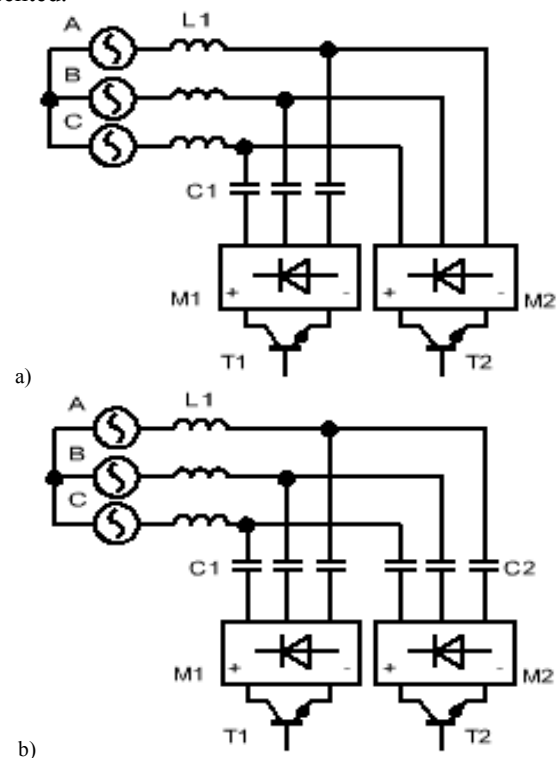


Fig. 1. Reactive power compensator.

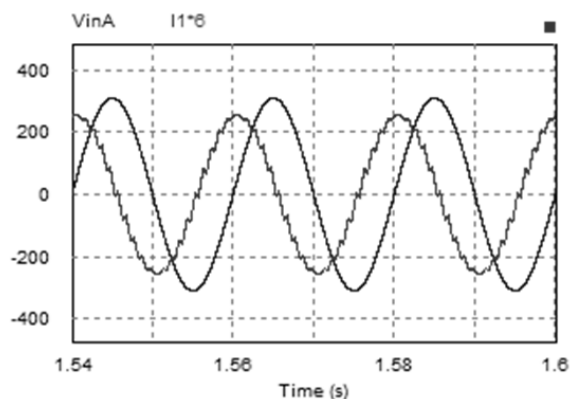


Fig. 2 The oscillograms of the input voltage and the current of the compensator.

In the case of three capacitors, a research was carried out for two values of 10 μF (relative reactive power 2.6) and 50 μF (relative reactive power 6.7). It was found that at low capacity levels the current control range is wider, with current lead observed at $M=[0;0.7]$, whereas for large capacitance values this range narrowed down to 2 times, but the current was more produced, as can be seen from Fig. 3.

In connection with the fact that in a circuit with three capacitors the current is not always capacitive. When switching the key T2, the reactance current of the grid is generated, the presence of which leads to a positive phase between the current and the voltage, this moment is shown on the diagram in the negative region. This problem can be solved by including additional three capacitors, as shown in Fig. 1b. The dependence of the generated reactive power from the modulation depth is shown in Fig. 4.

The additional capacitors in the last circuit are taken with nominal values about an order of magnitude larger, 0.0001 F (relative reactive power 2.2) and 0.00025 F (relative reactive power 4.7), respectively.

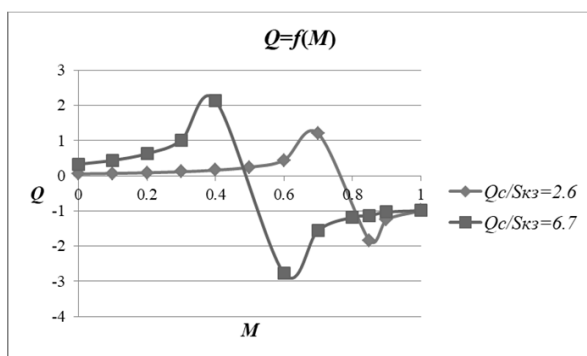


Fig. 3 Dependence of the output reactive power from the modulation depth for the compensator with the 3 capacitors.

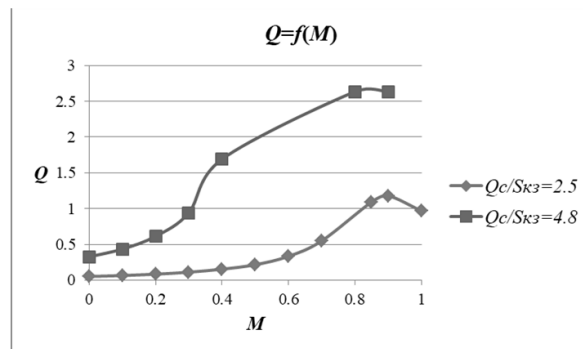


Fig. 4 Dependence of output reactive power from the modulation depth for a compensator with 6 capacitors.

III. ANALYTICAL CALCULATION BY THE ADE METHOD

Fig. 5 shows an AC voltage regulator with commutated capacitors and its replacement one phase circuit.

To construct a mathematical model of the compensator by the first harmonic and higher harmonics we use the direct method of calculating the ADE (1) and ADE2 [7] and in the end, the dependences of the output reactive power (relative to the reactor power) from the modulation depth are constructed, Fig. 6 [7]. Switching function of keys S1 and S2 carrying out the conversion between two states of the circuit is presented below:

$$\psi = 1 - M - (-1)^n \sum_{n=1}^{\infty} \left[\frac{2}{\pi n} \sin(2\pi n M) \cdot \cos(\omega n t) \right] \quad (1)$$

$$\psi_{\cos} = \frac{1-M}{2} + \frac{2 \sin(\pi n M) \sin(T n \omega_1) (8\pi^2 - T^2 n^2 \omega_1^2)}{\pi n T \omega_1 n (16\pi^2 - T^2 n^2 \omega_1^2)} \quad (2)$$

As can be seen from the presented cosine component of the commutation function (2), it is necessary to compose differential equations to construct a mathematical model and to transform them into algebraic ones. For this we "split" first harmonics of variables into their active (sinus) and reactive (cosine) components, orthogonal to each other. In the process of algebraization, we multiply the equations consecutively by $\cos(\omega t)$ and $\sin(\omega t)$ and averaged over the period of the first harmonic. As a result of the algebraization of this system of equations using the ADE2 method, we obtain the following

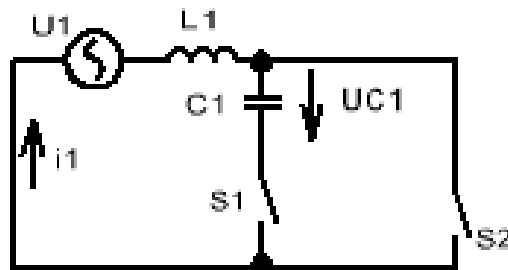


Fig. 5. Replacement power factor compensation circuit for one phase.

system of algebraic equations, in matrix form [4]:

$$\begin{pmatrix} 0 & 0 & -\psi_{\cos(1)}\omega L_1 & 0 & 0 & 0 \\ 0 & -R_1 & \psi_{\cos(1)} & 0 & \omega L_2 & 0 \\ -1 & 1 & 0 & 0 & 0 & -\omega C_1\psi_{\cos(1)} \\ \omega L_1 & 0 & 0 & 0 & 0 & 0 \\ 0 & \omega L_2 & 0 & 0 & R_1 & 0 \\ 0 & 0 & -\omega C_1 & 1 & -1 & 0 \end{pmatrix} \cdot \begin{pmatrix} I_{1(1)r} \\ I_{2(1)r} \\ U_{C1(1)r} \\ I_{1(1)a} \\ I_{2(1)a} \\ U_{C1(1)a} \end{pmatrix} = \begin{pmatrix} 0 \\ 0 \\ 0 \\ U_{1(1)a} \\ 0 \\ 0 \end{pmatrix} \quad (3)$$

In contrast to [4], it is necessary to get rid of R_1 and L_2 . The final expression is:

$$\begin{pmatrix} 0 & -\psi_{\cos(1)} & \omega L_1 & 0 \\ -1 & 0 & 0 & -\omega C_1\psi_{\cos(1)} \\ \omega L_1 & 0 & 0 & \psi_{\sin(1)} \\ 0 & -\omega C_1\psi_{\sin(1)} & 1 & 0 \end{pmatrix} \cdot \begin{pmatrix} I_{1(1)r} \\ U_{C1(1)r} \\ I_{1(1)a} \\ U_{C1(1)a} \end{pmatrix} = \begin{pmatrix} 0 \\ 0 \\ U_{1(1)a} \\ 0 \end{pmatrix} \quad (4)$$

Dependencies have been obtained for the case when the output current to the grid is ahead of the grid voltage. The values of the input current were received, from which the relative value of the reactive power of the grid was calculated to the power of the short circuit. A comparison with results is given obtained with the help of modeling, the greatest discrepancy is noticeable in the region of the transition from the zone of leading current to the zone of the lagging current.

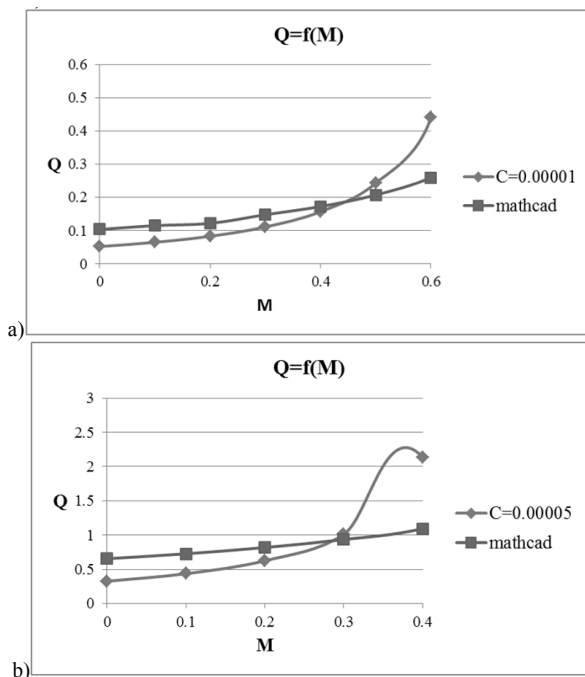


Fig. 6. Dependence of the output reactive power from the modulation depth for $C = 10 \mu\text{F}$ (a) and $C = 50 \mu\text{F}$ (b).

The quality of the generated capacitive current was evaluated and presented in the form of the dependence $THDi = f(M)$ in Fig. 7.

IV. THE DISCUSSION OF THE RESULTS

Comparison of the proposed and known compensators by reactive power of capacitors, power losses in semiconductors and their cost at the level of 100 kVAR were made (see Table I). The cost of the proposed compensators is equal to twice the cost of their components.

TABLE I
COMPENSATORS COMPARISON

| Parameter (at 100 kVAR) | M=0 | M=0.1 | M=0.2 | M=0.3 | M=0.4 | M=0.5 | M=0.6 |
|--------------------------------|-------|-------|-------|-------|-------|--------|--------|
| KPM-0,4-150-6-25 Y3 IP31 [8] | | | | | | | |
| Cost, \$ | 1000 | | | | | | |
| Compensator with 3 capacitors | | | | | | | |
| Q_r , kVAR | 55 | 69 | 89 | 123 | 18 | 299 | 63 |
| Losses in semiconductors, W | 3635 | 6362 | 9327 | 13012 | 19489 | 3291.1 | 7141.4 |
| Cost, \$ | ~1200 | | | | | | |

With the growth of the modulation depth, capacitors reactive power tends to a nominal value, but in the case of 6 capacitors this is more smoothed out that it can be seen from the table. As for losses on semiconductor elements, they reach up to 5% of the nominal 100 kVAR.

V. CONCLUSIONS

- Two circuits of reactive power compensators based on AC voltage regulators with commutated capacitors are analyzed.
- Schemes of reactive power compensators are investigated and expansion of a calculating direct method of energy parameters of converters on their models with variable parameters is determined. The effective values of higher harmonics of currents and voltages are obtained. This allowed us to estimate the distortion of the current and voltage curve, with respect to their first harmonics. This analysis showed the possibility of calculating the energy parameters in the schemes of reactive power compensators.

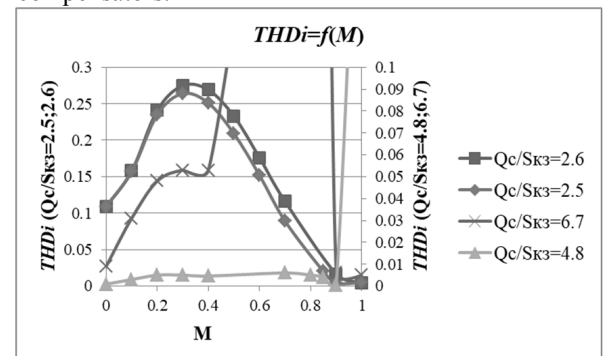


Fig. 7 Quality of generated current for case with 3 capacitors ($Q_c/S_{k3}=2.6; 6.7$) and 6 capacitors ($Q_c/S_{k3}=2.5; 4.8$).

3. Analysis of reactive power compensators has shown the possibility of regulating the generated capacitive current. The evaluation of the reactive power in relation to the short-circuit power gave a full range of control.
4. In addition, the harmonic ratio of the generated current was received for 4 cases (two versions of each circuit). The most effective option was a 6-capacitor with a larger capacity. There, the harmonic coefficient did not exceed 5% in the working control zone.
5. At 100 kVAR, the reactive power of the capacitors varied from 5.5 to 63 kVAR, which in relative units was from 6 to 65%. As for losses in semiconductors, they are not significant at such power levels and do not exceed 5% at the working control range $M = [0; 0.6]$.

REFERENCES

- [1] V. Vorotnitsky, Strategic way to increase the energy efficiency of networks. : News of electrical engineering. 3 (93) 2015
- [2] G.S. Zinoviev, Valve compensators of reactive power on the basis of a voltage inverter. In the book: Sovrem. problems of transforming technology. Theses dokl. Vses. STC, Part 2. Kiev: IED Academy of Sciences of the Ukrainian SSR, 1975, p. 247-252.
- [3] H. Akagi, Instantaneous reactive power compensators comprising switching devices without energy storage components. IEEE Trans. Ind. Appl., vol. IA-20, no. 3, pp. 625–630, May/Jun. 1984.
- [4] G.S. Zinoviev, AC voltage regulator. Pat. No. 2566668, op. 06/16/2014.
- [5] G.S. Zinoviev, Raising-lowering regulator of alternating voltage, patent number 2580677, op. 10.04. 2014.
- [6] A.V. Udovichenko, G.S. Zinoviev, "AC voltage regulators with switched capacitors," Proc. 2016 IEEE Inter Power Electronics and Motion Control Conference (PEMC), Varna, Bulgarian, 2016, pp. 44-49
- [7] Zinoviev GS The fundamentals of power electronics. - 5 th ed., M. : Yurayt, 2012 .. 667p.
- [8] Internet resource
https://www.ruselt.ru/catalog/production/kontaktornye_i_tiristornye_kompensatory/



Gennady S. Zinoviev – professor of the Industrial Electronics Department of the Novosibirsk State Technical University (NSTU), research supervisor of the Research Laboratory “Optimization of Energy in Converting Systems”. Author of the textbook on power electronics, two monographies devoted to electromagnetic compatibility of converters, more than 90 patents and over 200 publications.



Aleksey V. Udovichenko – Ph.D., assistant of Computer Engineering Department of Novosibirsk State Technical University. Research interests - energy-efficient AC voltage regulators, soft-start of engines, power electronics.

Performance Evaluation of Shunt Active Power Filter Based on Parallel Multilevel Inverters

Maksim A. Dybko, Vadim G. Tokarev, Sergey V. Brovanov, Sergey A. Kharitonov
Novosibirsk State Technical University, Novosibirsk, Russia

Abstract - This paper presents energy quality performance evaluation of an active power filter (APF) based on parallel multilevel NPC inverters. High power energy conversion systems are usually engage modular power converter structures. They can be parallel or cascade ones. In this research it is shown that usage of parallel structure for active power filtering provides several advantages such as power sharing, improved compensation quality and efficiency. In particular, three-level NPC converters in parallel connection with interleaved PWM for APF are considered. Technical considerations of the energy quality performance are presented for more common case of k inverters in parallel. Simulation results are presented to prove the theoretical conclusions.

Index Terms – Shunt active power filter, parallel multilevel converter, performance evaluation.

I. INTRODUCTION

ACTIVE POWER filters are the power electronic devices which are intended to ensure the required energy quality in a grid in conditions of significant non-linear and reactive loads. Currently, different issues of power quality are raised quite frequently in order to follow the hard electromagnetic compatibility requirements, regulated by the standards [1, 2]. Typical non-linear loads such as diode rectifiers, voltage regulators, electric drives etc., consume the current that contains higher order harmonics and reactive power. Consequently, distorted supply voltage has a significant negative influence on the other consumers. Especially it concerns some technological and scientific equipment that is power quality sensitive.

For the last decades, many solutions for the power conditioning have been presented in the literature [3-8]. For the high power applications, power conditioners, as many other power conversion systems are designed to have modular structure. Among the published papers some consider cascaded structures [3-5], others – parallel structures [6-9]. Paper [3] presents a high power static VAr compensator based on a number of two-level inverters connected in series by AC side. Authors of [4] and [5] proposed cascaded H-bridges inverters based active power filter. Both structures are used to form high voltage AC voltage by multiple steps, i.e. both structures implement multilevel AC voltage generation. These and other cascaded topologies are widely used for high voltage applications. However, they still have the same disadvantage: cascaded converter structure has lower fault tolerance compared to a parallel one. In other words, if any series link fails, the whole converter fails as well. That is why parallel topologies are considered as a competitive solution. An interesting APF

structure is proposed in [7]. The authors offer two different power converters: the main converter is intended to provide VAr compensation while the secondary one performs the harmonic compensation. Pure parallel converters with current sharing reactors are published in [6], [8, 9]. Usage of multilevel power converters as shown in [5, 7, 10] and [11], proves its effectiveness from the power quality point of view. In [11] the authors had shown that usage of parallel inverters allow better compensation quality than with a single power converter. This paper is devoted to estimation of the active power filters based on parallel connection using the current sharing reactors. It is shown that usage of multilevel power converter structure allows one to increase the bandpass of APF. Parallel inverters scheme also makes it possible to extend the APF bandpass in some cases. Detailed simulation model is used to verify the results of mathematical model.

II. PROBLEM DEFINITION

The considered power system is shown in Fig. 1. The one contains a primary power source, a nonlinear load and the active power filter. The primary power source (PPS) can be the AC grid, an autonomous energy source such as diesel generator or renewable energy source. It can also be a transformer secondary winding. As a base of the APF, N -level NPC converters are used. Multilevel NPC converters have shown their ability to generate the output voltage and current of higher quality, especially in parallel connection using current sharing reactors and the interleaved PWM strategy [12, 13].

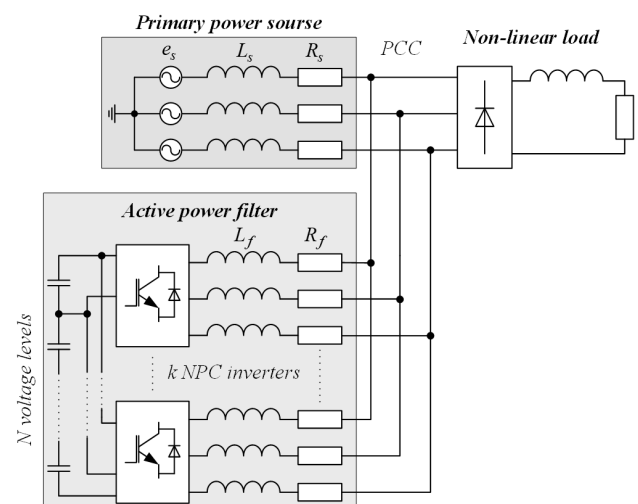


Fig. 1. Power supply system with an Active power filter.

The main task, described in this paper considers all the passive components depicted in Fig. 1. APF output inductances and PPS inductances define the power system bandpass together.

III. ENERGY QUALITY PERFORMANCE ESTIMATION

Let us denote the main factors to estimate the energy quality performance of an APF using the equivalent circuit shown in Fig. 2.

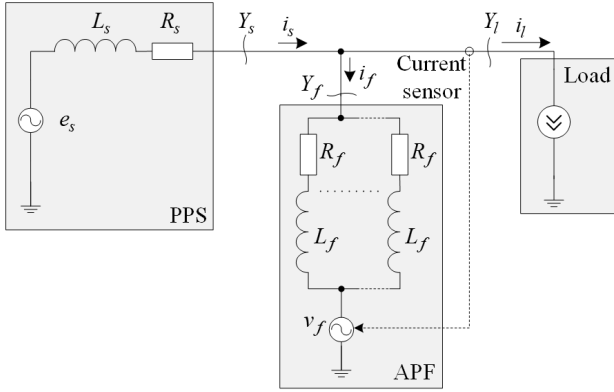


Fig. 2. Equivalent circuit to analyze the APF performance.

The energy quality performance factors are:

- APF bandpass: Δf ;
- TPower factor in the power source section (Y_s):
 $\chi_s = \frac{P_s}{S_s}$, where the apparent power is S_s and the active power is P_s ;
- Power factor in the load section (Y_l): $\chi_l = \frac{P_l}{S_l}$;
- APF Efficiency $\eta_f = \frac{\sqrt{S_f^2 - P_f^2}}{S_f}$, where the apparent power S_f and the APF losses P_f are measured in the section Y_f .

A. APF Bandpass Estimation

The Active power filters bandpass defines the higher frequency limit. The one shows which higher harmonic can be transferred as a compensating current component in PCC. Using Fig. 2, one can define the bandpass by impedances of the PPS and APF. Assume the filter's equivalent voltage source generates all the required harmonic current components including fundamental. The following equation can be written from Fig. 2 using the KCL:

$$i_s = i_f + i_l \quad (1)$$

In (1), component i_l is the load current and defined by the equivalent current source. The filter current i_f contains multiple harmonics. Impedances $\dot{Z}_s = R_s + j\omega L_s$ (PPS impedance) and $\dot{Z}_f = R_f + j\omega L_f$ (one of the APF inverters)

define the harmonic amplitudes. Obviously, the PPS impedance cannot be changed and it depends on PPS type. If PPS is an AC grid, its impedance much lower when the PPS is a transformer. The filter's impedance can be changed. Taking into account possibility of inverter parallel connection using the current sharing reactors as shown in Fig. 2, the current n -th harmonic component can be represented as follows:

$$i_f^{(n)} = \frac{v_f^{(n)}}{\dot{Z}_f^{(n)} + \dot{Z}_s^{(n)}} = \frac{v_f^{(n)}}{j\omega n \cdot \left(\frac{L_f}{k} + L_s \right) + \frac{R_f}{k} + R_s}, \quad (2)$$

where k denotes the parallel inverters count, $\omega = 2\pi f$, f is the fundamental frequency. Then, the admittance of the loop for n -th current harmonic component will be defined from (2):

$$Y^{(n)} = \left(j\omega n \cdot \left(\frac{L_f}{k} + L_s \right) + \frac{R_f}{k} + R_s \right)^{-1}. \quad (3)$$

The time constant of the circuit shown in Fig. 2 is as follows:

$$\tau = \frac{L_f + k \cdot L_s}{R_f + k \cdot R_s}. \quad (4)$$

The respective cut-off frequency defines the attenuation of the higher harmonics $f_c = 1/2\pi\tau$. Equations (3) and (4) show that in case of lower PPS impedance (e.g. high power AC grid) the cut-off frequency is defined by the filter parameters only. On the one hand, this frequency will remain the same whatever number k is, because the ratio L_f / R_f remains constant. On the other hand, the admittance of the loop will rise with rising k . Fig. 3 demonstrates frequency response of the admittance for k in range 1 to 4.

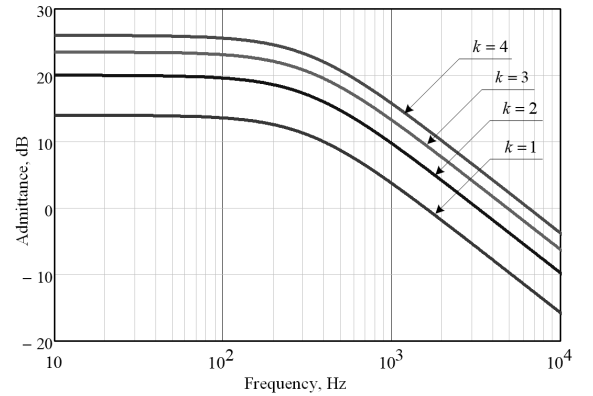


Fig. 3. Frequency response for lower PPS impedance.

Frequency responses in Fig. 3 are built for the case of PPS that is close to ideal power source (Numerical data are presented by Table I). It is seen that for the chosen frequency the admittance is higher in spite of equal cutoff frequency for all values of k . Fig. 4 shows the same curves for the case when the PPS impedance is much closer to the APF output impedance.

TABLE I
EQUIVALENT CIRCUIT PARAMETERS FOR IDEAL AND REAL PPS

| Case | R_s , Ohm | L_s , H | R_f , Ohm | L_f , H | k, f_c , Hz |
|-------|-------------------|-------------------|-------------|-------------------|--|
| Ideal | $1 \cdot 10^{-6}$ | $1 \cdot 10^{-8}$ | 0.2 | $1 \cdot 10^{-4}$ | $k = 1.4, f_c = 318$ |
| Real | $5 \cdot 10^{-2}$ | $1 \cdot 10^{-4}$ | 0.2 | $1 \cdot 10^{-4}$ | $k = 1, f_c = 198.9$ $k = 2, f_c = 159.2$ $k = 3, f_c = 139.3$ $k = 4, f_c = 127.3$ |

Fig. 4 shows that for a real primary power source, its impedance (grid or transformer winding) must be taken into account.

Note, although the cutoff frequency in the real case decreases, when inverter count k increases, the admittance can be higher for a selected frequency as in ideal case. The key difference between two cases lies in the range above the cutoff frequency.

Both of the cases allow us to conclude, usage of the parallel inverter structure provides higher compensation quality due to wide bandpass for the higher harmonic components.

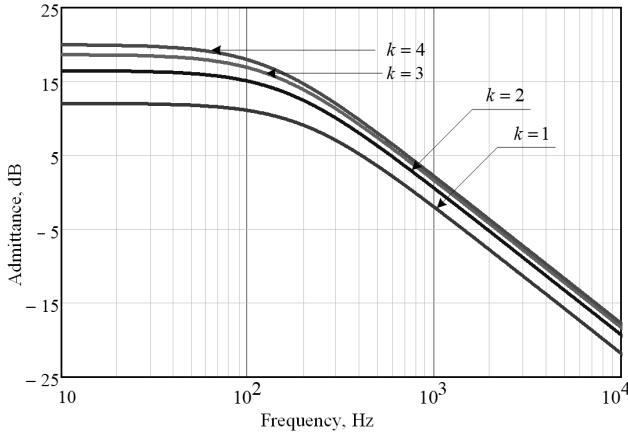


Fig. 4. Frequency response for significant PPS impedance.

B. APF Power Quality Estimation

To calculate the power quality factors designated at the beginning of this section, mathematical model based on the switching functions is used. The technique to implement the switching functions and spectral analysis of parallel multilevel converters was previously described in several papers [12-14]. In this section, only the addition concerning non-sinusoidal current generation and diode rectifier description is presented.

Diode bridge rectifier is a typical example of a nonlinear load, Fig. 5. The model can be reduced to one equivalent circuit with a few variable parameters, see Fig. 6.

Operation of the rectifier can be divided into six periods. In each period the equivalent circuit remains the same as depicted in Fig. 6 with different diodes open (D_p and D_n) and particular phase voltage sources connected (e_x and e_y),

where indices p, n, x and y can take the values: $p \in \{1, 2, 3\}, n \in \{4, 5, 6\}$,

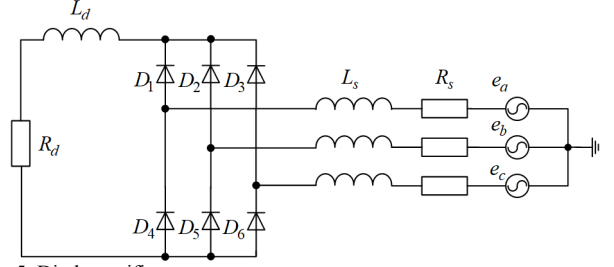


Fig. 5. Diode rectifier.

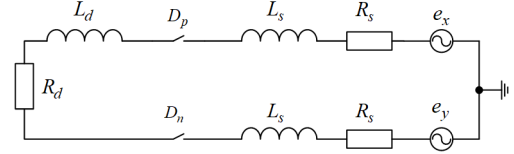


Fig. 6. Rectifier equivalent circuit.

$x, y \in \{a, b, c\}$. All the necessary parameters and variables for each of six periods of operation are summarized in Table II.

TABLE II
EQUIVALENT CIRCUIT PARAMETERS FOR DIODE RECTIFIER

| Per. | Duration | D_p | D_n | e_x | e_y |
|------|---|-------|-------|-------|-------|
| 1 | $\left[0; \frac{\pi}{6}\right] \cup \left[\frac{11\pi}{6}; 2\pi\right]$ | D_3 | D_5 | e_c | e_b |
| 2 | $\left[\frac{\pi}{6}; \frac{\pi}{2}\right]$ | D_1 | D_5 | e_a | e_b |
| 3 | $\left[\frac{\pi}{2}; \frac{5\pi}{6}\right]$ | D_1 | D_6 | e_a | e_c |
| 4 | $\left[\frac{5\pi}{6}; \frac{7\pi}{6}\right]$ | D_2 | D_6 | e_b | e_c |
| 5 | $\left[\frac{7\pi}{6}; \frac{3\pi}{2}\right]$ | D_2 | D_4 | e_b | e_a |
| 6 | $\left[\frac{3\pi}{2}; \frac{11\pi}{6}\right]$ | D_3 | D_4 | e_c | e_a |

In our task, the purpose of this model is to obtain the input line current as an APF target to be processed and compensated. As far as the equivalent circuit remains the same all the time, using the spectral method we can write the whole impedance for n -th harmonic:

$$\dot{Z}_{rect}^{(n)} = R_d + 2R_s + j \cdot n \cdot \omega \cdot (L_d + 2L_s) \quad (5)$$

Equivalent voltage applied to this impedance for phase A can be written as follows:

$$v_{ZA} = (e_a - e_b) \cdot (F_1 + F_5) + (e_a - e_c) \cdot (F_3 + F_6), \quad (6)$$

where $F_1 \dots F_6$ are the diode switching functions. They can be calculated as *signum* functions from the PPS voltages' comparisons. The equivalent voltages for phases B and C can be obtained by the same way. The voltage calculated by (6) is to be represented as Fourier series using the Fast Fourier transform. Then, the respective impedance should divide each resultant voltage harmonic to produce the current harmonics (example for phase A):

$$i_a^{(n)} = \frac{v_{Za}^{(n)}}{\dot{Z}_{rect}^{(n)}}. \quad (7)$$

To obtain the instantaneous values the inverse Fourier transform should be implemented. Thus, the non-linear load currents are calculated.

The next step is to simulate the inverter of the APF which generates the non-sinusoidal current. The basic equations for multilevel inverter mathematical models can be found in [13] and [14]. In this paper, only addition for APF operation is described. First, the PWM modulating signal must be modified:

$$v_{ref,a} = M^{(1)} \sin(\omega t) + M^{(hg)} \cdot v_a^*, \quad (8)$$

where $M^{(1)}$ is the modulation index for the fundamental, $M^{(hg)}$ is the modulation index for the compensating component, v_a^* is the compensating component. The last term can be obtained from the instantaneous power theory. This suggests calculation the instantaneous powers first:

$$\begin{pmatrix} p \\ q \end{pmatrix} = \begin{pmatrix} v_\alpha & v_\beta \\ v_\alpha & -v_\beta \end{pmatrix} \times \begin{pmatrix} i_{l\alpha} \\ i_{l\beta} \end{pmatrix}, \quad (9)$$

where p and q are the instantaneous real and imaginary powers, v_α and v_β are the PPS voltages measured at PCC and transformed into $\alpha\beta$ -frame, $i_{l\alpha}$ and $i_{l\beta}$ are the load currents, measured at the load side (Fig. 2) and transformed into $\alpha\beta$ -frame. Next step is to eliminate the average component from the real power:

$$\tilde{p} = p - \frac{1}{T} \int_0^T p dt \quad (10)$$

Then, the reference current components must be calculated in the $\alpha\beta$ -frame:

$$\begin{pmatrix} i_\alpha^* \\ i_\beta^* \end{pmatrix} = \frac{1}{v_\alpha^2 + v_\beta^2} \begin{pmatrix} v_\alpha & v_\beta \\ v_\beta & -v_\alpha \end{pmatrix} \times \begin{pmatrix} -\tilde{p} \\ -q \end{pmatrix}. \quad (11)$$

The resultant signals are need to be transformed into the dq -frame and integrated to obtain the references as it is done in the real control system:

$$v_d^* = \int i_d^* dt; v_q^* = \int i_q^* dt. \quad (12)$$

The last step is to transform these signals from dq -frame to the abc -frame.

After that, the inverter model is implemented in the exactly the same way as it is explained in [12]. The result of the inverter implementation is its output voltages with PWM: v_f . For the k parallel inverters, these voltages are represented as follows [13]:

$$v_f = \frac{1}{k} \sum_{i=1}^k v_{N,i} \quad (13)$$

where $v_{N,i}$ is the output voltage of i -th N -level inverter in parallel structure. This equation is applicable the best when the interleaved PWM technique is implemented.

Next, the circuit of the power supply system shown in Fig. 2 can now be described in this model, where the load current is taken from (7). Our goal is to find the current that will be emitted in PPS line to compensate the load current. This current is produced by the voltages v_f and e_s applied to the system impedance described in (2). For n -th harmonic component of the first term in (1), it can be written using (3):

$$i_f^{(n)} = \left(e_s^{(n)} - v_f^{(n)} \right) \cdot Y^{(n)} \quad (14)$$

Table III shows the numerical results for two types of APF: single and dual inverter implementation.

TABLE III
NUMERICAL RESULTS OF MATHEMATICAL MODEL

| | Current THD, % | Power factor χ |
|-----------------|----------------|---------------------|
| Load side | 23.078 | 0.974 |
| APF, single VSI | 10.970 | 0.994 |
| APF, dual VSI | 7.989 | 0.997 |

Fig. 7 illustrates the results of the mathematical calculation of APF based on two three-level inverters in parallel connection.

IV. SIMULATION RESULTS

To verify the mathematical model and take account of the other real system features a detailed simulation model was built in PSIM software, see Fig. 8. The model provides to simulate active power filter based on one or two parallel inverters taking account of the following physical implementation factors: dead time, microcontroller-based control system with integer arithmetic, voltage and current sensing with operational amplifiers links, limited performance of the microcontroller (data processing with interrupts), Figs. 9 and 10.

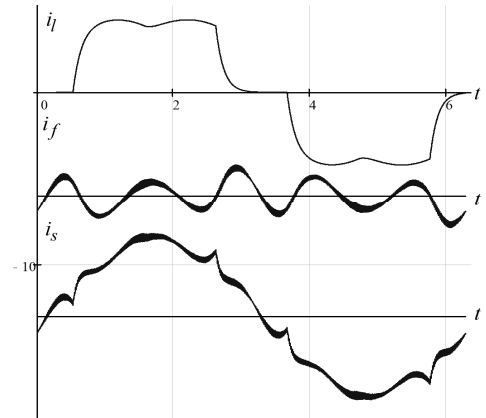


Fig. 7. Mathematical model waveforms from top to bottom: non-linear load current; APF current; grid current.

Digital control algorithm is implemented in a dynamic-link library file (DLL) that is connected to the simulation model in PSIM. The DLL-file contains all the files that are designed in Microsoft Visual Studio and they are identical to the ones for the MDK Keil project (microcontroller software development tool).

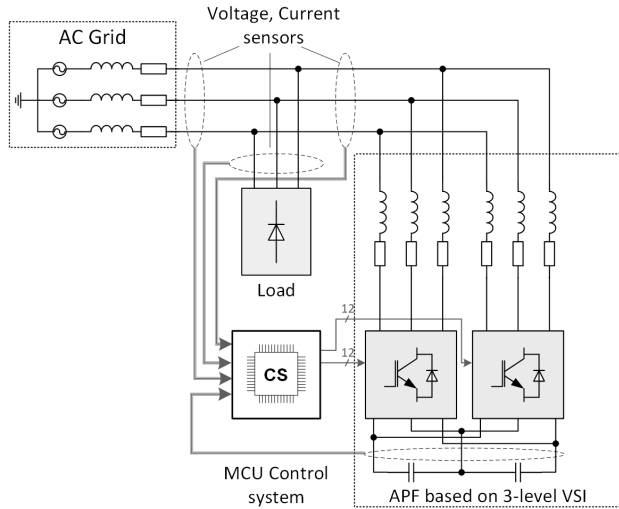


Fig. 8. PSIM model scheme .

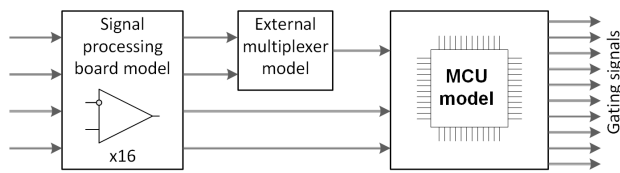


Fig. 9. Control system scheme.

The core of the control system implements the control, according to the instantaneous power theory with the decoupled inverter current control. A structure diagram of the instantaneous power calculation is on Fig. 11. The VSI decoupled current control is shown in Fig. 12.

Designations on Fig. 11 are the following: i_{sd} and i_{sq} are the actual line current values of the APF; $K_{pi} = \frac{1}{R_s}$ and

$K_{ii} = \frac{R_s}{L_s}$ are the PI-controller coefficients.

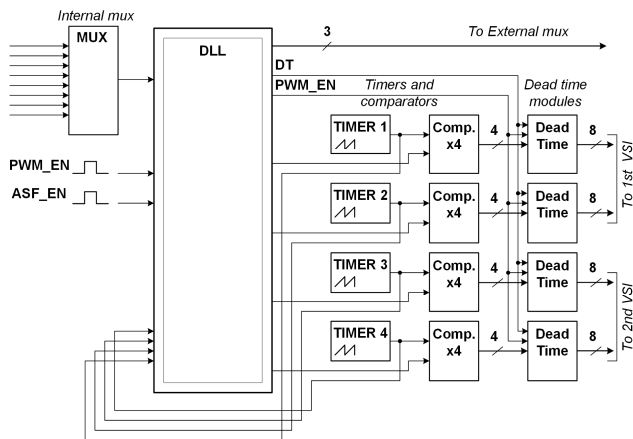


Fig. 10. Control system MCU core scheme.

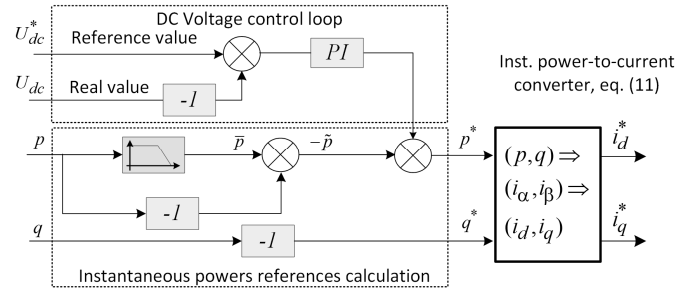


Fig. 11. Instantaneous power calculation and DC voltage control loop.

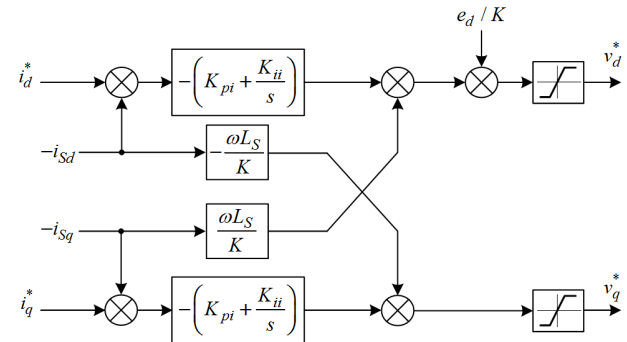


Fig. 12. Decoupled current control of the inverters in APF.

Parameters of the model are listed in Table IV.

 TABLE IV
SIMULATION MODEL PARAMETERS

| Item | Value | Comment |
|-----------------------------------|------------------------------------|------------------------------------|
| PPS output voltage, V, rms | 70 | Phase-to-ground |
| PPS inductance, mH | 2.0 | Autotransformer winding inductance |
| PPS resistance, Ohm | 0.01 | Autotransformer winding resistance |
| Load type | Diode bridge rectifier, see Fig. 5 | |
| Load power, W | 500 | |
| Load resistance R_d , Ohm | 30 | |
| Load inductance L_d , mH | 1.0 | |
| APF DC-link voltage, V | 270 | |
| APF PWM freq., Hz | 10000 | |
| APF Apparent power, VA | 2000 | per inverter |
| APF filter inductance L_f , mH | 1.0 | |
| APF filter resistance R_f , Ohm | 0.21 | |
| APF DC-link capacitance, uF | 1500 | 2 caps. per inverter |
| APF Dead time, uS | 0.5 | |

Fig. 13 illustrates the case when the APF operates with one three-level inverter. Fig. 14 shows operation in the same conditions, but with two inverters in parallel connection.

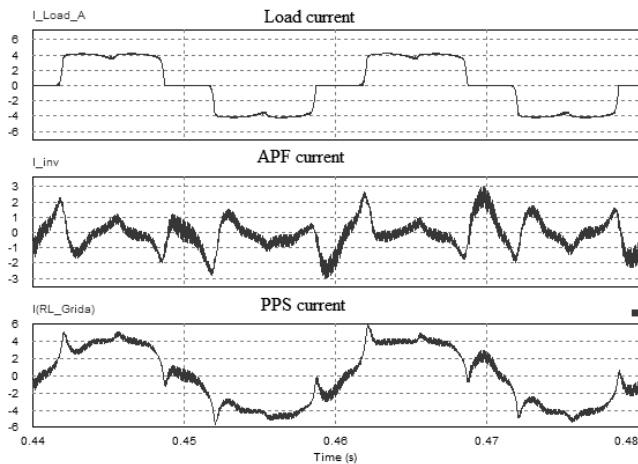


Fig. 13. Single inverter APF operation.

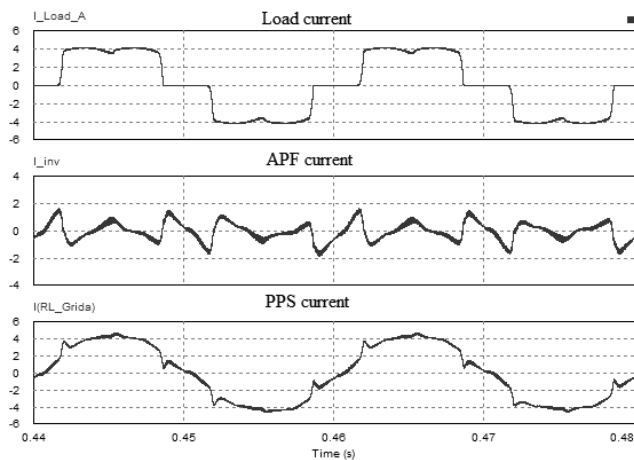


Fig. 14. Dual inverter APF operation.

As can be seen from Figs. 7, 13 and 14, parallel inverters allow to improve the compensation quality: for the first case THD of the PPS current is 15.8%, and power factor is 0.988, while for the second case these values are 11.8% and 0.993 respectively.

ACKNOWLEDGEMENT

This research is carried out under financial support of the Russian science foundation (project No. 17-79-10235).

CONCLUSIONS

The energy quality performance estimation was carried out for the active power filters with parallel inverters structure. It was shown that parallel connection of the multilevel inverters with interleaved PWM allows to increase the bandpass when the primary power source impedance is low and to increase the admittance for higher generated harmonics when the PPS impedance is comparable with the APF output impedance.

Mathematical model of the active power filter operating at the conditions of the nonlinear load has shown that reduction of the PPS current THD and improving the power factor. The simulation model has also shown better compensation quality improvement.

REFERENCES

- [1] IEEE Std 519-2014. "IEEE Recommended Practice and Requirements for Harmonic Control in Electric Power Systems."
- [2] European standard EN 50160:2010. "Voltage characteristics of electricity supplied by public distribution networks."
- [3] Z. Xi and S. Bhattacharya, "STATCOM Control and Operation with Series Connected Transformer Based 48-pulse VSC," IECON 2007 - 33rd Annual Conference of the IEEE Industrial Electronics Society, Taipei, 2007, pp. 1714-1719.
- [4] A. M. Massoud, S. J. Finney, A. J. Cruden and B. W. Williams, "Three-Phase, Three-Wire, Five-Level Cascaded Shunt Active Filter for Power Conditioning, Using Two Different Space Vector Modulation Techniques," in IEEE Transactions on Power Delivery, vol. 22, no. 4, pp. 2349-2361, Oct. 2007.
- [5] M. Waware and P. Agarwal, "Use of multilevel inverter for elimination of harmonics in high voltage systems," 2010 The 2nd International Conference on Computer and Automation Engineering (ICCAE), Singapore, 2010, pp. 311-315.
- [6] D. L. Popa and P. M. Nicolae, "Issues with high power shunt active filters operating with distorted mains voltages. Dual inverter topology," 2015 9th International Symposium on Advanced Topics in Electrical Engineering (ATEE), Bucharest, 2015, pp. 704-709.
- [7] M. Basu, S. P. Das and G. K. Dubey, "Parallel converter scheme for high-power active power filters," in IEE Proceedings - Electric Power Applications, vol. 151, no. 4, pp. 460-466, 7 July 2004.
- [8] E. C. dos Santos, C. B. Jacobina and A. M. Maciel, "Parallel connection of two shunt active power filters with losses optimization," 2010 Twenty-Fifth Annual IEEE Applied Power Electronics Conference and Exposition (APEC), Palm Springs, CA, 2010, pp. 1191-1196.
- [9] Chao He, C. Xie, Hui Yan, Guozhu Chen and Hua Yang, "Parallel converter scheme for large power high compensation Precision Shunt Active Power Filters," 2012 IEEE International Symposium on Industrial Electronics, Hangzhou, 2012, pp. 431-436.
- [10] S. Gierschner, D. Hammes, J. Fuhrmann, M. Beuermann and H. G. Eckel, "Fault-Tolerant Behaviour of the Three-Level Advanced-Active-Neutral-Point-Clamped Converter," PCIM Europe 2016; International Exhibition and Conference for Power Electronics, Intelligent Motion, Renewable Energy and Energy Management, Nuremberg, Germany, 2016, pp. 1-8.
- [11] M. A. Dybko and S. V. Brovanov, "Active power filter with battery energy storage based on NPC inverters," 2015 16th International Conference of Young Specialists on Micro/Nanotechnologies and Electron Devices, Erlagol, 2015, pp. 415-421.
- [12] M. Dybko et al., "Multilevel NPC Converters in Parallel Connection for Power Conditioning Systems", Applied Mechanics and Materials, Vol. 792, pp. 189-196, 2015.
- [13] M. Dybko and S. Brovanov, "Switching frequency circulating current analysis in parallel-connected multilevel NPC converters," 2014 16th International Power Electronics and Motion Control Conference and Exposition, Antalya, 2014, pp. 1195-1203.
- [14] M. A. Dybko, S. V. Brovanov and S. A. Kharitonov, "Mathematical simulation technique for power systems based on diode-clamped multilevel VSC," Eurocon 2013, Zagreb, 2013, pp. 941-948.



Maksim A Dybko received PhD degree from the Novosibirsk State Technical University, Novosibirsk in 2013. His research interests include power quality correction, multilevel converters, energy storage and control algorithms. He has 40 published works in the area of his interests.
E-mail: dybko@corp.nstu.ru



Vadim G. Tokarev (b. 1967) – senior lecturer at the computer engineering department, Novosibirsk State Technical University. His research interests include active power filters, voltage source converters, automation systems, and digital signal processing. He is a co-author of 5 scientific papers. Email: v.tokarev@corp.nstu.ru



Sergey V. Brovanov PhD, professor, Vice Rector for Academic Activities, Novosibirsk State Technical University. His research interests are currently focused on designing effective power converters. He is the author of 120 scientific papers. E-mail: brovanov@corp.nstu.ru



Sergey A. Kharitonov received doctor of sciences in Electrical Engineering from Novosibirsk State Technical University, Novosibirsk (NSTU), Ph. D work called as “Electric energy generating system for wind energetics and independent mobile objects (Analysis and synthesis)”. He is currently Professor and Head Department of Electronics and Electrical Engineering in the NSTU. His research interests include different application field of industrial electronics. E-mail: Kharitonov@corp.nstu.ru

Theoretical Aspects of the Common-mode Leakage Current Suppression in a Photovoltaic Power Generation System Based on Multi-level H-bridge Type Converters

Evgeniy V. Grishanov, Sergey V. Brovanov
Novosibirsk State Technical University, Novosibirsk, Russia

Abstract – Now days, power generation systems (PGS) based on a solar photovoltaic modules (batteries) and semiconductor converters (PV PGS) are widely used. Recent studies conducted by the international energy agency (IEA) shows that most of the PV PGS used in grid applications. For reducing weight and size factors of PV PGS from its structure eliminate the transformer. Some estimates show that the transformer can occupy up to half the volume and reach half the weight and cost of PV PGS without solar photovoltaic modules. However, the elimination of the transformer leads to common-mode leakage current (CLC) occur, which flows through the parasitic elements of the PV PGS circuit. Common-mode leakage current can be cause of some type's equipment failure. The common-mode leakage current extremely difficult to suppress in some cases with PV PGS designed on H-bridge multilevel converters. The algorithmic capabilities of common-mode leakage current suppression in the PV PGS based on H-bridge type multilevel converters were considered in this paper. Obtained results were verified by simulation.

Index Terms - Multilevel converters, space-vector PWM, H-bridge, common-mode leakage current, and power electronics.

I. INTRODUCTION

TODAY there is a problem of electrical energy shortage. This problem could increase due to the electricity consumption growing in future. This problem is very actual in some critical branches of human economic activity. The electrical energy shortage is particularly sensitive in remote private households. Usually low power single phase grids are required for these private households. Photovoltaic power generation systems are a solution of this problem for these remote private households [1]-[2]. The trend in development PV PGS is usage of multilevel semiconductor converters. Multilevel semiconductor converters allow significantly improving generated electric energy quality and reducing the weight and size factors of PV PGS [3]-[5]. It is noted, that H-bridge type multilevel converters have high quality of electrical energy conversion and technical maintenance [6]. Usually transformer is used for galvanic isolation in PV PGS. Transformer removing from PV PGS (Fig. 1) allows reduce the weight and size factors of those system but common-mode leakage current appears [7]. Common-mode leakage current leads to output generated voltage and current quality reduction and it is a cause of thin-film solar photovoltaic

modules failure. Moreover CLC is a cause of electric shock to service personnel.

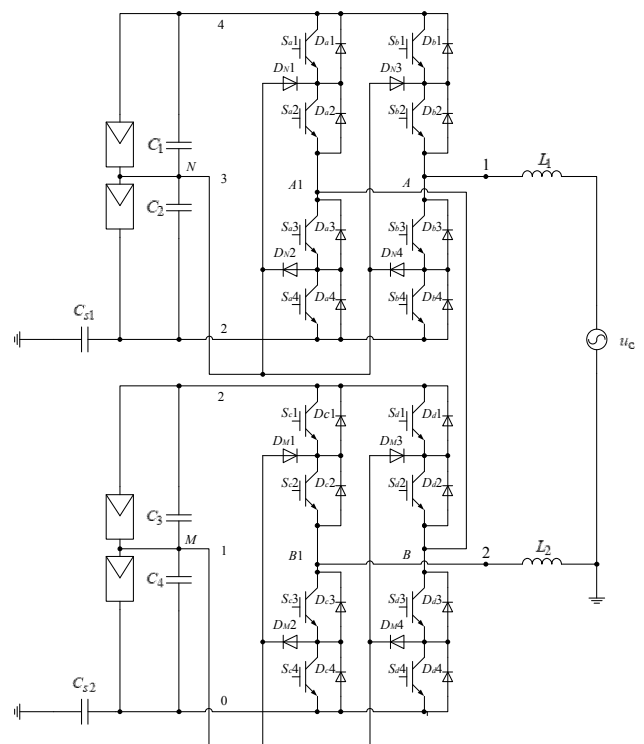


Fig. 1. PV PGS based on three level H-bridge type multilevel converter.

The available theoretical material of usage PV PGS based on H-bridge type multilevel converters is not complete and does not satisfy the current scientific trends [8].

II. PROBLEM DEFINITION

There are known some methods of common-mode leakage current reduction: usage of separating capacitor [9], additional switches installation in converter circuit [8], which allows the DC link disconnection from the load at certain intervals and other. But all these methods only reduce the common-mode leakage current and can't suppress it. Several solutions have been proposed in this paper that allows common-mode leakage current suppression in the PV PGS based on H-bridge type multilevel converters.

III.THEORY

First of all for purpose of common-mode leakage current suppression it required to be find sources of CLC. For this, it is necessary to consider PV PGS based on H-bridge type multilevel converters such as conventional PV PGS [7]. In order to identify the sources of CLC it is necessary to convert the PV PGS circuit to equivalent circuit shown in Fig.2, taking into account the expressions (1) and (2). u_{2A} , u_{2A1} , u_{0B} and u_{0B1} is equivalent voltage sources formed at converter terminals «A» и «A1» with respect to the bus «2» and at converter terminals «B» и «B1» with respect to the bus «0» respectively.

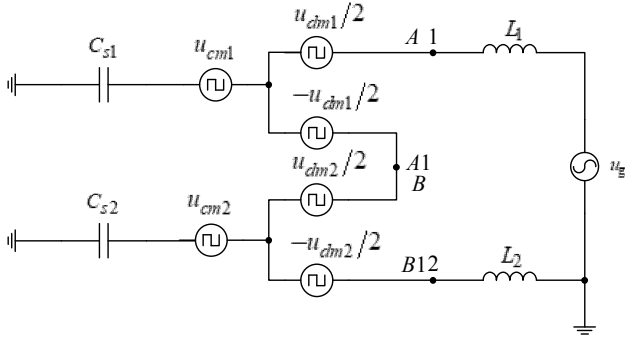


Fig. 2. Equivalent circuit PV PGS based on H-bridge type multilevel converters.

Expressions (1) and (2) shows common mode and differential mode voltages of H-bridge type converter:

$$u_{cm1} = \frac{u_{2A} + u_{2A1}}{2}; u_{cm2} = \frac{u_{0B} + u_{0B1}}{2}. \quad (1)$$

$$u_{dm1} = u_{2A} - u_{2A1}; u_{dm2} = u_{0B} - u_{0B1}. \quad (2)$$

If the DC bus voltages of both converters are equal (Fig. 2), then the next condition must be satisfied:

$$u_{dm1} + u_{dm2} = 0. \quad (3)$$

Grid is a low frequency voltage source and its output impedance is much smaller compared with impedance formed by common mode differential mode voltage sources u_{dm} and u_{cm} , which formed with PWM frequency. Consequently, the grid influence on the common-mode leakage current will be neglected from now on. At next step, it is shown that differential mode voltage sources combines and depend from difference the values of inductances L_1 and L_2 , as defined follows:

$$u'_{dm} = \frac{u_{dm}(L_2 - L_1)}{2(L_2 + L_1)}, \quad (4)$$

where $L_{12} = \frac{L_1 L_2}{L_1 + L_2}$ is equivalent inductance.

Equivalent common mode voltage sources can be defined in next expression:

$$u'_{cm1} = \frac{u_{cm1} X_{C_{s2}}}{X_{C_{s1}} + X_{C_{s2}}}, u'_{cm2} = \frac{u_{cm2} X_{C_{s1}}}{X_{C_{s1}} + X_{C_{s2}}}, \quad (5)$$

If conditions (3), (4) and (5) are carried out, that PV PGS circuit shown in Fig.2 can be easily simplify (Fig. 3).

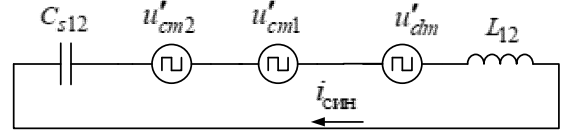


Fig. 3. Next type of equivalent circuit PV PGS based on H-bridge type multilevel converters.

As shown in Fig.3 common-mode leakage current sources are: equivalent common mode voltages u'_{cm1} , u'_{cm2} and equivalent differential mode voltage u'_{dm} . In this case, if equal values of the inductances L_1 and L_2 are ensured, then equivalent differential mode voltage u'_{dm} stay equal to zero and it influence on the common-mode leakage current will be neglected. But equivalent common mode voltage sources 1 and 2 leads to the common-mode leakage current occur. In that case common-mode leakage current defined by next expression:

$$I_{cm} = \frac{u'_{cm1} + u'_{cm2}}{\frac{1}{j2\pi f C_{s12}} + j2\pi f (L_{12})}, \quad (6)$$

where f is common-mode voltage source frequency, $C_{s12} = C_{s1} + C_{s2}$ is equivalent stray capacitance.

Substituting (6) in expression (5) of obtained common-mode leakage current in the following form:

$$I_{cm} = \frac{u_{cm1} C_{s1} + u_{cm2} C_{s2}}{(C_{s12}) \left(\frac{1}{j2\pi f C_{s12}} + j2\pi f (L_{12}) \right)}. \quad (7)$$

In case of $C_{s1} = C_{s2}$, for common-mode leakage current suppression the next condition must be satisfied:

$$u_{cm1} + u_{cm2} = const. \quad (8)$$

However, it should be noted that such a condition is rarely performed in practice. Then to suppress the common-mode leakage current, the following condition must be satisfied:

$$u_{cm1} = const; u_{cm2} = const. \quad (9)$$

There is need to develop control algorithm based on pulse-width modulation (PWM) to suppress for common-mode leakage current with conditions (8) or (9) satisfaction. Different types of PWM have individual features. When developing a control algorithm, they must be taken into account. The best option is to use a space-vector PWM (SPWM). It is known that SPWM based on usage of switching states (SS) which correspond to certain voltage levels. Switching states used for create reference vector V^* . Sequence of switching states should meet the requirement of reference vector V^* synthesis.

For creation of three level SPWM which can suppress CLC is needed define voltage levels u_{2A} , u_{2A1} , u_{0B} , u_{0B1} for switching states and satisfy conditions (3), (8) or (9). In addition, these voltages must satisfy the conditions [4]:

$$1) u_{dm} \in \left\{ U_{DC}; \frac{U_{DC}}{2}; 0; -\frac{U_{DC}}{2}; -U_{DC} \right\}, \text{ where } U_{DC} \text{ is DC link voltage.}$$

2) Voltages formed on output terminals of H-bridge converter should vary within the following bandwidth:
 $0 \leq [u_{2A} \vee u_{2A1} \vee u_{0B} \vee u_{0B1}] \leq U_{DC}$.

Voltage levels for SPWM with satisfaction condition (8) define by system of linear equations solution shown in Table I. Voltage levels for SPWM with satisfaction condition (9) define by system of linear equations solution shown in Table II. It should be noted, that DC link voltage of each converter in H-bridge is equal U_{DC} , and full output voltage is equal to

$2U_{DC}$. The converter that is suitable for solving the systems of linear equations presented in Table I corresponds to a single-phase five-level converter represented in Fig.1. The converter that is suitable for solving the systems of linear equations is presented in Table II corresponds to a single-phase nine-level converter represented in Fig. 4. However, it should be noted that for the formation of a three-level voltage, the use of a nine-level semiconductor converter is extremely inefficient.

TABLE I

| System of equations | $\begin{cases} u_{cm1} + u_{cm2} = U_{DC} \\ u_{dm1} + u_{dm2} = 0 \\ u_{dm1} - u_{dm2} = 2U_{DC} \end{cases}$ | $\begin{cases} u_{cm1} + u_{cm2} = U_{DC} \\ u_{dm1} + u_{dm2} = 0 \\ u_{dm1} - u_{dm2} = U_{DC} \end{cases}$ | $\begin{cases} u_{cm1} + u_{cm2} = U_{DC} \\ u_{dm1} + u_{dm2} = 0 \\ u_{dm1} - u_{dm2} = 0 \end{cases}$ | $\begin{cases} u_{cm1} + u_{cm2} = U_{DC} \\ u_{dm1} + u_{dm2} = 0 \\ u_{dm1} - u_{dm2} = -U_{DC} \end{cases}$ | $\begin{cases} u_{cm1} + u_{cm2} = U_{DC} \\ u_{dm1} + u_{dm2} = 0 \\ u_{dm1} - u_{dm2} = -2U_{DC} \end{cases}$ |
|---------------------|--|---|--|--|---|
| u_{2A} | U_{DC} | $U_{DC}/2$ | $U_{DC}/2$ | 0 | 0 |
| u_{2A1} | 0 | 0 | $U_{DC}/2$ | $U_{DC}/2$ | U_{DC} |
| u_{0B} | 0 | $U_{DC}/2$ | $U_{DC}/2$ | U_{DC} | U_{DC} |
| u_{0B1} | U_{DC} | U_{DC} | $U_{DC}/2$ | $U_{DC}/2$ | 0 |
| u_{cm1} | $U_{DC}/2$ | $U_{DC}/4$ | $U_{DC}/2$ | $U_{DC}/4$ | $U_{DC}/2$ |
| u_{cm2} | $U_{DC}/2$ | $3U_{DC}/4$ | $U_{DC}/2$ | $3U_{DC}/4$ | $U_{DC}/2$ |
| u_{dm1} | U_{DC} | $U_{DC}/2$ | $U_{DC}/2$ | $-U_{DC}/2$ | $-U_{DC}$ |
| u_{dm2} | $-U_{DC}$ | $-U_{DC}/2$ | $U_{DC}/2$ | $U_{DC}/2$ | U_{DC} |
| u_{dm} | $2U_{DC}$ | U_{DC} | 0 | $-U_{DC}$ | $-2U_{DC}$ |
| SS | (4;0) | (3;1) | (2;2) | (1;3) | (0;4) |

TABLE II

| System of equations | $\begin{cases} u_{cm1} = U_{DC}/2 \\ u_{cm2} = U_{DC}/2 \\ u_{dm1} + u_{dm2} = 0 \\ u_{dm1} - u_{dm2} = 2U_{DC} \end{cases}$ | $\begin{cases} u_{cm1} = U_{DC}/2 \\ u_{cm2} = U_{DC}/2 \\ u_{dm1} + u_{dm2} = 0 \\ u_{dm1} - u_{dm2} = U_{DC} \end{cases}$ | $\begin{cases} u_{cm1} = U_{DC}/2 \\ u_{cm2} = U_{DC}/2 \\ u_{dm1} + u_{dm2} = 0 \\ u_{dm1} - u_{dm2} = 0 \end{cases}$ | $\begin{cases} u_{cm1} = U_{DC}/2 \\ u_{cm2} = U_{DC}/2 \\ u_{dm1} + u_{dm2} = 0 \\ u_{dm1} - u_{dm2} = -U_{DC} \end{cases}$ | $\begin{cases} u_{cm1} = U_{DC}/2 \\ u_{cm2} = U_{DC}/2 \\ u_{dm1} + u_{dm2} = 0 \\ u_{dm1} - u_{dm2} = -2U_{DC} \end{cases}$ |
|---------------------|--|---|--|--|---|
| u_{2A} | U_{DC} | $3U_{DC}/4$ | $U_{DC}/2$ | $U_{DC}/4$ | 0 |
| u_{2A1} | 0 | $U_{DC}/4$ | $U_{DC}/2$ | $3U_{DC}/4$ | U_{DC} |
| u_{0B} | 0 | $U_{DC}/4$ | $U_{DC}/2$ | $3U_{DC}/4$ | U_{DC} |
| u_{0B1} | U_{DC} | $3U_{DC}/4$ | $U_{DC}/2$ | $U_{DC}/4$ | 0 |
| u_{cm1} | $U_{DC}/2$ | $U_{DC}/2$ | $U_{DC}/2$ | $U_{DC}/2$ | $U_{DC}/2$ |
| u_{cm2} | $U_{DC}/2$ | $U_{DC}/2$ | $U_{DC}/2$ | $U_{DC}/2$ | $U_{DC}/2$ |
| u_{dm1} | U_{DC} | $U_{DC}/2$ | $U_{DC}/2$ | $-U_{DC}/2$ | $-U_{DC}$ |
| u_{dm2} | $-U_{DC}$ | $-U_{DC}/2$ | $U_{DC}/2$ | $U_{DC}/2$ | U_{DC} |
| u_{dm} | $2U_{DC}$ | U_{DC} | 0 | $-U_{DC}$ | $-2U_{DC}$ |
| SS | (8;0) | (6;2) | (4;4) | (2;6) | (0;8) |

IV. EXPERIMENTAL RESULTS

Control algorithm based on SPWM for three level and nine level H-bridge type converters was created. The algorithm was used taking into account the peculiar properties of the

operation of H-bridge converters in the structure of PV PGS considered earlier.

To confirm the theoretically obtained results, simulation models of a single-phase five-level H-bridge converter and a single-phase nine-level H-bridge converter were created using the PSim software package. These models were used to verify the formation of the SPWM algorithm and

correspond common-mode voltage level at the output of the inverter and phase possibilities of leakage current suppression.

Fig. 5 shows the diagrams of the differential voltage, current generated into the grid, the common-mode leakage current, the sum of the common-mode voltages and the differential voltages of each converter in H-bridge. These diagrams were obtained for PV PGS based on single-phase five-level H-bridge converter in three level mode without CLC suppression. These diagrams were obtained by usage PSim software package. It is seen that sum of the common mode voltages is variable ($u_{cm1} + u_{cm2} \neq const$). Conditions (8) or (9) are not satisfied. Common-mode leakage current i_{cm} significantly degrades the current generated by the converter into the grid i_g .

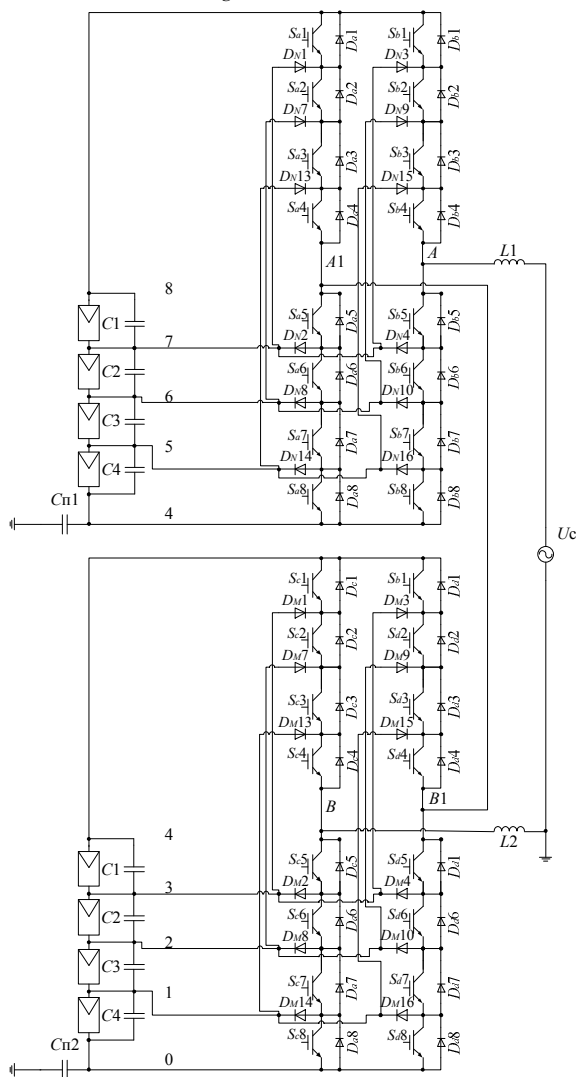


Fig. 4. PV PGS based on nine level H-bridge type multilevel converter.

Fig. 6 shows the diagrams of the differential voltage, current generated into the grid, the common-mode leakage current, the sum of the common-mode voltages and the differential voltages of each converter in H-bridge. These diagrams were obtained for PV PGS based on single-phase five-level H-bridge converter in three level mode with CLC

suppression. These diagrams were obtained by usage PSim software package. Received the sum of common-mode voltages $u_{cm1} + u_{cm2} = const$. Condition (8) is satisfied. Stray capacitance parameters are as follows: $C_{s1} = C_{s2}$. The common-mode leakage current i_{cm} is suppressed; its effect on the current generated by the converter into the grid i_g is diminutive.

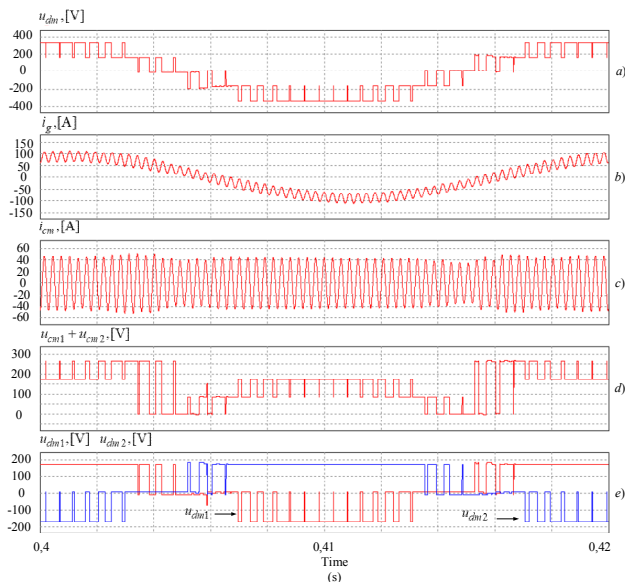


Fig. 5. Current and voltage diagrams of single-phase five-level H-bridge converter in three-level mode without suppression CLC: a) u_{dm} is differential mode voltage; b) i_g is current generated into the grid; c) i_{cm} is common-mode leakage current; d) $u_{cm1} + u_{cm2}$ is sum of common-mode voltages; e) u_{dm1} and u_{dm2} are differential mode voltages respectively.

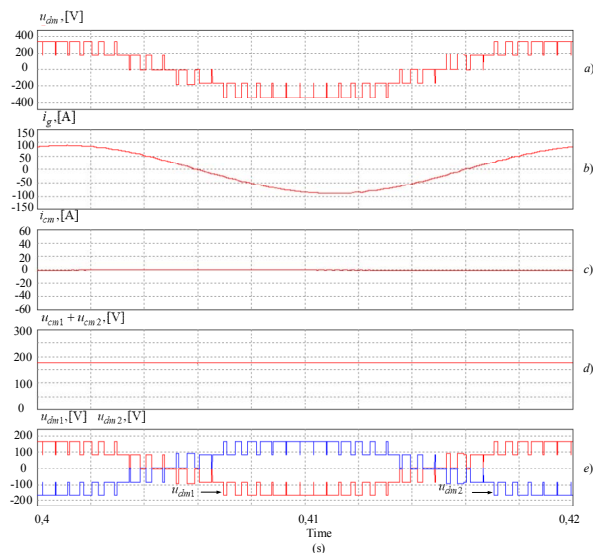


Fig. 6. Current and voltage diagrams of single-phase five-level H-bridge converter in three-level mode with suppression CLC and $C_{s1} = C_{s2}$: a) u_{dm} is differential mode voltage; b) i_g is current generated into the grid; c) i_{cm} is common-mode leakage current; d) $u_{cm1} + u_{cm2}$ is sum of common-mode voltages; e) u_{dm1} and u_{dm2} are differential mode voltages respectively.

Fig. 7 shows the diagrams of the differential voltage, current generated into the grid, the common-mode leakage current, the sum of the common-mode voltages and the differential voltages of each converter in H-bridge. These diagrams were obtained for PV PGS based on single-phase five-level H-bridge converter in three level mode with CLC suppression. These diagrams were obtained by using PSImsoftwa repackage. The sum of common-mode voltages $u_{cm1} + u_{cm2} = const$ is received. Condition (8) is satisfied. Stray capacitance parameters are as follows: $C_{s1} \neq C_{s2}$. The common-mode leakage current is not suppressed; its effect on the current generated by the converter into the grid is diminutive in 5 times compare with current shown in diagrams of Fig. 5.

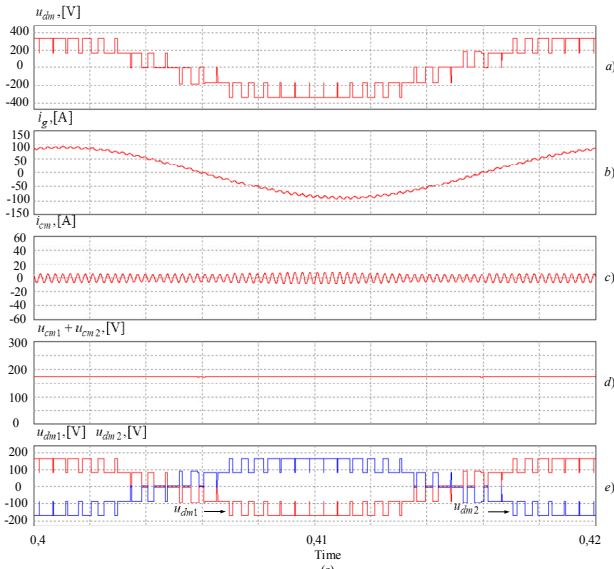


Fig. 7. Current and voltage diagrams of single-phase five-level H-bridge converter in three-level mode with suppression CLC and $C_{s1} \neq C_{s2}$: a) u_{dm} is differential mode voltage; b) i_g is current generated into the grid; c) i_{cm} is common-mode leakage current; d) $u_{cm1} + u_{cm2}$ is sum of common-mode voltages; e) u_{dm1} and u_{dm2} are differential mode voltages respectively.

Fig. 8 shows the diagrams of the differential voltage, current generated into the grid, the common-mode leakage current, the sum of the common-mode voltages and the differential voltages of each converter in H-bridge. These diagrams were obtained for PV PGS based on single-phase nine-level H-bridge converter in three level mode with CLC suppression. These diagrams were obtained by using PSImsoftwa repackage. Received the common-mode voltages $u_{cm1} = const$; $u_{cm2} = const$. Condition (9) is satisfied. Stray capacitance parameters are as follows: $C_{s1} \neq C_{s2}$. The common-mode leakage current i_{cm} is suppressed; its effect on the current generated by the converter into the grid i_g is diminutive.

V. DISCUSSION OF RESULTS

The algorithmic capabilities of common-mode leakage current suppression in the PV PGS based on H-bridge type multilevel converters were demonstrated. These opportunities are confirmed by simulation. It was demonstrated that conditions (8) and (9) can be satisfied by different types H-bridge converters. To satisfy condition (8) and to form a three-level output voltage, a five-level converter is needed. To satisfy condition (9) and to form a three-level output voltage, a nine-level converter is needed. As mentioned earlier that for the formation of a three-level voltage, the use of a nine-level semiconductor converter is extremely inefficient. Conditions (8) and (9) can be realized only in case with satisfied condition (3).

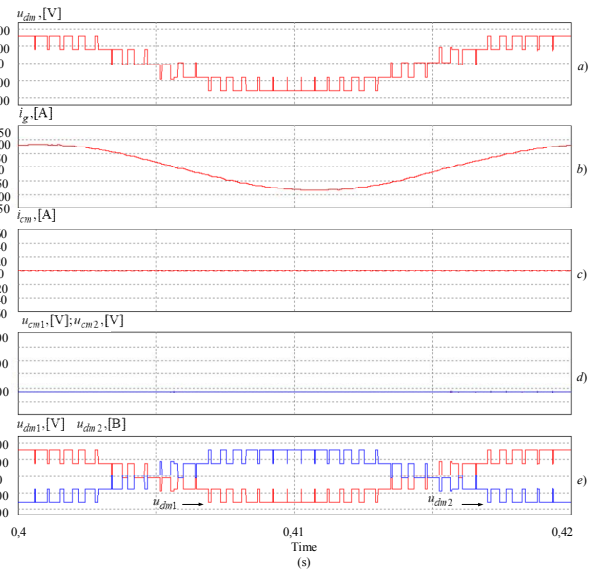


Fig. 8. Current and voltage diagrams of single-phase nine-level H-bridge converter in three-level mode with suppression CLC and $C_{s1} \neq C_{s2}$: a) u_{dm} is differential mode voltage; b) i_g is current generated into the grid; c) i_{cm} is common-mode leakage current; d) u_{cm1} and u_{cm2} are common-mode voltages respectively; e) u_{dm1} and u_{dm2} are differential mode voltages respectively.

VI. CONCLUSION

Common-mode leakage current suppression capabilities in the PV PGS based on H-bridge type multilevel converters were analyzed in this paper. Characteristic operating modes of the PV PGS based on H-bridge type multilevel converters are noted. Switching state voltages definition technique for reference vector synthesis in space-vector pulse-width modulation was presented.

VII. ACKNOWLEDGMENT

The reported study was funded by RFBR and Government of the Novosibirsk region according to the research project № 17-48-543169.

REFERENCES

- [1] Hu S., HeX., Cao F. A high-efficiency single-phase inverter for transformerless photovoltaic grid-connection //Energy Conversion Congress and Exposition (ECCE). – IEEE.– 2014. – pp. 4232-4236.
- [2] Hongpeng L., Yan R., Kuan L., Wei W., Dianguo X.. A Modified Single-Phase Transformerless Y-Source PV Grid-Connected Inverter //IEEE Access. – 2018.–pp. 1-9.
- [3] BharatirajaC.Munda J. L., Bayindir R., Tariq M.. A common-mode leakage current mitigation for PV-grid connected three-phase three-level transformerless T-type-NPC-MLI //Renewable Energy Research and Applications (ICRERA), 2016 IEEE International Conference on. – IEEE, 2016. – pp. 578-583.
- [4] Grishanov E. Brovanov S.V.. Technical aspects of common-mode leakage current suppression in pv-generation systems //Power Electronics and Motion Control Conference (PEMC) International. – IEEE, 2016. – pp. 505-510.
- [5] Vazquez G., Martinez-Rodriguez P.R., Sosa J.M., Escobar G., Juarez M.A.. Transformerless single-phase multilevel inverter for grid tied photovoltaic systems //Industrial Electronics Society, IECON 2014-40th Annual Conference of the IEEE. – 2014. – pp. 1868-1874.
- [6] Dybko M. A., Brovanov S. V. Usage of Spectral Models and Switching Functions for Cascaded H-bridges VSC Analysis // Proceedings и способыформированиякомбинацийсостоянияключейприразработке алгоритмавекторнойШИИМ.of Actual Problems of Electronic Instrument Engineering (APEIE).–2016.–pp. 94-98.
- [7] GubiaE., SanchisP.,UrsuaA., LopezJ. Ground currents in single-phase transformerless photovoltaic systems // Progress in photovoltaics: research and applications. – 2007. – Vol. 15, №7. – pp. 629–650.
- [8] Guo X., Jia X. Hardware-based cascaded topology and modulation strategy with leakage current reduction for transformerless PV systems //IEEE Transactions on Industrial Electronics. – 2016. – Vol. 63. – №. pp. – pp. 7823-7832.
- [9] Ground leakage current elimination in a transformerless unipolar modulation based single phase grid-connected photovoltaic system / A. Datta, G. Bhattacharya, D. Mukherjee, H. Saha // Power and Energy Engineering Conference. IEEE PES Asia. – Pacific. – 2013. – pp. 1–5.



Grishanov Evgeniy Valer'evichvich - (b. 1988)
– junior researcher, department of electronics
and electrical engineering, NSTU. His research
interests are currently focused on generation
systems based on NPC. He is the author of 14
scientific papers. (Address: 20, Karl Marx Av.,
Novosibirsk, 630073, Russia. E-
mail: e.grishanov@corp.nstu.ru).



Brovanov Sergey Viktorovich(b. 1964) – PhD,
professor, Vice Rector for Academic Activities,
Novosibirsk State Technical University. His
research interests are currently focused on
designing effective power converters. He is the
author of 120 scientific papers. (Address: 20,
Karl Marx Av., Novosibirsk, 630073, Russia.
E-mail: brovanov@corp.nstu.ru).

Dynamic and Energy Performances of Voltage Active Converter at Its Operation on Elevated Frequencies

Aleksandr A. Efimov

Saint-Petersburg State University of Aerospace Instrumentation, Saint-Petersburg, Russia

Abstract - For a three-phase voltage active converter, when it is supplied from an ideal 400 and 800 Hz network, a relay current control system is designed. The system provides control of the network currents and their phase shift relative to the network voltages, as well as stabilization of the output voltage at the levels of 270 and 540 V. In the MATLAB / Simulink environment, a simulation model of the system was created. The results of the simulation testify to its good dynamic and energy performance and output voltage converter high stabilization.

Keywords - Voltage active converter, mathematical modeling.

I. INTRODUCTION

THE stage in the development of aviation power supply systems is characterized by the use of high-energy permanent magnets in the latest developments, as well as the latest achievements of intelligent power electronics associated with the emergence of high-power, high-voltage power semiconductor devices, specialized signal microcontrollers that enable real-time implementation of pulse-modulation algorithms for controlling power converters electricity.

It is common knowledge that magnetoelectric generators (MEG) possess the best specific mass-dimensional parameters, which predetermines their advantageous application in the projected aviation electric power generation systems (AEPGS) [1-4]. Application of MEG in aviation power supply systems in conjunction with power semiconductor converters allows to create AEPGS up to several hundred kilowatts with high mass and energy parameters.

One of the promising high-power AEPGS is a generator with a layered structure of the inductor [1], in which, to ensure strength, the ferromagnetic sheets of the rotor package alternate with nonmagnetic inserts of titanium. At a maximum MEG rotation speed of 14,000 rpm, it is possible to perform a generator at a power of 360 kW with a specific active mass of 0.08 kg / kW, and at 24000 rpm - at a power of 400 kW at a specific power of 0.06 kg / kW. Advances in the development and creation of such high-powered aviation high-speed MEGs are obvious.

It is impossible to achieve an increase in the dynamic and energy performance of the entire AEPGS, without developing and exploring its second main element, a power semiconductor converter. However, work devoted to the development and investigation of high-power semiconductor

converters, which should provide the necessary quality of electric power in the entire range of changes in MEG rotation frequencies, is clearly not enough. This especially applies to the prospective AEPGS of an increased DC voltage of 540 V, the development of semiconductor converters for which insufficient attention is paid in the periodical literature.

II. PROBLEM DEFINITION

The purpose of this paper is to study the power and dynamic performances of a voltage active converter (VAC) with a power of several hundreds kVA, connected to an ideal source of alternating voltage with an "aviation" frequency of 400 Hz or 800 Hz operating in modes of a network voltage inverter (NVI) and voltage active rectifier (VAR), while ensuring the stability of the DC voltage at its output at the levels of 270 V and 540 V.

To achieve the purpose, the following tasks were set and solved in the work:

- selection of the power circuit of the VAC and determination of the parameters of its power part, as well as nominal values of the network power, voltage and frequency;
- justification of the control algorithm and synthesis of the structure of the automatic control system (ACS) and regulator parameters;
- development and implementation the VAC ACS simulation model in the MATLAB / Simulink environment;
- research of dynamic modes operation the VAC ACS and determination of the main energy performance indicators of the converter operation in the VAR and NVI modes;
- determination of accuracy DC voltage stabilization.

III. THEORY

A. The VAC Power Circuit Choice and Calculation its Parameters

Given the success of power electronics in the creation of powerful semiconductor switches, based on the simplicity, reliability and versatility of the three-phase bridge circuit, it was chosen as the semiconductor switch VAR implemented on IGBT modules. When determining the nominal values of power, frequency and voltage in the network, their two-fold change in operating conditions is taken into account. This corresponds to a two-fold change in the rotational speed of the MEG shaft in ASGEE under operating conditions [1-4].

For further analysis, the nominal power of the VAC was assumed to be equal 202.5 kVA, for which the nominal frequency of the supply voltage was 400 Hz. Taking into account the fact that the VAC should, as a minimum, provide twice the nominal power, it is assumed that it should be achieved, both at a frequency of the supply voltage 400 Hz and 800 Hz. The choice of the nominal value of the mains supply voltage requires some explanation. Because the VAC is a step-up converter, the nominal value of its supply voltage must be selected at the minimum frequency and stabilization its output voltage at 270 V. For the VAC operation in the linear mode, this rectified voltage should more than double the amplitude value mains phase voltage. Therefore, the effective value of the rated line network voltage U_{LN} was assumed equal to 160 V. This voltage provides stabilization of the rectified voltage at 270 V and 540 V at a frequency of the 400 Hz mains supply. With a double increase in the supply voltage (designated U_{LC}) and a frequency of 800 Hz, stabilization of the rectified voltage at the level of 540 V is ensured when the VAC is operated in linear mode.

To develop and create a VAC simulation model, an approximate calculation the mains filter (inductance and active resistance) parameters and the capacitance in the rectified voltage circuit was carried out. This calculation was carried out by the simplest procedure [5], since when the simulation model is implemented, the calculated parameter values can always be refined.

The calculated value of the inductance of the mains filter is determined by the formula:

$$L_f = \frac{U_{dn}}{6 \cdot \pi \cdot F_{pwm} \cdot \Delta I_c} = 24 \cdot 10^{-6} H$$

where $U_{dn}=270$ V - rated rectified voltage of the VAC;

$\Delta I_c = K_a \cdot I_{cn} \cdot \sqrt{2} = 50$ A - amplitude of pulsations of the VAC mains current;

$I_{cn} = 720.72$ A - the rated phase current of the network;

$K_h = 0.05$ - harmonic ratio of the mains current of the VAC;

$F_{pwm} = 12$ kHz - is the PWM carrier frequency.

To calculate the active resistance of the mains filter, we assume that the active losses in it make up 2% of the active phase power of the supply network, equal to 67.5 kW.

$$R_f = \frac{P_{1f}}{I_{cn}^2} = 0.0026 \text{ Om}.$$

Capacity in the rectified voltage circuit is calculated by the formula:

$$\tilde{N}_d = \frac{I_{cn} \cdot T_{PWM} \cdot \sqrt{3}}{0.05 \cdot U_{dn} \cdot \sqrt{2}} = 0.0054 F.$$

The network filter, capacitance, and load parameters calculated and selected for the VAC model are shown in Table I.

TABLE I
CALCULATED AND SELECTED PARAMETERS OF THE VAC
MODEL

| Parameter | Calculation | Selection |
|---|-------------|--|
| Inductance of the mains filter, H | 0.000024 | 0.00002 |
| Active resistance of the mains filter, Om | 0.0026 | 0.005 |
| Capacity in the load chain, F | 0.0054 | 0.005 |
| Load resistance, Om | 0.36 | 0.36 |
| EMF in the load circuit (when implementing NVI mode, in which a change in the sign of the load current is ensured by connecting the EMF), V | - | 400 V, $f_c = 400$ Hz 800 V, $f_c = 800$ Hz |

B. VAC Automatic Control System

The control of the VAC can be performed using various algorithms and ACS. This issue has been devoted to a huge number of publications, both domestic and foreign [5-15]. Based on the simplicity of implementation and the ability to provide quality control, both rectified voltage and the network current offset factor with respect to the phase voltage of the network, the relay current control algorithm ("current corridor" algorithm) was used in the work. In addition, the ACS contains a single proportional-integral PI-regulator of the rectified voltage [6]. As will be shown below, the current regulator in the relay mode provides an almost sinusoidal form of the supply network currents in the VAR and NVI modes. It proves to be better than the one provided by the PWM algorithm.

Taking into account the data presented in Table. I and the uncompensated time constant $T_\mu = 0.00008$ c, the transfer function of the PI regulator of the rectified voltage tuned to the symmetrical optimum has the following form:

$$W(p) = \frac{0.002p + 1}{0.0005p}. \quad (1)$$

The filter installed at the input of the ACS has a transfer function

$$W_f(p) = \frac{1}{0.002p + 1}. \quad (2)$$

C. The ACS Simulation Model

For the chosen control algorithm and calculated parameters of the power circuit of the VAC and the PI - controller, an imaging model of the ACS in the MATLAB / Simulink environment was developed, shown in Fig. 1. The parameters of the PI - controller and the input filter used in the model remained unchanged in all modes of operation and corresponded to (1) and (2). The parameters of the VAC and the load are shown in Table. I.

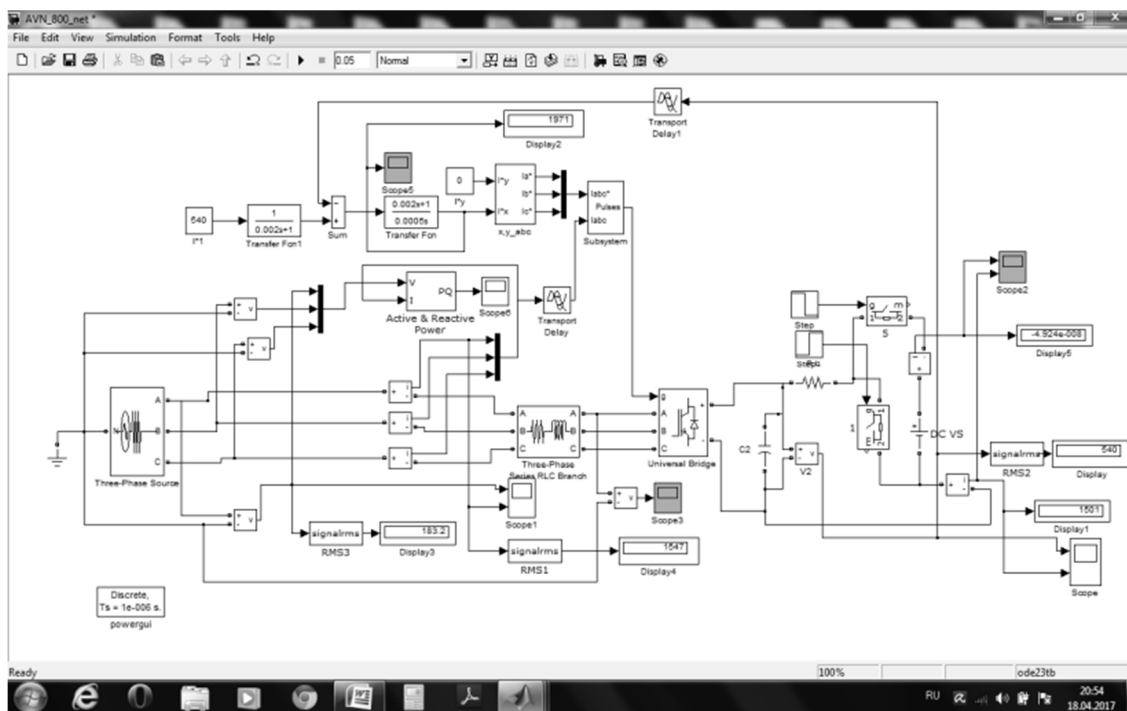


Fig. 1. Automatic control system simulation model.

IV. EXPERIMENTAL RESULTS

The developed simulation model made it possible to carry out studies of various operating modes of the VAC ACS. During the preparation of the article, the following modes of operation were modeled.

1. Testing of the control action $U_d^* = 270 \text{ V}$ with maintaining a single shift factor and stabilization of the rectified voltage of the VAR at 270 V at nominal parameters of the power network ($U_{LN} = 160 \text{ V}$, $f_c = 400 \text{ Hz}$).
2. Testing of the control action $U_d^* = 270 \text{ V}$ while maintaining the inductive shear factor and stabilization of the rectified voltage of the VAR at the level of 270 V at the nominal parameters of the supply network ($U_{LN} = 160 \text{ V}$, $f_c = 400 \text{ Hz}$).
3. Testing of the control action $U_d^* = 270 \text{ V}$ while maintaining the capacitive shear factor and stabilization of the rectified voltage of the VAR at 270 V with nominal parameters of the power supply network ($U_{LN} = 160 \text{ V}$, $f_c = 400 \text{ Hz}$).
4. Testing of the control action $U_d^* = 540 \text{ V}$, while maintaining a single shift factor and stabilizing the rectified voltage of the VAR at a level of 540 V at nominal parameters of the supply network ($U_{LN} = 160 \text{ V}$, $f_c = 400 \text{ Hz}$).
5. Testing of the control action $U_d^* = 540 \text{ V}$ while maintaining a single shift factor and stabilization of the rectified voltage of the VAR at 540 V with increased

parameters of the power supply network ($U_{LC} = 320$ V, $f_c = 800$ Hz).

6. Testing of the control action $U_d^* = 270$ V with maintaining a single shift factor and stabilization of the rectified voltage of the VAR at 270 V at nominal parameters of the power supply network ($U_{LN} = 160$ V, $f_c = 400$ Hz) and decreasing at time $t = 0.02$ c load resistance from 0.36 Ohms to 0.18 Ohms.
7. Testing of the control action $U_d^* = 540$ V while maintaining a single shift factor and stabilization of the rectified voltage of the VAR at 540 V at nominal parameters of the power supply network ($U_{LN} = 160$ V, $f_c = 400$ Hz) and decreasing at time $t = 0.04$ c load resistance from 0.36 Ohms to 0.23 Ohms.
8. Testing of the control action $U_d^* = 540$ V, while maintaining a single shift factor and stabilization of the rectified voltage of the VAR at 540 V with increased parameters of the supply network ($U_{LC} = 320$ V, $f_c = 800$ Hz) and decreasing at time $t = 0.04$ c load resistance from 0.36 Ohms to 0.23 Ohms.
9. Testing of the control action $U_d^* = 270$ V while maintaining a single shift factor and stabilization of the rectified voltage of the VAR at 270 V at nominal parameters of the power supply network ($U_{LN} = 160$ V, $f_c = 400$ Hz) and further conversion of the converter at time $t = 0.02$ s into the NVI mode.
10. Elimination of the control action $U_d^* = 540$ V while maintaining a single shift factor and stabilization of the

rectified voltage of the VAR at 540 V with increased parameters of the supply network ($U_{LC} = 320$ V, $f_c = 800$ Hz) and further conversion of the converter at time $t = 0.02$ s into the NVI model.

V. DISCUSSION OF RESULTS

It is not possible to present all simulation results, therefore in the future only some of the results will be shown. All the results of modeling the dynamic and energy parameters of

the VAC ACS operation, as well as the accuracy of stabilization of the rectified voltage, are summarized and presented in Table II.

In Fig. 2 - 4 show some of the results of modeling the stabilization mode of the rectified voltage of the VAR at the level of 270 V at the time of the master signal and the perturbation (when the load resistance is changed by a factor of 0.02 from the resistance of the load twice from 0.36 to 0.18 Ω) - the regime number 6.

TABLE II.
AVC ACS INDICATORS OBTAINED FROM MODELING

| Number of the mode | Energy indicators | | | | | Dynamic indicators | | Static accuracy |
|--------------------|-------------------|--------------|------------|--------|----------|--------------------|--------------|-----------------|
| | P_{net} , kW | Q_c , kVar | P_d , kW | EFF, % | K_{sh} | T_{up} , s | σ , % | % |
| 1 | 190.18 | 0 | 181.43 | 95.4 | 1.0 | 18 | 0 | 0.1 |
| 2 | 222.0 | +114.0 | 199.4 | 89.8 | +0.889 | 25 | +1.5 | 0.74 |
| 3 | 244.5 | -90.0 | 202.53 | 82.8 | -0.938 | 16 | 0 | 0.01 |
| 4 | 917.06 | 0 | 738.88 | 80.6 | 1.0 | 28 | 0 | 0.185 |
| 5 | 850.23 | 0 | 806.76 | 94.9 | 1.0 | 17 | 0 | 0.1 |
| 6 | 41673 | 0 | 376.42 | 90.3 | 1.0 | 19 | -22.2 | 0.63 |
| 7 | 1267.1 | 0 | 895.75 | 70.7 | 1.0 | 20 | -8.7 | 0.61 |
| 8 | 1346.5 | 0 | 1250.3 | 92.86 | 1.0 | 17 | -12.1 | 0.278 |
| 9 | -96.08 | 0 | -97.6 | 98.4 | 1.0 | 8.5 | +52.0 | 0.074 |
| 10 | -381.78 | 0 | -388.7 | 98.2 | 1.0 | 12 | +51.0 | 0.02 |

In Fig. 2 shows the oscillograms of the network phase voltage and phase current at a frequency of 400 Hz.

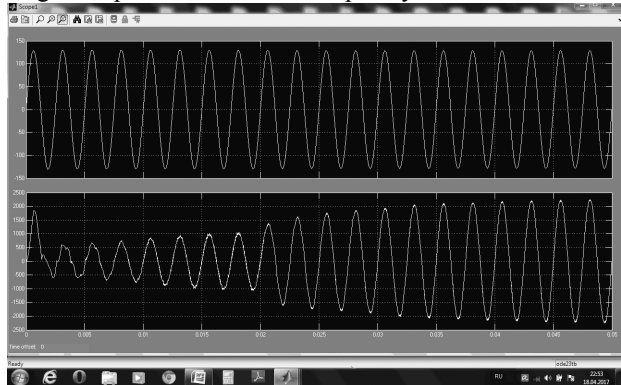


Fig. 2. Mains voltage and current (mains frequency 400 Hz).

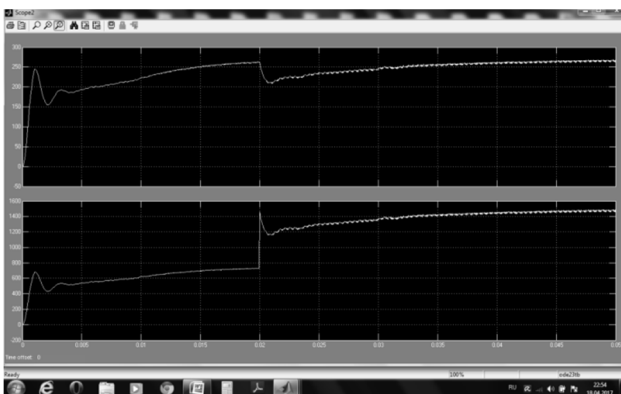


Fig. 3. Rectified voltage and current (mains frequency 400 Hz).

In Fig. 3. the oscillograms of the rectified voltage and current are shown, and in Fig. 4 - active and reactive power of one phase of the supply network. As can be seen from the presented oscillograms, the current of the supply network is practically sinusoidal, the reactive power is zero, because in the ACS, a single factor of the network current shift relative to the phase voltage was maintained.

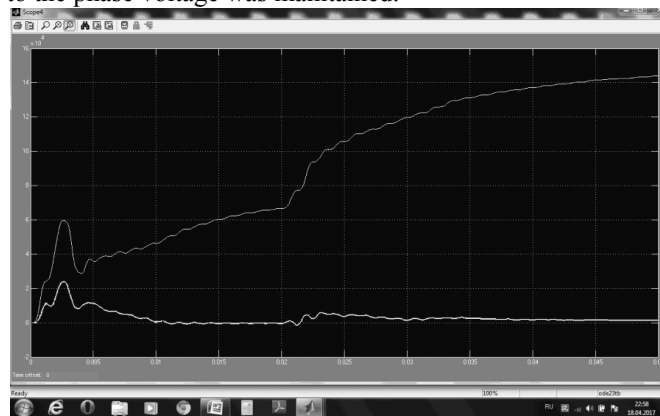


Fig. 4. Active and reactive power (mains frequency 400 Hz).

The results of modeling the mode of connection of the VAR to the power network with its parameters corresponding to the frequency of 800 Hz and the conversion of the converter to the NVI mode are shown in Fig. 5 - 7. VAC ACS in this mode provided stabilization of the output voltage at the level of 540 V. The source EMF in the

rectified voltage circuit connected at the time $t = 0.02$ s was set equal to 800 V - the regime number 10.

In Fig. 5 shows the oscillograms of the network phase voltage and phase current, which are in phase before $t = 0.02$ s, and after - in phase out.

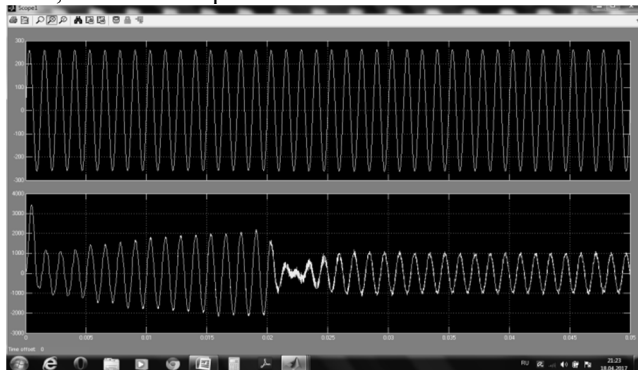


Fig. 5. Mains voltage and current (mains frequency 800 Hz).

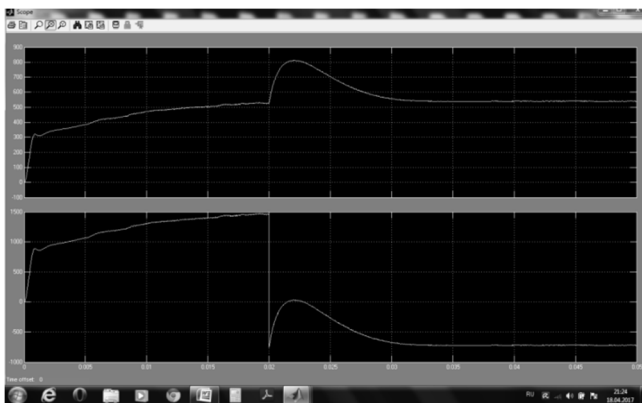


Fig. 6. Output load voltage and current (mains frequency 800 Hz).

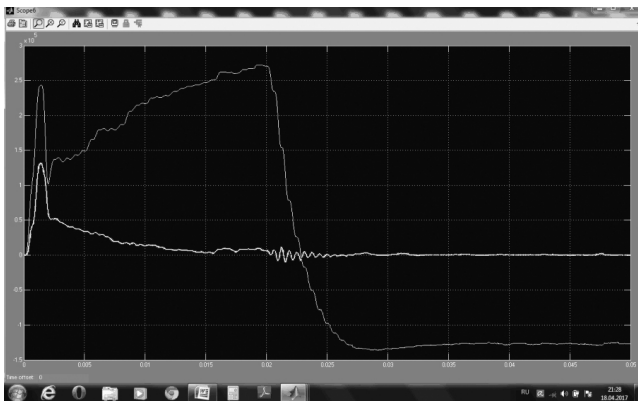


Fig. 7. Active and reactive power (mains frequency 800 Hz).

In Fig. 6 shows the oscillograms of the output voltage and current in the load circuit, and in Fig. 7 - active and reactive power of one phase of the supply network. From the oscillograms of Fig. 7, it is seen that up to time $t = 0.02$ s, the active power of one phase of the network is positive, and the reactive power tends to zero after decay of the transient process associated with the connection to the network. After this time, the active power becomes negative, which corresponds to the transfer of energy from the rectified voltage circuit to the supply network. The reactive power

after the oscillations associated with the transition to the NVI mode, tends to zero value.

VI. CONCLUSION

1. The synthesized automatic control system has sufficient robustness, ensuring good performance without changing the parameters of the regulator.

2. The simulation results obtained on the developed simulation model of the automatic control system testify to its good dynamic and energy parameters and high accuracy of stabilizing the output voltage of the converter operating in the modes of an active rectifier and a network voltage inverter.

3. These indicators characterize the "limiting" capabilities of the converter when powered by an ideal network. However, they are a definite guideline for the developers of aviation power supply systems.

4. The direction of further research is related to the development of an imitation model of the aviation power generation system, the power part of which consists of a magnetoelectric generator and an active voltage converter, prototyping this system, as well as conducting its experimental tests.

REFERENCES

- [1] Designing a generator with rare-earth magnets in the aircrafts power supply system / A. V. Levin, D. V. Levin, E. Ya. Livshits, B. S. Zechikhin. *Electricity*. No. 10, 2009. - pp. 41-47. (In Russian).
- [2] Kharitonov, S. A. The system "synchronous generator with excitation from permanent magnets - active rectifier" (mathematical model) / S. A. Kharitonov. *Electrical engineering*. No. 12, 2009. - pp. 33-41.
- [3] Kharitonov S. A. *Elektromagnitnyye protsessy v sistemakh generirovaniya elektricheskoy energii dlya avtonomnykh ob'yektov: monografiya*. [Electromagnetic processes in power generation systems for autonomous objects: monograph]. Novosibirsk: Izd. NSTU, 2011. - 536 p. (In Russian).
- [4] Garganeyev, A. G. Perspective aircraft power supply systems with fully electrified equipment. A. G. Garganeyev, S. A. Kharitonov // *Reports of TUSUR*. Tomsk: TUSUR publishing house. No. 2 (20), 2009. - pp. 185-192. (In Russian).
- [5] Efimov, A. A. Schreiner R. T. *Aktivnye preobrazovateli v reguliruemyykh elektroprivodakh peremennogo toka* [The Active Converters in Alternative Electric Drivers]. Novouralsk: NGTI Publ., 2001. 250 p. (In Russian).
- [6] German-Galkin, S. G. *Virtual'nyye laboratorii poluprovodnikovyykh sistem v srede Matlab-Simulink* [Virtual laboratories of semiconductor systems in the Matlab-Simulink environment]. SPb.: Lan Publishing House, 2013. - 448 p. (In Russian).
- [7] Predictive relay-vector control of active frequency converters in AC drive systems / R. T. Shreiner, A. A. Efimov, G. S. Zinoviev, K. N. Koryukov, I. A. Mukhamashin, A. I. Kalygin // *Electrical Engineering*. 2004. № 10. - pp.43-50.
- [8] Efimov A. A., Muhamatshin I. A. Control Active Converters in Energy Supply Systems and Electric Drive. *Izvestia RAN. Energetika*, 2005, no. 4, pp. 91-112. (In Russian).
- [9] Efimov A. A. Control Active Converters Consisting of Electromechanical Systems. *Izvestia GUAP. Aerokosmicheskoe priborostroenie*, Saint-Petersburg, GUAP Publ., 2012, iss. 2, pp. 58-67. (In Russian).
- [10] Skuryatin Yu. V., Belousov A. V., Denisevich N. A. Frequency converter with control on sliding modes, electromagnetically compatible with the network / *Proceedings of the IX International (XX All-Russian) Conference on Automated Electric Drive*. Perm: Publishing house of the

- Central Scientific and Technical University, 2016. pp. 301-305. (In Russian).
- [11] Operating modes of the power generation system of unstable frequency and stable voltage / A. V. Levin, S. F. Konyakhin, M. M. Yukhnin, S. A. Kharitonov, D. V. Korobkov, D. V. Makarov // Aviation Industry. - 2012. - №4. - pp. 2-8. (In Russian).
- [12] Kharitonov S. A. AC-AC converter without passive elements in DC link / S. A. Kharitonov, M. V. Balagurov, P. A. Bachurin // XIII International Conference of Young Specialists on Micro / Nanotechnologies and Electron Devices, EDM 2012: proc., Altai, Erlagol, 2-6 July 2012. - Novosibirsk: NSTU, 2012. - pp. 327-329. (In Russian).
- [13] Kharitonov S. A. AC-AC converter based on six-phase active rectifier and current source inverter / S. A. Kharitonov, M. V. Balagurov, P. A. Bachurin // XIV International Conference of Young Specialists on Micro / Nanotechnologies and Electron Devices, EDM 2013: proc., Altai, Erlagol, 1-5 July 2013. Novosibirsk: NSTU, 2013. - pp. 259-260. (In Russian).
- [14] Karaarslan and I. Iskender, "The analysis of AC-DC boost PFC converter based on peak and hysteresis current control techniques, "International Journal on Technical and Physical Problems of Engineering(IJTPE), Issue 7, Vol. 3, No. 2, pp. 100-105, June 2011.
- [15] Nguyen T., Lee H., "Dual Three-Phase Indirect Matrix Converter With Carrier-Based PWM Method", IEEE Transactions on Power Electronics, Vol. 29, No. 2, pp. 569-581, February 2014.



Efimov Alexander Andreevich (b. 1948) – Dr. Sc. Tech., Professor, professor of the department "Control in technical systems", SPb SUAI. His research interests are currently focused on electromechanical systems and power electronics. He is author of 190 scientific papers. (Address: apt. 203, build. 61, Kosmonavtov Ave., St. Petersburg, Russia, 196158. Email: efa33@aanet.ru).

Development of Set of Electric Energy Quality Factors

Gennady S. Zinoviev, *Member, IEEE*

Novosibirsk State Technical University, Novosibirsk, Russia

Abstract – The review and analysis of our proposals on the addition of the existing set of electrical energy quality factors describing the distortion of the network voltage form is made. First, there are a number of new factors of the quality of the non-sinusoidal voltage and current of the consumer. Secondly, these are new factors of the share participation of consumers in the general distortion of the network voltage and the methodology for calculating them. Thirdly, these are new factors of the share participation of consumers' currents in the general distortion of the current in the supply network and the methodology for calculating them.

Index Terms – Integral total harmonic distortion, differential total harmonic distortion, contribution to voltage distortion, contribution to current distortion, quality of electrical energy.

I. INTRODUCTION

THE PROBLEM of determining the factors of the quality of electrical energy included in the standards for the quality of electrical energy continues to be relevant. Periodic new reissues of the standards contain adjustments in the definition and measurement of some individual energy factors. The article considers our proposals to justify the introduction of additional factors of the quality of electrical energy in the new reprints of the standards for the quality of electrical energy. We are talking about indicators that additionally or more adequately characterize the manifestations of this type of substandard, such as distortion of the sinusoidal voltage of the supply by higher voltage harmonics. The purpose of introducing new factors of the quality of electrical energy is to obtain new or more adequate characteristics of damage from distortion of the sinusoidal voltage and current of the supply network.

Three aspects of the problem are considered, namely

1. Introduction of new factors of the quality of electrical energy;
2. Substantiation of a new technique for determining the degree of the inverse effect of currents of nonlinear consumers on their partial contributions to the overall distortion of the supply network voltage;
3. Substantiation of a new technique for determining the degree of the inverse effect of currents of nonlinear consumers on their partial contributions to the total current of the supply network.

II. ADDITIONAL FACTORS OF THE QUALITY OF THE SUPPLY NETWORK VOLTAGE

The main consumers of electrical energy of the common supply network are transformers, reactors, AC motors, capacitors. In the first approximation, the first three elements

of the network can be represented in the model in the form of an equivalent inductance (scattering, magnetization, resultant). The higher harmonics of the mains voltage contribute to the higher harmonics of the inductor current, inversely proportional to the numbers of the harmonics. Then the coefficient of harmonics of the inductor current K_{hc} , equal to the ratio of the effective value of the current of higher harmonics $I_{(hh)}$ to the effective value of the current of the first harmonic of inductance $I_{(1)}$ will be equal to

$$K_{hcL} = \frac{I_{(hh)}}{I_{(1)}} = \frac{\sqrt{\sum_{k=2}^{\infty} I_{(k)}^2}}{I_{(1)}} = \frac{\sqrt{\sum_{k=2}^{\infty} \left(\frac{U_{(k)}}{k\omega L} \right)^2}}{\frac{U_{(1)}}{\omega L}} = \sqrt{\sum_{k=2}^{\infty} \left(\frac{U_{(k)}}{kU_{(1)}} \right)^2} = \bar{K}_{hv} \quad (1)$$

Here there is the RMS value of higher current harmonics $I_{(hh)} = RMS(i_{hh}) = RMS(i - i_{(1)})$.

We named this coefficient the integral coefficient harmonics voltage of the first-order (the first of the system-forming series of integral coefficients harmonics of higher-order) [1-4]. This coefficient directly (without calculation) determines the coefficient of harmonic current inductance K_{hc} , characterizing the direct damage from distortion of the current by higher harmonics. Abroad, a little later, as far as we can judge from the available foreign literature, this indicator was introduced under the name weighted total harmonic distortion of WTHD [5].

Similarly to the derivation of formula (1) for the inductance current, a formula is obtained for the capacitor current. The higher harmonics of the mains voltage contribute to the higher harmonics of the capacitor current, directly proportional to the numbers of the harmonics. Then the harmonic coefficient of the capacitor current, equal to the ratio of the effective value of the current of the higher harmonics to the effective value of the current of the first harmonic of the capacitance, is equal to

$$K_{hcC} = \frac{I_{(hh)}}{I_{(1)}} = \frac{\sqrt{\sum_{k=2}^{\infty} I_{(k)}^2}}{I_{(1)}} = \frac{\sqrt{\sum_{k=2}^{\infty} (k\omega C U_{(k)})^2}}{\omega C U_{(1)}} = \sqrt{\sum_{k=2}^{\infty} \left(k \frac{U_{(k)}}{U_{(1)}} \right)^2} = \hat{K}_{hv} \quad (2)$$

Here, the effective value of the differentiated q-times of the higher-harmonic voltage is given by

$$U_{(hh)}^{(q)} = RMS\left(\frac{1}{dt} \frac{\dots}{q\text{-times}} \left(\frac{1}{dt} \left(\frac{u_{hh}}{dt}\right)\right)\right)$$

By analogy with (1), we named this coefficient as the differential coefficient of the voltage harmonics of first-order (the first of the system-forming series of differential coefficients of harmonics of higher orders) [1-4]. Knowing this coefficient directly (without calculation of current) determines the harmonic coefficient of the capacitor current, i.e., direct damage from distortion of the current by higher harmonics.

Two families of integral and differential coefficients of harmonics of voltage (current) can be combined into one under the name of q-order voltage (current) coefficients of harmonic, where positive values of q will generate integral coefficients harmonics of voltage (current), and negative values of q will generate differential coefficients of harmonics of voltage (current) of higher orders.

$$\overline{K}_{hv}^{(q)} = \frac{U_{(hh)}^{(q)}}{U_{(1)}} = \frac{\sqrt{\sum_{k=2}^{\infty} \frac{U_{(k)}^2}{k^2}}}{U_{(1)}} = \sqrt{\sum_{k=2}^{\infty} \left(\frac{U_{(k)}}{k^{(q)} U_{(1)}}\right)^2} \quad (3)$$

Here, the negative values of the exponent q correspond to the differentiation operation, that is, $U_{(hh)}^{(q)}$ is the effective value of the q-times differentiated voltage of the higher harmonics.

$$U_{(hh)}^{(q)} = RMS\left(\frac{1}{dt} \frac{\dots}{q\text{-times}} \left(\frac{1}{dt} \left(\frac{du_{hh}}{dt}\right)\right)\right)$$

Abroad, a little later, as far as we can judge from the available foreign literature, this indicator appeared under the name of the weighted total harmonic distortion of WTHD [5].

Thus, in order to simplify the determination of the damage in the consumer's current from the non-sinusoidal voltage of the supply, it was proposed to introduce the integral and differential coefficients harmonics of voltage of the first-order into the standards for the quality of electrical energy (voltage) $\overline{K}_{hv}^{(1)}$, $\widehat{K}_{hv}^{(1)}$ respectively.

$$\overline{K}_{hv}^{(1)} = \sqrt{\sum_{k=2}^{\infty} \left(\frac{U_{(k)}}{k U_{(1)}}\right)^2} \quad \widehat{K}_{hv}^{(1)} = \sqrt{\sum_{k=2}^{\infty} \left(k \frac{U_{(k)}}{U_{(1)}}\right)^2} \quad (4)$$

It has been shown [6-8] that the degree of the inverse influence of the consumer with non-sinusoidal current on the distortion of the network voltage form (with two types of network replacement schemes) is determined by the first-order differential of the current harmonics coefficient of the consumer.

$$\widehat{K}_{hc} = \frac{\widehat{I}_{(hh)}}{I_{(1)}} = \sqrt{\sum_{k=2}^{\infty} \left(k \frac{I_{(k)}}{I_{(1)}}\right)^2} \quad (5)$$

or fractional order (one second) when the impedance of the network depends on the frequency in form of one second degree

$$\widehat{K}_{hc}^{(1/2)} = \frac{\widehat{I}_{(hh)}^{(1/2)}}{I_{(1)}} = \sqrt{\sum_{k=2}^{\infty} k \left(\frac{I_{(k)}}{I_{(1)}}\right)^2} \quad (6)$$

In the standard this factor is called the partial weighted coefficient of harmonic components; [Partial weighted harmonic distortion (PWHd)].

These factors were used in the West in the IEC standard, and then were copied in the standard of Russia [9]. We have repeatedly raised the problem of introducing additional factors of the quality of electrical energy in our standards [10-13], but to this day this scientific problem has not found a response [14].

III. DEFINITION OF THE PARTIAL CONTRIBUTIONS OF INDIVIDUAL CONSUMERS TO THE GENERAL DISTORTION OF THE NETWORK VOLTAGE FORM

Used in the previous GOST for the quality of electrical energy [15], the method of determining the contributions of individual consumers to the general distortion of the voltage network form, as we have shown [13], did not always yield adequate results. The former method is not included in the new GOST [16], although a new method is not proposed in exchange.

The equation for the high-frequency component of the voltage in the node of the power system from two harmonics distorted currents has the form

$$u_{hh} = L \frac{di_{1h}}{dt} + L \frac{di_{2h}}{dt}$$

The following notations will be used in the paper:

$\hat{\cdot}$ – the icon on the variable indicates the derivative,

$\overline{\cdot}$ – the icon on the variable indicates the integral.

The equation is squared and integrated over the period:

$$\begin{aligned} \frac{1}{T} \int_0^T u_{hh}^2 dt &= \frac{1}{T} \int_0^T \left(L \frac{di_{1h}}{dt} \right)^2 dt + \frac{1}{T} \int_0^T \left(L \frac{di_{2h}}{dt} \right)^2 dt + \\ &+ \frac{1}{T} \int_0^T 2 \cdot L \frac{di_{1h}}{dt} \cdot L \frac{di_{2h}}{dt} dt \end{aligned}$$

We obtain the equation of the relation between the proper partial participations PP and the mutual participations MP of the loads in the general distortion of the network voltage, if we divide the right-hand side of the equation by the left-hand side of

$$PP^*(i_1) + PP^*(i_2) + MP^*(i_1; i_2) = 1 \quad (7)$$

$PP^*(i_i)$ – the relative own equity participation of the relevant branch adjacent to the node, in the general change in the quality of the voltage at the node.

$MP^*(i_1; i_2)$ – the relative mutual share of the two branches adjacent to the node, in the general change in the quality of the voltage in the node.

Define the coefficients of equity participation of each non-linear consumer in the general voltage distortion on the basis of equation (7):

$$K_1 = PP^*(i_1) + MP^*(i_1, i_2) \cdot \frac{PP^*(i_1)}{PP^*(i_1) + PP^*(i_2)} \quad (8)$$

the contribution of the first consumer to network distortions and,

$$K_2 = PP^*(i_2) + MP^*(i_1, i_2) \cdot \frac{PP^*(i_2)}{PP^*(i_1) + PP^*(i_2)} \quad (9)$$

the second consumer's contribution to network distortions.

From the above equations it can be seen that the resulting distortions in the quality of the voltage in the node of the power system are determined not only by the characteristics of the power objects adjacent to the node, but also by the pairwise characteristics of the power facilities. It is the mutual characteristics of the energy objects that determine the deterioration of the quality of electricity at the node when the new object is connected, since the coefficients of mutual participation MP may have negative or positive signs, in contrast to the coefficients of own participation PP, which are always positive. Therefore, the method of determining the consumer's share in the distortion of the quality of electricity by the previous GOST [15] by disabling individual loads, not taking this factor into account, was not always suitable, as confirmed by the results of modeling [13].

It is proposed to determine the share participation of consumers in the general distortion of the grid voltage according to formulas (8) and (9). In the new GOST [16] there is no method for determining the share participation of consumers in the general distortion of the network voltage.

IV. THE METHOD OF CALCULATING THE INTEGRATED QUALITY OF THE SUPPLY CURRENT THROUGH FACTORS OF THE QUALITY OF THE CURRENTS OF INDIVIDUAL CONSUMERS.

A technique is proposed for calculating the harmonic ratio of the network current through the coefficients of the current harmonics of individual consumers. Such a task was not raised before.

The scheme of the node of the power system (points of common connection-TCC) with several non-linear loads of electric energy is shown in Fig. 1. Here, the source of the resulting EMF (e.) the equivalent of a complex power system, the three branches of loads represented as current sources (i_1, i_2, i_3).

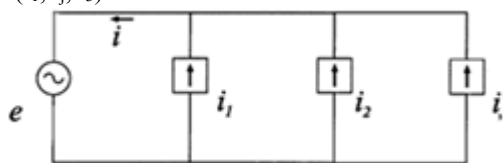


Fig. 1. Scheme of the power system node with three consumers.

Equations for instant high-frequency current components of the network and consumers are transformed by squaring the equation and integrating it over the period in accordance with the ADE method [3]. As a result, we obtain the following algebraic equation for the effective values of high-frequency (distorting) current components with two consumers

$$I_h^2 = \frac{1}{T} \int_0^T (i_h)^2 dt = I_{1h}^2 + I_{2h}^2 + \frac{2}{T} \int_0^T i_{1h} \cdot i_{2h} dt \quad (10)$$

We divide the equation into the effective value of the first harmonic of the network current, and after explicit transformations for the relative variables we obtain

$$K_g^2 = K_{g1}^2 K_{l1}^2 + K_{g2}^2 K_{l2}^2 + K_{g12}^2 K_{l1} K_{l2} \quad (11)$$

Where K_{g1}, K_{g2} the coefficients of the harmonics of consumer currents

$$K_{l1} = \frac{I_{1(1)}}{I_{(1)}}, K_{l2} = \frac{I_{2(1)}}{I_{(1)}} \quad \text{load factors according to the}$$

effective value of the first harmonic of individual consumers with respect to the effective value of the first harmonic of the network current.

K_{g12}^2 cross- harmonics coefficient of a pair of consumer currents.

The general formula for the cross- sectional harmonics coefficient of pairs of consumers currents has the form

$$K_{g12}^2 = \frac{2}{T} \int_0^T \frac{i_{j1} \cdot i_{l2}}{I_{j(1)} I_{l(1)}} dt \quad (12)$$

It should be noted that the new indicator - the cross-sectional harmonic coefficient - has a sign. This takes into account the fact that when the currents of two consumers are summed, the quality of the total current (its harmonic coefficient) can improve (the cross sectional harmonics coefficient is negative) or deteriorate (the cross harmonic coefficient is positive).

Now it is possible to construct formulas for determining the partial contributions of individual consumers to the distortion of the total current of the supply network. It is clear from the structure of formula (11) for current harmonics of the network that it is determined not only by the sum of the weighted harmonics coefficients of each consumer, but also the weighted cross sectional coefficients of the harmonics of consumer currents. Then, for the equity participation of K_1 of the first consumer in the general distortion of the current of the supply network, we obtain

$$K_1 = \frac{I_{1hc}^2}{I_h^2} = K_{g1}^2 K_{l1}^2 + K_{g12}^2 K_{l1} K_{l2} \frac{I_{1h}^2}{I_{1h}^2 + I_{2h}^2} \quad (13)$$

Here I_{1hc}^2 the virtual contribution of the square of the effective value of the current of the higher harmonics of the first consumer to the square of the effective value of the current of the higher harmonics of the network.

Similarly, we obtain a formula for the equity participation of the second consumer

$$K_2 = \frac{I_{2hc}^2}{I_h^2} = K_{g2}^2 K_{l2}^2 + K_{g12}^2 K_{l1} K_{l2} \frac{I_{2h}^2}{I_{1h}^2 + I_{2h}^2} \quad (14)$$

In this case, the amount of shares is equal to one. The method is easily generalized to any number of consumers.

Physically, the share participation of individual consumers shows the share of additional losses in the active power of the corresponding consumer in the total conductive losses in the supply network from the higher harmonics of consumer currents. The partial coefficients of harmonics of individual consumers used for these purposes will not give an adequate result, since these harmonics coefficients characterize the degree of additional losses of active power from the higher harmonics of consumers' currents, not in the network, but among consumers themselves, which is their own, and not the network problem.

It is proposed to use partial participation (13) and (14) in the standards for assessing the degree of negative influence of higher harmonics of individual consumers on the supply network. In addition, a measurement or calculation of the new cross-sectional harmonics of the pairs (12) of consumer currents is required.

V. CONCLUSION

1. Further development in the construction of indicators of the of electrical energy quality, characterizing the nonsinusoidal voltage and current has been made . New indicators are proposed for a deeper non-sinusoidal voltage characteristic, namely, integral and differential voltage coefficients. They allow us to predict the quality of the consumer's current without its calculation in typical elements of the electric network.
2. New definitions of the partial participation of consumers in the general distortion of the network voltage and the methodology for their calculation are proposed.
3. New definitions of partial participation of consumers' currents in the general distortion of the current of the supply network and the methodology for their calculation are proposed.

REFERENCES

- [1] G.S. Zinoviev, Method of direct calculation of the effective value of the current in a circuit with a non-sinusoidal voltage. Theoretical Electrical Engineering, Lviv, No. 43, 1987, p. 98-103 (in Russian).
- [2] G.S. Zinoviev, Direct method for calculating capacities in circuits with gate converters. Electricity, No. 6, 1989, p. 70-75 (in Russian).
- [3] G.S. Zinoviev, Direct methods for calculating the energy parameters of gate converters. Novosibirsk: Izd.-in NSU, 1990, 220p (in Russian).
- [4] G. S. Zinoviev, Concept of definition of electromagnetic compatibility factors of power converters with supply line and load. Proc. Conf. PEMC'96. Hungary, Budapest, 1996, p. 2.201-2.204.
- [5] J. Holtz, Pulse width modulation for electronic power conversion. Proc. IEEE, v.82, 1994, issue 8, p.1194-1214.
- [6] G.S. Zinoviev, Criteria for the efficiency of energy processes in gate converters, Preprint / IED, Ukrainian Academy of Sciences, No. 342.- Kiev, 1982, 31p (in Russian).
- [7] G. Zinoviev, Direct methods for calculating the energy parameters of gate converters, Novosibirsk, NSU. 1990, 220p (in Russian).
- [8] G.S. Zinoviev, Fundamentals of power electronics. 2 nd ed. Novosibirsk, NSTU, 2002, 672p (in Russian).

- [9] GOST 30804.3.12-2013 (IEC 61000-3-12: 2004) Electromagnetic compatibility of technical equipment. Norms of harmonic current components created by technical means with a current consumption of more than 16 A, but not more than 75 A (in one phase) (in Russian).
- [10] G.S. Zinoviev, A look at the problem of reactive power from the standpoint of an electrical engineer. Actual problems of electronic instrument making. Proceedings of MNTK. Novosibirsk: NETI, vol. 7, 1992, p.2-6 (in Russian).
- [11] G.S. Zinoviev, Results of solving some problems of electromagnetic compatibility of gate converters. Electrical engineering. № 11, 2000, p. 12-16 (in Russian).
- [12] G.S. Zinoviev, V.I. Popov, A new approach to assessing the electromagnetic compatibility of gate converters with a power network and load. Electricity, No. 8, 2007. - p. 29-34 (in Russian).
- [13] G.S. Zinoviev, Expansion of a set of indicators of energy efficiency of power electronics devices. Electrical engineering. - 2011. - No. 6. - p. 54-58 (in Russian).
- [14] The quality of electrical energy. Main. Editor Voropai N.I. Novosibirsk, Nauka, 2017. 219p (in Russian).
- [15] GOST 13109-97. Electric Energy. Electromagnetic compatibility. Norms of quality of electric energy in general-purpose power supply systems. - Moscow: Gosstandart, 1998 (in Russian).
- [16] GOST 32144-2013 Electrical energy. Electromagnetic compatibility. Norms of quality of electric energy in general-purpose power supply systems. - Moscow: Gosstandart, 2013 (in Russian).



Gennady S. Zinoviev is a professor of the Electronics and electrical engineering Department of the Novosibirsk State Technical University (NSTU), research supervisor of the Research Laboratory "Optimization of Energy in Converting Systems". Author of the textbook on power electronics, three monographies devoted to electromagnetic compatibility of converters, more than 110 patents and over 200 publications.
E-mail: genstep@mail.ru

Phase Current Curve Analyzing of Hysteresis-Synchronous Motor Powered With Autonomous Voltage Inverter

Alexander G. Garganeev¹, Alexey V. Kasheutov², Evgeny I. Kashin³

¹ National Research Tomsk Polytechnic University, Tomsk, Russia

² Science Research Institute of Automation and Electromechanics, Tomsk, Russia

³ Joint-stock company "Research and Production Facility "Polus", Tomsk, Russia

Abstract – Phase current curve and back electromotive force analysis results obtained for hysteresis-synchronous motor powered with autonomous voltage inverter are presented. The article shows filtering capabilities of a hysteresis-synchronous motor electromagnetic system applied in gyro-equipment for inertia navigation systems of stand-alone objects. A gyromotor phase current generation mathematical model for autonomous inverter commutation intervals is provided.

Index terms – Gyromotor, inverter, electrical winding, filtering, hysteresis.

I. INTRODUCTION

A HYSTERESIS-SYNCHRONOUS motor (HSM) is widely used as a gyrorotor kinetic moment former in inertia navigation systems of stand-alone objects with electromechanical gyroscopes, when the systems are powered by an autonomous voltage inverter (AVI) with classic 180-degree switch control and additional pulsed magnetic biasing module [1–6]. The AVI architecture meets well the gyrocomplex requirements such as high efficiency, speed and temperature condition stability, electromagnetic compatibility, gyroinstrument (GI) accuracy, reliability, price, etc. The AVI of the electromechanical systems (EMS) has informative properties that allow realizing sensorless motor control methods since the AVI is not only operates as a power converter but a device that generates a probing signal directly in operating mode, and a response of the signal contains the information about the motor variables and modes. [7–13]. This feature of the AVI well corresponds to the main mechatronic systems (MS) property: principal impossibility to implement the motor control methods without autonomous inverter. An AVI staircase voltage as the probing signal allows both to specify interrelation between HSM phase current form and magnetization processes and to take into account electromechanical considerations in a special gyroscopic system development.

II. PROBLEM DEFINITION

When designing the gyrodrive, the main task is to create a reliable and simple-constructed electric drive with minimal mass-dimensional parameters and GI errors that are caused by destabilizing factors of the motor. Whereas the HSM

potentially corresponds to the requirements, as mentioned earlier, the HMS electromagnetic processes analysis is required for circuitry and design solutions optimization and in particular for the AVI informative properties realization [7–11]. Back electromotive force (EMF) shape, HSM phase current and their relation to stator winding design peculiarities are to be analyzed.

III. THEORY

When the motor is powered by the 3-phase staircase voltage AVI, the phase current can be described by $I_1(\varphi)$, $I_2(\varphi)$, $I_3(\varphi)$ expressions accordingly to $0 \div \pi/3$; $\pi/3 \div 2\pi/3$; $2\pi/3 \div \pi$ switching intervals:

$$I_1(\varphi) = \frac{U_d}{3R_{\text{эKB}}} \left[1 - \frac{(1+a)(2-a)}{1+a^3} e^{-k\varphi} \right] - E_r \quad (1)$$

$$I_2(\varphi) = \frac{U_d}{3R_{\text{эKB}}} \left[2 - \frac{(1+a)^2}{1+a^3} e^{-k(\varphi - \frac{\pi}{3})} \right] - E_r \quad (2)$$

$$I_3(\varphi) = \frac{U_d}{3R_{\text{эKB}}} \left[1 + \frac{(1+a)(1-2a)}{1+a^3} e^{-k(\varphi - \frac{2\pi}{3})} \right] - E_r \quad (3)$$

where $R_{\text{эKB}}$ and $X_{\text{эKB}}$ are active and reactive HMS phase impedance respectively, $k = R_{\text{эKB}}/X_{\text{эKB}}$, $a = e^{\frac{R_{\text{эKB}}}{X_{\text{эKB}}} \frac{\pi}{3}}$, E_r is a rotor electromotive force, $\varphi = \omega_1 t$; ω_1 is a circular frequency, φ is an actual phase value, and U_d is a constant AVI input voltage [14].

The HSM rotor magnetic condition is defined by the $X_{\text{эKB}}$ impedance that includes such inductive resistances as stator winding dissipation resistance, mechanical gap resistance and rotor material active layer resistance X_r , which is magnetization function as well. The article [2] demonstrates the more rotor magnetization intensity the more EMF E_r and the less X_r . In fact, the EMF E_r is a back-EMF topologically and is a rotation EMF physically. The experiments showed a good harmonic composition of the HSM electromotive force. Total harmonic distortion was from 2.8% to 3.8% in different operation modes. Good filtering properties of the HSM electromagnetic system are caused by:

1) stator windings allocation in pole pitch and windings interconnection,

2) AVI output voltage symmetry, and
3) electromagnetic field propagation processes in ferromagnetic environment.

Usually, gyroscopic HSM has a winding with two slots per pole and phase ($q = 2$) and relative winding pitch $\beta = 5/6$. Also, fifth and seventh harmonic shorting coefficients are $k_{y5} = k_{y7} = 0.259$ [15]. Since the Y-connection of the HSM phase windings causes the absence of every third harmonic and filtering capability of the winding removes every fifth and every seventh harmonics together with all-order submultiple harmonics [16], a back-EMF of high quality sinusoidal shape is generated (Fig. 1).

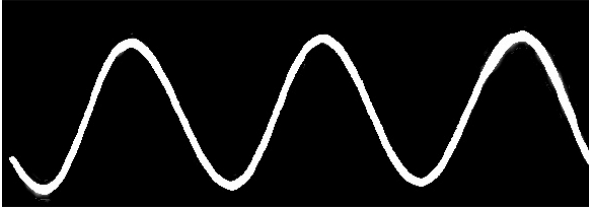


Fig. 1. HSM back electromotive force shape.

When the HSM rotor drops in synchronism, it is under constant field influence, winding type and rotor magnetization peculiarities that define a harmonic composition of the field. The amplitudes of all active harmonic components magnetizing the rotor reduce in factor of $\nu/k_{y\nu}$ respectively, where ν is a harmonic number. The fifth and the seventh harmonics are the most significant for $q = 2$ and $\beta = 5/6$. Since 7th harmonic is forward and 5th harmonic is backward, their phase shifts are as follows:

- phase A: $-5\Theta_r$ and $-5\Theta_r$;
- phase B: $-(240^\circ + 5\Theta_r)$ and $-(120^\circ + 7\Theta_r)$;
- phase C: $-(120^\circ + 5\Theta_r)$ and $-(240^\circ + 7\Theta_r)$.

Unlike rotor, the HSM stator is influenced by back-EMF higher harmonics which obeys the electromagnetic field laws, Maxwell equations, in particular, describing magnetization process dynamic [17–19]. The HSM analyzing aim comes to surface effect consideration when the electromagnetic field wave penetrates into the ferromagnetic half-space (stator) with the frequencies of 5th (2000 Hz) and 7th (2800 Hz) harmonics. If normal to stator surface coordinate is defined as z , electromagnetic wave behavior H in time t could be described as:

$$H(z, t) = H(z)e^{j\omega t} = H_m e^{-\lambda\sqrt{\frac{\omega}{2}}z} e^{j(\omega t - \lambda\sqrt{\frac{\omega}{2}}z)}, \quad (4)$$

where ω is a rotation frequency, $\lambda = 0,57\sqrt{\frac{\pi\mu}{\rho}}$, μ is

a magnetic conductivity, and ρ is resistivity.

A solution of the noted problem is the expression (4) real part:

$$H = H_m e^{-\lambda\sqrt{\frac{\omega}{2}}z} \cos\left(\omega t - \frac{\lambda z}{\sqrt{2\omega}}\right). \quad (5)$$

The expression (5) calculation results are presented in Fig. 2 for the HSM stator electrical steel 2421 with 0.18 mm thickness.

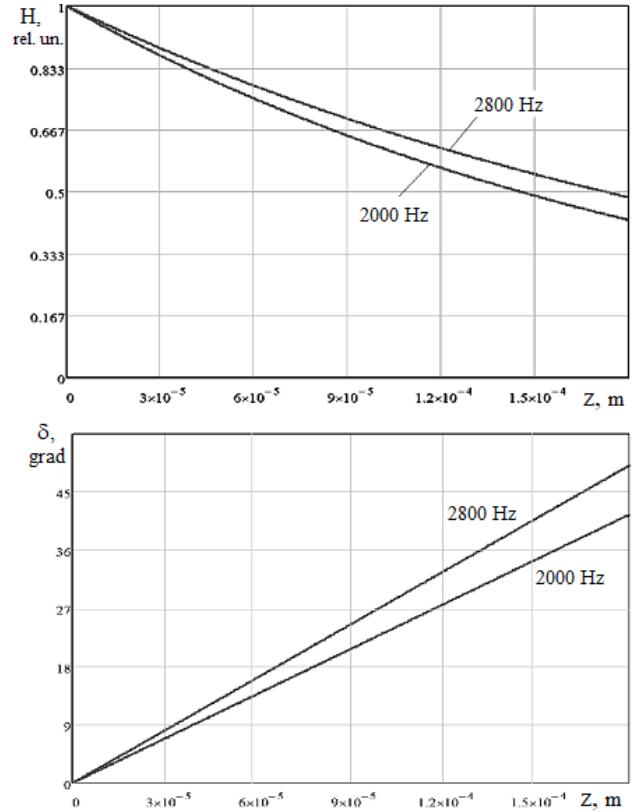


Fig. 2. Back-EMF field relative amplitude (top diagram) and phase (bottom diagram) of 5th and 7th harmonic penetrating into the stator.

Fig. 2 analyzing shows fifth and seventh harmonics additional reduce in factor of $1/k_{y\nu\Delta}$, for the fifth and seventh harmonics:

$$k_{5\Delta} = \frac{\int_0^{18} H(z) dz}{18} = 0,71, \quad k_{7\Delta} = \frac{\int_0^{18} H(z) dz}{18} = 0,67. \quad (6)$$

So total harmonic amplitude reducing factor can be described as:

$$k_{oc\Delta\nu} = k_{\Delta} k_{y\nu} / \nu. \quad (7)$$

As far as the field propagates into the stator steel sheet, the higher harmonics electromagnetic wave gathers phase-shift δ (expression (5))

$$\delta = \frac{\omega\lambda z}{\sqrt{2\omega}}, \quad (8)$$

that causes average sum of different amplitude and phase harmonic components takes part in back-EMF generation. According to Fig. 2, the fifth harmonic average value (δ_{av}) is $\delta_{5av} = 21^\circ$ and the seventh harmonic average value is $\delta_{7av} = 25^\circ$ for the corresponding frequencies. In terms of the fundamental harmonic, additional ν -th harmonic phase-shift δ_{av} is less in factor of ν .

So, the HSM phase current mathematical model $I_{\phi n}(\varphi)$, defined by equations (1) – (3), transforms to expression (9):

$$I_{\phi n}(\varphi) = \frac{U_d}{3R_{\Sigma KB}} F_n(\varphi) - \sum_{\nu=1}^{\infty} A \sin\left[\nu(\varphi - \Theta) - \alpha_{\nu} - \frac{\delta_{\nu cp}}{\nu}\right] \quad (9)$$

where $F_n(\varphi)$ is the AVI commutation function for n -th commutation interval, here is $n = 1$ on $0 \div \pi/3$; $n = 2$ on $\pi/3 \div 2\pi/3$; $n = 3$ on $2\pi/3 \div \pi$;

$$F_1 = 1 - \frac{(1+a)(2-a)}{1+a^3} e^{-k\varphi}; F_2 = 2 - \frac{(1+a)^2}{1+a^3} e^{-k(\varphi - \frac{\pi}{3})};$$

$$F_3 = 1 + \frac{(1+a)(1-2a)}{1+a^3} e^{-k(\varphi - \frac{2\pi}{3})}, \alpha_v = \arctg(vX_{\text{ЭКВ}}/R_{\text{ЭКВ}});$$

Θ is a rotor EMF phase relatively to the power voltage;

$$A = \frac{E_r k_{\text{ОСЛ.V}} B}{\sqrt{R_{\text{ЭКВ}}^2 + (vX_{\text{ЭКВ}})^2}},$$

where B is a harmonic series former function which exclude even harmonics and every third harmonic

$$B = \frac{1 - (-1)^v + 2 \sin \frac{\pi}{2} v \cdot \sin \frac{\pi}{6} v}{v}.$$

As for tooth harmonic (of 11th and 13th order), slots and tooth existence generates the harmonics that result in field curve distortion (Fig. 3), but does not influence to the back-

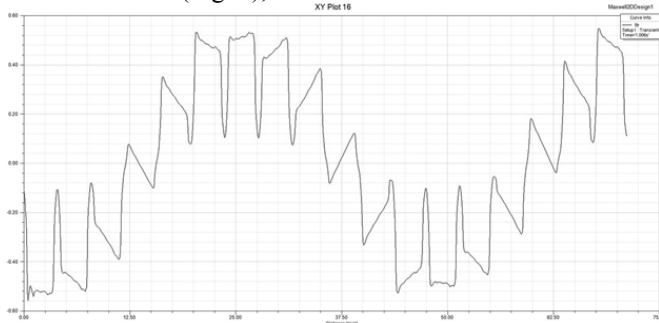


Fig. 3. HSM inductance shape on the mechanical gap pole pith.

EMF curve [15]. Moreover, when a hysteresis layer is magnetized by tooth harmonics, the field penetration in rotor thickness, having regard to the above, reduces harmonic influence in the rotor. For example, the rotor made of Fe-Ni-Al alloy reduces harmonics amplitude (expression (6)) in factor of 3.4 and 3.6 respectively, and when the rotor influences to a stator made of steel 2421, harmonics reduce more in 1.6 and 1.7 times respectively. In addition, hysteresis layer magnetic conductivity deviation, researched in paper [20], does not affect the values evaluated previously. An additional phase-shift of the harmonics penetrating into the rotor thickness achieves value of approximately 90° in depth of 2.5 mm, it means that the sum of the shift with a hysteresis shift angle could be understood as something like “slot skewing” in corresponding frequencies, that leads to additional tooth components reducing.

IV. EXPERIMENTAL RESULTS

A mathematical model of expression (9) was designed in *Mathcad* program as well as a corresponding imitation model was designed in *Multisim* environment to verify theoretical statements presented above. The current curve modeling took

into account preliminary measured HSM parameters such as rotor EMF (rotor alloy is Fe-Ni-Al), total inductive winding impedance, and stator winding active impedance excluding losses in steel (2421 steel with sheet thickness 0.18 mm). The results of current shape modeling, as validation criterion of previously noted reasoning, are presented in Fig. 4, and they show very good matching.

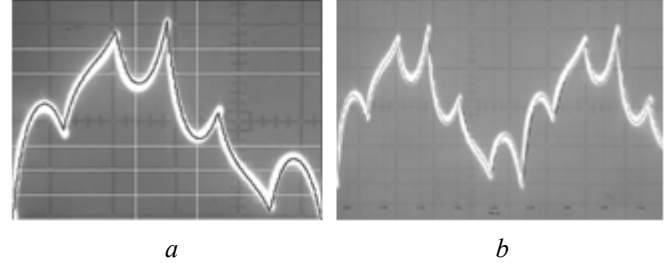


Fig. 4. Comparison of a real HSM current with phase current modeling results of *Mathcad* (a) and *Multisim* (b) (modeling curves was overlapped on the real oscillograms).

V. DISCUSSION OF RESULTS

The results of analysis specify the findings of articles [2,7] related to the phase current (I_ϕ) shape of the electrical machines powered with 180-degree switch control AVI, as the sum of two functions: I_{ei} AVI influence current exponent and sinusoidal current I_{2Er} of rotation EMF in commutation intervals. The mathematical model (9) more precisely describes electromagnetic processes in HSM MS from the electromagnetic field propagation peculiarities in ferromagnetic environments and stator winding parameters influence point of view. In the HSM MS realization processes, including AVI informative properties realization, it is more preferable to use the stator windings with two slots per pole and phase ($q = 2$), relative winding pitch $\beta = 5/6$, and Fe-Ni-Al rotor material because the resistivity $\rho = 0.5 \cdot 10^{-6} \text{ Ohm}\cdot\text{m}$ and relative magnetic conductivity $\mu_{\text{rel}} = 10$ combination of the Fe-Ni-Al alloy provides better field high harmonics filtration then, for example, $\rho = 50 \cdot 10^{-6} \text{ Ohm}\cdot\text{m}$ and $\mu_{\text{rel}} = 22$ combination of the Fe-Co-Cr alloy, that is expressed in worse values of back-EMF harmonic coefficient ($THD \approx 6\%$).

VI. CONCLUSION

Presented research shows that the hysteresis motor electromagnetic system has good filtering capabilities for the high-order field harmonic components. This fact allows calculating the HSM moment using the first harmonic components for different AVI output voltage shapes. The suggested mathematical model provides per-interval current evaluation methods not only for switch choosing but for speed and rotor position feedback signal generation, particularly, for gyrorotor oscillation suppression when using the corresponding points on the switching intervals.

REFERENCES

- [1] Delektorsky B.A. Controlled hysteresis electrodrive/ V.N. Tarasov, B.A. Delektorsky. – M.: Energoatomizdat, 1983. – 128 p. (in Russian)
- [2] Garganeev A.G. Mechatronic systems with hysteresis synchronic motors/ A.G. Garganeev, S.V. Brovanov, S.A. Haritonov. – Polytechnic University, 2012- 227 p.(in Russian).
- [3] Mastyaev N.Z. Hysteresis electromotors. Part.I/ N.Z. Mastyaev, I.N. Orlov – Moscow Power Engineering Institute, 1963. – 220 p. (in Russian).
- [4] Delektorsky B.A. Gyroscopic electromotors design / B.A. Delektorsky, N.Z. Mastyaev, I.N. Orlov. – Mashinostroenie, 1968. – 252 p. (in Russian).
- [5] Bertinov A.I. Aircraft automation electrical machine. – Oborongiz, 1961. – 430 p. (in Russian).
- [6] Tarasov V.N. Overexcitation device miniaturization in hysteresis electromotors // Moscow Power Engineering Institute Reports. 1976. – Rep.291. – Pages. 72 – 77. (in Russian).
- [7] Garganeev A.G. Autonomous inverter informative properties in electromechanics //Elektrichestvo, 2001- № 12. Pp.28 – 36. (in Russian)
- [8] RF Patent № 2164053. Rotation frequency stabilization method for alternate current motors (variants) / Garganeev A.G., Shehovtsov A.S., Shurygin Y.A. – Published in BI 2000, № 7. (in Russian).
- [9] RF Patent № 2207578. The method of synchronous motors rotor EMF definition and asynchronous motors rotor current definition (variants) / Garganeev A.G., Shurygin Y.A. – Published in BI 2003, №18. (in Russian).
- [10] RF Patent № 2193212. The method of alternate current motors inductive resistance definition / Garganeev A.G., Shurygin Y.A. – Published in BI 2002, № 32. (in Russian).
- [11] Garganeev A.G., Informative properties of mechatronic systems.: Tomsk State University of Control Systems and Radioelectronics Reports, 2012. (in Russian)
- [12] RF Patent № 2486649 Electromotor winding resistance control method in mechatronic system/ Garganeev A.G. – Published. 27.06.13. Bul. №18. – 5 p. (in Russian).
- [13] Simulation of the Drive System With Informative Properties of the Stand-alone Voltage Inverter[Electronic resource] / A. V. Kasheutov, A.G. Garganeev// Micro/Nano-technologies and Electron Devices, EDM 2017 : proceedings 17th International Conference of Young Specialists, 30 June-4 July 2017, Erlagol, Altai Republic, Russia, IEEE, 2017. P. 462 – 464.
- [14] Rudenko V.S. Converter equipment/ V.S. Rudenko, V.I.Senko, I.M. Chizhenko. – Kiev.: Visha shkola, 1978.– 423 p. (in Russian).
- [15] Voldek A.I. Electric machine. – Energia, 1974. – 840 p. (in Russian).
- [16] Zherve G.K. Electrical machine windings. – Leningrad. 1989. – 400 p. (in Russian).
- [17] Tamm I.E. Electricity theory bases. Book1, Part.2. – Gostehizdat, 1934. – 284 p. (in Russian).
- [18] Polivanov K.M. Electrotechnics theory bases. Part.3. – Energia, 1969. – 352 p. (in Russian).
- [19] Kifer I.I. Ferromagnetic materials testing/ I.I. Kifer, V.S. Pantushin. – Gosenergoizdat, 1955. – 240 p. (in Russian).
- [20] Mastyaev N.Z. Inductance high harmonics influence to hysteresis motor start moment /N.Z. Mastyaev, V.A. Tregeubov//Elektrichestvo. – 1977. – P.30 – 33. (in Russian).



Alexander G. Garganeev. Doctor of Science, is a Professor at Tomsk National Research Polytechnic University, the school of Energy and Power Engineering. He graduated from Tomsk Polytechnic University in 1978 with a degree in electrical equipment of aircrafts. His main research interests are electric drives, power electronics, process and industrial automation. He has over 200 scientific publications, including 5 monographs and 12 study guides.



Alexey V. Kasheutov, is a postgraduate student at Tomsk National Research Polytechnic University, the school of Energy and Power Engineering. His research interests are power and digital electronics, process automation, programming. He graduated from Tomsk State University of Control System and Radioelectronics in 2012 with a degree in complex protection of informatization objects.



Evgeny I. Kashin, is a postgraduate student in Tomsk National Research Polytechnic University, the school of Energy and Power Engineering. He graduated from Tomsk Polytechnic University in 2007 with a degree in electrical apparatus. His research fields are electrical machines, electrotechnical materials, technical and production process automatization.

A ZVS/ZCS Hybrid Driver Integrated Circuit in 250 nm BCD Technology for Energy-Efficient Switch Mode Power Supply Units

Andrey A. Antonov¹, *Member, IEEE*, Igor K. Surin^{1,2}, Igor V. Pichugin¹, Vladislav Yu. Vasilyev^{1,2}

¹SibIS LLC, Novosibirsk, Russia

²Novosibirsk State Technical University, Novosibirsk, Russia

Abstract – This work represents verification results of experimental samples of hybrid zero voltage/zero current switching driver integrated circuit (IC) developed for switch mode power supply units. The IC samples have been designed and manufactured in 250 nm BCD IC technology, which combines CMOS, bipolar and DMOS options. Hybrid voltage and current control method with addition of different gate voltage forming realized.

Index Terms – Power supply, soft switching, driver.

I. INTRODUCTION

SWITCHED MODE POWER SUPPLY (SMPS) units are inherent parts of telecommunication and electronic equipment, car electronics, renewable energy sources, industrial smart systems, etc. Main parameters that define SMPS are high reliability and controllability, stability in dynamic modes, electromagnetic compatibility, low level of output voltage ripple and noise, energy efficient conversion.

Fig. 1 represents the typical structural diagram of high-power isolated SMPS unit which meets all mentioned above features. This unit can be separated into two parts: power tract (PWR) part, and control and management circuitry (CTRL) part. PWR tract includes the following modules: input filter (IF), input rectifier and active power factor corrector (IR+APFC), voltage converter (VC), power transformer (galvanic isolation), output rectifier (OR), output filter (OF). CTRL part includes: secondary power supply (SPS), independent rectifier control module (RC), converter control module of VC (CC), output and secondary control circuit (O+SCC) with remote control input (RC).

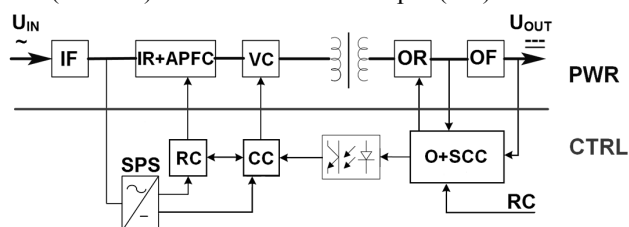


Fig. 1. Schematic diagram of modern SMPS unit.

Whereas PWR tract includes discrete power electronic devices (power MOSFETs and diodes), main components of CTRL section are complex integrated circuits (IC).

II. PROBLEM DEFINITION

There is an issue of interconnection between smart and sophisticated ICs and simple, but very powerful, power switch (like 50 A MOSFET). This issue can be described as follows: the more power and switching frequency PWR tract is, the more power is needed to maintain the system. There are two different ways to solve this issue. First, it is possible to make special interface circuits that transfer control signals to power units – power drivers. Second, it is possible to integrate power drivers into control IC chip die. Second way leads to the special control ICs that are more complex than existing ICs of these types. Another drawback is complicated design that includes high frequency digital circuitry, sensitive detector circuitry and high power circuitry on one IC chip die. First way allows to separate the interference problems by the price of increased component quantity. It is also preferable way for experimental setup and new SMPS units development because of constant control circuit core (microcontroller based). On the other hand, because of the SMPS units market growth and advances in hybrid IC manufacturing technologies, the second way of integrating different circuit types into single IC chip die brings some benefits with reliable solutions.

This work is connected with new high frequency control methods and hybrid technology research for future complex ICs development. The purpose of this study is to develop mainly power driver with essential additional circuitry onto single IC chip die (detector and digital) that allows to operate in main modes. Hybrid technology used in this work is 250 nm BCD technology (that combines CMOS, bipolar and DMOS options [1]. Manufacturer provides BSIM4 MOSFET SPICE model for accurate and predictive development of complex and mixed analog-digital ICs.

The purpose of this work is the verification of hybrid driver experimental sample ICs manufactured by 250 nm BCD technology. This driver is assumed to be a transitional step between simple buffer driver and complex control IC, suitable for SMPS unit control in different modes.

III. ZVS AND ZCS SOFT SWITCHING

Achieving switching frequencies more than 200 kHz in SMPS units with mentioned above parameters (such as high level of electromagnetic compatibility) and output power more than 200 W requires special technology different from

pulse-width modulation, which is known as soft-switching. The reasons of the latter include full control of power transistor's main functions (which are voltage, current passing, speed of current and voltage changing) and generation of appropriate command action that leads to low dynamic energy losses at switching, low level of electromagnetic interference, high level of faultless operation.

There are some different modes of soft-switching technology, known as resonant, Zero Current Switching, ZCS (turn-on at zero level of current, I) and Zero Voltage Switching, ZVS (turn-off at zero level of voltage, U) [2, 3].

ZCS mode assumes providing the conditions for the power switch voltage drop at relatively low level before and during on-time. ZVS mode assumes providing the conditions to redirect the current from switch's channel to external circuitry at near-zero level of voltage during off-time, Fig. 2. In this figure, the definitions are the following: U_K – input constant primary voltage, I_L – maximum current at nominal operation, U_D – voltage difference between source and drain (or collector and emitter), I_D – current function of time, E_{ON} and E_{OFF} – energy losses during transistor switching. Hence, low-level (near zero) voltage (U_D) is the mandatory condition of switching the transistor since this condition leads to the energy loss minimum E_{ON} and E_{OFF} .

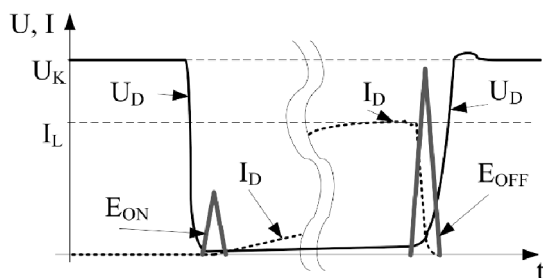


Fig. 2. ZCS/ZVS mode characterization schematic.

Fig. 3 shows a power switch converter configuration with the necessary elements for ZCS/ZVS mode implementation. The dashed line shows an example of a circuit supplement for deriving a DC/DC down-conversion circuit. Shunt capacitors form "bypass" channels for the I_L current when the transistors are off-state and together with the load form a capacitor recharge loop with resonant frequency $\omega_0 = 1/\sqrt{L(C_1 + C_2)}$.

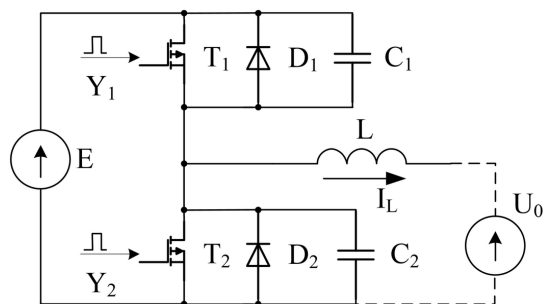


Fig. 3. Simplified schematic diagram of ZCS/ZVS converter.

Resonance processes of capacitor recharging are interrupted if any voltage level equal to the voltage of the primary source E is reached (this phenomenon is called automatic voltage fixation [4]). The second condition for interrupting

the resonance process occurs when the sign of the voltage across the capacitor $C1$ or $C2$ changes when the threshold level of the shunting diode is reached, making it possible to open the switch $T1$ or $T2$, respectively, at a voltage close to zero.

Fig. 4 shows a timing diagram of this process. Fig. 5 shows a strict sequence of switching in the converter structure and pauses forming to recharge capacitors [5].

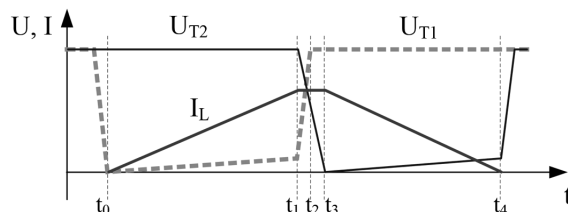


Fig. 4. Timing diagram of switching process.

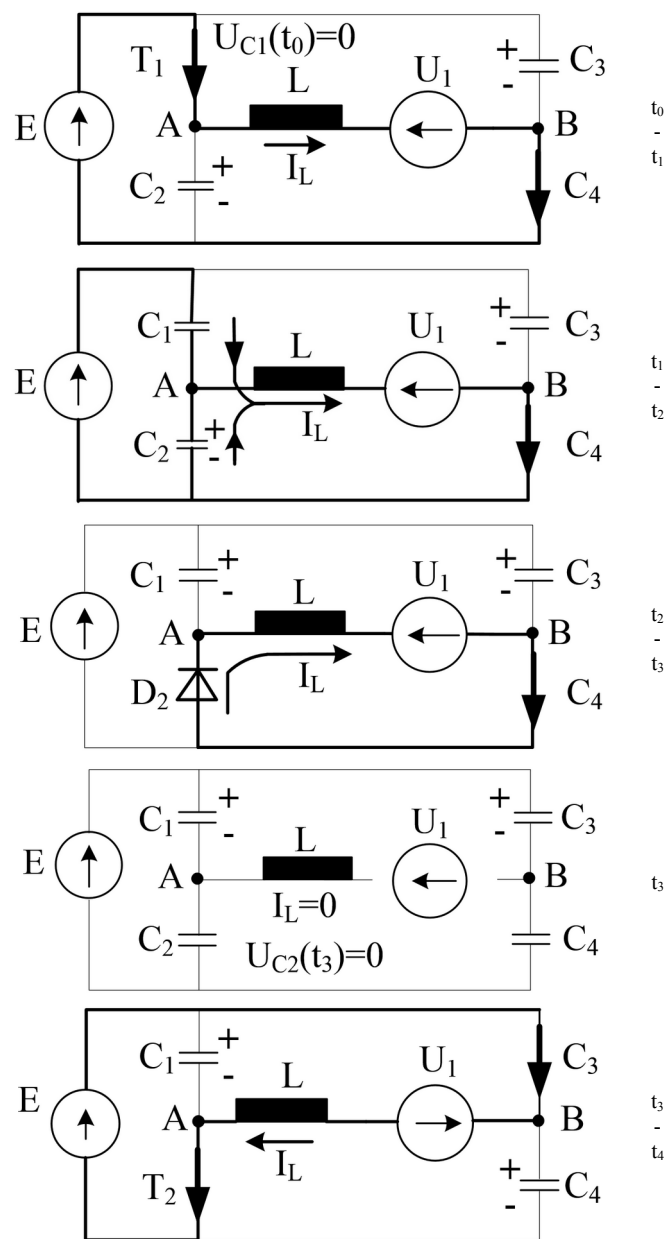


Fig. 5. State diagram of switching process.

From the in Fig. 5 it can be seen that the pause introduction before switching on the transistor T2 after reducing the current through diode D2 to zero (or a pause before turning on T1 after reducing the current through D1) allows to adjust the output parameters of the converter without disturbing the ZCS/ZVS mode.

Summing up the presented, the driver unit has been developed for main operational modes.

IV. ZCS/ZVS HYBRID DRIVER DESCRIPTION

This work represents the second iteration in our research devoted to driver control circuit and SMPS control methods implementation in silicon. We have described first iteration of ZVS driver in our previous work [6]. It is worth mentioning some different solutions that are used partly in this work. Mainly, the development of optimized power buffer amplifier [7] and some ideas from active output rectifier controller [8] and some blocks from multifunctional control unit ICs [9]

Fig. 6(a) represents simplified schematic diagram of the ZCS/ZVS driver with connection to power switch. The driver includes power buffer amplifier (BUF), several detector circuitry (voltage and current), basic digital circuitry (CORE) with start sequence and setup functions, parametric Miller discharge unit (M) and internal voltage converter. Fig. 6(b) represents basic operational principle that is power switch T voltage (U) and current (I) detection, creating appropriate GATE signal.

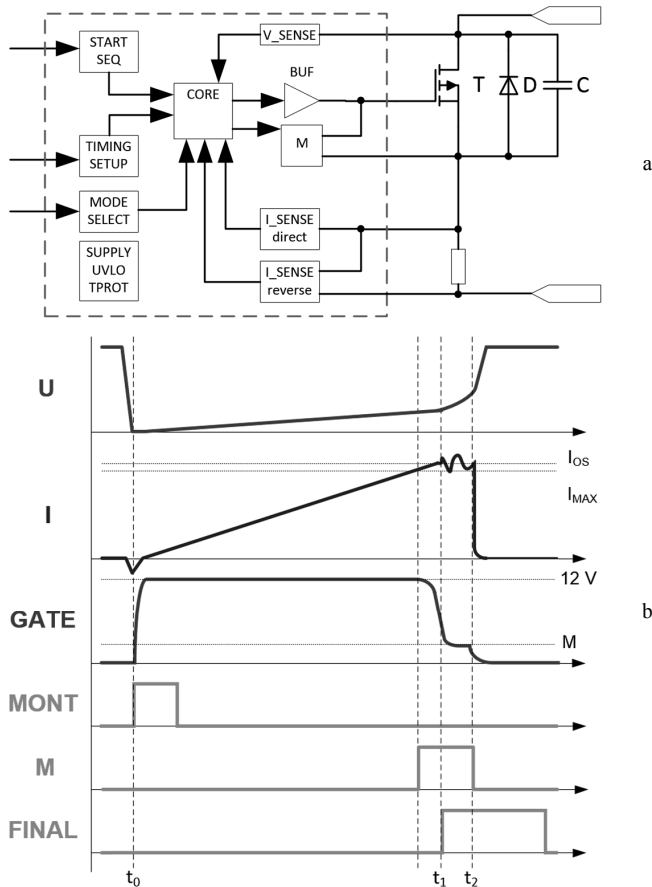


Fig. 6. Schematic diagram of ZCS/ZVS driver IC (a) and its basic operational principle (b).

It is worth mentioning that time intervals ($t_0 - t_2$) are equal to those in Fig. 4. Another feature is internal timings: ON time (MONT), parametric discharge (M) and end cycle protection (FINAL). Main feature is the ability to trace voltage and current that leads to ZCS different realization on turn-on stage and stable ZVS mode with overcurrent protection. To maintain full cycle power switch control the BUF unit is made as tristable. This allows to maintain “flying” gate voltage during conduction cycle and different gate discharge technique application that is essential for different switch types [10].

Voltage and current detection allows driver IC operates in ZCS/ZVS modes with hybrid voltage-current startup.

V. ZCS/ZVS DRIVER IC VERIFICATION

Experimental samples of ZCS/ZVS driver ICs have been manufactured using 250 nm BCD technology. Samples intend for packaging in 48 leads enclosure. Die area of driver IC have dimension of 1.85×1.85 mm. Fig. 7 illustrates the IC layout and the still image of ZCS/ZVS driver IC in enclosure. Table I represents main electrical characteristics of developed hybrid driver.

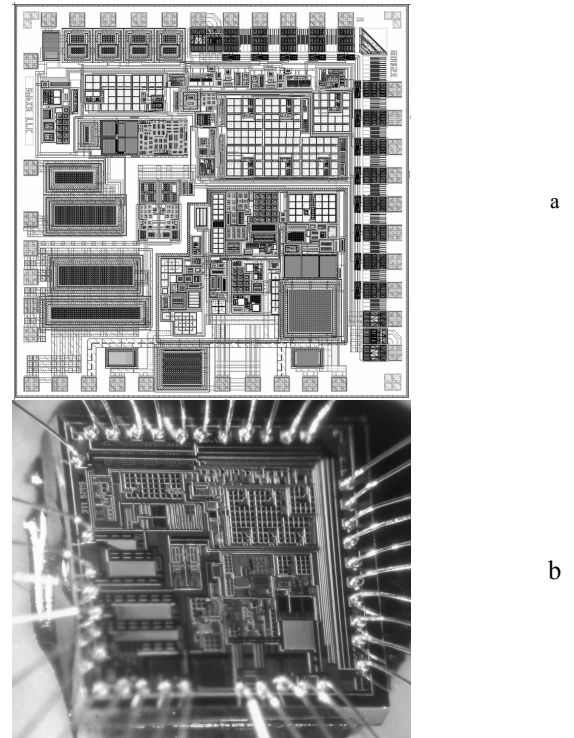


Fig. 7. ZCS/ZVS driver IC layout (a) and still image in enclosure (b).

TABLE I
PARAMETERS OF ZCS/ZVS DRIVER

| | |
|----------------------------------|--------------|
| Supply voltage (U_{CCI}), V | 12.5 – 30 |
| Output voltage (U_{GATE}), V | 12 |
| Maximum output current, A | +2/-4 |
| Operating frequency, kHz | 50 – 500 |
| Own current consumption, mA | Lower than 4 |
| Operating temperature, °C | -40 ... 85 |

Fig. 8(a) represents driver IC operation in PWM mode with constant gate driving in equivalent single switch test circuit. This mode allows to use driver as simple buffer IC. In this figure voltages presented as follows: gate voltage (1); IC internal voltage detector (2); IC internal current detector, equivalent to power switch's current (3); parametric discharge internal signal, suppressed in this mode (4).

Fig. 8(b) represents ZCS/ZVS operation mode with constant gate driving in equivalent test circuit. This mode allows driver IC to operate as a power circuit with fixed frequency soft switching. In this figure voltages presented as follows: gate voltage, difference from previous mode in active gate discharge during ZVS turn-off (1); IC internal voltage detector (2); IC internal current detector, equivalent to power switch's current (3); parametric discharge internal signal, active in this mode (4). As can be seen, active discharge is multi-phase, with 3 areas: parametric discharge with accordance to Miller effect, stable gate voltage fixation with current fixation, and robust discharge with power switch's current cut-off.

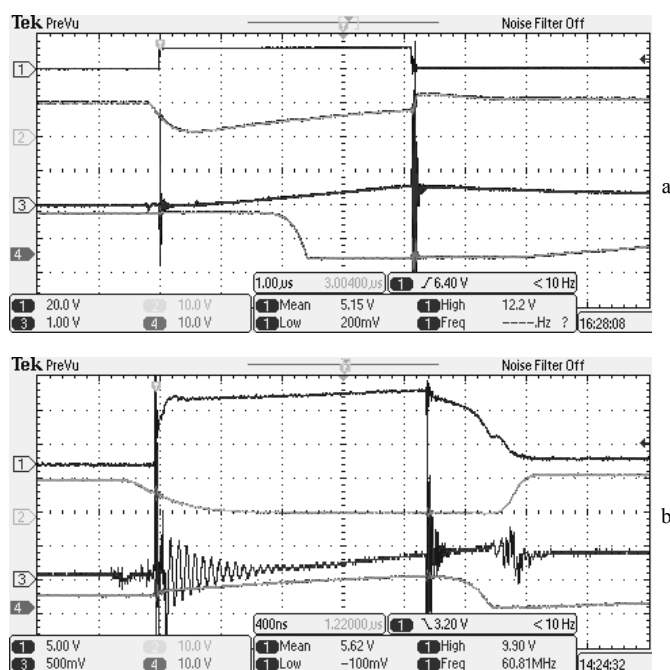


Fig. 8. PWM (a) and ZCS/ZVS (b) modes with constant gate driving.

Fig. 9 represents voltage/current diagrams of power switch operating in ZCS/ZVS mode with “flying gate” technique in equivalent single switch test circuit. As can be seen, gate charging time is fixed for a part of operational cycle. Parametric gate discharge also presented. Current fixation during active off-state followed by robust gate discharge with current cut-off and drain voltage rise. Some voltage spikes explained by ground sharing (test equivalent has 3 basic potentials that can be considered as “ground”) with float potentials and some particular features of equivalent setup circuitry (some drawbacks in clear visualization too). Oscillations are due to parasitic inductances and ground sharing. Despite these effects, the experimental setup shows good and predictable behavior and stable operation in ZCS/ZVS mode. Oscillations and voltage rise at the end of ZVS switch-off

cycle does not break the ZVS mode as can be seen from current waveform: at the time voltage rises the current flow in power switch is ended and directed to auxiliary elements. So, the power losses are minimized.

Fig. 10 represents different ZVS Miller setup (early robust discharge with BUF unit and appropriate holding time for lowering the switching energy and electromagnetic interference).

Fig. 11 represents the experimental verification of ZCS/ZVS hybrid driver operation in half bridge DC/DC converter. Two power switches with two developed driver ICs has been used. One can see that proper grounding and potentials isolation leads to clear picture without voltage spikes and noise. Verification has been made with converter frequency of 79 kHz. Full accordance to model behavior (Fig. 4) has been obtained. Current waveform includes linear areas of different polarity with constant current hold-up (equivalent to zero current in inductance L, see Fig. 5).

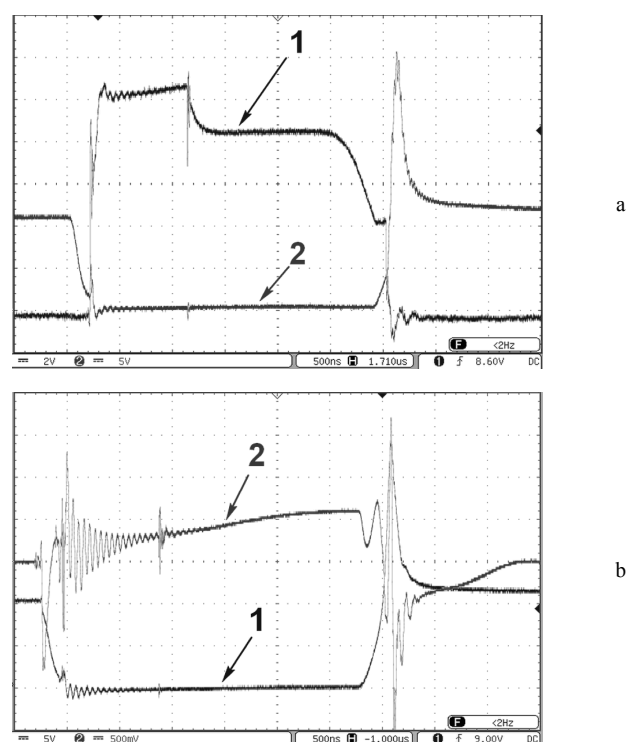


Fig. 9. Driver IC operation in ZCS/ZVS mode. Power switch voltages and current: gate (1) and drain (2) voltages (a); drain voltage (1) and drain current (2).

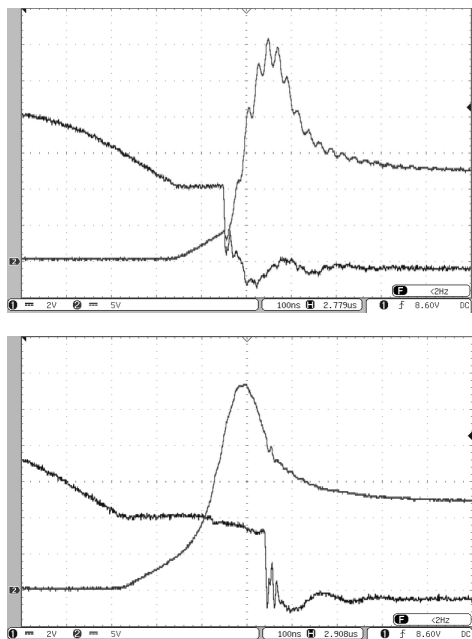


Fig. 10. Different hold-up time during ZVS switch-off. Insufficient (a) and normal discharge with accordance to Miller effect (b).

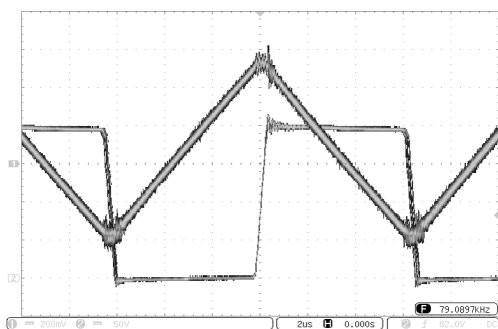


Fig. 11. Experimental verification of ZCS/ZVS operation in half bridge DC/DC converter (Fig. 3 and 4).

VI. DISCUSSION

Verification “in-silicon” of experimental samples of ZCS/ZVS hybrid driver IC shows their correspondence to the expected parameters. The stable operation in a temperature range of $-40...+85\text{ }^{\circ}\text{C}$ has been confirmed. Driver ICs sustained a 2000 V Electrostatic Discharge by the Russian industry standard OST 11 073.013-2008, part 7, method 502-1a (HBM 2000 V).

Results obtained indicate that using this IC it is possible to develop energy efficient SMPS units with several improvements: reducing in component count, lowering mass and dimension of SMPS units by higher the switching frequency, keeping stability maintained, keeping robust functionality in different load conditions by different switch control methods.

Future work is connected with complex control circuit IC. It is worth mentioning that gate voltage shaping is at the front edge of high frequency switching control methodology [11]. Our methodology is soft-switching ZCS/ZVS theory-based and realizing these control methods with several improvements in different gate driving technique: constant driving and partial cycle driving (“flying gate”). Nonetheless, we

agree that development of SMPS units is taking place towards switching frequency rising and power transistor inner processes accounting. First is hardly achieving without lowering switching energy losses while second is inextricably linked with different gate control techniques.

a

VII. CONCLUSION

Experimental samples of ZCS/ZVS hybrid driver IC have been manufactured using 250 nm TSMC BCD technology. IC chip die area is $1.85 \times 1.85\text{ mm}$ (3.43 mm^2). IC verification “in silicon” has confirmed the stable operation of manufacturing samples and full realization of soft-switching algorithms ZVS and ZCS in addition to simple PWM buffer amplifier function. Hybrid current/voltage and current-voltage control methodology with different gate driving technique has shown high reliability and stable power switch control by driver IC developed achieved.

REFERENCES

- [1] TSMC web page, section “Power IC” (web page) URL: http://www.tsmc.com/english/dedicatedFoundry/technology/power_ic.htm.
- [2] Arendt Wintrich, Ulrich Nicolai, Werner Tursky, Tobias Reimann. Application Manual Power Semiconductors. ISLE Verlag 2011.
- [3] Mohan N., Undeland T.M., Robbins W. P. In “Power electronics. Converters, applications and design”. John Wiley and Sons, Inc., 2003. pp.249-298.
- [4] Severns R.P, Bloom G.E. Modern DC-TO-DC Switchmode Converter Circuits. New York: Van Nostrand Reinhold, 1985, 342 pp.
- [5] In “Secondary Supply Units Incorporating Soft-Switching Technology for Power Keys” (Kozlyayev Yu.D.: Editor). Publishing House SB RAS, Novosibirsk, 2014. 113 Pages.
- [6] Antonov A.A., Karpovich M.S., Pichugin I.V., et.al.: ‘Designing and verification of integrated circuit driver for power transistor operation in AC/DC power supply units in zero voltage switching mode’. Proc. 2015 16th International Conference of Young Specialists on Micro/Nanotechnologies and Electron Devices EDM, 2015, pp.371-374, doi.: 10.1109/EDM.2015.7184565.
- [7] Antonov A.A., Karpovich M.S., Pichugin I.V., et al.: ‘Time Domain and ZCS Approximation in Tristable Digital Buffer Amplifiers Engineering for Power Converters’. Proc. of 18th International Conference of Young Specialists on Micro/Nanotechnologies and Electron Devices (EDM), 2017, pp.537-540, doi.: 10.1109/EDM.2017.7981813.
- [8] Ryzhkov V.A., Antonov A.A., Karpovich M.S., et al.: ‘Verification “In Silicon” of the Active Output Rectifier Controller IC in 250 nm BCD Technology for High-Efficiency Power Converters’. Proc. of 13th International Conference on Actual Problems of Electronic Instrument Engineering (APEIE), 2016, pp.41-45, doi.: 10.1109/APEIE.2016.7807076.
- [9] Antonov A.A, Karpovich M.S., Pichugin I.V., et al.: ‘Multi-Functional Control Integrated Circuits in 250 nm BCD Technology for High-Efficiency Power Converters’. Proc. of 17th International Conference of Young Specialists on Micro/Nanotechnologies and Electron Devices (EDM), 2016, pp.411–416, doi: 10.1109/EDM.2016.7538767.
- [10] Boehmer J., Schumann J., Eckel H.-G. ‘Effect of the miller-capacitance during switching transients of IGBT and MOSFET’. Proc. 15th International Power Electronics and Motion Control Conference (EPE/PEMC), 2012, pp. LS6d.3-1 - LS6d.3-5, doi: 10.1109/EPEPEMC.2012.6397498.
- [11] Dymond H.C. P., Wang J., Liu D., et al.: ‘A 6.7-GHz Active Gate Driver for GaN FETs to Combat Overshoot, Ringing, and EMI’. IEEE Transactions on Power Electronics, 2018, Vol.33, No.1, pp.581-594, doi.: 10.1109/TPEL.2017.2669879.



Andrey A. Antonov was born in Arkhara, USSR in 1988. He received B.S., M.S. and Ph.D. degrees in Electronics from Novosibirsk State Technical University (Russia) in 2010, 2012 and 2016, respectively.

From 2009 to 2010, he was a technologist with the Novosibirsk Semiconductor Factory. Since 2011, he has been an R&D engineer of SibIS LLC (Dachnaya 60/1, office room 417, Novosibirsk, 630082, Russia). He is the author of more than 20 articles, and 4 patents. His research interests include micro and nano electronics, power electronics, IC fabrication technology, power converters and renewable electronics, high frequency electronics, problems of electromagnetic compatibility.

Mr. Antonov was a recipient of several awards in the international conferences and the Russia Foundation for Assistance to Small Innovative Enterprises in Science and Technology (FASIE) grant in 2014.

E-mail: reaperrrr@mail.ru



Igor K. Surin was born in Ust-Ilimsk, USSR in 1990. He received B.S. and M.S. degrees in Electronics from Novosibirsk State Technical University (Russia) in 2013 and 2015, respectively. Since 2015, he has been a Ph.D. student in Novosibirsk State Technical University.

Since 2013, he has been an R&D engineer of SibIS LLC. He is the author of several articles. His research interests include micro and nano electronics, power electronics, IC fabrication technology, high frequency electronics, problems of electromagnetic compatibility.

E-mail: surinigork@gmail.com



Igor V. Pichugin received his Eng. in electronics from Novosibirsk State Technical University (Russia) in 1989.

Currently he is R&D engineer of SibIS LLC.

E-mail: pichugin@sib-is.ru.



Vladislav Yu. Vasilyev (Vassiliev) received his MS in chemistry from Novosibirsk State University (Russia), and his Ph.D. in physical chemistry and D.Sc. in solid-state chemistry from Russian Academy of Sciences in 1990 and 2002, respectively.

Currently he is Deputy Director of SibIS LLC and a professor at Novosibirsk State Technical University (Russia).

E-mail: vasiliev@sib-is.ru

Robust Voltage Tracking Control of Three-Phase Four-Wire Split DC Bus Inverter via Time-Scale Separation Technique

Valery D. Yurkevich, *Member, IEEE*, Gennagy S. Zinoviev, *Member, IEEE*
Novosibirsk State Technical University, Novosibirsk, Russia

Abstract — The problem of controller design is investigated for a three-phase four-wire split dc bus inverter with output filters and loads. The proposed time-scale separation technique for controller design gives the possibility to achieve a high accuracy of three-phase voltage generation subject to variations of source voltages or load resistors. The discussed approach to problem of three-phase inverter controller design provides high power quality with small harmonic distortion. The efficiency of the discussed design methodology is highlighted by simulation results.

Index Terms — Power systems, three-phase inverters, pulse-width modulation, PID control, time-scale separation method, singular perturbations.

I. INTRODUCTION

There are various renewable sources of electrical power energy such as solar batteries, wind power plants, hydroelectric resources, and fuel cells [1,2]. The connection of different distributed energy sources of renewable energy to the existing three-phase network is provided based on various types of three-phase inverters. In order to power system efficiency increase, the further development of control system design methods, particularly, for three-phase inverters is an important task. Robust voltage tracking control of three-phase inverters is required for the purpose of grid integration of renewable energy sources and providing high power quality of three-phase alternating current generation with small harmonic distortion [3-5]. The same problem exists for autonomous power supply systems [6-8].

Different control strategies of three-phase inverter controller design are used [9-17], for example, based on PID control [10], frequency domain method [11], sliding mode control [12,13], internal model principle [17]. The proposed controller design methodology in this paper is based on time-scale separation technique (or singular perturbation technique) developed in [18-21] where fast-time-scale and slow-time-scale dynamics are induced in the closed-loop system by proper selection of controller parameters. Then closed-loop system properties are examined via the method of singular perturbations [22,23]. The proposed approach gives the possibility to achieve a high accuracy of three-phase voltage generation under variations of load resistor or source voltage. The discussed design methodology of continuous-time controller is performed based on consideration of an equivalent average continuous-time mathematical model for the three-phase inverter under assumption of a high-frequency pulse-width modulator

(PWM). Therefore, Filippov's average method [24,25] and the geometric approach to PWM control in dynamical systems [26] are used for continuous-time controller design.

As an extension of [21], the application of the time-scale separation method for control of the three-phase four-wire inverter with a split dc bus is studied in this paper where internal resistances of DC sources are taken into account. First, the circuit of the three-phase four-wire inverter with the split dc bus is discussed. Second, the control problem is stated. Third, the mathematical model of the discussed three-phase inverter is described. Fourth, the controller design procedure via time-scale separation technique is presented. Finally, simulation results are included.

II. THE THREE-PHASE FOUR-WIRE SPLIT DC BUS INVERTER

A. The Circuit of the Three-Phase Inverter

The circuit of the three-phase four-wire split dc bus inverter with output filters and loads is shown on Fig. 1. This inverter includes three single-phase half-bridge inverters where interconnection between currents and voltages of these inverters exists due to the presents of the resistors $R_{dc,1}$ and $R_{dc,2}$. The currents and voltages in the circuit of the single-phase half-bridge inverter are highlighted on Fig. 2.

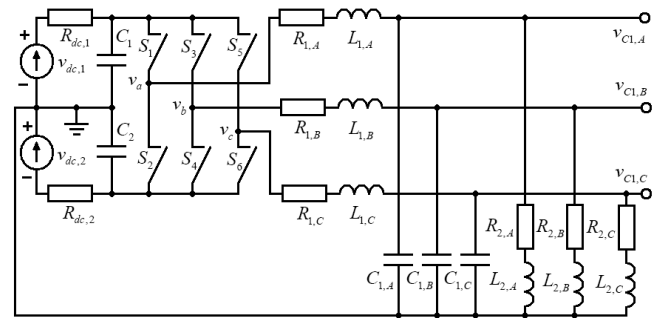


Fig. 1. The circuit of the three-phase four-wire split dc bus inverter with output filters and loads.

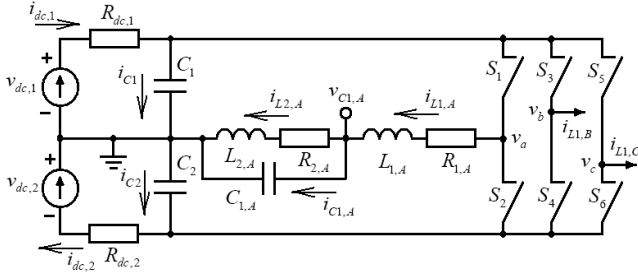


Fig. 2. The circuit of the single-phase half-bridge inverter with output filter and load.

B. Mathematical Model of the Three-Phase Inverter with Output Filters and Loads

The operation of the three-phase inverter in the continuous conduction mode is discussed in the course of the paper. In accordance with the circuits on Fig. 1 and Fig. 2, dynamics of the voltages v_{C1} and v_{C2} are described by

$$\begin{aligned} v_{dc,1} &= R_{dc,1} i_{dc,1} + v_{C1} \\ v_{dc,2} &= R_{dc,2} i_{dc,2} + v_{C2} \\ i_{dc,1} &= i_{C1} + i_{L1,A} \frac{1+\psi_A}{2} + i_{L1,B} \frac{1+\psi_B}{2} + i_{L1,C} \frac{1+\psi_C}{2} \\ i_{dc,2} &= i_{C2} - i_{L1,A} \frac{1-\psi_A}{2} - i_{L1,B} \frac{1-\psi_B}{2} - i_{L1,C} \frac{1-\psi_C}{2} \\ C_1 \frac{dv_{C1}}{dt} &= i_{C1} \\ C_2 \frac{dv_{C2}}{dt} &= i_{C2} \end{aligned} \quad (1)$$

where ψ_A , ψ_B , and ψ_C are the bipolar control variables generated by PWM which can take only two values in the set $\{-1, 1\}$. The switch S_1 conducts current and the switch S_2 is disconnected if the switching function $\psi_A = 1$. The switch S_1 is disconnected and the switch S_2 conducts current if the switching function $\psi_A = -1$. The same rules are used for the other switches.

From (1), by removing of i_{C1} , i_{C2} , $i_{dc,1}$, and $i_{dc,2}$, we get

$$\begin{aligned} C_1 \frac{dv_{C1}}{dt} &= \frac{1}{R_{dc,1}} [v_{dc,1} - v_{C1}] - \sum_{m=A,B,C} i_{L1,m} \frac{1+\psi_m}{2} \\ C_2 \frac{dv_{C2}}{dt} &= \frac{1}{R_{dc,2}} [v_{dc,2} - v_{C2}] + \sum_{m=A,B,C} i_{L1,m} \frac{1-\psi_m}{2} \end{aligned} \quad (2)$$

From the circuit on Fig. 2 we get the equations to describe the behavior of the currents $i_{L1,A}$, $i_{L2,A}$, and the voltage $v_{C1,A}$, that are

$$\begin{aligned} v_a &= v_{C1} \frac{1+\psi_A}{2} + v_{C2} \frac{1-\psi_A}{2} \\ v_a &= L_{1,A} \frac{di_{L1,A}}{dt} + R_{1,A} i_{L1,A} + v_{C1,A} \\ v_{C1,A} &= L_{2,A} \frac{di_{L2,A}}{dt} + R_{2,A} i_{L2,A} \\ i_{L1,A} &= i_{L2,A} + i_{C1,A} \\ C_{1,A} \frac{dv_{C1,A}}{dt} &= i_{C1,A} \end{aligned} \quad (3)$$

By removing of v_a and $i_{C1,A}$, we get

$$\begin{aligned} L_{1,A} \frac{di_{L1,A}}{dt} &= -R_{1,A} i_{L1,A} - v_{C1,A} + v_{C1} \frac{1+\psi_A}{2} + v_{C2} \frac{1-\psi_A}{2} \\ C_{1,A} \frac{dv_{C1,A}}{dt} &= i_{L1,A} - i_{L2,A} \\ L_{2,A} \frac{di_{L2,A}}{dt} &= -R_{2,A} i_{L2,A} + v_{C1,A} \end{aligned} \quad (4)$$

From (4), it follows that

$$\frac{d^2 v_{C1,A}}{dt^2} = f_A(i_{L1,A}, i_{L2,A}, v_{C1,A}, v_{C1}, v_{C2}) + g_A(v_{C1}, v_{C2}) \psi_A \quad (5)$$

where

$$\begin{aligned} f_A(i_{L1,A}, i_{L2,A}, v_{C1,A}, v_{C1}, v_{C2}) &= \\ \frac{1}{C_{1,A}} \left\{ \frac{R_{2,A}}{L_{2,A}} i_{L2,A} - \frac{R_{1,A}}{L_{1,A}} i_{L1,A} - \left[\frac{1}{L_{1,A}} + \frac{1}{L_{2,A}} \right] v_{C1,A} + \frac{v_{C1} - v_{C2}}{2L_{1,A}} \right\} \end{aligned} \quad (6)$$

and

$$g_A(v_{C1}, v_{C2}) = \frac{v_{C1} - v_{C2}}{2L_{1,A}} \quad (7)$$

where $v_{C1} > 0$ and $v_{C2} < 0$, then $g_A(v_{C1}, v_{C2}) > 0$.

Let us define the new variables such that

$$\begin{aligned} x_{1,A} &= v_{C1,A}, \quad x_{2,A} = dv_{C1,A} / dt, \quad x_{3,A} = i_{L2,A}, \\ x_4 &= v_{C1}, \quad x_5 = v_{C2}. \end{aligned} \quad (8)$$

From the second equation of (4) we get

$$i_{L1,A} = C_{1,A} x_{2,A} + x_{3,A}.$$

Then, by taking into account (4)-(8), the system (4) can be rewritten in the form

$$\begin{aligned} \dot{x}_{1,A} &= x_{2,A} \\ \dot{x}_{2,A} &= f_A(x_{1,A}, x_{2,A}, x_{3,A}, x_4, x_5) + g_A(x_4, x_5) \psi_A \\ \dot{x}_{3,A} &= \frac{1}{L_{2,A}} [x_{1,A} - R_{2,A} x_{3,A}] \end{aligned} \quad (9)$$

The same derivations can be done for the circuits of the phase B and the phase C, therefore ones are omitted in the paper. Let us denote

$$x_{1,B} = v_{C1,B}, \quad x_{2,B} = dv_{C1,B} / dt, \quad x_{3,B} = i_{L2,B}, \\ x_{1,C} = v_{C1,C}, \quad x_{2,C} = dv_{C1,C} / dt, \quad x_{3,C} = i_{L2,C}.$$

In accordance with (2) and (9), we get the mathematical model of the three-phase four-wire split dc bus inverter with output filters and loads in the form

$$\begin{aligned} \dot{x}_{1,A} &= x_{2,A} \\ \dot{x}_{2,A} &= f_A(x_{1,A}, x_{2,A}, x_{3,A}, x_4, x_5) + g_A(x_4, x_5)\psi_A \\ \dot{x}_{3,A} &= \frac{1}{L_{2,A}}[x_{1,A} - R_{2,A}x_{3,A}] \\ \dot{x}_{1,B} &= x_{2,B} \\ \dot{x}_{2,B} &= f_B(x_{1,B}, x_{2,B}, x_{3,B}, x_4, x_5) + g_B(x_4, x_5)\psi_B \\ \dot{x}_{3,B} &= \frac{1}{L_{2,B}}[x_{1,B} - R_{2,B}x_{3,B}] \\ \dot{x}_{1,C} &= x_{2,C} \\ \dot{x}_{2,C} &= f_C(x_{1,C}, x_{2,C}, x_{3,C}, x_4, x_5) + g_C(x_4, x_5)\psi_C \\ \dot{x}_{3,C} &= \frac{1}{L_{2,C}}[x_{1,C} - R_{2,C}x_{3,C}] \\ \dot{x}_4 &= \frac{1}{C_1} \left[\frac{1}{R_{dc,1}}[v_{dc,1} - x_4] - \sum_{m=A,B,C} [C_{1,m}x_{2,m} + x_{3,m}] \frac{1+\psi_m}{2} \right] \\ \dot{x}_5 &= \frac{1}{C_2} \left[\frac{1}{R_{dc,2}}[v_{dc,2} - x_5] + \sum_{m=A,B,C} [C_{1,m}x_{2,m} + x_{3,m}] \frac{1-\psi_m}{2} \right] \end{aligned} \quad (10)$$

From (10) it follows that interconnection between currents and voltages of the each phase exhibits as the dependence of functions $f_A, f_B, f_C, g_A, g_B, g_C$ from variables x_4 and x_5 .

III. THE THREE-PHASE INVERTER CONTROLLER DESIGN

A. The Three-Phase Inverter Tracking Regulation Problem

Block diagram of the discussed control system for the three-phase four-wire split dc bus inverter is shown on Fig. 3. The problem of controller design for each single phase m will be treated separately where $m = A, B, C$.

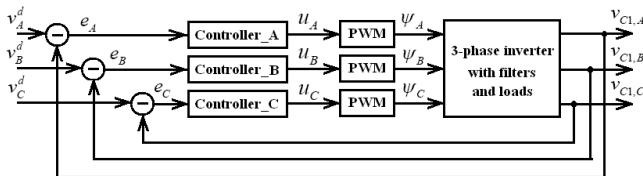


Fig. 3. Block diagram of control system for the three-phase four-wire split dc bus inverter.

Let the desired output voltage of the single phase is assigned by the sin function

$$v_m^d(t) = V_m^d \sin(\omega t + \varphi_m)$$

where V_m^d is the desired value of the output voltage amplitude, $V_m^d = \text{const} > 0$, ω is the network frequency, $\omega = 2\pi f$, for example, $f = 50$ Hz. The control objective is providing high tracking accuracy of the desired sin function $v_m^d(t)$ by the output voltage $v_m(t) = v_{C1,m}(t)$ of the inverter. So, the tracking control problem is stated as the following requirement:

$$|v_m^d(t) - v_{C1,m}(t)| \leq \varepsilon \quad (11)$$

where ε is an arbitrary small positive value and $m = A, B, C$.

B. Average Model of the Three-Phase Four-Wire Split DC Bus Inverter

It is assumed throughout the paper, that all pulse-width modulators on Fig. 3 are not saturated, then u_m belongs to the continuous interval $(-1, 1)$. The averaging is considered during the PWM sampling period T_s as replacement of the discontinuous control variable ψ_m by the continuous PWM input u_m such that

$$u_m(t) = \frac{1}{T_s} \int_t^{t+T_s} \psi_m(\tau) d\tau, \quad \forall m = A, B, C.$$

and $x_j(t)$ is replaced by $y_j(t)$ where

$$y_j(t) = \frac{1}{T_s} \int_t^{t+T_s} x_j(\tau) d\tau, \quad \forall j.$$

Assume that the PWM sampling period T_s has sufficiently small value in comparison with time constants associated with dynamics of (10). Then, by following to the Filippov's averaging approach [24,25] and the geometric approach to PWM control [26], the average model of the system (10) is given by

$$\begin{aligned}
 \dot{y}_{1,A} &= y_{2,A} \\
 \dot{y}_{2,A} &= f_A(y_{1,A}, y_{2,A}, y_{3,A}, y_4, y_5) + g_A(y_4, y_5)u_A \\
 \dot{y}_{3,A} &= \frac{1}{L_{2,A}}[y_{1,A} - R_{2,A}y_{3,A}] \\
 \dot{y}_{1,B} &= y_{2,B} \\
 \dot{y}_{2,B} &= f_B(y_{1,B}, y_{2,B}, y_{3,B}, y_4, y_5) + g_B(y_4, y_5)u_B \\
 \dot{y}_{3,B} &= \frac{1}{L_{2,B}}[y_{1,B} - R_{2,B}y_{3,B}] \\
 \dot{y}_{1,C} &= y_{2,C} \\
 \dot{y}_{2,C} &= f_C(y_{1,C}, y_{2,C}, y_{3,C}, y_4, y_5) + g_C(y_4, y_5)u_C \\
 \dot{y}_{3,C} &= \frac{1}{L_{2,C}}[y_{1,C} - R_{2,C}y_{3,C}] \\
 \dot{y}_4 &= \frac{1}{C_1} \left[\frac{1}{R_{dc,1}}[v_{dc,1} - y_4] - \sum_{m=A,B,C} [C_{1,m}y_{2,m} + y_{3,m}] \frac{1+u_m}{2} \right] \\
 \dot{y}_5 &= \frac{1}{C_2} \left[\frac{1}{R_{dc,2}}[v_{dc,2} - y_5] + \sum_{m=A,B,C} [C_{1,m}y_{2,m} + y_{3,m}] \frac{1-u_m}{2} \right] \quad (12)
 \end{aligned}$$

C. Tracking PID Controller

The average model (12) will be used below in order to controller design. Then, by following to the singular perturbation approach to controller design [18-21], consider the tracking PID-controller given by

$$\mu_m \ddot{u}_m + d_{1,m} \mu_m \dot{u}_m = k_m [T_m^{-2} e_m + a_{1,m}^d T_m^{-1} \dot{e}_m + \ddot{e}_m] \quad (13)$$

where e_m is the tracking error, $e_m(t) = v_m^d(t) - y_{1,m}(t)$. From (13), by Laplace transform, we get

$$u_m(s) = k_m \frac{s^2 + a_{1,m}^d T_m^{-1} s + T_m^{-2}}{\mu_m^2 s^2 + d_{1,m} \mu_m s} e_m(s).$$

So, the controller (13) corresponds to the proper transfer function and implemented without ideal differentiation. The distinctive feature of the controller (13) is that μ_m will be treated as the small parameter of the controller. The way for selection of parameters k_m , T_m , μ_m , $a_{1,m}^d$, and $d_{1,m}$ are highlighted below.

D. Two-Time-Scale Motions in the Closed-Loop System

Denote $u_{1,m} = u_m$, $u_{2,m} = \mu_m \dot{u}_m$ and rewrite the control law (13) in the form

$$\begin{aligned}
 \mu \dot{u}_{1,m} &= u_{2,m} \\
 \mu \dot{u}_{2,m} &= -d_{1,m} u_{2,m} + k_m [T_m^{-2} e_{1,m} + a_{2,m}^d T_m^{-1} e_{2,m} + \dot{e}_{2,m}] \quad (14)
 \end{aligned}$$

where

$$\begin{aligned}
 e_{1,m} = e_m &= v_m^d - y_{1,m}, \quad e_{2,m} = \dot{e}_m = \dot{v}_m^d - \dot{y}_{2,m}, \\
 \dot{e}_{2,m} &= \ddot{e}_m = \ddot{v}_m^d - \ddot{y}_{2,m} \quad (15)
 \end{aligned}$$

From (12) and (14), the average close-loop system of the m -th phase is given by

$$\begin{aligned}
 \dot{y}_{1,m} &= y_{2,m} \\
 \dot{y}_{2,m} &= f_m(y_{1,m}, y_{2,m}, y_{3,m}, y_4, y_5) + g_m(y_4, y_5)u_{1,m} \\
 \dot{y}_{3,m} &= \frac{1}{L_{2,m}}[y_{1,m} - R_{2,m}y_{3,m}] \\
 \mu \dot{u}_{1,m} &= u_{2,m} \\
 \mu \dot{u}_{2,m} &= -d_{1,m} u_{2,m} + k_m [T_m^{-2} e_{1,m} + a_{2,m}^d T_m^{-1} e_{2,m} + \dot{e}_{2,m}] \quad (16)
 \end{aligned}$$

From (16), by taking into account (15), we get

$$\begin{aligned}
 \dot{y}_{1,m} &= y_{2,m} \\
 \dot{y}_{2,m} &= f_m(y_{1,m}, y_{2,m}, y_{3,m}, y_4, y_5) + g_m(y_4, y_5)u_{1,m} \\
 \dot{y}_{3,m} &= \frac{1}{L_{2,m}}[y_{1,m} - R_{2,m}y_{3,m}] \\
 \mu \dot{u}_{1,m} &= u_{2,m} \\
 \mu \dot{u}_{2,m} &= -d_{1,m} u_{2,m} + k_m [T_m^{-2} (v_m^d - y_{1,m}) + a_{2,m}^d T_m^{-1} (\dot{v}_m^d - \dot{y}_{2,m}) + \ddot{v}_m^d - \ddot{y}_{2,m}] \quad (17)
 \end{aligned}$$

Replace $\dot{y}_{2,m}$ in the last equation of (17) by the right part of the second equation of (17). Hence, we get

$$\begin{aligned}
 \dot{y}_{1,m} &= y_{2,m} \\
 \dot{y}_{2,m} &= f_m(y_{1,m}, y_{2,m}, y_{3,m}, y_4, y_5) + g_m(y_4, y_5)u_{1,m} \\
 \dot{y}_{3,m} &= \frac{1}{L_{2,m}}[y_{1,m} - R_{2,m}y_{3,m}] \quad (18)
 \end{aligned}$$

$$\begin{aligned}
 \mu \dot{u}_{1,m} &= u_{2,m} \\
 \mu \dot{u}_{2,m} &= -k_m g_m(y_4, y_5)u_{1,m} - d_{1,m} u_{2,m} + \zeta_m(y_{1,m}, y_{2,m}, y_{3,m})
 \end{aligned}$$

where

$$\begin{aligned}
 \zeta_m(y_{1,m}, y_{2,m}, y_{3,m}) &= k_m [T_m^{-2} (v_m^d - y_{1,m}) + a_{2,m}^d T_m^{-1} (\dot{v}_m^d - \dot{y}_{2,m}) - f_m(y_{1,m}, y_{2,m}, y_{3,m})] \quad (19)
 \end{aligned}$$

The system (18) has the form of the singularly perturbed differential equations [22,23], where μ_m is the small positive parameter. If $\mu_m \rightarrow 0$, then fast and slow motions are induced in this system. From (18), the fast motion subsystem (FMS) in the form

$$\begin{aligned}
 \mu \dot{u}_{1,m} &= u_{2,m} \\
 \mu \dot{u}_{2,m} &= -k_m g_m(y_4, y_5)u_{1,m} - d_{1,m} u_{2,m} + \zeta_m(y_{1,m}, y_{2,m}, y_{3,m}) \quad (20)
 \end{aligned}$$

results, where $\zeta_m(y_{1,m}, y_{2,m}, y_{3,m})$ is the function of the frozen variables during the transients in (20).

Let us take, for simplicity, the gain coefficient k_m of the controller (13) with regards to condition

$$k_m = 1 / g_m(y_4, y_5) \quad (21)$$

then the FMS characteristic polynomial of (20) is given by

$$\mu_m^2 s^2 + d_{1,m} \mu_m s + 1$$

where FMS transients stability is achieved if $\mu_m > 0$ and $d_{1,m} > 0$. The damping of FMS transients is provided by selection of the parameter $d_{1,m}$, for example, take $d_{1,m} = 2$.

Let $\mu_m \rightarrow 0$, then we get steady state of the FMS (20), where

$$\begin{aligned} u_{1,m}^s &= u_{1,m} = (k_m g_m)^{-1} \zeta_m(y_{1,m}, y_{2,m}, y_{3,m}), \\ u_{2,m}^s &= u_{2,m} = 0. \end{aligned}$$

Hence, from (18), the slow motion subsystem (SMS)

$$\begin{aligned} \dot{y}_{1,m} &= y_{2,m} \\ \dot{y}_{2,m} &= T_m^{-2} (v_m^d - y_{1,m}) + a_{2,m}^d T_m^{-1} (\dot{v}_m^d - y_{2,m}) + \ddot{v}_m^d \\ \dot{y}_{3,m} &= \frac{1}{L_{2,m}} [y_{1,m} - R_{2,m} y_{3,m}] \end{aligned} \quad (22)$$

results.

From the first and second equations of (22) it follows that the behavior of the tracking error $e_m = v_m^d - y_{1,m}$ is described by

$$T_m^2 \ddot{e}_m + a_{1,m}^d T_m \dot{e}_m + e_m = 0 \quad (23)$$

where SMS transients stability is achieved in (23) by selection of the controller parameters T_m and $a_{1,m}^d$ such that $T_m > 0$, $a_{1,m}^d > 0$. The damping of SMS transients is provided by selection of $a_{1,m}^d$. For example, take $a_{1,m}^d = 2$.

The rate of time-scale separation between fast and slow transients is maintained in (18) if $\mu_m \ll T_m$, for example, take $\mu_m = T_m / 10$.

IV. SIMULATION RESULTS

Numerical simulation of the three-phase inverter was carried out based on Matlab/Simulink tools under varying values of the dc bus voltages $v_{dc,1}(t)$ and $v_{dc,2}(t)$. Parameters of the inverter were selected such that

$$\begin{aligned} R_{dc,1} &= R_{dc,2} = 1 \, \Omega, C_1 = C_2 = 10 \cdot 10^{-6} \, \text{F}, \\ R_{1,A} &= R_{1,B} = R_{1,C} = 1 \, \Omega, L_{1,A} = L_{1,B} = L_{1,C} = 0.005 \, \text{H}, \\ C_{1,A} &= C_{1,B} = C_{1,C} = 0.6 \cdot 10^{-6} \, \text{F}, R_{2,A} = R_{2,B} = R_{2,C} = 18 \, \Omega, \\ L_{2,A} &= L_{2,B} = L_{2,C} = 0.03 \, \text{H}. \end{aligned}$$

The nominal value of the dc voltage sources is assigned as $v_{dc}^0 = 360 \, \text{V}$. The desired output voltage $v_m^d(t)$ is defined by the sin function where

$$\begin{aligned} v_A^d(t) &= 220 \sin(100\pi t), \\ v_B^d(t) &= 220 \sin(100\pi t - 2\pi/3), \\ v_C^d(t) &= 220 \sin(100\pi t - 4\pi/3). \end{aligned}$$

The value of the PWM switching frequency f_s is defined as $f_s = 20 \cdot 10^3 \, \text{Hz}$, then the PWM sampling period is given as $T_s = 50 \cdot 10^{-6} \, \text{s}$.

In accordance with (7) and (21), the gain k_m of the controller (13) is assigned by

$$k_m = \frac{L_{1,m} C_{1,m}}{v_{dc}^0}.$$

The parameters $a_{1,m}^d$ and $d_{1,m}$ of the controller (13) were selected as $a_{1,m}^d = d_{1,m} = 2$ for all $m = A, B, C$.

Simulation results of (10) governed by the controller (13) with $e_m = v_m^d - x_{1,m}$ where the switching functions ψ_m are generated by the pulse-width modulators with bipolar voltage are shown on Figs. 4-7 when $\mu_m = T_s/3$ and $T_m = 10\mu_m$ for all $m = A, B, C$.

Note, it was shown in [21], the tracking errors e_A, e_B , and e_C can be reduced by $\mu_m \rightarrow 0$ for all $m = A, B, C$. So, by a proper selection of μ_m the requirement (11) can be maintained in the close-loop system.

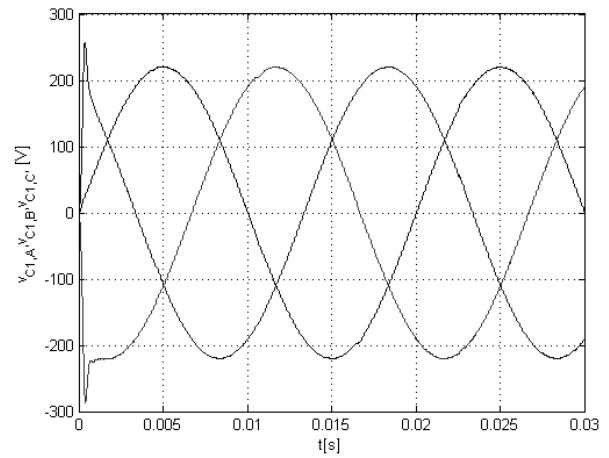


Fig. 4. Plots of $v_{C1,A}(t)$, $v_{C1,B}$, and $v_{C1,C}$ in the closed-loop control system.

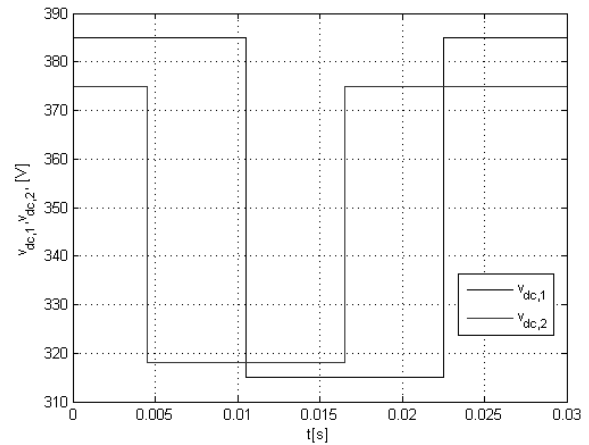


Fig. 5. Plots of $v_{dc,1}(t)$ and $v_{dc,2}(t)$ in the closed-loop control system.

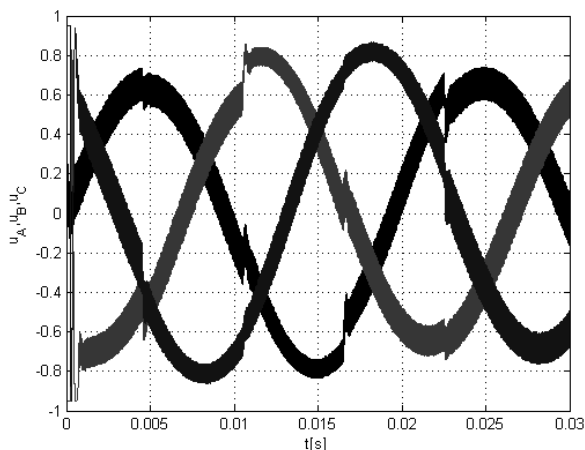


Fig. 6. Plots of $u_A(t)$, $u_B(t)$, and $u_C(t)$ in the closed-loop control system.

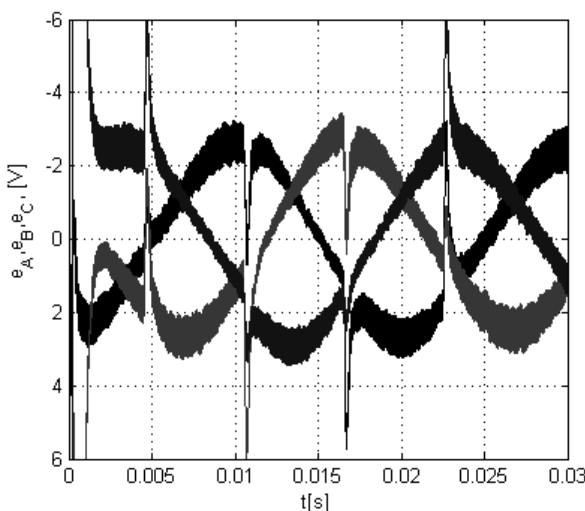


Fig. 7. Plots of the tracking errors $e_A(t)$, $e_B(t)$, and $e_C(t)$ in the closed-loop control system.

V. CONCLUSION

The presented results and numerical simulations for the three-phase four-wire split dc bus inverter with output filters and loads show that the proposed time-scale separation approach gives a clear procedure for selection of controller parameters and allows to achieve a high accuracy of three-phase voltage generation subject to variations of the source voltages or load resistors, as well as in the presence of internal resistances of DC sources.

REFERENCES

- [1] K. Tada, A. Umemura, R. Takahashi, J. Tamura, Y. Matsumura, D. Yamaguchi, H. Kudo, M. Niiyama, Y. Taki, "Frequency control of power system with solar and wind power stations installed by flow control of HVDC interconnection line," Proc. of 20th Int. Conf. on Electrical Machines and Systems (ICEMS), 2017, pp.1-5.
- [2] N. H. Behling, Fuel Cells: Current Technology Challenges and Future Research Needs (First ed.). Elsevier Academic Press, 2012.

- [3] M. Prodanovic, and T. C. Green, "Control and filter design of three-phase inverters for high power quality grid connection," IEEE Trans. on Power Electronics, vol. 18, no. 1, pp. 373–380, January 2003.
- [4] E. Twining, and D. Hohnes, "Grid current regulation of a three-phase voltage source inverter with an LCL input filter," in Proc. Power Electron. Spec. Conf., vol. 3, pp. 1189–1194, 2002.
- [5] J. Miret, M. Castilla, A. Camacho, L. Garcia de Vicuna, and J. Matas, "Control scheme for photovoltaic three-phase inverters to minimize peak currents during unbalanced grid-voltage sags," IEEE Trans. on Power Electronics, vol. 27, no. 10, pp. 4262–4271, 2012.
- [6] S. Kharitonov, D. Makarov, G. Zinoviev, D. Korobkov, A. Sidorov, "Variable frequency generation system for aircraft," IEEE Energy Conversion Congress and Exposition (ECCE)- USA: IEEE, 2014. - pp. 917-922.
- [7] G. S. Zinoviev, A. V. Sidorov, S. A. Kharitonov, "Three-phase AC voltage regulator as part of an autonomous system," Proc. of Int. Conf. on Actual problems of electronic instrument engineering (APEIE-2014), vol. 1. – pp. 762-765. doi: 10.1109/APEIE.2014.7040788
- [8] I.A. Bakhovtsev, D.V. Panfilov, "Three-phase three-level voltage source inverter construction based on quasi-Z-source cells," Proc. of 14th Int. Conf. of Young Specialists on Micro/Nanotechnologies and Electron Devices (EDM), Erlagol, Altai, 1–5 July 2013. – Novosibirsk, 2013. – pp. 322–327. – doi: 10.1109/EDM.2013.6642005.
- [9] M. P. Kazmierkowski, and L. Malesani, "Current control techniques for three-phase voltage-source PWM converters: A survey," IEEE Trans. Ind. Electron, no. 5, pp. 691–703, 1998.
- [10] Yu Zhang, Mingyong Li, and Yong Kang, "PID controller design for UPS three-phase inverters considering magnetic coupling," Energies, 2014, no. 7, pp.8036-8055 (doi:10.3390/en7128036)
- [11] Y. N. Dementyev, N. V. Kojain, A. D. Bragin, and L. S. Udut, "Control system with sinusoidal PWM three-phase inverter with a frequency scalar control of induction motor," 2015 Int. Siberian Conf. on Control and Communications (SIBCON), pp.1– 6, 2015.
- [12] Sameer Sabir, Qudrat Khan, M. Saleem, and Abdul Khaliq, "Robust voltage tracking control of three phase inverter with an output LC filter: A sliding mode approach," 13th International Conference on Emerging Technologies (ICET), pp.1–5, 2017.
- [13] M.Dai, M.N. Marwali, J.-W. Jung, and A. Keyhani, "A Three-Phase Four-Wire Inverter Control Technique for a Single Distributed Generation Unit in Island Mode," IEEE Trans. on Power Electronics, vol. 23, no. 1, January 2008, pp.322-331.
- [14] Lai Xiangdong, Zou Yunping, Quang Jianzhou, and Zhong Yanping, "Research on three-phase inverter control method with full-decoupling," 7th World Congress on Intelligent Control and Automation, pp.2377–2380, 2008.
- [15] Hyun-Sam Jung, Seung-Jun Chee, Seung-Ki Sul, Young-Jae Park, Hyun-Soo Park, and Woo-Kyu Kim, "Control of three-phase inverter for AC motor drive with small DC-link capacitor fed by single-phase AC source," IEEE Trans. on Industry Applications, vol. 50, no. 2, pp. 1074–1081, 2014.
- [16] Xin Chen, Chang-hua Zhang, Qi Huang, and Jin-song Meng, "Study on a novel control strategy of three-phase inverter under unbalanced load," 2nd IET Renewable Power Generation Conf. (RPG 2013), pp.1–4, 2013.
- [17] Samuel Oludare Bamgbose, Yonpeng Zhang, Lijun Qian, "Three-phase inverter synchronization control utilizing internal model principle," IEEE Int. Conf. on Consumer Electronics (ICCE), pp.439–442, 2015.
- [18] V.D. Yurkevich, "PWM controller design based on singular perturbation technique: A case study of buck-boost DC-DC converter," Proc. of the 18-th IFAC World Congress, Milan, Italy, pp. 9739–9744, August 28 - September 2, 2011.
- [19] V. D. Yurkevich, G. S. Zinoviev, and A. A. Gordeev, "PWM current controller design for multi-level DC-DC converter via singular perturbation technique," Proc. of Int. Conf. and Seminar of Young Specialists on Micro/Nanotechnologies and Electron Devices EDM 2011. 12-th Annual. Erlagol, Altai, pp. 390–398, June 30-July 4, 2011.
- [20] V.D. Yurkevich, "Tracking control of PWM non-affine nonlinear systems via singular perturbation approach," Proc. of 1st IFAC Conf on Modelling, Identification and Control of Nonlinear Systems (MICNON 2015), Saint Petersburg, Russia, pp. 854–859, 24-26 June 2015.
- [21] V.D. Yurkevich, "Controller Design via Time-Scale Separation Technique for a Three-Phase Four-Wire Inverter with a Split DC Bus," Proc. of 13 Int. forum on strategic technology (IFOST 2018), China, Harbin, 30 May – 1 June 2018. – Harbin : IEEE, pp. 893–897, 2018. – ISBN 978-1-5386-5073-8.

- [22] P.V. Kokotovic, H. K. Khalil, and J. O'Reilly, *Singular Perturbation Methods in Control: Analysis and Design*, Philadelphia, PA: SIAM, 1999.
- [23] Y. Zhang, D. S. Naidu, C. Cai, and Y. Zou, "Singular perturbations and time scales in control theory and applications: An overview 2002-2012," *Int. J. of Information Systems Sciences (IJISS)*, vol. 9, pp.1–36, January 2014.
- [24] A.F. Filippov, "Differential equations with discontinuous right hand sides," *Am. Math. Soc. Transl.*, vol. 42, pp. 199–231, 1964.
- [25] R.D. Middlebrook, and S. Cuk, "A general unified approach to modelling switching converter power stages," *Int. J. of Electronics*, vol. 42, no.6, pp. 521–550, 1977.
- [26] H. Sira-Ramirez, "A geometric approach to pulse-width-modulated control in nonlinear dynamical systems," *IEEE Trans. Automatic Control*, vol. 34, no. 2, pp. 184–187, 1989.



Valery D. Yurkevich is a professor in the Automation Department, Novosibirsk State Technical University. His areas of research are nonlinear control systems, digital control systems, flight control, distributed parameter control systems, robotics, switching controllers for power converters, singular perturbations in control



Gennady S. Zinoviev is a head of laboratory "Optimization of power converters", a professor in the Power Electronics Department, Novosibirsk State Technical University. His areas of research are power converters, power supply systems, multilevel voltage source inverters, controller design, current rectifiers, converters for advanced electric locomotives, power engineering.

Neural Network Load Current Observer for DC Converter

Miroslav V. Martinovich, Irina A. Belova, Vladimir A. Skolota, Ilya V. Zaev
Novosibirsk State Technical University, Novosibirsk, Russia

Abstract – A neural network load current observer is proposed for a boost DC converter with an autotransformer. The settlement relations for producing the training data are resulted, the requirements to a set of input signals of a neural network of the observer are formulated. Additional solutions are considered that ensure an increase in the accuracy and stability of the proposed observer under conditions of asymmetry of electromagnetic processes in the autotransformer. The structure of a neural network is received and its training is conducted for a specific set of converter parameters. Modeling of the observer's work as part of the converter for various loads and supply voltage has been done. The recommendations for using of proposed observer are made.

Index Terms – ANN, current observer, DC converter.

I. INTRODUCTION

IN MODERN POWER ELECTRONICS, DC voltage converters occupy a significant place, such as: in distributed and autonomous power engineering, in photovoltaics, incl. used in the aerospace industry; in consumer electronics; in AC converters with DC link. The use of precise and high-speed control systems allows, in addition to providing high dynamic characteristics of DC converters, also reduce the mass-dimensional parameters by reducing the installed capacity of the filter elements. For the operation of such control systems (in particular, adaptive and intelligent ones), as much information as possible on the current state of the system is needed, and the load current (or the resistance of the load) is one of such parameters; the presence of load current in the system increases its controllability.

At the same time, such sensors worsen some characteristics of the converter: the cost increases (which is especially important in consumer electronics), there are time costs for the digitization process on the ADC (which worsens the synchronization of measurements with the conversion clock cycles); the reliability of the system is reduced by increasing the number of components; the efficiency is reduced due to losses on the sensor.

Thus, obtaining information about the load current without the use of a physical sensor makes it possible to obtain the described advantages without the indicated drawbacks. For example, in [1], the load current observer is designed and used to control the active three-phase rectifier as part of a DC link converter; in [2], the load current observer is used in a control system in a multiplying DC converter, in [3] a nonlinear load resistance observer of an boost DC converter is proposed.

II. PROBLEM DEFINITION

To develop an observer to determine the load current of a boost DC converter with an autotransformer. Other electrical quantities are available for measurement that determine the behavior of the system within the pulse of the transformation.

III. THEORY

A. Mathematical Model of the Converter

The circuit of the converter for which the proposed observer is designed is shown in Fig. 1. The work of this converter is described in detail in [4]. We consider here the main aspects (the figures explaining the operation of the converter are taken, in particular, from [4]).

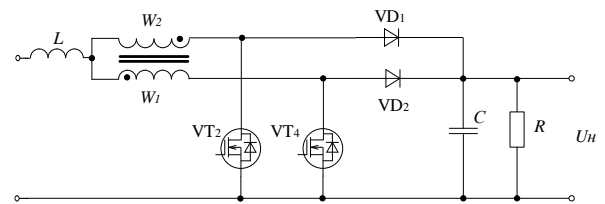


Fig. 1. Boost DC converter with autotransformer.

The operation of the converter circuit consists of four key switching zones, where each switching zone corresponds to the commutation functions k_1, k_2, k_3, k_4 , taking the values 0 and 1 (Fig. 2). The value D (pulse fill factor) determines the pulse width at the first and third clock cycles of the converter and takes values in the range from 0 to 1/2.

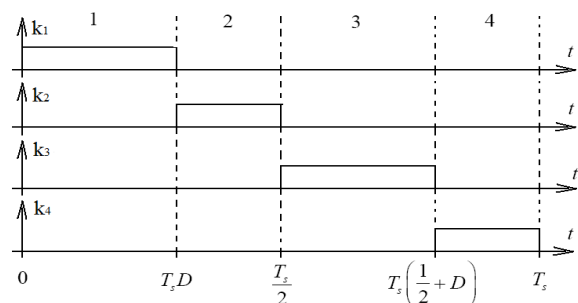


Fig. 2. The commutation functions.

The switching functions k_1, k_2 are formed at the output of the pulse width modulator (PWM) with the repetition period T_s (the switching period of the power switches VT2 and VT4), where D is the signal at the PWM input. The commutation functions k_3, k_4 repeat the commutation functions k_1, k_2 and are shifted in time with respect to them by $T_s/2$.

The substitution schemes for the converter for the first and second zones are shown in Fig. 3, for the third and fourth in Fig. 4.

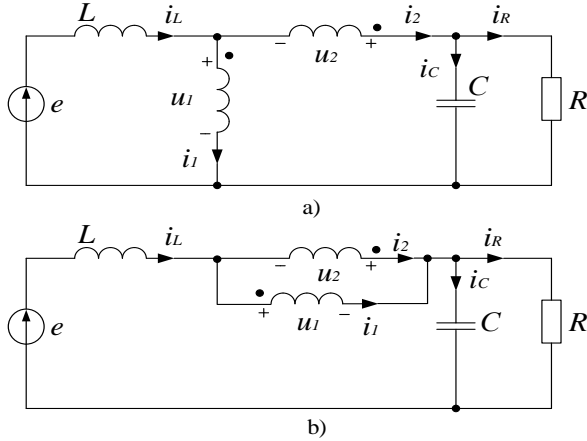


Fig. 3. Substitution schemes for (a) the first and (b) the second working zones.

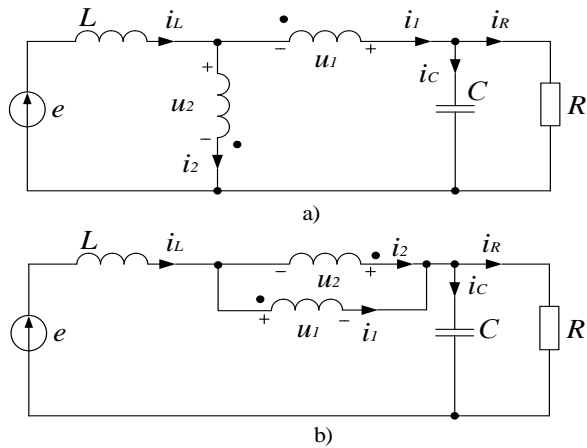


Fig. 4. Substitution schemes for (a) the third and (b) the fourth working zones.

When creating the mathematical model, the following assumptions were made: the inductor current of inductor L and the currents of transformer windings are continuous, there are no active losses in the inductor L and the capacitor C , the leakage inductance of the transformer windings is zero, the inductances of the primary and secondary windings of the transformer are equal to each other and the mutual induction coefficient $L_1=L_2=M=L_T$.

Under these assumptions, the differential equations describing the converter circuit at 1 and 3 work cycles are represented (1), and at 2 and 4 clock cycles (2).

$$\begin{cases} \frac{di_L}{dt} = \left[\frac{1}{L}e - \frac{1}{2L}u_C \right] k_1 \\ \frac{du_C}{dt} = \left[\frac{1}{2C}i_L - \frac{1}{RC}u_C \right] k_1 \end{cases} \quad (1)$$

$$\begin{cases} \frac{di_L}{dt} = \left[\frac{1}{L}e - \frac{1}{L}u_C \right] k_2 \\ \frac{du_C}{dt} = \left[\frac{1}{C}i_L - \frac{1}{RC}u_C \right] k_2 \end{cases} \quad (2)$$

From these expressions it is clear that independent physical quantities that can change during the operation of the converter, and determine its transient processes, are u_C, i_L, e, R ; knowing their instantaneous values at the beginning of the pulse of the transformation and the value of D , it is possible to calculate all the processes in the circuit during the pulse, and therefore, to control the converter most effectively. Because the current in the load i_R and R is related by Ohm's law, you can use i_R in this list instead of R , which can be more convenient in a practical sense.

In the steady state, (3) is satisfied for the average values of the currents and voltages, which, as we see, coincides with the analogous expressions for the boost converter. Also note that since $0 < D < 0.5$, then the coefficient of increase of this converter lies in the range 1...2.

$$\begin{cases} U_C = \frac{E}{1-D}, \\ I_L = \frac{U_C}{R(1-D)}. \end{cases} \quad (3)$$

B. The Principle of the Observer's Work

Consider the structure and functioning of the proposed neural network observer. In the course of the presentation, we present an increasingly complete scheme. The core of the proposed observer is the "neural network - Newton's method" bundle (Fig. 5).

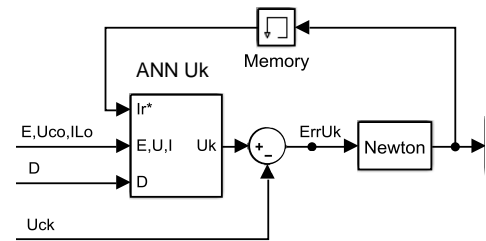


Fig. 5. Neural network observer.

At the input of the neural network «ANN Uk» five signals are fed: the current estimate of the load current I_r^* ; supply voltage E , the voltage on the capacitor $u_{C,0}$, the current in the inductor $i_{L,0}$ ($E, u_{C,0}, i_{L,0}$ are measured at the beginning of the current pulse), the duty factor D . At the output of the neural network, we get the value of the voltage at the end of the pulse ($u_{C,k}^*$) for the current estimate I_r^* .

Next, the discrepancy $ErrU_k$ is calculated between $u_{C,k}^*$ and $u_{C,k}$, which arrives at the input of the *Newton* block. If this discrepancy exceeds a certain predetermined threshold, the *Newton* block corrects the estimate I_r^* , until the discrepancy is less than this threshold (the *Memory* block ensures that the estimate I_r^* falls on the neural network input only for the next calculated clock cycle). Because the values $u_{C,0}$, $i_{L,0}$, D , $u_{C,k}$ change once per pulse, then the evaluation correction procedure for I_r^* is performed once per pulse.

Let's take a closer look at the functioning of the *Newton* block. At its output, we have the current estimate I_r . If the module of $ErrU_k$ signal exceeds a threshold, the Newton method is performed solving the equation $ErrU_k(I_r^*)=0$. In order to evaluate the derivative $d ErrU_k/d I_r^*$, the *Newton* block modifies I_r^* by a small amount ΔI_r^* the authors used the value 0.001A), the new I_r^* value is fed to the input of the neural network in the next calculation cycle, the output is $ErrU_{k+1}$ (value before this change we denote by $ErrU_{k0}$). The derivative estimate is $(ErrU_{k+1} - ErrU_{k0}) / \Delta I_r^*$. Using this estimate, the *Newton* block calculates a new I_r value, which is fed to the input of the neural network in the next calculation cycle. If the *ErrUk* module continues to exceed the threshold after this, the next iteration of the Newton method is performed. As the simulation showed, with a threshold value of $10^{-7}V$ it takes 3-4 iterations.

In order for the transient to not affect the rest of the circuit during the correction, upon completion of the correction process, the output of the *Newton* block is fixed by the block *A* on the rising edge of the signal from the *AND* block (Fig. 6).

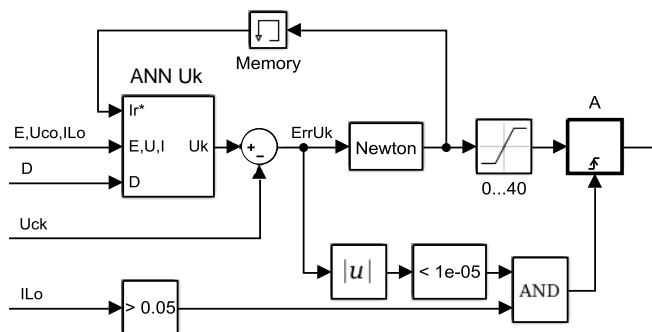


Fig. 6. Neural network observer with timing and protection against intermittent current (Observer 1).

This signal takes a value 1 when two conditions are fulfilled: first, the absolute value of the $ErrU_k$ signal is less than the threshold value (in the figure, the threshold $1e-5$ is selected), which means that the correction process is considered complete, and secondly, the value of the inductor current at the beginning of the pulse is greater than 0 (or a certain threshold value, for example, in Figure 0.05 is indicated). The last condition is due to the fact that the neural network is tuned to the continuous current mode.

The limiting block "0 ... 40" serves to limit the value of I_r^* at start-up and during transients with a step change of I_r .

One of the features of the scheme under consideration is that in the transient process, the windings of the autotransformer are loaded unequally, a magnetizing current

appears that differs from zero, and electromagnetic processes begin to differ significantly in zones 1-2 and 3-4. Because this feature was not taken into account when obtaining the final form of equations (1), (2), and the currents of the autotransformer windings are not measured in the circuit, then a component depending on the amplitude of the magnetizing current appears in the current obtained at the output of block A, and having the opposite sign in zones 1-2 and 3-4.

To take this into account, we add the calculation of the half-sum of the currents obtained during the last period of T_s , and this averaging is performed once for each $T_s/2$. Because duration 1-2 and 3-4 are equal, to calculate the average, half-sum of the currents calculated in these zones can be used (Fig. 7, block B delays one clock cycle of the signal arriving at its timing input, the adder and amplifier calculate half-sum).

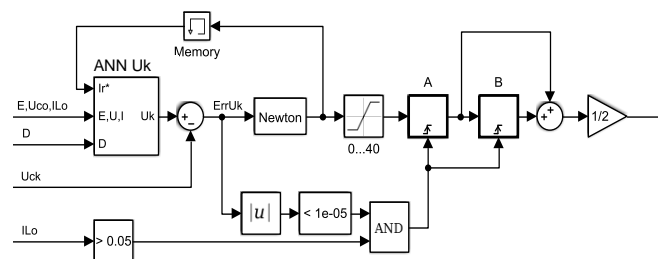


Fig. 7. Neural network observer taking into account the asymmetry of the processes in the autotransformer windings (Observer 2).

Another solution would be to take this unbalance into account at the stage of forming the equations, add to the circuit the sensor of an autotransformer current, and add appropriate inputs to the observer's neural network, which would lead to its complication and increase the time required to calculate it during converter operation.

Obviously, such a solution will lead to a delay in the calculated current in $T_s/2$ in the dynamics. To avoid this, in especially critical cases, when the load current changes abruptly, it is suggested that when the change in the calculated load current is greater than the double value of the expected magnetizing current, give the output not half the sum but the last calculated current (Fig. 8, here the modulus of difference of estimated currents is calculated on the last pulse and the previous one, and if it is above the threshold - in the figure the threshold 1 is selected, then send the last current to the output).

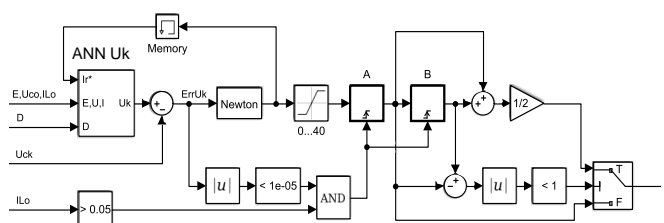


Fig. 8. Neural network observer taking into account the asymmetry of processes in the autotransformer windings and with improved dynamics (Observer 3).

The authors preferred the option with the calculation of the half-sum, which, as we shall see from the results of the experimental simulation, justified itself.

C. Principles of Operation of a Neural Network

The neural network is a direct calculation tool based on the so-called artificial neurons which organized into a network. Currently, the most commonly used type of artificial neuron is a formal neuron, described by the formula

$$y = Fa\left(\sum_{i=1}^N w_i x_i + b\right) \quad (4)$$

where

w_i, b – weights

x_i – input arguments (N - the number of input arguments of the neuron)

Fa – activation function (sigmoidal, stepwise, linear, etc.)

The generalized structure of a neural network, as a rule, contains one or several hidden layers, which are characterized by the same activation functions within the layer. Networks of direct propagation convey the results of the work of neurons in one direction, from the entrance to the exit; recurrent networks transmit information in the opposite direction, which gives the network dynamic properties.

To analyze and predict the time series at the input of the neural network, a time delay line is created, which forms the data for the time window.

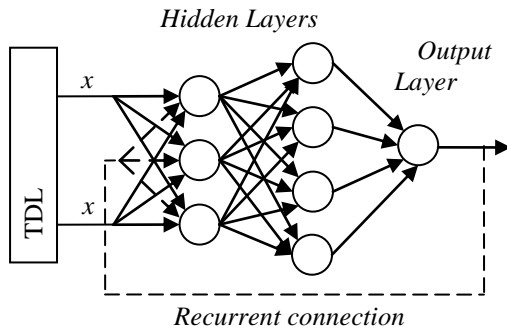


Fig. 9. Example of ANN.

To adjust the weights, a pre-prepared set of input and output data (offline training) or current input-output data (online training) is used; if it contains the desired network responses, then the training with the teacher (for approximation, classification and forecasting time series) is used, if not - then the training without a teacher (for clustering).

In this paper, a direct propagation network with no feedbacks and delay lines is used because the dynamic network properties are not used; pre-prepared data are used for training.

D. Data Preparation and Training

The data used in the training of the ANN is presented in the form of a table whose rows contain the quantities supplied to the ANN input ($u_{C,0}$, $i_{L,0}$, e_0 , I_r , D), and $u_{C,k}$ value to be obtained on its output (index 0 means that the values

were measured at the moment of the onset of the pulse of the converter, and the index k is measured at the end of the pulse).

To obtain these data, the solutions of the differential equations (1), (2) were used. D , $u_{C,0}$, $i_{L,0}$, $e_0=E$ were randomly assigned (it is unchanged on the pulse) and the average value of the load current I_r was calculated for invariable parameters of the system (C , L , T).

After that, the data was arranged in the order necessary to feed to the neural network (I_r , E , $u_{C,0}$, $i_{L,0}$, D and the desired result $u_{C,k}$).

After the preparation of the data, a neural network is constructed, input data is fed into its input, and using the Levenberg-Marquardt algorithm, we adjust the weights in order to minimize the root-mean-square difference between the desired $u_{C,k}$ value and the network operation result. If necessary, the network structure changes to increase its accuracy or reduce computational costs.

IV. EXPERIMENTAL RESULTS

To test the proposed schemes, an artificial neural network was constructed and trained (an array of ANN input and output data includes 6,000 lines, it was prepared in advance). Network structure: a fully connected network of direct propagation; input layer of 5 neurons, according to the number of input data ($u_{C,0}$, $i_{L,0}$, e_0 , I_r , D); a hidden layer of 20 neurons with the activation function tansig (5); output layer of 1 neuron with linear activation function ($u_{C,k}$).

$$\text{tansig}(x) = \frac{2}{1 + \exp(-2x)} - 1 \quad (5)$$

The modeling of the converter with the following parameters (L1, L2 - inductance of the autotransformer windings) was performed:

TABLE I
PARAMETERS OF THE SCHEME

| | |
|--------|-----------------|
| L | 100 mH |
| C | 30 mF |
| L1, L2 | 0.1 mH |
| R | 13.33...200 Ohm |
| E | 55-95 V |
| Uc.nom | 100 V |

The output signals of the observers were compared with the value of the average load current calculated for the previous pulse, which provides a comparison with a physically feasible meter providing an almost maximum measurement speed. Thus, the questions related to the errors caused by the failure of the process of measuring the current for a time comparable to the pulse, and questions of compensation for these errors are beyond the framework of the article.

Below are diagrams of two transient processes obtained by modeling the converter supplied 55V voltage sources (Fig. 10) and 95 V (Fig. 11). Transients are divided into zones: A -

start, B - intermittent or missing inductor current (in this zone the observer does not work and saves the last calculated value), C - step change in load, D, F - smooth load change, E - rated load, G is the minimum load.

The control system tends to stabilize the load voltage at the level of 100V, but for the convenience of presenting results during the transient process, the steady state is not achieved at any zone.

We see that Observer 1 (b), as indicated in Section III, forms an output with pulsations correlated in magnitude with magnetizing current of the autotransformer (g), where the average deviation from the measured value of the load current (e) is very close to 0. Output of Observer 2 (c) is devoid of these pulsations, but lags behind with a step change in the load.

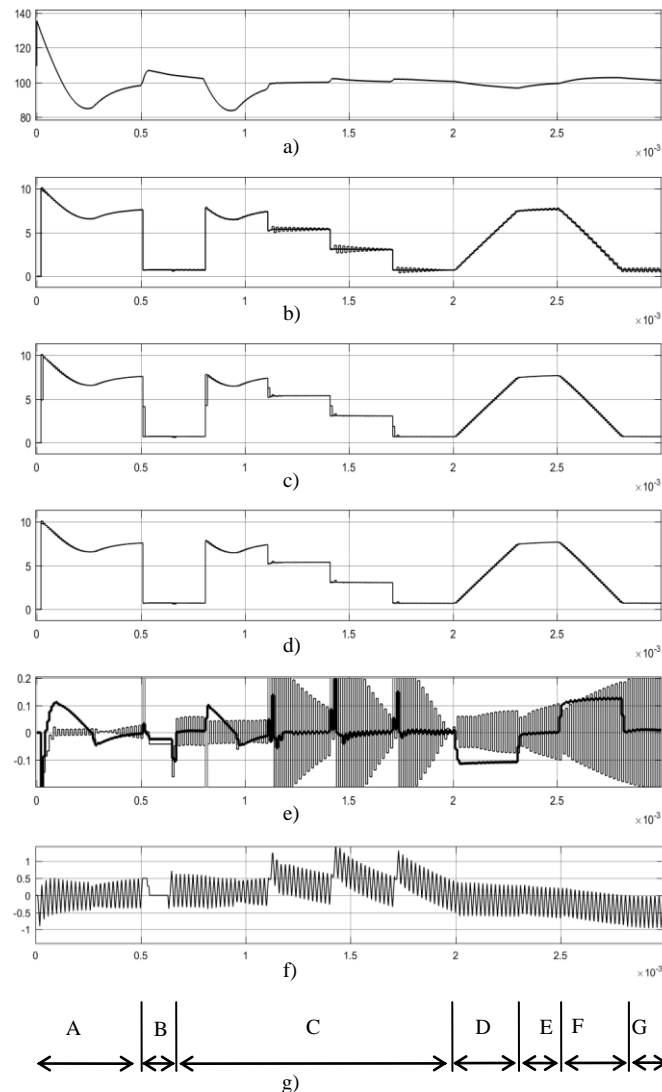


Fig. 10 Simulation at $E = 55$ V (a – u_C b – i_r and Observer 1, c – i_r and Observer 2, d – i_r and Observer 3, e – error of Observer 1 (gray) and error of Observer 3 (black), f – autotransformer magnetizing current, g - transition zones).

As you can see, in all modes (except for the pulses immediately following the step change in the load), the accuracy of the Observer 3 is no worse than 0.12A, and near the steady state is not worse than 0.01A.

Note that this accuracy is achieved, in particular, with a significant deviation of the load voltage from the nominal value (up to 135 V, zone A) and significant dynamics of this voltage ($\approx 300V / msec$, zone A), with the load current dynamics up to $4.2A / msec$ (zones D and F).

All observers are inoperative in the mode of intermittent inductor current of converter and in absence of this current (zone B), because the neural network is configured for continuous current mode.

Thus, the proposed scheme of the Observer 3 can be recommended for systems operating in the continuous current mode with step change of load.

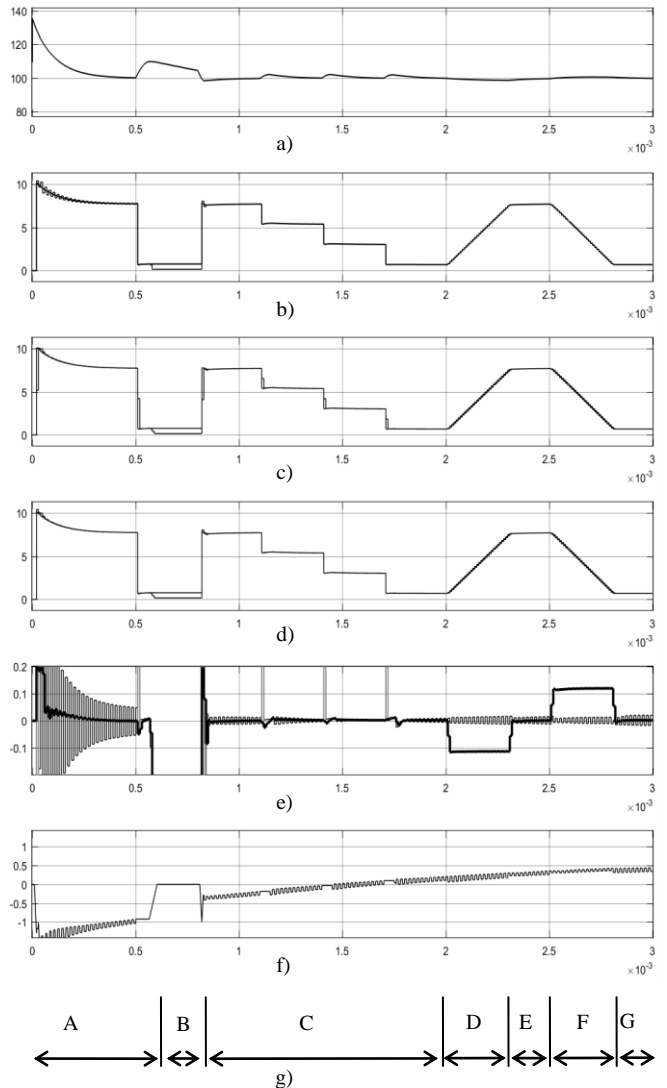


Fig. 11 Simulation at $E = 95$ V (a – u_C b – i_r and Observer 1, c – i_r and Observer 2, d – i_r and Observer 3, e – error of Observer 1 (gray) and error of Observer 3 (black), f – autotransformer magnetizing current, g - transition zones).

V. DISCUSSION OF RESULTS

As can be seen from the results of the simulation, the load current calculated by the proposed observer quite accurately reproduces the measured load current, without requiring a

procedure of numerical integration and measurement of additional current counts during the pulse.

In addition, the proposed observer, it seems to us, can be used to estimate the magnetization current, and, as a consequence, to correct the asymmetry of processes in the autotransformer winding

It can also be suggested to extend the application of the proposed approach by constructing an observer for the intermittent current mode.

VI. CONCLUSION

The load current observer is considered for the boost DC converter with an autotransformer, taking into account additional solutions ensuring an increase in the accuracy and stability of the observer's work in conditions of asymmetry of electromagnetic processes in the autotransformer. The proposed method for creating and tuning an artificial neural network has been tested and confirmed its efficiency. Modeling confirmed the theoretically suggested solutions. The proposed observer can be recommended for systems operating in the continuous current mode with a step change in load.

REFERENCES

- [1] Load current observer based feed-forward DC bus voltage control for active rectifiers, Z. Zhoua, C. Wanga, Y. Liub, P.M. Hollanda, P. Igic // Electric Power Systems Research, 2012, V. 84, pp.165– 173
- [2] On the Output Current Estimation of a DC-DC Multiplier Converter, J. C. Mayo-Maldonado, R. Salas-Cabrera, J. de-Leon-Morales, E. N. Salas-Cabrera, R. Castillo-Gutierrez, J. E. Martinez-Bernal, D. Soto-Monterrubio // Proceedings of the World Congress on Engineering and Computer Science 2011 Vol I, WCECS 2011, October 19-21, 2011, San Francisco, USA. pp.162–165
- [3] Milad Malekzadeh, Alireza Khosravi, Mehdi Tavan, "Observer based control scheme for DC-DC boost converter using sigma-delta modulator", COMPEL - The international journal for computation and mathematics in electrical and electronic engineering, <https://doi.org/10.1108/COMPEL-02-2017-0102>
- [4] Control system design of a battery discharge unit for space applications, V. D. Yurkevich, D. V. Makarov, D. V. Korobkov, S. A. Kharitonov, // IECON 2017 - 43rd Annual Conference of the IEEE Industrial Electronics Society, 2017, pp. 177–184.



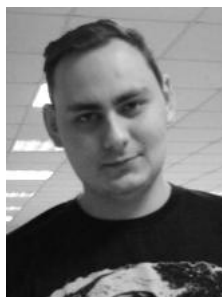
Miroslav V. Martinovich, PhD, ass.prof. NSTU.
martinovich_m@mail.ru



Irina A. Belova was born in Novosibirsk region, in 1991. Received Master's degree from the Novosibirsk State Technical University in 2015. Since 2015, a postgraduate student of the Department of Electronics and Electrical Engineering.



Vladimir A. Skolota was born in Novosibirsk region, in 1989. Received Master's degree from the Novosibirsk State Technical University in 2015. Since 2015, a postgraduate student of the Department of Electronics and Electrical Engineering.



Ilya V. Zaev – post-graduate student at Novosibirsk State Technical University. Interested at power engineering, resonant converters, neural networks. Email: rollproduce@gmail.com.

The Rule of Electric Drive Multi Criteria Optimization Solutions Choice

Yuriy P. Filyushov¹, Gennadiy M. Simakov², Boris V. Palagushkin³

¹Federal State Unitary Enterprise Production Association "Sever", Novosibirsk, Russia

²Novosibirsk State Technical University, Novosibirsk, Russia

³Siberian State University of Water Transport, Novosibirsk, Russia

Abstract – Effective control of the electric machine should provide the best combination of dynamic and energy properties of the electric drive in the conditions of existing restrictions. These properties are contradictory, causing a complex (multicriteria) approach to the synthesis of control. An integrated approach to synthesis requires formalization of the control problem. The article deals with the rule of choosing solutions of multicriteria optimization, on the basis of which the problem of effective control of an alternating current electric drive is formalized.

Index Terms – AC electric drive, generalized electric machine, the connection of the main properties of the electric machine by means of quality indicators, multi-criteria synthesis of control.

I. INTRODUCTION

THE HIGH - SPEED electric drive has reached a high level of perfection, providing high dynamic properties, satisfying a wide variety of technological tasks. At the same time, being an energy power plant, the electric drive should respond not only to dynamic, but also to energy requirements, taking into account the existing limitations [1].

Requirements to the electric drive [2] are due to increase the productivity of technological processes and to minimize energy losses.

II. PROBLEM DEFINITION

To solve the problem of effective control, it is necessary to compare the main properties of the electric drive, taking into account the reactive power, the loss in steel, copper losses, saturation of the magnetic system, the instantaneous power of the magnetic field during the formation of the electromagnetic moment, the efficiency of using voltage and power supplied to the motor windings.

These properties have contradictory character that complicates the solution of a problem of effective management [3], which providing the best combination of dynamic and power properties of the electric drive which is reached at the fullest use of the electric drive and a power supply. This control depends on several parameters of quality [4], which means a multi-criteria approach to motor control synthesis. Effective control should provide the best combination of dynamic and energy properties of the electric drive.

The choice of certain properties is determined by technological requirements. The difficulty lies in the fact that

no rule has been developed (optimality principle) that would allow us to answer the question, what solution is better for the implementation of the requirements imposed on the electric drive [5]. It is necessary to know the arguments that determine the control law, and establish a list of quality indicators that characterize the dynamic and power properties of the electric drive, depending on the taken arguments. By setting one quality criterion, restricting the field of admissible controls, it is necessary to define other local criteria whose indices under these conditions have the best value. Therefore, the solution of the problem of a multi-criterial approach to the synthesis of electric drive control [6], which provides the best combination of dynamic and power properties of the electric drive, requires its solution within the limits set by the constraints.

III. RELATION OF POWER AND ENERGY CHARACTERISTICS OF THE ELECTRICAL MACHINE

Consider the solutions selection rule making multi-criterial optimization of the drive operation, which provides the best combination of power and dynamic properties of the drive in specified limitations. The generalized electric machine is examined as an energy converter. The voltage vector U (1) determines the control of the electric machine:

$$U = RI + \omega D\Psi + \frac{d\Psi}{dt}; U = [u_d \quad u_q \quad u_{rd} \quad u_{rq}]^T; (1)$$

$$\Psi = [\psi_d \quad \psi_q \quad \psi_{rd} \quad \psi_{rq}]^T; R = \text{diag}\{R_s \quad R_s \quad R_r \quad R_r\};$$

$$I = L^{-1}\Psi; L_s = L_m + L_{\sigma}; L_r = L_m + L_{\sigma r};$$

$$L_m = \frac{\Psi_0}{I_0};$$

$$I_0 = \sqrt{(i_d + i_{rd})^2 + (i_q + i_{rq})^2}; \Psi_0 = \sqrt{(\Psi_d - L_{\sigma} i_d)^2 + (\Psi_q - L_{\sigma} i_q)^2},$$

D - rotation matrix; L - inductance matrix; L_{σ} , $L_{\sigma r}$ - inductance dissipation of stator and rotor windings; L_s , L_r - full inductances of stator and rotor windings; L_m - mutual inductance of stator and rotor windings, which determines instantaneous ratio of flux linkage in the air gap Ψ_0 to the magnetizing current I_0 . For a generalized electric machine,

the linkage of the flux linkage in the air gap and the magnetizing current has a linear relationship. The study is based on the mathematical model (1) represented by the Kirchhoff equations in the coordinate system d, q rotating with the rotor speed ω , oriented along the rotor current, $i_{rq}=0$, $i_{rd}=i_r$. To analyze the relationships of power and energy characteristics of [7], which are the electromagnetic torque, magnetic field energy, heat losses and the voltage applied to the windings of the electrical machine, the processes of electromechanical energy conversion are considered. These processes are inseparable linked with the accumulation of energy w in the motor windings (the energy of the magnetic field) and are described by the equation of the power balance P (2) of all control circuits.

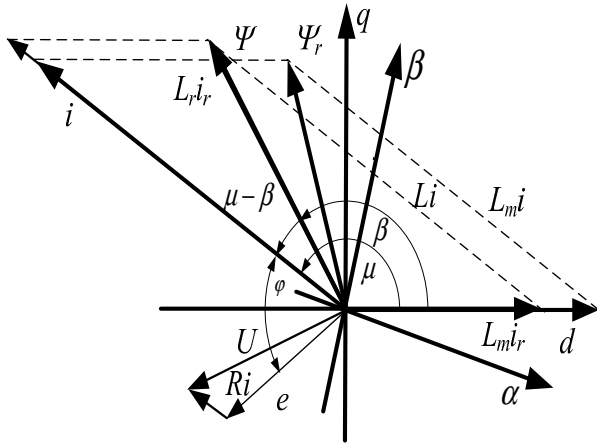


Fig. 1. Vector diagram of the operation of a generalized electrical machine.

From the presented equation follows, the state of the electric machine depends on four independent variables [8]. As independent variables can act: electromagnetic torque m , ω – rotor rotation velocity, β , ϕ – two arguments presented on Figure 1, which is sufficient to determine the position of all vectors. Among the above variables, m and ω are given conditions of technological task. Variables are arguments β , ϕ by which search is performed relations of basic properties drive operation.

$$P = \mathbf{I}^T \mathbf{R} \mathbf{I} + \omega \mathbf{I}^T \mathbf{D} \Psi + \mathbf{I}^T \frac{d\Psi}{dt} = \Delta P + \omega m + \frac{dw}{dt}; \quad (2)$$

$$w = \frac{1}{2} \Psi^T \mathbf{I}; \quad f(\phi, \beta) = \frac{2w}{m};$$

$$f(\beta, \phi) = \frac{1}{(\text{ctg } \beta + \text{tg } \phi)} \times \left(\frac{1}{\cos^2 \phi} + \frac{L_r L_s}{L_m^2 \sin^2 \beta} - 2 + 2 \text{tg } \phi \text{ ctg } \beta \right); \quad (3)$$

$$F(\phi, \beta) = \frac{\Delta P}{m};$$

$$F(\beta, \phi) = \frac{1}{(\text{ctg } \beta + \text{tg } \phi)} \times \left(\frac{R_s}{L \cos^2 \phi} + \frac{R_r}{L_m^2} \frac{L_s}{\sin^2 \beta} \right); \quad (4)$$

$$f_{\min} = \frac{2\sqrt{L_r L_s - L_m^2}}{L_m}; \quad (5)$$

$$\beta = \frac{\pi}{2}; \quad \phi = \arcsin \sqrt{\frac{L_r L_s - L_m^2}{L_r L_s}}$$

$$F_{\min} = \frac{2\sqrt{R_r R_s}}{L_m};$$

$$\phi = \beta = \arcsin \left(L_s \sqrt{\frac{R_r}{R_r L_s^2 + R_s L_m^2}} \right). \quad (6)$$

The connections of the power and energy characteristics of the electric machine are represented in the form of two functions of the energy state [9]. The surfaces of the values of the functions in the linear part of the magnetization characteristic are reflected in the Figure 2.

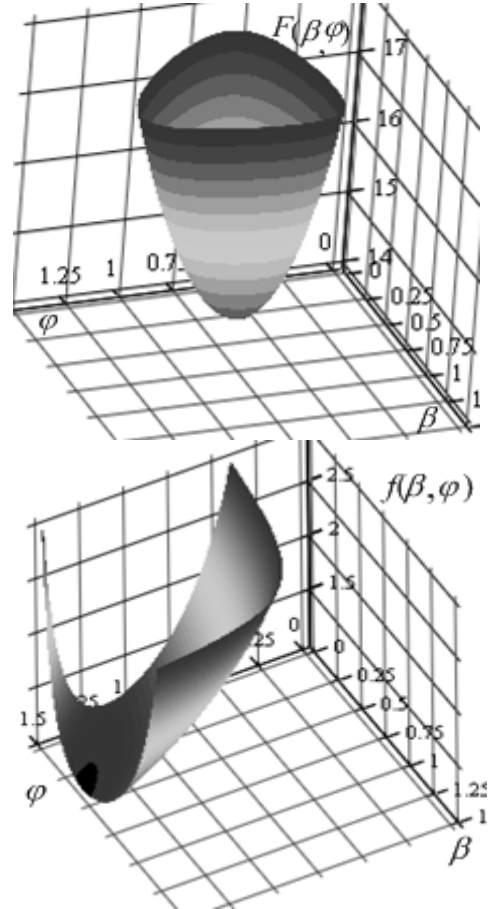


Fig. 2. The surfaces of the values of the first $f(\phi, \beta)$ and the second $F(\phi, \beta)$ functions of the energy state of the electric machine.

The first function of the energy state $f(\varphi, \beta)$ determines the relationship between the energy w accumulated in the windings of the electric machine and the electromagnetic moment (3), has no dimension.

The relationship between the heat losses and the electromagnetic moment m is represented as the second function (4) of the energy state $F(\varphi, \beta)$ [c-1]. The losses in steel are taken into account in tabular form. Studies show that surface values of each function has a minimum f_{min}, F_{min} , which is dependent upon the design of the electrical machine and is achieved at a certain position vectors [10]. Minimum of $f(\varphi, \beta)$ is achieved by some arguments β, φ (5). Minimum $F(\varphi, \beta)$ is achieved when arguments determines by equation (6). The established connections of power and energy characteristics of the electric machine allow interpreting the received results on other types of electric machines, considering losses in steel and saturation of a magnetic system of the engine.

IV. RELATIONS STRUCTURING OF BASIC PROPERTIES OF ELECTRIC DRIVE

Increasing the speed of the system by boosting control, the voltage and power applied to the motor windings are increased, which determines the increase in the intensity of energy conversion processes. Consider conditions of the electrical machine changes state in the minimum time while limiting the power supplied to the motor windings [11], considering the power balance equation (2) as the coupling equation (7):

$$\frac{dw}{dt} = -2w \frac{\omega + F(\beta, \varphi)}{f(\beta, \varphi)} + P_{ref}; \quad (7)$$

$$T_\delta = \frac{f(\beta, \varphi)}{\omega + F(\beta, \varphi)}; \quad (8)$$

$$\eta = \frac{m\omega}{m\omega + \Delta P} = \frac{\omega}{\omega + F(\beta, \varphi)};$$

$$T_\delta = \frac{f(\beta, \varphi)}{\omega} \eta [s]. \quad (9)$$

The time parameter T_δ , characterizing the rate of electromechanical energy conversion, can act as an indicator of the performance of the electric drive (8). It depends on the functions of the energy state $F(\varphi, \beta)$, $f(\varphi, \beta)$ and angular velocity of rotation of the rotor ω . The position of the vectors for which the function $f(\varphi, \beta)$ has a minimum value determines the condition for the highest intensity of energy conversion processes under power limitation. In these conditions, losses in the electric drive increase, which required establishing the dependence (9) of the energy

efficiency index η to the intensity index of the energy conversion processes T_δ . The desired ratio of the energy and dynamic properties of the electric drive (9) can be realized only at a sufficient value of the voltage, the value of which is always limited. Therefore, the evaluation of the properties will be incomplete without estimating the magnitude and efficiency of using the voltage u supplied to the motor windings. For this purpose, the third function (9) of the energy state $f_u(\varphi, \beta)$, is introduced, which establishes the relationship between the stator voltage modulus and the electromagnetic moment. Taking symbol $T_s = L_s/R_s$, the third energy state function $f_u(\varphi, \beta)$ is recorded by the equation (10):

$$f_u(\beta, \varphi) = \frac{u^2}{R_s m}, \quad u = \sqrt{u_d^2 + u_q^2}; \quad (9)$$

$$f_u(\beta, \varphi) = \frac{\text{tg } \varphi^2 + [1 + \omega T_s (\text{ctg } \beta + \text{tg } \varphi)]^2}{T_s (\text{ctg } \beta + \text{tg } \varphi)} [s]; \quad (10)$$

$$U_o = \frac{U_{min}}{U} = 2 \sqrt{\frac{\omega}{f_u(\beta, \varphi)}};$$

$$U_{min} = 2 \sqrt{R_s \omega m}. \quad (11)$$

The surface of the values of the function $f_u(\varphi, \beta)$ is shown in Figure 3. At a given rotor rotation speed, the arguments of the function $f_u(\varphi, \beta)$ can characterize the magnitude of the required voltage.

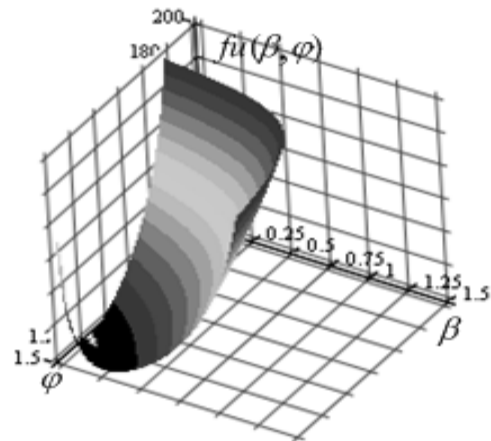


Fig. 3. The third function of the energy state, characterizing the relationship between the electromagnetic moment and the voltage applied to the motor windings.

To evaluate the efficiency of using the voltage U_o , the ratio U_{min} to the value of the voltage U required to implement a particular control method is selected (11), where U_{min} is the value of the minimum voltage required for transmission to the actuator of a given power at a fixed speed ω .

The combination of the arguments φ, β of functions (3-4) and (10) determines the basic properties of the electric machine, which are characterized by quality indicators.

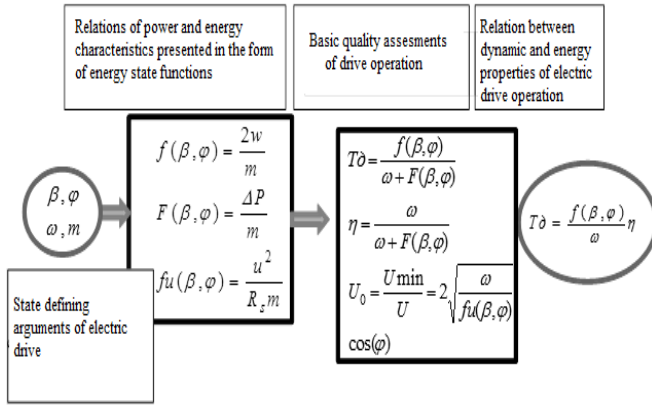


Fig. 4. Relations of indicators of the basic properties of the electric machine.

Arguments φ, β can act as a reference of the basic properties of the electric drive in the organization of the multidimensional control. Figure 4 shows a block diagram of the relations of the main properties of the electric drive from the arguments that determine the position of the vectors in the rotating coordinate system. The quality indicators are:

- coefficient of efficiency;
- an indicator of the intensity of energy conversion processes;
- efficiency indicator of voltage use;
- efficiency indicator of power use.

V. THE SOLUTION OF MULTI-CRITERIA OPTIMIZATION OF THE ELECTRIC DRIVE

Depending on the purpose and nature of the technological task, the established list of interrelated indicators of dynamic and energy quality properties makes it possible to make a rule of selecting solutions for multi-criteria optimization of the operation of the electric drive.

By setting one indicator, it is always possible to determine the arguments under which other quality indicators have the best value. Consider applying this rule to the following example. Let the time t_{ref} be set, during which it is necessary to form linearly the electromagnetic moment m_{ref} under the power limitation P_{ref} applied to the motor windings. The rotor speed is zero. Under these conditions, it is necessary to determine the arguments β, φ , at which the losses ΔP_{min} are minimal. For this purpose, the dimensionless value of the first function of the energy state $f(\beta, \varphi)$ is determined:

$$\frac{dw}{dt} = P_{ref} = \frac{f(\beta, \varphi)}{2} \frac{dm}{dt}; \quad f(\beta, \varphi) = \frac{P_{ref}}{2} \frac{t_{ref}}{m_{ref}};$$

$$\beta = f(\varphi); \quad \Delta P_{min} = F(\beta) M_{ref}. \quad (12)$$

The found value of the function $f(\beta, \varphi)$ allows to determine the relationship between the arguments φ, β in the range of values where the conditions of a given speed are fulfilled. In this area, it is necessary to determine those values of the arguments for which the second function $F(\beta, \varphi)$ has a minimum value. Substituting the obtained connection of the

arguments in (4), the second function of the energy state $F(\beta)$ is represented depending on one argument. The minimum of the function $F(\beta)$, shown in Fig. 5, determines the values of the arguments at which the minimum of heat losses is reached under the conditions of a given speed. For arguments that deliver the best ratio of the dynamic and energy properties of the electric drive, it is necessary to check the solution for compliance with other quality requirements (8 - 11) for different rotor speed, their indicators are presented in a structured form in Figure 4. In case of non-compliance (voltage or efficiency of power usage), speed should be reduced or, in conditions of speed limitation, increase losses by determining new values of the arguments.

The method of formalizing the management requirements ensuring the efficient use of an electrical machine and a power source for the implementation of the management goal is proposed based on the developed rule for multicriteria optimization.

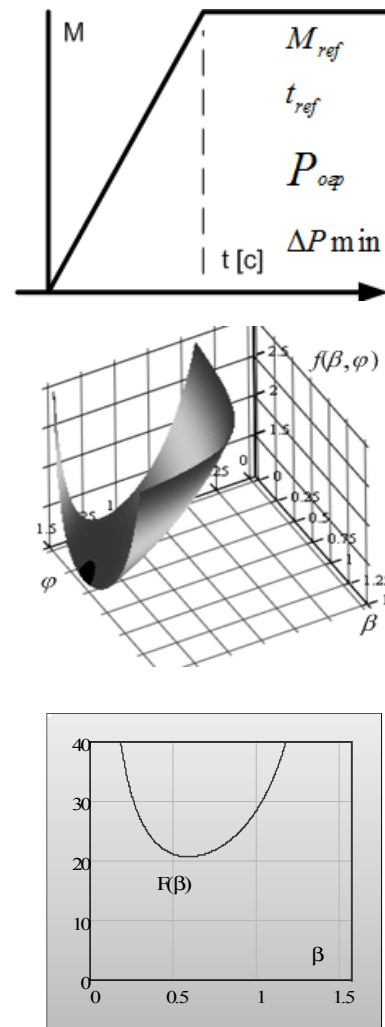


Fig. 5. An example of selecting multi-criteria optimization solutions.

VI. CONCLUSIONS

The task of solutions choosing for multicriteria optimization of an electric drive is an essential part of the developed concept of an integrated approach to the synthesis of multi-dimensional control of an electric drive of various types.

In accordance with technological requirements, formalization of the management task is carried out. The change of the arguments in the velocity or load functions is determined. Synthesis of multidimensional control of the electric drive, along with the formation of the electromagnetic torque allows regulate the energy properties of the electric drive. The concept includes the consideration by variational [12] methods of the conditions for changing the state of an electric machine in a minimum time [13], while limiting the bandwidth of the regulated variables. The standard behavior of the output values is achieved by inverse model design with output linearization [14]. The novelty and priority of control, the formalization of which was carried out on the basis of the developed rule, is confirmed by the patent for invention No. 2092967 of the Russian Federation, No. 02 P 21/00. This idea is based on the methodology for synthesizing multidimensional control of electric machines (synchronous machines with electromagnetic excitation, salient and non-salient synchronous machines with excitation from permanent magnets and asynchronous machines with squirrel cage rotor) of a high-speed electric drive. Without pre-magnetizing the magnetic system of the engine, improving the integral evaluation of the efficiency during the transient process by 6 to 8%, this control expands the consumer properties of the AC drive [15-16]. The area of application of control algorithms based on the developed concept can be metallurgical electric drives, metalworking industry, electric drive of railway transport, where the technological processes require high dynamic and energy demands under conditions of a significant change in the load.

REFERENCES

- [1] Ilyinskii N. F., Sarabato R. S. Scientific and technical aspects of increasing the efficiency of energy use in a mass electric drive. Automated electric drive / Under the general editorship of Ilyinskii N. F., Yunkova M. G. – M.: Energoatomizdat, 1986. – 448p.
- [2] Shubenko, V.A. Optimization of a frequency-controlled asynchronous electric drive over a minimum of current / Shubenko, V.A. Shreiner R.T., Mishenko V.A. // Electricity – 1970. – № 9. – pp. 23 – 26.
- [3] Filyushov Yu. P. The method of optimal synthesis of control actions of an alternating current machine /Electrotenika. 2012.№8.pp.28 – 34.
- [4] White, D., Woodson G. Electromechanical energy conversion. – M.: Energiya, 1964. – 527 p.
- [5] Shreiner R. T. Optimum frequency control of asynchronous electric drives / Shreiner R.T., Dmitrienko Yu.A. – Kishinev. 1982. – 224 p
- [6] Polakov, V. N. Extreme control of electric motors / Polakov V.N., Shreiner R.T.– Ekaterinburg: UGTU – UPI, 2006. – 420 p.
- [7] Polakov, V. N. Energy-efficient modes of regulated electric drives: torate thesis: 05.09.03 / Polakov, V. N. – Ekaterinburg. 2009 – 495 p.
- [8] Filyushov Yu. P. Synthesis of synchronous motor control structures in the system of the physical variables, ensuring a minimum reactive losses / Filyushov Yu. P. // Proceedings of the All - Russian Scientific and Technical Conference on Enhancing the Efficiency of Energy Production and Use in the Conditions of Siberia. – Irkutsk, 1994. – pp. 5 – 7.
- [9] Simakov G.M. Energy efficient management. Investigation of energy-efficient management of a high-speed asynchronous electric drive / Simakov G.M., Filyushov Yu.P., Filyushov V.Yu. // The Ninth International Conference on Automated Electric Drive AED 2016 – Perm, 2016. pp. 152 – 168.
- [10] Filyushov Yu. P. Optimization of electromagnetic processes an asynchronous squirrel cage machine // Electricity. 2011, № 5. pp 42-47.
- [11] Alekseev V.M. Optimal control. / Alekseev V.M., Tihomirov V.M., Fomin S.V. – M.: Nauka. General edition of physical and mathematical literature, 1979. – 430 p.
- [12] Voevoda A.A. Synthesis of the algorithm for controlling a multichannel object / Voevoda A. A., Filyushov Yu.P.//Bulletin RSREU. 2017.– №61.– pp.88– 95/
- [13] Filyushov V.Yu. Output linearization of three channel nonlinear object / Filyushov V.Yu. // Scientific bulletin of NSTU. – 2017. – chp. 66. – №1 – pp. 43 – 49.
- [14] Filyushov Yu.P. Optimizaion of electromagnetic processes in synchronous machine // Electricity. – 2011.– № 8.– pp. 57 – 62.
- [15] Filyushov Yu.P. Control of an asynchronous machine in conditions of minimum reactive power // Electrical engineering. – 2014. – № 2. – pp. 15 – 20.



Simakov Genadiy Mikhailovich
Novosibirsk State Technical University.
Doctor of Technical Sciences, professor of
department of [Electric Drive and
Automation of Industrial Units](#).
630073, Novosibirsk, pr. Karla Marksa, 20
E-mail: simskov44_86@mail.ru



Palaguchkin Boris Vladimirovich
Siberian State University of Water
Transport. Doctor of Technical Sciences,
professor. 630099, Novosibirsk region,
Novosibirsk, St. Schetinkina, 33
E-mail: info@nsawt.ru



Filyushov Yuriy Petrovich
Federal State Unitary Enterprise Production
Association «Sever». PhD in Technical
Sciences, Senior Engineer. Obyedineniy 3,
Novosibirsk, 630092, Russian Federation
E-mail: [filyushov@mail.ru](#)

Improvement of Controllable Zone-Phase Regulated Rectifiers by Structural Synthesis Methods Means

Vladlen V. Ivanov, Sergey V. Myatezh, Andrei V. Kapustin, Irina K. Alekseeva
Novosibirsk State Technical University, Novosibirsk, Russia

Abstract – The simple methods of structural synthesis are adapted for controllable zone-phase regulated rectifiers and illustrated by examples of single-phase and three-phase rectifiers circuits gaining. Capabilities of this method are demonstrated in case of zone-phase rectifiers circuit transformation from single phase circuits to three phase circuits. Also the directed search of further circuits development is carried out.

Index Terms – Structural synthesis, zone-phase rectifying.

I. INTRODUCTION

STRUCTURAL SYNTHESIS task formalization is complicated by power semiconductor devices volt-ampere characteristics non-linearity and necessarily of large amount possible semiconductors combinations accounting. That is the reason why most common rectifiers were invented by heuristic way [1-2]. At the same time, the objective of rectifiers with high power factor (χ) and efficiency (η) values creation and improvement objectives remain unresolved.

II. THE PROBLEM FORMULATION

The article set the goal to develop controllable three-phase rectifiers with zone-phase regulation using the methods of controllable and uncontrollable single-phase rectifiers structural synthesis [2].

III. THEORY

The greatest difficulty in controllable alternating current rectifiers with high power indicators invention is power factor χ and U_d regulating semiconductors opening angle α dependence.

The efforts to increase the value χ have caused to set up a special class of the controlled zone-phase of single-phase alternating current rectifiers.

Advantages of four-zone single-phase rectifier (curve 1) over common controllable rectifier (curve 2) in $\chi(U_d)$ dependance are demonstrated on Fig. 1.

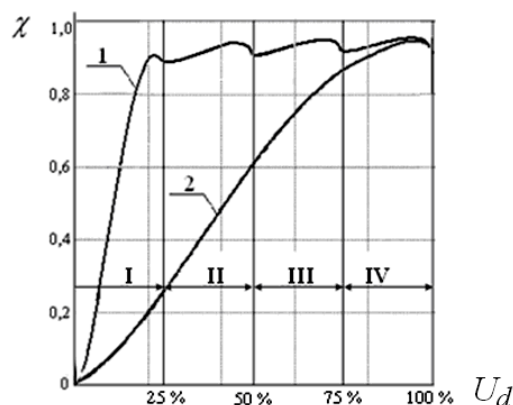


Fig. 1. Power factor and rectified voltage value dependence for single-phase alternating current controllable rectifiers.

However, known zone-phase rectifiers have their own disadvantages which don't allow the values χ and η to reach their own theoretical maximum, decreasing, in practice, these performance indicators by 10 – 15%.

The Structural synthesis method for alternating current rectifiers helps find ways to eliminate circuits disadvantages.

IV. IMPROVEMENT OF SINGLE-PHASE RECTIFIERS WITH ZONE-PHASE REGULATION BY STRUCTURAL SYNTHESIS METHOD

The synthesis method peculiarity of single-phase alternating current rectifier will be resulted rectified voltage that should be considered as maximum electric potential difference on topographic potential plane containing time base sweep of voltage represented in form of a vector diagram. In this case all accessible voltage vectors to be modified due to the single system peculiarity background will appear to be collinear.

With the aim of formalization of this method it is necessary to create generally accepted assumptions of elements' ideality used in rectifier setting up: PSD is immediately commutated becoming an ideal key without any losses available, transformer winding has no resistance and leakage inductance and so forth.

It is accepted, for synthesis convenience, that the magnitude of voltage vector corresponds to the produced by them secondary transformer winding and reflects their peak value.

Non-operational interval is illustrated by the dot line.

To achieve high value of rectifiers energy indicators it is necessary to involve transformers secondary windings in both positive and negative half-periods.

As a rule for each winding end to be connected with two powered PSDs divergently where no connection ends can create appropriate, from practical point of view, potential difference of constant signs on topographic potential plane (Fig. 2, a).

The projection on $\theta\varphi$ characterizes instant values of rectified voltage which helps us to get both the rectified voltage curve (Fig. 2, b) and the basic circuitry of the rectifier (Fig. 2, c).

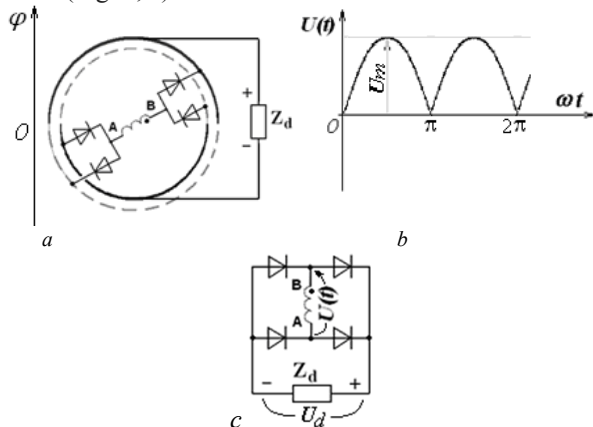


Fig. 2. Single phase full-wave rectifier: a – simplified topology, b – rectified voltage curve, c – electric circuit.

This is the way how the one-phase rectifier circuit as known as the Grets-Pollack circuit was deduced. One-phase bridge rectifier built on thyristors will have capability to change output voltage level by means of phase regulation method (Fig. 3)

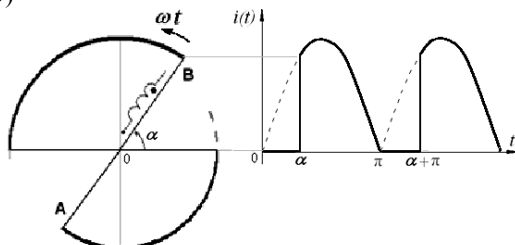


Fig. 3. Wave diagram construction of controllable zone rectifier with phase regulation output current.

Applying a signal opening towards PSD with the delayed-action at angle α , we are getting a picture of accessible potentials of a projection of diagonal maximum difference of which is time-base swept and will give a typical oscillogram of voltage output (or current, in case of active load) half-period average value of which is regulated by value change of α .

To provide U_d value regulation capability and acceptable χ values (as on Fig. 1) combination of amplitude and phase methods by way of secondary windings connection through semiconductors is used in practice. This is way how single-phase zone-phase rectifiers were invented.

It is sufficient to combine two or more bridge rectifiers to build a simple zone-phase regulator. Using aggregation as

the most common approach in the structural synthesis method given at Figure 4, a two stage single-phase rectifier was produced and in assumption of availability of active load shows the curves: 1 – of first step (zone/stage) and 2 – second step (zone/stage) of rectified voltage (or current).

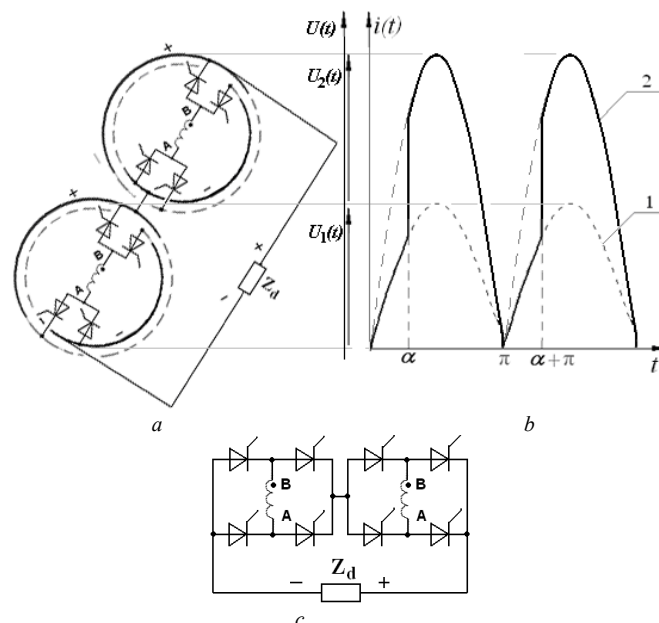


Fig. 4. Single-phase two-zone rectifier: a – simplified two bridge rectifiers serial connection topology; b – rectified voltage curves; c – principle electric circuit.

This is how single-phase rectifier with zone-phase regulation (Fig. 4, c), as known as Ogier scheme, was deduced [3]. Main disadvantage of this circuit is doubled number of serial connected semiconductor devices on the way of rectified current flow.

It doubles the capacity losses, decreases η value and restricts practical application.

To decrease capacity losses a number of PSD needs to be reduced being connected on the way of rectified current flow resulted in preserving of the potential distribution of dual zone rectifier on topographic plane. Such zones combination (merging) is feasible, for example, through their combination /merging as it is seen from Fig. 5.

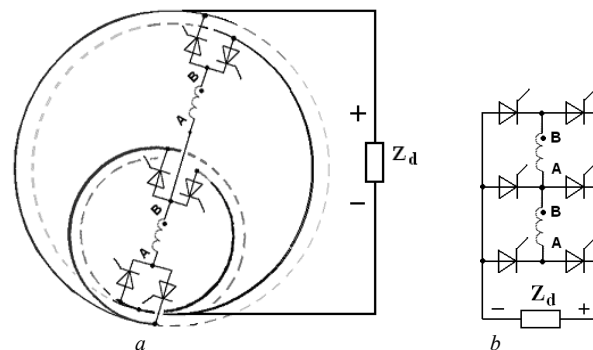


Fig. 5. Single-phase two-zone rectifier: a – topology deduced by way of two zones rotating windings vectors absorption (merger) b - principle electric circuit.

Due to combination (merging), we can reduce number of PSD in several times, which are step-by-step connected on the way of rectified current flow and increase of η value by value of reduced capacity losses in PSD. In practice η is increased at an average of 3 – 5 % based on real variables of feeding transformer. The rectifier at Fig. 5,b was widely practiced and known as bridge zone-phase rectifier. [3].

The only serious disadvantage of bridge zone-phase rectifiers is a continuous commutation (switch) processes, specified by obvious inserted commutation circuit as it is shown at Fig. 5.

Commutation process duration known as commutation angle γ_0 is determined by means of classical technique. [4]

$$\gamma_0 = \arccos \left(1 - \frac{I_d X_a}{\sqrt{2} U_\Sigma} \right), \quad (1)$$

where X_a is a resultant commutating reactance of commutation circuit, U_Σ is a combined stress in commutation circuit. Based on typical variables of feeding transformer the value is $\gamma_0 \approx 5^\circ - 10^\circ$.

Commutation of two circuit nesting results in general commutation duration which makes $\gamma_{01} + \gamma_{02}$. It doesn't only visibly distort the curve of rectified voltage but restricts the adjustment range α_p : on low limit from the value $\alpha_{p \min}$ and up to value $\alpha_{p \max}$ on high limit (Fig. 6).

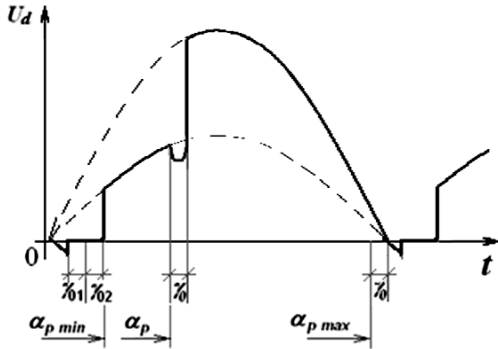


Fig. 6. Effect of commutation angles on the rectified voltage curve and the range of the zone-phase rectifier.

Besides, due to the continuous commutation the power factor is affected.

As it is known,

$$\chi = \nu \cdot \cos \varphi_1, \quad (2)$$

where ν is a distortion coefficient taking into account higher harmonics, $\cos \varphi_1$ takes into consideration a shift of basic harmonics against basic harmonics of voltage.

The [8] shows that

$$\cos \varphi_1 = \left(\frac{\cos(\alpha_p) + (2n-1)}{2n} \right) - \frac{\sqrt{2} U_2 (1 - \cos(\gamma_0))}{\pi \cdot u_{d0}}, \quad (3)$$

Where α_p is a delay angle of PSD opening, n is a number of rectifier's operational zone, U_2 is a – resultant voltage

connected to the operation of secondary windings, u_{d0} is a half-period average voltage without load.

The (1)th – (3)th formulas demonstrate that the bridge zone-phase rectifier, as the result of commutation process, the value χ can be decreased based on the calculations an additional 2-4%.

Thus, the bridge zone-phase rectifiers, in comparison with the Ogier circuit having higher value η , loses by χ value. PSD quantity reduction step-by-step connected on the way of rectified current flow results in inevitable nesting of commutation circuit in case of zones merging.

To eliminate this contradiction and find a way to further single-phase rectifiers with zone-phase regulation improvement it is necessary to place semiconductor devices out potentials geometric places of rotating winding vectors on the topographic potential plane as it shown in [3], or provide for secondary windings rotation. In this mode of rotation one group of secondary windings will work in positive half-period and other in negative. In this case there won't be potentials geometric places overlapping of rotating windings-vectors on first zones, as it shown on Fig. 7.

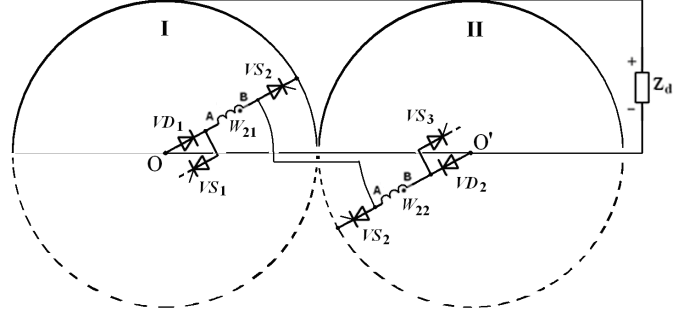


Fig. 7. Simplified topology of first regulation zone building for single-phase two-zone rectifier with secondary windings rotation.

Fig. 7. represents that secondary winding W_{21} works in positive half-period I and W_{22} works in negative half-period II. Such solution allows to avoid nested switching loops during work in younger first zone.

Only during the joint work of such rectifier all secondary winding parts in eldest second regulation zone the unavoidable overlapping of switching loops appears (Fig. 8). Such rectifier circuit solution is proposed in Fig. 9.

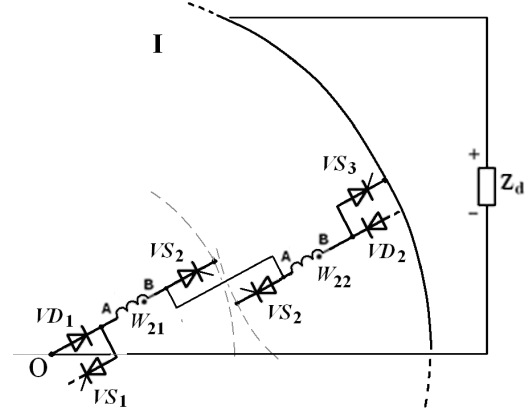


Fig. 8. The second zone simplified fragment building topology for single-phase two-zone rectifier positive half-period.

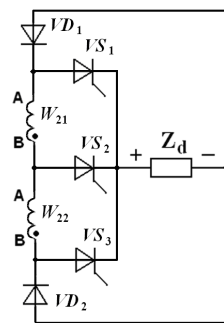


Fig. 9 Single-phase two-zone rectifier with secondary winding rotation on first zone principal circuit.

The concept of a similar solution for single-phase rectifiers is outlined in [6].

V. CONSTRUCTION OF SIMPLE THREE-PHASE RECTIFIER WITH ZONE-PHASE REGULATION

Structure of single-phase two-zone rectifier with secondary winding rotation allows to construct three-phase rectifier with zone-phase regulation. By way of assembly, admitting unbound three-phase circuits, the rectifier structure is repeated for each phase of three-phase grid.

This way allows to exclude unwanted switching contours and gives opportunity to apply thyristors without the risk of keeping them in the open state during the process of voltage level regulation and switching between zones.

Fig. 10, *a* represents three-phase two-zone rectifier as example.

Imitation modeling research results confirmed this three-phase rectifier working capacity and its structure work efficiency (on younger zones, due to the secondary windings rotation) which is expressed by the absence of double commutation angles.

Comparing secondary windings location features on topographic potential plane for bridge rectifiers zones construction (Fig. 2 – Fig. 5) and for rectifiers with secondary windings rotation construction (Fig. 5 – Fig. 7) it has to be noticed that, rotation requires complete symmetry of secondary windings.

It should be taken into account in the zone-phase rectifiers constructing process.

Three-phase two-zone rectifier work mode research (Fig. 10) show that its energy indicators are better than same indicators of three-phase controlled bridge rectifier with same parameters.

Thus, an almost identical value $\eta \geq 0,98$ over a wide range regulation U_d for the adopted model parameters of the three-phase traction rectifier unit $S = 1000 \text{ kVA}$, operating on a load with an inductive character $L \rightarrow \infty$, is explained by the identity of the structures formed when a rectified current flows for a bridge rectifier and a rectifier with rotation of the windings: two SPEs and one secondary winding transformer.

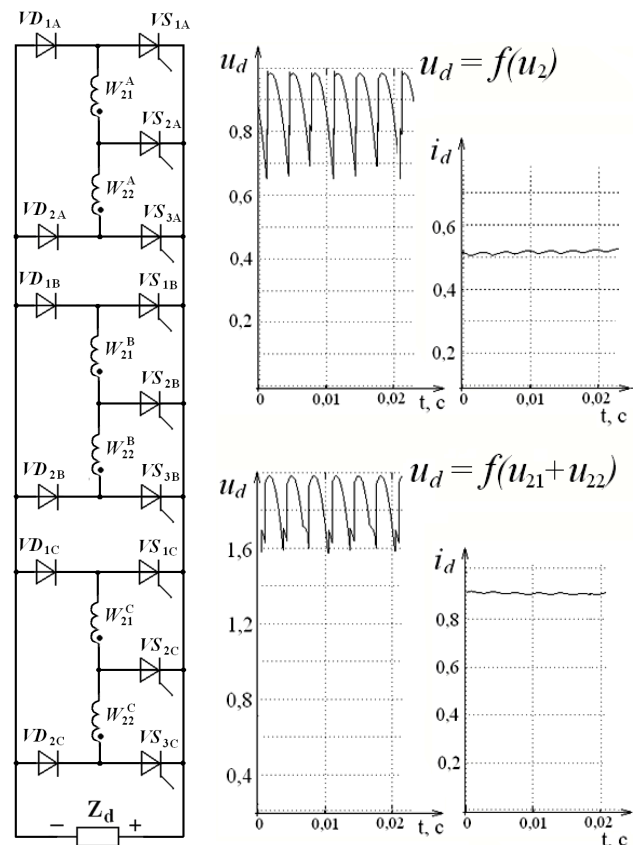


Fig. 10. Three-phase two-zone rectifier: *a* – principal electric circuit; *b* – voltage and current oscillograms, gained by imitation modeling.

At the same time, during work process at the youngest (first) rectifier zone with rotation of the windings, the value of χ , determined in accordance with (6) by the set value α_p , on average, 2 to 4% higher than same parameter of the controlled three-phase bridge rectifier. This can be explained by eliminating double switching angles. Herewith the second regulation zone χ value turns out much higher than same indicator values for three-zone bridge controlled rectifier.

This demonstrates zone-phase rectifiers advantages in their in their working process on elder zones, which also graphically characterize the dependencies $\chi(U_d)$ in Fig. 1.

In conclusion, it should be noticed that the structures shown in Fig. 7 - Fig. 10 have no fundamental limitations and allow to construct zone-phase rectifiers with each number of zones and only a limited amount of this publication does not allow to result in circuit solutions of rectifiers with larger number of zones.

VI. CONCLUSIONS

1. The simple positions adaptation ways of the method structural synthesis for the controlled and uncontrolled of single-phase alternating current rectifiers construction are presented.

2. A simple transition from uncontrolled single-phase rectification circuits to controlled three-phase rectification circuits with zone-phase control is shown.

3. The operability of three-phase rectifiers with zone-phase regulation and their operating efficiency, χ in comparison with conventional controlled rectifiers, determined by the indicators η and, has been confirmed.

REFERENCES

- [1] Rectifiers classification option per topological features / S.A. Yevdokimov, G.S. Zinovyev // Current issues of electronic instrument making: IXth International Conference Proceedings– Novosibirsk: NSTU Publisher, 2008. – V.7. – pp. 3-14. (in Russian).
- [2] Structural synthesis of multi-phase valve inverters / monograph, S.A. Yevdokimov, N.I. Shchurov. - Novosibirsk: NSTU Publisher, 2010. – 423p. (in Russian).
- [3] Improvement of single-phase alternating rectifiers by structural synthesis method / V. V. Ivanov, S. V. Myatezh, N. I. Shchurov, L. S. Atabaeva // The 18 international conference of young specialists on micro/nanotechnologies and electron devices, EDM 2017 : proc., Altai, Erlagol, 29 June – 3 July 2017. – Novosibirsk : NSTU, 2017. – P. 551 - 555. - ISBN 978-150906688-9. - DOI: 10.1109/EDM.2017.7981816.
- [4] Power electronics: monograph / G.S. Zinovyev. – M.: Yurajt Publisher, 2012. – 667p. (in Russian).
- [5] Research of four-zone converter in regenerative braking mode. Dzhaborov M.M., Myatezh S.V., Ivanov V.V. // Applied Mechanics and Materials. - 2015. – Vol. 698 : Electrical Engineering, Energy, Mechanical Engineering, EEM, 2014, pp. 101-105.
- [6] Regulator of rectified voltage: patent. Russian Federation RU №2035828, MPK: H02M7/12; G05F1/16/ Khakhulin V.A. // submitted: 02.03.1993; published: 20.05.1995.



Vladlen V. Ivanov, Russia.
Postgraduate of Electrotechnical Units
Department, Novosibirsk State Technical
University.
Basic direction of research activities is a system
development of electrical power semiconductor
converters.



Sergey V. Myatezh, Russia.
Associate Professor of Electrotechnical Units
Department, Novosibirsk State Technical
University.
Basic direction of research activities is
improvement of the semiconductor converters
engineering.



Andrey V. Kapustin, Russia.
Graduate student of Electrotechnical Units
Department, Novosibirsk State Technical
University.
Basic direction of research activities is a system
development of electrical power semiconductor
converters.



Irina K. Alekseeva, Russia.
Graduate student of Electrotechnical Units
Department, Novosibirsk State Technical
University.
Basic direction of research activities is a system
development of electrical power semiconductor
converters.

Power Generation System for Wind Turbines Based on Novel Multizone Converters

Alexander G. Volkov, *Member, IEEE*
Novosibirsk State Technical University, Novosibirsk, Russia

Abstract – A novel configurations of multizone current source converters are proposed in this paper for wind turbine power generation system using permanent magnet synchronous generator. The system consists of permanent magnet synchronous generator, diode rectifier in couple with buck converter or alternative multizone current source rectifier, and a pulse-width-modulated multizone current source inverter. Current source converter topologies with natural advantages in terms of quality of generated voltage in the entire range of regulation, controllable power factor, and reliable grid short-circuit protection is considered to be a promising power converter configurations for use in medium voltage high-power permanent magnet synchronous generator based wind turbine power generation systems. In this regard, two topologies of multizone current source inverters for medium-voltage wind turbine power generation system were proposed, investigated and analyzed in this paper. The advantages and disadvantages of these topologies are illustrated. The comparison was performed on the basis of analysis and simulation results in terms of grid-side voltage THD, grid power factor, DC current ripple factor, control characteristic and external characteristic. Also, reverse voltages of power semiconductor switches were analyzed.

Index Terms – Current source inverter, multizone current source inverter, permanent magnet synchronous generator, wind turbine power systems.

I. INTRODUCTION

WIND turbine power generation systems (WTPGS) annually undergo significant growth, which stimulates technological developments in the field of industry. Variable speed generators are often used for large turbines, since they can generate more energy with less structural stresses and acoustic emissions compared to systems with a fixed speed. Currently, the basic technology in the market of large wind turbines is the doubly fed induction generator (DFIG) with a partially rated rotor side converter. There are other topologies, and new ones are being developed with a lower cost, higher performance and reliability. In turn, direct-drive systems with a permanent magnet synchronous generator (PMSG) are of great interest due to the high efficiency of the generator, less weight and elimination of the gearbox. As for power electronic converters, most commercial power converters for WTPGS are realized on the basis of voltage source converters.

However, converters based on a current source inverter that have been successfully used in a high-power industrial drives [1], on the other hand, are also suitable for use in high-power wind turbine power generation systems with their

inherent advantages in terms of simple structure, the quality of the generated voltage, controllable power factor and reliable grid short-circuit protection [2, 3]. There are three main configurations of power converters based on a current source inverter for WTPGS.

The first configuration is a back-to-back system based on a current source converter technology, where the current source rectifier (CSR) is used as the first unit of the electrical energy conversion, and current source inverter with pulse-width modulation (PWM CSI) is used as the second power conversion unit [4]. This configuration provides most freedoms in the field of control, but the cost of semiconductor devices is relatively high, as well as the complex development of control system for this converters.

The second configuration employs uncontrolled diode rectifier and a thyristor current inverter. This solution is well established and the reliability is proven [5], but for modern WTPGS, the poor quality of the generated voltage, the lack of reactive power control and the additional costs of the compensation equipment leveling its low cost.

The third configuration is an inexpensive power converter solution based on the use of an uncontrolled diode rectifier with PWM current source inverter [6] for variable-speed wind turbine power generation systems. When compared with the configuration of an uncontrolled diode rectifier and a voltage source inverter with PWM, the advantages of a solution based on PWM CSI are disclosed. However, the uncontrolled diode rectifier has its limitations, since it cannot provide either maximum power point tracking (MPPT) on the generator side, nor the unity power factor (UPF) control on the grid-side in the full generator speed range. In order to improve the operation range for the turbine power generation system [7], another configuration was introduced with the addition of a buck converter between the diode rectifier and PWM CSI. An analysis confirms the necessity of using buck converter for achieving maximum power point tracking and unity power factor on the grid-side. In an onshore horizontal axis wind turbine, generator and converter are usually in the nacelle on the top of the tower, while the grid step-up transformer is placed at the bottom of the unit. The inductances of long cables coming directly from the generator to power converter unit can be used as input inductances of the current source inverter.

The purpose of the work is to research new schemes of three-phase multizone current source converters for wind turbine power generation systems based on a permanent magnet synchronous generator.

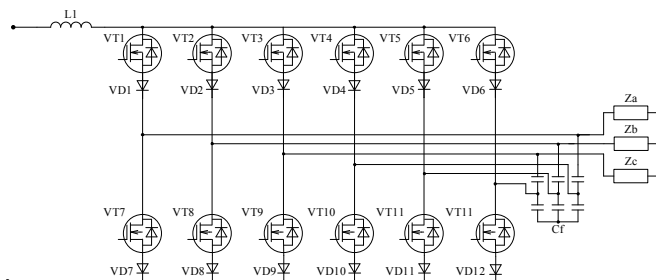


Fig. 5. Three-phase parallel scheme of a multizone current source inverter.

For WTPGS, parameters of generated output voltage and its quality are determined by the grid codes. In this paper, all energy characteristics are given with a unity grid power factor.

III. SIMULATION MODEL

Simulation of sequential and parallel schemes of multizone current source inverters was carried out in the power electronics simulation software package PowerSIM. To research the schemes shown in Fig. 4 and Fig. 5, let's set the constant voltage source at the input $E_d = 600V$, as well as the frequency of the pulse-width modulation of 50 KHz. To analyze the quality of the input current, the current source at the input of the converter will be replaced by an equivalent circuit, namely by the sequential inclusion of the constant voltage source and inductance.

For each phase, current pulses with sinusoidal pulse width modulation are applied. At the same time, closing through the capacitor, they create the required sinusoidal voltage on the load. For the analysis of the investigated schemes, the main energy characteristics of the multizone current source inverters were obtained with the following parameters: $E_d = 600V$, $L_d = 1mH$, $C_f = 100\mu F$.

Since investigated converters generating the output current and the output filter contains the parallel-connected capacitor divider same capacity, presented below energy characteristics will be equal for both test schemes with a single control strategy.

IV. EXPERIMENTAL RESULTS

Fig. 6 shows the control characteristic of the multizone current source inverter in the first and second zones for different values of the modulation.

As can be seen from the figure, the multizone current source inverter has a non-linear control characteristic in each of the control zones. Fig. 7 shows the external characteristic of the multizone current source inverter for the first and second zones with the modulation depth $M = 0.9$.

The advantage of the investigated topologies is the possibility of increasing the output voltage without additional equipment and investment, as well as grid short-circuit protection.

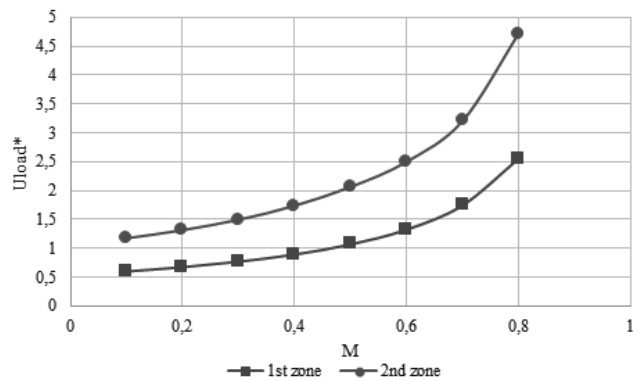


Fig. 6. Control characteristic of the multizone current source inverter in the first and second zones for different values of the modulation.

The disadvantages of this solution include external and non-linear control characteristics in both zones, as well as the impossibility of idle operation.

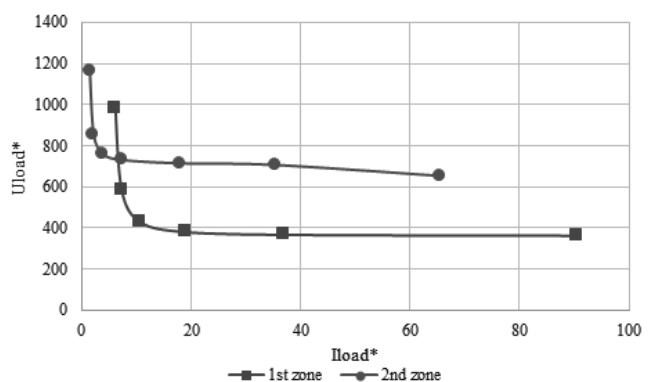


Fig. 7. External characteristic of the multizone current source inverter of the first and second zones.

The quality of the output-generated voltage is estimated by its total harmonic distortion. Fig. 8 shows a graph of the total harmonic distortion of the output generated voltage of a multizone current inverter for different values of the modulation.

The quality of the output-generated voltage of the investigated converters under identical experimental conditions is at the same level.

Better total harmonic distortion of the output voltage can be achieved by changing the control strategy, which will lead to an improvement in the quality of the output current, and, consequently, of the output voltage.

The quality of the input current is estimated by its DC current ripple factor. Fig. 9 shows the graph of the DC current ripple factor depending on the modulation in the first and second control zones.

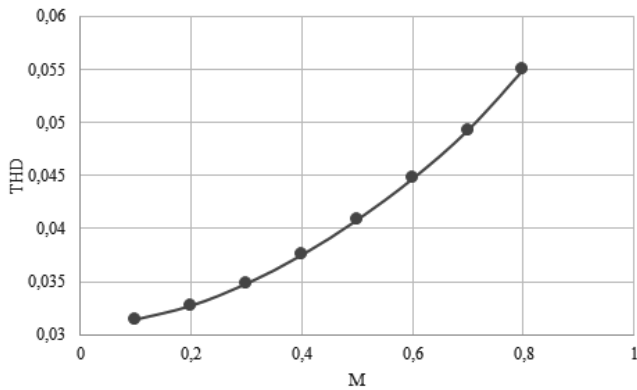


Fig. 8. The total harmonic distortion of the output voltage of the multizone current source inverter for different values of the modulation.

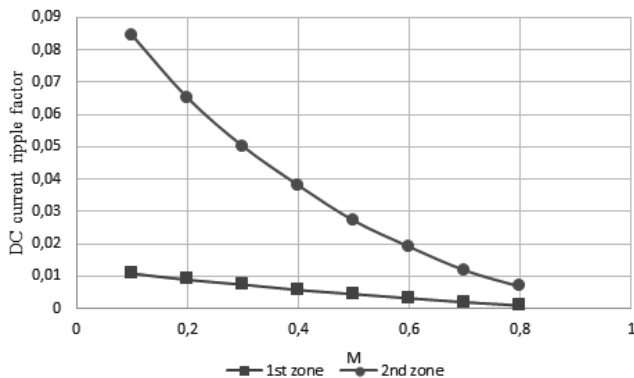


Fig. 9. DC current ripple factor of the multizone current source inverter of the first and second zones for different values of the modulation.

Also, reverse voltage of the power switches was analyzed. Using of a multizone current source inverter topologies provides the required output voltage quality, as well as a decrease of the power switches reverse voltage in comparison with the parallel scheme of the multizone current source inverter. Therefore, the transistors VT2 can be selected for a lower voltage class. Fig. 10 shows the reverse voltages on the transistors VT1 and VT2 of the sequential scheme of the multizone current source inverter. Fig. 11 shows the reverse voltages on the transistors VT1 and VT2 of the parallel scheme of the multizone current source inverter. For a visual representation, the switching frequency of the pulse width modulation was reduced by 10.

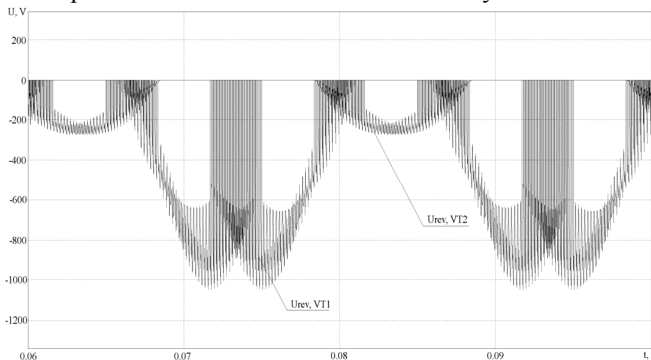


Fig. 10. The reverse voltages of the transistors VT1 and VT2 of the sequential scheme of the multizone current source inverter.

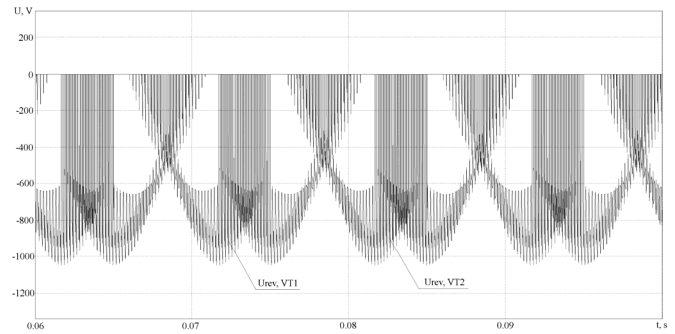


Fig. 11. The reverse voltages of the transistors VT1 and VT2 of the parallel scheme of the multizone current source inverter.

V. CONCLUSIONS

In this paper, novel configurations of multizone current source converters for medium-voltage high power wind turbine power generation system using permanent magnet synchronous generator are investigated. In multizone current source inverters, by changing the ratio of the load phase and capacitance of the output filters the magnitude of voltage can be changed in each of the converter zones. The transition from the lower to upper zone of a two-zone current source inverter provides an increase in value of the output voltage twice with the same values of capacitance divider maintains.

The main advantage of a current source inverter is the possibility to amplify output voltage with respect accordingly the input by several times. Changing the inverter load impedance results in to an increase or decrease voltage on it, and hence on the consumer load.

It is evident from aforementioned results that the investigated topologies of multizone converters have the same quality of generated electric AC power at a nominal modulation.

However, the reverse voltages of the power switches are reduced, respectively, the number this power switches is reduced in those cases where a serial connection of transistors is required.

The disadvantages of this solution include external and non-linear control characteristics in both zones, as well as the impossibility of idle operation.

For wind turbine power generation systems, the investigated schemes can be used as a second conversion unit of electrical energy, when powered by an uncontrolled diode rectifier, or by a buck converter, and also in an current source rectifier mode. By making a comparison between the system configurations using a single uncontrolled diode rectifier, or an uncontrolled rectifier in couple with buck converter, the configuration of the current source rectifier and the multizone current source inverter is considered the most promising topology for using in wind turbine power generation systems. Replacing the diode rectifier with a more expensive current source rectifier provides full control from both the permanent magnet synchronous generator-side and the grid-side. Thus, a fully controllable converter as a first conversion unit of electrical energy can significantly improve the quality of the generated voltage, the quality of the energy consumed and the maximum power point tracking throughout the full operating range.

ACKNOWLEDGEMENT

The reported study was funded by Russian Science Foundation (RSF) according to the research project № 17-79-10366.

REFERENCES

- [1] B. Wu, J. Pontt, J. Rodriguez, S. Bernet, and S. Kouro, "Current-Source Converter and Cycloconverter Topologies for Industrial Medium-Voltage Drives," *IEEE Transactions on Industrial Electronics*, Vol. 55, No.7, 2786-2797, 2008.
- [2] F. Blaabjerg, Z. Chen, R. Teodorescu, and F. Iov, "Power Electronics in Wind Turbine Systems," in *Power Electronics and Motion Control Conference*, 2006. IPEMC '06. CES/IEEE 5th International, 2006, pp. 1- 11.
- [3] Z. Chen, J. M. Guerrero, and F. Blaabjerg, "A review of the state of the art of power electronics for wind turbines," *IEEE Trans. Power Electron.*, vol. 24, no. 8, pp. 1859–1875, Aug. 2009.
- [4] Jingya Dai, Dewei Xu, Bin Wu, "A Novel Control System for Current Source Converter Based Variable Speed PM Wind Power Generators", *Power Electronics Specialists Conference, PESC 2007*, pp. 1852-1857, 2007.
- [5] Z. Chen, E. Spooner, "Current source thyristor inverter and its active compensation system," *IEE Proc.-Gener. Transm. Distrib.*, vol. 150, No. 4, July 2003.
- [6] J. Dai, B. Wu, D. Xu, N. R. Zargari and J. Wang, "Low Cost Current Source Converter Solutions for Variable Speed Wind Energy Conversion Systems," in *IEEE International Electric Machines and Drives Conference*, 2011.
- [7] X. Tan, J. Dai and B. Wu, "A Novel Converter Configuration for Wind Applications Using PWM CSI with Diode Rectifier and Buck Converter," in *IEEE International Electric Machines & Drives Conference*, 2011.
- [8] Volkov A. G. Development and Research of Three-phase Multizone AC-DC Converters / Volkov A.G., Zinoviev G.S. // Twelfth international conference and seminar on micro/nanotechnologies and electron device (EDM 2011). – Erlagol, Altai. – June 30 – July 4, 2011. – P. 377-380.
- [9] Volkov A. G., Zinoviev G.S., Multizone DC/AC converter. Patent of Russia since 19.11.2012 (RU 2523001) Bul. No 2012. (in russian)
- [10] Volkov A. G. Analysis of electromagnetic processes in the three phase multizone current source inverter / Volkov, A.G., Zinoviev, G.S., Sidorov, A.V., Kharitonov, S.A. // Source of the Document International Conference of Young Specialists on Micro/Nanotechnologies and Electron Devices (EDM 2014) . – 2014. – P. 415-418.



Alexander G. Volkov - Candidate of Technical Sciences, associate prof., Novosibirsk state technical university. His research interests are currently focused on power electronics, power converters, power generation and energy storage systems, active power filters. Since 2011, he is a senior researcher of Industrial Electronics Department of NSTU.

Area of scientific interests: developing and analysis of energy-saving and renewable energy technologies in industry. Currently he has over 35 published works.

E-mail: _bismark_@mail.ru

Prospects in the Field of Energy-Conversion Devices Design for High-Voltage Power Systems

Mariya M. Chernaya, 93024727, IEEE, Alexander V. Osipov, Yuriy A. Shinyakov, Maxim P. Sukhorukov
Tomsk State University of Control System and Radio Electronics, Tomsk, Russia

Abstract – In this paper the comparative analysis of the structures variants of spacecrafts power supply systems with the connection of accumulator battery charge and discharge devices to the output power bus and to the solar battery bus, based on the calculation of energy flows in the system and the calculation of weight dimension characteristics of the estimated components of the system was carried out. Recommendations for choosing the rational structure of space craft high-voltage power supply system in terms of improved specific weight dimension characteristics and requirements for its energy-converting devices design are presented. The need to develop energy-converting devices with high values of efficiency has been proved and the expediency of designing it on the basis of combined modules is justified. The integrated charge-discharge module for the high-voltage power supply system on the basis of the bridge boost converter with an active rectifier (1400 W), providing a reversible mode of operation, used to charge the accumulator battery, is proposed. Experimental studies of the charge-discharge module were carried out. It is proved that the module provides limitation of the battery discharge current (15 A), the implementation of transistors soft switching and the achievement of efficiency is not less than 96 %.

Index Terms – Spacecraft, high-voltage power supply system, energy-conversion devices, charging-discharge module, buck converter.

I. INTRODUCTION

STUDY and space exploration requires the development and improvement of spacecrafts (SCs) with different targets: intended for deep space exploration, for the formation of a global communication system, television and navigation, for studying weather conditions, the Earth's natural resources, for monitoring and transmitting information, etc.

Now and in the near future the main primary energy source of space crafts will be solar batteries (SB). In addition to the SB on the board of modern spacecrafts with long service life accumulator batteries (AB) are installed. SB and AB via energy-conversion devices (ECD) and control and monitoring equipment are connected to the common output stabilized load power buses. These components of SC power supply systems (PSS) require research and development, while for the full use of each of the SC PSS components it is necessary to study the entire system of spacecraft as a whole, which is up to 30 % by mass, volume, and cost of the spacecraft. Therefore, optimization of the existing and development of new methods and approaches for designing and creating SC PSS will significantly improve the technical and economic performance of the spacecraft.

Initially, the voltage level of the output stabilized power supply bus of the SC PSS was 27–28 V. The most widespread was the SC PSS on the basis of parallel and parallel-sequential structures. The choice of structure is largely due to the choice of the working orbit, operating conditions, load curve, targets and other technical requirements for the spacecraft [1].

Since the mid-90s of the 20th century new more stringent requirements for the projected SC PSS and spacecrafts have been formed, an increase in the number of tasks solved by spacecraft, an increase in its power-to-weight ratio and output power. The requirements in terms of the weight dimension characteristics of the SC PSS components and its efficiency, requirements for reducing the cost of development and manufacturing, increasing the level of reliability, radiation resistance, etc., have been raised. The transition to a high-voltage (100 V) power supply bus in the field of development and creation of SC PSS was made.

II. PROBLEM DEFINITION

The main problem associated with the use of SB with nonlinear I-V characteristics with a brightly expressed power maximum in high-voltage SC PSS is the possibility of achieving critical open-circuit (OC) voltage of the SB when SC exit from the shadow areas of the orbit and the maximum decrease in the SB panels temperature, which creates conditions for the occurrence of electrostatic discharges between the SB photodiode chains or current collector elements (for silicon SB – up to 300 V, for arsenide-gallium SB – up to 245 V). The geostationary spacecraft designers determined the optimal shunt structure of the PSS construction at that time, which made it possible to force the SB voltage [2, 3]. Examples of such high-power high-voltage SC PSS designed on the basis of arsenide-gallium SB, lithium-ion AB and shunt voltage stabilizers may be the Russian platform Express-2000 developed by the JSC Information Satellite Systems Academician M.F. Reshetnev, PSS of the European company Alcatel, made for the platform Spacebus-4000, Hughes PSS on the HS-702 platform, the Lockheed Martin PSS on the A-2100 AXX platform and others.

Despite the existing scientific and technical advance, the testing of the results and the successful implementation of shunt high-voltage SC PSS, it is not optimal to directly apply these results to the implementation of high-voltage SC PSS with different types of working orbits, load curve and operating conditions due to its low energy efficiency provided by a significant change in the I-V characteristic of

the SB by the influence of a change in the environmental conditions (temperature, illumination, etc.), and when applied parallel-sequential structures of SC PSS because of the possibility of accidents due to reaching critical levels of open-circuit voltage of cooled SB, as a result, low reliability of SC PSS.

It has been established that when designing high-voltage high-power SC PSS with various loading curves and operating conditions, it is necessary to carry out a number of complex scientific and technical works, taking into account the fulfillment of energy efficiency requirements, reliability and simplicity of the coordination of energy sources and loads in SC PSS, which requires new technical solutions, approaches and search for unified solutions in the field of development and creation of energy-conversion devices and SC PSS.

III. THEORY

A. Comparative Analysis of SC PSS Structures

For an arbitrary load curve of the spacecraft and taking into account the illumination and temperature curves of the SB, the calculation of the SB power generated graph according to the technique [4] is performed, which provides the energy balance in the SC PSS with the connection of the charge device (CD) and discharge device (DD) to the SB bus and in the SC PSS with the connection of the charge and discharge devices to the load power bus. The current power values generated by the SB are calculated under the condition of the maximum power point tracking mode. It is assumed that the SC PSS works either in the mode of simultaneous power supply of the load and the charge of AB from the SB or in the mode of simultaneous power supply of the load from the SB and AB.

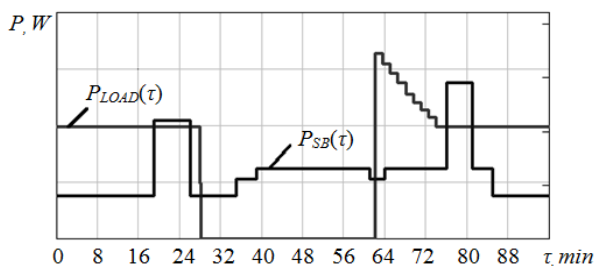


Fig. 1. The load curve $P_{LOAD}(\tau)$ and the curve of SB power $P_{SB}(\tau)$ in PSS.

The processes of distribution of energy flows in PSS (Fig. 1) were studied with a change of the ECD efficiency for the purpose of its comparative analysis, an assessment of the effect of the ECD efficiency on the weight dimension characteristics, and the determination of the optimal PSS structure. In Table I the calculated values of the masses (m , kg) of EDC, SB (including SB area S , m^2) and AB of alternatives PSS are given, provided by the efficiency of the CD, DD or voltage regulator (VR) is reduced in order to achieve the equality estimated in alternative versions of PSS mass. At $\eta_{VR} = 0,96$, $\eta_{CD} = 0,95$ and $\eta_{DD} = 0,95$ m_{sum} in the PSS with connection of charge and discharge devices to the load power bus is equal to 581.88 kg.

TABLE I
PARAMETERS OF THE SC PSS AT THE CHANGE OF POWER
CONDITIONING DEVICES EFFICIENCY

| Parameter | PSS with connection of CD and DD to SB bus | PSS with connection of CD and DD to the load power bus | | |
|------------------|--|--|--|---|
| | $\eta_{VR} = 0,96$, $\eta_{CD} = 0,95$, $\eta_{DD} = 0,95$ | $\eta_{VR} = 0,94$, $\eta_{CD} = 0,95$, $\eta_{DD} = 0,95$ | $\eta_{VR} = 0,96$, $\eta_{CD} = 0,89$, $\eta_{DD} = 0,95$ | $\eta_{VR} = 0,96$, $\eta_{CD} = 0,95$, $\eta_{DD} = 0,935$ |
| S_{SB} , m^2 | 73.37 | 74.85 | 75.46 | 73.88 |
| m_{SB} , kg | 220.11 | 224.56 | 226.38 | 221.62 |
| m_{AB} , kg | 227.72 | 218.62 | 214.83 | 221.20 |
| m_{DD} , kg | 45.426 | 43.61 | 43.61 | 44.31 |
| m_{CD} , kg | 50.789 | 48.76 | 50.15 | 49.09 |
| m_{VR} , kg | 43.16 | 51.81 | 52.24 | 51.14 |
| m_{sum} , kg | 587.21 | 587.35 | 587.20 | 587.36 |

It can be seen (Table I) that for equal values of the ECD efficiency of the PSS, a rational variant of the structure is the SC PSS with the connection of the charge and discharge devices to the load power bus. The advantage of such structure is that the input charger voltage of the charger and the output discharge voltage of the DD are determined by the level of the stabilized output voltage of the load power bus and for the high-voltage SC PSS do not exceed a level of 100 ± 2 V.

B. Charge-Discharge Module of Accumulator Battery

Since the distribution of energy flows in PSS between the SB, AB and the load, and as a consequence, the specific energy and weight dimension characteristics of PSS depends on the ECD efficiency, the actual task, the solution of which will allow achieving significant improvement in the characteristics of high-voltage SC PSS, taking into account the non-simultaneity of the processes charge and discharge of AB, is the development of energy-transforming devices that provide the possibility of reversible modes of operation: both discharge and charge AB modes, i.e. the development of integrated charge-discharge modules (CDM).

In Fig. 2 shows the circuit of CDM based on a bridge boost converter with an active rectifier, which provides limitation of the AB discharge current due to the introduction into the circuit of an additional transistor VT_{ADD} and a diode VD_{ADD} [5].

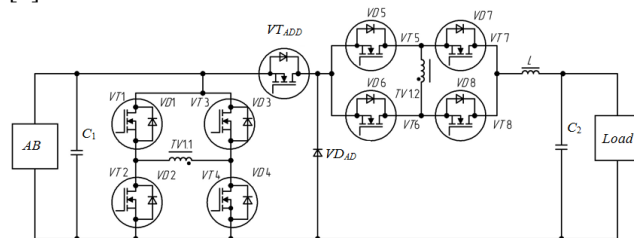


Fig. 2. Circuit of the module of CDD based on the boost AB energy converter.

The inverter and rectifier form a high-frequency link that converts part of the energy needed to form the required output voltage, which is the sum of the output voltage and the added high-frequency control voltage.

The control pulses of the rectifier transistors are formed by adding the control pulses of the inverter transistors that are located in diagonals. The voltage of the output bus of the load power is stabilized by the SB energy converter in charging mode. AB is the load, the output power bus is the power source and the current of inductor changes direction. The rectifier performs the function of a current inverter, and the inverter operates in the rectification mode [6].

IV. EXPERIMENTAL RESULTS

A prototype of the charge-discharge module on the basis of the boost AB energy converter for a high-voltage (100 V) SC PSS was developed (Fig. 3).

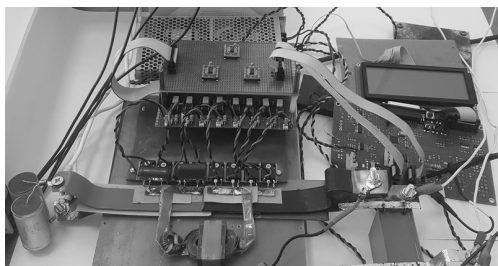


Fig. 3. The breadboard model of CDM.

In the CDM the limitation of the AB discharge current at a level of 15 A is realized. In this case, the converter with closed transistors of the inverter and open transistors of the rectifier comes to buck voltage converter. The maximum output power of the converter is 1400 W and the discharge AB voltage varies from 55 to 96 V.

The operation of the converter when the input voltage is changed is shown in Fig. 4.

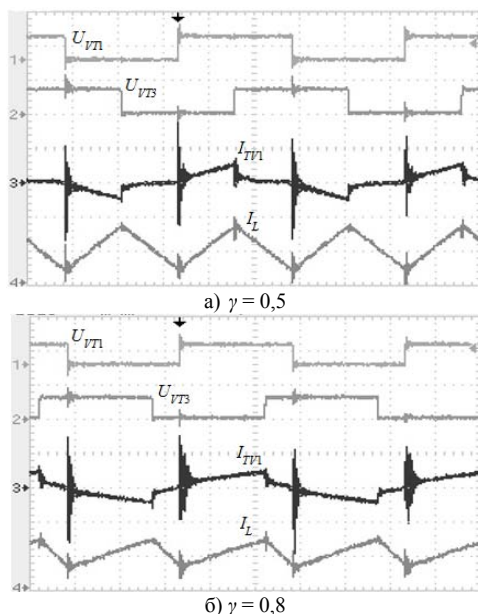


Fig. 4. The oscillograms of the inductor currents (8 A/div) and the transformer (16 A/div) and voltages of transistors (100 V/div) of the boost converter in the discharge mode.

The oscillograms of the inductor current, the current of the transformer, voltage of transistors with the stabilization of

the output voltage (100 V) are illustrated with the load resistance equal to 12 ohms for the various intervals (Fig. 4).

According to Fig. 4 it can be seen that the current of the transformer decreases as the input voltage increases, thereby reducing the static losses.

V. DISCUSSION OF RESULTS

In the course of the research it was established that for equal values of the ECD efficiency of SC PSS, a rational variant of the SC PSS structure is the PSS with the connection of the ECD in the energy conversion channel from the AB to the load power bus. At the same time, an equally important task for PSS developers is the development and creation of its energy-conversion devices with increased efficiency.

A promising version of the energy-conversion devices of PSS is the design of charge-discharge module based on a bridge boost converter with an active rectifier. During the experimental studies of the breadboard AB charge-discharge model, an efficiency of 96 % was achieved and it was obtained that in the discharge mode, the switching of the regulated rack transistors (VT3, VT4) occurs hard, and the inclusion of the remaining transistors of the converter is accompanied by a preliminary discharge of parasitic capacitances and occurs with a minimum switching loss. In the inverter it is achieved due to the inertia of the transformer inductor leakage current, and in the rectifier it is achieved due to the continuity of the current of the smoothing inductor. The switching of the rectifier transistors is hard in the charge mode, and in the inverter, only unconstrained rack transistors are rigidly switched.

VI. CONCLUSION

A promising direction in the field of development and creation of high-voltage high-power spacecrafts power supply systems is the design on the basis of integrated energy-conversion modules, in particular, on the basis of integrated accumulator battery charge-discharge modules.

The totality of the obtained research results allows to draw a conclusion that it is expedient to design high-voltage SC PSS when connecting charge-discharge modules to the output bus of the load power taking into account the implementation the maximum power point tracking mode. At the same time, an increase in the energy conversion devices efficiency will significantly improve the energy efficiency and minimize the weight dimension characteristics of SC power supply systems.

A breadboard model of the charge-discharge AB module was developed on the basis of a boost converter with an active rectifier and its experimental studies were carried out, confirming the possibility of limiting the discharge AB current, implementing a soft switching of transistors and reducing the transformer current with increasing input voltage, which reduces static losses and achieves an efficiency factor of (96 %).

The research was made to implement decree of the Government of the Russian Federation of 9 April, 2010 No.

218 and contract between ISS JSC and the Ministry of Education and Science of the Russian Federation of 01 December 2015 No. 02.G25.31.0182.

REFERENCES

- [1] Shinyakov Yu.A., Gurtov A.S., Gordeev K.G., Ivkov S.V. Choice of the structure of low-orbit space vehicles power systems // Bulletin of the Samara State Aerospace University, 2010. №. 1 (21). pp. 103-113. (in Russian).
- [2] Lesnykh A.N., Sarychev V.A. The research of high-voltage power supply systems for space crafts with boost converter // Bulletin of Siberian state aerospace university named after academician M.F. Reshetnev, 2006. №. 6 (13). pp. 63-66. (in Russian).
- [3] Raushenbach G. Reference book of the solar cells design / Tr. from English. – M.: Energoatomizdat, 1983. – 360 p.
- [4] Chernaya M.M. Research and development of energy-transforming devices of high-voltage power supply systems of space crafts: Dis. cand. of tech. sciences. Tomsk, 2017. 142 p. (in Russian).
- [5] Osipov A.V., Shkolny V.N., Shinyakov Yu.A., Yaroslavtsev E.V., Shemolin I.S. Serial resonant converter for battery power systems // Proceedings of TUSUR, 2017. V. 20. №. 2. pp. 103-110. (in Russian).
- [6] Zinoviev G.S. Fundamentals of Power Electronics. – Novosibirsk: NSTU Publ., 2000. – P.2. – 197 p. (in Russian).



Mariya M. Chernaya was born in in Jambul, Kazakhstan, in 1991. Graduated from the Faculty of Electronic Engineering of the Tomsk State University of Control Systems and Radioelectronics (TUSUR) in 2012. She defended her thesis for the degree of candidate of technical sciences in specialty 05.09.12. Since 2012, he works as a junior researcher at the Scientific Research Institute of Space Technology of TUSUR. He is the author of 18 publications, including 6 patents for inventions. Research interests: energy-conversion equipment, high-voltage power supply systems of space crafts, mathematical and simulation modeling of energy flow distribution processes.
e-mail: cmm91@inbox.ru.



Aleksandr V. Osipov is a senior researcher of the Scientific Research Institute of Space Technology of the TUSUR, candidate of technical sciences. Graduated from the Faculty of Electronic Engineering (TUSUR) in 1999. Defended a dissertation on the topic "High frequency induction heating systems of blanks before its plastic deformation" in 2004. Research interests: power electronics, power supply systems of space crafts, mathematic simulation and simulation modeling.
e-mail: ossan@mail.ru.



Yuriy A. Shinyakov was born in Russian Federation, in 1950. He graduated from the electrophysical faculty of the Tomsk Polytechnic Institute in 1972. In 2009 he received a doctorate in technical sciences in specialty 05.09.03. Since 2010 he is the Director of the Scientific Research Institute of Space Technology of TUSUR. He is the author of more than 150 publications. For his successful work he was awarded the medal "300 Years of the Russian Fleet" (1996). He has the title of "Honored Mechanical Engineer of the Russian Federation" (1999). In 2012 he was with the S.P. Koroleva medal. Research interests: energy-conversion equipment, power supply and control systems for underwater, ground and space applications.



Maxim Sukhorukov was born in Ust-Kamenogorsk, Kazakhstan, in 1987. Graduated of the Tomsk State University of Control Systems and Radioelectronics (TUSUR). Head of the Laboratory of Digital Control Systems of the Scientific Research Institute of Space Technologies TUSUR. Scientific interests: mathematical modeling, instrumentation, on-board radioelectronic equipment.
e-mail: max_sukhorukov@mail.ru.

Single-Cycle LCL-T Resonant Converter for Solar Battery

Sergey A. Zapolskiy¹, Aleksandr V. Osipov¹, Ivan M. Zhuravlev², Mikhail E. Khlystunov¹

¹Tomsk State University of Control Systems and Radioelectronics, Tomsk, Russia

²JSC Academician M.F. Reshetnev Information Satellite Systems Zheleznogorsk, Russia

Abstract – In this paper we consider single-cycle solar battery energy converter with resonant LCL-T circuit. It is shown that the using LCL-T converter allows to get in wide load range stabilized voltage from solar battery which is a current source. Besides, single-cycle mode allows excluding transformer from converter circuit and simplifying the topology, but increasing the resonant circuit current.

Index Terms – LCL-T converter, resonant converter, single-cycle converter, soft switching.

I. INTRODUCTION

THE CURRENT trend towards the increase of the unit power of spacecraft power supply systems (PSS) sets high requirements to its efficiency. Primary electrical source of spacecraft power supply is a solar battery (SB), which generates energy only on sunlight portion of the orbit. Besides the time of consuming spacecraft from SB much more than the time of power from accumulator battery. Therefore, it makes SB energy converter more significant. Currently applied DC-DC converters [1] have high switching losses in power transistors, which limits operating frequency and weight-size parameters of power elements. Besides attempts to obtain soft switching lead to using active [2] or passive [3] snubber circuits.

To solve the problem of the formation of soft switching is possible by application of resonant Converter with the soft-switching transistors. This allows to increase the efficiency and improve the energy efficiency of the supply system as a whole. However, it is necessary to consider that the feature of solar battery as an energy source is the presence of two plots of current-voltage characteristics (CVC): the stable voltage plot and the stable current plot. In space SB is operated in the current source mode and its voltage is limited to the level of the output voltage because of the possibility of breakdown in vacuum conditions. In addition, the load of the converter can vary in wide ranges. Therefore, the classical LC resonant converter is not effective to stabilize the voltage, because reducing the load requires wide control range and idle is emergency mode.

LCL-T converters performing parametric performing impedance conversion of the input source [4] are more effective. In the conversion of solar battery, which is a current source, the current of resonant circuit is stable. It leads to the parametric stabilization of the voltage on the resonant capacitor and the load, regardless of its resistance. Analysis of the characteristics of the resonant LCL-T converter constructed

according to the DAB topology in the stabilization mode of output voltage when powered by SB performed in [5]. It shows that the presence of the active rectifier is an indispensable condition of parametric stabilization. The DAB topology provides galvanic isolation and high efficiency range, but the presence of two full bridges and a power transformer leads to a significant increase in the size of the inverter.

II. PROBLEM DEFINITION

A solution of the reduction of the dimensions may be the use of single-cycle resonant converters without the power transformer [6]-[8]. Therefore, the analysis of the single-cycle converter with LCL-T circuit and its characteristics in the parametric stabilization of the output voltage in a wide range of load changes mode are presented in this paper.

III. THEORY

Resonant converters performing impedance (inductive-capacitive) transformation provide a sinusoidal current as well as the parametric stabilization of the output voltage with a stable current of the input source. Popular topologies of the respective resonant circuits are shown in Fig. 1. An element, carrying out impedance conversion, is a resonance capacitor parallel to the load and having stable voltage during the flow of it constant current. The easiest way is to use a Boucherot cell (Fig. 1A).

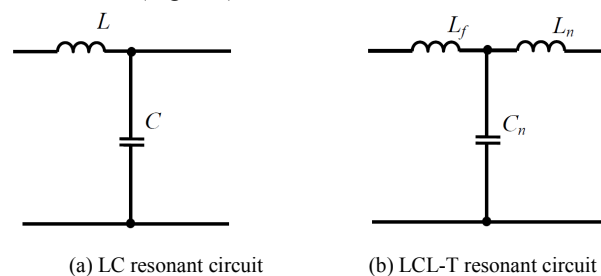


Fig. 1. Resonant circuit schemes.

However, the shunting capacitor current with load leads to the output voltage drift and instability. To compensate for the dependence on load is possible by introducing an additional inductor L_2 . As result, LCL-T circuit will have formed (Fig. 1, b). In that way its voltage drop eliminates this disadvantage. The foregoing is illustrated with a vector diagram (Fig. 2). Under the condition of equality of the inductances $L_f = L_n$ the voltage drop across the inductor L_n allows to form

angle $\pi/2$ between the rectifier current I_{rect} and the inverter current I_{inv} which does not depend on the load resistance. This condition ensures the equality $U_{Lf}=U_{rect}$ and the stability of the output voltage, since changing U_{inv} is compensated by the change of U_{Ln} . The current of the capacitor has a phase shift relative to the current inverter at the angle α determined by the load

$$\operatorname{tg} \alpha = \frac{U_{inv}}{U_{rect}} = \frac{I_{rect}}{I_{inv}} = \frac{\rho}{R},$$

where ρ is the characteristic impedance of the resonant circuit. Therefore, the control pulses and voltage of the transistors of the inverter and rectifier are shifted respectively by $\pi/2$.

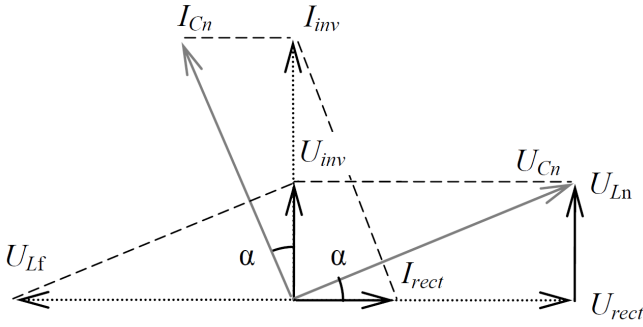


Fig. 2. Vector diagram of the resonant LCL-T converter.

The proposed single-cycle resonant converter is shown in Fig. 3. The principle of its work differs from the full-bridge topology in the influence on the resonance of the LCL-T circuit of unipolar voltage pulses generated by single-ended inverter which is made of transistors $VT1$, $VT2$. Transistors are opened one by one, so that the positive half wave of the circuit current is consumed from the inverter when the transistor $VT1$ is open, the negative half wave is closed by the transistor $VT2$, thus two intervals are formed: the interval of energy transfer from the source to the resonant circuit and the interval of short circuit current of the resonant circuit. The active rectifier operates in single-cycle mode transmitting the positive half-wave current to the load by the transistor $VT3$ and short-circuiting the negative half wave by the transistor $VT4$, i.e. half-wave rectification is implemented.

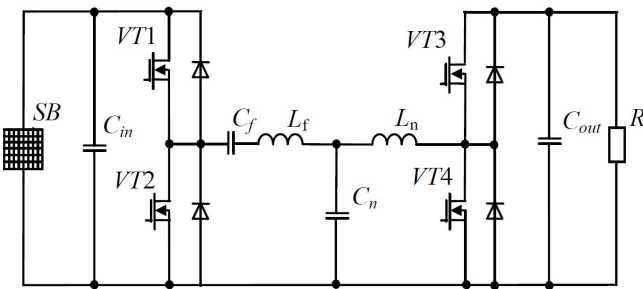


Fig. 3. Single-cycle resonant LCL-T converter.

Thus, in single-cycle converters the input source energy may be transferred to the load only during the half period, therefore, the amplitude of current in resonant circuit in π times higher than the average current SB

$$I_{inv} = \pi I_{SB},$$

and the first harmonic of the circuit output current is under resistance

$$R_{ac} = \frac{2}{\pi^2} R,$$

therefore, the voltage in the output of single-cycle converter is 4 times greater than the one in the output of two-cycle converter with the same wave resistance.

$$U_{out} = \frac{\pi^2}{2} I_{SB} \rho = \frac{\pi^2}{2} I_{SB} \rho.$$

In addition, the inverter voltage U_{inv} and the rectifier voltage U_{rect} have DC components, which requires using of the passing capacitor C_f in the inverter circuit.

Single-cycle resonant LCL-T Converter work diagrammes at different loads are shown in Fig. 4 and Fig. 5. When the load is close to the characteristic impedance $R \rightarrow \rho$ input voltage tends to the output $U_{SB} \rightarrow U_{out}$, and the angle of the load $\alpha \rightarrow \pi/4$ (Fig. 4). The increase in the load resistance in LCL-T converter reduces the voltage of SB and the amplitude of the first harmonic current of the rectifier, the output voltage remains constant (Fig. 5).

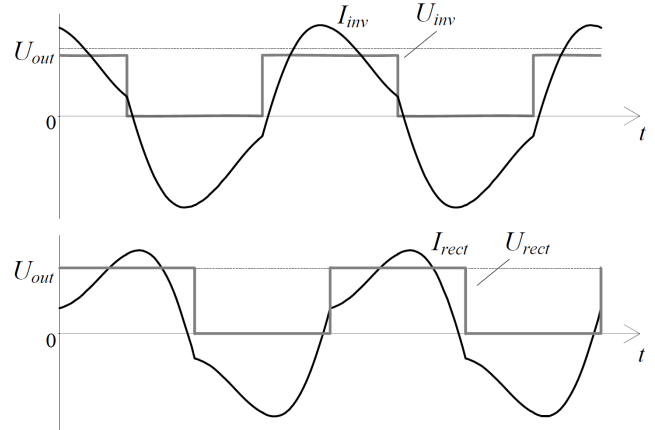


Fig. 4. Single-cycle resonant LCL-T converter parameters with $R \rightarrow \rho$.

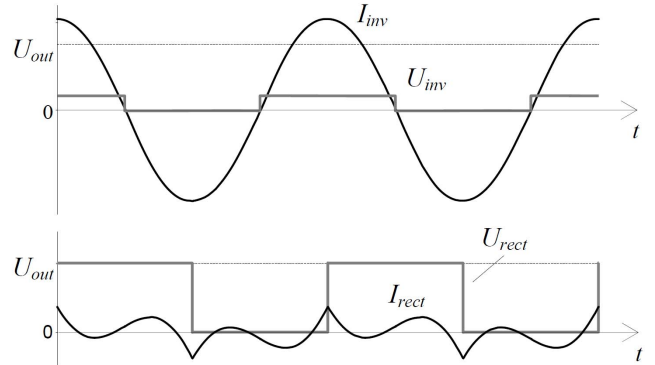


Fig. 5. Single-cycle resonant LCL-T converter parameters with $R \rightarrow \infty$.

When SB current changes, in the resonant converters the output voltage stabilization can be provided with pulse-width regulation, which is implemented by changing the duration of the inverter upper transistor $VT1$ on-state relative to the lower transistor $VT2$. In the result the energy transfer and short-circuiting intervals duration are changing (Fig. 6). Regulating characteristic is described by the ratio

$$U_{out} = \frac{\pi^2}{2} \cdot I_{SB} \cdot \rho \cdot \frac{1}{\sin^2\left(\frac{\pi\gamma}{2}\right)},$$

where γ is the relative inverter voltage pulse duration. One-sided character of pulse-width regulation leads to delay of the inverter current first harmonic relative to voltage and advance of the rectifier current first harmonic relative to its voltage by the same angle

$$\varphi = \frac{\pi(1-\gamma)}{2}.$$

This causes an increase of reactive power, the appearance of recuperation intervals in the converter and increases the losses. The solution may be a converter frequency adjustment to the resonant mode.

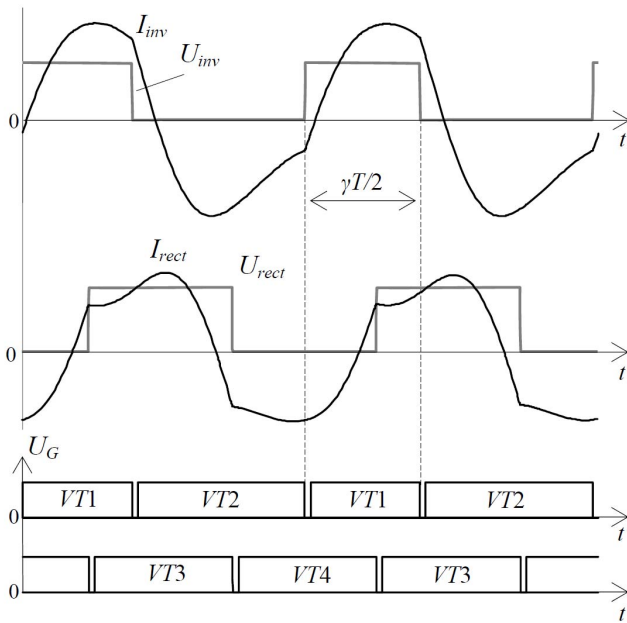


Fig. 6. Curve of the LCL-T resonant converter parameters with $\gamma=0.8$.

Transistors switching-modes of the single-cycle LCL-T converter is fundamentally no different from switching-modes of the full-bridge resonant converter. The soft-switching in the inverter is provided by the lagging current, in the rectifier is provided by the leading current. The difference is due to the fact that in the inverter it is necessary to switch transistors before the current crosses zero, thus turning-on will be provided at negative current, i.e. at the opened reverse diode and zero voltage. In the rectifier switching is implemented after the current crosses zero. Providing a soft switching in resonant converters discussed in more detail in [9].

IV. EXPERIMENTAL RESULTS

The prototype of the proposed single-cycle LCL-T converter based on two-phase topology was designed for experimental verification of the obtained results (Fig. 7). Two-phase topology is caused by a large number of spacecraft PSS solar panels, working with a common load and the desire to reduce voltage ripple in the output capacitor.

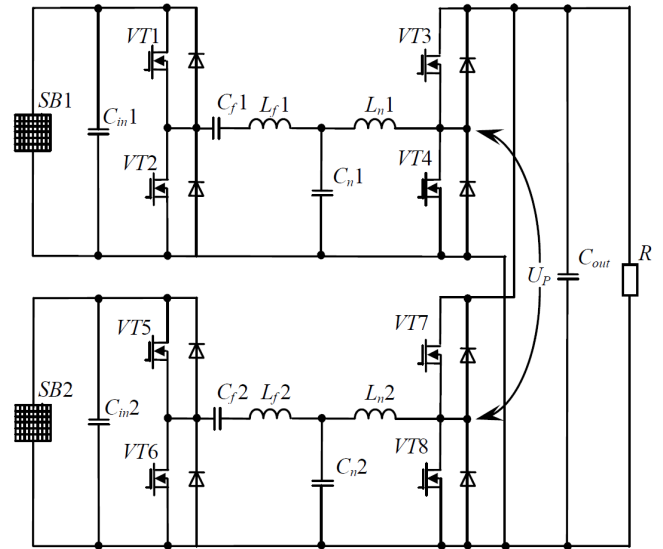


Fig. 7. Two-phase single-cycle resonant LCL-T converter.

The prototype consists of transistors IRFP4868, resonant inductors $L_{f1} = L_{n1} = L_{f2} = L_{n2} = 5.2 \mu\text{H}$, the magnetic core EILP 38/8/25, the resonant capacitor $C_{n1} = C_{n2} = 530 \text{ nF}$, with 5 capacitors K78-2-350-0.1 μF and one K78-2-350-0.033 μF . The calculated resonant frequency of LCL-T circuit is $f = 100 \text{ kHz}$. Received parameter waveforms of the

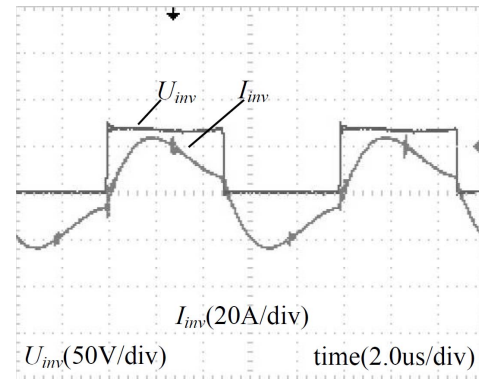


Fig. 8. The waveforms current and voltage curves of the inverter when $I_{SB1} = I_{SB2} = 7 \text{ A}$, $U_{out} = 100 \text{ V}$, $R = 12 \text{ Ohm}$.

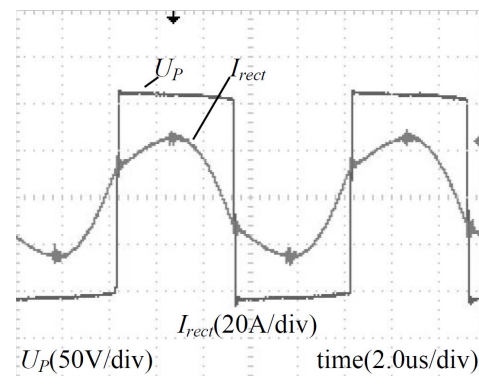


Fig. 9. The rectifier current and voltage between the inputs of the active rectifiers curves when $I_{SB1} = I_{SB2} = 7 \text{ A}$, $U_{out} = 100 \text{ V}$, $R = 12 \text{ Ohm}$.

resonant LCL-T converter with input current of one solar panel $I_{SB1}=I_{SB2}=7\text{ A}$, stabilized output voltage $U_{\text{out}}=100\text{ V}$ with the load $R=12\text{ Ohm}$ are shown in Fig. 8, Fig. 9.

Waverforms show a resonant mode converter performance. The inverter and the rectifier current forms are quasi-sinusoidal, due to the low quality factor and higher harmonics. An inverter current lagging and a rectifier current leading confirms transistors ZVS mode.

V. DISCUSSION OF THE RESULTS

The presented single-cycle LCL-T resonant converter has the parametric stabilization of the output voltage and has not the transformer, (which is presented in the full-bridge resonant converters), thus improving mass and dimension parameters. However, when the current of the resonant circuit is doubled, it leads to a significant increase in static losses. The use of multi-phase converter allows to aggregate the power of an arbitrary number of solar panels and reduce the ripple of the output filter.

VI. CONCLUSION

Thus, the presented single-cycle converter is effective in the spacecraft PSS with a large number of small capacity solar panels, which minimizes the static losses due to single-cycle mode of operation. In the spacecraft PSS with a large capacity of a single channel it is more reasonable to use full-bridge topologies.

The work is done within the implementation of the Decree of the Government of the Russian Federation of 09.04.2010, № 218, and the contract between the JSC Academician M.F. Reshetnev Information Satellite Systems and the Ministry of education and science of the Russian Federation from 01.12.2015 No. 02.G25.31.0182.

REFERENCES

- [1] Abdi B., Safaei A., Moghani J. S., Askarian A. An overview to soft-switching boost converters for photovoltaic // International Journal of Computer and Electrical Engineering. 2013. V. 5. No. 1. pp. 18-21.
- [2] Altintas N., Bakan A. F., Acsoy I. A novel ZVT-ZCT-PWM boost converter // IEEE Transactions On Power Electronics. 2014. V. 29. No. 1. pp. 256-265.
- [3] Bodur H., Bakan A.F. An improved ZCT-PWM DC-DC converter for high-power and frequency applications // IEEE Transactions On Industrial Electronics. 2004. V. 51. No. 1. pp. 89-95.
- [4] Milyakh A. N., Kubyshin B. E., Volkov I. V. Inductive-capacitive converters of voltage sources to current sources / Naukova Dumka, 1964. – 304 p. (in Russian)
- [5] Osipov A.V., Shinyakov Y.A., Shkolnyi V.N., Sakharov M.S. LCL-T resonant converter based on dual active bridge topology in solar energy applications // Journal of Aerospace Technology and Management. 2017. V. 9. No. 2. pp. 248-254.
- [6] Akshay K.R., Devendra P.R., Srinivasan D. A non-isolated bidirectional soft-switching current-fed resonant LCL DC/DC converter to interface energy storage in DC microgrid // IEEE Transactions on Industry Applications. 2016. V. 52. No. 2. pp. 1711-1722.
- [7] Kwon M., Oh S., Choi S. High gain soft-switching bidirectional DC-DC converter for eco-friendly vehicles // IEEE Transactions On Power Electronics. 2014. V. 29. No. 4. pp. 1659-1666.
- [8] Peretz M.M., Ben-Yaakov S. Digital control of resonant converters: resolution effects on limit cycles // IEEE Transactions On Power Electronics. 2010. V. 25. No. 6. pp. 1652-1661.
- [9] Osipov A.V., Shkolnyi V.N., Shiniakov Yu.A., Yaroslavlsev E.V., Shemolin I.S. Series resonant converter for discharge of batteries spacevehicles power systems // Proceedings of Tomsk State University of Control Systems and Radioelectronics. 2017. V. 20. – No. 2. pp. 103-110. (in Russian).



Sergey A. Zapolskiy was born in 1992 in Karaganda, Kazakhstan. In 2015, received a degree as engineer in industrial electronics in Tomsk State University of Control Systems and Radioelectronics (TUSUR). In 2016, he enrolled in TUSUR graduate school. Since 2015, he is working at the Research Institute of Space Technology of Tomsk University of Control Systems and Radioelectronics (TUSUR). Research interests: the power supply system of the spacecraft.



Alexander V. Osipov was born in 1978. in Semipalatinsk, a senior researcher of the Research Institute of Space Technology of Tomsk University of Control Systems and Radioelectronics (TUSUR), a candidate of technical Sciences. In 1999 graduated from the faculty of electronic engineering (TUSUR). He defended his thesis "High-frequency induction heating system parts before plastic deformation" in 2004. Research interests: power electronics, resonant converters, power supply systems.
e-mail: ossan@mail.ru



Ivan M. Zhuravlev, born in 1991. in Tomsk, Russia. In 2014, he received a degree as engineer in industrial electronics in Tomsk State University of Control Systems and Radioelectronics (TUSUR). In 2016, received a master's degree in industrial electronics (TUSUR). In 2016, he enrolled in TUSUR graduate school. 2016, works in JSC Academician M.F. Reshetnev Information Satellite Systems. Research interests: control system of the spacecraft.



Mikhail E. Khlystunov was born in 1994 in Samarskoe, Kazakhstan. In 2016 he received a Bachelor of Engineering and Technology degree in Industrial Electronics in Tomsk State University of Control Systems and Radioelectronics (TUSUR). In 2016, he enrolled in TUSUR master's program. Since 2016, he is working at the Research Institute of Space Technology of Tomsk University of Control Systems and Radioelectronics (TUSUR). Research interests: the power supply systems, control systems, space technology.

Universal Control System of a Semiconductor Electric Energy Converter on Programmable Logic Devices

Dmitri A. Matveyev, Alexander Yu. Balzamov, Yuri B. Fedotov, Sergey A. Nesterov
N. P. Ogaryev Mordovia State University, Saransk, Russia

Abstract – The article presents the results of the development of a universal control system for semiconductor power converters based on a programmable logic devices (PLD). As a result of the work done, shared functional modules for the various control systems of semiconductor converters were determined, the features of implementing modules on programmable logic were considered, and the algorithms for controlling converters on mathematical models were studied. The principal circuit diagram of the universal control system of the converter is synthesized on the basis of a combination of programmable logic devices and a microcontroller. The topologies of printed circuit boards and their layout in a single module of the universal control system of the converter are developed; the built-in microcontroller software was written and debugged in the assembler language. An experimental sample of the control system was made and its joint tests with a prototype of a low-power three-phase inverter equipped with a load simulator were carried out, oscillograms of control pulses and output voltage were obtained in various modes of inverter control.

Index Terms – semiconductor power converter, digital control system, programmable logic device, model, algorithm.

I. INTRODUCTION

THE RAPID development of wide range of semiconductor electric power converters caused by the creation of power semiconductor devices (PSD) with new features such as energy and frequency parameters. So the best examples of thyristors (T993-2000) operate at a voltage of 6 kV and a current of 2 kA for a single semiconductor device, and some IGB-transistors (FZ750R65KE3, MTKI-600-65TV) operate at a voltage of 6.5 kV and a current of 750 A.

Stable and trouble-free operation of PSD semiconductor electric power converters depends on the reliability of PSD and the reliability of control systems. Incorrect control signals forming due to a failure of the control system may cause damage or total failure of the converter PSDs that make approximately 60 % of the converter cost. It is also worth noting that control signals forming with floating time response adversely affects the PSD life time causing degradation of their characteristics, this is especially true if PSDs are connected in series or in parallel. In this regard, the study of methods and ways of control signals forming for converter valve units is an equally important task both from the position of the general design of the control system for

electric power converters, and from the position of the minimization of energy losses in transients during valve commutations.

II. PROBLEM DEFINITION

Most modern electric power converters carry out a multistage power transmission from the AC circuits to the DC circuit and back, wherein there are two power circuits: rectifier and inverter [1]. In different applications these circuits have variations in their circuitry, but 80% of them use common laws for the control system signals that control power valves.

This circumstance creates the initial conditions for the problem definition for the study and generalization of the most popular circuit solutions of digital control systems and optimization of control methods based on functional units mathematical models design. The ultimate goal is software and hardware implementation of a converter digital control system on the basis of programmable logic devices (PLD).

III. THEORY

The nomenclature of semiconductor converters includes a variety of apparatus for different branches of industry and energetic, the power capacities of these converters are in the range from a few kilowatts to tens of megawatts. In applications the converters can be divided into several areas [1]:

1. Back-to-back direct current converters for coupling inconsistent industrial networks.
2. Converters for dc drives.
3. Emergency power systems, battery charging sets.
4. Converters for electroplating baths.
5. Uninterruptible power supplies and their installations.
6. Converters for ac drives.

For the purpose of identifying general principles of the above listed converters structural analysis of the most common technical solutions for further development of requirements to design integrated control system was carried out. For example, in Fig. 1 presents a functional diagram of some of the most popular apparatus today of the power electronic apparatus — frequency converters (FC) for AC drives with variable frequency and output voltage.

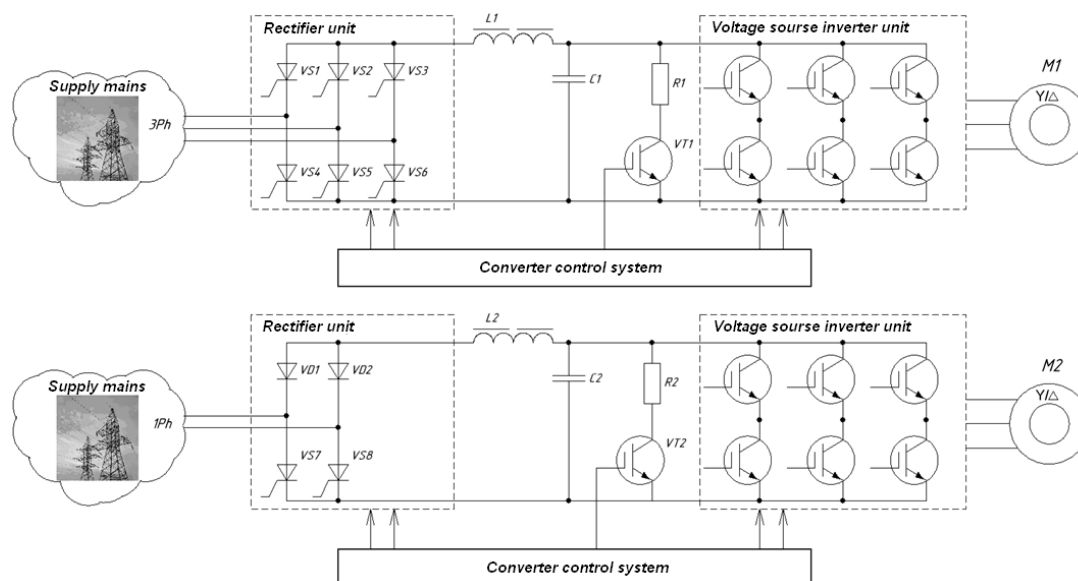


Fig. 1. Functional diagram of frequency converters (FC) for AC drives.

As loads are the drive motor windings with an explicit inductive character, then the output filter in this case is not required, current of the inverter is known to be sinusoidal in the case of the formation of the sinusoidal envelope signal of pulse-width modulation (PWM). This statement is subject to the Kostenko law (constancy of the ratio of the output voltage frequency to the amplitude). The input circuit of the converter can be designed based on uncontrolled, and the controlled rectifier, including rectifier with incomplete number of thyristors.

The main purpose of the controlled rectifier in the FC structure:

1. Provision of the high-speed protection feature. Failures when the inverter operation of the FC is associated with high reach-through breakdown currents (transistor or bypass diode breakdown) and short-circuit currents (phase short-circuit to pole, to case or to ground). High-speed disconnection from the power network can prevent large-scale development of the failure.

2. A smooth charge of dc-link capacitors. Capacitance value in dc-link of high power converters can reach ten thousands microfarads or more, which is determined by the reactive power of used motor. It is obvious that direct charging from the mains of such capacity in the initial moment of time is equivalent to a short circuit on the output of the rectifier, and the current surges will destroy the electrodes of the capacitors for a few hundred charge cycles.

One of the important distinctive elements of the structure of the converters is the presence of the brake key with the ballast resistor required to prevent overvoltage in the DC link caused by the process of electric braking in the transition of the electric motor to the generator mode. So overvoltage in the dc-link can reach four times the values of nominal voltage and lead to complete damage both of the rectifier and the inverter. The output stage of most frequency converters is based on the three-phase bridge inverter, controlled by a 6-channel pulse-width modulator that generates 3 mutually-counterphase signals for the transistors of each phase. In the particular case the duty cycle is modulated by three

sinusoidal envelopes, shifted by 120 el. degrees, the period and the amplitude of the envelope changes depending on the current speed setting for the rotor. Summarizing the results of the review of semiconductor converters, it is concluded that the bridge rectification and inversion circuits are used in 90% of the converter equipment apparatus, the base principles of formation of control signals remain unchanged and can be extended for each specific application with the aim of improving operating reliability. Combining elements of pulse-phase rectifier bridge control and elements of the PWM inverter bridge control into a single control system can ensure universal modular control system design for wide range of power converters for different applications can be ensured.

IV. EXPERIMENTAL RESULTS

A. Mathematical Simulation of the Control System Functional Units

For the purpose of a preliminary synthesis of the controller structure of the pulse-phase control system (PPCS) and study of its operating logic the combined simulation of the developed PPCS prototype and thyristor bridge was carried out in the simulation environment Sim Power System 9 (PSIM 9). The controller of three-phase bridge inverter on IGBT transistors with the load of three-phase induction motor having shaft rotation speed sensor was also simulated. During the study it was revealed that to increase efficiency of dc-link voltage usage it is acceptable to inject the third harmonic with amplitude up to 15% from the fundamental envelope frequency amplitude, in line load currents these components are suppressed and have no negative impact.

According to the obtained results of the preliminary modeling mathematical prototypes of control systems for the rectifier and the inverter were formed and the basic principles of their construction were defined. Further, the transition from mathematical models in PSIM environment

to the digital electronics element base was performed for subsequent implementation in a digital control system.

As the basis of construction programmable logic devices (PLD) were selected. The choice is determined by a number of reasons, one of which is a hardware implementation, with reference to the period of the reference sync that ensures the formation of control signals at precisely defined intervals. In contrast to the sequential software implementation of algorithms for microprocessor, in PLDs all processes are run in parallel and synchronously with the periods of the clock generator. The most significant is the low susceptibility to faults of the finite logical automaton implemented on the PLD basis, while software cyclic process handlers are prone to 'hang', for example, in the case of a stack overflow or

when you exit subroutines to the wrong address [2]. Thus, the further design of the integrated control system was carried out taking into account the peculiarities of its elements location in the form of synthesized logical structures in the PLD crystals. As rectifier and inverter control systems have no communication except for the configuration operating modes interface, it is advisable to allocate them to individual controllers and to carry out successive study of their configuration.

B. Three-Phase Rectifier Controller

Block diagram of a three-phase rectifier controller is shown in Fig. 2. Consider its composition.

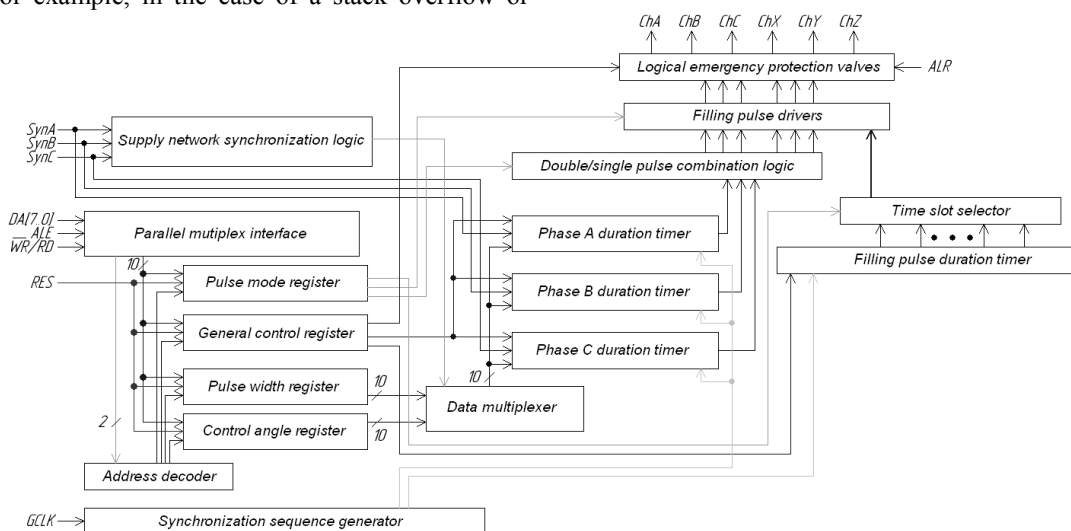


Fig. 2. Structural diagram of a pulse-phase controller of a three-phase rectifier.

A communication base of PPCS controller is a parallel 8-bit interface with multiplexed address and data bus. The interface is intended for operating modes configuration of the controller and the data exchange with the central processor of the integrated control system. The controller equipped with parallel interface is preferable, as it allows integrating the configuration registers of the PPCS controller in the address space of the I/O control microprocessor, as well as without significant difficulties adding and changing the number of peripheral control registers attended by parallel interface. Using the principle of multiplexing requires a smaller amount of involved outputs of the central processor, which will simplify subsequent tracing and layout of the printed circuit board of the integrated control system.

Implemented parallel interface block performs a 2-byte transferring, first, a destination address is sent to the internal buffer, where it is received by the internal address decoder, after which the data bytes is sent via internal bus to the destination register. The internal bus interconnects four software-accessible register to store configuration values, two of which have bit-oriented flag format, their adjusting determines the operation mode of the PPCS controller. The mode configuration allows configuring a single or dual pulse, setting the duration of the control impulse, choosing continuous control pulse or pulse filled with high frequency component, selecting the duration of the initial forcing impulse. In addition two lines of digital output are program-

accessible which can be used at the discretion of the user's discretion, for example, to control the contactor network connection or switching output polarity relay.

The next important unit of PPCS controller is a block of three timers, each of which counts time slots only to control one of three phases. To save the area occupied on the chip, the phase timers by turns count time intervals of angle of control and duration. The values of the counted time intervals by turns are fed to the timer from the respective registers using the data multiplexer under the control of the logic unit receiving synchronization from the mains supply. This block of logic plays the role of decoder and depending on the synchronization input status sends to multiplexer a signal to commutate communication link from the corresponding timer to a counting time interval register. Formed by three channels of the timer pulses arrive at the logic combination block, where the separation time intervals and the conversion of the three phase channels to six control channels, one for each half period of the phase performed. The logic combination block uses the mode register flag, switching step pulse overlaps from the next phase of the 6-channel system to get dual or single pulses. Next, the resulting pulse sequence is processed by the HF filling forming unit, for which the time intervals are formed by a separate timer and selector. This timer is significantly different from the phase timers, so as to save resources it is made on the basis of the fixed frequency set former, and cannot be software

reconfigured. To control the filling selection a program-accessible selector is used which allows applying a frequency from one of the timer fixed outputs to the filling unit. For the correct operation of PPCS controller synchronization former is required which converts a sinusoidal mains voltage to rectangular synchronizing sequence. It should be noted that the three-phase bridge scheme of the rectifier performs rectification of the line voltages, at the same time the rules of electrical safety demand that control system must either have galvanic insulation from live high-voltage circuits or use of protective earth as a potential common point. In this case, to obtain the synchronization an insulation transformer is used, which allows galvanic insulation, and synchronization from the line voltages. But in some cases the use of the transformer is difficult because of its weight and size parameters or impossibility of making interwinding insulation corresponding to the operating voltage. But it is possible to use resistive dividers of the phase voltages to obtain synchronization signals, with the formation of the line voltage synchronizing sequence from the phase voltage obtained by dividers.

In the structure of the control system shaper can be made on the basis of the three comparators covered by the hysteresis loop to prevent false switching. It is worth noting individually the use of only one polarity for the entire power supply circuit; this was achieved by shifting the input voltages to the positive polarity area by applying the virtual zero method to the resistive-capacitor divider. At the same time, the circuit has become insensitive to the presence of a constant component between the common point of the star connection of the three-phase network and the ground point, which also positively affects the stability of the synchronization former.

The last in the path of the fully formed PPCS signals is one of the most crucial elements of the entire controller — a block of emergency protection valves, the main purpose of which is to allow or prohibit the passage of generated pulses to the external pins of the controller chip, and also to act as a bus driver to increase the load capacity of external terminals.

A separate block in the block diagram of the implemented controller is a dedicated unit of the synchronizing sequence. This unit receives a clock signal through the external GCLK input, divides its frequency, and then distributes it to internal units, in particular upon its operation the controller's operation as a whole, as well as the duration of all generated time intervals depends.

The operation of all units of the described control system was simulated in the VSM ISIS7 Proteus environment. Further development of detailed models was carried out in the automated design and simulation environment of ALTERA Quartus II, which allows simulating the work of the derived configuration taking into account the features of the programmable logic chips, calculating the required logical capacity necessary for placement on a PLD. The results of the simulation fully confirmed the preliminary theoretical calculations. The total logical capacitance

required for configuring the rectifier controller was 134 logical macro cells.

C. Three-Phase Inverter Controller

Then, the block diagram of the three-phase inverter controller was developed, which is shown in Fig. 3. Just like in the structure of the rectifier controller, in this structure there is a parallel port with an address decoder for specifying operating modes, the circuit model of the port does not have any differences from the one mentioned above. Such a solution allows further comparatively simple combining of the address space of both controllers to obtain a single interface for accessing internal register files, both of the rectifier controller and the inverter. For communication with external devices, a synchronous serial port of the analog-to-digital converter (ADC) controller has been added, the main tasks of which are continuous interrogation of the channels and transmission of the conversion results via a serial bus for placement in internal memory cells [3]. Loaded values can later be used by the internal modules of the inverter controller or transmitted via a parallel multiplexed bus to an external device. In order to obtain a universal three-phase inverter controller, additional blocks were added to the block diagram, which were absent in the preliminary modeling stage. Thus, an acceleration-deceleration unit was added that includes an accumulator for generating a frequency change rate and a reverse counter that determines the current output frequency setting and receives clock pulses when overflow of the accumulator occurs. And also a block of dependent change in the amplitude of the envelope from the current frequency, based on the shifting multiplier. These units are designed for building control systems where the inverter is used as part of a frequency converter for an AC drive and can be disabled when using a control system in conjunction with an output stage inverter at an uninterruptible power supply.

For flexible adjustment of the inverter control system, 2 selectors available through the external interface are provided in its structure. Selectors choose the sources of amplitude and frequency setting that can be analog inputs of the ADC, internal registers of the parallel interface, or modules for controlling the electric drive.

The formation of the sinusoidal envelope period is made by counting the clock periods in the accumulating adder that come from the synchronizing sequence generator. When the adder overflows, its accumulation register is reloaded with a certain number that determines the required output frequency of the envelope, at the same time, the address counter of the sine table is incremented. In order to save internal memory resources, the table contains sine values only in the range of 180 degrees, with 8-bit amplitude sampling. To form an envelope in the range of more than 180 degrees (this is indicated by the transition of the highest digit of the address counter to the log 1), the original table data is multiplied by – 1. This action is performed in a 12-bit parallel multiplier together with multiplying by the value of the current amplitude reference.

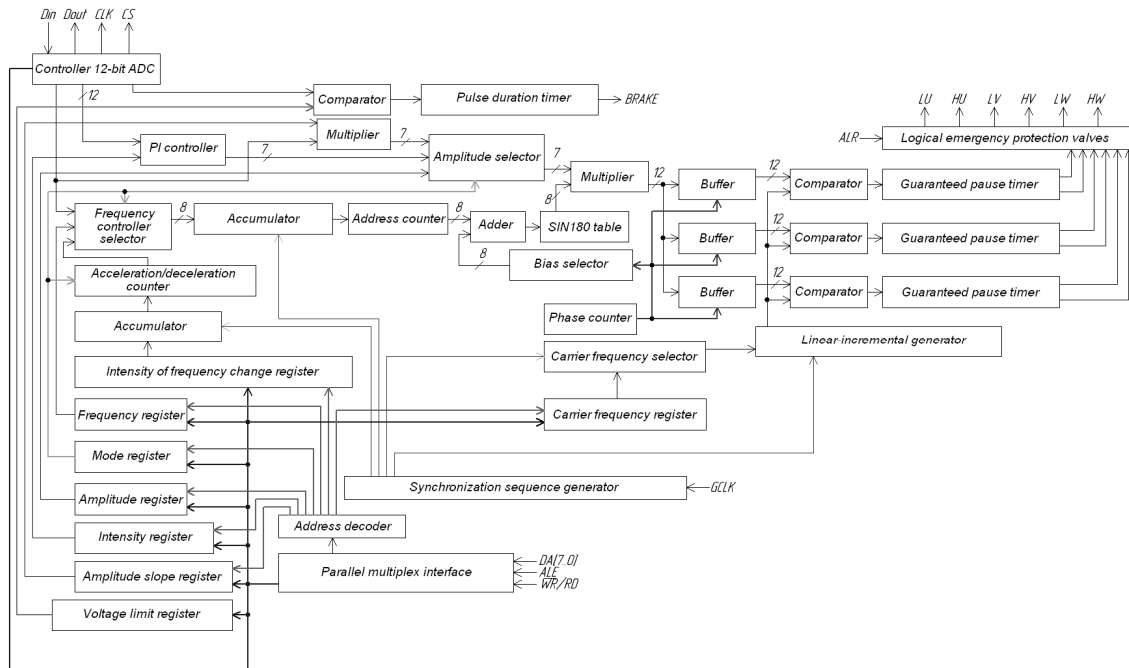


Fig. 3. Block diagram of the pulse-width controller with a sinusoidal envelope for a three-phase inverter.

In the structure of the inverter controller, there are buffers which store the current value of the modulation factor for each phase, which is updated each time the address counter of the sine table is changed. Also, these buffers together with the phase counter, offset selector and address adder are designed to organize the shift of sinusoidal envelopes in phases. It is organized as follows: simultaneously with the change of the base address counter, the operation of the phase counter is enabled, which sequentially selects increments to the current address in the sine table through the offset selector. Simultaneously, strobe signals are output to write the value from the table to the corresponding phase register. After all three buffer phase registers are reloaded with new values the phase counter is locked until the next step of the base address counter in the table. The last block is a pulse-width modulator consisting of three 12-bit code comparators and a linearly incrementing code generator that determines the carrier frequency of the modulation. From the output of each comparator, the signal goes to the guaranteed pause timer, which delays the switching front of the PWM signal received from the comparator for a fixed time, thereby introducing a guaranteed pause in the operation of the gates when they are mutually switched. The last in the path of the generated control signals of the inverter is a block with logic gates of emergency protection, which has priority control from an external protective device on the alarm ALR signal. This solution allows creating in the control system a two-level independent protection for disconnecting the converter under emergency operating conditions.

Based on the simulation results of the inverter control system, the logical capacitance required for configuring the on the PLD chip, which was 797 logical macro cells, was obtained.

D. Integrated Digital Control System

Based on the previously performed modeling results in the Quartus II environment, data were obtained on the logical capacity required for the hardware implementation of the converter control system, which is a total of 931 macro cells. This allows us to make a preliminary conclusion about the possibility of its placement with some margin in the volume of the chip of a programmable logic device (PLD) with CPLD structure and a maximum capacity of 1270 macro cells. At the same time, the remaining logical capacity in 339 macro cells is not enough to place an integrated microprocessor on the crystal with the goal of overall coordination of the entire control system. Thus, there are two possible ways of solving the problem [4]:

1. Use a more capacious FPGA array with FPGA architecture (EP1C3T144)
2. Use of a separate external microprocessor and FPGA with CPLD architecture (EPM1270T144).

The use of ALTERA PLD of the Cyclone series will require external configuration memory (EPCS4), as well as in addition to the main 5 V, 3.3 V power supplies, an additional 1.8 V power supply. At the same time, for convenience of debugging work, it is necessary to place an external program memory chip for the integrated microprocessor. It should also be noted that converting projects with a logical capacity of more than 1500 macro cells into the basis of basic matrix crystals (BMC) becomes difficult, and can serve as an obstacle to the transition to the production of semi-custom chips by third-party manufacturing plants. In the second variant, the use of an external microprocessor is more convenient for debugging in conjunction with a LSI of a programmable logic CPLD device. And compared to the first, this solution does not increase the number of chips on the PCB of the integrated control system, because the CPLD does not require a

configuration memory, and only one 3.3 V power supply is enough.

The general structural diagram of the complex control system is shown in Fig. 4, it consists of two basic elements: a

microprocessor and a converter LSI based on a CPLD architecture programmable logic device.

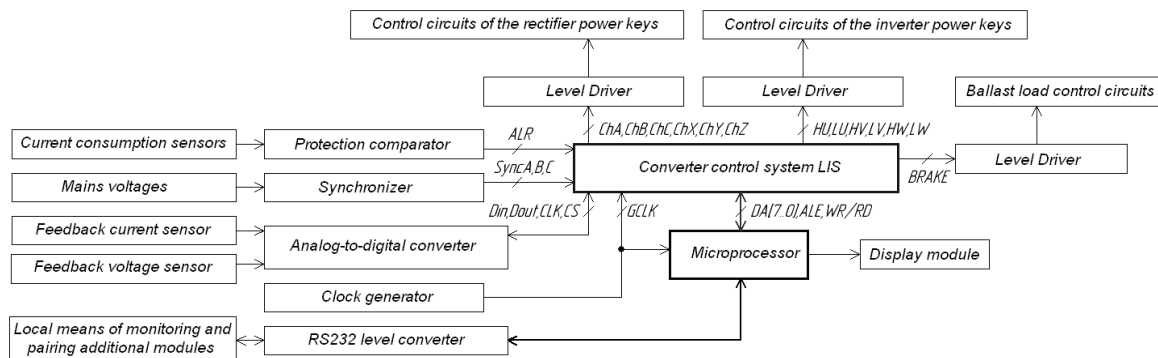


Fig. 4. General structural diagram of an integrated control system.

In this case, the microprocessor performs the peripheral functions of the control system, such as the formation of the operator menu structure, the maintenance of the display and the external serial interface. Also, the microprocessor is the master on the multiplexed parallel bus, which connects it to the internal registers of the hardware controllers of the rectifier and inverter, which are placed on the PLD chip. The Intel MCS-51 (C8051) architecture was chosen as an external microprocessor, since it is de facto an industrial standard, and is produced by a variety of different manufacturers, including the domestic industry [5]. In addition, it is possible to simply expand the external data memory, which can be used to interface with the parallel bus of the controller being implemented. With this construction of a complex control system, the microprocessor is completely freed from the rigid time constraints on the formation of control signals for power devices, and consequently, software malfunctions can not affect the correctness of the control signal output and entail an uncontrolled emergency situation.

As can be seen from the block diagram, the operating logic of the PLD configuration includes the functions of data collection from feedback circuits, such as current and voltage sensors. However, PLDs do not have analog units in their structures and operate only with digital signals. In this regard, the integrated control system must contain an external microcircuit of a multichannel analog-to-digital converter, connected via a serial interface with a maximum exchange rate 1.5 Mbit/s, which for a 12-bit ADC, taking into account the time of channel selection, will be ~ 90 kbps per channel. To prevent the development of fault currents associated with a short-circuit at the output of the power converter or overload, it is envisaged that there will be a hardware-implemented separately realized protection comparator that outputs a trip signal to the PLD output buffers, leading to an instantaneous termination of the control signal supply to the power devices regardless of the current state of the internal logic.

Since the PLD input have low load capacity and operate with logic levels of CMOS 3.3 V, the signals generated on them can not be directly used to control the power switches and can not be transmitted over a distance of more than a ten centimeters. To overcome this limitation, the structure of the

complex control system should contain level drivers that allow you to transmit control signals via external communications directly to the drivers of power devices.

Thus, a complete complex control system for a power converter containing one set of rectifier and one set of inverter can be fully implemented in a single-board version, including an operator interface and an external automated engineering process control system.

E. Implementation of the Control System

The design of a universal control system for semiconductor power converters was carried out on the basis of the conditions for ensuring broad compatibility with both primary current and voltage sensors and with drivers of power semiconductor devices. Simultaneously, when implementing the control system, the interaction with the operator problems was solved by creating a convenient man-machine interface that allows displaying the parameters of the system operation, the structure of the menu items and inputting the necessary initial data. To display and enter the current parameters, operating modes, as well as display menu items, there is a keyboard-display module made in two versions: resident-located in the case along with the motherboard, and remote-located outside the control system which can be used for remote control at a short distance. Operating of the keyboard and display is carried out by the peripheral controller on the main board of the system.

The control system also provides a number of opportunities for interaction with external control devices and automated control systems of the upper level, there is a port for connecting the ATISP in-circuit debugger or a remote keyboard/display module. The control system is clocked from two sources: the microcontroller is clocked from an internal oscillator stabilized by a 22.118 MHz quartz oscillator and a peripheral controller made on a PLD — from an external quartz oscillator with a frequency of 32.768 MHz. The choice of such frequencies is determined by the convenience of the frequency division multiplication of the fundamental frequency, in the case of the MK, to obtain a standard grid of transmission speeds of the UART port

(115200 bps, 57600 bps), and in the case of PLD time intervals multiple of 1 second.

The algorithm of the software executed on the resident microcontroller includes the process of initial initialization, activation of protections and preparation of the operator interface (display of menu lines on the display). The second part of the algorithm contains a branch tree that distributes the CPU time between several different tasks connected through the command handler. The branch tree forms the main program cycle, the execution of auxiliary and serving tasks is performed in the handlers of the corresponding interrupts. In accordance with the elements of the developed algorithm and the peculiarities of access to resources of the peripheral controller in assembler language, the target software for the AT89S8253 microcontroller with the advanced MCS-251 architecture was written, with the time of most instructions execution for 2 cycles of the clock generator [6].

Based on the results of the prototyping of circuitry solutions, the final setup of the hardware and its joint debugging with the software, printed circuit boards of the mock-up model of the universal control system based on PLDs were developed and traced. The model consists of two mainboards: the basic one, on which all the main components are located, and the display board, on which the keyboard, the valcoder, the OLED display are located. The boards are stacked one above the other, and are connected via a BLS pin interconnect connector. The layout of all boards is mainly made using electronic components of surface mounting (SMD), which allowed to increase the density of mounting and significantly reduce the volume of the enclosure occupied by the CS. For convenient connection of external cable connections, the connection terminals are arranged in a row from the top and bottom sides of the printed circuit board, and are made in the form of rupture screw terminals. Tracing of the signal lines of the base printed circuit board was carried out whenever possible in one layer, on the side of the surface mounting components, in the upper layer there are local transitions of the power lines and the distribution lines of the reference voltage. Most of the top layer is covered with a massive polygon connected to the "ground". This solution maximizes noise immunity by screening the signal distribution circuits located in the lower layer.

Photographs of the control system in assembled form are shown in Fig. 5 and 6.

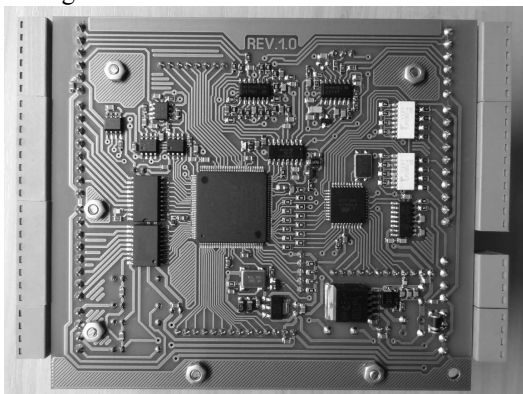


Fig. 5. Photo of the control system (view from the elements side).



Fig. 6. Photograph of the control system assembled.

V. DISCUSSION OF RESULTS

The experimental check of the functioning of the prototype model of the control system was carried out by the step-by-step study of the oscillograms of the converter control signals from the corresponding outputs of the control system in various modes and with various parameters for generating the output pulse sequences of the PSD control. So, in Fig. 7 shows the oscillogram on which 6 channels of control of the rectifier thyristors in the mode of doubling and high-frequency filling with a regulation angle of 1 ms and a total pulse width of 650 mks were captured.

Also, a check was made of the formation of six transistor control signals in a pulse-width modulated inverter and the quality of the sinusoidal envelope formed by the inverter. For this purpose, a number of experiments were carried out in which the output signals of the designed control system were fed to a low-power three-phase bridge inverter. The output of the inverter, in turn, was loaded onto an L-shaped low-pass filter designed to cut off the high-frequency PWM carrier, create a current loop and simulate the load. Fig. 8 shows the voltage waveforms taken at the output of the inverter (channel 1) and at the output of the filter (channel 2).



Fig. 7. Oscillogram of phase A of the supply network and 6 channels at the output of the control system with a pulse width of 650 mks.

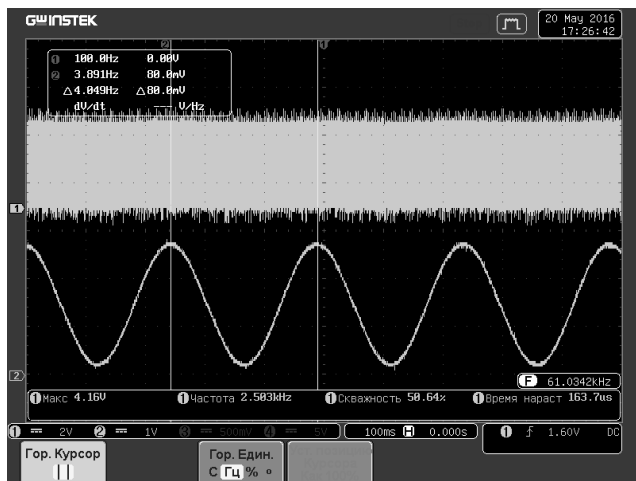


Fig. 8. Oscillogram of the sinusoidal envelope of the W phase obtained after the LPF in the mode of deep sinusoidal modulation with a frequency of 4 Hz.

VI. CONCLUSION

The considered universal control system for semiconductor power converters based on a combination of PLD with a microcontroller has a number of advantages (noise immunity, reliability, flexibility, compactness, etc.) and can be used after an appropriate adjustment in the vast majority of modern devices of power converter technology [7]. Particularly, it should be noted that it can be carried out entirely on the domestic element base.

The article was prepared as a part of applied research (AR) according to the Agreement on the provision of subsidy No. 14.574.21.0135 with the financial support of Russian Federation Ministry of Education and Science. The unique identifier of AR is RFMEFI57417X0135.

REFERENCES

- [1] Semyonov B.Yu. Power electronics: from simple to complex. – M.: SOLON-Press, 2005. – 416 p. (in Russian).
- [2] Cteshenko V. B. Altera PLD: element base, design system and hardware description languages. – M.: Publishing House "Dodeka XXI", 2007. – 576 p. (in Russian).
- [3] Stuart R. Ball. Analog interfaces of microcontrollers. – M.: Publishing House "Dodeka XXI", 2007. – 360 p. (in Russian).
- [4] Kostrov B. V., Ruchkin V. N. Architecture of microprocessor systems. – M.: Publishing House Dialog-MIFI, 2007. – 304 p. (in Russian).
- [5] Gladstein M. A. Microcontrollers of mixed signal C8051 from SiLab and their applications. User guide. – M.: Publishing House "Dodeka XXI", 2008. – 336 p. (in Russian).
- [6] Ernie Kasper. Programming in assembly language for microcontrollers of the 8051 family. – M.: Goryachaya liniya – Telecom, 2004. – 191 p. (in Russian).
- [7] Matveyev D. A., Balzamov A. Yu. Development of a control system for a semiconductor power converter on PLD // Practical power electronics, 2017. No 4 (68). pp. 18–26. (in Russian).



Dmitri A. Matveyev, born in 1988 in Voronezh, Russia, graduated from the faculty of Electronic Engineering of N. P. Ogarev Mordovia State University in 2010. Since 2010 he has been working in the "Electronic and software systems" innovative company. In 2014 he became a winner of the All-Russia competition called "Engineer of the year". The field of scientific interest is specialized high-performance units of control systems based on programmable logic matrices.



Alexander Yu. Balsamov, born in 1955 in Saransk, Russia, graduated from the faculty of Electronic Engineering of N. P. Ogarev Mordovia State University in 1977. In 1981 he got a degree of the candidate of technical science at Leningrad Electrotechnical Institute. Since 1982 he has been working at the Faculty of Electronic Engineering (later – the Institute of Electronics and Lighting Engineering) of Mordovia State University. In 1989 he received the academic title of Associate Professor. Currently he is an Associate Professor of the Department of Electronics and Nanoelectronics. The field of scientific interest is the development of microprocessor control systems and automated information systems for various purposes. A number of developments in which he took part were put in commercial operation at some enterprises and organizations of the Russian Federation.



Yuri B. Fedotov, born in 1951 in the village of Bogdanovka, Staroshaigovski district of Republic of Mordovia, graduated from the faculty of Electronic Engineering of N. P. Ogarev Mordovia State University in 1974. In 1985 he got a degree of the candidate of technical science at Moscow Power Engineering Institute. Since 1987 he has been working at the Faculty of Electronic Engineering (later – the Institute of Electronics and Lighting Engineering) of Mordovia State University. In 1994 he received the academic title of Associate Professor. Currently he is a Head of the Department of Electronics and Electrical Engineering. The field of scientific interest is the power electronic units modeling and development. A number of developments in which he took part were put in commercial operation at some enterprises and organizations of the Russian Federation.



Sergey A. Nesterov, born in 1949 in Saransk, Russia, graduated from the faculty of Electronic Engineering of N. P. Ogarev Mordovia State University in 1972. In 1977 he got a degree of the candidate of technical science at Leningrad Electrotechnical Institute. Since 1977 he has been working at the Faculty of Electronic Engineering (later – the Institute of Electronics and Lighting Engineering) of Mordovia State University. In 1985 he received the academic title of Associate Professor. Currently he is an Associate Professor of the Department of Electronics and Electrical Engineering. The field of scientific interest is the power electronic units modeling and development. A number of developments in which he took part were put in commercial operation at some enterprises of the Russian Federation.

Mathematical Analysis of Multiport Converter Operation Modes

Vadim E. Sidorov, Dmitri A. Shtein, Ilya V. Zaev, Maxim A. Khoroshev
Novosibirsk State Technical University, Department of Electronics and Electrical Engineering,
Novosibirsk, Russia

Abstract– Multi-port converters are used in spacecraft where an important criterion is the weight and size indicators. In this paper topology of multi-port converter, which ensures required work modes is proposed. Mathematical analysis of electromagnetic processes was conducted and dependences of the output voltage and current of the battery were obtained.

Index Terms – Multi-port converter, solar panel, control method, DC-DC converter.

I. INTRODUCTION

NOWADAYS MULTI-PORT converters are widely used for power supplying of autonomous objects such as spacecrafts, vehicles and distant objects.

In general, multiport converters perform function of simultaneous or alternating load supplying from different, independent sources of energy and also distribute excess energy between energy sources. Energy sources, for instance, are storage batteries, solar panels, fuel elements, wind generators and etc. The main problem in designing of converters described above is a specific of each power source which expressed at volt-ampere and volt-watt characteristics.

Among the various topological solutions of multi-port converters, it is possible to distinguish converters with separated functional blocks of energy conversion. This blocks are well-known topologies. The main advantage of similar converter topologies in independent control of each energy sources power consumption. This allows consider non-linear characteristics of each energy source and works at wide voltage range. The disadvantage of similar converters is large weight, dimensions and implementations complexity [1, 2].

There are also converters with the presence or absence of galvanic isolation between the sources of energy and the load can be distinguished. Galvanic isolation at similar converters allows conforming voltage levels of sources and load. And it increases electrical safety of converters using too. The main galvanic isolations disadvantage is using additional intermediate conversion blocks such as DC-AC and AC-DC to ensure passing energy through transformer. This is significantly affects increasing of weight and dimensional characteristics [3, 4].

An alternative topological solution is non-galvanically isolated converters, in which functional blocks are combined. That is, the load power and power redistribution between the sources occurs through the same circuit elements. This

allows you to significantly simplify the design, reduce the weight and dimensions [5].

II. PROBLEM DEFINITION

The result of previous studies was a multiport converter with integrated functional blocks [6]. It consisted of two inductances, three transistors and one diode, which made its weight and dimensions low. But the main disadvantage was the lack of ability to charge the battery with low battery voltage and high power consumption, if solar battery has enough power for this.

In result of search new topologic multiport solution was developed to eliminate this disadvantage.

III. DESCRIBING OF MULTIPORT CONVERTER TOPOLOGY

In this paper presented a new topology of converter with united functional blocks without galvanic isolation. Energy sources are solar panel (SP) and accumulator battery (AB).

Configuration of converter presented at Fig. 1.

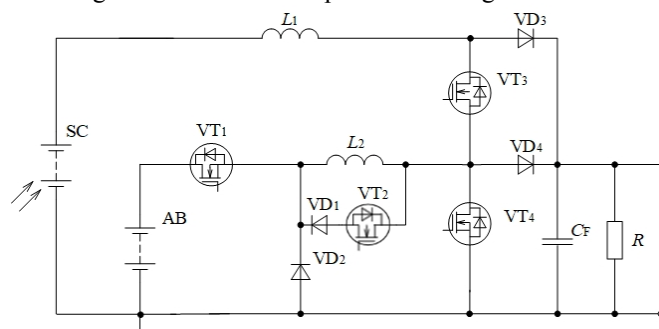


Fig. 1. Configuration of multiport converter.

Presented converter can ensure next work modes:

1. Load supplied from AB.
 2. Limitation of the AB current during a short-circuit of the load;
 3. Load supplied from SP;
 4. Load supplied from SP and stabilization of AB current.
- Describing of each work modes presented down below.

IV. CONVERTER WORKMODES

1. Load supplied from AB.

At this mode voltage on SP is absent and all load power is consumed from the battery. Transistor VT_1 is constantly in a conducting state, transistors VT_2 and VT_3 are closed.

Regulation and stabilization of load voltage is carried out by switch VT_4 . Equivalent circuit of converter with taking into account the open state of power switches is presented at Fig. 2.

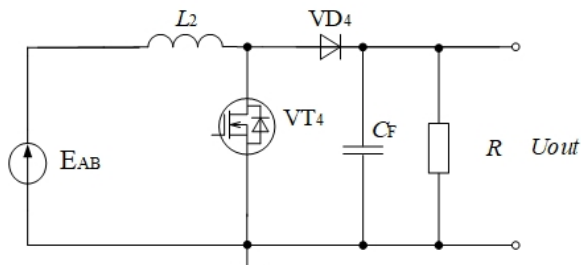


Fig. 2. shows that equivalent circuit at this mode presents a conventional boost converter.

2. When load is short-circuited, limitation of the battery current is realized by controlling transistor VT_1 . When transistor VT_1 at off-state, inductance L_2 current flows through the diode VD_2 .

3. At «load supplied from SP» mode, the battery disconnects from work, transistors VT_1 and VT_2 are closed, a transistor VT_4 is constantly in a conducting state. Stabilization of load voltage and limitation of SP current is carried out by switching VT_3 .

Equivalent circuit of the voltage converter with taking into account equivalent circuit of solar panel is presented at Fig. 3.

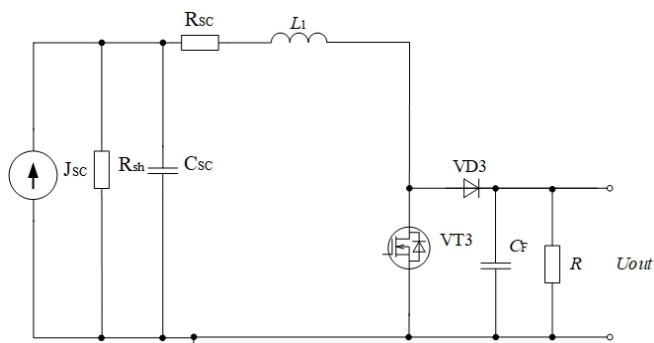


Fig. 3. shows that equivalent circuit at this mode is shunt regulator of solar panel current.

When the power of solar panel is insufficient to power the load due to low illumination, the transistor VT_3 is completely closed, and the load power can be provided simultaneously from the solar panel and the battery.

4. When load of the converter supplied from SP, battery charge can be realized by using excess of power. The algorithm of work at this mode is described in detail down below.

V. ALGORITHM OF WORK AT LOAD SUPPLIED FROM SP AND STABILIZATION OF ABCURRENT MODE

When it becomes necessary to start charging the battery transistor VT_4 passes from a permanently conducting state to

a switched. In this mode power switch $vt1$ is closed, but reversed diode of this switch is conduct. Current flows to the battery through this diode. Transistor VT_2 is on conduction state and shunt inductance L_2 through diode VD_1 . Stabilization of load voltage and stabilization of AB charge current is carried out by switching power transistors VT_3 and VT_4 .

Equivalent circuit of the voltage converter with taking into account equivalent circuit of SP and AB is presented at Fig. 4.

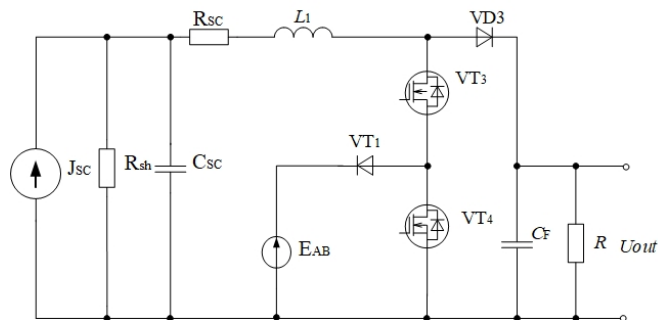


Fig. 4. Equivalent circuit of «load supplied from SP and stabilization of AB current».

Proposed converter operation algorithm consists of 3 operating states. Each of power switches VT_3 , VD_2 , VT_4 , VT_1 correspond to switching functions that take values 0 and 1, as shown in Fig. 5. Controlled parameters are duty ratios D_1 and D_2 and determining the relative durations of the conducting state of the transistor VT_3 and VT_4 , respectively, and taking values in the range from 0 to 1. Period of switching functions is equal to T .

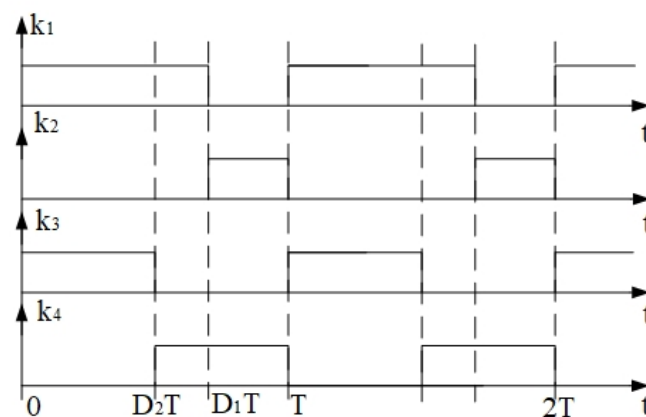


Fig. 5. Graph of commutation functions.

VI. ANALYSIS OF ELECTROMAGNETIC PROCESSES IN A CONVERTER

When analyzing electromagnetic processes, it was assumed that there is no loss in capacitors and inductances. Taking these assumptions into account, systems of differential equations are compiled for three operation states circuit in matrix form.

The matrix system of differential equations for the first working cycle:

$$\begin{bmatrix} \frac{du_{c_{sc}}}{dt} \\ \frac{di_{L_1}}{dt} \\ \frac{du_{out}}{dt} \end{bmatrix} = \begin{bmatrix} -\frac{1}{R_{SH} \cdot C_{SC}} & -\frac{1}{C_{SC}} & 0 \\ \frac{1}{L_1} & -\frac{R_{SC}}{L_1} & 0 \\ 0 & 0 & -\frac{1}{R \cdot C_F} \end{bmatrix} \cdot \begin{bmatrix} u_{c_{sc}} \\ i_{L_1} \\ u_{out} \end{bmatrix} + \begin{bmatrix} \frac{1}{C_{SC}} & 0 \\ 0 & 0 \\ 0 & 0 \end{bmatrix} \cdot \begin{bmatrix} J_{SC} \\ E_{AB} \end{bmatrix}. \quad (1)$$

The matrix system of differential equations for the second working cycle:

$$\begin{bmatrix} \frac{du_{c_{sc}}}{dt} \\ \frac{di_{L_1}}{dt} \\ \frac{du_{out}}{dt} \end{bmatrix} = \begin{bmatrix} -\frac{1}{R_{SH} \cdot C_{SC}} & -\frac{1}{C_{SC}} & 0 \\ \frac{1}{L_1} & -\frac{R_{SC}}{L_1} & 0 \\ 0 & 0 & -\frac{1}{R \cdot C_F} \end{bmatrix} \cdot \begin{bmatrix} u_{c_{sc}} \\ i_{L_1} \\ u_{out} \end{bmatrix} + \begin{bmatrix} \frac{1}{C_{SC}} & 0 \\ 0 & -\frac{1}{L_1} \\ 0 & 0 \end{bmatrix} \cdot \begin{bmatrix} J_{SC} \\ E_{AB} \end{bmatrix}. \quad (2)$$

The matrix system of differential equations for the third working cycle:

$$\begin{bmatrix} \frac{du_{c_{sc}}}{dt} \\ \frac{di_{L_1}}{dt} \\ \frac{du_{out}}{dt} \end{bmatrix} = \begin{bmatrix} -\frac{1}{R_{SH} \cdot C_{SC}} & -\frac{1}{C_{SC}} & 0 \\ \frac{1}{L_1} & -\frac{R_{SC}}{L_1} & -\frac{1}{L_1} \\ 0 & \frac{1}{C_2} & -\frac{1}{R \cdot C_F} \end{bmatrix} \cdot \begin{bmatrix} u_{c_{sc}} \\ i_{L_1} \\ u_{out} \end{bmatrix} + \begin{bmatrix} \frac{1}{C_{SC}} & 0 \\ 0 & 0 \\ 0 & 0 \end{bmatrix} \cdot \begin{bmatrix} J_{SC} \\ E_{AB} \end{bmatrix}. \quad (3)$$

In general form, the matrix equations are as follows:

$$\frac{dx}{dt} = A_1 \cdot x + B_1 \cdot v; \quad (4)$$

$$\frac{dx}{dt} = A_2 \cdot x + B_2 \cdot v; \quad (5)$$

$$\frac{dx}{dt} = A_3 \cdot x + B_3 \cdot v. \quad (6)$$

The matrix coefficient can be written as follows:

$$A = D_2 \cdot A_1 + (D_1 - D_2) \cdot A_2 + (1 - D_1) \cdot A_3; \quad (7)$$

$$B = D_2 \cdot B_1 + (D_1 - D_2) \cdot B_2 + (1 - D_1) \cdot B_3. \quad (8)$$

Combine the equations (4-8) in one equation:

$$\frac{dx}{dt} = A \cdot x + B \cdot v.$$

Then the general solution for the mean values is as follows:

$$X = -A^{-1} \cdot B \cdot v. \quad (9)$$

Using expression (9), the expression for the average value of the load voltage can be found:

$$U_{out} = \frac{R \cdot (1 - D_1) \left[(D_2 - D_1) \cdot E_{AB} + J_{SC} \cdot R_{SH} \right]}{R \left(D_1^2 - 2 \cdot D_1 + \frac{R_{SH} + R_{SC}}{R} + 1 \right)},$$

And expression for the average charge current of AB:

$$I_{AB} = I_{L_1} \cdot (D_1 - D_2) = \frac{\left[J_{SC} \cdot R_{SH} + (D_2 - D_1) \cdot E_{AB} \right] \cdot (D_1 - D_2)}{R \left(D_1^2 - 2 \cdot D_1 + \frac{R_{SH} + R_{SC}}{R} + 1 \right)}.$$

Neglecting the relatively small internal resistance of SP, and also assuming that the term $J_{SC} \cdot R_{SH}$ is much larger than the term $(D_2 - D_1) \cdot E_{AB}$ simplified expressions for the load voltage and charging current AB can be obtained:

$$U_{out} = \frac{(1 - D_1) \cdot J_{SC} \cdot R_{SH}}{\left(D_1^2 - 2 \cdot D_1 + \frac{R_{SH}}{R} + 1 \right)}, \quad (10)$$

$$I_{AB} = \frac{J_{SC} \cdot R_{SH} \cdot (D_1 - D_2)}{R \left(D_1^2 - 2 \cdot D_1 + \frac{R_{SH}}{R} + 1 \right)}. \quad (11)$$

Converting expression (10), the dependence of the duty ratio D_1 can be obtained:

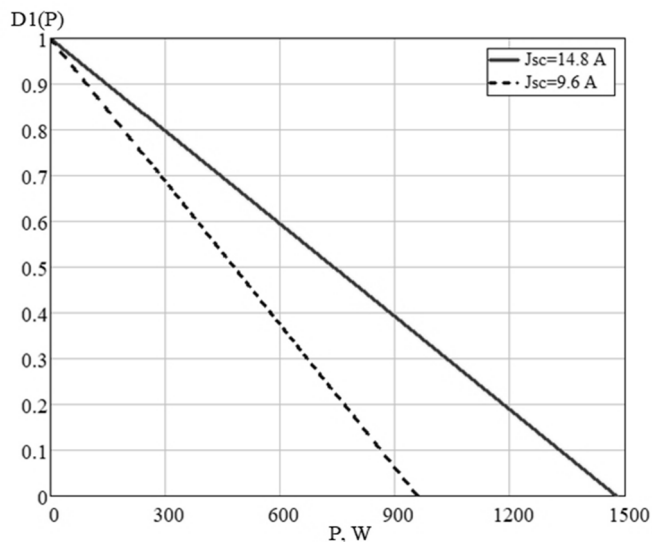
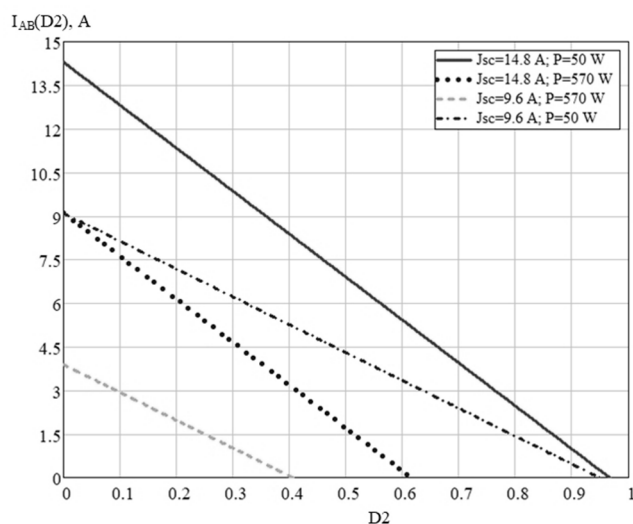
$$D_1 = 1 - \frac{J_{SC} \cdot R_{SH} - \sqrt{4 \cdot R_{SH} \cdot U_{out}^2 - R \cdot J_{SH}^2 \cdot R_{SH}^2}}{2 \cdot U_{out}} \quad (12)$$

Expression (12) can be rewritten:

$$D_1 = 1 - \frac{J_{SC} \cdot R_{SH} - \sqrt{4 \cdot R_{SH} \cdot P_{out} - J_{SH}^2 \cdot R_{SH}^2}}{2 \cdot U_{out}} \quad (13)$$

Fig. 6. shows dependence of duty ratio D_1 from load power with various values of solar panel short-circuit current. This factor depends on solar panel lifetime. The dependences were obtained under the condition that the load voltage is stabilized and equals 100 V. Figure shows that dependence is linear.

Dependence of AB charge current from duty ratio D_2 shows that regulation of current can realized in wide range. At the same time, the regulating characteristic has a linear character at any load power and the service life of the solar panel.

Fig. 6. Duty ratio D_1 vs. load power.Fig. 7. AB charge current vs. D_2 .

VII. CONCLUSION

Proposed topology of a multiport converter ensures necessary work modes, including simultaneous supplying of the load from solar panel and charge of the battery by excessive power.

According to the algorithm of work, circuit can simply go from one operation mode to another. In battery charging mode, there is no serial switching of the two inductors, since it is shunted with power keys in this mode. This topology can realize parallel supply by solar panel and accumulator battery too.

According to obtained regulation characteristics, regulation of battery charge current ensured by linear law in wide range at any load and any point of solar panel lifetime. It should be noted that the battery charge current does not depend on the battery voltage.

This circuit contains only two inductors, four transistors and four diodes. It means that this topology have reduced weight and dimensional characteristics in comparison with analogic topologies.

ACKNOWLEDGEMENT

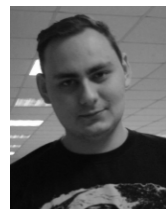
The reported study was funded by RFBR according to the research project №18-38-00281.

REFERENCES

- [1] Solero L., Lidozzi A., and Pomilio J. A. Design of multiple-input power converter for hybrid vehicles. In Proc. IEEE Appl. Power Electron. Conf., 2004, pp. 1145–1151.
- [2] Tao H., Kotsopoulos A., Duarte J. L., and Hendrix M. A. Transformer coupled multiport ZVS bidirectional DC–DC converter with wide input range. IEEE Trans. Power Electron., vol. 23, no. 2, pp. 771–781, Mar. 2008.
- [3] Peng F. Z., Li H., Su G. J., and Lawler J. S. A new ZVS bidirectional DC–DC converter for fuel cell and battery applications. IEEE Trans. Power Electron., vol. 19, no. 1, pp. 54–65, Jan. 2004.
- [4] Tao H., Kotsopoulos A., Duarte J. L. and Hendrix M. A. Family of multiport bidirectional DC-DC converters. IEEE Proc.-Electr. Power Appl., Vol. 153, No. 3, May 2006, pp. 451 – 457.
- [5] Korobkov D. V., Rechetnikov A. N., Shtein D. A., Geist A. V., Sekushenko T. S., Klassen S. V. Simulation of the multiple port DC-DC converter, 18th International Conference of Young Specialists on Micro/Nanotechnologies and Electron Devices (EDM 2017), Altai, Erlagol, 2017, pp. 429-434.
- [6] Sidorov V. E., Shtein D. A., Korobkov D. V., Zaev I. V., Khoroshev M. A., Design mathematic analysis of the multiport converter operation algorithm.



Vadim E. Sidorov was born in 1995. He is a first year MS. Dg. student at the Novosibirsk State Technical University. His research interests include the improvement of power electronics, DC-DC converters and electric drive systems.
E-mail: reksarpk@gmail.



Ilya V. Zaev – Phd student of Novosibirsk state technical university. research interests: Power electronic, resonant converter, neural network.
Email: rollproduce@gmail.com.



Maxim A. Khoroshev – was born in 1993, Phd student of Novosibirsk state technical university. research interests: Power electronic, power generation and accumulation systems, active power filters.
Email: imxoiam1@gmail.com



Dmitry A. Shtein was born in Novosibirsk, Russia, in 1990. He received the B.S. and M.S. degree from the Novosibirsk State Technical University in 2011 and 2013, respectively. Since 2012, he has been working at the Institute of Power Electronics of NSTU.
Research interests: multi-level power converters, autonomous power supply systems, renewable energy and digital control systems.
E mail: Dmitry_Shteyn@mail.ru

Development of Boost Converter Mathematical Model with an Additional Inductance (1C2-2L)

Denis A. Kurochkin, Andrei V. Geist, Dmitry A. Shtein, Alexander G. Volkov, *Member, IEEE*
Novosibirsk State Technical University, Novosibirsk, Russia

Abstract—In various power supply systems, both in autonomous and in stationary, the mass and dimensions of the devices are very important. The purpose of this work is researching of boost converter with additional inductance, mathematical model creating of this converter and comparison it with the classical boost converter.

Index Terms—DC/DC converter, boost converter, mathematical model.

I. INTRODUCTION

IN THE PRESENT day, single-cycle pulse converters are widely used. They are popular due to their simplicity, high efficiency and wide range of output voltage regulation. However, with all their advantages, schemes are not ideal and often have large weight and size parameters, due to stringent requirements for the quality of electricity produced. All this makes engineers to conduct their research and development to find alternative solutions. In this paper, one of these solutions is proposed.

II. PROBLEM DEFINITION

In this paper, boost converter with an additional inductance 1C2-2L is considered. 1C2-2L means: a single-cycle converter of the second kind. Scheme of proposed converter is shown in Fig. 1.

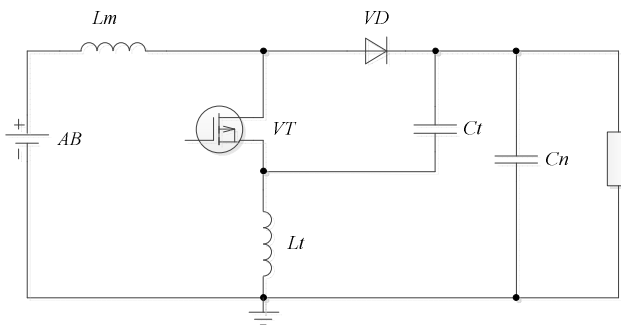


Fig. 1. Scheme of 1C2-2L converter.

The inclusion of additional capacitance and inductance in the scheme is designed to reduce the ripple of the output voltage. The purpose of this work is to develop a mathematical model of the 1C2-2L converter scheme and comparison in terms of energy parameters with the classical boost converter.

III. THEORY

Fig. 1 shows an equivalent circuit the 1C2-2L converter. The operation of the circuit consists of two cycles of key switching. At the first operation cycle, the replacement scheme takes the form shown in Fig. 2a. In Fig. 2b, a replacement circuit is shown for the second cycle of operation.

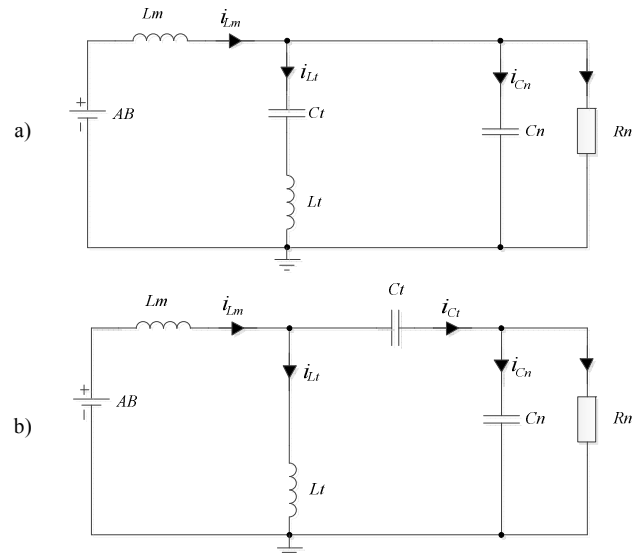


Fig. 2. Replacement schemes of 1C2-2L converter on key switching intervals.

Each of the replacement schemes is described by a system of equations compiled according to Kirchhoff's law for circuits and nodes. As a result, two systems of equations (1) and (2) are obtained that describe the circuit at two switching intervals.

$$\begin{cases} Lm \cdot \frac{di_{Lm}}{dt} = E_{AB} - u_{Ct} - u_{Cn} \\ Lt \cdot \frac{di_{Lt}}{dt} = u_{Cn} - u_{Ct} \\ Ct \cdot \frac{du_{Ct}}{dt} = i_{Lm} - i_{Lt} \\ Cn \cdot \frac{du_{Cn}}{dt} = i_{Lm} - i_{Lt} - i_{Rn} \end{cases} \quad (1)$$

$$\begin{cases} Lm \cdot \frac{di_{Lm}}{dt} = u_{AB} - u_{Cn} \\ Lt \cdot \frac{di_{Lt}}{dt} = u_{Cn} - u_{Ct} \\ Ct \cdot \frac{du_{Ct}}{dt} = -i_{Lt} \\ Cn \cdot \frac{du_{Cn}}{dt} = i_{Lm} - i_{Lt} - i_{Rn} \end{cases} \quad (2)$$

Each of the systems describes its own interval, and depends on the switching function. The relative duration of the enabled key state is D . In the first interval, the switching function is equal to one. On the second interval this function is equal to zero. In more detail, the derivation of expressions is described in the article [1].

$$\begin{cases} U_{AB} - U_{Ct} \cdot D - U_{Cn} = 0 \\ U_{Ct} - U_{Cn} = 0 \\ I_{Lm} \cdot D - I_{Lt} = 0 \\ I_{Lm} - I_{Lt} - I_{Rn} = 0 \end{cases} \quad (3)$$

From the system of equations (3) it is possible to derive expressions for the average values of the currents in the inductances and voltages on the capacitors.

$$I_{Lt_{av}} = \frac{U_{AB} \cdot D}{Rn \cdot (1-D)^2} \quad (4)$$

$$I_{Lm_{av}} = \frac{U_{AB}}{Rn \cdot (1-D)^2} \quad (5)$$

$$U_{Cn_{av}} = \frac{U_{AB}}{(1-D)} \quad (6)$$

$$U_{Ct_{av}} = \frac{U_{AB}}{(1-D)} \quad (7)$$

The mathematical model contains two systems of differential equations (1), (2) allowing determining the instantaneous values of currents and voltages with some assumptions, which are described below.

A. Dependence of Output Current Ripple on the Inductance Lm

On the first switching interval, take the assumption that the voltage drop across the additional inductance (Lt) is insignificant compared to the voltage drop at the input inductance (Lm). This assumption is further confirmed by the model. The current pulsations at the first interval will be determined as follows:

$$i_{Lm_{-1}}(t) = \frac{1}{Lm} \cdot \int U_{AB} dt = \frac{U_{AB}}{Lm} \cdot t \quad (8)$$

The current in the inductor cannot change abruptly. The pulsating component of the current in the inductor is shorted in the capacitor Cm . The shape of the current in this section represents a straight line. One can find an expression describing the pulsating component of the current on the second interval. Knowing the start and end points of the first interval (8), we form the equation of a straight line with two points.

$$i_{Lm_{-2}}(t) = \frac{U_{AB}}{Lm} \cdot \frac{D}{(1-D)} \cdot (T-t) \quad (9)$$

The resulting current expression describes the pulsation component of the inductor current. This function will have a minimum and maximum value at the points $t = 0$ and $t = T \cdot D$. This function has a nonzero average value, which must be taken into account in subsequent calculations. Still need to take into account the average value of the current in the

inductor. The result of the transformations will be a system of equations describing the current of the inductance.

$$\begin{cases} i_{Lm_{-1}}(t) = U_{AB} \cdot \left[\frac{t}{Lm} - \frac{D \cdot T}{2 \cdot Lm} + \frac{1}{Rn \cdot (1-D)^2} \right] \\ i_{Lm_{-2}}(t) = U_{AB} \cdot \left[\frac{D}{(1-D)} \cdot \frac{(T-t)}{Lm} - \frac{D \cdot T}{2 \cdot Lm} + \frac{1}{Rn \cdot (1-D)^2} \right] \end{cases} \quad (10)$$

The resulting current is continuous and has a triangular shape. To find the magnitude of the current ripple amplitude, we take the expression for the current ripple in the first interval (10). We substitute in the expression the time of the beginning and the end of the interval. Further, find the difference of the expression for the maximum value and the expression for the minimum value.

$$\Delta I_{Lm} = i_{Lm_{-1}}(T \cdot D) - i_{Lm_{-1}}(0) = \frac{U_{AB}}{Lm} \cdot T \cdot D \quad (11)$$

B. Dependence of Output Voltage Ripple on the Output Capacitance Cn

The capacitor does not pass a constant current. Only the pulsating component of the inductor current (Lm) is shorted through the capacitor. The voltage on the capacitor will be defined as the current integral in the inductance Lm (8) (9) without a constant component (5):

$$u_{Cn}(t) = \frac{1}{Cn} \cdot \int (I_{Lm}(t) - I_{Lm_{av}}) dt \quad (12)$$

In the second interval, the voltage is determined in the same way, but in the calculation of the indefinite integral an arbitrary constant is added. On the first interval, for convenience of calculation, it is assumed to be zero. The voltage across the capacitor is continuous. This constant is equal to the shift of the second interval relative to the end of the first interval at the point $t = T \cdot D$. The result of the transformations is a system of equations describing the voltage pulsations on the capacitor Cn . It is necessary to take into account the average value of the ripple, which arises because of the inequality of the intervals duration, and the average value of the voltage across the capacitor (6).

$$\begin{cases} u_{Cn_{-1}}(t) = \frac{U_{AB}}{2 \cdot Lm \cdot Cn} \cdot [t^2 - D \cdot T \cdot t] - \frac{U_{AB} \cdot D \cdot T^2}{12 \cdot Lm \cdot Cn} \cdot [1 - 2 \cdot D] + \frac{U_{AB}}{(1-D)} \\ u_{Cn_{-2}}(t) = \frac{U_{AB}}{Lm \cdot Cn} \cdot \left[\frac{D \cdot T \cdot t}{(1-D)} - \frac{D \cdot t^2}{2 \cdot (1-D)} - \frac{D^2 \cdot T^2}{2 \cdot (1-D)} - \frac{D \cdot T \cdot t}{2} \right] - \\ - \frac{U_{AB} \cdot D \cdot T^2}{12 \cdot Lm \cdot Cn} \cdot [1 - 2 \cdot D] + \frac{U_{AB}}{(1-D)} \end{cases} \quad (13)$$

To find the maximum and minimum voltage on the capacitor Cn , it is necessary to find the points of maximum and minimum of the functions of two intervals (13). We take the derivative of each expression. We equate them to zero. It is necessary to find the moments of time in the interval at which the voltage reaches its maximum and minimum values. Substituting them into expressions for the instantaneous value of the voltage, we get that the result of the difference of these expressions is the expression for finding the amplitude of the voltage ripple on the capacitor Cn .

$$\Delta U_{Cn} = u_{Cn-2}(t_{\max}) - u_{Cn-2}(t_{\min}) = \frac{U_{AB} \cdot T^2 \cdot D}{8 \cdot Lm \cdot Cn} \quad (14)$$

C. The Dependence of Capacitor Ct Voltage Ripple on the Value of This Capacitor

In order to determine the voltage on the capacitor, it is necessary to find the current flowing through this capacitor. It can be seen from the system of equations (1) that the current flowing through the capacitor is the difference of the inductance Lm current (10) and Lt current. The current pulsations in the inductance Lt are insignificant, which is confirmed by the experiment, therefore we will use only the constant component of the current flowing through it (4). In the second interval, we also neglect pulsations. In this interval, the average inductor current Lt (4) flows through the capacitor.

It is necessary to integrate and divide both these expressions by the value of the capacitor Cm. A system of equations is obtained that describes the voltage pulsations on the capacitor Ct. As in the previous case, the integration does not take into account the constant equal to the displacement of the expression relative to the end of the first interval at the point $t = T \cdot D$. Just as for the capacitor Cn, it is necessary to take into account the average value of the pulsation component and the constant component of the voltage across the capacitor (7).

$$\begin{cases} u_{Ct(1)}(t) = \frac{U_{AB}}{Ct} \cdot \left[\frac{t^2}{2 \cdot Lm} - \frac{D \cdot T \cdot t}{2 \cdot Lm} + \frac{t}{Rn \cdot (1-D)} \right] \\ - \frac{U_{AB} \cdot T \cdot D \cdot [T \cdot D^2 \cdot Rn \cdot (D-1) + 6 \cdot Lm]}{12 \cdot Lm \cdot Ct \cdot Rn \cdot (D-1)} + \frac{U_{AB}}{(1-D)} \\ u_{Ct(2)}(t) = \frac{U_{AB} \cdot D \cdot (t-T)}{Ct \cdot Rn \cdot (1-D)^2} - \\ - \frac{U_{AB} \cdot T \cdot D \cdot [T \cdot D^2 \cdot Rn \cdot (D-1) + 6 \cdot Lm]}{12 \cdot Lm \cdot Ct \cdot Rn \cdot (D-1)} + \frac{U_{AB}}{(1-D)} \end{cases} \quad (15)$$

The resulting system (15) describes the voltage across the capacitor Ct. The function reaches its maximum value when $t = T$, and the minimum value when $t = T \cdot D$. Substituting in any expression the value of time, we can find expressions for the maximum and minimum voltage on the capacitor. Their difference will be an expression for determining the voltage ripple on the capacitor Ct.

$$\Delta U_{Ct} = u_{Ct-2}(T) - u_{Ct-2}(T \cdot D) = \frac{U_{AB} \cdot T \cdot D}{Ct \cdot Rn \cdot (1-D)} \quad (16)$$

D. The Dependence of the Current Ripple in the Inductance Lt on the Value of This Inductance

To determine the current in the inductance Lm, it is necessary to find the voltage on this inductance. Let us look at the systems of equations (1) and (2). At any time, the voltage across the inductance is the voltage difference between the capacitors Ct and Cn. The system of equations describing the voltage ripple for the inductance Lt is the

difference between the two systems of equations, (15) and (13). In order to find the current in the additional inductance, it is necessary to integrate and divide by the value of the inductance, both expressions of the obtained system. It is necessary to take into account the constant component of the pulsation, as well as the constant component of the current in the throttle Lt (4). The result will be a system of equations that describes the current in the additional inductance Lt.

Expressions for the current in the additional inductance are large, and are not given in this article. It is necessary to find the range of current ripple. For this, we find the points of maximum and minimum for two intervals. From the roots of the equation obtained, only those roots that fall into the interval (0, T) are needed. The expression for finding the ripple current in the additional inductance Lt is the difference of the expressions for the maximum and minimum current.

IV. SIMULATION

A. Parameters Calculation

In the simulation, we will follow the technical specification: $U_{AB_min} = 55 \text{ V}$, $U_{AB_max} = 96 \text{ V}$, Output voltage $U_n = 100 \text{ V}$, pulsation of output voltage - 0.5%, Output power 700 W. The pulsation of the current drawn from the battery is less than 30%. Switching frequency is $f = 50 \text{ KHz}$

$$D = \frac{U_n - U_{AB}}{U_n} = 0.45$$

Knowing this, we use formulas (4), (5), (6) and (7), and calculate the average values of currents and voltages on the elements of the scheme.

$$\begin{aligned} I_{Lt_av} &= 5.73 \text{ A;} \\ I_{Lm_av} &= 12.73 \text{ A;} \\ U_{Cn_av} &= U_{Ct_av} = 100 \text{ V.} \end{aligned}$$

Since the switching frequency is 50 kHz, the period $T = 20 \mu\text{s}$. The current pulsations of the inductance are 30% of the average value, this is $\Delta I_{Lm} = 3.8 \text{ A}$. Using expressions (11) and (14), we calculate the inductance Lm and the capacitance of the output capacitor.

$$\begin{aligned} Lm &= \frac{U_{AB}}{\Delta I_{Lm}} \cdot T \cdot D = 130 \mu\text{H} \\ Cn &= \frac{U_{Cn} \cdot T^2 \cdot D}{8 \cdot Lm \cdot \Delta U_{Cn}} = 19 \mu\text{F} \end{aligned} \quad (17)$$

We take the value of the additional capacitance $Ct = 40 \mu\text{F}$, and the value of the additional inductance $Lt = 10 \mu\text{H}$. For such values of pulsation of current in the additional inductance will be: $\Delta I_{Lt} = 0.45 \text{ A}$, and in the additional capacity: $\Delta U_{Ct} = 1.6 \text{ V}$. With the same initial data, we calculate the elements for the classical boost converter. For this we turn to the "Fundamentals of Power Electronics" [2].

$$L = \frac{U_{AB}}{\Delta I_{Lm}} \cdot T \cdot D = 130 \mu\text{H} \quad (18)$$

$$C = \frac{U_c \cdot T \cdot D}{R \cdot \Delta U_{Cn}} = 126 \mu\text{F}$$

We also calculate the capacity of the input filter, the impedance of which is an order of magnitude lower than the impedance of the battery, in order not to consume the pulsating component of the current from the battery. The impedance of the battery at 50 kHz is $Z_{AB} = 500 \text{ m}\Omega$.

$$C_\phi = \frac{1}{2 \cdot \pi \cdot f \cdot \frac{Z_{AB}}{10}} = 63 \mu\text{F}$$

We will use this filter to simulate both schemes.

B. Simulation in the PSIMSoftware Package

In the PSIMsoftware package, imitation models of converters were built. And the calculated values for all elements are taken into account. The oscillograms of currents and voltages for elements of both circuits are obtained. For 1C2-2L converter, oscillograms were obtained using a mathematical model. All the data obtained are shown below.

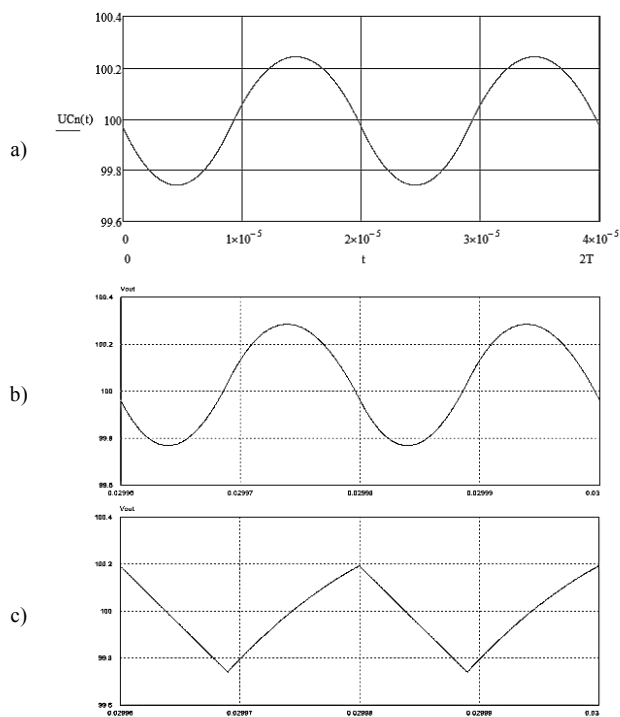


Fig.3. Voltage oscillogram of the scheme output, a – mathematical model, b – converter with additional inductance imitation model, c – boost converter imitation model.

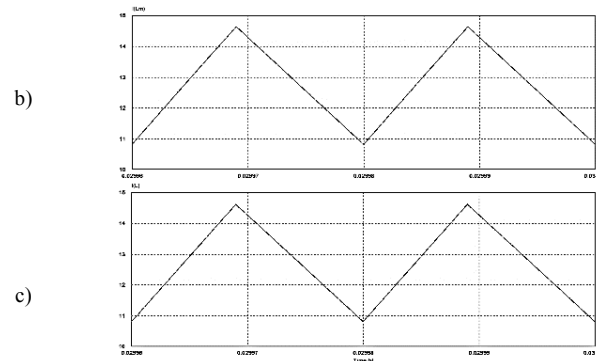
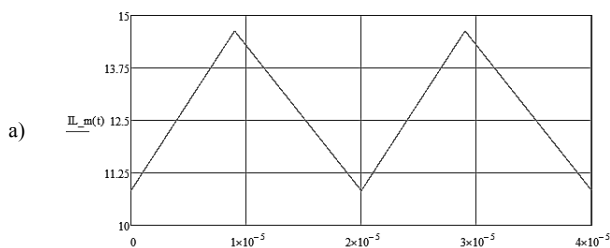


Fig.4. Oscillograms of the current in the input inductance, a – mathematical model, b – converter with additional inductance imitation model, c – boost converter imitation model.

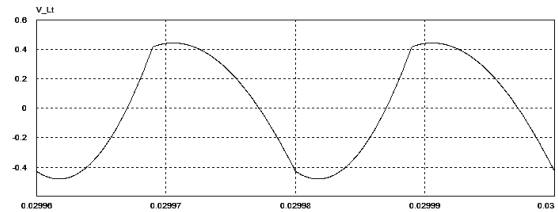


Fig.5. Voltage oscillograms of additional inductance.

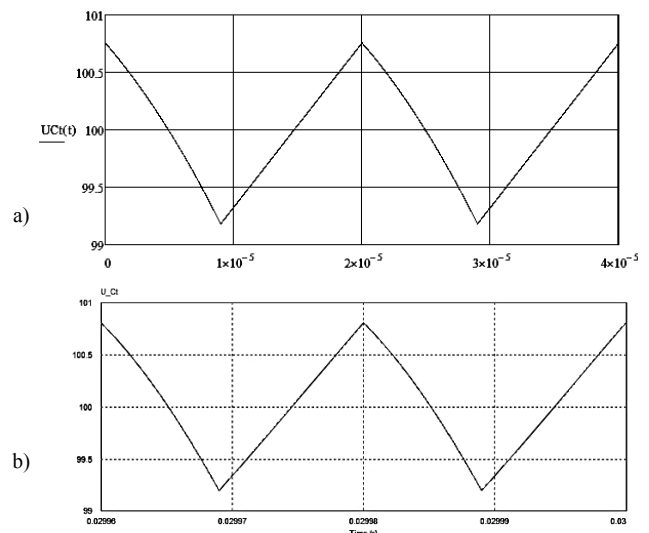
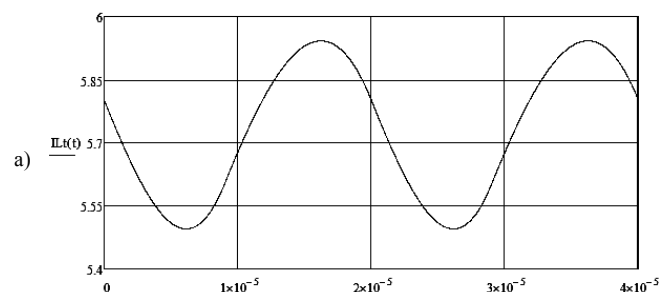


Fig.6. Voltage oscillograms of additional capacitance, a – mathematical model, b – converter with additional inductance imitation model.



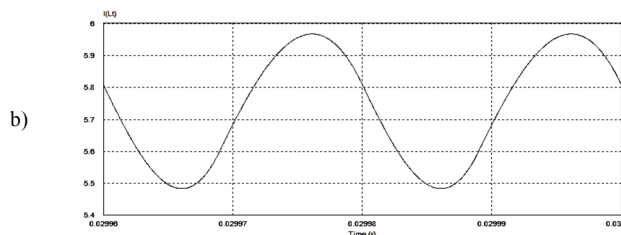


Fig.7. Oscillograms of the current in the additional inductance, a – mathematical model, b – converter with additional inductance imitation model.

TABLE I

SCOPE PULSATING OF VOLTAGES TO THE CIRCUIT ELEMENTS

| Parameter | Math. Model | 1C2-2L (Psim) | Boost (PSIM) |
|--------------------|-------------|---------------|--------------|
| $\Delta U_{Cn}(V)$ | 0.50 | 0.51 | 0.49 |
| $\Delta I_{Lm}(A)$ | 3.80 | 3.82 | 3.82 |
| $\Delta U_{Ct}(V)$ | 1.57 | 1.61 | - |
| $\Delta I_{Lt}(A)$ | 0.45 | 0.48 | - |

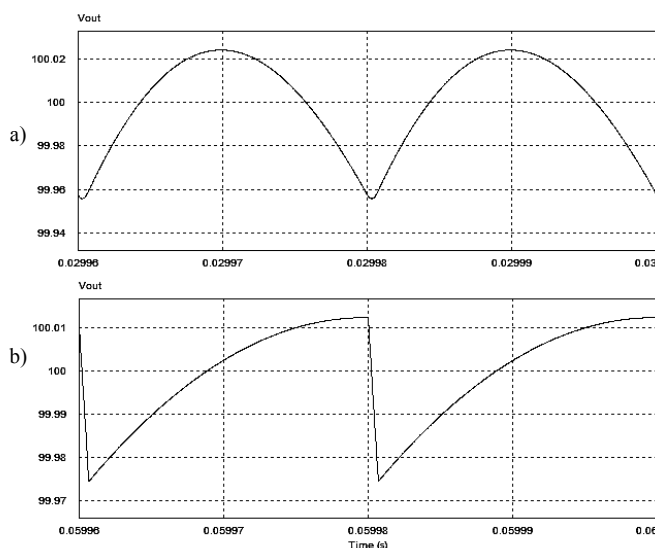


Fig.8. Voltage oscillograms of scheme output ($U_{AB} = 96 V$), a – converter with additional inductance imitation model, b – boost converter imitation model.

V. DISCUSSION OF RESULTS

The oscillograms shown in Fig.3a and Fig.3b show that the mathematical model corresponds to the model built in the software package PSIM. Some differences, in particular, in the magnitude of the ripple range are a consequence of the assumptions made when creating a mathematical model, see Table I. The same can be seen in Fig.4a and Fig.4b, in Fig.6a and Fig.6b and in Fig.7a and Fig.7b, see Table I. From this it can be concluded that the mathematical model describes the scheme quite accurately. Despite the assumptions made at its creation. The expressions that describe the dependence of the ripple of the current or voltage in the elements on the values of these elements can be used to calculate the parameters of the circuit of the boost converter with additional inductance.

From the oscillograms shown in Fig.3b and Fig.3c, it can be seen, that the shape of the output voltage pulsation of the converter with the additional inductance is close to the

sinusoidal, whereas the pulsations in the boost converter have a triangular shape. The magnitude of the pulsation in the circuit with the additional inductance $\Delta U_{Cn} = 0.51B$, and in the boost converter scheme $\Delta U_{Cn} = 0.49B$. The output capacitance of the boost converter $C = 129 \mu F$, while the total used capacitance in the 1C2-2L converter is $60 \mu F$. This is more than 2 times lower. Also, the additional capacity can be reduced, but its value should not be less than the value of the output capacitance. This allows to use in the 1C2-2L converter more than 3 times less capacitors than in the boost converter. Fig.5b and Fig.5c show that the shape and the ripple of the input current of the converter with the additional inductance and of the boost converter are not different. The inductance of the input is $130 \mu H$ in both circuits. In the 1C2-2L converter has an additional inductance of $10 \mu H$. This slightly increases the mass of the device.

As can be seen from Fig. 5, the magnitude pulsation of the voltage on the additional inductance is small, and the average value is zero. The assumption that was made when deriving formulas is possible.

Also from Fig.8, it is seen that the circuit operates at an input voltage of $96.5 V$. The magnitude pulsation of the output voltage of the converter with the additional inductance $\Delta U_{Cn} = 0.07 B$, and of the boost converter $\Delta U_{Cn} = 0.04 B$.

VI. CONCLUSION

A converter with additional inductance is a good substitute for the classical boost converter. It has some disadvantages, in particular extra inductance. Also, a more complex system for calculating circuit elements. But with its use, the number of capacitors used is significantly reduced. There is no need to redesign the control system, because the transfer characteristic are the same. The created mathematical model corresponds to the scheme and the obtained expressions for calculating circuit elements can be applied when creating this converter.

In the future, it is planned to assemble a real model of the two circuits, to perform a numerical comparison of the mass of the devices, the quality of the output voltage and its harmonic composition. And also compare the dynamics of these two converters.

REFERENCES

- [1] A.V. Geist, A.V. Sidorov, D.V. Korobkov, "DC/DC Boost Converter with Additional Inductance for the Space Power Supply System" Novosibirsk State Technical University, Novosibirsk, Russia 2012r.unpublished.
- [2] R.W. Erickson, "Fundamentals of Power Electronics". USA, New York, 1997. — 883 p.
- [3] V.S. Moin, "Stabilized transistor transducers", Moscow. 1986. — 376 p.
- [4] O. Mourra, A. Fernandez, F. Tonicello, "Buck Boost Regulator (B²R) for spacecraft Solar Array Power conversion". in Applied Power Electronics Conference and Exposition (APEC), Palm Springs, CA, USA, 2010, pp 1313-1319.



Denis A. Kurochkin was born in 1996. He is a bachelor student of the fourth year of studies at the Novosibirsk State Technical University. Research interests: power electronics, DC-DC converters, autonomous power supply systems, digital and analog control systems.
E mail: Denis963258@gmail.com



Andrei V. Geist was born in Zarinsk, Russia, in 1984. He received the B.S. and M.S. degrees from the Novosibirsk State Technical University, in 2005 and 2007, respectively. Since 2007, he is a lecturer at the department of Electronics and electrical engineering of NSTU. The subject of his thesis is Operation modes analysis and application of multi-level converter for aircraft power generation systems. His main research interests are DC-AC power converters, boost DC-DC converter and its control algorithms.
E-mail: andrey.geist@gmail.com



Dmitry A. Shtein was born in Novosibirsk, Russia, in 1990. He received the B.S. and M.S. degree from the Novosibirsk State Technical University in 2011 and 2013, respectively. Since 2012, he has been working at the Institute of Power Electronics of NSTU. Research interests: multi-level power converters, autonomous power supply systems, renewable energy and digital control systems.
E mail: Dmitriy_Shteyn@mail.ru



Alexander G. Volkov - Candidate of Technical Sciences, associate prof., Novosibirsk State Technical University. His research interests are currently focused on power electronics, power converters, power generation and energy storage systems, active power filters. Since 2011, he is a senior researcher of Industrial Electronics Department of NSTU.
Area of scientific interests: developing and analysis of energy-saving and renewable energy technologies in industry. Currently he has over 35 published works.
E-mail: _bismark_@mail.ru

Analysis of Dynamic Processes in the Electric Power Generating System of Variable Frequency for Aircrafts

Maxim A. Khoroshev, Denis V. Makarov, Ilya V. Zaev, Vadim E. Sidorov
Novosibirsk State Technical University, Novosibirsk, Russia

Abstract – This article describes the analysis of dynamic processes in the system electric power generation system of variable frequency for aircraft. Based on the well-known mathematical model for a continuous system, a mathematical model for small deviations is developed. The frequency characteristics are obtained. A two-channel two-loop closed-loop control system for the generation system was developed, using the principle of development of systems of subordinate regulation and frequency methods of synthesis of regulators.

Index Terms – Dynamic process, optimal control, parallel semiconductor converter, magnetoelectric generator.

I. INTRODUCTION

THE DESIRE to improve the technical and economic performance of next-generation aircraft sets a number of complex problems for aviation specialists that require new methods for building on-board power systems. Thus, the most promising direction in this area of research is the creation of an aircraft with a single centralized secondary power supply system that provides all the energy needs of on-board equipment. This concept was put forward as a result of research to improve the energy efficiency of aircraft and is called "Fully electric aircraft." [1] Unlike the established technique for creating on-board energy systems in which three types of secondary systems are used:

- hydraulic system;
- power supply system;
- pneumatic system,

in a centralized system, electrical energy will be used to power the most energy-intensive systems that have traditionally used hydraulic and pneumatic energy for their operation.

According to experts, the use of a centralized power supply system will allow:

- reduce fuel consumption by 8-12%;
- to reduce the total take-off mass by 6-10%;
- Reduce operating costs by 5-10%;
- Increase the average raid by 5-6%;
- Reduce the cost of the life cycle by 3-5%;
- Reduce maintenance time by 4-4.5%.

However, the desire to create systems in which electrical equipment prevails over equipment operating from other

types of energy, carries a number of difficulties. One of these problems is the search for a compromise between the desire to reduce the existing mass-dimension indicators of power supply systems and improve the quality of generated electrical energy. On this issue, today, there are numerous discussions.

II. PROBLEM DEFINITION

With the advent of the concepts "Fully electric aircraft" and "More electric aircraft," the improvement of the quality of electrical energy in aircraft power supply systems has become one of the most important tasks in the aviation industry. Moreover, with the increase in the electrical equipment capacity of aircraft, the requirements for power supply systems are tightened each time, so there is a growing need for new methods of building such systems. To date, a wide range of scientists and engineers are conducting research on the further electrification of airborne equipment of aircraft.

Thus, the power of electric supply systems on a separate aircraft can reach 1 MW [1]. This amount of power can be compared with the total power consumption of a small settlement. It is easy to assume that consumers in such a system can be very diverse, from those for whom the quality of electrical energy does not play a special role, to precision devices, power failures for which they can lead to incorrect operation or failure.

At the moment, the document regulating the quality of electrical energy on aircraft is GOST R 540073 - 2010 "ELECTRICAL SUPPLY SYSTEMS OF AIRCRAFT AND HELICOPTERS" [2]. This document describes all the currently permitted types of aircraft power supply systems, dynamic processes, possible tolerances for voltage dips and splashes, types of loads, etc. are described.

Among the types of power supply systems for aircraft, a new system of variable frequency 115 / 200V, 380-720 Hz is of great interest. This system was proposed in the course of improving the electrical equipment of aircraft, in which the stability of the frequency of the supply voltage ceased to be a critical factor [3]. The proposed type of power supply system has opened new ways to the creation of power generation systems. Moreover, the development of power electronics has made it possible to create such systems more flexible,

and a large number of studies are being conducted in this direction to date.

One way to build such a system is to use a synchronous generator (SG) with excitation from permanent magnets in its composition. The peculiarity of the operation of such a generator is that the magnitude of the voltage at its terminals depends on the frequency of rotation of the shaft and the load, therefore a voltage regulator must necessarily be used in the composition of such a system. Due to the high technical base of modern power electronics, it is most rational, as a voltage regulator, to use a semiconductor converter.

Schemes based on a synchronous generator and a semiconductor converter are conventionally called "SG-SC" generation systems for electric energy.

Fig. 1. shows a schematic diagram of an electric power generation system (EPGS) of the "SG-SC" type of alternating voltage of variable frequency. As seen from the scheme, the role of the voltage regulator is performed by a three-phase inverter in reverse mode.

The voltage regulation at the clamps of the SG occurs by generating a sinusoidal current by a semiconductor converter shifted in phase by $\pi / 2$ or $-\pi / 2$. As a result, due to the reaction of the armature, the total magnetic flux of the synchronous generator increases or decreases, as shown in publications [4,5,6]. A publication [7] proposes a method for synchronizing the control system with a variable frequency of the generated voltage. In this article, it is proposed to develop a mathematical model of the SGSE of a variable voltage of variable frequency.

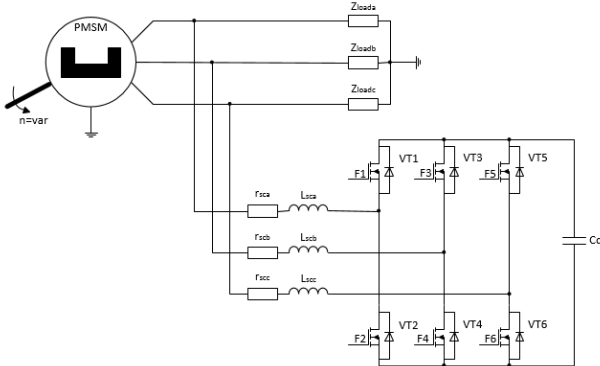


Fig. 1. Schematic diagram type «SG-SC» variable voltage variable frequency.

III. THEORY

A. Small-Signal Model

It is necessary to obtain a dynamic model for analyzing the dynamic properties of the EPGS. There are two main ways to represent transforming impulse systems as dynamic objects. The first approach, in which the power part working with PWM or PFM, is considered as a discrete link, allows to reveal the features of the entire discrete system, in particular, to determine the stability boundaries by the exact model. Unfortunately, the initial consideration of the power part of

the converter as a discrete dynamic link leads to great difficulties.

The second approach of representing the power part of a pulse converter operating with any type of PWM, with an analog or discrete processor in the control part, is based on replacing the power part as a discrete link with a continuous one. In addition to the transition to a continuous link, as a mathematical model, a further change is practically useful: the transition from a nonlinear link to a linear one. The obtained model, continuous and linear, is available for analysis of dynamic properties by known methods [8].

A continuous EPGS model is represented by equations (1-5).

$$U_{sgd} = u_{dc} \frac{1}{2} M_d + r_{sc} I_{scd} + L_{sc} \frac{dI_{scd}}{dt} - \omega L_{sc} I_{scq}; \quad (1)$$

$$U_{sgq} = u_{dc} \frac{1}{2} M_q + r_{sc} I_{scq} + L_{sc} \frac{dI_{scq}}{dt} + \omega L_{sc} I_{scd}; \quad (2)$$

$$C_d \frac{du_{dc}}{dt} = \frac{3}{4} (M_d I_{scd} + M_q I_{scq}); \quad (3)$$

$$E_d = U_{sgd} + r_{sg} \left(I_{scd} + \frac{U_{sgd}}{R_{load}} \right) + L_{sg} \frac{d \left(I_{scd} + \frac{U_{sgd}}{R_{load}} \right)}{dt} - \omega L_{sg} \left(I_{scq} + \frac{U_{sgd}}{\omega L_{load}} \right); \quad (4)$$

$$E_q = U_{sgq} + r_{sg} \left(I_{scq} + \frac{U_{sgd}}{\omega L_{load}} \right) + L_{sg} \frac{d \left(I_{scq} + \frac{U_{sgd}}{\omega L_{load}} \right)}{dt} + \omega L_{sg} \left(I_{scd} + \frac{U_{sgd}}{R_{load}} \right); \quad (5)$$

The next step, on the way to analyzing the dynamic properties and synthesis of the control system, will be the linearization of the system of equations. As is known, any nonlinear system (continuous or impulse) can be replaced linear within a sufficiently small neighborhood with respect to its operating point. Thus, it is necessary to consider the behavior of the system in a small deviation.

To perform this procedure, each member of the system of equations (1-5) is represented as the sum of the mean value and its infinitesimal deviation. The principle of linearization consists in eliminating nonlinear components from the equations [9]. Thus, simplifying the expression, we obtain a system of equations (6-10):

$$\hat{u}_{Crd} = u_{dc} \frac{1}{2} \hat{m}_d + \hat{u}_{dc} \frac{1}{2} M_d + r_{lm} \hat{i}_{lmd} + L_{lm} \frac{d\hat{i}_{lmd}}{dt} - \omega L_{lm} \hat{i}_{lmq}; \quad (6)$$

$$\hat{u}_{Crq} = u_{dc} \frac{1}{2} \hat{m}_q + \hat{u}_{dc} \frac{1}{2} M_q + r_{lm} \hat{i}_{lmq} + L_{lm} \frac{d\hat{i}_{lmq}}{dt} + \omega L_{lm} \hat{i}_{lmd}; \quad (7)$$

$$C_d \frac{d\hat{u}_{dc}}{dt} = \frac{3}{4} (\hat{m}_d I_{lmd} + M_d \hat{i}_{lmd} + \hat{m}_q I_{lmq} + M_q \hat{i}_{lmq}); \quad (8)$$

$$\hat{e}_d = \hat{u}_{crd} + r_{cr} \left(\hat{i}_{md} + \frac{\hat{u}_{crd}}{R_H} \right) + L_{cr} \frac{d \left(\hat{i}_{md} + \frac{\hat{u}_{crd}}{R_H} \right)}{dt} - \omega L_{cr} \left(\hat{i}_{mq} - \frac{\hat{u}_{crd}}{\omega L_H} \right); \quad (9)$$

$$\hat{e}_q = \hat{u}_{crq} + r_{cr} \left(\hat{i}_{mq} + \frac{\hat{u}_{crd}}{\omega L_H} \right) + L_{cr} \frac{d \left(\hat{i}_{mq} - \frac{\hat{u}_{crd}}{\omega L_H} \right)}{dt} + \omega L_{cr} \left(\hat{i}_{md} + \frac{\hat{u}_{crd}}{R_H} \right); \quad (10)$$

Equations (6-8) map the continuous linearized dynamic SC model, equations (9.10) to the continuous linearized dynamic SG model.

The model obtained allows us to analyze the dynamic processes taking place in the EPGS of a variable frequency. In parallel with the dynamics analysis, it is necessary to construct a closed-loop control system to stabilize the DC voltage level in the DC link and the AC voltage amplitude at the generator terminals.

B. Synthesis of a Closed-Loop Control System

The subordinate control system is a multi-loop structure with cascade controllers. The number of regulators and control loops equals the number of adjustable parameters. The name of the system is explained by the fact that the output signal of the regulator included in the external circuit is the master for the regulator included in the internal circuit, i.e. one controller is subordinate to another [10].

An important advantage of the systems of subordinate regulation is that the regulators are set independently and sequentially from the internal circuit to the external one. In the case of a variable-frequency EPGS with a parallel active voltage rectifier, the slave control system contains two dual-loop control channels. The first channel contains two series-connected regulators, where the external circuit is a voltage regulation loop in the DC link, and the internal one is the current control loop of the semiconductor converter. The second channel also contains two regulators, where the external controller controls the voltage at the generator terminals, and the second channel controls the reactive current of the semiconductor converter.

In Fig. 2. A block diagram of the closed-loop control system of a variable-frequency EPGS is presented. In it, compensation is introduced for the cross-links of the currents of the coordinates d and q.

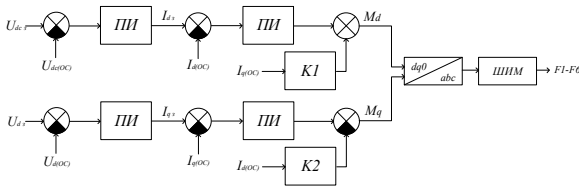


Fig. 2. Block diagram of the closed-loop control system of a EPGS variable frequency.

To realize this structure, it is necessary to obtain its own transfer functions for each control loop, analyze the dynamic properties of the loop and plot the amplitude and phase characteristics, introduce compensating links for each circuit to obtain the required parameters.

C. Frequency Characteristics

It is convenient to begin the analysis of the dynamic properties of the system from a semiconductor converter. As can be seen from equations (6.7) in the expression for the voltage of the d-coordinate, there is an effect of the current of the q-coordinate and vice versa. This mutual influence is called "cross-connection". In order to get rid of the interaction of the current components, it is necessary to compensate the control signal. In this case, the control signal will change as follows:

$$M_d = M_d^* + \frac{2}{u_{dc}} \omega L_{mn} I_{mq}; \quad (11)$$

$$M_q = M_q^* - \frac{2}{u_{dc}} \omega L_{mn} I_{md}; \quad (12)$$

We rewrite equations (6.7) with allowance for the compensation of cross-links.

$$\hat{u}_{crd} = u_{dc} \frac{1}{2} (\hat{m}_d^* + \frac{2}{u_{dc}} \omega L_{mn} \hat{i}_{mq}) + r_{mn} \hat{i}_{md} - \omega L_{mn} \hat{i}_{mq} + \quad (13)$$

$$+ \hat{u}_{dc} \frac{1}{2} (M_d^* + \frac{2}{\hat{u}_{dc}} \omega L_{mn} I_{mq}) + L_{mn} \frac{d \hat{i}_{md}}{dt};$$

$$\hat{u}_{crq} = u_{dc} \frac{1}{2} (\hat{m}_q^* - \frac{2}{u_{dc}} \omega L_{mn} \hat{i}_{md}) + \omega L_{mn} \hat{i}_{md} + \quad (14)$$

$$+ \hat{u}_{dc} \frac{1}{2} (M_q^* - \frac{2}{\hat{u}_{dc}} \omega L_{mn} I_{md}) + r_{mn} \hat{i}_{mq} + L_{mn} \frac{d \hat{i}_{mq}}{dt}.$$

From the system of equations (13,14) we obtain the transfer function "control-current" for each coordinate of the basis dq. For this, all small deviations are equated to zero, except for the current component and the control signal.

$$G_{idmd}(s) = \frac{\hat{i}_{md}}{\hat{m}_d} = -u_{dc} \frac{1}{2} \left(\frac{1}{sL_{mn} + r_{mn}} \right); \quad (15)$$

$$G_{iqmq}(s) = \frac{\hat{i}_{mq}}{\hat{m}_q} = -u_{dc} \frac{1}{2} \left(\frac{1}{sL_{mn} + r_{mn}} \right); \quad (16)$$

The resulting transfer functions reflect the dependence of the current of the converter with the perturbation of the control signal. For the known SGE parameters it is possible to construct the amplitude-frequency and phase-frequency characteristics (AFC and PFC).

Since the transfer functions on channel d and q are the same, we will analyze one of them.

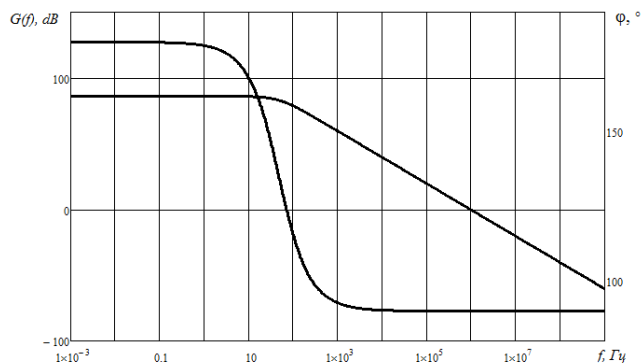


Fig. 3. AFC and PFC of the transfer function of the «control-current».

In Fig. 3. The AFC and PFC of the open transfer function "control-current" are depicted. The amplitude of the transfer function will be zero at a frequency of about 1 MHz. Also, it is seen that the gain at low frequencies has a finite value. According to the PFC form, it is seen that at the inflection point, the phase of the signal changes by 90 degrees.

The classical approach to the construction of closed control systems is the introduction of compensating links that change the frequency characteristics of the transfer functions. The AFC and PFC should be adjusted in such a way that the unity gain factor is at a frequency of at least 10 times smaller than the switching frequency of the PWM to ensure the implementation of Kotel'nikov's theorem, and the phase of the signal at the frequency of the unit gain does not decrease less than -180 degrees for system stability. For the resulting control-current transfer function, we introduce the compensating proportional-integral link of the form:

$$G_{pi}(s) = K_{id} + \frac{1}{sT_{id}}, \text{ where} \quad (17)$$

K_{id} – proportional gain

T_{id} – time constant of the integrating link;

Changing the coefficients of the proportional-integral link in such a way that the unit gain of the transfer function was at a frequency at least 10 times lower than the switching frequency of the switches, and also the phase of the signal at this frequency was not less than -180 degrees, we obtain a compensated transfer function "Control-current". The AFC and PFC of this transfer function are shown in Fig. 4.

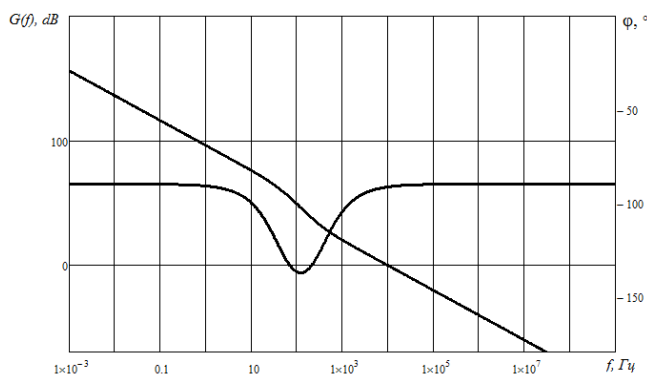


Fig. 4. AFC and PFC of the transfer function of the «control-current» with the added proportional-integral link.

The transient response of the obtained compensated transfer function is shown in Fig. 5.

The obtained indicators of the quality of the transient process fit into the criteria for evaluating such systems.

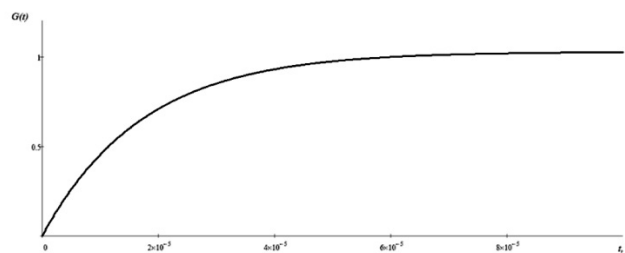


Fig. 5. Transient characteristic of the transfer function «control-current» with the added proportional-integral link.

The next transfer function to be analyzed is responsible for the voltage response in the DC link when the SC current is perturbed by the coordinate d.

On the basis of equation (8), dividing the voltage control channels at the generator terminals and the voltage in the DC link, we obtain the transfer function "DC voltage – SC current" (18):

$$G_{ucid}(f) = \frac{\hat{u}_{dc}}{\hat{i}_{ind}} = \frac{3}{4C_d s}. \quad (18)$$

The resulting transfer function is an integrator. The AFC and PFC of this function are shown in Fig. 6.

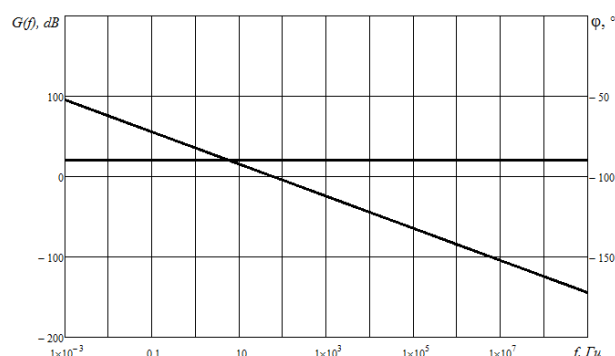


Fig. 6. AFC and PFC of the transfer function «DC voltage – current».

Based on the received frequency characteristics, we can conclude that the system is stable throughout the frequency range, and, to increase the speed, it makes sense to introduce a proportional link. However, to reduce the astatic error, it is necessary to introduce a compensating proportional-integral link.

The obtained AFC and PFC with compensating link are shown in Fig. 7.

The parameters of the proportional-integral link are chosen in such a way that the frequency of the unit gain of the transfer function is at least 10 times smaller than the frequency of the unity gain of the current-control transfer function, thereby satisfying the principles of subordinate regulation [11].

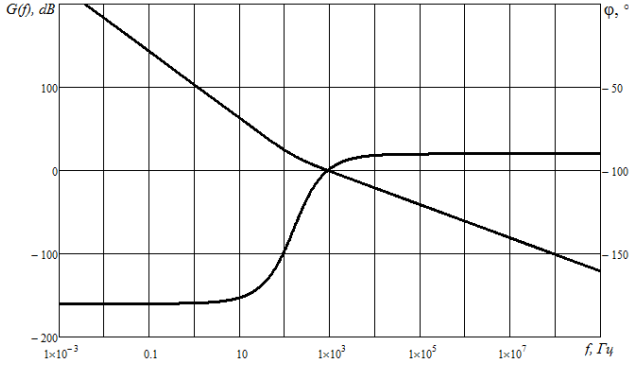


Fig. 7. AFC and PFC of the transfer function "DC voltage – SC current" with the added proportional-integral link.

The transient characteristic of the transfer function "DC voltage – SC current" is shown in Fig. 8.

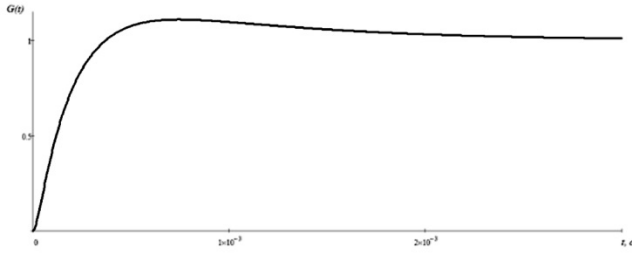


Fig. 8. Transient characteristic of the transfer function "DC voltage – SC current" with the added proportional-integral link.

The next transfer function to be analyzed is responsible for the relationship between the voltage at the generator terminals and the current of the semiconductor converter in coordinate q. The expression for this transfer function looks as shown in (19).

$$G_{udiq}(f) = \frac{\hat{u}_{CFd}}{\hat{i}_{mq}} = \frac{(r_{CF} + sL_{CF})^2 + \omega_{\min} L_{CF}}{1 + \frac{r_{CF} + sL_{CF}}{R_H} + \frac{\omega_{\min} L_{CF}}{\omega_{\min} L_H}} \dots \dots \frac{r_{CF} + sL_{CF}}{\omega_{\min} L_{CF}} \left(\frac{\omega_{\min} L_{CF}}{R_H} - \frac{r_{CF} + sL_{CF}}{\omega_{\min} L_H} \right) \quad (19)$$

The built-in AFC and PFC for the transfer function (19) are shown in Fig. 9.

The AFC of the transfer function (19) has a complex shape in the mid-frequency region, reflecting the interaction of the load inductance currents and the stator winding of the synchronous generator. In the low-frequency region, it has a finite low gain (less than one).

AFC and PFC of the transfer function "SG voltage – SC current" with a compensating proportional-integral link are shown in Fig. 10.

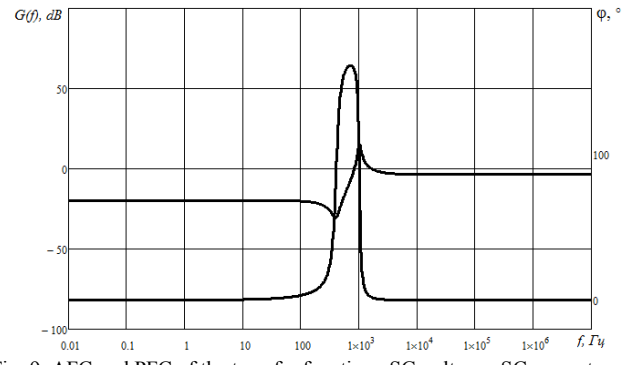


Fig. 9. AFC and PFC of the transfer function «SG voltage – SC current».

The compensating link changes the AFC in Fig. 10. so that in the region of the crossing through zero, the shape of the curve had a slope of 20 dB / dec. in both directions to increase the stability of the system.

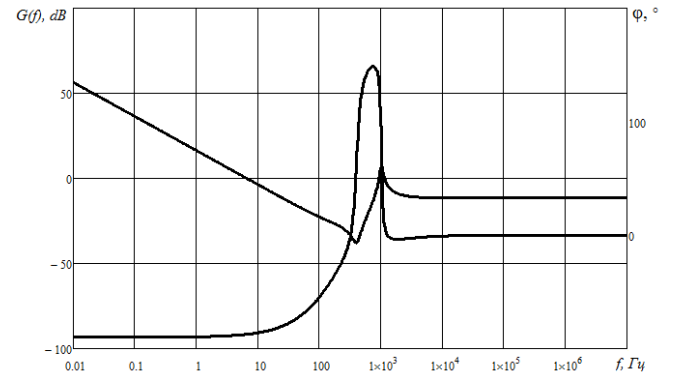


Fig. 10. AFC and PFC of the transfer function «SG voltage – SC current» with the added proportional-integral link.

As can be seen from Fig. 10., the phase margin has a positive value at the frequency of the crossing through zero. The transition characteristic is of an oscillatory character at the initial stage of work. In this case, the effect of the second-order aperiodic link in the numerator of the transfer function is affected. It is worth noting that this behavior of the transfer function in a closed control system will be compensated by the mutual influence of control channels [12].

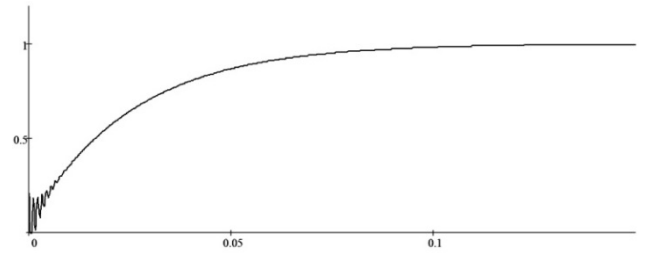


Fig. 11. Transient characteristic of the transfer function "SG voltage – SC current" with the added proportional-integral link.

IV. SIMULATION

Simulation modeling is carried out for a model, compiled in the package of applied programs of mathematical modeling «PSIM».

The first numerical experiment was carried out when the reference signal was applied to the current q of the

coordinate. In Fig. 12. The transient process in the current i_q is shown. As can be seen from the oscillogram, the shape of the transient process coincides with the transient characteristic presented in Fig. 5.

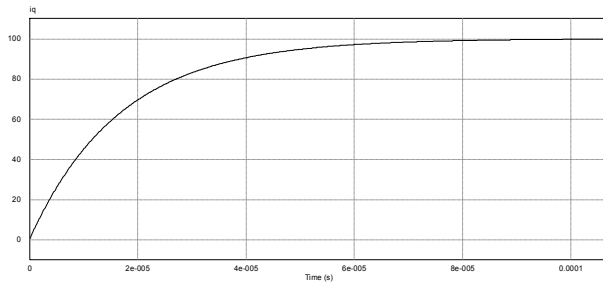


Fig. 12. Oscillogram of the transient in the current i_q .

The oscillogram presented in Fig. 13., demonstrates the transient process of voltage in the DC link when reference signal has stepped-up. Comparing the forms of the transition process and the transition characteristic shown in Fig. 8., we can make sure the results are identical.

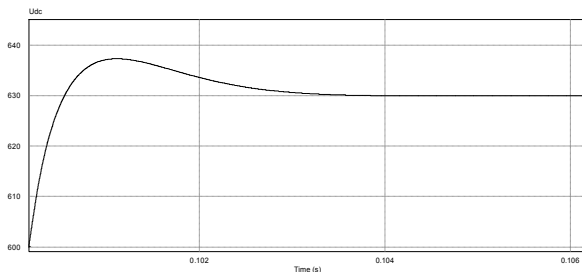


Fig. 13. Oscillogram of the voltage transient in the DC link u_{dc} .

Fig. 14 shows an oscillogram of the voltage transient process at the generator terminals when reference signal has stepped-up. The result obtained in the form of the transition process is similar to that shown in Fig. 11.

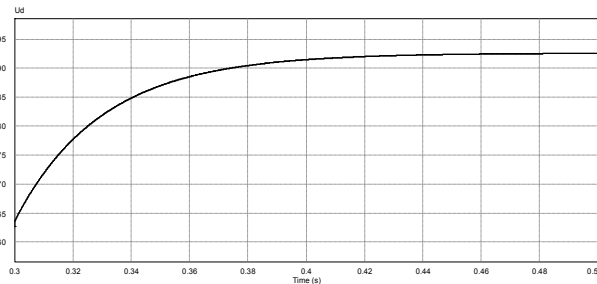


Fig. 14. Oscillogram of the voltage transient on the generator terminals u_d .

The obtained oscillograms of the transient processes fully correspond to the calculated parameters.

The following experiment was carried out for the analysis of dynamic processes in the mode of voltage stabilization at the generator terminals during a step-down and a step-up of load. In Fig. 15 shows an oscillogram of the transient process.

Transient parameters:

- Step-down of load from 160% to 10% of the nominal:
 - regulation time: 2,5 ms;
 - peak of voltage: 260V.
- Step-up of load from 10% to 160% of the nominal:
 - regulation time: 1,5 ms;
 - peak of voltage: 40V.

A numerical experiment was also performed with a smooth change in the frequency of the generated voltage at the terminals of the SG from the minimum value of 360 Hz to the maximum 780 Hz. The oscillogram of this transient process is shown in Fig. 16.

Transient parameters:

- Increasing the frequency from 360Hz to 780Hz:
 - transient time: 10mc;
 - regulation time: 12mc;
 - peak of voltage: 180B.

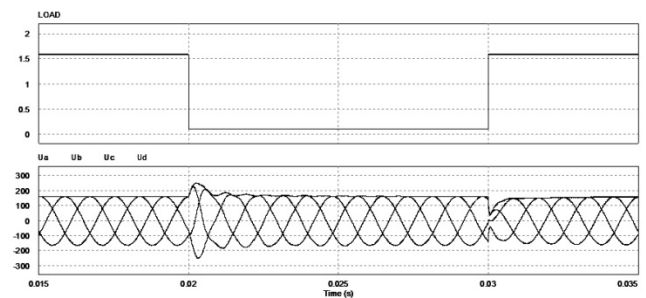


Fig. 15. Oscillogram of transients during discharge and load build-up, load level (a), three-phase voltage at SG terminals (b).

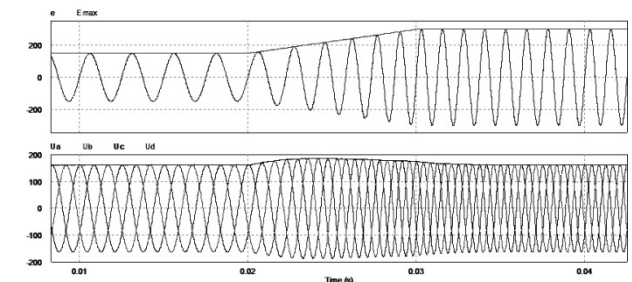


Fig. 16. Oscillogram of transient processes with a smooth increase in the frequency of the generated voltage, idling EMF (a), three-phase voltage at the SG terminals (b).

V. DISCUSSION OF RESULTS

As a result of the simulation, the transient processes shown in Fig. 12 - 14. These oscillograms confirm the theoretical data obtained in Chapter III. When simulating the EPGS for the voltage stabilization mode at the clamps of the SG, the experiment with the discharge and the load sketch showed satisfactory results in terms of the stability of the control system, however, the obtained parameters of peak voltages do not satisfy GOST. It should be noted that a more precise setting of the regulators can give a better result, in comparison with the received one. The experiment with changing the frequency of the generated voltage showed acceptable results. The parameters of the transient process satisfy GOST.

VI. CONCLUSION

In this paper, we investigate dynamic processes in the electric power generation system for aircraft. From the mathematical model, a model is obtained for small deviations

over which its frequency characteristics are investigated. The synthesis of the automatic control system has been carried out and the regulators have been calculated by the frequency method. In the course of numerical experiments, adequate results were obtained that satisfied theoretical data.

ACKNOWLEDGEMENT

The reported study was funded by RFBR according to the research project № 18-38-00281.

REFERENCES

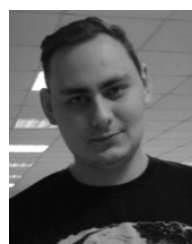
- [1] Kutahov V. P. Polnostyu elektricheskij samolet/ V. P. Kutahov, V.A. Kargopol'cev, S.A. Voronovich // Aviapanorama. - 2009. - № 2 (74). - S.14-17.
- [2] GOST 54073 – 2010. Sistemy elektrosnabzheniya samoletov i vertoletov. Obshchie trebovaniya i normy kachestva ehlektroehnergii.
- [3] Barvinskij A. P., Kozlova F. G. EHlektrooborudovanie samoletov: Ucheb. dlya sred. spec. ucheb. zavedenij — 2-e izd., pererab. i dop.— M.: Transport, 1990.—320s.
- [4] But D. A. Beskontaktnye elektricheskie mashiny: Ucheb. posobie dlya ehlektromekh. i ehlektroehnerg. spec. vuzov. – M.: Vyssh. shk., 1990. – 416 s.: il.
- [5] Kharitonov S.A., Korobkov D.V., Makarov D.V., Garganeev A.G. / stabilizaciya napryazheniya sinhronnogo generatora s postoyannymi magnitami pri peremennoj nagruzke // Doklady Tomskogo gosudarstvennogo universiteta sistem upravleniya i radioehlektroniki. 2012. – № 1-1. – S. 139-146.
- [6] Aviacionnaya sistema generirovaniya elektroenergii / S. A. Haritonov, D. V. Korobkov, D. V. Makarov, A. V. Levin, S. F. Konyahin, M. M. YUhnin // Nauchnyj vestnik Novosibirskogo gosudarstvennogo tekhnicheskogo universiteta. - 2013. - №1. - S. 147-162.
- [7] Makarov D. V., Kharitonov S. A., Khoroshev M. A. Method of synchronization in power supply //Actual Problems of Electronics Instrument Engineering (APEIE), 2016 13th International Scientific-Technical Conference on. – IEEE, 2016. – T. 3. – C. 17-21.
- [8] Chaplygin E.E. Spektral'noe modelirovanie preobrazovatelej s shirotno-impul'snoj modulyaciej: Ucheb. Posobie. – M.: MEI, 2009. – 56 s.
- [9] Erickson, Robert W.. Fundamentals of Power Electronics. Second Edition. Secaucus, NJ, USA: Kluwer Academic Publishers, 2000. p 877.
- [10] Vasil'ev K. K. Teoriya avtomaticheskogo upravleniya (sledyashchie sistemy): Uchebnoe posobie.–2-e izd.– Ul'yanovsk, 2001. – 98 s.
- [11] Middlebrook R.D. Small-Signal Modeling of Pulse-Width Modulated Switched-Mode Power Converters / Proceedings of the IEEE. – Vol. 76. – No. 4. – 1988. – pp. 343-354
- [12] Neal Clements, Giri Venkataramanan, T.M. Jahns Design Considerations for a Stator Side Voltage Regulated Permanent Magnet AC Generator // Energy Conversion Congress and Exposition, 2009. ECCE 2009. IEEE. - pp.2763 - 2770.



Denis V. Makarov– (b. 1986) – Candidate of Technical Sciences, associate prof., Novosibirsk state technical university. His research interests are currently focused on power electronics, power converters, power generation and accumulation systems, active power filters. He is author of 40 scientific papers.
Email: armature.current@gmail.com



Maxim A. Khoroshev – was born in 1993, Phd student of Novosibirsk state technical university. research interests: Power electronic, power generation and accumulation systems, active power filters. Email: imxoiam1@gmail.com



Ilya V. Zaev – Phd student of Novosibirsk state technical university. research interests: Power electronic, resonant converter, neural network.
Email: rollproduce@gmail.com



Vadim E. Sidorov was born in 1995. He is a first year MS. Dg. student at the Novosibirsk State Technical University. Since 2017, he is a laboratory assistant of Institute of Power Electronics of NSTU. His research interests include the improvement of power electronics, DC-DC converters, electric drive systems.
E-mail: rekspark@gmail.com

Signal-Adaptive Current Controller in the Cascade System of Rotor Radial Displacement Updating

Ilya S. Dymov, Denis A. Kotin
Novosibirsk State Technical University, Novosibirsk, Russia

Abstract – The paper is devoted to the equivalent transfer function calculation of signal-adaptive controller of the electromagnet excitation current, which is an inner control loop in cascade control system of automatic correction system of rotor radial position updating of micro electric drive, using in ultraprecision processing systems. A new approach of solving the problem of stabilizing the rotating element of motor, based on active current updating of the spatial position is offered. The calculation of automatic control algorithm is done using the method of signal-adaptive inverse model. The paper describes the way of constructive implementation of this method, structural synthesis methodology of control law, as well as the results of simulation, confirming potential of conducted research.

Index Terms – Active stabilization, signal-adaptive current controller, active magnetic bearings.

I. INTRODUCTION

MODERN developments in the field of perfecting of methods of stabilization of the axial and radial displacements in case of using close control equipment are aimed at research of fundamentally new kinds of bearings, where for creating of a corresponding response magnetic and electric fields are used. As far as the main mechanical vibration source in electric plants leading to an unacceptable operation in loss of accuracy is rotating rotor of DC or AC electric motor using such bearings for high-precision systems will allow to improve operational capability and reduce defective products. Today active magnetic bearings (AMB), where rotor position relative to the stator is controlled by the feedback system, which provides stability of radial position of axis of rotation, are of most practical interest [1,2].

Main advantages of AMB are absence of mechanical contact between rotating and stationary part of electric motor under normal operational mode, and a possibility to control a toughness and amortization of AMB system during the process operation. Contactless interworking excludes depreciation of electric motor structural components, lowers starting torques, and load torques, excludes necessity of lubricant, and provides a longer operating life. Variation of elasticity and damping characteristics of magnetic system allow to greatly lower vibration and disturbance actions related to it, and force moments caused by rotor residual dynamic unbalance.

In spite of clear advantages of AMB they do not have wide acceptance for several reasons [3]. First, there is a design and engineering implementation complexity of AMB in the structure of electric motor. Second, there is a necessity of

count of failure possibility. Therefore, any high-precision devices with magnetic bearings include safety bearing assembly. This assembly consists of supplementary bearings, designed for restraint of radial rotor displacement and exclusion its contact with stator surface at switching-off of AMB by running down of a rotating rotor to full-stop or return to operation of AMB.

II. PROBLEM DEFINITION

Operating performance of the high-precision advanced equipment improvement connected with reducing accruing radial displacement by implementation of new methods of control system synthesis becomes priority objective for development of laser setups, high-precision turning, scabbling, grinding workstations, stabilization and orientation systems of the space vehicles. Therefore, the main task is to develop and investigate adaptive controller of the active stabilization system of the spatial position of the rotating element of the electric motor in the cascade system.

III. THEORY

A. Method of Active Stabilization of the Radial Displacement

The method of active exclusion of the radial displacement of the rotor is based on contactless stabilization of the spatial position of the rotating element without modernization of electric motor. Rotor of the motor is supported by typical bearing assembly in construction. In the process of machine rotor preparation for realization of the active stabilization method, mounting of magnetic circle of the required thickness on the surface is needed. As a control object there are used two pairs of electromagnets, mounted in mutually perpendicular planes. Each pair of electromagnets mounted in its own plane, provides reversible deflection behavior in terms of cancel out the radial displacements of the rotation axis according to the coordinate, depending on the signals from the sensors of displacement of the rotor position [4]. Thus balancing process of the rotating rotor is being performed non-stop according to created electromagnetic action.

Function diagram of design and process control system of active stabilization is presented in Fig. 1.

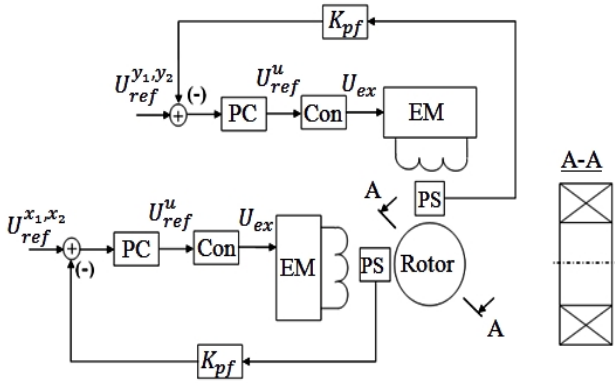


Fig. 1. Function diagram showing method of active stabilization of the rotor.

The legend of Fig. 1 is as follows:

- $U_{ref}^{x_1, x_2, y_1, y_2}$ – the reference signals on the desired radial displacement in the plane X and Y respectively, V;
- PC – the spatial position controllers;
- Con – the converter;
- U_{ref}^u – the reference signal for the converter voltage, V;
- U_{ex} – the output voltage of the converter (excitation voltage of the electromagnet), V;
- EM – the electromagnet – a control object (CO);
- PS – the spatial position sensors of the rotor, registering the radial displacement in the plane X and Y ;
- K_{pf} – the coefficient for radial displacement feedback in planes X and Y .

As the spatial position sensors of the rotor, registering the radial displacement in the plane X and Y we assume implementation of photovoltaic converters of combined type, which information element can provide high accuracy of axial displacement measurement by the help of self-correction of angular error of measuring raster [5].

B. Method of Signal-Adaptive Inverse Model

Method of signal-adaptive inverse model (SAIM) is a way of synthesis of robust single-channel and multichannel control systems with different-rate processes, which generate direct adaptive control algorithms (without midline identification of parameters deviation) with signal (non-parametric) self-tuning. Systems synthesized by SAIM method have a low-sensitivity to external and parametric disturbances and to variation behavior of CO [6]. Interpretation of conceptual issues of this method is fully described in [7].

If we write a mathematical model of CO in standard form:

$$x^{(n)} = a(t, \mathbf{x}) + b(t, \mathbf{x})u, \quad (1)$$

where $a(\cdot)$ – unchangeable part of the mathematical model of CO; $b(\cdot)$ – changeable part of the mathematical model of CO; x – output (controlled) variable; t – time parameter;

$x^{(n)} = \frac{d^n x}{dt^n}$ – higher derivative of controlled coordinate,

explicitly dependent from control action u ;

$\mathbf{x} = [x, x^{(1)}, x^{(2)}, \dots, x^{(n-1)}]^T$ – a vector of canonical, for principles of controlling of motions in invariant varieties, of state coordinates.

In this case, necessary and sufficient condition of realizability of control objective, consisting in tracking output of n times differentiating reference time-varying function, that is always true for objects in terms of (1) when limitations on a control and state coordinates are absent, is their mathematical models reversibility with respect of control action.

C. Method of Cascade Control

Synthesis of the automatic control system of stabilization of the radial position by cascade control method represents the group of some guidelines [8]:

1. The development of the flow diagram of the system is started from the inner control loop. It includes an uncompensated part of the control object followed by an overcome circuit.
2. For the output variable of the first overcome circuit is developed a closed loop with feedforward compensator – controller.
3. Control loops of the output variables of all next circuits are closed each with its own controller in order. Feedbacks do not cross against each other.
4. The type definition and calculation of the controller is also carried out consequently, starting from the inner to the default settings.
5. In the synthesis of the controller of each external loop, inner control loop is approximated by a first-order circuit with the corresponding response time. This is considered uncompensated at this stage.

The finding of controllers and their parameters calculation is reduced to bring the transfer function of each loop in accordance with the set requirements, for example, an equation of desired motion path. Synthesis carried consequently, starting with the inner control loop.

IV. EXPERIMENTAL RESULTS

Let's make the digital simulation of radial displacement of the rotor centering system of a motor in a part of micro electric drive. A general flow diagram of adaptive current controller of the electromagnet for the approach of active stabilization of radial displacement of the rotor is presented in Fig. 2.

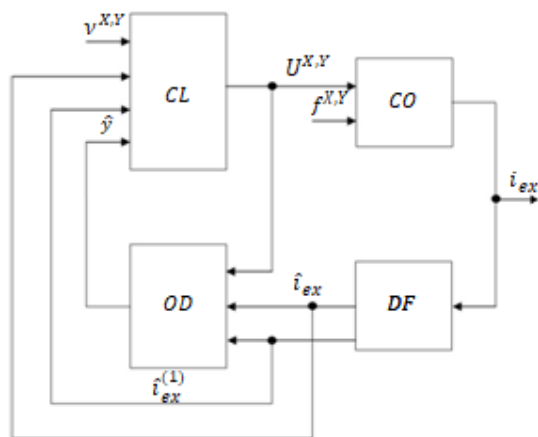


Fig. 2. General flow diagram of current control loop, synthesized by SAIM method.

The legend of Fig. 2 is as follows:

- $v^{X,Y}$ – the reference signals on the radial displacement in planes X and Y respectively, V;
- CL – subsystem of a control law;
- CO – subsystem of CO;
- DF – subsystem of differential filter (DF);
- OD – subsystem of a disturbances observer;
- $U^{X,Y}$ – produced voltage on a CO, V;
- $f^{X,Y}$ – disturbance action acting on a CO;
- \hat{y} – disturbances estimation, including both parametric and signal disturbances, V;
- i_{ex} – output coordinate, excitation current of the electromagnet;
- $\hat{i}_{ex}, \hat{i}_{ex}^{(1)}$ – estimations of the excitation current and it first-order derivative.

In further discussion about active stabilization system, description of the control system will be provided only in one plane for one electromagnet (for the rest of electromagnets description is the same).

A mathematical model of electromagnetic processes in magnetizing coil of an electromagnet is represented as a following differential equation:

$$U = i_{ex}R + L \frac{di_{ex}}{dt}. \quad (2)$$

Flow diagram of the CO subsystem is presented in Fig. 3.

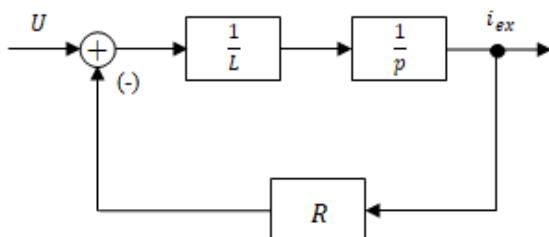


Fig. 3. Flow diagram of the CO subsystem.

The legend of Fig. 3 is as follows:

- i_{ex} – excitation current of the electromagnet, A;
- R – resistance of a magnetizing coil, Ω ;

- L – inductance of a magnetizing coil, H;
- U – voltage applied to the electromagnet, V.

On the other hand, for synthesis adaptive current controller, mathematical representation of the electromagnet in operational notation is as follows:

$$i_{ex}(p) = (U(p) - Ri_{ex}(p)) \frac{1}{Lp}. \quad (3)$$

The components of an equation (3) can be divided into two parts: known (unchangeable) and unknown (changeable) in accordance with (1):

$$\begin{cases} a(t, x) = -\frac{i_{ex}R}{L}, \\ b(t, x) = \frac{1}{L}. \end{cases} \quad (4)$$

To simplify synthesis procedure of a control law, let's reduce the first equation of a system (4) to the following view:

$$a_0(t, x) = a_{01}\dot{i}_{ex} - a_{00}i_{ex}, \quad (5)$$

where a_{01}, a_{00} – coefficients, located ahead of \dot{i}_{ex} and i_{ex} respectively.

According to equation (3) and condition under which it is necessary to provide motion of a CO in accordance with sample processes an equation of desired motion path looks as follows:

$$\dot{i}_{ex} = \Omega_d U - i_{ex} A_1, \quad (6)$$

where $A_1 = 1.41$ – the shape form of a proof linear setting to the Butterworth, determining the oscillatory transient of the excitation current; $\Omega_d = \frac{1}{T_d}$ – geometric average root,

determining the rate of response of the current control process; $T_d = 0.1 \frac{L}{R}$ – desired time response, s.

Thus, the control law for a system of adaptive current controller of the electromagnet will be defined by the following equation:

$$U = \frac{1}{b_0} ((-\Omega_d - a_0)i_{ex} + \Omega_d v - \hat{y}), \quad (7)$$

where \hat{y} – “disturbances” estimation, created by observer.

Flow diagram of the control law subsystem is presented in Fig. 4.

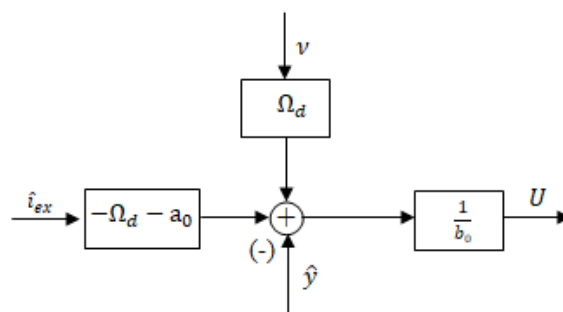


Fig. 4. Flow diagram of the control law subsystem.

For a noise level reduction in the channel of a control action creation setting DF, which should be a low-pass filter that is at least per unit higher than a degree of a highest derivative estimated by its using, in a control system structure is needed. In this case, mathematical formulation of DF looks as follows:

$$T_F A_1 \frac{d\hat{i}_{ex}}{dt} + \hat{i}_{ex} = i_{ex}, \quad (8)$$

where $T_F \leq \frac{\mu}{K_{dm}}$ – filter time constant, s; $K_{dm} = 6 \dots 10$ – splitting ratio of a motions; $\mu > 0$ – small parameter, defining the rate of signal adaptation process of control algorithm (7).

Flow diagram of the DF subsystem presented in Fig. 5.

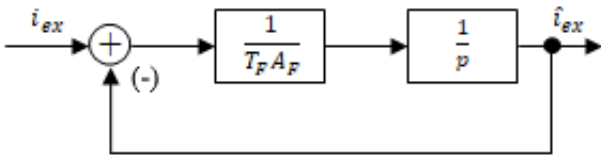


Fig. 5. Flow diagram of the DF subsystem.

Flow diagram of the disturbances observer subsystem is presented in Fig. 6.

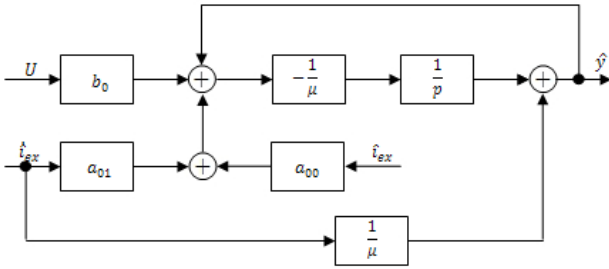


Fig. 6. Flow diagram of the disturbances observer subsystem.

For further finding of radial displacement controller structure of active stabilization system it is necessary to convert gained adaptive controller to equivalent transfer function. Let's create a general flow diagram of SAIM method for it.

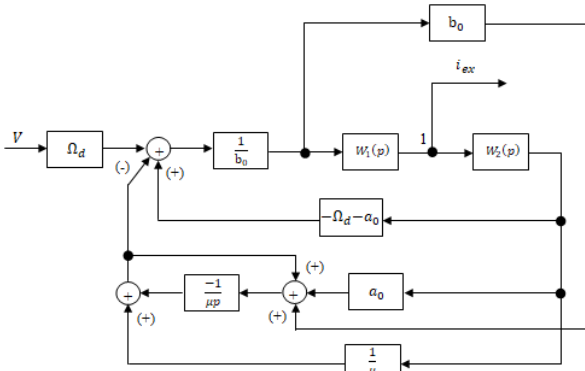


Fig. 7. Reduced flow diagram of the signal-adaptive excitation current control loop.

The legend of Fig. 7 is as follows:

- $W_1(p) = \frac{1}{Lp} - \text{CO transfer function};$
- $W_2(p) = \frac{1}{(T_F A_F)p} - \text{DF transfer function}.$

Since flow diagram in Fig. 7 is multi-loop, then firstly it is necessary to remove crossfeeds using nodes shifting rules or summers, and then with the help of structural reconstructions fundamental rules reduce flow diagram to single-loop and write transfer function. Based on the above, let's move node 1 from input circuit with transfer function $W_2(p)$ to its output (see Fig. 8).

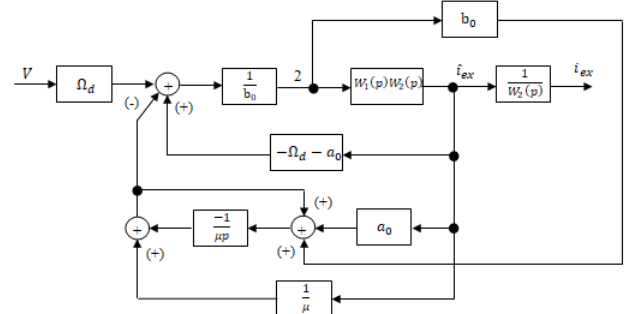


Fig. 8. Reconstructed reduced flow diagram of the current control loop.

Let's move node 2 from input circuit with transfer function $W_1(p)W_2(p)$ to its output (see Fig. 9).

According to flow diagrams reconstructions rules, let us convert the structure to the view as it is shown in Fig. 10.

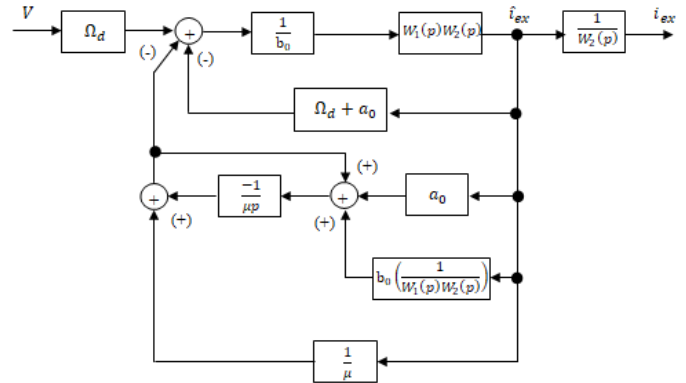


Fig. 9. Reconstructed flow diagram of the current control loop.

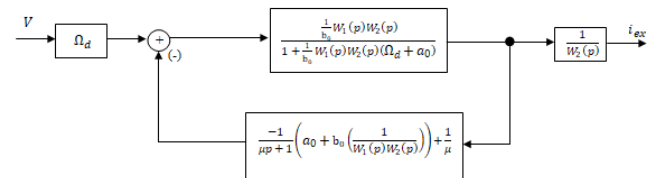


Fig. 10. Equivalent flow diagram of the signal-adaptive excitation current control loop.

Based on Fig. 10 transfer function of excitation of the electromagnet current control loop is:

$$W_3(p) = \frac{\mu \Omega_d / W_2(p)}{1 + \mu \left(\left(1 - \frac{1}{\mu p + 1} \right) \left(\frac{1}{W_4(p)} + a_0 \right) + \Omega_d \right)}, \quad (9)$$

$$\text{where } W_4(p) = \frac{W_1(p)W_2(p)}{b_0}.$$

The results of a digital simulation is the excitation current transient during supply unit step-type signal, at that equivalent controller parameters are equal to real signal-adaptive controller and were not changed during simulation modeling.

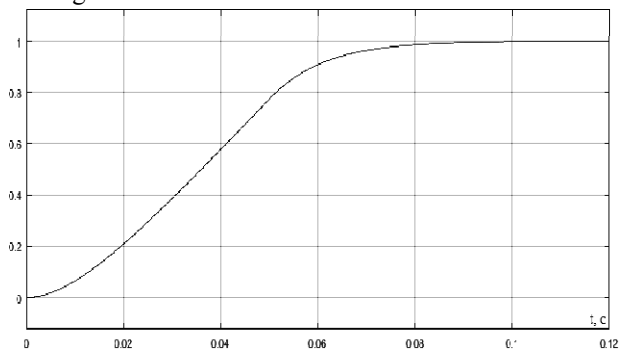


Fig. 11. Equivalent signal-adaptive excitation current control loop transient.

V. DISCUSSION OF RESULTS

Analyzing the results of digital simulation of equivalent signal-adaptive excitation current controller of method of an active stabilization of the radial displacements of the electric drive rotor it is possible to draw the following conclusions:

- 1) Type of transient represents first-order circuit behavior, that fulfills equation of desired motion path.
- 2) Setting time $t=0.071$ s and lack of overshoot allows to use received transfer function as an inner control loop, according to cascade control system guidelines.

VI. CONCLUSION

Based on received transients, we can draw a conclusion that received equivalent transfer function of the electromagnet excitation current control loop of system of an active stabilization of the radial displacements of the rotor can be used for synthesis of next loops, since control loop can be approximated by a first-order circuit with the corresponding response time. Thus, using calculation of the controller rules for the cascade control system with SAIM method using a signal-adaptive controller of the radial displacements of active stabilization system that has all the advantages of using methods will be calculated.

REFERENCES

- [1] Zhuravlev Y.N. Active magnetic bearings: Theory, calculation, application. – St. Petersburg: Polytechnic, 2003. – 206 p.

- [2] Bogdanova Y.V., Guskov A.M. Modeling of dynamics of electric spindle rotor on magnetic bearings // Science and Education. Bauman Moscow State Technical University. – 2015. – № 01 – pp. 201–220.
- [3] Polyakov M.V. Determination of Safety Rotor Displacement Zone for Active Magnetic Bearing Reaction Wheel // Bulletin of the Reshetnev Siberian State Aerospace University. – 2016. – Vol. 17. – № 4 – pp. 1005–1014.
- [4] Ilya S. Dymov, Denis A. Kotin. Signal-Adaptive Controller for Micro Electric Drive Rotor Radial Displacement Updating // 18 International Conference of Young Specialists on Micro/Nanotechnologies and Electron Devices EDM 2017: Proceedings, Erlagol, Altai Republic – 29 June – 3 July, 2017. – Novosibirsk: NSTU, 2017. – P. 572 – 578.
- [5] Kiryanov A.V., Zhmud V.A., Tomilov I.N., Kotin D.A., Tereshkin D.O., Ostanin A.V. Accuracy enhancement of circular laser pattern generator for precision angle measurement structures // Science Bulletin of the Novosibirsk state technical university. – 2013. – № 3 (52). – pp. 46–50.
- [6] Pankratov V.V. Synthesis method of robust control algorithms based on adaptive inverse models // Automated electromechanical systems: Proceedings. – Novosibirsk: NSTU, 2008. – pp. 14 – 27.
- [7] Pankratov V.V., Zima E.A., Nos O.V. Special sections of modern automatic control theory: Study guide. – Novosibirsk: NSTU, 2007. – 219 pp.
- [8] V.V. Pankratov. Automatic control of the elect drives: study guide. Part I. Coordinates regulation of the DC-motor electric drives. – Novosibirsk: NSTU, 2013. – 200 p.



Ilya S. Dymov was born in Novosibirsk, Russia, in 1992. Received a Bachelor's degree in 2014 and a Master's degree in 2016 at Novosibirsk State Technical University. Nowadays author is a postgraduate student at the same university. Research interests: adaptive control systems. E-mail: ildymov@mail.ru



Denis A. Kotin was born 1984. Cand. of Tech. Sc., Associate Professor, Head of the Department of Electric Drive and Industry Automation at Novosibirsk State Technical University. Research interests: automatic control of AC electric drives and power electronic devices. E-mail: d.kotin@corp.nstu.ru

Digital Pulse-Width Modulator with Asynchronous Change of Compare Register Value and Short Delay Time*

Vagiz A. Kabirov, Valery D. Semyonov, Nikita P. Vintonyak, Danila B. Borodin, Sergey S. Tyunin
Tomsk State University of Control Systems and Radioelectronics, Tomsk, Russia

Abstract– This paper presents an analysis of signal delay time in implementation of digital pulse-width modulators (DPWM). The paper demonstrates that the most essential component of delay time in a digital modulator is the time required for implementation of DPWM, and that it is almost always understood that the DPWM is a type 1 PWM. It is shown that the maximum delay time in such approach to DPWM implementation within the range cannot be less than one PWM conversion period. A new approach to DPWM implementation is proposed, suggesting an increase of the number of signal measurements within a PWM period and an asynchronous change of the compare register value in the digital comparator. Signal delay in the proposed DPWM is reduced N times, where N is the number of signal measurements within a PWM period. The proposed approach essentially results in implementation of a DPWM as a type 2 PWM.

IndexTerms– Digital control systems for switching converters, pulse-width modulation, phase frequency characteristic.

I. INTRODUCTION

DIGITAL control systems (DCS) used to control switching voltage converters have a number of advantages over analog systems, as discussed in [1-5].

At the same time, replacement of an analog control system in a switching converter with a digital control system results in inferior dynamic properties and precision of the switching converter due to delays and the quantization effect caused by the operating algorithm of the digital PWM [Error! Reference source not found., Error! Reference source not found.], ADC and the digital correction element [Error! Reference source not found.].

[Error! Reference source not found.] offers an observation that implementation of microcontroller-based digital CS creates a pure time delay element in a small-signal model of a switching voltage converter (1).

$$W_{DCS}(p) = e^{-t_{DCS} \times p} \quad (1)$$

According to the authors, the time delay t_{DCS} introduced by the DCS consists of the following components: delay t_{ADC} in ADC measurements, delay t_{CALC} in calculations of coefficients for the correction element and delay t_{DPWM} in implementation of a digital pulse-width modulator (DPWM). Delay t_{ADC} in ADC measurements can be neglected due to its small value compared to the other components. Delay t_{CALC} in calculations accounts for half of the DPWM period if coef-

ficient values are calculated at the output of the correction element in the middle of the previous DPWM period, after measurement and conversion of the signal, as shown in expression (2).

$$t_{CALC} = 0,5 \times T_{PWM} \quad (2)$$

Delay t_{DPWM} introduced by the DPWM accounts for half of the DPWM period as well [6], which the authors believe makes it possible to set the total delay to one DPWM period.

Fig. 1 shows a small-signal diagram for a switching voltage converter with a single negative feedback, demonstrating the point of connection of the pure time delay element W_{DCS} , as discussed in [Error! Reference source not found.].

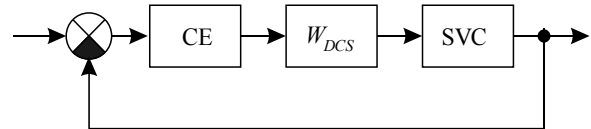


Fig. 1. Small-signal switching converter model.

However, simulation and experimental testing of DPWM-based switching converters made it possible to observe a significant divergence of phase-frequency characteristics of actual systems from those systems where the PWM delay was described by the expression (1). A more detailed study of the DCS operation showed that the delay t_{DPWM} introduced by the DPWM is a variable within the range from 0 to T_{PWM} , and the constant component of the signal b changes at the output of the correction element.

II. PROBLEM STATEMENT

The objectives of this paper are: to analyze the pure time delay in a DPWM; to establish the dependency of pure time delay on calculated parameters of the operating point of the converter and to analyze the potential ways to bring the delay time closer to the values found in analog control systems.

*The research has been carried out under Agreement №02.G25.31.0182 dated December 1, 2015 between JSC Information Satellite Systems and the Ministry of Education and Science of the Russian Federation.

III. THEORY

Operation of a DCS implemented through a MC-based software-hardware platform, as proposed in [Error! Reference source not found.], is characterized by timing diagrams shown in Fig. 2.

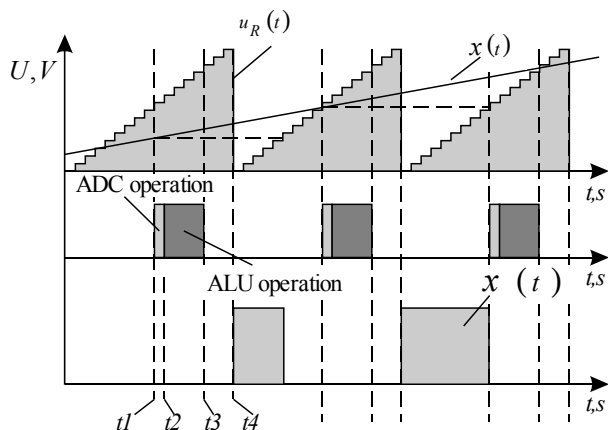


Fig. 2. DCS operation diagram.

The above diagrams demonstrate the PWM generation algorithm that currently enjoys the widest use. At the time point t_1 shifted by $0.5 T_{PWM}$ relative to the start of the modulating ramp signal generation, as recommended by [6] above, the analog-to-digital converter (ADC) starts its operation. At this point, the analog signal is captured to the memory-storage cell of the ADC (analog signal capture). At the time point t_2 , the ADC finishes its conversion and hardware-interrupts the microcontroller MC, with the MC's ALU starting its operation until the time point t_3 . Two mathematical operations are performed in this time interval: calculation of error between the measured ADC signal and the signal from the generator U_3 , and calculation of the output signal from the correction element CE, based on the error. At the time point t_3 , the output signal from the correction element (CE) is calculated and written to the "latch register". At the time point t_4 , one period of modulating signal generation ends, and the next one begins. The calculated value of the CE output signal is taken from the "latch register" and fed to the compare register of the timer generating the DPWM signal. Saving the calculated value of the CE output signal in the latch register until the end of the DPWM period makes it possible to avoid the occurrence of two output pulses in the modulator within the same period.

Fig. 2 offers a good demonstration of the delays caused by the ADC operation. A sum of these time intervals does not exceed and can be significantly less than $0.5 T_{PWM}$. The delay itself is related to the elimination algorithm used to prevent formation of a double pulse at the output of the modulator.

Analytical determination of the delay t_{DPWM} introduced by the DPWM implementation can present a challenge. Therefore, we shall rely on experimental determination of such delay based on the frequency DPWM characteristics obtained with the help of a mathematical simulation model of the DPWM.

Fig. 3 shows a simulation model of the DPWM. It consists of a ramp generator (R), a zero order hold device (ZOH) and a comparator C. The working period and phase of the hold device coincide with the working period of the ramp genera-

tor. The hold device ZOH simulates the operation of an ideal ADC that instantaneously measures the analog signal $x(t)$ at the time point coinciding with the start of the DPWM, while comparison of the measured signal to the saw-tooth voltage $z(t)$ with the help of the comparator C simulates the operation of an ideal type 2 digital PWM [7]. The proposed simulation model implements a type 1 PWM algorithm, without regard to delay times t_{ADC} and t_{ALU} .

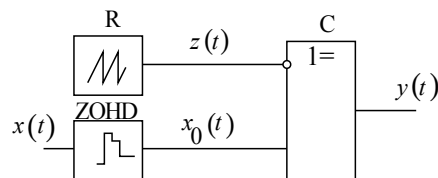


Fig. 3. DPWM simulation model.

The following signal is fed to the DPWM input:

$$x(t) = A \times \cos(2 \times \pi \times f \times t) + b \quad (4)$$

where: A is the amplitude of the variable component of the harmonic signal, b is the constant component of the input signal.

In small-signal models of PWM converters, the constant component b determines the operating point of the converter where the pulse system is linearized, and the amplitude A determines the amplitude of harmonic deviation from the operating point. The amplitude, by definition, should be small and theoretically tend to zero, but in practice, in experiments it can fall within the range from 1 to 20% of the value of the constant component b . The sum value of the components b and A should also not exceed the saw-tooth voltage in order to eliminate PWM saturation. The output signal $y(t)$ of the DPWM (response signal) is assumed to be the first DPWM output signal harmonic.

The simulation model shown in Fig. 3 can be represented in Mathcad as follows.

We shall write the modulating signal from the ramp generator output as follows:

$$z(t) = f_{\Pi} \times t - \text{floor}(f_{\Pi} \times t) \quad (5)$$

where: f_{Π} is the DPWM operation frequency (in experiments, f_{Π} is taken to be 100 kHz).

The modulating signal is a ramp signal with a variation range of 0 to 1.

The zero-order hold device output signal can be represented by the expression:

$$x_0(t) = \begin{cases} n \leftarrow \text{floor}(f_{\Pi} \times t) \\ t_n \leftarrow \frac{n}{f_{\Pi}} \\ x(t_n) \end{cases} \quad (6)$$

DPWM output signal:

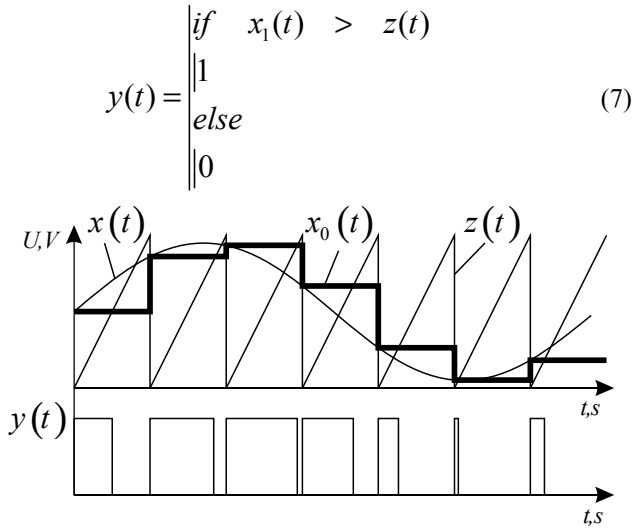


Fig. 4. DPWM operation diagrams.

For illustrative purposes, Fig. 4 shows diagrams of functions $x(t)$, $x_0(t)$, $z(t)$ and $y(t)$ with a large value of the amplitude A .

Thereafter, the output signal $y(t)$ is decomposed into a Fourier series in Mathcad with the help of the FFT function.

By adjusting the frequency f of the input harmonic signal $x(t)$ and finding the phase ϕ of the first harmonic of the output signal $y(t)$, we shall form the phase-frequency characteristic (PFC) of the DPWM $\phi(f)$, Fig. 5, with its measurements given in electrical degrees for the sake of convenience. It can be seen in the Figure that at low frequencies, the PFC family presents as lines at various angles, the size of which is proportional to the value b of the constant component of the input signal. Such PFC has an ideal pure time delay element. For illustrative purposes, the PFC of such element with the delay time T_{Π} , equaling the PWM period, is represented by a line with a maximum angle. The graph shows the numerical values of parameters A and b of the test input signal (4). Changing the amplitude A of the variable component of the test signal has virtually no effect on the PFC (unless the PWM becomes saturated), and the value of the constant component b determines the angle of the PFC, which, in its turn, determines the delay t_{DPWM} in DPWM implementation. Further frequency increase results in divergent oscillations of the PFC, overlapping the characteristic of the ideal delay element. That phenomenon is associated with errors of the FFT function algorithm that occur when finding the first harmonic at aliquant frequencies. The error becomes significantly smaller with the increase of the number of periods of the output signal $y(t)$ decomposed into a Fourier series, and the PFC becomes linear. The PFC family can be approximated by the expression (3)

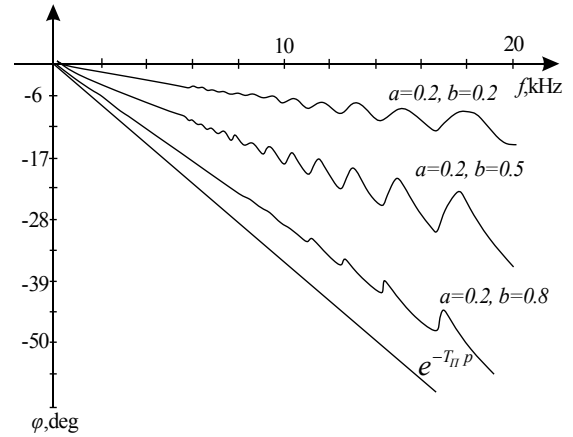


Fig. 5. DPWM PFC.

$$t_{DPWM} \approx \frac{T_{PWM}}{b_m} \times b \quad (3)$$

where: b_m is the saw-tooth voltage amplitude, and b is the constant component of the test signal that serves as a parameter of the operating point for the mode.

It follows from the above that the DPWM is an element with a changeable-time delay, and that the maximum DCS delay during capture of the analog signal (ADC start) in the middle of the DPWM cycle should be set to $t_{DCS} 1.5 T_{PWM}$.

The resultant value of the pure time delay t_{DCS} causes a significant deterioration of frequency characteristics in a small-signal model of an uncorrected automatic control system, and, more precisely, its phase-frequency characteristic [8,9]. Ultimately, that makes it impossible to achieve dynamic properties of the switching converter that would be similar to those of analog system-controlled switching converters.

A DCS based on a specialized digital IC or a FPGA (gate-array chip) makes it possible to implement a different logic for pulse-width signal generation (PWM) and significantly accelerate calculation of the CE output signal. Fig. 6 shows a proposed operation algorithm of a modified DCS (MDCS) that would allow a significantly reduced time delay t_{DCS} , introduced by the DCS.

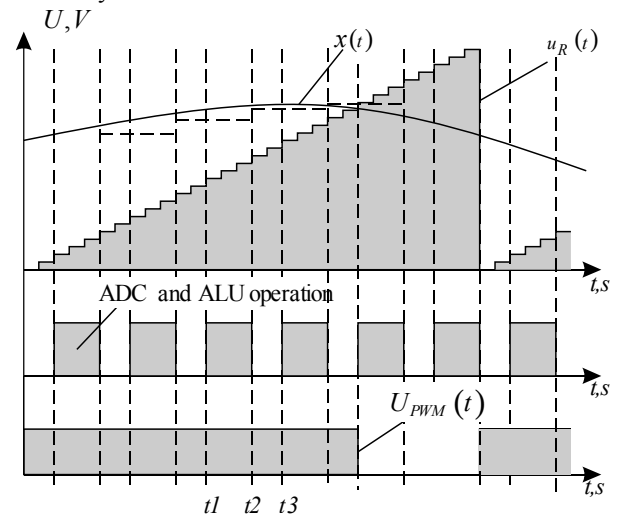


Fig. 6. Algorithm of MDCS operation.

The time t_1 determines the DSC start (storage of the analog signal), the time t_2 determines the end of the CE output signal calculation, and the time t_3 determines the start for the next ADC conversion. In a real system, the time interval t_3-t_2 can be made negligible compared to the input signal change period. As shown in the Figure, the time interval t_3-t_2 is set to be final in order to illustrate the delay of the measured signal $x_0(t)$ compared to the original $x(t)$.

The time interval t_2-t_1 represents the delay caused by the ADC operation and calculation of the CE output signal. Within the range, the speed of the CE output signal calculation can be reduced to a single cycle of the generator timing the FPGA. At the generator's frequency of 200 mGz, the calculation time will be $t_{ALU} = 5$ ns. Contemporary successive-approximation ADC (e.g., AD7356) can draw up to 5×10^6 samples per second, enabling a delay of $t_{ADC} = 200$ ns. Thus, some 50 samples (measurements) can be drawn within a single period of the PWM modulator.

In order to estimate the time delays introduced by the proposed MDCS, without regard to the delays introduced by the ADC t_{ADC} and ALU t_{ALU} , we shall also rely on the method of experimental determination of frequency characteristics in a simulation model of the MDCS modulator. The simulation model of the MDCS modulator has the same form as the DPWM. The difference between simulation models of DPWM and MDCS is in the operation frequency of the zero order hold device, which is determined by the number N of measurements of the input $x(t)$ signal within a PWM period.

In such a case, the output signal from the zero order hold device of the MDCS can be written as the following expression:

$$x_0(t) = \begin{cases} n \leftarrow \text{floor}(N \times f_{\Pi} \times t) \\ t_n \leftarrow \frac{n}{N \times f_{\Pi}} \\ x(t_n) \end{cases} \quad (8)$$

where: N is the number of signal measurements within a PWM period.

Figure 7 shows a PFC family of the MDCS with the number of measurements $N=2$. The resultant dependencies of the MDCS PFC are the same in nature as the DPWM PFC. The pure time delay also increases with increase of the constant component b of the input signal, but its maximum value is $N=2$ times smaller than the DPWM period, which is confirmed by the phase characteristic of the ideal delay element, with a delay time of $T_{\Pi}/2$. With the value of the constant component b tending to unity, the MDCS PFC tends to the PFC of the pure delay element where the delay time equals half of the PWM operating period.

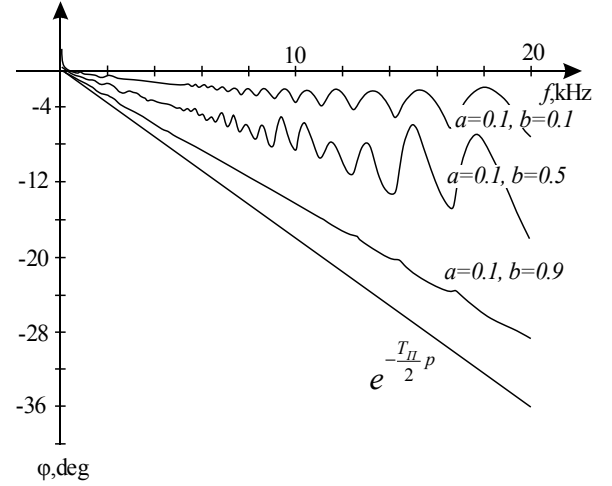


Fig. 7. MDCS PFC with the number of quantizations in the PWM period $N=2$.

Increase of the number of measurements N in the PWM period results in a phase delay reduced N times at any values of A and b . The transfer function of the pure delay element determining the maximum phase deviation at $b \rightarrow 1$ is defined with the expression:

$$W(p) = e^{-\frac{T_{\Pi}}{N} p} \quad (9)$$

Increase of the number of quantizations in the PWM period makes it possible to reduce the pure time delay in the automatic switching converter control system N times.

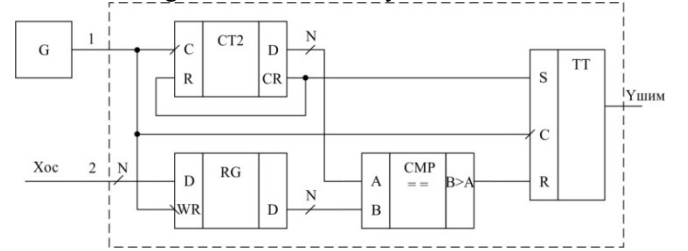


Fig. 8. Functional diagram of a DPWM with asynchronous change of the compare register.

Fig. 8 shows a functional diagram of a DPWM with asynchronous change of the compare register value. It includes: binary counter CT2, latch register RG, comparator CMP and a clocked RS-trigger TT. A DPWM with asynchronous change of the compare register has two inputs and one output: input 1 of timing generator, input 2 of the signal being modulated and PWM output (Y_{PWM}). The diagram is rather simple and demonstrates a digital implementation of a type 2 analog pulse-width modulator PWM-2 [7]. An important aspect of the diagram is the function of the latch register RG. Data storage in the register RG and operation of the clocked RS-trigger should be spread out in time to prevent false action of the circuit due to the race condition. For that purpose, the latch register is timed by the trailing edge of the generator's signal (G), while the clocked RS-trigger is timed by the leading edge.

IV. EXPERIMENTAL RESULTS

To check the validity of the expressions, a simulation model of a shunt voltage regulator was developed (Fig. 9), consisting of a current source ($J1$), Butterworth filter ($C1$, $C2$, $R1$), throttle ($L1$), ideal wrench ($S1$), ideal diode ($VD1$), output filter ($C3$), load resistance (R_H), voltage meter ($V.M.1$), load voltage controller (G), subtracter-adder, subsystem of the correction element (CE) and the PWM subsystem. In the process of simulation, the PWM subsystem is substituted, i.e. the type of the control system is changed, in order to compare their characteristics. All other elements of the simulation model remain the same.

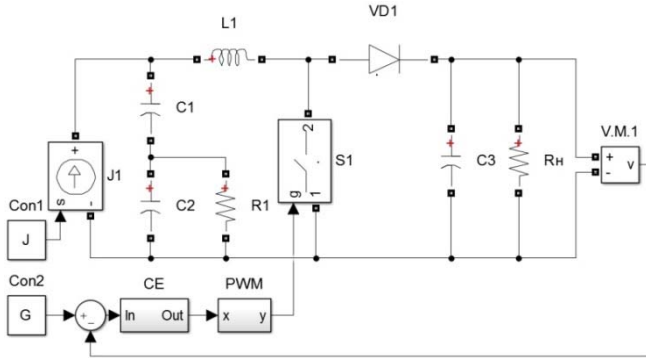


Fig. 9. Model of a shunt voltage regulator in MATLAB/Simulink.

Fig. 10 shows oscillograms of transient processes in simulation models of three shunt switching stabilizers with various types of control systems. A load current jump was used for the disturbance effect. Fig. 10 a) shows a transient process in a stabilizer with an analog PWM-2-based control system. Fig. 10 b) shows a stabilizer with a type 1 digital modulator DPWM-1-based control system; Fig. 10 c) shows a stabilizer with a control system based on a DPWM with asynchronous change of the compare register (analog DPWM-2). All of the control systems used the same correction element with the same parameters.

The above oscillograms of transient processes, recorded under pulsed load current increments, offer a good demonstration of damping oscillations in output voltage, which indicates a small phase margin for the voltage stabilization loop. The smallest damping of oscillations, meaning the smallest phase margin, is observed in a DPWM-2 shunt voltage stabilizer (Fig. 9 a), and the largest phase margin, meaning the highest damping of oscillations, is observed in the "analog PWM" shunt voltage stabilizer (Fig. 9 c), which validates our estimate of delay time for the PFC in Fig. 6-7.

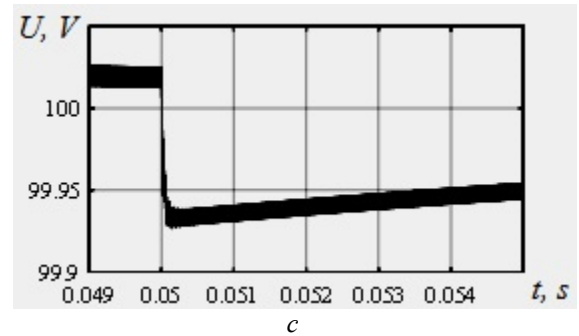
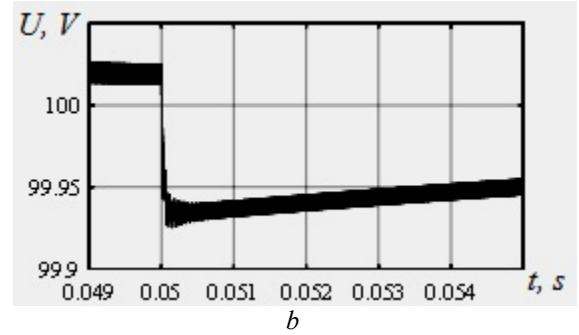
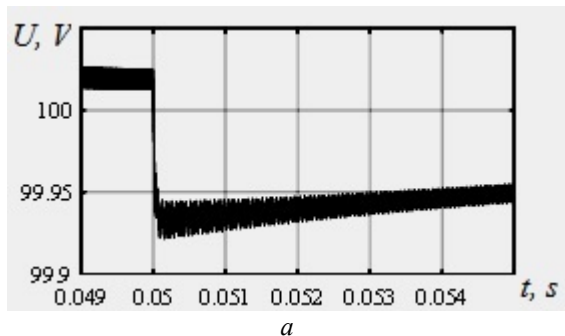


Fig. 10. Output voltage of shunt stabilizer simulation models with progressive load current increments. *a* – DPWM-based control systems. *b* – control system based on DPWM with asynchronous change of the compare register. *c* – "analog PWM"-based control system.

V. RESULTS AND DISCUSSION

The results obtained allow the authors to conclude that signal delay in DPWM is mainly due to the underlying algorithm of type 1 PWM, which makes it fundamentally impossible to achieve a delay that is under one cycle of PWM signal formation. Implementation of a control system for a switching converter based on a DPWM with asynchronous change of the compare register makes it possible to improve its dynamic properties. Within the range, by increasing the number of signal measurements to 10-20 by using a DPWM with asynchronous change of the compare register, it is possible to achieve the same dynamic properties as when using an "analog" PWM.

VI. SUMMARY AND CONCLUSION

– Implementation of digital PWM based on conventional approaches in power electronics makes it possible to reduce the maximum delay time, which is equivalent to pure delay, only down to over one period of the PWM modulator, even when state-of-the-art fast-acting microcontrollers are used.

– When using the proposed DPWM with asynchronous change of the compare register, it becomes possible to reduce pure delay to the time required for the ADC to convert the input analog signal to digital, which ultimately makes it possible to accelerate the performance of closed-loop electrical conversion systems N times, where N is the number of signal measurements within a PWM period.

REFERENCES

- [1] RaduEtz, Stefan R. Daraban, Dorin M. Petreus, Adina R. Rusu. A Comparison between Digital and Analog Control for a Buck Converter// IEEE Electronics Technology International Spring Seminar – Warsaw, May 2010.
- [2] Maksimovic D., Zane R., Erickson R. Impact of Digital Control in Power Electronics// Proceedings of ISPSD, pp. 13-22, May 2004.
- [3] Yan-Fei Liu, P.C.Sen. Digital Control of Switching Power Converters// IEEE Conference on Control Applications Toronto, Aug 2005.
- [4] Ahmad, H., Bakkaloglu, B. A DC-DC digitally controlled buck regulator utilizing first-order $\Sigma\Delta$ frequency discriminators// Conference Proceedings – IEEE Applied Power Electronics Conference and Exposition – APEC, art. no. 4522745, pp. 346-352, 2008.
- [5] Junhong Zhang, Jih-Sheng Lai, Wensong Yu Bidirectional DC-DC converter modeling and unified controller with digital implementation// Applied Power Electronics Conference and Exposition, 2008. APEC 2008. Twenty-Third Annual IEEE.
- [6] Junhong Zhang Bidirectional DC-DC power converter design optimization, modeling and control// Dissertation submitted to the faculty of the Virginia Polytechnic Institute and State University in partial fulfillment of the requirements for the degree of Doctor of Philosophy In Electrical Engineering, 2008. Blacksburg, Virginia
- [7] Kobzev A. V. Modulation Power Sources in Electronics (in Russian) / A. V. Kobzev, G. Ya. Mikhalechenko, N. M. Muzychenko – Tomsk: Radio i Svyaz, 1990. – 336 pp.
- [8] Shinyakov Yu.A., Semenov V.D., Kabirov V.A., Torgaeva D.S., Sukhorukov M.P., Cevastyanov R.S. Methodology to synthesis of digital regulator for solar battery energy conversion channel in the spacecraft power supply system// Conference: 2017 International Multi-Conference on Engineering, Computer and Information Sciences (SIBIRCON), September 2017
- [9] Borovikov Yu. S., Kobzev A. V., Semyonov V. D., Sulaimanov A. O., Temchuk A. I., Fedotov V. A. Signal Amplifiers for Real-Time Models (in Russian)// Proceedings of Tomsk State University of Control Systems and Radioelectronics 2(28) 2013 p. 70



Vagiz A. Kabirov was born in 1983 in Tomsk, Russia. In 2000 he enrolled to Tomsk State University of Control Systems and Radioelectronics (TUSUR), graduating in 2005 with a Specialist degree in Industrial Electronics. Starting in 2005, he has been working at the TUSUR Department of Industrial Electronics as the Head of the Laboratory of Project-Based Group Learning. Co-authored 17 utility model patents and over 40 papers published in various publications.



Valery D. Semyonov was born in 1949 in Novosibirsk region. In 1966 he enrolled to Tomsk Polytechnic Institute, graduating in 1972 with a Specialist degree in Electric Equipment of Aircraft. From 1975 till 1992 he worked at Research Institute of Automatics and Electromechanics, Tomsk State University of Control Systems and Radioelectronics (TUSUR) as an Engineer, Junior Researcher, Senior Researcher, Head of Laboratory, Head of Division. In 1982 he presented his Candidate thesis in AC Voltage Stabilizers with High-Frequency Boost Element. In 1992 took the position of Associate Professor, in 2010 became Professor at the TUSUR Department of Industrial Electronics. Throughout his teaching career, he taught courses in Basics of Converter Equipment, Electric Power Electronics. Currently he teaches courses in Semiconductor Switches in Main Circuits, Pulse Modulation Systems for Master students majoring in Electronics and Nanoelectronics. Co-authored three monographs, four teaching guides, over 50 inventor's certificates and patents and over 150 papers in various publications. Supervises research in Power Electronics for four PhD students. Four of his former PhD students have successfully pre-

sented their theses and obtained the Candidate of Science degrees. Currently he is the Head of the Laboratory of Pulse Modulation Power Systems.



Nikita P. Vintonyak was born in 1991 in Severodonetsk, Lugansk region. In 2008 he enrolled to Tomsk State University of Control Systems and Radioelectronics, graduating in 2013 with a Specialist degree in Industrial Electronics. In 2013 he became a PhD student at TUSUR University with a program in Power Electronics. Starting in 2012, he has been working at the Laboratory of Pulse Modulation Power Systems. The Laboratory develops and tests various types of power sources. Has over 20 papers published in various publications.



Danila B. Borodin was born in 1991 in Kemerovo, Russia. In 2013 he obtained a Bachelor degree in Electronics and Microelectronics at Tomsk State University of Control Systems and Radioelectronics, in 2015 obtaining a Master of Engineering and Technology degree. In 2015 he started a PhD program at TUSUR. Starting in 2013, he has been working at the Laboratory of Pulse Modulation Power Systems. The Laboratory develops and tests various types of power sources for civil use. Has 6 papers published in various regional and interuniversity publications.



Sergey S. Tyunin was born in 1989 in Tomsk, Russia. In 2013 he obtained a Specialist degree in Industrial Electronics at Tomsk State University of Control Systems and Radioelectronics, in 2015 obtaining a Master of Engineering and Technology degree. In 2015 he started a PhD program at TUSUR. Starting in 2015, he has been working at the Laboratory of Pulse Modulation Power Systems. The Laboratory develops and tests various types of power sources for civil use. Has 8 papers published in various regional and interuniversity publications. Has a utility model patent.

Soft Capture of Movable Target by Robot-manipulator

Nikolai V. Kramarenko

Novosibirsk State Technical University, Novosibirsk, Russia

Abstract – A plane model of a manipulator with two degrees of freedom consisting of two pivotally connected rod links is considered. The drive motors are located in the hinge joints. At the end of the last rod is gripper. An arbitrary trajectory along which the target moves is known in advance. The aim of this work is to develop such a control algorithm by motion of the manipulator, which provides for a specified time the soft capture of the target by the manipulator, without exceeding the limits of moments and the capacities of the drives. Based on the mathematical solution of the problem, an algorithm for manipulator control is developed, which is implemented in the form of an intellectual simulator used for training students.

Index Terms – mechatronics, controlled movement of the mechanism.

I. INTRODUCTION

MANAGEMENT tasks with mechanical devices arise in various areas technology, especially in robotics. Widespread in the industry got robot manipulators. A manipulative robot is an automated system consisting of a mechanical part and an associated software control device. The mechanical part of the manipulator is a multi-link spatial mechanism with several degrees of freedom, carrying a Tong or a replaceable tool with which you can move objects in the workspace, or perform technological operations [1]. The purpose of this work is to teach students to develop algorithms for controlling mobile mechanical objects to perform various technical tasks.

II. PROBLEM STATEMENT

The design scheme of the manipulator is shown in Figure 1. The manipulator is controlled by two motors in the hinges O and A . The part D moves along a known arbitrary trajectory specified by the coordinate method. The initial fixed position of the manipulator is specified by the rotation angles of the links $\varphi_{10}, \varphi_{20}$, the position of the parts D_0 - by coordinates $x_D(0), y_D(0)$. By the time τ is required to achieve the combination of points M and D with a given δ_0 relative error of misalignment of their coordinates [2]:

$$\delta = \frac{\Delta x(\tau)}{\Delta x(0)} = \frac{\Delta y(\tau)}{\Delta y(0)} \leq \delta_0 \quad (1)$$

At the same time, during the whole time of the chase ($0 \leq t \leq \tau$), we will require the fulfillment of the constraints on the moments M and capacities N , developed in the drives:

$$M_{01} \leq M_{01}^{\max}; \quad M_{A2} \leq M_{A2}^{\max}. \quad (2)$$

$$N_0 \leq N_0^{\max}; \quad N_A \leq N_A^{\max}. \quad (3)$$

To simplify the task, we believe that the manipulator works in a horizontal plane, in this case, its own weight does not affect the dynamics of the mechanism. We also believe that the control moments do not depend on the parameters of the movement of the mechanical part of the manipulator and are determined only by the currents supplied to the drives.

It is required to determine the control moments developed by the engines in the hinges O and A , as functions of time, as well as to determine the necessary power of these engines from the soft touch of the Tong M of the part D .

III. THEORY

To solve the problem it is necessary, firstly, to obtain the differential equations of motion of the links, and secondly, to develop an algorithm for changing the values of the control moments.

The first task is not difficult, it can be solved in different ways. For example, in the literature on robotics [1, 3] the method of Lagrange equations of the second kind is more often used, and in the theory of mechanisms and machines – the method of kinetostatics [2, 4]. Here we solve this problem via the Lagrange equation of the second kind. First, let's write down the basic kinematic relations for the manipulator [5]:

$$\bar{V}_M = \bar{V}_{M,nep} + \bar{V}_{M,omu} = \bar{V}_D + \Delta\bar{V}, \quad \Delta\bar{V} = k\Delta\bar{r}. \quad (4)$$

$$\omega_1 = \frac{V_{Mx}l_{2x} + V_{My}l_{2y}}{l_{1x}l_{2y} - l_{1y}l_{2x}}, \quad \omega_2 = \frac{V_{Mx}l_{1x} + V_{My}l_{1y}}{l_{1x}l_{2y} - l_{1y}l_{2x}}. \quad (5)$$

Here \bar{V}_D is the velocity vector of the part D (see Fig. 1); $\Delta\bar{V}$ - the vector of the relative velocity of approach of the part and Tong, directed at the part; $k = \frac{1}{\tau} \ln \frac{1}{\delta}$ - control parameter, which provides the capture of the part to the point of time τ ; ω_1, ω_2 - angular velocity links manipulator OA and AM , respectively.

The equations of motion of the manipulator links are obtained from two Lagrange equations of the second kind

$$\frac{d}{dt} \left(\frac{\partial T}{\partial \dot{q}_j} \right) - \frac{\partial T}{\partial q_j} = Q_j \quad (j = 1, 2), \quad (6)$$

in which independent generalized displacements are:

$$q_1 = \varphi_1, \quad q_2 = \psi_2 = \varphi_2 - \varphi_1. \quad (7)$$

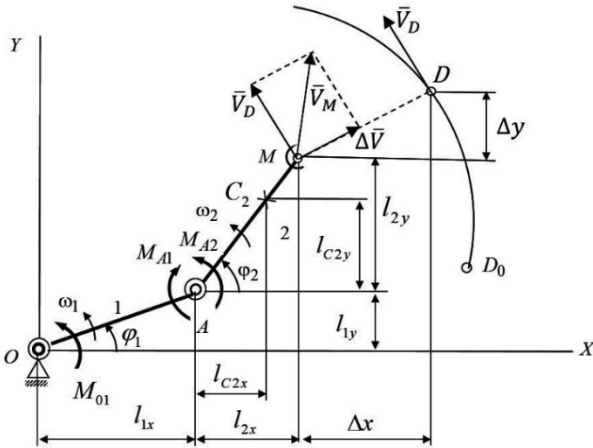


Fig. 1. Arbitrary position of the manipulator.

Solving equations (6, 7) with respect to the control moments in the drives, we obtain:

$$M_{01} = \varepsilon_1 J_{012} + \varepsilon_2 J_{A2} + (\varepsilon_1 + \varepsilon_2) J_{m12} \cos \psi_2 + (\omega_1^2 - \omega_2^2) J_{m12} \sin \psi_2. \quad (8)$$

$$M_{A2} = \varepsilon_1 J_{m12} \cos \psi_2 + \varepsilon_2 J_{A2} + \omega_1^2 J_{m12} \sin \psi_2. \quad (9)$$

Here $\varepsilon_1, \varepsilon_2, \omega_1, \omega_2$ - angular accelerations and velocities of links 1 and 2, the coefficients J_{012}, J_{A2}, J_{m12} are the reduced moments of inertia.

Engine power in the hinges O and A are determined by the moments:

$$N_0 = M_{01} \omega_1; \quad (10)$$

$$N_A = M_{A2} \omega_{\psi 2} = M_{A2} (\omega_2 - \omega_1). \quad (11)$$

To solve the second problem of developing an algorithm for changing the values of the control moments it is necessary to take into account the conditions (1) - (3). If the drives had unlimited power, it would be possible to take the speed of the Tong M by the formula (4). In this case, the manipulator control algorithm does not differ from the point control algorithm M [5]. If the power of the drives is limited, they may not provide the required speed (4) point M , and the part D will not be caught. To take into account the limitations of the power of the drives, we introduce the convergence parameter b [6], which will change the equation (4):

$$\bar{V}_M = b * (\bar{V}_D + \Delta \bar{V}). \quad (12)$$

In order to find the optimal value of parameter b we will reduce it from 1 to 0. If the new value of b , the algorithm chase. At the same time, the Tong speed (12), the required moments (8, 9) and the power in the drives (10, 11) are calculated at each time and adjusted according to the conditions (2, 3). At the end of the chase time, the error of the solution (1) is calculated. If the resulting error does not exceed the specified error δ_0 , it is considered that the part is caught. If the error of the solution is higher than the set value

δ_0 , the value of the convergence parameter b decreases and the cycle repeats.

IV. PROGRAM REALIZATION AND RESULTS NUMERICAL EXPERIMENTS

Following the results of the given decision the program simulator which allows to visualize process of a pursuit [6] was developed. Figure 2 shows the design of the program screen.

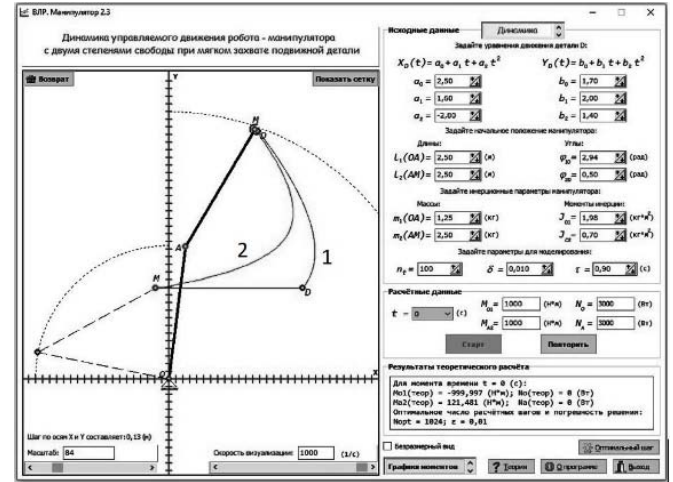


Fig. 2. Window the software simulator of the chase.

Input parameter values are entered in the right part of the window. After the program is launched, the left part of the screen shows the chase animation preserving the trajectory of the part (line 1) and Tong (line 2).

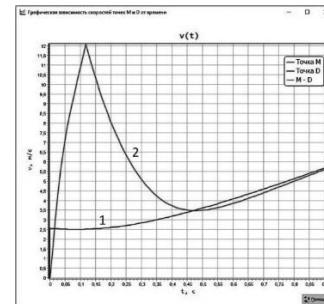


Fig. 3. Detail (1) and Tong (2) speeds.

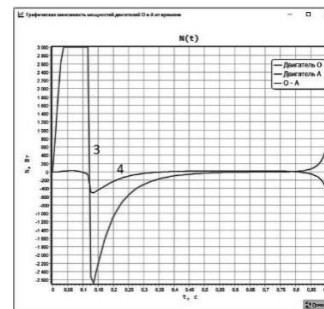


Fig. 4. Power to the drive.

After the chase is over, you can switch the screen to the mode of viewing the graphs of speeds (Fig. 3), moments and capacities in the drives (Fig. 4).

V. DISCUSSION OF RESULTS

From Figure 2 it can be seen that the chase is divided into two stages - first Tong moves sharply closer to the part, and then moves for a long time next to the part to align the speeds. At the same time, Figure 3 shows that at the first stage the Tong speed (line 2) is much higher than the speed of the part (line 1), and then their speeds are smoothly aligned. Figure 4 shows that in the first stage of the chase, the drive in the O hinge (line 3) operates at the limit mode first to accelerate, then to slow down the rotation of the OA link, and the drive in the A hinge (line 4) consumes much less power. In the second stage of the chase, both drives operate at very low capacities.



Kramarenko Nikolai graduated from Novosibirsk electrotechnical Institute in 1974 with a degree in "dynamics and strength of machines". He worked at the Department of "aircraft strength" engineer, Junior researcher. Then moved team leader at the CDB engineering, where he was engaged in calculations of the spatial load-bearing structures for stiffness and strength. In 1987 he defended his thesis. At the Novosibirsk Shoe factory he developed an automated system for design and technological preparation of Shoe production as head of the CAD Bureau. In the years of perestroika left the profession. In 2005 he returned to NSTU, works as an associate Professor at the Department of "aircraft strength", conducts courses on theoretical and applied mechanics, similarity methods. Actively engaged in the introduction of computers in the educational process.

VI. CONCLUSIONS AND CONCLUSION

The proposed control algorithm handling robot that provides a soft capture the details of a gripper of the manipulator under given constraints on points and facilities in the engines. Based on the algorithm developed software simulator, which visualizes the process of the chase and explore the graphs of the velocities of the part and the gripper, and the capacity of the control actuators. The developed software simulator can be used as an intelligent simulator both in training and in improving the skills of specialists in the field of robotics. For students, this simulator can be used as a virtual laboratory work [7].

The students mastering of the technique of building control algorithms for the simplest two-link mechanism will allow them to develop control algorithms for more complex mechatronic devices in their professional activities.

REFERENCES

- [1] Zenkevich S. L., iushchenko A. S. basic control of manipulation robots: Textbook for universities. 2nd ed., rectified. and EXT., M.: Izd-vo MG TU im. H. E. Bauman, 2004. - 480 p. (in Russian).
- [2] Novozhilov, I. V., Zatsepin M. F. Model calculations in theoretical mechanics at the base of the computer. - Moscow: Higher school, 1986. 136 p. (in Russian).
- [3] Mechanics of industrial robots: textbook for higher educational institutions in 3 kN./Ed. by K. V. Frolov, and E. I. Vorobyov. kN.3: Basics of design/ E. I. Vorobyov, A.V. Babich, K. p. Zhukov – etc. - m: Higher school, 1989. - 383 p. (in Russian).
- [4] Artobolevsky I. I. Theory of mechanisms and machines. M., 1975. (in Russian).
- [5] Kramarenko N. B. Kinematics of the controlled motion of the robot manipulator with two degrees of freedom with a soft grip of the movable part/ N. V. Kramarenko, P. A. Lakiza / / Nauka. Industry. Defense: Tr. 17 overgrown. science.- tech. Conf., Novosibirsk, 20-22 APR. 2016 in 4 t. - Novosibirsk: publishing house of NSTU, 2016. – Vol.1. C. 220-225. (in Russian).
- [6] Kramarenko N. Dynamics of the manipulator robot with two motors of limited power with a soft grip of the movable part/ N. V. Kramarenko, P. A. Lakiza / / Nauka. Industry. Defense: Tr. 18 overgrown. science.- tech. Conf., Novosibirsk, 19-21 APR. 2017 in 4 t. - Novosibirsk: publishing House of NSTU, 2017. – Vol.1. – Pp. 171-176. (in Russian).
- [7] Algorithms for controlling the movements of the point and the robot manipulator: tutorial/N. In. Kramarenko, A. A. Rykov. - Novosibirsk: publishing house of NSTU, 2016. - 87 p. (in Russian).

Comparative Analysis of Mathematical Models for the Coefficient of Conductor Resistance Increase due to Higher Harmonics

Vadim Z. Manusov, Viktor V. Khripkov

Novosibirsk State Technical University, Department of Industrial Power Supply System, Novosibirsk, Russia

Abstract – The influence of higher harmonic components of the alternating current (AC) on the increase of resistance of current-carrying cable cores and wires is shown. It is caused by forcing the current to the conductor surface, that is called the skin effect. The comparative analysis of various mathematical models was carried out. After that, coefficients of the increase of AC conductor resistance in relation to direct current (DC) resistance were determined. Obtained coefficients can be used for correct and reliable calculations of active power losses in electrical networks and power supply systems.

Index Terms – Alternating current, higher harmonics, conductor resistance, skin effect.

I. INTRODUCTION

ONE OF SIGNIFICANT reasons of uncertain calculations of active power losses is distortion of sinusoidal waveforms of current and voltage. This is caused by the fact that power consumers include devices having nonlinear current-voltage characteristics. A nonsinusoidal waveform of current and voltage is caused by occurrence of higher harmonic components related to the fundamental frequency ($f = 50\text{Hz}$).

The following problems should be considered:

- To analyze models considering the skin effect of current forcing proposed by the International Electrotechnical Commission (IEC) and other authors;
- To measure a spectrum of higher harmonics by experimental investigations;
- To carry out comparative analysis of resistance increase by calculations using different methods;
- To determine coefficients of AC resistance increase for a conductor with frequency in comparison with DC resistance and AC resistance at the fundamental frequency ($f = 50\text{Hz}$).

Higher harmonics are generated by power consumers with nonlinear current-voltage characteristics. The structure of nonlinear power consumers strongly depends on the type of an industrial plant. The main source of higher harmonics at metallurgical plants are frequency converters that are concentrated high-power harmonic sources. Their total installed capacity amounts 80-90% of total equipment power. Frequency converters, having the single rated power of up to 20 MW, are also used for supplying modern continuous hot rolling mills. At the present time, inverters are widely used for electrified industrial transport [1].

In addition, inverters are widely applied as power sources for welding units using electric arc welding and electric resistance welding at many industrial plants. Welding rectifiers are generally supplied from 0.38 kV networks. Power of welding machines for automatic welding by single-phase current of fundamental frequency reaches 1.5 MVA, while for three-phase arc welding it reaches several MVA. The percentage of welding machines at some workshops of automotive and machinery plants may reach 80% of total electrical loads [2].

II. PROBLEM DEFINITION CURRENT FORCING BY THE SKIN EFFECT

When an alternating current flows through wires and cables, it is forced to the conductor surface that is called the skin effect. This effect is especially observed in the presence of higher harmonics in the network, that is caused by nonlinear current-voltage characteristics, as was said before. At the present time, power transmission in low- and medium-voltage distribution networks is realized through aerial bundled cables (ABC) and cable lines. Both systems involve proximity effects of phase conductors.

Different methods of considering the skin effect [2, 3] based on the fundamental Umov–Poynting formula are considered in various publications.

Exact mathematical expressions describing the influence of electric current frequency on conductor resistance are given in the theory of an electromagnetic field [3]. For example, conductor resistance is determined using the Umov–Poynting theorem. For this purpose, it is necessary to calculate the flux of the Umov–Poynting vector through the lateral surface of the conductor along the 1-m length and divide it by the squared electric current flowing through a conductor. As a result, the complex impedance of a conductor per unit length can be determined:

$$-\oint [\vec{E}^* \cdot \vec{H}] d\vec{s} = P + jQ = I^2 R + jI^2 X = I^2 Z, \quad (1)$$

$$Z = R + jX = \frac{-\oint [\vec{E}^* \cdot \vec{H}] d\vec{s}}{I^2}. \quad (2)$$

Impedance of the conductor of the cylindrical form per 1-m length is expressed by

$$Z = \frac{\dot{E}_a \cdot \dot{H}_a \cdot 2\pi a \cdot 1}{I^2} = \frac{\sqrt{w\gamma\mu} b_0 e^{-j45^\circ} e^{j\beta_0}}{2\pi\gamma a b_1 e^{j\beta_1}}. \quad (3)$$

Then, AC resistance can be determined as

$$R_n(f) = \frac{\sqrt{w\gamma\mu} b_0}{2\pi\gamma a b_1} \cos(\beta_0 - \beta_1 - 45), \quad (4)$$

where w – angular frequency of electric current; b_0 – modulus of the zero-order Bessel function of the first kind; b_1 – modulus of the first-order Bessel function of the first kind; β_0 – argument of the zero-order Bessel function of the first kind; β_1 – argument of the first-order Bessel function of the first kind; γ – conductivity of an electric conductor; μ – magnetic permeability; a – radius of an electric conductor.

Equation (4) gives exact results, but involves complicated mathematical functions, therefore it is not used in engineering calculations. In practice, simpler mathematical expressions, that approximate the dependence of conductor resistance on electric current frequency, can be used.

1. The International Electrotechnical Commission (IEC) recommends the following formula in IEC 60287-1-1 [4]:

$$R_n(v) = R(1 + y_s + y_p), \quad (5)$$

where $R_n(v)$ – AC conductor resistance at frequency v , corresponding to the n -th harmonic; R – DC resistance of a conductor; y_s – the skin effect factor; y_p – the proximity effect factor for conductors.

The value of y_s is proposed to be calculated by the following equations depending on the value of x :

for $0 < x \leq 2,8$

$$y_s = \frac{x^4}{192 + 0,8x^4} \quad (6)$$

for $2,8 < x \leq 3,8$

$$y_s = -0,136 - 0,0177x + 0,0563x^2 \quad (7)$$

for $x > 3,8$

$$y_s = 0,354x - 0,733 \quad (8)$$

or to be determined graphically depending on the parameter x that is equal to

$$x = \sqrt{\frac{8\pi f k}{R}} 10^{-7}, \quad (9)$$

where k – experimental factor ($k = 1$) [4] depending on the type of a conductor; R – DC resistance of a conductor at maximum permissible temperature T_{max} .

$$R = \frac{\rho[1 + \alpha(T_{max} - 20)](1 + k_0)}{F}, \quad (10)$$

where ρ – DC resistivity of a conductor at 20 °C, Ohm·m; α – temperature coefficient of resistance, 1/°C; k_0 – assembly coefficient [5]; T_{max} – maximum operating

temperature, °C – determined by the type of insulation and specified by standards or technical specifications for a considered cable type; F – conductor size, m^2 .

The proximity effect factor y_p for three-core cables or three single-core cables is given by

$$y_p = \frac{x_p^4}{192 + 0,8 \cdot x_p^4} \cdot \left(\frac{d_c}{s}\right)^2 \cdot \left[0,312 \left(\frac{d_c}{s}\right)^2 + \frac{1,18}{\frac{x_p^4}{192 + 0,8 \cdot x_p^4} + 0,27} \right], \quad (11)$$

where d_c – the diameter of a conductor, mm; s – the distance between conductor axes, mm; x_p is determined as

$$x_p = \sqrt{\frac{8\pi f k_p}{R}} 10^{-7}, \quad (12)$$

where k_p – experimental factor ($k_p = 0,8$) [4].

2. The increase of AC resistance with frequency can be calculated using the simplified expression [1]:

$$R_n(v) = R_0 \sqrt{n}, \quad (13)$$

where R_0 – DC resistance of a conductor; n – the harmonic number.

In other words, it is assumed that DC resistance of a conductor is increasing proportionally to the square root of the harmonic number.

3. To take into account the dependence of conductor resistance on frequency, the following equation is proposed in [6]:

$$\frac{R_n(v)}{R_0} = k_{sv} + k_{pv}, \quad (14)$$

where k_{sv} , k_{pv} – factors of the skin effect and the proximity effect. These factors have the same physical meaning as factors y_s , y_p in IEC 60287-1-1 [3].

The value of k_{pv} for cable lines is given by

$$k_{pv} = 0,59 \cdot \frac{k_{sv} - 1}{k_{sv} - 0,73}. \quad (15)$$

The value of k_{sv} is calculated as

$$k_{sv} = \begin{cases} 1 + \frac{x^4}{3} \text{ for } x \leq 1; \\ x + 0,25 + \frac{0,47}{x} \text{ for } x \geq 1 \end{cases}, \quad (16)$$

where $x = 0,128 \cdot \sqrt{\frac{n}{R_0}}$ is the intermediate parameter.

III. ANALYSIS OF THE FREQUENCY SPECTRUM OF THE REAL ELECTRICAL NETWORK

During experimental investigations, values of higher harmonics were measured in the real electrical network. It was found that traditional harmonics of the 1-, 3-, 5-, 7-, 9-, 11-order prevail in the network with the probability close to 1.0, harmonics of the 13-, 15-, 25-order are observed with the probability of about 0.5, and unrepresentative even harmonics of the 2- and 26-order are observed with the probability of about 0.3. Other harmonics are random values and not considered below. The spectrum of measured harmonic components of voltages and currents is presented in Figure 1.

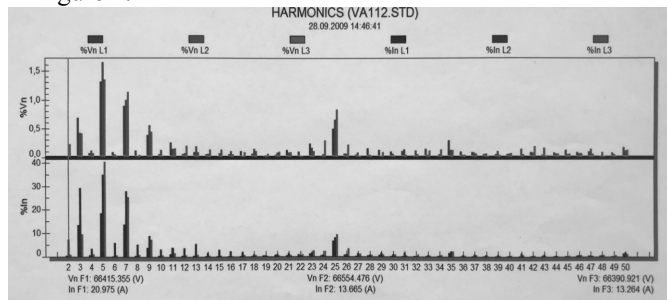


Fig. 1. Spectrum of higher harmonics.

Coefficients of resistance increase with frequency for higher harmonics of frequent occurrence were determined based on mathematical models given above. As these models can be applied for conductors of various sizes in different ways, therefore the basic sizes of 120 mm², 150 mm², 240 mm², 300 mm², 400 mm² were chosen for calculations.

A relative coefficient of resistance increase with frequency of harmonic components is given by the ratio of

$$k_f = \frac{R_n(v)}{R_0}. \quad (17)$$

Coefficients of resistance increase with frequency are calculated for higher harmonics of frequent occurrence using (5) and presented in Tables 1, 2, 3 below.

TABLE I
CABLE OF 150 MM²

| No. of harmonic | 1 | 2 | 3 | 5 | 7 | 9 | 11 | 13 | 15 | 25 | 26 |
|-------------------------|-------|-------|-------|-------|-------|-------|-------|-------|-------|-------|-------|
| f, Hz | 50 | 100 | 150 | 250 | 350 | 450 | 550 | 650 | 750 | 1250 | 1300 |
| R _n , Ohm/km | 0.244 | 0.248 | 0.252 | 0.268 | 0.288 | 0.312 | 0.337 | 0.364 | 0.390 | 0.502 | 0.511 |
| R ₀ , Ohm/km | 0.206 | 0.206 | 0.206 | 0.206 | 0.206 | 0.206 | 0.206 | 0.206 | 0.206 | 0.206 | 0.206 |
| K _f , p.u. | 1.186 | 1.206 | 1.225 | 1.299 | 1.398 | 1.514 | 1.638 | 1.765 | 1.891 | 2.435 | 2.479 |

TABLE II
CABLE OF 240 MM²

| No. of harmonic | 1 | 2 | 3 | 5 | 7 | 9 | 11 | 13 | 15 | 25 | 26 |
|-------------------------|-------|-------|-------|-------|-------|-------|-------|-------|-------|-------|-------|
| f, Hz | 50 | 100 | 150 | 250 | 350 | 450 | 550 | 650 | 750 | 1250 | 1300 |
| R _n , Ohm/km | 0.154 | 0.160 | 0.166 | 0.187 | 0.212 | 0.239 | 0.264 | 0.287 | 0.307 | 0.379 | 0.384 |
| R ₀ , Ohm/km | 0.129 | 0.129 | 0.129 | 0.129 | 0.129 | 0.129 | 0.129 | 0.129 | 0.129 | 0.129 | 0.129 |
| K _f , p.u. | 1.19 | 1.240 | 1.287 | 1.451 | 1.647 | 1.850 | 2.044 | 2.222 | 2.382 | 2.941 | 2.978 |

TABLE III
CABLE OF 300 MM²

| No. of harmonic | 1 | 2 | 3 | 5 | 7 | 9 | 11 | 13 | 15 | 25 | 26 |
|-------------------------|-------|-------|-------|-------|-------|-------|-------|-------|-------|-------|-------|
| f, Hz | 50 | 100 | 150 | 250 | 350 | 450 | 550 | 650 | 750 | 1250 | 1300 |
| R _n , Ohm/km | 0.124 | 0.131 | 0.139 | 0.162 | 0.188 | 0.213 | 0.236 | 0.255 | 0.272 | 0.324 | 0.327 |
| R ₀ , Ohm/km | 0.103 | 0.103 | 0.103 | 0.103 | 0.103 | 0.103 | 0.103 | 0.103 | 0.103 | 0.103 | 0.103 |
| K _f , p.u. | 1.201 | 1.273 | 1.345 | 1.575 | 1.828 | 2.071 | 2.289 | 2.478 | 2.641 | 3.148 | 3.178 |

For electrical networks with overhead transmission lines it is reasonable to use the Umov–Poynting formula or its approximate analogue:

$$\frac{R_n(v)}{R_0} = \begin{cases} 1 + \frac{x^4}{3} & \text{for } x \leq 1; \\ x + 0.25 + \frac{0.47}{x} & \text{for } x \geq 1 \end{cases}, \quad (18)$$

where $x = 0.1 \sqrt{\frac{n}{R_0}}$ is the intermediate parameter used for calculations. Coefficients of resistance increase are given in Tables 4, 5, 6.

TABLE IV
WIRE OF 150 MM²

| No. of harmonic | 1 | 2 | 3 | 5 | 7 | 9 | 11 | 13 | 15 | 25 | 26 |
|-------------------------|-------|-------|-------|-------|-------|-------|-------|-------|-------|-------|-------|
| f, Hz | 50 | 100 | 150 | 250 | 350 | 450 | 550 | 650 | 750 | 1250 | 1300 |
| R _n , Ohm/km | 0.206 | 0.207 | 0.208 | 0.210 | 0.219 | 0.224 | 0.235 | 0.244 | 0.251 | 0.323 | 0.330 |
| R ₀ , Ohm/km | 0.206 | 0.206 | 0.206 | 0.206 | 0.206 | 0.206 | 0.206 | 0.206 | 0.206 | 0.206 | 0.206 |
| K _f , p.u. | 1 | 1.005 | 1.009 | 1.019 | 1.065 | 1.086 | 1.143 | 1.183 | 1.217 | 1.566 | 1.601 |

TABLE V
WIRE OF 240 MM²

| No. of harmonic | 1 | 2 | 3 | 5 | 7 | 9 | 11 | 13 | 15 | 25 | 26 |
|-------------------------|-------|-------|-------|-------|-------|-------|-------|-------|-------|-------|-------|
| f, Hz | 50 | 100 | 150 | 250 | 350 | 450 | 550 | 650 | 750 | 1250 | 1300 |
| R _n , Ohm/km | 0.129 | 0.132 | 0.135 | 0.147 | 0.152 | 0.160 | 0.177 | 0.184 | 0.198 | 0.248 | 0.253 |
| R ₀ , Ohm/km | 0.129 | 0.129 | 0.129 | 0.129 | 0.129 | 0.129 | 0.129 | 0.129 | 0.129 | 0.129 | 0.129 |
| K _f , p.u. | 1 | 1.025 | 1.050 | 1.137 | 1.180 | 1.242 | 1.374 | 1.426 | 1.532 | 1.925 | 1.963 |

TABLE VI
WIRE OF 300 MM²

| No. of harmonic | 1 | 2 | 3 | 5 | 7 | 9 | 11 | 13 | 15 | 25 | 26 |
|-------------------------|-------|-------|-------|-------|-------|-------|-------|-------|-------|-------|-------|
| f, Hz | 50 | 100 | 150 | 250 | 350 | 450 | 550 | 650 | 750 | 1250 | 1300 |
| R _n , Ohm/km | 0.103 | 0.105 | 0.107 | 0.118 | 0.126 | 0.140 | 0.152 | 0.165 | 0.174 | 0.218 | 0.222 |
| R ₀ , Ohm/km | 0.103 | 0.103 | 0.103 | 0.103 | 0.103 | 0.103 | 0.103 | 0.103 | 0.103 | 0.103 | 0.103 |
| K _f , p.u. | 1 | 1.019 | 1.038 | 1.145 | 1.227 | 1.361 | 1.479 | 1.597 | 1.690 | 2.116 | 2.153 |

Characteristic curves are shown in Figures 2, 3.

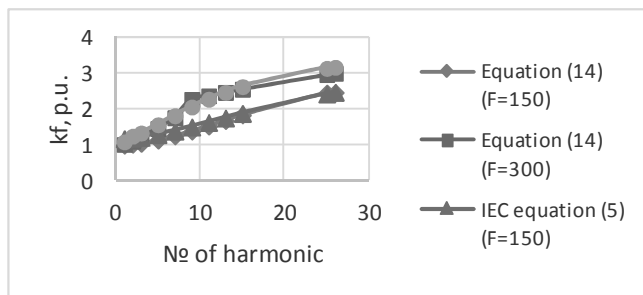


Fig. 2. Dependence of the coefficient of resistance increase on harmonic frequency for cable lines.

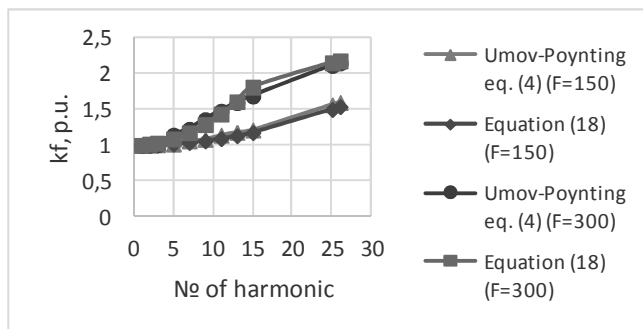


Fig. 3. Dependence of the coefficient of resistance increase on harmonic frequency for overhead lines.

It is evident that curves plotted with the use of (5) and (14) for cable lines and curves plotted with the use of (4) and (18) for overhead lines have a good coincidence in the full spectrum of harmonic frequencies.

IV. NEW MODEL CONSIDERING RESISTANCE INCREASE BY HIGHER HARMONICS FOR ABC AND CABLES

V.Z. Manusov, the author of this paper, has proposed the new mathematical model of the dependence of conductor resistance on frequency as the cube root of frequency:

$$R_n(\nu) = R_0 \sqrt[3]{n}. \quad (19)$$

As this model involves multiplication of DC resistance by a harmonic number, while a coefficient of resistance increase includes division by the same DC resistance, then coefficient k_f for all conductor sizes will be one and the same being proportional to $\sqrt[3]{n}$. In this case, a coefficient of resistance increase for all conductor sizes does not change with the size of a conductor, thus being constant for every harmonic number and for any conductor sizes (Tab. 7).

TABLE VII
COEFFICIENT OF RESISTANCE INCREASE FOR THE MODEL $\sqrt[3]{n}$

| No. of harmonic | 1 | 2 | 3 | 5 | 7 | 9 | 11 | 13 | 15 | 25 | 26 |
|-----------------|----|-------|-------|-------|-------|-------|-------|-------|-------|-------|-------|
| f, Hz | 50 | 100 | 150 | 250 | 350 | 450 | 550 | 650 | 750 | 1250 | 1300 |
| Kf, p.u. | 1 | 1.260 | 1.442 | 1.710 | 1.913 | 2.080 | 2.224 | 2.351 | 2.466 | 2.924 | 2.962 |

As shown below in Figure 4, calculations become considerably simpler without any degradation of accuracy.

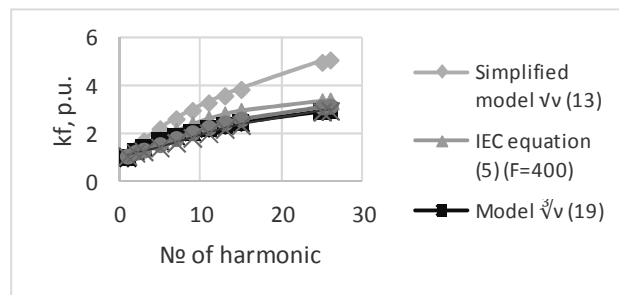


Fig. 4. Comparative analysis of the new formula $\sqrt[3]{n}$ with known mathematical expressions.

VI. CONCLUSION

It was shown that mathematical models based on (5) and (14) give close results, therefore the IEC equation should be used for proximate SSIW and cables of all conductor sizes. The model based on the quadratic dependence of resistance on frequency gives rough approximation with a significant error after the 5th harmonic. The simplified model using the square root of frequency is not applicable. The formula proposed by authors of this paper and based on the cubic dependence is rather simple and allows obtaining results with a good correspondence with the mathematical model of IEC 60287-1-1 in the full range of conductor sizes.

REFERENCES

- [1] Zhezhenlenko I.V. Higher harmonics in power supply systems of industrial enterprises. – Moscow: Energoatomizdat, 6th edition, 2010. (in Russian).
- [2] Zhezhenlenko I.V. [et al] Selected problems of nonsinusoidal regimes in electrical networks of enterprises. – Moscow: Energoatomizdat, 2007. (in Russian).
- [3] Bessonov L.A. Theoretical basics of electrical engineering: Electromagnetic field. – Moscow: Vysshaya shkola, 1986. (in Russian).
- [4] IEC 60287-1-1. Electric cables. Calculation of the current rating. Part 1-1: Current rating equations (100% load factor) and calculation of losses. General. – 2014.
- [5] Larina E.T. Power cables and cable lines: Textbook for Higher Education Institutions. – Moscow: Energoatomizdat, 1984. (in Russian).
- [6] Geraskin O.T., Cherepanov V.V. Application of computer engineering for calculation of higher harmonics in electrical networks. – Moscow: VIPKEngo, 1987. (in Russian).



Manusov Vadim Zinovevich. Novosibirsk State Technical University, Department of Industrial Power Supply System, manusov36@mail.ru, Doctor of Sciences (Engineering), Professor. The main direction of research: the use of artificial intelligence techniques for the planning and optimization of electric power systems modes. The author of more than 300 scientific papers, including 4 monographs.



Khripkov Viktor Vladimirovich. Novosibirsk State Technical University, Department of Power Supply System, hripkov91@yandex.ru, graduate student. The main direction of research: the use of artificial intelligence techniques for the planning and optimization of electric power systems modes.

Motion Control Algorithms for Points*

Anatoly A. Rykov, Peter Y. Isakov
Novosibirsk State Technical University, Novosibirsk, Russia

Abstract – The paper considers one of the methods of pointing to a moving target, the method of parallel approach. The movement of the target is considered known, and the kinematic characteristics of the point are determined depending on which meeting is to occur - soft or hard. The force necessary to accomplish the task is also determined.

Index Terms – Pointing method, controlled point movement.

I. INTRODUCTION

THE PROBLEMS of controlling the approach of material points arise in various fields of technology. For example, in aviation such a task arises when the missile is aimed at a target, in space - when the shuttle rocket is pointed at the station, in robotics - when the grip is fixed on the moving part.

In aviation, the method of guidance is usually called the method of forming the trajectory of approaching a fighter or missile with a target. There are several methods of guidance. In this article, we will consider one of the methods for injecting a point (a fighter, a rocket) onto a mobile target: the method of parallel approach [1].

II. FORMULATION OF THE PROBLEM

Calculation of kinematic and dynamic parameters of the point is illustrated by examples of methods for targeting a mobile target. The law of movement of the target (point D) is given. Under the method of guidance is understood the way of movement of the point, which ensures hit in the target. Trajectory of the movement of the point to hit the target can be many, but in practice try to choose one of them, which under the given conditions will ensure reliable performance of the task. In calculating the trajectory of the point, the time of motion of the point before the collision with the target are determined.

Common methods of guidance: the method of parallel approach, the chase method and the method of guidance along the ray [1]. In this paper, we restrict our attention to the method of parallel approximation.

III. THEORY

A. Equations of Motion of Hard Touch

Suppose that the point M_0 - the position of the point at the moment of its transition to the guidance by the method of parallel approach; the position of the goal at the same moment.

By the method of parallel approach is meant the method of guidance, in which the line «point M – target D» remains during the movement parallel to its initial position, i.e. this line moves in space (see Fig. 1).

Designate a vector MD in terms of $\Delta\vec{r}$ - relative-range vector. Then it follows from Fig. 1 that

$$\Delta\vec{r} = \vec{r}_D - \vec{r}_M, \quad (1)$$

there \vec{r}_D and \vec{r}_M - radius-vectors, drawn from the origin of the fixed coordinate system, respectively in target D and in point M. Differentiate (1) by time, taking into account that

$$\Delta\vec{r} = \Delta r \cdot \vec{\tau}, \quad \frac{d\vec{\tau}}{dt} = \vec{\omega} \times \vec{\tau},$$

there $\vec{\tau}$ - unit vector:

$$\frac{d\Delta r}{dt} \vec{\tau} + \Delta r (\vec{\omega} \times \vec{\tau}) = \vec{V}_D - \vec{V}_M, \quad (2)$$

there $\vec{\omega}$ - angular velocity of the relative-range vector $\Delta\vec{r}$.

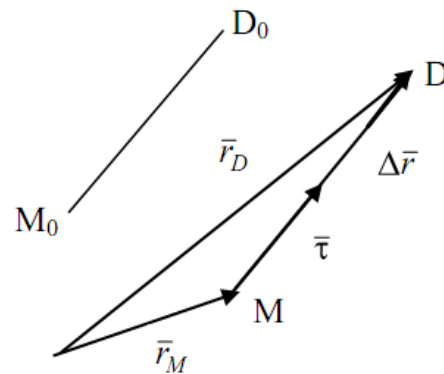


Fig. 1. Position of the line MD while movement.

Notice, that (2) is valid for any method of guidance. In this case, since the MD line moves steadily, then $\omega = 0$. Then from (2) will get

$$\frac{d\Delta r}{dt} \vec{\tau} = \vec{V}_D - \vec{V}_M \quad (3)$$

From expression (3) is seen, that vectors $\vec{\tau}$, \vec{V}_D , \vec{V}_M lie in one plane. Consider the instantaneous position of these vec-

*UDC 621.865.8(075.8)

tors (Fig. 2). Project expression (3) onto the line, perpendicular to MD (on the n-axis).

$$\sin \varphi = (V_D / V_M) \sin \alpha. \quad (4)$$

In expression (4) V_D and α are functions of time. Project (3) on MD (on the τ -axis):

$$\frac{d\Delta r}{dt} = V_M \cos \varphi \left(\frac{V_D}{V_M} \frac{\cos \alpha}{\cos \varphi} - 1 \right) \quad (5)$$

Since usually $V_M > V_D$, we have from (5) $\sin \alpha > \sin \varphi$, and first, $\cos \alpha < \cos \varphi$. Then it follows from (5), that

$$\frac{d\Delta r}{dt} < 0,$$

those. In the method of parallel approach, the distance between the point M and the target D all the time decreases and at some instant of time there will be a collision. This moment of time T is found from condition

$$\Delta r(T) = 0.$$

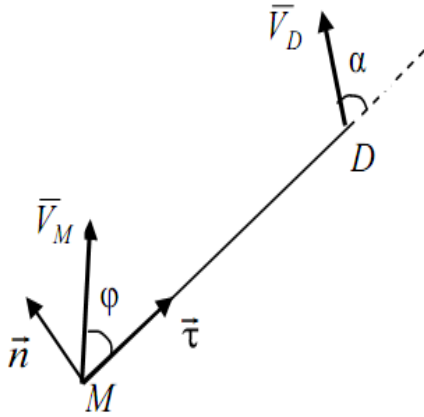


Fig. 2. Instant position of velocity vectors.

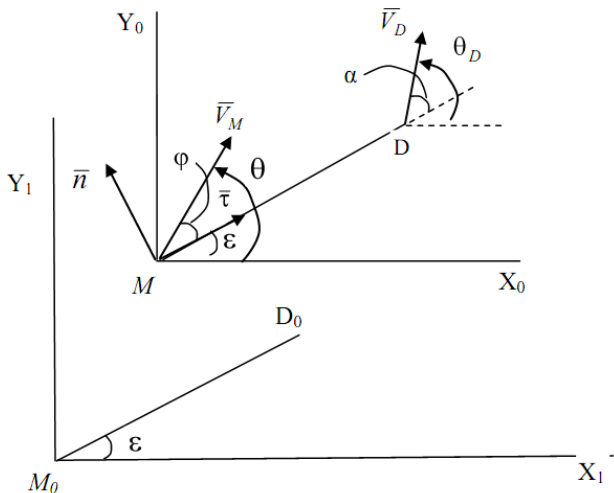


Fig. 3. Position of coordinate systems.

Consider the calculation of the trajectory of the point M in this method of guidance for motion in the plane. Let the frame of reference X_0MY_0 be connected with the exact M

(see Fig. 3). The axes of this system are always parallel to the axes of system $X_1M_0Y_1$, connected by the Earth. Angle ϵ remains constant throughout the guidance time and is equal to its value at the time of launch. It follows from Fig. 3 that

$$\varphi = \theta - \epsilon, \quad \alpha = \theta_D - \epsilon \quad (6)$$

Substituting (6) into (4) and (5), we obtain two equations

$$\begin{aligned} V_M \sin(\theta - \epsilon) &= V_D \sin(\theta_D - \epsilon), \\ \frac{d\Delta r}{dt} &= V_D \cos(\theta_D - \epsilon) - V_M \cos(\theta - \epsilon), \end{aligned} \quad (7)$$

in which three functions are unknown $V_M(t)$, $\Delta r(t)$, $\theta(t)$.

Express $\sin \theta$ in terms of the velocity of V_M with the aid of the first equation of (7)

$$\sin \theta = \sin(\theta - \epsilon + \epsilon) =$$

$$= \cos \epsilon \frac{V_D}{V_M} \sin(\theta_D - \epsilon) + \sin \epsilon \sqrt{1 - \frac{V_D^2}{V_M^2} \sin^2(\theta_D - \epsilon)}$$

Finally obtain the system of equations:

$$\begin{aligned} \frac{d\Delta r}{dt} &= V_D \cos(\theta_D - \epsilon) - V_M \sqrt{1 - \frac{V_D^2}{V_M^2} \sin^2(\theta_D - \epsilon)}, \\ \theta &= \epsilon + \varphi = \epsilon + \arcsin[(V_D / V_M) \sin(\theta_D - \epsilon)], \\ \frac{dx_M}{dt} &= V_M \cos \theta, \\ \frac{dy_M}{dt} &= V_M \sin \theta. \end{aligned} \quad (8)$$

The last two equations determine the position of the point M in a fixed reference frame.

Thus, we have three ordinary differential equations of the first order that are nonlinear with respect to the functions $V_M(t)$, $\Delta r(t)$, $x(t)$, $y(t)$, and the algebraic equation for determining the angle $\theta(t)$. The velocity of the point M $V_M(t)$ programmed depending on the task:

- Either it is necessary to make a soft touch (i.e., at a tangent with zero relative speed),
- Or a tough encounter (defeat of the goal).

Initial conditions:

$$V_M(0) = V_0, \quad \Delta r(0) = \Delta r_0, \quad x_M(0) = x_0, \quad y_M(0) = y_0.$$

The initial values of the coordinates of the point x_0 , y_0 can be set equal to zero: $x_M(0) = 0$, $y_M(0) = 0$. The initial value of the speed of the point M $V_0 = V_M(0)$ and define the equations of motion of the target $x_D = f_1(t)$, $y_D = f_2(t)$. Then the initial value for the relative distance Δr_0 is determined by the formula

$$\Delta r_0 = \Delta r(0) = \sqrt{f_1^2(0) + f_2^2(0)}.$$

The angle ϵ , which remains constant in this method during the entire time of motion is determined by the formula

$$\epsilon = \arctg(f_2(0) / f_1(0)).$$

For printing, we show the time of movement t , coordinates of target D and its speed x_D , y_D , V_D , coordinates of a

point M and its speed x_M, y_M, V_M . The calculation ends at $\Delta r = 0$.

B. Algorithm for the Analytical Calculation of a Rigid Tangency

We consider the case of a rigid tangency of points M and D with constant velocity vectors of these points during their motion. Note that in this method of targeting the vectors $\Delta \vec{r}$ and $\Delta \vec{V}$ are directed along a straight line MD.

1. Set the initial data

move point D (target):

$$x_D = f_1(t), \quad y_D = f_2(t) \quad y_{D0}, \quad x_{D0}, \quad \theta_D, \quad V_D$$

The initial position of the point M:

$$x_M(0) = 0, \quad y_M(0) = 0, \quad V_M = V \gg V_D$$

calculate time-independent constants

$$\varepsilon = \arctg(y_{D0} / x_{D0}),$$

$$(\Delta r)_0 = \sqrt{x_{D0}^2 + y_{D0}^2},$$

2. Time cycle: while $\Delta r > 0.01$

3. For the next step in time, calculate:

3.1. the new position of point D (target)

$$x_D, \quad y_D, \quad V_{dx}, \quad V_{dy}, \quad V_D$$

3.2. angle of inclination of the target's velocity vector

$$\theta_D = \arcsin(V_{dy} / V_D)$$

3.3. the angle of inclination of the velocity vector of the point M

$$\theta = \varepsilon + \arcsin((V_D / V_M) \sin(\theta_D - \varepsilon))$$

3.4. the projection of the velocity of the point M

$$V_{Mx} = V_M \cos(\theta), \quad V_{My} = V_M \sin(\theta)$$

3.5. the position of the point M

$$x_M = x_M + V_{Mx} \cdot dt,$$

$$y_M = y_M + V_{My} \cdot dt$$

3.6. relative range

$$\Delta r = \sqrt{(x_D - x_M)^2 + (y_D - y_M)^2}$$

4. Issue and draw current results

$$(x_D, y_D) \quad (x_M, y_M) \quad t \quad \Delta r$$

Example 1 - a tough encounter

Equations of motion of the target: $x_D = 3 \cdot \cos(t/3)$ m,
 $y_D = 3 \cdot \sin(t/3)$ m.

The point M leaves the origin $x_M = 0, \quad y_M = 0$. In Fig. 4 shows the trajectories of the point M and the goal D before the encounter.

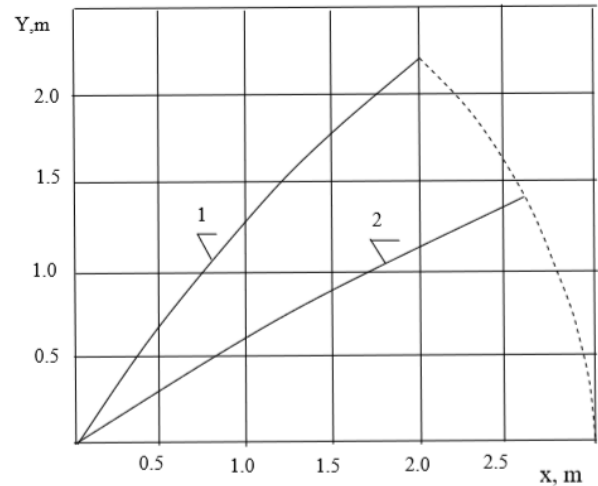


Fig. 4. A tough meeting point and goal.

The dashed line shows the trajectory of the target. Trajectories of the motion of point M: solid line 1 corresponds to the speed of point M 1.2 m / s, solid line 2 corresponds to the speed of the point M 2 m / s. As the speed of the point M decreases, the meeting place shifts to the left and the time until the meeting increases. At $V_M = 2$ m/s the time of motion of the point M before the encounter is 1.49 s and with $V_M = 1.2$ m/s - 2.5 s.

C. Equations of Soft Touch Motion

Formulas representing the equations of motion of soft cushion remain the same as in the case of hard touch (p.A), only it is necessary to enter the control parameter k. [2]-[3].

Define the control parameter.

As a strategy for controlling the motion of point M, we take two positions:

- firstly, the relative velocity vector must be directed along the discrepancy vector Δr to the point D,
- secondly, in modulus, the relative velocity vector should decrease as we approach the point D, so that at the time of the meeting we provide a soft touch with zero relative velocity.

We introduce the positive constant k as follows:

$$\Delta \vec{V} = k \cdot \Delta \vec{r} \quad \Delta \vec{V} = \vec{V}_M - \vec{V}_D \quad (11)$$

$$\Delta V_x = k \cdot \Delta x, \quad \Delta V_y = k \cdot \Delta y$$

Define it for the coordinate x:

$$V_{Mx} - V_{Dx} = k \cdot (x_D - x_M)$$

$$\frac{dx_M}{dt} - \frac{dx_D}{dt} = k \cdot (x_D - x_M)$$

$$-\frac{d}{dt}(x_D - x_M) = k \cdot (x_D - x_M)$$

$$\frac{d(\Delta x)}{dt} = -k \cdot \Delta x$$

A similar equation is obtained for the coordinate

$$y: \frac{d(\Delta y)}{dt} = -k \cdot \Delta y$$

Replace the notation:

$$(\Delta x, \Delta y) = z \Rightarrow \frac{dz}{dt} = -k \cdot z$$

Solve the last equation:

$$\begin{aligned} \frac{dz}{z} &= -k \cdot dt \\ \ln z &= -kt + C_1 \\ z &= e^{-kt+C_1} = e^{C_1} e^{-kt} = C_2 e^{-kt} \end{aligned} \quad (12)$$

The unknown constant C_2 is found from the initial condition, when the discrepancies $\Delta x(0)$ and $\Delta y(0)$ are known:

$$z(0) = C_2 e^{-k \cdot 0} = C_2 \Rightarrow z = z(0) e^{-kt} \quad (13)$$

By the condition of the problem, at the instant of time $t = \tau$, the mismatch $z = (\Delta x, \Delta y)$ must satisfy the relation:

$$\frac{z(\tau)}{z(0)} = \delta \quad (14)$$

Comparing the dependences (13) and (14) for $t = \tau$,

$$\begin{aligned} z(\tau) &= z(0) e^{-k\tau} \\ z(\tau) &= z(0) \cdot \delta \end{aligned}$$

find

$$\begin{aligned} e^{-k\tau} &= \delta \\ -k\tau &= \ln \delta \end{aligned}$$

And finally

$$k = \frac{1}{\tau} (-\ln \delta) = \frac{1}{\tau} \ln \frac{1}{\delta} > 0 \quad (15)$$

The control parameter k , which determines the speed of the point M according to the formulas (11), should be positive; the quantity δ is much less than unity. The smaller the relative error in approaching δ (14), the larger the parameter k , which determines the speed of the point M. For example, for $\tau=10$ sec we get:

$$\begin{aligned} \delta = 0.1 &\rightarrow k = \frac{1}{10} \ln 10 = 0.230 \\ \delta = 0.01 &\rightarrow k = \frac{1}{10} \ln 100 = 0.460 \\ \delta = 0.001 &\rightarrow k = \frac{1}{10} \ln 1000 = 0.691 \end{aligned}$$

D. Algorithm for Analytical Calculation of Soft Touch

1. Set the initial data

The equations of motion of the target and the projection of target velocity on the axis

$$\begin{aligned} x_D &= f_1(t), \quad y_D = f_2(t) \\ V_{Dx} &= \dot{f}_1(t), \quad V_{Dy} = \dot{f}_2(t) \end{aligned}$$

Calculate the initial position and speed of the target

$$x_{D0} = f_1(0), \quad y_{D0} = f_2(0)$$

$$V_{Dx0} = \dot{f}_1(0), \quad V_{Dy0} = \dot{f}_2(0), \quad V_{D0} = \sqrt{V_{Dx0}^2 + V_{Dy0}^2}$$

$$\theta_{D0} = \arcsin(V_{Dy0} / V_{D0})$$

The initial position of the point M and the velocity of the point

$$\begin{aligned} x_{M0} &= x_0, \quad y_{M0} = y_0 \\ V_{M0} &= V_{D0} \end{aligned}$$

Calculate angle ε of the slope of the MD line to the x axis is

$$\begin{aligned} (\varepsilon - \text{const}) \\ \varepsilon = \arctg((y_{D0} - y_{M0}) / (x_{D0} - x_{M0})) \end{aligned}$$

set two control parameters: the time to move to the meeting τ

and parameter $\delta \ll 1$ ($\delta = 0.1 \ 0.01 \ 0.001$).

Compute the third control parameter k

$$k = \frac{1}{\tau} \ln \frac{1}{\delta} > 0$$

The number of time steps for calculating n

Then the time step $\Delta t = \tau / n$

2. Time cycle. For the next step, calculate:

2.1. new position and speed of the target D, the angle of inclination of the target velocity vector to the x axis

$$\begin{aligned} x_D &= f_1(t), \quad y_D = f_2(t) \\ V_{Dx} &= \dot{f}_1(t), \quad V_{Dy} = \dot{f}_2(t), \quad V_D = \sqrt{V_{Dx}^2 + V_{Dy}^2} \\ \theta_D &= \arcsin(V_{Dy} / V_D) \end{aligned}$$

2.2. the new position of the point M, the velocity and the angle of inclination of the velocity vector of the point M to the x axis

$$\theta = \varepsilon + \arcsin((V_D / V_M) \sin(\theta_D - \varepsilon))$$

$$\begin{aligned} x_M &= x_{M0} + V_m \cos(\theta) dt \\ y_M &= y_{M0} + V_m \sin(\theta) dt \end{aligned}$$

2.3 the coordinate mismatch and the velocity of the point M

$$\begin{aligned} dx &= x_D - x_M, \quad dy = y_D - y_M, \quad dr = \sqrt{dx^2 + dy^2} \\ V_{Mx} &= V_{Dx} + k \cdot dx, \quad V_{My} = V_{Dy} + k \cdot dy \\ V_M &= \sqrt{V_{Mx}^2 + V_{My}^2} \end{aligned}$$

3. Issue and draw current results

$$\begin{aligned} t \ (x_D, y_D) \quad (x_M, y_M) \quad (V_{Dx}, V_{Dy}, V_D) \\ (V_{Mx}, V_{My}, V_M) \end{aligned}$$

Example 2 - soft touch

Let the goal move according to equations

$$x_D = 3 \cdot \cos(t/3) \text{ m}, \quad y_D = 3 \cdot \sin(t/3) \text{ m}.$$

Initial target position:

$$x_{D0} = 3 \text{ m}, \quad y_{D0} = 0.$$

Initial target speed:

$$V_{Dx0} = 0, \quad V_{Dy0} = 1, \quad V_{D0} = 1 \text{ m/s}.$$

The point M leaves the origin ($x_{M0} = 0$, $y_{M0} = 0$) with velocity $V_{M0} = V_{D0} = 1 \text{ m/s}$. Set the time to meet with $\tau = 1 \text{ s}$, the control parameter $\delta = 0.1$, the number of steps $n = 200$.

Figure 5 shows the calculated trajectories of point M (line 1) and goal D (line 2) before they meet. As can be seen from the Fig. 6, the velocity modulus of the point M at the initial instant of time acquires a jump, and by the time of approaching the target ($t = 1 \text{ s}$) it is close to the target velocity both in modulus and in direction.

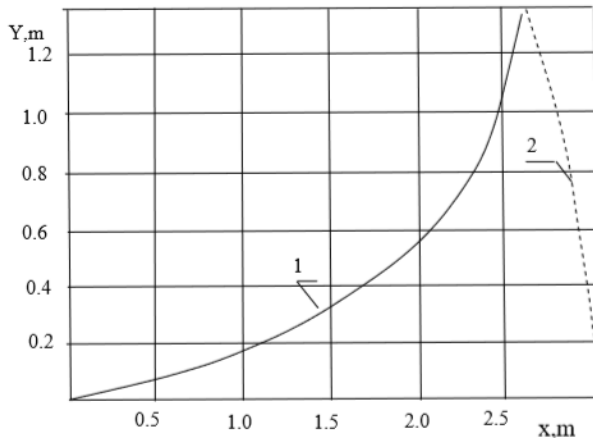


Fig. 5. Trajectories of the motion of point (1) and goal (2).

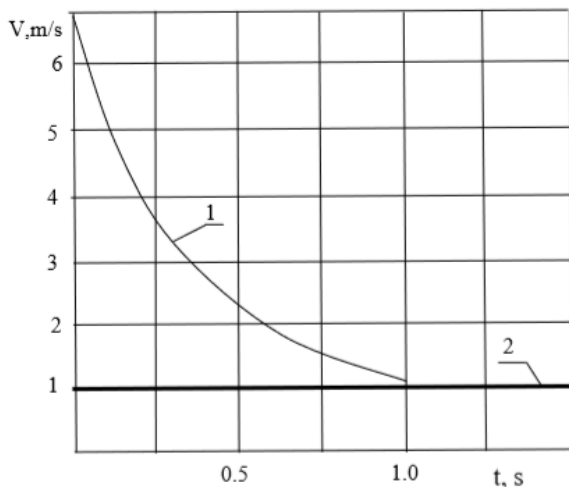


Fig. 6. The velocities of point (1) and goal (2).

Having determined the speed function of the point M necessary for meeting with the target D, we can find the mass of the point M and find the force that will ensure the obtained dependence of the velocity of the point M. This force P can be found from the equation of motion of the point for the given pointing method:

$$m \frac{dV_M}{dt} = P - mg \sin \theta$$

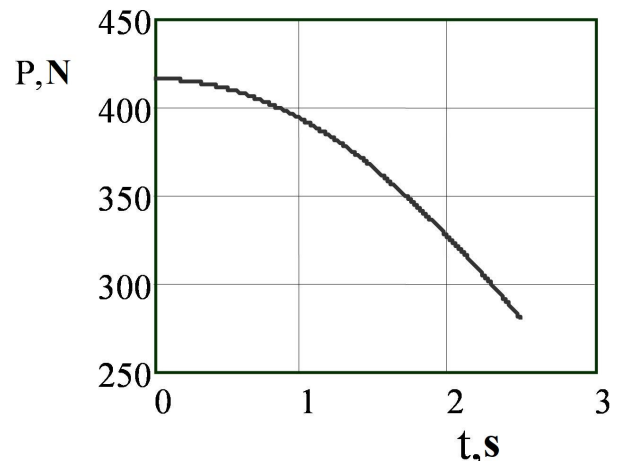


Fig. 7. Dependence of force on time.

Figure 7 shows the time dependence of the force P for a rigid meeting of the point M with the target D. The velocity of the point M remains constant in absolute value at all times and equal to $V_M = 1.2 \text{ m/s}$, the mass of the point M is $m = 50 \text{ kg}$.

IV. FINDINGS AND CONCLUSION

On the example of the method of aiming at a target, the method of parallel approach, two algorithms for directing are given. The first algorithm demonstrates a rigid meeting of a point with a goal (defeat of the target). The second algorithm realizes a soft touch of the point with the goal (with zero relative speed).

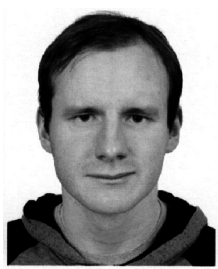
REFERENCES

- [1] Theory and methods of aviation management: Textbook. In two parts / S.Ya. Pan'kov, Yu.E. Zaburayev, A.M. Matveyev; under obs..red. V.A. Meshcheryako-va. - Ulyanovsk: UAVUGA, 2006.-190 p.
- [2] Zenkevich S.L., Yushchenko A.S. Fundamentals of manipulation robots management: A textbook for high schools. - 2 nd ed., Corrected. and additional. Moscow: Izd. MSTU. NE Bauman, 2004. - 480 p.
- [3] Novozhilov IV, Zatselin MF Typical calculations on theoretical mechanics on the basis of a computer. - M.: High School, 1986. - 136 p.



Rykov Anatoly Ar-kadievich

In 1968 he graduated from the Novosibirsk State University of Mechanics and Mathematics in specialty " Mechanics". Since 1975 he worked as an assistant at the Department of Theoretical Mechanics of the NSTU. In 1982 he defended his thesis on "Development and research of devices for the formation of impact pulses". At the present time he works as an assistant professor on the department Strength of flying machines of the NSTU.



Isakov Peter Yurievich

In 2016 he entered the NSTU at the Mechanical-technological Faculty. Now he is a second year Bachelor's degree.

Influence of the Topology of the Distributed Series Compensation Devices on Power Transformer Losses

Pavel A. Rashitov¹, Evgeniy A. Vershanskiy¹, Michail I. Petrov¹
¹National Research University «MPEI», Moscow, Russia

Abstract – This paper studies the effect of topologies of distributed series compensation devices on the value of losses in a power transformer. The analytical expressions for the calculation of the current in the secondary winding of the transformer of distributed series compensation devices have been derived. The calculations for finding the dependence of the value of in the transformer secondary winding losses on the line current for different topologies of the distributed series compensation device have been explained.

Index Terms – distributed series compensation devices, injection rate, reactance.

I. INTRODUCTION

THE CONTROL of power flows in electrical networks is one of the most important functions ensuring the reliability and efficiency of electric power systems. The alternative to traditional power flow control devices (FACTS devices) are distributed series compensation devices. The main idea of the distributed series compensation devices lies in creating the controlled effect on the reactance of the power line section, which is equivalent to the effecting on the linear parameters of the overhead line (OL). Their main advantage in relation to FACTS devices is the fast installation on the power line and mobility, which allows their use for elimination of the local bottlenecks in the electric power system in the medium term, with subsequent dismantling and transfer to other facilities [1, 2]. The distributed series compensation devices with mounting directly to the OL wire were named distributed compact series compensation devices (DCSC) [3].

The operation principle of DCSC lies in the installing of the transformer, which primary winding is the wire of the OL. The energy taken from the line is reserved in the energy store. With the help of the converter, a voltage drop, that is shifted on 90° or -90° with respect to current, is created on the primary winding. It is equivalent to including the reactive element in the line cut. The ability of the DCSC to influence on the redistribution of power flows in power transmission lines is achieved by the possibility of bringing in of the both capacitive (capacitive injection) and inductive (inductive injection) reactance in the transmission lines.

II. PROBLEM DEFINITION

There are two principles of bringing in distributed compact series compensation devices into the resistance line. The first principle is based on the operation of the parallel oscillatory circuit, formed by the transformer magnetization inductance and the capacitor this is connected in parallel with the transformer secondary winding. The character and magnitude of the input reactance depends on the size of the connected capacitance. The second principle is based on the formation of voltage, due to the presence of an energy storage device and a bridge converter on the secondary side of the transformer that lags or leads the line current by 90° , this corresponds to the introduction of the capacitive or inductive reactance [4]. The object of the paper is the analysis of the transformer losses for two principles of bringing in DCSC reactance into the line.

III. THEORY

Distributed compact series compensation device, based on the first principle of bringing in reactance into the line, can be represented as a simple parallel oscillatory circuit. Fig. 1 shows the structure of the parallel connection of the magnetization inductance and the capacitor.

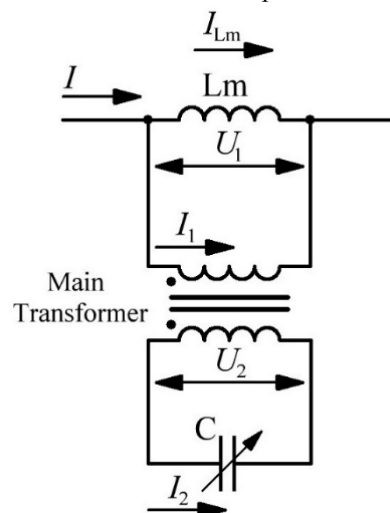


Fig. 1. Scheme of the oscillating circuit with the ideal transformer.

We can write a system of equations of currents and voltages for this scheme:

$$\begin{cases} I = I_1 + I_{Lm} \\ I_2 = \frac{I_1}{K_{tr}} \\ U_2 = I_2 \cdot \frac{1}{j \cdot \omega \cdot C} \\ U_1 = I_{Lm} \cdot j \cdot \omega \cdot Lm \\ U_1 = \frac{U_2}{K_{tr}} \end{cases} \quad (1)$$

Lm – the magnetization inductance of the power transformer, C – capacitance on the secondary side, K_{tr} – ideal transformer ratio, ω – network angular frequency.

Based on the system of equations (1), it is possible to determine the dependence of the equivalent reactance brought by the DCSC into the transmission line on the capacitance value of the condenser:

$$X_{eq} = \frac{U_1}{I} = \frac{j \cdot \omega \cdot Lm}{1 - \omega^2 \cdot Lm \cdot C \cdot K_{tr}^2}.$$

The value of the capacitance C determines the character and magnitude of the reactance of the wire section of the overhead line, on which DCSC is mounted. If $C < \frac{1}{\omega^2 \cdot Lm \cdot K_{tr}^2}$, then the

brought reactance has an inductive character, otherwise capacitive.

The voltage drop on the equivalent resistance of the DCSC (booster voltage) should not lead to the saturation of the magnetic circuit of the DCSC power transformer with any current flowing through the power line. The maximum permissible booster voltage is determined by the dimensions of the magnetic circuit and is limited by the saturation induction of the magnetic core material (B_s):

$$|U_{1max}| = B_s \cdot S_{mag} \cdot \omega, \quad (2)$$

where S_{mag} – is the cross-sectional area of the magnetic core.

The maximum equivalent reactance is dependent on the line current and is determined by the maximum allowable booster voltage:

$$X_{eqmax} = \frac{|U_{1max}|}{I} = \frac{B_s \cdot S_{mag} \cdot \omega}{I}. \quad (3)$$

At the nominal line current (I_{nom}), the maximum equivalent reactance (nominal reactance) is equal to the resistance of the magnetization of the power transformer:

$$X_{nom} = j \cdot \omega \cdot Lm. \quad (4)$$

The relative change of the resistance of the parallel oscillatory circuit in comparison with the nominal reactance can be represented as the injection coefficient (K_{inj}):

$$K_{inj} = \frac{X_{eq}}{X_{nom}} = \frac{1}{1 - \omega^2 \cdot Lm \cdot C \cdot K_{tr}^2}.$$

Fig. 2 shows the dependence of the injection coefficient on the capacitance connected to the secondary side of the DCSC power transformer in the cases of absence and presence of losses in the circuit [5].

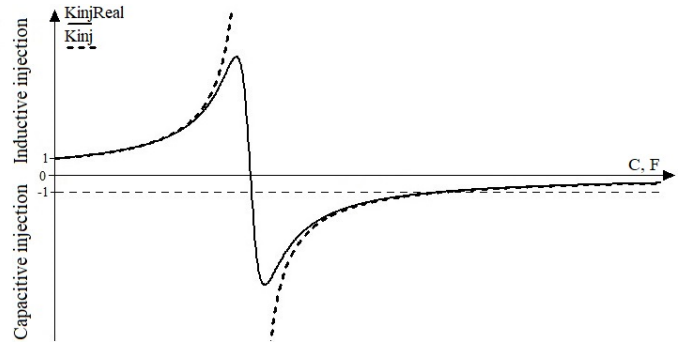


Fig. 2. The dependence of the injection coefficient on the capacity ($K_{injReal}$ - injection coefficient in the case of presence of losses in the circuit, K_{inj} - injection coefficient in the case of absence of losses in the circuit).

If the injection coefficient is positive DCSC brings in inductive reactance into the line, when the injection coefficient is negative – the capacitive reactance.

Dependence in Fig. 2 shows the possible values of the injection coefficient. This dependence takes into account the changes of the condenser capacitance, but doesn't take into account the limitations associated with saturation of the magnetic core. The dependence of the maximum possible injection coefficient on the line current can be obtained from expressions (3) and (4) (Fig. 3).

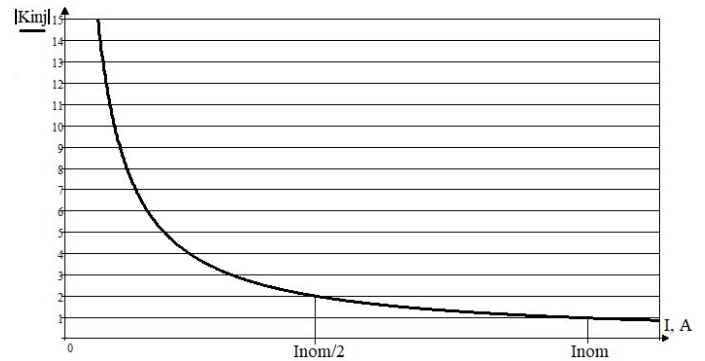


Fig.3. The dependence of the maximum possible injection coefficient on the line current.

When working with the maximum injection coefficient, the current of the magnetization inductance is determined as follows:

$$I_{Lm} = I \cdot |K_{injmax}| = I \cdot \frac{X_{eqmax}}{X_{nom}} = I \cdot \frac{|U_{1max}|}{I \cdot X_{nom}} = I_{nom}. \quad (5)$$

From (5) we can define K_{injmax} as: $K_{injmax} = \pm \frac{I_{nom}}{I}$. The secondary winding current at the maximum injection coefficient depending on the line current is determined as:

$$I_2 = (1 - K_{injmax}) \cdot \frac{I}{K_{tr}} = (1 \pm \frac{I_{nom}}{I}) \cdot \frac{I}{K_{tr}} = \frac{I \pm I_{nom}}{K_{tr}}. \quad (6)$$

Fig. 4 shows the dependence of the transformer secondary winding current on the line current.

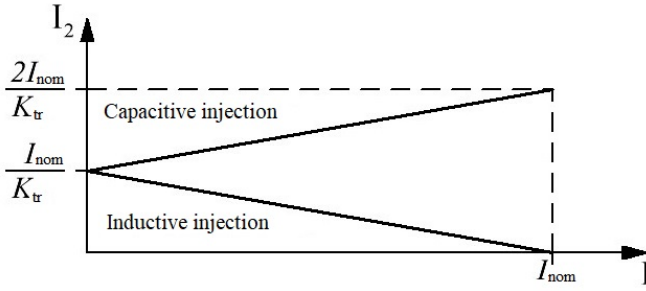


Fig. 4. The dependence of the current in the secondary winding of the transformer on the current in the line.

From the dependence, it can be seen that during the injection of inductive reactance, the current of the secondary winding changes linearly from I_{nom}/K_{tr} to 0 as the line current increases from 0 to I_{nom} . With capacitive injection, during the increase of the line current in the transformer secondary winding changes from I_{nom}/K_{tr} to $2I_{nom}/K_{tr}$. With capacitive injection, the current in the secondary winding of the transformer exceeds the rated current of the secondary winding (I_{nom}/K_{tr}), which leads to the losses rise and to the necessity of the increase of the transformer secondary winding cross section.

Fig. 5 shows DCSC based on the second principle of bringing in reactance into the line.

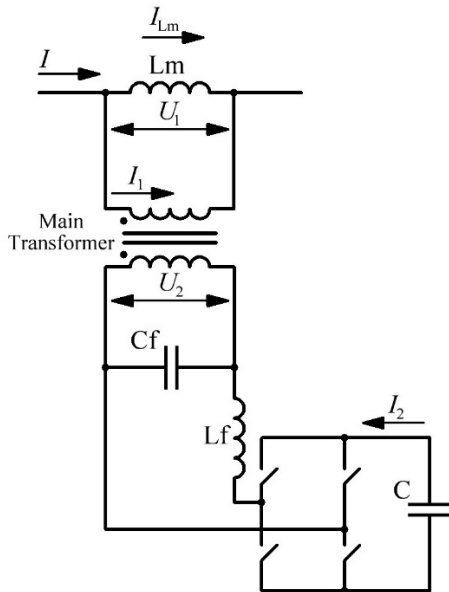


Fig. 5. Structure of DCSC with bridge converter and energy storage.

The operation of this type of DCSC is based on the formation of voltage in the secondary winding of the transformer using a bridge converter and a capacitive energy storage device, which in this case is acting as a constant voltage source. The generation of the voltage that lags or leads the line current by 90° corresponds to the introduction of reactance of a capacitive or inductive character.

If X_{nom} in this scheme is equal to the magnetization inductance impedance of the power transformer, all expressions that have been derived above will be valid for this circuit, including the dependence of the secondary current on the line current.

The change of the transformer magnetization inductance value won't affect on the operation of the circuit, but the dependence of the current of the secondary winding on the line current will be changed. In order to reduce the secondary current in capacitive injection, the magnetization inductance should be made as large as possible, ideally $L_m \rightarrow \infty$. Then the expression for the secondary winding current for a different injection character takes the following form:

$$I_2 = \frac{I}{K_{tr}}. \quad (7)$$

Fig. 6. shows the dependence of the secondary current on the line current.

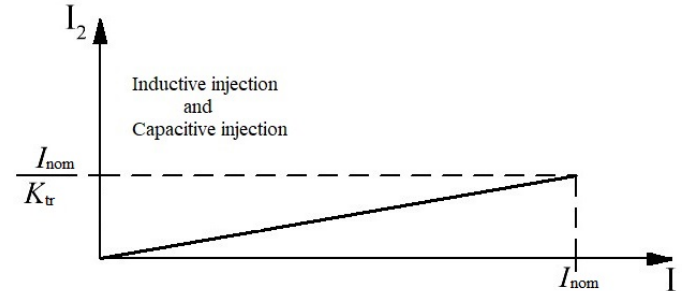


Fig. 6. The dependence of the current in the secondary winding of the transformer on the current of the line.

The dependence shows that during the injection of the reactance with increasing of the line current from 0 to I_{nom} , the secondary winding current varies linearly from 0 to I_{nom}/K_{tr} , regardless of the character of the injection.

IV. EXPERIMENTAL RESULTS

Example of calculation.

Initial data:

$R_2 = 0.44 \text{ Ohm}$, $K_{tr} = 50$, $B_S = 1.7 \text{ T}$, $d_{in} = 50 \text{ mm}$, $d_{out} = 80 \text{ mm}$, $l = 1.2 \text{ m}$, $\omega = 314 \text{ rad/s}$, $I_{nom} = 750 \text{ A}$.

1) The magnetic core of the DCSC transformer is a thick-walled cylinder, where d_{in} is the inner diameter, d_{out} is the outer diameter, l is the length. Let's determine the cross-sectional area of the magnetic core $S_{mag} = l \cdot \frac{d_{out} - d_{in}}{2} = 0.018 \text{ m}^2$.

2) Initial date identify the value of $|U_{1max}| = 9.6 \text{ B (2)}$.

3) The ratio of the power losses in the secondary winding to the reactive power of the DCSC is determined as follows:

$$\Delta\eta = \frac{P_{los2}}{Q} = \frac{I_2^2 \cdot R_2}{I \cdot |U_{1max}|} \cdot 100\%$$

The coefficient $\Delta\eta$ is related to losses in the secondary winding of the transformer and shows how much the efficiency of the entire device decreases.

Let's calculate the values of the secondary winding current and the coefficient $\Delta\eta$ for two principles of introduction of reactance of capacitive and inductive character for the line current that varies from the minimum value to the nominal value, using formulas (6) and (7).

The calculation results for the two principles of introduction are given in Table I and Table II.

TABLE I

MAIN CIRCUIT VALUES FOR DIFFERENT LINE CURRENT DURING THE FUNCTIONING OF THE DCSC BASED ON THE FIRST PRINCIPLE OF INTRODUCTION OF REACTANCE TO THE LINE

| Inductive injection | | | Capacitive injection | | |
|---------------------|----------|------------------|----------------------|----------|------------------|
| I, A | I_2, A | $\Delta\eta, \%$ | I, A | I_2, A | $\Delta\eta, \%$ |
| 50 | 14 | 17.94 | 50 | 16 | 23.43 |
| 100 | 13 | 7.74 | 100 | 17 | 13.23 |
| 150 | 12 | 4.39 | 150 | 18 | 9.89 |
| 200 | 11 | 2.77 | 200 | 19 | 8.26 |
| 250 | 10 | 1.83 | 250 | 20 | 7.23 |
| 300 | 9 | 1.24 | 300 | 21 | 6.73 |
| 350 | 8 | 0.84 | 350 | 22 | 6.33 |
| 400 | 7 | 0.56 | 400 | 23 | 6.05 |
| 450 | 6 | 0.37 | 450 | 24 | 5.86 |
| 500 | 5 | 0.23 | 500 | 25 | 5.72 |
| 550 | 4 | 0.13 | 550 | 26 | 5.63 |
| 600 | 3 | 0.07 | 600 | 27 | 5.56 |
| 650 | 2 | 0.03 | 650 | 28 | 5.52 |
| 700 | 1 | 0.006 | 700 | 29 | 5.49 |
| 750 | 0 | 0 | 750 | 30 | 5.49 |

TABLE II

MAIN CIRCUIT VALUES FOR DIFFERENT LINE CURRENT DURING THE FUNCTIONING OF THE DCSC BASED ON THE SECOND PRINCIPLE OF INTRODUCTION OF REACTANCE TO THE LINE

| Inductive injection | | | Capacitive injection | | |
|---------------------|----------|------------------|----------------------|----------|------------------|
| I, A | I_2, A | $\Delta\eta, \%$ | I, A | I_2, A | $\Delta\eta, \%$ |
| 50 | 1 | 0.09 | 50 | 1 | 0.09 |
| 100 | 2 | 0.18 | 100 | 2 | 0.18 |
| 150 | 3 | 0.27 | 150 | 3 | 0.27 |
| 200 | 4 | 0.37 | 200 | 4 | 0.37 |
| 250 | 5 | 0.46 | 250 | 5 | 0.46 |
| 300 | 6 | 0.55 | 300 | 6 | 0.55 |
| 350 | 7 | 0.64 | 350 | 7 | 0.64 |
| 400 | 8 | 0.73 | 400 | 8 | 0.73 |
| 450 | 9 | 0.82 | 450 | 9 | 0.82 |
| 500 | 10 | 0.91 | 500 | 10 | 0.91 |
| 550 | 11 | 1 | 550 | 11 | 1 |
| 600 | 12 | 1.09 | 600 | 12 | 1.09 |
| 650 | 13 | 1.19 | 650 | 13 | 1.19 |
| 700 | 14 | 1.28 | 700 | 14 | 1.28 |
| 750 | 15 | 1.37 | 750 | 15 | 1.37 |

The dependence of the ratio of the power losses in the secondary winding to the reactive power of the DCSC on the line current for the two principles of bringing in capacitive and inductive reactance in the line is shown in Fig. 7.

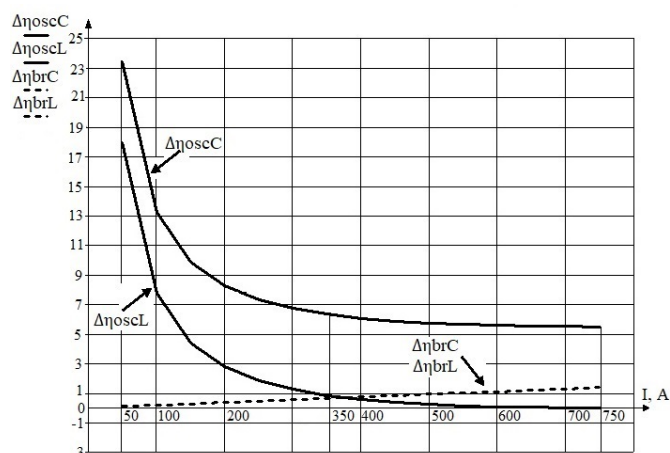


Fig. 7. The dependence of the ratio of the loss power in the secondary winding to the reactive power of the DCSC on the line current ($\Delta\eta_{oscC}$ for the first principle for capacitive injection, $\Delta\eta_{oscL}$ for the first principle for inductive injection, $\Delta\eta_{brC}$ for the second principle for capacitive injection, $\Delta\eta_{brL}$ for the second principle for inductive injection).

The dependence shows that when using the first principle of injection inductive reactance into the line, with the increase of the line current from 50 A to $I_{nom} = 750$ A, the coefficient $\Delta\eta$ decreases from 17.94% to 0%, that is, the efficiency of the entire device increases. With capacitive injection, the coefficient $\Delta\eta$ changes from 23.43% to 5.49% with increasing of the line current. If the second principle is used for capacitive or inductive injection, the coefficient $\Delta\eta$ increases from 0.09% to 1.37% with the increasing of the line current from 50 A to $I_{nom} = 750$ A, which leads to the efficiency decrease. Comparing the two principles of bringing in reactance into the line, it can be concluded that at the nominal current in the line during inductive injection using the first principle, the reduction in efficiency of the device is 1.37% less than for the second principle, and during capacitive injection, 4.12 % more.

Losses during capacitive injection for the first principle are higher than for the second principle. Losses during inductive injection for the first principle with increasing line current reduce, and for the second principle they rise. However, at line currents of up to the half of the nominal value, the reduction in device efficiency is less when the second principle is used, regardless of the character of the injection.

V. DISCUSSION OF RESULTS

The introduction of the capacitive reactance into line in the use of DCSC based on the operation of a parallel oscillatory circuit with the increase of line current the current in the secondary winding rises from the rated current to twice the rated current. On the other hand, when the inductive reactance is brought in into the line, the current in the secondary winding of the power transformer decreases from nominal value to zero. With the use of DCSC based on the generation of the booster voltage, an increase in the line current when injected into a reactive line of capacitive or inductive character causes an increase in the current in the secondary winding from zero to nominal value.

The losses in the secondary winding of the transformer are estimated with the help of the coefficient $\Delta\eta$, that determines

the efficiency of the transformer operation. With line currents up to the half of the nominal, the coefficient $\Delta\eta$ of DCSC's topology based on the booster voltage formation is less, regardless of the type of injection, than of the DCSC based on the oscillatory circuit. At currents greater than half of the nominal the coefficient $\Delta\eta$ for inductive injection in the DCSC's topology based on the oscillatory circuit, the losses in the transformer become smaller than in the topology based on the formation of the booster voltage.

VI. CONCLUSION

1. The analytical expressions for calculation of the current in the secondary winding of the DCSC transformer for different topologies for different injection's character have been derived.
2. In the capacitive injection mode, the losses in the DCSC transformer that is based on the parallel oscillation circuit is greater than in the DCSC that is based on the booster voltage generation over the entire range of power line operating currents.
3. In the inductive injection mode, the losses in the DCSC transformer based on the parallel oscillatory circuit is greater than in the DCSC based on the booster voltage generation when the transmission line currents are lower than half of the nominal value.

The study was performed at National Research University "Moscow Power Engineering Institute" within the framework of the project "Development and experimental approbation of the technical solutions for the creation of the stand-alone semiconductor control devices for series compensation to improve the reliability of overhead transmission lines (RFMEFI57417X0140)" with the financial support of the Ministry of Education and Science of the Russian Federation.

REFERENCES

- [1] D. Divan, W. Brumsickle, R. Schneider, B. Kranz, R. Gascoigne, D. Bradshaw, M. Ingram and I. Grant. A Distributed Static Series Compensator System for Realizing Active Power Flow Control on existing Power Lines // IEEE PSCE Conference Records, Oct 2004, pp. 642-649.
- [2] D.I. Panfilov, P.A. Rashitov, M.I. Petrov. Optimization of weight and dimensions of longitudinal compensation devices for electric transmission lines 110-220 kV // 2017 IEEE 58th International Scientific Conference on RTUCON, Oct 2017, pp. 1-7.
- [3] D.I. Panfilov, Y.G. Shakaryan, M.G. Astashev, P.A. Rashitov, A.V. Antonov. Small devices for longitudinal compensation in overhead power lines // Russian Electrical Engineering, Volume 88, Issue 7, 1 July 2017, pp. 471-474.
- [4] M.G. Astashev, D.I. Panfilov, D.A. Seregin, A.A. Chernyshev. Analysis of the operating modes of an autonomous serial control power flow for overhead power lines // Nauka Publishers (Moscow), 2017, pp. 39-52. (in Russian)
- [5] D.I. Panfilov, P.A. Rashitov, M.I. Petrov. Analysis of element's parameters influence on characteristics of distributed compacts series compensators // 2017 18th International Conference of Young Specialists on EDM, June-July 2017, pp. 455-459.



Rashitov Pavel Ahmatovich – Russia, 1984, PhD. Finished the Electrotechnical Faculty of the «NRU «MPEI» in 2008. In 2011 he has defended the dissertation «Research and development of control algorithms for high-power semiconductor phase shifter devices for energy facilities of the United National Electric Power Network of Russia» (specialty 05.09.12 - Power Electronics). Currently he works as the associate professor at the Industrial Electronics Department of the «NRU «MPEI».



Vershanskiy Evgeniy Aleksandrovich – Russia, 1994, finished magistracy of the Industrial Electronics Department of the «NRU «MPEI» in 2017. Currently he is a PhD student of the same department.



Petrov Michail Igorevich – Russia, 1991, finished magistracy of the Industrial Electronics Department of the «NRU «MPEI» in 2014. Currently he is a PhD student of the same department.

Soft Switching Stacked-up Boost Push-Pull Converter

Aleksandr V. Osipov¹, Aleksandr A. Lopatin², Raimzhan A. Latypov², Ilya S. Shemolin¹

¹Tomsk State University of Control Systems and Radioelectronics, Russia

²JSC Academician M.F. Reshetnev Information Satellite Systems, Zheleznogorsk, Russia

Abstract – This work describes boost type push-pull converter with active rectification based on center tapped topology. It is shown that active rectification not only reduce static losses but makes converter bidirectional, which can be used to charge accumulator battery as well. Besides that active rectification makes transfer function linear down to the idle by recuperation input filter energy. Control method to minimize static losses has been proposed. Commutation transitions have been analyzed. It is shown that inductor current reversal due to active rectifier employed provides resonant discharge of intrinsic capacitances and soft commutation for switching transitions of low side transistors. Soft commutation of high side transistors is provided by inductor current inertia. Prototype has been developed to verify analysis validity. Soft commutation has been confirmed. Efficacy achieved is 98.5%.

Index Terms – Stacked-up converter, push-pull converter, soft switching, zero voltage switching (ZVS).

I. INTRODUCTION

STACKED-UP BOOST converters are widely employed in power supply systems to provide constant voltage from accumulator battery having relatively high efficiency due to the partial power flow conversion. The latter means limited conversion range. This way application efficiency depends on match between source voltage range to the output one. Spacecraft power supply system usually have upper input voltage level close to output one.

Stacked-up boost converters have been investigated in [1] – [5], push-pull low output voltage ones with reduced switch count [3] – [5]. It is shown in [3] that inductor can be placed either at the input or at the output. In the latter case switches do not experience double input voltage, such topology is well suited for higher input voltages. Besides that, inductor at the input means lesser time-voltage product thus smaller inductance.

Widely used push-pull topology variation, having coupled smoothing inductor with direct power transfer to the output namely the Weinberg one [6], which can be galvanically decoupled [7]. Double winding inductor while unloading transformer is deemed unfavorable.

Common problem of such topologies is hard commutation thus limiting conversion frequency thus increasing size (volume or weight). That is why contemporary practice is to employ soft switching transitions like Zero Voltage Switching (ZVS) etc. Snubbing or damping circuits passive as well as active are utilized but transfer of the energy during commutation is basically a source of an additional losses [8]. Yet another

way would be use of resonant converters [9,10] but the elements constituting resonant tank do bring additional mass or volume thus being detrimental. Taking into account that soft commutation is usually related to reversal of the current through the switch just before the turning switch on, which is usually obtained by intrinsic components already present in the converter. For instance: use of magnetizing current of the power transformer for ZVS, commutation inductor in push-pull boost converter [11], creating conditions for soft commutation using smoothing inductor together with the active rectifier by ripples well exceeding nominal current [12].

II. PROBLEM DEFINITION

Increasing current ripples in the input inductor to achieve negative instantaneous value seems to be the most reasonable approach to provide ZVS conditions because no additional components are needed while active rectification further lowers losses. It could be assumed that soft commutation can be achieved not only in basic boost topology but in stacked-up ones as well.

This way the purpose of the current work is to investigate of a current recuperation mode commutation processes in push-pull boost converter.

III. THEORY

Diode based center tapped variation of push-pull boost converter is widely used. Such a circuit with active rectifiers is shown at Fig.1. Converter is inductor fed. Two totem pole channels are switched by phase shifted signals with fixed dead time. As a result at each period two distinct phases exist: boost one and direct transfer one, when input inductor is directly connected to the output capacitor C .

Boost phase exists when bottom switch in one channel and top switch in another channel are closed: VT_1 , VT_4 or VT_2 , VT_3 . As a result voltage applied to the winding is equal to the sum of battery and inductor ones. This way output voltage doubles the input one. One may say that additional voltage is added to or stacked up over the input one

$$V_{OUT} = 2(V_{IN} + V_L) = 2V_{TVm},$$

where V_L – inductor voltage, V_{TVm} – center tap voltage.

The other words boost phase makes center tap voltage equal to the half of the output one. If such voltage is lower than input one current in the inductor will rise.

When both top switches are closed direct transfer phase exists: inductor is directly tied to the output capacitor thus making

ing output voltage equal to the sum of input and inductor ones

$$V_{OUT} = V_{IN} + V_L = V_{TVm}.$$

Conversely inductor current will fall.

It is worth noting that current in windings stays at the half value of the input one which makes it different from a full bridge topology where current is zero at the very same conversion phase. Simultaneous closing of the bottom switches is prohibited.

To regulate output voltage pulse widths of such phases have to be changed, diagrams are presented at Fig. 2. Transfer function can be derived using volt-time product equality in an inductor

$$V_{OUT} = \frac{V_{IN}}{1 - \gamma/2},$$

where γ – relative duration of boost phase in respect to conversion period.

It should be mentioned that use of an active rectifier allows to preserve inductor's current continuity and to linearize transfer function irrespective to the load including idle.

Static losses then depend on relative duration of boost phase γ . Summary of the static losses is proportional to the relative duration γ at constant load. Relative static losses per transistor P_{loss_VT} are governed by the equation

$$P_{loss}^* = \frac{P_{loss}}{P_{loss_VT}} = \frac{3}{2}\gamma + \frac{1}{2}.$$

Static losses at the direct transfer phase are determined by drop across two upper transistors connected in parallel. This is different from boost phase when transistors are connected in series.

Power transferred through the transformer depends on the relative duration γ and is described by the expression

$$P_{TV}^* = \frac{P_{TV}}{P_{OUT}} = \frac{\gamma}{4\left(1 - \frac{\gamma}{2}\right)},$$

its maximum value does not exceed half the output power P_{OUT} .

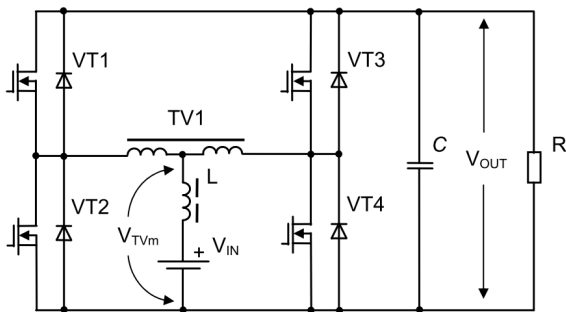


Fig. 1. Push-pull stacked-up boost converter with active rectification

Processes in such converter have been analyzed in inductor current recuperation mode. Current and voltage diagrams are shown at Fig. 2.

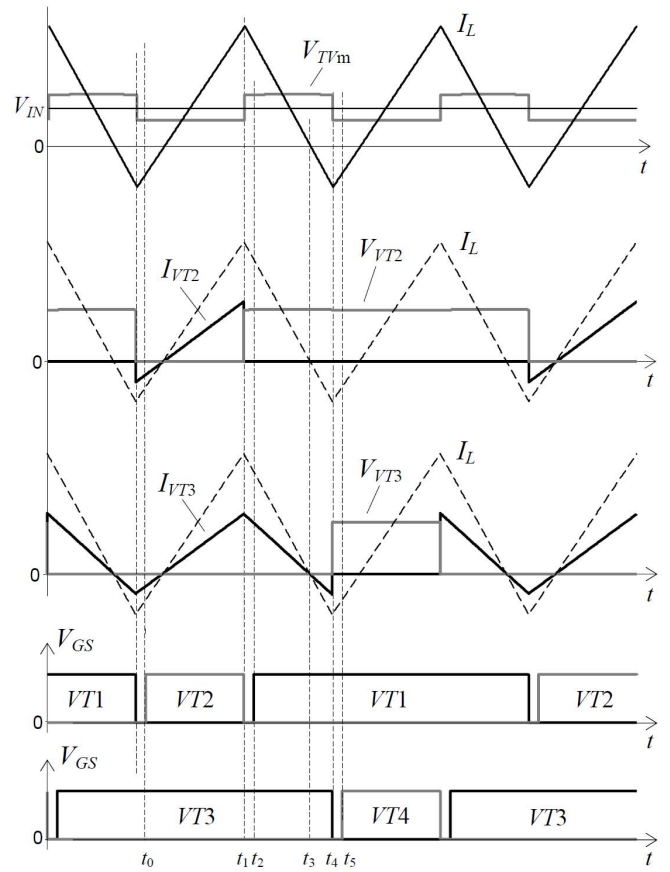


Fig. 2. Converter operation at $\gamma = 0.5$

At time interval (t_0-t_1) $VT2$, $VT3$ are closed, as a result each winding experiences $V_{OUT}/2$ and a current in each winding is equal to $I_L/2$ and a half of the inductor current is flowing into the load and another half is circulated in short circuited winding. At the moment t_1 $VT2$ is off and current in the winding flows into $VT1$, discharging its parasitic capacitance and turning on body diode. At this moment converter start to operate in direct transfer phase, in which voltage across windings becomes zero, current flows into the load and inductor's current is falling. At the moment t_2 $VT1$ is turned on at Zero Voltage Condition when body diode is conducting, this does not change operating mode. At the moment t_3 inductor current changes direction as well as a current does in $VT1$, $VT3$. This allows to discharge parasitic capacitance of $VT4$ at the moment t_4 when $VT3$ is turned off. This way at a moment t_5 $VT4$ is turned on at zero voltage, and Fig. 2 showing moment t_0 of zero voltage turning on of $VT2$.

This way in such boost converter, if the reverse inductor current exists all transistors are switching at zero voltage (ZVS).

IV. EXPERIMENTAL RESULTS

The hardware prototype has been made to verify simulation results for the proposed stacked-up converter. The converter consists of two channels made of IRFP4668, a center tapped transformer with $N1/N2=1$ using EILP38 N87core, input inductor using the same core. An output capacitor C

value is $30\mu\text{F}$. To minimize leakage inductance windings are bifilar wound using copper foil. Flux density B amplitude is 0.14 T at $f = 40\text{ kHz}$. Fig. 3 and Fig. 4 shows: low side transistor current I_{VT2} , inductor current I_L , center tap voltage V_{TVm} for a different inductance values given $V_{OUT} = 100\text{ V}$, $V_{IN} = 75\text{ V}$, $f = 40\text{ kHz}$, $R = 18\text{ Ohm}$, $\gamma = 0.5$.

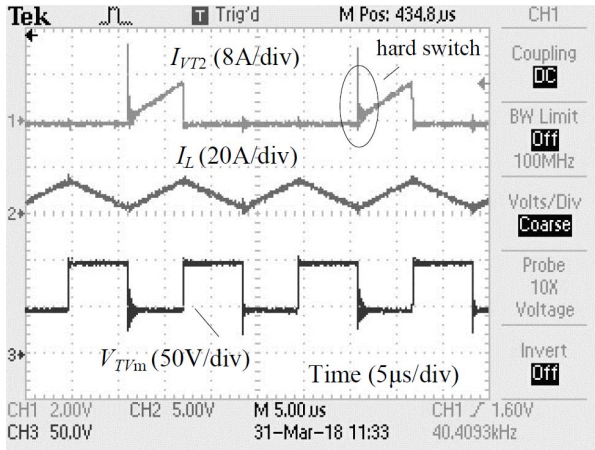


Fig. 3. Converter parameters' waveforms at $V_{OUT} = 100\text{ V}$, $V_{IN} = 75\text{ V}$, $f = 40\text{ kHz}$, $R = 18\text{ Ohm}$, $\gamma = 0.5$, $L = 12.5\text{ }\mu\text{H}$

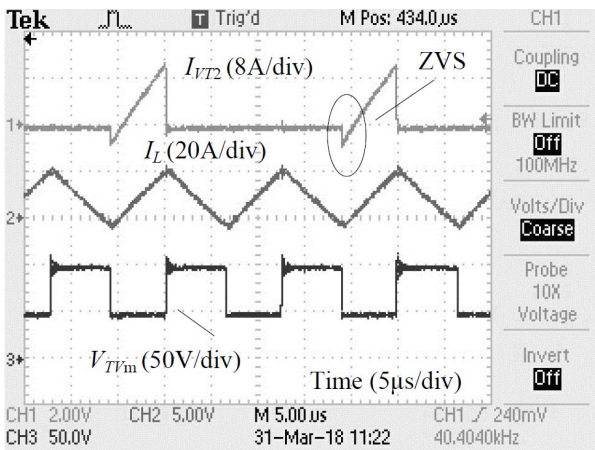


Fig. 4. Converter parameters' waveforms at $V_{OUT} = 100\text{ V}$, $V_{IN} = 75\text{ V}$, $f = 40\text{ kHz}$, $R = 18\text{ Ohm}$, $\gamma = 0.5$, $L = 6.2\text{ }\mu\text{H}$

At $L = 12.5\text{ }\mu\text{H}$ no recuperation of inductor current occurs which corresponds to hard commutation of $VT2$ causing instantaneous discharge of drain-source capacitances and, subsequently, electromagnetic interference (Fig. 3). Reducing inductance L down to $6.2\text{ }\mu\text{H}$ is enough to achieve negative current through the inductor (Fig. 4), which is sufficient to discharge a drain-source capacity of the lower transistor $VT2$ and turning on its body diode to provide ZVS. Real waveforms do confirm soft switching at a particular inductor value. In the soft-switch mode efficiency achieved is 98.5%.

V. DISCUSSION OF RESULTS

Given boost converter topology seems to be advantageous due to low transformer's voltage and inductance values because only part of the output power is converted and range of regulation is limited. However placing inductor at the input does increase current through one.

It should be noted, that soft switching in this converter is provided by increased inductor current ripples, which can increase an input capacitive filter. Multi-phase or interleaved converters seems to be a reasonable cure. Besides inductor current ripples change in the process of regulation, which is narrows the possible soft-switching range. The solution of this problem is the variation of frequency with fixed commutation current value of transistor.

Increasing ripples even further net negative input current could be achieved which means that converter shown is bidirectional. ZVS mode is maintained as well.

VI. CONCLUSION

As shown above soft commutation of the transistors along with low static losses, use of stacked-up topology improves overall efficiency in respect to basic boost topology making it advantageous in battery powered systems.

The study was performed during the execution of a complex project (number 02.G25.31.0182) with the financial support of the Russian Government (Ministry of Education of Russia).

REFERENCES

- [1] Park K.-B., Moon G.-W., Youn M.-J. Nonisolated high step-up stacked converter based on boost-integrated isolated converter // IEEE Transactions on Power Electronics. 2011. V. 26. No. 2. pp. 577-587.
- [2] Li W., He X. Review of nonisolated high-step-up DC/DC converters in photovoltaic grid-connected applications // IEEE Transactions on Power Electronics. 2011. V. 58. No. 4. pp. 1239-1250.
- [3] Forouzesh M., Siwakoti Y.P., Gorji S.A., Blaabjerg F., Lehman B. Step-up DC-DC converters: a comprehensive review of voltage-boosting techniques, topologies, and applications // IEEE Transactions on Power Electronics. 2017. V. 32. No. 12. pp. 9143-9178.
- [4] Chen R.T., Chen, Y.Y. Single-stage push-pull boost converter with integrated magnetics and input current shaping technique // IEEE Transactions on Power Electronics. 2006. V. 21. No. 5. pp. 1193-1203.
- [5] Tofoli F.L., De Castro Pereira D., De Paula W.J., De Sousa Oliveira J'unior D. Survey on non-isolated high-voltage step-up DC-DC topologies based on the boost converter // IET Power Electronics. 2015. V. 8. No. 10. pp. 2044-2057.
- [6] Weinberg A.H., Rueda Boldo P. A high power, high frequency, DC to DC converter for space applications // Power Electronics Specialists Conference, 1992. PESC '92 Record., 23rd Annual IEEE, V. 2. pp. 1140-1147.
- [7] Thottuvelil V.J., Wilson T.G., Owen Jr. H.A. Analysis and design of a push-pull current-fed converter // in Proc. of PESC'81 - IEEE Power Electronics Specialists Conference Proceedings. 1981. pp. 192-203.
- [8] Mao H., Lee F.C.Y., Zhou X., Dai H., Cosan M., Boroyevich D. Improved zero-current-transition converters for high-power applications // IEEE Transactions on Industry Applications. 1997. V. 33. No. 5. pp. 1220-1232.
- [9] Corradini L., Seltzer D., Bloomquist D., Zane R., Maksimovic D., Jacobson B. Minimum current operation of bidirectional dual-bridge series resonant DC/DC converters // IEEE Transactions on Power Electronics. 2012. V. 27. No. 7. pp. 3266-3276.
- [10] Osipov A.V., Yaroslavl'tsev Y.V., Burkin Y.Y., Sviridov V.V. // Boost type series resonant converter with flexible structure for power supplies. Bulletin of the Tomsk Polytechnic University, Geo Assets Engineering. 2018. V. 329. No. 2. pp. 27-37. (in Russian).
- [11] Dixon R.C., Dement'ev Yu.N., Mikh'alchenko G.Ya., Mikh'alchenko S.G., Semenov S.M. Dynamic properties of a two-phase boost converter with soft-switching transistors technology // Bulletin of the Tomsk Polytechnic University, Geo Assets Engineering. 2014. V. 324. No. 4. pp. 96-101. (in Russian).

- [12] Waffler S., Kolar J.W. A novel low-loss modulation strategy for high-power bidirectional buck + boost converters // IEEE Transactions on Power Electronics. 2009. V. 24. No. 6. pp. 1589-1599.



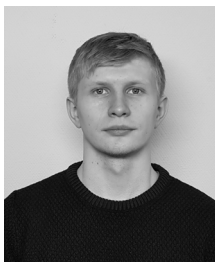
Aleksandr V. Osipov was born in 1978 in Semipalatinsk, is a senior researcher of the Scientific Research Institute of Space Technology of the Tomsk State University of Control Systems and Radioelectronics (TUSUR), candidate of technical sciences. Graduated from the Faculty of Electronic Engineering (TUSUR) in 1999. Defended a dissertation on the topic «High frequency induction heating systems of blanks before its plastic deformation» in 2004. Research interests: power electronics, resonant converters, power supply systems.
e-mail: ossan@mail.ru.



Aleksandr A. Lopatin was born in 1977 in Krasnoyarsk, the head of the development of power on-board equipment in the JSC "Information Satellite Systems", candidate of technical sciences. In 1999 he graduated from the Krasnoyarsk State Technical University with a degree in Electrification of Industrial Enterprises. In 2006 he defended his thesis on the topic "Indirect Adaptive Control of a Direct Current Electric Drive". Area of scientific interests: microprocessor-based automatic control systems, pulse converters of direct voltage, power supply systems for space vehicles.



Raimdzhan A. Latypov, was born in 1992 in Bishkek, Kyrgyzstan. In 2015 he obtained a Specialist degree as an Industrial Electronics Engineer from Tomsk State University of Control Systems and Radioelectronics (TUSUR University). In 2015 he began his studies as a PhD student at TUSUR University. Starting in 2015, he has been working at JSC "Information Satellite Systems". His main research interests are spacecraft power systems.



Ilya S. Shemolin, was born in 1993. in Almaty, Kazakhstan. In 2016 he obtained a bachelor's degree as an engineer in industrial electronics from the Tomsk State University of Control Systems and Radioelectronics (TUSUR University). In 2015 he began his studies as a master's student at TUSUR University. Starting in 2017 he has been working at the Research Institute of Space Technologies. Area of scientific interests: power supply systems for space vehicles.

Virtual Instrument for Assessment of Simulated Signal Integrated Harmonics Factors

Nikolay N. Lopatkin, *Member, IEEE*,
Ivan S. Lucenko,
Yuriy A. Chernov

Shukshin Altai State Humanities Pedagogical University (ASHPU), Biysk, Russia

Abstract – The block diagram of the LabVIEW virtual instrument for the assessment of simulated signal integrated harmonics factors is presented. This virtual device version is equipped with the input module for waveform data points import from PSIM output text file. The examples of measurement and use of the integrated harmonics factors values of the investigated voltage for estimating the harmonic distortion of the load circuit current are shown.

Index Terms – Weighted THD, n-order integrated voltage (current) harmonics factor (IHF), method of the differential equations algebraization (ADE), LabVIEW virtual instrument, PSIM.

I. INTRODUCTION

THE SIGNAL harmonic content analysis remains the most needed research operation in radio engineering, electronics and communications systems as well as in electrical engineering and power electronics when it relates to electromagnetic compatibility and efficiency issues [1]-[4].

The conventional factor of voltage harmonics K_{hu} (HF), i.e. the classical voltage THD, is excellent in characterization of the impacting voltage itself only, since it can provide the adequate valuation of the response harmonic contents only for the circuit with the pure active (resistive) load.

The well-known weighted THD (WTHD) factor [5] is used approximately since 2000. It is the most used element of the system of the weighted THD factors for the induction motor load with the frequency-dependent parameters.

The integrated voltage harmonics factors (IHF) were offered by Professor G.S. Zinoviev (NETI, now NSTU, Novosibirsk) much earlier, namely 35 years ago, and they produces weighted (by the harmonic number) summation of harmonics, thereby modeling the effect of the amplitude-frequency characteristic action of the corresponding order idealized electric integrating circuit [6]-[11]. The IHF factors are closely related to the method of the differential equations algebraization (ADE) which allows finding asymptotically with the preset accuracy the closed analytical form expressions for the mathematical relations between the voltages and/or currents RMS values, using the coefficients of the integral-differential equation, that includes these voltages and currents, without solving it [6], [8].

Similar to the THD definitions, the n-order voltage IHF, $\overline{K}_{hu}^{(n)}$, is calculated as follows [6]-[8]:

$$\overline{K}_{hu}^{(n)} = \frac{\overline{U}_{(hh)}^{(n)}}{\overline{U}_{(1)}^{(n)}} = \frac{\overline{U}_{(hh)}^{(n)} \cdot \omega^n}{U_{(1)}}, \quad (1)$$

$$\overline{K}_{hu}^{(n)} = \frac{\sqrt{\left(\overline{U}^{(n)}\right)^2 - \left(\overline{U}_{(1)}^{(n)}\right)^2}}{U_{(1)} / \omega^n} = \sqrt{\left(\frac{\overline{U}^{(n)} \cdot \omega^n}{U_{(1)}}\right)^2 - 1}, \quad (2)$$

$$\overline{K}_{hu}^{(n)} = \frac{\sqrt{\left(\overline{U}_{(hh)}^{(n)}\right)^2}}{U_{(1)} / \omega^n} = \sqrt{\sum_{k=2}^{\infty} \left(\frac{U_{(k)}}{k^n \cdot U_{(1)}}\right)^2}, \quad (3)$$

where for estimated voltage u values $U_{(k)}$, $\overline{U}_{(1)}^{(n)}$, $\overline{U}_{(hh)}^{(n)}$

and $\overline{U}^{(n)}$ are the RMS value of the k harmonic component and RMS values of the results of the n -fold indefinite integral taking of the instantaneous values of the fundamental component $\overline{u}_{(1)}^{(n)}$, of the high harmonics component $\overline{u}_{(hh)}^{(n)}$

and of the whole voltage $\overline{u}^{(n)}$, correspondingly; ω is the angular frequency of the fundamental component. Since the process without a DC component is being considered,

$$\overline{u}^{(n)} = \overline{u}_{(1)}^{(n)} + \overline{u}_{(hh)}^{(n)}. \quad (4)$$

The conventional voltage THD (HF, K_{hu}) corresponds to $n = 0$. The similar way the differentiated voltage harmonics factors (DHF) [6] have been introduced.

In accordance with (3), the n -order integrated voltage harmonics factors IHF can be also referred to as the n -order weighted THD [11]:

$$\overline{K}_{hu}^{(n)} = WTHD^{(n)}. \quad (5)$$

The IHF factors make it possible to evaluate beforehand the load circuit voltages and currents and their quality indices, such as the load (end user) current THD value. In this, these IHF indices relate not to some particular load circuit parameters and their some particular values, but to the impacting voltage itself (imposed to this load circuit).

II. PROBLEM DEFINITION

One of the main research techniques for electronic circuits now is computer simulation. The friendly user interface and fast speed of simulation of power electronics devices, control systems for electric drive and power conversion systems are provided by the widespread simulation software PSIM developed by Powersim (France) [12]. This software is much faster and much cheaper than Matlab/Simulink system.

Despite the growing number of optional add-on modules available to address specific needs in various applications and giving the flexibility to tailor PSIM for user's own needs, the National Instruments LabVIEW software-hardware environment (Laboratory Virtual Instrument Engineering Workbench) is more attractive as a simulation tool. LabVIEW is used as the standard tool for investigation in industry, scientific researches and education. LabVIEW Programming Structures, such as "For Loop", "While Loop", "Case structure", "Sequence structure", are providing great opportunities. At last, LabVIEW is very promising in terms of both data analysis and moving towards carrying out the real nature measurements [13].

In addition to the regular virtual instrument (VI) "Distortion Measurements Express VI", making it possible to easily estimate the signal THD after specifying the order number N of the highest counted harmonic component, the LabVIEW environment provides the enough wide range of designing means for the harmonic contents monitoring [14]-[16]. However, the need for the consideration of the above mentioned integrated harmonics factors is not satisfied.

Our previous papers proved efficiency of the before offered LabVIEW virtual instrument for IHF assessment of signals constructed within LabVIEW VI itself. In particular, the meander, trapezoidal and triangle waveforms signals have been synthesized and analyzed by means of this VI, the IHF and some DHF estimation results have been compared with analytical ones obtained via harmonic synthesis [17], [18]. The multilevel voltage source inverter (MLVSI) output voltage IHF assessments have been accomplished via controller signals waveforms in [19], [20].

Despite the obvious progress achieved, LabVIEW has natural limitation for our research, namely, it is not intended for any electronics, electrical engineering and power electronics circuits simulation, so we have not here any ready for use models of electric circuit elements, their connections, power switches etc.

The purpose of this paper is to present the LabVIEW virtual instrument for the assessment of simulated signals integrated harmonics factors, which is equipped with the input module for waveform data points import from PSIM output text file. Thus, the capability of the PSIM power elements voltages and currents waveforms processing in advanced LabVIEW environment, avoiding supplementary PSIM modules, is shown.

Also some examples of measurement and use of the integrated harmonics factors values of the investigated voltage for estimating the load circuit THD are demonstrated.

III. LABVIEW VIRTUAL INSTRUMENT

The core part block diagram of the LabVIEW virtual instrument for the voltage harmonics integrated factors evaluation is presented in Fig. 1.

The "IFH-meter" is implementing operations of (1) as definition, which provides the most accurate results [17]. The virtual instruments "Tone Measurements Express VI" and "Simulate Signal Express VI" are used here, respectively, to define the parameters of the fundamental component $u_{(1)}$ and to synthesize it for the further obtaining instantaneous higher harmonics component signal $u_{(hh)}$. The direct current voltage components (the mean values) are eliminated before each integrating and RMS calculating operations.

For multiple data updating, the "IFH-meter" software graphic code can be placed in "For Loop" cyclic structure.

The "Table data converter" operates in the current version as follows (see Fig. 1). The "Open/Create/Replace File" function through the "File path" control opens the output PSIM file, the "Scan From File" function passes the all lines except the first one (the only numeric data). Then the other "Scan From File" function, placed in the "For Loop" structure, reads one line from the file and, according to the specified format template, converts it to output variables. The decimal separator character must be specified for decimal fractions. The above-mentioned function runs as many times as the data lines in the file are. This number is defined here by using the "Read Lines from file" VI and the "Spreadsheet String to Array", "Array Size" and "Index Array" functions. After the data reading at the output of the cycle, two arrays are formed: the time values array and the corresponding signal values array (waveforms elements). At last, the signal time is being scaled up to the original one. The "Scale Delta t" VI is used for this operation, its inputs are supplied with the data signal array, needed to be scaled up, and the scaling parameter. The scaling parameter must be close to the original time step, so the difference between the first two elements of the time array from the two more "Index Array" functions is used. The supplementary "Multiply", "Round to Nearest" and "Divide" functions eliminate insignificant digits which were remaining due to PSIM simulation features.

The "Samples per second" dialog box value of the "Simulate Signal Express VI" in the "IFH-meter" must be set equal to the resulting sampling frequency of the "Table data converter", which in turn is equal to the scaling parameter inverse value and is defined after the first virtual instrument launching.

The "Table data converter" can be also expanded to read from PSIM file more than one signal data columns and rebuild corresponding waveforms in LabVIEW virtual instruments.

The IHF factors measurements results obtained via the offered VI and comparisons between the results for the signal, generated within LabVIEW VI (used as references while the relative error values calculating) and the signal, imported from the PSIM model, are summarized in Table I below. The measured waveform examples correspond to the executed phase-to-neutral voltage of the MLVSI with nearest vector selecting instantaneous space vector control [20].

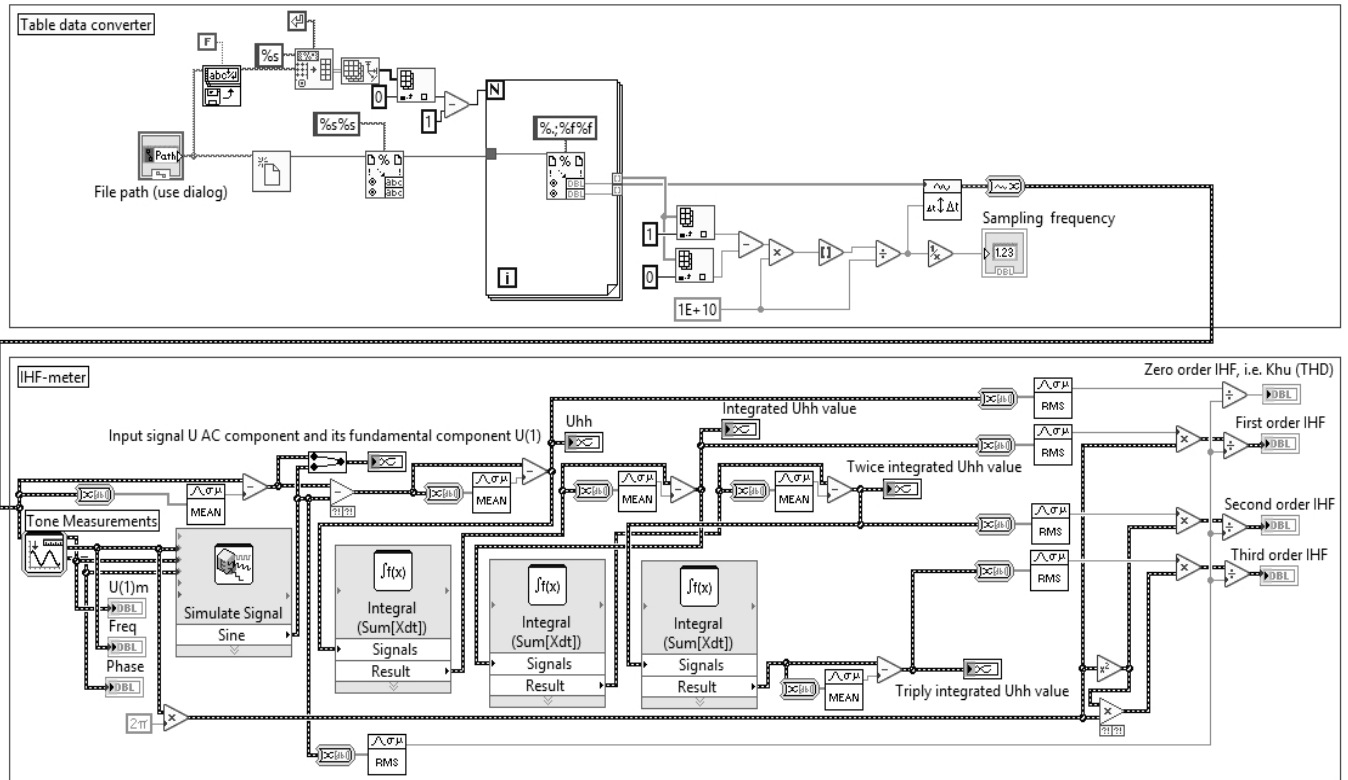


Fig. 1. LabVIEW virtual instrument for voltage harmonics integrated factors evaluation.

Here m_{aY} is the phase voltage amplitude modulation index:

$$m_{aY} = U/U_d = U^*, \quad (6)$$

where U and U^* are the value and the relative value of the reference voltage space vector magnitude, equal to the reference phase voltage amplitude, U_d is the input DC voltage of the unit (base) level.

The Table I pictures display also sine wave lines of the fundamental components (50 Hz) of the investigated voltage waveforms.

The four amplitude modulation index values have been arbitrarily selected ones. The LabVIEW simulations were carried out under the sampling frequency 1MHz, i.e. with the time step equal to 0.000001 s. The PSIM simulation results and their relative errors are given for the time step 0.000001 s and the time step 0.0000001 s in the first and in the second lines of the table cells, respectively.

The adequate estimation of the zero- to third-order IHF for the PSIM-imported waveforms is demonstrated for cases in which their simulation step has been set to 0.0000001 s. The more accurate estimation of the third-order IHF needs time step value of an order of magnitude below those used here.

In addition to the higher resolution simulating at reduced time step values, the following two simple conditions of the PSIM signal simulations should be followed to obtain the most accurate their measurement results in the LabVIEW virtual instrument:

- A steady-state mode of an investigated electromagnetic process should be considered.

- The X axis (time) settings of the Simview (the waveform display program of the PSIM) should correspond to the only selected fundamental period. The using of the first period is strongly discouraged because of its accessory signal spike and absence of the zero time moment data.

IV. USE OF INTEGRATED VOLTAGE HARMONICS FACTORS

The set of the main needed for the further calculations IHF factors is being determined on the results of the ADE procedure, applied to differential equations that have been derived from some particular load circuits.

The simplified equivalent phase circuits of the MLVSI, as the examples of the circuits with nonsinusoidal voltage source, are shown in Fig. 2, where $u_{EXEan}(t)$ is the phase “a” executed phase-to-neutral (“n”) voltage; L_a and R_a are the prospective phase “a” load inductance and resistance, L_f and C_f are the elements of phase “a” MLVSI output LC filter; i_a is the phase “a” load current.

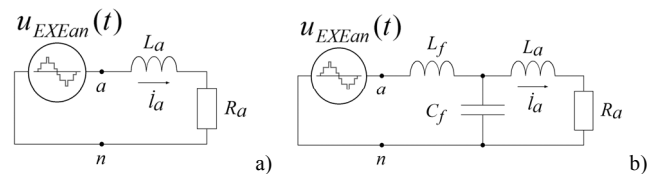
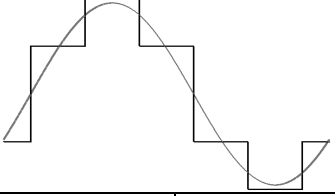
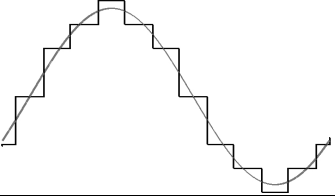
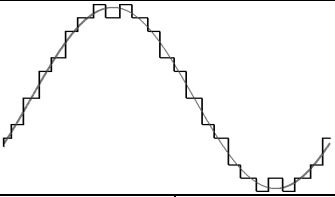
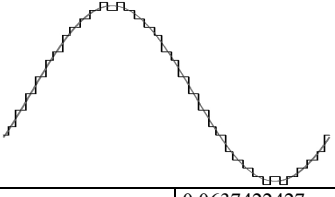


Fig. 2. MLVSI simplified equivalent phase circuits: phase RL load circuit a), phase RL load circuit with MLVSI output filter b).

TABLE I
COMPARISON OF MEASUREMENTS RESULTS

| m_{aY} | Result parameters | Origin environment of simulated signal | | Relative error, % |
|----------|------------------------------------|---|---|-------------------|
| | | LabVIEW virtual instrument controller model | PSIM power circuit model (high and low simulation time step values) | |
| 0.612 | Waveform |  | | - |
| | $\overline{K}_{hu}^{(0)} = K_{hu}$ | 0.3108050252 | 0.3121464292 0.3110606880 | 0.43 0.08 |
| | $\overline{K}_{hu}^{(1)}$ | 0.0463705 | 0.0465907 0.046412 | 0.47 0.09 |
| | $\overline{K}_{hu}^{(2)}$ | 0.00856205 | 0.00881988 0.00857771 | 3.01 0.18 |
| | $\overline{K}_{hu}^{(3)}$ | 0.00165464 | 0.00253593 0.00168449 | 53.3 1.80 |
| 1.26 | Waveform |  | | - |
| | $\overline{K}_{hu}^{(0)} = K_{hu}$ | 0.1685503522 | 0.1692846183 0.1686142347 | 0.44 0.04 |
| | $\overline{K}_{hu}^{(1)}$ | 0.0156507 | 0.0157639 0.0156509 | 0.72 0.0013 |
| | $\overline{K}_{hu}^{(2)}$ | 0.00229352 | 0.00254504 0.00229306 | 10.97 0.02 |
| | $\overline{K}_{hu}^{(3)}$ | 0.000410563 | 0.00113811 0.000410463 | 177.2 0.02 |
| 2.16 | Waveform |  | | - |
| | $\overline{K}_{hu}^{(0)} = K_{hu}$ | 0.1074704251 | 0.1075494956 0.1075015846 | 0.07 0.03 |
| | $\overline{K}_{hu}^{(1)}$ | 0.00918433 | 0.0091874 0.00918118 | 0.03 0.03 |
| | $\overline{K}_{hu}^{(2)}$ | 0.00143054 | 0.00143456 0.00143031 | 0.28 0.02 |
| | $\overline{K}_{hu}^{(3)}$ | 0.00026185 | 0.000274415 0.000261956 | 4.80 0.04 |
| 3.45 | Waveform |  | | - |
| | $\overline{K}_{hu}^{(0)} = K_{hu}$ | 0.0636369244 | 0.0637422427 0.0636811972 | 0.17 0.07 |
| | $\overline{K}_{hu}^{(1)}$ | 0.0025928 | 0.00260175 0.00259187 | 0.35 0.04 |
| | $\overline{K}_{hu}^{(2)}$ | 0.000182188 | 0.000258368 0.000182235 | 41.81 0.03 |
| | $\overline{K}_{hu}^{(3)}$ | 0.0000177959 | 0.000181097 0.000020644 | 917.6 16.00 |

The simplest MLVSI load circuit (Fig. 2, a) produces the first order differential equation and reduced integral equation derived from it:

$$L_a \cdot \frac{di_a}{dt} + R_a \cdot i_a = u_{EXEan}, \quad i_a + a_1 \cdot \overline{i}_a^{(1)} = b_1 \cdot \overline{u}_{EXEan}^{(1)}, \quad (7)$$

$$a_1 = R_a / L_a, \quad b_1 = 1 / L_a,$$

here and after the rest values designations completely correspond to description of (3). Let's here treat the $\overline{K}_{hu}^{(n)}$ as the n-order IHF of $u_{EXEan}(t)$.

After the ADE technique applying, the phase "a" load current i_a THD value, K_{hia} , can be defined as asymptotic quantity, being approximately calculated as the sum of the finite series with alternating members signs:

$$K_{hia} = I_{a(hh)} / I_{a(1)} \approx \sqrt{(a_1^2 + \omega^2) \cdot \sum_{n=1}^{N_f} \left\{ (-1)^{n-1} \cdot \left(\frac{a_1^{n-1}}{\omega^n} \cdot \overline{K}_{hu}^{(n)} \right)^2 \right\}}, \quad (8)$$

where N_f is the approximation level, related to the "filter hypothesis" [6], [8], namely $\overline{i}_{a(hh)}^{(n \geq N_f)} \equiv 0$. So, the first approximation $N_f = 1$ corresponds to

$$K_{hia} \approx \overline{K}_{hu}^{(1)} \cdot \sqrt{1 + \left(\frac{a_1}{\omega} \right)^2}. \quad (9)$$

The MLVSI phase load circuit with LC filter (Fig. 2, b) leads to the third order reduced integral equation and $N_f = 1$ approximation i_a THD result:

$$i_a + a_1 \cdot \overline{i}_a^{(1)} + a_2 \cdot \overline{i}_a^{(2)} + a_3 \cdot \overline{i}_a^{(3)} = b_3 \cdot \overline{u}_{EXEan}^{(3)}, \quad (10)$$

$$a_1 = \frac{R_a}{L_a}, \quad a_2 = \frac{1}{C_f} \cdot \left(\frac{1}{L_f} + \frac{1}{L_a} \right), \quad a_3 = \frac{R_a}{L_f \cdot C_f \cdot L_a},$$

$$b_3 = \frac{1}{L_f \cdot C_f \cdot L_a},$$

$$K_{hia} \approx \overline{K}_{hu}^{(3)} \cdot \sqrt{1 + \frac{a_1^2 - 2 \cdot a_2}{\omega^2} + \frac{a_2^2 - 2 \cdot a_1 \cdot a_3}{\omega^4} + \frac{a_3^2}{\omega^6}}. \quad (11)$$

Thus, the demanded IHF indices order numbers are strongly dependent on the whole load circuit order and configuration, as well as on the approximation level N_f . In our case, the first three coefficients with $n = 1 \dots 3$ are needed for the simplest circuit current i_a THD evaluation at the approximation level $N_f = 3$ according to (8), and the last of them is the main index for the load circuit with MLVSI output LC filter (and the only index at the level $N_f = 1$).

Let us consider an example of a current THD value calculations via an impacting voltage IHF values and

compare these results with the results of PSIM current waveform measurement in PSIM itself (by the internal means of the Simview) and in the offered LabVIEW virtual instrument. Suppose the Fig. 2, a load circuit has the parameters $R_a = 48.13 \text{ Ohm}$, $L_a = 0.14 \text{ H}$, and the imposed voltage is again the PSIM-simulated phase-to-neutral voltage of the MLVSI with nearest vector selecting instantaneous space vector control [20], here under $m_{aV} = 3.45$ (see Table I).

The LabVIEW VI measurement result and the ADE calculations results for the first three approximation levels according to (8) and their corresponding ratio errors, relative to the internal PSIM (Simview) THD estimate, are reflected in Table II. The investigated PSIM waveform, transmitted to the LabVIEW VI, of the MLVSI phase RL load current is shown in Fig. 3.

Despite the almost negligible current waveform distortion value, it has been successfully detected and estimated by the offered LabVIEW virtual instrument for the assessment of simulated signal integrated harmonics factors.

An even higher results precision has been reached through the ADE method calculation under $N_f > 1$, i.e. with using the few impacting voltage IHF values, preliminary measured via the same virtual instrument.

TABLE II
COMPARISON BETWEEN MEASUREMENTS AND
CALCULATIONS RESULTS

| Value origin | | Load current waveform THD value (K_{hia}) | Relative error,% | |
|------------------------|------------------------------|--|---------------------|-------|
| Simview measurement | | 0.0038314100 | Reference value | |
| LabVIEW VI measurement | | 0.003828600977765 | 0.073 | |
| ADE calculations | Approximation level N_f | 1 | 0.00384218048256077 | 0.281 |
| | | 2 | 0.00383079097362870 | 0.016 |
| | | 3 | 0.00383096625679934 | 0.012 |

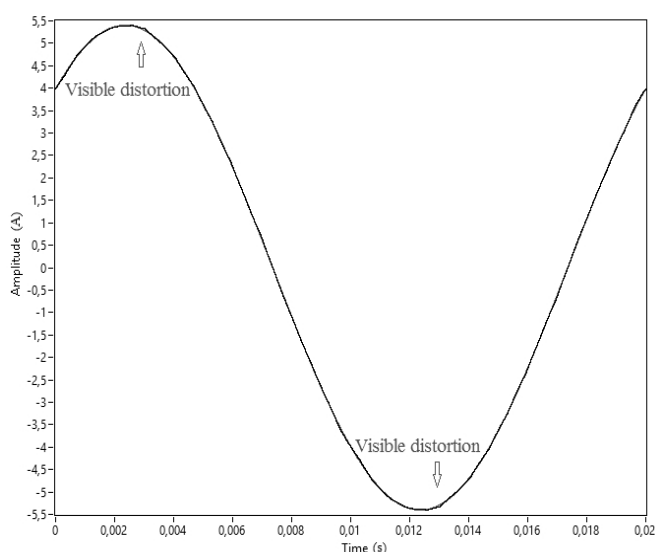


Fig. 3. From PSIM to LabVIEW transmitted power circuit waveform of phase RL load current and its fundamental component (mostly coinciding lines).

V. CONCLUSIONS

The LabVIEW virtual instrument for the assessment of simulated signals integrated harmonics factors, equipped with the input module for waveform data points import from PSIM output text file, is offered and proved to be effective.

The role of the integrated voltage harmonics factors in circuits with nonsinusoidal voltage source for load variables quality evaluation is demonstrated. Some examples of measurement and use of the integrated harmonics factors values of the investigated voltage for estimating the load circuit current THD are presented.

REFERENCES

- [1] Arrilaga J., Bradely D.A., and Bodger P.S. Power System Harmonics. John Wiley & Sons, 1985.
- [2] Arrilaga J., Bradely D., and Bodger P. Harmonics in Electrical Systems (translation from English edition, 1985). Moscow: Jenergoatomizdat, 1990. 320 p. (in Russian).
- [3] Arrilaga J., Watson N.R. Power System Harmonics. Second Edition. John Wiley & Sons, 2003.
- [4] Zinoviev G.S. Electromagnetic Compatibility of Power Electronics Devices (Electric Power Aspect). Textbook. Novosibirsk: NSTU, 1998. 91 p. (in Russian).
- [5] Holms D.G., Lipo T.A. Pulse Width Modulation for Power Converters. Piscataway, NJ: IEEE Press, 2003.
- [6] Zinoviev G.S. Power Electronics. Textbook for undergraduate students. Fifth edition. Moscow: Jurajt, 2012. 667 p. (in Russian).
- [7] Zinoviev G.S. Efficiency Criteria of Energy Processes in Valve Converters. Preprint 342 of Institute of Electrodynamics of Academy of Sciences of the Ukrainian SSR, Kiev, 1983. 31 p. (in Russian).
- [8] Zinoviev G.S. Direct Methods of Calculation of Power Indicators of Valve Converters. Novosibirsk: NSU, 1990. 220 p. (in Russian).
- [9] Zinoviev G.S. The results of solving some problems of electromagnetic compatibility of valve converters // Jelektrotehnika (Electrical Engineering), Iss. 11, 2000, pp. 12-16 (in Russian).
- [10] Lipko V.A., Zinoviev G.S. The family of extended power quality factors // EDM'2015, 16-th International Conference of Young Specialists on Micro/Nanotechnologies and Electron Devices (EDM), Erlagol, Altai, 25 June - 3 July, 2015. Proceedings, pp. 553-556.
- [11] Zinoviev G.S., Dybko M.A., Brovanov S.V., Kharitonov S.A. Unified analysis technique for energy quality factors estimation of NPC multilevel VSC for energy storage systems // 2013 15th European Conference on Power Electronics and Applications (EPE). France, Lille, September 2-6, 2013. Proceedings, pp. 1-9.
- [12] PSIM user's guide. Version 11.1. Release 2. Powersim Inc., November 2017. Available: <https://powersimtech.com/drive/uploads/2017/11/PSIM-User-Manual.pdf>.
- [13] Automation of Physical Researches and Experiments. Computer measurements and Virtual Instruments Based on LabVIEW 7 (30 Lectures) / Edited by P.A. Butyrin. Moscow: DMK Press, 2005. – 264 p. (in Russian).
- [14] Bath S.K., Kumra S. Simulation and measurement of power waveform distortions using LabVIEW // 2008 IEEE International Power Modulators and High Voltage Conference, Proceedings, pp. 427-434, Las Vegas, NE, USA, 27-31 May, 2008.
- [15] Saiteja S., Vinodkumar D.V.V.S., Srikanth T., Bhaskar Rao Y. LabVIEW based harmonic analyser // The International Journal of Engineering and Science (IJES), vol. 4, iss. 6, pp. 86-89, June, 2015. Available: <http://www.theijes.com/papers/v4-i6/Version-2/L0462086089.pdf>.
- [16] Swarupa N., Vishnuvardhini C., Poongkuzhali E., Sindhu M.R. Power quality analysis using LabVIEW // International Journal of Research in Engineering and Technology (IJRET), vol. 3, iss. 9, pp. 322-331, September, 2014. Available: <http://esatjournals.net/ijret/2014v03/i09/IJRET20140309051.pdf>.
- [17] Lopatkin N.N., Chernov Y.A. Virtual instrument for nonconventional total harmonic distortion factors evaluation // SIBCON-2016, 2016 International Siberian Conference on Control and Communications (SIBCON), Russia, Moscow, May 12-14, 2016. Proceedings (pp. 1-6).

- [18] Lopatkin N.N., Chernov Y.A. Differential and integral factors of harmonics LabVIEW estimation // EDM'2016, 17th International Conference of Young Specialists on Micro/Nanotechnologies and Electron Devices (EDM), Erlagol, Altai, 30 June - 4 July, 2016. Proceedings, pp. 493-498.
- [19] Lopatkin N.N. Voltage source multilevel inverter voltage quality comparison under multicarrier sinusoidal PWM and space vector PWM of two delta voltages // 2017 International Multi-Conference on Engineering, Computer and Information Sciences (SIBIRCON). Russia, Novosibirsk, Novosibirsk Akademgorodok, September 18-24, 2017. Proceedings, pp. 439-444.
- [20] Lopatkin N.N. Voltage THD and integrated voltage harmonics factors of three-phase multilevel voltage source inverter with nearest vector selecting space vector control // ICIEAM-2018, 2018 International Conference on Industrial Engineering, Applications and Manufacturing (ICIEAM), IEEE Conference # 43496. Russia, Moscow, Moscow Polytechnic University, May 15-18, 2018. Proceedings. Paper 3.4.40 (pp. 1-6), in press.



Lopatkin Nikolay Nikolaevich is the graduate of the industrial electronics department of the NETI (now NSTU), 1988, the candidate of engineering sciences, NSTU, 1998, the lecturer of the mathematics, physics and informatics department of Shukshin Altai State Humanities Pedagogical University (ASHPU), Biysk. His research interests include multilevel converters and control of them, quality indexes of electrical energy processes and improvement of them.
E-mail: nikolay_lopatkin@mail.ru



Lucenko Ivan Sergeevich received a Bachelor's degree of Education (Physics and Informatics) from Shukshin Altai State Humanities Pedagogical University (ASHPU), Biysk, in 2018. His training and scientific interests include computer modelling of physical processes (in particular, LabVIEW simulation of electromagnetic processes in electrotechnical systems) and supercomputer programming.



Chernov Yuriy Aleksandrovich received a Bachelor's degree of Education (Physics and Informatics) from Shukshin Altai State Humanities Pedagogical University (ASHPU), Biysk, in 2018. His training and scientific interests include computer modelling of physical processes, in particular, LabVIEW simulation of electromagnetic processes in electrotechnical systems.

Assessment of Output Voltage Quality of Three-Phase Multilevel Inverter with Nearest Vector Selecting Space Vector Control

Nikolay N. Lopatkin, *Member, IEEE*

Shukshin Altai State Humanities Pedagogical University (ASHPU), Biysk, Russia

Abstract – The paper presents the nearest vector selecting space vector control (SVC) of any arbitrary MLVSI circuit with any arbitrary number of the equal feeding DC voltage levels. The linear mode LabVIEW model for the SVC digital controller is designed in two variants of the reference signals sampling. The MLVSI output voltage THD and integrated voltage harmonics factors (IHF), needed for computing of the load circuit voltages and currents and their quality indices, are estimated as functions of the sampling frequency index).

Index Terms – Multilevel inverter, voltage space vector control (SVC), integer and fractional parts of delta voltages relative values, n-order integrated voltage harmonics factors (IHF), LabVIEW simulation.

I. INTRODUCTION

THE SIGNIFICANT progress has been achieved in inverters output voltage and power increasing mostly due to the multilevel voltage source inverters (MLVSI) [1]-[6].

Since the high MLVSI levels number makes it possible to avoid high switching frequency PWM while providing high output voltage quality, the so-called pseudo-modulation techniques [7] becomes the most promising for industrial applications. In particular, the space vector control (SVC) with the nearest vector selecting [8], [9] may be convenient modulation technique for present and future industrial medium and high voltage adjustable speed drive converters with enough high number of levels.

The new nearest vector selecting algorithm has been developed in the context of the space vector algorithm of two delta voltages [10]-[13] which uses barycentric and affine (oblique-angled) coordinates on triangles of three nearest vectors to the reference one [14]. The offered technique uses both the integer parts and the fractional parts of the reference delta voltages relative values as the coordinates of the reference voltage space vector. This approach to the SVC for any arbitrary MLVSI circuit with any arbitrary number of the equal feeding DC voltage levels needs no preliminary finding of anything coefficients and holding them in look-up tables [15].

II. PROBLEM DEFINITION

The thorough research has been accomplished to estimate the THD and the integrated voltage harmonics factors (IHF) of the resulting MLVSI voltage for the nearest vector selecting SVC [16] in its continuous variant. This case of the analog control might be treated as digital control with the tending to zero sampling period duration, and it shows the boundaries of voltage quality for this kind of SVC upon non-zero sampling period, in particular THD and IHF exact hypothetical lower limits.

The above mentioned IHF factors of various orders were offered by Professor G.S. Zinoviev (NETI, now NSTU, Novosibirsk) more than 30 years ago, and they produces weighted (by the harmonic number) summation of harmonics, thereby modeling the effect of the amplitude-frequency characteristic action of the corresponding order idealized electric integrating circuit [17]. The n-order voltage IHF can be defined as follows:

$$\bar{K}_{hu}^{(n)} = \frac{\sqrt{\left(\bar{U}_{(hh)}^{(n)}\right)^2}}{U_{(1)}/\omega^n} = \sqrt{\sum_{k=2}^{\infty} \left(\frac{U_{(k)}}{k^n \cdot U_{(1)}}\right)^2}, \quad (1)$$

where for estimated voltage u values $U_{(k)}$ and $\bar{U}_{(hh)}^{(n)}$ are the RMS value of the k harmonic component and RMS value of the result of the n -fold indefinite integral taking of the instantaneous value of the high harmonics component $\bar{u}_{(hh)}^{(n)}$, correspondingly; ω is the angular frequency of the fundamental component. The block diagram of the used LabVIEW virtual instrument for the assessment of simulated signals integrated harmonics factors and THD (the IHF-meter) and the IHF clear and concise description, which is concerning their values obtaining and application, are given in [18], [19] and [16].

The purpose of this paper is to provide the MLVSI output voltages quality estimate while the reference voltages sampling is impacting on them. Here we will confine ourselves to consideration of the two variants of the reference sinusoidal signals sampling under few phase voltage amplitude modulation index values.

III. LABVIEW SVC DIGITAL CONTROLLER MODEL

The The LabVIEW SVC digital controller model with the two versions of the quantized reference signals builder is presented in Fig. 1. The SVC controller is intended for any three-phase MLVSI with any arbitrary levels number N under linear mode, i.e. under the condition that the equal feeding DC voltage levels are physically available in sufficient numbers.

Each of the two waveforms builders of the sampled reference delta voltages u_{REFSbc}^* and u_{REFSab}^* (Fig. 1, a and b) has the input control elements to specify the desirable values of the output frequency f_{out} , the sampling frequency index (or the sample rate) m_{fs} and the phase voltage amplitude modulation index m_{aY} . Here the sampling frequency index has been introduced by analogy with PWM frequency modulation index,

$$m_{fs} = f_s / f_{out}, \quad (2)$$

f_s is the sampling frequency; the phase amplitude modulation index is defined as follows:

$$m_{aY} = U / U_d = U^*, \quad (3)$$

where U is the value of the reference voltage space vector magnitude, equal to the reference phase voltage amplitude,

U_d is the input DC voltage of the unity (base) level. Throughout the paper, all the voltages marked with an asterisk (*) are the corresponding relative values, in relation to U_d .

The difference between the two variants of the quantized reference signals builder is demonstrated in Fig. 2 and Fig. 3 for $m_{aY} = 3.14$. The illustrating figures are shown here for a comparatively low value of the sampling frequency index, $m_{fs} = 42$ ($f_s = 2100$ Hz for $f_{out} = 50$ Hz). The sampling is supposed to be performed for the midpoint of each the cycle.

The sampling cycle number time-dependent function $k(t)$ of Fig. 1,a is shown in Fig. 2,a and corresponds to the equation

$$k(\alpha) = \left\lfloor \left(\frac{\alpha}{2\pi} - \left\lfloor \frac{\alpha}{2\pi} \right\rfloor \right) \cdot m_{fs} \right\rfloor + 1, \quad (4)$$

where $\lfloor w \rfloor$ is the integer part of w , i.e. the rounding down w to the closest integer number, taking into account the sign (the “floor” function).

The respective sampled reference voltage u_{REFSbc}^* is shown in Fig. 2,b and is described as follows:

$$u_{REFSbc}^*(\alpha) = m_{aY} \cdot \sqrt{3} \cdot \sin\left(\frac{2\pi \cdot k(\alpha) - \pi}{m_{fs}}\right). \quad (5)$$

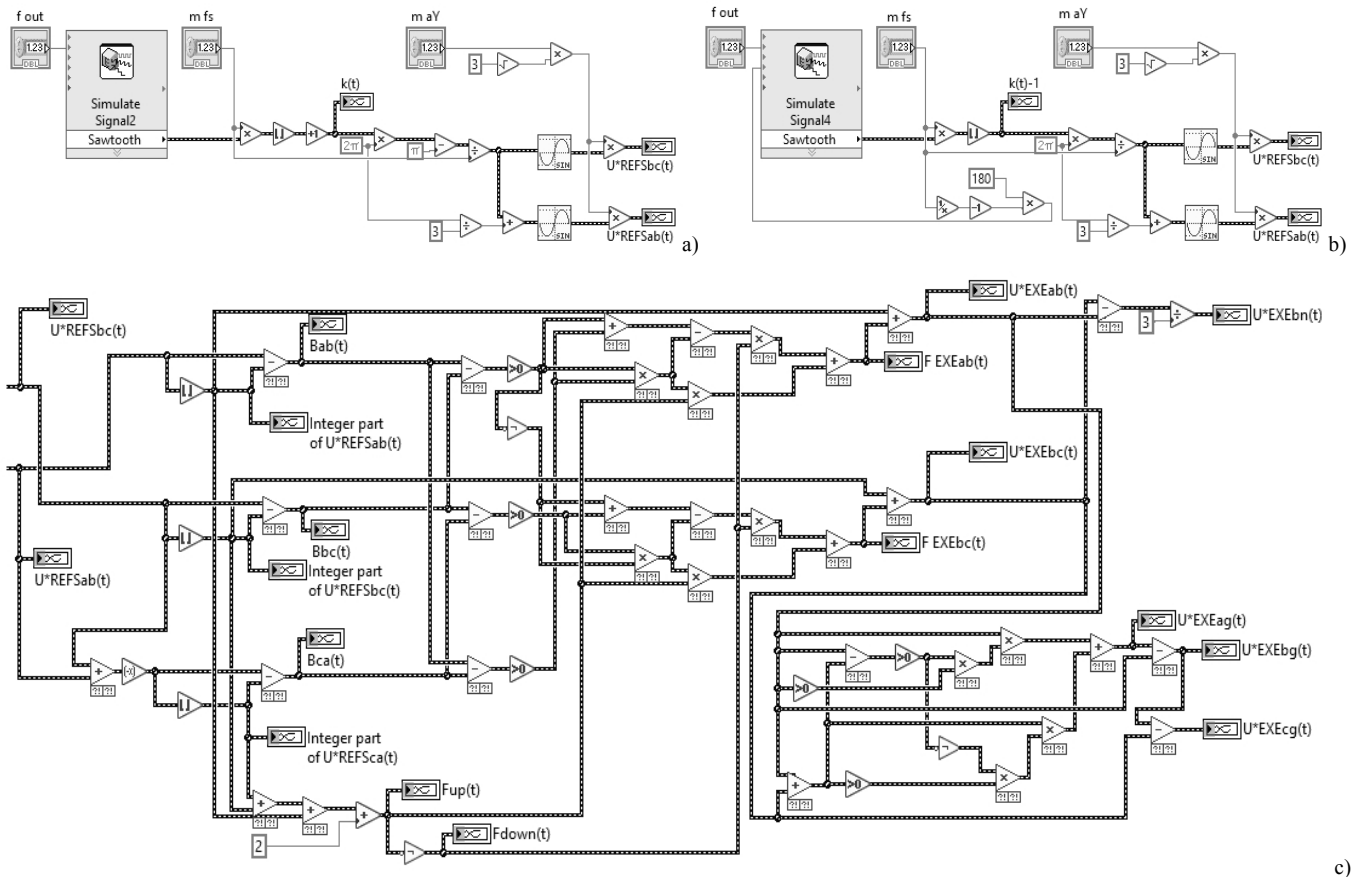


Fig. 1. LabVIEW SVC digital controller model for three-phase multilevel voltage source inverter with arbitrary level number N under linear mode: a) first version of quantized reference signals builder; b) second version of quantized reference signals builder; c) core part of SVC controller.

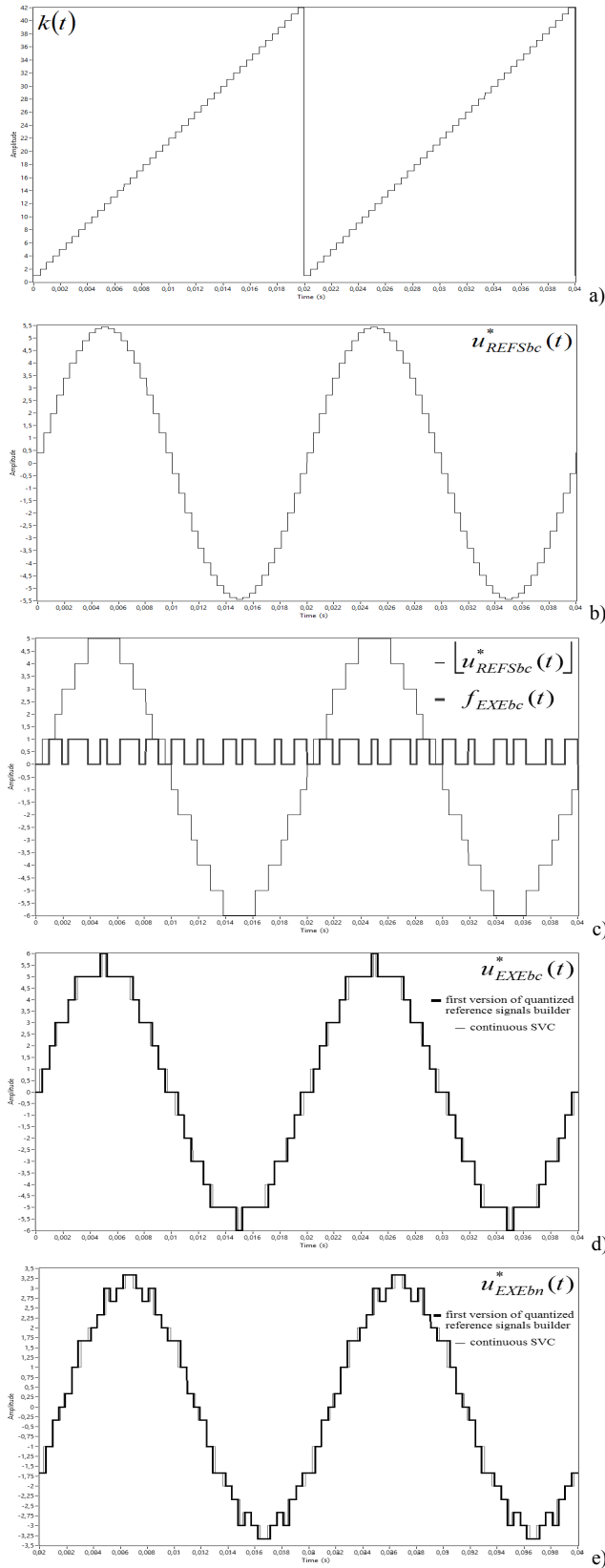


Fig. 2. LabVIEW-simulated digital SVC controller signals waveforms for first variant of quantized reference signals builder under $m_{ay} = 3.14$, $m_{is} = 42$: a) sampling cycle number time-dependent function, b) sampled reference delta voltage, c) executed delta voltage components, d) executed delta voltage, e) executed phase-to-neutral voltage.

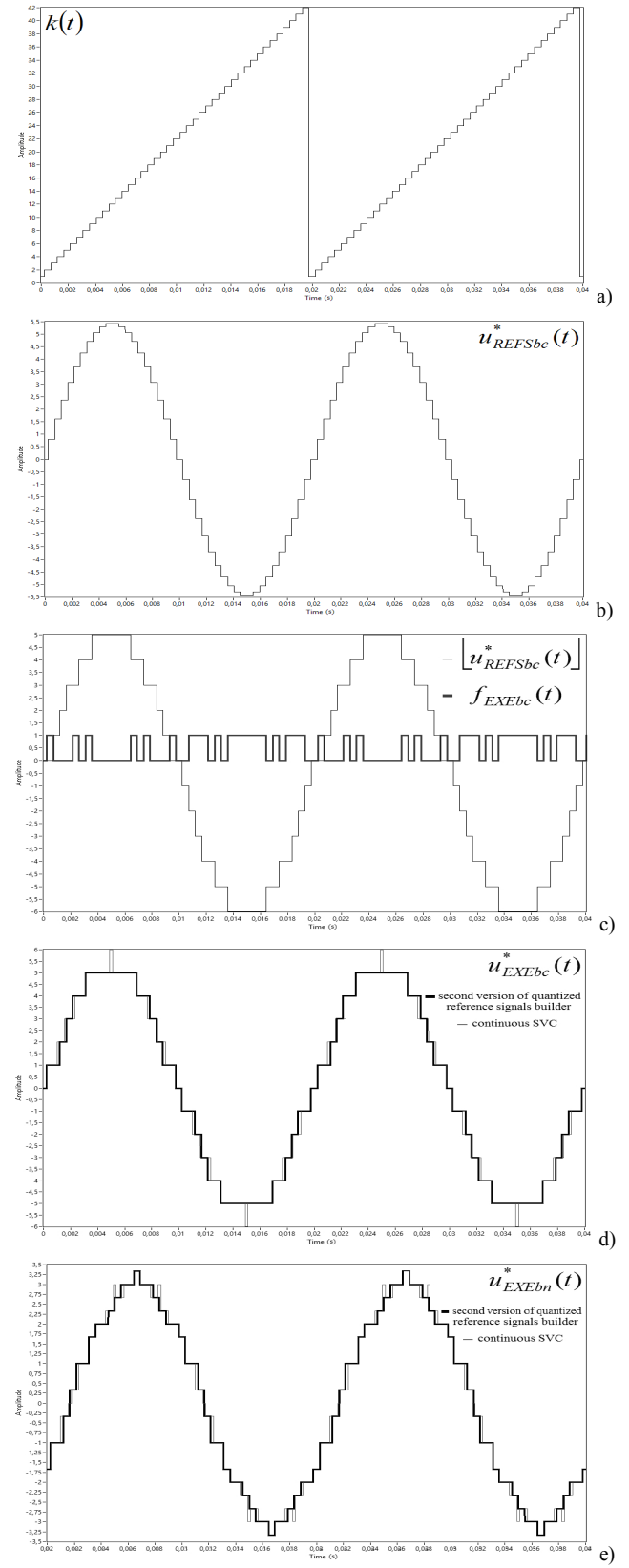


Fig. 3. LabVIEW-simulated digital SVC controller signals waveforms for second variant of quantized reference signals builder under $m_{ay} = 3.14$, $m_{is} = 42$: a) sampling cycle number time-dependent function, b) sampled reference delta voltage, c) executed delta voltage components, d) executed delta voltage, e) executed phase-to-neutral voltage.

The same cycle number function $k(t)$ of Fig. 1,b is shown in Fig. 3,a and corresponds to the equation

$$k(\omega) = \left\lfloor \left(\frac{\omega + \pi/m_{fs}}{2\pi} - \left\lfloor \frac{\omega + \pi/m_{fs}}{2\pi} \right\rfloor \right) \cdot m_{fs} \right\rfloor + 1; \quad (6)$$

the respective sampled reference voltage u_{REFSbc}^* is shown in Fig. 3,b and is described by equation

$$u_{REFSbc}^*(\omega) = m_{aY} \cdot \sqrt{3} \cdot \sin\left(\frac{2\pi \cdot (k(\omega) - 1)}{m_{fs}}\right). \quad (7)$$

So, the first sampled value for $k(\omega) = 1$ generates the sampled reference voltage u_{REFSbc}^* waveform with the quarter-wave symmetry but having different behavior at $\omega = 0$: the waveform just is jumping from some negative to some positive value in case of the first variant of the quantized reference signals builder (see Fig. 2, b), and the waveform has the zero value level for the second variant (see Fig. 3, b).

The core part of SVC controller (Fig. 1, c) has replicated the respective Matlab/Simulink model [15] and has already been used [16].

The main used in [10]-[13], [15] the delta voltage two-component formation principle is kept in the offered approach (see Fig. 2, c and Fig. 3, c):

$$u_{EXEgh}^*(t) = \lfloor u_{REFSgh}^*(t) \rfloor + f_{EXEgh}(t), \quad (8)$$

where the relative value of the being executed output delta voltage $u_{EXEgh}^*(t)$ and its two components are instantaneous functions of current time, the relative value of the sampled reference delta voltage $u_{REFSgh}^*(t)$ and its integer part $\lfloor u_{REFSgh}^*(t) \rfloor$ are here both the stepped functions, and $f_{EXEgh}(t)$ is the pulse function that can possess only the values 0 and 1 (see [15]).

As can be seen from Fig. 2, d and Fig. 3, d as well as from Fig. 2, e and Fig. 3, e, the resulting executed delta and phase-to-neutral voltages can be quite different for the two variants of the quantized reference signals builder, so the quantitative study of harmonic factors for some m_{aY} range is needed.

IV. SIMULATION RESULTS

The LabVIEW-simulated curves of the MLVSI output voltage THD (K_{hu}) and first to third orders IHF indices ($\overline{K}_{hu}^{(n)}$ for $n = 1 \dots 3$) dependences on the sampling frequency index are presented in Fig. 4 for the two variants of the quantized reference signals builder. Here the sampling frequency index values are assigned as follows:

$$m_{fs} = 6 \cdot (2k - 1), \quad k \in N, \quad k \leq 50, \quad (9)$$

namely, $m_{fs} = 6; 18; 30; \dots 594$.

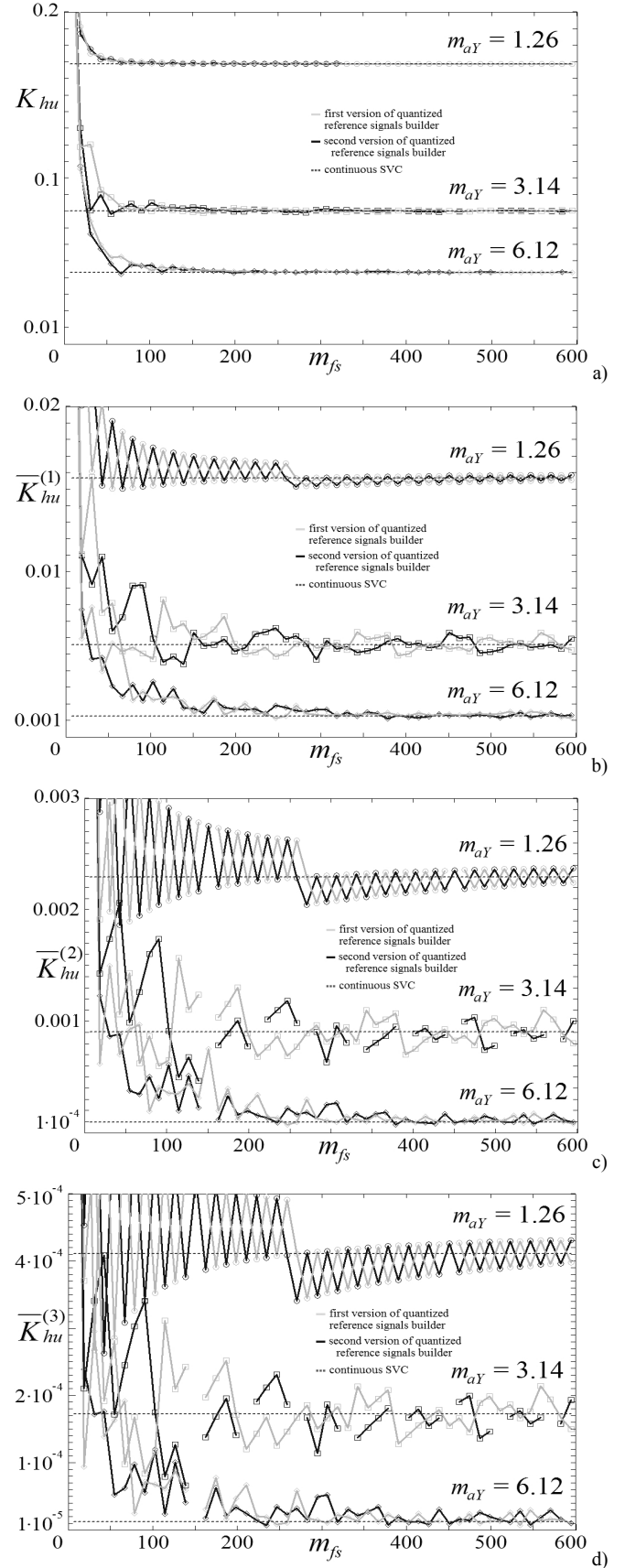


Fig. 4. LabVIEW-simulated THD (a) and first three orders IHF (b, c and d) dependences on the sampling frequency index m_{fs} for the two variants of the reference sinusoidal signals sampling under phase voltage modulation index m_{aY} values 1.26, 3.14 and 6.12.

The points in Fig. 4, c and d, where the IHF-meter results have been distorted a lot due to the mean values poor elimination and the consequent wrong values of the twice and thrice integrated high harmonics component signal, have been removed.

As can be seen from Fig. 4, the higher the IHF order is, the higher the relative difference values between the results of the continuous SVC and the results obtained through the reference sinusoidal signals samplings under the comparatively low values of the sample rate are. The two variants of the reference sinusoidal signals sampling compete with each other, having their advantages on successive sub-ranges of the sampling frequency index.

Beginning from some not very high m_{fs} value the resulting output voltage waveforms of the both sampling variants come close to the respective continuous SVC waveform. The rising and falling edges positions are still changing, whereas the quantity of the steps (and levels) and appropriate MLVSI semiconductor devices switchings number, power losses and efficiency remain unchanged.

The numeric data on the values of the delta voltage IHF indices for those same selected phase voltage amplitude modulation index m_{aY} values (1.26, 3.14 and 6.12) under three m_{fs} values (594, 1050 and 2106) are placed in Table I. Here the respective sampling period values, corresponding to equation

$$T_s = \frac{1}{f_s} = \frac{1}{f_{out} \cdot m_{fs}}, \quad (10)$$

are 33.7, 19.0 and 9.5 μs for $f_{out} = 50$ Hz.

As can be noted, the harmonic content of the resulting output voltage under the digital SVC can be both some better and some worse compared to the continuous SVC results. The minus sign of the relative difference corresponds to each case when the IHF value under digital SVC is less than the respective continuous SVC value.

Because the continuous SVC doesn't provide the THD and IHF indices exact hypothetical lower limits, one can choose the first or the second sampling variant on the basis of the convenient combination of the output voltage and current quality and the computational effort.

Thus, freed up microprocessor computing resources can be directed to processing of other data needing the more fast response (some close-loop control process), equipment diagnostics etc.

The MLVSI output voltage zero to third orders IHF values dependences on the phase voltage amplitude modulation index, obtained with m_{aY} step equal to 0.1 for $m_{fs} = 2106$, show the almost perfectly matching of the three curves, corresponding to the continuous SVC [16] and the offered first and second digital control versions.

TABLE I
MLVSI OUTPUT VOLTAGE ZERO TO THIRD ORDERS IHF VALUES

| Control parameters | | | Harmonic distortion factors | | | | | | | |
|--|----------------|------------------|------------------------------------|------------------------|---------------------------|------------------------|---------------------------|------------------------|---------------------------|------------------------|
| Phase amplitude modulation index m_{aY} | SVC type | | Total harmonic distortion | | First order IHF | | Second order IHF | | Third order IHF | |
| | | | $\overline{K}_{hu}^{(0)} = K_{hu}$ | Relative difference, % | $\overline{K}_{hu}^{(1)}$ | Relative difference, % | $\overline{K}_{hu}^{(2)}$ | Relative difference, % | $\overline{K}_{hu}^{(3)}$ | Relative difference, % |
| 1.26 | Continuous SVC | | 0.168545478476 | Reference values | 0.0156516 | Reference values | 0.00229402 | Reference values | 0.000410701 | Reference values |
| 3.14 | | | 0.08005172801897 | | 0.00557263 | | 0.000905254 | | 0.000172267 | |
| 6.12 | | | 0.04297928868022 | | 0.00124104 | | $9.33371 \cdot 10^{-5}$ | | $1.17979 \cdot 10^{-5}$ | |
| | Digital SVC | | | | | | | | | |
| | m_{fs} | Sampling version | | | | | | | | |
| 1.26 | 594 | First | 0.1685921795594 | 0.028 | 0.0155368 | -0.733 | 0.00224511 | -2.132 | 0.000397773 | -3.148 |
| | | Second | 0.168562837729 | 0.010 | 0.0158566 | 1.310 | 0.00237453 | 3.510 | 0.000431322 | 5.021 |
| | 1050 | First | 0.1685755016019 | 0.018 | 0.0157453 | 0.599 | 0.0023306 | 1.595 | 0.000420116 | 2.292 |
| | | Second | 0.1685576909653 | 0.007 | 0.015559 | -0.592 | 0.00225558 | -1.676 | 0.000400596 | -2.460 |
| | 2106 | First | 0.1685444948277 | -0.0006 | 0.0156905 | 0.249 | 0.00230975 | 0.686 | 0.000414783 | 0.994 |
| | | Second | 0.1685511336482 | 0.003 | 0.0155952 | -0.360 | 0.00227081 | -1.012 | 0.00040462 | -1.481 |
| 3.14 | 594 | First | 0.08034833064616 | 0.371 | 0.00525211 | -5.752 | 0.00080445 | -11.135 | 0.000150248 | -12.782 |
| | | Second | 0.08030508472647 | 0.316 | 0.00594045 | 6.600 | 0.00100288 | 10.784 | 0.000193258 | 12.185 |
| | 1050 | First | 0.08006783183935 | 0.020 | 0.00554331 | -0.526 | 0.000901308 | -0.436 | 0.000171946 | -0.186 |
| | | Second | 0.07991167002516 | -0.175 | 0.00575464 | 3.266 | 0.000950793 | 5.031 | 0.000181122 | 5.140 |
| | 2106 | First | 0.08003706167006 | -0.018 | 0.00574116 | 3.024 | 0.000951101 | 5.065 | 0.000181962 | 5.628 |
| | | Second | 0.0800637600696 | 0.015 | 0.00553381 | -0.697 | 0.000892399 | -1.420 | 0.000169269 | -1.740 |
| 6.12 | 594 | First | 0.0431100254879 | 0.304 | 0.00114584 | -7.671 | $8.20884 \cdot 10^{-5}$ | -12.052 | $1.05187 \cdot 10^{-5}$ | -10.843 |
| | | Second | 0.04295165208329 | -0.064 | 0.00129807 | 4.595 | $9.36154 \cdot 10^{-5}$ | 0.298 | $9.9086 \cdot 10^{-6}$ | -16.014 |
| | 1050 | First | 0.04290933884246 | -0.163 | 0.00124815 | 0.573 | $8.84255 \cdot 10^{-5}$ | -5.262 | $9.36313 \cdot 10^{-6}$ | -20.637 |
| | | Second | 0.04304862937807 | 0.161 | 0.00130852 | 5.437 | 0.000128814 | 38.009 | $2.15247 \cdot 10^{-5}$ | 82.445 |
| | 2106 | First | 0.04300843038659 | 0.068 | 0.00122182 | -1.549 | $8.42402 \cdot 10^{-5}$ | -9.746 | $8.78956 \cdot 10^{-6}$ | -25.499 |
| | | Second | 0.04299999011319 | 0.048 | 0.00126862 | 2.222 | 0.000104895 | 12.383 | $1.50046 \cdot 10^{-5}$ | 27.180 |

V. CONCLUSIONS

The digital implementation of the space vector control algorithm with the nearest vector selection for the three-phase arbitrary MLVSI circuit with any arbitrary number N of the equal feeding DC voltage levels is tested by LabVIEW simulation. The offered space vector control technique uses both the integer part and the fractional part of the reference delta voltages relative values as the coordinates of the reference voltage space vector and needs no preliminary finding of anything coefficients and holding them in look-up tables.

The two variants of the reference sinusoidal signals sampling has been considered. The impact of the reference voltages sample rate on the SVC output voltages quality is assessed.

The offered approach and the obtained curves of the zero to third orders IHF indices dependences on the sampling frequency index can be interesting and helpful to industrial engineers who designs some system “MLVSI - filter - load circuit” for particular load circuit parameters values and uses the SVC technique.

The sampling frequency reduction makes it possible to provide the room for manoeuvre within the existing computing resources budget while keeping the most important for the concrete task weighted THD (IHF) values within some acceptable limits.

REFERENCES

- [1] Rodriguez J., Lai J.-S., Peng F.Z. Multilevel inverters: a survey of topologies, controls, and applications // IEEE Transactions on Industrial Electronics, Vol. 49, Iss. 4, August 2002, pp. 724-738.
- [2] Kouro S., Malinowski M., Gopakumar K., Pou J., Franquelo L.G., Wu Bin, Rodriguez J., Pérez M.A., and Leon J.I. Recent advances and industrial applications of multilevel converters // IEEE Transactions on Industrial Electronics, Vol. 57, Iss. 8, Aug. 2010, pp. 2553-2580.
- [3] Gonzalez S.A., Verne S.A., Valla M.I. Multilevel Converters for Industrial Applications. CRC Press, 2013.
- [4] Luo F.L., Ye H. Advanced DC/AC Inverters: Applications in Renewable Energy. CRC Press, 2013.
- [5] Ge B., Peng F.Z., and Li Y. Multilevel Converter/Inverter Topologies and Applications, Chapter 14 in Power Electronics for Renewable Energy Systems, Transportation and Industrial Applications, First Edition. Wiley-IEEE Press, 2014. Edited by H. Abu-Rub, M. Malinowski and K. Al-Haddad, pp. 422-462.
- [6] Wu Bin, Narimani M. High-Power Converters and AC Drives. Second Edition. Wiley-IEEE Press, 2017.
- [7] Leon J.I., Kouro S., Rodriguez J., Wu Bin. The essential role and the continuous evolution of modulation techniques for voltage-source inverters in the past, present, and future power electronics // IEEE Transactions on Industrial Electronics, Vol. 63, Iss. 5, May 2016, pp. 2688-2701.
- [8] Rodriguez J., Moran L., Correa P., Silva C. A vector control technique for medium-voltage multilevel inverters // IEEE Transactions on Industrial Electronics, Vol. 49, Iss. 4, August 2002, pp. 882-888.
- [9] Rodriguez J., Moran L., Pontt J., Correa P., Silva C. A high-performance vector control of an 11-level inverter // IEEE Transactions on Industrial Electronics, Vol. 50, Iss. 1, February 2003, pp. 80-85.
- [10] Lopatkin N.N. Simple delta voltages space vector PWM algorithm for voltage source multilevel inverters // 2016 2-nd International Conference on Intelligent Energy and Power Systems (IEPS), Kyiv, Ukraine, June 7-11, 2016, Proceedings, pp. 149-154.
- [11] Lopatkin N.N. Output voltage simulation of multilevel inverter with space vector modulation of two delta voltages // Tekhnichna Elektrodynamika (Technical Electrodynamics), edition of National Academy of Sciences of Ukraine, Kyiv, Iss. 5, 2016, pp. 20-22 (in Russian).
- [12] Lopatkin N.N. Voltage quality comparison of space vector PWM voltage source multilevel inverter under symmetric and nonsymmetric switching sequence variants: voltage waveforms, spectra and THD // ICIEAM-2017, 2017 3rd International Conference on Industrial Engineering, Applications and Manufacturing (ICIEAM), IEEE Conference #40534, Russia, St. Petersburg, Peter the Great Saint-Petersburg Polytechnic University, May 16-19, 2017, Proceedings, pp. 1-8.
- [13] Lopatkin N.N. Simple space vector PWM scheme with quarter-wave symmetric output voltage waveform for three-phase multilevel inverter // 2017 International Multi-Conference on Engineering, Computer and Information Sciences (SIBIRCON), Russia, Novosibirsk, Novosibirsk Akademgorodok, September 18-24, 2017, Proceedings, pp. 433-438.
- [14] Lopatkin N.N. Some new representations of the multilevel inverter voltage space vector in the complex plane // SIBCON-2015, 2015 International Siberian Conference on Control and Communications (SIBCON), Russia, Omsk, May 21-23, 2015, Proceedings, 222em.pdf (pp. 1-11).
- [15] Lopatkin N.N. New implementation of nearest vector selecting space vector control for three-phase multilevel voltage source inverter // ICIEAM-2018, 2018 International Conference on Industrial Engineering, Applications and Manufacturing (ICIEAM), IEEE Conference #43496, Russia, Moscow, Moscow Polytechnic University, May 15-18, 2018, Proceedings, paper 3.4.39 (pp. 1-7), in press.
- [16] Lopatkin N.N. Voltage THD and integrated voltage harmonics factors of three-phase multilevel voltage source inverter with nearest vector selecting space vector control // ICIEAM-2018, 2018 International Conference on Industrial Engineering, Applications and Manufacturing (ICIEAM), IEEE Conference #43496, Russia, Moscow, Moscow Polytechnic University, May 15-18, 2018, Proceedings, paper 3.4.40 (pp. 1-6), in press.
- [17] Zinoviev G.S. Power Electronics. Textbook for undergraduate students. Fifth edition. Moscow: Jurajt, 2012. 667 p. (in Russian).
- [18] Lopatkin N.N., Chernov Y.A. Virtual instrument for nonconventional total harmonic distortion factors evaluation // SIBCON-2016, 2016 International Siberian Conference on Control and Communications (SIBCON), Russia, Moscow, May 12-14, 2016. Proceedings, pp. 1-6.
- [19] Lopatkin N.N., Chernov Y.A. Differential and integral factors of harmonics LabVIEW estimation // EDM'2016, 17th International Conference of Young Specialists on Micro/Nanotechnologies and Electron Devices (EDM), Erlagol, Altai, 30 June - 4 July, 2016, Proceedings, pp. 493-498.



Lopatkin Nikolay Nikolaevich is the graduate of the industrial electronics department of the NETI (now NSTU), 1988, the candidate of engineering sciences, NSTU, 1998, the lecturer of the mathematics, physics and informatics department of Shukshin Altai State Humanities Pedagogical University (ASHPU), Biysk. His research interests include multilevel converters and control of them, quality indexes of electrical energy processes and improvement of them.
E-mail: nikolay_lopatkin@mail.ru

Aggregate Factors of Switchings and Integrated Voltage Harmonics of Three-Phase Multilevel Voltage Source Inverter with Nearest Vector Selecting Space Vector Control

Nikolay N. Lopatkin, *Member, IEEE*

Shukshin Altai State Humanities Pedagogical University (ASHPU), Biysk, Russia

Abstract – The paper deals with the model of the nearest vector selecting space vector control (SVC) of any arbitrary MLVSI circuit with any arbitrary number of any equal feeding DC voltage levels. Using the LabVIEW simulation results for instantaneous SVC, the aggregate factors of switchings and integrated voltage harmonics (ASIH) dependences on phase voltage amplitude modulation index are obtained and compared with the corresponding results of the quarter-wave symmetric space vector PWM (SVPWM).

Index Terms – Multilevel inverter, voltage space vector control (SVC), integer and fractional parts of delta voltages relative values, n-order integrated voltage harmonics factors (IH), n-order aggregate switchings and integrated voltage harmonics factors (ASIH).

I. INTRODUCTION

THE MULTILEVEL voltage source inverters (MLVSI) circuits and the techniques for control of them are the two wings, which provide now the rise of the medium and high voltage three-phase adjustable speed drives [1-6].

Notwithstanding the importance of the circuitry solutions, the modulation technique is their general resource belonging to every of the MLVSI circuits in some adapted form and making it possible to provide high quality output AC voltage and current, high output capability, low losses in power switches, low cost of components or acceptable combinations of the parameters values of the MLVSI.

The high MLVSI levels number avoided pulse width modulation (PWM) with too high switching frequency while providing high output voltage quality. Moreover, the so-called pseudo-modulation techniques [2] becomes the most promising for industrial applications. In particular, the space vector (SV) control (SVC) with the nearest vector selecting [7]-[10] may be convenient modulation technique for present and future industrial medium and high voltage adjustable speed drive converters with enough high number of levels. Originally, the SVC was described for cascaded multilevel inverter (CMLI) control [7]-[10], but obviously, it is equally attractive for use in a variety of MLVSI circuits, again, for the case of high number of levels.

The new nearest vector selecting algorithm has been developed in the context of the space vector algorithm of two delta voltages [11]-[15] which uses barycentric and affine

(oblique-angled) coordinates on triangles of three nearest vectors to the reference one [16]. The offered technique uses both the integer parts and the fractional parts of the reference delta voltages relative values as the coordinates of the reference voltage space vector. This novel approach to the SVC for any arbitrary MLVSI circuit with any arbitrary number of the equal feeding dc voltage levels in itself needs no preliminary finding of anything coefficients and holding them in look-up tables [17].

The offered scheme applies no special operations radically different from used in the traditional one. But it utilizes the conventional space vector PWM (SVPWM) attribute, namely “modulating triangle” of the three vectors nearest to the reference voltage SV (NTV).

As have been shown in [16], the fractional parts of the reference delta voltages relative values are not only the duty cycles of the three nearest vectors NTV in SVPWM, but also the barycentric coordinates on corresponding triangle for the reference voltage SV endpoint. So, the closer to unity the fractional value of certain relative delta voltage is, the closer to the related vertex the reference voltage SV endpoint is. The highest value of the three barycentric coordinates on the NTV triangle points to the appropriate vertex as the vertex, closest to the reference point, and such a way one can choose the space vector nearest to the reference vector endpoint. Due to the fractional parts of the reference delta voltages relative values are mapped to the possible nearest vectors, the closest to the reference voltage space vector is being selected easily through the comparisons of the three fractional values for maximum value detection in one of the two triangles [17].

The main used in [11]-[15] delta voltage two-component formation principle is kept in the offered technique:

$$u_{EXEY}^*(t) = \lfloor u_{REFxy}^*(t) \rfloor + f_{EXEY}(t), \quad (1)$$

where the relative value of the being executed output delta voltage $u_{EXEY}^*(t)$ and its two components are instantaneous functions of current time, the stepped function $\lfloor u_{REFxy}^*(t) \rfloor$ is the integer part of the relative value of the reference delta voltage $u_{REFxy}^*(t)$ (all relative values are in relation to input dc voltage U_d of the unity level), and $f_{EXEY}(t)$ is the pulse function that can possess only the values 0 and 1.

II. PROBLEM DEFINITION

The controller LabVIEW model of the SVC instantaneous version [17] has been developed (see Fig. 1), and the simulated curves of the output voltage THD and first to third orders integrated harmonics factors (IHF) dependences on amplitude modulation index have been obtained [18]. The SVC controller replicates the respective Matlab/Simulink model [17], based on the above mentioned new delta voltages coordinates approach. The used IHF-meter (see Fig. 2) has proven before to be an enough reliable and precision simulation instrument [19], [20]. It implements one of the time-domain IHF definitions [21], which makes it possible to process directly the input signal high harmonics component u_{hh} .

The joint approach and attributes of the offered quarter-wave symmetric SVPWM [13]-[15] and SVC techniques have made to compare their THD and IHF simulated results for the lowest values of the SVPWM frequency modulation index. The SVC advantage in the THD values and drawback in the IHF indices values at some amplitude modulation index sub-ranges have been noted. Thus, the SVC and the quarter-wave symmetric SVPWM can compete against each other in the MLVSI load current quality issues.

Our preferences can be based on the taking into account the switching losses value of the MLVSI which is directly proportional to the switchings (commutations) number in the MLVSI phase leg per the output voltage cycle N_{swph} .

It seems reasonable that further study and comparison should consider the aggregate indices, which take into account both the voltage quality and the price of its achieving. This paper provides the so-called aggregate switchings and integrated voltage harmonics factors (ASIHf) dependences on amplitude modulation index in two sub-ranges, both for the SVC and the quarter-wave symmetric SVPWM and some their intercomparisons results.

III. AGGREGATE FACTORS OF SWITCHINGS AND INTEGRATED VOLTAGE HARMONICS

The considered here ASIHf indices have already been used for the SVPWM-controlled MLVSI output voltage assessment in a small amplitude modulation index range [14]. As we have noticed, issues [22] and [23] were the first to propose the aggregate indices taking into account both the voltage harmonics and the number N_{swph} of the per cycle switchings in the MLVSI phase leg output voltage.

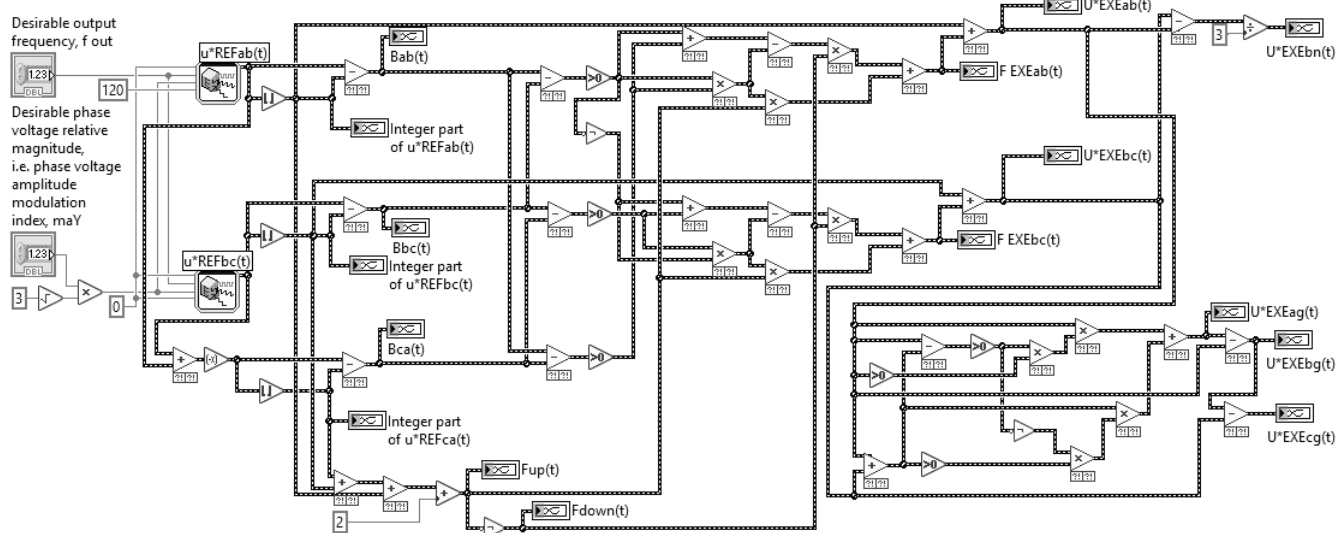


Fig. 1. LabVIEW “instantaneous SVC” controller model for three-phase multilevel voltage source inverter with arbitrary level number.

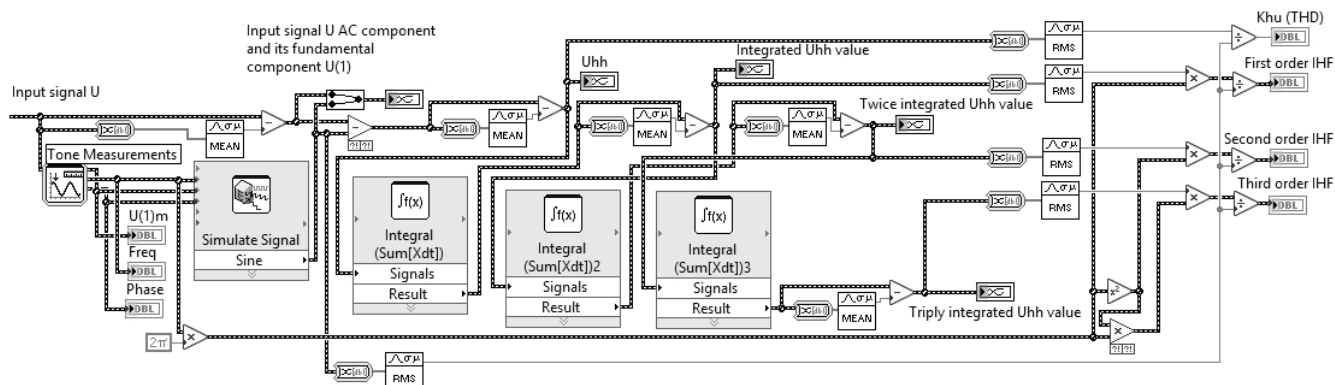


Fig. 2. LabVIEW virtual metering instrument for zero to third orders integrated harmonics factors assessment.

The most general n -th order aggregate switchings and integrated voltage harmonics factor has been defined with using the singlefold multiplying of the n -th order voltage IHF $\overline{K}_{hu}^{(n)}$ by the switchings number:

$$\overline{K}_{hu-aggr-sw}^{(n)} = N_{swph} \cdot \overline{K}_{hu}^{(n)}. \quad (2)$$

The estimated n -th order ASIHF calculation can be performed by using the approximation as follows:

$$\overline{K}_{hu-aggr-sw}^{(n)} \approx \frac{\overline{K}_{hu-aggr-sw}^{(0)}}{(N_{swph})^n} = \frac{N_{swph} \cdot K_{hu}}{(N_{swph})^n} = \frac{K_{hu}}{(N_{swph})^{n-1}}, \quad (3)$$

where K_{hu} is harmonics factor (THD).

The comparatively recent paper [24] presents a rather different output voltage index, the so-called normalized integral (weighted) harmonic factor of n -th order:

$$\overline{K}_{hu_norm}^{(n)} = (N_{swph})^n \cdot \overline{K}_{hu}^{(n)}. \quad (4)$$

These normalized indices eliminate the IHF dependence on the frequency modulation index, and they should depend only on the amplitude modulation index. Such the coefficients are helpful and suitable for the group harmonics consideration, and they are now frequently used in the design

of filters. But due to analog of left part of (3) for $\overline{K}_{hu}^{(n)}$, all the normalized reduced integral harmonic factors add up to the level of the zero order IHF, i.e. THD:

$$\overline{K}_{hu_norm}^{(n)} \approx \overline{K}_{hu}^{(0)} = K_{hu}. \quad (5)$$

Processing the weighted THD (the first order IHF) produces the same values for the first order normalized integral harmonic factor and the first order aggregate switchings and integrated voltage harmonics factor:

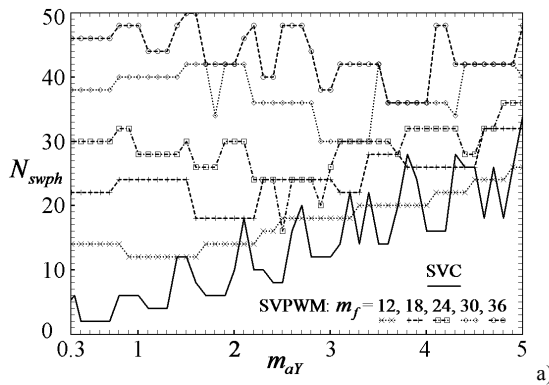
$$\overline{K}_{hu-aggr-sw}^{(1)} = \overline{K}_{hu_norm}^{(1)} = N_{swph} \cdot \overline{K}_{hu}^{(1)}. \quad (6)$$

As can be seen from (4) for $n=0$, the switchings number inherently can not be taken into account for the THD itself.

So, ASIHF, related to (2), continue to be the only adequate generalized indices, reflecting these two the most important voltage generating aspects.

IV. SIMULATION RESULTS AND DISCUSSION

The switchings (commutations) number in the MLVSI phase leg per the output voltage cycle N_{swph} dependences on



the phase voltage amplitude modulation index m_{aY} , with step equal to 0.1, are presented in Fig. 3, a and b, respectively, for the two sub-ranges: $m_{aY}=0.3..5$ and $m_{aY}=5..10$.

Here the phase voltage amplitude modulation index is defined as follows:

$$m_{aY} = U/U_d = U^*, \quad (7)$$

where U and U^* are the value and the relative value of the reference voltage space vector magnitude, equal to the reference phase voltage amplitude, U_d is the input dc voltage of the unit level (the base for all the voltages, marked with an asterisk *).

So, the delta voltage amplitude modulation index can be expressed as follows:

$$m_{a\Delta} = \sqrt{3} \cdot U^* = U_{\Delta}^* = \sqrt{3} \cdot m_{aY}, \quad (8)$$

and the amplitude modulation depth M , frequently used for the particular number N of the MLVSI levels, can be defined and related to the phase voltage amplitude modulation index by the equations:

$$M = U/U_{\max} = \frac{U}{(N-1) \cdot U_d} = \frac{U^*}{N-1} = \frac{m_{aY}}{N-1}, \quad (9)$$

where U_{Δ}^* is the amplitude relative value of the reference delta voltages, U_{\max} is the maximum value of the voltage space vector magnitude provided by the N -level MLVSI.

Also in these two and the further provided figures the quarter-wave symmetric SVPWM [13]-[15] dependences are shown for the five lowest frequency modulation index m_f values: 12, 18, 24, 30 and 36, to be compared to the instantaneous SVC results. Here frequency modulation index is defined conventionally:

$$m_f = f_c/f, \quad (10)$$

f_c and f are the clock and modulating frequencies, respectively.

The zero to third orders ASIHF indices curves of their dependences on the phase voltage amplitude modulation index are presented in Fig. 4 and Fig. 5, respectively, for the same two phase voltage amplitude modulation index sub-ranges: $m_{aY}=0.3..5$ and $m_{aY}=5..10$.

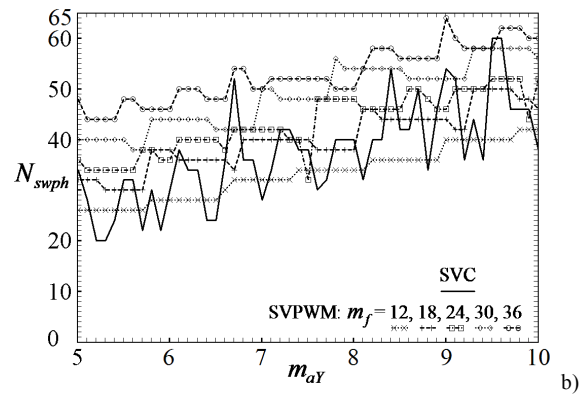


Fig. 3. Simulated results of the multilevel inverter phase leg per cycle switchings numbers: a) for the the range $m_{aY}=0.3..5$; b) for the range $m_{aY}=5..10$.

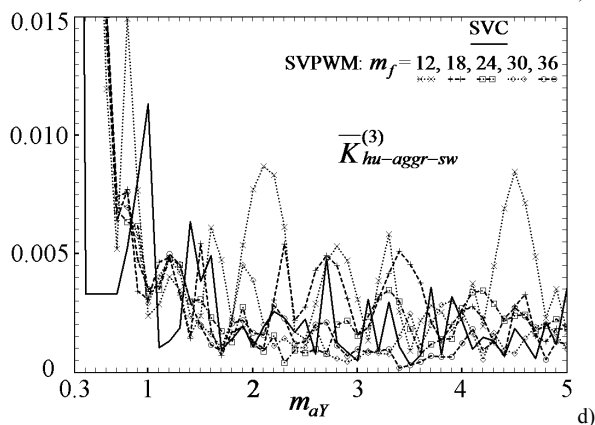
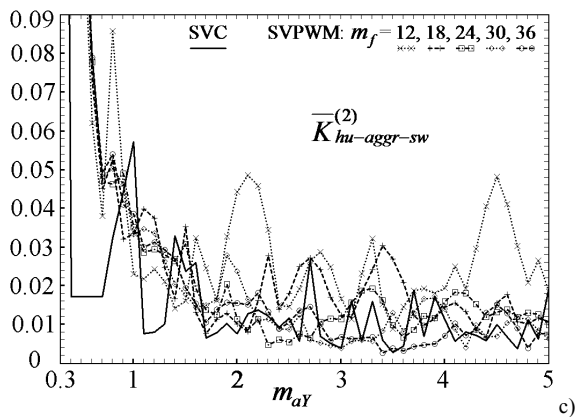
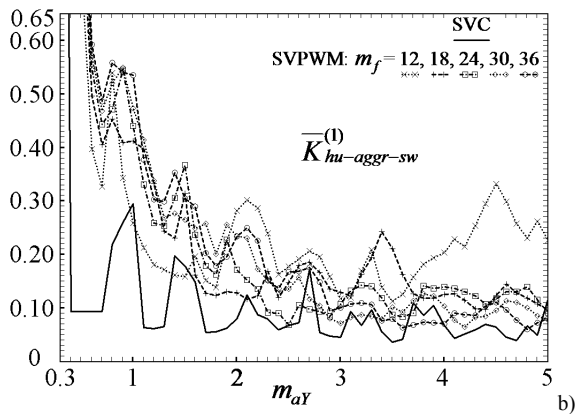
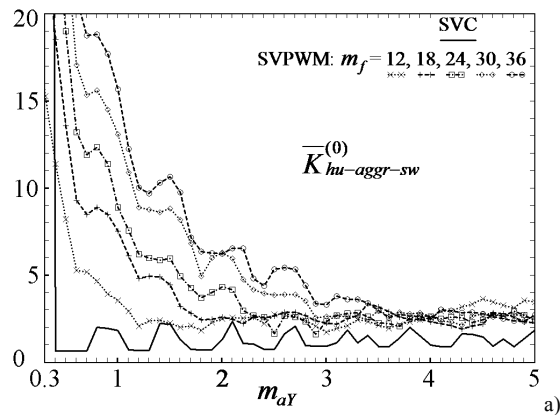


Fig. 4. Simulated zero-order (a) and first to three orders aggregate factors of switchings and integrated voltage harmonics (b, c and d) dependences on the phase amplitude modulation index $m_{a\gamma}$ for the instantaneous SVC and the quarter-wave symmetric SVPWM (under the five lowest values of the frequency modulation index) in the range $m_{a\gamma} = 0.3 \dots 5$.

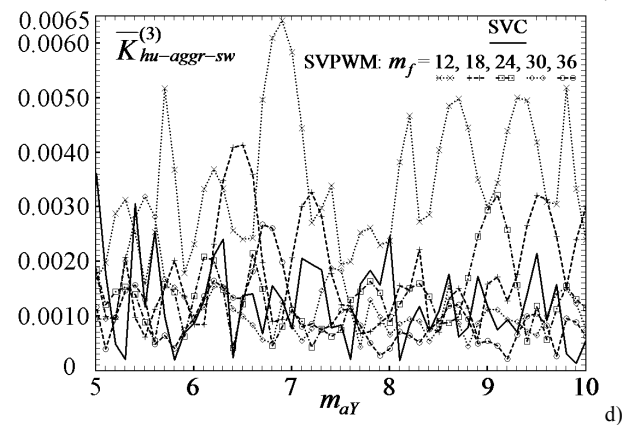
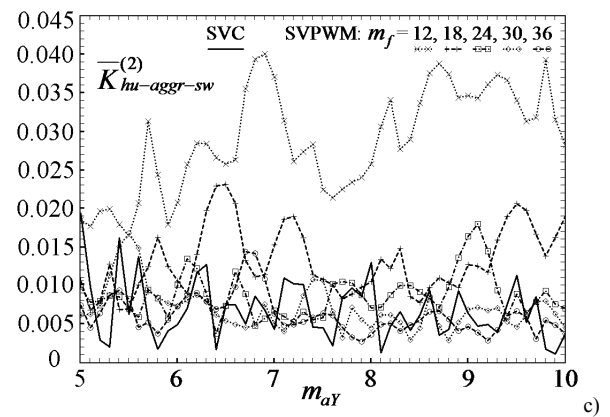
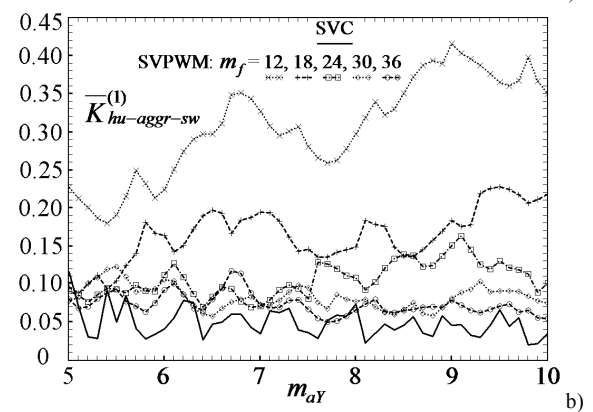
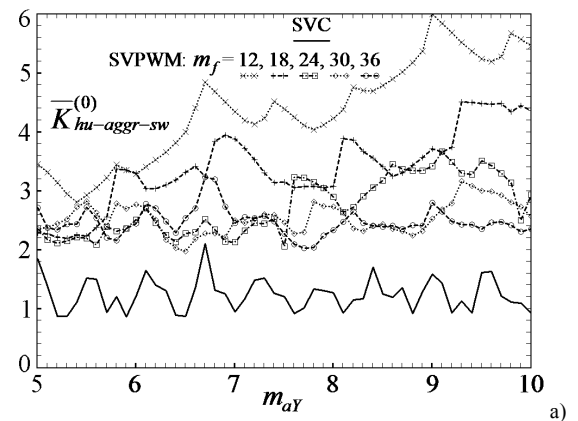


Fig. 5. Simulated zero-order (a) and first to three orders aggregate factors of switchings and integrated voltage harmonics (b, c and d) dependences on the phase amplitude modulation index $m_{a\gamma}$ for the instantaneous SVC and the quarter-wave symmetric SVPWM (under the five lowest values of the frequency modulation index) in the range $m_{a\gamma} = 5 \dots 10$.

The sub-range $m_{aY} = U^* < 1/3$ is the zero-SV proximity zone, i.e. the dead band, for which all the MLVSI output instantaneous voltages are equal to zero.

The zero order ASHF corresponds to the THD, and similar to the THD curves [18], the Fig. 4, a and Fig. 5, a demonstrate the SVC absolute superiority over the considered SVPWM modes in the zero order ASHF values throughout the whole amplitude modulation index range, despite the relating to SVC per cycle switchings numbers are mostly higher than the corresponding SVPWM results for $m_f = 12$ in the second m_{aY} sub-range (see Fig. 3, b).

Equally sustainable competitive SVC advantage (with few exceptions) can be observed in the first-order ASHF values.

But in values of the second-order and, especially, the third-order ASHF the quarter-wave symmetric SVPWM successfully competes with SVC, at the frequency modulation index values, sequentially increasing with the growth of the amplitude modulation index value. This SVC drawback is caused by the high magnitude of fluctuations in second and third orders IHF values. It should be noted that, beginning from the first order ASHF, values of these aggregate indices become the ambiguous functions of the amplitude modulation index (and also of the frequency modulation index for SVPWM).

Due to the proportion (3) of the ASHF coefficients, the more the order ASHF is, the less values of this ASHF and its contribution to the corresponding output voltage or current THD are (just like in case of IHF values [21]).

But where the ac filters installation is envisaged, the respective order ASHF indices are playing a growing role, and the above considered best SVPWM frequency modes should be applied.

Based on the joint approach and attributes of the before offered quarter-wave symmetric SVPWM and this novel SVC technique, the target might be to combine use of SVC and SVPWM with the output voltages quarter wave symmetry, applying one of the specified techniques depending on the range of amplitude modulation index values to obtaining voltage of the best quality of two alternatives with low dynamic losses in power semiconductor switches.

V. CONCLUSIONS

The n-order aggregate switchings and integrated voltage harmonics factors are used for the output voltage analysis of the three-phase multilevel inverter under the space vector control with the nearest vector selecting. These aggregate factors should be treated as the supplementary instrumentation for the comparison of the modulation algorithms for voltage generating which takes into account both the voltage quality and the price of its achieving. They must be further studied and developed to be correlated with the total power losses and the efficiency factor of the entire MLVSI circuit, including the output filter.

Based on the LabVIEW-simulated IHF results, curves of the ASHF indices (from zero to third orders) dependences on the phase voltage amplitude modulation index (in its

range from 0.3 to 10) are obtained for the SVC scheme and for the quarter-wave symmetric SVPWM (at the five low values of the frequency modulation index) for intercomparison.

Due to the SVC advantage in the zero and first orders aggregate indices, it can be strictly recommended for the loads which need no filter system. Otherwise, the choice of one of the two considered control techniques can be made via the above mentioned dependences curves by an industrial engineer who designs some system “MLVSI - filter - load circuit” for particular load circuit parameters values (they specify the most important orders numbers of IHF and ASHF) and for selected amplitude modulation index ranges.

The supplementary researches are needed to solve the problem of MLVSI combined SVC and SVPWM control on the base of the general approach, operating with the integer and fractional parts of the reference delta voltages relative values. Such the control would preliminary assess the considered aggregate (voltage quality and dynamic losses) factors and apply the most suitable control technique.

REFERENCES

- [1] Rodriguez J., Lai J.-S., Peng F.Z. Multilevel inverters: a survey of topologies, controls, and applications // IEEE Transactions on Industrial Electronics, Vol. 49, Iss. 4, August 2002, pp. 724-738.
- [2] Leon J.I., Kouro S., Rodriguez J., Wu Bin. The essential role and the continuous evolution of modulation techniques for voltage-source inverters in the past, present, and future power electronics // IEEE Transactions on Industrial Electronics, Vol. 63, Iss. 5, May 2016, pp. 2688-2701.
- [3] Stynski S. and Malinowski M. Space Vector Modulation in Three-Phase Three-Level Flying Capacitor Converter-Fed Adjustable Speed Drive. Chapter 10 in Advanced and Intelligent Control in Power Electronics and Drives. Springer, Switzerland, 2014, 410 p., 2014. Edited by T. Orłowska-Kowalska, F. Blaabjerg and J. Rodriguez, pp. 335-374.
- [4] Wu Bin, Narimani M. High-Power Converters and AC Drives. Second Edition. Wiley-IEEE Press, 2017.
- [5] Gonzalez S.A., Verne S.A., Valla M.I. Multilevel Converters for Industrial Applications. CRC Press, 2013.
- [6] Kouro S., Malinowski M., Gopakumar K., Pou J., Franquelon L.G., Wu Bin, Rodriguez J., Pérez M.A., and Leon J.I. Recent advances and industrial applications of multilevel converters // IEEE Transactions on Industrial Electronics, Vol. 57, Iss. 8, Aug. 2010, pp. 2553-2580.
- [7] Rodriguez J., Moran L., Silva C., Correa P. A high performance vector control of a 11-level inverter // IPENC 2000, 3rd International Power Electronics and Motion Control Conference, Beijing, China, August 15-18, 2000, Proceedings, pp. 1116-1121.
- [8] Rodriguez J., Correa P., Moran L. A vector control technique for medium voltage multilevel inverters // APEC 2001, 16th Annual IEEE Applied Power Electronics Conference and Exposition, Anaheim, CA, USA, March 4-8, 2001, Proceedings, pp. 173-178.
- [9] Rodriguez J., Moran L., Correa P., Silva C. A vector control technique for medium-voltage multilevel inverters // IEEE Transactions on Industrial Electronics, Vol. 49, Iss. 4, August 2002, pp. 882-888.
- [10] Rodriguez J., Moran L., Pontt J., Correa P., Silva C. A high-performance vector control of an 11-level inverter // IEEE Transactions on Industrial Electronics, Vol. 50, Iss. 1, February 2003, pp. 80-85.
- [11] Lopatkin N.N. Simple delta voltages space vector PWM algorithm for voltage source multilevel inverters // 2016 2-nd International Conference on Intelligent Energy and Power Systems (IEPS), Kyiv, Ukraine, June 7-11, 2016, Proceedings, pp. 149-154.
- [12] Lopatkin N.N. Output voltage simulation of multilevel inverter with space vector modulation of two delta voltages // Tekhnichna Elektrodynamika (Technical Electrodynamics), edition of National Academy of Sciences of Ukraine, Kyiv, Iss. 5, 2016, pp. 20-22 (in Russian).

- [13] Lopatkin N.N. Voltage quality comparison of space vector PWM voltage source multilevel inverter under symmetric and nonsymmetric switching sequence variants: voltage waveforms, spectra and THD // ICIEAM-2017, 2017 3rd International Conference on Industrial Engineering, Applications and Manufacturing (ICIEAM), IEEE Conference # 40534, Russia, St. Petersburg, Peter the Great Saint-Petersburg Polytechnic University, May 16-19, 2017, Proceedings, pp. 1-8.
- [14] Lopatkin N.N., Zinoviev G.S. Voltage quality comparison of space vector PWM voltage source multilevel inverter under symmetric and nonsymmetric switching sequence variants: voltage harmonics integral factors // ICIEAM-2017, 2017 3rd International Conference on Industrial Engineering, Applications and Manufacturing (ICIEAM), IEEE Conference # 40534, Russia, St. Petersburg, Peter the Great Saint-Petersburg Polytechnic University, May 16-19, 2017, Proceedings, pp. 1-7.
- [15] Lopatkin N.N. Simple space vector PWM scheme with quarter-wave symmetric output voltage waveform for three-phase multilevel inverter // 2017 International Multi-Conference on Engineering, Computer and Information Sciences (SIBIRCON), Russia, Novosibirsk, Novosibirsk Akademgorodok, September 18-24, 2017, Proceedings, pp. 433-438.
- [16] Lopatkin N.N. Some new representations of the multilevel inverter voltage space vector in the complex plane // SIBCON-2015, 2015 International Siberian Conference on Control and Communications (SIBCON), Russia, Omsk, May 21-23, 2015, Proceedings, 222em.pdf (pp. 1-11).
- [17] Lopatkin N.N. New implementation of nearest vector selecting space vector control for three-phase multilevel voltage source inverter // ICIEAM-2018, 2018 International Conference on Industrial Engineering, Applications and Manufacturing (ICIEAM), IEEE Conference # 43496, Russia, Moscow, Moscow Polytechnic University, May 15-18, 2018, Proceedings, paper 3.4.39 (pp. 1-7), in press.
- [18] Lopatkin N.N. Voltage THD and integrated voltage harmonics factors of three-phase multilevel voltage source inverter with nearest vector selecting space vector control // ICIEAM-2018, 2018 International Conference on Industrial Engineering, Applications and Manufacturing (ICIEAM), IEEE Conference # 43496, Russia, Moscow, Moscow Polytechnic University, May 15-18, 2018, Proceedings, paper 3.4.40 (pp. 1-6), in press.
- [19] Lopatkin N.N., Chernov Y.A. Virtual instrument for nonconventional total harmonic distortion factors evaluation // SIBCON-2016, 2016 International Siberian Conference on Control and Communications (SIBCON), Russia, Moscow, May 12-14, 2016. Proceedings, pp. 1-6.
- [20] Lopatkin N.N., Chernov Y.A. Differential and integral factors of harmonics LabVIEW estimation // EDM'2016, 17th International Conference of Young Specialists on Micro/Nanotechnologies and Electron Devices (EDM), Erlagol, Altai, 30 June - 4 July, 2016, Proceedings, pp. 493-498.
- [21] Zinoviev G.S. Power Electronics. Textbook for undergraduate students. Fifth edition. Moscow: Jurajt, 2012. 667 p. (in Russian).
- [22] Bakhovtsev I.A., Zinoviev G.S. Energy conversion quality analysis of PWM autonomous voltage inverter // Power thyristor converters, Interuniversity collection of scientific papers, edition of Novosibirsk Institute of Electrical Engineering (NETI), Novosibirsk, 1987, 162 p., edited by G.V. Grabovetskiy, pp. 3-12 (in Russian).
- [23] Zinoviev G.S. Direct Methods of Calculation of Power Indicators of Valve Converters. Novosibirsk: NSU, 1990. 220 p. (in Russian).
- [24] Bakhovtsev I.A., Zinoviev G.S. Generalized analysis of output power of multiphase multilevel PWM voltage source inverters // Electricity, Iss. 4, 2016, pp. 26-33 (in Russian).



Lopatkin Nikolay Nikolaevich is the graduate of the industrial electronics department of the NETI (now NSTU), 1988, the candidate of engineering sciences, NSTU, 1998, the lecturer of the mathematics, physics and informatics department of Shukshin Altai State Humanities Pedagogical University (ASHPU), Biysk. His research interests include multilevel converters and control of them, quality indexes of electrical energy processes and improvement of them.

E-mail: nikolay_lopatkin@mail.ru

Development of a Sound Recognition System Using STM32 Microcontrollers for Monitoring the State of Biological Objects

Vali Kh. Abdrakhmanov¹, Renat B. Salikhov², Konstantin V. Vazhdaev^{1,2}

Physical-Technical Institute, Bashkir State University, Ufa, Russia¹

Architectural and Construction Institute of Ufa State Petroleum Technological University, Ufa, Russia²

Abstract – The analysis of the main trends in the development of automation in the field of beekeeping, in particular the use of modern network technologies, sound recognition technologies for monitoring the state of bee-families. Considered the main existing recognition technologies, requirements for the hardware of monitoring systems. The possibility of implementing a prototype based on the Arduino platform with Wi-Fi modules ESP8266, advantages and disadvantages of this solution was considered. As a result, the conclusion of the feasibility of using the 32-bit STM32 microcontroller with a core ARM Cortex-M4, and for developing a prototype device - the STM32F4DISCOVERY evaluation board. The features of development of projects on STM32, a choice of software for development are also considered.

Index Terms – monitoring the state of bee families, algorithms for artificial neural networks (neuronet), algorithms for fast Fourier transform (FFT), speech recognition technology, Arduino Due, IoT, ARM Cortex-M4, STM32F4DISCOVERY, STM32Cube, CooCox IDE.

I. INTRODUCTION

Automation in beekeeping would help solve several problems. Let's consider the main relatively easily solved problems. Diagnosis of the state of beekeeping by sounds produced by a bee hive. In the summer period, you can determine the different stages in the life of the hive: calm state, ventilation, singing of the uterus, swarm output, flying bees, etc. Especially important is the ability to recognize the singing of the uterus; during the swarming period, the probability of bee-losses and beekeepers during this period are forced to constantly monitor the apiary, not having the opportunity to go off for a while somewhere. In addition, many experienced beekeepers carry out various measures to eliminate swarming (make so-called layers, etc.), which can be quite labor-intensive. During the wintering period, it is also possible to determine the condition of the bee-family by sounds, for example, to determine the situation of lack of food, disease of bees, violation of the temperature regime in the winter hut, increased humidity, etc., which require intervention by the bee-fisherman. To monitor the condition of the bee family, in addition to the sound signals of the hive, it is also advisable to remove the temperature in the hive, because The increased temperature during the wintering of the whitefish reveals the disturbance of the bees. Also, the humidity in the hive is important - a change in humidity can also be an alarm.

II. PROBLEM DEFINITION

Judging by the publications in the network, it can be noted that automation in the field of beekeeping in European countries is widely introduced. This is due to the fact that beekeeping develops mainly not only for the products of beekeeping, but because of the need for pollination of agricultural plants, in addition bees play an important role in maintaining the stability of the entire biosphere. There are known foreign developments in monitoring systems of bee colonies: for example, Apis - the development of Portuguese beekeepers [1], which allows you to monitor the status of hives remotely, directly from your smartphone. This system can significantly facilitate the life of both a beginner beekeeper and a professional, and the main thing is to significantly reduce the physical interference in the life of the bees themselves. The Apis monitoring system aims to make a "smart hive" from each hive with a built-in temperature and humidity sensor, bee counter and weights. All-important statistical data is sent to a computer, smartphone, or tablet. In addition, the European Union is completing the development of a device for remote monitoring of the health of bees by monitoring the sounds produced by them in the hive. The initiators of this project were the University of Trent (UK) and the Association of Farmers of Great Britain (BFA). For the implementation of the project from the EU budget allocated 1.4 million euros [2].

There are also domestic developments [3], where it is proposed alongside monitoring, to realize also the regulation of temperature and humidity in the hive (by installing an electric heater in the hole of the lower tap) during wintering, and also in the spring-summer period prior to the beginning of June Moment, when stable warm weather is established in the central part of Russia) - at this time there is a sharp temperature drop, which requires large energy costs from the bee colony. The main element of the monitoring and diagnostics device is the Atmel microcontroller. It is connected to digital temperature sensors DS1620, humidity HIH4000 and electret microphone SG72.

To diagnose the condition of bee families by sounds, you can use known and widely used speech recognition technologies, with two fundamentally different recognition methods: T2SI (text-to-speaker-independent, "person-independent", anyone can be speaking) and SD (speaker -dependent, the one who taught the system should speak). Obviously, in our device, the more easy to implement SD method will be more

appropriate. The possibility of using a free voice recognition service from Google servers such as Google ASR or YandexSpeechKit [4] was considered, but this requires a constant network connection, that for a battery device with Wi-Fi modules ESP8266 [5], known for their high power consumption, is unacceptable.

In addition, it must be said that these programs use a more complex "human-independent" T2SI method, whereas in our case, SD (speaker-dependent) is sufficient. Thus, it is clear that Google ASR or YandexSpeechKit speech recognition services can not be adapted to recognize the sounds of bees, and it would be necessary to develop their own service with their server. It is possible to refuse the transfer of all data to the server. The operating system for mobile devices Android 4.1 allows this, because there is a system of offline - speech recognition; Internet access is not required. Moreover, the quality of recognition is reduced. But in our case, using Android - the device will be redundant and expensive, in this case it is desirable to avoid redundancy, because first of all, you need to minimize power consumption.

EasyVR Shield 3.0 speech recognition software [6] (shown in Fig. 1) was also considered, but this is too expensive a solution for beekeeping (price 50 Euro).

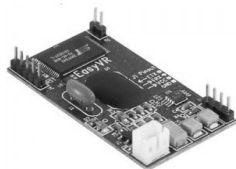


Fig. 1. EasyVR Shield 3.0

III. PROPOSED IDEAS FOR DEVELOPMENT

After analyzing the state of the problem, it is possible to propose a fairly budgetary solution using the Arduino platform, with the Wi-Fi module ESP8266 [5], the microphone module [7], the Micro SD card [8] needed to store the samples (shown in Fig. 2), the DS18B20 digital temperature sensor. The sampling frequency for the audio signal is usually taken at 48 kHz, but for the sounds of the hive it is sufficient to take the frequency band of 70..600Hz [9], and then it is obvious that the requirements for the microphone module bandwidth are low - for the electret condenser microphone CZN used in the microphone module [7] 20Hz..14kHz. Also, the sampling frequency of the signal can be reduced, which will reduce the memory and speed requirements of the controller in comparison with the known task of speech recognition, for example.



Fig. 2. Wi-Fi module ESP8266-07, microphone module, SPI - reader module for micro SD card.

Thus, we propose to implement monitoring on the sounds of the bee-family and the temperature in the hive. We believe that the implementation of the regulation of temperature and

humidity in the spring-summer period will be too time-consuming (it is necessary to tie the wires across the whole apiary) for widespread introduction, but the ability to determine the state of swarming (the so-called singing of the uterus) will be called for by beekeepers - After the swarm period, the modules can be disabled and completely removed from the apiary. We also consider excessive and laborious control of the weight of the hive.

For recognition, it is proposed to use algorithms of artificial neural networks (ANN) [10], with a preliminary expansion of the frequency spectrum, for which use the algorithms for Fast Fourier Transform (FFT) - there are libraries of 8-bit conversion [11]. Thus, we propose to implement monitoring on the sounds of the bee-family and the temperature in the hive.

It is proposed to periodically extract small samples of the signal from the microphone module, digitize it using an Arduino board, and only if a change in the state of the bee-family is detected (for example, the singing of the uterus has been fixed) to include a Wi-Fi module. This will minimize the power consumption of the device, which is especially important due to the use of autonomous power. In view of the fact that large volumes of RAM are required for selection, high processing speed is suggested to be used by Arduino Due [12] based on the 32-bit ARM Cortex-M3 86MHz ARM, 512K flash + 96K RAM. Clones Arduino Due from Chinese manufacturers can cost relatively under-the-go - from 15USD. The use of the Arduino platform is usually due to the low cost and a large number of ready-made modules with libraries for their connection. In addition, you can easily find a lot of information on devices already implemented on this base. The lack of hardware support for digital processing of signals, support of operations for floating-point numbers, the need for large computing power with low power consumption leads to the decision about the advisability of using 32-bit microcontrollers with the ARM Cortex-M4 core.

The emergence and wide distribution of sufficiently budget 32-bit microcontrollers STM32 with the ARM Cortex-M4 core, which differs by the built-in instructions for Digital Signal Processing (DSP) and Floating Point Unit (FPU) , allows them to be used for our development. And, despite the high power and speed due to the peculiarities of the timing system in ARM microcontrollers, it is possible to significantly reduce power consumption. Particularly convenient for developing a prototype device is the STM32F4DISCOVERY board [13] (shown in Fig. 2), based on the STM32F407VGT6 microcontroller [14] (Cortex M4, 168MHz, flash 1MB, RAM 192Kb). Of course, the presence of DSP and FPU is especially valuable, which will speed up the processing of sound, but also significantly higher clock frequency, a large amount of RAM, as well as the presence of a board-based digital microphone (ST MEMS sensor MP45DT02).

In addition, there is an audio DAC with an amplifier of class D, which you can try to use to reproduce pre-recorded in memory samples of the uterus sounds in a calm state in order to calm, while digging, for example. Thus, it becomes possible to investigate the influence on the behavior of bees with the help of standard uterus sounds, which could possi-

bly stop the swarming or slow it down. It is also possible to use the ST MEMS LIS302DL motion sensor on the board and the outputs of the digital accelerometer in three axes for registration to change the position of the hive in space, some vibrations and shock loads. This can be useful for recording the fall or inclination of a hive when colliding with large animals, which can happen. For example, during a summer migration, and also for recording the torture of penetration into the hive of rodents, which can occur in the winter when the hive is in the hibernation. It is also important that the controller has a controller module 10/100 Ethernet MAC, which will allow you to connect to the global network Internet and display all current information - on the smart background of the beekeeper, for example. This connection is good for using the module in the hibernate, and for working in the summer conditions, of course, it is more convenient to use wireless connection with Wi-Fi modules ESP8266 [5] widely used in the Internet of things (IoT) and the "Smart House" [15-18].

When choosing a microcontroller for development, often follow the experience of its previous developments on 8-bit widespread AVR and PIC [19] or Arduino platform [15,18]. At the same time, for developing software, it is convenient for beginners to get acquainted with the STM32 family by using the newly developed program - the CubeMX initialization code generator [20] from STMicroelectronics manufacturer for setting (initializing) the core and peripherals, connecting libraries, generating an empty project. After the project is generated, you can transfer it to a convenient development environment for the CooCox IDE [21]. Thus, it is relatively easy to read and start working with STM32.

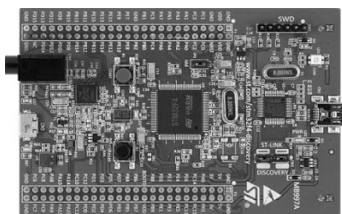


Fig. 3. STM32F4DISCOVERY

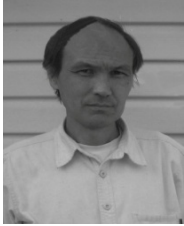
IV. CONCLUSIONS

The analysis of the main trends in the development of automation in the field of beekeeping is done, in particular the use of modern network technologies, sound recognition technologies for monitoring the state of bee-families. The main existing recognition technologies, requirements for the hardware of monitoring systems are considered. The possibility of implementing a prototype based on the Arduino platform with Wi-Fi modules ESP8266, advantages and disadvantages of this solution were considered. As a result, the conclusion was made about the advisability of using 32-bit microcontrollers STM32 (shown in Fig. 3) with the ARM Cortex-M4 core, and for developing a prototype device - the STM32F4DISCOVERY evaluation board. Also features of development of projects on STM32, a choice of software for development are considered.

REFERENCES

- [1] Apis is a system for monitoring the health and activity of your bees. [Online]. Available: <http://rodovid.me/pchelovodstvo/apis-sistema-monitoringa-zdorovya-i-aktivnosti-vashi-pchel.html>
- [2] Monitoring the well-being of bees at a distance. It's already coming! [Online]. Available: <http://bashkirskimed.ru/medovi-spravochnik/428-kontrol-samochuvstviya-pchel-na-rasstoyanii-eto-uzhe-gryadet.html>
- [3] V.V. Semenov, A.R. Ganeev Automatic monitoring and management of the family's state // Beekeeping, №9 2011. C.50
- [4] SpeechKit Speech Technology: Speech Recognition and Speech Synthesis. [Online]. Available: <https://tech.yandex.ru/speechkit/>
- [5] ESP8266 Module WIFI for Arduino. [Online]. Available: <http://www.ebay.com/itm/ESP8266-Receive-AP-STA-Hot-Wireless-Send-Transceiver-Module-WIFI-For-Arduino>
- [6] EasyVR Shield 3.0 per Arduino Modulo Riconoscimento Vocale - Speech recognition. URL:http://www.ebay.com/itm/EasyVR-Shield-3-0-per-Arduino-Modulo-Riconoscimento-Vocale-Speech-recognition-/121925584067?_ul=RU
- [7] Microphone Sensor AVR PIC High Sensitivity Sound Detection Module For Arduino. [Online]. Available: <http://www.ebay.com/itm/201414878181>
- [8] Micro SD Storage Board. [Online]. Available: <http://www.ebay.com/itm/Micro-SD-Storage-Board-Micro-SD-TF-Card-Memory-Shield-Module-SPI-For-Arduino-UR>
- [9] Sounds of bees. [Online]. Available: <http://epz.ru/stroitelstvo/paseka/zvuki-pchyl>
- [10] Artificial neural networks. [Online]. Available: <http://robocraft.ru/blog/algorithm/558.html>
- [11] Modified 8bit FFT. [Online]. Available: <http://forum.arduino.cc/index.php?topic=38153.msg282965#msg282965>
- [12] Arduino Due. [Online]. Available: <https://www.arduino.cc/en/Main/ArduinoBoardDue>
- [13] STM32F407VG. High-performance foundation line, ARM Cortex-M4 core with DSP and FPU, 1 Mbyte Flash, 168 MHz CPU, ART Accelerator, Ethernet, FSMC. [Online]. Available: <http://www.st.com/en/microcontrollers/stm32f407vg.html>
- [14] STM32F4DISCOVERY. [Online]. Available: <http://www.st.com/en/evaluation-tools/stm32f4discovery.html>
- [15] Development of automation tools using WI-FI-modules ESP8266 and LPWAN-technologies. Abdrakhmanov V. Kh., Vazhdaev K. V., Salikhov R. B. Electrical and data processing facilities and systems. 2017. T. 13. № 4. P. 98-108
- [16] Salikhov R. B., Abdrakhmanov V. Kh., Vazhdaev K. V. System of monitoring and remote control of temperature conditions, climate and heat consumption. In Actual Problems of Electronics Instrument Engineering (APEIE), 2016 13th International Scientific-Technical Conference on (Vol. 3, pp. 171-174). IEEE.
- [17] Intelligent system of living areas on the basis of information-measuring control systems. Vazhdaev K.V., Abdrakhmanov V.Kh., Salikhov R.B. / Electrical and data processing facilities and systems. - 2016. - No. 2. - T 12. - P. 70-75.
- [18] Research into the possibility of applying information and measurement technologies and the Internet of things (IoT) in the agro-industrial complex. Abdrakhmanov V. Kh., Vazhdaev K. V., Salikhov R. B. Electrical and data processing facilities and systems. 2017. T. 13. № 2. P. 85-95
- [19] Abdrakhmanov V. Kh., Bikbaev N. N., Salikhov R. B. Development of low-cost electronic training boards based on universal microcontroller. In Actual Problems of Electronics Instrument Engineering (APEIE), 2016 13th International Scientific-Technical Conference on (Vol. 1, pp. 319-325). IEEE.
- [20] STM32Cube initialization code generator. URL:<http://www.st.com/en/development-tools/stm32cubemx.html>

[21]CooCox IDE. Free/open ARM Cortex-M Development Tool-chain.
[Online]. Available: <http://www.coocox.org/>



Vali Kh. Abdrakhmanov in 1998 he was graduated from Ufa State Aviation Technical University (UGATU). In 2003 defended his Ph.D. thesis in the USATU, then worked as an assistant professor at the Department of Industrial Electronics at the Faculty of Aviation Instrumentation of the USATU. Now he works as an assistant professor of the Department of Info communication Technologies and Nanoelectronics at the Physics -Technical Institute of the Bashkir State University, Ufa. His field of scientific interests is automation and control systems.



Renat B. Salikhov graduated in 1981 National Research Nuclear University NNRU. In 1987, he defended his Ph.D. thesis in the field of solid-state physics. He was the head of the laboratory of fiber-optic transducers OKB "Charger" in the 1990s, assistant professor of general physics at the Bashkir State Pedagogical University in the 2000s. At present, he is the head of the department of info communication technologies and Nanoelectronics of the Physical and Technical Institute of the Bashkir State University. Area of interest in research and development - condensed matter physics, nanotechnology and electronics.



Konstantin V. Vazhdaev was graduated from Ufa State Aviation Technical University (USATU) in 1998. In 2003 defended his Ph.D. thesis in the USATU. Then he worked as an assistant professor at the Department of Information and Measurement Technology of the Faculty of Aviation Instrumentation UGATU. Currently, he works as an assistant professor of the Department of Infocommunication Technologies and Nanoelectronics at the Physico-Technical Institute of the Bashkir State University, city of Ufa. His field of scientific interests is information and measurement technology.

Personal Computer User's Activity Monitoring Software Development for the Enterprise Business Process Optimizing

Evgeny A. Basinya^{1,2}, Sergei V. Kazarbin^{1,2}

¹Research Institute of Information and Communication Technologies, Novosibirsk, Russia

²Novosibirsk State Technical University, Novosibirsk, Russia

Abstract - The paper presents one of the possible approaches to optimize the business processes of the enterprise by monitoring the activity of users of personal computers. Problems of existing solutions are reviewed. Open source software development for the employee time tracking is described.

Index Terms - User activity monitoring, idle time and active time monitoring, remote work.

I. INTRODUCTION

AT PRESENT, the employees' work monitoring is an important tool for optimizing the business processes of an enterprise. The check point system, time sheets and books do not always accurately reflect the work activities of the employee. Recording the actual work activity and the employee computer activity can be used as an important supplementary tool for managing the operations of the enterprise[1].

Currently, there are many solutions that carry out this task. The comparative analysis of the existing solutions using the application environment virtualization ("sandboxes"), the active and passive traffic analysis technologies and the computer programs (packet sniffers, scanners) have revealed a number of significant problems[2-4]:

- 1) local storage of the data in an unencrypted or weakly encrypted form. For example, using the DES (Data Encryption Standard) algorithm;
- 2) unauthorized sending of the information to the developer's server in the hidden mode;
- 3) unauthorized abuse of software permissions that have an access to the camera, microphone and other equipment;
- 4) use of a vulnerable technology stack during the development process (for example, Adobe AIR);
- 5) use of the network protocols and technologies that are not functionally necessary. For example, setting up an encrypted virtual channel with a suspicious IP addresses;
- 6) closed source distribution.

These disadvantages may be the result of the developer's mistakes or the intentionally integrated tools for the hidden collection of confidential information.

Despite the closed source, the use of the traffic interception and the analysis tools can detect a network activity, even if the data transfer is not expected by the settings and is not

specified in the documentation or in the user agreement. Running the product in a sandbox allows to track an unauthorized access to different system files, registry branches, and hardware which reasonably allows to suspect such software in the collection, analysis and transfer of the confidential data to the software developer's server.

In addition to these existing disadvantages in terms of the information security, some different solutions offered on the market also vary in a number of functional problems. Most products provide reports that lack information, and the event logs are presented in a form that is difficult to be analyzed due to large and often excessive number of records. Some products do not support or incorrectly monitor the remote work of users through the terminal connections and remote access protocols in general. No product supports the integration with a firewall, this prevents the system administrator and managers from receiving the necessary information about the user's activities. In addition, agents for collecting information are not provided to the firewall and the intrusion detection and prevention system.

It is also important to point out that the existing solutions for the user activity monitoring that are in a high demand of are characterized by an expensive license.

II. PROBLEM DEFINITION

In this work, the task was to develop a free software product for employee time tracking for personal computers running the Windows operating system, distributed with open source, eliminating the identified vulnerabilities of competitors and having the following functionality:

- 1) ensuring information security of user data using a symmetric-key encryption algorithm AES with 256-bit key length;
- 2) no tools for collection of confidential data acquisition and computer control;
- 3) creating informative reports with graphical analytics;
- 4) parsing of Windows event logs;
- 5) correct work with remote access protocols and technologies;
- 6) verification of the security of the connection (for example, HTTP (HyperText Transfer Protocol and HTTPS (HyperText Transfer Protocol Secure));
- 7) portability of the software;

- 8) work in hidden mode for the user, the program is opened only by pressing the key combination specified and entering the password;
- 9) further integration of the interaction module with the gateway / firewall developed by the Research Institute of Information and Communication Technologies [5].

III. SOFTWARE DEVELOPMENT

The development of the software for employee computer

time was conducted taking into account these identified problems. The solution developed determines the time of work in general and calculates both the time of work and inactivity with the window of a certain program. The user activity is any use of the mouse or the keyboard. If for a sufficiently long period of time (by default - more than 60 seconds.) the user has not performed any actions, this period is considered idle. The rest of the time during the operation of the software is defined as user activity. The information about the process that created the window, the process description, and the window title are saved (Fig. 1).

In case of working with the Internet browser, the time of working with each tab and the protocol used is fixed.

| Process name | Process description | Window title | Work time | Idle time |
|--------------|---|--------------|-----------|-----------|
| devenv | Microsoft Visual Studio 2017 | - | 04:04:54 | 01:01:34 |
| explorer | Explorer | - | 00:09:54 | 01:16:34 |
| chrome | Google Chrome | - | 01:51:38 | 00:27:15 |
| notepad++ | Notepad++ : a free (GNU) source code editor | - | 00:03:33 | 00:00:00 |
| mintty | MSYS2 terminal | - | 00:07:09 | 00:00:00 |
| Mattermost | Mattermost | - | 00:04:07 | 00:00:00 |
| KeePass | KeePass | - | 00:00:30 | 00:00:00 |
| WINWORD | Microsoft Word | - | 00:29:37 | 00:00:00 |
| TOTAL: | | | 06:51:22 | 02:45:23 |

Fig. 1.Graphical window.

A number of the most popular browsers are supported, for each of them the title of the window contains the title of the current tab, the title of the web page usually describes the content of the page (Fig. 2).

| Process name | Process description | Window title | Work time | Idle time |
|--------------|---------------------|---|-----------|-----------|
| TM.GUI | TM.GUI | - | 00:08:15 | 00:00:00 |
| explorer | Explorer | - | 00:01:40 | 00:00:00 |
| chrome | Google Chrome | - | 00:03:37 | 00:00:00 |
| firefox | Tor Browser | - | 00:00:39 | 00:00:00 |
| firefox | Tor Browser | HTTPS Google - Tor Browser | 00:00:07 | 00:00:00 |
| firefox | Tor Browser | HTTP Novosibirsk State Technical University - Tor Browser | 00:00:00 | 00:00:00 |
| firefox | Tor Browser | HTTPS Welcome! VK - Tor Browser | 00:00:16 | 00:00:00 |
| firefox | Tor Browser | HTTPS Yandex - Tor Browser | 00:00:15 | 00:00:00 |
| firefox | Firefox | - | 00:00:43 | 00:00:00 |
| TOTAL: | | | 00:14:56 | 00:00:00 |

Fig. 2.Graphical window

It is possible to generate an activity report for a certain period and export it from the program. The program works in a hidden mode for the user. To open the main window, you must use a secret key combination and enter a password. The password can be changed later in the settings (Fig. 3).

Settings

Passwords:

DB password: password

Password: password

Time:

Interval to check idle (second) 60

Save Cancel

Fig. 3.Settings window.

Information about the activity and idle for the selected period is presented in the graphical window of the program in the form of a list of programs and browser tabs with which the user has worked, including the amount of time specified in the form of activity and idle. The data are also presented in the graphical form for further analysis (Fig. 4).

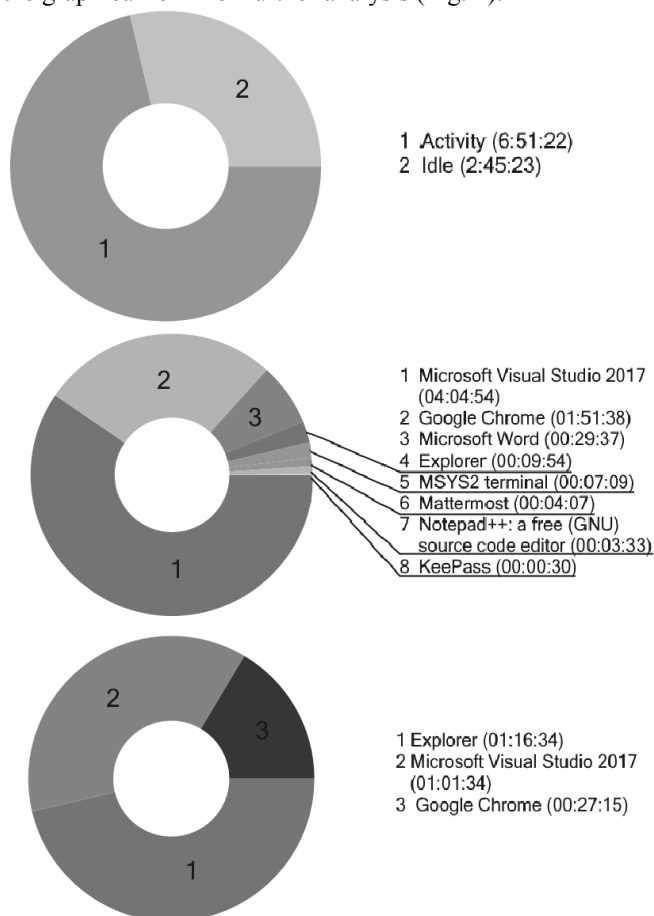


Fig. 4. An example of a graphical analytics.

The configuration and stored data are stored in an encrypted form. For the encryption, the AES encryption algorithm is used. This algorithm is currently considered strong enough and has an acceptable execution speed. The encryption allows you to protect the confidentiality and integrity of data. The password that is used to generate the encryption keys is set during the first run of the program.

For the correct remote access monitoring, connection and disconnection events of the RDP session are logged.

IV. CONCLUSION

In the present work, the free software product was developed for employee time tracking for a personal computers running the Windows operating system, distributed with open source.

The following tasks have been completed:

- 1) information security of user data is ensured using a symmetric-key encryption algorithm AES with 256-bit key length;

- 2) there are no tools for collection of confidential data acquisition and computer control;
- 3) informative reports with graphical analytics are provided;
- 4) parsing of Windows event logs is provided;
- 5) correct work with the remote access protocols and technologies is provided;
- 6) connection security (http and https) is verified;
- 7) implemented work in hidden mode for the user, the program is opened only by pressing the key combination specified and entering the password;
- 8) work is currently in progress to integrate the module of interaction with the firewall developed by the Research Institute of Information and Communication Technologies;
- 9) work is currently in progress to prevent the falsification of the user activity.

The advantage of the developed solution is its portability, when the installation is not required. An embedded database is used, the program requires the .NET Framework version 4 or later. The required version of the platform is installed in the operating system Windows 8 and later releases and can be installed in earlier versions of the operating systems of the Windows family.

The software was implemented in the full, proper quality and successfully tested in more than 50 enterprises with more than 70 employees. At the moment, the work is under way to integrate the interaction module with the gateway being developed by the Research Institute of Information and Communication Technologies.

REFERENCES

- [1] Reznichenko D.A. Automation of the process of accounting for employees' activity // Economics and management of innovative technologies. 2016. № 6 [WEB resource]. URL: <http://ekonomika.snauka.ru/2016/06/11853> (visit date: 21.02.2018).
- [2] Basinya E. A. Protection against the falsification of information resources / E. A. Basinya, S. V. Kazarbin // Perspective development of science, techniques and technology: Proc. 6th intern. sci. conf., Russia, Kursk, 20-21 Oct. 2016. - Kursk, 2016. - P. 16-19. (In Russian)
- [3] Basinya E. A. Design and study of the metadata management system for images / E. A. Basinya, A. V. Safronov // Actual problems of electronic instrument engineering (APEIE-2016) : materials of the. 13th intern. sci. conf., Russia, Novosibirsk, 3-6 Oct. 2016. - Novosibirsk: Publ. NSTU, 2016. - Vol. 9. - P. 155-157. - ISBN 978-5-7782-2991-4. (In Russian)
- [4] Basinya E. A. On encryption and anonymization with the issues of information security / E. A. Basinya, G. A. Frantsuzova, A. V. Gunko // Computer technologies in science, production, social and economic processes: materials of the 14th intern. sci. conf., Russia, Novocherkassk, 12 Dec. 2013 - Novocherkassk: SRSPU(NPI), 2014. - P. 165-168. (In Russian)
- [5] Research Institute of Information and Communications Technologies: [WEB resource]. N., 2016. URL: <https://nii-ikt.ru/>. (visit date: 23.04.2018).
- [6] Basinya E. A. Methods of self-organization in providing network security / E. A. Basinya, G. A. Frantsuzova, A. V. Gunko // Global Science and Innovation: materials of the 1st intern. sci. conf., USA, Chicago, 17-18 Dec. 2013. - Chicago: Accent Graphics communications 2013. - Vol. 2. - P. 386-389.
- [7] Frantsuzova G. A. Self-organizing system for the computer network traffic management: a method of countering network threats / G. A. Frantsuzova, A. V. Gunko, E. A. Basinya // Software Engineering. - 2014. - iss. 3. - P. 16-20. (In Russian)



Basinya Evgeny Alexandrovich defended his PhD thesis in 2015. He continued his teaching and research activities as an associate professor at the automation department in the Novosibirsk State Technical University. In 2016, he set up the Research Institute of Information and Communications Technologies with the support of the Foundation for Assistance to Small Innovative Enterprises in Science and Technology and is now its director.



Kazarbin Sergei Vladimirovich is engaged in scientific activities and software development under the leadership of E.A. Basinya, starting with the bachelor's and master's degrees of the Novosibirsk State Technical University. The Gold medal winner of the Interuniversity Olympiad "Network Security & Technologies - 2017", conducted by D-Link, the Research Institute of Information and Communication Technologies and the Siberian State University of Geosystems and Technologies in 2017.

Implementation of an Intrusion Detection and Prevention System Module for Corporate Network Traffic Management

Evgeny A. Basinya^{1,2}, Yuliya K. Ravtovich^{1,2}

¹Research Institute of Information and Communication Technologies, Novosibirsk, Russia

²Novosibirsk State Technical University, Novosibirsk, Russia

Abstract – The paper addresses an algorithm of functioning of an intrusion detection and prevention system module, based on the principles of disguise and modification of the information system parameters. An implementation of an integrated local area network security control system using the designed module is described. The proposed concept allows providing protection of the corporate computer networks and information systems from a range of network attacks (impersonation, imposition of improper route, distributed denial of service, man-in-the-middle attacks, etc).

Index Terms – Intrusion Detection and Prevention System, network security, falsification of system parameters.

I. INTRODUCTION

AT THE PRESENT time providing information security is one of the key trends in the field of information and communication technologies. A number of corporate networks security threats is constantly increasing, whilst existing data transfer protection tools are not capable to provide reliable network security since their functioning is based on linear reaction logics. An example is the vulnerability of the Border Gateway Protocol (BGP), which is widely used in the Internet network. This protocol neither contains mechanisms to protect the integrity and reliability of the route data nor provides the authentication of partners involved in the data exchange. The absence of such protection means causes the susceptibility of the BGP protocol leading to the risk of transmitted data confidentiality violation, the conduct of Man-in-the-Middle and Denial of Service attacks [1, 2]. Depletion of network resources, its overload and other malfunctions may become a result of carrying out the mentioned attacks. In that regard, the development of local area networks (LAN) security control algorithm and implementation of an Intrusion Detection and Prevention System (IDS/IPS) module on its basis is a relevant task. The use of non-standard methods of information systems protection allows levelling the faults of the already existing approaches and, as a result, significantly improves security of the corporate networks [3]. A new approach proposed in this paper is to protect information systems from the instruments of active and passive traffic analysis by hanging imitation, giving false information and realizing a hidden redirection of the information flows of the attacker.

II. PROBLEM DEFINITION

The aim of the work is the implementation of an Intrusion Detection and Prevention System module falsifying the system parameters and its response to external disturbances. Accomplishment of this purpose contains a range of tasks, including the study of existing network threats and methods of their implementation, as well as LAN protection means. Additional tasks are the development of a module for falsifying the system's response to an intrusion attempt with the ability to identify the attacker, implementation of an integrated LAN security control system using the module proposed and testing the implemented system.

III. DESCRIPTION OF THE ALGORITHM

In order to obtain the information about the network and define the potential attack targets, an attacker may use various methods of vulnerabilities check. These methods include mechanisms of passive and active traffic analysis, namely: sniffing, scanning and probing [4]. Sniffing is listening to the network, which is carried out through specialized programs that accept all transmitted packets regardless of their destination. The purpose of scanning is collecting information about the computers connected to the network and identifying the services running. Probing is a technology for active vulnerability analysis based on simulating attacks and is performed on the basis of the information obtained during the preliminary scanning. These processes allow to make a list of information system's vulnerabilities and to determine the possible sequence of attacks.

The proposed approach to protect information systems and resources from the described methods is the disinformation of the attacker. This approach underlies the developed LAN security control algorithm, which includes the use of non-standard methods to counter network threats: the modification of system parameters, hanging imitation and a hidden redirection of the attacker's datagrams for further study and identification of the intruder.

A block diagram of the algorithm is shown in Fig.1:

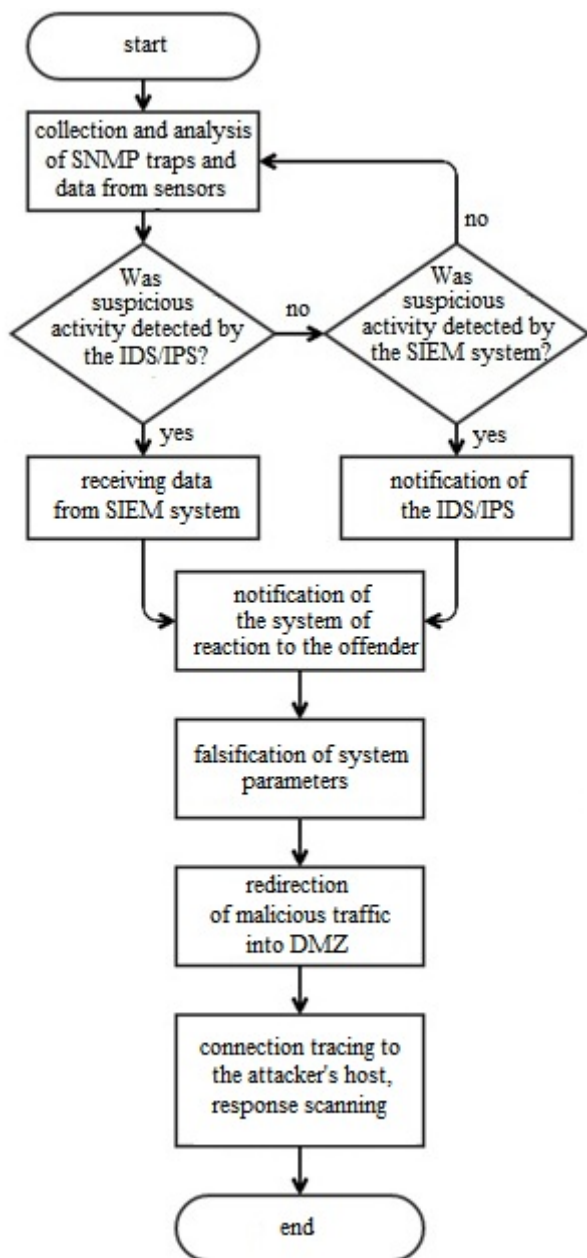


Fig. 1. A block diagram of the algorithm.

The sequence of actions performed by the security system depends on which component of this system has identified a suspicious activity: Security Information and Event Management System (SIEM) or IDS/IPS. In accordance with the developed algorithm, false information is produced about the services used and the operating system. If potential security threats are identified, malicious traffic is being redirected. Thus, an imitation of the hang of the connection is created, which forces the attacker to spend time and computing resources. A feature of the proposed solution is the ability to implement all types of response actions, including connection tracing to the attacker's host, response scanning and probing, through the Tor (The Onion Router) overlay network in order to ensure anonymity. The redirection of the information flows through the overlay network allows avoiding the identification of the host that initiated this activity. However, it should be noted that such

measures go beyond the legal fold in a number of countries, so in this algorithm their application is optional.

A significant feature of the developed algorithm is connection tracing in order to identify the anonymous connection attempts by associating the IP address from which it is accessed with known IP addresses of proxy servers and VPN services. In addition, using a script written in Python, it is possible to test the connection attempts from the Tor exit nodes.

The described algorithm significantly allows to increase the level of LAN security due to the timely collection, analysis and correlation of network events, filtering of incoming, outgoing and transit traffic and the recording of existing network threats.

Based on the algorithm considered an IDS/IPS system module has been developed, which has been subsequently integrated into the LAN security control system, the concept of which is described below.

IV. DESCRIPTION OF THE MODULE

The LAN security control algorithm resulted in the Intrusion Detection and Prevention System module, which was later introduced in the complex security system, which has a multi-level client-server architecture that allows a high level of flexibility, scalability and performance. In the comparative study, Linux CentOS 6.5 was chosen as the server operating system for reliability, fault tolerance and security, as well as additional components:

- 1) the Intrusion Detection and Prevention System Bro;
- 2) the integrated firewall based on Netfilter;
- 3) the Rsyslog Server as a logging system;
- 4) the Security Information and Event Management System PreludeOSS;
- 5) the system of reaction to the offender.

These software products are distributed through open sources and have been chosen due to their flexibility and efficiency in comparison with their analogues. The scheme for implementing the protection system is shown in Fig. 2:

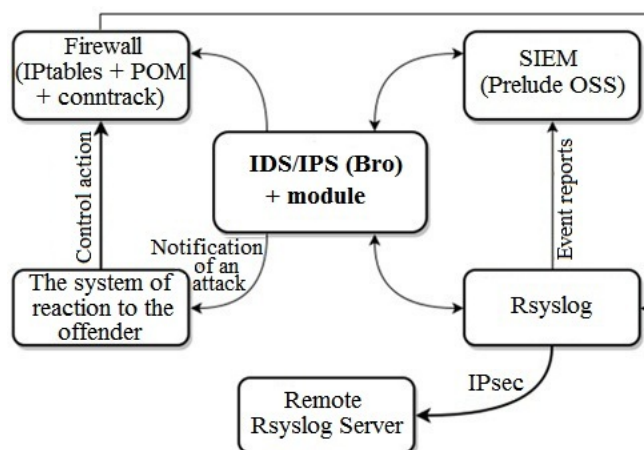


Fig. 2. The scheme for implementing the protection system.

The components of this system are considered below.

A. *The Intrusion Detection and Prevention System*

Intrusion Detection and Prevention systems use different approaches to secure events analysis. The most well-known are anomaly-based, behavior-based and the signature-based detection, as well as identification of self-similarity. Each of these approaches has a number of shortcomings and cannot be used independently. For example, the anomaly-based method does not require detailed information on attacks for their detection, but it does not allow to obtain unambiguous results in case of using encryption means and overlay technologies. The application of misuse detectors does not allow to identify complex distributed attacks due to the use of strictly defined signatures, so this method is only applicable to detect the already known attacks [5, 6]. The optimal approach to monitoring and analyzing events is to combine the methods described with an intelligent-adaptive approach.

Bro is a network IDS/IPS developed by Vernon Paxson in 1998 that combines various methods for determining attacks. In this intrusion detection and prevention system both signature-based and anomaly-based detection are used. In addition, Bro enables to define custom security policies for detecting the malicious traffic. This system consists of several interacting modules, the principal among them being the packet capture engine, the Event Engine and the Policy Script Interpreter. The packet capture engine reads the network traffic using the libcap library and then sends the received packet stream to the event engine to generate primary network activity data. Further, the script interpreter in accordance with the FIFO order, registers the handler for each event occurred. After that, the script corresponding to the handler determines the action necessary to detect malicious activity, and the rule used in case of its detection.

In order to fully cover the entire LAN and monitor insider threats, it is necessary to place IDS/IPS sensors in each segment of the network. For each sensor, it is recommended that the port is selected on the switches and subsequently traffic is mirrored from the other ports using the Port Mirroring function. Further, traffic from the port to which the sensor is connected needs to be redirected to the IDS/IPS system for analysis.

B. *Firewall*

The developed system uses an integrated firewall based on Netfilter, which includes an IPtables packet filter in combination with patch-o-matic (POM) scripts and a conntrack connection tracer. POM at present is used as a term meaning the expansion of Linux based firewall functions, so this system uses its contemporary analogue called Xtables-addons, which does not require patching the Linux kernel. Similar extensions exist for FirewallD, which replaced IPtables in CentOS 7 and later versions. In that regard, it is worth noting that the rejection of the use of FirewallD does not adversely affect the developed system, because the functionality and capabilities of IPtables allow to perform equally qualitative filtering of incoming, outgoing and transit traffic.

The IPtables packet filter is a part of the Netfilter firewall built into the Linux kernel and it allows to filter traffic according to the predefined rules. The IPtables architecture includes three general terms: the chain, the table, and the rule. Chains can be basic (created by default - PREROUTING, INPUT, FORWARD, OUTPUT and POSTROUTING) and are user-defined ones. PREROUTING is a chain designed for initial processing of incoming packets; INPUT processes incoming packets destined for this host; FORWARD processes all packets passing through the firewall; OUTPUT is designed to handle outbound packets; POSTROUTING provides final processing of outgoing packets. For the independent creation, configuration or destruction of chains, user-space utility iptables is provided.

The chains under consideration contain the following standard tables: raw, mangle, nat, and filter. The raw table is designed for passing packets before they are sent to the connection tracer. It enables to specify packets that do not need to be processed by the state detection mechanism by marking them as “notrack”. This table is contained in the chains PREROUTING and OUTPUT. The mangle table is designed for modifying the headers of IP packets (TOS - Type of Service, TTL - Time To Live) and is contained in all the basic chains. Nat is a table required to perform Network Address Translation (NAT): Destination Network Address Translation (DNAT), Source Network Address Translation (SNAT), MASQUERADE—similar to SNAT address translation capable of working with dynamic IP addresses. Only the first packet from the chain passes the Nat table; address translation or masking is applied automatically to the remaining packets. Nat is contained in the chains PREROUTING, OUTPUT and POSTROUTING.

After the packet arrives at the firewall, it enters the network device and passes a number of kernel checks. Next, the IP datagram passes the PREROUTING chain and, depending on its purpose, is passed either to the FORWARD or the INPUT chain. After passing the INPUT chain, the packet is transferred to the local application, then, if necessary, the response packet is formed and sent to the OUTPUT chain. After passing the OUTPUT chain (or the FORWARD in case the packet was transit), the packet is sent to the postprocessing chain POSTROUTING.

The conntrack state detection mechanism is a Netfilter component that provides a classification of packets by their connections. The functions of this module include tracking the states of both individual and connected connections (for example, ICMP responses to TCP packets).

The transmitted packets can be assigned four states: new, related, established, and invalid. The new status means that the packet belongs to a new connection. The established status is set if the connection already exists; to obtain this status it is enough that the host of the network transmits the packet and receives a response from the other host. Packages belonging to child connections (having established status) are marked as related, and those that cannot be explicitly identified receive the invalid status.

To manage the conntrack module, a conntrack-tools package is provided, which includes a conntrack tool that provides tracking the establishment of new connections and

monitoring changes to the existing ones. It also allows editing the connection tables and filtering the output. In addition, conntrack-tools include the conntrackd daemon, which is designed for synchronizing the state tables with other nodes.

The use of connection state detection mechanism allows to create reliable rule sets and perform a stateful filtering of traffic, which enables to manage without searching in the rule set by using the "keep state" option.

The extension of IPtables capabilities requires the installation of additional modules that allow to counter network threats.

Xtables-addons differs from its predecessor patch-o-matic in its simplicity of installation and maintenance due to the absence of necessity to rebuild the Linux kernel and IPtables. In addition, the compatibility problem is solved: for the correct functioning of this set of modules, it is necessary to use the kernel 2.6.17 version and higher and IPtables 1.4.3 version.

The developed system uses three Xtables-addons tools: tarpit, delude and chaos.

The tarpit tool is used to create a trap for the attacker: after opening an incoming TCP connection, the TCP window size is set to zero, which prevents the attacker from correctly closing the connection until the timeout expires. These actions create an imitation of the connection hanging and cause the attacker to spend time and computing resources without exerting undesirable influence on the protected system.

The delude tool is used to emulate open ports: in response to a request to establish a connection by sending SYN packets (Sequence Number) SYN/ACK packets (Acknowledgment Number) are sent, which creates a simulation of the open port that receives the connection; in response to other packets, an RST packet (reset) is sent to terminate the connection. This application of the delude tool effectively counteracts port scanning by misleading an attacker.

The chaos tool performs one of the following operations: tarpit, delude, reject (resetting connection and sending the notification of unavailability of the node) and drop (resetting connection without sending the notification of unavailability of the node) for all new TCP connections with the indicated probability [7, 8].

C. Centralized Logging Server

System events registration is performed by using a centralized Rsyslog server, to which events from various network devices are redirected.

The main Rsyslog configuration file is *rsyslog.conf*, which includes a number of modules, configuration directives, templates and a ruleset.

Modules are divided into functional groups: input modules responsible for receiving messages from various sources (*imudp* – using of UDP protocol, *imsock* – receiving local messages via a socket, *imklog* – receiving kernel messages, *imtcp*, *imrelp* – using TCP and RELP protocols), output modules used to write messages (*omsnmp* – sending SNMP traps, *onmail* – sending messages by e-mail, *onmysql*,

ompgsql – writing to MySQL and PostgreSQL databases), parser modules, string generator modules and message modification modules.

The configuration directives define the general parameters of the *rsyslogd* daemon, for example, the loading of modules (*\$ModLoad*) or the maximum size of the queue (*\$MainMessageQueueSize*).

Templates allow defining the format of output messages and using dynamic log file names. Templates are set before they are used in the rules.

The rules consist of a selector and an action, separated by a tab or space. The selector is a record formed as *facility.priority*. Facility may be represented as *authpriv*, *cron*, *daemon*, *kern*, *lpr*, *mail*, *news*, *syslog*, *user*, *uucp* and *local0-local7*. Priority is set as *emerg*, *alert*, *crit*, *err*, *warn*, *notice*, *info* and *debug*. Before logging each message is checked against the selectors. Messages are suitable with the facility equal to those specified in the selector and a priority is equal to or higher than specified. If a match is established, the action specified in the rule is executed.

Rsyslog allows using variable values as a selector (*msg*, *hostname*, *fromhost*, *fromhost-ip*, *syslogtag*), which provides performing the filter of the events based on the RainerScript language and the filter based on message properties. The basis of RainerScript language is the "if then else" construction.

Thus, after the message arrives in the Rsyslog system by some input module, it passes a check against the selectors specified in the rules. In the case of matching the selector, before the action is performed, the message is transformed using the appropriate template. If the template is not specified, the one indicated in the global parameters or the default template is applied. After applying the action defined by the rule, the message is sent to the specified location (in this case in the MySQL database using the *onmysql* output module).

D. Security Information and Event Management System

The SIEM-system is used as an auxiliary tool for IDS/IPS in the network security control system. SIEM is not capable of effectively countering attempts to penetrate the network and other types of network threats on its own. These systems analyze and correlate events coming from different sources and allow identifying complex distributed attacks based on accumulated statistics. Deviation from norms is detected by using its own correlation rules.

In the developed system, the Prelude OSS is used as the SIEM-system. The commercial version of the Prelude provides more functionality, including the ability to send data to SIEM through the SDEE (Security Device Event Exchange) standard; however, in this study, the priority is to use the free version of the program. Among the advantages of this system is the flexibility, scalability and connectivity of any source that writes the log.

Architecture of Prelude includes a manager, an LML (Log Monitoring Lackey) agent, the correlation module, the database storing the system-processed events, and the interface subsystem Prewikka. The manager is the main component of the system that accepts normalized events

from LML agents and outside systems and writes the received information to the database. The security events management agent is responsible for receiving logs from various systems and translating them into a single standard view (normalization). The correlation module correlates the events arriving to the manager, in accordance with the set of rules compiled by the system administrator. Due to the connection the Python scripts to this module, the system administrator has the ability to describe any correlation rules.

Events are sent to the Prelude system through SNMP traps. To process the data from the sources, Intrusion Detection Message Exchange Format (IDMEF) is used.

The scheme of the Prelude system functioning is shown on Fig. 3:

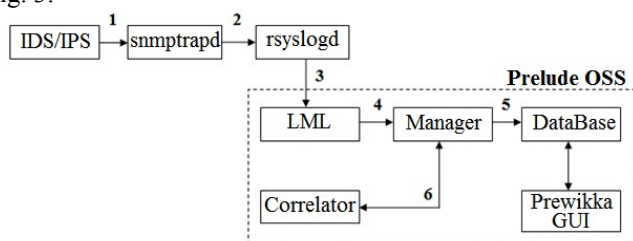


Fig. 3. The scheme of the Prelude system functioning.

- 1) IDS/IPS detects an attack and sends SNMP-trap;
- 2) SNMP-trap is transmitted to syslog;
- 3) Rsyslogd writes the received message to a file;
- 4) The security events management agent normalizes the log and maps the required values to standard IDMEF fields;
- 5) The normalized event is passed to the manager, which writes the event to the database and after that it becomes possible to display it through Prewikka.
- 6) Events received from the IDS / IPS can also be sent to the correlation module.

In the designed system the Prelude OSS system collects information from the Rsyslog server and the Bro system. Prelude provides an opportunity to identify violations of network security policies and create reports on incidents. In the event that suspicious activity is detected, the Prelude sends information about the intruder to the IDS/IPS.

V. CONCLUSION

This paper describes a possible approach to the protection of information systems from active and passive traffic analysis tools, and also the work of the Intrusion Detection and Prevention System module functioning on the basis of the developed algorithm.

The proposed solution involves non-standard means of implementing information security of corporate networks that impede to predict the security system response and cause an attacker spend time and computer resources to accurately analyze the vulnerabilities of the system. These results are achieved by simulating the hang of the connection, giving false information about the system being attacked and performing a hidden redirection of the information flows of the attacker. The developed system provides protection of the network either from common network threats (DoS and DDoS attacks, MitM attacks) or previously unknown ones.

In addition, the described module makes it possible to actively protect information resources by performing a series of response actions that allow identifying the attacker and forcing him to stop the attack [9].

Using the described concept of implementing complex protection of computer networks in combination with known methods of protecting the data transfer process will significantly reduce the threats of interception of data and the removal of the node from the state of availability.

The research was carried out with the support of the Foundation for Assistance to Small Innovative Enterprises in Science and Technology, a state non-profit organization in the form of a federal state budget institution established in accordance with Resolution No. 65 of the Government of the Russian Federation on February 3, 1994.

REFERENCES

- [1] Basinya E. A. On encryption and anonymization with the issues of information security / E. A. Basinya, G. A. Frantsuzova, A. V. Gunko // Computer technologies in science, production, social and economic processes: materials of the 14th intern. sci. conf., Russia, Novocherkassk, 12 Dec. 2013. – Novocherkassk: SRSPU(NPI), 2014. – P. 165-168. (In Russian)
- [2] Basinya E. A. Protection against the falsification of information resources / E. A. Basinya, S. V. Kazarbin // Perspective development of science, techniques and technology : Proc. 6th intern. sci. conf., Russia, Kursk, 20-21 Oct. 2016. – Kursk, 2016. – P. 16–19. (In Russian)
- [3] Basinya E. A. Methods of self-organization in providing network security / E. A. Basinya, G. A. Frantsuzova, A. V. Gunko // Global Science and Innovation: materials of the 1st intern. sci. conf., USA, Chicago, 17–18 Dec. 2013. – Chicago: Accent Graphics communications 2013. – Vol. 2. – P. 386-389.
- [4] Frantsuzova G. A. Self-organizing system for the computer network traffic management: a method of countering network threats / G. A. Frantsuzova, A. V. Gunko, E. A. Basinya // Software Engineering. – 2014. – iss. 3. – P. 16-20. (In Russian)
- [5] Detecting distributed network traffic anomaly with network-wide correlation analysis [Text] / Li Zonglin [et al.] // EURASIP Journal on Advances in Signal Processing. – 2009. – Vol. 2009. – Art. 2. – (Special issue on signal processing applications in network intrusion detection systems).
- [6] Ma, Ruhui Network anomaly detection based on wavelet fuzzy neural network with modified QPSO [Text] / Ruhui Ma, Yuan Liu, Xing Lin // International Journal of Distributed Sensor Networks. – 2009. – Vol. 5, iss. 1. – P. 49.
- [7] Basinya E. A. Design and study of the metadata management system for images / E. A. Basinya, A. V. Safronov // Actual problems of electronic instrument engineering (APEIE-2016) : materials of the. 13th intern. sci. conf., Russia, Novosibirsk, 3–6 Oct. 2016. – Novosibirsk: Publ. NSTU, 2016. – Vol. 9. – P. 155-157. – ISBN 978-5-7782-2991-4. (In Russian)
- [8] Basinya E. A. Implementation and research of an Intrusion Detection and Prevention System module / E. A. Basinya, Y. K. Radvovich // Modern materials, techniques and technologies. – 2016. – iss. 2 (5). – P. 26–32. (In Russian)
- [9] Research Institute of Information and Communications Technologies: [WEB resource]. N., 2016. URL: <https://nii-ikt.ru/>. (visit date: 23.04.2018).



Basinya Evgeny Alexandrovich defended his PhD thesis in 2015. He continued his teaching and research activities as an associate professor at the automation department in the Novosibirsk State Technical University. In 2016, he set up the Research Institute of Information and Communications Technologies with the support of the Foundation for Assistance to Small Innovative Enterprises in Science and Technology and is now its director.



Ravtovich Yuliya Konstantinovna is engaged in scientific activities and software development under the leadership of E.A. Basinya, starting with the bachelor's and master's degrees of the Novosibirsk State Technical University. Gold medal winner of the all-Russian scientific conference "Science. Technologies. Innovations" in the section "Automation and Information Security", conducted by the Novosibirsk State Technical University in 2016.

A Polynomial Method for Synthesizing a Two-channel Regulator Stabilizing a Three-mass System

Kurbonmurod M. Bobobekov

Novosibirsk State Technical University, Novosibirsk, Russia

Abstract – The method of synthesizing linear multichannel regulators for multichannel objects using matrix polynomial expansion, along with classical synthesis methods, such as synthesis in the state space, using full and reduced order observers, and others, is finding increasingly widespread. In the polynomial method of synthesizing multichannel regulators, as a rule, a transition from polynomial representations to matrix numeric ones is used, which in some cases leads to equations with a degenerate Sylvester matrix. In this paper, based on the results obtained by Chen, Kailath and other authors, a detailed formalized synthesis algorithm is presented based on the formalization of algorithms for the synthesis of multichannel systems, analysis of calculations of numerous examples of multichannel regulators. The proposed algorithm allows us to find the general solution of a system of linear equations. As a result, we obtained polynomial regulator matrices containing free parameters that can be set arbitrarily. In other words, when setting free parameters of the controller, it becomes possible to obtain a variety of polynomial matrices of the "numerator" and "denominator" of the regulator, which makes it possible to provide additional properties of the automatic control system. The proposed algorithm synthesizes a two-channel regulator that stabilizes the three-mass system and provides exactly the desired characteristic polynomial matrix of the system.

IndexTerms – Matrix transfer function, right matrix polynomial decomposition, the coprime decomposition, polynomial matrices, linear equation, synthesis of multichannel systems, Sylvester matrix, algorithm for synthesis of multichannel regulators, matrix characteristic equation.

I. INTRODUCTION

MANY TECHNICAL systems are systems that regulate several variables, or, we might say, multi-channel systems. In connection with the continuous development of technical systems and their complication, the regulators used for them become more and more complex, and therefore more expensive in cost and labor-intensive in operation. However, at the present time, the developed control algorithms do not always correspond to the tasks set. Thus, the task of formalizing the synthesis of multi-channel controllers is quite relevant.

In the theory of automatic control, the problem of synthesizing linear multichannel regulators occupies a special place, for example, because of the use of matrix equations, polynomial matrix calculus, because of the complication of such classical concepts as zeros and poles of multi-channel systems, the transition from the characteristic polynomial to the characteristic matrix, etc.

Methods of synthesis of multichannel systems are described in many works (textbooks), for example, in the works

of the following domestic and foreign authors: Andreyev YU.N., Aleksandrov A.A., Voronov V.V., Gayduk A.R., Kim D.P., Chen C.T., Kailath T., Doyle J.C., Dorf R.C., Antsaklis P.J. and etc. Research in this area can be found in dissertations, for example in dissertations Meleshkin A. I., Voronov V. V., Shoby E. V. [4–6] and others.

This paper is a continuation of the author's research [7-13, 17, 20, 22, 24] and is devoted to the analysis and synthesis of linear multichannel control systems by the polynomial method. A technique is proposed for the synthesis of multichannel regulators using the matrix polynomial fraction of the transfer function of an object on the basis of the theorems given in [1, Theorem 9.M2, p.296] and on the basis of the algorithms given in the above dissertations [4-6], and in the works author's [7-9, 17]. Synthesis algorithms in the above-mentioned works were illustrated by the example of synthesis of a two-channel regulator stabilizing a three-mass system in two coordinates. Unfortunately, the desired characteristic matrix of the system is implemented approximately, for example, [6, pp.77, 15, p.49], which indicates the possibility of improving synthesis algorithms.

II. PROBLEM DEFINITION

In this paper, we propose a synthesis algorithm that makes it possible to eliminate the shortcomings of previously developed algorithms. The efficiency of the proposed algorithm is demonstrated by the example of synthesis of a two-channel regulator stabilizing a three-mass system.

In algorithms [1, 4-6, 15, 16], as a rule, linearly dependent rows are set to zero in order to reduce the Sylvester matrix to a non-degenerate form. Also in a number of works [6, 15, 16] pre-set the column degrees of polynomial matrices of the "denominator" Y and the "numerator" X of the regulator, and then some columns are set to zero, which sometimes allows us to find a solution of the system of linear equations and, consequently, to synthesize the regulator. Such solutions, in fact, are particular solutions of a system of equations including the Sylvester matrix. A very important question is the correct choice of the row degrees of the regulator m_i , assuming that the object description is used in the form of a right polynomial fraction.

$$W_{ob}(s) = N_r(s)D_r^{-1}(s),$$

where $W_{ob}(s)$ – matrix transfer function of the object with p inputs and p outputs, $N_r(s)$ and $D_r(s)$ – polynomial matrices corresponding to right decomposition.

In this paper, it is suggested that linearly dependent rows of the Sylvester matrix not be deleted, but transferred to the right with the corresponding columns of the matrix from unknown coefficients

$$(Y_0 \ X_0 \ Y_1 \ X_1 \ \dots \ Y_m \ X_m),$$

where Y_i and X_i matrix order $p \times p$ – "coefficients" of matrix

$$\text{polynomials } Y(s) = \sum_{i=0}^m Y_i s^i, \quad X(s) = \sum_{i=0}^m X_i s^i.$$

As a result, we obtain a general solution of a system of linear equations, including free parameters that allow us to satisfy additional requirements for an automatic control system.

When solving the problem of synthesizing multi-channel controllers, there are different options for selecting the polynomial matrices of the controller $Y(s)$ and $X(s)$, for example, if the object is given in the form of a left fraction, then the regulator is selected in the form of a right fraction and vice versa. Consider the system "regulator – object – a unity feedback". In our case, the object is given in the form of a right polynomial fraction of $W_{ob}(s) = N_r(s)D_r^{-1}(s)$, and the regulator is chosen in the form of a left fraction $W_r(s) = Y_l^{-1}(s)X_l(s)$. In our case, the object is given in the form of a right polynomial fraction of $W_{ob}(s) = N_r(s)D_r^{-1}(s)$, and the regulator is chosen in the form of a left fraction of $W_r(s) = Y_l^{-1}(s)X_l(s)$. The transfer function of a closed system can be written as:

$$W_{cl}(s) = N_r(s)(Y_l(s)D_r(s) + X_l(s)N_r(s))^{-1} X_l(s),$$

where $Y_l(s)D_r(s) + X_l(s)N_r(s)$ – is equal to the desired characteristic matrix $C(s)$. To solve the problem, go from a polynomial equation to a system of linear equations with matrix coefficients of the form

$$(Y_0 \ X_0 \ Y_1 \ X_1 \ \dots \ Y_m \ X_m) \mathfrak{R}_m = (C_0 \ C_1 \ \dots \ C_{m+\mu}).$$

Here \mathfrak{R}_m – Sylvester matrix. Further, we use the notation:

$$\bar{C} = (C_0 \ C_1 \ \dots \ C_{m+\mu}), \quad \mathfrak{S} = (Y_0 \ X_0 \ Y_1 \ X_1 \ \dots \ Y_m \ X_m).$$

III. ALGORITHM OF THE SYNTHESIS OF REGULATORS

More often the object under investigation is described in the form of differential equations. In order to consider the synthesis problem, it is necessary to go from the differential equations to the Laplace image, namely, the derivative " d/dt " is replaced by the operator " s ". Further, it is easy to obtain the left polynomial matrix fraction $D_l^{-1}(s)N_l(s)$, and then, calculate by left fraction the right polynomial fraction

$$D_l^{-1}(s)N_l(s) \rightarrow N_r(s)D_r^{-1}(s).$$

After this, we can consider the problem of synthesizing the regulator. However, you first need to check the following requirements for the object: coprime (mutual simplicity), strict propriety, and column reducibility of the matrix $D_r(s)$ of a right polynomial fraction.

Below is the algorithm for synthesizing multi-channel regulators for the case when an object is described as a right polynomial fraction.

The algorithm for synthesizing multichannel regulators consists of the following steps:

- Knowing the column degrees μ_i and the row degrees ν_i object, we select the row degrees m_i of the regulator and write out the polynomial matrices of the numerator and denominator of the regulator

$$X(s) = X_0 + X_1 s + \dots + X_m s^m, \quad Y(s) = Y_0 + Y_1 s + \dots + Y_m s^m.$$

- Select the structure and degree of the characteristic polynomial matrix of the system $C(s)$: $f \triangleq \max_i(f_i)$, where

$$f_i = m_i + \mu_i, \quad i = \overline{1, p} \text{ and write it:}$$

$$C(s) = C_0 + C_1 s + \dots + C_f s^f.$$

- Create a system of linear equations $\mathfrak{S}\mathfrak{R}_m = \bar{C}$.

- Check the rank of the matrix \mathfrak{R}_m , delete the zero columns of the matrices \mathfrak{R}_m and \bar{C} and denote by: $\mathfrak{R}_m \rightarrow \tilde{\mathfrak{R}}_m$, $\bar{C} \rightarrow \bar{C}_1$. If no zero columns, then skip this step.

- Create a system of linear equations of the form $\mathfrak{S}\tilde{\mathfrak{R}}_m = \bar{C}_1$.

- Find the linearly dependent rows of the matrix $\tilde{\mathfrak{R}}_m$ from top to bottom (delete the lines in turn); transfer to the right linearly dependent rows from the matrix $\tilde{\mathfrak{R}}_m$ with the corresponding columns from the matrix \mathfrak{S} and create a system of linear equations $\mathfrak{S}_1 \hat{\mathfrak{R}}_m = \bar{C}_2$. Here

$$\bar{C}_2 = \bar{C}_1 - (j_1 r_1 + \dots + j_k r_i),$$

where $j_1 r_1$ – the product of the first column of the matrix \mathfrak{S} and the first row of the matrix $\tilde{\mathfrak{R}}_m$, ..., $j_k r_i$ – the product of the k 'th column of the matrix \mathfrak{S} and the i 'th row of the matrix $\tilde{\mathfrak{R}}_m$, (r_1, \dots, r_i – linearly dependent rows).

- Solve the equation $\mathfrak{S}_1 \hat{\mathfrak{R}}_m = \bar{C}_2$: $\mathfrak{S}_1 = \bar{C}_2 \hat{\mathfrak{R}}_m^{-1}$

- Restore \mathfrak{S} to \mathfrak{S}_1 : (corresponds to return from $\hat{\mathfrak{R}}_m$ to $\tilde{\mathfrak{R}}_m$ and from \bar{C}_2 to \bar{C}_1).

- Write the polynomial matrices $X(s)$ and $Y(s)$; computation check – by the known $N(s)$, $D(s)$, $X(s)$ and $Y(s)$ calculation of the characteristic polynomial matrix $C(s)$. **End of algorithm.**

The efficiency of the synthesis algorithm is demonstrated using the example of calculating a regulator stabilizing a three-mass system consisting of three masses m_i , $i = \overline{1, 3}$ in series connected by springs with rigidity k_i , $i = \overline{1, 3}$. The coordinates y_i , $i = \overline{1, 3}$ are directed from top to bottom and the numbering corresponds to the numbers of masses. It is assumed that to the masses m_1 and m_2 , two control signals

are applied (force) - u_1 and u_2 . The output quantities are the coordinates of the masses y_1 and y_2 , counted from the equilibrium state. The system is described by three second-order differential equations [14, 16]:

$$\begin{aligned} m_1 s^2 y_1 + d_1 s y_1 + (k_1 + k_2) y_1 - k_2 y_2 &= u_1, \\ -k_2 y_1 + m_2 s^2 y_2 + d_2 s y_2 + (k_2 + k_3) y_2 - k_3 y_3 &= u_2, \\ -k_3 y_2 + m_3 s^2 y_3 + d_3 s y_3 + k_3 y_3 &= 0. \end{aligned}$$

where d_i , $i = \overline{1, 3}$ – coefficient of damping. Set the following object parameters [14]:

$$m_1 = m_2 = m_3 = 1, \quad d_1 = d_2 = d_3 = 0 \quad k_1 = k_2 = 2 \text{ и } k_3 = 4.$$

IV. EXAMPLE

If we go over to Laplace images, we obtain the left matrix polynomial fraction of the transfer function of the object

$$\underbrace{\begin{bmatrix} s^2 + 4 & -2 \\ -2(s^2 + 4) & (s^2 + 6)(s^2 + 4) - 16 \end{bmatrix}}_{D_l} y(s) = \underbrace{\begin{bmatrix} 1 & 0 \\ 0 & s^2 + 4 \end{bmatrix}}_{N_l} u(s)$$

The paths of the transition from the left polynomial fraction to the right one are given in [14].

The object is given in the form of a right matrix polynomial fraction with two inputs and two outputs 2×2 [5, 6, 15, 16]:

$$D_r(s) = [d_r^{ij}(s)]_{2 \times 2}, \quad N_r(s) = [n_r^{ij}(s)]_{2 \times 2}, \quad (1)$$

where

$d_r^{11}(s) = 16(s^2 + 4)$, $d_r^{12}(s) = -2(s^2 + 4)$, $d_r^{21}(s) = -32$,
 $d_r^{22}(s) = s^4 + 10s^2 + 8$, $n_r^{11}(s) = 16$, $n_r^{12}(s) = 0$, $n_r^{21}(s) = 0$,
 $n_r^{22}(s) = s^2 + 4$. Thus column degrees (column indices) of the object are equal $\mu_1 = 2$, $\mu_2 = 4$, we select $\mu = \max(\mu_1, \mu_2) = 4$. Row degrees (rowindex) ν_i are determined by left fraction [14] – $\nu_1 = 2$, $\nu_2 = 4$, whence $\nu = \max(\nu_1, \nu_2) = 4$. The sum of the column degrees of the object is equal to the degree of the determinant $\mu_1 + \mu_2 = n = \det D_r(s) = 6$, that is, the matrix $D_r(s)$ is the column reduced. We write out the right polynomial representation of the object:

$$\begin{aligned} D_r(s) &= D_0 + D_1 s + D_2 s^2 + D_3 s^3 + D_4 s^4, \\ N_r(s) &= N_0 + N_1 s + N_2 s^2 + N_3 s^3 + N_4 s^4. \end{aligned} \quad (2)$$

Here

$$\begin{aligned} D_1 = D_3 = 0, \quad D_4 &= \text{diag}\{0, 1\}, \quad D_0 = \begin{bmatrix} 64 & -8 \\ -32 & 8 \end{bmatrix}, \quad D_2 = \begin{bmatrix} 16 & -2 \\ 0 & 10 \end{bmatrix}, \\ N_1 = N_3 = N_4 &= 0, \quad N_0 = \text{diag}\{16, 4\}, \quad N_2 = \text{diag}\{0, 1\}. \end{aligned}$$

To form a system of linear equations of the form

$$Y(s)D(s) + X(s)N(s) = C(s), \quad (3)$$

including the polynomial matrices of the regulator $X(s)$, $Y(s)$ and the desired characteristic polynomial matrix $C(s)$,

we select the row degrees of the regulator by formula $m_i \geq \nu - 1$ [3]: we take $m = m_1 = m_2 = \nu - 1 = 3$. We can write out the polynomial matrices of the "numerator" and "denominator" of the regulator

$$\begin{aligned} X(s) &= X_0 + X_1 s + X_2 s^2 + X_3 s^3, \\ Y(s) &= Y_0 + Y_1 s + Y_2 s^2 + Y_3 s^3. \end{aligned}$$

To calculate the desired matrix, we calculate the column degrees of $C(s)$ for each channel $f_i = m_i + \mu_i$ where $i = 1, 2$. The structure of the characteristic matrix is given by the diagonal structure. Thus, the column degrees of $C(s)$ are equal $f_1 = m_1 + \mu_1 = 5$ and $f_2 = m_2 + \mu_2 = 7$. This enable find the proper regulator. Set the roots of the first $\{-1, -1, -1, -1, -1\}$ and on the second channel $\{-1, -1, -1, -1, -1, -1, -1\}$, i.e

$$C(s) = \text{diag}\{(s+1)^5, (s+1)^7\}, \quad (4)$$

whence

$$C(s) = C_0 + C_1 s + C_2 s^2 + C_3 s^3 + C_4 s^4 + C_5 s^5 + C_6 s^6 + C_7 s^7.$$

Here $C_0 = \text{diag}\{1, 1\}$, $C_1 = \text{diag}\{5, 7\}$, $C_2 = \text{diag}\{10, 21\}$,

$C_3 = \text{diag}\{10, 35\}$, $C_4 = \text{diag}\{5, 35\}$, $C_5 = \text{diag}\{1, 21\}$,

$C_6 = \text{diag}\{0, 7\}$, $C_7 = \text{diag}\{0, 1\}$.

We pass from the polynomial matrix equation to the system of linear equations (3) with numerical coefficients, for which we equate the matrix coefficients at s with the same degrees:

$$\Im \mathfrak{R}_m = \bar{C}, \quad (5)$$

where

$$\Im = (Y_0 \mid X_0 \mid Y_1 \mid X_1 \mid Y_2 \mid X_2 \mid Y_3 \mid X_3),$$

$$\mathfrak{R}_m = \begin{pmatrix} D_0 & D_1 & D_2 & D_3 & D_4 & O & O & O \\ N_0 & N_1 & N_2 & N_3 & N_4 & O & O & O \\ O & D_0 & D_1 & D_2 & D_3 & D_4 & O & O \\ O & N_0 & N_1 & N_2 & N_3 & N_4 & O & O \\ O & O & D_0 & D_1 & D_2 & D_3 & D_4 & O \\ O & O & N_0 & N_1 & N_2 & N_3 & N_4 & O \\ O & O & O & D_0 & D_1 & D_2 & D_3 & D_4 \\ O & O & O & N_0 & N_1 & N_2 & N_3 & N_4 \end{pmatrix},$$

$$\bar{C} = (C_0 \mid C_1 \mid C_2 \mid C_3 \mid C_4 \mid C_5 \mid C_6 \mid C_7).$$

Here O – the zero matrix of order 2×2 , $Y_0, Y_1, Y_2, Y_3, X_0, X_1, X_2, X_3$ – unknown parameters (matrix) of order 2×2 controller with elements y_{ij}^k and x_{ij}^k . In expanded form the matrix with unknown coefficients \Im and the matrix \bar{C} take the form:

$$\Im = \begin{bmatrix} 1 & 2 & 3 & 4 & 5 & 6 & 7 & 8 \\ y_{11}^0 & y_{12}^0 & x_{11}^0 & x_{12}^0 & y_{11}^1 & y_{12}^1 & x_{11}^1 & x_{12}^1 \\ y_{21}^0 & y_{22}^0 & x_{21}^0 & x_{22}^0 & y_{21}^1 & y_{22}^1 & x_{21}^1 & x_{22}^1 \end{bmatrix}$$

$$\bar{C} = \begin{bmatrix} 1 & 0 & 5 & 0 & 10 & 0 & 10 & 0 & 5 & 0 & 1 & 0 & 0 & 0 & 0 & 0 \\ 0 & 1 & 0 & 7 & 0 & 21 & 0 & 35 & 0 & 35 & 0 & 21 & 0 & 7 & 0 & 1 \end{bmatrix}$$

Also, if we substitute the values of N_i and D_i (these are the matrix coefficients for the right expansion) from (2) into the Sylvester matrix \mathfrak{R}_m , we get a matrix order $2p(m+1) \times (\mu+m+1)p = 16 \times 16$, the rank of which is fourteen. The number of zero columns can be calculated from the formula $\alpha = p\mu - n = 2$, which corresponds to the columns of the 13th and 15th matrices \mathfrak{R}_m and \bar{C} . After their delete, the rank remains equal 14; we introduce the new denote $\mathfrak{R}_m \rightarrow \tilde{\mathfrak{R}}_m$, $\bar{C} \rightarrow \bar{C}_1$; equation (5) is transformed

$$\mathfrak{Z}\tilde{\mathfrak{R}}_m = \bar{C}_1.$$

The matrix $\tilde{\mathfrak{R}}_m$ became the order 16×14 , and the matrix \bar{C}_1 – order 2×14 . Further, in order for the matrix $\tilde{\mathfrak{R}}_m$ to become square, it is necessary to transfer two linearly dependent rows to the right; rows must be chosen such that the rank of the matrix $\tilde{\mathfrak{R}}_m$ remains equal to 14. In [6, 15, 16], a special case is considered when the transferred rows are nullify. In Table I provides information on which lines can be moved to the right (when you delete these lines in turn, the rank does not decrease); they are marked "+". For example, at cross out the 1st row, (look at the left the table), for example, the 5th row (look at the column) at the intersection is "+" – these rows can be crossed out. From the analysis of Table I it follows that there are several solutions.

TABLE I
THE ROWS, ALLOWED FOR TRANSFER (DELETE)

| № rows | 1 | 3 | 4 | 5 | 7 | 8 | 11 | 15 |
|--------|---|---|---|---|---|---|----|----|
| 1 | | – | – | + | + | + | – | + |
| 3 | | | – | + | + | + | – | + |
| 4 | | | | + | + | + | – | + |
| 5 | | | | | – | – | + | – |
| 7 | | | | | | – | + | – |
| 8 | | | | | | | + | – |
| 11 | | | | | | | | + |
| 15 | | | | | | | | |

For example, rows 1 and 7 of the matrix $\tilde{\mathfrak{R}}_m$ we transfer to the right with the corresponding columns of the matrix \mathfrak{Z} ; after the transfer we denote $\mathfrak{Z} \rightarrow \mathfrak{Z}_1$, $\tilde{\mathfrak{R}}_m \rightarrow \hat{\mathfrak{R}}_m$, $\bar{C}_1 \rightarrow \bar{C}_2$ and we obtain:

$$\mathfrak{Z}_1 \hat{\mathfrak{R}}_m = \bar{C}_2, \quad (6)$$

where $\bar{C}_2 = \bar{C}_1 - (q_1 + q_2)$,

$$q_1 = \begin{pmatrix} y_{11}^0 \\ y_{21}^0 \end{pmatrix} (64 - 8 \ 0 \ 0 \ 16 - 2 \ 0 \ 0 \ 0 \ 0 \ 0 \ 0 \ 0 \ 0),$$

$$q_2 = \begin{pmatrix} x_{11}^1 \\ x_{21}^1 \end{pmatrix} (0 \ 0 \ 16 \ 0 \ 0 \ 0 \ 0 \ 0 \ 0 \ 0 \ 0 \ 0 \ 0 \ 0 \ 0 \ 0).$$

Because the matrix $\hat{\mathfrak{R}}_m$ square and nonsingular, it is easy to find the \mathfrak{Z}_1 from (6) – $\mathfrak{Z}_1 = \bar{C}_2 \hat{\mathfrak{R}}_m^{-1}$. As a result, we obtain

$$\mathfrak{Z}_1 = \begin{bmatrix} 0 & 0,0625 - y_{11}^0 & 2y_{11}^0 & 0,312 - x_{11}^1 & 0 \\ 26,2 & 52,4 - y_{21}^0 & 2y_{21}^0 - 52,1 & -x_{21}^1 - 9,38 & -4,69 \end{bmatrix}$$

$$\begin{bmatrix} 0,625 - 2x_{11}^1 & 0,312 & 0 & 0,312 - y_{11}^0 & 0,625 \\ -2x_{21}^1 - 7,62 & 0 & 7 & 14 - y_{21}^0 & -61,2 \end{bmatrix}$$

$$\begin{bmatrix} 0,0625 - x_{11}^1 & 0 & x_{11}^1 + 0,25 & 0,125 \\ 0 & 1 & x_{21}^1 + 11,4 & 15,7 \end{bmatrix},$$

where y_{11}^0 , y_{21}^0 , x_{11}^1 и x_{21}^1 free controller parameters that can be set arbitrarily. We restore \mathfrak{Z} to \mathfrak{Z}_1 , $\tilde{\mathfrak{R}}_m$ to $\hat{\mathfrak{R}}_m$ and also we return from \bar{C}_2 to \bar{C}_1 ; we write out the matrix of unknowns \mathfrak{Z}

$$\mathfrak{Z} = \begin{bmatrix} y_{11}^0 & 0 & 0,0625 - y_{11}^0 & 2y_{11}^0 & 0,312 - x_{11}^1 & 0 \\ y_{21}^0 & 26,2 & 52,4 - y_{21}^0 & 2y_{21}^0 - 52,1 & -x_{21}^1 - 9,38 & -4,69 \end{bmatrix}$$

$$\begin{bmatrix} x_{11}^1 & 0,625 - 2x_{11}^1 & 0,312 & 0 & 0,312 - y_{11}^0 & 0,625 \\ x_{21}^1 & -2x_{21}^1 - 7,62 & 0 & 7 & 14 - y_{21}^0 & -61,2 \end{bmatrix}$$

$$\begin{bmatrix} 0,0625 - x_{11}^1 & 0 & x_{11}^1 + 0,25 & 0,125 \\ 0 & 1 & x_{21}^1 + 11,4 & 15,7 \end{bmatrix}.$$

If we set free parameters equal:

$$y_{11}^0 = 1, \ y_{21}^0 = 0, \ x_{11}^1 = -0,688, \ x_{21}^1 = -9,38,$$

then we obtain polynomial matrices of the regulator:

$$Y(s) = \begin{bmatrix} 0,0625s^3 + 0,312s^2 + s + 1 & 0 \\ 0 & s^3 + 7s^2 - 4,69s + 26,2 \end{bmatrix},$$

$$X(s) = \begin{bmatrix} -0,44s^3 - 0,69s^2 - 0,69s - 0,94 \\ 2s^3 + 14s^2 - 9,38s + 52,4 \end{bmatrix} \cdot \begin{bmatrix} 0,125s^3 + 0,625s^2 + 2s + 2 \\ 15,69s^3 - 61,2s^2 + 11,125s - 52,125 \end{bmatrix}.$$

It can be make sure that the calculated regulator provides exactly (in contrast to, for example, [15]) the required characteristic matrix of the system, for which it suffices to substitute $X(s)$ and $Y(s)$ in $Y(s)D(s) + X(s)N(s)$, which should equal $C(s)$.

V. CONCLUSION

The paper compares the algorithms of polynomial synthesis of multichannel regulators proposed in [1–3] and developed in dissertational works [4–6]. Further formalization of the synthesis algorithm is given in [7–9], whose application for single-channel systems is described in [10–13], and for a multichannel object that is a three-mass system, which can be considered as a generalization of the two-mass system [19, 21–23], calculations are given in this paper. These calculations differ significantly from the calculations given in [14–16], which make it possible to provide approximately the desired characteristic matrix of the system. In [17, 24] it was proposed to use a two-parameter regulator to autonomization the system. To further develop the method, one can use the results given in [18–24].

In all the papers, the synthesis problem is solved on the basis of the theorem proved in [1, p.296]. The main requirements of the theorem - is coprime polynomial matrix right fraction, strictly proper of the object, a column of reducibility $D(s)$. In all methods, the transition from polynomial matrix equations to numerical matrix equations is used, the key in these equations is the Sylvester matrix. Chen suggests using the operator $[q, r] = qr(S')$, which allows finding line-dependent rows in the direction from top to bottom, and then removes them; by removing the zero columns, the Sylvester matrix becomes square and non-degenerate, which allows us to calculate the parameters of the regulator. This corresponds to the search for a specific solution – when zeroing the "extra" parameters of the regulator.

On the basis of algorithms for the synthesis of regulators in the above quoted works, a detailed algorithm for calculating multichannel regulators by a polynomial method is proposed based on the use of the Sylvester matrix, taking into account various possible variants of specifying the characteristic polynomial of a closed system, setting the regulator and allowing us to find the general solution of equation matrix of Sylvester. The proposed algorithm considers the case missed in the above works: in this paper, the linearly dependent rows of the Sylvester matrix with the corresponding columns from the matrix with unknown coefficients (regulator parameters) are transferred to the right-hand side of the system of linear equations. As a result, free parameters appear in the solution, which can be used in some way. Thus, an algorithm for the

synthesis of multichannel regulators is proposed for cases previously unaccounted.

REFERENCES

- [1] C.T. Chen, Linear system theory and design. 3rd ed. New York Oxford: Oxford University Press, 1999. – 334 P.
- [2] P. J. Antsaklis, A. N. Michel, Linear systems, New York: McGraw-Hill, 1997, 685 P.
- [3] Kailath. T. Linear Systems / T. Kailath – Englewood Cliffs, N.J.: Prentice Hall, 1980. – 350 P.
- [4] Meleshkin A.I. Modal synthesis of regulators of reduced order. Work of the Technical Sciences Candidate: Spec. 05.13.01 / E.V.Shoba; Novosibirsk State Technical University. – Novosibirsk, 1999. – 166 p. (In Russian).
- [5] Voronoy V.V. A polynomial method for calculating the multi-channel controllers low order. Work of the Technical Sciences Candidate: Spec. 05.13.01 / V.V.Voronoy; Novosibirsk State Technical University. – Novosibirsk, 2013. – 173 p. (In Russian).
- [6] Shoba E.V. The modal method for the synthesis of multi-channel dynamic systems using a polynomial expansion. Work of the Technical Sciences Candidate: Spec. 05.13.01 / E.V.Shoba; Novosibirsk State Technical University. – Novosibirsk, 2013. – 192 p. (In Russian).
- [7] Voevoda A. A., Bobobekov K.M. Solution of an overdetermined linear system of equations for polynomial synthesis of regulators // Modern technologies. System analysis. Modeling. 2017. Vol. 56, – no. 4. pp. 84–99. (In Russian).
- [8] Bobobekov K. M. About structural transformations of multichannel linear systems in the matrix polynomial representation // Science bulletin of the Novosibirsk state technical university, Novosibirsk. – 2017, no. 2 (67), pp. 7–25. (In Russian).
- [9] Voevoda A.A., Bobobekov K.M. Synthesis of linear multichannel regulators using structural transformations // Bulletin of the Astrakhan state technical university, 2017 no. 3, pp. 7–20. (In Russian).
- [10] Troshina G.V., Voevoda A.A., Bobobekov K.M. The Active Identification of Parameters for the Unstable Object // The 11th International Forum on Strategic Technology 2016. June 1 – June 3, 2016 Novosibirsk State Technical University, 2016. pp. 594 – 596.
- [11] Troshina G.V., Voevoda A.A., Bobobekov K.M. The Parameters Determination of the Inverted Pendulum Model in the Automatic Control System // Proc. of the XIII Intern. Conf. "Actual problems of electronic instrument engineering (APEIE-2016)" Novosibirsk. Novosibirsk State Technical University. 2016. P. 180 – 182.
- [12] Troshina G.V., Voevoda A.A., Bobobekov K.M. The periodic signals application for the estimation of the unstable object parameters // IOP Conf. Series: Journal of Physics: Conference series. – 2017. – Vol. 803. – Art. 012166 (5 p.). – URL: <http://iopscience.iop.org/article/10.1088/1742-6596/803/1/012166/pdf> (date: 26.04.2018).
- [13] Troshina G.V., Voevoda A.A., Bobobekov K.M. Unstable object parameters estimation with one input and two outputs in automatic control system // 18th International Conference of young specialists on micro/nanotechnologies and electron devices, EDM 2017: proc., Altai, Erlagol, 29 June – 3 July 2017. – Novosibirsk : NSTU, 2017. – P. 138–141.
- [14] Voevoda A.A., Shoba E.V. About diagonally decoupling for multi-input multi-output systems. Pt. 1 // Transaction of scientific papers of the Novosibirsk state technical university, Novosibirsk. – 2010, no. 2 (60), pp. 16–25. (In Russian).
- [15] Voevoda A.A., Shoba E.V. About diagonally decoupling for multi-input multi-output systems. Pt. 2 // Transaction of scientific papers of the Novosibirsk state technical university, Novosibirsk. – 2010, no. 3 (61), pp. 41–50. (In Russian).
- [16] Voevoda A. A., Chekhonadskikh A. V., Shoba E. V. Modal synthesis method using a polynomial expansion: traffic separation in the stabilization of three-mass system // Science bulletin of the Novosibirsk state technical university, Novosibirsk. – 2011, no. 2 (43), pp. 39–46. (In Russian).

- [17] Voevoda A.A., Bobobekov K.M. Avtonomnost' i astatizm v mnogokanal'noy sisteme s dvukhparametricheskimi regulyatorami // Transaction of scientific papers of the Novosibirsk state technical university, Novosibirsk. – 2017, no. 3 (89), pp. 7–31.
- [18] Bobobekov K.M. About rationing polynomials denominator object and regulator during polynomial method of synthesis // Transaction of scientific papers of the Novosibirsk state technical university, Novosibirsk. – 2016, no. 4 (86), p. 7–24. (In Russian).
- [19] Voevoda A.A. Stabilization of two-mass systems: modal synthesis method using polynomial factorization // Science bulletin of the Novosibirsk state technical university, Novosibirsk. – 2010, no. 1 (38), pp. 195–198. (In Russian).
- [20] Voevoda A.A., Bobobekov K.M. About the necessary conditions of existence of the solution in polynomial method of synthesis of single-channel systems // Transaction of scientific papers of the Novosibirsk state technical university, Novosibirsk. – 2017, no. 4 (90), pp. 7–21. (In Russian).
- [21] Voevoda A.A. Stabilization of the two-mass system: polynomial method of synthesis of two-channel system // Transaction of scientific papers of the Novosibirsk state technical university, Novosibirsk. – 2009, no. 4 (58), p. 121–124. (In Russian).
- [22] Bobobekov K.M. A polynomial method for the synthesis of single-channel two-mass system // Transaction of scientific papers of the Novosibirsk state technical university, Novosibirsk. – 2016, no. 4 (86), p. 25–36. (In Russian).
- [23] Voevoda A.A., Bobobekov K.M. Simulation of multichannel systems with singular objects in a polynomial matrix representation // International Scientific-Practical Conference "Independence – the basis for the development of the country's energy", December 22–23, 2017 – Bokhtar: IET Publishing, 2017. pp. 214–218. (In Russian).
- [24] Voevoda A.A., Bobobekov K.M. Calculation of controller parameters for the stabilization of the inverted pendulum by corner deviation // Transaction of scientific papers of the Novosibirsk state technical university, Novosibirsk. – 2016, no. 3 (85), pp. 18–32.



Bobobekov Kurbonmurod, specialist of the mechanical engineering technology, Tajik Technical University of the academician M. S. Osimi. The postgraduate student of the Automation department in Novosibirsk State Technical University (2015). The science interests and competence field are automation theory, control systems synthesis. He is the author of 25 science papers.

Development of a Monitoring and Management System for the Study of Energy-intensive Processes of Processing Agricultural Raw Materials

Alexey P. Borisov

Altai State Technical University, named by I.I. Polzunova, Barnaul, Russia

Abstract – The article is devoted to the development of a software and hardware complex for studying the grinding processes on a pendulum deformer and air movement in a cyclone separator, as well as the management of these processes. The hardware and software complex is based on Arduino and Raspberry Pi, as well as developed software that allows monitoring and monitoring of the grinding and separation process. The results of the research showed that the pendulum deformer makes it possible to determine the vitreousness of the grain with an error of no more than 2%, and also, due to the use of a new grinding method, to obtain a greater extraction of endosperm, and, consequently, to obtain more flour and croupodun products. The efficiency of the cyclone separator exceeded 99.5%, while the air flow rate was $376 \text{ m}^3 / \text{h}$, $472 \text{ m}^3 / \text{h}$ and $516 \text{ m}^3 / \text{h}$, and ΔP less than 600 Pa. The velocity in the inlet branch of the screw insert was 18-20 m / s, and at the exit of the screw insert the airflow velocity is 50-70 m / s.

Index Terms – Arduino, Raspberry Pi, grinding, separation, monitoring, control, management.

I. INTRODUCTION

THE ALTAI TERRITORY is one of the main regions that determine the country's grain potential. In this regard, the work that is carried out to improve the technological processes aimed at creating new methods for processing grain into flour are relevant, and this urgency can be most fully felt in the agro-industrial complex of the Altai Territory. The processes of grinding grain materials and separation of grinding products form the basis of many industries in various industries: food processing, processing of agricultural and feed mill products. Most of the energy resources are spent on these processes, they determine the yield and quality of the finished products.

In the technology of processing grain into flour, grinding and separation of the solid phase from the aerodisperse flow are the most important processes on which the rational use of grain, the yield of flour, baking and other advantages of the final product depend.

Grain and intermediate products, obtained during its processing, are crushed in rolling mills at modern flour mills. The efficiency of the grinding process, both in individual stages and throughout the technological process of grinding grain, essentially characterizes the state of the overall technological process of flour-milling, the rational use of basic technological equipment, determines the quality of

flour and the technical and economic indicators of the production process.

The basic process that changes the mechanical parameters of products in flour mills is the grinding of grain and grain products. It should be remembered that it is closely associated with other processes of grain processing, in particular - with sorting, which is the basis for the production of high-quality flour. The quality of grain is estimated by several indicators, characterizing its baking and flour-milling properties. Vitreousness is the most important indicator used in modern practical technology, which characterizes the ability of grain to croup. The properties of the grain depend on the tuning of the grinding machines of the entire line, so these properties must be known, in order to obtain a greater yield of flour and croup-din products. For example, depending on the vitreousness of the grain, various methods of preparing wheat for varietal grinding are used and the regime of the milling process is established. Vitreous wheat, in contrast to mealy, is easier to grind, gives thin and lean bran, more grits in the grapple process, of which then more flour is produced first grades. Glass vitreous grain affects the methods used to prepare grain for milling. Wheat with a greater vitreousness is easier to grind, bran is obtained from it, more thin and lean than with mealy, in the grapple process, more grits are obtained, which allows obtaining a higher yield of flour of the first grades [1].

Since grinding is an explosive production and dust flour emits into the environment, the grinding process is dedusted. Federal laws "On Environmental Protection" of 10.01.2002 No. 7-FZ; No. 96-FZ of 04.05.1999 "On the Protection of Atmospheric Air" regulate the necessity and procedure for the use of gas purification facilities at sites that have a negative impact on the environment.

The basis for dedusting milling enterprises are cyclones. In order to purify air volumes on a production scale, so-called "gravity dust separators", which have the working name "Cyclones", are used. Elements of the "Cyclones" design transform the airflow, informing him of rotational or translational motion.

Compared to other types of dust separators, cyclones have the following advantages: simplicity of construction, reliability, satisfactory efficiency, strength and ease of repair; wide throughput, as well as relatively low aerodynamic drag. The actual production conditions make their adjustments to the calculated values of cyclone efficiency. Thus, failure to

meet the condition for the airflow rate to match the optimal value, reduces the efficiency of purification to 80% [2].

II. FORMULATION OF THE PROBLEM

Proceeding from the foregoing, the aim of the work is to develop an automated complex that allows grain grinding and dedusting of this process while increasing the productivity of flour and crouppod products, as well as increasing the efficiency of process air.

The tasks of the work include:

1. Development of a system for monitoring and controlling the grinding process.
2. Development of a monitoring and control system for the separation process.
3. Carrying out of researches on experimental installations of grinding and separation with the help of the developed complex.

III. THEORY

Numerous studies of domestic, foreign scientists and practitioners show that in those cases when the energy costs for grinding a unit of grain mass are given, the data of different researchers differ significantly from each other.

This is explained by the fact that the calculated indices of the specific energy consumption (energy attributed to the newly formed surface) characterize only the strength characteristics of the initial grain material, and not the efficiency of the technological process for obtaining processed products with specified quality indicators.

An important characteristic of grain, except for glassiness, is hardness. This characteristic is paid attention at the practical grinding of grain crops. The importance of hardness was noticed by Kazakhstan scientists in their scientific works.

Due to the fact that the research of grain properties within the laboratories is extremely important for the development of flour milling, mainly in the Altai Territory, which occupies key positions in Russia in the agricultural sector, in view of all the same shortcomings, roller machines do not perform the research role with a maximum effectiveness.

As it was said earlier, roller equipment is used as the main equipment of grain processing enterprises for flour production, the main working part of which is a pair of rollers making rotational movement with different speeds towards each other. This process is partially automated and lasts continuously, but also such production has its drawbacks, namely the high power consumption (up to tens of millions of kWh per year). Also, roller machines have other disadvantages, such as: complex technology; large costs for the production of a rolling mill bed, re-grinding grain, and so on.

Despite the sufficient complexity of the process for obtaining flour in mill production, the production of endosperm from the grains is not more than 63-68%, although the endosperm in it is up to 85%. At present, the processes of additional obtaining of endosperm are perfected

only by increasing the number of machines or creating multi-roll machines, which only increases energy consumption.

The most energy-consuming parts of the grinding process are the first and second torn systems, where engines up to 17.5 kW are installed, and on subsequent grinding and grinding systems it reaches 7.5 kW. In large mills the machine stock is up to 15 machines and more, which indicates the complexity and energy intensity of this process.

The main provisions of studies of aeromechanical processes in swirling flows on the mechanisms of particle separation, the behavior of the dispersed phase, and also bibliography in the field of gas dedusting are given in the reference manual of J. Perry; A.A. Rusanova; public publications VA. Schwab; V. Ostrich; A. Gupta, D. Lily, N. Saireda; A.N. Shtym; E.P. Volchkova, V.I. Terekhova; I.I. Smulsky and others.

One of the works of Schwab, the most influential Russian scientist in the field of gas dedusting, is primarily devoted to a detailed study of the theory of a swirling turbulent flow in the separation element of an air-centrifugal classifier.

The analysis of certain numerical solutions and experimental data for air-centrifugal classifiers is reduced primarily to the study of the fields of the averaged velocity in the interdisk space, since in this part the initial fraction of the powder is divided into small and coarse fractions.

The main drawback of the existing studies related to the development and modernization of inertial gas scrubbers is the absence of working models for the structuring of the dispersed phase in the apparatus, along with the absence of parallel tests, to compare the created dust separator with popular, widely known apparatuses, conducted with the same initial conditions, on one and the same dust. At the same time, questions related to the operating conditions of the dust separator in a particular production are omitted, which leads to the fact that the values of the recommended apparatus for this technology are significantly lower than those obtained under laboratory conditions. It is noteworthy that the most common group and battery cyclone gas scrubbers have performance indicators much lower than those calculated for the fractional efficiencies determined in the laboratory for each element with its own dust receiver.

An alternative to rolling machines is a pendulum deformer, Doctor of Technical Sciences, Professor VL. Zlochevsky [3]. Its principle of operation and grinding of grain differs from that in roller machines. The deformer unfolds the grain along the furrow, without disturbing the structure of the grain. This method allows you to conduct grain research during shredding and adjust the entire line of roller machines. The pendulum deformer lacks the disadvantages of roller mechanisms: it is not so large, it has less power consumption, is cheap enough in production and better suited for the role of a device for studying the properties of grain.

On the basis of the foregoing, the purpose of the work is defined as the study of the properties of grain material with the help of a developed laboratory installation

At the moment, the existing system consists of the following elements:

- Pendulum deformer.
- Microcomputer Raspberry Pi B +.

- Software for a personal computer.

The general view of the connection between all nodes is shown in Fig.1.

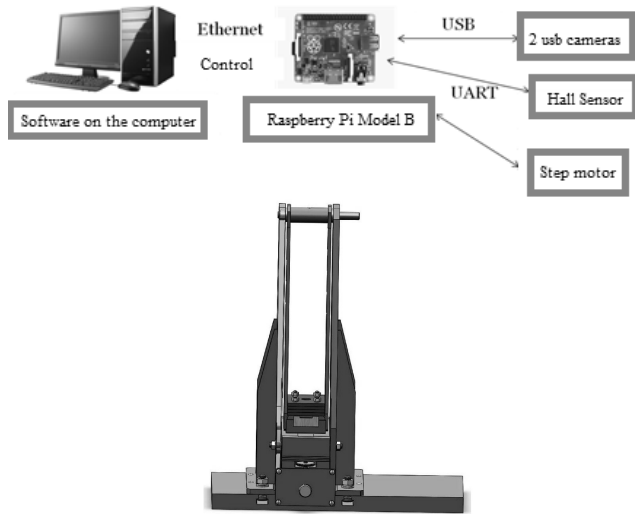


Fig. 1. System setup.

The grain deformer is designed to investigate the physical properties of grains, for example, such as vitreousness or strength.

The pendulum deformer consists of the base on which the stand is mounted. On the stand with a shaft to which a stepper motor is connected, a pendulum is mounted. The curved deck is fixed on the pendulum. Based on the substrate, located under the pendulum. The substrate has a concave structure. To the substrate, as well as to the pendulum, a stepper motor is connected. Its necessity consists in that it regulates the height of the substrate, thereby changing the angle of the grain meeting with the surface of the pendulum and the degree of grain refinement.

A distinctive feature of the pendulum deformer from roller is that it does not require constant rotation of the working cylinder. Also, in this installation, the problem with overheating of the grains and working surfaces was solved, since the whole grinding process proceeds very quickly, and the working surfaces of the pendulum do not touch each other.

The possibility of qualitative grinding of grain depends on which part of the substrate it was located in. The most rational is the location in the center of the supporting surface, since at the point of plummet the pendulum surface reaches the highest speed and guaranteed grinding of the grain.

In order to minimize the kinetic energy during the grinding of grain, it is necessary to make an extremely slow deformation of the grain, gradually increasing the external forces, which is achieved by a pendulum surface when the potential energy is transferred to the kinetic energy when the pendulum surface moves, so that at each instant of time each grains, given its structure, in equilibrium. In other words, under deformation, the effect of the applied external forces must be balanced by the internal stresses arising in this process. When this condition is satisfied, the grain will perform a quasi-static process. Such a process is preliminary for dividing the grain into parts by cutting. This leads to a

reduction in energy consumption for grinding and stabilization of the temperature factor.

Determination of the energy of grain destruction is based on the identification of unambiguous values of the stored potential energy that can be obtained at the extreme points of the pendulum surface with a damped oscillatory process. It is also necessary to take into account the energy losses due to friction. Thus, the sequence of actions of the method:

- retraction of the pendulum surface by a certain angle α_1 by means of a stepper motor controlled from a personal computer;

- placing the test grain on the support surface;

- release of the pendulum surface;

- fixing the angle α_2 on the opposite side;

- Calculation of energy costs of the pendulum deformer, glassiness and strength of grain.

It should be noted that the definition of losses is possible in two ways:

- making an analytical calculation using known theoretical information;

- calculating the losses for the standard oscillation of the pendulum, which was taken to a given angle.

In this paper, the first method is used, although it is possible that in the future the second method will be used.

It is known that for a pendulum:

$$E = m \cdot g \cdot l_m \cdot (1 - \cos \alpha),$$

where m is the mass of the pendulum, E is the potential energy stored by the pendulum, α is the pendulum deflection angle, l_m is the reduced length of the pendulum. Proceeding from the fact that the decrement of the pendulum decay equals:

$$d = \ln \left(\frac{\alpha_1}{\alpha_2} \right) = \beta T,$$

where T is the period of oscillation,

it is possible to calculate the energy dissipated in one period:

$$E_p = m \cdot g \cdot l_m \cdot (\cos \alpha_2 - \cos(e^{-\beta T} \alpha_1)).$$

Therefore, in order to determine the energy value for the destruction of the grain, it is necessary to calculate the damping decrement and the period of natural oscillations of the pendulum for a given angle of initial deviation, and also fixing the extreme positions of the surface of the pendulum.

To determine the angular position of the pendulum surface, an industrial encoder was first used to convert the value of the angle into a sequence of pulses. However, due to the low resolving power (0.25°), as well as the high cost of the copies with higher resolution, it was decided to abandon this method of angle measurement. An alternative to the encoder was the non-contact magnetic proximity sensor KMA200 from NXP, which indicated a resolving power of at least 0.04° in digital mode. As it turned out, in the analog mode it is possible to obtain higher values, which was the reason for choosing the analog mode of the sensor operation. The analog interface of the sensor is a differential analog output, varying within 5..95% of the supply voltage, depending on the angular position of the magnet. Experimentally, it was

possible to obtain the resolution of the sensor at the analog output 0.01° [4].

To control the grinding process with the help of a pendulum deformer and control its characteristics, the sensors use a Raspberry Pi model B + microcomputer with the control of the developed program. The Raspberry Pi model B + microcomputer controls the lifting of the pendulum surface and the adjustment of the reference surface by means of synchronous stepper motors and the transfer of all collected information from a contactless angle sensor to a computer. The software installed on the computer allows you to view the incoming information in an accessible format, and also allows you to control the pendulum deformer using the command system for the microcontroller and, accordingly, control the stepper motors. Also, the speed and acceleration of the pendulum surface are calculated based on the data obtained from the angular position sensor KMA200.

USB-cameras are used to determine the perfect work of the pendulum deformer. For this we use the formula proposed by P.A. Rebinder:

$$A_p = k_v \cdot k_n \cdot V_m + \alpha_{nog} \cdot \Delta S$$

where, A_p - energy consumption for destruction; k_v - coefficient that takes into account what part of the volume of the particle is deformed; k_n is a coefficient characterizing the physical and mechanical properties of the body being destroyed; V_m is the volume of the body being destroyed; α_n - the specific surface energy of the body being destroyed; ΔS is the new surface formed during the fracture.

Using the openCV library, the grain area is calculated before grinding and after grinding, which allows the software to perform calculations using the Rebinder formula. Images are obtained with USB cameras, by constantly comparing the photos until they become the same, that is, the grinding process stops. On the basis of these photographs, namely the photograph of the grain after grinding, information is taken on the area of the crushed grain, which in turn is used in calculating the work of the pendulum deformer.

The software (Fig. 2) for controlling the hardware of the complex is written in the C # programming language. To connect the microcomputer with the software and with the pendulum deformer, a wired connection is used via the Ethernet port [5].

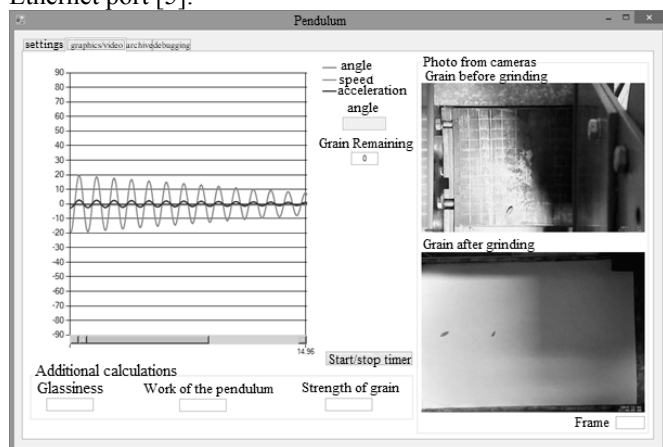


Fig. 2. Main program screen, graphics / video tab.

The development of a cyclone separator on the basis of an air-screw insert [6] located on the cyclone exhaust pipe and located in a confuser with a perforated surface made it possible to create a fundamentally new method that has no analogues. In the laboratory, currently has an efficiency of 95-99.9%, which is higher than foreign analogs.

In order to improve the efficiency of the cyclone, it is necessary to maintain constant monitoring of its technical parameters.

Parameters selected for monitoring: air speed, amount of dust in the air, air pressure and temperature. Monitoring parameters will occur at the inlet and outlet of the cyclone separator. To monitor these parameters, specially developed software will be used that will allow monitoring of data in real time and save them for further processing. In addition, the program will implement the automation function to control the fan speed in a wide range [7].

The general algorithm of operation is as follows (Fig. 3):

1. Arduino collects data from pressure, speed, dust meter and main engine characteristics.
2. Arduino composes the data as a string and sends it to the server.
3. The server converts the string into a json-object and sends the data to display to the client.
4. The client receives the data that is displayed for it in the interface.

In case the user wants to change the speed of the engine:

1. The desired speed is sent from the client to the server.
2. The server sends data to the Arduino microcontroller.
3. Arduino applies the received data and changing the parameters of the engine, thereby changing the speed of its operation.

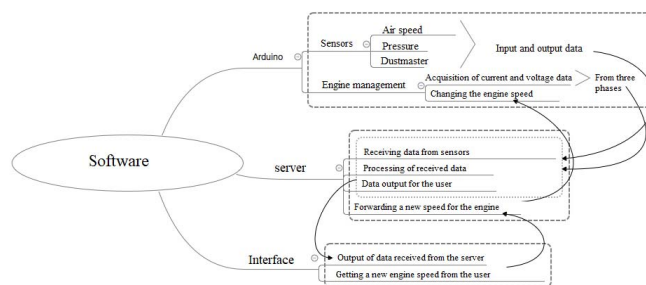


Fig. 3. General algorithm of the application.

The scheme of information flows is presented in Fig. 4.

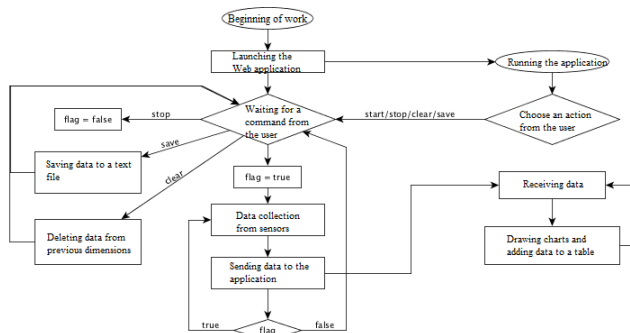


Fig. 4. Information flows of the application.

The software consists of two programs: one written for the microcontroller Arduino, the second for the computer [8].

The program interface is presented in Fig. 5.

Figure 6 shows graphs of the dependence of the speed obtained from the wind sensors on time.

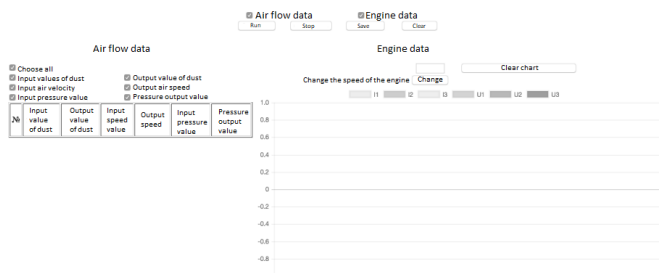


Fig. 5. The interface of the program.

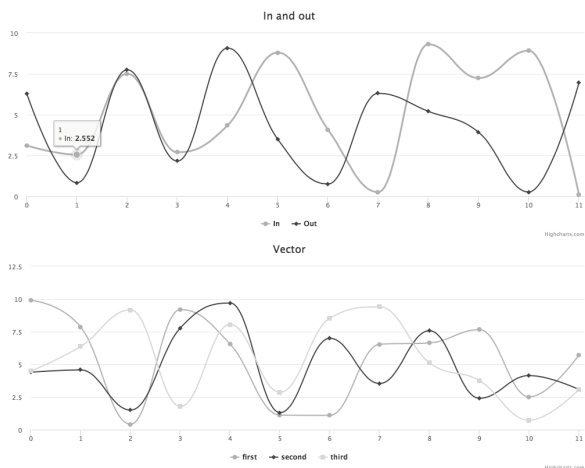
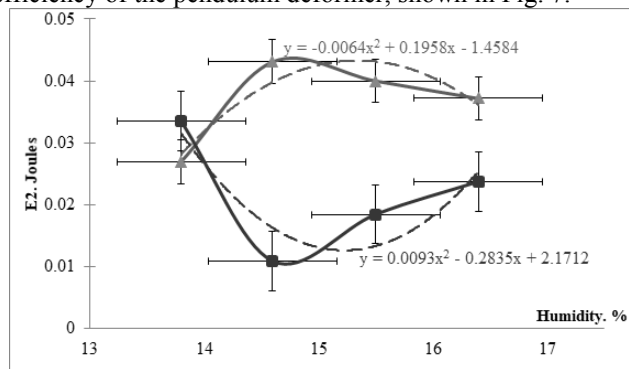


Fig. 6. Graphs of the vector velocity field.

IV. EXPERIMENTAL RESULTS

A series of experiments revealed a regime of maximum efficiency of the pendulum deformer, shown in Fig. 7.



—■— The vertical arrangement of the grain, the deviation of the surface from the vertical by 45 degrees, the location of the grain on the supporting surface, shifted from the plumb zone by 40 mm down.

—▲— The horizontal arrangement of the grain, the deviation of the surface from the vertical by 30 degrees, the location of the grain on the supporting surface, shifted from the plumb zone by 40 mm down.

Fig. 7. Range of rational use of the pendulum deformer.

At the current time, there are the following grain characteristics and tuning of the pendulum deformer, which were experimentally verified and confirmed:

1) Position of the grains on the deck (in the beginning, in the middle, in the end).

2) Angle of deviation of the pendulum (deviates by 30°, 40°, 45°);

3) The angle of rotation of the grain in the square of the deck (can lie - vertically, horizontally, diagonally).

For the successful implementation of the experiment, the Latin square method was applied. Thus, the number of experimental studies was reduced to 9 regimes.

Analysis of the experimental data shows:

1. Depending on the selected regime for one grain, the energy consumption for the destruction of grain materials is from 0.01 to 0.05 J. When grinding on a roller machine, the energy costs are on the order of 0.114-3.24 J per grains.

2. Since in grains 1, 6, 8 the grain lies at the beginning of the deck, the kinetic energy reserve is minimal and there is no grain breakage. Therefore, these regimes are not rational.

3. Mode No. 9 has the greatest deviation of the pendulum surface and the grain is located at the beginning of the reference surface, then the greatest energy consumption (on average 0.042 J) and the maximum speed of the pendulum movement from all modes are observed.

4. Since the grain is located in the middle of the support surface, where the largest values of speed and kinetic energy, due to the location of this zone at the point of the plumb and the angle of the deviation of the pendulum surface 40°, the most rational is mode No. 5, having throughout the experiments average values of energy consumption 0.026-0.028 J (Fig. 8).

Thus, the characteristics of the rational operating mode of the pendulum deformer are the deviation of the pendulum deformer by an angle of 40°, the horizontal arrangement of the grain material, and its location along the center of the support surface.

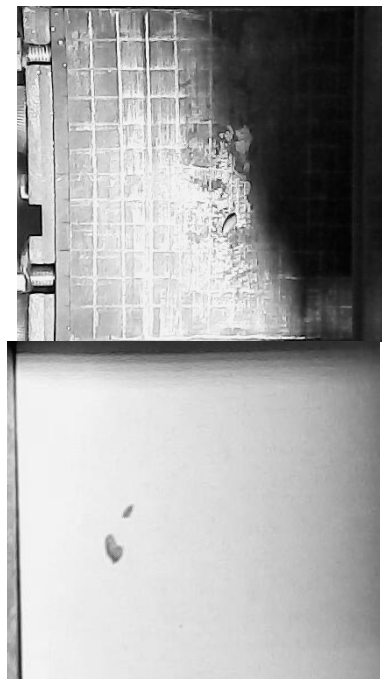


Fig. 8. Grain before and after grinding.

To study the glassiness of the software in the beginning "learns" on different batches of grain with known

parameters. Proceeding from the studies on grinding grain (Fig. 9), it can be concluded that, with a decrease in glassiness, energy consumption for grain refinement is reduced. The error in measuring the vitreousity is not more than 2%.

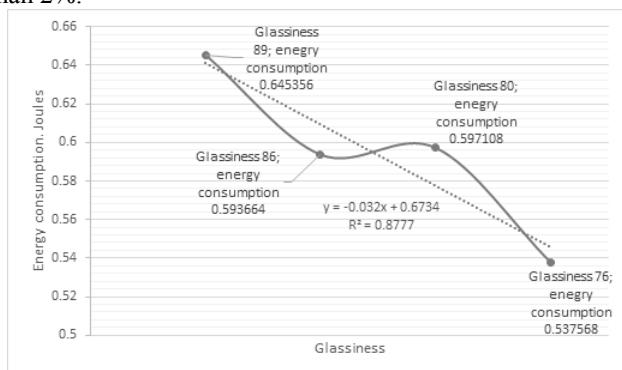


Fig. 9. Dependence of energy consumption on grinding grain from vitreousness.

The conducted laboratory tests using the monitoring and control system for the cyclone separator showed very satisfactory results both in terms of efficiency and aerodynamic resistance of the cyclone. On flour dusts, the efficiency of the cyclone separator in question exceeded 99.5%, with an air flow of 376 m³ / h, 472 m³ / h and 516 m³ / h, and ΔP less than 600 Pa. The velocity in the inlet branch of the screw insert was 18-20 m / s, and at the exit of the screw insert the airflow velocity is 50-70 m / s.

V. THE DISCUSSION OF THE RESULTS

At the moment, the only way to determine the glass's vitreousity is the manual method specified in GOST 10987-76 Grain. Methods for determining the vitreousity. This method is quite labor-intensive for a person, because requires concentration and attention in determining the vitreousity, which leads to natural fatigue, loss of attention and deterioration in the accuracy of determining the glassiness. Therefore, the development of an automated method would simplify the determination of the basic parameters of grain materials. The proposed method is automatic, allowing, with an error of not more than 2%, to determine the vitreousness of the grain. The cost of grinding one grain by the proposed method is 0.05 J, when grinding on a roller machine is 3.24 J for one grain.

In comparison with the known cyclones-separators, which have an efficiency of 80%, the developed complex allows to increase the efficiency up to 99.9%.

VI. CONCLUSION

The developed pendulum deformer with a monitoring and control system makes it possible to determine glass vitreousity with an error of no more than 2%, and also, due to the use of a new grinding method, to obtain a greater extraction of endosperm, and, consequently, to obtain more flour and crouppodun products.

On flour dusts, the efficiency of the cyclone separator in question exceeded 99.5%, with an air flow of 376 m³ / h, 472

m³ / h and 516 m³ / h, and ΔP less than 600 Pa. The velocity in the inlet branch of the screw insert was 18-20 m / s, and at the exit of the screw insert the airflow velocity is 50-70 m / s.

REFERENCES

- [1] Lyukshin V S, Barsuk A V and Fazleev R R 2015 IOP Conf. Ser.: Mater. Sci. Eng. 91 012047 doi: 10.1088/1757-899X/91/1/012047
- [2] Xu W W, Li Q, Zhao Y L, Wang J J and Jin Y H 2016 IOP Conference Series: Materials Science and Engineering 129 012022 doi:10.1088/1757-899X/129/1/012022
- [3] Zlochevskiy V L, Zlochevskiy A V 2005 A method of forming a grinding cereals, Patent RF № 2263544 (in Russian)
- [4] Borisov AP Development of a software-hardware complex for studying the process of grinding by a pendulum deformer // 2018 IOP Conf. Ser.: Mater. Sci. Eng. 289 012004
- [5] Edakin NV, Borisov A.P. Automatic control of the process of grain refinement. // Certificate of state registration of the computer program №2016610021, filed. 06.11.15, publ. 11.01.16. (in Russian).
- [6] Zlochevskiy V.L. Aerovoltaic cyclone separator, Patent RF № 2442662, 2012 (in Russian)
- [7] Borisov AP Software and hardware complex for research and management of the separation process // 2018 IOP Conf. Ser.: Mater. Sci. Eng. 289 012039
- [8] Nikolaeva VK, Borisov A.P. Program for controlling and controlling airflow in the cyclone separator. // Certificate of state registration of the computer program №2017662653, filed. 26.09.17, publ. 11.13.17. (in Russian).



Borisov Alexey Pavlovich, a graduate of the Altai State Technical University. I.I. Polzunova. He defended his thesis on the topic "Modes of the process of grain destruction through a pendulum shredder." Grantee of the City Hall of Barnaul, 2008, the winner of the "UMNIK" program with the theme "Development of an automated control system for the process of destruction of grain material", 2010, Diploma of the I degree. Teacher of the year - 2015 in the FGBOU V AltGTU them. I.I. Polzunova, 2015, Diploma UMO IB for the scientific management of the research work of the student who took the I place on the results of the All-Russian open competition in 2016 for the best scientific work of students in the field of Information Security for the project "Development of access control system based on NFC technology", 2016, Winner in the nomination "Best Global Project" at the 1st Fair of Startups "Our Business-2016", 2016, Winner of the RFBR grant together with the Altai Territory with the project "Theoretical and Experimental Studies of the Formation of the "The diploma of the Governor of the Altai Territory for the II place in the regional competition" The Best Informatization Projects in the Altai ", September 27, 2017, No. 89-rg, Diploma of the Governor of the Altai Territory for the III place in the regional contest "Best Projects " Informatization in the Altai ", September 27, 2017, No. 89-rg, Diploma of the winner of the contest " Best Teacher of AltSTU ", 2017, Gratitude for conscientious work in the system of higher education, high professionalism and exemplary performance of official duties from administrations eniya Communications and Mass Media of the Altai Territory, 2017, a letter of thanks for the pursuit of excellence in research activities of Altai State Technical University, 2018

CMOS Current Logic Elements: Application Features for Processing Analog and Digital Signals

Nikolay V. Butyrlagin¹, Nikolay I. Chernov¹, Nikolay N. Prokopenko^{1,2}, *Member, IEEE*, Vladislav Ya. Yugai¹

¹Don State Technical University, Rostov-on-Don, Russia

²Institute for Design Problems in Microelectronics of Russian Academy of Sciences, Zelenograd, Russia

Abstract – Features of the design and circuit technology implementation of CMOS current logic elements (TLE), including multi-valued logic elements are considered. An unconventional method for processing analog and digital current signals of sensors in automatic systems of extreme control based on the use of TLE "minimum" and "maximum" with three or more input variables is investigated. The CMOS TLE description of this class is described, as well as the results of their computer simulation when working with analog, as well as binary and ternary digital current signals.

Index Terms – Automatic systems of extreme regulation, current logic, current logic element "minimum" with three input variables, current logic element "maximum" with three input variables.

I. INTRODUCTION

THE CURRENT state of microelectronics is characterized by the approximation of the technological parameters of the LSI components to the maximum permissible values (transistor sizes, the width of the conductors of communication lines, etc.) and by the full use of the capabilities of Boolean algebra to improve the parameters of circuit solutions. Therefore, intensive searches for other alternative principles for constructing digital structures (DS) are being conducted, incl. multivalued elements [1].

One of the modern ways to improve the technical characteristics of the DS in the framework of known technologies is the use of the current element base [2]. The perspective of the current approach is determined by the following factors:

- the mathematical apparatus of the logical synthesis of current logic elements is well known and developed. This is a linear algebra [3];
- current non-resistive circuit realization of logic circuits determines the high technological efficiency of the TLE [4];
- difference representation of the output signal determines the high operational characteristics of the TLE under severe operating conditions [5];
- current approach determines the possibility of creating not only two-valued, but multivalued logic elements and computing structures based on them [5];
- the properties of multivalued TLE allow them to work not only with discrete but also with analog signals, which allows them to be used as analog elements of automation (for example, the AND, OR and their multivalued "minimum" and "maximum" analogues can be used to extract the largest or smallest signals from a given group), for example, for

processing sensor signals [6-8]. The use of multi-valued logic provides higher technical, technological and operational characteristics in the construction of a number of devices for digital signal processing and automatic control systems [9-13].

II. PROBLEM DEFINITION

In this paper, we describe the logical synthesis and circuit design of the current logical elements of the main functionally complete system (AND, OR, NOT) and their many-valued generalizations (\min , \max , $x \oplus i$). The possibility of using current logic devices "minimum" and "maximum" as elements of the separation of the minimum or maximum continuous signals is also considered.

III. THE DISCRETE INTERPRETATION

A. Logical Element "Minimum"

The logical operation of determining the "minimum" of n input variables x_1, x_2, \dots, x_n in the mathematical apparatus of linear algebra is described for $n = 2$ as follows [14-20]: In the mathematical tool of linear algebra, the logic operation "minimum" for three input variables (x_1, x_2, x_3) is described by the expression [21]:

$$x_1 x_2 = x_1 \div (x_1 \div x_2). \quad (1)$$

If $n = 3$, then

$$\begin{aligned} \min(x_1, x_2, x_3) &= \min[x_1, \min(x_2, x_3)] = \\ &= x_1 \div \{x_1 \div [x_2 \div (x_2 \div x_3)]\}. \end{aligned} \quad (2)$$

In equation (1) and (2) the symbol \div denotes the operation "truncated difference":

$$x_1 \div x_2 = \begin{cases} x_1 - x_2 & \text{under } x_1 > x_2 \\ 0 & \text{under } x_1 \leq x_2 \end{cases}. \quad (3)$$

In general case

$$\begin{aligned} \min(x_1, x_2, \dots, x_n) &= \\ &= x_1 \div (x_1 \div (x_2 \div \dots \div (x_{n-1} \div x_n) \dots)). \end{aligned} \quad (4)$$

In the circuit of the logic element "minimum", the output signal takes a value corresponding to the minimum value of one of the input signals. The scheme of such an element for $n = 3$ is shown in Fig. 1.

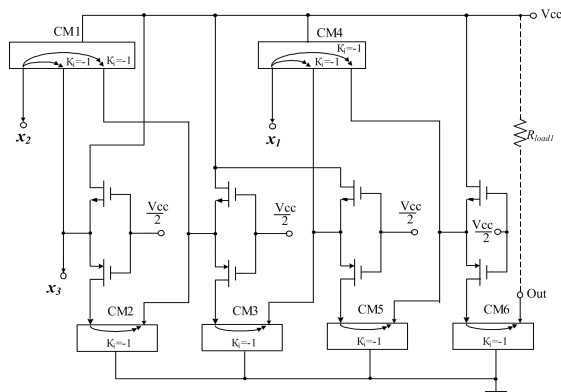


Fig. 1. The “minimum” logic element for three variables.

Fig. 2 shows the results of computer simulation of the “minimum” element (Fig. 1) with binary and ternary input current signals (I_{x1}, I_{x2}, I_{x3}).

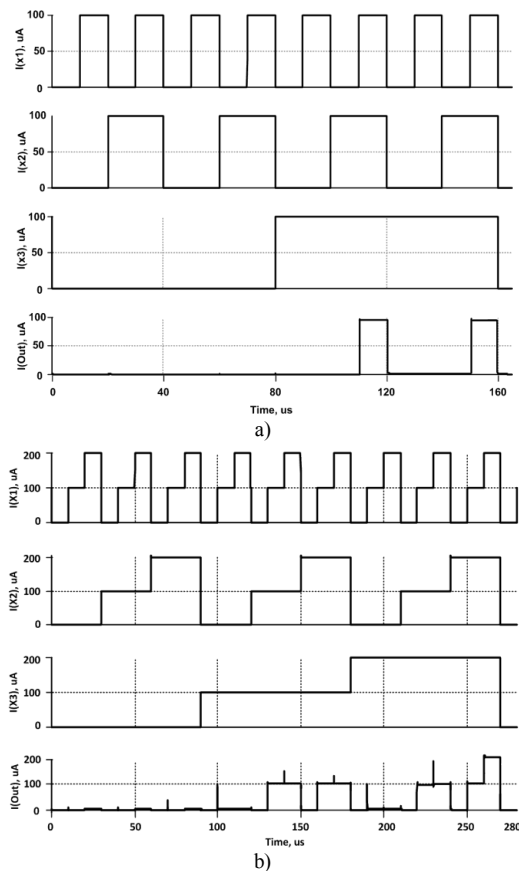


Fig. 2. Time diagrams of the logic element “minimum” when operating with binary (a) and ternary (b) signals.

B. Logical Element "Maximum"

In the mathematical apparatus of linear algebra, the logical operation "maximum" for the n input variables x_1, x_2, \dots, x_n for $n = 2$ is described by the expression [21]:

$$x_1 \vee x_2 = x_1 + (x_2 \div x_1) \quad (5)$$

If $n = 3$, then

$$\begin{aligned} \max(x_1, x_2, x_3) &= \max[x_1, \max(x_2, x_3)] = \\ &= x_1 + \{[x_2 + (x_3 \div x_2)] \div x_1\}. \end{aligned} \quad (6)$$

In general case

$$\max(x_1, x_2, \dots, x_n) = x_1 + (x_2 + (\dots(x_n \div x_{n-1}) \div \dots) \div x_1).$$

The output signal of the logic element $\max(x_1, x_2, x_3)$ takes a value equal to the maximum value of one of three input signals x_1, x_2 and x_3 . It should also be noted that equation (6) is valid for any values of input variables, including for analog signals. The scheme shown in Fig. 3 corresponds to equation (6).

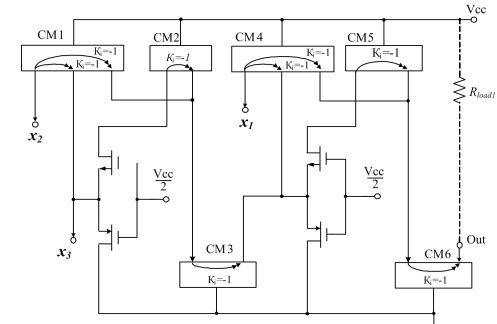


Fig. 3. The “maximum” logic element for three variables.

The scheme (Fig. 3) contains 6 current mirrors CM1-CM6. The sources of current signals are connected to the inputs In.1, In.2, In.3, the output current signal is formed in the equivalent load R_{load1} .

Fig. 4 presents the results of computer simulation of the “maximum” element (Fig. 1) with binary and ternary input current signals (I_{x1}, I_{x2}, I_{x3}).

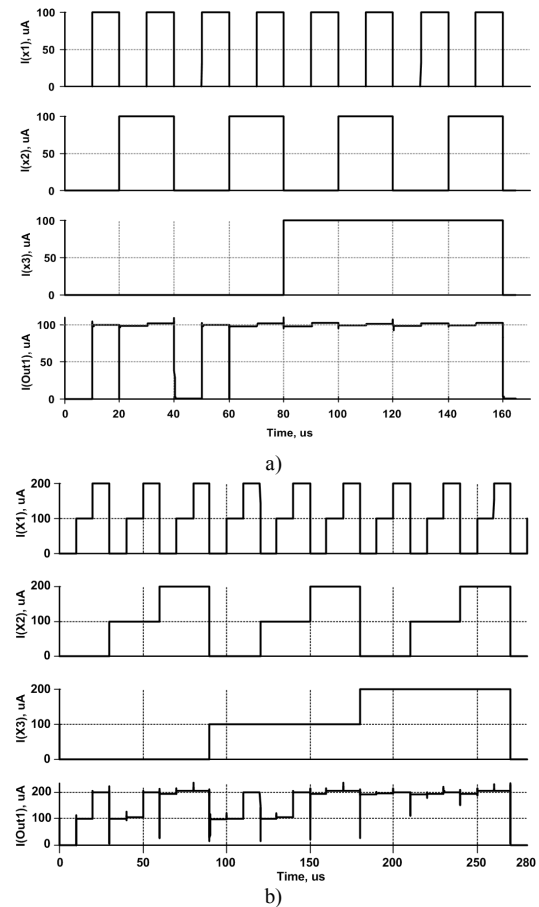


Fig. 4 Time diagrams of the logic element “maximum” when operating with binary (a) and ternary (b) signals.

C. Current Cyclic Shift Element

The binary (Boolean) inversion operation (NOT)

$$\bar{x} = x \oplus 1 = x \ominus 1,$$

in linear algebra can be described as

$$x \oplus 1 = x + 1 - 2 \lfloor \frac{x+1}{2} \rfloor$$

$$x \ominus 1 = x - 1 + 2 \lfloor \frac{x-1}{2} \rfloor$$

The cyclic shift operation is considered as a generalized inversion representation. In Fig. 5 shows CMOS elements of direct ($x \oplus 1$) (a) and inverse ($x \ominus 1 = x \oplus 2$) (b) cyclic shifts.

Fig. 5 shows CMOS elements of forward (a) and reverse (b) cyclic shifts, realized on the basis of the elements “minimum” and “maximum”. Besides, cyclic shift operations are considered as a generalized representation of the inversion.

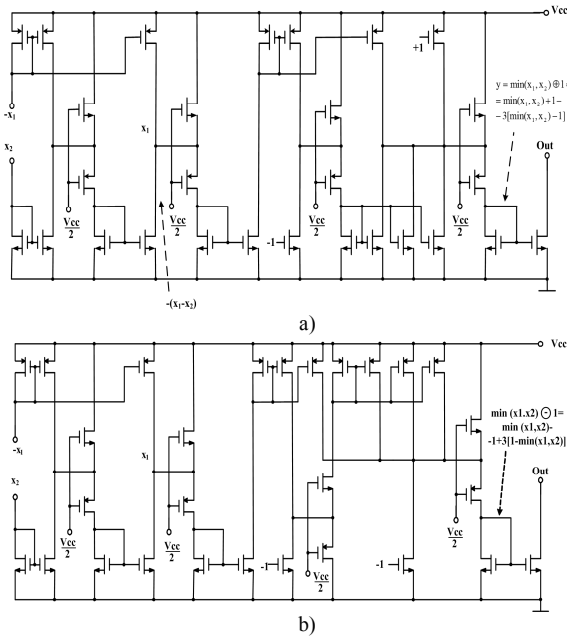


Fig. 5. CMOS elements of forward (a) and reverse (b) cyclic shift.

The set of elements $\min(x_1, \dots, x_n)$, $\max(x_1, \dots, x_n)$ and $x \oplus 1 = x \ominus 1$, has a functional completeness and, therefore, allows to realize any logical function of given values and number of arguments. On the basis of the functionally complete set of elements discussed above, it becomes possible to construct not only combinational circuits, but also memory elements - both binary triggers and multi-valued memory elements.

IV. THE ANALOG INTERPRETATION

The “minimum” element can also be used to processing of analog signals.

Fig. 6 presents the results of computer simulation of the three-valued element “minimum” (Fig. 1) with three input sawtooth current signals (I_{x1}, I_{x2}, I_{x3}).

In the section $0-t_1$ of the time diagram (Fig. 6), the output signal is equal to the input current I_{x1} , since here the current $I_{x1} < (I_{x3}, I_{x2})$. In the section t_1-t_3 , the output signal corresponds to the input current I_{x2} , since $I_{x2} < (I_{x1}, I_{x3})$. In the section t_3-t_5

the output signal is equal to the input current I_{x3} , due to the fact that the current $I_{x3} < (I_{x1}, I_{x2})$. In the section t_5-t_6 the output signal corresponds to the input current I_{x1} , since the current $I_{x1} < (I_{x3}, I_{x2})$.

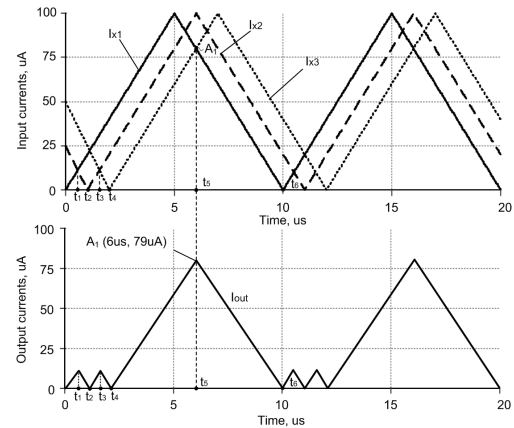


Fig. 6. Time diagrams of the input and output currents of the logic element “minimum” with input sawtooth signals.

Fig. 7 shows the results of computer simulation of the three-valued element “maximum” (Fig. 3) with binary and ternary input current signals (I_{x1}, I_{x2}, I_{x3}).

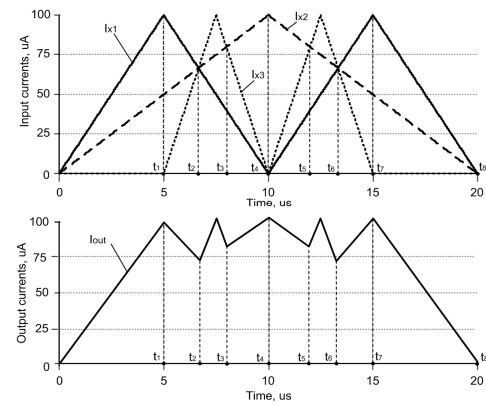


Fig. 7. Time diagrams of the input and output currents of the logic element “maximum” with input sawtooth signals.

In the section $0-t_2$ of the time diagram (Fig. 7), the output signal is equal to the input current I_{x1} , since here the in equation $I_{x1} > (I_{x3}, I_{x2})$ is satisfied. In the section t_2-t_3 , the output signal corresponds to the input current I_{x3} , since here $I_{x3} > (I_{x1}, I_{x2})$. In the section t_3-t_5 , the output signal is equal to the input current I_{x2} , due to the fact that the current $I_{x2} > (I_{x1}, I_{x3})$. In the section t_5-t_6 , the output signal corresponds to the input current I_{x3} , since the inequality $I_{x3} > (I_{x1}, I_{x2})$ is fulfilled. In the section t_6-t_8 , the output signal is equal to the input current I_{x1} , since $I_{x1} > (I_{x3}, I_{x2})$.

Computer simulation confirms the operability of the proposed converters of current signals.

V. CONCLUSIONS

The new method for current signal processing based on the current logic elements “minimum” and “maximum” with three input variables has been considered.

The output current signal of the proposed logic elements “minimum” and “maximum” takes the value of either the

maximum or minimum value of one of the input current signals x_1, x_2, x_3 .

On the basis of current logic elements “minimum” and “maximum” the circuitry of three-digit logic elements of forward and reverse cyclic shifts for construction of multi-valued memory elements is developed.

The possibility operations of proposed elements with using discrete and analog input signals are shown.

ACKNOWLEDGEMENT

The reported study was funded by RFBR according to the research project No. 18-37-00061.

REFERENCES

- [1] Volgin L.I., Zarukin A.I. The Synthesis and the Circuitry of Analog Electronic Means in the Element Basis of Amplifiers and Current Followers, endorsed by L.I. Volgina. Ulyanovsk: USTU, 2005, 200 p. (in Russian).
- [2] Rivetti A. CMOS: Front-End Electronics for Radiation Sensors (Devices, Circuits and Systems), CRC Press, 2015, p. 726.
- [3] Wada K., Kimerling L.C. Photonics and Electronics with Germanium, Wiley, 2015, p. 336.
- [4] Hintenhaus P. Engineering Embedded Systems: Physics, Programs, Circuits, Springer, 2016, p. 310.
- [5] Klaassen Klaas B. Electronic Measurement and Instrumentation, Cambridge University Press, 1996, p. 335.
- [6] Chernov N.I. The effectiveness of the apparatus of linear spaces in the logical synthesis of digital structures, Proceedings of the international scientific and technical conferences «Intelligent systems (IEEE AIS'05)» and «Intelligent CAD (CAD-2005)», vol.1, pp. 420-424. (in Russian).
- [7] Chernov N.I., Nazarov S.P. Logic synthesis of multi-bit adders based on linear algebra, Izvestiya SFEDU, Engineering Sciences, 2007, vol. 73, no. 1, pp. 230-235. (in Russian).
- [8] Chernov N.I., Yugai V.Ya., Prokopenko N.N., Butyrlagin N.V. Basic Concept of Linear Synthesis of Multi-Valued Digital Structures in Linear Spaces, Proceedings of IEEE East-West Design & Test Symposium (EWDTS'2013). Rostov-on-Don, Russia, September 27-30, 2013, Kharkov National University of Radioelectronics, pp. 146-149.
- [9] Prokopenko N.N., Chernov N.I., Yugai V.Ya. Base Concept of Linear Synthesis of Multivalued Digital Structures within Linear Spaces, Proceedings of the IS & IT13 Congress. The Scientific Edition in four volumes. Moscow, PhysMathLit, 2013, vol. 1, pp. 284-289 (in Russian).
- [10] Prokopenko N.N., Chernov N.I., Yugai V.Ya. The Linear Logic Synthesis of k-Valued Digital Structures in the Analogous Circuitry Basis, Proceedings of IEEE East-West Design & Test Symposium (EWDTS'2014), Kiev, Ukraine, September 26-29, 2014. – Kharkov National University of Radioelectronics. – pp. 348-351.
- [11] Prokopenko N.N., Budyakov P.S., Chernov N.I., Yugai V.Ya. Schematic Design of Digital IC at the Base of Linear Algebra, ICSES 2014 International Conference on Signals and Electronic Systems, September 11-13, 2014, Poznan, Poland. pp.1-6. DOI: 10.1109/ICSES.2014.6948728. WOS:000348648600021.
- [12] Prokopenko N.N., Chernov N.I., Yugai V.Ya. Linear synthesis - is a new approach to the logical design of k-valued digital structures, Problems of development of perspective micro and nanoelectronic systems - 2015. Proceedings / under the general editorship of academicians of RAS A.L. Stempkovskiy, IPPM RAS, Moscow, 2015.
- [13] Prokopenko N.N., Chernov N.I., Yugai V.Ya., Butyrlagin N.V. The linear concept of logical synthesis of digital IP-modules of control and communication systems, International Siberian Conference on Control and Communications, SIBCON-2015, Omsk, Russia, 21-23 May, 2015.
- [14] Prokopenko N.N., Chernov N.I., Yugai V.Y. Synthesis of k-valued digital IP-modules for robots and sensor systems based on linear transformations of current logic signals, SPIIRAS Proceedings, vol. 2, Ed. 45, 2016, pp. 172-189. DOI: 10.15622/SP.45.11
- [15] Prokopenko N.N., Chernov N.I., Yugai V.Ya., Budyakov P.S. Logic functions representation and synthesis of k-valued digital circuits in linear algebra, 2016 24-nd Telecommunications Forum (TELFOR 2016), Belgrade, Serbia, 22-23 November 2016, pp. 1-4. DOI: 10.1109/TELFOR.2016.7818892.
- [16] Prokopenko N.N., Chernov N.I., Yugai V.Ya., Butyrlagin N.V. The Linear Synthesis of the K-Valued Digital Element Base with the Current Logic Signals: the Principle of Generalization, Selected Articles of the VII All-Russia Science&Technology Conference MES-2016 “Problems of Advanced Micro- and Nanoelectronic Systems Development”, 2017, Part I, Moscow, IPPM RAS, pp. 22-27.
- [17] Prokopenko N.N., Chernov N.I., Yugai V.Ya., Butyrlagin N.V. The Multifunctional Current Logical Element for Digital Computing Devices, Operating on the Principles of Linear (Not Boolean) Algebra, IEEE East-West Design & Test Symposium (EWDTS'2016), Yerevan, Armenia, 14 – 17 Oct. 2016. DOI: 10.1109/EWDTS.2016.7807723.
- [18] Prokopenko N.N., Chernov N.I., Yugai V.Ya., Butyrlagin N.V. The Element Base of the Multivalued Threshold Logic for the Automation and Control Digital Devices, on International Siberian Conference on Control and Communications, SIBCON-2017, Astana, Kazakhstan, 29-30 June, 2017. DOI: 10.1109/SIBCON.2017.7998508.
- [19] Chernov N., Yugai V., Prokopenko N., Butyrlagin N. Threshold Synthesis of Digital Structures in Current-Mode Logic, Proceedings of IEEE East-West Design & Test Symposium (EWDTS'2017), Novi Sad, Serbia, September 29 - October 2, 2017. pp. 584-587. DOI: 10.1109/EWDTS.2017.8110146.
- [20] Chernov N.I., Prokopenko N.N., Butyrlagin N.V. The Method of Analog-to-Digital Conversion of the Sensor Current Signals on the Base of the Multivalued Adder, IEEE II International Ural Conference on Measurements “Uralcon 2017”, 16-19 October 2017, Chelyabinsk, Russia.
- [21] Chernov N.I., Prokopenko N.N., Yugai V.Ya., Butyrlagin N.V. The Application of Multi-Valued Logic Elements “Minimum” and “Maximum” for Processing Current Signals of Sensors, 24-th IEEE International Conference on Electronics, Circuits and Systems (ICECS), 5-8 December 2017, Batumi, pp. 450-453.



Nikolay V. Butyrlagin,
born in Donetsk of Rostov region, Russia on the 27th of March, 1989. He is a Candidate of Technical Sciences, associate professor, junior researcher. His area of expertise is analog microelectronics, analog-to-digital circuitry.
E-mail: nbutyrlagin@mail.ru .



Nikolay I. Chernov,
born in Konstantinovka village of Petrovskiy district of the Stavropol Territory, Russia on the 21st of October, 1945. He is a Doctor of Engineering, Professor. His research interests are analog microelectronics, analog-to-digital circuitry.
E-mail: chernovni@yandex.ru .



Nikolay N. Prokopenko,
born in Koltunovka village of Sovetskiy district of Stavropol Territory, Russia on the 1st of January, 1949. He is a Doctor of Engineering, Professor. His area of expertise is analog microelectronics, analog-to-digital circuitry.
E-mail: prokopenko@sssu.ru



Vladislav Ya. Yugai,
born in Tashkent region, Uzbekistan on the 18th of May, 1950. He is a Candidate of Technical Sciences, associate professor. His research interests are analog microelectronics, analog-to-digital circuitry.
E-mail: yugtag@gmail.com .

Basic Parameters and Characteristics of the Op-Amp Based on the BiJFet Array Chip MH2XA030 Intended for the Design of Radiation-Hardened and Cryogenic Analog ICs

Oleg V. Dvornikov¹, Valentin L. Dziatlau², Vladimir A. Tchekhovski², Nikolai N. Prokopenko^{3,4}, *Member, IEEE*, Anna V. Bugakova³, *Student Member, IEEE*

¹JSC “Minsk Scientific and Research Instrument-Making Institute”, Minsk, Belarus,

²“Research Institute for Nuclear Problems of Belarusian State University”, Minsk, Belarus

³Don State Technical University, Rostov-on-Don, Russia

⁴Institute for Design Problems in Microelectronics of RAS, Zelenograd, Russia

Abstract – Features of the schematic design of two types of operational amplifiers (Op-Amp) on the new BiJFet array chip (AC) MH2XA030 are considered. The topology, the electric circuits of the Op-Amp and the results of their computer simulation are given. The brief information about the AC MH2XA030, intended for the accelerated creation of analog integrated circuits (IC) of automation devices, which retain their operational integrity under the influence of penetrating radiation and extremely low temperatures (up to -197°C) is presented.

Index Terms – Analog integrated circuits, array chip, radiation hardness, cryogenic electronics, operational amplifier.

I. INTRODUCTION

THE OP-AMP is the main functional node of modern microelectronic analog equipment, which determines (in many cases) static and dynamic parameters of automation devices [1-13]. In the problems of space device engineering and high-energy physics, the Op-Amps are required that enable the work under severe operating conditions [14-22].

As a rule, the Op-Amp is part of many ACs and structured arrays (SA) widely used in the creation of specialized analog ICs (especially for their low-volume production [23-32]).

Previously, for the production of specialized radiation-hardened ICs, we created the SA MH2XA010 [27-29] and the array chip (AC) ABMK-2.1 [27,30], in which complementary bipolar transistors (BJT) with high cutoff frequency of amplification, field effect transistors with p-n-junction and a p-type channel (p-JFet), semiconductor resistors and MOS capacitors were used.

Approbation of the microcircuits MH2XA010 and ABMK-2.1 in the design of a number of microelectronic products revealed a high level of their electrical parameters [31,32]. Experimental studies also established [33,34] that on the base of the microcircuits MH2XA010 and ABMK-2.1 it is possible to create analog devices that are proof against the action of gamma quanta ⁶⁰Co with an

absorbed dose up to 3 Mrad, a fast-electron flux up to 3×10^{14} el / cm² with an energy of 4 MeV, heavy charged particles with linear energy losses of at least 68 MeV·cm² / mg (Si).

On the other hand, the studies revealed structural and circuit features of the microcircuits MH2XA010 and ABMK-2.1, which can limit the scope of their use, namely [31,34]:

- the offset voltage of the Op-Amp, which does not exceed 5 mV under normal conditions, leads to the need to adjust the quiescent output voltage of the analog devices at a high amplification gain;
- the fast response of the Op-Amp (the unity gain frequency is about 200 MHz) and the comparator (the delay is less than 5 ns) in many applications is excessive and it is desirable to reduce it while reducing the current consumption.

II. PROBLEM DEFINITION

In 2018 the identification of the features of the previously developed SA and AC has made it possible to create the SA MH2XA030, in which the limitations inherent in the microcircuits MH2XA010 and ABMK-2.1 are eliminated.

The goal of the article, which is aimed at the developers of low-temperature and radiation-hardened analog microcircuits, is a brief review of the design of the new AC MH2XA030 (2018), as well as a discussion of the results of computer simulation of two modifications of the Op-Amp (OAMP1, OAMP2) based on the SA.

III. DESIGN OF MICROCIRCUITS ON THE AC MH2XA030

The concept of the AC involves not only the development of the semiconductor element topology [23-32], but also the creation of the necessary design tools, namely: Spice models of active and passive elements located on the AC, recommendations for schematic design, circuit-topological libraries of components.

A. Construction of the AC

The AC MH2XA030 developed is an upgrade of ABMC-2.1 [30,32] aimed at introducing the p-JFet into each macrocell, a significant increase in the maximum resistance and the number of semiconductor resistors, and also the number of bond sites.

The AC MH2XA030 contains eight macrocells (Fig. 1).

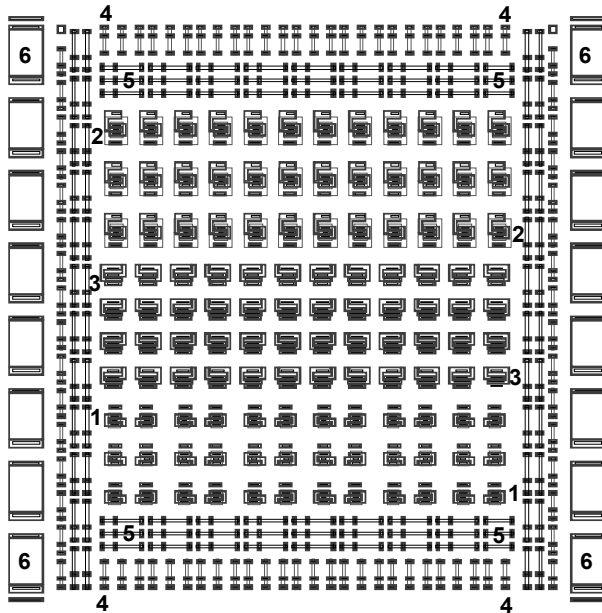


Fig. 1. Simplified topology of the macrocell of the AC MH2XA030.

On the perimeter of the AC there are complex functional bond sites (122 pcs.), which are used to connect the semiconductor element with conductors to the package traverses or as the following active elements: PADN – two multi-emitter high-power n-p-n transistors; PADP – two multi-emitter high-power p-n-p transistors; PADJ – a low-noise p-JFet.

In total, 64 high-power n-p-n transistors, 60 high-power p-n-p transistors and 60 low-noise p-JFets are located on the AC.

Each macrocell (Fig. 1) includes:

- 36 low-power n-p-n transistors (1 in Fig. 1) with a topological emitter size of $7 \mu\text{m} \cdot 1.5 \mu\text{m}$ arranged as a matrix of their 3 rows and 12 columns;
- 36 low-power vertical p-n-p transistors (2 in Fig. 1) with an emitter size of $7 \mu\text{m} \cdot 1.5 \mu\text{m}$ (a matrix of their 3 rows and 12 columns);
- 48 low-power p-PTTs (3 in Fig. 1) with a gate size of $16.5 \mu\text{m} / 1.5 \mu\text{m}$ (a matrix of 4 rows and 12 columns);
- 84 resistors of the 2R4um type (4 in Fig. 1), each of which gives a resistance of 0.735 k Ω , 1.05 k Ω , 2.45 k Ω , 3.5 k Ω , by performing various interconnections;
- 96 resistors of the 2RR4um type (5 in Fig. 1), each of which gives resistance of 3.51 k Ω , 5.2 k Ω , 10.8 k Ω , 16 k Ω ;
- 16 MOS-capacitors (6 in Fig. 1), each of which has a capacity of 1.07 pF.

The total resistance of all AC resistors is 14.64 M Ω , and the total capacitance of all capacitors is 136.96 pF.

The macrocell in Fig. 1 is surrounded by a screening contact to the p-type substrate, which enables to eliminate the parasitic interaction through the substrate.

The emitter area of the low-power BJTs of the MH2XA030 is almost 2 times smaller than the transistors' are of the AC MH2XA010, therefore analog components of the AC MH2XA030 at the current consumption of 2 times smaller will have almost the same fast response as the components of the AC MH2XA010.

A single Op-Amp can be implemented on one macrocell, so an analog device with a complexity of up to 8 Op-Amps can be created on the AC MH2XA030.

B. Schematic design tools

It is known [35] that not all commercial CAD systems and firm libraries of Spice-parameters of transistor models are suitable for circuit simulation of the effect of penetrating radiation and cryogenic temperature on the parameters of analog microcircuits. To consider simultaneously the effect of radiation and low temperatures, it was proposed to use CAD LTSpice, built-in LTSpice standard models with averaged temperature coefficients, as well as the developed mathematical expressions that establish the relationship between model parameters, semiconductor and radiation exposure, and describe a nonmonotonic change in the BETA p-JFet parameter [35,36]. The developed models allow describing the existing manufacturing tolerance β by changing the parameter BFscale, the effect of the absorbed dose of gamma radiation and the neutron flux – parameters of the model D_G and F_N , respectively. The use of these tools ensured satisfactory coincidence of the results of measurements and simulation of the current-voltage characteristics (CVC) of the BJT (Fig. 2-6).

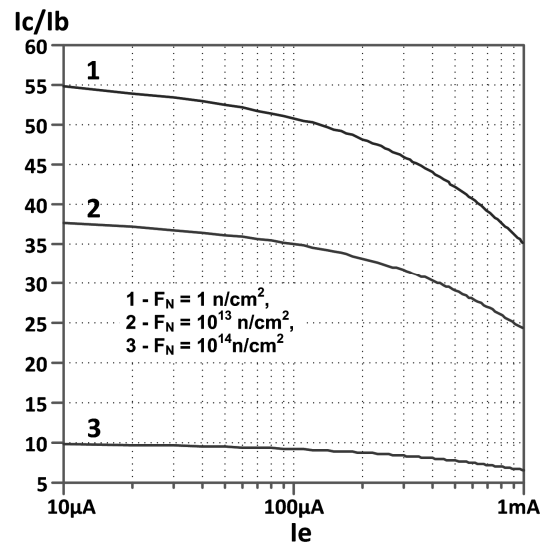


Fig. 2. Dependence of the low-power p-n-p-transistor AC on the emitter current at $T = 30 \text{ }^{\circ}\text{C}$ and different neutron fluxes F_N .

Thus, Fig. 2-6 shows the simulation results of the CVC transistors of the AC MH2XA030 under the influence of temperature T , neutron flux F_N and absorbed dose of D_G gamma quanta in the LTSpice program. The following notations are used in these figures and hereinafter:

- $\beta = I_C/I_B$; I_E , I_C , I_B , I_D – current of emitter, collector, base, drain of the corresponding transistors ;
- V_{GS} , V_{SD} , V_{CB} , V_{EB} – voltage of gate-source, source-drain, collector-base, emitter-base;
- V_{TH} – JFet cutoff voltage.

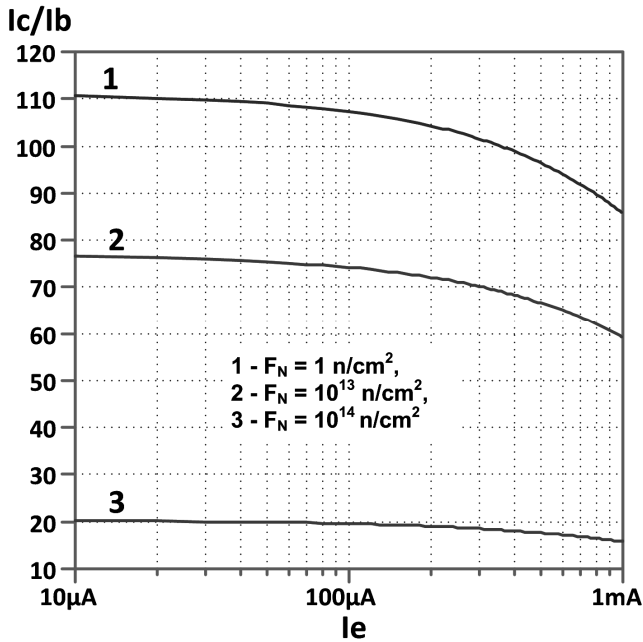


Fig. 3. Dependence of the β of the low-power n-p-n-transistor AC on the emitter current at $T = 30^\circ\text{C}$ and different neutron fluxes F_N .

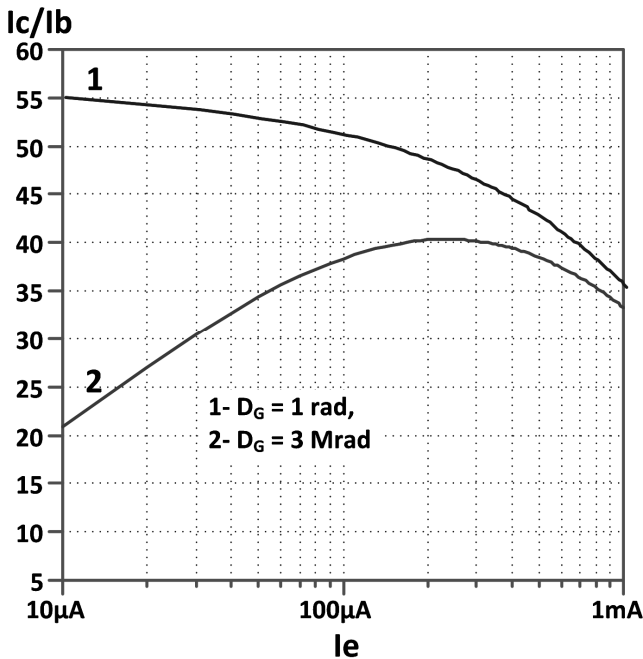


Fig. 4. Dependence of the β of the low-power p-n-p-transistor AC on the emitter current at $T = 30^\circ\text{C}$ and different absorbed doses of gamma radiation D_G .

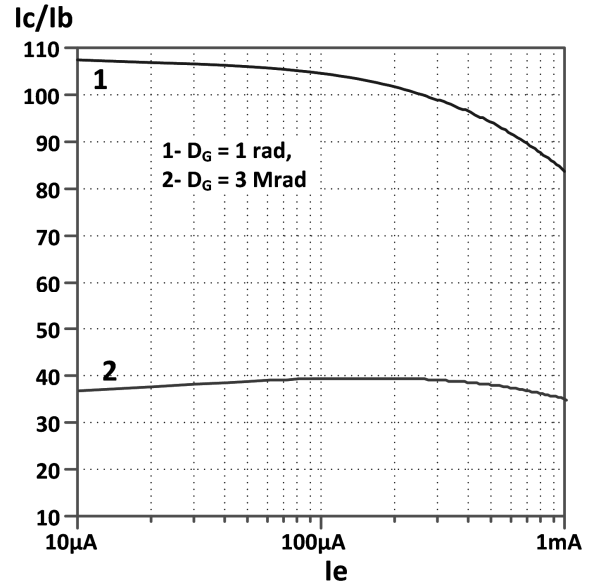


Fig. 5. Dependence of the β of the low-power n-p-n-transistor AC on the emitter current at $T = 30^\circ\text{C}$ and different absorbed doses of gamma radiation D_G .

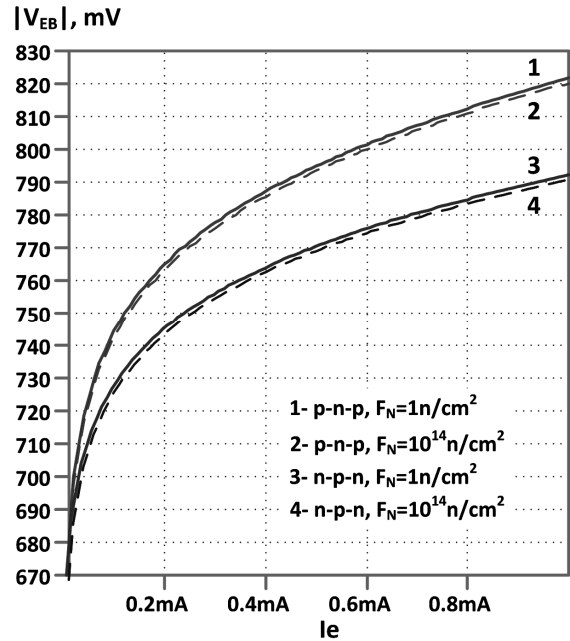


Fig. 6. Dependence of the absolute value of the voltage on the forward-biased emitter junction $|V_{EB}|$ of the low-power transistors AC on the emitter current at $T = 30^\circ\text{C}$ and different neutron fluxes F_N .

IV. RECOMMENDATIONS ON THE SCHEMATIC DESIGN OF THE OP-AMP ON THE AC

When developing the radiation-hardened Op-Amps on the field effect and bipolar transistors, it is advisable to consider the following factors.

First of all, for the transistors it is recommended to perform simulation and analysis of the dependencies: $I_D = f(V_{GS})$ at $V_{SD} = \text{Const} \geq V_{TH}$; $\beta = f(I_E)$ at the collector-base voltage $V_{CB} = 1\text{ V}$; the voltage on the forward-biased emitter junction V_{EB} on I_E , i.e. $V_{EB} = f(I_E)$ at $V_{CB} = 1\text{ V}$. Simulation should be performed under the following conditions:

- the permissible manufacturing tolerance of the cutoff voltage due to the measurement of the parameter $V_{TOValue} = 1.3; 1.44; 1.925$, which corresponds to $V_{TH} = 1.35 \text{ V}; 1.5 \text{ V}; 2 \text{ V}$;
- admissible manufacturing tolerance β ($BFscale = 0.75, 1, 1.25$);
- at the absorbed dose of gamma radiation $D_G = 1 \text{ rad}$ (normal conditions), 100 krad, 1 Mrad, 2 Mrad, 3 Mrad;
- at the neutron flux $F_N = 1 \text{ n/cm}^2$ (normal conditions); 10^{13} n/cm^2 ; 10^{14} n/cm^2 .

Studying the simulation results of the CVC of transistors makes it possible to reveal features that must be taken into account in the schematic synthesis of the radiation-hardened analog ICs. Thus,

- gamma radiation practically does not affect the parameters of the p-JFet, and the influence of the neutron flux is manifested, mainly, at $F_N > 10^{14} \text{ n/cm}^2$. Thus, the cutoff voltage equal to 1.5 V under normal conditions decreases to 0.88 V at $F_N = 10^{15} \text{ n/cm}^2$;
- the effect of gamma radiation and neutron flux do not lead to a significant change in the voltage on the forward-biased emitter junction V_{EB} of the low-power transistors with emitter currents exceeding $10 \mu\text{A}$;
- the strongest drop of the β of the transistors of the AC MH2XA030 occurs at the effect of the neutron flux $F_N = 10^{14} \text{ n/cm}^2$ in comparison with the influence of the absorbed dose $D_G = 3 \text{ Mrad}$. Therefore, as the worst case in the simulation of the radiation hardness, it is recommended to use the value of the model parameter $F_N = 10^{14} \text{ n/cm}^2$ and partially compensate for the drop of the β by choosing the operating mode or applying the circuits of composite transistors.

V. RADIATION-HARDENED OP-AMP OAMP1 IN THE STRUCTURE OF THE AC MH2XA030

Two types of Op-Amps OAMP1, OAMP2 have been developed on the AC MH2XA030. The topology of OAMP1 amplifier is shown in Fig. 7.

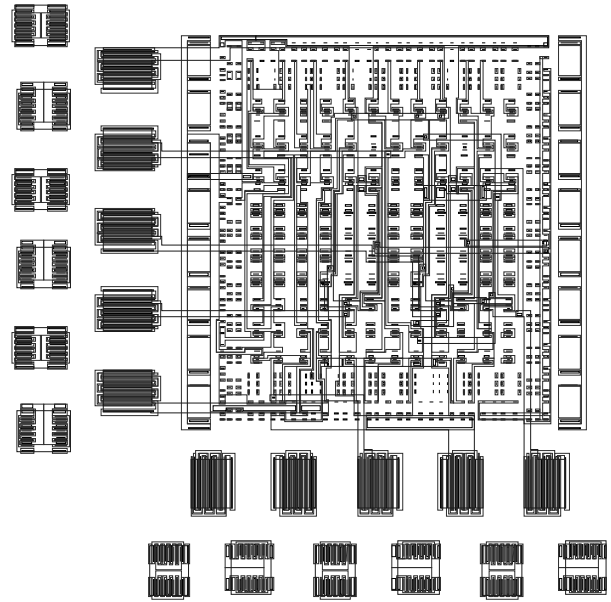


Fig. 7. Simplified topology of amplifier OAMP1 on the AC MH2XA030.

Op-Amp OAMP1 (OAMP2) consists of the voltage controlled current source (VCCS) and the output emitter follower. OAMP1 includes the VCCS shown in Fig. 8, and one output stage Q51-Q54, where the nodes with the same names Bp, Bn, Ou1, Vcc, Vee are interconnected.

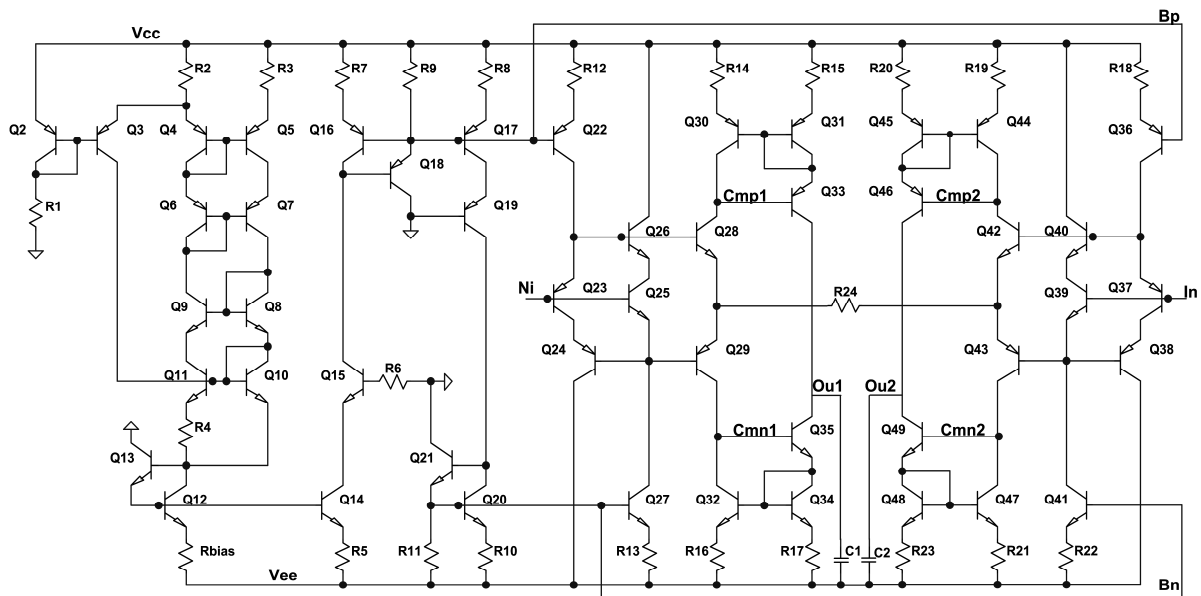


Fig. 8. The electrical diagram of the VCCS, which is part of OAMP1 (OAMP2).

Amplifier OAMP1 is similar to the Op-Amp of the AC MH2XA010 [29,37], although the operating current level of transistors is almost 2 times lower here ($I_{R4} = 61.08 \mu\text{A}$, $I_{R12} \approx I_{R13} \approx I_{R14} \approx I_{R16} \approx I_{R25} \approx I_{R26} \approx 110 \mu\text{A}$, $I_{EQ52} = I_{EQ54} \approx$

$215 \mu\text{A}$). However, the current density of the transistors of OAMP1 and Op-Amp of the AC MH2XA010 is the same.

The transfer characteristics of the Op-Amp are shown in Fig. 9. It follows that the voltage gain $K_V = 7210$, and the offset voltage of OAMP1 corresponds to $642 \mu\text{V}$.

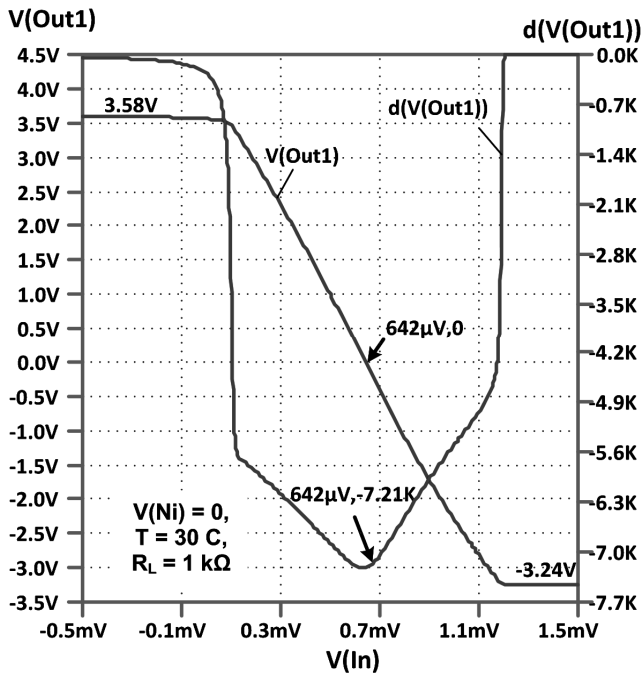


Fig. 9. Dependence of the output voltage and amplification gain of Op-Amp OAmpl on the input voltage $V(\text{In})$.

Fig. 10 shows the amplitude and phase frequency characteristics of OAmpl. The unity gain frequency of the Op-Amp is 50.5 MHz with a phase margin of 56.5°.

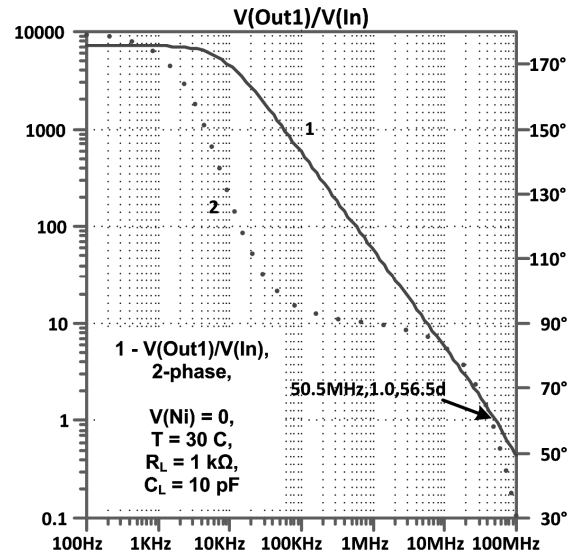


Fig. 10. Amplitude and phase frequency characteristics of Op-Amp OAmpl.

VI. THE OP-AMP WITH PARAPHASE OUTPUT OF OAMP2

Operational amplifier OAmpl2 has a paraphase output and includes a VCCS (Fig. 8), two output stages Q51-Q54 and Q56-Q59 and a differential stage (DS) of the negative feedback loop for the common-mode signal (NF) (Q61-Q70 in Fig. 11).

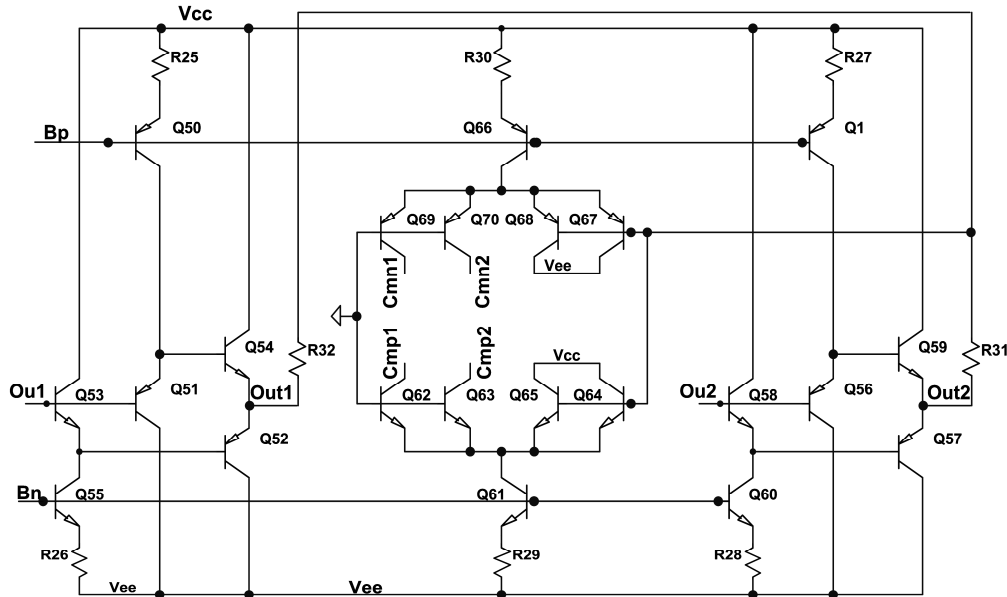


Fig. 11. The method of introducing a negative feedback for the common-mode signal in Op-Amp OAmpl2 [38].

First input of the DS (Q62, Q63, Q69, Q70 bases) is connected to the zero-potential bus, the second input (Q64, Q65, Q67, Q68 bases) – to the output of resistive divider R31, R32, setting the average voltage between the outputs of OAmpl2 (Out1 and Out2 nodes). The outputs of the DSs Cmp1, Cmp2, Cmn1, Cmn2 (collectors of the transistors Q62, Q63, Q69, Q70, respectively) are connected to the

inputs of “current mirrors” Cmp1, Cmp2, Cmn1, Cmn2 of the VCCS.

The NF effect on the static characteristics of OAmpl2 is illustrated in Fig. 12 and Fig. 13, which shows the transfer characteristics of OAmpl1 and OAmpl2 when the value of the BFscale model parameter varies from 0.75 to 1.25.

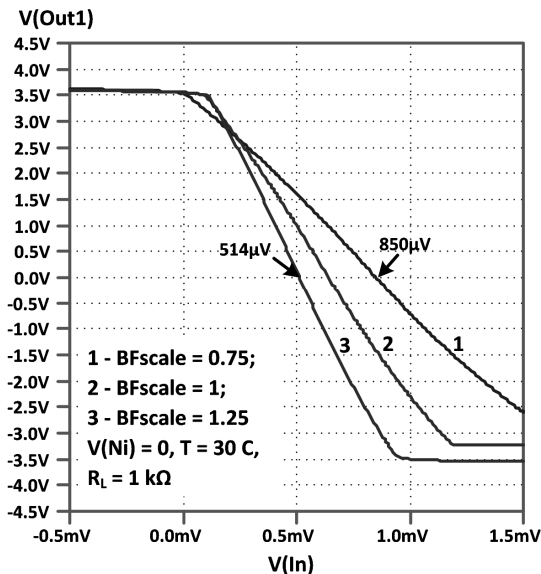


Fig. 12. Dependence of the output voltage $V(Out1)$ on the input $V(In)$ at different values of the BFscale parameter for amplifier OAmpl1.

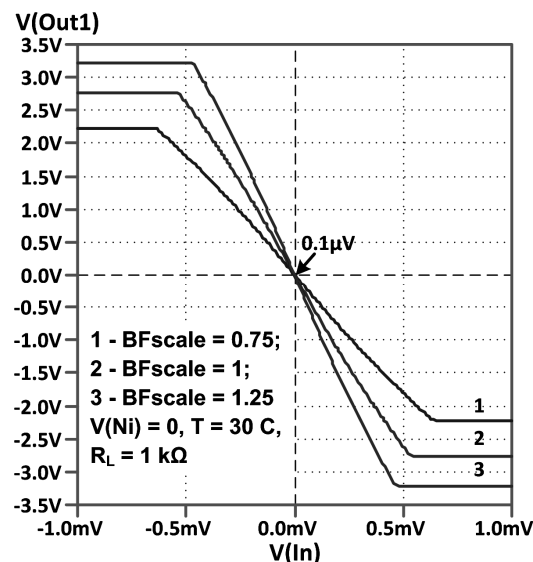


Fig. 13. Dependence of the output voltage $V(Out1)$ on the input $V(In)$ at different values of the BFscale parameter for amplifier OAmpl2.

This change in BFscale causes the same change of the β in both n-p-n- and p-n-p- transistors within the range of $\pm 25\%$ and leads to the change in the offset voltage of OAmpl1 from 514 μV to 850 μV , while the offset voltage of OAmpl2 remains at the level of 0.1 μV (Fig. 13).

Thus, the introduction of the NF for the common-mode signal stabilizes the static mode of the Op-Amp at the permissible manufacturing tolerance of the parameters of the integral elements, the effect of temperature and penetrating radiation [38].

VII. THE SIMULATION RESULTS OF OAMP1 AND OAMP2

Table 1 shows the simulation results of the designed Op-Amps at the temperature of 27 °C.

TABLE I
THE SIMULATION RESULTS OF THE DESIGNED OP-AMP AT
THE POWER SUPPLY OF $\pm 5 V$

| Parameter name | Op-Amp name | |
|---|-------------|------------|
| | OAmpl1 | OAmpl2 |
| Current consumption, mA | 1.79 | 2.51 |
| Input amplifier, μA | 1.28 | 1.28 |
| Offset voltage, μV | 642 | 0.1 |
| Voltage gain | 7214 | 5936 |
| Maximum output voltage, V | -3.24/3.58 | -2.77/2.77 |
| Unity gain frequency, MHz | 50.5 | 46.06 |
| Phase margin at the unity gain, degrees | 56.5 | 53.1 |
| Fourier density of the noise voltage $nV/Hz^{0.5}$ | 3.14 | 3.14 |

VIII. CONCLUSION

For the design of radiation-hardened and cryogenic analog ICs, incl. Op-Amps, a set of tools has been created, containing: BiJFet AC MH2XA030, Spice-models of active and passive elements, as well as the recommendations for schematic design of the analog ICs.

Operational amplifiers OAmpl1 (OAmpl2) have been developed on the AC MH2XA030, which are characterized by the following parameters: current consumption – 1.79 mA (2.51 mA), input current – 1.28 μA , voltage gain – about 7 000 (6 000), offset voltage – 642 μV (0.1 μV), the unity gain frequency – more than 50 (45) MHz. The main fields of application of the Op-Amp are space device engineering and high-energy physics.

ACKNOWLEDGMENT

In the development of amplifiers OAmpl1, OAmpl2, as well as their computer simulation, the results of scientific research conducted at the expense of the grant of the Russian Science Foundation (project No. 16-19-00122) were used.

REFERENCES

- [1] Filanovsky I.M., Ivanov V.V. Operational Amplifier Speed and Accuracy Improvement: Analog Circuit Design with Structural Methodology // Kluwer Academic Publishers. New York. Boston. Dordrecht. London. 2004. 194 p.
- [2] Sedra A.S., Smith K.C. Microelectronic Circuits // 5th ed. – New York: Oxford University Press. 2004. 1392 p.
- [3] Huijsing J. Operational Amplifiers. Theory and Design // 3rd ed. – Springer International Publishing. 2017. 423 p. DOI: 10.1007/978-3-319-28127-8
- [4] Dostal J. Operational amplifiers // 2nd ed. (EDN Series for Design Engineers) – Butterworth-Heinemann. 1993. 387 p.
- [5] Dehghani R. Design of CMOS Operational Amplifiers // Boston: Artech House. 2013. 205 p.
- [6] Franco S. Design With Operational Amplifiers And Analog Integrated Circuits // New York: McGraw-Hill. 2015. 733 p.
- [7] Zumbahlen H. ed. Linear Circuit Design Handbook // Newnes, 2008. 960 p.
- [8] Shea J.J. Op Amp Applications Handbook [Book Review] // in IEEE Electrical Insulation Magazine. V. 22, No. 6. pp. 52-52. Nov.-Dec. 2006. DOI: 10.1109/MEI.2006.253434
- [9] Nordholt E. H. Operational amplifiers // in Proceedings of the IEEE, V. 70. No. 4. pp. 413-413, Apr. 1982. DOI: 10.1109/PROC.1982.12323

- [10] Allen P.E. Operational amplifiers and linear integrated circuits // in Proceedings of the IEEE. V. 71. No. 9. pp. 1116-1116, Sept. 1983. DOI: 10.1109/PROC.1983.12732
- [11] Dessai S.R., Keny P., Gaitonde U., Chandra M.V.S. Design of CMOS based Programmable Gain Operational Amplifier // RSM 2013 IEEE Regional Symposium on Micro and Nanoelectronics, Langkawi. 2013. pp. 139-142. DOI: 10.1109/RSM.2013.6706492
- [12] Prokopenko N.N., Budyakov A.S. Architecture and circuitry of the high speed operational amplifiers // Shakhty: SRSUES. 2006. 232 p. (in Russian)
- [13] Anisimov V.I., Kapitonov M.V., Prokopenko N.N., Sokolov Yu.M. Operational Amplifiers with the direct coupling of stages // L. "Energiya". 1979. 148p. (in Russian)
- [14] Newell M.A., Stern R., Hykes D., Bolotin G., Gregoire T., McCarthy T., Buchanan C., Cozy S. Extreme Temperature (-170C to +125C) Electronics for Nanorover Operation // Aerospace Conference, 2001, IEEE Proceedings. Mar., 10-17 2001. DOI: 10.1109/AERO.2001.931205
- [15] Lee I., Johnston A.H. Comparison of total dose effects on micropower op-amps: bipolar and CMOS // 1998 IEEE Radiation Effects Data Workshop. NSREC 98. Workshop Record. Held in conjunction with IEEE Nuclear and Space Radiation Effects Conference (Cat. No.98TH8385), Newport Beach, CA. 1998. pp. 132-136. DOI: 10.1109/REDW.1998.731492
- [16] Kruckmeyer K., Trinh T. ELDRS Characterization up to 300 Krad of Texas Instruments High Speed Amplifiers, LM7171 and LM6172 // 2015 IEEE Radiation Effects Data Workshop (REDW), Boston, MA. 2015. pp. 1-5. DOI: 10.1109/REDW.2015.7336707
- [17] Kruckmeyer K., McGee L., Brown B., Hughart D. Low Dose Rate Test Results of National Semiconductor's ELDRS-free Bipolar Amplifier LM124 and Comparators LM139 and LM193 // 2008 IEEE Radiation Effects Data Workshop, Tucson, AZ. 2008. pp. 110-117. DOI: 10.1109/REDW.2008.27
- [18] Chen D. *et al.* Radiation Performance of Commercial SiGe HBT BiCMOS High Speed Operational Amplifiers // 2010 IEEE Radiation Effects Data Workshop, Denver, CO. 2010. pp. 5-5. DOI: 10.1109/REDW.2010.5619511
- [19] Guckenberger D., Hiemstra D.M. Simultaneous cryogenic temperature (77 K) and total dose ionizing radiation effects on COTS amplifiers // 2001 IEEE Radiation Effects Data Workshop. NSREC 2001. Workshop Record. Held in conjunction with IEEE Nuclear and Space Radiation Effects Conference (Cat. No.01TH8588), Vancouver, BC. 2001. pp. 14-18. DOI: 10.1109/REDW.2001.960442
- [20] Chen Yu., Mojaradi M., Westergard L., Aranki N., Kolawa E., Blalock B. A case study: Design for reliability for a rail-to-rail operational amplifier for wide temperature range operation for Mars missions // IEEE International Reliability Physics Symposium, Phoenix, AZ. 2008. pp. 121-125. DOI: 10.1109/RELPHY.2008.4558872
- [21] Dvornikov O.V., Prokopenko N.N., Pakhomov I.V., Ignashin A.A., Bugakova A.V. Precision Radiation-Hardened BiJFET OP AMP for Low-temperature Analog Interfaces Sensors // The scientific and practical journal National Research Nuclear University "MEPhI", Global Nuclear Safety. 1(22). pp. 36-45. (in Russian)
- [22] Gulin A.I., Dvornikov O.V., Prokopenko N.N., Bugakova A.V. Design of the radiation-hardened BiJFET OP-AMP for operation in analogue interfaces of sensors at low temperatures // J. Sensors and systems. 2017. No. 12. pp.3-10. (in Russian)
- [23] Teifel J., Flores R.S., Pearson S., Begay C., Ma K.K., Palmer J., ViArray Standard Platforms: Rad-Hard Structured ASICs for Digital and Mixed-Signal Applications // 2012 IEEE Aerospace Conference. Mar. 3-10, 2012. DOI: 10.1109/AERO.2012.6187235
- [24] Analogue arrays from Sweden, SLA description, 1999 Dec., pp. 1-4.
- [25] Stoica A., Keymeulen D., Mojaradi M., Zebulum R., Daud T., Progress in the Development of Field Programmable Analog Arrays for Space Applications," 2008 IEEE Aerospace Conference, Big Sky, MT, 2008. pp. 1-9. DOI: 10.1109/AERO.2008.4526474
- [26] Suda N., Suh J., Hakim N., Cao Y., Bakkaloglu B. A 65 nm Programmable ANalog Device Array (PANDA) for Analog Circuit Emulation // IEEE Transactions on Circuits and Systems I: Regular Papers, 2016 Feb. V. 63. No. 2. pp. 181-190. DOI: 10.1109/TCSI.2015.2512718
- [27] Dvornikov O.V., Prokopenko N.N., Butyrlagin N.V., Bugakova A.V., Perspectives of application of new chips of analog master slice array (AGAMC-2.1) and configurable structured array (MH2XA010) of crystals (JSC MNIPI, Minsk) in the radiation-hardened sensor systems of robots and analog processors // SPIIRAS Proceedings. 2016. issue 2(45). pp. 157-171. DOI: <http://dx.doi.org/10.15622/sp.45.10> (in Russian)
- [28] Dvornikov O.V., Prokopenko N.N., Pakhomov I.V., Butyrlagin N.V., Bugakova A.V. Design of the radiation-hardened analog processors and signal converters of the sensors systems based on basic structural crystal MH2XA010 // J. Radioengineering. 2016. No. 2. pp. 107-113. (in Russian)
- [29] Dvornikov O.V., Dyatlov V.L., Prokopenko N.N., Chekhovskii V.A. Configurable Structured Array for Fabrication of Radiation-Hardened Analog Interfaces // Journal of Communications Technology and Electronics. 2017. V. 62. No. 10. pp. 1193-1199.
- [30] Dvornikov O.V., Chekhovsky V.A., Dyatlov V.L., Prokopenko N.N., New microcircuit of the master slice array MSA-2.1 for the design of the radiation-hardened analog and analog-digital interfaces of the sensor systems // J. Radioengineering. 2016. No. 6. pp.163-168. (in Russian)
- [31] Dvornikov O.V., Bugakova A.V., Prokopenko N.N., Dziaulau V.P., Pakhomov I.V. The microcircuits MH2XA010-02/03 for signal processing of optoelectronic sensors // 2017 18th International Conference of Young Specialists on Micro/Nanotechnologies and Electron Devices (EDM), Erlagol. 2017. pp. 396-402. DOI: 10.1109/EDM.2017.7981781; WOS:000412127000087
- [32] Dvornikov O.V., Tchekhovskii V.A., Prokopenko N.N., Bugakova A.V. The Design of the Circuits of Radiation-Hardened Charge-Sensitive Amplifiers Based on the Structured Array (MH2XA010) and Array Chip (AC-2.1) // 2016 13th International Scientific-Technical Conference on Actual Problems of Electronics Instrument Engineering (APEIE). Novosibirsk. 2016. pp. 253-258. DOI: 10.1109/APEIE.2016.7802268; WOS:000392622500064
- [33] Dvornikov O.V., Tchekhovskii V.A., Dziaulau V.L., Prokopenko N.N. Influence of Ionizing Radiation on the Parameters of an Operational Amplifier Based on Complementary Bipolar Transistors // Russian Microelectronics. 2016. V. 45. No. 1. pp. 54-62. DOI: 10.1134/S1063739716010030.
- [34] Dvornikov O.V., Dziaulau V.L., Prokopenko N.N., Chekhovskii V.A., Pakhomov I.V., Bugakova A.V. The Static Parameters of the Comparators and the Charge-Sensitive Amplifiers of the MH2XA010 Structured Array at Gamma Emission Influence // The scientific and practical journal National Research Nuclear University "MEPhI", Global Nuclear Safety. 2017-2(23). pp. 38-46. (in Russian)
- [35] Dvornikov O.V., Dziaulau V.L., Prokopenko N.N., Petrosiants K.O., Kozhukhov N.V., Tchekhovskii V.A. The Accounting of the Simultaneous Exposure of the Low Temperatures and the Penetrating Radiation at the Circuit Simulation of the BiJFET Analog Interfaces of the Sensors // 2017 International Siberian Conference on Control and Communications (SIBCON), Astana. 2017. pp. 1-6. DOI: 10.1109/SIBCON.2017.7998507; WOS:000426785900084.
- [36] Dvornikov O.V., Grishkov V.N. Radiation hardened analog IC design. Part 1. Radiation effects simulation in the "Spice-like" programs // Problems of Perspective Micro- and Nanoelectronic Systems Development - 2010. Proceedings / edited by A. Stempkovsky, Moscow, IPPM RAS. 2010. pp. 301-306. (in Russian)
- [37] Dvornikov O.V., Chekhovskii V.A., Dyatlov V.L., Prokopenko N.N. A Configurable Analog Integrated Circuit with Programmable Parameters // Instruments and Experimental Techniques. 2016. V. 59. No. 4. pp. 539-543. DOI: 10.1134/S0020441216030143
- [38] Dvornikov O.V., Prokopenko N.N., Pakhomov I.V., Bugakova A.V. The Drivers of the Communication Lines based on Radiation Hardened Structured Array MH2XA010 // 2016 IEEE East-West Design & Test Symposium (EWDTS), Yerevan. 2016. pp. 290-293. DOI: 10.1109/EWDTS.2016.7807728; WOS:000400700700107



Oleg V. Dvornikov was born in 1958 in Minsk, Belarus. He received a degree of candidate of technical sciences in 1994 (BSUIR, Minsk), a degree of Doctor of Technical Sciences in 2008 (BSUIR) in the design and simulation of analog microcircuits.

From 1982 to 1985 he worked at JSC "Integral", from 1985 to the present time he works at JSC Minsk Research Instrument-Making Institute (JSC MNIPI). From 1992 to 2012 he worked part-time at BSUIR as an assistant professor, professor.

Since 2008 - Senior Scientific Officer of JSC "MNIPI", part-time – Senior Scientific Officer of the Scientific Research Institute of the Yakut State University. The author of 2 monographs, 19 teaching and methodical works, more than 150 articles and 80 inventions. Scientific interests include the design of analog microcircuits and sensor interfaces, circuit simulation, the study of radiation resistance. Member of international projects: CMS at the Large Hadron Collider at the European Center for Nuclear Research (Geneva, Switzerland), D0 at the accelerator-collider Tevatron in the National Accelerator Laboratory, Enrico Fermi (Batavia, USA). He has the following awards: Thanks-you letter of Apr.10, 2000 from the Fermi National Accelerator Laboratory (Batavia, Illinois, USA) for the development and serial shipments of 1700 printed circuit boards with 8-channel specialized microcircuits Ampl-8.3 and Disk-8.3. Diploma of the second degree from Feb. 19, 2010 Joint Institute for Nuclear Research (Dubna, Russia) for the work "Development, creation and application of mini-drift tubes with recording electronics in experiments on high-energy physics." Diploma of the first degree for the victory in the nomination "The best innovative project in the field of instrumentation, domestic element base" at the XXI International Exhibition and Congress HI-TECH'2015 (St. Petersburg, 2015).



Valentin L. Dziatlau, was born in 1987, in Chausy, Mogilev region, Belarus. He received his master's degree in 2011 at the Belarusian State University of Informatics and Radioelectronics. From 2011 to 2018 he worked at JSC Minsk Research Instrument-Making Institute (JSC MNIPI). From 2011 to 2018 he worked at JSC Minsk Research Instrument-Making Institute (JSC MNIPI). Since 2017 he has been working in the research institutions of the Belarusian State University: the Research Institute for Applied Physical Problems, the National Center for Particle Physics and High Energy, the Institute of Nuclear Problems (Research Institute of Nuclear Problems). Author of more than 34 articles and 4 inventions. Scientific interests include the research of analog microcircuits, radiation resistance, sensor interfaces, circuit simulation, automation of measurements of parameters of microcircuits and element base.



Vladimir A. Tchekhovski, was born in 1960 in Minsk, Belarus. Graduate of Minsk Radio Engineering Institute, specialty "Design and manufacture of electronic computing equipment". Since 1985 he has been working in the research institutions of the Belarusian State University: the Research Institute for Applied Physical Problems, the National Center for Particle Physics and High Energy, the Institute of Nuclear Problems (Research Institute of Nuclear Problems). Since 2015 - Head of the Laboratory of the Research Institute of the Belarusian State University. Author of more than one hundred articles and scientific papers. Scientific interests: development of programmable analog microelectronic products for harsh operating conditions, including radiation-resistant ones; analog microcircuits, automated measurement of



parameters of microcircuits, methods of testing of microcircuits for radiation resistance. Member of international projects: CMS (CERN, Switzerland), MPD (NICA, JINR, Russian Federation). Co-author of CERN's official technical documentation for the CMS muon detector: "Technical Design Report" (CERN / LHC 97-32 CMSTDR 3 15.12.97, chapters 4.3.4.4), "ME1 / 1 Engineering Design Review" (1999-035 CMSDOCUMENT, June 21-23.1999).

Nikolay N. Prokopenko (M'2012) was born in 1949 in the village Koltunovka, Stavropol Territory (Russia). PhD in Engineering Science (1975, SPSETI, the city of Leningrad), Doctor of Engineering Science (2001), Taganrog Radio Engineering University). Research interests: microelectronics, automation and computer facilities, instrument engineering, communication systems and telecommunications.

At the present time he is a head of the Department "Information Systems and Radio Engineering" of DSTU, a head of Scientific and Research Laboratory of Design Problems in Extreme Microelectronics of IPPM RAS and DSTU, President of the Section of Academic Science and Innovations of Rectors' Board of Higher Educational Institutions of Rostov region. He is the author and co-author of 20 monographs, more 200 articles and 500 inventions. Member of the IEEE. Honored Inventor of the Russian Federation.

Member of the program committee of the international symposium EWDTS (since 2014). Co-chair of the section of the All-Russian Conference Designing Microelectronic Systems (MES, Zelenograd) (since 2016). Counselor at the rector of the DSTU on issues of scientific and innovative work. Chairman of the section "ADP-2 Imaging" at the conference 24th IEEE International Conference on Electronics, Circuits and Systems (ICECS'2017, Batumi, Georgia).



Anna V. Bugakova (SM'2017) was born in 1992 in Shakhty, Russia. Received a Bachelor's Degree in information service (2015) and a Master's Degree in the area of intelligence information systems (DSTU, 2017).

Since 2017, she has been a PhD student of DSTU in the field of 05.13.05 "Elements and Devices of Computer Engineering and Control Systems". In 2013-2017, she was being a research assistant of DSTU, since 2017, she has been an engineer of DSTU. The scientific interest is an analog and A/D microcircuitry.

She has awards of DSTU for high indexes in research work and Diplomas of arrangements committees of IEEE conferences and symposiums for the effective reporting.

She has awards of DSTU for high indexes in research work, Diplomas of IEEE organizing committees and symposiums (EWDTS, TELFOR, etc.) for successful presentation of reports. Since 2017 is laureate the Russian President's scholarship to the young scientist and PhD students in the field of "Space technologies related to telecommunications, including GLONASS, and the program for the development of ground infrastructure."

The Peculiarities of Application of the Potential Fields Method for the Problems of Local Navigation of Mobile Robots

Alexander B. Filimonov¹, Nikolay B. Filimonov²

¹Moscow Technological University (MIREA), Moscow, Russia

²Lomonosov Moscow State University, Moscow, Russia

Abstract – The methodology of application of linear-quadratic optimization for problems of sequential regulation, where it is necessary to watch the dynamic processes in the environment is considered in the paper. The generalized scheme of control system combining the principles of the construction of classical single-loop regulation systems and stabilization systems with feedback condition is in its base. The proposed solutions represent the idea of conversion of stabilization problems for tracking problems in connection with class of systems with zero steady-state tracking error.

Index Terms – Mobile robots, local navigation, planning of movements, artificial potential fields, the problem of local minimums, the problem of going around the obstacles.

I. INTRODUCTION

ONE of the urgency problem of mobile robotics is the problem of robot's navigation in the working space that is the analysis of the current situation and the autonomous (that is without the man's participation) choice of the route by robot. The process of the navigation of the mobile robot (MR) includes the following steps: the preparation of the map of the external environment, the localization of robot in space and the planning of its route conducting to purpose.

The problems of global and local navigation of MR [1] are recognized. The *global navigation* is involved with the questions of the definition of absolute coordinates of robot on the map and the transfer to the given points of this map on the long routes. Here the trajectory is adapted still before the beginning of the movement on the base of the received information. The *local navigation* is involved with the decision of the following group of the problems: the definition of the coordinates of objects with respect to some (often start) point, the planning of robot's transfer in the working space and keeping the obstacles from collision (going around the obstacles) during the movement.

We emphasize that the planning defines here the only small interval of trajectory, in final point of which the further trajectory is chosen.

The working space of robot denoted later by W they call the enclosing space where it operated. The problems of the route planning (route planning) and the movement planning (movement planning) are distinguished.

The method of artificial potential fields, which also named "virtual force fields" is relative to the number of popular

methods of local MR navigation. Its idea was proposed in the paper [2]. Among the first papers developing the given method let us note [3]. Rather full representation concerning the peculiarities of its use in mobile robotics the papers [4–15] are given. In doing so the papers using the method of potential fields in scenario of real time strategy for computer games (see, for example [16]) we may evolve especially.

II. PROBLEM DEFINITION

The electric fields are the physical similar to the artificial potential fields. They suppose that robot disposes by the map of the environment and is provided with the navigation system making possible to define its coordinates rather exactly. The functional structure of robot has the generation module of virtual field $U(\mathbf{q})$, which enters into the informational base of MR and is used to control algorithms for calculation of virtual forces being used to the control algorithms so to attract robot to the aim and was repelled from beforehand well-known obstacles. If the new obstacles come from in the path of robot's movement, then the virtual field becomes renewed.

The route is the continuous curve in the working space:

$$\mathbf{c}:[0,1] \rightarrow W$$

If the route is parametrized by time t , then $\mathbf{c}(t)$ is the trajectory and by means of its differentiation we can calculate the routes and accelerations of MR. The determination of possible trajectory is called the trajectory planning or the movement planning.

In the report the plane problem $W \subseteq \mathbf{R}^2$ is considered, then robot is as mass point and so its orientation may be disregarded.

Three aspects of the potentials method are discussed in the report: the choice of the structure of virtual fields, the problem of local minimums and strategy of going around of the obstacles.

III. METHOD OF THE ARTIFICIAL POTENTIAL FIELDS

The potential field $U(\mathbf{q})$ is formed by superposition of two fields: the attracting field, which is produced by the aim, and the repelling one being formed by the obstacles:

$$U(\mathbf{q}) = U_{att}(\mathbf{q}) + U_{rep}(\mathbf{q}). \quad (1)$$

Then we'll suppose, that the field $U(\mathbf{q})$ is differentiated one. The potential force in the position $\mathbf{q}=(x,y)$ is as anti-gradient of the function $U(\mathbf{q})$:

$$F(\mathbf{q}) = -\nabla U(\mathbf{q}),$$

where

$$\nabla U(\mathbf{q}) = \text{col} \left(\frac{\partial U(\mathbf{q})}{\partial x}, \frac{\partial U(\mathbf{q})}{\partial y} \right).$$

According to (1) the virtual force being made by the field we also may decompose into two components: the attracting and the repelling forces:

$$F(\mathbf{q}) = F_{att}(\mathbf{q}) + F_{rep}(\mathbf{q}), \quad (2)$$

where

$$F_{att}(\mathbf{q}) = -\nabla U_{att}(\mathbf{q}),$$

$$F_{rep}(\mathbf{q}) = -\nabla U_{rep}(\mathbf{q}).$$

The virtual force (2) may be used for control by robot's movement, directing it to the aim and preventing the collisions with the obstacles. There are three ways of such its use [11]:

- the controlling input \mathbf{u} of robot is formed according to the law:

$$\mathbf{u} = F(\mathbf{q});$$

- in the scheme of kinematic control the force field gives the desired speed of robot's movement:

$$\dot{\mathbf{q}} = F(\mathbf{q}).$$

- in the scheme of dynamic control robot is considered as large point to which the given force is operated:

$$\ddot{\mathbf{q}} = F(\mathbf{q}).$$

The attracting potential. In the capacity of the attracting potential we usually take (see, for example, [4–6] the parabolic function:

$$U_{att}(\mathbf{q}) = \frac{1}{2} k_a d(\mathbf{q})^2, \quad (3)$$

where $k_a > 0$ is constant, $d(\mathbf{q})$ is Euclidean distance of MR up to the aim, which is said to be in point \mathbf{q}_{goal} :

$$d(\mathbf{q}) = \|\mathbf{q} - \mathbf{q}_{goal}\|.$$

Here and further $\|\bullet\|$ is Euclidean vector norm.

The repelling potential. The repelling potential must be very large near the obstacle and must not influence on the robot's movement far from it. The following way of the repelling potential task [9–11] is very extended:

$$U_{rep}(\mathbf{q}) = \begin{cases} \frac{1}{2} k_r \left(\frac{1}{d(\mathbf{q})} - \frac{1}{\rho_0} \right)^2, & d(\mathbf{q}) \leq \rho_0; \\ 0, & d(\mathbf{q}) > \rho_0. \end{cases} \quad (4)$$

where $k_r > 0$, $d(\mathbf{q})$ is minimum distance up to the obstacle. Thus the given field creates the “potential barrier” around the width obstacle ρ_0 where the potential is increased sharply during the approach to the obstacle.

IV. CHOICE OF THE POTENTIAL FIELD STRUCTURE

The field (3) generates the potential forces

$$F_{att}(\mathbf{q}) = -k_a (\mathbf{q} - \mathbf{q}_{goal}),$$

where

$$\|F_{att}(\mathbf{q})\| = k_a \|\mathbf{q} - \mathbf{q}_{goal}\|.$$

Let us note the important characteristic of the following solution: being formed gravitational pull is changed essentially in process of robot's movement and under approach to the aim it tends to zero so that the MR movement will be slow down at the end of the route. It inevitably will reduce to the unwarranted tightening of general time of MR movement to the goal position.

To remove the given undesirable effect the authors propose to use the attracting potential fields of the other form [17, 18]:

$$U_{att}(\mathbf{q}) = \frac{1}{2} k_a d(\mathbf{q}).$$

In this case we'll get the attracting force

$$F_{att}(\mathbf{q}) = -k_a \frac{\mathbf{q} - \mathbf{q}_{goal}}{d(\mathbf{q})},$$

the absolute value of which will be constant:

$$\|F_{att}(\mathbf{q})\| = k_a.$$

V. THE PROBLEM OF LOCAL MINIMUMS

The problem of local minimums in the method of potential fields is known widely [6, 9–11]. The configuration of the environment can reduce to the occurrence of the potential holes of the different geometric structure and they take a position of the traps for MR.

In the kinematic control scheme robot moves to the direct of the field's antigradient:

$$\dot{\mathbf{q}}(t) = -\nabla U(\mathbf{q}(t)).$$

i.e. it follows the trajectory of gradient descent.

At the point of local minimum \mathbf{q}^* gradient of the potential function is equal to zero

$$\nabla U(\mathbf{q}^*) = 0,$$

that is robot will stop after hit in it.

We have another picture in the scheme of the dynamic control: MR picked up speed and on the strength of its inertia it will be overcome the small potential holes. To analyze the given schemes it is appropriate to turn into the experiment of numerical solution of unconditional optimization problems of nonconvex goal functions. The different methods of

search of global minimum for such functions are developed in the optimization theory. The method of “heavy small ball”, the physical analog of which is the process of the rolling down of the small ball along inclined surface reduced to the numerical of these functions. If the small ball is heavy it by-pass the small hollows mechanically. The more is mass of the small ball, the more deeply may be the hollows which it by-pass during the movement. Evidently the scheme of dynamic control by robot is identical to the given method although has the principle difference: we a priori know the point of global minimum of the potential field $\mathbf{q} = \mathbf{q}_{goal}$.

And also we must take into account that robot tests the action of resistance forces for the movement from side of the external environment in the real conditions.

But the schemes of the dynamic control do not guarantee overcoming deep potential holes by MR during the movement. Let us note the character of the trajectories' movement of MR captured the potential hole: in the neighborhood of the local minimum robot will be perform recursive-forward or cyclic movement along closed curve and as a result it will not be able to continue the movement to the aim.

It is interesting the historical aspect of the development of the potential fields method. In the first papers in this area of the investigation the trajectory of robot was calculated in consequence of the integration of differential movement equations of the second order. But during the process of the investigations it was found to be the inertia factor may reduce to impractical forms of the trajectories near the extensive obstacles and as a result of multiple repulsions MR from the obstacles its trajectory will be take a position of ‘rugged’ trajectory too much [6]. In view of this later was turned to the models of the movement of the first order.

Thus the problem of the first origin in the potential fields can't be solved completely by means of use of the simple models of the movement of the first or the second order and points to necessary of the complication of control algorithms MR.

In connection with this the following problems are actual:

- 1) diagnostics of the capture of robot's trajectory of the movement by the potential hole;
- 2) output of robot from the potential hole.

The situation of MR hit into the potential hole in case of the application of the kinematic control schemes one may diagnose by means of the operating check its trajectory speed: the chance answer it when speed and speeding up are found to be lower of some threshold levels in the process of the motion. In the schemes of the dynamic control the situation of hit into the hole is diagnosed by means of the detection of the fact of the trajectory localization in some limited zone of the working space. It is necessary to accumulate and develop data observation during some sliding time interval for it.

The authors propose the general approach for solution of two key problems for mobile robotics: the output of robot from the potential hole and going around the obstacles.

VI. THE STRATEGY OF GOING AROUND THE OBSTACLES

The problem of going around the obstacles may be classified under two subproblems:

- 1) the detection of the obstacle in the path of the robot's movement;
- 2) the organization of going around the obstacles.

The very popular way of going around the obstacles by robot is the method of “Vector Fields Histogram” suggested in the paper [19]. It makes possible to discover the obstacles and go around them during the movement. The peculiarities and possibilities of the given method are presented in monographs [6, 10, 11].

The new way of going around the obstacles is proposed in the given report. It may be useful for mobile robotics. The idea of *separated* use in control algorithms of two maps of the potential fields $U(\mathbf{q})$ and $U_{rep}(\mathbf{q})$ in situated in its base. The force lines of the first potential field and equipotential lines (isolines) of the second one are considered as analogues with the navigation isolines on the navigation maps for navigation, for example, magnetic meridians and the Earth parallels.

The force fields lines $U(\mathbf{q})$ are used for building of the route of MR movement.

Isolines of the repelling field are described by the equation

$$U_{rep}(\mathbf{q}) = C,$$

where $C > 0$ is constant.

The map of isolines of $U_{rep}(\mathbf{q})$ function permits to solve two problems. In the first place it makes possible to check the situations of coming together robot with obstacles. Secondly the field isolines represent information about the obstacle's geometry and are situated in the base of the structure of going around the given obstacle, that is the robot's movement is aligned with isoline and hence is governed by the equation

$$\langle \dot{\mathbf{q}}, \nabla U_{rep}(\mathbf{q}) \rangle = 0,$$

where the corner brackets \langle , \rangle are used for the notation of scalar vectors product.

VII. CONCLUSION

The questions of local navigation of mobile robots are considered. The method of the artificial potential fields belongs to the number of the popular methods of local navigation of robots. The peculiarities of the given method are analyzed in the paper. The question of the choice structure of the attracting potential fields is researched. The problem of local minimums in the potential fields method is touched upon. The analysis of the kinematic and dynamic aspects of control by robot's transfer is conducted. The new way of going around the obstacles in motion of robot to the aim is suggested.

In the work [20] is discussed the problem of the structure's formation in group of the moving objects is discussed. Two variants of statement of the problem are considered: kinemat-

ic and dynamic. The kinematic variant leads to one from the base problems of combinatorial optimization, that is the problem about assignments. The proposed solutions of the dynamic problem are based on the method of virtual force fields.

REFERENCES

- [1] Bobrovsky S.N. Navigation of mobile robots // Journal PC Week. 2004. No 9, pp. 60-63 (in Russian).
- [2] Khatib O., Le Maitre J.-F. Dynamic Control of Manipulators Operating in a Complex Environment // Proceedings RoManSy'78, 3rd CISM-IFTOMM Symp., 1978, pp. 1-24.
- [3] Andrews J.R., Hogan N. Impedance Control as a Framework for Implementing Obstacle Avoidance in a Manipulator. In David E. Hardt and Wayne J. Book, ed. Control of Manufacturing Processes and Robotic Systems. 1983, pp. 243-251.
- [4] Khatib O. Real-time obstacle avoidance for manipulators and mobile robots // The International Journal of Robotics Research. 1986. Vol. 5 (1), pp. 90-98.
- [5] Ge S.S., Cui Y.J. New Potential Functions for Mobile Robot Path Planning. IEEE Transactions on Robotics and Automation. 2000. Vol. 16. № 5. - P. 615-620.
- [6] Platonov A.K. Kiril'chenko A.A., Kolganov M.A. The Potential Field Approach in the Path Finding Problem: History and Perspectives // Preprint, Inst. Appl. Math., the Russian Academy of Science. 2001. No 40. - 32 p. (in Russian).
- [7] Howard A., Mataric M.J., Sukhatme G.S. Mobile Sensor Network Deployment Using Potential Fields: a Distributed, Scalable Solution to the Area Coverage // Proceedings of the 6th International Symposium on Distributed Autonomous Robotics Systems. - Fukuoka, Japan, June 2002, pp.113-126.
- [8] Pozna C., Precup R.-E., Koczy L.T., Ballagi A. Potential Field-Based Approach for Obstacle Avoidance Trajectories // The IPSI BgD Transactions on Internet Research. 2002. Vol. 8. № 2, pp. 40-45.
- [9] Siegwart R., Nourbakhsh I.R. Introduction to Autonomous Mobile Robots. - Cambridge: MIT Press. 2004. - 321 p.
- [10] Choset H., Lynch K.M., Hutchinson S., Kantor G.A., Burgard W., Kavraki L.E., Thrun S. Principles of Robot Motion: Theory, Algorithms and Implementations. - Cambridge: Howie MIT Press. 2005. - 603 p.
- [11] Coenen S.A.M. Motion Planning for Mobile Robots - A Guide // Control Systems Technology. 2012, pp. 79.
- [12] Chepizhenko V.I. The Analysis of Use of the Potential Field Methods for the Solution of Navigation and Confluent Problems // Cybernetics and Computerized Technology. 2012. No 1, pp. 15-24 (in Russian).
- [13] Li F., Tan Y., Wang Y., Ge G. Mobile Robots Path Planning Based on Evolutionary Artificial Potential Fields Approach // Proceedings of the 2nd International Conference on Computer Science and Electronics Engineering. 2013. - pp. 1314-1317.
- [14] Local Autonomous Robot Navigation Using Potential Fields / M.A. Padilla Castaneda, J. Savage, A. Hernandez, F. Arambula Cosio. Motion Planning, Xing-Jian Jing (Ed.). 2008. [Electronic resource] http://www.intechopen.com/books/motion_planning/local_autonomous_robot_navigation_using_potential_fields
- [15] Beloglazov D.A., Gajduk A.R., Kosemko E.Iu., etc. The Group Control by the Moving Objects in Indefinite Mediums. By edit. V.Kh. Pshikhopov. M. PHYSMATLIT. 2015. - 305 p. (in Russian).
- [16] Hagelback J., Johansson S.J. Using Multi-agent Potential Fields in Real-time Strategy Games. Proceedings of 7th International Joint Conference on Autonomous Agents and Multi-agent Systems (AAMAS 2008), Padgham L., Parkes D. (eds.). Vol. 2. Estoril, Portugal, May 2008. - P. 631-638.
- [17] Filimonov A.B., Filimonov N.B. Some aspects of use of the potential fields method in the problems of local navigation of mobile robots. Control problems and simulation in complex systems: The papers of XIX International conference. Samara. Sam SC RAS. 2017, pp. 242-247 (in Russian).
- [18] Filimonov A.B., Filimonov N.B. Methodology of artificial potential fields in the problems of local navigation of mobile robots. Intellectual systems, control and mechatronics: The materials of the third All-Russian conference of the young scientist, post-graduates and students. Sevastopol. Sev.SU. 2017, pp. 157-160 (in Russian).
- [19] Borenstein J., Koren Y. Real-time Obstacle Avoidance for Fast Mobile Robots in Cluttered Environments. IEEE Int. Conf. Robotics and Automation. 1990, pp. 572-577.
- [20] Filimonov A.B., Filimonov N.B. Formation Shaping in Group of Moving Objects on the Basis of the Method of Virtual Force Fields // Journal of Advanced Research in Technical Science. North Charleston, USA: SRC MS, CreateSpace. 2018. Issue 9-1, pp. 67-72.



Filimonov Aleksandr Borisovich – professor of Moscow Technological University (MIREA), the department of automatic control systems. Dr. of eng. sc. (system analysis, control and information processing, 2003). Research interests: theory of control system, intellectual technologies of information processing and control processes, multi-agent information control systems. The number of publications - 250.
E-mail: filimon_ab@mail.ru;
Phone: +79032929125.



Filimonov Nikolay Borisovich – professor of Lomo-nosov Moscow State University, the department of physics and mathematical methods of control. Dr. of eng. sc. (system analysis, control and information processing, 2009). Research interests: theory of control system, polyhedral optimization of control processes, intellectualization of automatic systems. The number of publications - 260.
E-mail: nbfilimonov@mail.ru;
Phone: +79165147102.

PI2D-Controllers Synthesis for Nonlinear Nonstationary Plants

Galina A. Frantsuzova
Novosibirsk State Technical University, Novosibirsk, Russia

Abstract – PID controller modification by adding an additional differentiation channel is presented in the paper. The resulting linear controller is proposed to be called the PI2D controller. It is proposed to move the differential channel in the feedback to eliminate the undesirable effects from differentiation. It is shown that such controller division into two components entails the appearance of two control loops in the system. In accordance with this fact, it is proposed to calculate the PI2D controller coefficients in the two stages. At the first stage, it is recommended to use the basic relation of the localization method for calculating the inner contour. It is proposed to apply a modal approach in the outer control loop synthesis. It is shown that the calculated PI2D controller provides the stabilization of the second order nonlinear non-stationary plants. The results of numerical simulation of the system in the MatLab are presented. They illustrate the PI2D controller main properties.

Index Terms – Control, PI2D-controller, nonlinear plant, localization method.

I. INTRODUCTION

ALTHOUGH ones of the first industrial controllers are typical PID-regulators, they are still widely used in the industry and have not lost their relevance at the present time [1 - 5]. The reasons for such a high popularity are the construction simplicity and industrial application, the properties and operating principle, the suitability for the most practical problems and their low cost. All of the above is an indisputable advantage of the typical controllers.

Despite the fact that a large number of the recommendations on the tuning [1, 3, 4], calculation [2, 5, 7] and the optimizing of the controllers parameters [6] have been developed to date, a universal technique for their synthesis has not yet been proposed. Often, after calculating the PID-controller, it is necessary to refine its parameters and perform their manual adjustment. The typical controllers do not provide the required quality in the automatic system if the external factors (load changes, ambient temperatures, etc.) have a significant effect on the plant or its parameters change over time.

The typical PID controller completely solves the stabilization problem for the nonlinear first order plants [1 - 6]. Due to a practical convenience, such controllers are also used for the higher order plants. However, the requirements to the system both in the dynamic properties and in the perturbations suppressing are compulsorily weakened, especially if there are the nonlinearities in the system.

It is possible to significantly expand the traditional PID-controllers application scope by using the additional chan-

nels. On the PID controller based, the various controllers with different properties are offered: P2ID [8, 9], a fractional-order controller [10], controller with weight coefficients by mistake, etc. [6]. First of all, the modification assumes such controller transformation, so that it becomes robust [11 - 14].

The localization method [15 - 18] is an effective approach to the controller synthesis for a class of the nonlinear plants with the external perturbations. The resulting controller has the robustness property both in relation to the nonlinear characteristics and to the action of external perturbing factors.

In this paper, we present an original PI2D controller obtained by adding to the typical PID controller an additional channel of the double differentiation. Moreover it was suggested to separate the individual controller components and transfer the differential channel in the feedback. It was leaded to the two control-loops appearance in the system. In accordance with this fact, it is proposed to calculate the PI2D controller coefficients in the two stages. The inner contour structure corresponds to the system based on the localization method, therefore for its calculation it is possible to use this method relations [15 - 17]. It is proposed to apply a modal approach in the outer control loop synthesis.

The purpose of this paper is to investigate the system with PI2D-controller and develop a calculating procedure the controller coefficients based on the localization method relationships for a class of the second order nonlinear non-stationary plants.

II. PROBLEM DEFINITION

We consider the stabilization problem for a nonlinear, non-stationary second-order plants with the model in the form

$$\ddot{y} = f(t, \dot{y}, y) + b(t, \dot{y}, y)u, \quad (1)$$

where $y \in R^1$ - plant output variable; $u \in R^1$ - control variable; functions $f(t, \dot{y}, y)$ and $b(t, \dot{y}, y)$ - are continuous and differentiable ones, have the bounded derivatives; their values can vary within a certain range depending on the system operating conditions: $|f(\cdot)| \leq f_{\max}$, $0 < b_{\min} \leq |b(\cdot)| \leq b_{\max}$. Also, the functions dependence on the time reflects the perturbations affect on the plant.

It is necessary to calculate a linear robust controller to ensure the requirements for the process quality in the system. These requirements are specified in the form of the estimates

for a transient time, overshoot and permissible error in the static regime.

III. THEORY

A. Controller Description

We will consider a modified typical PID controller with an added channel of the double differentiation. As a result, we obtain a PI2D controller [8, 9] with a transfer function of the form

$$W_{PI2D}(s) = k_p + \frac{k_i}{s} + k_{D1}s + k_{D2}s^2 \quad (2)$$

where k_p , k_i , k_{D1} and k_{D2} - the proportional, integral and differential components coefficients, respectively.

The main problem in the PI2D controller implementation is the error signal derivative channel (differential component) [2, 11]. This channel increases the gain with increasing the frequency, and this leads to the following undesirable effects at the system output.

1. As the high-frequency component of the error signal rises, the useful signal-to-noise ratio decreases. This fact entails a control system destabilization.
2. If a step signal is applied to the system input, then the large amplitude pulses occur at the moment of a sudden change in the error level. The delta-like pulses presence can lead to serious consequences: from a quiet breakdown to a loud explosion of an installation.

There are several options for a partial elimination of the undesirable effects associated with the differential component, such as the low-frequency filters use, the differential channel transfer into the feedback. Let's consider the PI2D controller possibilities that transfer function (2) can be represented in the form

$$W_{PI2D}(s) = k_{D2} \left[\frac{c_0}{s} + (s^2 + c_2s + c_1) \right], \quad (3)$$

where the coefficients are notated:

$$\begin{cases} c_0 = k_i / k_{D2}, \\ c_1 = k_p / k_{D2}, \\ c_2 = k_{D1} / k_{D2}. \end{cases} \quad (4)$$

Here, the integral component and the proportional-differential part were singled out. The differential component in the system with the PI2D-controller is transferred to the feedback channel for the entering and tracking modes (Fig. 1). As you can see, the system contains a nonlinear control plant and a linear controller.

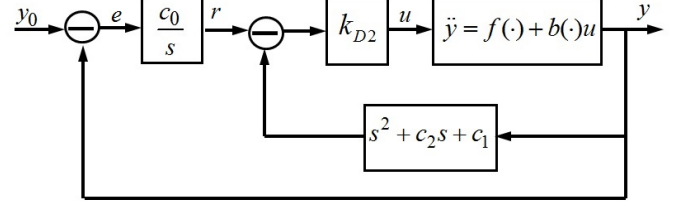


Fig. 1. Block diagram of the system with a separated PI2D-controller.

This system has two control loops, therefore it is proposed to calculate the controller in the two stages.

B. PI2D Controller Design

Now, if we consider the system structure (Fig. 1), it is clear that the inner contour fully corresponds to the structure of the system based on the localization method [16, 17]. Since this method is oriented to nonlinear non-stationary plants, it is first proposed to calculate the inner contour taking into account the localization method relations.

In accordance with the system structure (Fig. 1), we write the equation for the proportional-differential part of the controller (3) in the form

$$u = k_{D2} [r - c_1y - c_2\dot{y} - \ddot{y}]$$

or

$$u = k_{D2} [F(y, \dot{y}, r) - \ddot{y}], \quad (5)$$

where $F(y, \dot{y}, r) = r - c_1y - c_2\dot{y}$ can be considered as a function corresponding to the desired contour behavior.

Substituting (5) into the plant equation (1), we obtain after the transformation the contour description in the form

$$\ddot{y} = \frac{1}{1 + b(\cdot)k_{D2}} f(t, \dot{y}, y) + \frac{1}{1 + b(\cdot)k_{D2}} F(y, \dot{y}, r)$$

It is clear that in the limit for $k_{D2} \rightarrow \infty$ the contour behavior describes the desired equation

$$\ddot{y} = F(y, \dot{y}, r). \quad (6)$$

For the practical calculations k_{D2} we will use the localization method recommendations [16], that is, will choose a coefficient depending on the required accuracy in the form

$$b_{\min} k_{D2} \approx 20 \dots 100. \quad (7)$$

After the inner contour dynamics is subordinated to the linear equation (6), its model can be represented as a transfer function

$$W_{inner}(s) = \frac{y}{r} = \frac{1}{s^2 + c_2s + c_1}.$$

Now we consider the calculation of the outer contour (Fig. 2). It does not depend on the plant time-varying parameters and the nonlinear characteristics (1).

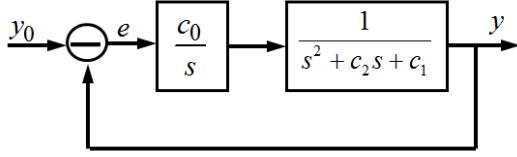


Fig. 2. Block diagram of the outer contour.

To calculate the controller coefficients $c_i, i = \overline{0,2}$, we use the linear control theory, namely the modal approach [17]. In accordance with it, we define the characteristic equation of the outer contour in the form

$$A(s) = s^3 + c_2s^2 + c_1s + c_0 = 0. \quad (8)$$

Next, we form the desired characteristic equation on the basis of the specified requirements for the system processes according to the modal approach

$$D(s) = s^3 + d_2s^2 + d_1s + d_0 = 0. \quad (9)$$

As can be seen from the comparison (8) and (9), the coefficients of the PI2D-controller (3) are equal to the coefficients of the desired characteristic equation (9), i.e. $c_i = d_i, i = \overline{0,2}$. If this is necessary, the original parameters of the PI2D controller k_p, k_i, k_{D1} can be calculated from (4).

C. Recommendations for Controller Implementation

The PI2D controller implementation assumes the special devices use for obtaining differential components. For this purpose, if there is no a measurement noise, it is proposed to use a linear device (the so-called differentiating filter [16, 17]) with the following transfer function:

$$W_f(s) = \frac{1}{\mu^2 s^2 + 2d\mu s + 1}, \quad (10)$$

where μ - device time constant; d - damping factor. The choice of a numerical value μ must provide transients in the filter an order of faster than in the system. The damping coefficient is chosen from the oscillations absence condition, i.e., as a rule, in the range $d \approx (0,5 \dots 0,7)$.

When using the device (10), the proportional-differential part of the controller in the feedback channel is described by the transfer function

$$W_{DP}(s) = \frac{s^2 + c_2s + c_1}{\mu^2 s^2 + 2d\mu s + 1}.$$

Its implementation does not cause the difficulties. The block diagram of the system is shown in Fig 3.

It should be noted that if there is a measurement noise, then it is necessary to increase the order of the device (10) similarly to the localization method recommendations. For example, a third-order device can be used to obtain the first and second order output derivatives.

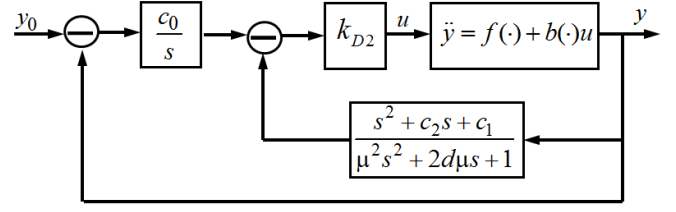


Fig. 3. Block diagram of the system with the real differentiation.

IV. EXPERIMENTAL RESULTS

Let's look at the properties of a system with a PI2D-controller (3). To this end, we consider a following model plant

$$\ddot{y} = -a_1 y^2 \dot{y} - a_2(t) \dot{y} + bu + M(t),$$

where $a_1 = -2$; $b = 4$; $M(t) = M_m(t - t_0)$ - perturbation; $M_m = 10$; $t_0 = 1c$; parameter $a_2(t)$ can vary in the range $0 \leq a_2(t) \leq 3$.

The requirements for the transient system processes are as follows: $t_n \leq 4c$; $\sigma \leq 10\%$; the static error is missing. In accordance with them, the desired equation (9) is formed as follows

$$D(s) = s^3 + 6s^2 + 13s + 10 = 0.$$

Thus, the controller parameters in feedback are calculated by means the relations (4): $c_0 = 10$, $c_1 = 13$ и $c_2 = 6$. The controller coefficient k_{D2} is chosen from the relation $bk_{D2} = 100$, as a result $k_{D2} = 25$. The differentiating filter (10) parameters are as follows: $\mu = 0.01$ и $d = 0.5$.

The closed-system simulation scheme in the MatLab is shown in Fig. 4.

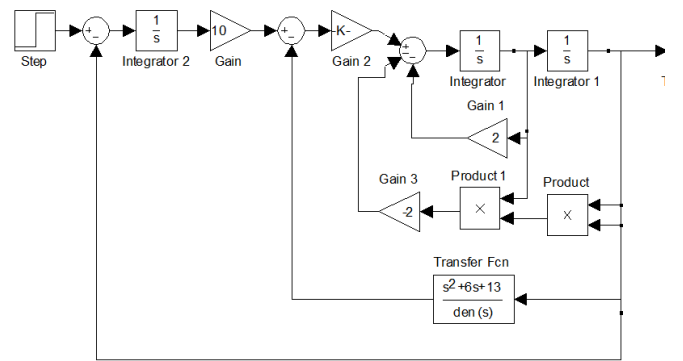


Fig. 4. The closed-system simulation scheme.

The graphs show the transient response (Fig. 5) and the control in the system (Fig. 6 and Fig. 7) for constant parameter values and the external perturbations absence. It can be seen that this controller ensures the processes quality that satisfy the specified requirements. The oscillations in the initial control area (Fig.6 and Fig. 7) are the fast processes

due to the differentiating device (10) with a small time constant.

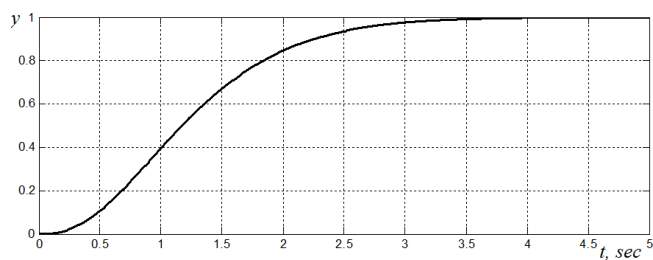


Fig. 5. The closed-system transient characteristic.

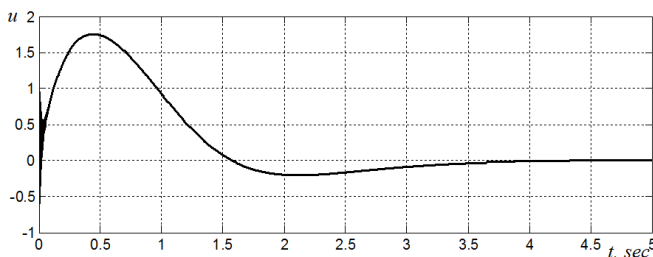


Fig. 6. The control change in the system.

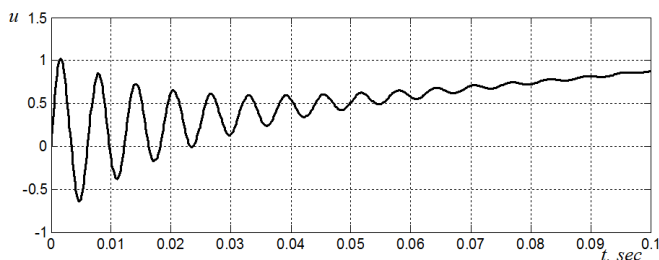


Fig. 7. The initial control area.

The graphs presented in Fig. 8 and Fig. 9 illustrate the control under the abrupt disturbance action $M(t)$ and the time-varying parameter $a_2(t)$ changing, respectively. The type of the parameter $a_2(t)$ change is shown in Fig. 10.

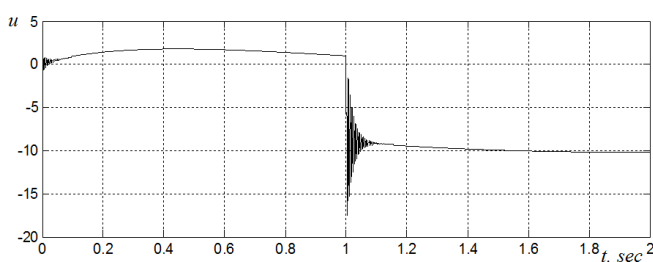


Fig. 8. The perturbation influence on the control.

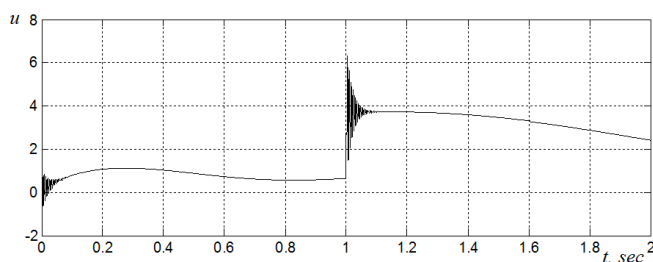


Fig. 9. The non-stationary parameter influence on the control.

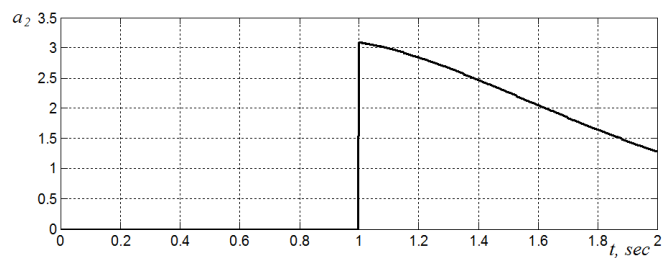


Fig. 10. The graph of the time-varying parameter $a_2(t)$.

Thus, both the non-stationary parameters and the external perturbation are rapidly processed in the inner loop, which is clearly seen from Fig. 8 and Fig. 9. In this case, even a significant change in the nonlinear plant parameters has no effect on the output variable of the system with the PI2D controller. The process satisfies the specified requirements and corresponds to Fig. 5.

Thus, the proposed PI2D-controller is robust and ensures the system invariance with respect to the parameters variation in a wide range.

VI. CONCLUSION

The possibility of applying the localization method to the parameters calculation for the PI2D controller is considered. Such a controller can be used to solve the technical problem of stabilizing the low-order control systems. The advantage of the presented approach is that the calculated controller coefficients don't depend on the plant properties. This allows ensuring the required dynamic quality in the system under conditions of the nonlinear characteristics and the plant non-stationary parameters, as well as the external uncontrolled disturbances influence.

We also note that the proposed controller type can effectively operate in the mode of the out stepwise input influences.

REFERENCES

- [1] PID control (PID controller) on practical examples. - URL: <http://pidcontrollers.narod.ru/pidregulator/chapter3page18.html> (in Russian).
- [2] Nikulin E.F. Fundamentals of the atomic control theory. Frequency methods of the systems analysis and synthesis. - St. Petersburg: BHV - Petersburg, 2004. 631p. (in Russian).
- [3] Denisenko V.V. PID-regulators: principles of construction and modification // STA, 2006. № 4. pp. 66-74. (in Russian).
- [4] Shlyaher M. Automatic control technology for practitioners. - Moscow: JUMO, 2006. 273 p. (in Russian).
- [5] Dorf R., Bishop R. Modern control systems / Trans. from engl. - Moscow: Laboratory of Basic Knowledge, 2002. 832 p. (in Russian).
- [6] Zhmud V.A., Dimitrov L.V., Taichenachev A.V., Semibalamut V.M. Calculation of PID-regulator for MISO system with the method of numerical optimization // Intern. Siberian conf. on control and communications (SIBCON), Kazakhstan, Astana 29–30 June 2017. – Astana. 2017. pp. 670-676.
- [7] Nikulin G.L., Frantsuzova G.A. Synthesis of the electromechanical power steering system // Autometry, 2008. № 5. pp. 93-99. (in Russian).
- [8] Vostrikov A.S. The controller synthesis problem for an automation systems: state and prospects // Autometry. 2010. v.46. № 2(37). pp. 3-19. (in Russian).
- [9] Kotova E. P., Frantsuzova G. A. Application PI2D controller in automatic control systems // Intern. Siberian conf. on control and communi-

- cations (SIBCON), Kazakhstan, Astana 29–30 June 2017. – Astana. 2017. pp. 692-695.
- [10] Zhmud V.A., Zavoryn A.N. Fractional-exponent PID-controllers and ways of their simplification with increasing control efficiency //Automation and software engineering, 2013. № 1 (3). pp. 30–36. (in Russian).
- [11] Vostrikov A. S., Frantsuzova G. A. Synthesis of PID-controllers for nonlinear nonstationary plants //Journal Optoelectronics, Instrumentation and Data Processing, 2015, v. 51. is. 5. pp. 471–477.
- [12] Hlava J., Zemtsov N., Frantsuzova G. Application of PID controller based on the localization method for ancillary service provision /Intern. Siberian Conf. on Control and Communications, Russia, Moscow, 12-14 June 2016. – Moscow. 2016. pp.1 – 6. DOI: 10.1109/SIBCON.2016.7491747
- [13] Frantsuzova G.A., Zemtsov N.S., Hubka L., Modrak O. Calculation of robust PID-controller //Actual problems of electronic instrument engineering (APEIE–2014), 2–4 October 2014, Russia, Novosibirsk. – Novosibirsk. 2014. v. 1. pp. 675-678.
- [14] Frantsuzova G.A., Zemtsov N.S. The parameters calculation of a robust PID-controller based on the localization method // Bulletin of the South Ural State University. Series: Computer technologies, control, radioelectronics, 2013. v. 13, № 4. pp. 134-138. (in Russian).
- [15] Vostrikov A.S., Utkin V.I., Francuzova G.A. Systems with the state-vector derivative in the control //Automation and Remote Control, 1982. № 3. pp. 22-25. (in Russian).
- [16] Vostrikov A.S. The control systems synthesis by the localization method. - Novosibirsk: NSTU, 2007. 252 p. (in Russian).
- [17] Vostrikov A.S., Французова Г.А. Automatic control theory. - Moscow, Urait Publ., 2017. 278 p. (in Russian).
- [18] Frantsuzova G.A., Zemtsov N.S. The application of the localization method for calculating a robust PID controller // Scientific Bulletin of the Novosibirsk State Technical University, 2013. № 3. Pp.18-23 (in Russian).



Frantsuzova Galina Aleksandrovna – Doctor of Technical Sciences, professor of Novosibirsk State Technical University Automatics department. Her research interests are currently focused on analysis and design methods for nonlinear control systems with nonstationary parameters. She is author of more than 200 scientific papers.

Email: frants@ac.cs.nstu.ru

Features of Estimation of Resistance of Separate Grades of Wheat to Influence of Various Stress Factors on Change of Biological Potentials

Andrey V. Gunko¹, Gennady V. Seroklinov²

¹Novosibirsk State Technical University, Novosibirsk, Russia

²Siberian Federal Scientific Center of Agrobiotechnologies of RAS, Krasnoobsk, Russia

Abstract – The results of experiments on measurement of biological potentials of separate grades of wheat in the conditions of influence of the most typical stress factors are discussed: the increased and under temperature, salinization of the soil, influence of herbicides and toxins, existence of sporous diseases of cereals. The purpose of researches is the choice of informational and significant parameters of the measured signals that allowing to estimate resistance of concrete grades to influence of the listed stress factors.

As a result of the conducted researches it was shown that for different types of stress factors various parameters of signals are informative, at the same time their statistical characteristics improve at multi-fold carrying out an experiment with one sprout. At the same time numerous influence of unstable elevated temperature can lead to death of a sprout owing to what multiple carrying out experiments demands automation of process of formation of temperature influences.

Index Terms - Biopotential, stressors, information-significant parameters.

I. INTRODUCTION

WHEN THE PLANT is exposed to various environmental factors, such as temperature, soil salinity, spore infestation, and others, which are stresses for the plant, processes occur in the plant that cause the appearance of electrical signals. In case of non-destructive actions, these electrical signals (biopotentials) are defined as the action potential (AP), which characterizes the plant's reaction to the actions of the stressor [1].

Experimental studies on the effect of stressors on biopotentials of cereals (wheat and barley) were implemented using an automated system for carrying out experiments of Avto-ExpI [2] developed for the study of biological structures. Nowadays, it has been established [3] that the resistance of barley seedlings of various varieties to an increase and decrease in temperature can be estimated from the average (by group) value of the maximum and minimum of the centered biopotential signal smoothed by the low-frequency filter, to the mean deviation and dispersion. It was also noted there that in the conditions of chloride salinity the values of these parameters are lower, and a significant amount of mean deviation may be caused by imperfection of the technique of signal measuring. Further studies have shown [4] that repeated

exposure to the same sample leads to an improvement in the statistical characteristics of the biopotential signal. However, beyond the scope of the studies, there has been an assessment of the effect of spore infection and the complex effect of stressors (spore infection + chloride salinity). Thus, the task of selecting informationally significant parameters of the biopotential signal under the influence of previously unexplored stressors in conditions of a limited number of prepared wheat germs is topical.

II. PROBLEM DEFINITION

In the framework of this work, it is required to select the statistical characteristics of the signals of the biopotentials of wheat seedlings, allowing one to assess the resistance of wheat varieties to chloride salinization, sporogenous infections and toxins, and to determine the possibility of reducing the number of samples due to repeated exposure to samples increasing and decreasing temperatures.

III. THEORY

The changes occurring in the metabolism of plants under the influence of stressors are manifested in the disruption of the functioning of enzyme systems regulating the entire complex energy exchange complex, which leads to the emergence of processes that contribute to counteracting plants to unfavorable environmental factors. These processes are accompanied by a change in the ionic conductivity of plant cells, which is characterized by a change in its biopotentials. In particular, with chloride salinization, the internal resistance of the plant decreases due to the addition of additional ions from the nutrient solution. While exposing to spore infections, the internal resistance of the plant increases due to a decrease in intercellular conductivity.

There is an assumption that all electrical signal-induced functional changes in the plant lead to its adaptation to repeated stress factors, as they will be formed in conditions of functional changes in the vital activity of the plant. It can be expected that when the experiment is repeated, the biopotential signal will have a smaller amplitude and a smoother shape.

IV. EXPERIMENTAL RESULTS

At the begin we estimate the change in the statistical characteristics of various parameters of a centered biopotential signal smoothed by a low-frequency filter, which occurs when high and low temperatures are applied to the wheat germ, in the absence of other stressors. Actually, the signals measured on the same sample of wheat germ of «Omskaya 18» grade with triple exposure to increased temperature are shown on Fig. 1. The statistical characteristics of the signals, taken from a group of 5 sprouts, are given in Tab. I and illustrated by a histogram on Fig. 2.

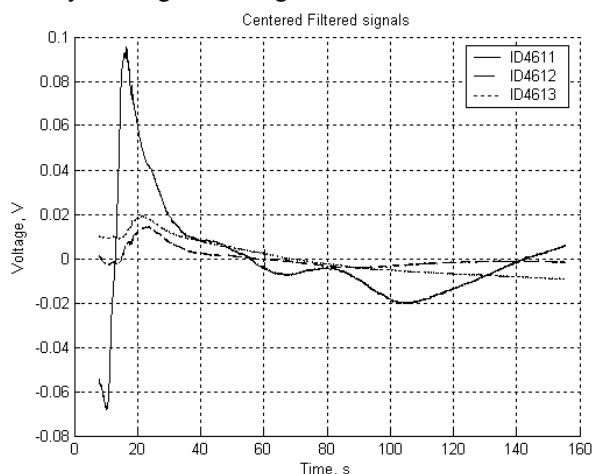


Fig. 1. The graphs of the filtered centered signals of the biopotentials of wheat germ variety «Omskaya 18» at the first (ID4611), the second (ID4612) and the third (ID4613) exposure to elevated temperature.

TABLE I

STATISTICAL CHARACTERISTICS AT THE REPEATS OF EXPERIMENTS ON THE EXPOSURE TO HEAT

| Repeat | 1 | 2 | 3 |
|----------------|----------|----------|----------|
| maxcf | | | |
| Mean Value | 0.068148 | 0.026979 | 0.018298 |
| Standard Error | 0.020341 | 0.009276 | 0.006189 |
| Average Error | 0.015086 | 0.006269 | 0.004262 |
| Dispersion | 4.14E-04 | 8.61E-05 | 3.83E-05 |

The effect of decreasing temperature in the absence of other stressors results in practically the same results, and therefore is not illustrated here.

Investigation of the effect of *chloride salinization* of the nutrient solution during the growth of seedlings showed that the signals of biopotentials after repeated experiments with one sample also improve its shape (see Fig. 3).

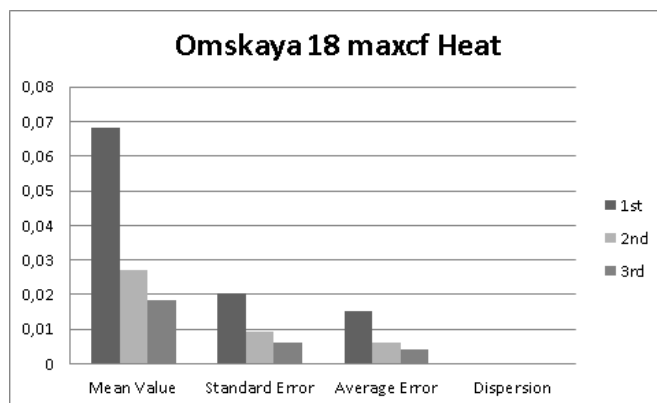


Fig. 2. Histogram of the characteristics of the maximums of the filtered centered signals of the biopotentials of wheat germs of the «Omskaya 18» with the first, second and third exposure of increased temperature.

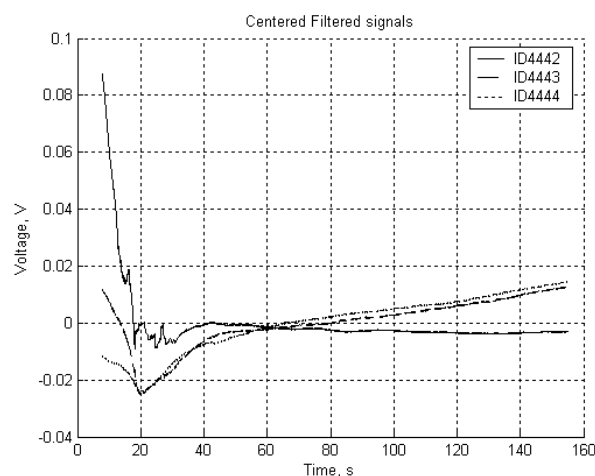


Fig. 3. The graphs of filtered centered signals of the biopotentials of wheat germ variety «Novosibirskaya 44» at the first (ID4442), the second (ID4443) and the third (ID4444) exposure by increased temperature.

Significant decrease in the statistical characteristics of signal parameters during repeated experiments is observed for maximums of centered filtered signals as for increasing as for decreasing of temperature. The corresponding characteristics for seedlings of wheat «Novosibirskaya 44» under the influence of increasing temperature are given in Tab. II and are illustrated by the histogram in Fig. 4, and when exposed by decreasing temperature - in Tab. III and in Fig. 5.

Effects on sprouts by a *spore suspension* showed that the signals of biopotentials in repeated experiments with one sample also improve its shape (see Fig. 6).

There is also a decrease in the statistical characteristics of signal parameters during repeated experiments is observed for the same parameters for different types of exposure. When the increasing temperature is applied, the statistical characteristics of the maximum of filtered centered signal are improved (see Tab. IV and Fig. 7), as when exposed by decreasing temperature (see Tab. V and Fig. 8).

TABLE II
STATISTICAL CHARACTERISTICS AT THE REPEATS OF
EXPERIMENTS ON THE EFFECTS OF HEAT IN CHLORIDE
SALINIZATION

| maxcf \ Repeat | 1 | 2 | 3 |
|----------------|----------|----------|----------|
| Mean Value | 0.046461 | 0.006504 | 0.007172 |
| Standard Error | 0.033796 | 0.003979 | 0.004696 |
| Average Error | 0.027429 | 0.002765 | 0.003195 |
| Dispersion | 0.001142 | 1.58E-05 | 2.21E-05 |

TABLE III
STATISTICAL CHARACTERISTICS AT THE REPEATS OF
EXPERIMENTS ON THE EFFECTS OF COLD IN CHLORIDE
SALINIZATION

| maxcf \ Repeat | 1 | 2 | 3 |
|----------------|----------|----------|----------|
| Mean Value | 0.007883 | 0.001998 | 0.002353 |
| Standard Error | 0.005087 | 0.000511 | 0.000469 |
| Average Error | 0.003958 | 0.000426 | 0.000384 |
| Dispersion | 2.59E-05 | 2.62E-07 | 2.20E-07 |

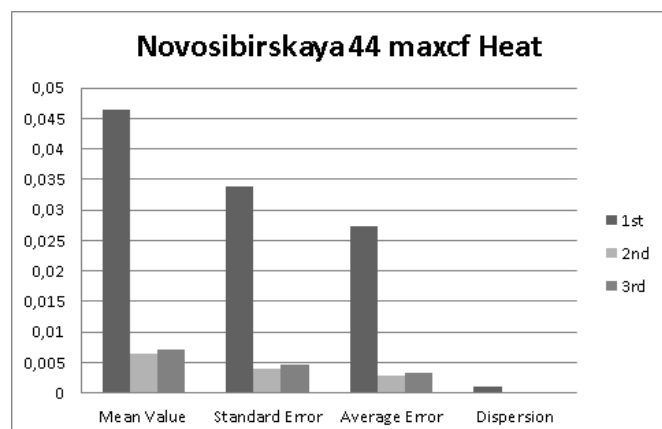


Fig. 4 Histogram of the characteristics of the maximums of the filtered centered signals of the biopotentials of wheat germs of the «Novosibirskaya 44» with the first, second and third exposure by increased temperature.

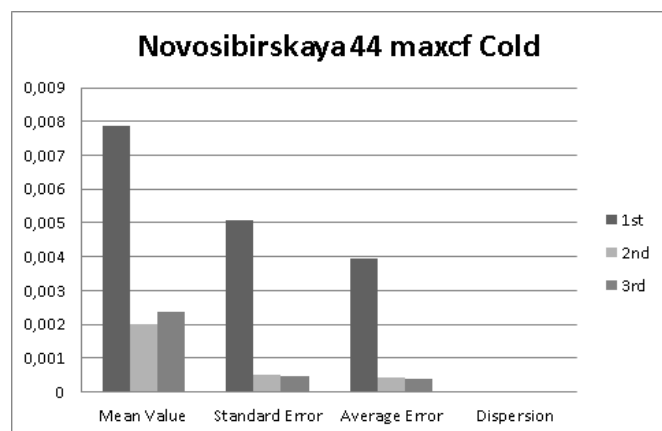


Fig. 5. Histogram of the statistical characteristics of the maximums of the filtered centered signals of the biopotentials of wheat germs of the «Novosibirskaya 44» with the first, second and third exposure by decreased temperature.

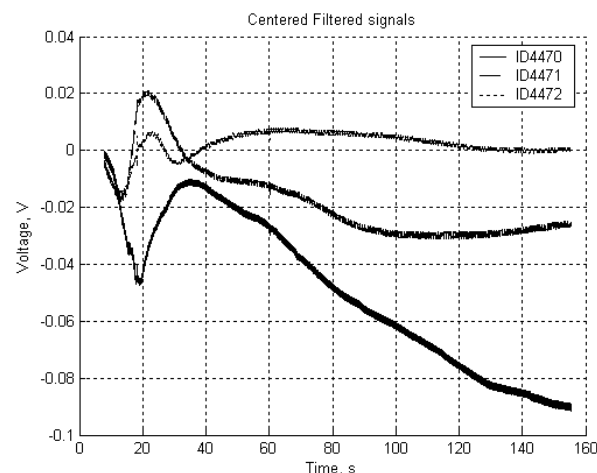


Fig. 6. The graphs of filtered centered signals of biopotentials of wheat germ variety «Novosibirskaya 18» at the first (ID4470), the second (ID4471) and the third (ID4472) exposure by increased temperature.

TABLE IV
STATISTICAL CHARACTERISTICS AT THE REPEATS OF EXPER-
IMENTS ON THE EFFECTS OF HEAT IN SPORE SUSPENSION

| maxcf \ Repeat | 1 | 2 | 3 |
|----------------|----------|----------|----------|
| Mean Value | 0.068574 | 0.034198 | 0.021924 |
| Standard Error | 0.037896 | 0.020255 | 0.007427 |
| Average Error | 0.02773 | 0.016151 | 0.005454 |
| Dispersion | 0.001436 | 0.00041 | 5.52E-05 |

TABLE V
STATISTICAL CHARACTERISTICS AT THE REPEATS OF EXPER-
IMENTS ON THE EFFECTS OF COLD IN SPORE SUSPENSION

| maxcf \ Repeat | 1 | 2 | 3 |
|----------------|----------|----------|----------|
| Mean Value | 0.028557 | 0.014483 | 0.013521 |
| Standard Error | 0.013834 | 0.009283 | 0.006208 |
| Average Error | 0.01102 | 0.00635 | 0.004624 |
| Dispersion | 0.000191 | 8.62E-05 | 3.85E-05 |

Simultaneous effects on seedlings of chloride salinization and spore suspension showed that the signals of biopotentials in two experiments with one sample also improve its shape (see Fig. 9), and later the loss of viability of the seedling is observed.

Here again, a decrease in the statistical characteristics of the signal parameters in repeated experiments is observed for the same parameters for different types of exposure. In particular, when the temperature is increased, the statistical characteristics of the maximums of the filtered centered signal are improved (see Fig. 10), and when the temperature is increased, the maximums are improved (see Fig. 11).

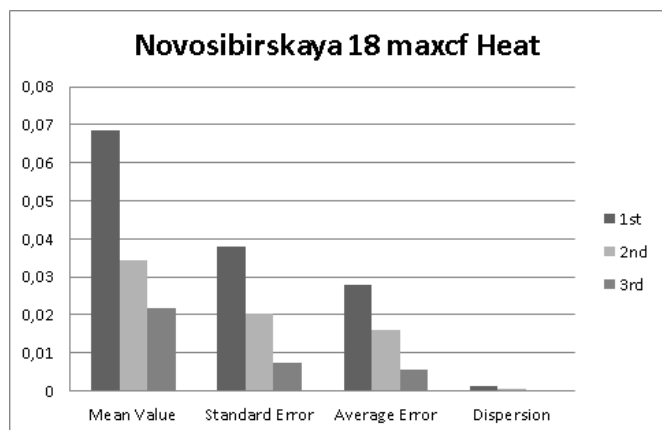


Fig. 7. Histogram of the statistical characteristics of the maximums of the filtered centered signals of biopotentials of wheat germs of the «Novosibirskaya 18» with the first, second and third exposure by increased temperature.

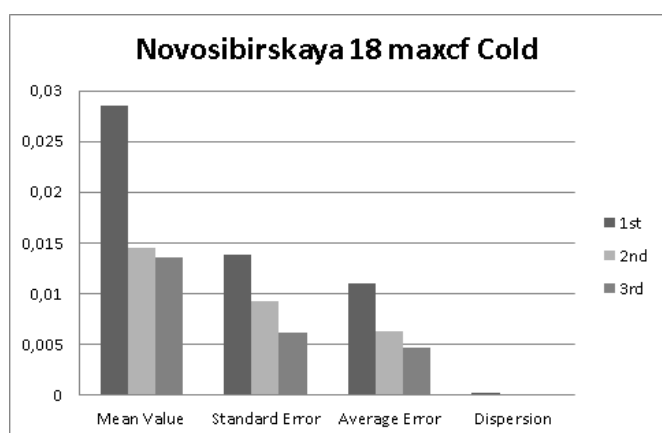


Fig. 8. Histogram of the statistical characteristics of the maximums of the filtered centered signals of biopotentials of wheat germs of the «Novosibirskaya 18» with the first, second and third exposure by decreased temperature.

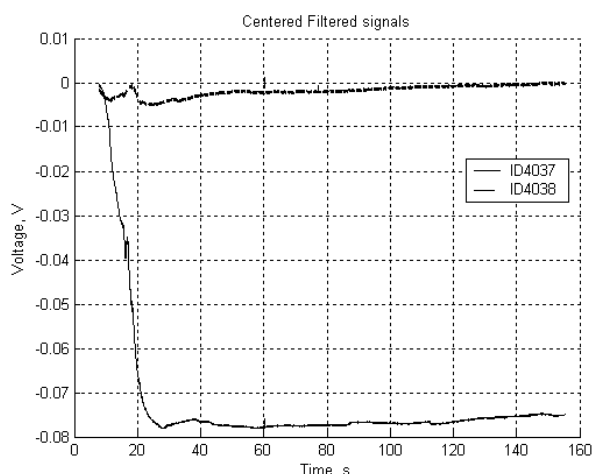


Fig. 9. The graphs of filtered centered signals of the biopotentials of wheat germ variety «Novosibirskaya18» at the first (ID4037) and the second (ID4038) exposure by increased temperature.

Simultaneous effects on seedlings of chloride salinization and spore suspension clearly shown the resistance of various grade of wheat germs for those stressors. In Tab. VI are shown the statistical characteristics of the minima of the filtered centered signals of biopotentials of the four wheat

grades under the action of the increased temperature, and on Fig. 12 is the histogram of the mentioned characteristics.

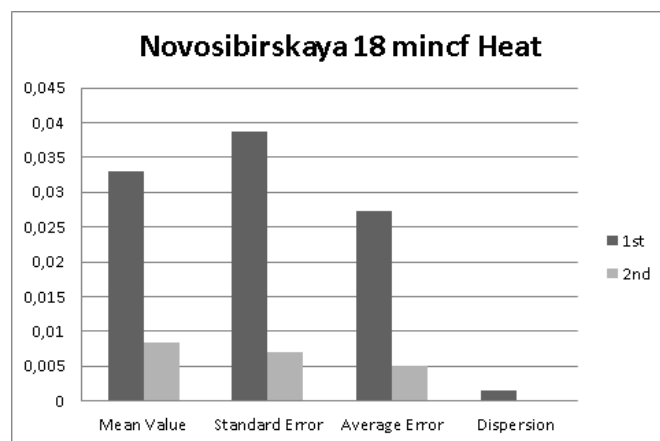


Fig. 10. Histogram of the statistical characteristics of the minima of the filtered centered signals of biopotentials of wheat germs of the «Novosibirskaya 18» with the first and second exposure by increased temperature.

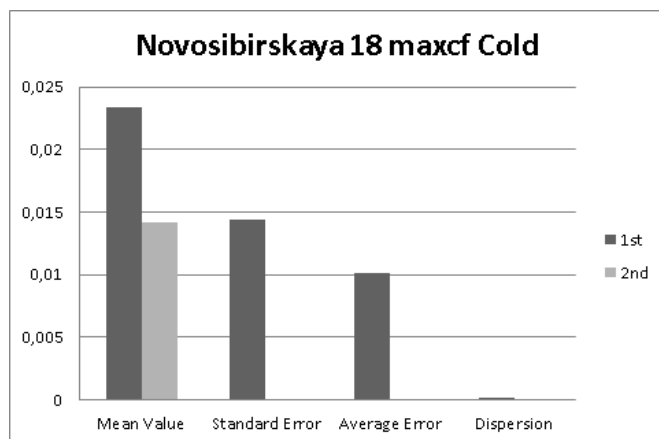


Fig. 11. Histogram of the statistical characteristics of the maximums of the filtered centered signals of biopotentials of wheat germs of the «Novosibirskaya 18» with the first and second exposure by decreased temperature.

Simultaneous effects on seedlings of chloride salinization and spore suspension clearly shown the resistance of various grade of wheat germs for those stressors. In Tab. VI are shown the statistical characteristics of the minima of the filtered centered signals of biopotentials of the four wheat varieties under the action of the increased temperature, and on Fig. 12 is the histogram of the mentioned characteristics.

TABLE VI
STATISTICAL CHARACTERISTICS OF VARIOUS GRADES ON THE EFFECTS OF HEAT WITH CHLORIDE SALINIZATION AND PROCESSING OF SPORE SUSPENSION.

| Grade | Omskaya 18 | Svetlanka | N-skaya 18 | N-skaya 44 |
|----------------|------------|-----------|------------|------------|
| mincf | | | | |
| Mean Value | 0.0327955 | 0.0352834 | 0.043501 | 0.0521788 |
| Standard Error | 0.0243076 | 0.0257085 | 0.0305377 | 0.0565715 |
| Average Error | 0.0188236 | 0.0210505 | 0.026122 | 0.0400785 |
| Dispersion | 5.91E-04 | 6.61E-04 | 9.33E-04 | 3.20E-03 |

In Tab. VII one can see the statistical characteristics of the maximums of the filtered centered signals of biopotentials of

the same wheat grades under the action of a decreasing temperature on Fig. 13 - histogram of the characteristics of the signal maximums when exposed to decreasing temperature.

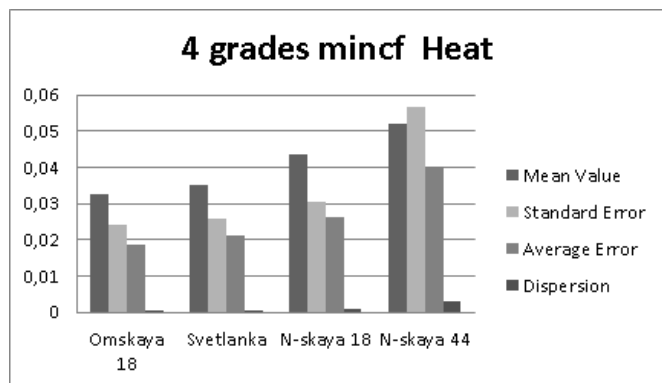


Fig. 12. Histogram of the statistical characteristics of the minima of the filtered centered signals of biopotentials of wheat germs of four grades when exposed by increasing temperature.

TABLE VII

STATISTICAL CHARACTERISTICS OF VARIOUS GRADES ON THE EFFECTS OF COLD WITH CHLORIDE SALINIZATION AND PROCESSING OF SPORE SUSPENSION.

| Grade maxcf | Omskaya 18 | Svetlanka | N-skaya18 | N-skaya 44 |
|----------------|------------|-----------|-----------|------------|
| Mean Value | 0.03572833 | 0.0170622 | 0.0288925 | 0.0125172 |
| Standard Error | 0.03040496 | 0.0012853 | 0.0146692 | 0.0057429 |
| Average Error | 0.02219044 | 0.0009542 | 0.0118447 | 0.0046856 |
| Dispersion | 9.24E-04 | 1.65E-06 | 2.15E-04 | 3.30E-05 |

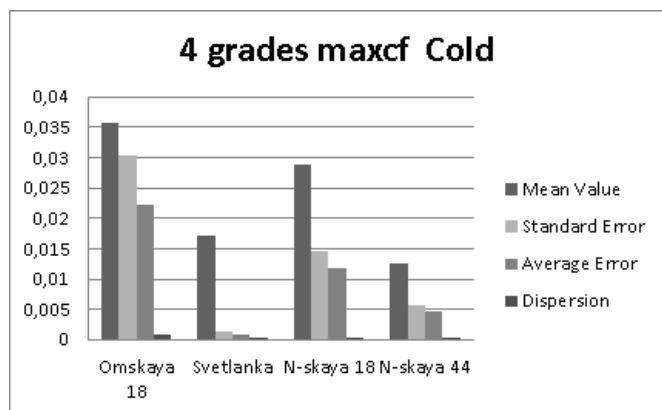


Fig. 13. Histogram of the statistical characteristics of the maximums of the filtered centered signals of the biopotentials of wheat germs of four grades when exposed by increasing temperature.

V. DISCUSSION OF RESULTS

The presented results show that:

1. In the absence of stressors other than exposure to temperature, repeated experiments with one seedling lead to a decreasing of the statistical characteristics of the signal maximum when exposed to both heat and cold.

2. With chloride salinization of the nutrient solution during the growth of seedlings, multiple experiments lead to a de-

crease in the statistical characteristics of the signal maximum when exposed to heat. When exposed to cold with an increase in the number of repetitions, also the statistical characteristics of the maximum decreasing.

3. When processing seedlings with a spore suspension, repeated experiments lead to a decreasing of the statistical characteristics of the signal maximum when exposed to heat. When exposed to cold with an increase in the number of repetitions, the statistical characteristics of the maximum of the biopotential signal decreasing.

4. With chloride salinization and seedling treatment with a spore suspension, repeated experiments result in a decreasing in the statistical characteristics of the maximum of the signal when exposed to heat. With further repetitions of the experiment with the same sample, the results deteriorate substantially, which may be related to the loss of viability of the sprout from the action of the increasing temperature. When the exposed of cold, then increasing with the number of repetitions, the statistical characteristics of the minimum with respect to the temperature of the signal of the biopotential decrease.

5. The combination of chloride salinization and processing with a spore suspension allows to compare grades of wheat with respect to resistance to the action of a set of stressors.

6. In order to assess the resistance of different grades of wheat to the action of the set of stressors, it is necessary to continue this research. In this case, it is necessary to evaluate the expediency of carrying out a larger number of repeats of experiments with a single sprout to increase the statistical reliability of the results of studies with a reduction in the number of samples studied.

VI. CONCLUSION

As a result of the studies, it was shown that for the set of stressors, various parameters of signals are informative, while their statistical characteristics improve upon repeated experimentation with one seedling. At the same time, repeated exposure to an unstable high temperature can lead to the death of the seedling, as a result of which repeated experiments require the automation of the formation of temperature effects.

REFERENCES

- [1] Bos D.C. Selected works on the irritability of plants. - Moscow: "Science", 1964, 2 T, 395 p. (in Russian).
- [2] Seroklinov G.V., Gunko A.V., Dobrovolsky N.A. Software of the automated measuring complex. // Methods and technical means of research of physical processes in agriculture: the works of the SibPTI State Unitary Enterprise Rosselkhozakademia. - Novosibirsk: SibPTI, 2011. pp 152-156. (in Russian).
- [3] Seroklinov G.V., Gunko A.V. Information technology in the study of plant biopotentials under the action of stressors. Computational technologies. 2016. Vol. 21. No. S1. pp. 94-103. (in Russian).
- [4] Seroklinov G.V., Gunko A.V. Adaptation of samples of cereals as the method of increase in informational content of data in the study of biopotentials. // Intellectual analysis of signals, data and knowledge: methods and means: collection of articles of the All-Russian scientific and practical conference, Novosibirsk, 14-17 October 2017. - Novosibirsk: NSTU, 2017. pp 217-222. (in Russian).



Gunko Andrey Vasilievich - Candidate of Technical Sciences, Associate Professor of the Automation Department of the NSTU. The field of scientific interests is the automation of technological processes in various industries, the development of means for collecting and automating the processing of experimental research results.



Seroklinov Gennady Vasilievich - Candidate of Science, Leading Researcher of the Laboratory for the Study of Physical Processes in Agrophytocenoses of the Siberian Federal Scientific Center for Agrobiotechnologies of the Russian Academy of Sciences. The field of scientific interests is the automaticization of technological processes for the production and processing of agricultural products, the automation of experimental studies of biological structures.

Speed Regulation of Single-Phase Engines Used in Agriculture

Tatiana M. Halina, Maya I. Stalnaya, Ilya A. Ivanov, Tatyana I. Rybalkina, Elizaveta D. Ryazanova
Polzunov Altai State Technical University (AltSTU), Barnaul, Russia

Abstract – The use of an asynchronous single-phase motor in agriculture is associated with a number of difficulties, namely the difficulty of starting and speed control. In this paper, several solutions to this problem are presented, using special designed conversion devices.

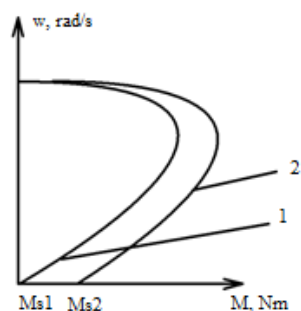
Index Terms – Frequency converter; transistor converter, single-cycle converter, push-pull converter.

I. INTRODUCTION

ELECTRIC ALTERNATING current machines, especially low-power engines (up to 5 kW), are widely distributed in the agricultural industry, such as single-phase asynchronous motors. These motors are powered by a single-phase AC power line. Moreover, the stator generates a pulsating magnetic field and the torque is absent, when feeding the AC supply voltage to both stator windings simultaneously. Then, a capacitor is installed to start the motor in the circuit of one of the phases, providing a phase shift between the supply voltages, thereby creating a rotating magnetic field. However, the capacitor used to start a single-phase asynchronous motor has large dimensions, and the material used in its design is in most cases paper, which reduces the durability of the device and its reliability.

II. PROBLEM DEFINITION

Thus, the main disadvantage of a single-phase asynchronous motor when feeding from a single-phase circuit is its lack of starting torque (Fig. 1, curve 1), which leads to the need for additional devices leading to its start-up. The starting torque is zero (M_{s1}) in the absence of such devices and the starting torque has a relatively small value (M_{s2}) at the capacitor start (Fig. 1, curve 2).



1 - without additional equipment; 2 - using a capacitor

Fig. 1. Mechanical characteristics of single-phase and two-phase asynchronous motor.

The solution to the above problem is the use of frequency converters. These devices are able to provide starting and braking of the engine, as well as smooth adjustment of the engine speed.

Two types of frequency converters are known: single-ended ones - converting AC power to alternating voltage of the required frequency, and push-pull ones - converting the alternating voltage of the network into a constant and then into an alternating voltage of the required frequency.

III. SINGLE-CYCLE CONVERTER

Single-ended frequency converters are universally used in low-power engines, since they do not require balancing, they require a simpler circuit to control them than to control push-pull frequency converters. For example, a single-ended frequency converter is a semiconductor device for regulation the speed of a single-phase asynchronous motor [1], that is represented in Fig. 2.

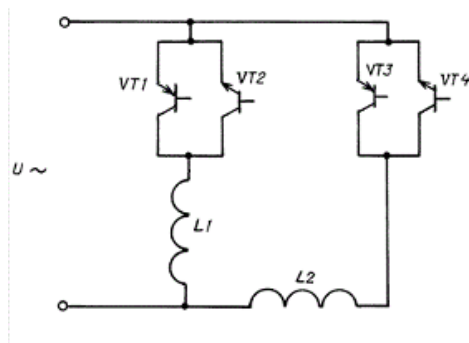


Fig. 2. Semiconductor device for regulating the speed of a single-phase asynchronous motor.

The described single-ended frequency converter consists of reversible semiconductor switches made on transistors VT1, VT2, VT3, VT4 and intended for connection with stator windings of single-phase asynchronous motor and consisting of two transistors of different conductivity.

The work of the semiconductor device for regulating the speed of a single-phase asynchronous motor is carried out as follows. The control pulses are applied to the transistors in the following sequence (shown in Fig. 3b) to ensure the rotation of the stator magnetic field in accordance with the vector diagram shown in Fig. 3a.

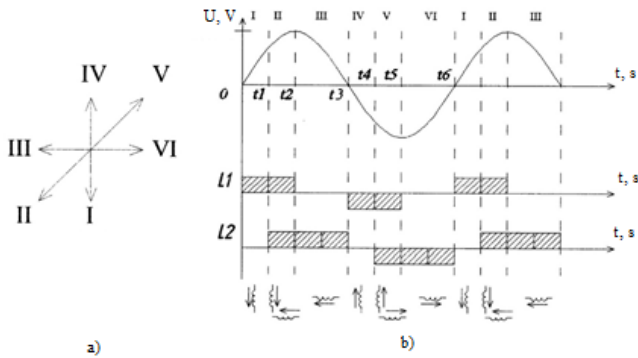


Fig. 3. Operation of a semiconductor device for regulating the speed of a single-phase asynchronous motor.

So, the transistor VT1 opens (Fig. 2) to create the first vector of the stator magnetic field (Fig. 3a) in the positive time interval t_1 (Fig. 3b). The current flows through the winding L1 in the forward direction indicated in Fig. 3a. The transistors VT1 and VT3 are opened to create the second vector of the stator magnetic field in the positive time interval t_2 . Subsequent opening of the transistors to create vectors of the stator magnetic field occurs in accordance with Fig. 3. The current flows through the windings L1 and L2 in the forward direction. The subsequent vectors of the stator magnetic field are created in a similar way. To implement the reverse function, the transistors are switched in the reverse order. This semiconductor device for regulating the speed of a single-phase asynchronous motor, possessing high reliability and economy indicators, is capable of performing non-condenser start-up, engine reverse and speed control.

Developed triac reducer is operated by a single-phase alternating voltage network. Also, it is used for a single-phase asynchronous motor (Fig. 4) in addition to the frequency converter presented above.

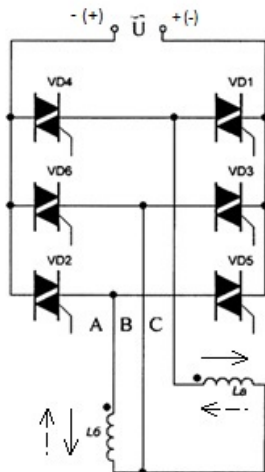


Fig. 4. Triac reducer operated by a single-phase AC voltage network for a two-phase asynchronous motor.

Triacs forming a bridge circuit are used as semiconductor switches in this design. The triacs are connected directly to the AC single-phase voltage network.

This device can operate the engine in two modes: at maximum speed and half-maximum speed.

It is necessary to follow the vector diagram shown in Fig. 5a to operate the frequency converter (triac reducer) in the mode at maximum speed. So, the control signal is applied to the triacs VD1 and VD6, the current flows through the stator winding La in the forward direction indicated in Fig. 4 by a solid arrow in the time interval t_1 in the positive half-width of the supply voltage. The control signal is applied to the triacs VD5 and VD6, and the triac VD1 is closed, then the current flows through the stator winding Lb in the reverse direction indicated in Fig. 4 by the dotted arrow in the negative half-time t_2 . The subsequent vectors of the stator magnetic field are created in a similar way. The triacs are opened in reverse order to implement the reverse function.

Operation in the mode of half-maximum speed is similarly shown in Fig. 5b. The control signal is applied to the triacs VD1 and VD6 in the positive half-time t_1 , Fig. 4, they open, the current flows through the stator winding La in the forward direction. The control signal is applied to the triacs VD4 and VD5 in the negative half-time t_2 . The triacs VD1 and VD6 are closed, the triacs VD4 and VD5 open. Then the current flows through the stator winding La in the forward direction, and through the winding Lb in the opposite direction. The subsequent vectors of the stator magnetic field are created in a similar way. The triacs are opened in reverse order to implement the reverse function.

Thus, this device allows starting and controlling speed of an asynchronous single-phase motor. Since this circuit uses one set of triac transistors that start and reverse, hence the operating costs are reduced.

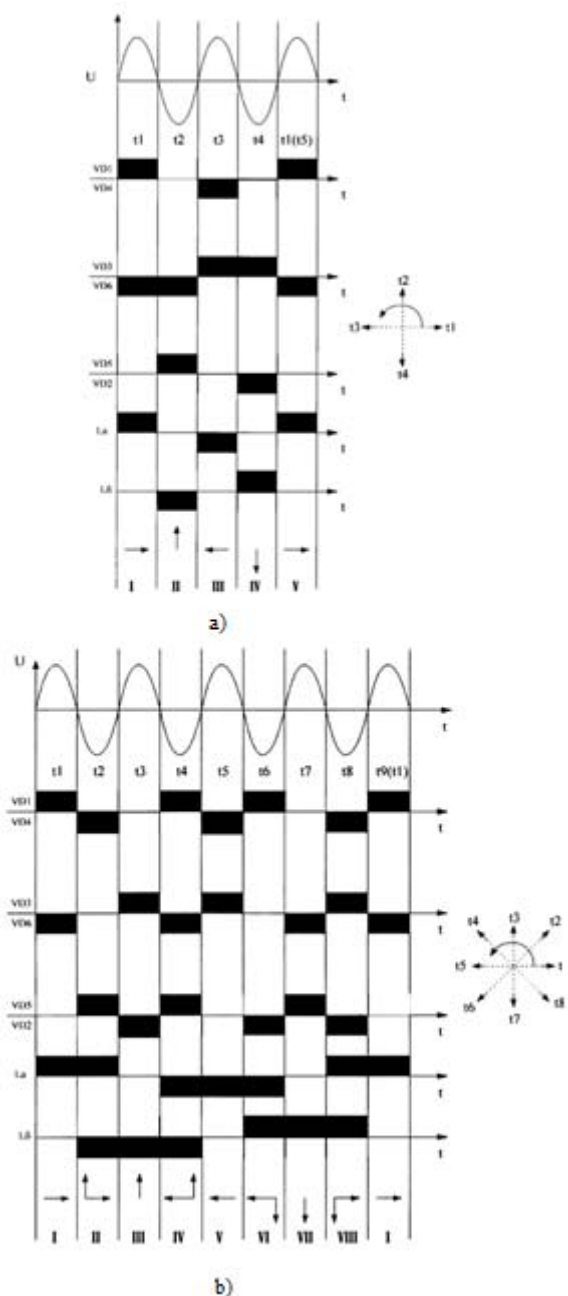


Fig. 5. Operation of a triac gearbox driven by a single-phase AC voltage network for a two-phase asynchronous motor:
a) engine operation at maximum speed.
b) engine operation at half-maximum speed.

IV. PUSH-PULL FREQUENCY

Push-pull frequency converters are widely used due to a number of their advantages, these frequency converters provide a wide and smooth frequency control range and smooth control of the rotation speed of an asynchronous single-phase motor, which is achieved due to the possibility of converting from DC voltage any alternating voltage of the required frequency.

One of the push-pull converters is the developed frequency converter [3], the transistor reversing frequency converter "for a single-phase motor", its circuit is shown in Fig. 6. A

method for controlling transistors through an optocoupler [4, 5] is used in this frequency converter, which greatly simplifies a control system for transistors by eliminating isolated power supplies to provide control currents through transistors.

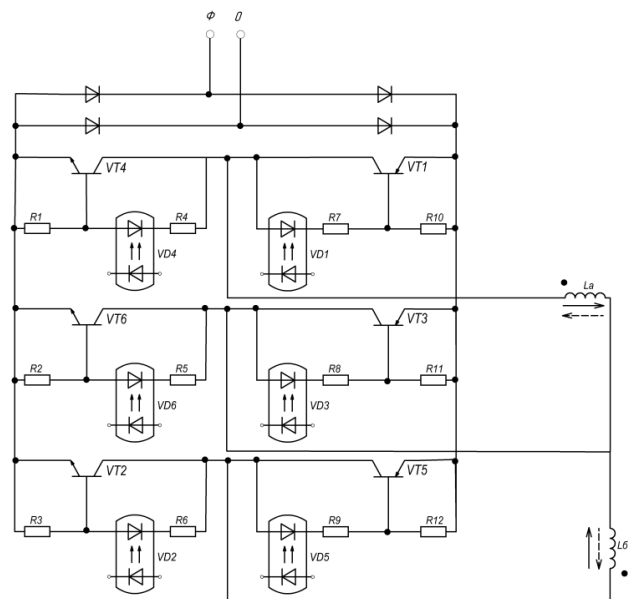


Fig. 6. Transistor reversing frequency converter for single-phase motor.

The per-cycle operation of a transistor reversing frequency converter for a single-phase motor is shown in Fig. 7. It is necessary to include transistors in the sequence shown in Fig. 7b to determine the vectors of the stator magnetic field in the order shown in Fig. 7a.

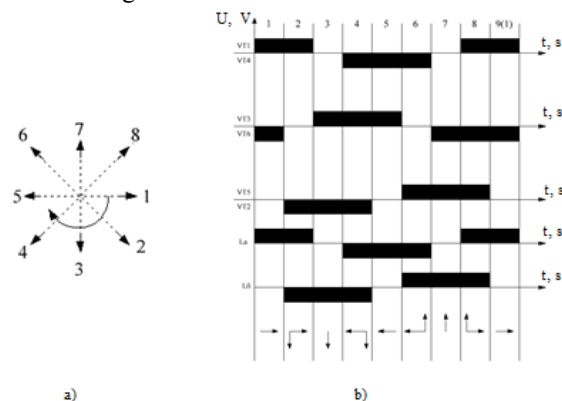


Fig. 7. Operation of a transistor reversing frequency converter for a single-phase motor.

A control signal is sent to the optocouplers VD1 and VD6 (Fig. 6) to create the first vector (Fig. 7a) of the stator magnetic field), thus the corresponding optocouplers VT1 and VT6 will be opened (Fig. 7b). The control signal is applied to the optocouplers VD1 and VD2 to create the second position of the stator magnetic field vector, the signal is removed from the optocoupler VD6 and the transistor VT6 is closed, the transistors VT1 and VT2 are open. The current flows through the stator winding La in the forward direction indicated in Fig. 6 by a solid arrow and through the stator winding Lb in the reverse direction indicated in Fig. 6 by the dotted arrow. Further, the opening of the bus couplers takes

place in the order shown in Fig. 7b. The reverse function is performed by turning the transistors on in reverse order.

Thus, a transistor reversing frequency converter for a single-phase motor is capable of performing such functions as starting, reverse of the motor. This frequency converter has the following number of advantages. First, for the discovery of transistors, there is no need for isolated power supplies. Secondly, this device carries out a power isolation between the control system of transistors and the power part of the circuit. Thirdly, from the above mentioned advantages it follows that this device has increased reliability, since there is no additional equipment (additional power supplies).

Reverse-current braking is applied with the engine reverse in all the considered schemes, which is performed by changing the alternation of the opening of the semiconductor switches, and dynamic braking by applying a constant voltage to the stator windings of the motor.

V. CONCLUSION

The considered converters can perform such functions as: starting and braking, reverse and speed control of an asynchronous motor. At the same time, they have a simple design, increased reliability and reduced operating costs.

REFERENCES

- [1] Pat. 2420857 Russian Federation, H02P 1/42. Semiconductor speed control device of single-phase two-winding asynchronous motor [Text] / Stalnaya M. I., Cheremisin P. S., Skornyakov, A. A., Goncharov D. Yu.; The applicant and patent holder: The federal state institution of higher education «Polzunov Altai State Technical University» - 2010123977/07; claimed. 11/06/2010; publ. 10/06/2011.
- [2] Pat. 177672 Russian Federation, H02P 21/12. Simistor reducer driven by a single-phase alternating voltage network for two-phase asynchronous motor [Text] / Stalnaya M. I., Ivanov E. A., Chirskaya V.E., Sharipov N. B.; The applicant and patent holder: The federal state institution of higher education «Polzunov Altai State Technical University» - 2017125969; claimed. 19/07/2017; publ. 06/03/2018.
- [3] Pat. 176148 Russian Federation, H02P 21/12. Transistor reverse frequency Converter for two-phase motor [Text] / Stalnaya M. I., Ivanov E. A., Petrin M. S.; The applicant and patent holder: The federal state institution of higher education «Polzunov Altai State Technical University» - 2017125970; claimed. 19/07/2017; publ. 10/01/2018.
- [4] Pat. 174897 Russian Federation, H03K 17/041. Independent solid-state switch on p-n-p type transistor [Text] / Stalnaya M. I., Ivanov E. A., Rybalkina T. I., Ryazanova E. D.; The applicant and patent holder: The federal state institution of higher education «Polzunov Altai State Technical University» - 2017124134; claimed. 06/07/2017; publ. 09/11/2017.
- [5] Pat. 174898 Russian Federation, H03K 17/041. Independent semiconductor switch on a type n-p-n transistor [Text] / Stalnaya M. I., Ivanov E. A., Rybalkina T. I., Ryazanova E. D.; The applicant and patent holder: The federal state institution of higher education «Polzunov Altai State Technical University» - 2017124133; claimed. 06/07/2017; publ. 09/11/2017.
- [6] Gorbachev G.N., Chaplygin E.E. Industrial Electronics: A Textbook for Universities / G.N. Gorbachev, E.E. Chaplygin; Ed. V.A. Labuntsova. - M.: Energoatom-publishers, 1988. - 319 p.
- [7] Braslavsky I.Ya. Energy-saving asynchronous electric drive: Textbook / I.Ya. Braslavsky, Z.Sh. Ishmatov, V.N. Poles. Ed. AND I. Braslavsky. - M.: Academy, 2004. - 256 p.
- [8] Bocharov L.N. Calculation of electronic devices on transients / L.N. Bocharov, S.K. Zhebryakov, I.F. Kolesnikov. - M.: Energy, 1978. - 208 p.
- [9] Pat. 164966 Russian Federation, IPC H 02 P 27/06. Wide-regulating transistor frequency converter for an alternating-current motor [Text] / Stalnaya M.I., Eremochkin S.Y., Borisov A.P., Titova A.A., Korolev D.A.; The applicant and patent holder: The federal state institution of higher education «Polzunov Altai State Technical University» - 2016108693/07; claimed. 10/03/16; publ. 27/09/2016.
- [10] Pat. 174897 Russian Federation, H 03K 17/041. Independent semiconductor switch with n-p-n transistor / Stalnaya M.I., Ivanov I.A., Rybalkina T.I., Ryazanova E.D.; The applicant and patent holder: The federal state institution of higher education «Polzunov Altai State Technical University» - 2017124133/08; claimed. 06/07/17; publ. 11/11/2017.
- [11] Bocharov L.N. Inverse switching of the transistor / L.N. Bocharov. - Moscow: Energia, 195. - 56s.
- [12] Eremochkin S.Yu. Investigation and calculation of the mechanical characteristics of a three-phase asynchronous short-circuited electric motor, starting and operating from a single-phase network by means of vector-algorithmic commutation of stator windings // Polzunovskii vestnik. 2013. № 4-2. Pp. 72-77.
- [13] Eremochkin S.Yu. Single-phase three-phase electric drive for agricultural electrified machines // Agricultural Bulletin of the Urals. 2012. №7. Pp. 49-52.
- [14] Khalina T.M., Stalnaya M.I., Eremochkin S.Yu. Estimation of efficiency of use of three-phase electric motors of agricultural electrified machines in a single-phase network under vector-algorithmic control // Energy supply and energy saving in agriculture: Proceedings of the 8th International Scientific and Technical Conference - Moscow, May 16 - 17, 2012. M.: GNU VIESKh Rosselkhozakademii, 2012. - Part 3. - P. 334-339.



Tatiana M. Halina.

She graduated from the Altai Polytechnic Institute with a degree in Electric Power Supply of Industrial Enterprises (with honors) in 1975. In 1986 she defended her thesis on the topic "The calculation and application areas of the static stability of power" in Azerbadzhanskom Institute of Oil and Chemistry. M. Azizbayov in 2005, defended his doctoral thesis on "multi-electrode system of low-temperature composite electric radiators for agriculture" in the Altai State Technical University.

Published more than 170 works. According to the corporation SPRINGER list ranked by relevance and scientific article citation Halina TM ranked 10th in the world. Member of the editorial board of the journal "Problems of Energy" of the Azerbaijan Academy of Sciences. Member of the Organizing Committee of the International Conference "Physical Problems of Energy" TPE-2004, Iran; TPE-2006 -Турция, TPE-2008 - Romania, 2010 - Spain. The surveys published seven research papers and made seven presentations at international conferences "Physical problems of power engineering" TPE -2004, Iran; TPE-2006 - Turkey, TPE-2008 - Romania, 2010 - Spain TPE 2013- Norway. "Technical and physical problems of energy" THREE 2015-Romania.

Author of a monograph published in the Russian Academy of Sciences.

Awards: Certificate of honor of the Administration of the Altai Territory - 2013; Veteran of Labor of the Altai Territory-2010.



Maya I. Stalnaya.
She has been working at the University since 1967. She has the title "Honored Inventor of the Altai Territory". Veteran of Labor of AltSTU and Altai Territory. He reads lecture courses "Automated electric drive", "Synthesis of discrete control systems", "Elements of analog automatics", "Diagnostics of discrete control systems" and much more. Published more than 200 scientific papers and received more than 70 patents in the field of automated electric drive.



Ilya A. Ivanov.
Student. Participant of scientific and park conferences at the Russian and regional level, participant of the XVII International Scientific and Technical Conference "AC electric drives" - ACED 2018 .. There are several indexed publications in the SKOPUS database, received more than 15 patents.



Tatyana I. Rybalkina.
Student. She is a participant in scientific and practical conferences at the regional and regional levels. There are several patents.



Elizaveta D. Ryazanova.
Student. She is a participant in scientific and practical conferences at the regional and regional levels. There are several patents.

Using the Numerical Optimization Method for Tuning the Regulator Coefficients of the Two-Wheeled Balancing Robot

Andrei Yu. Ivoilov¹, Vadim A. Zhmud¹, Vitaly G. Trubin¹, Hubert Roth²

¹Novosibirsk State Technical University, Novosibirsk, Russia

²University of Siegen, Siegen, Germany

Abstract – This article is devoted to tuning the regulator coefficients of the automatic stabilization system of a two-wheeled balancing robot. When calculating the regulator coefficients analytically, it is necessary to set the desired distribution of the system roots. This distribution can be defined based on general requirements for the quality of the system transient processes such as the maximum level of overshoot and the maximum duration of the transient process that define the sector in the complex plane within which the roots should be placed. But the issue of choosing the distribution within this sector remains open. This task becomes even more complicated if there are nonlinearities in real devices. It is shown that the root distribution in the form of Newton binomial gives not a good enough result because it is not possible to correct the transient process towards more speed or less oscillation on this case. The technique that allows tuning the coefficients of the regulator of the stabilization system by performing the numerical optimization procedure is proposed in the paper. In this case, it is possible to change the form of the transient process depending on the specific requirements for the system by changing the form of the cost function. The results of the work are confirmed by numerical simulation and experimentally.

Index Terms – Automatic control system, regulator, numerical optimization, regulator coefficients tuning, robot, microcontroller, desired dynamics equation.

I. INTRODUCTION

THIS article is devoted to tuning the regulator coefficients of the automatic stabilization system of a two-wheeled balancing robot. When calculating the regulator coefficients analytically, it is necessary to set the desired distribution of the system roots. This distribution can be defined based on general requirements for the quality of the system transient processes such as the maximum level of overshoot and the maximum duration of the transient process that define the sector in the complex plane within which the roots should be placed. However, the issue of choosing the distribution within this sector remains open. This task becomes even more complicated if there are nonlinearities in real devices. Along with analytical methods of calculating regulators [18–22], there are different non-analytic ones. Among them methods of empirical tuning and methods of numerical optimization can be distinguished [1–11]. In this paper, we propose a technique based on the numerical optimization method, which allows tuning the coefficients of the control

system regulator and obtaining transient processes that correspond to certain requirements for the system.

II. THE DEVICE DESCRIPTION

The appearance of the two-wheeled balancing robot is depicted in Fig. 1. This device is a platform on which boards with control and power electronics are placed. The stators of the DC motors are rigidly mounted on the platform. The shaft of each motor is connected to its wheel. The main task of stabilization system of this device is to maintain the vertical position of the robot by the wheels rotation.

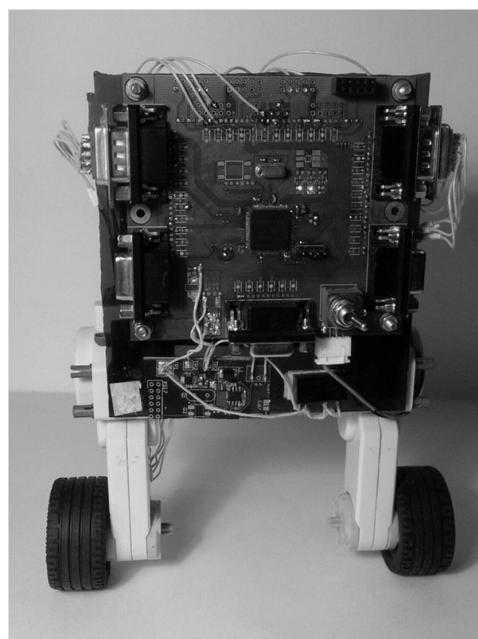


Fig. 1. The device appearance.

The structural scheme of the robot is shown in Fig. 2. Two Lego NXT servomotors are the actuators of the system. These devices are the direct current motors with embedded reducers and quadrature encoders. The encoders have the resolution of 180 pulses per rotation, which allows estimate the relative rotation angle of the motor shaft with the accuracy of not less than 2 degrees. The control of each servomotor is carried out by the full bridge circuit based on 4 MOSFETs and its driver circuits. This circuit allows control the motor rotation with a reversing ability.

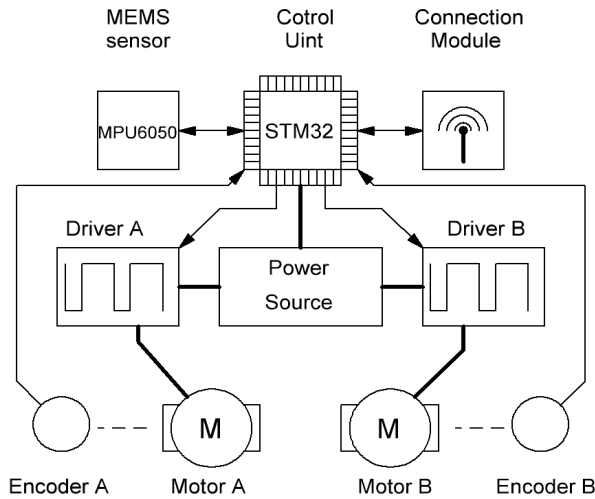


Fig. 2. The structural scheme of the robot.

The MPU6050 measuring module which includes 2 three-axis MEMS sensors – an accelerometer and a gyroscope is applied for estimation of the robot tilt angle. Presently only gyro sensor is applied in the robot stabilization system in practice [12]. Detailed information about operation and applying features of the MPU6050 module is given in articles [13, 14].

The core of the device is the STM32F205VET6 microcontroller from STMicroelectronics. The control program of the microcontroller collects the system sensors data and calculates the control action of the stabilization system. In addition to the described blocks, the device also includes wired and wireless data transmission blocks. Two Li-Ion batteries with a total voltage of 8.4 V. power the device.

III. THE CONTROL SYSTEM DESCRIPTION

Consider the operation of the automatic stabilization system of the two-wheeled balancing robot. The structural diagram of this system is depicted on the Fig. 3. Details of the rationale for choosing the system structure and the calculation of its regulator are given in [12]. Here we give only a brief description of the principle of its operation and the final form of the equations. The expressions of the transfer functions of the system are given below and the numerical values of their parameters are presented in the Table I.

$$W_\varphi(s) = \frac{k_o s}{s^3 + a_2 s^2 + a_1 s + a_0}$$

$$W_\alpha(s) = k_\alpha \frac{s^2 + b_0}{s^2}$$

$$W_K(s) = \frac{K_d s^2 + K_p s + K_i}{s}$$

$$W_H(p) = \frac{H_p s^2 + H_i s + H_{ii}}{s^2}$$

TABLE I
THE TRANSFER FUNCTIONS PARAMETERS VALUES

| Parameter | Value |
|------------|-------|
| a_0 | -490 |
| a_1 | -52.3 |
| a_2 | 9.9 |
| k_o | -2.8 |
| b_0 | -49.5 |
| k_α | -7.07 |

The choosing such structure of the system is due to need to compensate an angular speed sensor (MEMS gyro sensor) disadvantage called the zero drift. This disadvantage is expressed in a gradual increase in the tilt angle estimation error, which is depicted, on the structural diagram by the sensor error signal Err_g and the integrator block. Over time, this leads to a loss of stability of the system if it does not provide a way to compensate for this error. The system presented allows you to do this. Indeed if we derive the transfer function of the system output relative to the error signal we obtain the following expression:

$$W_e = - \frac{k_o k_a K(s) B(s)}{(A(s) + k_o K(s)) s^3 + k_o k_a H(s) B(s)}$$

where

$$A(s) = s^3 + a_2 s^2 + a_1 s + a_0$$

$$B(s) = s^2 + b_0$$

$$H(s) = H_p s^2 + H_i s + H_{ii}$$

$$K(s) = K_d s^2 + K_p s + K_i$$

Upon the completion of the transient processes this expression will take the following form:

$$W_e = - \frac{k_o k_a K_i b_0}{k_o k_a H_{ii} b_0} = \frac{K_i}{H_{ii}}$$

Thus, the incremental error of the tilt angle estimation is compensated. In theory, using an ideal angular speed sensor for stabilization of the system would be sufficient if the regulator “Controller 2” was proportional and the regulator “Controller 1” would have the same form. This means that the system order is higher than the theoretical one precisely because of the need to compensate the gyro sensor zero drift.

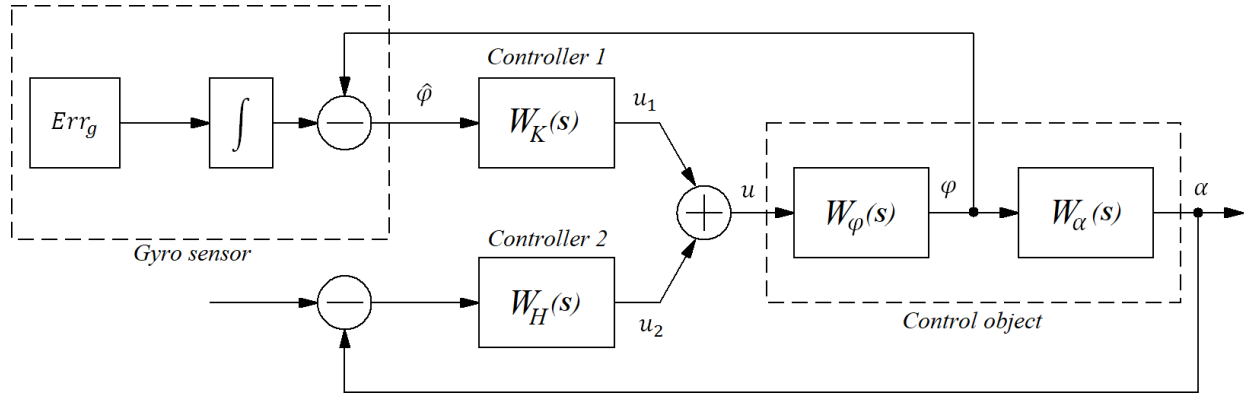


Fig. 3. The structural diagram of the system.

The expressions for the calculation of the regulator coefficients are given below.

$$a_2 + k_o K_d = a^*_5 \quad (1)$$

$$a_1 + k_o K_p + k_o k_a H_p = a^*_4 \quad (2)$$

$$a_0 + k_o K_i + k_o k_a H_i = a^*_3 \quad (3)$$

$$k_o k_a (H_{ii} + b_0 H_p) = a^*_2 \quad (4)$$

$$k_o k_a b_0 H_i = a^*_1 \quad (5)$$

$$k_o k_a b_0 H_{ii} = a^*_0 \quad (6)$$

The coefficients a^*_i are the coefficients at the powers of the desired dynamics equation of the system:

$$A^*(s) = s^6 + \sum_{i=0}^5 a^*_i s^i \quad (7)$$

IV. THE PROBLEM DEFINITION

To calculate the control system described above, it is necessary to choose the roots distribution of the desired equation (7), and to calculate the values of the regulator coefficients. However, in fact the choosing the desired equation is not a trivial task. Usually the distribution of the roots of this equation is chosen based on the general constraints to the system quality indicators such as the maximum value of the overshoot and maximum transient time. These parameters define the sector on the complex plane within which the roots should be placed. But the issue of the distribution of the roots inside this sector remains open. There are almost no recommendations on the choice of the desired equation in the literature. The rational for the choosing the desired equation roots is given, for example, in [15, 16]. In practice, the choice of the desired equation is associated with a number of difficulties, such as, for example, the presence of the nonlinearities in a real device. The behavior of the system can be very different from the predicted one if there are such nonlinearities as the limitation of the control action, the dry friction, and the backlash of the actuators. This complicates the choice of the roots distribution. Often the distribution of the roots in the Newton binomial form is chosen as the desired one but the quality of the system processes obtained can be far from the optimal in

this case. In the presence of the nonlinearities described above, the real object can become unstable as shown in [12]. In the control system under consideration [12], the following distribution of the desired dynamics equation roots was chosen by the empirical way:

$$p_1 = p_2 = -50; p_3 = p_4 = p_5 = p_6 = -1$$

This in accordance with expressions (1-6) gives the values of the regulator coefficients, which are presented in Table II. The graphs of the transient processes of the system during the initial condition adjustment are depicted in Fig. 4 – 6. As it can be seen from the figures the system compensates the gyro sensor zero drift and provides the stability of the device. However, the transient processes of the system have a sufficiently high duration. If, for example, the speed of the system is a priority requirement then such system parameters may be unacceptable. In other cases, the system may have other requirements. Thus, the research problem can be formulated as follows: it is necessary to propose a method that allows calculating the coefficients of the system regulator or tuning them in accordance with the specific requirements for the system. The solving this task can be achieved on the one hand by the reasonable choice of the desired dynamics equation with the subsequent calculation of the regulator coefficients on the other hand by tuning using some method the regulator coefficients calculated earlier. To solve the task by any of these approaches, a numerical optimization method can be used, both for choice the desired roots distribution, and for tuning the regulator.

TABLE II
THE ORIGINAL SYSTEM REGULATOR COEFFICIENT VALUES

| Parameter | Value |
|-----------|-------|
| K_i | -4040 |
| K_p | -1170 |
| K_d | -33.6 |
| H_p | -15.8 |
| H_i | -10.3 |
| H_{ii} | -2.55 |

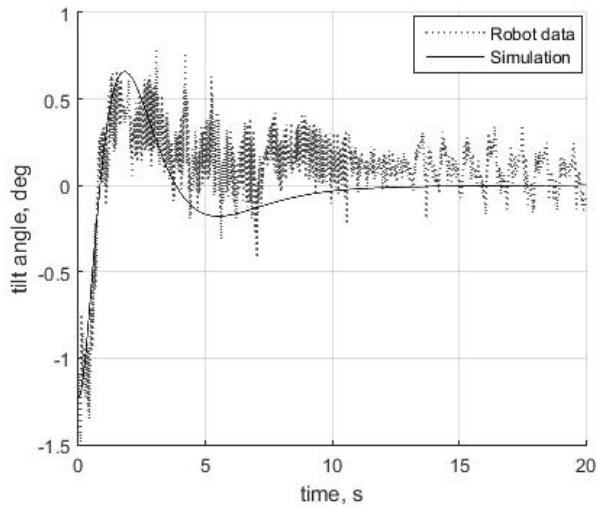


Fig. 4. The process of the tilt angle relative to vertical in the original system.

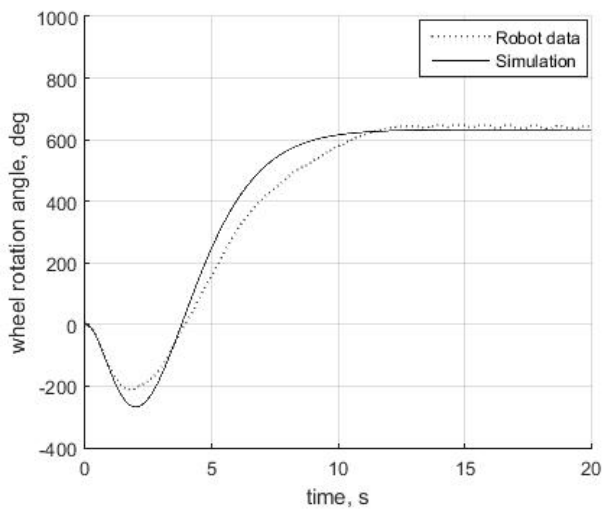


Fig. 5. The process of the wheel rotation angle in the original system.

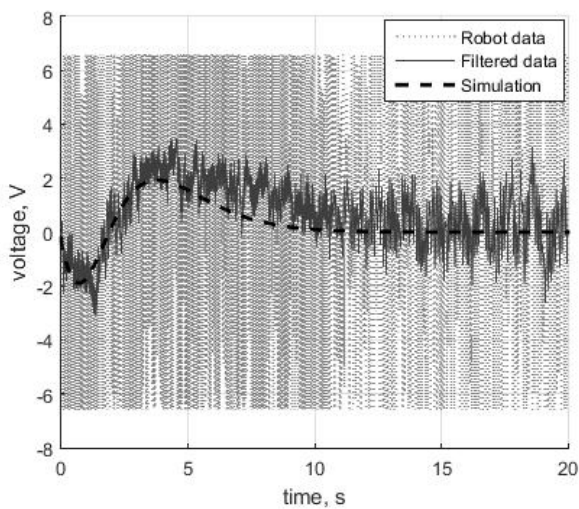


Fig. 6. The process of the voltage in the original system.

V. ABOUT THE DISTRIBUTION OF THE ROOTS

Consider the system with the roots distribution in a Newton binomial form. We calculate the regulator coefficients for the different values of the roots. The results of the calculation are given in the Table III. Let us perform the numerical simulation of the processes in the system. As an example we will investigate the response to the system on the impulse disturbance:

$$M(t) = \begin{cases} 1, & t \leq 0.01c \\ 0, & t > 0.01c \end{cases} \quad (8)$$

TABLE III
THE NEWTON BINOMIAL COEFFICIENT VALUES

| Root value | $p = -3$ | $p = -5$ | $p = -8$ |
|------------|----------|----------|----------|
| K_i | -378 | -1200 | -5250 |
| K_p | -75.8 | -223 | -843 |
| K_d | -2.89 | -7.18 | -13.6 |
| H_p | -1.25 | -9.89 | -68.1 |
| H_i | -1.49 | -19.1 | -201 |
| H_{ii} | -0.744 | -15.9 | -268 |

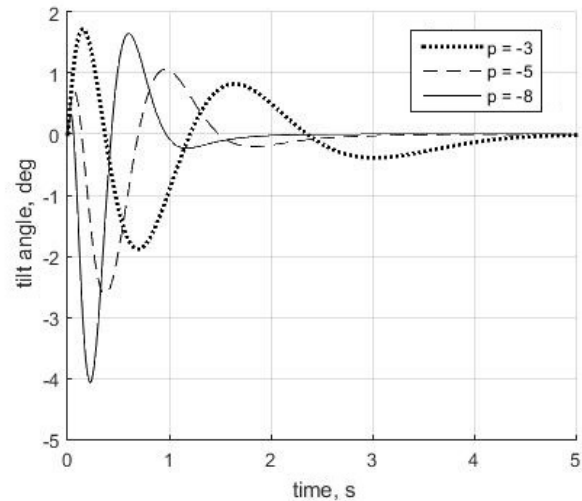
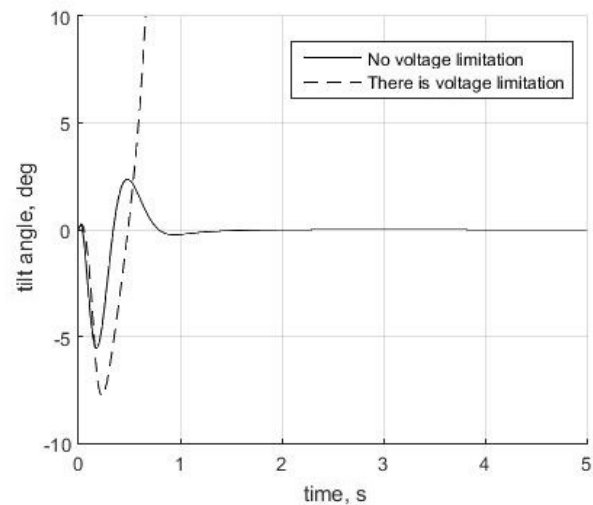


Fig. 7. The system simulation for the Newton binomial roots.

Fig. 8. The system behavior at the $p = -10$ with and without control action constraint.

This type of action corresponds to the action of disturbances on the real device (impacts or pushes). The simulation results are depicted in Fig. 7. We note that for smaller and larger values of the roots the system obtained at the calculation loses the stability. But if we remove the constraint of the control action the system calculated for larger root values becomes stable which is shown in Fig. 8. This is the property of this type of nonlinearity. Next, we apply the calculated values of the coefficients in the real device. The response of the robot to the disturbance and its adjustment of the initial conditions are depicted in Fig. 9 and 10. As it can be seen from the figures although the processes form corresponds to the simulation results in general (the process speed increases as the absolute value of the system roots increases) the processes quality in the real device is not correspond to the predicted one. The only acceptable system with the reservations is the system with the value of the root of $p = -5$. Thus we can give the following conclusions:

- The distribution of the roots in the Newton binomial form allows setting only general gain of the system not the relation between the speed and the oscillation value at the given gain factor.
- There is a limit cycle with the significant amplitude at the small value of the general system gain ($p = -3$) and also the system stability is not high.
- At the large value of general gain, the system begins to be affected by the control action constraint: the system also has a limit cycle although the high stability remains.

Thus it is necessary to choose the roots distribution more thoroughly to obtain a better quality of the processes.

VI. THE REGULATOR COEFFICIENTS TUNING TECHNIQUE

The alternative to choosing the distribution of the roots of the desired dynamics equation of the system is the tuning existing values of the regulator coefficients to obtain the system processes with an acceptable quality. We will use the numerical optimization method in the VisSim software to tuning the coefficients of the system regulator. We note that it is not required to define the global optimum of the system in this case, it is only necessary to obtain the processes with the acceptable quality. In the course of the simulation, we will also investigate the response of the system to the impulse disturbance of the form (8). The adjustment of the regulator coefficients will be performed in two stages:

1. We determine first four coefficients of the regulator and assuming that the remained two coefficients are equal to the zero. The angular speed sensor is an ideal in this case (the error signal of the gyro sensor is also equal to the zero).
2. We determine two remained coefficients of the regulator taking into account the presence of the error of the tilt angle measurement.

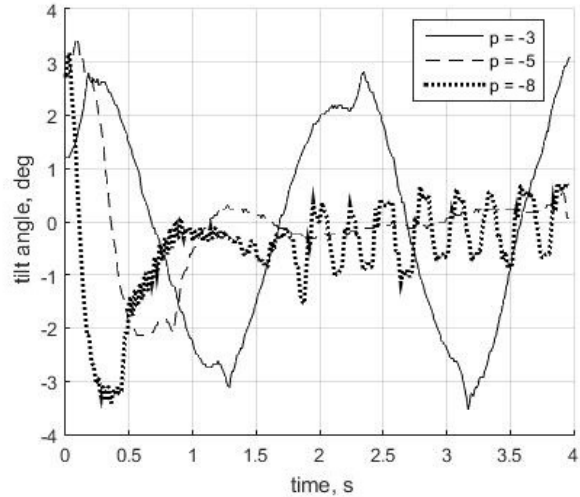


Fig. 9. The real device processes with the Newton binomial roots: the initial conditions adjustment system response.

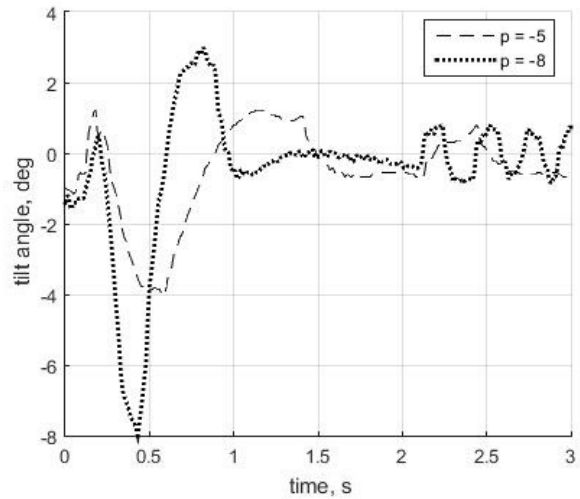


Fig. 10. The real device processes with the Newton binomial roots: the disturbance system response.

A. The Stage 1

We use the simplified structural diagram of the system depicted in the Fig. 11 to calculate the values of the regulator coefficients with which the optimization procedure will start. The transfer function of the tilt angle of the robot relative to the input in this system has the following form:

$$\overline{W}_\varphi(s) = \frac{k_o(K_d s^2 + K_p s + K_i)}{s^3 + (a_2 + k_o K_d)s^2 + (a_1 + k_o K_p)s + (a_0 + k_o K_i)}$$

The expressions for calculation of the regulator coefficients have the following form:

$$\begin{aligned} a_2 + k_o K_d &= a^*_2 \\ a_1 + k_o K_p &= a^*_1 \\ a_0 + k_o K_i &= a^*_0 \end{aligned}$$

where a^*_i is the coefficients at the desired dynamics polynomial powers.

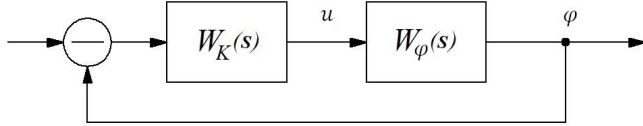


Fig. 11. The simplified system.

The values of the coefficients obtained from the equation set by the distribution of the roots in the Newton binomial form can be used as the start values of the optimization procedure. And we apply the following value of the proportional coefficient of the regulator “Controller 2”:

$$H_p = \frac{K_d}{2}$$

It is necessary to define the cost function of the system to perform the optimization. Minimization of value of this function is the goal of the optimization. We choose the form of the cost function described in [17]:

$$f(t) = \int |e(t)|^M t^N dt$$

where $e(t)$ is the system error, M and N are the integer indices of the power. Since the system error make larger contribution to the value of the cost function in the latter stages on the transient process this form of the cost function can be applied to obtain the more efficient in speed processes. Setting different values of the M and N power indices it is possible to change the form of the obtained processes towards more speed or less oscillation. We choose the current tilt angle value as the system error $e(t)$ since the goal of the operation of the system is to ensure the zero value of this angle. When performing the optimization, we will specify different values of the power indices of M and N . We perform a numerical optimization of the system in the VisSim software in accordance with the simulation scheme shown in Fig. 12. The optimization results are shown in Fig. 13 and 14. The values of the regulator coefficients obtained for different values of the parameters N and M , as well as their initial values, are given in Table IV. Note that for the case of $M = 4$ and $N = 1$, an incorrect result was obtained, because at the end of the transient process the device continues to move along the surface, which is shown in Fig. 14 (wheel rotation angle increases with time). To solve this problem, we choose the current value of the angular velocity of the wheel as the error of the system instead the tilt angle value, and repeat the optimization procedure for $M = 4$ and $N = 1$. It can be seen from the figures that the best system for speed is the system 1, and the system 5 is the best in terms of the level of oscillation. We take the values of the regulator coefficients of these systems and continue the adjustment in stage 2. Note that although the oscillation of the initial system is lower than in system 5, in the last one the transient time is much shorter, while the level of oscillation is slightly higher, so we will adopt this system.

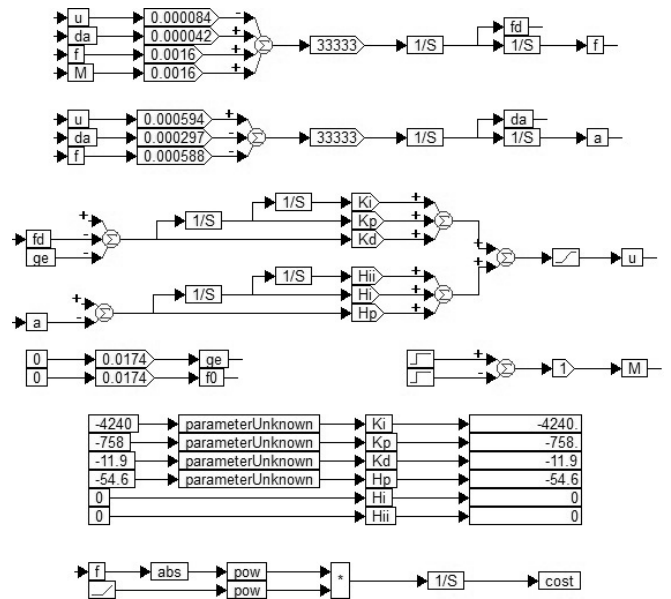


Fig. 12. The simulation scheme for the stage 1.

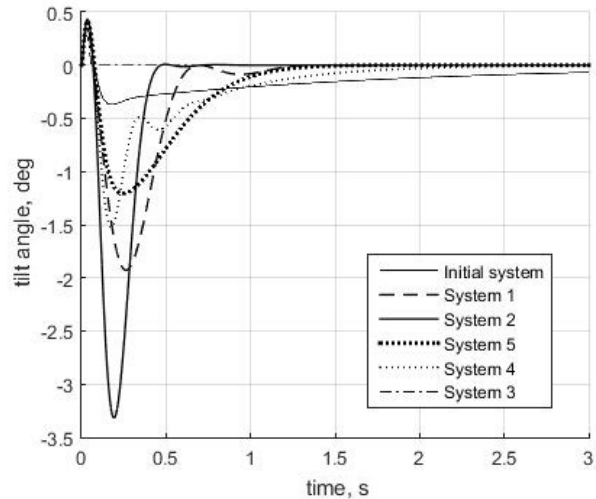


Fig. 13. The stage 1 tuning results: the tilt angle.

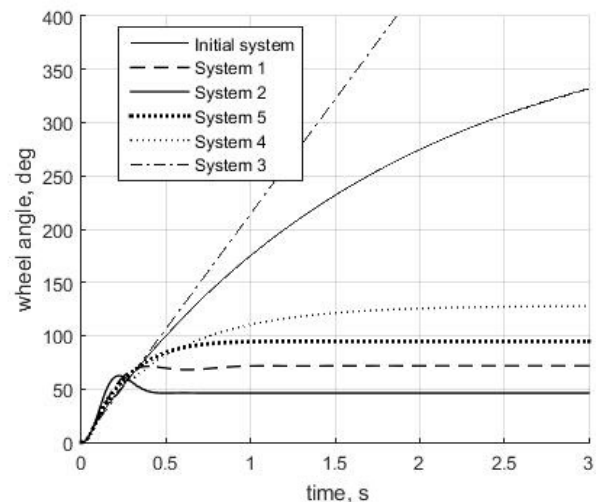


Fig. 14. The stage 1 tuning results: the wheel angle.

TABLE IV
 THE STAGE 1 TUNING RESULT

| - | - | 1 | 2 | 3 | 4 | 5 |
|------------|---------|----------|----------|----------|----------|----------|
| The system | Initial | M=1, N=1 | M=1, N=4 | M=4, N=1 | M=4, N=4 | Modified |
| K_i | -9820 | -4720 | -4240 | -36300 | -6190 | -3550 |
| K_p | -983 | -757 | -758 | -104000 | -583 | -650 |
| K_d | -28.6 | -31.1 | -11.9 | -481 | -13.3 | -14.2 |
| H_p | -14.3 | -39.1 | -54.6 | -0.126 | -28.7 | -22.3 |
| H_i | 0 | 0 | 0 | 0 | 0 | 0 |
| H_{ii} | 0 | 0 | 0 | 0 | 0 | 0 |

B. The Stage 2

For the final adjustment of the regulator coefficients, we use the optimization diagram shown in Fig. 15. The main difference between this scheme and the previous one is that an error in measuring the tilt angle by a gyro sensor has been introduced into this system. In accordance with this diagram, we will perform the tuning three factors of the regulator "Controller 2". We take the value of the coefficient H_p obtained in stage 1 as the initial value. And the initial values of the coefficients H_i and H_{ii} are taken to be half that of H_p :

$$H_i = \frac{H_p}{2}$$

$$H_{ii} = \frac{H_p}{2}$$

At the second stage of the tuning procedure, we keep those values of the cost function M and N parameters, at which the coefficients of the system regulators were obtained in stage 1. But we take the current value of the wheel angular velocity as the error signal $e(t)$. The optimization results are shown in Fig. 16 and 17. The values of the regulator coefficients obtained for different values of the parameters N and M , as well as the initial values of the coefficients in [12], are given in Table V. It can be seen from the figures that processes in systems with adjusted coefficients have a faster response time than the original system. At the same time, the system 5 has a level of oscillation close to the initial system at a better speed: the first peak has a somewhat larger value, while the second peak is slightly smaller. Thus, it can be concluded that the described procedure allows obtaining better processes, in comparison with those obtained empirically. And the technique allows obtaining processes that are more efficient in terms of speed or level of oscillation, depending on the specific requirements for the system.

 TABLE V
 THE STAGE 2 TUNING RESULT

| - | - | 2 | 5 |
|------------|----------|----------|----------|
| The system | Original | M=1, N=4 | Modified |
| K_i | -4040 | -4240 | -3550 |
| K_p | -1170 | -758 | -650 |
| K_d | -33.6 | -11.9 | -14.2 |
| H_p | -15.8 | -35.4 | -20.9 |
| H_i | -10.3 | -55.7 | -22.6 |
| H_{ii} | -2.55 | -32.3 | -9.48 |

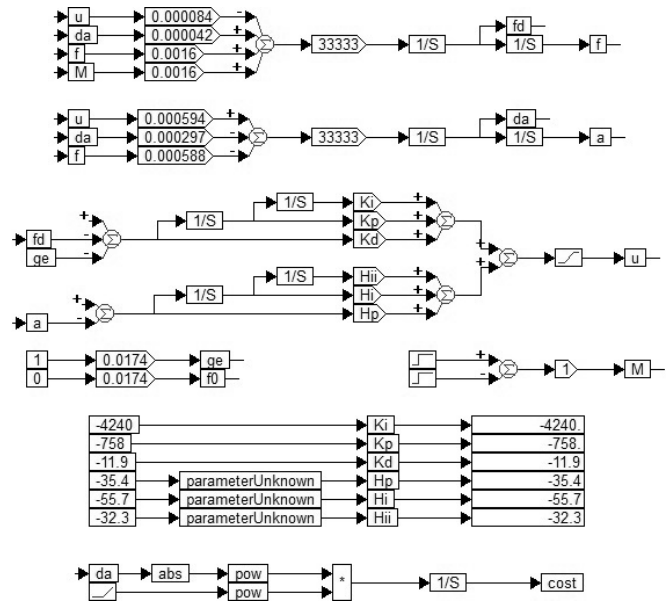


Fig. 15. The simulation scheme for the stage 2.

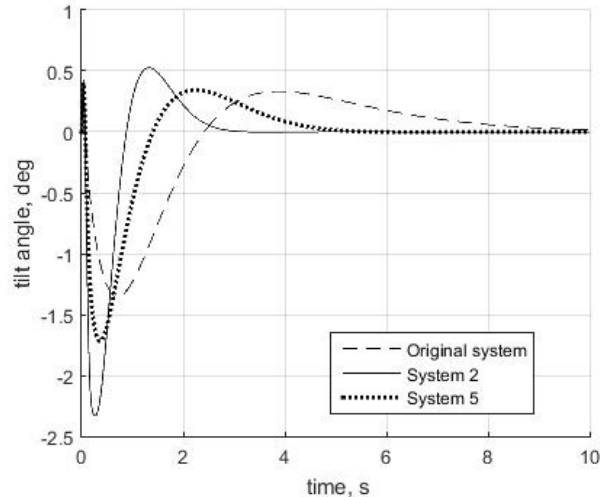


Fig. 16. The stage 2 tuning results: the tilt angle.

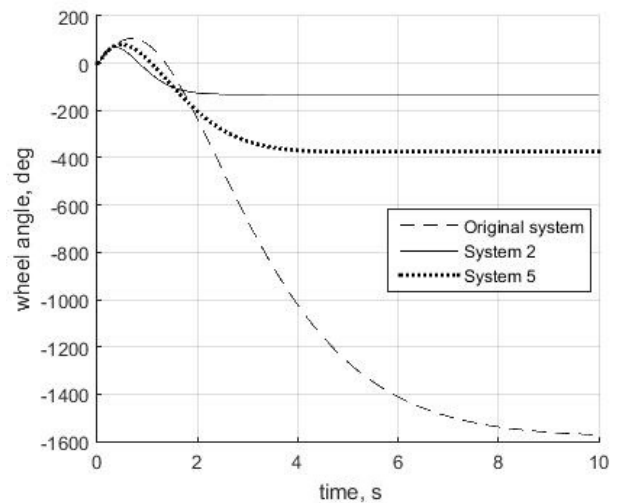


Fig. 17. The stage 2 tuning results: the wheel angle.

VII. THE EXPERIMENTS

The previously obtained values of the regulator coefficients were applied in the control system of the real device. The results of the operation of the systems obtained, as well as of the original system, at adjustment of the initial conditions and adjustment of the disturbance are shown in Fig. 18 – 21. It can be seen from the graphs that the processes in real systems correspond to the results of simulation in general. It should be noted, however, that limit cycle are presented in tuned systems. For a system with the highest speed, the magnitude of these oscillations is more significant. At the same time, the level of the static error in the wheel rotation angle in tuned systems is much lower than in the original system. Thus, it can be concluded that the proposed technique allows you to obtain processes in accordance with specific requirements for the system for a real device.

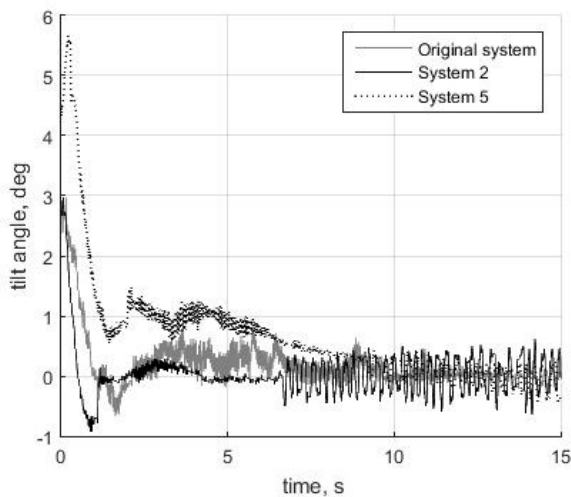


Fig. 18. The experiment results: the tilt angle at the initial conditions adjustment.

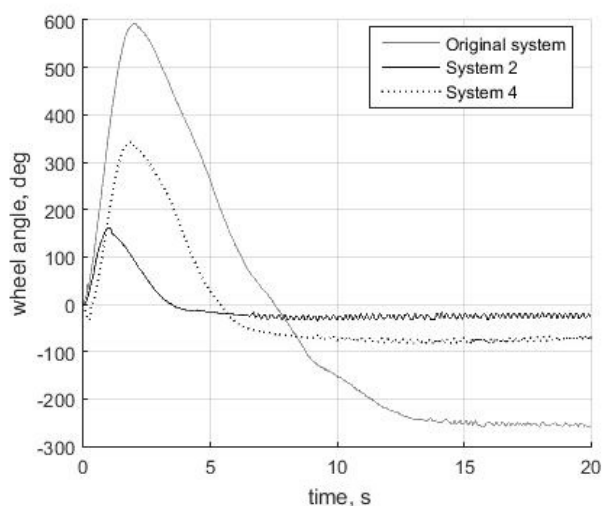


Fig. 19. The experiment results: the wheel angle at the initial conditions adjustment.

VIII. CONCLUSION

The paper considers the choice of the desired distribution of the roots of the system and its impact on the quality of its operation. It is shown that the choice of the roots distribution in the form of a Newton binomial allows you only obtain the stable processes in the system and set its general amplification. But within the given gain, it is not possible to specify the preferred requirement for processes such as high speed, small oscillation, or its compromise. Therefore, such a distribution cannot be considered acceptable. As a result of the research, a technique based on the numerical optimization method was proposed. It is shown that this technique allows you to configure processes in the system in accordance with specific requirements for the system by changing the type of cost function used in system optimization. The results of the research are confirmed by numerical simulation and experimentally.

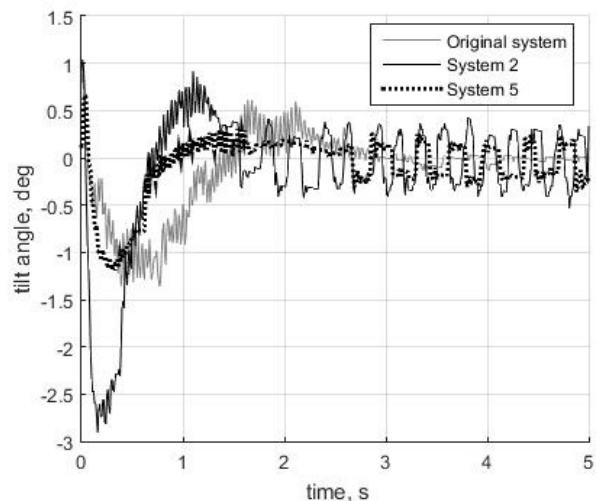


Fig. 20. The experiment results: the tilt angle at the disturbance adjustment.

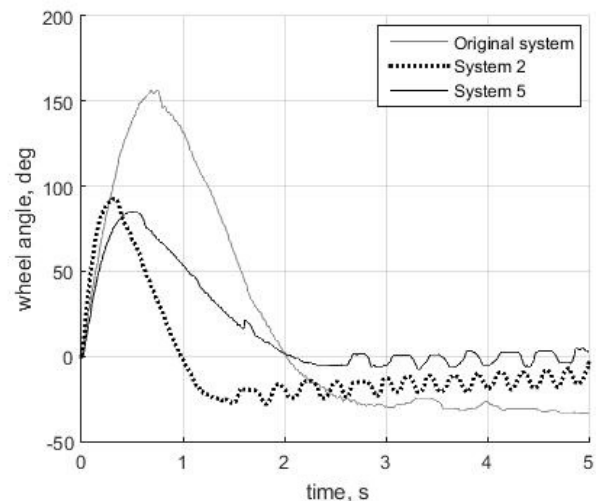


Fig. 21. The experiment results: the wheel angle at the disturbance adjustment.

REFERENCES

- [1] Toscano R. "A simple robust PI/PID controller design via numerical optimization approach". Journal of Process Control. vol. 15, no. 1, pp. 81-88, Feb. 2005.
- [2] Zhmud V.A. and Liapidevskiy A.V. "The Design of the Feedback Systems by Means of the Modeling and Optimization in the Program VisSim 5.6/6.0". Proc. Of The 30th IASTED Conference on Modelling, Identification, and Control ~ AsiaMIC 2010 ~November 24 – 26, 2010 Phuket, Thailand. P. 27–32.
- [3] Sanchis R., Romero J. and Balaguer P. "Tuning of PID controllers based on simplified single parameter optimization". International Journal of Control. vol. 83, no. 9, pp. 1785-1798, Jul. 2010.
- [4] Zhmud V.A., Dimitrov L.V. and Yadrishnikov O.D. "Calculation of regulators for the problem of mechatronics by means of numerical optimization method". 12th International Conference on Actual Problems on Electronic Instrument Engineering APEIE 2014. Proceedings.
- [5] Zhmud V. A., Semibalamut V. M. and Vostrikov A. S. "Feedback systems with pseudo local loops". Testing and measurement: techniques and applications: proc. of the 2015 intern. conf. on testing and measurement techniques (TMTA 2015), Thailand, Phuket Island, 16–17 Jan. 2015. – London: CRC Press, 2015. – P. 411–416. – 200 copy. – ISBN 978-1-138-02812-1-8.
- [6] Walton C., Phelps C., Gong Q. and Kaminer I. "A Numerical Algorithm for Optimal Control of Systems with Parameter Uncertainty". IFAC-PapersOnLine. vol. 49, no. 18, pp. 468-475, 2016.
- [7] Diaz-Rodriguez I., Han S., Keel L., Bhattacharyya S. "Advanced Tuning for Ziegler-Nichols Plants". IFAC-PapersOnLine. vol. 50, no. 1, pp. 1805-1810, Jul. 2017.
- [8] Zhmud V. and Zavorin A. "The design of the control system for object with delay and interval-given parameters". International Siberian conference on control and communications (SIBCON–2015): proc., Omsk, 21–23 May, 2015. – Omsk: IEEE, 2015. – Art. 130 (6 p.). – This work was supported by the Russian Ministry of Education and Science, project number 2014/138, the theme name is: "New structures, models and algorithms for the management of breakthrough technology systems based on high-tech results of intellectual activity". – ISBN 978-1-4799-7102-2. – DOI: 10.1109/SIBCON.2015.7147060.
- [9] Jin M., Lee J., Chang P., Kim M. and Kang S. "Automatic Gain Tuning for Robust PID Control Using Time-Delay Control". IFAC-PapersOnLine. vol. 50, no. 1, pp. 4318-4323, Jul. 2017.
- [10] Zhmud V.A., Yadrishnikov O.D. and Semibalamut V.M. "Control of the objects with a single output and with two or more input channels of influence". WIT Transaction on Modelling and Simulation. Vol.59, 2015. WIT Press. www.witpress.com, ISSN 1743-355X. P. 147 – 156.
- [11] Quirynen R. "Numerical Simulation Methods for Embedded Optimization". Ph.D. dissertation, Faculty of Engineering Science., KU Leuven, Leuven, Belgium, 2017. Available: <http://ftp.esat.kuleuven.be/pub/SISTA/ida/reports/17-18.pdf>.
- [12] Ivoilov A.Yu., Zhmud V. A. and Trubin V. G. "The tilt angle estimation in the inverted pendulum stabilization task". 2018 Moscow Workshop on Electronic and Networking Technologies (MWENT). Moscow, 14-16 march, 2018.
- [13] Fedorov D., Ivoilov A., Zhmud V., and Trubin V. "Development of Deflection Angle Stabilizing System for Balancing Robot". Journal of Advances in Management Sciences & Information Systems. – 2015. №1. – P. 65-82. – ISSN 2371-1647.
- [14] Ivoilov A. Y., Zhmud V. A., Trubin V. G. and Dimitrov L. V. Detection of unrevealed non-linearities in the layout of the balancing robot. International Siberian conference on control and communications (SIBCON) : proc., Moscow, 12-14 May 2016. – Moscow: IEEE, 2016. – 9 p. – ISBN 2380-6516.
- [15] Lebedev S. K., Gnezdov N. E. and Kolganov A. R. "Dynamic Model Selection For Vector Control Systems of AC Electric Drives". XVI mezhdunarodnaja nauchno-tekhnicheskaja konferentsiya "Electroprivody peremennogo toka" [XVI International Science Conference "AC Electric Drives"]. Ekaterinburg, 05-09 October 2015.
- [16] Kim D.P. "Algebraicheskiye metody siteza sistem avtomaticheskogo upravleniya" [Algebraic synthesis methods of the automatic control systems], Russia: FIZMATLIT, 2014.
- [17] Ivoilov A.Yu., Zhmud V.A. and Roth H. "The Dynamic Accuracy Increasing for a Controlling System by Means of the Modified Algorithm of Numerical Optimization of the Regulator". 2018 Moscow Workshop on Electronic and Networking Technologies (MWENT). Moscow, 14-16 march, 2018.
- [18] Kotova E. P. and Frantsuzova G. A. "Application PI2D controller in automatic control systems". Int. Siberian conference on control and communications (SIBCON): proc., Kazakhstan, Astana. 2017.: S. Seifullin Kazakh Agrotechn. Univ., 2017. P. 692-695.
- [19] Zemtsov N. S., Hlava J., Frantsuzova G. A. "Using the robust PID controller to manage the population of thermostatically controlled loads". Int. conf. on industrial engineering, applications and manufacturing (ICIEAM): proc., Chelyabinsk, 2017. IEEE, 2017. 4 p.
- [20] Hlava J., Zemtsov N. and Frantsuzova G. "Application of PID controller based on the localization method for ancillary service provision". Int. Siberian conf. on control and communications (SIBCON): proc., Moscow, 2016.IEEE, 2016. 6 p.
- [21] Suvorov D. A., Frantsuzova G. A. and Zemtsov N. S. "Using the localization method for once-through boiler control". Int. Siberian conf. on control and communications (SIBCON–2015): proc., Omsk, 2015. IEEE. 5 p.
- [22] Frantsuzova G. A., Zemtsov N. S., Hubka L., Modrak O. "Calculation of robust PID-controller" Actual problems of electronic instrument engineering (APEIE–2014): 2014 г. : V. 7. Novosibirsk. NSTU. P. 32-35.



Ivoilov Andrey Yurievich – PhD-student of Department of Automatics of NSTU.
E-mail: iau13hv@mail.ru
630073, Novosibirsk,
str. Prosp. K. Marksa, h. 20



Zhmud Vadim Arkadievich – Head of the Department of Automation in NSTU, Professor, Doctor of Technical Sciences.
E-mail: oao_nips@bk.ru
630073, Novosibirsk,
str. Prosp. K. Marksa, h. 20



Trubin Vitaly Gennadievich – Head of the department. lab. Automatics Department of NSTU, Director of KB Automatics.
E-mail: trubin@ngs.ru



Roth Hubert – Head of the Department of Automatic Control Engineering of University of Siegen, Professor, Doctor of Sci., Germany
E-mail: hubert.roth@uni-siegen.de

Adaptive System for Automatic Control of Output Effort of Electromagnetic Sausage-Filler

Vitaliy A. Kargin, Andrei V. Volgin, Alexei P. Moiseev
Saratov State Agricultural University name N.I. Vavilov, Saratov, Russia

Abstract – A promising direction in the development of machines for filling sausage meat is the use of a pulsed power electric drive, which is based on an engine with a linear trajectory of motion of the working member. In this case, the use of a linear electromagnetic engine is preferable due to the simplicity of design, small dimensions, reliability in operation, determined by the absence of excitation windings, relatively high specific parameters. To maintain the output parameters of an electromagnetic sausage-filler with a linear electromagnetic engine (pressure, speed of movement of the filling piston), it is necessary to provide a variation in the output force. In most known electromechanical pulse systems with linear electromagnetic engines powered from alternating current sources, the control of the output tractive force is provided by varying the duration of the voltage supply pulse. The voltage level of the supply pulse is not regulated and limited by the values of the line or phase voltage of the power supply. The article proposes a system using a programmable logic controller and a strain gauge as a feedback element, which makes it possible to smoothly move the armature of a linear electromagnetic engine with simultaneous automatic correction of the output traction force depending on the change in load parameters.

Index Terms – Sausage-filler, linear electromagnetic engine, strain gauge.

I. INTRODUCTION

ONE of the main conditions for solving the problems of providing high-quality agricultural products is the introduction of new and improvement of available technical means. In particular, technological equipment, currently used in small meat processing plants, often does not meet modern requirements. So, for example, for processes of forced filling of sausage shells with minced meat, pneumatic, hydraulic devices with linear displacement of the working organ are used, which are characterized by multistage energy conversion, relatively high equipment price, high qualification of maintenance personnel, etc. [1].

A promising direction in the development of machines for filling sausage meat is the use of a pulsed power electric drive, which is based on an engine with a linear trajectory of motion of the working member. [2,3,4]. In this case, the use of a linear electromagnetic engine (*LEME*) is preferable due to the simplicity of design, small dimensions, reliability in operation, determined by the absence of excitation windings, relatively high specific parameters. [3,5].

Linear electromagnetic engines that realize discrete consumption and conversion of electrical energy into mechanical work for a power source represent an impulse

load. Pulse metering of the flow transmitted by the source to the *LEME* of energy is provided by special electric converters, due to which the energy of the source enters the winding of the engine in the form of unipolar voltage and current pulses [3,5].

II. PROBLEM DEFINITION

To maintain the output parameters of the electromagnetic sausage-filler with *LEME* (pressure, speed of movement of the filling piston), it is necessary to provide a variation in the output force F_t , which can be achieved by affecting the duration of energy consumption (operating cycle t_c) or the amount of power input p in the *LEME* winding by changing the applied voltage u for given properties of the winding. In most known electromechanical pulse systems with *LEME*, powered by alternating current sources, the control of the output traction force F_t is provided by changing the duration of the voltage supply pulse, which is performed, for example, by manually tuning the parameters of the timing RC-chain [3]. The voltage level of the supply pulse is not regulated and limited by the values of the line or phase voltage of the power supply. Thus, it is important to ensure the smoothness of start and stroke of the armature of the *LEME* of the sausage-filler by automatically adjusting the consumed energy while changing the load properties.

III. IMPLEMENTATION OF AUTOMATIC CORRECTION OF OUTPUT EFFECT F_t OF *LEME*

To achieve smoothness of the armature stroke of *LEME*, an approach for the implementation of automatic correction of the output force F_t of a linear electromagnetic engine is proposed. The functional diagram of the electrical converter with a programmable logic controller is shown in Fig. 1 [6].

The supply of the electromagnetic working machine *EWM* is carried out from the power supply PS through the solid-state relay SSR (Fig.1). The discrete power supply is provided by the switching element SE, the activation and deactivation of which is linked to the limit position of the armature and the control buttons CB [3,6].

Automatic correction of the output traction force F_t is provided by smooth variation of the voltage on the engine winding by changing the control voltage on the solid-state relay SSR.

Fig. 2 shows a nomogram describing the operation of the adaptive system with automatic correction of the output traction force F_t . At the initial time, the voltage applied to

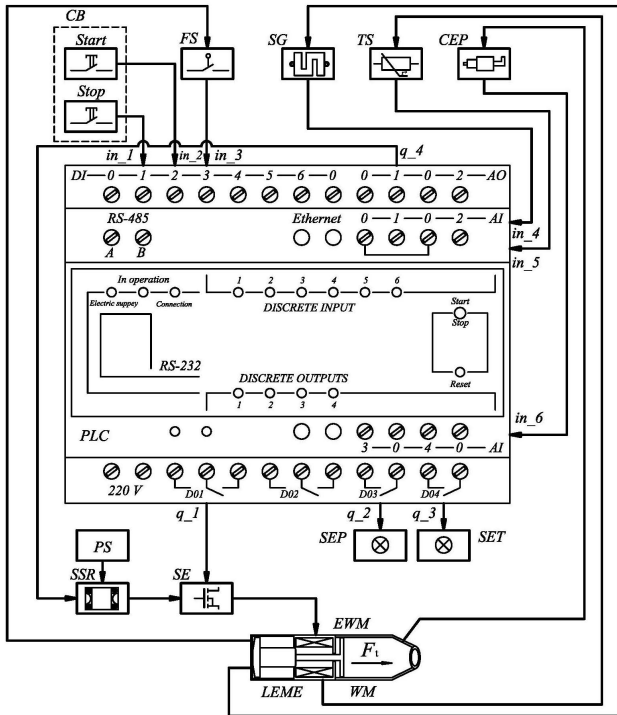


Fig. 1. Automatic control system for the smooth armature stroke of LEME: CB – control buttons; SG – strain gauge; TS – temperature sensor; CEP – converter of excess pressure; PS – power supply; SSR – solid-state relay; SE – a switching element; EWM – electromagnetic working machine; WM – working member; LEME – linear electromagnetic engine; SEP – signaling of excess of the pressure in the sausage cylinder; SET – signaling excess of the temperature of the motor winding; PLC – programmable logic controller.

the LEME winding through the solid-state relay SSR with control from the programmable logic controller PLC is

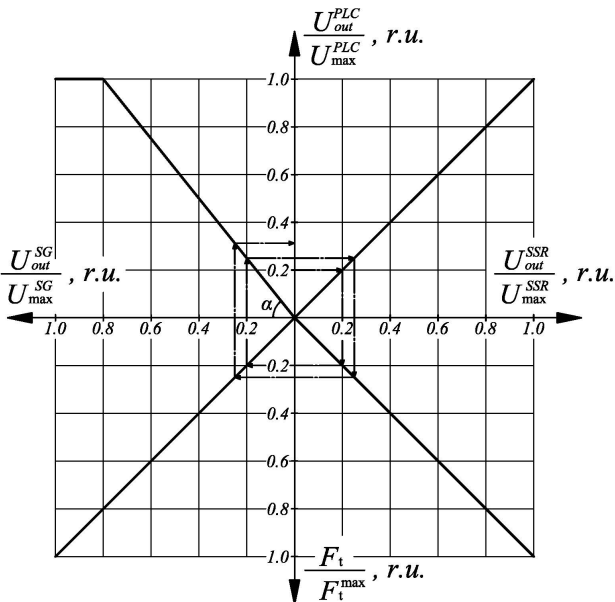
$$U_{out}^{SSR} = 0.2U_{max}^{SSR} \text{ (Fig. 2).}$$


Fig. 2. A nomogram describing the operation of the adaptive system with automatic correction of the output traction force.

The armature of the engine with the working member WM under the action of electromagnetic force starts smooth movement by the piston, while compressing the strain gauge SG (Fig. 1). The converted value of F_t in the voltage change

U_{out}^{SG} of the strain gauge SG is fed to the analog input of the PLC, where in accordance with the program an output analog signal of the control voltage U_{out}^{PLC} of the solid-state relay SSR is formed (dashed line in the nomogram Fig. 2). The voltage on the winding rises, increasing the value of the output traction force F_t until the working member starts to move [6,7].

Thus, a voltage is applied to the LEME winding, at which the necessary force is provided to move the conveyor and a smooth running of the LEME armature is achieved.

PLC programming is carried out in the CoDeSys environment using the standard library of function blocks [8,9], the aggregate and connection scheme of which are presented in Fig. 3 – Fig. 8.

The designations of the global inputs and outputs of the controller are given in the Tab. 1.

TABLE I
GLOBAL INPUTS AND OUTPUTS
OF THE PROGRAMMABLE LOGIC CONTROLLER

| Name | Type of signal | Designation | Number of input/output |
|---|----------------|----------------|------------------------|
| INPUTS | | | |
| Drive start button | discrete | <i>start</i> | in_1 |
| Drive stop button | discrete | <i>stop</i> | in_2 |
| Limit switch | discrete | <i>SQ</i> | in_3 |
| Strain gauge | analogue | <i>d_str</i> | in_4 |
| Temperature sensor | analogue | <i>d_temp</i> | in_5 |
| Converter of excess pressure | analogue | <i>d_press</i> | in_6 |
| OUTPUTS | | | |
| Control of the switching element | discrete | <i>LEME-d</i> | q_1 |
| Signaling excess of the temperature of the motor winding | discrete | <i>Lamp_TS</i> | q_2 |
| Signaling of excess of the pressure in the sausage cylinder | discrete | <i>Lamp_PS</i> | q_3 |
| Solid-state relay control | analogue | <i>LEME-a</i> | q_4 |

The condition for starting the sausage-filler is the logical unit (TRUE) of the discrete input *in_1* (the closed contact of the “Start button” - *Start*) and the logical zeroes (FALSE) of the digital inputs *in_2* and *in_3* (the open contacts of the Stop button – “Stop” and the limit switch *SQ*), inversion of which is carried out with the help of the function block NOT and is fed to the AND block. At the input CLK of the R-trigger “Rtrig”, a signal TRUE is generated.

At the output of Q «Rtrig» a logical unit is set [9]. The discrete output of PLC *q_1* (LEME-d) with the connected winding of the linear electromagnetic engine (Fig. 3).

The LEME is switched off by pressing the «Stop» button (*in_2*) or by the limit switch *SQ* (*in_3*) (Fig. 4). To ensure a smooth start and armature stroke of LEME the signal from the strain gauge is fed to the analog input of the controller

in_4 (d_str) and is compared in the GT functional unit with the specified U_{str} (Fig. 5, a). If the value of the signal in_4 is

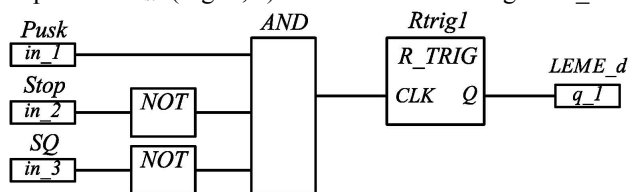


Fig. 3. Logic scheme for controlling the starting the electromagnetic sausage-filler.

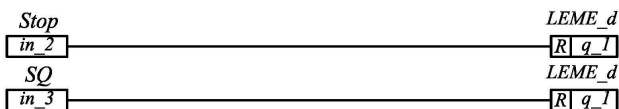


Fig. 4. Logic scheme for controlling the stopping the electromagnetic sausage-filler.

greater than U_{str} , the output of the GT block appears $TRUE$, the *Blinker1* (rectangular pulse generator) function block is started and the *ADD* block (addition) is activated at the specified frequency, increasing the current value of the local current output by ΔU_c .

When the analog signal is reduced from the strain gauge in_4 (d_str), the output from the GT block goes to the logical state $FALSE$ and, if this value falls below the specified U_{str} , the logical unit appears at the output of the LT comparator. The *Blinker2* function block (rectangular pulse generator) is started and the *SUB* (subtraction) unit is switched on at the set frequency, reducing the current value of the local current output by ΔU_c (Fig. 5, b) [8,9].

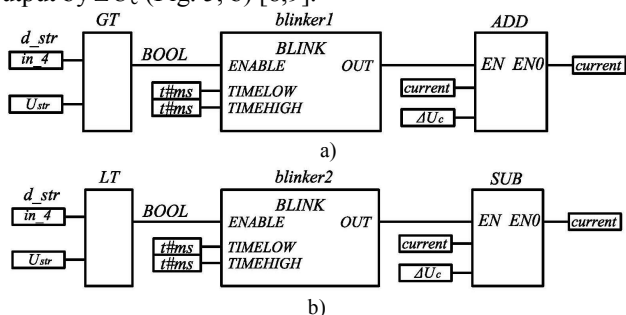


Fig. 5. Logic control circuits for smooth start and armature stroke of LEME

IV. CONCLUSION

Thus, by changing the *current* value to ΔU_c , it is possible to smoothly change the voltage at the analog output q_4 ($LEME_a$) and, as a consequence, at the input of the solid state-relay *SSR* and the *LEME* winding, the tractive effort is increased or decreased in accordance with the load (Fig. 6).

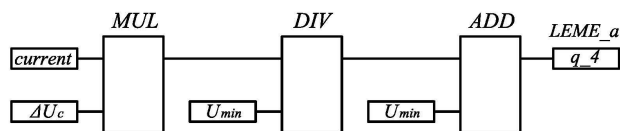


Fig. 6. Logical scheme for controlling the analog output of the PLC.

The logic diagram presented in Fig. 6 describes the following mathematical expression:

$$U_n = \frac{\text{current} \cdot \Delta U_n}{U_{\min}} + U_{\min},$$

where U_c – analog output voltage q_4 ($LEME_a$) PLC, ΔU_c – output voltage increment value; U_{\min} – minimum output voltage q_4 ($LEME_a$) PLC; *current* – current local output value.

The automatic control system is equipped with drive protection from emergency operation modes. In particular, to protect against overheating of the *LEME* winding and overpressure in the stuffing cylinder, feedback signals are used, respectively, from the temperature sensor *TS* and the *PS* pressure sensor. (Fig. 7) [10].

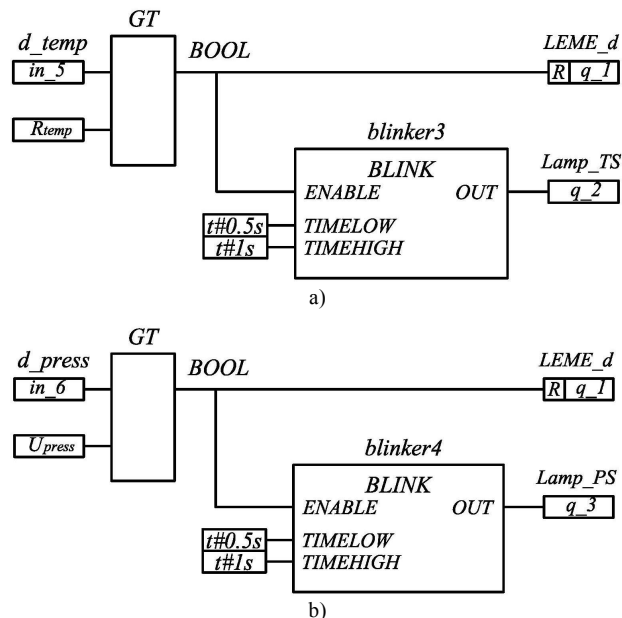


Fig. 7. Logical circuits for protecting the electromagnetic drive from overheating of the *LEME* winding (a) and overpressure in the sausage cylinder (b)

When the temperature of the *LEME* winding or the pressure in the sausage cylinder is exceeded, the signals, respectively, from the temperature sensor *TS* or *PS* pressure sensor (Fig. 7) are fed to the analog inputs of the controller in_5 (d_temp) and in_6 (d_press), and are compared in GT function blocks with given values (Fig. 7). If the values of signals in_5 and in_6 will exceed the values set by the operator, $TRUE$ appears on the output of the GT block, the engine (q_1 - $LEME_d$) is turned off, the *Blinker3* or *Blinker4* (rectangular pulse generator) function blocks are started and a light alarm is switched on q_2 - *Lamp_TS* or q_2 - *Lamp_PS*.

Adjustment of the speed of moving speed of working member is carried out by the operator during programming, by setting the proportionality coefficient k of the PLC controller's P-law (Fig. 8) [11]:

$$k = tg\alpha = \frac{U_{\text{out}} / U_{\text{out}}^{\max}}{U_{\text{in}} / U_{\text{in}}^{\max}},$$

where U_{out} , U_{in} – output and input voltage of the PLC; U_{out}^{\max} , U_{in}^{\max} – maximum values of the output and input voltage of the PLC, $tg\alpha$ – slope ratio of the static characteristic (Fig. 8).

Thus, a control system using a programmable logic controller and a strain gauge as a feedback element will make it possible to perform a smooth armature stroke of the *LEME*

with simultaneous automatic correction of the output traction force depending on the change in the load parameters.

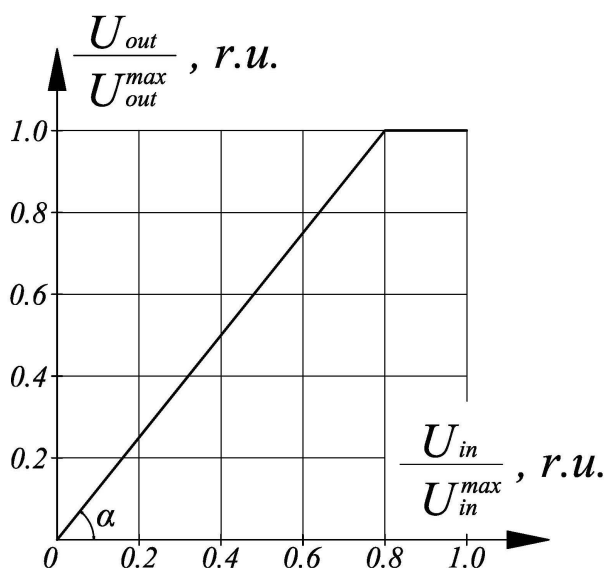


Fig. 8. Adjustment characteristic of moving speed of working member.

REFERENCES

- [1] Usanov K M, Kargin V A, Zubarev S M 2009 Classification and analysis of devices for forced filling with sausage shells. *Technology and products of healthy nutrition: in the collection of the III International Scientific and Practical Conference* 3 37-43 (in Russian).
- [2] Usanov K M, Volgin A V, Chetverikov E A, Kargin V A, Moiseev A P, Ivanova Z I 2017 Strike action electromagnetic machine for immersion of rod elements into ground *IOP Conf. Series: Earth and Environmental Science* 87 032050.
- [3] Usanov K M, Ugarov G G, Moshkin V I 2006 *Linear pulse electromagnetic drive of machines with autonomous power: monograph*. (Kurgan: Publishing house of Kurgan state University press) (in Russian).
- [4] Ugarov G G, Neiman V Y 2002 Trends in the development and use of handheld percussion machines with Electromechanical energy conversion *Russian Electromechanics* 2 37-43 (in Russian).
- [5] Usanov K M, Moshkin V I, Kargin V A, Volgin A V 2015 *The linear electromagnetic motors and actuators pulse processes and technologies: monograph*. (Kurgan: Publishing house of Kurgan state University press) (in Russian).
- [6] Kargin V A, Volgin A V, Moiseev A P, Logacheva O V 2018 Electrical converter with self-tuning of the output force of an electromagnetic molding of sausages. *Bulletin of the Altai State Agrarian University* 2 176-180 (in Russian).
- [7] Kargin V A, Moiseyev A P, Volgin A V, Belova N N 2014 Control system for the smooth running of the armature of the LEMD feed distributors by means of automatic adjustment of the output force. *Proceedings of the International Academy of Agrarian Education* 37 15-18 (in Russian).
- [8] Petrov And In 2004 Programmable Controllers. *Standard languages and techniques of applied design* (Moscow: SOLON-Press) (in Russian).
- [9] CoDeSyS 2.3 Programming User's Guide - Edition RU 2.4, for CoDeSyS v 2.3.6x.
- [10] Usanov K M, Zmeev A Y, Kargin V A, Moiseyev A P, Volgin A V 2014 *Technical means of automation: textbook* (Saratov: Saratov State SAU Publishing House) (in Russian).
- [11] Borodin I F, Andreev S A 2005 *Automation of technological processes and automatic control systems: a textbook* (Moscow: KolosS) (in Russian).



Kargin Vitaliy Aleksandrovich – candidate of tech. Sciences, assistant professor of the department of "Engineering physics, electrical machinery and electrotechnology". «Saratov State Agricultural University name N.I. Vavilov». Candidate's thesis on the topic "Improving the technology of immersing longitudinally unstable rod elements at APC facilities using a portable pulsed electromagnetic drive" was defended in 2007. The experience of scientific and pedagogical work is 15 years.



Volgin Andrei Valerievich – candidate of tech. Sciences, assistant professor of the department of "Engineering physics, electrical machinery and electrotechnology". «Saratov State Agricultural University name N.I. Vavilov». Candidate's thesis on the topic "Intensification of unloading bunker devices due to reduction of impulse electromagnetic systems" was defended in 2005. The experience of scientific and pedagogical work is 17 years.



Moseev Alexei Petrovich – candidate of tech. Sciences, assistant professor of the department of "Engineering physics, electrical machinery and electrotechnology". «Saratov State Agricultural University name N.I. Vavilov». Candidate's thesis on the topic "Application of linear electromagnetic drives in washers feed conveyor belts" was defended in 2011. The experience of scientific and pedagogical work is 17 years.

Cascade Synthesis of External Perturbations Observers Based on Virtual Models

Svetlana A. Krasnova^{1,2}

¹V.A. Trapeznikov Institute of Control Sciences of Russian Academy of Sciences, Moscow, Russia

²Bauman Moscow State Technical University, Moscow, Russia

Abstract – The formation of a combined control based on estimates of external uncontrolled influences is one of the methods for the synthesis of invariant systems. The method of expanding the state space due to the dynamic model simulating the action of external disturbances and the construction on its basis of a dynamic compensator or perturbation observer is the most developed in the theory of automatic control. However, in practice it is difficult to construct an adequate dynamic model of external perturbations. An alternative method for estimating external influences that does not require the extension of the state space is to use state observers with discontinuous corrective actions functioning in the sliding mode or their continuous analogues. Within the framework of this approach, in the paper, the original method for estimating the derivatives of external disturbances based on virtual dynamic models composed by sequential differentiation of a part of the derivative of state variables of the control plant, to which the estimated disturbances acting, is proposed. Note that real differentiation of signals is not performed. Virtual models are not introduced into the regulator, only dynamic observers of perturbations derivatives are present in the feedback loop. Observers are built as replicas of virtual models and in fact are differentiators. Procedure for cascade synthesis of observers of perturbations derivatives with piecewise linear correcting actions is developed. In this procedure, the method of separation of motions in virtual space of observation errors is realized. Not only the observer's variables, but also their corrective actions, serve as estimates of the derivatives of external perturbations.

Index Terms – Nonlinear systems, external perturbations, state observer, the method of separation of motions.

I. INTRODUCTION

THE PROBLEM of providing invariance to external perturbations is an actual task of automatic control. Different approaches to its solution within the framework of various methods are known under specific assumptions about the type of external perturbations and the channels of their action on the control plant.

One of the methods of ensuring invariance is the synthesis of combined control, which consists of two terms. Stabilizing feedback on the state vector is the first term. The second term is used to compensate for external matched disturbances belonging to the control space, and derivatives of external unmatched disturbances under the assumption of their smoothness. Within the framework of this approach, these or other dynamic models need to be introduced into the feedback loop to obtain current estimates of external disturbances and their derivatives. The method of synthesis

of invariant systems in the presence of a dynamic model, that simulates the effect of external disturbances, and the construction on its basis of a dynamic compensator or disturbances observer, is most developed in the theory of automatic control [1–6]. However, if the nature of external disturbances changes significantly in the control process, then an adequate dynamic model of external disturbances can not be made.

In the particular case where the parameters of the control plant are known and the state vector is fully measured, the current information on external influences can be obtained by directly assessing their effect on the control plant via state observer with discontinuous corrective actions, functioning in sliding mode [7–9], or its prelimit realization with continuous corrective actions [10–12]. Such observers can be used as differentiators. The idea is that with the help of S-shaped corrective actions the stabilization of observation errors and their derivatives with a given accuracy in a finite time is ensured, and corrective actions work out external limited disturbances and give their estimates in real time. In Section 3, A the basic method of synthesizing the state observer for nonlinear systems, affine by perturbations, is presented. Estimation of external disturbances is carried out with the help of piecewise-linear correcting actions.

The main result is presented in Section 3, B. In the framework of this approach, we propose an original method for estimating the derivatives of external perturbations on the basis of virtual dynamic models, compiled by successive differentiation derivatives of the state variables of the control plant to which the estimated disturbances acting. We note at once that real differentiation of signals is not carried out. We design state observers (differentiators) as replicas of these virtual models and implement the cascade principle. The method of separation of motions [3–4] in the space of observation errors is realized as a result of cascade synthesis of continuous corrective actions. Namely, in each i -th block of the state observer for the virtual model obtained after the i -th differentiation, the estimates of external disturbances and their derivatives up to $(i-1)$ -th order obtained in the previous blocks are used, and disturbances derivatives of i -th order are estimated by means of corrective actions. These signals, in turn, are used to generate corrective actions in the $(i+1)$ -th block of the state observer of the virtual model, and to estimate $(i+1)$ -th derivative of the external disturbance, etc.

Simulation results of the control system of inverted pendulum position under the action of an external unmatched disturbance are given to illustrate the developed algorithms (see Section 4).

II. PROBLEM DEFINITION

Let us consider non-linear control systems under the action of external, uncontrolled disturbances

$$\dot{x} = f(x, u) + Q(x)\eta, \quad (1)$$

where $x \in X \subset R^n$ is measured state vector, $u \in R^r$ is the control vector, $\eta(t) \in R^p$ is a vector of external disturbances, which are assumed by the unknown smooth functions of time, bounded together with their derivatives in the general case up to the n -th order, and

$$\text{rank} Q(x) = \text{rank} Q_1(x) = p < n \quad \forall x \in X, Q = \begin{pmatrix} Q_1 \\ Q_2 \end{pmatrix}. \quad (2)$$

In this paper we solve the problem of estimating the external disturbances $\eta(t)$ and their derivatives up to the $(n-1)$ -th order for current diagnostics and/or combined control design. We do not detail the control purpose and the control law, but we assume that the elements of the vector-function $f(x, u)$ and the matrix $Q_1(x)$ are smooth, satisfy the Lipschitz condition and limited in the control process:

$$\|Q_1(x(t))\eta(t)\|_\infty \leq F_0, \left\| \frac{d^i}{dt^i} Q_1(x)\eta(t) \right\|_\infty \leq F_{0i} \quad \forall t \geq 0, \quad (3)$$

where F_0, F_{0i} ($i = \overline{1, n}$) are known constants, their values are determined from the worst possible case when the purpose and law of control, as well as the features of the operation environment of the control plant are detailed. For simplicity of exposition, here and below, the norms of vectors appear in the constructions. Without loss of generality, the following results can be applied to obtain more accurate componentwise estimates.

In the next section, a cascade procedure for the synthesis of state observers with piecewise linear correcting effects is developed to solve the problem.

III. THEORY

A. A Basic Algorithm for Estimating External Perturbations

Let us show that the estimates of the external disturbances can be obtained without an extension of the state space using an autonomous dynamic model simulating external perturbations. Let us represent system (1)–(2) in the form of two subsystems via rows permutation as follows

$$\dot{x}_1 = f_1(x, u) + Q_1(x)\eta, \dot{x}_2 = f_2(x, u) + Q_2(x)\eta, \quad (4)$$

where

$$\dim x_1 = \text{rank} Q_1(x) = p \quad \forall x \in X, \dim x_2 = n - p.$$

Assuming the elements of the vectors $x(t)$ and $u(t)$ to be known functions of time, we construct a state observer on the basis of the first subsystem (4) in the form

$$\dot{z}_0 = f_1(x, u) + v_0, \quad (5)$$

where $z_0, v_0 \in R^p$ are the state vector and the vector of correcting actions of the observer. In view of (4)–(5) let us

write the system with respect to observation errors

$$\varepsilon_0 = x_1 - z_0 \in R^p \text{ as}$$

$$\dot{\varepsilon}_0 = Q_1(x)\eta - v_0. \quad (6)$$

The idea is that with the help of corrective actions $v_0(\varepsilon_0)$, where $\varepsilon_0(t)$ are measured signals, the stabilization of observation errors and their derivatives is ensured in system (6). Then, by virtue of the static equations, the correcting actions will work out external perturbations and serve as their estimate.

As is known, the static equations

$$\varepsilon_0(t) = \dot{\varepsilon}_0(t) = 0$$

are solved in finite time $t \geq t_0 > 0$ via observers with discontinuous corrective actions operating in a sliding mode [7–9]. However, the sliding modes observers can give a low quality (singularity) evaluated signals, if the computing resources are limited.

A new paradigm is the observer design with continuous, limited S-shaped corrective actions as smooth sigma-functions $\sigma(kx) = 2/(1 + e^{-kx}) - 1$ [10] or non-smooth saturation functions [11], which, on the one hand, provide a better quality of evaluation, but, on the other hand, a stabilization of observation errors and their derivatives with a given accuracy:

$$\|\varepsilon_0(t)\|_\infty \leq \delta_0,$$

$$\|\dot{\varepsilon}_0(t)\|_\infty \leq \delta_0 \Rightarrow v_0(t) \approx Q_1(x(t))\eta(t) \quad \forall t \geq t_0 > 0. \quad (7)$$

We use in the following constructions simple in tuning S-shaped, piecewise-linear corrective actions of the form

$$v_0 = M_0 \text{sat}(k_0 \varepsilon_0),$$

where

$$\text{sat}(k_0 \varepsilon_0) = \text{col}(\text{sat}(k_0 \varepsilon_{01}), \dots, \text{sat}(k_0 \varepsilon_{0p})),$$

$$M_0 \text{sat}(k \varepsilon_{0i}) = \begin{cases} M_0 \text{sign} \varepsilon_{0i}, & |\varepsilon_{0i}| > 1/k_0, \\ M_0 k_0 \varepsilon_{0i}, & |\varepsilon_{0i}| \leq 1/k_0, \end{cases} \quad (8)$$

which have two configurable parameters: $M_0 = \text{const} > 0$ is the amplitude of corrective actions, $k_0 = \text{const} > 0$ is high gain.

Obviously, if $1/k_0 < \|\varepsilon_0(0)\|_\infty < \infty$, then in closed system (6), (8) for a finite time $t_0 \geq 0$ observation errors fall into the region

$$\|\varepsilon_0(t)\|_\infty \leq 1/k_0$$

when the sufficient condition [7–12]

$$\begin{aligned} \varepsilon_0^T \dot{\varepsilon}_0 = \varepsilon_0^T (Q_1(x)\eta - M \text{sign} \varepsilon_0) &\leq \|\varepsilon_0\| (F_0 - M) < 0 \Rightarrow \\ &\Rightarrow M_0 > F_0 \end{aligned} \quad (9)$$

is satisfied, and if $\|\varepsilon_0(0)\|_\infty \leq 1/k_0$ (in particular $z_0(0) = x_1(0) \Rightarrow \varepsilon_0(0) = 0$), then the observation errors do not leave this region.

For $\forall t \geq t_0$ the dynamics of observation errors and their derivatives is described by the following differential

equations

$$\begin{aligned}\dot{\varepsilon}_0 &= Q_1(x)\eta - M_0 k_0 \varepsilon_0, \\ \ddot{\varepsilon}_0 &= \frac{d}{dt} Q_1(x)\eta(t) - M_0 k_0 \dot{\varepsilon}_0.\end{aligned}$$

In view of (3) and the given equations we find the lower bound for the choice of the high gain, so that both inequalities (7) are satisfied at the already chosen value of the amplitude $M_0^* > F_0$ (9):

$$\begin{aligned}\varepsilon_0^T \dot{\varepsilon}_0 &\leq \|\varepsilon_0\| (F_0 - M_0^* k_0 \|\varepsilon_0\|) < 0, \\ \dot{\varepsilon}_0^T \ddot{\varepsilon}_0 &\leq \|\dot{\varepsilon}_0\| (F_{01} - M_0^* k_0 \|\dot{\varepsilon}_0\|) < 0 \Rightarrow \\ \Rightarrow k_0^* &= k_0 > \frac{\max\{F_0, F_{01}\}}{M_0^* \delta_0}, \quad 0 < \delta_0 < 1/k_0^*.\end{aligned}\quad (10)$$

Thus, the current estimates of external disturbances will be obtained via correcting actions in finite time with a given accuracy:

$$\begin{aligned}\eta(t) &\approx \bar{\eta}(t) = Q_1^{-1}(x(t))v_0(t) \quad \forall t \geq t_0, \\ \|\eta(t) - \bar{\eta}(t)\|_\infty &\leq \|Q_1^{-1}(x(t))\|_\infty \delta_0 = \bar{\delta}_0.\end{aligned}\quad (11)$$

If condition (2) does not hold in system (1) and

$$\text{rank} Q(x) = \text{rank} Q_1(x) = p_0 < p,$$

then the problem of componentwise estimation of the perturbation vector has no solution. In this case, similarly via observer (5), where $z_0, v_0 \in R^{p_0}$, the problem of estimating linear combinations of external perturbations of the greatest possible rank is solved and

$$v_0(t) \approx Q_1(x(t))\eta(t).$$

Note, that for incomplete measurements of the state vector $x(t)$, it is possible to solve within the framework of this approach the problem of estimating and unmeasured state variables, and external perturbations, if they do not narrow the observed space [7–12].

Further, the obtained estimates (11) are used to synthesize the corrective actions of the state observers of virtual models with the purpose to evaluate the current values of the derivatives of external disturbances in the general case to the $n-1 \geq v$ -th order.

In the next section, it will be shown that in the basic algorithm, it is necessary to ensure stabilization with a given accuracy not only of the first, but also of the higher derivative of observation errors ε_0 up to $(v+1)$ -th order by appropriately selecting the high gain to ensure a given accuracy of estimating the derivatives of perturbations of the v -th order.

In view of (3) from sufficient conditions, similar to (10), we obtain the following estimates up to damped eigenfrequencies of higher derivatives:

$$\begin{aligned}\varepsilon_0^{(i)T} \varepsilon_0^{(i+1)} &\leq \|\varepsilon_0^{(i)}\| (F_{0i} - M_0^* k_0 \|\varepsilon_0^{(i)}\|) < 0 \quad (i = \overline{2, v+1}) \Rightarrow \\ \Rightarrow k_0^* &> \frac{\max\{F_0, F_{01}, \dots, F_{0, v+1}\}}{M_0^* \delta_0} \Rightarrow \\ \Rightarrow \|\varepsilon_0^{(i)}(t)\|_\infty &\leq \delta_0 \quad \forall i = \overline{0, v+1}, \quad \forall t \geq t_0.\end{aligned}\quad (12)$$

B. Estimation of Derivative Perturbations on the Basis of Virtual Dynamic Models

Suppose that for combined control, estimates of the derivatives of external disturbances in the general case up to the $n-1 \geq v$ -th order are required. We show that this problem can be solved on the basis of virtual dynamic models

To estimate the first derivatives of perturbations, we will compile a virtual dynamic model for the virtual output $y_1(t) = Q_1(x)\eta \approx v_0(t)$ (7) in the form

$$\dot{y}_1 = H(x, u, \eta)\eta + Q_1(x)\eta_1, \quad (13)$$

where

$$\dot{\eta} = \eta_1 \in R^p, \quad \eta_i = \eta_{i+1}, \quad H(x, u, \eta) = \frac{d}{dt} Q_1(x).$$

In system (13) under $t > t_0$ only the perturbation derivatives $\eta_1(t)$ are unknown. For their estimation, we construct an observer as a replica of the virtual system (13) in view of (11), namely:

$$\dot{z}_1 = H(x, u, \bar{\eta})\bar{\eta} + v_1. \quad (14)$$

On the basis of (13)–(14) we form a system with respect to observation errors $\varepsilon_1 = y_1 - z_1 \in R^p$ as

$$\dot{\varepsilon}_1 = \Delta H_1 + Q_1(x)\eta_1 - v_1, \quad v_1 = M_1 \text{sat}(k_1(v_0 - z_1)), \quad (15)$$

where elements of a vector function

$$\Delta H_1 = H(x, u, \eta)\eta - H(x, u, \bar{\eta})\bar{\eta}$$

according to a priori assumptions, satisfy the Lipschitz condition:

$$\|\Delta H_1\|_\infty \leq L_1 \bar{\delta}_0.$$

Under the conditions similar to (3), (9), (12), namely, if $\forall t \geq 0$ the following estimates

$$\|Q_1(x(t))\eta_1(t)\|_\infty \leq F_1, \quad (16)$$

$$\left\| \frac{d^i}{dt^i} (\Delta H_1(t) + Q_1(x)\eta_1(t)) \right\|_\infty \leq F_{1i}, \quad i = \overline{1, v}$$

are valid, then choosing the amplitude of corrective actions as

$$M_1^* > L_1 \bar{\delta}_0 + F_1 \quad (17)$$

the observation errors for finite time fall into the region

$$\|\varepsilon_1(t)\|_\infty \leq \delta_0 + 1/k_1,$$

where the shift by δ_0 conditioned by expressions (6), (7), (12):

$$v_0 = y_1 - \dot{\varepsilon}_0 \Rightarrow v_0 - z_1 = \varepsilon_1 - \dot{\varepsilon}_0. \quad (18)$$

Thus, corrective action (15) and its derivatives in the indicated region are representable in the form

$$v_1 = M_1 \text{sat}(k_1(\varepsilon_1 - \dot{\varepsilon}_0)),$$

$$v_1^{(i)} = M_1 k_1 (\varepsilon_1^{(i)} - \varepsilon_0^{(i+1)}), \quad i = \overline{0, v},$$

and the choice of the high gain in the form

$$k_1^* > \frac{\max\{L_1 \bar{\delta}_0 + F_1, F_{11}, \dots, F_{1v}\}}{M_1^* \delta_1}, \quad 0 < \delta_1 < 1/k_1^* \quad (19)$$

will provide the convergence of the observation errors of

system (15) and their derivatives in the region

$$\|\mathcal{E}_1^{(i)}(t)\|_\infty \leq \delta_0 + \delta_1 \quad \forall i = \overline{0, v}, \quad \forall t \geq t_1 > t_0,$$

$$\|Q_1(x)\eta_1 - v_1\| = \|\dot{\mathcal{E}}_1(t) - \Delta H_1\|_\infty \leq \delta_0 + \delta_1 + L_1\bar{\delta}_0 \Rightarrow v_1(t) \approx Q_1(x(t))\eta_1(t). \quad (20)$$

Thus, we have current estimates of the first derivatives of external perturbations with the help of corrective actions as

$$\eta_1(t) \approx \bar{\eta}_1(t) = Q_1^{-1}(x(t))v_1(t), \quad (21)$$

$$\|\eta_1(t) - \bar{\eta}_1(t)\|_\infty \leq \|Q_1^{-1}(x(t))\|_\infty (\delta_0 + \delta_1 + L_1\bar{\delta}_0) = \bar{\delta}_1.$$

Note 1. Within the framework of these constructions, in the current estimates of external perturbations (11) and their derivatives (21), the measured signals $v_0(x_1(t) - z_0(t))$, $v_1(v_0(t) - z_1(t))$ appear directly. This requires high-quality measurements $x(t)$ or their pre-filtering in the presence of noise in the measurement channels.

This drawback is inherent in any observers of reduced dimensionality. Such observers require high quality estimation and accurate knowledge of the parameters of the control plant [13–14]. These disadvantages can be partially circumvented by constructing an observer of full dimension, namely, use an observer's signal (14)

$$z_1(t) \approx Q_1(x(t))\eta(t) \quad \forall t \geq t_1, \\ \|z_1(t) - Q_1(x(t))\eta(t)\|_\infty \leq \delta_0 + \delta_1 \quad (22)$$

to estimate the linear combination of external perturbations (11). Estimation accuracy (22) will be worse than (11), where $\|v_0 - Q_1(x)\eta\|_\infty \leq \delta_0$, but better quality (smoothness) of the reconstructed signals can be expected due to the filtering properties of dynamic subsystem (14).

These constructions are successively repeated for the estimation of the higher derivatives of perturbations. So, for estimating the second derivatives, we compose a virtual dynamic model similarly based on the virtual output $y_2 = Q_1\eta_1$ in the form

$$\dot{y}_2 = H(x, u, \eta)\eta_1 + Q_1(x)\eta_2, \quad (23)$$

relevant observer

$$\dot{z}_2 = H(x, u, \bar{\eta})\bar{\eta}_1 + v_2 \quad (24)$$

and the system with respect to observation errors

$$\mathcal{E}_2 = y_2 - z_2 \in R^p \text{ as}$$

$$\dot{\mathcal{E}}_2 = \Delta H_2 + Q_1(x)\eta_2 - v_2, \quad (25)$$

where

$$\Delta H_2 = H(x, u, \eta)\eta_1 - H(x, u, \bar{\eta})\bar{\eta}_1, \\ \|\Delta H_2\|_\infty \leq L_{21}\bar{\delta}_0 + L_{22}\bar{\delta}_1.$$

Under conditions similar to (16)–(19), by means of piecewise linear correcting actions

$$v_2 = M_2 \text{sat}(k_2(v_1 - z_2)),$$

where $y_2 \approx v_1$ (20), the convergence of the state variables of system (25) and their derivatives for a finite time $\forall t \geq t_2 > t_1$ into the regions

$$\|\mathcal{E}_2^{(i)}(t)\|_\infty \leq \delta_0 + \delta_1 + \delta_2 \quad (0 < \delta_2 < 1/k_2^*) \quad \forall i = \overline{0, v-1},$$

$$\|Q_1(x)\eta_2 - v_2\| = \|\dot{\mathcal{E}}_2(t) - \Delta H_2\|_\infty \leq \delta_0 + \delta_1 + \delta_2 + L_{21}\bar{\delta}_0 + L_{22}\bar{\delta}_1 \Rightarrow v_2(t) \approx Q_1(x(t))\eta_2(t)$$

is ensured. Consequently, for $\forall t \geq t_2$ we have an alternative with respect to (20) for estimating the linear combinations of the first perturbation derivatives in the form

$$z_2(t) \approx y_2(t) = Q_1(x)\eta_1, \|z_2 - Q_1(x)\eta_1\|_\infty \leq \delta_0 + \delta_1 + \delta_2$$

(see Note 1), as well as the current estimates of the second derivatives of the perturbations

$$\eta_2(t) \approx \bar{\eta}_2(t) = Q_1^{-1}(x(t))v_2(t), \|\eta_2(t) - \bar{\eta}_2(t)\|_\infty \leq \quad (26)$$

$$\leq \|Q_1^{-1}(x(t))\|_\infty (\delta_0 + \delta_1 + \delta_2 + L_{21}\bar{\delta}_0 + L_{22}\bar{\delta}_1) = \bar{\delta}_2,$$

etc. The order of the virtual model depends on the need for estimates of the higher derivatives of disturbances for control purposes and current diagnostics.

Estimates (11), (21), (26) should be taken into account when assigning the accuracy of estimation

$$0 < \delta_i < 1/k_i^*, \quad i = \overline{0, v}$$

at each i -th step.

IV. EXPERIMENTAL RESULTS

To illustrate the approach, we consider the problem of controlling the angular position of an inverted pendulum under the action of an external unmatched disturbance. We use the following mathematical model of control plant taking into account the dynamics of the actuator

$$\dot{x}_1 = x_2, \\ \dot{x}_2 = a_{21} \sin x_1 - a_{22}x_2 + a_{23}(x_3 + \eta), \quad (27) \\ \dot{x}_3 = -a_{32}x_2 - a_{33}x_3 + b_3u,$$

where x_1 [rad] is the angular position of the pendulum (controlled variable), x_2 [rad/s] is the angular velocity, x_3 [N·m] is the torque applied to the pendulum on the suspension axis, which develops by an actuator with continuous control u ; $a_{21} = g/l$, $a_{22} = \kappa/l$, $a_{23} = 1/(ml^2)$, $g = 9.8$ [m/s²] is the acceleration of gravity; m [kg], l [m] is the mass and length of the pendulum, respectively; κ [N·s/m²] is coefficient of viscous friction; a_{32} , a_{33} , b_3 are positive transmission gains. All state variables are measured without noise.

In system (14) $\eta(t)$ is an unknown time function that characterizes the action of external, bounded perturbation with bounded derivatives

$$|\eta(t)| \leq F_0, |\dot{\eta}(t)| \leq F_1, |\ddot{\eta}(t)| \leq F_2 \quad t \geq 0.$$

The task is to synthesize a combined control providing tracking the output variable for a given, valid trajectory $g(t)$; $g(t)$, $\dot{g}(t)$, $\ddot{g}(t)$ are known limited time functions.

To solve this problem, we represent system (27) in the

canonical input-output form [9] with respect to tracking error $e_1 = x_1 - g$ and its derivative $e_2 = x_2 - \dot{g}$ as

$$\dot{e}_1 = e_2, \dot{e}_2 = e_3, \quad (28)$$

$$\dot{e}_3 = \psi(x, t) + bu, \quad b = a_{23}b_3,$$

where $e_3 = a_{21} \sin x_1 - a_{22}x_2 + a_{23}(x_3 + \eta) - \ddot{g}$,

$$\psi = a_{21}x_2 \cos x_1 - a_{22}(e_3 + \ddot{g}) - a_{23}(a_{32}x_2 + a_{33}x_3 - \dot{\eta}) - \ddot{g},$$

and design a basic law of combined control as

$$u = -(\psi(x, t) + l_1 e_1 + l_2 e_2 + l_3 e_3) / b, \quad (29)$$

where $l_i = \text{const} > 0$ are coefficients of the Hurwitz polynomial. Closed system (28)–(29)

$$\dot{e}_1 = e_2, \dot{e}_2 = e_3, \dot{e}_3 = -l_1 e_1 - l_2 e_2 - l_3 e_3$$

is stable, and the asymptotic convergence to zero of the tracking error

$$\lim_{t \rightarrow +\infty} e_1(t) = 0$$

is ensured.

It is necessary to obtain signal estimates $\eta(t), \dot{\eta}(t)$ for the implementation of control law (29).

First, for estimating an external disturbance $\eta(t)$ we construct a state observer as a replica of the second equation of system (27) in the form

$$\dot{z}_0 = a_{21} \sin x_1 - a_{22}x_2 + a_{23}x_3 + v_0 \quad (30)$$

and write the system with respect to the observation error $\varepsilon_0 = x_2 - z_0$ as

$$\dot{\varepsilon}_0 = a_{23}\eta - v_0.$$

The choice of the parameters of the piecewise linear corrective action $v_0 = M_0 \text{sat}(k_0 \varepsilon_0)$ in a form similar to (9), (12), namely,

$$M_0^* > a_{23}F_0, \quad k_0^* > \frac{\max\{F_0, F_1, F_2\}}{M_0^* \delta_0}, \quad 0 < \delta_0 < 1/k_0^*,$$

will ensure the stabilization of the observation error and its derivative (7) and allow us to obtain an estimate of the external disturbance for a finite time in the following form:

$$|a_{23}\eta(t) - v_0(t)| = |\dot{\varepsilon}_0(t)| \leq \delta_0 \quad \forall t \geq t_0. \quad (31)$$

Secondly, we use a virtual output $y_1 = a_{23}\dot{\eta}$ to compile a virtual model

$$\dot{y}_1 = a_{23}\dot{\eta},$$

and on its basis construct a state observer

$$\dot{z}_1 = v_1, \quad v_1 = M_1 \text{sat}(k_1(v_0 - z_1)), \quad y_1 \approx v_0 \quad (32)$$

and write the system with respect to the observation error $\varepsilon_1 = y_1 - z_1$ as

$$\dot{\varepsilon}_1 = a_{23}\dot{\eta} - v_1.$$

The choice of the parameters of the piecewise linear corrective action in a form similar to (17), (19), namely

$$M_1^* > a_{23}F_1, \quad k_1^* > \frac{a_{23} \max\{F_1, F_2\}}{M_1^* \delta_1}, \quad 0 < \delta_1 < 1/k_1^*,$$

will allow us to obtain the derivative estimate for a finite time in the following form

$$|a_{23}\dot{\eta}(t) - v_1(t)| = |\dot{\varepsilon}_1(t)| \leq \delta_0 + \delta_1 \quad \forall t \geq t_1 > t_0. \quad (33)$$

Variables $e_3(t), \psi(t)$ in the law of combined control (29) are formed with the help of estimates (31), (33) as

$$\begin{aligned} e_3(t) &= a_{21} \sin x_1(t) - a_{22}x_2(t) + a_{23}x_3(t) + v_0(t) - \ddot{g}(t), \\ \psi(t) &= a_{21} \cos x_1(t) \cdot x_2(t) - a_{22}(e_3(t) + \ddot{g}(t)) - \\ &\quad - a_{23}(a_{32}x_2(t) + a_{33}x_3(t)) + v_1(t) - \ddot{g}(t). \end{aligned} \quad (34)$$

Simulation of closed system (27), (29), (30), (32), (34) was performed by Matlab–Simulink with the following parameters:

$$a_{32} = 2, \quad a_{33} = 10, \quad b_3 = 10, \quad m = 1, \quad l = 1, \quad \kappa = 8,$$

$$x_i(0) = 1, \quad z_0(0) = x_2(0) \Rightarrow \varepsilon_0(0) = 0,$$

$$g = \sin(0.5t), \quad \eta(t) = 0.5 \sin 2t, \quad l_1 = 125, \quad l_2 = 75,$$

$$l_3 = 15, \quad M_0^* = 2, \quad M_1^* = 2, \quad k_0^* = 100, \quad k_1^* = 50.$$

The simulation results confirm the effectiveness of the developed approach. In Fig. 1–2 the plots of the external perturbation $a_{23}\eta(t)$, its derivative $a_{23}\dot{\eta}(t)$ and estimation errors $a_{23}\eta(t) - v_0(t)$, $a_{23}\dot{\eta}(t) - v_1(t)$ are shown.

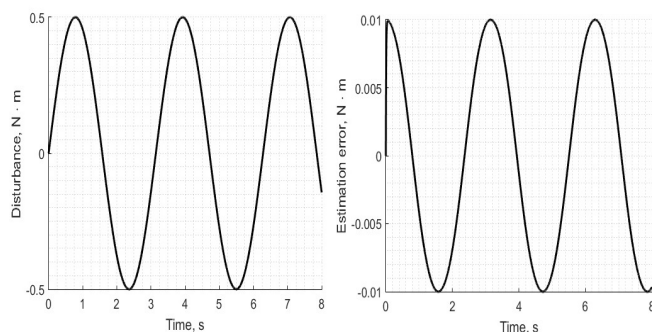


Fig. 1. Plots of external perturbation $a_{23}\eta(t)$ and estimation error

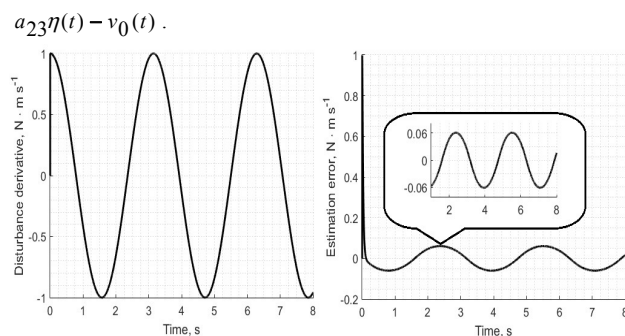


Fig. 2. Plots of perturbation derivative $a_{23}\dot{\eta}(t)$ and estimation error

$$a_{23}\dot{\eta}(t) - v_1(t).$$

As can be seen from the figures, inequalities

$$|a_{23}\eta(t) - v_0(t)| \leq 0.01 \quad \forall t \geq 0, \quad (35)$$

$$|a_{23}\dot{\eta}(t) - v_1(t)| \leq 0.06 \quad \forall t \geq 0.1[s]$$

are satisfied.

In Fig. 3 the plots of the angular position $x_1(t)$ of the pendulum, the given trajectory $g(t)$ and tracking error $e_1(t) = x_1(t) - g(t)$ are shown. A stabilization of the

tracking error $|e_1(t)| \leq 0.01$ [rad] is achieved less than 2 [s]. Stability error caused by observation errors (35).

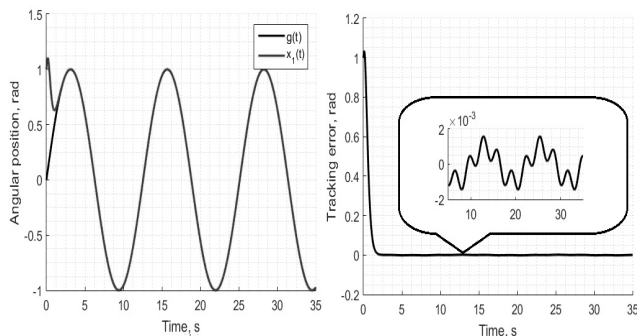


Fig. 3. Plots of angular position of the pendulum $x_1(t)$, given trajectory $g(t)$ and tracking error $e_1(t)$.

Note 2. In the framework of this approach, we could use a different version of the information providing basic control law (29). It is possible to directly obtain estimates of the variables $e_3(t)$, $\psi(t)$ with the help of an observer with piecewise linear corrective actions, constructed on the basis of the second and third equations of system (28), namely:

$$\begin{aligned} \dot{z}_2 &= z_3 + v_2, \quad v_2 = M_2 \text{sat}(k_2(e_2 - z_2)), \\ \dot{z}_3 &= bu + v_3, \quad v_3 = M_3 \text{sat}(k_3(v_2 - z_3)). \end{aligned} \quad (36)$$

With an appropriate choice of parameters of corrective actions, stabilization with a specified accuracy of observation errors $\varepsilon_2 = e_2 - z_2$, $\varepsilon_3 = e_3 - z_3$ and their derivatives

$$\dot{\varepsilon}_2 = \varepsilon_3 - v_2, \quad \dot{\varepsilon}_3 = \psi(x, t) - v_3,$$

is provided. This allows us to obtain, at a finite time, sequentially estimates

$$e_3(t) \approx z_3(t), \quad e_2(t) \approx v_2(t), \quad \psi(t) \approx v_3(t)$$

and realize the control law (29) in the form

$$u = -(v_3 + l_1 e_1 + l_2 e_2 + l_3 z_3) / b.$$

In this case, the structure of the regulator is simplified, but there are certain difficulties in obtaining estimates of change of variables $\varepsilon_3(t)$, $\psi(t)$, $\dot{\psi}(t)$, necessary for setting the parameters of the observer (36).

V. CONCLUSION

In the proposed approach to estimation external perturbations and their derivatives of the ν -th order, the observer of the type (5), and ν observers of the type (14), (24) are required. These observers, in fact, are differentiators, i.e. they evaluate the current values of the right-hand sides of the corresponding differential equations, if they are smooth and bounded. Once again, we note that in these constructions, real differentiation of signals is not carried out.

The synthesis procedure is decomposed into independently solvable one-dimensional subtasks in each block of dimension p . The parameters of bounded everywhere piecewise linear corrective actions are chosen on the basis of inequalities. This approach does not require the expansion of

the state space and the compilation of real dynamic models of external perturbations. Virtual dynamic models like (13), (23) are used only as a basis for constructing state observers and are not introduced into the feedback loop. To implement the developed approach, the worst estimates for the ranges of changes in the components of the control plant, external disturbances and their derivatives are sufficient. They can be obtained from objective considerations.

ACKNOWLEDGMENT

This work is financially supported in part by the Russian Foundation for Basic Research, project no. 18-01-00846A.

REFERENCES

- [1] Wonham W.M. Linear Multivariable control: a geometric approach. – New York: Springer-Verlar, 1979. – 356 p.
- [2] Nikiforov V.O. Adaptive nonlinear tracking with complete compensation of unknown disturbances // European J. of Control. 1998. V. 4. No. 2. pp. 132–139.
- [3] Yurkevich V.D. Output regulation of pulse-width-modulated nonlinear nonaffine-in-control systems via singular perturbation // IFAC Proc. Volumes. January, 2011. V. 44. No. 1. pp. 1374–1379.
- [4] Utkin V.A., Utkin V.I. Design of invariant-system by the method of separation of motions // Automation and Remote Control, 1983. V. 44. No. 12. pp. 1559–1668.
- [5] Darouach M., Boutat-Baddas L., Zerrougui M. H0-observer design for a class of Nonlinear singular systems // Automatica, 2011. V. 47. No. 11. pp. 2517–2525.
- [6] Malikov A.I. State Estimation and Stabilization of Continuous Systems with Uncertain Nonlinearities and Disturbances // Automation and Remote Control, 2016. V. 77. No. 5. pp. 764–778.
- [7] Krasnova S.A. Cascade design of the state observer for nonlinear systems in the presence of external perturbation // Automation and Remote Control, 2003. V. 64. No. 1. pp. 1–22.
- [8] Krasnova S.A., Kuznetsov S.I. Incontrollable perturbations on nonlinear dynamic systems: estimation on moving modes // Automation and Remote Control, 2005. V. 66. No. 10. pp. 1580–1593.
- [9] Krasnova S.A., Utkin A.V. Analysis and synthesis of minimum phase nonlinear SISO systems under external unmatched perturbations // Automation and Remote Control, 2016. V. 77. No. 9. pp. 1665–1675.
- [10] Krasnova S.A., Mysik N.S. Cascade synthesis of a state observer with nonlinear correction influences // Automation and Remote Control, 2014. V. 75. No. 2. pp. 263–280.
- [11] Krasnova S.A., Utkin A.V. Sigma function in observer design for states and perturbations // Automation and Remote Control, 2016. V. 77. No. 9. pp. 1676–1688.
- [12] Krasnova S.A., Utkin V.A., Utkin A.V. Block Approach to Analysis and Design of the Invariant Nonlinear Tracking Systems // Automation and Remote Control, 2017. V. 78. No. 12. pp. 2120–2140.
- [13] Luenberger D.B. Observers of multivariable systems // IEEE Transactions on Automatic Control, 1966. V. AC-11. pp. 190–197.
- [14] Delshad S.S., Johansson A., Darouach M., Gustafsson T. Robust state estimation and unknown inputs Reconstruction for a class of nonlinear systems: multiobjective approach // Automatica, 2016. V. 64. pp. 1–7.



Krasnova Svetlana Anatolyevna, Doctor of Technical Sciences, Chief Researcher, V.A. Trapeznikov Institute of Control Sciences RAS; Professor, Bauman Moscow State Technical University. Research interests: sliding modes; the theory of state observers; electromechanical systems, block approach to the analysis and synthesis for control systems of various purposes under incomplete information. Author over 200 scientific and methodical works.

A Powerful Single-Mode Diode Laser with Automated Control as the Source of Pumping of the Ytterbium Laser

Sergey A. Kuznetsov¹, Victor S. Pivtsov^{1,2}, Anastasia V. Semenko^{1,2}

¹Institute of Laser Physics SB RAS, Novosibirsk, Russia

²Novosibirsk State Technical University, Novosibirsk, Russia

Abstract – A powerful single-mode distributed bragg reflector tapered diode laser with a low-noise automatic power supply has been developed. The output characteristics of the tapered diode laser are investigated. Using such laser as a pumping source, the free running mode of a Yb:KYW laser is obtained and investigated. It is shown that a compact precision femtosecond frequency synthesizer based on a Yb:KYW laser pumped by a diode laser of the similar type can be created.

Index Terms - Distributed bragg reflector tapered diode laser.

I. INTRODUCTION

NUMEROUS publications are devoted to studies of femtosecond ytterbium crystalline lasers pumped by diode lasers. Multimode diode pumping has been mostly used (see, for example, [1] – [2]). Femtosecond mode, as a rule, was achieved with the help of SESAM (Semiconductor saturable absorber mirror). Lasers with pulse repetition rates of < 100 MHz have been investigated. The average output power of such lasers is from 100 mW to several W. Publications of the results of studies of femtosecond ytterbium crystalline lasers pumped by low-power single-mode diode lasers with open and fiber output are also available [3] - [7]. The power of such diode lasers in a continuous mode is <1 W. The average output power of femtosecond ytterbium lasers with such pumping is from several tens of mW to hundreds of mW. A stable regime emerges both with and without the use of a SESAM. Compact femtosecond lasers have high pulse repetition rate (> 100 MHz). Lasers with such pulse repetition rates have a beam waist diameter of generating radiation of several tens of microns. Pumping can be focused to a spot with such a diameter only from single-mode lasers, whose radiation has diffraction divergence. Therefore, efficient femtosecond lasers with a repetition rate of > 100 MHz have been developed only with such pumping. With the use for pumping of a powerful single-mode diode laser (Distributed Bragg Reflector Tapered Diode Laser, DBR TDL, power up to 12 W), a femtosecond mode of a crystalline ytterbium laser with an average output power of up to 2.2 W and a pulse repetition rate of 1 GHz was obtained [8, 9]. A stable and self-starting mode was obtained using a SESAM. Such powerful compact ytterbium lasers hold much promise for the development of femtosecond optical frequency synthesizers and precision systems on their basis, which are

presently very important. In these publications, a femtosecond mode was obtained, and energy, time and spectral characteristics were presented. However, optimal schemes of femtosecond ytterbium lasers for their use in synthesizers have not been considered or studied. Also, the pumping system and the electronic part of the power supply and control have not been described. The present article is devoted to solving the above problems.

II. PROBLEM DEFINITION

A multimode pumping radiation beam cannot be fully matched in the active element with a generation beam of a compact laser having a waist of several tens of microns. This limits the laser efficiency. In addition, the transverse distribution of such radiation is not smooth. This nonsmoothness varies with time and pumping power. The stability of the mode-locking regime depends on the degree of nonsmoothness up to the inability of obtaining a stable regime. For a laser of typical size the waist is 100 and more microns. In this case pumping and generation beams can be matched, the effect of nonsmoothness is smaller, and it is realistic to obtain a stable regime. Therefore, for a stable mode-locking regime in a compact laser pumping by a single-mode laser source of sufficient power is necessary. As such a source, single-mode diode lasers of the DBR TDL type (manufactured by Ferdinand-Braun-Institute, Berlin, Germany) with a radiation wavelength of 981 nm (the center of the Yb:KYW crystal absorption line) and a maximum output power of 6 W were used. For this it was necessary to develop a low-noise power supply, optimize the characteristics of radiation of the DBR TDL laser and the ytterbium laser cavity, and study the resulting characteristics of the free running mode of this laser.

III. EXPERIMENTAL RESULTS AND THEIR DISCUSSION

From the literature and our experience of work with femtosecond lasers we know that for a stable mode-locking regime and reliable stabilization of the spectral components of radiation the pumping radiation noise must not exceed 1E-4 of the total power. The DBR TDL laser consists of three sections: a passive distributed Bragg reflector (DBR), a ridge waveguide (RW), and a tapered amplifier section (TA) with a

cone angle of 6° in a single chip. The current of the RW and TA sections was controlled individually. The cathode of the sections is common. For stability of the DBR TDL spectral characteristics, the chip temperature must be maintained with an accuracy of 0.1°C . Commercial power supply with a set of metrological and functional characteristics necessary for the application is absent. The use of separate sources for each of the chip parts complicates the operation, makes the computer control more difficult, and considerably increases the cost of optical pumping. For this reason, a power supply and thermostabilization source for the DBR TDL has been developed (Fig. 1).



Fig. 1. Exterior view of the DBR TDL laser with power supply.

The power supply and thermostabilization source is used to power the DBR TDL and stabilize its temperature. In the development, current drivers for the laser diodes with the necessary metrological characteristics are used. In addition to the drivers, the source has two independent channels: one for the circuits of the thermal stabilizer and the optical amplifier driver and the other for the diode laser, a distributed microprocessor control system consisting of two microcontrollers, an analog thermostabilization controller, UART digital interfaces with galvanic isolation, and a UART-USB interface converter.

The built-in software of the microcontroller of the laser diode and optical amplifier channels provides (upon receipt of the corresponding command from the personal computer) the system switching on/off, the formation of linearly increasing or decreasing signals at the input of the current control with programmable signal variation rates, setting of starting and operating current of the diode and optical amplifier, thermostabilization switching on/off, and setting and monitoring of the object temperature. In case of an emergency (detection of a breakage, short circuit, out of tolerance temperature), the microcontroller immediately turns off the current driver and puts the circuit in a safe state. The operational parameters of the optical amplifier, laser diode, and thermal stabilizer channels can be stored in the

nonvolatile memory of the microcontroller and used in further work.

In addition to the modes of independent control of the thermal stabilizer and optical amplifier mostly employed at the stage of the source adjustment, an automatic operation mode for use of the source on the setup is provided.

In this case, upon receiving the corresponding command from the computer or pressing the start button, the following set sequence of actions is performed: switch-on of the thermal stabilizer, switch-on of the diode laser when a set temperature is reached, and switch-on of the optical amplifier when the diode laser channel is ready. When a shutdown command is received or when the shutdown button is pressed, the reverse sequence of actions is performed.

In the automatic operation mode, analysis of emergency situations is supplemented by analysis of the state of the laser diode channel and detection of the absence of communication with the microcontroller of the laser diode channel. Also, when an emergency situation is detected in the optical amplifier channel, an emergency shutdown command is sent to the laser diode channel.

Characteristics of the power supply for the DBR TDL:

Laser diode channel:

- Output current 0 ... 200 mA.
- Starting output current 0 ... 200 mA.
- Resolution of the output current setting of $5\ \mu\text{A}$.
- Integral rms current noise value in the frequency range 0.1 Hz ... 0.5 MHz – $2\ \mu\text{A}$.

- Temperature instability – no more than $1\text{E-}4/^\circ\text{C}$.

Optical amplifier channel:

- Output current 0 ... 10 A.
- Starting output current 0 ... 10 A.
- Resolution of the output current setting of 2.5 mA.
- Temperature instability – no more than $2\text{E-}4/^\circ\text{C}$.

Thermostabilization channel:

- The reference temperature is $+10^\circ\text{C}$... $+40^\circ\text{C}$.
- Absolute temperature setting error: 2°C .
- Temperature maintenance instability, reproducibility: not worse than 0.1°C .
- The maximum output voltage: 4.5 V.
- The maximum output current in the heating mode: 1 A.
- The maximum output current in cooling mode: 3 A.



Fig. 2. Graphic interface of the diode laser control program

A top-level program was written to manage the controller. The program is executed in the Windows 10 operating system. To visualize data and manage the controller, a graphic interface of the program has been developed. Its principal view is shown in Fig. 2. The main task is graphic representation of the current averaged characteristics: the laser current, the optical amplifier current, and the chip temperature. An extended form of the graphic interface of the program is available, which provides the most complete functional of the program. The program has been debugged and tested. The total code is about two thousand lines. The executable file size is 3 Mb.

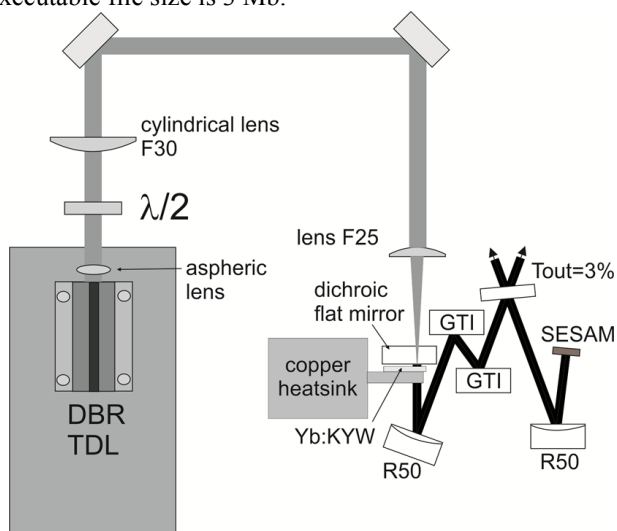


Fig. 3. The experimental setup.

Fig. 3 shows a general scheme of the femtosecond ytterbium laser. Since the cross-section of the laser output radiation was $\sim 400 \times 100 \mu\text{m}$, that is, there was significant astigmatism, the

radiation was collimated separately along the both axes: the fast axis, by an aspherical lens with a focal length of 3.1 mm, and the slow axis, by the same aspherical and cylindrical lens with a focal length of 30 mm. Since the astigmatism of the DBR TDL laser can vary slightly from sample to sample and depends on the current, a cylindrical lens was placed on the linear translator to adjust its position as the current varies. Since the cross-section of the laser output radiation is elliptical in shape, it will have the same shape in the focal plane. In this case, it will not be possible to fully match the pumping and radiation beams, which will decrease the laser efficiency. Since DBR TDL lasers have quasi-diffraction divergence ($M^2 = 1.1 \dots 1.2$) with significant astigmatism, optimization of the correcting and focusing system is required for each sample. A half-wave plate was used to rotate the polarization. Direct measurement of the noise characteristics of the DBR TDL laser radiation with the power source developed by the authors has shown that the amplitude of fluctuations of the laser output power does not exceed 0.1 % (the noise level of the photodetector).

According to the certificate, the DBR TDL laser operates at a wavelength of 980.4 nm at a temperature of 25°C. At a radiation power of 5 W, the central lobe of the transverse distribution must have $\sim 76\%$ of the power ($M^2 = 1.1$), and the spectrum width at half-height must be $< 20 \text{ pm}$.

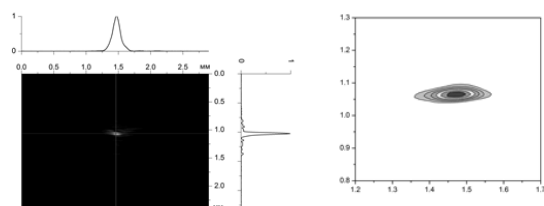


Fig. 4. The cross-section of the intensity distribution of the DBR TDL laser.

Using a CCD camera, a snapshot of the transverse profile of the DBR TDL laser intensity distribution was obtained (Fig. 4). The intensity distribution transverse profile was recorded after the cylindrical lens. Since it is difficult to exactly adjust the focal length of the cylindrical lens to compensate for astigmatism, the intensity distribution transverse profile in the focal plane of an aspherical lens will have the shape of an elongated ellipse. This form is not efficient for pumping. A minimum waist size in the crystal was achieved by changing the distance between the lenses. All results were obtained under these conditions. One can see in Fig. 4 that the transverse distribution is smooth, without appreciable ruggedness, and close in shape to Gaussian distribution. This is very important, because the stability of the mode-locking regime at non-smoothness becomes much worse. It should be noted that the maximum possible efficiency of pumping of a compact femtosecond laser (intermode frequency: $> 1 \text{ GHz}$) can only be obtained with precise compensation of astigmatism and transformation of the elliptical beam shape into a circular

one.

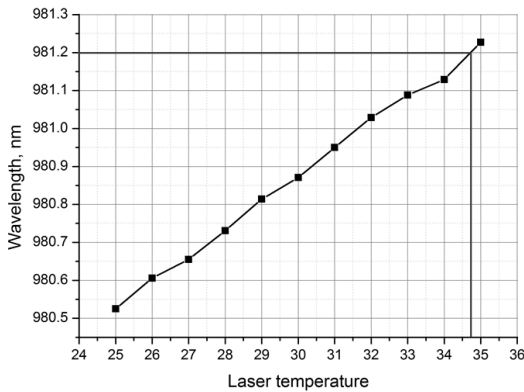


Fig. 5. Wavelength of the DBR TDL laser versus temperature (maximum current $I_{TA}=10A$).

The ytterbium laser was optimized in the free running mode. Therefore, the dispersion mirrors (GTI) and the nonlinear semiconductor mirror (SESAM) (Fig. 3) were replaced by dense dielectric mirrors. As an active element we used Yb: KYW 1 and 1.5 mm thick crystals with an activator concentration of 10 wt. % cut along the C axis. Since the maximum of the Yb: KYW crystal absorption line is at a wavelength of 981.2 nm, the DBR TDL laser was tuned to this wavelength by increasing the temperature of the diode.

Fig. 5 shows the laser wavelength versus temperature for the maximum current $I_{TA} = 10 A$. The tuning was about 0.06 nm per 1°C. Fig. 6 presents the wavelength tuning versus the amplifier current. The tuning was about 0.018 nm per ampere. Thus, a temperature of 34.6°C was taken as the operating one. The housing was designed with a power reserve and, therefore, the laser operated without water cooling.

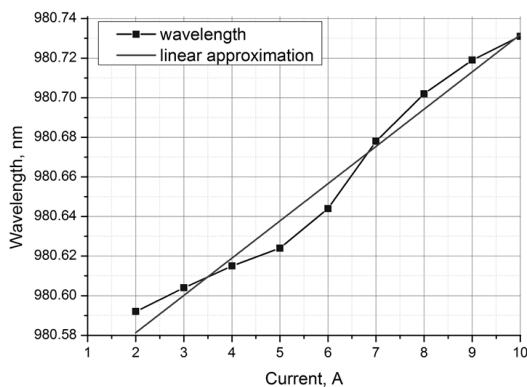


Fig. 6. The DBR TDL laser wavelength versus the amplifier current I_{TA} (diode temperature: 28°C).

Fig. 7 shows the DBR TDL laser power incident on the crystal versus the amplifier current. The Yb:KYW laser power in the free running mode versus the crystal thickness and the use of output mirrors with a transmission of 1%, 2%, 3%, and 4% was studied.

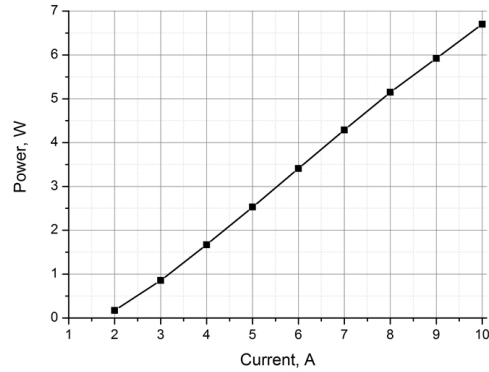


Fig. 7. The DBR TDL laser power incident on the crystal versus the amplifier current.

The best results were obtained with a 1.5 mm crystal. From Figs. 8 and 9 we see that the optimal transmittance of the output mirror was 3 %, and the effective and total optical efficiency was 64.9 % and 61 %, respectively. Only one paper [8] presents the efficiency of a laser with pumping of up to 5 W: the effective and total optical efficiency is 28 % and 20 %, respectively, which is much less than our results. The peculiarities of using a DBR TDL laser for pumping or optimizing the parameters of the cavity of a compact ytterbium laser have not been studied. As the crystal thickness increases from 1 mm to 1.5 mm, the total optical efficiency increases insignificantly. However, in this case the cavity dispersion increases, which is undesirable. Thus, a thickness of about 1 mm is optimal for a Yb:KYW crystal with an activator concentration of 10 wt. %.

It should be noted that all experimental results were obtained without cooling the Yb:KYW crystals, that is, at room temperature. At a maximum pumping laser power of 6 W, there was a slight increase in the temperature of the copper cooler, while the output power remained stable for some hours. The use of a Peltier element and a water cooling system to decrease the crystal temperature to 15°C increased

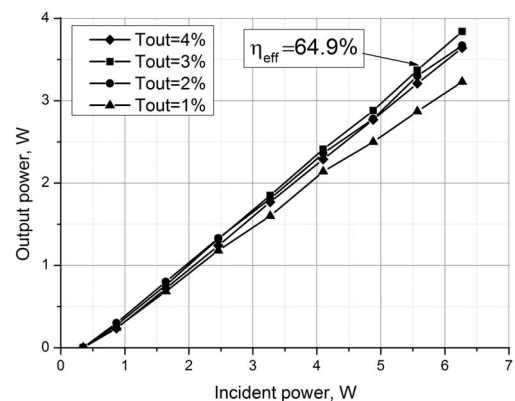


Fig. 8. The laser generation power versus the incident power for a 1.5 mm Yb: KYW crystal and various transmittance of the output mirror.

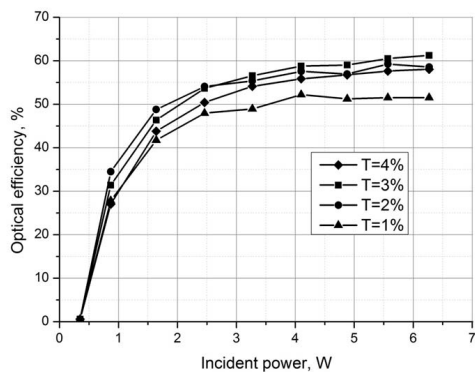


Fig. 9. The total optical efficiency of the laser versus the incident power for a 1.5 mm Yb: KYW crystal and various transmittance of the output mirror.

the power level by 1.5 % at the maximum power of the pumping laser.

IV. CONCLUSION

A powerful single-mode diode laser of the DBR TDL type with a low-noise automatic power supply has been developed. The output characteristics of the laser have been investigated and optimized. It has been shown that they hold much promise as sources of pumping of compact femtosecond ytterbium lasers. The free running mode of a Yb:KYW laser pumped by a DBR TDL radiation was investigated. Record efficiency for compact lasers with pumping by DBR TDL laser radiation has been obtained. Conditions for obtaining limiting efficiency and a scheme of formation of pumping radiation have been determined. The use of a SESAM mirror to start the mode-locking regime of the Yb:KYW laser will make it possible to create a fully automated compact precision femtosecond frequency synthesizer, which was problematic with multimode pumping [10, 11].

This work was supported by the Russian Foundation for Basic Research (project no. 16-02-00639-a); the equipment of the "Femtosecond Laser Complex" was used.

REFERENCES

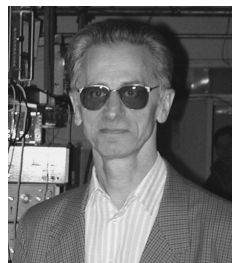
- [1] Paunescu G., Hein J., Sauerbrey R. Appl. Phys. B, 2004, 79, 555.
- [2] Liu J., Wang W. W., Liu C.C., et al. Laser Phys. Lett., 2010, V. 7, p. 104.
- [3] Lagatsky A. A., Brown C. T. A., Sibbert W. OPTICS EXPRESS, 2004, V. 12, No. 17, p. 3928.
- [4] Lagatsky A. A., Sarmani A. R., Brown C. T. A., et al. Opt. Lett., 2005, V.30, p.3234.
- [5] Wasylczyk P., Wnuk P. and Radzewicz C. OPTICS EXPRESS, 2009, V. 17, No. 7, p. 5630.
- [6] Schratwieser Th., Leburn Ch. and Reid D. Opt. Lett., 2012, V.37, p.1133.
- [7] Endo M., Ozawa A. and Kobayashi Y. OPTICS EXPRESS, 2012, V. 20, No. 11, p. 12191.
- [8] Pekarek S., Fiebig C., Stumpf M., et al. OPTICS EXPRESS, 2010, V. 18, No. 16, p. 16320.
- [9] Pekarek S., Sudmeyer Th., Lecomte S., et al. OPTICS EXPRESS, 2011, V. 19, No. 17, p. 16491.

[10] Kuznetsov S.A., Pivtsov V.S. A highly efficient, compact Yb:KYW laser for mobile precision systems // Quantum Electronics 2014, V. 44 No. 5, pp. 444–447.

[11] Kuznetsov S.A., Pivtsov V.S., Semenko A.V. and Bagayev S.N. Highly efficient multimode diode-pumped Yb:KYW laser // Journal of Physics: Conference Series. 2017, V.793 (1), 012016.



Sergey A. Kuznetsov received a B.Sc. degree in physics from Novosibirsk State Technical University in 1995 and a M.Sc. degree in physics from Novosibirsk State Technical University in 1997. He is a researcher of the Institute of Laser Physics SB RAS, Novosibirsk, Russia. His research interests are femtosecond lasers, optical standards, and spectroscopy.



Victor S. Pivtsov graduated from Novosibirsk State University in 1969, received a PhD degree in physics in 1981. He is currently a laboratory head and a Senior Researcher of the Institute of Laser Physics SB RAS, Novosibirsk, Russia. His research interests are nonlinear optics, lasers, spectroscopy, and experimental physics.



Anastasia V. Semenko received a B.Sc. degree in physics from Novosibirsk State Technical University in 2017. She is currently a master student of the Faculty of Physics and Technology of Novosibirsk State Technical University.

Experimental Installation for the Investigation of the Influence of the Methods of Feeding on the Relative Humidity of Capillary-Porous Materials with the Built-in Software

Ludmila V. Larina, Dmitry V. Rusljakov, Olga B. Tikhonova
Don State Technical University, Rostov-on-Don, Russia

Abstract - The article deals with the peculiarities of management of the processes of hydrothermal treatment (humidification, drying, wet-heat treatment) of capillary-porous materials, including crops under conditions of low pressure (vacuum). In traditional technologies, only one of the above-mentioned processes is provided in specialized installations, during which the temperature or pressure [1,2] are controlled separately, if the process takes place in a sealed chamber, and these parameters are controlled, first of all, based on the requirements of safe operation of the installations. In the considered experimental setup it is possible to perform in parallel-sequential processes of humidification, drying, wet-heat treatment under reduced pressure (vacuum) [3, 4]. In this set-up with integrated program management monitored and regulated not the individual parameters - temperature and pressure, and their interrelation, which characterize the condition of the working environment of steam under reduced pressure. The temperature sensors T and pressure P are connected to the computer, where their readings are compared with the program [5], which reflects the dependence $P=f(T)$ for the state of the working environment of each process [6]. In the event of misalignment parameters (pressure and temperature) that characterize the condition of the working medium in the chamber, a signal is supplied to the solenoid valve control, which, actuating, ensures the flow of portions of water in the steam generator, located at the bottom of the working chamber, before the onset of harmonization between the indicators of T and P. When drying, the temperature rise is ahead of the pressure increase and the water portion is not required, so the temperature level of the resulting dry steam is maintained.

Index Terms – Vacuum-thermal treatment, experimental installation, microcontroller, capillary-porous material, software.

I. INTRODUCTION

WITH THE use of preliminary evacuation of the internal microcavities of the grain through its porous membrane, to reduce the time spent on moistening the grain before grinding it, one should take into account the moisture transfer through the capillaries (microcavities) of the grain envelope in the gaseous phase, (in the form of steam) as a more efficient [1,2]. Such moisture transfer can be realized on an experimental setup for studying the kinetics of vacuum-hydrothermal treatment with different methods of feeding steam to the test samples.

II. PROBLEM DEFINITION

The experimental installation is a chamber with a volume of 0.09 m³ with a hermetically sealed cover, connected via a control slide, a moisture filter with a vacuum pump (type 2NVR-5DM, a capacity of 5 l / s, a pressure range at the inlet from atmospheric to 0.02 MPa, 0.55 kW). To equalize the pressure with the atmospheric chamber is equipped with an air inlet valve. To maintain the temperature of the working medium inside the chamber, a tubular electric heater (TET) with a power of 1 kW is installed in it. The voltage applied to the heater was regulated by the power supply circuit of the stand. The supply of moisture to the samples in the chamber during the study of moistening processes was carried out in two ways:

- connection of the evacuated chamber through the inlet valve with a separate reservoir - the steam generator, in which there was water, heated in different experiments to different temperatures (Fig. 1);
- evaporation of the heated water from the open surface of the container with water installed in the chamber (Fig. 2).

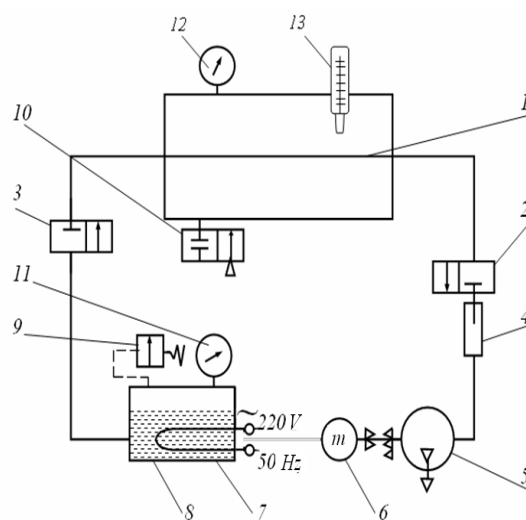


Fig.1. Schematic diagram of an installation for vacuum-hydrothermal treatment with a steam generator outside the chamber: 1 - humidifying vacuum chamber; 2 - shut-off gate valve; 3 - the valve for the admission of steam; 4 - trap for trapping condensate; 5 - the vacuum pump; 6 - the electric motor; 7 - electric heater; 8 - steam generator; 9 - safety valve; 10 - the valve for an admission of air; 11 - manometer; 12 - a vacuum gauge; 13 - thermometer.

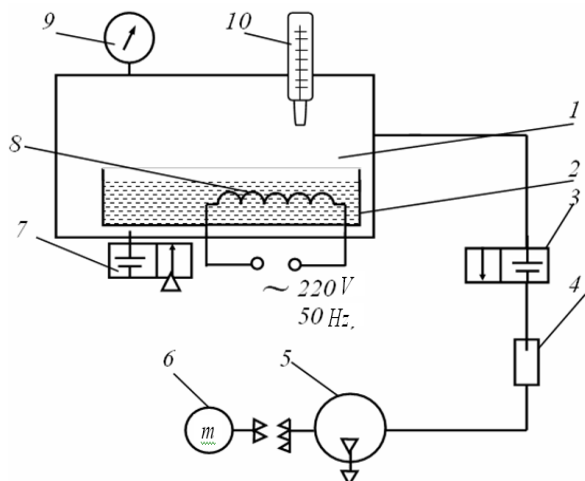


Fig. 2. Schematic diagram of the installation for vacuum-hydrothermal treatment with a steam generator inside the chamber: 1 - humidifying vacuum chamber; 2 - a bath with water; 3 - shut-off gate valve; 4 - trap for trapping condensate; 5 - the vacuum pump; 6 - the electric motor; 7 - the valve for an admission of air; 8 - electric heater; 9 - a vacuum gauge; 10 - thermometer.

To measure the pressure inside the working chamber, an electronic pressure sensor with an analog output type 26PCAFA6D from Honeywell (USA) was used [3-5, 6]. The basis of the piezoresistive sensor with the analog output of this series is a strain-sensitive element. These are four identical piezoresistors implanted in the grooves that are etched onto the surface of the silicon membrane and connected by a bridge circuit. External pressure causes deformation of the membrane, which leads to imbalance of the bridge. The value of the created disagreement voltage UBOD. (useful signal) is directly proportional to the applied pressure.

To measure the temperature of the working medium inside the lower chamber, a DS1820 temperature sensor from DALLAS (USA) was used [7, 8]. The digital 12-bit semiconductor sensor contains a temperature sensor and an analog-to-digital converter on a semiconductor crystal. The sensor does not need calibration and a converter and can be not only a temperature sensor but also a thermostat, which can be realized in the internal settings of the sensor when programming and installing it.

A personal computer was used as recording equipment.

A block diagram of the hardware of the experimental installation for vacuum hydrothermal processing using the above-described sensors is shown in Fig. 3.

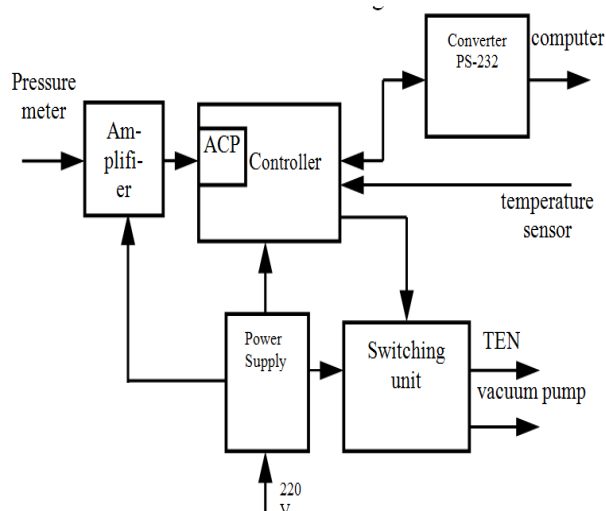


Fig. 3. Block diagram of the hardware of the experimental setup.

The main computing device of the unit is the microcontroller of the AVR family. The operation of the unit was carried out as follows: the amplifier increased the differential signal from the pressure sensor, after which it entered the ADC and the controller, where it was digitized with 12-bit accuracy twice per second. The digital data from the temperature sensor directly entered the controller (sensor accuracy 0.5°C) twice per second. Based on the received data, the controller generates a control law for the TEN and vacuum pump in two modes: automatic and manual.

Automatic mode provides the values of the parameters within the specified limits, and in manual mode the operator switches on and off the heater and the vacuum pump.

To collect and display experimental data, the device was connected to a PC through a special RS-232 level converter.

To control the operation of the plant, a program was developed [9] "Information-control shell of an experimental installation for hydrothermal treatment of hides". The program is designed to generate control actions (depending on the selected operating mode) in accordance with the table specified by the user of two pressure and temperature parameters for the pilot plant control system for hydrothermal treatment of the leather.

In automatic or manual control mode, when humidifying, it is necessary to observe the ratio of temperature and pressure according to the equation (Fig. 4) [10].

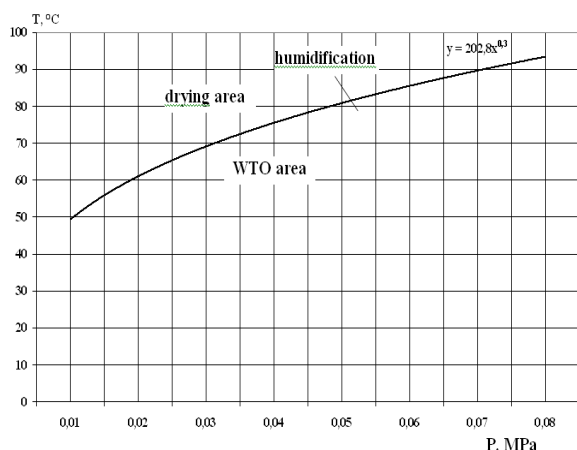


Fig. 4. The graph of the temperature dependence of water vapor in a state of saturation from pressure [10].

III. CONCLUSIONS

To effectively control the processes of vacuum-hydrothermal treatment of capillary-porous materials[7], which include the shells of a number of grain crops[8], the assignment of scientifically based optimal technological regimes to achieve the required processing quality, it is necessary to use the built-in software described above.

The results of the calculation of the theoretical weight gain of moisture are given in Table I, taking into account the fact that the share of moisture in capillaries accounts for 12% of the total grain volume[9].

TABLE I
VALUES OF THEORETICAL MOISTURE GAIN IN
MICROCAPILLARIES DEPENDING ON THE PARAMETERS AND
TIME OF VACUUM-SORPTION HUMIDIFICATION

| Main settings vacuum-sorption humidification | Humidification time, s | | | |
|---|------------------------|--------------------|--------------------|--------------------|
| | 120 | 240 | 360 | 480 |
| Mean value of pressure, Pa | $25 \cdot 10^3$ | $30 \cdot 10^3$ | $40 \cdot 10^3$ | $50 \cdot 10^3$ |
| Average temperature, °C | 55 | 57 | 58 | 59 |
| Average value of vapor density, kg / m ³ | $16 \cdot 10^{-2}$ | $19 \cdot 10^{-2}$ | $26 \cdot 10^{-2}$ | $36 \cdot 10^{-2}$ |
| Average rate of thermal motion molecules, m / s | $6,23 \cdot 10^2$ | $6,24 \cdot 10^2$ | $6,24 \cdot 10^2$ | $6,26 \cdot 10^2$ |

| | | | | |
|---|-----------------------|-----------------------|-----------------------|-----------------------|
| Average mean free path molecules, m | $0,4 \cdot 10^{-6}$ | $0,37 \cdot 10^{-6}$ | $0,28 \cdot 10^{-6}$ | $0,22 \cdot 10^{-6}$ |
| Diffusion coefficient, m ² / s | $0,83 \cdot 10^{-4}$ | $0,76 \cdot 10^{-4}$ | $0,58 \cdot 10^{-4}$ | $0,45 \cdot 10^{-4}$ |
| Moisture volume of microcapillary, m ³ | $3,51 \cdot 10^{-14}$ | $5,25 \cdot 10^{-14}$ | $5,84 \cdot 10^{-14}$ | $6,09 \cdot 10^{-14}$ |
| Theoretical moisture gain of microcapillaries, % | 6,9 | 10,3 | 11,5 | 12,0 |

As can be seen from the above data, with the increase in moisture time, the intensity of steam condensation due to capillary-sorption phenomena falls. The above-described experimental setup with a built-in programmer is used by the authors in the implementation of the method of hydrothermal treatment grain oats, including hydration of the grain, differing is the fact that the process of moistening the grain to produce wet saturated steam produced inside the chamber by heating the water in the lower part of the chamber to a temperature of 60-80°C at a residual pressure of 0.03-0.05 MPa and ends when the residual pressure of 0.06-0.08 MPa, this eliminates the presence of surface moisture due to condensation of steam inside the capillaries and the need for re-vacuuming to remove it[10].

REFERENCES

- [1] M. G. Korniliev, V. N. Kovalnogov and A. N. Zolotov, "Modeling and analysis of the efficiency of the conventional drying of capillary-porous bodies with ultrasound," 2016 2nd International Conference on Industrial Engineering, Applications and Manufacturing (ICIEAM), Chelyabinsk, 2016, pp. 1-4. DOI: 10.1109/ICIEAM.2016.7911655
- [2] Y. Sokolovsky, I. Kroshnyy and V. Yarkun, "Mathematical modeling of visco-elastic-plastic deformation in capillary-porous materials in the dressing process," 2015 Xth International Scientific and Technical Conference "Computer Sciences and Information Technologies" (CSIT), Lviv, 2015, pp. 52-56. DOI: 10.1109/STC-CSIT.2015.7325429
- [3] Larina, L., Ruslyakov, D., Tihonova, O., Morozov, S. (2017). Development of the control algorithm of processes of intensive hydrothermal impact on capillary and porous materials in the conditions of the vacuum - materials Web of Conferences Volume 132 (2017) XIII International Scientific-Technical Conference "Dynamic of Technical Systems" (DTS-2017), Rostov-on-Don, Russian Federation, September 13-15, 2017.
- [4] Larina, L., Ruslyakov, D., Tihonova, O. (2017). Investigation of the influence of the microcapillary structure of natural skins on relative humidity in vacuum-sorption humidification. - MATEC Web of Conferences Volume 132 (2017) XIII International Scientific-Technical Conference "Dynamic of Technical Systems" (DTS-2017), Rostov-on-Don, Russian Federation, September 13-15, 2017.
- [5] Certificate of state registration of computer program No. 2010617180 "Information control shell of the experimental setup for hydrothermal treatment of skin" / Tarara I. V., Larina L. V., Smimov V. V. / application No. 2010614416, publ., 20 July 2010 was Declared. 27.10.2010, the applicant and the patent holder of the South Grew. state University of Economics and service.
- [6] Chaiyo, K., Rattanadecho, P., 2013: Numerical analysis of heat-mass transport and pressure building of unsaturated porous medium in a rectangular waveguide subject to a combined microwave and vacuum system. Int. J. Heat Mass Tran. 65: 826-844.

- [7] Larina, L., Ruslyakov, D., Tihonova, O. (2017). Innovative ways of development of heat power equipment for agricultural production (scientific article) Pecs Innovative technologies in science and education (ITNO-2017): materials of the V International Scientific and Practical Conference (Divnomorskoe village, September 11-15, 2017) / rare. D.V. Ruda [and others]; The Don state. tech. un-t. - Rostov-on-Don: DSTU-Print, 2017. - 597 p.
- [8] Larina, L., Ruslyakov, D., Tihonova, O. (2016). Justification of the system approach to the design of heat power equipment (scientific article) Pecs Scientific Spring-2017: I Vseros. (with the participation of citizens of foreign states-in) scientific. Conf. students, graduate students and young scientists. Engineering: Materials (Shakhty, May 20, 2017): scientific. electron. ed. / rare: S. G. Stradanchenko [and others]; ИСОиП (branch) ДДТУ in Shakhty. - Mines: ISOiP (branch) of DSTU, 2016. - 1 electron. opt. disk (CD-ROM). - Ver. from the disc label. - Electron. Dan. (9.71 MB). - ISBN 978-5-906786-11-1
- [9] Larina, L., Ruslyakov, D., Tihonova, O. (2017). Modeling of heat exchange processes in capillary-porous materials (scientific article) Pecs Scientific Spring-2017: I Vseros. (with the participation of citizens of foreign states-in) scientific. Conf. students, graduate students and young scientists. Engineering: Materials (Shakhty, May 20, 2017): scientific. electron. ed. / rare: S. G. Stradanchenko [and others]; ИСОиП (branch) ДДТУ in Shakhty. - Mines: ISOiP (branch) of DSTU, 2016. - 1 electron. opt. disk (CD-ROM). - Ver. from the disc label. - Electron. Dan. (9.71 MB). - ISBN 978-5-906786-11-1
- [10] Larina, L., Ruslyakov, D., Tihonova, O. (2017). The choice of the rational design of the device for the intensified heat treatment of capillary-porous materials (scientific article) Pecs Scientific Spring-2017: I Vseros. (with the participation of citizens of foreign states-in) scientific. Conf. students, graduate students and young scientists. Engineering: Materials (Shakhty, May 20, 2017): scientific. electron. ed. / rare: S. G. Stradanchenko [and others]; ИСОиП (branch) ДДТУ in Shakhty. - Mines: ISOiP (branch) of DSTU, 2016. - 1 electron. opt. disk (CD-ROM). - Ver. with these-disc mice. - Electron. Dan. (9.71 MB). - ISBN 978-5-906786-11-1



Ludmila V. Larina,
born in Shakhty of Rostov Region, on the
25th of May, 1954.
She is Candidate of Technical Sciences, assistant
professor (docent). Her research interests are control
and monitoring in technical systems, heat and
mass transfer.



Dmitriy V. Ruslyakov,
born in Shakhty of Rostov Region, on the
21st of May, 1986.
He is Candidate of Technical Sciences, assistant
professor (docent). His research interests are control
and monitoring in technical systems, heat and
mass transfer.
E-mail: ruslyakof@yandex.ru



Olga B. Tikhonova,
born in Shakhty of Rostov Region, on the
16th of June, 1969.
She is Candidate of Technical Sciences, assistant
professor (docent). Her research interests are control
and monitoring in technical systems, heat and
mass transfer.

Intelligent Control System for Process Parameters Based on a Neural Network

Elena A. Muravyova, Marsel I. Sharipov

Ufa State Petroleum Technological University, Branch in Sterlitamak, Russia

Abstract – A neural network for control systems of raw material dosing in dry cement production process with the use of a closed cycle has been developed. The artificial neural network is intended to control motor speed of belt-conveyor weighers and the separator of the cement milling unit intended for the production of three-component cement of various grades. The developed neural network is designed to solve the problem with an appreciable error in the output quantity of cement in comparison with the set capacity; in addition, there is a task of increasing the control system performance and increasing its fault tolerance. The control system uses a two-layer unidirectional network with a sigmoidal function of activating the neurons of the hidden layer and a linear function of activating the neurons of the output layer. The network was trained on 50 examples within 120 epochs. The neural network is developed in the Matlab environment using the Matlab Neural Network Toolbox application. The process control is carried out by SCADA-system through OPC-server intended to provide communication between the neural network and a controlled object.

Index Terms – Artificial neural network, ANN, controlling the motor speeds, the cement grinding unit, separator.

I. INTRODUCTION

THE ARTICLE considers a cement grinding unit intended for production of a three-component cement of various grades.

To ensure stable operation of the grinding unit with high and constant capacity its optimal load is necessary. This primarily means that it is necessary to avoid high fluctuations in the dust-and-gas stream.

For this purpose the grinding unit is equipped with an automated process control system keeping the amount of raw materials and grits loaded into the mill at the most constant level.

The cement mill has three batch weighers (one for each type of raw materials).

In the process lines of cement grinding the basket stab air separators are installed. The cage rotating separator is designed for separation of fine-grained material into thin and coarse fractions, i.e. a separation of the material into ready cement and grits, which is returned to the mill, takes place in the separator.

II. PROBLEM DEFINITION

This technological process has a significant drawback - a large error in the amount of cement at the outlet relative to the given capacity, i.e. the readings of the ready product flow sensor do not correspond to the set quantity. This is due to

the fact that there are minor production losses such as shrinkage, weathering and losses during feeding the material from one production process to another, and so on.

This problem is proposed to be solved by increasing or decreasing the mass amount of the initial components by controlling the belt weighers speed and the separator speed using an artificial neural network (ANN). For this purpose, it is necessary to create an ANN which in accordance with the set values calculates the required current frequency for the motors of the belt weighers and the separator.

The use of an artificial neural network to solve the existing problems is based on the fact that ANN has a number of important advantages, namely [1]:

- Adaptation to changes – the neural networks can adapt to a changing environment;
- Fault tolerance - they can produce correct results even with significant damage to their components;
- Ultra-high speed performance.

III. DEVELOPMENT OF THE NEURAL NETWORK

The ANN was developed in the Matlab 9.0.0.341360 (R2016a) environment. When solving the problem the Matlab Neural Network Toolbox was used. The Neural Network Toolbox is a complete MATLAB environment for handling the applied problems using neural networks.

The process of building the neural network model can be formally divided into 5 main stages (Fig. 1) [2].

IV. DATA ACQUISITION

To solve a problem using a neural network it is necessary to collect data for training. The training data set is a set of observations for which the values of input and output variables are specified.

To create a training set for our neural network we will use the following formulas:

- induction motor rotation speed

$$n = \frac{60 \cdot v}{\pi \cdot D}, \quad (1)$$

where D - diameter of drive drum;

v - rotation speed.

- Equipment performance

$$Q = v \cdot P, \quad (2)$$

where P - material weight.

- Current frequency

$$f = \frac{p \cdot n}{60}, \quad (3)$$

where p - number of pairs of poles (in our case equal to 2);
n - rotation frequency.

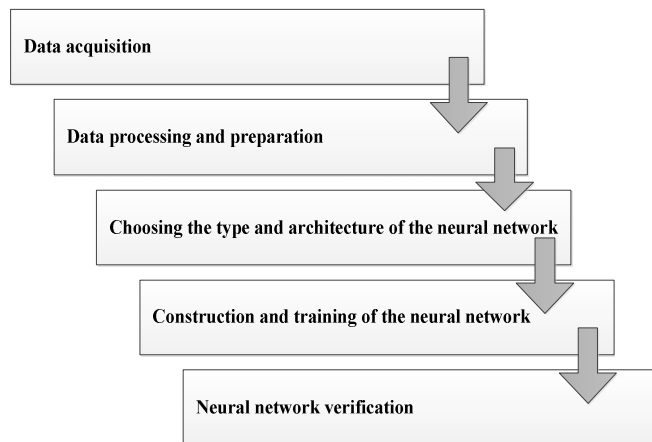


Fig. 1. Stages of building the neural network model.

Combining the above formulas we obtain a formula by which we calculate the current frequency necessary to control the belt weighers speed and the separator speed for cement grinding. As a result of combination, the following formula was obtained

$$f = \frac{2 \cdot Q}{P \cdot \pi \cdot D}, \quad (4)$$

Next, we prepare data for training the neural network.

V. DATA PROCESSING AND PREPARATION

Using the above formula we create a table with data training set. It will consist of 50 examples (Tab. I).

10 values will be given to the neural network input:

- 1) Specified capacity of the cement grinding unit (t) - Qset;
- 2) True capacity of the cement grinding unit (t) - Qtrue;
- 3) Percentage of clinker mass to total capacity (%) - x1;
- 4) Percentage of clay mass to total capacity (%) - x2;
- 5) Percentage of slag mass to total capacity (%) - x3;
- 6) Percentage of mass of grains from the separator to total capacity (%) - x4;
- 7) Clinker weight on the weigher - p1;
- 8) Gypsum weight on the weigher - p2;
- 9) Slag weight on the weigher - p3;
- 10) Grits weight in the separator - p4.

At the output, the neural network should calculate 4 values of current frequency:

- 1) f1 - current frequency for clinker weigher motor (Hz);
- 2) f2 - current frequency for gypsum weigher motor (Hz);
- 3) f4 - current frequency for clinker weigher motor (Hz);
- 4) f5 - current frequency for separator motor (Hz).

VI. CHOOSING THE TYPE AND ARCHITECTURE OF THE NEURAL NETWORK

The choice of the neural network structure affects the features of the output functions of the ANN; The ANN structure

determines the location and the number of interneuronal connections and accordingly the number of link weights which must be adjusted after the training. There is no unambiguous procedure for selecting the number of hidden layers and neurons thereof, and the question of how successful one or another choice is often solved based on experimental results of ANN training and testing [7].

Our network will consist of 2 layers - hidden layer and output layer.

The first step is to select the neural network structure. A two-layer unidirectional network with a sigmoidal function of hidden layer neurons activation and a linear function of output layer neurons activation will be used (created by the fitnet function). Such network allows arbitrarily closely to solve the problems of multidimensional approximation under condition of data consistency and sufficient number of neurons in the hidden layer (net = fitnet(hiddenLayerSize, trainFcn)) [4].

Next, we must select the number of neurons in the hidden layer. Choosing the right amount is a very important step. Too small amount - and the network will not be able to train. Too big amount will result in increase in network training time to a practically unreal value. There is no easy way to determine the required number of elements in the hidden network layer. In our case, the required number of neurons in the hidden layer equal to 16 was experimentally established (hiddenLayerSize = 16). This experiment was carried out as follows: first, the number of neurons in the hidden layer was chosen equal to 10 proceeding from the fact that the number of neurons in the hidden layer cannot be less than the amount of input data; further, the number of neurons increased by 1, until training error became minimal.

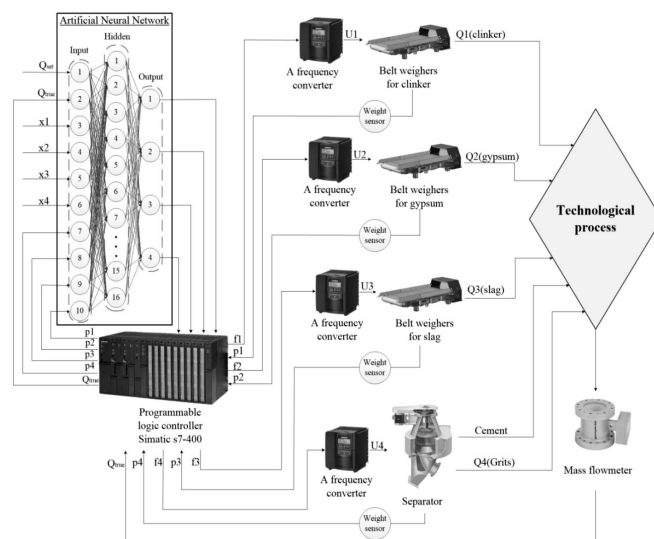


Fig. 2. ANN structural workflow.

The network was trained according to the modified back propagation of error algorithm:

trainFcn = 'trainbr'.

TABLE I
DATA TRAINING SET[illegible]

TrainBR is a network training function which modifies weight values and displacements in accordance with the Levenberg-Marquardt optimization algorithm. In this case, a combination of error squares and weights is minimized, and then a corrected combination is determined which provides an improvement in network's generalizing capacity.

We then select the network training parameters [3].

We set the maximum number of training epochs which determines the number of epochs (time interval) after which the training will be terminated:

```
net.trainParam.epochs = 1000.
```

Let's choose the number of epochs between the shows equal to five:

```
net.trainParam.show = 5.
```

We set the training termination criterion - the value of a deviation by which the training will be considered as completed:

```
net.trainParam.goal = 0.0001.
```

Next, we divide the data into a training set (Training), a test set which is used to evaluate the network's generalizing capacity (Validation) and to stop learning when generalization ceases improving and the test set does not affect the training but serves to check data which was not used in network training (Testing):

```
net.divideParam.trainRatio = 60/100;
```

```
net.divideParam.valRatio = 35/100;
```

```
net.divideParam.testRatio = 5/100.
```

VII. CONSTRUCTION AND TRAINING OF THE NEURAL NETWORK IN MATLAB

Next, we implement and train the neural network in Matlab. For this purpose we open the data editor by clicking the "Import data" button and we load the data for training the neural network. The input data of the neural network is called "input", and the output data is "output" [5].

Next, in the command line, we need to enter the obtained neural network program code to control the speed of belt weighers motors and separator motor of the cement grinding unit.

```
% input - input data.
% output - target data.
x = input';
t = output';
trainFcn = 'trainbr';
% Создание нейронной сети
% Количество нейронов в скрытом слое
hiddenLayerSize = 16;
net = fitnet(hiddenLayerSize,trainFcn);
net.SampleTime=0.01;
% Максимальное количество эпох тренировки
net.trainParam.epochs = 1000;
% Количество эпох между графиками
net.trainParam.show = 5;
% Условие остановки по отклонению от эталона
net.trainParam.goal = 0.0001;
% Setup Division of Data for Training, Validation, Testing
net.divideParam.trainRatio = 60/100;
net.divideParam.valRatio = 35/100;
net.divideParam.testRatio = 5/100;
% Обучение нейросети
[net,tr] = train(net,x,t);
% View the Network
view(net)
```

Fig. 3. ANN program code in Matlab.

After clicking the Enter button the neural network begins the training.

Figure 4 of the neural network structure is showing that 10 values are given to the ANN input and the number of output values is 4. Also, the figure 4 shows the network consisting of two layers - hidden consisting of 16 neurons and the output layer.

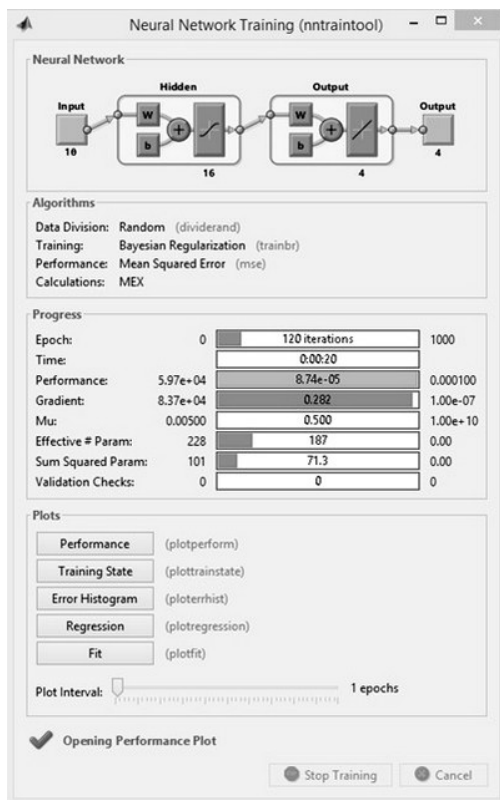


Fig. 4. Neural network training.

In the network training box (Fig. 4), when clicking the Performance button you can see the network training schedule showing the behavior of the learning error (Fig. 5).

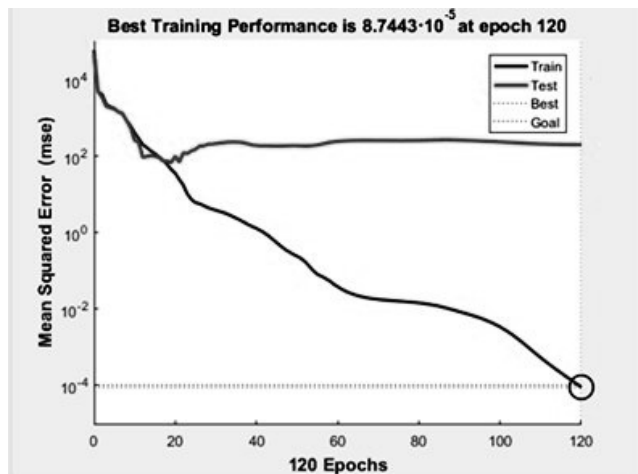


Fig. 5. Mean square error.

The graph in figure 5 shows that over 120 epochs the mean square error of $8.7443 \cdot 10^{-5}$ has been achieved. The training function uses early stopping against retraining. MSE is a network performance function. It shows the performance in accordance with the mean square error.

Figure 6 shows the training state graphs - Training State. The graph "val fail" shows the error change on the control set. The gradient graph shows a gradient change in learning error functional by the network weights. The mu graph reflects the change in the training parameter μ of the Levenberg-Marquardt method [6].

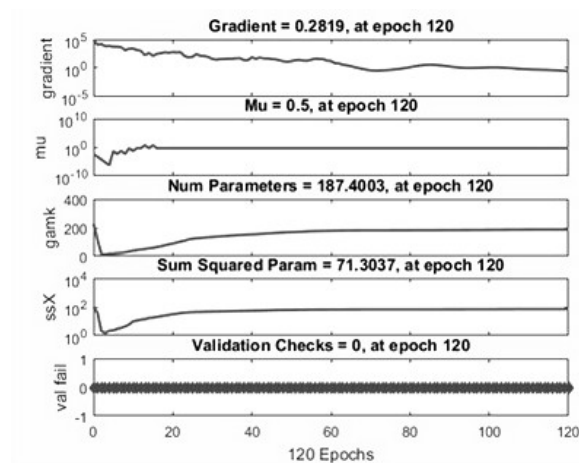


Fig. 6. Network training graphs.

As a result of the training, a neural network is obtained, which without resetting the link weights produces output signals when any stack of input signals from the training set is given to the network input.

VIII. NEURAL NETWORK VERIFICATION

To test the neural network we give 10 values to the input using the command `sim(net,[Qset;Qtrue;x1;x2;x3;x4;p1;p2;p3;p4])`. Data for verification are presented in the Table II.

After the test we obtained output values that have a minimum error. It means that the parameters of the neural network were chosen correctly.

IX. CONCLUSION

As a result, an artificial neural network to regulate the speed of the belt weigher motors and the separator motor of the cement grinding unit intended for production of three-component cement of various grades was developed and researched.

A two-layer unidirectional network with a sigmoidal function of hidden layer neurons activation and a linear function of output layer neurons activation was used. The network has trained on 50 examples over 120 epochs.

As a result of the training, a neural network was obtained which without resetting the link weights produces output signals when any stack of input signals from the training set is given to the network input.

The neural network was developed in the Matlab R2016a environment using the Matlab Neural Network Toolbox. The use of the obtained artificial neural network is possible in conjunction with a SCADA system using the OPC server.

TABLE II

VERIFICATION DATA

| Input | | | | | | | | | | Output | | | |
|-------------------------|--------------------|------------------|----|----|----|-----------|--------|--------|--------|--------------------------|------|------|------|
| Specified capacit. t | True capacit. t | Percentage, % | | | | Weight, t | | | | Current frequency, Hz | | | |
| Qset | Qtrue | x1 | x2 | x3 | x4 | p1 | p2 | p3 | p4 | f1 | f2 | f3 | f4 |
| 40 | 39 | 90 | 4 | 1 | 5 | 0.04 | 0.0016 | 0.0003 | 0.002 | 50.3 | 55.9 | 74.5 | 55.9 |
| 20 | 24 | 80 | 5 | 2 | 13 | 0.015 | 0.0011 | 0.0005 | 0.0028 | 59.6 | 50.8 | 44.7 | 51.9 |
| 39 | 38 | 80 | 6 | 1 | 13 | 0.04 | 0.002 | 0.0005 | 0.0049 | 43.6 | 65.4 | 43.6 | 57.8 |

REFERENCES

- [1] Haykin S., Neural Networks: A Comprehensive Foundation, 2nd Edition. – Pearson Education, 1999. – 1104 p.;
- [2] Terehov V.A., Efimov D.V., Tjukin I.U. Nejrosetevye sistemy upravleniya [Neural network control systems]. Moscow, IPRZhR Publ., 2002, 480 p. (In Russian);
- [3] Medvedev V.S., Potemkin V.G., Neural Network MATLAB, Moscow, 2001. – 630 p. (In Russian);
- [4] Akhmetov B.S., Gorbachenko V.I., Neural Network, Laboratory Practice, Almaty, 2015;
- [5] Vasenkov D.V. Methods of teaching of artificial neural networks // Computer Tools in Education. 2007. No. 1. P. 20-29. (In Russian);
- [6] Krug P.G., Neural networks and neurocomputers, a textbook for the course «Microprocessors», Publishing MEI, Moscow, 2002. – 176 p. (In Russian);
- [7] Mochalov I. A., Artificial neural networks in control and information processing problems – Moscow, 2004. –145 p. (In Russian).
- [8] Muravyova E. Intellectual control of oil and gas transportation system by multidimensional fuzzy controllers with precise terms / Muravyova E., Sagdatullin A., Emekeev A. // Applied Mechanics and Materials. 2015. T. 756. C. 633.
- [9] Muravyova E. The analysis of opportunities of construction and use of avionic systems based on cots-modules / Muravyova E., Bondarev A., Kadyrov R., Rahman P. // ARPN Journal of Engineering and Applied Sciences / 01.2016. Vol. 11.
- [10] Muravyova E.A. Simulation of Multidimensional Non-Linear Processes Based on the Second Order Fuzzy Controller / Muravyova E.A., Solovev K.A., Soloveva O.I., Sultanov R.G., Charikov P.N. // Key Engineering Materials, Vol. 685, pp. 816-822, Mar. 2016.
- [11] Reliability Model of Fault-Tolerant Dual-Disk Redundant Array / Rahman P. A., Muraveva E. A., Sharipov M. I. // Key Engineering Materials. Vol. 685, pp 805-810.
- [12] Muravyova E.A. The Questions of Circuitry Design when Forming the Switching Functions of the Control System of the Matrix Frequency Converter / Muravyova E.A., Bondarev A.V., Kadyrov R.R., Shulaeva E.A. // Indian Journal of Science and Technology. V. 8(S10), December 2015. PP. 1-8.
- [13] Muravyova E. Modelling of Fuzzy Control Modes for the Automated Pumping Station of the Oil and Gas Transportation System / Muravyova E. Sagdatullin, A., Sharipov, M. // IOP Conference Series: Materials Science and Engineering, 2016. – 132 (1), 012028.
- [14] Muravyova E.A. System-integrative approach to automation of the oil and gas fields design and development control / Muravyova E.A., Sagdatullin, A.M., Emekeev, A.A. // Neftyanoe khozyaystvo - Oil Industry, 2015. (3), PP. 92-95.
- [15] Muravyova E.A. Fuzzification concept using the any-time algorithm on the basis of precise term sets // Industrial Engineering, Applications and Manufacturing (ICIEAM) : International Conference on Industrial Engineering, Applications and Manufacturing, 16-19 May 2017 / IEEE. - CIP6., 2017.
- [16] Muravyova E.A. Two fuzzy controller synthesis methods with the double base of rules: Reference points and training using // Industrial Engineering, Applications and Manufacturing (ICIEAM) : International Conference on Industrial Engineering, Applications and Manufacturing, 16-19 May 2017 / IEEE. - CIP6., 2017.
- [17] Muravyova E.A. Simulation of salt production process // IOP Conference Series: Earth and Environmental Science : IPDME 2017 / IOP Publishing. - 2017. - Vol. 87. - 052018.
- [18] Muravyova E.A. Chlorine condenser-evaporator simulation // IOP Conference Series: Earth and Environmental Science : IPDME 2017 / IOP Publishing. - 2017. - Vol. 87. - 082032.
- [19] Muravyova E.A. Fuzzy controller adaptation // IOP Conference Series: Earth and Environmental Science : IPDME 2017 / IOP Publishing. - 2017. - Vol. 87. - 082033.
- [20] Muravyova E.A., Sharipov M. I. Method of fuzzy controller adaptation // Proceedings of the International Conference "Actual Issues of Mechanical Engineering" 2017 (AIME 2017). November 2017. doi:10.2991/aime-17.2017.82.
- [21] Muravyova E.A., Shulaeva E.A., Charikov P.N., Kadyrov R.R., Sharipov M.I., Bondarev A.V., Shishkina A.F. Optimization of the structure of the control system using the fuzzy controller // 9th International Conference on Theory and Application of Soft Computing, Computing with Words and Perception, (ICSCCW 2017), 22-23 August 2017, Budapest, Hungary. Procedia Computer Science. Volume 120, 2017, PP. 487-494.



Muravyova Elena Aleksandrovna. Doctor of Engineering Sciences, Associate Professor, Head of the Chair «Automated Process and Information Systems» FSBEI HE USPTU, Branch in Sterlitamak, Russian Federation.

E-mail: muraveva_ea@mail.ru



Sharipov Marsel Ilgizovich. Candidate of Engineering Sciences, Associate Professor of the Chair «Automated Process and Information Systems» FSBEI HE USPTU, Branch in Sterlitamak, Russian Federation.

E-mail: muraveva_ea@mail.ru

Development of the Stabilizing Algorithm for Pendulum Systems Based on Modal Technique

Olga A. Votrina, Galina V. Sablina

Department of Automation, Novosibirsk State Technical University, Novosibirsk, Russia

Abstract – The objective of this paper is to discuss the stabilization problem of electromechanical oscillatory systems via modal synthesis technique. The use of such method is suitable only when mathematical model containing physical characteristics of real object is calculated. In this paper, objects of research are two types of model systems: torsional pendulum and horizontal spring pendulum. The regulator based on the modal synthesis was suggested to solve the problem of model high oscillation level. Such regulator with other elements of stabilizing system gave the opportunity to reach predetermined requirements of transient process quality. Simulating stabilizing system by means of Matlab Simulink integrated environment allowed us to prove that the system completes predetermined initial conditions in a required transient time.

Index Terms – Mathematical model; stabilizing system; regulator; torsional pendulum; horizontal spring pendulum; MATLAB Simulink; transient process; modal synthesis technique; electromechanical oscillatory systems; automatic control theory.

I. INTRODUCTION

TODAY THE PROBLEM of high oscillation systems stabilizing is urgent. Such systems have worse quality than their alternatives with low level of oscillation. The object does not complete disturbances under the impact of external forces and transient process requirements are not met.

In recent years, many papers dedicated to solving the problem of stabilizing pendulum systems with high oscillation level appeared in local and international literature [2-11]. To solve such problem, the preliminary verification of object mathematical model qualities will be suggested in this paper. Hereafter, the use of algorithm based on modal technique, which, as is known, is reputable for stabilizing systems in the mode of initial conditions and disturbances completion [1], will also be suggested.

II. PROBLEM DEFINITION

The paper is related to design of stabilizing algorithms for two types of pendulum systems: dual-mass torsional pendulum and horizontal spring pendulum. Such object types are applied in many fields of science and engineering. For instance, torsional pendulums are applied for high-level earthquakes forecasting in mountainous areas as well as for precise measuring of gravitational constant g . Whereas spring pendulums are applied as an accelerometer in ballistic missile control system. They are also used as a basic

mechanism of artillery and air ammunition contact fuse. The use of stabilizing algorithms in instruments based on pendulum systems will lead to increase of accuracy, efficiency and operation speed.

III. MATHEMATICAL MODELS DESCRIPTION

Dual-mass torsional pendulum consists of a laterally based disk suspended from its mass center by a thin spring fiber and another disk suspended from the first disk [12]. Second fiber is fixed in mass centers of the first and second disks (see Fig. 1).

In the Figure 1, physical parameters of the torsional pendulum model system are indicated: I_1, I_2 - disk masses moment of inertia in reference to lateral axis; C_1, C_2 - fiber factors of rigidity under torsion; φ_1, φ_2 - disks angles of rotation over lateral axis; U - applied momentum.

Horizontal spring pendulum is a system, which consists of solids with m_1 and m_2 masses connected together by springs with forces C_1 and C_2 (see Fig. 2).

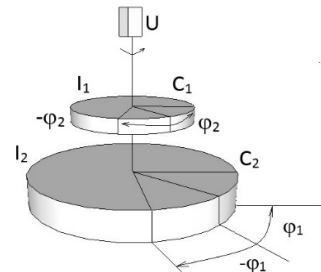


Fig. 1. Schematic representation of the torsional pendulum.

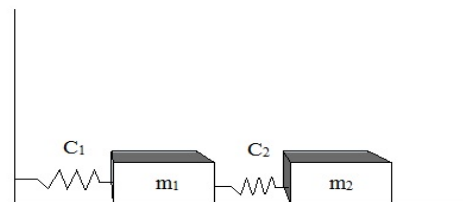


Fig. 2. Schematic representation of the spring pendulum.

Mathematical model of the torsional pendulum is described via system of linearized second-order differential equations:

$$\begin{cases} I_1 \ddot{\varphi}_1 = R_1 \dot{\varphi}_1 - C_1 \varphi_1 + C_2 (\varphi_2 - \varphi_1) + U, \\ I_2 \ddot{\varphi}_2 = R_2 \dot{\varphi}_2 - C_2 (\varphi_2 - \varphi_1), \end{cases} \quad (1)$$

where R_1, R_2 – resistant forces coefficients.

Mathematical model of the horizontal spring pendulum is also described via system of linearized second-order differential equations:

$$\begin{cases} m_1 \ddot{s}_1 = -r_1 \dot{s}_1 - C_1 s_1 + C_2 (s_2 - s_1) + U, \\ m_2 \ddot{s}_2 = -r_2 \dot{s}_2 - C_2 (s_2 - s_1), \end{cases} \quad (2)$$

where r_1 и r_2 - damping factors, s_1 и s_2 - pendulum solids displacements, U - control input.

After several transformations and setting state vector components for the torsional pendulum that can be written as:

$$x_1 = \varphi_1, x_2 = \dot{\varphi}_1, x_3 = \varphi_2, x_4 = \dot{\varphi}_2, \quad (3)$$

the state variables form of the model for torsional pendulum is obtained:

$$\begin{cases} \dot{x}_1 = x_2, \\ \dot{x}_2 = -\left(\frac{C_1}{I_1} + \frac{C_2}{I_1}\right)x_1 - \frac{R_1}{I_1}x_2 + \frac{C_2}{I_1}x_3 + \frac{1}{I_1}U, \\ \dot{x}_3 = x_4, \\ \dot{x}_4 = \frac{C_2}{I_2}x_1 - \frac{C_2}{I_2}x_3 - \frac{R_2}{I_2}x_4, \\ y_1 = x_1, \\ y_2 = x_3. \end{cases} \quad (4)$$

State variables for the horizontal spring pendulum can be set in a form:

$$x_1 = s_1, x_2 = \dot{s}_1, x_3 = s_2, x_4 = \dot{s}_2. \quad (5)$$

The state variables form of the model for horizontal spring pendulum:

$$\begin{cases} \dot{x}_1 = x_2, \\ \dot{x}_2 = -\frac{C_1}{m_1}x_1 - \frac{r_1}{m_1}x_2 + \frac{C_2}{m_1}(x_3 - x_1) + \frac{1}{m_1}U, \\ \dot{x}_3 = x_4, \\ \dot{x}_4 = -\frac{r_2}{m_2}x_4 - \frac{C_2}{m_2}(x_3 - x_1), \\ y_1 = x_1, \\ y_2 = x_3. \end{cases} \quad (6)$$

IV. SYNTHESIS TASK FORMULATION

Synthesis task formulation for the torsional pendulum model takes place in the form of equations below:

$$\begin{cases} \lim_{t \rightarrow \infty} \varphi_1(t) = 0, \\ \lim_{t \rightarrow \infty} \varphi_2(t) = 0. \end{cases} \quad (7)$$

Synthesis task formulation for the horizontal spring pendulum model can be written as:

$$\begin{cases} \lim_{t \rightarrow \infty} s_1(t) = 0, \\ \lim_{t \rightarrow \infty} s_2(t) = 0. \end{cases} \quad (8)$$

In both cases, the following requirement should be meat:

$$t_n \leq t_n^*,$$

where t_n^* - desired transient time.

In other words, it is need to stabilize rotation angles of torsional pendulum disks and displacements of horizontal spring pendulum solids in equilibrium state fulfilling the transient process requirements.

V. STABILIZING ALGORITHMS DESIGN

During the pendulum mathematical models verification the fact of object stability, complete controllability and observability was shown [1]. Equilibrium states sets for both objects are of the form that determined the resolvability of synthesis tasks. Therefore, we can start the stabilizing task solving.

On the first stage of stabilizing system, constructing the control law based on modal synthesis technique [1] was set of the form:

$$U = -Kx, \quad (9)$$

where $K = [k_1, k_2, k_3, k_4]$ - regulator undefined coefficients vector, $x = [x_1, x_2, x_3, x_4]$ - full state vector. Substitution of the control law in equations (4) and (6) allowed us to obtain closed-loop characteristic equations for both model objects.

Closed-loop equation for torsional pendulum model is of the form:

$$\begin{aligned} A_3(p) = p^4 + \left(\frac{R_1}{I_1} + \frac{R_2}{I_2} + \frac{1}{I_1}k_2\right)p^3 + \left(\frac{C_1}{I_1} + \frac{C_2}{I_1} + \frac{C_2}{I_2} + \right. \\ \left. + \frac{R_1 R_2}{I} + \frac{1}{I_1}k_1 + \frac{R_2}{I}k_2\right)p^2 + \left(\frac{R_1 R_2}{I} + \frac{C_1 R_2}{I} + \frac{C_2 R_2}{I} + \right. \\ \left. + \frac{R_2}{I}k_1 + \frac{C_2}{I}(k_2 + k_4)\right)p + \frac{C_1 C_2}{I} + \frac{C_2}{I}(k_1 + k_3) = 0, \end{aligned} \quad (10)$$

where $I = I_1 \cdot I_2$.

At the next stage, the desired equation of the form below was set according transient process requirements:

$$C(p) = (p - \lambda_1^*) \dots (p - \lambda_4^*) = p^4 + c_4 p^3 + c_3 p^2 + c_2 p + c_1 = 0, \quad (11)$$

where $\lambda_1^*, \lambda_2^*, \lambda_3^*, \lambda_4^*$ - desired roots set.

After that via equating such coefficients of closed-loop characteristic equation and desired equation, where the power of operator was the same, design ratios for regulator-undefined coefficients calculating were obtain:

$$\begin{cases} c_4 = \frac{R_1}{I_1} + \frac{R_2}{I_2} + \frac{1}{I_1} k_2, \\ c_3 = \frac{C_1}{I_1} + \frac{C_2}{I_1} + \frac{C_2}{I_2} + \frac{R_1 R_2}{I} + \frac{1}{I_1} k_1 + \frac{R_2}{I} k_2, \\ c_2 = \frac{R_1 R_2}{I} + \frac{C_1 R_2}{I} + \frac{C_2 R_2}{I} + \frac{R_2}{I} k_1 + \frac{C_2}{I} (k_2 + k_4), \\ c_1 = \frac{C_1 C_2}{I} + \frac{C_2}{I} (k_1 + k_3). \end{cases} \quad (12)$$

Closed-loop equation for the horizontal spring pendulum model is written as:

$$\begin{aligned} A_3(p) = p^4 + \left(\frac{r_1}{m_1} + \frac{r_2}{m_2} + \frac{1}{m_1} k_2 \right) p^3 + \left(\frac{C_1}{m_1} + \frac{C_2}{m_1} + \frac{C_2}{m_2} + \right. \\ \left. + \frac{r_1 r_2}{M} + \frac{1}{m_1} k_1 + \frac{r_2}{M} k_2 \right) p^2 + \left(\frac{r_1 C_2}{M} + \frac{r_2 C_1}{M} + \frac{r_2 C_2}{M} + \right. \\ \left. + \frac{r_2}{M} k_1 + \frac{C_2}{M} (k_2 + k_4) \right) p + \frac{C_1 C_2}{M} + \frac{C_2}{M} (k_1 + k_3) = 0, \end{aligned} \quad (13)$$

where $M = m_1 \cdot m_2$.

Hereafter design ratios for regulator-undefined coefficients calculating were get:

$$\begin{cases} c_4 = \frac{r_1}{m_1} + \frac{r_2}{m_2} + \frac{1}{m_1} k_2, \\ c_3 = \frac{C_1}{m_1} + \frac{C_2}{m_1} + \frac{C_2}{m_2} + \frac{r_1 r_2}{M} + \frac{1}{m_1} k_1 + \frac{r_2}{M} k_2, \\ c_2 = \frac{r_1 C_2}{M} + \frac{C_1 r_2}{M} + \frac{C_2 r_2}{M} + \frac{r_2}{M} k_1 + \frac{C_2}{M} (k_2 + k_4), \\ c_1 = \frac{C_1 C_2}{M} + \frac{C_2}{M} (k_1 + k_3). \end{cases} \quad (14)$$

At the next step two state estimation filters were added to the stabilizing system that allow us to measure full state vector because measurements of only two components of state vector are available in fact.

Filters transfer function is of the form below:

$$W_\phi(p) = \frac{1}{T_\phi^2 p^2 + 2dT_\phi p + 1}, \quad (15)$$

where d – damping factor, which is set in range $[0.5 \dots 0.8]$ to provide desired oscillation level of processes, filter time constant is chosen on the basis of ratio $T_\phi \leq 0.1t_n^*$, so that processes in filter will finish ten times faster than processes in objects under control [3].

The final stage of stabilizing system designing consists of closed-loop systems simulation via MATLAB Simulink integrated environment.

In the Figure 3, the simulation circuit of torsional pendulum stabilizing system is shown. In the Figure 4, the same circuit of horizontal spring pendulum stabilizing system is shown.

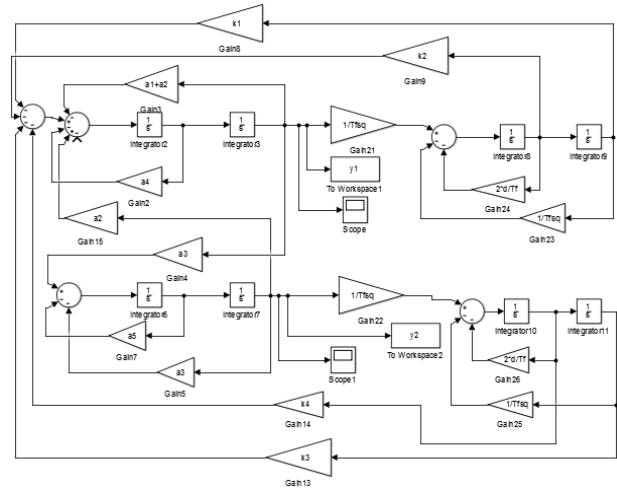


Fig. 3. Simulation circuit of the torsional pendulum stabilizing system.

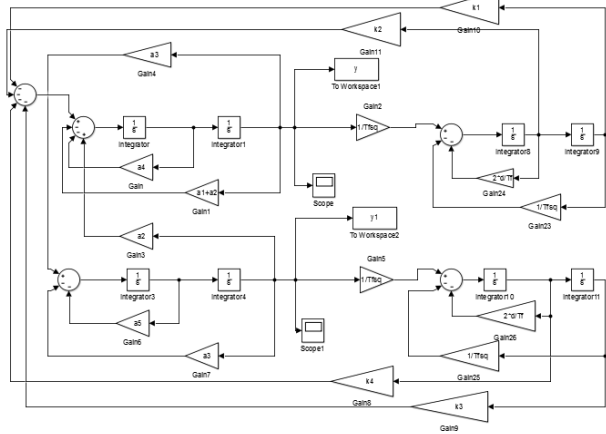


Fig. 4. Simulation circuit of the horizontal spring pendulum stabilizing system

As you can see by transient process plots (see Fig. 5,6), both objects inside the stabilizing system complete predetermined initial conditions with required transient processes quality ($t_n^* = 3c$).

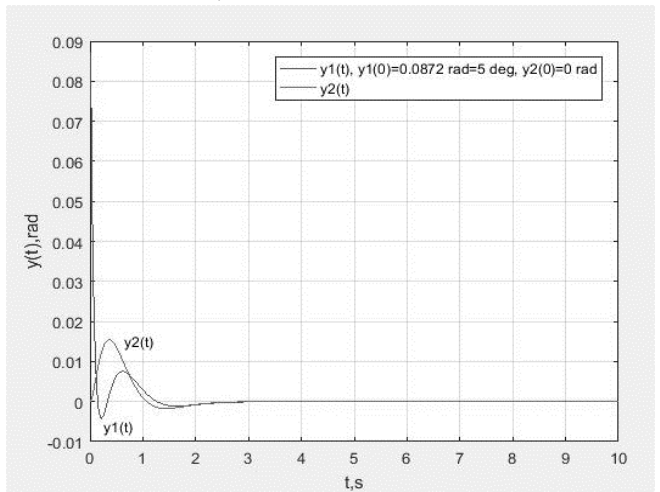


Fig. 5. Transient processes in closed-loop stabilizing system of the torsional pendulum.

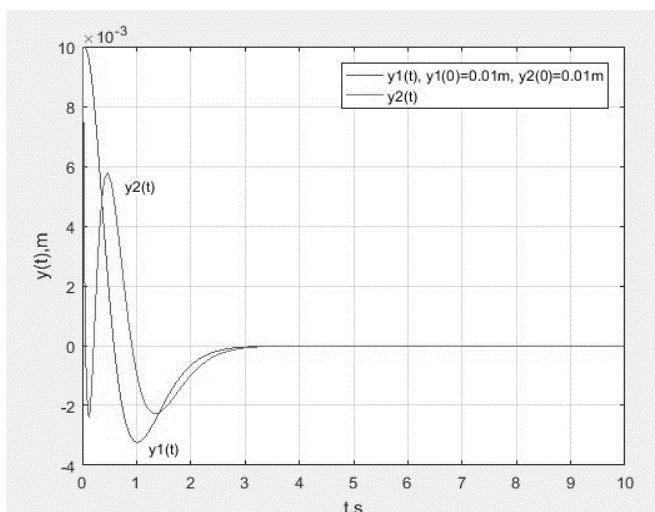


Fig. 6. Transient processes in closed-loop stabilizing system of the horizontal spring pendulum.

VI. CONCLUSION

The stabilization problem resolvability of two pendulum systems - dual-mass torsional pendulum and horizontal spring pendulum - was discussed in this article. Transformation of the mathematical model to a form, which is appropriate for further research of its characteristic properties, was fulfilled.

The pendulum mathematical models verification proved the fact of object stability, complete controllability and observability.

A set of equilibrium states of the system was obtained and analyzed. The fact, that discussed problems of dual-mass torsional pendulum and horizontal spring pendulum stabilization have possible decision, was proved.

The controller, based on the Modal Technique, was designed. As a result, stabilizing algorithms for dual-mass torsional pendulum and horizontal spring pendulum based on modal synthesis technique were suggested.

Stabilizing systems simulation by means of MATLAB Simulink integrated environment showed that predetermined initial conditions were completed in closed-loop systems with required transient process quality that is the evidence of suggested algorithms effectiveness.

REFERENCES

- [1] A.S. Vostrikov, G.A. Frantsuzova. Control Theory: Study Guide / Vostrikov A.S., Frantsuzova G.A. – Novosibirsk: NSTU, 2003. – 364 p. (in Russian)
- [2] G.V. Sablina, D.I. Hodakova. "Study of the properties of the model system "rotating pendulum"". Collection of scientific works of NSTU. Novosibirsk, 2009. Vol.3(57). p. 25-32. (in Russian)
- [3] Real time digital super-high accuracy vibrations measurements: Methods, devices and mathematical modeling for the metrology. Zhmud, V., Liapidevskiy, A. Proc. of the 30th IASTED Conference on Modelling, Identification, and Control - AsiaMIC 2010 -November 24 – 26, 2010 Phuket, Thailand. p. 343–347. G.V. Sablina About one method of model system "Suspended mass" synthesis / Sablina G.V. // Actual problems of electronic instrument engineering (APEIE-2014) : 12th international conference Novosibirsk, 2–4 Oct. 2014: 7 Vol. –

Novosibirsk : NSTU, 2014. – Vol. 7. – p. 68-71. – 100 p. – ISBN 978-1-4799-6019-4, ISBN 978-5-7782-2516-9. (in Russian)

- [4] Synthesis of double inverted pendulum on the cart system on the sliding modes method basis / G. V. Sablina, I. V. Stazhilov, A. I. Sazhin // International Siberian conference on control and communications (SIBCON-2015) : proc., Omsk, 21–23 May, 2015. – Omsk : IEEE, 2015. – 5 p. - ISBN 978-1-4799-7102-2.
- [5] Feedback systems with pseudo local loops. Zhmud, V., Semibalamut, V., Vostrikov, A. 2015 Testing and Measurement: Techniques and Applications - Proceedings of the 2015 International Conference on Testing and Measurement: Techniques and Applications, TMTA 2015, p. 411-417.
- [6] Designing and research of the real sliding mode in the inverted pendulum modelling / G. V. Sablina, A. I. Sazhin // 11 International forum on strategic technology (IFOST 2016) : proc., Novosibirsk, 1–3 June 2016. – Novosibirsk : NSTU, 2016. – Pt. 1. – P. 571-575. - ISBN 978-1-5090-0853-7. - DOI: 10.1109/IFOST.2016.7884182.
- [7] Development of rotating pendulum stabilization algorithm and research of system properties with the controller / G. V. Sablina, I. V. Stazhilov, V. A. Zhmud // Actual problems of electronic instrument engineering (APEIE-2016) : 13th international sc. and tech. conference, Novosibirsk, 3–6 Oct. 2016 : 12 vol. – Novosibirsk : NSTU, 2016. – Vol. 1, Pt. 3. – p. 165-170. – 100 p. - ISBN 978-5-7782-2991-4.
- [8] Use of bypass channel for feedback control of oscillatory object well-known as difficult one for control [Electronic resource] / V. A. Zhmud, G. V. Sablina, V. G. Trubin, L. V. Dimitrov // International Siberian conference on control and communications (SIBCON) : proc., Moscow, 12-14 May 2016. – Moscow : IEEE, 2016. – 6 p. - 1 electron-optical disc (CD-ROM)SIBCON. - Title with the label. - ISBN 2380-6516. – Research completed with support of Ministry of Education and Science of the Russian Federation - project 2014/138.
- [9] Calculation of regulators for the problems of mechatronics by means of the numerical optimization method/Zhmud, V., Dimitrov, L., Yadrishnikov, O. 20.15.2014 12th International Conference on Actual Problems of Electronic Instrument Engineering, APEIE 2014 – Proceedings 7040784, p. 739-744.
- [10] Detection of unrevealed non-linearities in the layout of the balancing robot [Electronic resource] / A. Y. Ivoilov, V. A. Zhmud, V. G. Trubin, L. V. Dimitrov // International Siberian conference on control and communications (SIBCON) : proc., Moscow, 12-14 May 2016. – Moscow : IEEE, 2016. – 9 p. - 1 electron-optical disc (CD-ROM). - Title with the label. - ISBN 2380-6516. - Research completed with support of Ministry of Education and Science of the Russian Federation - project 2014/138. - 10.1109/SIBCON.2016.7491853
- [11] O.A. Votrina, G.V. Sablina. Mathematical Model Application for Pendulum Based Systems Stabilizing./Information Technologies in Simulation and Control: Techniques, Methods, Solutions: Proceedings of the 1st Scientific Conference, Togliatti, 12-14 Dec. 2017 r. - Togliatti, TSU, 2017.- Pt.1 – p. 59-66. (in Russian)



Olga A. Votrina, Undergraduate student of Department of Automation in Novosibirsk State Technical University, author of 4 science papers
E-mail: olga_votrina@mail.ru



Galina V. Sablina, Associated professor of Department of Automation in Novosibirsk State Technical University, Cand.Tech.Sci., author of more than 40 science papers, including 3 schoolbooks.
E-mail: sablina@corp.nstu.ru

System of Monitoring and Remote Control of Microclimate in Greenhouses

Renat B. Salikhov, Alena A.Zainitdinova
Bashkir State University, Institute of Physics and Technology, Ufa, Russia

Abstract – The article presents the idea of developing an active home greenhouse model for growing plants and flowers in an autonomous mode with the ability to remotely monitor and remotely control the process of plant care using energy-saving technologies and modern intelligent systems.

Index Terms – Sensors, controller, interface, monitoring.

I. INTRODUCTION

In our time, it is difficult to find a person who has not heard about the term "Internet of things" or IoT. Let's imagine that all objects and devices surrounding us (household appliances and utensils, clothes, products, cars, industrial equipment, etc.) are equipped with miniaturized identification and sensory (sensitive) devices. Then, if you have the necessary communication channels with them, you can not only track these objects and their parameters in space and time, but also manage them, and also include information about them in the united "smart planet".

To solve the problems of energy and resource saving, the widespread use of modern automated monitoring and control systems for the heat consumption of residential buildings, production sites, warehouses, agricultural greenhouses, etc., and the regulation of the microclimate in these premises is urgent. For simple and budgetary solutions for remote monitoring and management, the global Internet network is well suited, because of its widespread prevalence in Russia (almost all residential buildings, residential premises at enterprises and educational institutions) and relative ease of implementation [1-4].

II. PROBLEM DEFINITION

We will highlight the main components of the centralized automatized "Smart Greenhouse" system, which ensure its successful functioning. The most important and necessary components of the system: are control software and hardware platform, microcontroller executive modules, various sensors (temperature, lighting, humidity).

A promising electronic control unit of the "Smart Greenhouse" system is the software-hardware platform under the Arduino trademark. It is an electronic designer and a convenient platform for rapid development of electronic devices for beginners and professionals (Fig.1). The platform is very popular all over the world due to the convenience and simplicity of the programming language, as well as open architecture and software code. The device is programmed via USB without the use of programmers. Arduino allows a

computer to go beyond the virtual world to physical and interact with it. Devices based on Arduino can receive information about the environment through various sensors, and can also control various actuators. Thus, the ability to implement the simplest "smart greenhouse" system becomes available to everyone.

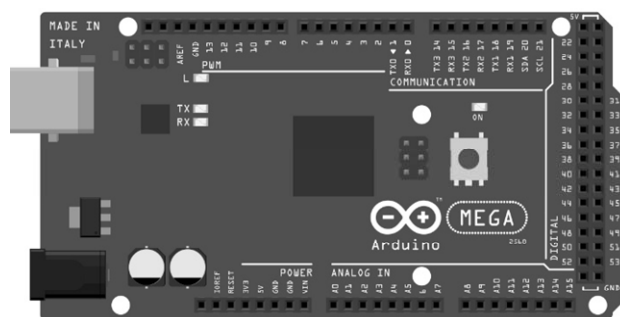


Fig. 1. Arduino Mega.

The executive units of the Smart Hothouse system are mainly built on the basis of AVR microcontrollers with RISC architecture, working along with a discrete transceiver or a wireless communication system on a chip. Depending on the system construction, the complexity of the firmware and the required form factor, the ARM-microcontroller can be 8- or 32-bit. The wider internal buses and perfect peripherals of the 32-bit microcontroller provide faster control system performance than the 8-bit controller. For applications with the "Run Fast, Then Sleep (RFTS)" work cycle, the use of a 32-bit device provides a shorter work period and increased energy efficiency.

III. DEVELOPMENT TOOLS

When creating a block diagram of the device (shown in Fig. 2), it repulsed from the functional of the device. Namely, the device must perform automatic monitoring of such parameters of the greenhouse as temperature and humidity; the device must be able to transmit this data remotely. And also it is necessary to collect mechanisms that correct the parameters of the greenhouse. It is also important that the device has the possibility of auto irrigation.

Elements of the structural diagram:

1) To process the sensor readings and control the functionality, we select the controller. All the readings of the sensors will be processed by him and thanks to the written program to influence this or that functionality of the device.

2) For visual I / O information, we need a display where we could see all the immediate parameters of the device.

3) To regulate temperature and humidity, we need devices that will help you to know their current value. Therefore, in this work we use the device with a humidity and temperature sensor.

4) Since in the device's functionality there is watering in time, we need a timer, which also will appear as a real-time clock.

5) Remote monitoring and management will be implemented using a communication module, for example, a Wi-Fi module.

6) To directly adjust the current temperature, you need an actuator (for example, from satellite antennas). And since a large current is needed to control the actuator, we need a relay. To enable watering, we use e-valves, which also require a large current and for this we also use a relay. To open and close the cold water valve that enters the tank, we use an electromagnetic valve, which is also controlled from the relay.

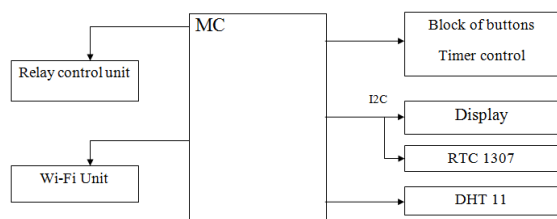


Fig.2. Structural scheme.

IV. HARDWAREIMPLEMENTATION

After considering the main hardware and software used in modern automation systems to connect to the Internet, the optimal methods of solving the problem were chosen - we choose the controller as the control unit. For the project, the Arduino Uno controller was chosen. (Fig. 3a).

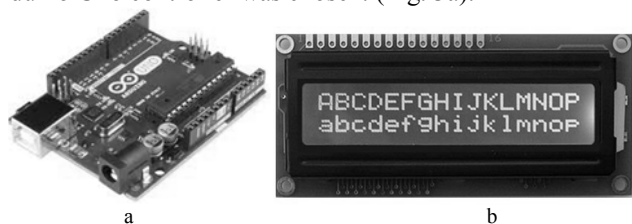


Fig.3. a) Arduino Uno, b) liquid crystal display (LCD) 1602.

This controller is selected for several reasons:

- 1) Low cost.
- 2) A large number of available libraries.
- 3) Ease of use and mastery.

There are no drawbacks critical for this work. The controller has 14 digital and 6 analog ports.

Arduino Uno can be powered via a USB connection or from an external power source. The power supply is automatically selected.

As a display, we use LCD 1602 (Fig.3b).

The model is chosen from the simplicity of working with it, the price is low, there are libraries ready. Places on the screen are enough to write a menu.

In order to connect the display to the serial interface, we use a simple 8-bit micro-circuit PCF8574. It simultaneously implements an I2C bus and an expander of parallel I / O ports.

To PCF8574 (module i2c) you can connect up to 8 parallel lines. We will only use 7, because we connect the OLED-display in 4-bit mode

Since we need to measure temperature and humidity, we need a sensor cheap, not very accurate, as for a training project. Such a sensor is DHT11 (Fig.4a). Its advantages such as: low price, ready-made libraries cover the shortcoming in the form of low accuracy.

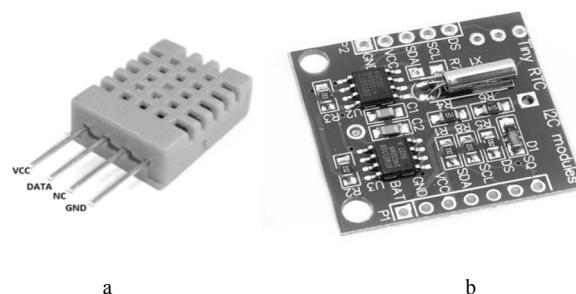


Fig.4. a) Temperature and humidity sensor DHT11, b)real time clock module ds1307.

The supply voltage is 5V. This sensor has a digital signal. And the temperature and humidity are given to them by one signal wire (S). DHT11 communicates with a host, such as Arduino, using its own protocol. Due to the fact that the sensor makes measurements only on request, energy efficiency is achieved: while there is no communication, the sensor consumes very little current.

Since we will need to run some of the functions after a long period of time and at the same time to make it automatically, and not under human control, that's why we need a timer. RTC 1307 is selected (Fig.4b), because it is widespread, easy to use, as there are ready-made libraries, a cheap module.

The real-time clock module must be connected to the SCL / SDA terminals referring to the I²C bus. It is also necessary to connect power lines (Vcc) and ground (GND).

The SDA / SCL lines have their own separate pins on the Arduino, but inside they are somehow connected to general purpose pins. If we consider Arduino Uno, the SDA line corresponds to pin A4, and SCL to A5.

In the kit with the module is supplied a cable with mother contacts, which is more convenient to connect to TroykaShield. However, the individual SDA and SCL pins on it are not output, so we connected directly through the A5 and A4 pins.

Wi-Fi module implements the function of monitoring and remote control via the network. we chose the ESP8266 module (Fig.5).

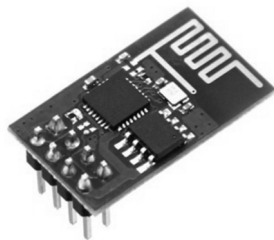


Fig.5. Wi-Fi module Esp8266.

The ESP8266 module is connected to the Arduino via a serial interface. You can use both Software Serial and Hardware Serial. The variant of connection of the module is selected in the module settings panel. The module is controlled by AT commands.

The electromagnetic relay block is used to control a powerful electric load: a water opening valve and an actuator for opening windows, for ventilation and a gate valve for supplying water to the tank (Fig.6 a).

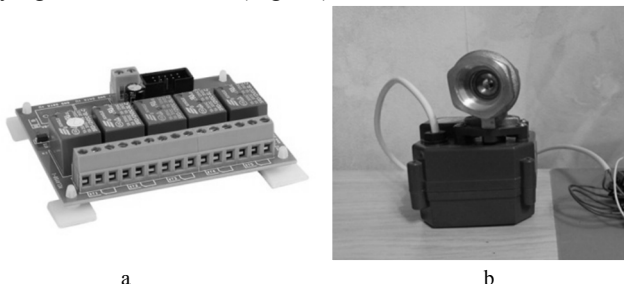


Fig.6. a) Block of electromagnetic relays, b)electromagnetic valve.

The electromagnetic valve (Fig.6b) is used to supply water to the tank, where it is heated to a comfortable temperature (and then used for irrigation)

To model the electrical circuit, the program Proteus (computer-aided design), version 8.6, was chosen. We use it for convenience, and to understand correctly whether the stand will work, when we sew the original project. In Figure 7, a part of the menu where the temperature and humidity in the greenhouse is displayed, with a single push of a button on the PB0 port, can also be switched to display the time, date and timer. A final Wi-Fi module will also be attached to the final qualification work, which will allow controlling the device for a distance, but since Proteus does not have its model, I left the ports for its implementation.

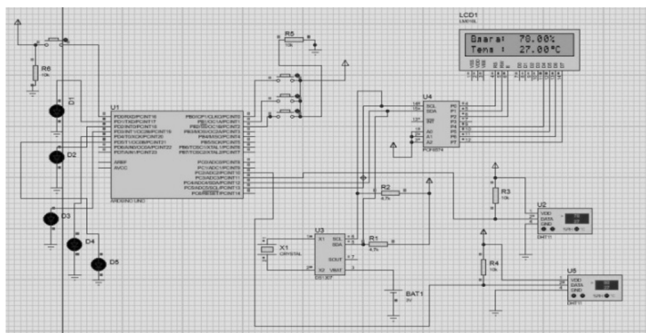


Fig.7.Electrical circuit diagram.

V. CONCLUSION

Thus, the developed system is implemented on the most modern element base used for building devices with an Ethernet interface, multifunctional, easily rebuilt for specific applications and is optimal from the point of view of implementation costs.

The expected results of the project are the creation of a commercial kit for building a smart greenhouse, with the help of which it will be possible to automate any greenhouse or home flower garden. The management of the greenhouse will be quite understandable even for older people who cannot work with a computer.

REFERENCES

- [1] Salikhov R.B., Abdrakhmanov V.Kh., Vazhdaev K.V., System of monitoring and remote control of temperature conditions, climate and heat consumption // 13th International Scientific-Technical Conference on Actual Problems of Electronic Instrument Engineering, APEIE 2016 – Proceedings 3,7807047, 171-174.
- [2] Salikhov R.B., Yusupov A.R., Lachinov A.N., Rakhmееv R.G., Gadiev R.M., Salazkin S.N., Chemical sensors based on nano-polymer films // Measurement Techniques. 2009. V. 52. № 4. 427-431.
- [3] Gadiev R.M., Lachinov A.N., Salikhov R.B., Kornilov V.M., Yusupov A.R., The conducting polymer/polymer interface // Applied Physics Letters. 2011. 98(17),173305.
- [4] Salikhov R.B., Lachinov A.N., Polymer thin film chemical sensors // Advances in chemical sensors Edited by Wen Wang. Rijeka, 2012. 215-234.



Renat B. Salikhov received the university degree and Ph.D. degree in physics from the National Research Nuclear University MEPhI, Moscow, Russia in 1981 and 1987, respectively. He is a Head of Infocommunication Technologies and Nanoelectronics Department of Institute of Physics and Technology of Bashkir State University, Ufa. His long-established research activities are in the fields of solid state physics, nanotechnology and electronics.



Alena A. Zainitdinova received a bachelor's degree Bashkir State University, Ufa, Russia in 2017. She studies at the magistracy of the Physics and Technology of Bashkir State University in Ufa. Her research activities belong to the field of electronics info and communication technologies.

Towards the Distributed Temperature Sensor with Potential Characteristics of Accuracy

Oleg V. Stukach^{1,2}, Ivan A. Ershov¹, Igor V. Sychev³

¹National Research Tomsk Polytechnic University, Tomsk, Russia

²National Research University Higher School of Economics, Moscow, Russia

³R&D “Kipline”, Novosibirsk, Russia

Abstract – The idea behind this paper was stimulated by known of the theory of automatic control definition concern potential pulse characteristics. It is used for increase of metrological accuracy of the distributed temperature sensor. All known works used averaging of the pulse response or its processing on certain algorithms for reduction of an error of transformation. It is bad idealization of used pulse signals for simplification of calculations. Thus it is supposed by default that risetime and decrease of pulse top do not influence to accuracy. The given approach does not consider an error due the transitive characteristic for any signal transferred through system with finite number of elements. It is shown that in actual life it mismatches the validity. A new distributed temperature sensor structure with the characteristics nearly to so-called potentially achievable is proposed. It is offered to use the mathematical theory of potentially achievable pulse characteristics for definition of limitations of accuracy of the pulse converter. Thus our approach is a refusal of signal idealization otherwise use the constructive methods of approximation. The new approach allows to consider transient parameters: the risetime duration, cut-off, deadtime, and peak overshoot. In turn, it minimized an error related with methods of temperature calculation. For modeling the reflected signal is presented in the form of Lanne polynomials. The second polynomial Remez algorithm has been used for finding of peak overshoot. Finally, in the paper the operation principle of distributed temperature sensor is resulted. The methods related decreasing of noise influence to measurement are designated. Some practical advice on increase accuracy of measurement by distributed temperature sensor is given.

Index Terms – optical distributed temperature sensor, distributed temperature sensor, optical fiber, accuracy of measurement, metrological accuracy, transient characteristic.

I. INTRODUCTION

MODERN technologies are related to constant search and perfection of measurement methods [1]. A new direction is measurement of temperature and small moving by means of the fiber-optical interrogators. Up to now this technology is expensive and distinguished by weak repeatability of characteristics from unit to unit, but progress in this area is visible. Technology perfection is necessary due clear advantages of optical sensors by sensitivity and accuracy in comparison with electromechanical methods of measurement [2]. Thus, at accounting of expenses some people do not consider that one sensor is capable to support measurements on tens kilometers that will allow to refuse a large amount discrete sensors. Also the fiber-optical sensor

will spend continuous measurements by all length of a sensitive element.

The good review of physical principles of measurement tools based on the fiber-optical sensor is presented in papers [3–6]. Temperature measurement is based on the spectrum analyze of the back-scattered light in optical fiber. The transformed pulse is proportional to energy of the scattered molecules transverse to new levels of energy. So-called stokes and anti-stokes components of spectrum are used at temperature measurement. The stokes component arises at transition of a molecule of glass in the raised level. This component has the big wave length in comparison with wave length of a light source. The anti-stokes component arises at transition of molecule from the raised level in the basic. The amplitude of the component depends on local temperature. Thus, using intensity stokes and anti-stokes, it is possible to temperature measurements on all optical fiber.

The measurement system scheme for the fiber-optical sensor is presented in Fig. 1 [4]. The laser source radiates a pulse signal on the electro-optical converter. Further the signal passes through a splitter and gets to the optical fiber. The back-diffused light from the optical fiber transfer through the filter which allocates stokes and anti-stokes components. They transfer into the optics-electron converter and analog-digital converter ADC. Next the signal is processed by digital devices for delivery to the operator in the convenient form.

The considerable quantity of measurements with their subsequent averaging is carried out due low intensity of the diffused light. Use of average leads to loss of accuracy due a high dispersion and digital processing of individual random errors, high or low values that not characterized the given sample. These values periodically appear in sample at the large dispersion, so average value is displaced. There is no proposition to assume that the measured values have normal distribution [7]. The rational decision of the problem is use the median values which is less sensitive to extremes and does not depends on the distribution law [8].

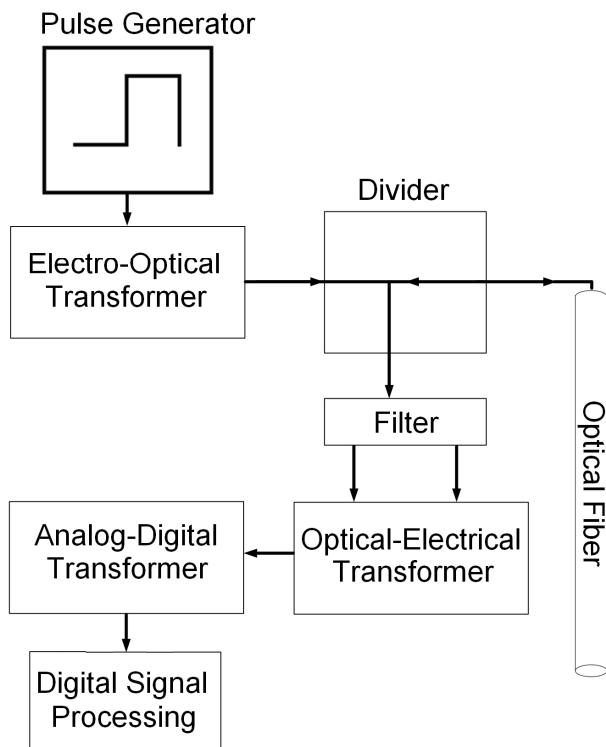


Fig. 1. Scheme of the measurement system of the fiber-optical sensor.

II. PROBLEM DEFINITION

At calculation and modeling of characteristics of the fiber-optical temperature sensor the pulse response from a photodetector is approached to ideal theoretical model. Thus, the developer of the distributed temperature sensor (DTS) directly at a design stage has no information of a possible achievable accuracy of the device. At the further digital signal processing it follows the ignoring of influence of risetime duration and peak overshoot that in turn leads to more measurement error. Therefore, it is of interest to consider this influence for the purpose of estimation of the upper limitation of achievement of measurement accuracy. It will be the top limitation because we will use a concept of the “potential characteristics”, extremely achievable in the real physical systems.

By definition, the potential pulse characteristic of the physically realized system is such pulse characteristic which at some peak overshoot has minimal risetime and may be designed in hardware unlike an ideal rectangular pulse [9]. At modeling of DTS with potentially achievable characteristics but not ideal pulse, we can specify the top limitations of accuracy.

III. THE POTENTIAL CHARACTERISTICS OF SYSTEM

An ideal pulse signal transferred through the physical system with finite number of elements has the transitive characteristic that is deviation from the ideal signal. But for DTS modeling the ideal signals have no physical sense especially in view of small intensity of a scattered light in

fiber. It is necessary to define of the potential accuracy connected with real pulse in DTS.

It is known that Lanne-optimum systems have potential characteristics [10]. At the defined peak overshoot δ it has the minimal time of risetime (Fig. 2). For the attenuation account it is necessary to define a function of the signal attenuation. Since the maximum value of peak overshoot is under interest, it is necessary to make the given characteristic as constant and equal δ .

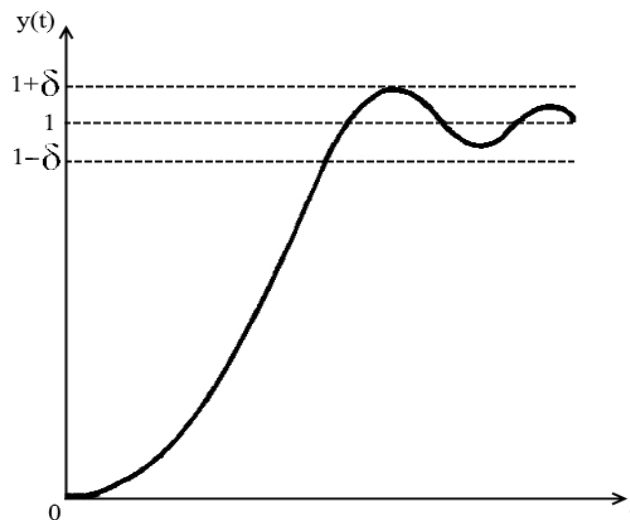


Fig. 2. The potential pulse characteristic.

It is shown in [10] that the potential characteristic may be obtained in a kind:

$$y(t) = \sum_{k=1,3,\dots}^{2n+1} a_k \sin(kt), \quad (1)$$

where a_k is coefficients of Lanne.

The second polynomial Remez algorithm is used for a finding of value of peak overshoot. It is based on theorem what it is possible always to receive function of error for approximation $\delta^* = 2\delta$ as a result of performance:

$$\left| 1 - \sum_{k=1,3,\dots}^{2n+1} a_k \sin(kx) \right| \leq \delta^*, \quad (2)$$

where $x \in [k; \frac{\pi}{2}]$.

From (2) it is follows:

$$1 - \sum_{k=1,3,\dots}^{2n+1} a_k \sin(kx_{n+1}^{(0)}) = (-1)^{n+1} \delta^*. \quad (3)$$

Therefore, solving system of the linear equations (3) in any $n+1$ point $x_1^{(0)}; x_2^{(0)}; \dots; x_{n+1}^{(0)} = \frac{\pi}{2}$ on the interval $[0; \frac{\pi}{2}]$, we

find coefficients $a_1^{(0)}; \dots; a_{2n+1}^{(0)}$.

Further it is required to investigate on extreme the difference:

$$\Delta(x) = \left[1 - \sum_{k=1,3,\dots}^{2n+1} a_k^{(0)} \sin(kx) \right] \quad (4)$$

for a finding of combination of points $x_1^{(1)}; x_2^{(1)}; \dots; x_{n+1}^{(1)}$, at which $\Delta(x)$ has alternating signs.

The given values are used for system of equations similar (2). Repeating the given algorithm, we find the polynomial of the best approximation giving the maximum value on the module δ^* .

For receiving of the potential accuracy the transients should be averaged as shown in Fig. 3. In this case we receive the minimum peak overshoot defining accuracy of temperature definition. Noise of a photodetector and in the reflected signal is considered in Fig. 3.

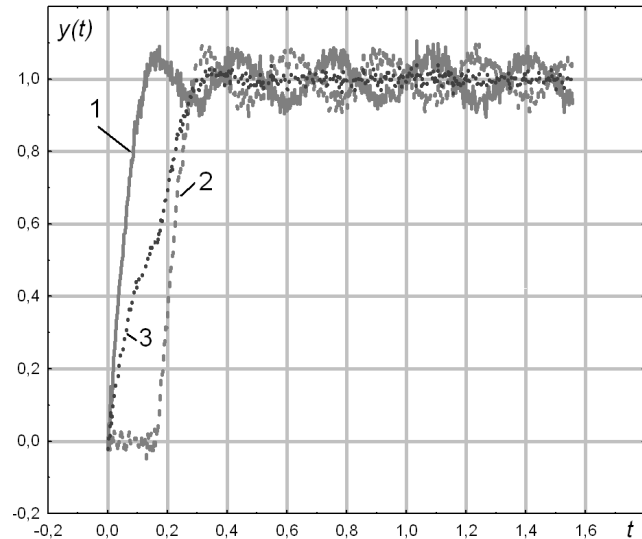


Fig. 3. Averaging of potential characteristics (model). 1, 2 is the reflected signals, 3 is average value.

For DTS model it has been chosen $n=19$, thus Lanne coefficients are equal: $a_1=1.271$, $a_3=0.41772$, $a_5=0.24361$, $a_7=0.16666$, $a_9=0.1226$, $a_{11}=0.09285$, $a_{13}=0.07167$, $a_{15}=0.05561$, $a_{17}=0.04303$, $a_{19}=0.07873$. Value of peak overshoot was chosen $\delta=0.03$ for the worst case. The arithmetic average and median was calculated:

$$S(\varepsilon) = [\varepsilon \cdot N_1(1)] \cdot y_1(t) + [\varepsilon \cdot N_2(1)] \cdot y_2(t), \quad (5)$$

where N is normally distributed random variable with root-mean-square deviation 1 and average 0, ε is noise level, y_1 and y_2 is values of potential transitive characteristics 1 and 2 (see Fig. 3). Results of modeling are shown in Fig. 4.

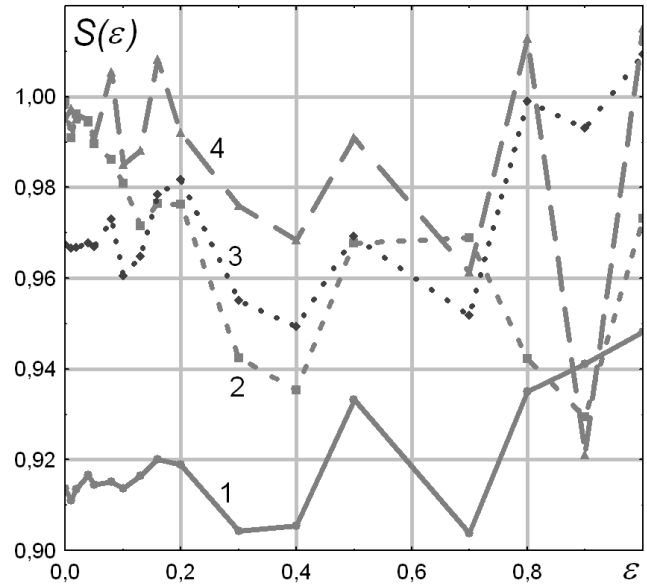


Fig. 4. Dependences of average values of potential characteristics for different noise levels ε (model). 1, 3 is mean, 2, 4 is median, 1, 2 is y_1+y_2 , 3, 4 is y_1 .

It is visible that at median averaging of registered pulses the ideal value $1(\varepsilon)$ is essentially achievable for potential characteristics of DTS. Herewith accuracy of temperature measurement in DTS depends only on the noise level.

IV. DISCUSSION

- Accuracy of temperature measurement depends on the noise level. But maintenance of its constant value is more important than decrease in the general noise level because of it is possible always to line up coefficients of calibration function for the necessary accuracy of measurement.
- Disorder of average values increase with growing of noise.
- For the potential characteristics the median evaluation of pulses are more correct.
- Rigorous synchronization for averaging pulses closed to the potential characteristics can lead to measurement of temperature with greater extent of accuracy. It is do not reach in devices without Lanne-optimum characteristics.

V. CONCLUSIONS

DTS are innovative tools which only begin to make popularity among consumers. For this reason it is necessary aspires to achievable measurement accuracy as much as possible. Up to now many DTS structures are developed with minimal influence of noise on accuracy. Many methods demand perfection of hardware. But the theory of potential pulse characteristics allows to achieve the temperature measurement near the physical limitations. Therefore, design of algorithms of signal processing raising measurements accuracy in optical DTS remains urgent.

ACKNOWLEDGMENT

Authors thank Russian Foundation for Basic Researches for financing of the project 18-37-00018 and National Research Tomsk Polytechnic University.

REFERENCES

- [1] Goncharenko A.M., Vasilev V.A., Zhmud V.A. "Method of sensitivity rise of laser vibrometers". *Avtometriya*, 2003. Vol. 39, Issue 2. P. 43–47.
- [2] P.S. Marinushkin, V.A. Bakhtina, I.A. Podshivalov et al. "Design Issues for MEMS-Based Pedestrian Inertial Navigation Systems". *Science & Education. Bauman Moscow State Technical University*. No. 06, June 2015. P. 157–173. – DOI: 10.7463/0615.0786740. – <http://dx.doi.org/10.7463/0615.0786740>.
- [3] Allwood G., Wild G., Hinckley S. "Optical Fiber Sensors in Physical Intrusion Detection Systems: A Review". *IEEE Sensors Journal*. July 2016. V. 16. № 14. P. 5497–5509. DOI 10.1109/JSEN.2016.2535465.
- [4] O.V. Stukach, I.V. Sychev. "Signal Processing in the Distributed Temperature Sensors by Raman Backscatter: Review of New Outcomes". *Radioengineering*, 2018. No 3. P. 86–92. – ISSN 0033-8486. – <http://www.radiotec.ru/number/1764> (in Russian)
- [5] Barmasov S.V., Zhmud V.A. "A phase-locked loop system for the difference frequency of two lasers". *Instruments and Experimental Techniques*. 2000. Vol. 43, Issue 3, May/June. P. 381–383.
- [6] A. Ukil, H. Braendle, P. Krippner. "Distributed Temperature Sensing: Review of Technology and Applications". *IEEE Sensors Journal*. May 2012. V. 12. No. 5. P. 885–892. DOI: 10.1109/JSEN.2011.2162060. – <http://ieeexplore.ieee.org/document/5955066/>.
- [7] B.N. Sun, J. Chang, J. Lian, Z.L. Wang, G.P. Lv, X.Z. Liu, W.J. Wang, S. Zhou, W. Wei, S. Jiang, Y.N. Liu, S. Luo, X.H. Liu, Z. Liu, S.S. Zhang. Accuracy improvement of Raman distributed temperature sensors based on eliminating Rayleigh noise impact // *Optics Communications*. 2013. V. 306. P. 117–120. <http://dx.doi.org/10.1016/j.optcom.2013.05.049>.
- [8] Kuznetsova E.Yu. "Fiber-Optic Sensor for Temperature Measurement". *Youth and Modern Information Technologies: Proceedings of the XII Conf. Tomsk, November, 12–14, 2014*. Vol. 1. P. 55–56. – <http://elibrary.ru/item.asp?id=23097467>.
- [9] O.V. Stukach, "A Novel Darlington Amplifier Optimized for Wideband". In the *Proceedings of the 1st European Wireless Technology Conference. - Wireless Technology, 2008. EuWiT 2008. European Conference on. Amsterdam, the Netherlands, 28-29 October 2008*. P. 155–157. <https://ieeexplore.ieee.org/document/4753830/>
- [10] Lanne A.A. "The Potential Characteristics of the Linear Filtering Circuits". *Moscow, Svaz*. 1974. 58 p.



Oleg V. Stukach (SM'01, IEEE, M'03, EuMA) received the Diploma degree (Hons.) in radio engineering and the Doctor of Technical Sciences degree in modeling, numerical methods, and software in 1988 and 2010, respectively. He joined the Engineering School of Infocom and Robotics in Tomsk Polytechnic University and Higher School of Economics, Moscow in 2018. He has published more than 250 technical works in microwaves, photonics, quality measurement, and theory of control.
E-mail: tomsk@ieee.org



Ivan A. Ershov (S'18) received the B.S. degree from the Tomsk Polytechnic University, Tomsk, Russia. In 2017 he is with Engineering School of Infocom and Robotics in TPU as M.S. student. He is the author of 10 papers proposed Internet of Measurement as concept of modern metrology platform. His research interests include practical and legislative metrology, statistical data analysis, optical sensors.
E-mail: zaragik@yandex.ru



Igor V. Sychev received the Engineering degree from Amur State University, Blagoveshensk, Russia and Hasso-Plattner-Institut, Potsdam, Germany. Now he is CEO of R&D "Kipline", Novosibirsk, Russia. His research interests include control systems, software development, and measurement technique.
E-mail: hr@kipline.ru

Analysis of Errors in Micromechanical Devices

Vera L. Tklich, Rimma Ia. Labkovskaia, Olga I. Pirozhnikova, Maria E. Kalinkina, Aleksei S. Kozlov
St. Petersburg National Research University of Information Technologies, Mechanics and Optics
(ITMO University), St. Petersburg, Russia

Abstract– The work is devoted to the analysis of various types of errors in micromechanical accelerometers, RR-type gyroscopes with a movable electrode, differential capacitive sensors of motion the seismic mass of a micromechanical gyroscope with compensation of external actions. Were investigated the static errors of MEMS-accelerometers of the type LSM303DLH. Were developed the algorithmic and software for modeling of experimental investigation of these errors. Were considered various methods of stability improvement of micromechanical gyroscopes to mechanical influences leading to errors. Was proposed new method for interference suppression which interfaced with non-linear changes of interstice and the effect of sticking electrodes of a flat capacitor of variable capacitance. Was evaluated the efficiency of the proposed solutions aimed at improving the accuracy of micromechanical devices.

Index Terms –Micromechanical devices, mathematical modeling, error, accelerometer, gyroscope, stability.

I. INTRODUCTION

AT THE PRESENT stage of development and improvement of microelectronics by the perspective direction development of microelectromechanical systems (MEMS) or in the English equivalent is “Micro Electro Mechanical Systems” (MEMS).

MEMS-accelerometers and micromechanical gyroscopes belong to the class of inertial sensors with a wide field of utilization: from problems of ensuring turn of the display of tablet computers to the integrated with satellite navigation systems miniature strapdown systems of determination of parameters of orientation and the coordinates of move flying, land, underwater and surface objects [1],[2].

The analysis revealed that the main causes of inaccuracy of measurements of the MEMS-accelerometer are temperature, vibration and crisscross acceleration.

Thus, changes in ambient temperature lead to changes in dielectric permittivity, as well as the size of the gap between the pendulum and the covers.

The crisscross acceleration leads to additional deformation of the elastic elements of the suspension and affects the movement of the pendulum. But since the movement of the pendulums along the y axis, they coincide with the axis of sensitivity, they are compensated by the torque sensor, without making errors. While the pendulums movements along the z axis change the effective area of the overlap of movable and stationary electrodes, which can lead to accidental error. To prevent this error, it is possible to increase the area of electrodes on the MEMS-accelerometer cover.

The most important parameters of MEMS-accelerometers are: accelerations range, sensitivity, nonlinearity in

percentages of full scale, noises, temperature drift of zero and sensitivity. The sensitivity of the accelerometer is determined by the resonant frequency of the mechanical subsystem and depends on the quality of the electronic converter. Temperature drift of sensitivity is mainly due to the change in the coefficient of elasticity, as well as thermal expansion. It is influenced by the technological errors that occur in the manufacture of the sensor [3].

II. PROBLEM DEFINITION

The physical model of the accelerometer is a inertial mass suspended on spring, with one degree of freedom along the measuring axis. The inertial mass of such accelerometer, for example, of LSM303DLH model (see Fig.1) under the action of accelerating force acquires acceleration proportional to mass m and acceleration \vec{a} . The main characteristics of these accelerometers include: supply voltage, zero offset, temperature drift, noise density and operating temperature range [4].



Fig. 1. STMicroelectronics LSM303DLH.

Features [4]

- Analog supply voltage: 2.5 V to 3.3 V
- Digital supply voltage IOs: 1.8 V
- Power-down mode
- 3 magnetic field channels and 3 acceleration channels
- ± 1.3 to ± 8.1 gauss magnetic field full-scale
- ± 2 g/ ± 4 g/ ± 8 g dynamically selectable fullscale
- 16-bit data out
- I²C serial interface
- 2 independent programmable interrupt

generators for free-fall and motion detection

- Embedded self-test
- Accelerometer sleep-to-wakeup function
- 6D orientation detection

Applications [4]

- Compensated compassing
- Map rotation
- Position detection
- Motion-activated functions
- Free-fall detection
- Intelligent power-saving for handheld devices
- Display orientation
- Gaming and virtual reality input devices
- Impact recognition and logging
- Vibration monitoring and compensation

Description

The LSM303DLH [4] is a system-in-package featuring a 3D digital linear acceleration sensor and a 3D digital magnetic sensor. The various sensing elements are manufactured using specialized micromachining processes, while the IC interfaces are realized using a CMOS technology that allows the design of a dedicated circuit which is trimmed to better match the sensing element characteristics. The LSM303DLH has a linear acceleration full-scale of $\pm 2 \text{ g} / \pm 4 \text{ g} / \pm 8 \text{ g}$ and a magnetic field full-scale of $\pm 1.3 / \pm 1.9 / \pm 2.5 / \pm 4.0 / \pm 4.7 / \pm 5.6 / \pm 8.1$ gauss, both fully selectable by the user. The LSM303DLH includes an I²C serial bus interface that supports standard mode (100 kHz) and fast mode (400 kHz). The internal self-test capability allows the user to check the functioning of the whole module in the final application. The system can be configured to generate an interrupt signal by inertial wakeup/free-fall events, as well as by the position of the device itself. Thresholds and timing of interrupt generators are programmable on the fly by the end user. Magnetic and accelerometer parts can be enabled or put in power-down mode separately. The LSM303DLH is available in a plastic land grid array (LGA) package, and is guaranteed to operate over an extended temperature range from -30 to $+85$ °C.

TABLE I
DEVICE SUMMARY

| Part number | Temp. range [°C] | Package | Packing |
|-------------|------------------|---------|---------------|
| LSM303DLH | -30 to +85 | LGA-28 | Tray |
| LSM303DLHTR | | | Tape and reel |

Fig. 2 shows a triaxial accelerometer. The sensitivity of the x and y axes, which are located in the lateral plane, is provided by the formation of a capacitance between the inertial mass, which is joined to the frame by means of elastic suspensions, and the areas under the bond sites. The sensitivity of the z axis can't be provided by these means because of the high rigidity of the elastic suspensions. To decision this problem, it is necessary to introduce a single constructive element in the form of a metal plate, which will perform the functions of a capacitive plate, an elastic metal

suspension and an anchor [5]. When the acceleration changes in the normal direction the capacitive plate deviates, while the inertial mass is deviated very little. Thus, in the role of the inertial mass, in this case, is used capacitive plate, and the inertial mass is used as a capacitive plate. All the construction is closed with a protective plate. The sensitivity of this accelerometer on the three axes is achieved by introducing only an insignificant addition in the construction, which favorably distinguishes it from similar accelerometers, which are a set of separate one-component accelerometers enclosed in a single case.

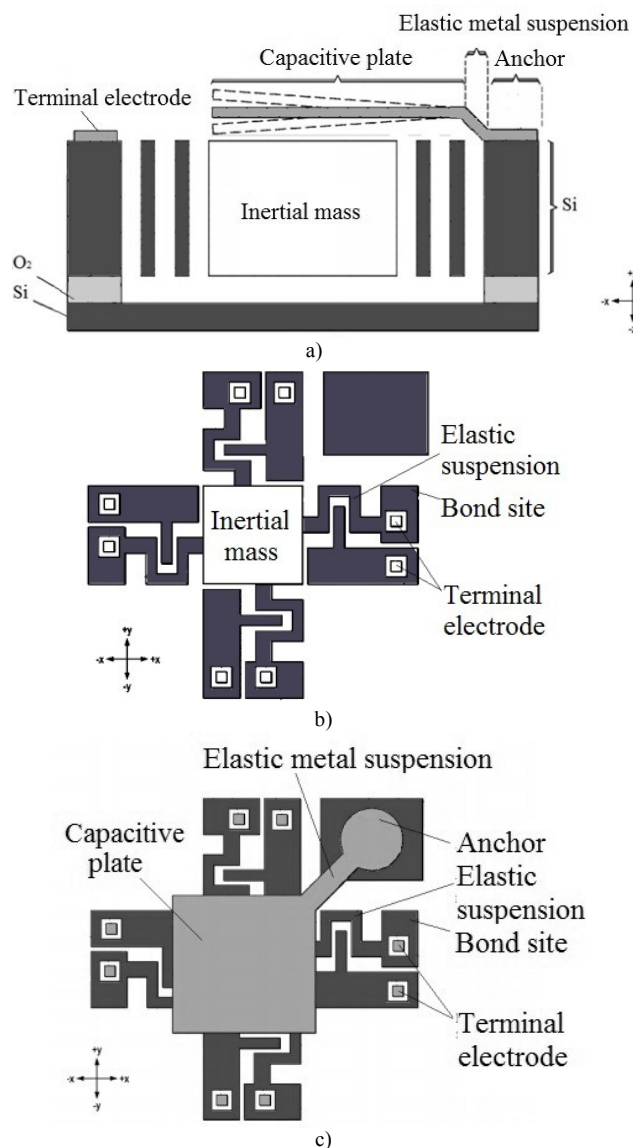


Fig. 2. Construction of the axial accelerometer: a - diagram of the device in a section; b - top view without metal plate; c - top view.

MEMS-sensors have small weight and dimensions, low power consumption and cost, high resistance to vibration and shock resistance. However, their disadvantage is not always high accuracy, which is due, among other things, the lack of adequate mathematical models of the errors of these devices [6]. For gyroscopes and accelerometers MEMS-industry main technological characteristics are: dynamic

range, sensitivity, frequency response and noise components [3]. To determine the systematic errors in calibrating it is possible to provide a sufficient degree of accuracy to fix microcircuits on the tiltrotary table, which allows to orient the axes of the accelerometers relative to the earth's axis. When calculating the systematic error, it is also necessary to take into account the factors of influence of temperature and supply voltage.

III. ERRORS OF MEMS ACCELEROMETER AND THEIR CLASSIFICATION

One of the main reasons of the error in measuring of the micromechanical accelerometer is the change in the ambient temperature [1]. The additional offset zero due to the variation of the ambient temperature can be calculated from the formula:

$$\Delta W_T = k_T \cdot \Delta T = k_T \cdot T \cdot t \quad ,$$

where k_T – thermal drift of zero shifts of accelerometers;

ΔT – temperature change during test time;

T —speed of change in temperature;

t – test time.

It is known that the accuracy of measurements is limited not only by the systematic error, but also by the spectral composition of the measurement noise. For example, MEMS sensors measure flicker-noise that stains measurement noise [3].

Accelerometers, like gyroscopes, suffer from bias and displacement drifts, errors of unequalization, drifts due to temperature and acceleration, and drift of sensitivity [1],[2]. The most important characteristics of accelerometers for their comparative analysis are displacement and its drifts, instability of displacement, and noise. Sensitivity drift and other parameters can also be taken into account.

IV. STATICERRORSCALCULATION OF THE SENSING ELEMENT

A. Cross Couplings

Whereas that in the accelerometer, the stiffness along the non-measuring axes is three orders of magnitude higher than in the measuring axis. Consequently, the displacement of the pendulum along these axes is so small that it is possible to neglect cross couplings.

B. Error of Locating Calculation of the Sensing Element

Choose the maximum error of locating $a_b = 12'$, then the sensitivity to linear accelerations along the non-measuring axes and z:

$$\Delta_{y_{max}} = \Delta_{z_{max}} = K_{CT} \cdot \cos(90 - a_h) = K_{CT} \cdot \sin a_h,$$

where

$$\Delta_{v \text{ } zmax} = K_{CT} \cdot \cos(89,8) = 3,5 \cdot 10^{-3} \cdot K_{CT}.$$

Whereas that the acceleration along the lateral axes is equal to the maximum measured acceleration (measuring range), the total relative error of locating:

$$\delta_{\Delta\Sigma} = 2 \cdot \delta_{\Delta_{y,z \max}} = 2 \cdot \frac{K_{\text{ст}} \cdot a_{y,z} \cdot \sin \alpha_{\delta}}{K_{\text{ст}} \cdot a_{\text{изм}}} \cdot 100 \% =$$

$$2 \cdot (\sin \alpha_{\bar{6}}) \cdot 100 \%,$$

where $\delta_{\Delta_{\Sigma}} = 2 \cdot \sin(0,2) \cdot 100 \% = 0,7 \%$.

C. Error of Nonlinearity Calculation of the Sensing Element

The capacitive transducer of the accelerometer (Fig. 3) is a differential capacitance $C_1 - C_2$ with one movable 1 and two fixed 2 plates. Movable plate (pendulum), supported by elastic suspension - a flat spring 3, is moved by the measured acceleration \ddot{y} an angle $\pm\alpha$ (δ_{cm} - the center of mass moving of the pendulum, l_{cm} - distance from the swing axis to the center of mass).

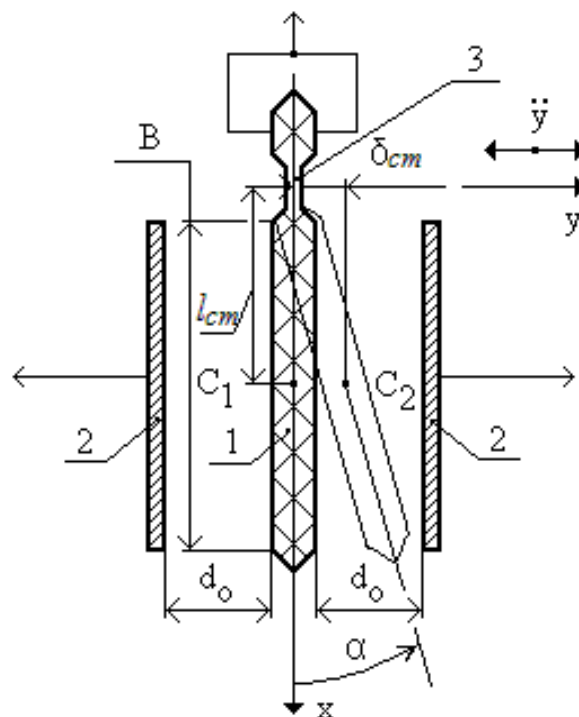


Fig. 3. Analytical model.

When the pendulum moves, the capacitances C_1 and C_2 change their values. Express the functional dependence of the values of these capacitances on the angle $\pm\alpha$ with the known design parameters of the capacitive sensing element. Capacitance of a flat capacitor:

$$C = \frac{\varepsilon \cdot \varepsilon_0 \cdot S}{d_0},$$

where $S = B \cdot b$ – plated distance, $d_0 = 20 \cdot 10^{-6}$ m – initial distance between the plates, $\varepsilon \approx 1$ – dielectric constant of the working gap filled with nitrogen N , B and b – respectively, the

length and width of the plates, $\varepsilon_0 = 8,85 \cdot 10^{-12} \text{ F/m}$ – dielectric constant.

Divide the side of the capacitance plate in length (along the axis) on n equal parts $\Delta x: B = n \cdot \Delta x$. Capacity of each part in the initial state:

$$\Delta C = \frac{\varepsilon \cdot \varepsilon_0 \cdot \Delta S}{d_0} = \frac{\varepsilon \cdot \varepsilon_0 \cdot \Delta x \cdot b}{d_0}.$$

When the middle plate deviates by an angle α all ΔS will be equal to each other, and the electric gaps between the different parts will be different.

$$\begin{aligned}\Delta S_n &= b \cdot \Delta x \cdot \cos \alpha, \\ d_n &= d_0 \pm x \cdot \sin \alpha,\end{aligned}$$

where x – distance to ΔS , signs “+” and “-” for C_1 and C_2 respectively. Dependence of the part of capacitance from the angular displacement:

$$\Delta C_{1,2} = \frac{\varepsilon \cdot \varepsilon_0 \cdot b \cdot \Delta x \cdot \cos \alpha}{d_0 \pm x \cdot \sin \alpha}. \quad (1)$$

When $\alpha < 1^\circ$ equation (1) can be simplified:

$$\Delta C_{1,2} = \frac{\varepsilon \cdot \varepsilon_0 \cdot b \cdot \Delta x}{d_0 \pm x \cdot \alpha}. \quad (2)$$

To obtain the total capacity integrate equation (2) (the limits of integration are approximately):

$$\begin{aligned}C_{1,2} &= \int_0^B \left(\frac{\varepsilon \cdot \varepsilon_0 \cdot b}{d_0 \pm x \cdot \alpha} \right) dx = \varepsilon \cdot \varepsilon_0 \cdot b \cdot \int_0^B \frac{dx}{d_0 \pm x \cdot \alpha} = \\ &= \left\{ \begin{aligned} d(d_0 \pm x \cdot \alpha) &= \pm \alpha dx, \\ dx &= \pm \frac{d(d_0 \pm x \cdot \alpha)}{\alpha} \end{aligned} \right\} = \frac{\varepsilon \cdot \varepsilon_0 \cdot b}{\pm \alpha} \cdot \int_0^B \frac{d(d_0 \pm x \cdot \alpha)}{d_0 \pm x \cdot \alpha} = \\ &= \pm \frac{\varepsilon \cdot \varepsilon_0 \cdot b}{\alpha} \cdot (\ln |d_0 \pm B \cdot \alpha| - \ln |d_0|). \end{aligned}$$

Best possible:

$$\begin{aligned}C_1 &= \frac{\varepsilon \cdot \varepsilon_0 \cdot b}{\alpha} \cdot \ln \left| 1 + \frac{B}{d_0} \cdot \alpha \right| \\ C_2 &= -\frac{\varepsilon \cdot \varepsilon_0 \cdot b}{\alpha} \cdot \ln \left| 1 - \frac{B}{d_0} \cdot \alpha \right| = \frac{\varepsilon \cdot \varepsilon_0 \cdot b}{\alpha} \cdot \ln \left| \frac{d_0}{d_0 - B \cdot \alpha} \right| \end{aligned} \quad (3)$$

Expand the equation (3) in a power series in powers α [7]:

$$\begin{aligned}C_1 &= \frac{\varepsilon \cdot \varepsilon_0 \cdot b}{\alpha} \cdot \left(\frac{B}{d_0} \cdot \alpha - \frac{B^2}{2 \cdot d_0^2} \cdot \alpha^2 + \frac{B^3}{3 \cdot d_0^3} \cdot \alpha^3 - \frac{B^4}{4 \cdot d_0^4} \cdot \alpha^4 + \dots \right) = \\ &= \frac{\varepsilon \cdot \varepsilon_0 \cdot b \cdot B}{d_0} \cdot \left(1 - \frac{B}{2 \cdot d_0} \cdot \alpha + \frac{B^2}{3 \cdot d_0^2} \cdot \alpha^2 - \frac{B^3}{4 \cdot d_0^3} \cdot \alpha^3 + \dots \right), \\ C_2 &= -\frac{\varepsilon \cdot \varepsilon_0 \cdot b}{\alpha} \cdot \left(-\frac{B}{d_0} \cdot \alpha - \frac{B^2}{2 \cdot d_0^2} \cdot \alpha^2 - \frac{B^3}{3 \cdot d_0^3} \cdot \alpha^3 - \frac{B^4}{4 \cdot d_0^4} \cdot \alpha^4 - \dots \right) = \\ &= \frac{\varepsilon \cdot \varepsilon_0 \cdot b \cdot B}{d_0} \cdot \left(1 + \frac{B}{2 \cdot d_0} \cdot \alpha + \frac{B^2}{3 \cdot d_0^2} \cdot \alpha^2 + \frac{B^3}{4 \cdot d_0^3} \cdot \alpha^3 + \dots \right) \end{aligned}$$

Differential algorithm for converting angular displacement into an electrical signal [7]:

$$\begin{aligned}U_1 &= k_{tg} \cdot (C_1 - C_2) \cdot U_{rp} = \\ &= k_{tg} \cdot \left(\frac{\varepsilon \cdot \varepsilon_0 \cdot b}{\alpha} \cdot \ln \left| 1 - \frac{B^2}{d_0^2} \cdot \alpha^2 \right| \right) \cdot U_{rp} = \\ &= -k_{tg} \cdot \left(\frac{\varepsilon \cdot \varepsilon_0 \cdot S \cdot B}{d_0^2} \cdot \left(\alpha + \frac{B^2}{2 \cdot d_0^2} \cdot \alpha^3 + \frac{B^4}{4 \cdot d_0^4} \cdot \alpha^5 + \dots \right) \right) \cdot U_{rp} \end{aligned} \quad (4)$$

Differential-logometric algorithm for converting angular displacement into an electrical signal:

$$\begin{aligned}U_2 &= k_{tg} \cdot \left(\frac{C_1 - C_2}{C_1 + C_2} \right) \cdot U_{rp} = \\ &= k_{tg} \cdot \left(\frac{\varepsilon \cdot \varepsilon_0 \cdot b}{\alpha} \cdot \ln \left| 1 - \frac{B^2}{d_0^2} \cdot \alpha^2 \right| \right) \cdot U_{rp} = \\ &= k_{tg} \cdot \left(\frac{\ln \left| 1 - \frac{B^2}{d_0^2} \cdot \alpha^2 \right|}{\ln \left| \frac{d_0 + B \cdot \alpha}{d_0 - B \cdot \alpha} \right|} \right) \cdot U_{rp} \end{aligned} \quad (5)$$

where k_{tg} – transducer gain, U_{rp} – reference potential [3].

V. DISCUSSION OF RESULTS

The differential-logometric algorithm (5) is preferred, since it eliminates multiplicative errors: the dependence of ε and geometric dimensions on temperature, and compensation of the initial unbalance of the measuring circuit is necessary for both algorithms (4) and (5). Practically complete nonlinearity (non-linearity of the third order) for a

differential-logometric algorithm is 3 times less than for a differential:

$$\delta_3(U_1) = \frac{k_3 \cdot \alpha^3}{k_1 \cdot \alpha} = \frac{1}{2} \cdot \frac{B^2}{d_0^2} \cdot \alpha^2,$$

$$\delta_3(U_2) = \frac{k_3 \cdot \alpha^3}{k_1 \cdot \alpha} = \frac{1}{6} \cdot \frac{B^2}{d_0^2} \cdot \alpha^2,$$

where k_1 and k_3 – respectively, the steepness of the static characteristic and the cubic nonlinearity coefficient of the angular displacement transducer for the expansion of the functions (4) and (5) in the power series [3].

VI. CONCLUSION

The authors developed the algorithmic and software for researching the statistical errors of the MEMS sensor using the example of the LSM303DLH micromechanical accelerometer.

The development of algorithmic support was based on the research of parameters such as standard deviation, mathematical expectation, covariance, correlation. The software was created in the Delfi 7.0 software environment for calculating parameters, as well as outputting graphs of accelerometer readings and frequency histograms for sampling observed values when testing the hypothesis of the normality of the population distribution according to Pearson's agreement criterion. The program provides information retrieval from information outputs of microcircuits, transfer of digital codes to physical quantities, writing data to data files and their static processing.

The adequacy of theoretical mathematical models [6] and analysis of static errors is confirmed by experimental data.

REFERENCES

- [1] Kalinkina M.E., Kozlov A.S., Labkovskaia R.Ia., Pirozhnikova O.I., Romanova A., Tkalic V.L. Development of mathematical model of accelerometer errors // Book of abstract of Congress of Young Scientists. Electronic issuing [Electronic resource] – http://kmu.ifmo.ru/collections_article/7178/razrabotka_matematicheskoy_modeli_pogreshnostey_akselerometra.htm
- [2] Vdovichenko M.Iu., Kalinkina M.E., Kozlov A. S., Labkovskaia R.Ia., Pirozhnikova O.I., Tkalic V.L. Analysis of errors of micromechanical gyroscopes // Book of abstract of Congress of Young Scientists. Electronic issuing [Electronic resource] – http://kmu.ifmo.ru/collections_article/7192/analiz_pogreshnostey_mikromekhanicheskikh_giroskopov.htm
- [3] Raspopov V.Ya. Micromechanical instruments: manual. - M.: Mechanical engineering, 2007. – p. 400 (in Russian).
- [4] LSM303DLH Sensor module: 3-axis accelerometer and 3-axis magnetometer // Doc ID 16941 Rev. 1, December 2009, p. 47 [Electronic resource] – <https://www.sparkfun.com/datasheets/Sensors/Magneto/LSM303%20Datasheet.pdf>
- [5] Process for manufacturing high-sensitivity capacitive and resonant integrated sensors, particularly accelerometers and gyroscopes, and sensors made therefrom, US 6090638 A.
- [6] Demin, A. Applying math modelling methods for forecasting the engineering system states – SPb.: ITMO University, 2016. — 108 c.
- [7] Rogozhin A.D. Principles of creation of integral pressure sensors // Radio-electronic and telecommunicationaly systems and devices: Interuniversity collection of scientific works. Issue 4. N - Novgorod: NGTU, 1998, pp. 101 – 109 (in Russian).

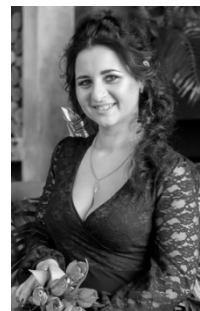


Vera L. Tkalic defended her thesis for the degree of Doctor of Technical Science on the theme: “Elastic Sensitive Elements of Control Systems: Principles of Construction, Analysis and Mathematical Modeling” in 2001 and received the degree of Doctor of Technical Sciences on specialty 05.13.05 “Elements and devices of computer facilities and control systems”.

In 2003 was promoted title of professor.

Currently during 15 years she has been working as a professor at the Faculty of Security of Information Technology at ITMO University.

List of Vera L. Tkalic scientific works exceeds 200 names (including 19 patents).



Rimma Ia. Labkovskaia defended her thesis for the degree of Candidate of Technical Science on the theme “Research and development of analysis methods statics and dynamics of membrane and plate sensing elements of sensors control systems” in 2014 and received the degree of Candidate of Technical Sciences on specialty 05.13.05 “Elements and devices of computer facilities and control systems” in 2015.

Rimma Ia. Labkovskaia works as an associate professor at the Faculty of Security of Information Technology at ITMO University.

List of Rimma Ia. Labkovskaia scientific works exceeds 100 names (including 15 patents).



Olga I. Pirozhnikova defended her thesis for the degree of Candidate of Technical Science on the theme “Development of a methodology for assessing the level of security and mathematical models of components of a comprehensive system for ensuring the security of information facilities” in 2015 and received the degree of Candidate of Technical Sciences on specialty 05.13.19 “Methods and systems of information security, information security (technical science)”. Olga I. Pirozhnikova works as an assistant at the Faculty of Security of Information Technology at ITMO University.

List of Olga I. Pirozhnikova scientific works exceeds more than 65 names (including 13 patents).



Maria E. Kalinkina graduated ITMO University in 2014. In 2016 entered the postgraduate course on specialty 05.13.05 “Elements and devices of computer facilities and control systems”, dissertation advisor – Vera L. Tkalic.

List of Maria E. Kalinkina scientific works exceeds 10 names.



Aleksei S. Kozlov after graduating Master's degree programme in ITMO University in 2015 entered the postgraduate course on specialty 05.13.05 “Elements and devices of computer facilities and control systems”, dissertation advisor – Vera L. Tkalic.

List of Aleksei S. Kozlov scientific works exceeds more than 45 names (including 6 patents).

Robust Control Algorithm for Turbine – Generator Unit

Anton V. Utkin, Victor A. Utkin

V.A. Trapeznikov Institute of Control Sciences of Russian Academy of Sciences, Moscow, Russia

Abstract – This paper presents a solution to the problems of robust control for turbine-generator system under the action of external unmatched disturbances, parametric uncertainty in the model, and an incomplete set of measuring sensors.

Index Terms – Nonlinear systems, tracking problem, turbine-generator unit, unmatched disturbances, parametric uncertainties.

I. INTRODUCTION

THE MATHEMATICAL models describing thermal power plants are multidimensional and multiply connected nonlinear dynamical systems with a large number of physical parameters that are not subject to direct measurements. In this paper we consider a nonlinear model of a steam turbine plant [1], which includes a turbine-generator aggregate and a steam supply actuator to change the turbine's power (DC motor). As external disturbances, the load of the generator and the pressure of the vapor before the valve are considered. Only the speed of rotation of the turbine unit and the corresponding driving force are measured.

At present, the algorithms for control in energy plants are based on the methods of linearization of the initial nonlinear system [2] and robust stabilization [3,4] with the subsequent analysis of the stability of the system on the basis of the Lyapunov functions. It should be noted that within the framework of these approaches it is possible to ensure the operability of the control system only in a small vicinity of the operating point. For large deviations of the phase point of the closed loop system from the steady state, the system loses its operability. This can result to emergency situations of different levels in the power systems. The use of adaptive control methods for energy systems and H_∞ [5] is difficult due to the presence of external unmatched disturbances and incomplete measurements of state variables.

In this paper, we propose a solution to the problems of robust control for turbine-generator system under the action of external, unmatched disturbances, parametric uncertainty in the model, and an incomplete set of measuring sensors. In such conditions, the solution of control problem for these objects requires the involvement and development of special methods.

The main idea of this paper is to present a mathematical model of the control plant in the form of an equivalent input-output system in a new coordinate basis of mixed variables. Mixed variables are combinations of state variables, external disturbances, reference signals and their derivatives. This

approach allows us to linearize a nonlinear model by feedback [6-9]. The block control principle in the tracking problem and methods of systems with deep feedbacks and discontinuous controls are also used in the paper. The application of these methods makes it possible to ensure robust and invariant properties of closed loop systems [10-12].

To obtain information about the state vector and variables of the linearized model, observers of states and disturbances of a special type are used [13, 14].

The paper has the following structure. Section 2 describes the model of the control plant, formalizes the formulation of the control problem. In Section 3, within the framework of the block approach, under conditions of complete certainty, decomposition procedures for the synthesis of basic laws of discontinuous control are presented, formed in terms of input-output subsystems and providing tracking of output variables for reference signals. In Section 4, for the information support of basic control laws, methods for constructing special robust observers of a state vector with piecewise linear correcting actions are presented. Observers are based on the transformed subsystems and serve for estimating mixed variables and uncertainties. Section 5 proposes continuous control algorithms for DC motor with pulse-width modulation (PWM). Section 6 presents the numerical simulation results.

II. PROBLEM DEFINITION

A mathematical model of the dynamics of a steam turbine unit includes a description of a number of physical processes [1]. The dynamics of the rotating masses is described by Newton's second law

$$J\dot{\omega} = N_1 - N_G, \quad (1)$$

where ω is the turbine speed, N_1 is the power (or torque) of the turbine, N_G is the power (or torque) of the resistance on the shaft of the turbine or on the rotor shaft of the generator, brought to the shaft of the turbine, J is the moment of inertia of the rotating masses of the unit.

To describe the process of generating a mechanical power by a steam turbine without taking into account the intermediate superheating of steam, one can use the energy balance equation:

$$T_h \dot{N}_h = -N_h + k_h P_T q_1,$$

where N_h is the output power of the unit, transmitted to the generator [MW]; T_h is the turbine time constant, determined

by the delay in the conversion of steam energy into mechanical energy; q_1 is the governor valve position; P_T is the steam pressure before the valve, which regulates the supply of steam directly to the turbine; $k_h = \text{const} > 0$.

When considering the intermediate overheating of the steam, the total power on the turbine shaft is determined by the powers transferred to the turbine shaft by a high-pressure cylinder (HPC) and a low-pressure cylinder (LPC).

The equation of power generation of LPC is introduced into the model:

$$T_l \dot{N}_l = -N_l + N_h,$$

where N_l is the generated power, T_l is the time constant.

Let $C = \text{const}$ is the fraction of the HPC power in the total power of the turbine, then the process of generating the total power $N_1 = CN_h + (1 - C)N_l$ with respect to the variables N_1 , N_l is described by equations of the form

$$\begin{aligned} \dot{N}_1 &= d_1 N_1 + d_2 N_l + g_1 P_T q_1, \\ \dot{N}_l &= d_3 (-N_l + N_1), \end{aligned} \quad (2)$$

where $d_1 = \frac{T_h - (T_l + T_h)C}{CT_h T_l}$, $d_2 = \frac{(1 - C)(C^2 T_l + T_h)}{CT_h T_l} > 0$,

$$g_1 = \frac{Ck_h}{T_h} > 0, \quad d_3 = \frac{1}{CT_l} > 0, \quad 0 < C < 1.$$

The time constant of HPC is rather small $T_h = 0,1 \div 0,3$ [s], and the time constant of LPC is an order of magnitude greater $T_l = 3 \div 7$ [s] due to the large volume of steam in the super heater.

The steam supplied to the steam turbine when opening the valve, controlled by the actuator - DC motor drive. This process is described by a system of nonlinear equations:

$$\begin{aligned} \dot{q}_1 &= q_2, \\ \dot{q}_2 &= a_{21}(q_3 q_4 - m_{L1}), \\ \dot{q}_3 &= a_{32}(-q_2 q_4 - a_{31} q_3 + u_1), \\ \dot{q}_4 &= 0, \end{aligned} \quad (3)$$

where q_1 is the angle position DC motor (governor valve), [rad]; q_2 the angular velocity, [rad/s]; q_3 is the stator current, [A]; $q_3 q_4$ is electrical moment, m_{L1} is the load moment, [Nm]; q_4 is magnetic flux, [Wb], a_{ij} are constructive coefficients of DC motor; u_1 is stator voltage, [V].

Next, we formulate the problem of joint control of a steam generator and a turbine with two cylinders, described by equations (1), (2) and (3). The purpose of the control is to ensure the rotation frequency $\omega(t)$ of the unit at a given reference value $\omega_d(t)$ with a given accuracy by maintaining a power balance in the equation of mechanical motion (1). Let $e_1(t) = \omega(t) - \omega_d(t)$ is a tracking error, then the purpose of control is to ensure

$$|e_1(t)| \leq \Delta_1 \quad \forall t > t_1^* > 0. \quad (4)$$

The models (1)-(3) can be represented as two subsystems. In the first subsystem we include the dynamics equations of the turbogenerator (1) - (2), which are write with respect to the tracking error $e_1(t)$ and supplemented by an integral link:

$$\begin{aligned} \dot{e}_0 &= e_1, \quad \dot{e}_1 = \frac{1}{J}(N_1 - N_G) - \dot{\omega}_d, \\ \dot{N}_1 &= d_1 N_1 + d_2 N_l + g_1 P_T q_1, \\ \dot{N}_l &= d_3 (N_1 - N_l). \end{aligned} \quad (5)$$

The input of a differential equation for a variable $e_0(t)$ and its further use in feedback will give the property of astaticism to a closed loop system.

In the second subsystem of the model of the turbine-generator aggregate we will write the dynamic model of the actuator (3).

The tracking problem (4) is solved in the following limiting assumptions:

1) Only the variable $e_1(t)$ is available to direct measurements, the signals $N_1(t)$, $N_G(t)$, $N_l(t)$, $\dot{\omega}_d(t)$ are bounded and unknown;

2) The parameters of the model (5) and (3) are assumed to be unknown.

These assumptions are explain the formulation of the tracking problem with a given accuracy.

III. CONTROLLER DESIGN

In this section, within the framework of the block approach [6, 7], decomposition procedures for feedback synthesis in the system (5) and (3) have been developed that provide the solution of the tracking problem with a given accuracy (4).

Step 1.1. In the second equation of the subsystem (5), the variable $(N_1 - N_G)/J$ is assumed to be a fictitious control and is selected in a form $(N_1 - N_G)/J = -k_1 e_1 - k_0 e_0 + \dot{\omega}_d$ to ensure the stability of the proper motions of the variables e_0, e_1 . We introduce a mismatch between the selected and the real fictitious control:

$$\bar{N}_1 = \frac{1}{J}(N_1 - N_G) + k_1 e_1 + k_0 e_0 - \dot{\omega}_d.$$

Taking into account the performed non-degenerate transformation of variables, the first two equations of the subsystem (5) take the form

$$\dot{e}_0 = e_1, \quad \dot{e}_1 = -k_1 e_1 - k_0 e_0 + \bar{N}_1. \quad (6)$$

Step 1.2. The stabilization problem of variable \bar{N}_1 is solved, which is described by an equation of the form

$$\dot{\bar{N}}_1 = b q_1 + f(\cdot) \quad (7)$$

where $b = \frac{g_1 P_T}{J}$,

$$f(\cdot) = \frac{1}{J}(d_1 N_1 + d_2 N_l - \dot{N}_G) + k_1 \dot{e}_1 + k_0 e_1 - \ddot{\omega}_d.$$

We choose a control in the form $q_1 = y_d$, where

$$y_d = [d_1 N_1 + d_2 N_l - \dot{N}_G + J(k_1 \dot{e}_1 + k_0 e_1 + k_2 \bar{N}_1 - \ddot{w}_d)] / g_1 P_T.$$

Taking into account the mismatch between the selected and real control

$$e_{10} = q_1 - y_d \quad (8)$$

we obtain an equation with stable proper motions:

$$\dot{\bar{N}}_1 = -k_2 \bar{N}_1 + e_{10}.$$

Thus, the subsystem (5) with closed local constraints takes the form

$$\begin{aligned} \dot{e}_0 &= e_1, \quad \dot{e}_1 = -k_1 e_1 - k_0 e_0 + \bar{N}_1, \\ \dot{\bar{N}}_1 &= -k_2 \bar{N}_1 + e_{10}, \\ \dot{N}_l &= -d_3 N_l + d_3 (J(\bar{N}_1 - k_1 e_1 - k_0 e_0 + \dot{w}_d) + N_G), \end{aligned} \quad (9)$$

where the last equation (9) can be treated as a subsystem of internal zero dynamics. Its proper motions are stable ($d_3 > 0$), therefore, the values of the variable $N_l(t)$ are bounded. This fact is a condition for the physical realizability of the tracking system [10].

At the second stage, the tracking problem in the DC motor model (3) with respect to the variable (8) is formulated

$$\begin{aligned} \dot{e}_{10} &= q_2 - \dot{y}_d, \\ \dot{q}_2 &= a_{21}(q_3 q_4 - m_{L1}), \\ \dot{q}_3 &= a_{32}(-q_2 q_4 - a_{31} q_3 + u), \\ \dot{q}_4 &= 0. \end{aligned} \quad (10)$$

Step 1. In the first equation (10) we introduce a transformation of variable $e_{20} = q_2 - \dot{y}_d + k_{10} e_{10}$, and the equation takes the form

$$\dot{e}_{10} = -k_{10} e_{10} + e_{20}. \quad (11)$$

Step 2. The second step solves the problem of stabilizing the variable e_{20} described by equation

$$\dot{e}_{20} = a_{21}(q_3 q_4 - m_{L1}) - \ddot{y}_d + k_{10} \dot{e}_{10}.$$

The next transformation of the variable $e_{30} = a_{21}(q_3 q_4 - m_{L1}) - \ddot{y}_d + k_{10} \dot{e}_{10} + k_{20} e_{20}$ converts the second equation (10) to the form

$$\dot{e}_{20} = -k_{20} e_{20} + e_{30} \quad (12)$$

Step 3. At the third step, we consider the problem of stabilizing a variable e_{30} described by equation (under the assumption that $\dot{q}_4 = 0$)

$$\dot{e}_{30} = f(\cdot) + bu, \quad (13)$$

where $b = a_{21} a_{32} q_4 > 0$ and

$$f = -a_{21} a_{32} q_4 (q_2 q_4 + a_{31} q_3) - a_{21} \dot{m}_L - \ddot{y}_{1d} + k_1 \dot{e}_1 + k_2 \dot{e}_2.$$

Control law can be selected as a discontinuous function

$$u = -M \text{sign}(e_{30}), \quad (14)$$

$$M = \text{const} > 0$$

When the amplitude of the discontinuous control (14) is sufficiently large, it is possible to organize a sliding mode in

a finite time t_c along the surface $e_{30} = 0$. This solves the tracking problem.

The conditions for the existence of a sliding mode in the last system (13), (14) have the form of an inequality $bM > f$. For the given condition for the existence of a sliding mode, it is necessary to have an upper limitation of the variable $|f| \leq F = \text{const}$ and constraint of parameter $b > b_{\min} = \text{const}$. In the close loop system (11) - (13) by feedback (14), the process of stabilization breaks up into a consecutive stabilization of the variables

$$\bar{\eta} = 0 \Rightarrow \lim_{t \geq t_c} e_{30} \rightarrow 0 \Rightarrow \lim_{t \rightarrow \infty} e_{20} \rightarrow 0 \Rightarrow \lim_{t \rightarrow \infty} e_{10} \rightarrow 0.$$

Stabilization of the variable $e_1 \rightarrow 0$ in system (9) after the stabilization of the variable $e_{10} \rightarrow 0$ also breaks up into a sequence of tasks

$$\lim_{t \rightarrow \infty} e_{10} \rightarrow 0 \Rightarrow \lim_{t \rightarrow \infty} \bar{N}_1 \rightarrow 0 \Rightarrow \lim_{t \rightarrow \infty} (e_1, e_0) \rightarrow 0.$$

To implement control law (14), it is necessary to estimate the variable e_{30} , which is obtained later using a special observer.

IV. OBSERVER DESIGN

In this section the problem of estimating e_{30} a variable by measuring the variable e_1 in the system (9) (without the last equation) and (11) - (12) is considered. Equations (9), (11) - (12) can be written in the combined form:

$$\begin{aligned} \dot{e}_0 &= e_1, \\ \dot{e}_1 &= -k_1 e_1 - k_0 e_0 + \bar{N}_1, \\ \dot{\bar{N}}_1 &= -k_2 \bar{N}_1 + e_{10}, \\ \dot{e}_{10} &= -k_{10} e_{10} + e_{20}, \\ \dot{e}_{20} &= -k_{20} e_{20} + e_{30}. \end{aligned} \quad (15)$$

With respect to the system (15), a state observer is constructed on the measured variables e_0, e_1 which makes it possible to obtain an estimate of the variable e_{30} with a given accuracy.

In this case, the variable e_{30} is regarded as a bounded disturbance $|e_{30}| \leq E_3 = \text{const}$.

Further constructions are based on an obvious result.

We consider a first-order system $\dot{x} = \eta - u$, where x is the state variable, u is a piecewise-linear bounded control of the form

$$u = M \text{sat}(\alpha x) = \begin{cases} M \text{sign} x, & |x| > \Delta; \\ \alpha x, & |x| \leq \Delta, \Delta = M / \alpha, \end{cases}$$

$$M, \alpha = \text{const} > 0; \quad |\eta(t)| \leq N, \quad |\dot{\eta}(t)| \leq N^1, \dots, |\eta^k(t)| \leq N^k,$$

$$N^{(i)} = \text{const}, \quad M > F.$$

Lemma. In the first-order system $\dot{x} = \eta - u$, in the finite time the following relations are satisfied:

$$\begin{aligned}
 1) \quad & \left| x^{(i-1)} \right| \leq \frac{N^{i-1}}{\alpha} = \delta_{i-1}, \quad i = 1, 2, \dots, k \Rightarrow |x| \leq \frac{N}{\alpha} = \delta_0, \\
 2) \quad & \alpha x^{(i-1)} = \eta^{(i-1)} - x^{(i)}, \quad \left| x^{(i)} \right| \leq \frac{N^i}{\alpha} = \bar{\delta}_i \Rightarrow \\
 & \Rightarrow \alpha x = \eta + \bar{\delta}_1, \quad \left| \bar{\delta}_1 \right| \leq \frac{N^{(1)}}{\alpha}.
 \end{aligned}$$

Proof.

1. We show that when $x(0) > \Delta$, for a finite time t_k , the variable falls into a linear zone $x(t > t_k) \leq \Delta$.

Consider the Lyapunov function candidate $V = 0.5x^2$.

Further outside the neighborhood Δ , we find its derivative and estimate.

$$\dot{V} = x(-M \operatorname{sign}(x) + \eta(t)) < -(M - N)|x| < 0,$$

$$\text{if } |x| > \Delta = \frac{M}{\alpha}.$$

Estimates of the convergence time in a linear zone are obtained in the form of successive actions with the derivative of the Lyapunov function:

$$\begin{aligned}
 \dot{V} &< -(M - N)|x| = -\sqrt{2M}V^{1/2} \Rightarrow \\
 \Rightarrow V(t) &= \left(-\frac{\sqrt{2M}}{2}t + V^{1/2}(0) \right)^2 = \Delta \Rightarrow \\
 \Rightarrow t_k &< \frac{2}{\sqrt{2M}} \left(V^{1/2}(0) - \Delta^{1/2} \right),
 \end{aligned}$$

where $\bar{M} = M - N$

2. Next we write down the derivative of Lyapunov function in the linear zone ($x(t \geq t_k) \leq \Delta$) and we estimate the neighborhood of zero outside which the Lyapunov function is negative

$$\dot{V} = x[-\alpha x + \eta(t)] \leq -\alpha x^2 + N|x| < 0 \Rightarrow |x| < \frac{N}{\alpha} = \delta_0.$$

Thus, the variable converges to a neighborhood $|x| \leq \delta_0$ that is given by an arbitrarily small choice of the slope of the saturation function α . Let us write the equation for the i -th derivative of the system $\dot{x} = \eta - u$:

$$x^{(i)} = -\alpha x^{(i-1)} + \eta^{(i-1)}.$$

Hence the first and then the second statement of the lemma are successively correct.

End of proof.

In the first stage, based on the first three equations of the system (15) and the measurements of variables $e_0(t)$, $e_1(t)$, to estimate the variable $\bar{N}_1(t)$ and the signal e_{10} , we construct a state observer of the form:

$$\begin{aligned}
 \dot{z}_1 &= -k_1 z_1 - k_0 e_0 + v_1, \\
 \dot{z}_2 &= -k_2 z_2 + v_2.
 \end{aligned} \quad (16)$$

In this case the variable e_{10} is treated as an external limited disturbance.

Corrective actions of the observer will be chosen in the form of linear functions with saturation

$$v_1 = M_1 \operatorname{sat}(\alpha_1 e_1), \quad v_2 = M_2 \operatorname{sat}[\alpha_2 (\bar{\alpha}_1 e_1 - z_2)],$$

where $\bar{\alpha}_1 = \alpha_1 + k_1$, $\bar{\alpha}_2 = \alpha_2 + k_2$

Next, we write the equations for the observation errors $\varepsilon_1 = e_1 - z_1$, $\varepsilon_2 = \bar{N}_1 - z_2$:

$$\begin{aligned}
 \dot{\varepsilon}_1 &= -k_1 \varepsilon_1 + \bar{N}_1 - M_1 \operatorname{sat}(\alpha_1 \varepsilon_1), \\
 \dot{\varepsilon}_2 &= -k_2 \varepsilon_2 + e_{10} - M_2 \operatorname{sat}[\alpha_2 (\bar{\alpha}_1 \varepsilon_1 - z_2)].
 \end{aligned} \quad (17)$$

Under the assumption

$$|\bar{N}_1(t)| \leq E_N, \quad |\dot{\bar{N}}_1(t)| \leq E_N^1, \quad |\ddot{\bar{N}}_1(t)| \leq E_N^2,$$

$|e_{10}| \leq E_{10}$, $|\dot{e}_{10}| \leq E_{10}^1$ (here and below E are known constants), and $M_1 > \bar{N}_1$, $M_2 > e_{20}$ according to the lemma, in a finite time the following relations hold:

$$\begin{aligned}
 |\varepsilon_1| &\leq \frac{E_N}{\bar{\alpha}_1}, \quad \bar{\alpha}_1 \varepsilon_1 = \bar{N}_1 - \dot{\varepsilon}_1, \\
 |\dot{\varepsilon}_1| &\leq \frac{E_N^1}{\bar{\alpha}_1}.
 \end{aligned} \quad (18)$$

In other words, the variable ε_1 with the growth of the coefficient α_1 stabilizes with a given accuracy and also the relation is satisfied $\bar{\alpha}_1 \varepsilon_1 \approx \bar{N}_1$.

The second equation (17) can be written in the form

$$\begin{aligned}
 \dot{\varepsilon}_2 &= -k_2 \varepsilon_2 + e_{10} - M_2 \operatorname{sat}[\alpha_2 (\bar{N}_1 - \dot{\varepsilon}_1 - z_2)] = \\
 &= -\bar{\alpha}_2 \varepsilon_2 + e_{10} + \alpha_2 \dot{\varepsilon}_1.
 \end{aligned}$$

and the following relations are satisfied

$$\begin{aligned}
 |\varepsilon_2| &\leq \frac{E_{10} + \alpha_2 \dot{\varepsilon}_1}{\bar{\alpha}_2} \leq \frac{E_{10}}{\bar{\alpha}_2} + \frac{\alpha_2 E_N}{\bar{\alpha}_1 \bar{\alpha}_2}, \\
 \bar{\alpha}_2 \varepsilon_2 &= e_{10} - \alpha_2 \dot{\varepsilon}_1 - \dot{\varepsilon}_2, \\
 |-\alpha_2 \dot{\varepsilon}_1 - \dot{\varepsilon}_2| &\leq \alpha_2 \frac{E_N^1}{\bar{\alpha}_1} + \frac{E_{10}^1}{\bar{\alpha}_2} + \frac{\alpha_2 E_N^2}{\bar{\alpha}_2 \bar{\alpha}_1}.
 \end{aligned} \quad (19)$$

Thus, based on the choice of amplitudes and amplification factors of corrective actions (according to relations (18) and (19), the problem of estimating of a variable e_{10} with a given accuracy from the available variable for measurement $\varepsilon_1 = e_1 - z_1$ is solved:

$$e_{10} \approx \bar{\alpha}_2 \varepsilon_2 \approx \bar{\alpha}_2 (\bar{\alpha}_1 \varepsilon_1 - z_2) \quad (20)$$

Knowing the estimation of the variable e_{10} , in the second stage the observation problem for the variable e_{30} in the model (15) is solved.

Let us construct a state observer of the form:

$$\begin{aligned}
 \dot{z}_{10} &= -k_{10} z_{10} + v_{10}, \\
 \dot{z}_{20} &= -k_{20} z_{20} + v_{20}
 \end{aligned} \quad (21)$$

The corrective actions of the observer are chosen in the form of linear functions with saturation

$$\begin{aligned}
 v_{10} &= M_{10} \operatorname{sat}(\alpha_{10} \varepsilon_{10}), \\
 v_{20} &= M_{20} \operatorname{sat}[\alpha_{20} (\bar{\alpha}_{10} \varepsilon_{10} - z_{20})].
 \end{aligned} \quad (22)$$

where $\bar{\alpha}_{10} = \alpha_{10} + k_{10}$, $\bar{\alpha}_{20} = \alpha_{20} + k_{20}$.

We write, in view of equations (16), (21), and (22), equations with respect to observation errors

$$\begin{aligned} \varepsilon_{10} &= e_{10} - z_{10}, \quad \varepsilon_{20} = e_{20} - z_{20}: \\ \dot{\varepsilon}_{10} &= -k_{10}\varepsilon_{10} + e_{20} - M_{10}\text{sat}(\alpha_{10}\varepsilon_{10}), \\ \dot{\varepsilon}_{20} &= -k_{20}\varepsilon_{20} + e_{30} - M_{20}\text{sat}[\alpha_{20}(\bar{\alpha}_{10}\varepsilon_{10} - z_{20})]. \end{aligned} \quad (23)$$

Under the assumption

$$\begin{aligned} |e_{10}| &\leq E_{10}, \quad |\dot{e}_{10}| \leq E_{10}^1, \\ |e_{20}(t)| &\leq E_{20}, \quad |\dot{e}_{20}(t)| \leq E_{20}^1, \quad |\ddot{e}_{20}(t)| \leq E_{20}^2, \\ M_{10} &> E_{20}, \quad M_{20} > e_{30} \end{aligned}$$

and according to the lemma, the relations similar to (18) and (19) hold for finite time: (we note that the system (23) is a replica of the system (17))

$$|\varepsilon_{10}| \leq \frac{E_{20}}{\bar{\alpha}_{10}}, \quad \bar{\alpha}_{10}\varepsilon_{10} = e_{20} - \dot{\varepsilon}_1, \quad |\dot{\varepsilon}_1| \leq \frac{E_{20}^1}{\bar{\alpha}_{10}} \quad (24)$$

$$\begin{aligned} |\varepsilon_{20}| &\leq \frac{E_{30} + \alpha_{20}\dot{\varepsilon}_{10}}{\bar{\alpha}_{20}} \leq \frac{E_{30}}{\bar{\alpha}_{20}} + \frac{\alpha_{20}E_{20}}{\bar{\alpha}_{20}\bar{\alpha}_{10}}, \\ \bar{\alpha}_{20}\varepsilon_{20} &= e_{30} - \alpha_{20}\dot{\varepsilon}_{10} - \dot{\varepsilon}_{20}, \\ |-\alpha_{20}\dot{\varepsilon}_{10} - \dot{\varepsilon}_{20}| &\leq \alpha_{20}\frac{E_{20}^1}{\bar{\alpha}_{10}} + \frac{E_{30}}{\bar{\alpha}_{20}} + \frac{\alpha_{20}E_{20}^2}{\bar{\alpha}_{20}\bar{\alpha}_{10}}. \end{aligned} \quad (25)$$

To construct the control law (14), we define the estimate of the variable: e_{30} : $e_{30} \approx \bar{\alpha}_{20}\varepsilon_{20} \approx \bar{\alpha}_{20}(\bar{\alpha}_{10}\varepsilon_{10} - z_{20})$ and, after substituting (20) we finally have:

$$e_{30} \approx \bar{\alpha}_{20}[\bar{\alpha}_{10}\bar{\alpha}_2(\bar{\alpha}_1\varepsilon_1 - z_2) - z_{20}]. \quad (26)$$

The resulting estimate of variable (26) is further used for the synthesis of discontinuous control (14).

The discontinuous control (14) implements directly the voltage inverter control algorithm. In practice, the electric drive DPT with key control of the inverter using the WPM scheme is often used. The reference signals in this case must satisfy the smoothness conditions. In addition, the complete servo motor drive usually includes position or speed sensors for the motor shaft, as well as stator current sensors.

In this paper, the model state variables and the parameters of the actuator (3) are not known and can not be evaluated due to the absence of sensors. The torque on the motor shaft is also not known. The synthesis of continuous controller under conditions of parametric uncertainty and the action of external disturbances is given in the next section.

V. CONTINUOUS CONTROL DESIGN

Let us return to the problem of stabilizing the system (13)

$$\dot{e}_{30} = f(\cdot) + bu, \quad (13)$$

where $b = a_{21}a_{32}q_4 > 0$,

$$f = -a_{21}a_{32}q_4(q_2q_4 + a_{31}q_3) - a_{21}\dot{m}_L - \ddot{y}_{1d} + k_1\dot{e}_1 + k_2\dot{e}_2.$$

Under the assumption that $q_4 > 0$, $|\dot{q}_4| \leq Q = \text{const}$,

$|f| \leq F = \text{const}$, $|\dot{f}| \leq F^1 = \text{const}$ we expand the state space

by introducing the integrating element $\dot{z} = v$.

Then, assuming that $u = z$ the extended system is written in the form

$$\dot{e}_{30} = f(\cdot) + bz, \quad \dot{z} = v. \quad (27)$$

When entering the transformation of variable

$$\bar{z} = z + \frac{1}{b}f(\cdot) + k_{30}e_{30}, \quad k_{30} = \text{const} > 0$$

system (27) can be rewritten as:

$$\dot{e}_{30} = -k_{30}e_{30} + \bar{z}, \quad \dot{\bar{z}} = v + g(\cdot), \quad (28)$$

where $g = \frac{1}{b}\dot{f} - \frac{\dot{b}}{b^2}f + k_{30}\dot{e}_{30}$.

Given that $b \neq 0$, $|\dot{b}|, |f|, |\dot{f}|, |\dot{e}_{30}| < \infty$ we also have the boundedness of the variable $|g| \leq E_g = \text{const}$.

With respect to system (28), the problem of stabilizing the second subsystem is posed, which can be solved in several ways.

Applying discontinuous virtual control:

$$\begin{aligned} v &= -M\text{sign}(\bar{z}), \\ M &= \text{const} > 0, \end{aligned} \quad (29)$$

when $M > E_g$ in the system (28) the sliding mode exists along the manifold $\bar{z} = 0$ and the variable $e_{30} \rightarrow 0$ converges to zero.

For realizing the control (29), it is required the estimation of the variable \bar{z} and knowledge of the constraint $|g| \leq E_g = \text{const}$.

As a reference signal to a voltage inverter operating in PWM, a variable z is used that is continuous and available for measurement.

To obtain estimates of variables z and g we construct a state observer by analogy with the ones suggested above:

$$\begin{aligned} \dot{z}_{11} &= -k_{30}z_{11} + v_{11}, \\ \dot{z}_{21} &= v + v_{21} \end{aligned} \quad (30)$$

where

$$\begin{aligned} v_{11} &= M_{11}\text{sat}(\alpha_{11}\varepsilon_{11}), \quad v_{21} = M_{21}\text{sat}[\alpha_{21}(\bar{\alpha}_{11}\varepsilon_{11} - z_{21})], \\ \bar{\alpha}_{11} &= \alpha_{11} + k_{30}. \end{aligned}$$

By (28) and (30), the equation in errors $\varepsilon_{11} = e_{30} - z_{11}$, $\varepsilon_{21} = \bar{z} - z_{21}$ has the form:

$$\begin{aligned} \dot{\varepsilon}_{11} &= -k_{30}\varepsilon_{11} + \bar{z} - M_{11}\text{sat}(\alpha_{11}\varepsilon_{11}), \\ \dot{\varepsilon}_{21} &= -M_{21}\text{sat}[\alpha_{21}(\bar{\alpha}_{11}\varepsilon_{11} - z_{21})] + g. \end{aligned} \quad (31)$$

Under the assumption

$$|\bar{z}| \leq E_{\bar{z}}, \quad |\dot{\bar{z}}| \leq E_{\bar{z}}^1, \quad |\ddot{\bar{z}}| \leq E_{\bar{z}}^2, \quad |g| \leq E_g, \quad |\dot{g}| \leq E_g^1,$$

$M_{11} > E_{\bar{z}}$, $M_{21} > E_g$ and according to the lemma, the relations similar to (18) and (19) hold for finite time:

$$|\varepsilon_{11}| \leq \frac{E_{\bar{z}}}{\bar{\alpha}_{11}}, \quad \bar{\alpha}_{11}\varepsilon_{11} = \bar{z} - \dot{\varepsilon}_1, \quad |\dot{\varepsilon}_1| \leq \frac{E_{\bar{z}}^1}{\bar{\alpha}_{10}}, \quad (32)$$

$$|\varepsilon_{21}| \leq \frac{E_g + \alpha_{21}\dot{\varepsilon}_{11}}{\bar{\alpha}_{21}} \leq \frac{E_g}{\bar{\alpha}_{21}} + \frac{\alpha_{21}E_{\bar{z}}}{\bar{\alpha}_{11}\bar{\alpha}_{21}},$$

$$\begin{aligned} \bar{\alpha}_{21}\varepsilon_{21} &= g - \alpha_{21}\dot{\varepsilon}_{11} - \dot{\varepsilon}_{21}, \\ |-\alpha_{21}\dot{\varepsilon}_{11} - \dot{\varepsilon}_{21}| &\leq \alpha_{21} \frac{E_{\bar{z}}^1}{\bar{\alpha}_{11}} + \frac{E_g^1}{\bar{\alpha}_{21}} + \frac{\alpha_{21}E_{\bar{z}}^2}{\bar{\alpha}_{21}\bar{\alpha}_{11}}. \end{aligned} \quad (33)$$

Using the relations (32) and (33), we can make the following conclusions

1. For the implementation of discontinuous virtual control (29), the estimates $\bar{z} \approx z_{21}$ are used: The amplitude of the discontinuous controller $M > E_g$ can be selected based on a highly overrated estimate E_g , since there are no physical limitations on the choice of virtual controls.
2. Using also the estimate

$$g \approx \bar{\alpha}_{21}[\bar{\alpha}_{11}\bar{\alpha}_{21}(\bar{\alpha}_{11}\varepsilon_{11} - z_{21}) - z_{21}],$$

one can design a continuous virtual control of the form

$$v = -k_{31}\bar{z} - g, \quad k_{31} = \text{const} > 0 \quad (34)$$

This solves the problem of stabilizing the system (28).

VI. EXPERIMENTAL RESULTS

For simulation we use the constant pressure P_T and the following scenario for change of variable N_G :

$$P_T = 18,18 \text{ MPa}, \quad N_G = \begin{cases} 500 \text{ MW}, & t \in [0, 60) \cup [120, 150) \\ 450 \text{ MW}, & t \in [60, 120). \end{cases}$$

Initial conditions:

$$\omega(0) = 49.5 \text{ Hz}; \quad N_{ld}(0) = 490 \text{ MW}; \quad q_i(0) = 0, i = \overline{1,3}; \quad z_{ij}(0) = 0.$$

The parameters of the plant:

$$J = 20 \text{ N/m}^2; \quad T_h = 0,2 \text{ s}; \quad T_l = 5 \text{ s}; \quad C = 0,7; \quad k_h = 30,9; \quad a_{21} = 0,5 (\text{kgm}^2)^{-1}; \quad a_{31} = 5,5 \Omega; \quad a_{32} = 2 \text{ Gn}^{-1}$$

The parameters of controller:

$$\begin{aligned} k_1 &= 0,5; k_2 = 5; k_{10} = 20; k_{20} = 30; k_{11} = 40; \\ M_1 &= 20; M_2 = 50; M_{10} = 200; M_{20} = 200; M_{11} = 500; \\ \alpha_i &= 1000, i = \overline{1,5}. \end{aligned}$$

Figures 1-5 show the transient processes of the main technological parameters of the plant.

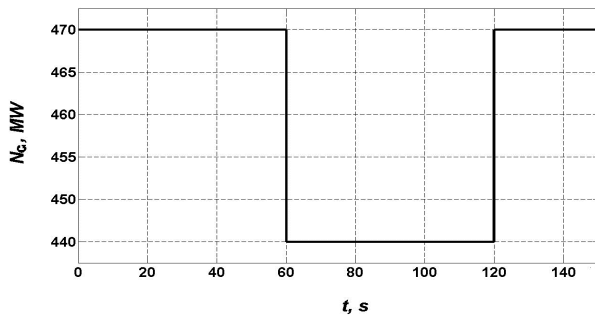


Fig.1. Simulated resistance on the shaft of the turbine.

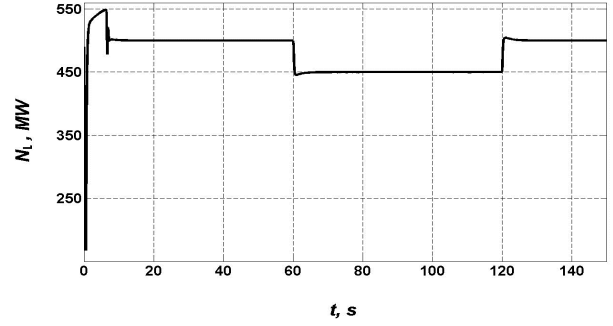


Fig.2. The generated power of the unit reaction.

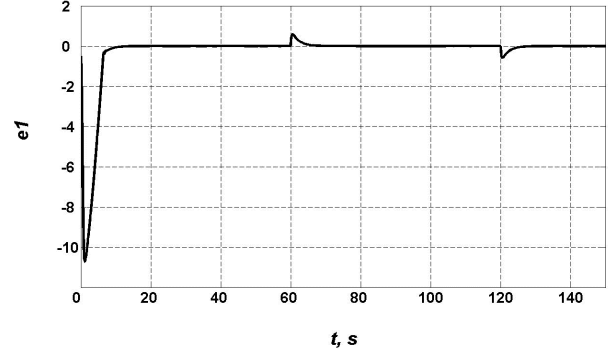


Fig.3. Tracking error transient.

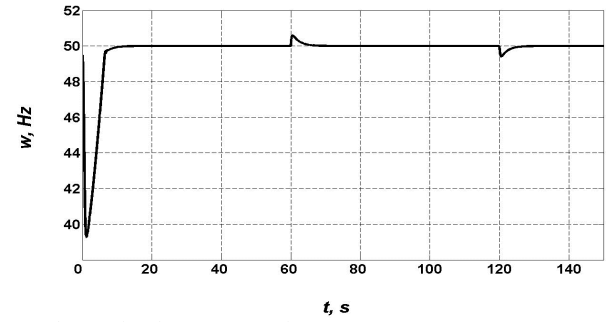


Fig.4. The rotation frequency transient.

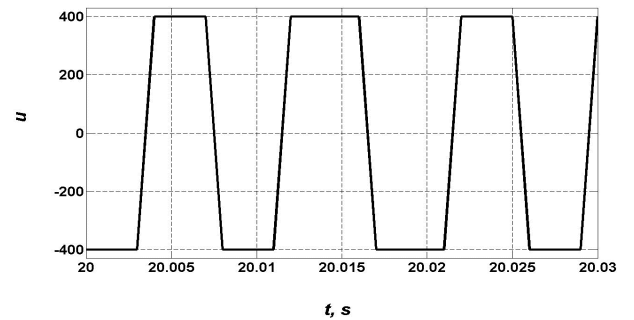


Fig.5. Discontinuous control (switching frequency is approximately 100Hz).

The analysis of transient processes shows the effectiveness of the proposed control algorithms for the turbine-generator system in the conditions of functional and parametric uncertainties of the model, and also under the influence of external disturbances and incomplete information about the state vector.

VII. CONCLUSIONS

In this paper, a new approach to the synthesis of robust and invariant systems using a block approach and special observers was demonstrated using the example of the synthesis of a control system for a steam turbine – generator unit. In the basis of the proposed control algorithms lies the representation of the initial model of the control object in the form of an input-output representation with respect to tracking errors. Further, with the aid of the special observers estimates of the state vector of the transformed system are obtained, with the use of which the controller are synthesized. It should be noted that in this paper too restrictive assumptions are made about both the control object model and the parameters available for measurement. In practice, additional information on the parameters and signals available for measurement and, in particular, the operation of protective automation should be taken into account. At present, the Russian Federation has just started to design and test high-capacity turbine – generator units. In this regard, there are no experimental data on the operation of such units in the Russian Federation. Modeling in this work was carried out using data, including experimental data, presented in foreign publications (see the list of references). In the future, the developed control algorithms can be useful in the automation of high-capacity turbine – generator units and in the Russian Federation.

ACKNOWLEDGMENT

This work is financially supported in part by the Russian Foundation for Basic Research, project no. 18-01-00846A.

REFERENCES

- [1] Merkurjev G.V., Shargin Yu.M. Stability of power systems. «Center for Training Energy Personnel». St. Petersburg. 2006.
- [2] P. W. Bolek, J. Sasiadek, T. Wisniewski. Adaptive backstepping control of a power plant station model. IFAC 15-th Triennial World Congress. 2002. pp.1650-1655.
- [3] Zheng, K., J. Bentsman, and C. W. Taft. Full Operating Range Robust Hybrid Control of a Coal-Fired Boiler/Turbine Unit. Journal of Dynamic Systems Measurement, and Control. 2008. vol. 130. no. 4, 041011-1–041011-14.
- [4] Krasnova S.A., Sirotina T.G. and Utkin V.A. A structural approach to robust control // Automation and Remote Control. 2011. Vol. 72. no. 8. pp. 1639–1666.
- [5] Tan, W., Marquez, H. J., Chen, T. and Gooden, R. K. H_∞ control design for an industrial boiler, Proceeding of ACC Conference. 2001. pp.2537-2542.
- [6] Utkin V.A. Invariance and Independence in Systems with Separable Motion // Automation and Remote Control. 2001. Vol. 62. № 11. pp. 1825–1843.
- [7] Utkin A.V. Method of state space expansion in the design of autonomous control // Automation and Remote Control. 2007. Vol. 68. № 16. pp. 1006–1022.
- [8] Krasnova S.A., Utkin V.A., Utkin A.V. Block Approach to Analysis and Design of the Invariant Nonlinear Tracking Systems //Automation and Remote Control. 2017. Vol. 78. № 12. pp. 2120–2140.
- [9] A. G. Akhobadze, S. A. Krasnova. Tracking in linear MIMO systems under external perturbations // Automation and Remote Control. 2009. Vol. 70. № 6. pp. 933–957.
- [10] Utkin V. A., Utkin A. V. Problem of Tracking in linear systems with parametric uncertainties under unstable zero dynamics // Automation and Remote Control. 2014. vol. 75. no. 9. pp. 1577–1592.
- [11] Loukianov A.G., H.Caballero-Barragan, L.Osuna-Ibarra, O.Espinosa-Guerra, B.Castillo-Toledo. Robust control for uncertain linear delay systems via sliding mode control // Int. Journal of Robust and nonlinear Control. March 2017. Vol. 89. Issue 17. pp. 4825-4845.
- [12] Alexander G. Loukianov, Jorge Rivera Dominguez, Bernardino Castillo-Toledo. Robust sliding mode regulation of nonlinear systems. Automatica. 2018 Vol. 89, 241-246.
- [13] Utkin, V.A., Method of Motion Separation in the Observation Problems //Automation and Remote Control. 1990. no. 3. pp. 27-37.
- [14] Krasnova S.A., Mysik N.S. Cascade synthesis of a state observer with nonlinear correction influences // Automation and Remote Control. 2014. vol. 75. no. 2. pp. 263–280.



Utkin Anton Viktorovich.
Candidate of technical sciences. Senior researcher of the Institute of control sciences of RAS. Author of more than 60 papers in the field of control theory.



Utkin Viktor Anatolievich.
Doctor of Technical Sciences, Professor, main researcher of the Institute of control sciences of RAS. Author of more than 210 papers in the field of control theory, including 5 monographs and 3 textbooks on mathematics.

Decomposition Principle in the Problem of Synthesis of State Observers for SISO Systems under the Action of External Disturbances

Anton V. Utkin¹, Svetlana A. Krasnova^{1, 2}

¹V.A. Trapeznikov Institute of Control Sciences of Russian Academy of Sciences, Moscow, Russia

²Bauman Moscow State Technical University, Moscow, Russia

Abstract – The problem of reference signal tracking of system's output is considered for a linear SISO system in the case of incomplete measurements and the action of external unmatched disturbances. Under the assumption of smoothness of external disturbances, the original mathematical model is presented in the equivalent quasi-canonical form of the input-output relative to the tracking error. In terms of the mixed variables of the new coordinate basis, which are linear combinations of state variables, external disturbances and their derivatives, the basic combined control law is synthesized, providing asymptotic stabilization of the tracking error invariant with respect to external disturbances. The main result of the paper is estimation method of linear combinations of unmeasured variables for feedback law under the assumption that only tracking error is measured. The problem is solved in a "narrow" setting and there is no extension of the state space, except for the observation subsystem, and the introduction of exogenous dynamic models simulating external disturbances is not required. The developed original method of synthesis of the full-dimensional observer of the state without corrective actions realizes the principle of a full decomposition. The observer setting requires the direct assignment of eigenvalues of the system coefficients matrix of observation errors. In this case the given accuracy of estimation of mixed variables and external disturbances for the basic control law is provided.

Index Terms – Tracking, external disturbances, invariance, state observer, decomposition.

I. INTRODUCTION

THE PROBLEM of synthesis of invariant tracking systems in conditions of incomplete information has a long development history and still remains relevant. The lack of sensors in the control system stimulates the development of new approaches to the synthesis of state observers, and also observers of external disturbances. The developed section of the theory of invariance consists of methods of dynamic compensation [1, 2], based on the extension of the state space by introducing a model of an exogenous system that describes the dynamics of external disturbances, and the use of estimates of its variables for the synthesis of feedback. The known methods for solving the observation problem in the presence of external disturbances suggest the use of a generator of disturbances and can be supplemented by adaptation algorithms under parametric uncertainty of the exogenous model [3–4]. These methods can't be used for control plants with significantly varying disturbances.

In this paper, the problem of synthesis of an invariant tracking system in relation to a linear one-dimensional control plant in the conditions of incomplete information is considered in a "narrow" setting, i.e., there is no other expansion of the state space, except for the observation subsystem, and the introduction of exogenous dynamic models simulating external disturbances is not provided.

In the considered system the relative degree of external disturbances is less than the relative degree of control, i.e. there is a case of so-called unmatched disturbances that do not belong to the control space [5]. This means that external disturbances are not directly compensable, and the disturbed system is not observable with respect to measurements only of the output variable [6–8]. Description of the control plant model and problem statement are given in section 2.

Under incomplete measurements, the synthesis of a closed-loop feedback system includes two aspects. In section 3(a), a procedure is developed for the synthesis of the basic law of combined control in terms of the equivalent input-output model, composed with respect to the tracking error under the assumption of the smoothness of external disturbances. It is essential that in the new coordinate basis of mixed variables, that are linear combinations of state variables, external disturbances and their derivatives, the relative degree of disturbances not involved in the transformations and the relative degree of control are the same. This means that the external disturbances will be compensated directly (in the presence of their estimates), and the system becomes observable with respect to tracking error [5, 8].

Section 3(b) presents the main result. For estimation of mixed variables and disturbances the decomposition synthesis of the state observer without corrective actions on the basis of the transformed system is developed. This approach is based on the principle of constructing a low-dimensional observer [9], which was transform to full decomposition in [10] and, in the presence of disturbances, makes it possible to obtain estimates of non-measurable variables with a given accuracy by directly assigning eigenvalues of the coefficient matrix of the system written with respect to observation errors. The new result is full-dimensional observer design of the specified type. It is shown that the current estimates of the external disturbances (without its dynamic model) with any given accuracy can be obtained by measuring only observation errors.

II. PROBLEM DEFINITION

A mathematical model of a linear stationary dynamical SISO system is

$$\dot{x} = Ax + bu + Q\eta, y_1 = d^T x, \quad (1)$$

where $x \in R^n$ is state vector, $u \in R$ is the control input, $y_1 \in R$ is output (measured and controllable) variable, $\eta \in R^p$ is external disturbance vector, $A \in R^{n \times n}$, $Q \in R^{n \times p}$, $b, d \in R^{n \times 1}$ are matrices and vectors with known constant elements, $b \neq \vec{0}$, pair (d^T, A) is observable, i.e.

$$H_{n \times n} = \begin{pmatrix} d^T \\ d^T A \\ \dots \\ d^T A^{n-1} \end{pmatrix}, \det H \neq 0. \quad (2)$$

Let us consider the problem of synthesis of combined feedback of state and disturbances for tracking problem for output variable $y_1(t)$ with reference signal $g(t)$ under the following assumptions:

1) only output variable $y_1(t)$ is measured without any noises;

2) external disturbances $\eta(t) = \text{col}(\eta_1(t), \dots, \eta_p(t))$ assumed to be unknown, smooth bounded time functions with bounded derivatives in general case of up to n -th order:

$$|\eta_j^{(i)}(t)| \leq Q_{ij} \quad \forall t \geq 0, i = \overline{0, n}; j = \overline{1, p}; \quad (3)$$

3) $g(t)$ – smooth bounded time function with bounded derivatives of up to $(n+1)$ -th order:

$$|g^{(i)}(t)| \leq G_i \quad \forall t \geq 0, i = \overline{1, n+1}. \quad (4)$$

Function $g(t)$ is not known, there are only its current values, and as a consequence, there is no current information about its derivatives. In inequalities (3)–(4) Q_{ij}, G_i are positive constants, which are chosen for the worst case scenario;

4) relative degree of inputs $v_u \in N$ of system (1) (minimum order of y_1 input derivative with respect to system (1) that contains explicit input summand):

$$v_u = \min \{i \in \overline{1, n} : d^T A^{(i-1)} b \neq 0\} = n. \quad (5)$$

Assumption (5) is introduced to simplify the presentation of the main result – the synthesis of the observer in the presence of external disturbances. The proposed approach can be extended to the more general case of systems (1) with a lower relative degree $1 \leq v_u < n$ where variables of internal dynamics are bounded either by problem statement or by feedback [11];

5) relative degree with respect to external disturbances $v_\eta \in N$ of system (1) (minimum order of y_1 input derivative with respect to system (1) that contains

disturbance summand) is lower than relative degree with respect to input:

$$v_\eta = \min \{i \in \overline{1, n} : d^T A^{(i-1)} Q \neq \vec{0}\}, 1 \leq v_\eta < v_u = n. \quad (6)$$

The matching condition

$$\text{rank } b = \text{rank}(b \ Q) = 1 \quad (7)$$

is not performed, and external disturbances can't be directly compensated. Under the assumptions made, the solution of the problem involves two aspects:

1) synthesis of the basic law of combined control in the conditions of full measurement of variables, external disturbances and their derivatives;

2) information support of the basic control law by obtaining current estimates of the state variables and external disturbances that are required for feedback synthesis with the help of the state observer using only measurements of tracking errors:

$$e_1(t) = y_1(t) - g(t), e_1 \in R. \quad (8)$$

III. THEORY

A. Basic Combined Control Law Synthesis

A constructive method for solving the tracking problem is a nonsingular transformation of the system variables (1), that leads to an equivalent input-output model that directly reflects the relationship of the input and output variables, and further synthesis of the feedback on the variables of the new coordinate basis [1–3, 5, 8]. This method is used as the basis for further constructions and the central premise is assumption of smoothness not only of the reference signal (4), but of external disturbances (3). This fact makes it possible to involve external disturbances in non-degenerate transformations to a new coordinate basis of mixed variables and to obtain an equivalent input-output model taking into account smooth disturbances. By virtue of (2), (5) there is a transformation of variables

$$y = Hx + \bar{H}\eta_{n-1}^* = H(x + A_\eta \eta_{n-1}^*), \quad (9)$$

where $\eta_{n-1}^* = \text{col}(\eta, \dot{\eta}, \dots, \eta^{(n-2)})$, $y = \text{col}(y_1, \dots, y_n)$, $y_i = y_1^{(i-1)}$,

$$\bar{H}_{n \times q(n-1)} = \begin{pmatrix} 0 & 0 & \dots & 0 & 0 \\ d^T Q & 0 & \dots & 0 & 0 \\ d^T A Q & d^T Q & \dots & 0 & 0 \\ \dots & \dots & \dots & \dots & \dots \\ d^T A^{n-3} Q & d^T A^{n-4} Q & \dots & d^T Q & 0 \\ d^T A^{n-2} Q & d^T A^{n-3} Q & \dots & d^T A Q & d^T Q \end{pmatrix},$$

by means of which system (1) is reduced to a quasi-canonical form of the input-output type

$$\dot{y}_i = y_{i+1}, i = \overline{1, n-1}; \dot{y}_n = a^T y + q_n^T \eta_n^* + b_n u, \quad (10)$$

$$a^T = d^T A^n H^{-1} = (a_1 \ a_2 \ \dots \ a_n), b_n = d^T A^{n-1} b \neq 0,$$

$$q_n^T \eta_n^* = q_n^{*T} \eta_n^* - d^T A^n H^{-1} \bar{H} \eta_{n-1}^*,$$

$$\eta_n^* = \text{col}(\eta, \dot{\eta}, \dots, \eta^{(n-2)}, \eta^{(n-1)}),$$

$$q_n^{*T} = (d^T A^{n-1} Q \quad d^T A^{n-2} Q \quad \dots \quad d^T A Q \quad d^T Q).$$

In system (10) the matching conditions similar to (7) are satisfied, i.e. the linear combination of external disturbances $q_n^T \eta_n^*$ belongs to the control space and can be compensated by the combined control if their current estimates are obtained. Due to the canonical structure of system (10), the procedure for the synthesis of the tracking system is quite obvious. The system (10) for tracking error (8) and its derivatives is as follows

$$e_i = y_i - g^{(i-1)}, i = \overline{1, n}: \quad (11)$$

$$\dot{e}_i = e_{i+1}, i = \overline{1, n-1}; \dot{e}_n = a^T e + f(t) + b_n u, \quad (12)$$

where $e = \text{col}(e_1, \dots, e_n)$ is the state vector; $g_n^* = \text{col}(g, \dot{g}, \dots, g^{(n)})$, $c^T = (a^T \quad -1)$. Linear combination of inputs $f(t) = c^T g_n^* + q_n^T \eta_n^*$ is treated as external disturbance; equations (3)–(4) define limitations

$$|f(t)| \leq F, |\dot{f}(t)| \leq F_1. \quad (13)$$

The canonical system (12) is easy for the synthesis of combined feedback. Vector a^T components match with the coefficients of the characteristic polynomial of the matrix of the system, and with the help of the stabilizing component of the control action they can be corrected. External disturbance $f(t)$ are matched and if there are current estimates, it can be compensated directly. The basic law of combined control

$$u = -b_n^{-1} (f + (a^T + k^T) e) \quad (14)$$

leads to closed loop system $\dot{e}_i = e_{i+1}$, $i = \overline{1, n-1}$, $\dot{e}_n = -k^T e$, where by vector $k_{1 \times n}^T$ the spectrum of the closed-loop system matrix is provided, which determines the desired characteristics of the tracking error stabilization

$$\lim_{t \rightarrow +\infty} e_i(t) = 0. \quad (15)$$

Let us emphasize once again that in this argumentation the assumption of smoothness of external disturbances was the determining factor and it allowed us to extend the class of systems in which it is possible to provide equation (15) invariant in asymptotic to the action of external disturbances. In the case of nonsmooth disturbances, the substitution of variables (9), (11) is not valid, and the requirement to comply with the matching condition is necessary to ensure (15), (7) or in general case $\nu_u \leq \nu_\eta$. If these conditions are not met, it is possible to provide only ε -invariance of the output variable to external disturbances provided that all state variables are directly measurable [12].

The following section presents the original method of synthesis of the observer of mixed variables and disturbances of system (12). Note that these constructions can be extended to nonlinear SISO systems, led to the form (12) [5].

B. Decomposition Synthesis of Combined Variables and External Disturbances Observer

In order to implement the basic law of combined control it is necessary to obtain current estimates of external disturbances and their derivatives g_n^* , η_n^* and combined variables (11) or its components as well.

In the presence of external unmatched disturbances in the case of (5)–(6) variables of the system (1) are unobservable relative to measurements y_1 [6–7]. So we can't solve the problem of estimating the state variables and external disturbances separately on the basis of system (1) without the input of exogenous dynamic models of reference signals and disturbances [1–3]. The use of generator of reference signals is quite common in practice. But the formation of adequate dynamic model that simulates external disturbances is not possible if the parameters of the operation of the control object change significantly.

On the other hand, quasi-canonical form (12) is observed with respect to tracking error measurements (8). In this regard, a new concept emerged: to obtain estimates of mixed variables directly using a state observer based on transformed system (12). The use of special corrective actions in this observer (in the form of discontinuous functions and the organization of the sliding mode or their pre-limit implementations in the form of S-shaped continuous, limited functions) makes it possible without expanding the state space to solve the problem of estimation external disturbances concentrated in the last equation of system (12) [5–6, 8, 10–11]. In these observers the method of motion separation is realized and by means of the choice of parameters of corrective actions on the basis of inequalities consistently, from top to down stabilization of observation errors and their derivatives are provided. Corrective actions of the current equation are used for forming of corrective action in the following block. Simulation results illustrate the proposed approach effectiveness. However, the eigenvalues of observation errors at the beginning of the transient process are unstable. The estimation of the variables causes some computational difficulties and leads to overestimated lower estimates when choosing parameters of corrective actions of the observer. In the following section we propose an original approach to the synthesis of state observers for systems (12) based on the principle of full decomposition. In this case, the observer will not contain the above-mentioned shortcomings. The basis for the state observer design is system (12), previously reduced to a special quasi-triangular form with specified eigenvalues on the main diagonal.

Lemma 1. By nonsingular coordinate transformation

$$s = Te, \det T \neq 0, \quad (16)$$

where the transition matrix has a lower triangular form

$$T_{n \times n} = \begin{pmatrix} 1 & 0 & 0 & \dots & 0 & 0 \\ -l_2 & 1 & 0 & \dots & 0 & 0 \\ a_{31} & -l_3 & 1 & \dots & 0 & 0 \\ \dots & \dots & \dots & \dots & \dots & \dots \\ a_{n1} & a_{n2} & a_{n3} & \dots & -l_n & 1 \end{pmatrix},$$

$$a_{n,n-2} = (a_n - l_n)(-l_n) - a_{n-1}, \quad (17)$$

$$a_{n,n-j} = (a_n - l_n)a_{n,n-j+1} - a_{n-j+1}, j = \overline{3, n-1};$$

$$a_{i,i-2} = (l_{i+1} - l_i)(-l_i) + a_{i+1,i-1},$$

$$a_{i,i-j+1} = (l_{i+1} - l_i)a_{i,i-j+2} + a_{i+1,i-j+2},$$

$$i = \overline{n-1, 4}, j = \overline{4, n-1}; a_{31} = (l_4 - l_3)(-l_3) + a_{42},$$

system (12) can be presented as

$$\dot{s}_1 = l_2 s_1 + s_2, \quad \dot{s}_i = l_{i1} s_1 - (l_i - l_{i+1}) s_i + s_{i+1}, i = \overline{2, n-1};$$

$$\dot{s}_n = l_{n1} s_1 - (l_n - a_n) s_n + f + b_n u, \quad (18)$$

where $l_{21} = (l_2 - l_3)(-l_2) - a_{31}$;

$$l_{i1} = (l_i - l_{i+1}) a_{i1} - a_{i+1,1}, i = \overline{3, n-1}; \quad (19)$$

$$l_{n1} = (l_n - a_n) a_{n1} + a_1.$$

Statement of Lemma 1 can be proven directly by providing the transformation $TAT^{-1} = \bar{A}$, where A is Frobenius matrix of system (12) with elements $a^T = (a_1 \ a_2 \ \dots \ a_n)$ in the last row, \bar{A} is uppertriangle matrix of the system (18) with non-zero first column. In transition matrix (17) elements $a_{ij}, i = \overline{3, n}, j = \overline{1, i-2}$ are chosen in a special way to provide in matrix \bar{A} elements from i -rows and j -columns $i = \overline{3, n}, j = \overline{2, i-1}$, to be equal to zero. Parameters $l_i > 0$ ($i = \overline{2, n}$) are chosen as high gains at the observer synthesis stage.

Transformation (16)–(18) is a simplified analogue of transformation from [10] for linear systems that are presented in block observation form with respect to output vector and it is the evolution of lower dimension Luenberger observer design method [9] that provide full decomposition of the procedure of synthesis of the observer for perturbed system. Our goal is to obtain estimates not only of the transformed state variables, but also of the external disturbances. Therefore, in contrast to [10], it is proposed to construct an observer of full dimension on the basis of system (18) without corrective actions, but with compensation of the measured variable $s_1 = e_1$:

$$\dot{z}_1 = l_2 z_1 + z_2 + l_1 (s_1 - z_1),$$

$$\dot{z}_i = l_{i1} s_1 - (l_i - l_{i+1}) z_i + z_{i+1}, i = \overline{1, n-1}; \quad (20)$$

$$\dot{z}_n = l_{n1} s_1 - (l_n - a_n) z_n + b_n u,$$

where $z_i \in R$ ($i = \overline{1, n}$) are observer state variables. With respect to (18), (20) we get equations system for observation errors $\varepsilon_i = s_i - z_i \in R$ with uppertriangle matrix

$$\dot{\varepsilon}_i = -(l_i - l_{i+1}) \varepsilon_i + \varepsilon_{i+1}, i = \overline{1, n-1}; \quad (21)$$

$$\dot{\varepsilon}_n = -(l_n - a_n) \varepsilon_n + f(t),$$

where eigenvalues are on the main diagonal. The problem of state observer synthesis is reduced to the stabilization of system (21) by the choice of parameters $l_i, i = \overline{1, n}$. It can be shown that due to the structure of system (21) in this problem the principle of complete decomposition is realized.

Lemma 2. Let in system (21) the condition (13) to be

satisfied. Then for any finite initial conditions $\varepsilon_i(0) < \infty$

($i = \overline{1, n}$) $\exists t_1 > 0: \forall t > t_1$ stabilization of system variables (21) is provided with a given accuracy

$$|\varepsilon_i(t)| = |s_i(t) - z_i(t)| < \Delta_i \quad \forall t > t_1, i = \overline{n, 1} \quad (22)$$

with sequential selection of parameters $l_i > 0, i = \overline{n, 1}$ to fulfill inequalities

$$l_n > \frac{F}{\Delta_n} + a_n, \quad (23)$$

$$l_i > \frac{F}{(l_{i+1} - l_{i+2}) \dots (l_{n-1} - l_n)(l_n - a_n) \Delta_i} + l_{i+1}, i = \overline{n-1, 1}.$$

The statement of Lemma 2 follows from the analysis of the solutions of system (21). It is obvious that when the necessary conditions

$$l_i > l_{i+1}, i = \overline{1, n}, l_{n+1} := a_n \quad (24)$$

are met for variables of system (21), the following estimates

$$|\varepsilon_n(t)| \leq \frac{F}{l_n - l_{n+1}} + \alpha_n(t); \quad (25)$$

$$|\varepsilon_i(t)| \leq \frac{|\varepsilon_{i+1}|}{l_i - l_{i+1}} + \alpha_i(t), i = \overline{n-1, 1}$$

are valid, where $\alpha_i(t) = |\varepsilon_i(0)| \exp(-(l_i - l_{i+1})t)$ are infinitesimals of different orders if $t \rightarrow +\infty$: $\lim_{t \rightarrow +\infty} \alpha_i(t) = 0$. So there are time moments

$t_1 > t_2 > \dots > t_n > 0$, when observer parameters are chosen in the form of (23) conditions (22) are successively executed:

$$|\varepsilon_n(t)| < \frac{F}{l_n - l_{n+1}} < \Delta_n \quad \forall t > t_n > 0;$$

$$|\varepsilon_i(t)| < \frac{\Delta_{i+1}}{l_i - l_{i+1}} < \frac{F}{(l_i - l_{i+1}) \dots (l_n - l_{n+1})} < \Delta_i$$

$$\forall t > t_i > t_{i+1}, n = \overline{n-1, 1}.$$

The synthesis procedure is decomposed into successively solvable one-dimensional tasks, and the estimation of the state of system (18) is provided with given accuracy (22).

To obtain estimates of the combined variables of system (12) from the control law (14), it is necessary to perform the real time inverse transformation with direct measurements $e_1 = s_1$ in order to reduce errors in estimating the system state variables (12) in the form of:

$$e(t) \approx T^{-1} \bar{z}(t) = T^{-1}(s(t) - \bar{\varepsilon}(t)), \quad (26)$$

where $\bar{z} = \text{col}(s_1, z_2, \dots, z_n)$, $\bar{\varepsilon} = \text{col}(0, \varepsilon_2, \dots, \varepsilon_n)$, vector $T^{-1} \bar{\varepsilon}$ defines estimation accuracy e_2, \dots, e_n .

Let us present the main result. We will show that using an observer (20) we can also obtain estimate of the external disturbance $f(t)$ without involving its dynamical model.

Lemma 3. Let condition (13) to be satisfied in system (21). Then for any finite initial conditions $\varepsilon_i(0) < \infty$ ($i = \overline{1, n}$) $\exists t_0 > t_1: \forall t > t_0$ the following assessment is made:

$$|f(t) - l^* \varepsilon_1(t)| \leq \Delta_0 \quad (27)$$

where $l^* = (l_1 - l_2)(l_2 - l_3) \dots (l_n - a_n)$,

$$\Delta_0 \leq F_1 \left(\frac{1}{l_1 - l_2} + \frac{1}{l_2 - l_3} + \dots + \frac{1}{l_n - a_n} \right). \quad (28)$$

Proof. From system (21) it follows that

$$\varepsilon_i = \frac{\varepsilon_{i+1} - \dot{\varepsilon}_i}{l_i - l_{i+1}}, \quad i = \overline{2, n-1}; \quad \varepsilon_n = \frac{f(t) - \dot{\varepsilon}_n}{l_n - a_n}.$$

Substituting these expressions into the first equation of system (21), we obtain the relations for the disturbance $f(t)$, measured observation error $\varepsilon_1(t) = e_1(t) - z_1(t)$ and observation errors' derivatives from system (21):

$$\begin{aligned} f = & (l_1 - l_2)(l_2 - l_3) \dots (l_n - a_n) \varepsilon_1 + \\ & + (l_2 - l_3)(l_3 - l_4) \dots (l_n - a_n) \dot{\varepsilon}_1 + \\ & + (l_3 - l_4)(l_4 - l_5) \dots (l_n - a_n) \dot{\varepsilon}_2 + \dots + (l_n - a_n) \dot{\varepsilon}_{n-1} + \dot{\varepsilon}_n. \end{aligned} \quad (29)$$

Variable $v(t) = l^* \varepsilon_1(t)$, that can be interpreted as a virtual corrective action for the observer (20), serves as an evaluation of the disturbance (27). To determine the accuracy of the estimation, we perform an analysis of the solutions of the auxiliary system describing the dynamics of the derived observation errors:

$$\begin{aligned} \ddot{\varepsilon}_i = & -(l_i - l_{i+1}) \dot{\varepsilon}_i + \dot{\varepsilon}_{i+1}, \quad i = \overline{1, n-1}; \\ \ddot{\varepsilon}_n = & -(l_n - a_n) \dot{\varepsilon}_n + \dot{f}(t). \end{aligned}$$

For the variables of this system the estimates similar to (25) are available. Therefore, there is such time moment $t_0 > t_1$, that $\forall t > t_0$ conditions $|\dot{\varepsilon}_n(t)| < F_1 / (l_n - a_n)$,

$$|\dot{\varepsilon}_i(t)| < \frac{F_1}{(l_i - l_{i+1})(l_{i+1} - l_{i+2}) \dots (l_n - a_n)}, \quad i = \overline{n-1, 1}$$

are met. After substituting these estimates into the expression (29), we obtain (28). Taking into account (26), (27) in closed loop systems with a state observer (20), the basic law of combined control is realized in the form of

$$u = -b_n^{-1} (l^* (e_1(t) - z_1(t)) + (a^T + k^T) T^{-1} \bar{z}(t)) \quad (30)$$

and due to (22), (28) is not providing (15), but providing closed loop system $\dot{e}_i = e_{i+1}$, $i = \overline{1, n-1}$, $\dot{e}_n = -k^T e + \varphi(t)$,

where $|\varphi(t)| \leq |b_n^{-1}| (l^* \Delta_0 + |(a^T + k^T) T^{-1} \bar{e}(t)|)$, and solving tracking problem with a given accuracy

$$|e_1(t)| \leq \delta \quad \forall t > t_0. \quad (31)$$

Thus, when assigning the accuracy of the observation (22), attention should be paid to (26), (28) and to the technical requirements for the accuracy of the tracking system in the established mode (31).

Let's give an algorithm for setting up proposed observer.

1. To determine estimates of the disturbance and its derivative (13).

2. Assign the accuracy of evaluation of the converted variables (22), select big coefficients based on inequalities (23) and taking into account (28).

3. For l_i , $i = \overline{1, n}$ calculate the transition matrix elements

(17), compose the inverse matrix T^{-1} and evaluate the accuracy of the tracking (31). If estimate (31) satisfies the technical requirements, proceed to clause 4, otherwise return to clause 2. For small dimension systems the closed loop analysis can be carried out using analytical expressions, and for systems of large dimension it is easier to perform numerical analysis via appropriate software.

4. Calculate correction gains (19) and synthesize an observer (20).

5. Synthesize feedback law with the output values and variables of the observer in form (30).

VI. CONCLUSION

The proposed method of synthesis of the state and disturbance observer without dynamic model of the external disturbances, based on the complete systems decomposition, provides easy parameters adjustment and seems promising. This method can be extended to linear and nonlinear systems with many inputs and many outputs if the model can be represented as a component of the input-output, similar to (12). The main disadvantage of the method is the need for an accurate knowledge of the parameters of the control object. This can be overcome by another management law based on suppression of external disturbances instead of accurate compensation. Another way of improving the method is the variation of observer dimension (20), namely, lowering, if it is not necessary to restore external disturbances or, conversely, to increase dimension due to fictitious dynamics of the derivative of the last variable.

The work is partially supported by RFBR project 18-01-00846A.

REFERENCES

- [1] Wonham W.M. Linear Multivariable control: a geometric approach. – New York: Springer-Verlar, 1979. – 356 p.
- [2] Utkin V.A., Utkin V.I. Design of invariant-system by the method of separation of motions // Automation and Remote Control, 1983. V. 44. No. 12. pp. 1559–1668
- [3] Fradkov A.L., Miroshnik I.V., Nikiforov V.O. Nonlinear and adaptive control of complex systems. – Dordrecht: Kluwer Academic Publ., 1999. – 510 p.
- [4] Glumov V.M., Zemlyakov S.D., Rutkovskii V.Y. Adaptive coordinate-parametric control for nonstationary plants: Certain results and development trends // Automation and Remote Control, 1999. V. 60. No. 9. pp. 839–851.
- [5] Krasnova S.A., Utkin A.V. Analysis and synthesis of minimum phase nonlinear SISO systems under external unmatched perturbations // Automation and Remote Control, 2016. V. 77. No. 9. pp. 1665–1675.
- [6] Krasnova S.A. Cascade design of the state observer for nonlinear systems in the presence of external perturbation // Automation and Remote Control, 2003. V. 64. No. 1. pp. 1–22.
- [7] Floquet T., Barbot J.P. An observability form for linear system with unknown inputs // Int. J. Control, 2006. No. 79. pp. 132–139.
- [8] Akhobadze A.G., Krasnova S.A. Tracking in linear MIMO systems under external perturbations // Automation and Remote Control, 2009. V. 70. No. 6. pp. 933–957.
- [9] Luenberger D.B. Observers of multivariable systems // IEEE Transactions on Automatic Control, 1966. V. AC-11. pp. 190–197.
- [10] Utkin V.A. Method of separation of motions in observation problems // Automation and Remote Control, 1990. V. 51, No. 3. pp. 300–308.

- [11] Utkin V.A., Utkin A.V. Problem of tracking in linear systems with parametric uncertainties under unstable zero dynamics // Automation and Remote Control, 2014. V. 75. No. 9. pp. 1577–1592.
- [12] Utkin V.A. Invariance and independence in systems with separable motion // Automation and Remote Control, 2001. V. 62. No. 11. pp. 1825–1843.



Utkin Anton Viktorovich.

Candidate of technical sciences. Senior researcher of the Institute of control sciences of RAS. Author of more than 60 papers in the field of control theory.



Krasnova Svetlana Anatolyevna.

Doctor of Technical Sciences, Chief Researcher, V.A. Trapeznikov Institute of Control Sciences RAS; Professor, Bauman Moscow State Technical University. Research interests: sliding modes; the theory of state observers; electromechanical systems, block approach to the analysis and synthesis for control systems of various purposes under incomplete information. Author and co-author over 200 scientific and methodical works.

Reduction of the Matrix Polynomial Decomposition of the Transfer Function to a Coprime form Using the Sylvester Matrix

Alexander A. Voevoda, Kurbonmurod M. Bobobekov
Novosibirsk State Technical University, Novosibirsk, Russia

Abstract – Is considered bringing of the matrix polynomial decomposition of the transfer function of the object to a coprime form. Violation requirements coprime decomposition leads to the appearance in the same roots "numerator" and "denominator" as in single-channel systems and in multi-channel systems. To check on the relatively coprime compiled of the system of linear homogeneous equations: in other words, a matrix of Sylvester and the desired matrix vector of the "elements" coprime decomposition. Then, using the $[q, r] = qr(R)$ command of the *Matlab* package, where R is the Sylvester matrix, the linearly dependent columns are checked in the direction from left to right. If the diagonal elements of r are non-zero, then the original polynomial matrices are coprime, and if there are zeros on the diagonal, we look for the right coprime polynomial matrices. Is proposed an algorithm for calculating a coprime decomposition is presented and one example illustrating algorithm.

Index Terms – Matrix transfer function, left and right matrix polynomial decomposition, coprime decomposition, the not coprime decomposition, polynomial matrices, linear equation, Sylvester matrix, the singular matrix, search algorithm coprime.

I. INTRODUCTION

CONSIDER the calculation of the polynomial decomposition of the transfer function to the coprime (relatively prime) form. Failure to meet the requirements coprimality can lead to problems associated with the emergence of latent instability of automatic control systems, uncontrollability or non-observability [1-4]. Such difficulties can be excluded by transforming the polynomial decomposition to a relatively prime form. It is proved that for the existence of a solution of the polynomial matrix equation that arises in the search for a controller guaranteeing a given characteristic polynomial in a single-channel case or a given characteristic polynomial matrix in a multichannel case, a mutually simple decomposition is required. To check for relatively prime, it is convenient to go from polynomial matrix equations to matrix equations with numerical coefficients [1-3].

A coprime decomposition can be obtained on the basis of an algorithm whose essence consists by searching the linearly dependent columns of the Sylvester matrix from left to right. To do this, you can use the QR -decomposition: in the *Matlab* package, the corresponding operator qr . Assume, and it is really so, that the Sylvester matrix of the rows is greater than or equal to the number of columns. The essence of the

QR -decomposition is as follows: for an $n \times m$ ($n \geq m$) matrix S there exists an $n \times n$ orthogonal matrix \bar{Q} such that

$$\bar{Q}S = R,$$

where R – upper triangular matrix of the same order as S – $n \times m$. Because \bar{Q} "converts" the rows of the matrix S , linear independence of the columns of S "is preserved" in the columns of R . In other words, if any column R is linearly dependent on the columns to its left, the column in S will be the same. Since R is an upper triangular matrix, its m -th table is linearly independent of the columns on the left side if and only if its m -th entry on the diagonal is not zero. Thus, analyzing R linear independence column S , from left to right, it can be obtained by direct verification. Because \bar{Q} is orthogonal, we have $\bar{Q}^{-1} = \bar{Q}' = Q$ and $\bar{Q}S = R$, i.e. $S = QR$. This procedure is called QR – decomposition. In *Matlab*, Q and R can be obtained by using the command $[q, r] = qr(S)$.

For scalar transfer functions, we can use either the rank operator or the qr -decomposition to determine the number μ of linearly independent n – columns. In the matrix case, the use of the *rank* operator is inconvenient and it is proposed to use the QR – decomposition.

An algorithm for calculating a coprime decomposition and examples confirming the operability of the proposed algorithm are given. This paper is a continuation of the studies begun in [5, 6] and continued in [7-18], and based on the basic results obtained in Chen's papers.

II. PROBLEM DEFINITION

We will make the assumption that the matrix transfer function, for example, of an object, a left fraction, not necessarily as a coprime polynomial fraction

$$W_{ob}(s) = D^{-1}(s)N(s).$$

We pose the problem of finding a *coprime fraction*

$$W_{ob}(s) = \bar{N}(s)\bar{D}^{-1}(s),$$

that is, we have the equality

$$W_{ob}(s) = D^{-1}(s)N(s) = \bar{N}(s)\bar{D}^{-1}(s).$$

Obviously, it is fair

$$D(s)(-\bar{N}(s)) + N(s)\bar{D}(s) = 0. \quad (1)$$

This problem will be considered in the next section.

III. REDUCE TO THE COPRIME FORM

The polynomial matrices included in (1) can be written in the form of polynomials with matrix coefficients whose elements are real numbers:

$$\begin{aligned} D(s) &= D_0 + D_1 s + \dots + D_{n-1} s^{n-1} + D_n s^n, \\ N(s) &= N_0 + N_1 s + \dots + N_{m-1} s^{m-1} + N_m s^m, \\ \bar{D}(s) &= \bar{D}_0 + \bar{D}_1 s + \dots + \bar{D}_{n-1} s^{n-1}, \\ \bar{N}(s) &= \bar{N}_0 + \bar{N}_1 s + \dots + \bar{N}_{n-1} s^{n-1}. \end{aligned}$$

Here D_i , N_i , \bar{D}_i and \bar{N}_i – numeric matrices order $p \times p$, p – number of channels and $m \leq n$. The matrices D_i and N_i are known to us and it is only necessary to determine \bar{D}_i and \bar{N}_i . Substituting D_i , N_i , \bar{D}_i and \bar{N}_i in (1), we write out the system of linear equations

$$\underbrace{\begin{bmatrix} D & N & D & N & \vdots & D & N \\ D_0 & N_0 & 0 & 0 & \vdots & 0 & 0 \\ D_1 & N_1 & D_0 & N_0 & \vdots & 0 & 0 \\ \dots & \dots & D_1 & N_1 & \vdots & D_0 & N_0 \\ D_n & N_n & \dots & \dots & \vdots & D_1 & N_1 \\ 0 & 0 & D_n & N_n & \vdots & \dots & \dots \\ 0 & 0 & 0 & 0 & \vdots & D_n & N_n \end{bmatrix}}_{\mathfrak{R}} \underbrace{\begin{bmatrix} -\bar{N}_0 \\ -\bar{D}_0 \\ -\bar{N}_1 \\ -\bar{D}_1 \\ \dots \\ -\bar{N}_{n-1} \\ -\bar{D}_{n-1} \end{bmatrix}}_x = 0, \quad (2)$$

where \mathfrak{R} – Sylvester matrix order $2n \times 2n$ – blocks, columns, which we denote by d_i and n_i : $D = (d_1, d_2, \dots, d_p)$ and $N = (n_1, n_2, \dots, n_p)$.

We now discuss some general properties of the matrix \mathfrak{R} under the assumption that it is necessary to find linearly independent columns \mathfrak{R} from left to right. This leads us to the fact that each D –column in each D –block column is linearly independent of the D –columns on the left (because of the downward shift). The situation for N –columns, however, is different. Recall that there every N –block column has p N –columns. We use the N_i –column to denote the i –th N –column in each N –block column. This leads to the fact that if the N_i –column in some N –block column is linearly depends on the columns of the left-hand-side (LHS) N –columns, then all subsequent N_i –columns, because of the repeatability of the structure \mathfrak{R} , will be linearly dependent on it's LHS columns. Let, μ_i , $i = 1, 2, \dots, p$ be the number of linearly independent N_i –columns in \mathfrak{R} . We call them *column indices* $W_{ob}(s)$. The first N_i –column, linearly dependent on LHS columns, is called the *primary dependent* N_i –column. It is clear that the $(\mu_i + 1)$ –th N_i –column is the primary dependent column.

We form the matrix \mathfrak{R}_i , $i = 1, 2, \dots, p$, which includes the primary linearly dependent column $(\mu_i + 1)$ and compute the monic null vector x_i ; i takes the values $i = 1, 2, \dots, p$.

From such normalized vectors we can obtain a right coprime fraction. The resulting matrix $D(s)$ has the smallest possible column degree. In addition $\bar{D}(s)$ automatically will be column reduced. The following example illustrates the procedure just cited.

Example. Find the right coprime polynomial matrix fraction $\bar{N}(s)\bar{D}^{-1}(s)$ by a given left the matrix polynomial fraction of the object

$$\begin{aligned} W_{ob}(s) &= \begin{bmatrix} (s+1)^2 & 0 \\ 3(s+2)^2 & (s+2)^3 \end{bmatrix}^{-1} \times \begin{bmatrix} s+1 & 2(s+1) \\ 3(s+2)^2 & 4(s+2)^2 \end{bmatrix} = \\ &= \begin{bmatrix} s^2+2s+1 & 0 \\ 3s^2+12s+12 & s^3+6s^2+12s+8 \end{bmatrix}^{-1} \times \\ &\quad \times \begin{bmatrix} s+1 & 2s+2 \\ 3s^2+12s+12 & 4s^2+16s+16 \end{bmatrix}, \quad (3) \end{aligned}$$

not necessarily coprime. The polynomial matrices $D(s)$ and $N(s)$ from the above left fraction $D^{-1}(s)N(s)$ can be represented as matrix polynomials

$$D(s) = \underbrace{\begin{bmatrix} 1 & 0 \\ 12 & 8 \end{bmatrix}}_{D_0} + \underbrace{\begin{bmatrix} 2 & 0 \\ 12 & 12 \end{bmatrix}}_{D_1} s + \underbrace{\begin{bmatrix} 1 & 0 \\ 3 & 6 \end{bmatrix}}_{D_2} s^2 + \underbrace{\begin{bmatrix} 0 & 0 \\ 0 & 1 \end{bmatrix}}_{D_3} s^3, \quad (4)$$

$$N(s) = \underbrace{\begin{bmatrix} 1 & 2 \\ 12 & 16 \end{bmatrix}}_{N_0} + \underbrace{\begin{bmatrix} 1 & 2 \\ 12 & 16 \end{bmatrix}}_{N_1} s + \underbrace{\begin{bmatrix} 0 & 0 \\ 3 & 4 \end{bmatrix}}_{N_2} s^2 + \underbrace{\begin{bmatrix} 0 & 0 \\ 0 & 0 \end{bmatrix}}_{N_3} s^3. \quad (5)$$

In our case, $n=3$ and channels two – $p \times p = 2 \times 2$. We form the Sylvester matrix (2) order $2n \times 2n = 6 \times 6$ –blocks: the 1-st and 2-nd D and N –block columns ($N = (n_1 \ n_2)$ and $D = (d_1 \ d_2)$), located beside we supplement from below by zero matrices in order to the number of rows equal to $2n = 6$ –blocks. The next block columns corresponding to the third and fourth columns are obtained from the first and second block columns with a downward shift by one position and complemented from above by zero matrices. Similarly, the procedure will continue as long as the amount of D and N –block columns becomes equal to $2n = 6$. Also, we form a block column x order $2n \times 1 = 6 \times 1$ blocks (or 12×2) of the matrix coefficients of the polynomials $\bar{N}(s)$ and $\bar{D}(s)$ (2)

$$\underbrace{\begin{bmatrix} D & N & D & N & D & N \\ D_0 & N_0 & 0 & 0 & 0 & 0 \\ D_1 & N_1 & D_0 & N_0 & 0 & 0 \\ D_2 & N_2 & D_1 & N_1 & D_0 & N_0 \\ D_3 & N_3 & D_2 & N_2 & D_1 & N_1 \\ 0 & 0 & D_3 & N_3 & D_2 & N_2 \\ 0 & 0 & 0 & 0 & D_3 & N_3 \end{bmatrix}}_{\mathfrak{R}} \underbrace{\begin{bmatrix} -\bar{N}_0 \\ -\bar{D}_0 \\ -\bar{N}_1 \\ -\bar{D}_1 \\ -\bar{N}_2 \\ -\bar{D}_2 \end{bmatrix}}_x = 0,$$

where O – zeromatrix order $p \times p = 2 \times 2$, \bar{N}_i and \bar{D}_i – the sought a coprime polynomial matrices order $p \times p = 2 \times 2$. After substituting the matrices D_i and N_i from (4) and (5), the Sylvester matrix will be the form:

$$\mathfrak{R} = \begin{bmatrix} 1 & 0 & 1 & 2 & 0 & 0 & 0 & 0 & 0 & 0 & 0 & 0 \\ 12 & 8 & 12 & 16 & 0 & 0 & 0 & 0 & 0 & 0 & 0 & 0 \\ 2 & 0 & 1 & 2 & 1 & 0 & 1 & 2 & 0 & 0 & 0 & 0 \\ 12 & 12 & 12 & 16 & 12 & 8 & 12 & 16 & 0 & 0 & 0 & 0 \\ 1 & 0 & 0 & 0 & 2 & 0 & 1 & 2 & 1 & 0 & 1 & 2 \\ 3 & 6 & 3 & 4 & 12 & 12 & 12 & 16 & 12 & 8 & 12 & 16 \\ 0 & 0 & 0 & 0 & 1 & 0 & 0 & 0 & 2 & 0 & 1 & 2 \\ 0 & 1 & 0 & 0 & 3 & 6 & 3 & 4 & 12 & 12 & 12 & 16 \\ 0 & 0 & 0 & 0 & 0 & 0 & 0 & 0 & 1 & 0 & 0 & 0 \\ 0 & 0 & 0 & 0 & 0 & 1 & 0 & 0 & 3 & 6 & 3 & 4 \\ 0 & 0 & 0 & 0 & 0 & 0 & 0 & 0 & 0 & 0 & 0 & 0 \\ 0 & 0 & 0 & 0 & 0 & 0 & 0 & 0 & 0 & 1 & 0 & 0 \end{bmatrix}$$

$d_1 \quad d_2 \quad n_1 \quad n_2 \quad d_1 \quad d_2 \quad n_1 \quad n_2 \quad d_1 \quad d_2 \quad n_1 \quad n_2$

where d_1, d_2, n_1 and n_2 – column height of eight. Then we use the qr -decomposition to find the linearly dependent columns in the order from left to right in the matrix \mathfrak{R} . Calculations in the Matlab package can be done in this way:

```
>>D0=[1 0; 12 8]; D1=[2 0; 12 12]; D2=[1 0; 3 6];
D3=[0 0; 0 1]; N0=[1 2; 12 16]; N1=[1 2; 12 16];
N2=[0 0; 3 4]; N3=zeros(2); O=zeros(2);
c1=[D0; D1; D2; D3; O; O]; c2=[N0; N1; N2; N3; O; O];
c3=[O; D0; D1; D2; D3; O]; c4=[O; N0; N1; N2; N3; O];
c5=[O; O; D0; D1; D2; D3]; c6=[O; O; N0; N1; N2; N3];
R=[c1 c2 c3 c4 c5 c6];
[q, r]=qr(R); %Calculation of the orthogonal matrix q and
% upper triangular matrix r such that  $q^{-1}R=r$ 
```

We need only the matrix r , and we do not show the matrix q . As a result, we obtain the matrix r :

$$r = \begin{bmatrix} d_1 & x & x & x & x & x & x & x & x & x & x & x \\ & d_2 & x & x & x & x & x & x & x & x & x & x \\ & & n_1 & x & x & x & x & x & x & x & x & x \\ & & & n_2 & x & x & x & x & x & x & x & x \\ & & & & d_1 & x & x & x & x & x & x & x \\ & & & & & d_2 & x & x & x & x & x & x \\ & & & & & & 0 & x & x & x & x & x \\ & & & & & & & 0 & x & x & x & x \\ & & & & & & & & 0 & x & x & x \\ & & & & & & & & & d_1 & x & x \\ & & & & & & & & & & d_2 & x \\ & & & & & & & & & & & 0 \\ & & & & & & & & & & & 0 \end{bmatrix}$$

Here, instead of numbers not on the diagonal, represented the "x". We analyze the linear dependence of the columns of the matrix \mathfrak{R} by means of the matrix r : we see that all D -columns are linearly independent of the columns on the left, since their elements corresponding to the diagonal are non-zero. As for N -columns, then in the matrix only by the one linearly independent n_1 and n_2 column (the third – $\mu_1 = 1$ and the 4-th – $\mu_2 = 1$). Therefore, the primary linearly dependent n_1 -column from left to right is the n_1 -column is in the 7-th column of the matrix (briefly $\mu_1 + 1$). Still remain n_2 -columns: Total only one linearly independent n_2 -columns from left to right, that is, $\mu_2 = 1$; The primary linearly dependent n_2 -column is the n_2 -column located in the 8-th column of the matrix (briefly $\mu_2 + 1$). We found two ($p = 2$) linearly dependent n_i -columns (briefly $\mu_1 + 1$, $\mu_2 + 1$). Therefore, there is no need to analyze the remaining 11-th and 12-th linearly dependent columns.

Thus, from an analysis of the form of the matrix r , it follows that it is necessary to take the columns from the 1-st to the 7-th when forming the matrix \mathfrak{R}_1 from the matrix \mathfrak{R} and because the 9-th, 11-th and 12-th rows are zero, they are discarded. Let's find the first column a null vector using the command `null`:

```
>>R1=R; %We copy the matrix R
R1(:,12)=[]; R1(:,11)=[]; R1(:,10)=[];
R1(:,9)=[]; R1(:,8)=[]; % Delete the extra columns
R1(12,:)=[]; R1(11,:)=[]; R1(9,:)=[]; %Deleting zero
%rows
x1=null(R1); %compute null vector
x1b=x1/x1(7) % normalize it
```

As a result, we get

$$x_{1b} = [-1 \quad -3 \quad 7 \quad -3 \quad 0 \quad 0 \quad 1]'$$

The first on the left is a linearly dependent 7-th column used. The next linearly dependent 8th column, corresponding to $\mu_2 + 1$ – the first linearly dependent n_2 -column of matrix \mathfrak{R}_2 , allows to form from the columns from left to right on the 8-th inclusive \mathfrak{R}_2 matrix:

```
>>R2=R;
R2(:,12)=[]; R2(:,11)=[]; R2(:,10)=[];
R2(:,9)=[]; R2(:,7)=[]; % Delete the extra columns
R2(12,:)=[]; R2(11,:)=[]; R2(9,:)=[]; %Deleting zero
%rows
```

```
x2=null(R2);
x2b=x2/x2(7)
```

As a result, we get

$$x_{2b} = [-2 \quad -4 \quad 10 \quad -4 \quad 0 \quad 0 \quad 1]'$$

Combine the vectors x_{1b} and x_{2b} :

$$\begin{bmatrix} -\bar{N}'_0 & \bar{D}'_0 & -\bar{N}'_1 & \bar{D}'_1 & -\bar{N}'_2 & \bar{D}'_2 \end{bmatrix}' =$$

$$= \begin{bmatrix} -1 & -3 & 7 & -3 & 0 & 0 & 1 & 0 & 0 & 0 & 0 & 0 \\ -2 & -4 & 10 & -4 & 0 & 0 & 0 & 1 & 0 & 0 & 0 & 0 \end{bmatrix}.$$

We can write down the right coprime polynomial matrix fraction

$$\bar{D}(s) = \begin{bmatrix} s+7 & 10 \\ -3 & s-4 \end{bmatrix}, \quad \bar{N}(s) = \begin{bmatrix} 1 & 2 \\ 3 & 4 \end{bmatrix},$$

where, the matrix transfer function of the object

$$W_{ob}(s) = \bar{N}(s)\bar{D}^{-1}(s) = \begin{bmatrix} 1 & 2 \\ 3 & 4 \end{bmatrix} \times \begin{bmatrix} s+7 & 10 \\ -3 & s-4 \end{bmatrix}^{-1}.$$

We perform the check

$$W_{ob}(s) = D_l^{-1}(s)N_l(s) = \bar{N}(s)\bar{D}^{-1}(s) = \begin{bmatrix} \frac{1}{s+1} & \frac{2}{s+1} \\ \frac{3s}{s^2+3s+2} & \frac{4s-2}{s^2+3s+2} \end{bmatrix}.$$

Of course, other ways of finding a coprime fractional can be used, for example, by reducing the polynomial matrix by unimodal transformations to the upper triangular form [18].

III. ALGORITHM FOR SEARCHING COPRIME FRACTION OF TRANSMISSION FUNCTION

Suppose that given a left matrix polynomial decomposition (fractional) of the transfer function

$$W_{ob}(s) = D^{-1}(s)N(s),$$

where

$$D(s) = \sum_{i=0}^n D_i s^i, \quad N(s) = \sum_{i=0}^m N_i s^i,$$

such that $\deg N(s) \leq \deg D(s)$, that is $m \leq n$, $\dim D_i = \dim N_j = p \times p$, where p – number of channels. Note, that $n \geq 1$. Below we use the concepts: N – block columns and D – block columns:

$$N = (N_0^t, N_1^t, \dots, N_p^t)^t = (n_1 \ n_2 \ \dots \ n_p),$$

$$D = (D_0^t, D_1^t, \dots, D_p^t)^t = (d_1 \ d_2 \ \dots \ d_p).$$

Two block columns D and N , located beside, are supplemented by zero matrices of order $p \times p$ for $n \geq 2$ from below so that the number of (block) elements in the columns is equal to $2n$ blocks.

In the algorithm, we study the equation (2), which includes the Sylvester matrix \mathfrak{R} and the vector of matrix coefficients from the coprime fraction of the matrix transfer function

$$x = (-\bar{N}_0^t \ \bar{D}_0^t \ | \ -\bar{N}_1^t \ \bar{D}_1^t \ : \ -\bar{N}_{n-1}^t \ \bar{D}_{n-1}^t)^t = (x_1 \ x_2 \ \dots \ x_p).$$

The **algorithm** consists of the following actions.

1. Drawing up the Sylvester matrix \mathfrak{R} order $2n \times 2n$ – blocks: the first and second D and N – block columns that are located beside are complemented from below by zero matrices in order that the number of rows is $2n$ – blocks. The next block columns corresponding to the 3-rd and 4-th col-

umns are obtained from the 1-st and 2-nd block columns with a downward shift by one position and complemented from above by zero matrices. Similarly, we construct $2n$ "pieces" D and N – block columns. Sylvester's matrix is formed. We form the block column x from the matrix coefficients of $\bar{N}(s)$ and $\bar{D}(s)$ polynomials order $2n \times 1$ blocks.

2. Compute of the linearly dependent columns of the matrix \mathfrak{R} in the direction from left to right, for which we use the command $[q, r] = qr(\mathfrak{R})$, which gives two matrices – q and r ; for further calculations, the matrix q is not required. The presence of linearly dependent columns corresponds to the zero element on the diagonal in the upper triangular matrix r .

3. If all the diagonal elements of the matrix r are not zero, or one zero, then the polynomial matrices $N(s)$ and $D(s)$ are coprime and, consequently, an **exit from the algorithm**; if there are zero elements – we are looking for coprime polynomial matrices $\bar{N}(s)$ and $\bar{D}(s)$ – transition to the next step.

4. Formation of the matrix \mathfrak{R}_1 :

– since all n pieces of D – block columns of \mathfrak{R} are linearly independent of all the columns on the left, we determine the quantities $\mu_1, \mu_2, \dots, \mu_p$ of linearly independent n_1, n_2, \dots, n_p – columns from the left to the right in the matrix \mathfrak{R} ;

– the matrix \mathfrak{R}_1 consists of linearly independent columns of the matrix \mathfrak{R} taken from the left to the right, including the first linearly dependent n_1 ($\mu_1 + 1$ – column), n_2 ($\mu_2 + 1$ – column), \dots , n_p ($\mu_p + 1$ – column) – dependent column;

– if in the matrix \mathfrak{R}_1 there is zero row / rows, then its / them are deleted – the matrix \mathfrak{R}_1 is formed;

5. We form the vector x_1 , or x_2 , or \dots , x_p : depends on which column n_1 , n_2 , or \dots , n_p is linearly dependent in the matrix \mathfrak{R}_1 – if n_1 then find x_1 , and if n_2 then x_2 etc. For the block vector x_i , we delete as many last elements as the columns are deleted when the matrix \mathfrak{R}_1 is formed.

6. To determine the non-zero solution x (consists of the matrix coefficients of the coprime fractions of the numerator and the denominator of the matrix transfer function of the equation $\mathfrak{R}_1 x_1 = 0$, or $\mathfrak{R}_1 x_2 = 0$, or $\dots \mathfrak{R}_1 x_p = 0$), we use the Matlab **null** (\mathfrak{R}_1) command – the vector x_i belongs to the kernel \mathfrak{R}_1 ;

– the vector found we normalize the elements of the vector x_i divide by the last element of it and denote it by x_{ib} (can be called the **monic null vector**).

7. Formation of a matrix \mathfrak{R}_2 consisting of linearly independent columns of the matrix \mathfrak{R} (the previous linearly dependent column is removed) taken from the left to the right, including the first linearly dependent n_i – column (if in the

matrix \mathfrak{K}_1 the n_2 –column was linearly dependent, then in the matrix \mathfrak{K}_2 – the first linear-dependent column – n_1 or vice versa).

8. Are performed steps 4 through 7 for all channels, that is, we perform calculations for the matrices $\mathfrak{K}_1, \mathfrak{K}_2, \dots, \mathfrak{K}_p$.

9. We write out the coprime polynomial matrices of the transfer function $\bar{N}(s)$ and $\bar{D}(s)$. Those columns that have been removed from the matrices $\mathfrak{K}_1, \mathfrak{K}_2, \dots, \mathfrak{K}_p$, the corresponding elements of the vectors x_1, x_2, \dots, x_p we are filled with zeros.
End of algorithm.

IV. CONCLUSION

The problem of coprimality plays an important role in the solution of the synthesis problem, both in single-channel systems [9, 11, 15, 17], and in multichannel systems [7, 8, 10–14, 16, 18]: the coprimality of polynomial matrices makes it possible to use the so-called Sylvester matrix, or its minor modifications, in the synthesis of multichannel regulators. In addition, if the polynomials of the numerator and the denominator of the object's transfer function in single-channel systems have the same roots, or the polynomial matrices are not coprime (they have a common matrix polynomial non-unimodal multiplier), this can lead to latent ACS instability or uncontrollability / non-observability of the system. If the Sylvester matrix is not singular, and this corresponds to the coprimality of the polynomial matrix fraction, then there exists a solution to the problem of synthesis of a multichannel regulator, which reduces to the solution of a linear algebraic equation. In other words, a null vectors of the Sylvester matrix are found. To do this, we use the QR -decomposition to find linearly dependent columns.

Based on the analysis of several examples of the search right coprime polynomial matrix fractions $\bar{N}(s)$ and $\bar{D}(s)$, an algorithm for calculating a coprime fraction is formulated.

REFERENCES

- [1] C.T. Chen, Linear system theory and design. 3rd ed. New York Oxford: Oxford University Press, 1999.
- [2] P. J. Antsaklis, A. N. Michel, Linear systems, New York: McGraw-Hill, 1997, 685 p.
- [3] Kailath. T. Linear Systems / T. Kailath – Englewood Cliffs, N.J.: Prentice Hall, 1980. – 350 P.
- [4] Gaiduk A. R. Theory and methods of analytical synthesis of automatic control systems (polynomial approach) – M.: FIZMATLIT, 2012. – 360 P.
- [5] Voronov V.V. A polynomial method for calculating the multi-channel controllers low order. Work of the Technical Sciences Candidate: Spec. 05.13.01 / V.V. Voronov; Novosibirsk State Technical University. – Novosibirsk, 2013. – 173 p. (In Russian).
- [6] Shoba E.V. The modal method for the synthesis of multi-channel dynamic systems using a polynomial expansion. Work of the Technical Sciences Candidate: Spec. 05.13.01 / E.V. Shoba; Novosibirsk State Technical University. – Novosibirsk, 2013. – 192 p. (In Russian).
- [7] Voevoda A. A., Bobobekov K.M. Solution of an overdetermined linear system of equations for polynomial synthesis of regulators // Modern technologies. System analysis. Modeling. 2017. Vol. 56, – no. 4. pp. 84–99. (In Russian).
- [8] Voevoda A.A. Stabilization of the two-mass system: polynomial method of synthesis of two-channel system // Transaction of scientific papers of the Novosibirsk state technical university, Novosibirsk. – 2009. no 4 (58). p. 121–124. (In Russian).
- [9] Bobobekov K.M. About rationing polynomials denominator object and regulator during polynomial method of synthesis // Transaction of scientific papers of the Novosibirsk state technical university, Novosibirsk. – 2016. no 4 (86). p. 7–24. (In Russian).
- [10] Voevoda A.A. Stabilization of two-mass systems: modal synthesis method using polynomial factorization // Science bulletin of the Novosibirsk state technical university, Novosibirsk. – 2010, no. 1 (38), pp. 195–198. (In Russian).
- [11] Voevoda A.A., Bobobekov K.M. About the necessary conditions of existence of the solution in polynomial method of synthesis of single-channel systems // Transaction of scientific papers of the Novosibirsk state technical university, Novosibirsk. – 2017, no. 4 (90), pp. 7–21. (In Russian).
- [12] Bobobekov K. M. About structural transformations of multichannel linear systems in the matrix polynomial representation // Science bulletin of the Novosibirsk state technical university, Novosibirsk. – 2017, no. 2 (67), pp. 7–25. (In Russian).
- [13] Voevoda A. A. Matrix transfer functions (Basic concepts): Part 1 – Part 3 A summary of lectures on the course "Designing of control systems" for 4–5 courses faculty of Automation and Computer Engineering (special 2101) / Voevoda A.A.; Eds. Vostrikov A.S.; Novosibirsk State Technical University – Novosibirsk: NSTU, 1994. – 94 P.
- [14] Voevoda A.A., Bobobekov K.M. Synthesis of linear multichannel regulators using structural transformations // Bulletin of the Astrakhan state technical university, 2017 no. 3, pp. 7–20. (In Russian).
- [15] Bobobekov K.M. A polynomial method for the synthesis of single-channel two-mass system // Transaction of scientific papers of the Novosibirsk state technical university, Novosibirsk. – 2016. no 4 (86). p. 25–26. (In Russian).
- [16] Voevoda A.A., Bobobekov K.M. Simulation of multichannel systems with singular objects in a polynomial matrix representation // International Scientific-Practical Conference "Independence – the basis for the development of the country's energy", December 22–23, 2017 – Bokhtar: IET Publishing, 2017. pp. 214–218. (In Russian).
- [17] Voevoda A.A., Bobobekov K.M. Calculation of controller parameters for the stabilization of the inverted pendulum by corner deviation // Transaction of scientific papers of the Novosibirsk state technical university, Novosibirsk. – 2016, no. 3 (85), pp. 18–32.
- [18] Voevoda A.A., Shoba E.V. About diagonally decoupling for multi-input multi-output systems. Pt. 1 // Transaction of scientific papers of the Novosibirsk state technical university, Novosibirsk. – 2010, no. 2 (60), pp. 16–25. (In Russian).
- [19] Voevoda A. A., Chekhonadskikh A. V., Shoba E. V. Modal synthesis method using a polynomial expansion: traffic separation in the stabilization of three-mass system // Science bulletin of the Novosibirsk state technical university, Novosibirsk. – 2011, no. 2 (43), pp. 39–46. (In Russian).



Voevoda Alexander, professor of the Automation department in Novosibirsk State Technical University, professor, doctor of technical sciences. The science interests and competence field are automation theory, optimization. He is the author of 260 science papers including 1 patent.



Bobobekov Kurbonmurod, specialist of the mechanical engineering technology, Tajik Technical University of the academician M. S. Osimi. The postgraduate student of the Automation department in Novosibirsk State Technical University (2015). The science interests and competence field are automation theory, control systems synthesis. He is the author of 25 science papers.

A stabilized Algorithm of Nonparametric Identification for a System with High-level Noise Measurement of Input Signal

Yury E. Voskoboinikov^{1,2}, Danila A. Krysov²

¹Novosibirsk State University of Architecture and Civil Engineering (SIBSTRIN), Novosibirsk, Russia

²Novosibirsk State Technical University, Novosibirsk, Russia

Abstract – In this paper the problem of nonparametric identification of a dynamical system is solved. The mathematical model of a system is represented by the Volterra integral equation of the first kind. This is the ill-posed problem because Hadamard's conditions are not met. In this case, it is usually considered that the input signal of the identified system is accurately specified, and the output signal is recorded with a random error. However, such a requirement is rarely satisfied in practice, since both the input and output signals of the system are measured and recorded by measuring instruments of the same accuracy class. Consequently, both the input and output signals are specified with random measurement errors. In this article, a new regularizing identification algorithm based on the discrete Fourier transform is constructed. The algorithm takes into account the high noise level of the input signal as in the construction of the regularized solution well as in the choice of the regularization parameter. An iterative algorithm for calculating the discrete Fourier transform coefficients of a regularized solution is proposed. This algorithm has a high rate of convergence. The choice of the regularization parameter is based on the verification of statistical hypotheses. This approach allows estimating accurately the optimum value of the parameter even there is a large measurement's noise level of the input signal. The researches of this algorithm showed its higher accuracy than similar algorithms, which do not take into account the noise of the input signal measurement. The proposed algorithm can be generalized for a stable solution of the Fredholm equation of the first kind with an ill-defined kernel.

Index Terms – Nonparametric identification, regularizing algorithm, Volterra integral equation of the first kind, discrete Fourier transform, choice of the regularization parameter.

I. INTRODUCTION

MORE OFTEN, the Volterra integral equation of the first kind with a difference kernel is used as a mathematical model of stationary dynamical system:

$$\int_0^t k(t-\tau)\varphi(\tau)d\tau = f(t), \quad (1)$$

where $k(\tau)$ is the impulse response function (IPF) of the dynamic system, $\varphi(\tau)$ and $f(t)$ – input and output signals of the system. Equation (1) relates two problems:

- *inverse measurement problem*, when it is necessary to construct an estimate for the input signal $\varphi(\tau)$ from the reg-

istered values of the functions $k(\tau)$, $f(t)$, i.e. to solve equation (1) with respect to the function $\varphi(\tau)$;

- *the problem of nonparametric identification* [1], where it is necessary to construct an estimate for the IPF system from the recorded values of the functions $\varphi(\tau)$, $f(t)$.

Both the first and the second problems belong to the class of ill-posed problems when the Hadamard correctness conditions can be violated. In particular, the errors in specifying the right-hand side $f(t)$ of equations influence to the instability of the solution of the integral equation (1) [2,3].

In the numerical solution of equation (1), its discretization is performed using the formula of rectangles. This further allows us to use the discrete Fourier transform (DFT). For the problem of nonparametric identification, such a discretization gives a system of equations:

$$\Phi k = f, \quad (2)$$

where the matrix Φ is formed from the values of the input signal. This matrix can be ill conditioned (and possibly singular matrix). This creates difficulties in solving the system (2).

To find the unique and stable solution of the inverse measurement problem (the solutions of equation (1) with respect to the function $\varphi(\tau)$), various regularization methods are used both deterministic and statistical [4]. In this case, as a rule, it is assumed that the right-hand side is known with some error, and the kernel $k(\tau)$ of equation (1) is specified exactly. The same methods can also be used to solve the problem of nonparametric identification. For this case, the kernel of the equation will be the input signal of the system $\varphi(\tau)$. A similar assumption is made that the input signal of the identified system is specified exactly. However, such a requirement is rarely satisfied in practice. Both the input and output signals of the system are measured and recorded by instruments of approximately the same accuracy class. Consequently, both the input and output signals are specified with random errors: measurement noises.

II. PROBLEM DEFINITION

It was shown in [5] that if the relative noise level of the measurement of the input signal is less or commensurable with the relative noise level of the output signal of the identified system, then a regularizing algorithm can be used. It does not take into account the errors of the input signal, including the choice of regularization parameter. If the noise level of the measurement of the input signal was more than the noise level of the output signal measurement (at times), the algorithm for estimating the optimal parameter of regularization, constructed on the basis of the optimality criterion, led to overestimated values, as well as another selection algorithm based on the principle of the residual.

There are two problems are solved in this paper:

- construction the regularizing algorithm based on the discrete Fourier transform (DFT), which takes into account the measurement noise of the input signal of the system being identified;
- construction a method for estimating the optimal regularization parameter of the algorithm, minimizing the root-mean-square error of identification.

III. THEORY

Assume that the measured values of the input and output signals $\tilde{\varphi}(\tau)$ and $\tilde{f}(t)$ admit representations:

$$\tilde{\varphi}_j = \varphi(\tau_j) + \zeta(\tau_j), j = 1, \dots, N_\varphi;$$

$$\tilde{f}_i = f(t_i) + \eta(t_i), i = 1, \dots, N_f.$$

where $\zeta(\tau_j)$, $\eta(t_i)$ – random values (measurement noise) with zero means and variances σ_ζ^2 and σ_η^2 . Values $\eta(t_i)$, $\zeta(\tau_j)$ are not correlated with each other. Hereinafter, the sign “~” means that the given value is distorted by the measurement noise.

A. The Regularization Algorithm for Identification

The construction of a regularized solution can be represented by the following “enlarged” steps (for more details, see [6]):

Step 1. To form periodic sequences $\tilde{f}_p(i)$, $\tilde{\varphi}_p(i)$, $i = 0, \dots, N-1$ (where N is the period size) by discrete values $\tilde{f}_i = f(t_i)$, $\tilde{\varphi}_j = \varphi(\tau_j)$ and to calculate from these DFT sequences, i.e. to calculate the coefficients of the DFT $\tilde{F}_p(l)$, $\tilde{\Phi}_p(l)$, $l = 0, \dots, N-1$.

Step 2. To calculate the coefficients of the DFT $K_{p\alpha}(l)$, $l = 0, \dots, N-1$, of the regularized solution.

Step 3. To calculate the periodic regularized solution $k_{p\alpha}(i)$, $i = 0, \dots, N-1$ by computation the inverse DFT from the sequence $\{K_{p\alpha}(l)\}$ and to form the vector of the non-periodic regularized solution k_{α_j} , $j = 0, \dots, N_k-1$, as an es-

timate for the values of the impulse response function at discrete instants of time: $k(\tau_j)$, $j = 0, \dots, N_k-1$.

The accuracy of identification is determined by the method of calculating the $K_{p\alpha}(l)$ at the second step of the regularization algorithm.

If the input signal of the system is accurately specified or the measurement noise is negligible (see [6]), then in step 2 the following expression is used:

$$K_{p\alpha}(l) = \frac{\Phi_p^c(l)}{|\Phi_p(l)|^2 + \alpha \cdot Q_p(l)} \cdot \tilde{F}_p(l), \quad (3)$$

where α is the regularization parameter, $\Phi_p^c(l)$ is the complex conjugate of $\Phi_p(l)$. Elements of the sequence $\{Q_p(l)\}$ are formed by the rule:

$$Q_p(l) = \begin{cases} Q(l \cdot \Delta_\omega), & l = 0, \dots, N/2; \\ Q((N-l) \cdot \Delta_\omega), & l = N/2 + 1, \dots, N-1, \end{cases}$$

where $\Delta_\omega = 2\pi/(N\Delta_t)$ – is the discretization step in the frequency domain. The function $Q(\omega)$ can be treated as a frequency characteristic of a stabilizing functional: it must be a non-decreasing function of the frequency ω and most often $Q(\omega) \rightarrow \infty$ at $\omega \rightarrow \infty$. If the order of regularization r is given, then for sufficiently large ω the asymptotics $Q(\omega) \approx \omega^{2r}$ is valid.

On the basis of the approach for solving the inverse measurement problem (described in [6,7]), one can obtain a non-linear equation with respect to the required DFT coefficients $K_{p\alpha}(l)$:

$$K_{p\alpha}(l) = \frac{\tilde{\Phi}_p^c(l)}{|\tilde{\Phi}_p(l)|^2 + \alpha(\sigma_\zeta^2 |K_{p\alpha}(l)|^2 + \sigma_\eta^2)} \cdot \tilde{F}_p(l),$$

where $l = 0, 1, \dots, N-1$. The dispersion relation $\theta = \sigma_\zeta^2 / \sigma_\eta^2$ is introduced. Then the equation is rewrote as:

$$K_{p\alpha}(l) = \frac{\tilde{\Phi}_p^c(l)}{|\tilde{\Phi}_p(l)|^2 + \alpha(1 + \theta |K_{p\alpha}(l)|^2)} \cdot \tilde{F}_p(l), \quad (4)$$

Note that it is easier to set the ratio θ than the variances σ_ζ^2 , σ_η^2 separately. So, if the noise level $\eta(t)$ is twice the level $\zeta(t)$, then the ratio $\theta = (0.5)^2 = 0.25$.

It can be shown that the nonlinear equation (4) has a unique solution for the values $\alpha \geq 0$, $\theta \geq 0$.

To find the solution $K_{p\alpha}^*(l)$ of a non-linear equation with a fixed regularization parameter α any algorithm for solving a non-linear equation can be used. For example, a simple iteration scheme:

$$K_{p\alpha}^{(n+1)}(l) = \frac{\tilde{\Phi}_p^c(l)}{|\tilde{\Phi}_p(l)|^2 + \alpha(1 + \theta |K_{p\alpha}^{(n)}(l)|^2)} \cdot \tilde{F}_p(l),$$

where $n = 0, 1, \dots$. The "start point" $K_{p\alpha}^{(0)}(l)$ is defined as:

$$K_{p\alpha}^{(0)}(l) = \frac{\tilde{\Phi}_p^c(l)}{|\tilde{\Phi}_p(l)|^2 + \alpha \cdot Q_p(l)} \cdot \tilde{F}_p(l), \quad l = 0, 1, \dots, N-1. \quad (5)$$

The termination condition for $(n+1)$ iteration has the form:

$$\left[\frac{\sum_{l=0}^{N-1} |K_{p\alpha}^{(n+1)}(l) - K_{p\alpha}^{(n)}(l)|^2}{\sum_{l=0}^{N-1} |K_{p\alpha}^{(n)}(l)|^2} \right] \leq 0.01 \quad (6)$$

The computational experiment showed that for the fulfillment of condition (6) no more than 5-8 iterations are required.

Note that if the input signal is specified exactly, i.e. $\sigma_\zeta^2 = 0$ and $\theta = 0$, then expression (4) coincides with expression (3) (as expected).

B. Selection of the Regularization Parameter

The problem of choosing the regularization parameter α is the main one when using regularizing algorithms in practice. If the value of α is low then a noise components will appear in the solution $k_\alpha(\tau)$. This is due to the noise of the measurements of the input and output signals. If the value α is too high, the informative components of the function $k(\tau)$ will be "removed" from the solution $k_\alpha(\tau)$. Therefore, as the optimal value α_{opt} is took the value that provide the minimum to the root-mean-square error function [6]:

$$\Delta(\alpha) = M_{\eta, \zeta} \left[\|k_\alpha - \bar{k}^+\|^2 \right],$$

where $M_{\eta, \zeta}[\cdot]$ is the operator of mathematical expectation for the measurement noise ensembles, the vector \bar{k}^+ is the normal pseudo solution calculated from the exact values of the input and output signals. The DFT coefficients of it are determined by the expression:

$$\bar{K}_{p\alpha}^+(l) = \frac{\Phi_p^c(l)}{|\Phi_p(l)|^2} \cdot F_p(l), \quad l = 0, 1, \dots, N-1.$$

The calculation α_{opt} requires the specification of certain characteristics of the function $k(\tau)$. (in particular, the exact values of the identifiable IPF), which in practice are not known. Therefore, several algorithms for the choice of the regularization parameter were proposed for solving inverse measurement problems for a precisely defined kernel of the equation (1). The algorithms allow to estimate α_{opt} (for example, [8,9]). In [4, 10], an optimality criterion for a linear regularizing algorithm was proposed for estimation, which later became the theoretical basis for constructing evaluation algorithms for α_{opt} by solving practical problems (for example, see [6]). In the paper the basic concepts and relationships

needed to understand this criterion when solving the problem of nonparametric identification are given.

Suppose that the input signal of the identified system is specified exactly and introduce statistics:

$$\rho_W(\alpha) = \tilde{f}^T V_\eta^{-1} e_\alpha, \quad (7)$$

where $e_\alpha = \tilde{f} - \Phi k_\alpha$ is the residual vector, Φ is the matrix of the system of equations (2), k_α is the vector composed of the values of the regularized solution $k_\alpha(\tau_j)$, $j = 0, \dots, N_k - 1$, V_η is the covariance matrix of the noise vector of the output signal measurement. (in the case of uncorrelated noise $V_\eta = \sigma_\eta^2 \cdot I$, I is the identity matrix). Then, as an estimate for α_{opt} we can take the quantity α_W , which inequality

$$\vartheta_m(\beta/2) \leq \rho_W(\alpha_W) \leq \vartheta_m(1 - \beta/2), \quad (8)$$

where $\vartheta_m(\beta/2)$, $\vartheta_m(1 - \beta/2)$ is the quantile χ^2 -distributions with $m = N_f$ degrees of freedom of the levels $\beta/2$ and $1 - \beta/2$, β is the probability of error of the first kind (usually 0.05) when testing the statistical hypothesis about the optimality of the α_W . It is shown that α_W more accurately estimates α_{opt} compared with other algorithms of the choice of the regularization parameter (for more details, see [6,11]).

Let us try to use this criterion to select the regularization parameter when solving the considered identification problem with an inaccurately given input signal. To do this, we replaced the covariance matrix V_η in the statistics (7) by the covariance matrix $V_{\eta'}(k_\alpha)$ of the "equivalent" error vector of the right-hand side:

$$\begin{aligned} \tilde{\rho}_W(\alpha) &= \tilde{f} \cdot (V_{\eta'}'(k_\alpha))^{-1} \cdot e_\alpha = \\ &= \tilde{f} \cdot [\sigma_\eta^2 \cdot I + \sigma_\zeta^2 \cdot K_\alpha K_\alpha^T]^{-1} \cdot e_\alpha \end{aligned} \quad (9)$$

where the matrix K_α is composed by the values k_α from the regularized solution vector. To calculate α_W , that satisfies the inequality:

$$\vartheta_m(\beta/2) \leq \tilde{\rho}_W(\alpha) \leq \vartheta_m(1 - \beta/2) \quad (10)$$

we applied to the iterative procedure for the quantity $\gamma = 1/\alpha$ of the form:

$$\gamma^{(n)} = \gamma^{(n-1)} - \frac{\tilde{R}_W(\gamma^{(n-1)}) - m}{\tilde{R}_W'(\gamma^{(n-1)})}, \quad n = 1, 2, \dots; \quad \gamma^{(0)} \ll 1, \quad (11)$$

where $m = N_f$, $\tilde{R}_W(\gamma) = \tilde{\rho}_W(1/\gamma)$, $\tilde{R}_W'(\gamma) = \frac{d}{d\gamma} \tilde{R}_W(\gamma)$. As a value α_W is assumed $\alpha_W = 1/\gamma_W$, $\gamma_W = \gamma^{(n)}$ where $\gamma^{(n)}$ satisfies condition

$$\vartheta_m(\beta/2) \leq \tilde{R}_W(\gamma^{(n)}) \leq \vartheta_m(1 - \beta/2). \quad (12)$$

It means that the iteration procedure (11) is interrupted as soon as condition (12) is satisfied. Usually $\gamma^{(0)} \approx 10^{-15}$ and no more than 4-5 iterations of the procedure (11) are required for the calculation α_W .

An effective algorithm for calculating $\tilde{R}_W(\gamma)$ through the DFT coefficients is proposed:

$$\tilde{R}_W(\gamma) = N \cdot \sum_{l=0}^{N-1} \frac{\gamma |\tilde{\Phi}_p(l)|^2 + (1 + \theta |K_{p\alpha}^*(l)|^2) \cdot Q_p(l)}{(C_\sigma \sigma_\xi^2 |K_{p\alpha}^*(l)|^2 + \sigma_\eta^2)},$$

where $C_\sigma = \frac{N_\varphi}{N_f} \cdot N^2 \cdot \Delta_t^2$ is the factor that establishes the relationship between the variances of measurement noise and the variances of the DFT coefficients of these noises, Δ_t the step of discretization of equation (1). The coefficients of the DFT $K_{p\alpha}^*(l)$ are solutions of the nonlinear equation (4) for $l = 0, \dots, N-1$. An analogous formula can also be given for calculating the derivative $\tilde{R}'_W(\gamma)$. The calculation of the regularization parameter in the space of the DFT coefficients significantly saves the computational costs of constructing the estimate α_W .

Let's give a graphic interpretation of the algorithm for choosing the regularization parameter and introduce the relative identification error as a function of the parameter

$$\gamma = 1/\alpha: \delta_k(\gamma) = \frac{\|k_\gamma - \bar{k}^+\|}{\|\bar{k}^+\|}. \text{ In Fig. 1, the solid line}$$

shows the function of the relative identification error $\delta_k(\gamma)$, the point curve – the value $\tilde{R}_W(\gamma)$, dashed lines – values $\vartheta_m(\beta/2)$, $\vartheta_m(1-\beta/2)$.

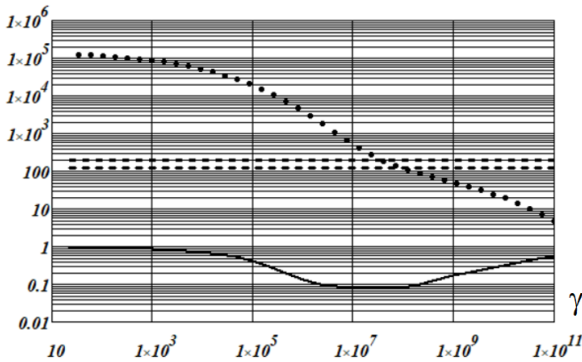


Fig. 1. Selection of the regularization parameter.

Values γ , for which the $\tilde{R}_W(\gamma)$ are between these two lines are values γ_W . Inequality (12) is satisfied for them. It can be seen that these values satisfy to the area of the minimum identification error.

IV. EXPERIMENTAL RESULTS

To answer the question - what is the gain in accuracy of identification given by the algorithm of choice of the regularization parameter in comparison with the algorithm that does not take into account the noise of the input signal measurement – numerous computational experiments were performed. The most interesting results of these experiments are presented.

As the impulse response function, the "vibrational" IPF was used. The graph of these function is shown in Fig. 2. The input signal was set by two functions: "narrowband" – solid curve in Fig. 3 (titled INPUT1) and "broadband" – the dotted curve in Fig. 3 (titled INPUT2). This choice of input signals was due to the fact that, for a broadband signal, the conditionality of the system (2) decreases and, all other things being equal, the accuracy of the estimation of the IAP increases.

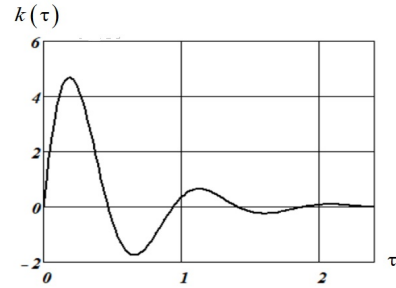


Fig. 2. Impulse response function $k(\tau)$.

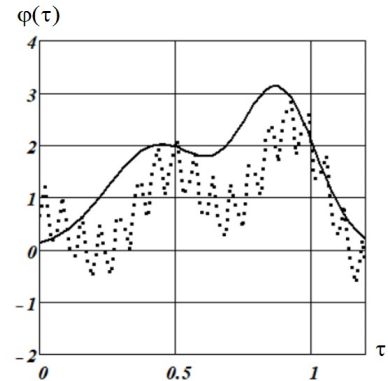


Fig. 3. Input signals of the identified system.

Number of samples identified $k(\tau_j)$ is $N_k = 100$. number of samples of the input signal $\varphi(\tau_j)$ is $N_\varphi = 60$. $N_f = N_\varphi + N_k - 1 = 159$ and $N = 256$. Discretization step is $\Delta_t = 0.022$. The relative noise levels of the right-hand side δ_f and the noise of the measurement of the input signal δ_φ were determined by the relations: $\delta_f = \frac{\|\mathbf{n}\|}{\|\mathbf{f}\|}$, $\delta_\varphi = \frac{\|\mathbf{s}\|}{\|\varphi\|}$, where \mathbf{f} , φ are the vectors of dimension N_f , N_φ , composed of the values $f(t_i)$, $\varphi(\tau_j)$ respectively. $\|\cdot\|$ is the Euclidean norm of the vector. The accuracy of the constructed regularized solution was determined by the relative error:

$$\delta_k(\alpha) = \frac{\|k_\alpha - \bar{k}^+\|}{\|\bar{k}^+\|}.$$

Initially, we illustrate the increase in the identification error with an inaccurately given input signal of the system being identified. In Fig. 4 shows the graphs for IPF2 and INPUT1: the solid curve corresponds to the relative noise levels of the measurement $\delta_f = 0.02$, $\delta_\phi = 0.0$ (the input signal is specified exactly), stroke – $\delta_f = 0.02$, $\delta_\phi = 0.10$. It can be seen that with an inaccurately given input signal, the identification error increases and the values α_{opt} are significantly (by an order of magnitude) different.

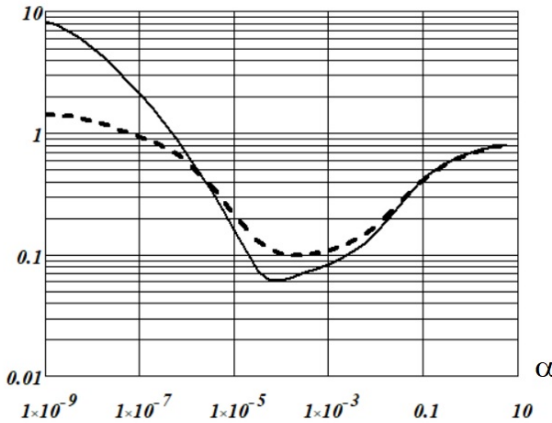


Fig. 4. Graphs of relative identification errors.

To answer the question of what kind of gain in accuracy of identification the given algorithm of choosing the regularization parameter gives, the efficiency coefficient was set. The coefficient is determined by the relation:

$$K_{eff} = \frac{\|k_{\bar{\alpha}_W} - \bar{k}^+\|}{\|k_{\alpha_W} - \bar{k}^+\|}, \quad (13)$$

where $k_{\bar{\alpha}_W}$ is the regularized solution constructed with the regularization parameter $\bar{\alpha}_W$, which was found by the criterion of optimality, but without allowance for the noise of the measurement of the input signal (statistics (7)). k_{α_W} is the regularized solution constructed with the regularization parameter α_W , which calculated by the proposed selection algorithm (statistic (9)). If K_{eff} more than 1, then the choice of the regularization parameter proposed by the algorithm is preferable. We note that the coefficient K_{eff} is a random variable whose value varies from one realization of measurement noise to another. Therefore, as a non-random characteristic, a sample mean \bar{K}_{eff} was used, defined by the expression:

$$\bar{K}_{eff} = \frac{1}{N_{sam}} \sum_{l=1}^{N_{sam}} K_{eff}^{(l)},$$

where $K_{eff}^{(l)}$ is the efficiency coefficient calculated from the realization l of measurement noise. The sample size in the experiment is $N_{sam} = 50$.

In Table. I shows the values \bar{K}_{eff} for two input signals and different δ_ϕ : (0.02, 0.05, 0.10, 0.15). The relative noise level of the output signal measurement is $\delta_f = 0.02$.

TABLE I
AVERAGE VALUES OF EFFICIENCY COEFFICIENT

| δ_ϕ | INPUT1 | INPUT2 |
|---------------|--------|--------|
| 0.02 | 1.02 | 1.01 |
| 0.05 | 1.19 | 1.17 |
| 0.10 | 1.44 | 1.39 |
| 0.15 | 1.86 | 1.82 |

V. DISCUSSION OF RESULTS

First of all, we note the effect of "self-regulation", which is caused by the noise of the input signal measurement and is as follows: in the area of small values of regularization parameter the solution error with inaccurately specified input (Fig. 4, dashed curve) less solution error with accurate input (Fig. 4, solid curve). The magnitude of this decrease is proportional to the noise level of the input signal. This effect can be explained by the fact that at small α the random noise of the input signal performs a kind of regularization – the squares $|\tilde{\Phi}_p(l)|^2$ of the DFT coefficients of the noisy kernel for large values of l prevail in the denominator of expression (3) over the values of the stabilizer $\alpha Q_p(l)$. This reduces the calculation error $K_{pa}(l)$ for these values of l and causes a decrease in the general error of the regularized solution.

Analysis of the data in the table shows that if the noise level of the measurement of the input signal is greater than the noise level of the output signal measurement, then the choice of the regularization parameter proposed by the algorithm constructed on the basis of the optimality criterion is preferable. When this difference is greater, the gain in the accuracy of identification is greater too. So, for the ratio $\delta_f / \delta_\phi = 7.5$ the identification accuracy is increased by $\approx 80\%$.

VI. CONCLUSION

The results of the computational experiment show that for the identification schemes of stationary dynamic objects, where the noise level of the input signal measurement is significantly higher than the noise level of the output signal, the proposed regularization algorithm and the algorithm for estimating the optimal regularization parameter should be used. These algorithms use the DFT as the computing basis, which causes their high computational efficiency and can process signals containing several thousand samples. Algorithms can be generalized for solving the Fredholm equation of the first kind with an inaccurately given kernel.

REFERENCES

- [1] Greblicki W., Pawiak M. Nonparametric system identification. – Cambridge University Press, 2008. – 400 p.
- [2] Tikhonov A.N., Arsenin V.YA. Methods for the Solution of Ill-Posed Problems. Moscow, Nauka Publ., 1979, 278 p. (in Russian)
- [3] Tikhonov A.N., Goncharky A.V., Stepanov V.V., Yagola A.G. Numerical Methods for the Solution of Ill-Posed Problems. Moscow, Nauka Publ., 1990, 231 p. (in Russian)
- [4] Voskoboinikov Yu.E., Preobrazhenskij N.G., Sedel'nikov A.I. Mathematical processing of the experiment in molecular gas dynamics. Novosibirsk, Nauka Publ., 1984, 238 p. (in Russian)
- [5] Voskoboinikov Yu.E., Krysov D.A. Nonparametric identification of a dynamic system with an inaccurate input signal // Automatics and software enginry, 2017, no. 4, pp. 86–93. (in Russian)
- [6] Voskoboinikov Yu.E. Stable algorithms for solving inverse measurement problems. Novosibirsk, NSUACE (SIBSTRIN), 2007, 184 p. (in Russian)
- [7] Voskoboinikov Yu.E., Litasov V.A. A stable image reconstruction algorithm for inexact point-spread function // Avtometriya – Optoelectronics, Instrumentation and Data Processing, 2006, no. 6, pp. 13–22. (In Russian)
- [8] Lukas M. A. Comparison of parameter choice methods for regularization with discrete noisy data // Inverse Problem. 2000. V. 14, № 2. P. 161–184. (in Russian)
- [9] Urmanov A.M. Information complexity-based regularizing parameter selection for solution of ill-posed inverse problems / A. M. Urmanov, A. V. Gribok, H. Bozdogan, J. W. Hines, R. E. Uhrig // Inverse problems. – 2002. – V. 18, № 3.
- [10] Voskoboinikov Yu.E. Estimation of the optimal parameter of the regularizing image recovery algorithm // Optoelectronics, Instrumentation and Data Processing. 1995. No 3. P. 64–72. (in Russian)
- [11] Voskoboinikov Yu.E. Numerical realization and comparison of four ways of choosing the regularization parameter in stable deconvolution algorithms // Science bulletin of the Novosibirsk state technical university. 2004. No 2 (17). P. 27–44. (in Russian)



Voskoboinikov Yury Evgenievich, Dr. Sci. in Physics and Mathematics. Professor, Honored worker of Higher school of Russian Federation, Full Member of MAI, RAE, man HSE, Professor of automation Department of NSTU. Head of the Department of applied mathematics of the new Novosibirsk State University of Architecture and Civil Engineering construction (Sibstrin). Author of more than 300 scientific publications, 6 monographs devoted to solving incorrect problems of data interpretation and signal and image processing, 16 textbooks and teaching AIDS. voscob@mail.ru



Krysov Danila Alekseevich, postgraduate student, Department of Automatics, Novosibirsk State Technical University. Author of several scientific articles. Area of scientific interests: wavelet filtration, identification of systems.

Additional Simplification of the Precision Frequency Synthesizer

Vadim A. Zhmud^{1,2}, Lubomir V. Dimitrov³, Audrey Yu. Ivoylov¹

¹Novosibirsk State Technical University, Novosibirsk, Russia

²Institute of Laser Physics SB RAS, Novosibirsk, Russia

³Technical University of Sofia, Sofia, Bulgaria

Abstract – The development and creation of frequency synthesizers is extremely important for laser physics problems, primarily for absolute frequency measurements. Numerous technical solutions for these purposes are known, but specific requirements, including the absence of jumps in the switching of the control code and the smoothness of the phase change of the generated signal, make it necessary to abandon the use of most known technical means for these purposes and develop individual devices based on new technical solutions. To the greatest extent these requirements are met by synthesizers on the basis of a method combining phase auto-tuning and frequency summation. The accuracy of such synthesizers is enhanced by the addition of identical blocks, which are seen as extremely simple. However, as it turns out, these blocks are still quite complex. Therefore, their addition is associated with a noticeable rise in price. This paper offers a new original solution to this problem by developing such refinement blocks that do not contain phase-locked loop subsystems. The synthesizer contains a simple block generating only two reference frequencies, several identical blocks containing synchronized switches, frequency adders, frequency dividers and filters, and the technical requirements for all these nodes are extremely simple. High characteristics of the device as a whole are achieved due to the organization of the signal conversion algorithm in it. The chosen frequency ratios greatly simplify the filters. The theoretical substantiation of the working capacity of all technical solutions, confirmed by modeling, is given, as well as the functional scheme of the synthesizer.

Index Terms – Frequency synthesizer, precision oscillator, frequency feedback, phase-locked loop, laser systems, frequency control, phase control.

I. INTRODUCTION

PRECISE measurements, fundamental metrology and other laser physics problems require extremely precise generation of a given frequency signal, as well as a very precise and smooth tuning of this frequency with a very small step [1–5]. Previously, these tasks were solved with the creation of a highly stable controlled generator, but this did not meet the requirements for frequency stability, although it ensured sufficient smoothness of its frequency changing. Modern devices of laser physics states such high demands of such generators that they can be satisfied only by means of digital frequency synthesis, which is performed in frequency synthesizers [6–13]. This is a completely different class of devices in which the generation frequency is determined not by the input control voltage, but precisely specified by the

input code. Changing of the code to the least significant digit should cause the frequency to change to the minimum step, and this change should occur without sudden phase changes. This is one of the most essential and elusive requirements.

Novosibirsk State Technical University and Institute of Laser Physics of SB RAS have developed a number of devices in which similar synthesizers are used, and the progress of such devices depends to a great extent on the progress in the development of frequency synthesizers. One of the latest versions of this synthesizer is described in [14]. This device still has some drawbacks, for the overcoming of which, studies have been performed. The results are described in this paper. These studies are aimed at creating a frequency synthesizer characterized by smoother transient processes in frequency switching, as well as greater reliability, simplicity and better possibilities for reducing the control step, i.e. improve accuracy.

II. PROBLEM DEFINITION

The prototype of the synthesizer is made on a combinational principle with the band-quartz frequency stabilization. Its functional diagram is shown in Fig. 1.

The device contains standard (reference) quartz oscillator of frequency $F_0 = 10 \text{ MHz}$, several counters for obtaining multiple frequencies: $F_1 = 1 \text{ MHz}$, $F_2 = 6.25 \text{ kHz}$ and $F_3 = 125 \text{ kHz}$, interface for inputting the control code and a number of similar summation and division units. Each such node contains a phase locked loop (PLL), a frequency adder and a divider-counter. Each node performs the conversion of the input frequency to the frequency with the increments determined by the control code. With this purpose, the PLL generates a frequency according to the ratio

$$F_{out} = F_{in} \times (140 + \Delta_i).$$

Here the input frequency is close to $F_2 = 6.25 \text{ kHz}$. After multiplying by 140, the output frequency is close to $F = 875 \text{ kHz}$. At the output of the first node, the output frequency is then added to the frequency $F_3 = 125 \text{ kHz}$, resulting in a frequency close to $F_1 = 1 \text{ MHz}$, this frequency is divided by 8. The result is a frequency that is again close to the original value of $F_3 = 125 \text{ kHz}$, but already contains the obtained frequency additive divided by 8. The frequency addition is initially multiples of $F_3 = 125 \text{ kHz}$, since it is this value, to which the frequency of the controlled oscillator is tuned after it is divided into the corresponding code supplied to this node.

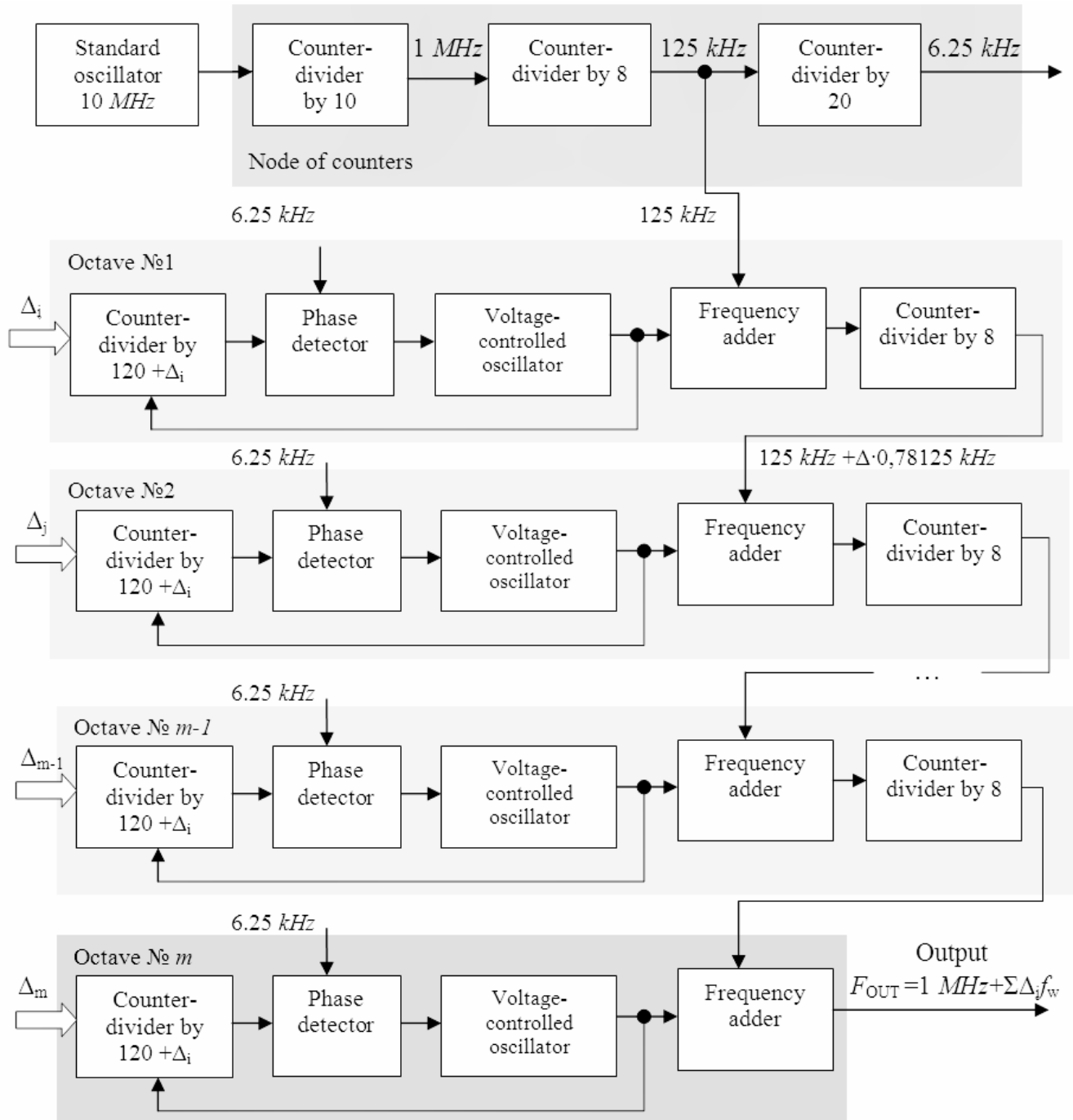


Fig. 1. Functional diagram of the synthesizer.

Thus, after the first conversion from frequency $F_1 = 1 \text{ MHz}$, the frequency $F_{01} = 1 \text{ MHz} + x$ is formed, where x takes one of the following values:

$$\begin{aligned} x_0 &= 0 \text{ kHz}, \\ x_1 &= F_2 = 6,25 \text{ kHz}, \\ x_2 &= 2F_2 = 12,5 \text{ kHz}, \\ x_3 &= 3F_2 = 18,75 \text{ kHz}, \\ x_4 &= 4F_2 = 25 \text{ kHz}, \\ x_5 &= 5F_2 = 31,25 \text{ kHz}, \\ x_6 &= 6F_2 = 37,5 \text{ kHz}, \\ x_7 &= 7F_2 = 43,75 \text{ kHz}. \end{aligned}$$

After dividing by 8, the frequency is formed, which is 8 times smaller, hence, the frequency increments become 8

times smaller. This frequency is used in the second transformation, where a new increment is added, and so on.

The frequency adder is a consecutive connection of a multiplier of signals and a high-pass filter. The filter passes the total frequency to its output and does not pass the difference frequency.

Thus, because of the summation of frequencies, the frequency $F_1 + x_i$ is formed on the first node, which can be called an octave. At the output of the second octave, a frequency equal to $F_1 + y_j + 0,1 x_i$ is formed. At the output of the third octave, a frequency equal to $F_1 + z_k + 0,1 y_j + 0,01 x_i$ is generated, etc. Thus, each octave shifts the previously obtained frequency increment 8 times down and adds a new

increment, while maintaining the value carrier frequency $F_1 = 1 \text{ MHz}$. This allows the reducing of the amount of the frequency setting step by adding standard nodes (octaves). All nodes of the octave are identical, which facilitates the manufacture and debugging of the synthesizer.

The last node does not contain a divider counter, since in applications in laser systems, the specified carrier frequency is the frequency that is required.

The disadvantage of the device is the need to use a large number of PLL systems with feedback control [15–20]. These PLL are used to form a frequency that is equal to the sum of the selected carrier frequency and the added frequency multiplied by the discrete value of the additive at the current step selected from the set from 0 to 7.

III. THEORY

With the use of quart instead of octave, the additive will be multiplied by a value from 0 to 3, while dividing by the divisor-counter should be performed not in 8 times, but only in 4 times.

Such a modification would increase the number of identical blocks, but significantly simplify them. Accordingly, if in the above scheme, to obtain the frequency $F_1 = 1 \text{ MHz}$, it is required to add two frequencies, representing, respectively, seven eighths and one eighth of the required value (and after dividing by 8, one eighth is obtained again), then the modification would require adding the frequencies, equal, respectively, to three fourth and to one fourth of the desired value of the frequency.

It is possible to develop this approach further, and to use a twofold increase in the frequency with addition and then dividing the frequency only by half. In this case, the additive at each step will vary only from 0 to 1, i.e. only one of the two fixed frequencies is required.

In the previous version of the synthesizer, shown in Fig. 1, a PLL system and a divider-counter are used to form the frequency with the addition. Of course, such a node has great potential, but it is more complicated. If only one of the two frequencies is required, then instead of the PLL system, a conventional frequency switch can be used. Arbitrary frequency switching, as a rule, generates a phase jump at the moment of switching, but with the chosen ratios of the used frequencies, this jump can be eliminated. Indeed, for example, if it is necessary to switch frequencies that are related to each other like 3: 4, then from time to time their phases may coincide, for example, with a certain initial synchronization, after every three periods of a lower frequency, they will again be in the same phase, since this interval will be exactly equal to four periods of higher frequency.

Fig. 2 shows the graphs of two frequencies, $F_{11} = 3f_0$ and $F_{12} = 4f_0$. It can be seen that these graphs regularly pass through states of identical phases. In this case, these points correspond to a signal value equal to zero and a close (albeit unequal) value of the derivatives of this signal. If these oscillations are not so well synchronized initially, then with the periodicity equal to four periods of frequency $F_{11} = 3f_0$ or, which is identical, three periods of frequency $F_{12} = 4f_0$,

the situation is repeated that the values of these signals coincide, and the derivative of the signal with frequency F_{11} is equal to third of the derivative signal with a frequency of F_{12} . These moments can be identified by analyzing these signals. The switching control circuit can be arranged so that the switching occurs only at these instants.

Fig. 3 shows the result of operation of such a switching circuit. In the first half of this graph, the signal has a frequency of $F_{12} = 4f_0$, and in the second half of this graph it has a frequency of $F_{11} = 3f_0$. Switching occurs smoothly, without jumps.

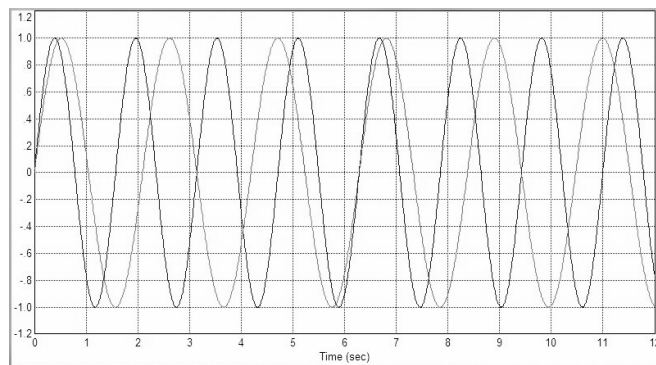


Fig. 2. An illustration of the fact that the frequencies $3f_0$ and $4f_0$ regularly pass through a state with the same phase.

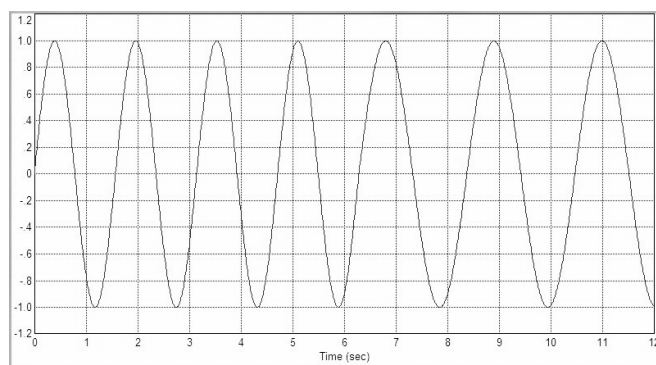


Fig. 3. The result of switching of the signals at the moment of coincidence of their phases: there is no jump.

Fig. 4 shows the result of multiplying this signal by a signal with a frequency $F_{12} = 4f_0$. Fig. 5 shows the same signal over a longer time interval. The result of high-frequency filtering of this signal is shown in Fig. 6. It can be seen that the signal obtained is quite similar to a harmonic signal, although its frequency changes abruptly at the moment of switching ($t = 12 \text{ s}$).

Figures 7 and 8 show similar signals when summing a signal previously shown in Fig. 4, with a signal with a frequency $F_{11} = 3f_0$. It can be seen that even in this case the filtering is carried out quite effectively; there are no problems with jumps of the signal, although the frequency changes abruptly at the same time. Thus, the combination of these graphs shows that it is possible to jump the frequency of the signal abruptly without the appearance of jumps in the form of this signal, and it is also possible to efficiently convert the received signal, namely, to add it to another signal of a close frequency by multiplying with subsequent high-pass filtering.

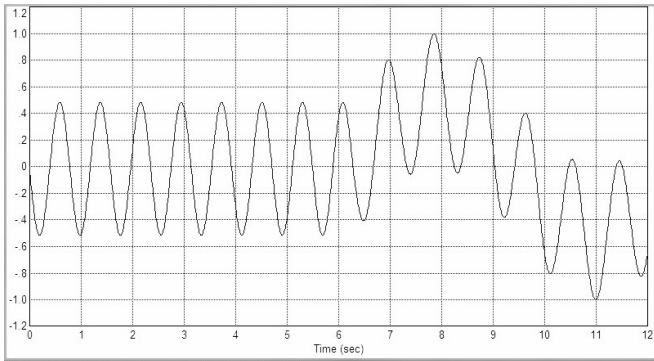


Fig. 4. The result of the conversion of the signal shown in Fig. 4, by multiplying it by a signal whose frequency is $4f_0$.

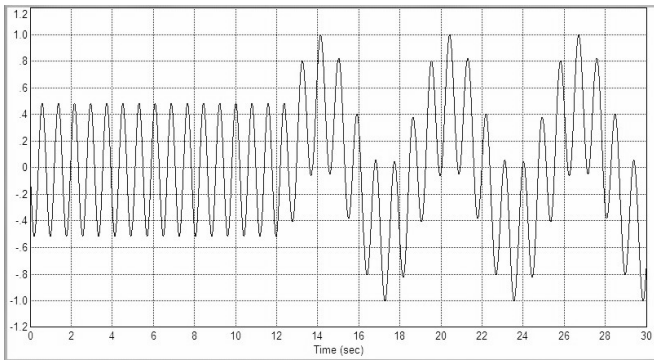


Fig. 5. The same signal as in Fig. 4, for a longer time interval.

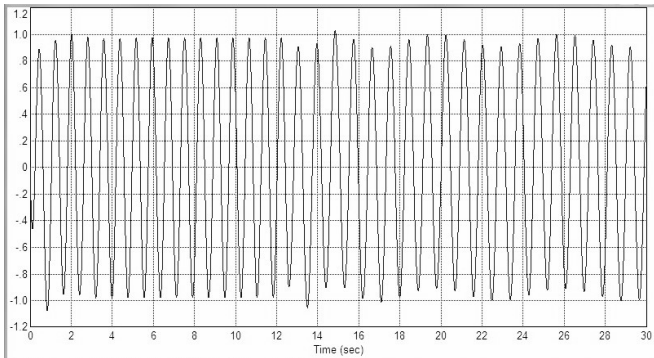


Fig. 6. The result of filtering of the signal shown in Fig. 5.

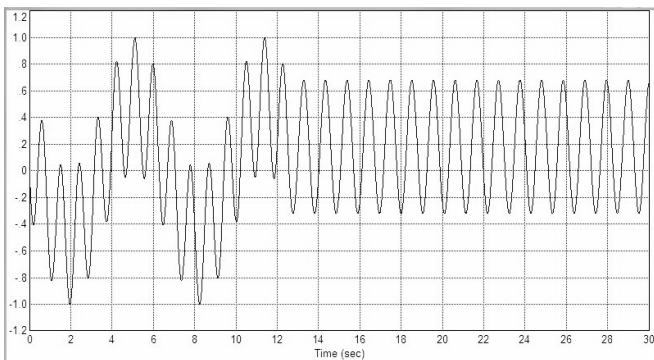


Fig. 7. The result of converting of the signal shown in Fig. 4, by multiplying it by a signal whose frequency is $3f_0$.

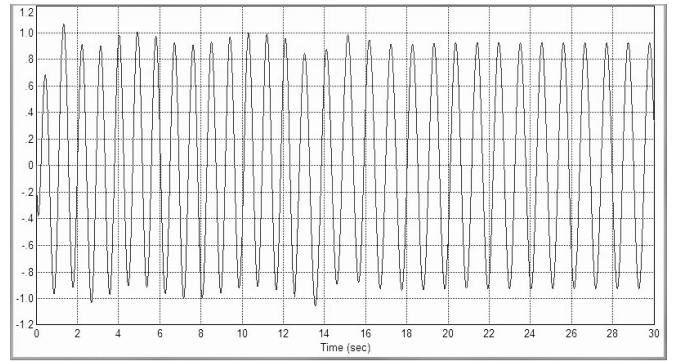


Fig. 8. The result of filtering the signal shown in Fig. 7.

IV. FUNCTIONAL DIAGRAM OF THE PROPOSED SYNTHESIZER OF FREQUENCIES

Fig. 9 shows a functional diagram of the proposed frequency synthesizer. The device contains a former of two frequencies with a multiplicity of 2: 3. In this case, frequencies of 500 kHz and 750 kHz are formed. The device also contains the required number of frequency refining nodes (octaves). Each such node contains a switch, a frequency adder, divider-counter by two and a filter. In this case, the frequency adder consists of a frequency multiplier, a high-pass filter and an end comparator, which converts the signal into a digital one. The output filter of each divider-counter serves to convert a rectangular signal into a harmonic signal.

In the first block, depending on the value of the least significant digit Δ_1 of the incoming code, the switch applies a frequency of 500 kHz to the input of the adder, if this bit is zero, or 750 kHz, if this bit is equal to one. Further, this frequency is added to the input frequency of 500 kHz, resulting in a frequency equal to 1000 kHz, if the code is zero, or 1250 kHz, if the code is equal to one. This frequency is divided in half, which gives $F_{21} = 500 \text{ kHz} + \Delta_1 \cdot 125 \text{ kHz}$.

The following node works in a similar way, but for the addition, it uses frequency F_{21} . As a result, the output of this unit generates a frequency equal to $F_{22} = 500 \text{ kHz} + \Delta_2 \cdot 125 \text{ kHz} + \Delta_1 \cdot 62.5 \text{ kHz}$. Further on the next block this frequency is again used as input, resulting in a new frequency $F_{23} = 500 \text{ kHz} + \Delta_3 \cdot 125 \text{ kHz} + \Delta_2 \cdot 62.5 \text{ kHz} + \Delta_1 \cdot 31.25 \text{ kHz}$. Each subsequent node reduces the previous additions by a factor of two and adds its own frequency addition, depending on the value of the corresponding digit controlling the output frequency of the synthesizer.

The end node does not contain a divider counter, since laser systems require a synthesizer at a carrier frequency of 1 MHz, which is the case in this case.

The obvious advantages of the proposed frequency synthesizer are its following features:

1. Absence of PLL subsystems, which greatly simplifies its scheme.
2. The ability to arbitrarily reduce the control step, i.e. to increase the accuracy of the prescribed frequency by adding identical simple nodes.
3. Extremely simple conditions for calculating all filters.

4. There is no need to debug nodes with a well-established prototype of one node (due to simplicity and identity), which simplifies replication and operation, as well as repair.

5. The extremely small number of required sample frequencies (only two), which can easily be obtained from a single frequency, and as a consequence, the possibility of an external reference of the standard frequency.

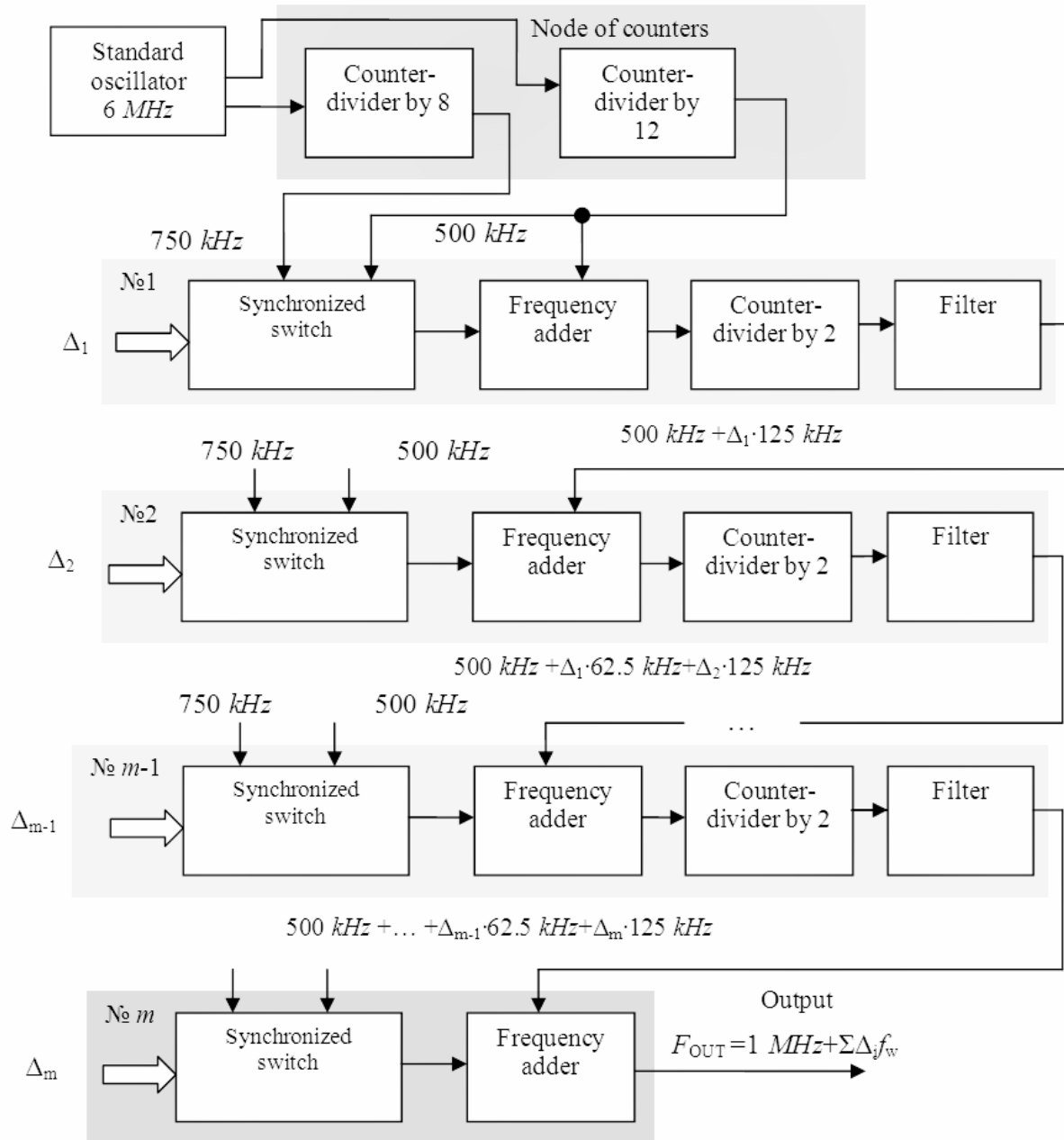


Fig. 9. Functional diagram of the synthesizer.

IV. EXPERIMENTAL RESULTS

Multiple simulations with different initial code values and when switching them to different new values have shown that in the signals formed in the intermediate blocks called octaves, there are no phase jumps, and the frequency changes abruptly to the desired value. In the output signals of these units, the frequency changes more smoothly, but phase jumps are also absent. In the final signal, phase jumps are also absent. This simulation result is not unexpected, since

the phase jumps are eliminated by the very principle of signal formation.

V. DISCUSSION OF RESULTS

This simulation result is not unexpected, since the phase jumps are eliminated by the very principle of signal formation. The structure according Fig. 9 is simple, effective and has high potential accuracy because the step of control can be decreased as fine as necessary by simple addition of the similar nodes.

VI. CONCLUSION

The paper proposes a new scheme for a precision synthesizer of frequency with an extremely small step. This scheme is easily manufactured, tuned and replicated. It is simpler than all the known and previously proposed and developed devices, including ones, developed by the authors of this publication. The circuit, like its prototypes, allows the increasing of the accuracy (i.e. reducing of the pitch of the frequency grid) by adding of the identical nodes, but these nodes are extremely simple due to the lack of PLL subsystems. The described synthesizer can be used in precision phase-locked loop systems as part of signal processing equipment. The control step can be arbitrarily reduced. The generated frequency is characterized by the accuracy and stability of the standard generator. This is especially important when creating systems for fundamental laser metrology (in absolute frequency measurements).

VII. ACKNOWLEDGEMENTS

The Russian Ministry of Education and Science supported this work. The Russian Scientific Foundation (Project No. 16-12-00052) has supported this work.

REFERENCES

- [1] Bagaev S.N., Belkin A.M., Dychkov A.S. et al. "Absolute frequency measurement of molecular Iodine reference line near 732 nm used for high precision spectroscopy of Muonium". Russian-German Laser Symposium. Novosibirsk, 27.06–1.07.97. Technical digest. p. P12–P13.
- [2] Bagaev S.N., Belkin A.M., Dychkov A.S. et al. "Frequency reference in the 732-nm region for precision laser spectroscopy of muonium". 2000 Quantum Electronics. 30(7), c. 641–646.
- [3] Bagayev S.N., Belkin A.M., Dychkov A.S. et al. "Absolute Frequency Measurements in Precision Laser Spectroscopy of Muonium". In collection: Proceedings of SPIE – The International Society for Optical Engineering Proceedings of the 1998 Nonlinear Optical Phenomena and Coherent Optics in Information Technologies, ICONO-98. Moscow, RUS, 1999. P. 310–318.
- [4] Zhmud V.A., Barmasov S.V. and Gitel'son V.D. "An electronic system for stabilizing the frequency of the He-Ne laser to the methane absorption lines". 1999 Instruments and Experimental Techniques. 42(4), c. 551–557.
- [5] Zhmud V., Dimitrov L. and Yadrishnikov O. "Calculation of regulators for the problems of mechatronics by means of the numerical optimization method" 12th International Conference on Actual Problems of Electronic Instrument Engineering, APEIE 2014 – Proceedings. 7040784, p. 739–744.
- [6] Efimov A.S. and Zhmud' V.A. "A frequency synthesizer with the supersmall step for the systems of frequency and phase autotuning". 1996 Optoelectronics, Instrumentation and Data Processing (Avtometriya). (2), P. 21–25.
- [7] DAC38RFxx Dual-Channel, Single-Ended, 14-Bit, 6- and 9-GSPS, RF-Sampling DAC With JESD204B Interface and On-Chip GSM PLL. <http://www.ti.com/general/docs/lit/getliterature.tsp?baseLiteratureNumber=SLASEF4&fileType=pdf>
- [8] Frequency Synthesiser Types. URL: <http://www.radio-electronics.com/info/rf-technology-design/pll-synthesizers/frequency-synthesiser-introduction-types.php>
- [9] What is an RF Frequency Synthesiser: technology & types. URL: <https://www.electronics-notes.com/articles/radio/frequency-synthesizer/synthesizer-types-introduction.php>
- [10] Ask the Applications Engineer – 30: PLL Synthesizers. Fox A. <http://www.analog.com/en/analog-dialogue/articles/pll-synthesizers.html>
- [11] M. Farazian et al., Fast Hopping Frequency Generation in Digital CMOS. Springer Science+Business Media New York 2013. Architectures for Frequency Synthesizers. URL: http://www.springer.com/cda/content/document/cda_downloaddocument/t/9781461404897-c2.pdf?SGWID=0-0-45-1355443-p174127461
- [12] Lu T-Y, Chen W-Z (2008) A 3-to-10GHz 14-band CMOS frequency synthesizer with spurs reduction for MB-OFDM UWB system. IEEE ISSCC digest of technical papers, pp 126–601, Feb 2008.
- [13] Liang C-F, Liu S-I, Chen Y-H, Yang T-Y, Ma G-K (2006) A 14-band frequency synthesizer for MB-OFDM UWB application. IEEE ISSCC digest of technical papers, pp 428–437, Feb 2006.
- [14] Zhmud V.A., Dimitrov L.V. and Ivoilov A. Yu. Precision Frequency Synthesizer. Automatics & Software Engineering. 2018. № 1 (23). P. 20–32. <http://www.jurnal.nips.ru/sites/default/files/AaSI-1-2018-2.pdf>.
- [15] Zhmud V.A., Dimitrov L.V. and Yadrishnikov O.D. "Calculation of regulators for the problem of mechatronics by means of numerical optimization method". 12th International Conference on Actual Problems on Electronic Instrument Engineering APEIE 2014. Proceedings.
- [16] Zhmud V. A., Semibalamut V. M. and Vostrikov A. S. "Feedback systems with pseudo local loops". Testing and measurement: techniques and applications: proc. of the 2015 intern. conf. on testing and measurement techniques (TMTA 2015), Thailand, Phuket Island, 16–17 Jan. 2015. – London: CRC Press, 2015. – P. 411–416.
- [17] Kotova E. P. and Frantsuzova G. A. "Application PI2D controller in automatic control systems". Int. Siberian conference on control and communications (SIBCON): proc., Kazakhstan, Astana. 2017.: S. Seifullin Kazakh Agrotechn. Univ., 2017. P. 692–695.
- [18] Zhmud V. A., Hlava J., Frantsuzova G. A. "Using the robust PID controller to manage the population of thermostatically controlled loads". Int. conf. on industrial engineering, applications and manufacturing (ICIEAM): proc., Chelyabinsk, 2017. IEEE, 2017. 4 p.
- [19] Hlava J., Zemtsov N. and Frantsuzova G. A. "Application of PID controller based on the localization method for ancillary service provision". Int. Siberian conf. on control and communications (SIBCON): proc., Moscow, 2016. IEEE, 2016. 6 p.
- [20] Suvorov D. A., Frantsuzova G. A. and Zemtsov N. S. "Using the localization method for once-through boiler control". Int. Siberian conf. on control and communications (SIBCON–2015): proc., Omsk, 2015. IEEE. 5 p.



Zhmud Vadim Arkadievich – Head of the Department of Automation in NSTU, Professor, Doctor of Technical Sciences.
E-mail: oao_nips@bk.ru

630073, Novosibirsk,
str. Prosp. K. Marksa, h. 20



Dimitrov Lubomir Vankov - Vice-Rector of the Technical University of Sofia (Sofia, Bulgaria), Doctor of Science, Professor, Honorary Doctor of the NSTU.
E-mail: lubomir_dimitrov@tu-sofia.bg

Bul. "St. Kliment Ohridski" 8, 1756 Studentski
Complex, Sofia, Bulgaria



Ivoylov Andrey Yurievich – PhD-student of Department of Automatics of NSTU.
E-mail: iau13hv@mail.ru

630073, Novosibirsk,
str. Prosp. K. Marksa, h. 20

Providing of Smooth Switching of Sine Signals for Precision Frequency Synthesizer

Vadim A. Zhmud^{1,2}, Lubomir V. Dimitrov³, Andrey Yu. Ivoylov¹

¹Novosibirsk State Technical University, Novosibirsk, Russia

²Institute of Laser Physics SB RAS, Novosibirsk, Russia

³Technical University of Sofia, Sofia, Bulgaria

Abstract – Laser systems are widely used to create highly stable frequency standards, as well as for absolute frequency measurements. One of the most important components of such systems is a precision frequency synthesizer. Despite the fact that there are many ready-made developments in this area, most of them do not meet the highest requirements for such synthesizers in terms of smooth frequency switching without any jumps in the phase or amplitude. Modern developments in this area are sometimes too complicated. Simplification of such devices while providing these characteristics lies in the ways of abandoning the phase subsystems of auto-tuning in the intermediate nodes of such systems, replacing it with simple switches of different frequencies, depending on the value of the frequency that is required to synthesize. However, the switching of signals of different frequencies inevitably must cause jumps in the generated signal at the moment of switching. This approach seems to contradict the task posed. This paper investigates ways of solving the problem of smooth switching of signals in such a way that the frequency undergoes a change at the output of the switch, but there would be no phase jumps in the generated signal. An analysis of the ways of solving this problem is given, a functional diagram for the switch providing the required smooth switching is provided, reliable and correct operation of the switch is confirmed by the results of the simulation.

Index Terms – Frequency synthesizer, precision oscillator, frequency feedback, phase-locked loop, laser systems, frequency control, phase control

I. INTRODUCTION

ONE of the most important uses of laser systems is to use them as sources of the most stable frequency. In laser systems, many transformations of optical frequencies are carried out, including phase binding of one laser to another, obtaining difference frequencies in the radio frequency range, controlling these frequencies by affecting the frequency of laser radiation, and so on. One of the key subtasks is the precise control of the frequency of the radiation, which is achieved by linking the resulting difference frequency to the reference frequency, which is formed by a synthesizer with an extremely small control step [1–6]. To solve these problems, synthesizers has been

developed [7–14]. However, not every synthesizer can be used in such a task, but only those that allow unlimited reduction of the control step due to the growth of identical nodes [7, 14]. The latest developments in this field are still unnecessarily complicated, since they require the use of a large number of feedback phase-control subsystems [15–16] for intermediate controlled of generators, which are used in the said identical nodes [14]. The functional scheme of such a synthesizer can be simplified to a sufficient degree, however, this requires solving the problem of switching two frequencies in such a way that at the moment of switching no jumps occur in the signal being generated, i.e. so that the signal at the output of the switch eventually smoothly changes its frequency, but does not change its value sharply. This paper is devoted to solving this problem.

II. PROBLEM DEFINITION

A simplified functional diagram of the proposed synthesizer is shown in Fig. 1. In this device, the reference oscillator generates only two frequencies, namely: $F_1 = 500 \text{ kHz}$ and $F_2 = 750 \text{ kHz}$. In addition, it has the necessary number of frequency refining nodes. Each such node contains a switch, which is a problem that is discussed in this article, as well as relatively simple elements: a frequency adder, a divider-by-two counter and output filter. The frequency adder consists of a frequency multiplier, a high-pass filter, and an end former (comparator or trigger) that converts the signal to a digital one. The output filter of each divider-counter serves to convert a rectangular signal into a harmonic signal.

The operating principle of this synthesizer can be understood from the functional diagram.

Fig. 2 shows the simulation process of the frequency conversion scheme in the software *VisSim*. When this structure is running, each frequency changes from a larger value to a smaller value by jumps. First the switch controlled by the highest digit of the code, makes switching. Then the next one, and so on, the switch operated by the low-order bit is switching at the end. The simulation result is shown in Fig. 3.

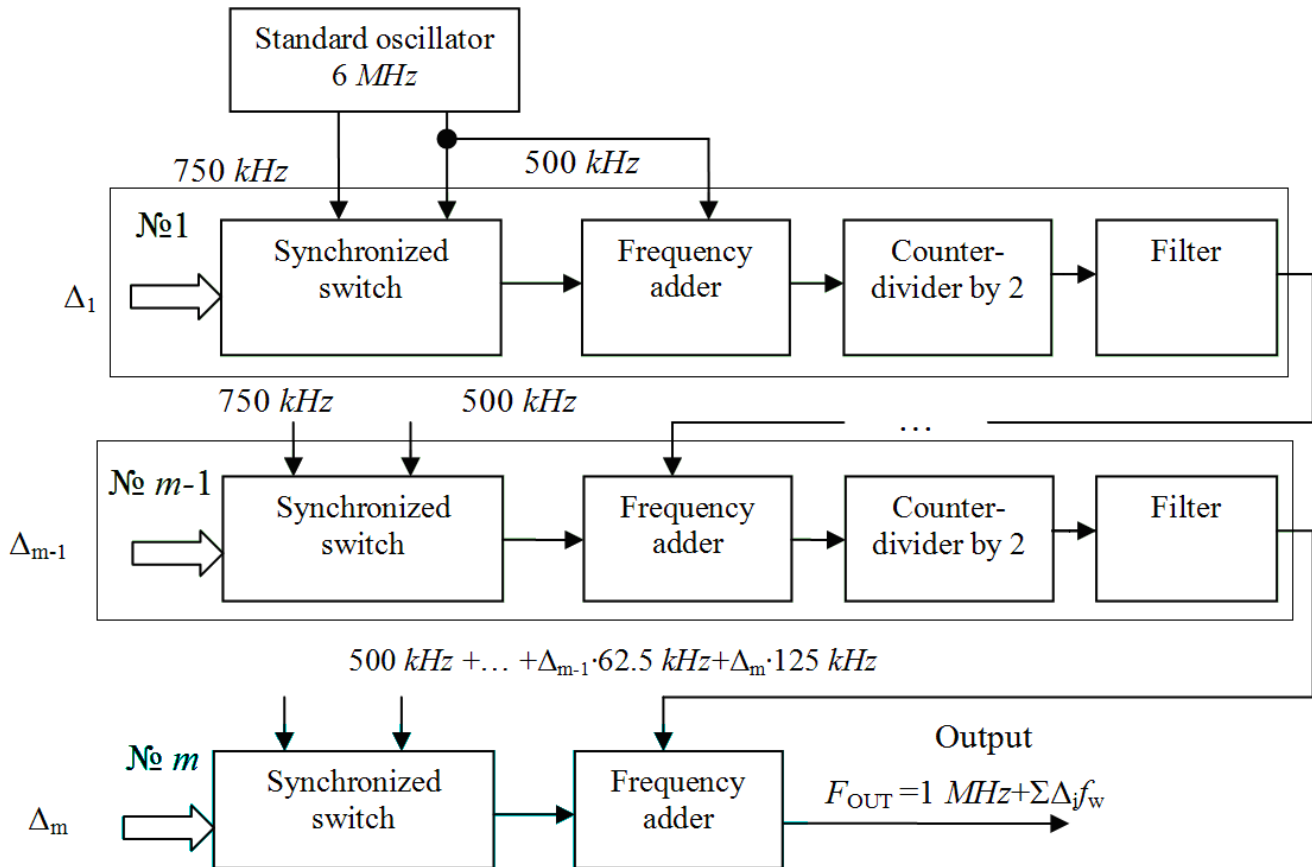


Fig. 1. Functional diagram of the synthesizer.

It can be seen that the operation of the key of the highest digit gives the greatest jump, the jump from the operation of each subsequent digit is half the jump from the preceding digit and so on. Depending on the input code, any frequency between $F_{\min} = 1$ and $F_{\max} = 1.5$ MHz can be obtained.

Thus, the problem of frequency synthesis is completely solved except for the sub problem of switching signals of two frequencies in such a way that there is no phase jump. In this case, the switching takes place relatively fixed frequencies $F_1 = 500$ kHz and $F_2 = 750$ kHz.

Both these signals are generated from the sample oscillator, which allows ensuring the following conditions: these signals have the same amplitude, every third pass through the zero of the frequency signal F_1 coincides with every second pass through zero of the frequency signal F_2 , as shown in Fig. 4. The switch can be developed, that switches signals only at these moments, and at other times switching is prohibited.

The statement of the problem can be complicated by setting such a requirement that the switching occurs smoothly even if the initial synchronization is not carried out. Such an extension of the functions of the switch allows switching without jumps signals of such frequencies that are not multiples, which will in the future not be tied to the first condition. It gives additional possibilities for frequencies choosing. This can simplify the synthesizer with some special requirements for it.

It is possible to estimate how often the phases of two harmonic signals coincide. Simple reasoning leads to the

conclusion that this situation will be repeated with a period corresponding to the difference frequency. The closer the frequencies that have to be switched, the less often there are moments when switching without phase jumps is possible. If the frequencies differ by 10%, then switching is possible once for ten periods of a lower frequency, which corresponds to eleven periods of a higher frequency. If the frequencies differ by 1%, switching is possible once for approximately one hundred periods.

With the chosen frequency ratio, the possibility of switching them without phase jumps is repeated at intervals equal to two periods of a lower frequency, which is equal to three periods of a higher frequency, i.e. approximately every 6.67 ms. This can be considered a sufficiently high speed. In the control system of a laser spectrometer, switching frequencies must be performed less frequently than once per second. Thus, the proposed technical solution more than 100 times the speed corresponds to the task.

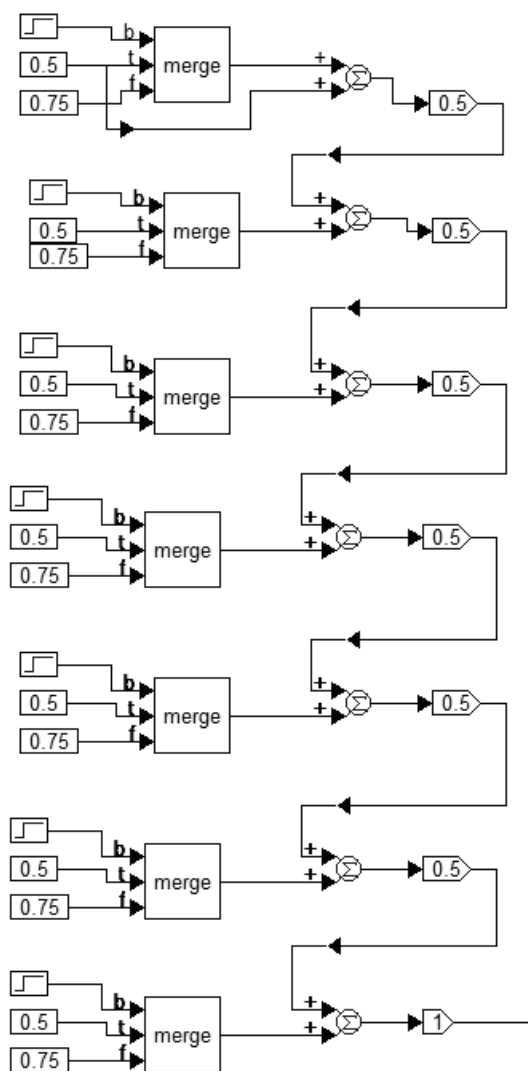


Fig. 2. The scheme for modeling the process of forming the desired frequency in the synthesizer.

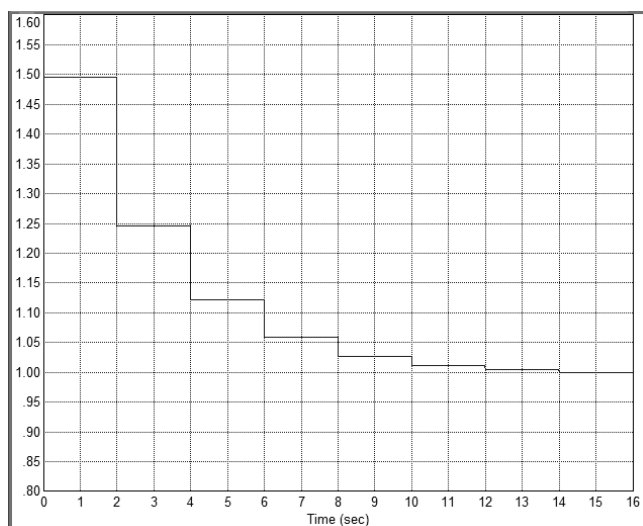


Fig. 3. The result of modeling the process of forming the desired frequency in the synthesizer.

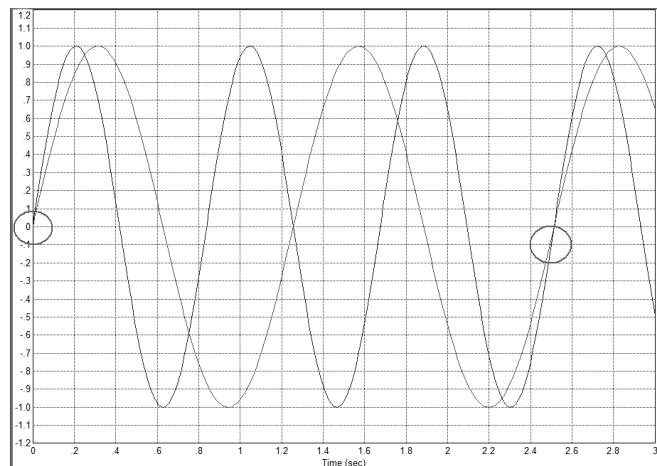


Fig. 4. An illustration of the fact that with the initial synchronism of frequencies $F_1 = 500 \text{ kHz}$ and $F_2 = 750 \text{ kHz}$, the synchronization situation is regularly repeated (the time units on the graph are conditional).

III. THEORY

If the first requirement is fulfilled and the signals of the switched frequencies are synchronized initially, as shown in Fig. 4, then the logic of operation of the synthesizer should ensure the detection of such states of both these signals, when the values are simultaneously close to zero, and the values of their derivatives coincide in sign. It can be noted that in this case the ratios of the absolute values of these derivatives are correlated in the same way as their frequencies are related, i.e. as two to three.

If the signals are not synchronized initially, then this condition should be slightly modified. The switching should be carried out at the moments when the values of these signals are close to each other, and the values of their derivatives coincide in sign and correlate as two to three.

IV. EXPERIMENTAL RESULTS

The device for recognizing this situation and generating a switching signal is shown in Fig. 5. It contains a signal difference calculator, a difference calculator with a coefficient, a differentiating device, two absolute value calculators, an adder with three inputs, scale amplifiers and a logic inverter. Also on the device, signal lines x , y , z are indicated to use these signals in other parts of the switch. An additional offset of -0.02 is applied to the adder with three inputs. This makes it possible to form a signal not strictly at the moment of equalization of the zero of the calculated signal, but on a somewhat longer interval, otherwise the generated signal would have zero duration. The received signals are shown in Fig. 6.

The signal generated in the device of Fig. 5 is then used to synchronize the switching signal. For this purpose, a trigger with dynamic synchronization input can be used, but in the software *VisSim* such a trigger was not found, so the sampling-and-hold device was used. The circuit of this device and the generated signal are shown in Fig. 7.

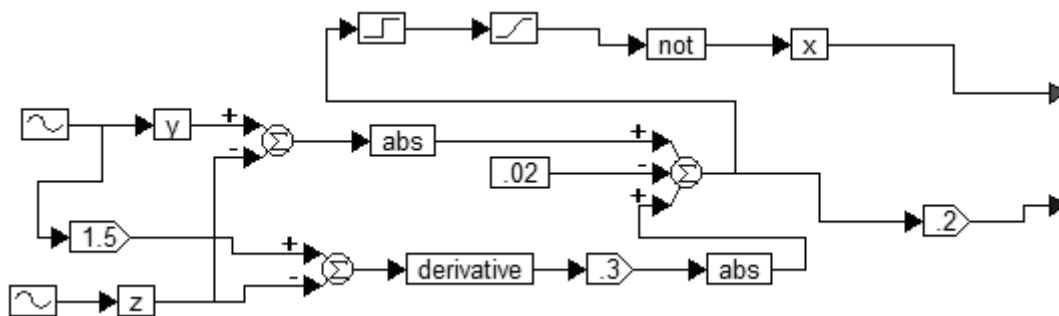


Fig. 5. Device for generating a switching signal: the lower output is analog signal to be analyzed, the upper output is digital signal to control switch.

Further, the generated signal, whose front coincides with the moment of equality of the switched signals and the required ratio of their derivatives, is used to switch signals.

Fig. 8 shows the switch circuit and the signal at its output. It can be seen that at the time $t = 2.5$ s (conditional time), when a short pulse is formed, shown in Fig. 6, the circuit forms the front of the switching signal shown in Fig. 7. It is at this moment when the signal frequency is switched.

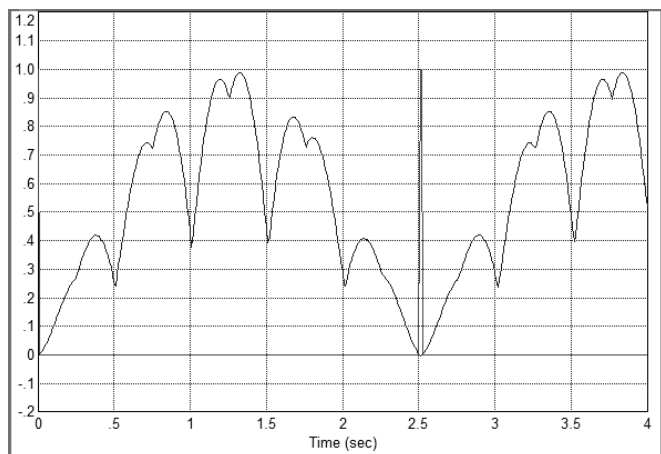


Fig. 6. Signals in the device according to Fig. 5: sharp pulse is formed when the smooth signal is close to zero.

For the purity of the experiment, another initial shift can be specified in one of the switched signals, or in the both. For example, let's set the first signal to a shift equal to 1.2 s. In this case, the values of the switched signals will coincide not with their zero value, but with the other, which is approximately 0.8 at the time approximately 2.6 seconds. It is at this moment that the circuit is switching. Fig. 9 shows the operation of the switch in both directions. According to the prescribed signal, the switch had to switch the frequency from the larger one to the smaller one at the instant of time equal to 1 s, and then from the lower frequency to the larger one at the time point equal to 4.5 s. The circuit of Fig. 7 generated a control signal starting at about 2.6 s, and terminating at zero at about 5.2 s. It was at these moments that a switch was made.

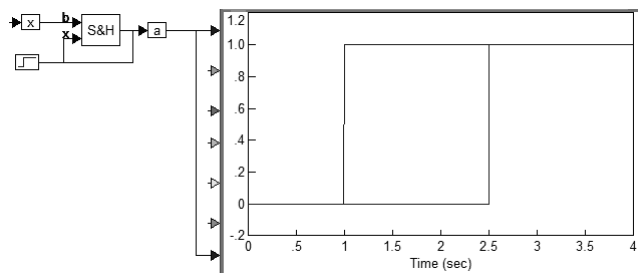


Fig. 7. Synchronization device and signals generated in it

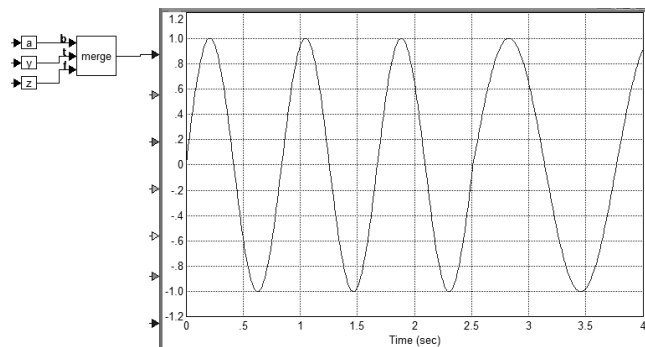


Fig. 8. Switching unit and the signal it generates.

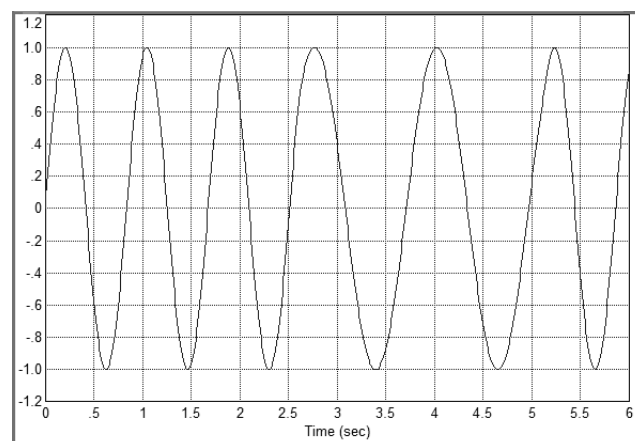


Fig. 9. The result of switching the signal from a higher frequency to a smaller one and back.

V. DISCUSSION OF RESULTS

The paper has proposed the method of switching harmonic signals of a fixed frequency for the forming of a signal with the variable frequency. This required the absence of phase jumps. The proposed method has been tested by modeling,

which has confirmed its operability and full compliance with the results obtained with those requirements that were put forward in the development of this device. If the frequencies are correlated as integers, then the initial synchronization of the switched signals may occur or may not. Modeling has confirmed that the proposed device works successfully regardless of such synchronization, hence such synchronization is not required. The proposed device can be successfully applied in the development of precision frequency synthesizers.

VI. CONCLUSION

The paper substantiates the possibility of creating a new scheme for a precision synthesizer of frequency with an extremely small step. The most acute issue of creating such a device is the smooth switching of signals having different frequencies. It is shown that for a fixed frequency ratio this problem can be successfully solved even if the signals are not initially synchronized. The external switching command in the form of a rectangular pulse only prepares the switching. The switching itself takes place at the most favorable moments, when the signals coincide in magnitude, and their derivatives have the same sign, and the ratio between them corresponds to the frequency of the switched frequencies. A block diagram is proposed that is assembled in the software *VisSim*, which allowed to simulate the operation of the switch and to demonstrate the efficiency of the proposed scheme on the received signals.

VII. ACKNOWLEDGEMENTS

The Russian Ministry of Education and Science supported this work. The Russian Scientific Foundation (Project No. 16-12-00052) has supported this work.

REFERENCES

- [1] Bagaev S.N., Belkin A.M., Dychkov A.S. et al. "Absolute frequency measurement of molecular Iodine reference line near 732 nm used for high precision spectroscopy of Muonium". Russian-German Laser Symposium. Novosibirsk, 27.06–1.07.97. Technical digest. p. P12–P13.
- [2] Bagaev S.N., Belkin A.M., Dychkov A.S. et al. "Frequency reference in the 732-nm region for precision laser spectroscopy of muonium". 2000 Quantum Electronics. 30(7), c. 641–646.
- [3] Bagayev S.N., Belkin A.M., Dychkov A.S. et al. "Absolute Frequency Measurements in Precision Laser Spectroscopy of Muonium". In collection: Proceedings of SPIE - The International Society for Optical Engineering Proceedings of the 1998 Nonlinear Optical Phenomena and Coherent Optics in Information Technologies, ICONO-98. Moscow, RUS, 1999. P. 310–318.
- [4] Bagayev, S.N., Belkin, A.M., Dychkov, A.S. et al. "High-stable compact Nd:YAG/¹²⁷I₂-laser system for precision measurements". 1996 Technical Digest - European Quantum Electronics Conference. P. 44
- [5] Zhmud, V.A., Barmasov S.V. and Gitel'son, V.D. "An electronic system for stabilizing the frequency of the He-Ne laser to the methane absorption lines". 1999 Instruments and Experimental Techniques. 42(4), P. 551–557.
- [6] Zhmud V., Dimitrov L., Yadrishnikov, O. "Calculation of regulators for the problems of mechatronics by means of the numerical optimization method". 12th International Conference on Actual Problems of Electronic Instrument Engineering, APEIE 2014 – Proc. P. 739–744.
- [7] Efimov, A.S. and Zhmud', V.A. "A frequency synthesizer with the supersmall step for the systems of frequency and phase autotuning". 1996 Optoelectronics, Instrumentation and Data Processing (Avtometriya). (2), P. 21–25.
- [8] DAC38RFxx Dual-Channel, Single-Ended, 14-Bit, 6- and 9-GSPS, RF-Sampling DAC With JESD204B Interface and On-Chip GSM PLL. <http://www.ti.com/general/docs/lit/getliterature.tsp?baseLiteratureNumber=SLASEF4&fileType=pdf>
- [9] Frequency Synthesizer Types. URL: <http://www.radio-electronics.com/info/rf-technology-design/pll-synthesizers/frequency-synthesizer-introduction-types.php>.
- [10] Leenaerts D, van de Beek R, Van der Weide G, Bergervoet J, Harish K, Waite H, Zhang Y, Razzell C, Roovers R, Res P et al (2005) A SiGe BiCMOS 1ns fast hopping frequency synthesizer for UWB radio. IEEE ISSCC digest of technical papers, 2005. P. 202–593.
- [11] Lee J, Chiu D (2005) A 7-band 3–8 GHz frequency synthesizer with 1 ns bandswitching time in 0.18 μ m CMOS technology. IEEE ISSCC digest of technical papers. 2005. P. 204–593.
- [12] Lu T-Y, Chen W-Z (2008) A 3-to-10GHz 14-band CMOS frequency synthesizer with spurs reduction for MB-OFDM UWB system. IEEE ISSCC digest of technical papers. 2008. P. 126–601.
- [13] Liang C-F, Liu S-I, Chen Y-H, Yang T-Y, Ma G-K (2006) A 14-band frequency synthesizer for MB-OFDM UWB application. IEEE ISSCC digest of technical papers. 2006. P. 428–437.
- [14] Zhmud V.A., Dimitrov L.V. and Ivoilov A. Yu. Precision Frequency Synthesizer. *Automatics & Software Engineering*. 2018. № 1 (23). P. 20–32. URL: <http://www.jurnal.nips.ru/sites/default/files/AaSI-1-2018-2.pdf>.
- [15] Zhmud V.A., Dimitrov L.V. and Yadrishnikov O.D. "Calculation of regulators for the problem of mechatronics by means of numerical optimization method". 12th International Conference on Actual Problems on Electronic Instrument Engineering APEIE 2014. Proceedings.
- [16] Zhmud V. A., Semibalamut V. M. and Vostrikov A. S. "Feedback systems with pseudo local loops". Testing and measurement: techniques and applications: Proc. of the 2015 Intern. Conf. on testing and measurement techniques (TMTA 2015), Thailand, Phuket Island, 16–17 Jan. 2015. – London: CRC Press, 2015. – P. 411–416.



Zhmud Vadim Arkadievich – Head of the Department of Automation in NSTU, Professor, Doctor of Technical Sciences.
E-mail: oao_nips@bk.ru

630073, Novosibirsk,
str. Prosp. K. Marksa, h. 20



Dimitrov Lubomir Vankov – Vice-Rector of the Technical University of Sofia (Sofia, Bulgaria), Doctor of Science, Professor, Honorary Doctor of the NSTU.
E-mail: lubomir_dimitrov@tu-sofia.bg

Bul. "St. Kliment Ohridski" 8, 1756 Studentski
Complex, Sofia, Bulgaria



Ivoylov Andrey Yurievich – PhD-student of Department of Automatics of NSTU.
E-mail: iau13hv@mail.ru

630073, Novosibirsk,
srt. Prosp. K. Marksa, h. 20

Control of Object in the Loop with Feedback Using Imperfect Sensors of Position and Acceleration

Vadim A. Zhmud^{1,2}, Lubomir V. Dimitrov³, Vitaly Trubin¹, Hubert Roth⁴

¹Novosibirsk State Technical University, Novosibirsk, Russia

²Institute of Laser Physics SB RAS, Novosibirsk, Russia

³Technical University of Sofia, Sofia, Bulgaria

⁴University of Siegen, D-57068, Siegen, Germany

Abstract – The paper discusses the problem of balancing robot control with negative feedback loop. The regulator (controller) can be calculated by numerical optimization. Sensors of the controlled value are imperfect. Orientation angle sensor (gyroscope) has a limited speed, as well as binary quantization noise. An acceleration sensor (accelerometer) has the average value drift and Gaussian noise. None of these sensors is sufficient to effectively stabilize the balancing of the robot, but using them both in a single control loop can achieve the required accuracy of control in static and dynamic. Method of combining the two sensors to more accurately determine the value of a single, previously developed in theory, has been tested with simulation and with realization in acting model of the robot. The results are confirmed by their practical use with good effect, which one can see on video by the reference link.

Index Terms – Control, automation, feedback, servo loop, robot, balancing robot, gyroscope, accelerometer, inverse pendulum, regulator, controller

I. INTRODUCTION

THE development of robots working in real time is advisable not only to the scientific and research purposes, but also for the purpose of teaching students. The main problems are worked through in the low-power and small-size models. Advantages of this design are that each part of such robot can be researched and modified, and the entire device may be repeated in increased size and power. The main problems of the development of such a system do not depend on the size. Complex tasks can be worked through on cheap models, and clearly demonstrated to the students. An example could be a two-wheeled balancing robot that maintains balance under the influence of uncontrollable external disturbance.

There are many papers giving instructions how to built self-made balancing robot [2–5]. These papers contain sufficient information for construction of hardware, but nothing about the software and tuning of regulators. The only paper containing few words about the tuning of PID-regulators writes: “PID requires that the gains K_p , K_i , and K_d values be “tuned” to optimal values. Engineers use software like MATLAB to compute these values automatically. Unfortunately, we can’t use MATLAB in our case because it would further complicate the project. We will tune the PID values manually instead. I’ve outlined the steps on how to do

this” [5]. This paper gives the poor instructions for manual tuning.

Monograph [6] and papers [7–11] give tools for effective calculation of PID-regulator, which are sufficient for any designer having basic knowledge in electronics.

These methods should use mathematical model of the object which is in the most cases is unknown. This paper discusses all problems occurring in the resolving of the task of the regulator calculation for balancing robot.

II. PROBLEM DEFINITION

One of the most acute problems of debugging such robot is to ensure the required accuracy of real-time control. This problem is solved by using feedback systems, the main elements of which are the object, sensor of its output value and the controller (regulator); all of them included into the closed loop. Object of control in this case is the electromechanical part comprising electric actuating wheel, and the mass of the robot itself, which must be maintained in balance. A feature of the object is that the centre of mass is located far above the axis of rotation of the wheels; hence, without the action of the robot feedback it is unstable and can maintain balance only due to the effective feedback operation.

A typical model of the system is given by a system of equations in the Laplace transforms. Model of object is given by the following equation:

$$X(s) = W(s)U(s) + H(s). \quad (1)$$

Here, each function of the argument s , except $W(s)$, is Laplace transform of the corresponding function of time, $X(s)$ corresponds to the output value, $U(s)$ corresponds to the control signal at the input of the object, $H(s)$ is the unknown disturbance which the system should suppress by the action feedback, $W(s)$ is transfer function of the object.

Model of the regulator action is given by the following equation:

$$U(s) = W_R(s)E(s). \quad (2)$$

Here $W_R(s)$ is transfer function of the regulator; $E(s)$ is Laplace transform of control errors. In stabilization, systems error is usually equal to the output value $X(s)$ with a negative sign, because it requires that the output value (the deviation

from equilibrium) would be zero. In control, systems prescribed value (setting) $V(s)$ takes place, which is added to the output value in the adder. The adder equation has the form:

$$E(s) = V(s) - X(s). \quad (3)$$

Two regimes can be in the system. First is changing of setting. Second is changing of disturbance. Hence, two kinds of error exist, and the system must suppress the both. In the system with the only loop, system dynamic and static error depends on the loop gain. The error because of step disturbance changing is similar to the error because of the step changing of setting. Therefore the quality and accuracy of the system can be evaluated by it working in the first regime.

In most cases, the developer considers that the output value is available for measurement. In practice, this is not always the case. Therefore, for implementation of the system sensor of the output value is used with the corresponding transfer function $W_s(s)$, and the equation (3) in this case has the form:

$$E(s) = V(s) - W_s(s)X(s). \quad (4)$$

The task of designing the system becomes more complicated if it is impossible to select a sensor that allows the required static and dynamic accuracy. In this case, to ensure the accuracy of static, it is necessary to use some sensor, and for providing a dynamic accuracy, the use of another sensor is necessary. The problem of using two or more sensors to control one value was considered in our papers [1–11]. This paper offers the investigation of particularities in solving the problems of this class, which is due to the fact that even under control with ideal sensor system it is not a simple task. Therefore, the differences of real sensor from the ideal one makes system design very difficult. Methods of regulator design are investigated with modeling.

III. FEATURES OF THE OBJECT MODEL

Object model is not linear, but near the equilibrium state, and it can be regarded as linear. The transfer function of the object contains the delay and second-order filter. Joint properties of the filter and delay link result in that the object has a tendency to oscillate.

Objects model is defined as follows:

$$X(s) = \frac{\exp(-0.2s)}{s^3 + s^2 + s + 1} U(s). \quad (5)$$

Here we use the time scale of 1:10 i.e. the time is given in tenths of a second.

We use numerical optimization method for designing PID-regulator on the assumption of an ideal sensor of the output value, that is, assuming $W_s(s) = 1$. The transfer function of the PID-regulator is:

$$W_R(s) = K_P + K_I / s + sK_D. \quad (6)$$

Here the coefficients K_P , K_I and K_D are required to determine in the numerical optimization procedure. Fig. 1 shows the structure for simulation and numerical optimization of regulator in program *VisSim*. This cost (objective) function used to optimize regulator has the form:

$$\Psi = \int_0^T t |e(t)| dt. \quad (7)$$

Here T is time simulation of the transition process, t is time (as an argument in the simulation), $e(t)$ is the control error as a function of time. In Fig. 1, wires marked with identical names are connected (these are the features of the program *VisSim*). Blocks “parameterUnknown” and “cost” are capable of optimizing the coefficients of the regulator. The resultant optimization coefficients are, respectively: $K_P = 0.02607$, $K_I = 0.337$ and $K_D = 1.016$. Fig. 2 shows the resulting transient response.

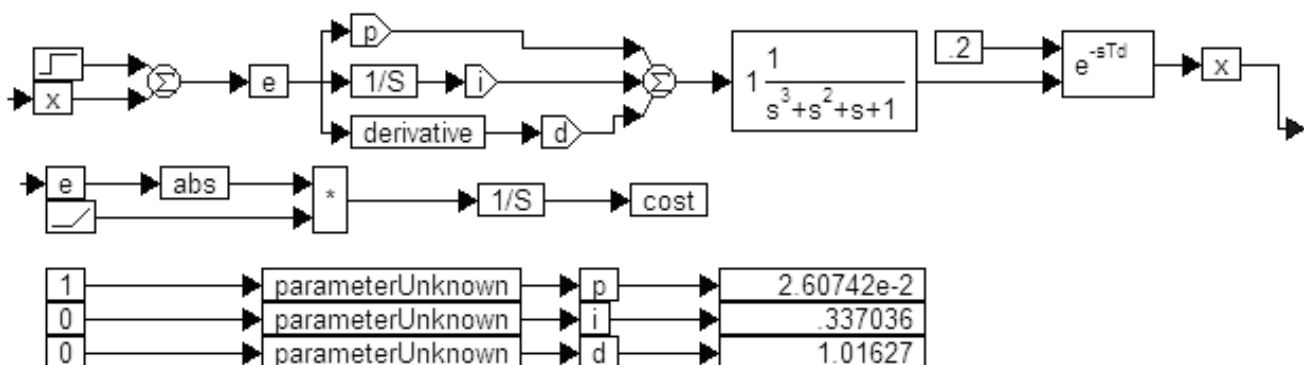


Fig. 1. The structure of system with balancing robot as an object.

It can be seen that the static error is zero, because the output value become equal to setting value. But the quality of the system is not too high, because the overshoot is about 17%, and in the process has more than five oscillations.

To verify that the object is of great complexity, increase the delay time up to five times. The simulation result is shown in Fig. 3. We see that as a result, two coefficients of regulator become negative, and only integral channel coefficient remains positive. These coefficients are, respectively: $K_P = -0.253$, $K_I = 0.1541$ and $K_D = -0.127$. At the start of the transient process of the system, shown in Fig. 4, there is reverse overshoot by about 17%.

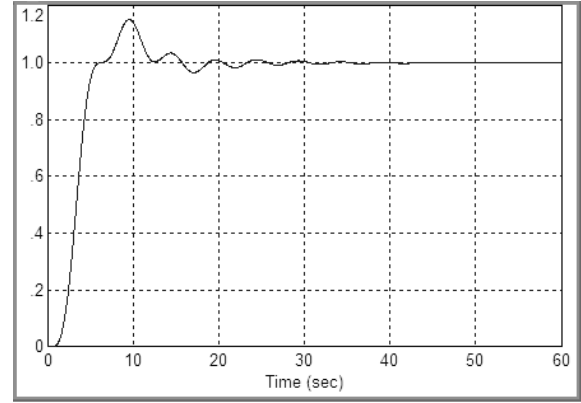


Fig. 2. The transient process obtained in the system of Fig. 1.

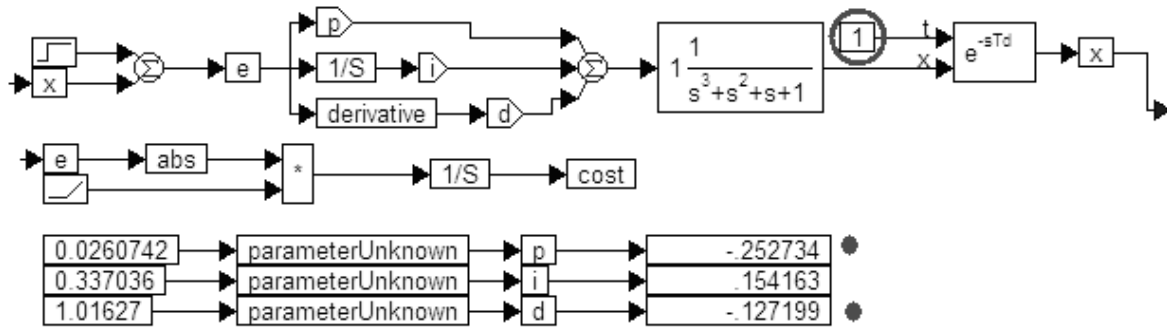


Fig. 3. The structure with increased delay which gives two negative coefficients (marked with dots).

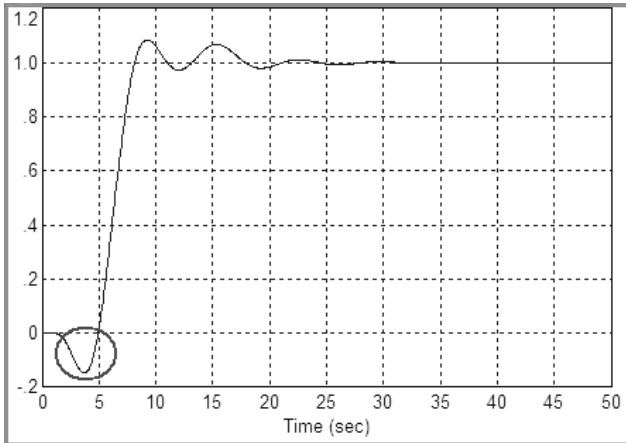


Fig. 4. The transient process in the case shown at Figure 3 has the reverse overshoot (marked with ellipse).

Thus, it is clear that the control of the object requires careful tuning of the regulator, because small changes of the model parameters, even with optimal controller system, tend to the reverse overshoot, which is typical for the system that is near the boundary of stability. If such a system of control is not designed properly, it will lose stability as it is evidenced by the negative coefficients of proportional and differentiating channels of the regulator.

IV. FEATURES OF SENSORS MODELS

To determine the deviation angle of balancing robot from the vertical line, sensors of different nature may be used, but they are far from ideal.

For example, to determine the angle of deflection gyroscope may be used. However, its performance is limited; moreover it has a quantization noise. Fig. 5 is a characteristic view of the output signal from the gyroscope (line 1) when its ideal output signal should have the form of a line 2.

Object model is not linear, but near the equilibrium state and it can be regarded as linear. The transfer function of the object contains the delay and second-order filter. Joint properties of the filter and delay link result in that the object has a tendency to oscillate.

Objects model is defined as follows:

$$X(s) = \frac{\exp(-0.2s)}{s^3 + s^2 + s + 1} U(s). \quad (5)$$

Here we use the time scale of 1:10 i.e. the time is given in tenths of a second.

We use numerical optimization method for designing PID-regulator on the assumption of an ideal sensor of the output value, that is, assuming $W_s(s) = 1$. The transfer function of the PID-regulator is:

$$W_R(s) = K_P + K_I / s + s K_D. \quad (6)$$

Here the coefficients K_P , K_I and K_D are required to determine in the numerical optimization procedure. Fig. 1 shows the structure for simulation and numerical optimization of regulator in program *VisSim*. This cost (objective) function used to optimize regulator has the form:

$$\Psi = \int_0^T t |e(t)| dt. \quad (7)$$

The resultant optimization coefficients are, respectively: $K_P = 0.02607$, $K_I = 0.337$ and $K_D = 1.016$. The resulting transient response is shown in Fig. 2.

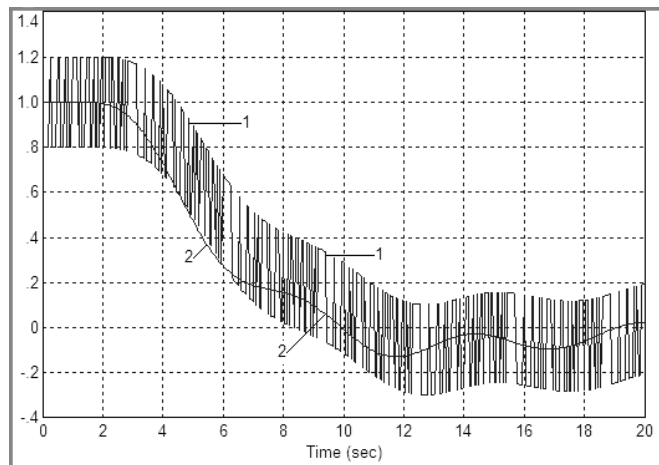


Fig. 5. The output signal of the gyroscope (model) is line 1, and its ideal view is line 2.

Model of gyroscope then may be represented by a transfer function as a filter with a time constant of 0.1 seconds (i.e. 1 unit in the selected time scale) with the addition of a binary noise generator. With all this, the following parameters of the binary noise generator are used: the length of the register is equal to six, the amplitude is 0.01 and the update period is 0.5. In this case, the noise of the gyroscope is obviously more than in real situation.

As seen in the previous section, the requirements for the sensors are extremely high. Using a gyroscope to control creates an excessively large noise in the signal derivative. This leads to substantial fluctuations in the steady state, the value of which is about 5%. Therefore, for the difference channel it is expedient to use velocity meter (accelerometer with integrator) which is available in the form of special chip. The model of the accelerometer should have two differences from the ideal sensor: high-frequency Gaussian noise and low frequency drift. High-frequency noise is insignificant impact due to low-frequency filter contained in the object model and due its low value. This noise does not give the zero offset. Low frequency drift gives zero offset, but it should not be a disadvantage when using it to generate an error signal in derivative tract. However, this signal cannot be used for signal generation in other control tracts, particularly in an integrating path, as the zero drift is too big, and its integration would result in linearly increasing errors.

To get the speed, which is derivation of the position, the signal from the accelerometer also can be used, where signal is proportional to the acceleration, which is the derivation of the speed. Hence the speed can be calculated as time integral of the acceleration. This method is very good from the point of view of the high-frequency noises, because the integration decreases them. Nevertheless, this sensor is not very good from the point of view of the drift, because the integration increases it many times. This way can give the sensor of the velocity (speed) with big drift. It can be names velocity meter.

For modeling of a drift of the velocity meter, a low-frequency signal from the output of the generator with small amplitude can be used. Fig. 6 illustrates an output signal of the velocity meter (line 1) when compared with the derivative actual output robot signal (line 2). Options of the generator that simulates the drift of the velocity meter are frequency is 0.0314 (i.e. half the period of this signal is equal to 100) and the amplitude is 0.1. It would be possible to offer a low-pass filter to eliminate drift, for example, such a filter, as shown in Fig. 7. However, such a filter while effectively removes low-frequency drift, also distorts the RF signal input as it introduces additional derivation. For clarity, Fig. 8 shows the output of this filter (line 1) versus the true derivative signal (line 1).

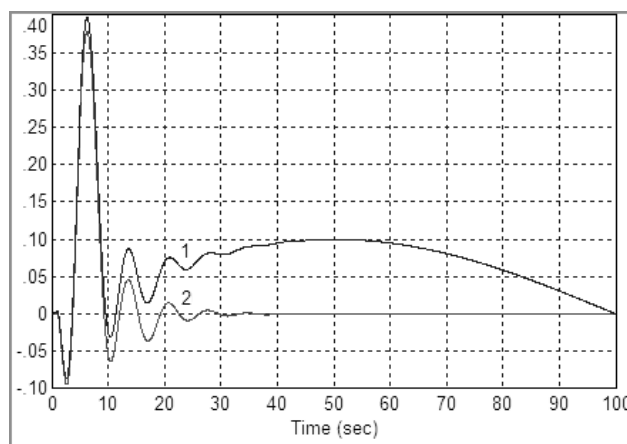


Fig. 6. The output of the velocity meter (from the mathematical model of the sensor) together with the drift (line 1) and the true speed of the object (the line 2).

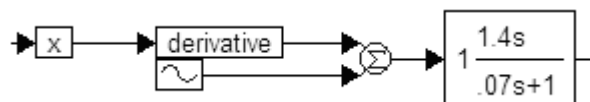


Fig. 7. The model of the velocity meter and the filter .

On this basis, it is proposed not using the filter while output signal from the velocity meter feeds directly the derivative channel of PID-regulator. Also it is proposed to refuse the use of the reference signal in this path, i.e. the feedback signal of the speed is supplied to the object directly, passing the adder.

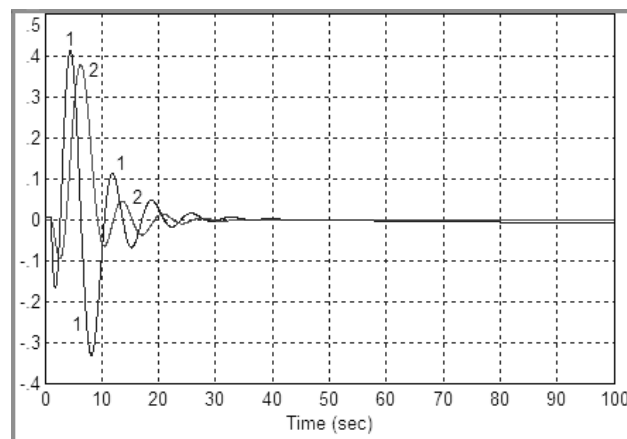


Fig. 8. Exit the filtered signal from the velocity meter (line 1) and the true velocity of the object (the line 2).

V. PROPOSED SOLUTIONS AND RESULTS

The peculiarity of the proposed solutions is optimization of system with model which takes into account all the features of both sensors.

In accordance with the recommendations given in [7, 11], the use of large delay in the object model is proposed, while optimizing to get a robust system. Such a system will have a sufficiently high stability, and even if some of the coefficients of the object model or the controller will differ from the calculated ones, the system will remain stable.

Fig. 9 shows the corresponding structure for modeling and optimization, and the optimization results. With all this, two

negative coefficients are also obtained in the result, namely: $K_P = -0.04766$, $K_I = 0.173667$ and $K_D = -0.418727$. The resulting transient response is shown in Fig. 10.

To demonstrate the robustness of the resulting system, the amplitude of both types of noise in the sensor was increased 10 times. The resulting process in such a system is shown in Fig. 11 (line 1), for comparison, the line 2 shows a graph with the initial process corresponding to Fig. 10. We see that there are oscillations in the amplitude of about 6%, but the system remains stable. The overshoot in the system did not increase.

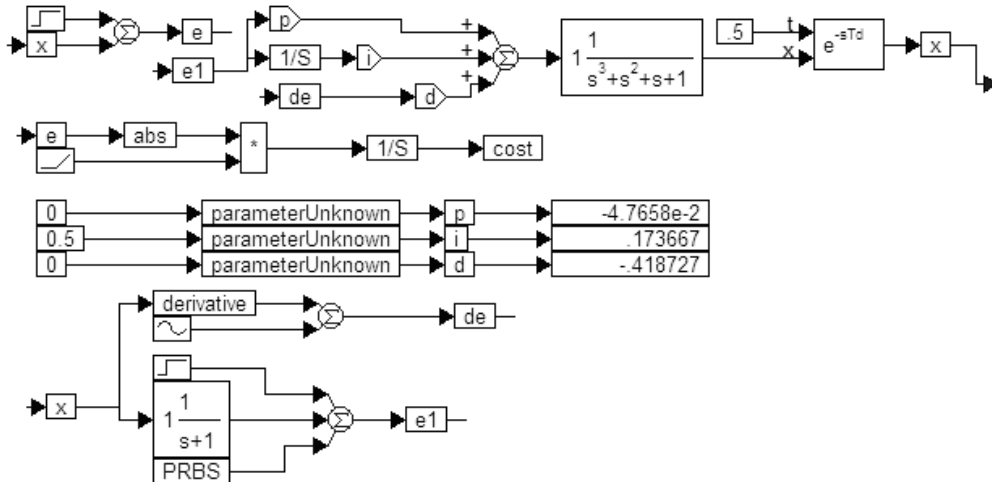


Fig. 9. The structure for the regulator optimization with real models of the sensors.

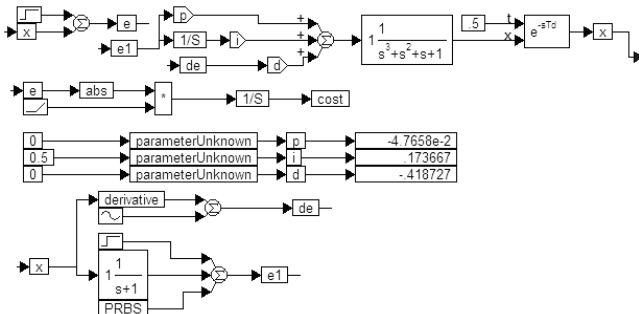


Fig. 10. The transient process in the system by the structure shown in Fig. 9.

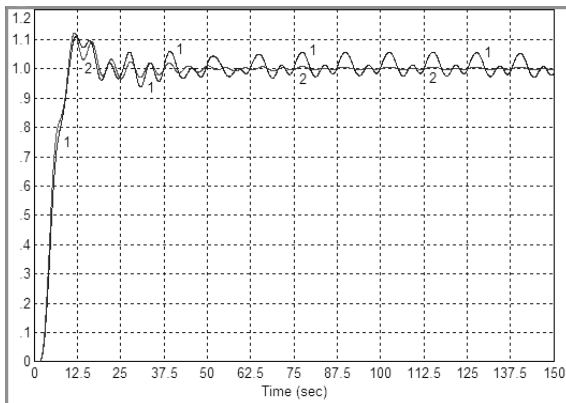


Fig. 11. The transient process in the case where both types of noise increased in amplitude in 10 times (line 1), line 2 shows the original curve.

VI. FEATURES OF THE METHOD WITH WORSENING IN THE PERFORMANCE OF THE OBJECT AND THE SENSOR

For additional test it is helpful to return to the original values of noise and to increase the time constant of the filter in the model of the gyroscope 10 times, increasing delay in the object model 2.5 times (up to 5 s). Carrying out re-optimization of the regulator, the result values of the coefficients are as following: $K_P = -0.121$, $K_I = 0.05$ and $K_D = -0.315$. The result of such a system is shown in the form of a transient process in Fig. 12. As shown, the increase in the oscillation amplitude is initially about 5%, but gradually oscillation fades to a negligible value of about 1%, and the system remains stable. Overshooting in the system also did not increase, although the duration of the transient process increased.

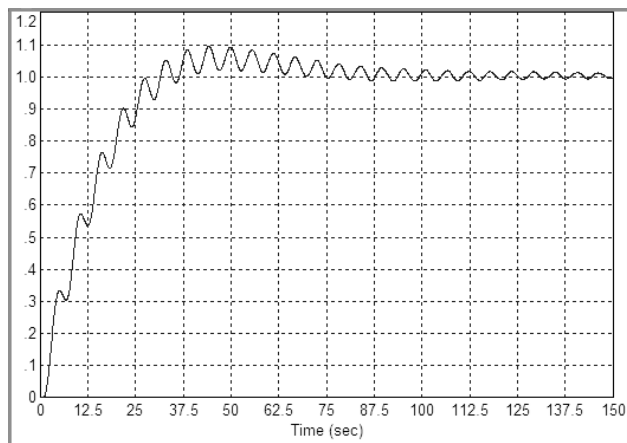


Fig. 12. The transient process in the system with a reduced speed of the object and the sensor (gyroscope).

VII. DISCUSSION OF RESULTS

The results of this paper are used in the developed balancing robot. The dimensions and appearance of the robot can be evaluated from Fig. 13.



Fig. 13. The window on the website [12], which is clickable to view a video about its working.

At the website [12] there is a video, which shows the work of the developed robot in the working off the disturbance, which is administered by the asymmetrical placement of its cargo. It can be seen that the robot successfully fulfils this hindrance, without losing balance.

VI. CONCLUSION

The paper has developed the method for control with the suppressed backward overshooting.

The conclusions of success operating of the discussed robot are as following:

1. Combination of the two sensors can combine their advantages and remove their drawbacks.
2. The acceleration sensor is advisable to use. Integrating of its signal gives the velocity. It is proposed to supply this signal directly to the regulator without a subtractor that calculates the control error.

3. Calculation of the regulator should be done with all the parameters of the real sensors. In addition, it is advisable to introduce an additional delay to the object model during the optimization procedure. It provides robust properties of the system.

4. This example shows the effectiveness of the proposed solutions.

VIII. ACKNOWLEDGEMENTS

The Russian Ministry of Education and Science supported this work. The Russian Scientific Foundation (Project No. 16-12-00052) has supported this work.

REFERENCES

- [1] 2-Wheel Self Balancing Robot by Using Arduino and MPU6050. URL: <http://www.instructables.com/id/2-Wheel-Self-Balancing-Robot-by-using-Arduino-and/>
- [2] How to Build a Self-Balancing Autonomous Arduino Bot. URL: <http://makezine.com/projects/arduoller-self-balancing-robot/>
- [3] Self-Balancing Robot. URL: <http://www.instructables.com/id/Self-Balancing-Robot/>
- [4] Chappie-Self-Balancing Robot. URL: <http://www.instructables.com/id/Chappie-Self-Balancing-Robot/>
- [5] How to Build an Arduino Self-Balancing Robot. URL: <https://diyhacking.com/build-arduino-self-balancing-robot/>
- [6] Zhmud V. A. Designing of the precision automatic control systems: monograph / V. A. Zhmud, L. Dimitrov. - Novosibirsk : KANT, 2017. - 126 p.
- [7] V. A. Zhmud, O. D. Yadrishnikov, V. M. Semibalamut Control of the objects with a single output and with two or more input channels of influence. Computational Methods and Experimental Measurements 17. – Wit Press, 2015. – P. 145-156. – WIT Transactions on Modelling and Simulation. Vol 59. – DOI: 10.2495/CMEM150131. - ISBN 9781845649227.
- [8] Modern key technologies in automatics: Structures and numerical optimization of regulators. Zhmud, V., Yadrishnikov, O., Poloshchuk, A., Zavorin, A. 2012. Proceedings - 2012 7th International Forum on Strategic Technology, IFOST 2012.
- [9] The design of the feedback systems by means of the modeling and optimization in the program VisSim 5.0/6. Zhmud, V., Liapidevskiy, A., Prokhorenko, E. 2010. Proceedings of the IASTED International Conference on Modelling, Identification and Control. PP. 27–32.
- [10] V. Zhmud, O. Yadrishnikov. Numerical optimization of PID-regulators using the improper moving detector in cost function. Proceedings of the 8-th International Forum on Strategic Technology 2013 (IFOST-2013), vol. II, 28 June – 1 July. Mongolian University of Science and Technology, Ulaanbaator, Mongolia. IEEE organized. 2013. P. 265–270. <http://www.must.edu.mn/IFOST2013/>
- [11] V.A. Zhmud, A.V. Polishchuk, A.A. Voevoda, R.V. Rao. The Tuning of the PID-Regulator for Automatic Control System of Thermo Energetic Equipment // Proceedings of the Fifth International Conference on Advances in Mechanical Engineering (ICAME-2011), June 06-08, 2011. Surat – 395 007, Gujarat, India. p. 254-263.
- [12] Web site of the Department of Automation in Novosibirsk State Technical University, page “Science work”. URL: <http://ait.cs.nstu.ru/content/nauchnaja-deyatelnost>, <https://www.youtube.com/watch?v=mQOP4kzWKwk>



Zhmud Vadim Arkadievich – Head of the Department of Automation in NSTU, Professor, Doctor of Technical Sciences.
E-mail: oao_nips@bk.ru

630073, Novosibirsk,
str. Prosp. K. Marksa, h. 20



Dimitrov Lubomir Vankov – Vice-Rector of the Technical University of Sofia (Sofia, Bulgaria), Doctor of Science, Professor, Honorary Doctor of the NSTU.
E-mail: lubomir_dimitrov@tu-sofia.bg

Bul. "St. Kliment Ohridski "8, 1756 Studentski
Complex, Sofia, Bulgaria



Trubin Vitaly Gennadievich – Head of the department. lab. Automatics Department of NSTU, Director of KB Automatics.
E-mail: trubin@ngs.ru

630073, Novosibirsk,
srt. Prosp. K. Marksa, h. 20



Roth Hubert – Head of the Department of Automatic Control Engineering of University of Siegen, Professor, Doctor of Sci., Germany
E-mail: hubert.roth@uni-siegen.de

Adolf-Reichwein-Strasse 2, Siegen, Germany

Smart Phase Locking of the Frequency of Two Identical Lasers to Each Other

Vadim A. Zhmud^{1,2}, Aleksey V. Taichenachev², Lubomir V. Dimitrov³, Vladimir M. Semibalamut⁴

¹Novosibirsk State Technical University, Novosibirsk, Russia

²Institute of Laser Physics SB RAS, Novosibirsk, Russia

³Technical University of Sofia, Sofia, Bulgaria

⁴Sibirean Branch of Geo physical service SB RAS, Novosibirsk, Russia

Abstract – The paper considers the main aspects of ensuring phase-locked looping of two lasers to each other. This problem is extremely important for laser physics. In traditional systems, this binding was carried out by using two circuits, namely frequency tuning and phase tuning. The tuning loop provides capture conditions, but in capture mode, it interferes with the operation of the phase loop and reduces the accuracy of the entire system. In addition, this solution is unnecessarily cumbersome, which increases the cost of the system and complicates its implementation, configuration and use. The proposed technical solution is based on the use of other types of phase detectors, namely, frequency-phase detectors. To be able to use them, a pulse shaper must be introduced into the system, which converts the input harmonic signals containing amplitude modulation and high frequency noises, and probably, low-frequency noise, to standard fixed-level signals with sharp edges. In this case, the propagation of fronts due to the remnants of high-frequency noise is strictly unacceptable, which requires the use of a Schmitt trigger, and for its effectiveness requires a relatively constant amplitude of the input signal. If this is not the case, an automatic level stabilization system is required. All these changes in the aggregate are still simpler than using two auto tuning circuits. In addition, it provides great ease of implementation, customization and use. Basic circuit diagrams of the main nodes are presented, as well as the relationships and method for adjusting the regulator in order to ensure high accuracy of the phase-locked loop.

Index Terms – Regulators, automatics, phase-locked loop, frequency auto-tuning, lasers, laser systems, frequency measurements, laser physics, laser spectroscopy, optoelectronics, electronics.

I. INTRODUCTION

PHASE-LOCKED LOOP (PLL) of one laser to another is extremely important in laser physics [1–13]. It is used to synthesize various frequencies without losing the accuracy of their formation. In this case, the frequency of the slave laser is adjusted to the frequency of the leading laser with a certain predetermined frequency difference, for example, 1 MHz. This difference should be kept accurate to the phase.

One can raise the question of why lasers do not adjust to each other with a zero frequency difference, because only in this case the system can be correctly called a phase-locked loop. The answer to this is that, firstly, such systems are also being made, but they are used for other purposes, namely for the coherent addition of radiation from several lasers.

Secondly, such systems are extremely difficult to set up, it is a special task that is solved by other methods [10]. Therefore, this article does not consider such systems.

This problem arises with absolute frequency measurements and for an accurate study of the absorption spectra of various media. The optical part of the system combines the parts of the beams from two lasers on one photodetector. This article discusses only the electronic part of this system.

Traditionally, in such systems, two feedback loops were used, one of which carried out frequency tuning, and the other provided phase self-tuning of the frequency.

The reason for this decision was that only one phase loop was not enough to ensure capture and retention. The phase detector was traditionally made on the basis of signal multipliers with a low-pass filter at the output, so if the frequencies of the two signals arriving at its inputs differed significantly, the output signal averaged zero. Therefore, automatic capture in the system without an additional frequency loop did not occur. In addition, in case of disruption of tracking, the capture was not restored.

A simplified functional diagram of such a system is shown in Fig. 1.

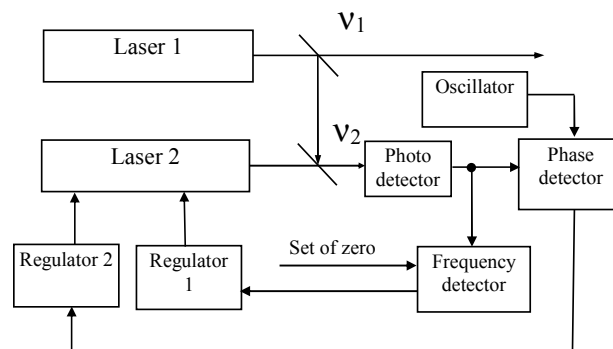


Fig. 1. Functional diagram of the traditional PLL system of two lasers.

II. PROBLEM DEFINITION

In such a system, the beat signal at the difference frequency $\Delta F = \nu_2 - \nu_1$ is formed at the output of the photodetector. This signal is simultaneously fed to the phase detector and to the frequency detector. In the absence of phase locking, the phase-locked loop does not work, and this was the reason for using the auxiliary frequency loop. In the frequency circuit, the signal from the photodetector is

converted into a signal proportional to the frequency. For this, it is sufficient, for example, to convert a harmonic signal into a series of pulses of a fixed duration, which is much shorter than the period of their follow-up. Further, these pulses are fed to the low-pass filter. At the output of the filter, in this case the average signal is proportional to the frequency. Also, in the frequency detector, it is possible to set the frequency at which the output signal will be zero. To this end, a certain fixed voltage is subtracted from the received signal, which coincides with the voltage corresponding to the desired frequency. Thus, the frequency detector is tuned so that, at the desired frequency, its output signal is zero. More precisely, this can be done by external adjustment. A more correct solution would be to use two identical frequency detectors, the second of which would apply voltage from the reference oscillator. Then the signals from these frequency detectors should be subtracted from one another. A difference signal would be a differential frequency detection signal, which is required for the operation of frequency-independent self-tuning. However, this decision was not used because of its excessive complexity. Instead of the second frequency detector, a fixed voltage was used, which could be manually adjusted.

A signal proportional to the difference frequency passes through the first regulator to the laser to control its frequency. The ability to control the frequency of the laser is provided by installing one of its mirrors on the piezoelectric modulator, at the output of the regulator a high-voltage amplifier is used. In this way, the frequency of the radiation of the driven laser can be varied by changing the voltage applied to it.

The frequency circuit provides approximate equality of the difference frequency to the desired value. In this case, a non-zero signal appears at the output of the phase detector, and the phase loop of the auto-tuning is turned on.

The reference generator generates a reference frequency signal FR. On the phase detector, the phase of the signal from the photodetector is compared with the phase of the reference signal. An error signal that is proportional to the phase difference taking into account the sign does not come from the second regulator, where it amplifies and enters the additional inputs of the slave laser. This signal provides additional control over the frequency of the radiation of the driven laser in such a way that the difference frequency coincides with the frequency of the sample oscillator to the phase accuracy.

III. IMPLEMENTATION OF THE ELECTRONIC PART OF THE SYSTEM

For the successful operation of such a system, the gain of the frequency loop must be several orders of magnitude smaller than the gain of the phase circuit. But even in this case, the frequency loop degrades the accuracy of the systems, since in the phase-locked loop its signal is not needed, it must be strictly zero. In practice, this condition is satisfied only approximately.

A system with two circuits is difficult to manufacture, configure and operate, has an unnecessarily high cost and does not provide the required accuracy.

This paper solves the problem of providing phase-locked loop without the use of a frequency loop.

IV. THEORY

The main difficulties in creating a PLL are related, first, to detecting a phase error, and secondly, to ensure the required dynamic properties of a closed system with the help of a regulator.

The first problem concerns the phase detector, the second - to the output part and the regulator.

Overcoming the difficulties of phase detection is provided by two key decisions.

First, it is proposed to use a frequency-phase detector instead of just a phase detector. Such a detector is known, but it requires a high signal-to-noise ratio at the input, since it operates only on the fronts of the input signals, from which the second problem is generated.

Secondly, to solve the noise problem, two or more different methods can be used, depending on the task.

The most effective method is to filter the signal received at the output of the photodetector, as well as use the Schmitt trigger to form rectangular pulses, in which the parasitic propagation of the fronts from the action of the remnants of high-frequency noise is eliminated. The Schmitt trigger is effective only if its threshold is certainly higher than the maximum noise level, and at the same time it is certainly below the minimum signal level. In most problems of laser physics, this is automatically provided, since the signal is formed in light beams obtained directly from the laser, and not in scattered beams, where the presence of noise is particularly large. If you have to work with a significantly noisy signal, you can recommend the use of an automatic level control system directly between the filter at the output of the photodetector and the Schmitt trigger. In cases where this measure is not sufficient, we can recommend the use of a tracking filter, although such cases are quite rare in practice.

Thus, the recommended circuit is somewhat simpler and contains only a phase loop of auto-tuning, as shown in Fig. 2.

In this case, a rectangular shaped shaper appears in the phase loop, and a frequency-phase detector circuit replaces the phase detector circuit.

The principle of the frequency-phase detector is based on the operation of two triggers. Initially, both flip-flops are set to zero. The pulses from the sample generator set the first trigger to a single state, and the pulses from the output of the shaper set the second trigger to a single state. The coincidence circuit determines the moment when both flip-flops are set to a single state and after a short delay both reset both flip-flops, after which their operation is repeated using the same algorithm.

Also in the frequency-phase detector there is a differential amplifier that generates a signal proportional to the difference of the signals of these flip-flops. Therefore, if the pulses from the sample generator outperform the pulses from the former in time, then, for example, positive pulses are

formed at the output of the amplifier. If these impulses lag behind, negative pulses are formed at the output.

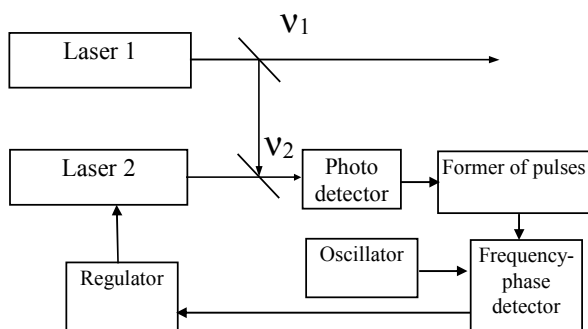


Fig. 2. Modified functional circuit of the traditional PLL system of two lasers.

After averaging the low-pass filter, a positive or negative signal is formed at the output of the detector. If the phases of the two input signals coincide, the output signal of the detector is zero. The advantage of such a detector is that even if the input signals differ greatly in frequency, a signal is generated at its output, the sign of which indicates which of the input signals has a high frequency, and if the frequencies

coincide, the component proportional to the frequency difference is strictly zero. Only a component proportional to the phase difference remains.

Such a scheme provides for capture only on one side, in contrast to the scheme shown in Fig. 1. This is an additional advantage of this system.

V. REALIZATION OF THE PROPOSED ELECTRONIC PART OF THE DEVICE

Fig. 3-6 show schematic diagrams of individual blocks of the PLL system, development of the Institute of Laser Physics of the SB RAS.

The system uses two control channels, in accordance with the methodology previously described in [14, 15].

For this purpose, in the driven laser, both reflecting mirrors are mounted on piezoelectric modulators. One of the channels is characterized by a higher speed, but a smaller control range. This channel is called “fast channel”. The other channel has a large control range, but less speed, it is called “slow channel”.

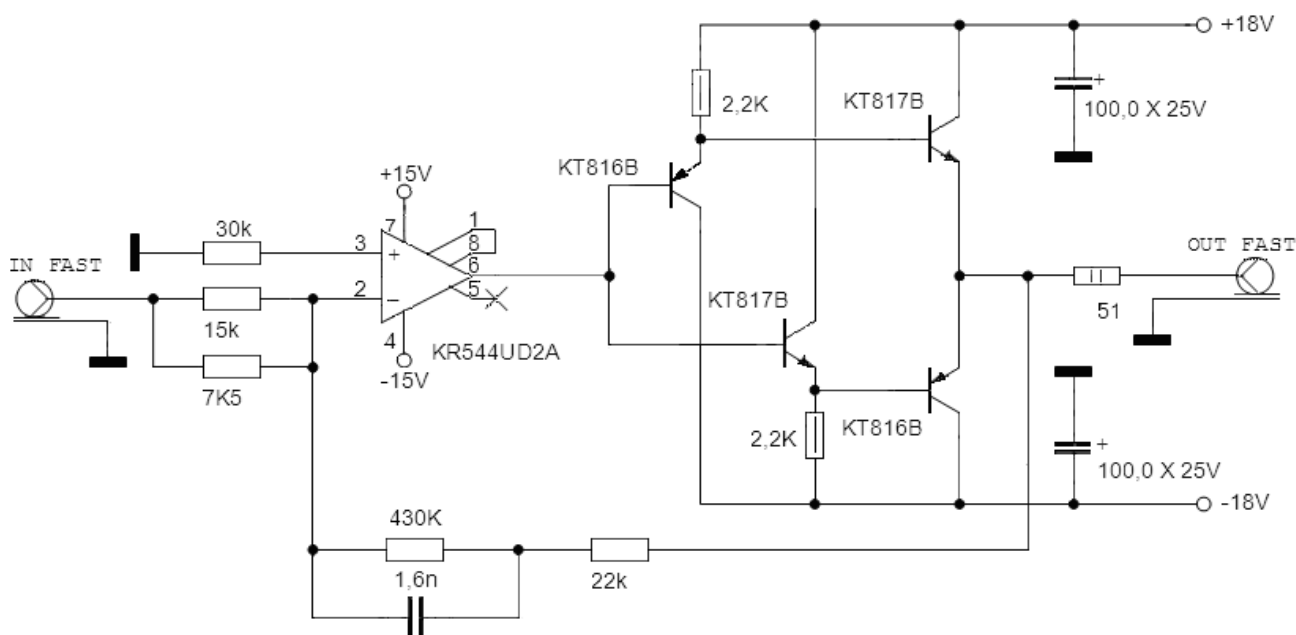


Fig. 3. Schematic diagram of a fast gain channel.

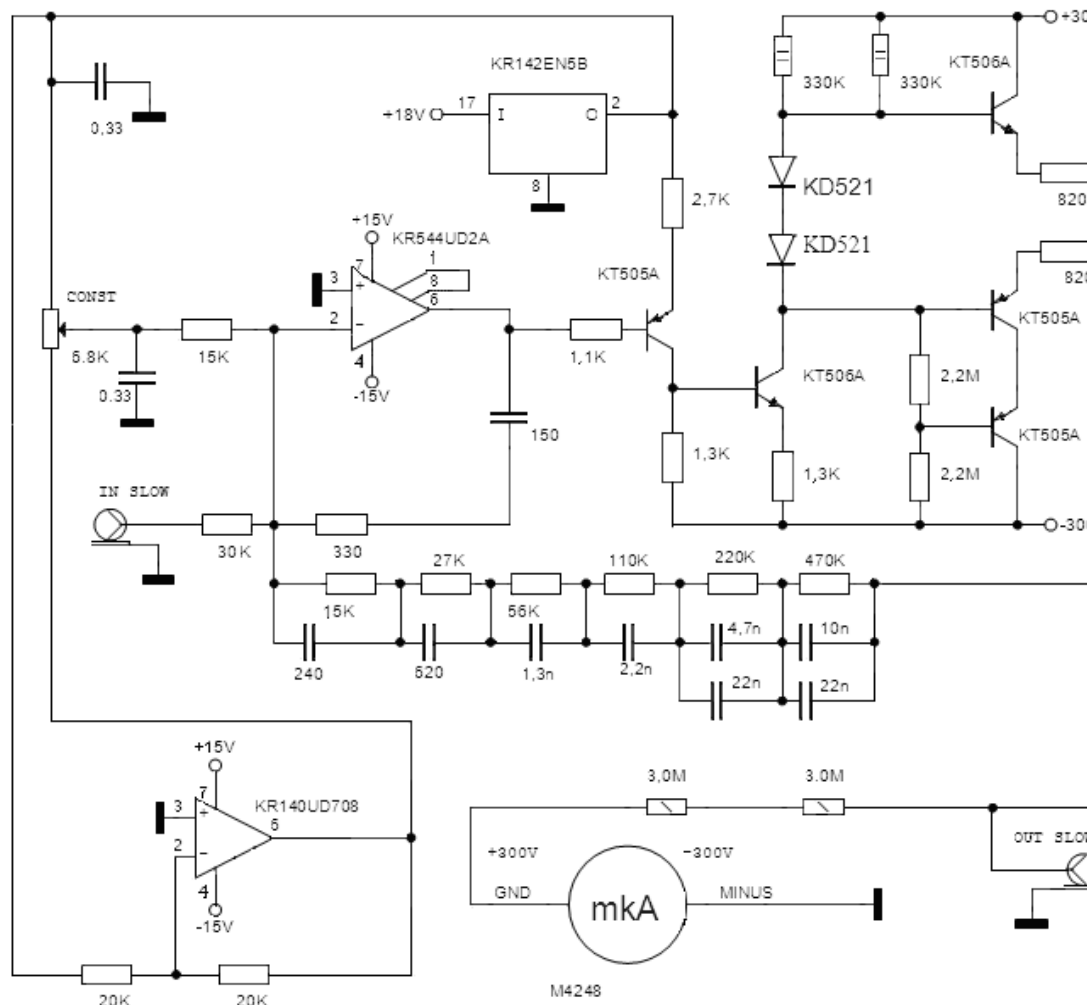


Fig. 4. Schematic diagram of a slow gain channel.

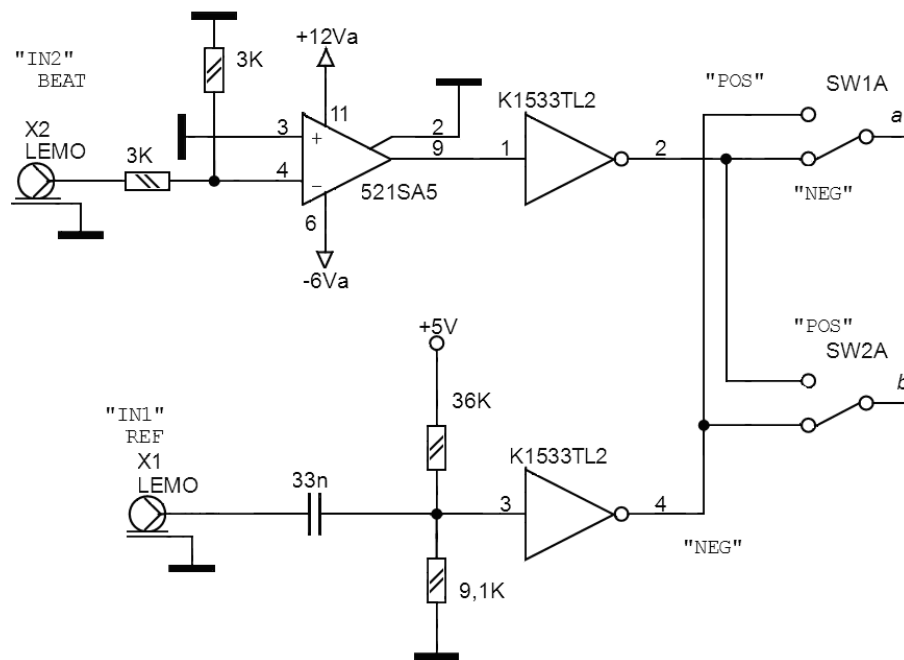


Fig. 5. Schematic diagram of the phase detector, part 1.

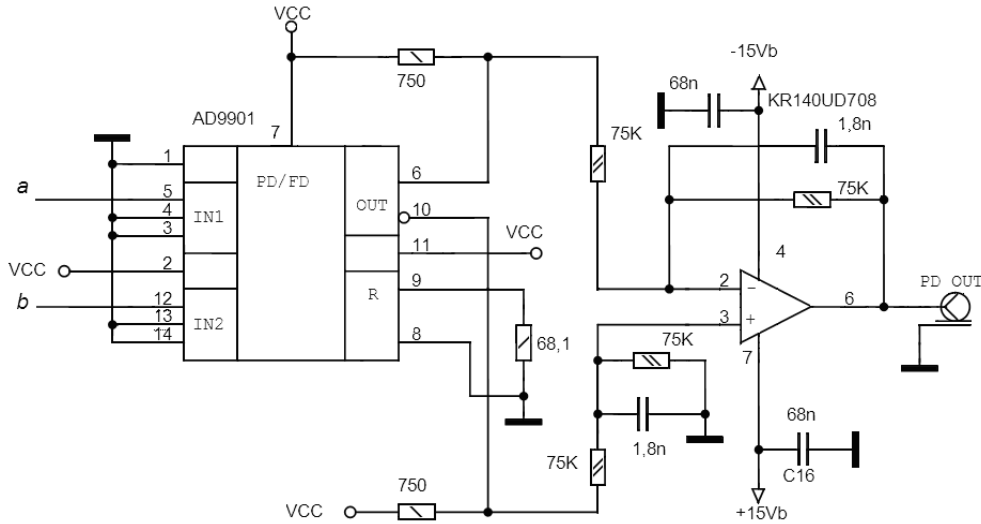


Fig. 6. Schematic diagram of the phase detector, part 2.

VI. REGULATOR DESIGN

The low-frequency deviations of the laser frequency have a large amplitude, and with increasing frequency the amplitude of the frequency noise drops sharply. Slow disturbances should be suppressed by a slow modulator and do not affect the fast modulator, which otherwise enters the signal-limiting mode. The distribution of motions along the modulators is provided by the form of the frequency response of the control channels. To form them to the unchanged part of the object add regulators. It is necessary to synthesize the frequency response of two channels - fast and slow. The transfer function of the object through different channels is different and the main inertial links in it are described by the integrator, as well as by the second-order links corresponding to the frequency response of the piezoelectric modulators.

The main tasks of synthesis of regulators for PLL:

- 1) ensuring stability when expanding the band;
- 2) providing the maximum sharp increase in the gain with decreasing frequency;
- 3) the energy distribution of the transient process of the system from the frequency spectrum between the fast and slow channels.

The logarithmic frequency response of the object on both channels has an initial slope of the first order due to the serial connection of the links that convert the voltage to the frequency (the laser with the modulator) and the phase into the voltage (phase detector). The relationship between frequency and phase is described by an integral relationship, so the object contains an integrator. According to the methodology outlined above, the fast channel controller must have a zero slope. As the gain increases, the frequency of the unit gain of the fast channel increases. The system is stable until it approaches the cutoff frequency of the next inertial link. This link is a fast modulator, since the frequency FF of the cutoff of the LF filter at the output of the PFD should exceed the resonance frequency of this modulator FB. At FB = 50 kHz, it is recommended that FF = 100 kHz.

It is possible for the FAP in a fast channel to be limited to a proportional regulator, and to increase the frequency response with a decrease in frequency due to a slow channel. For a better transition of the system from the search mode to the tracking mode, it is advisable to provide an additional increase in the frequency response of the fast channel. In this case, the system is efficient and without a slow channel, and it only provides a larger range of retention. The raising of the frequency response of the fast channel should begin only with a frequency an order of magnitude smaller than the frequency of the unit gain of the fast loop.

If the transfer function of the fast modulator is

$$W_{EM} = \frac{K_1}{1 + 2\xi T_1 p + T_1^2 p^2}, T_1 = \frac{1}{2\pi F_B}. \quad (1)$$

In this case, the transfer function of the LF filter should look like:

$$W_{\Phi PQ} = \frac{K_2}{1 + 2T_2 p}, T_2 = \frac{1}{2\pi F_\Phi} = \frac{1}{\alpha}, \alpha = 1, 2 \dots 2. \quad (2)$$

The fast channel regulator is given in the form

$$W_{PBK} = \frac{K_3(1 + \tau_0 p)}{(1 + T_4 p)(1 + T_3 p)}; \quad (3)$$

$$T_3 > T_2, T_4 = \beta T_1, \beta = 10 \div 30, \tau_0 = 10^N T_1, N = 2 \dots 5. \quad (4)$$

The transfer function of the slow modulator is

$$W_{PMK} = \frac{K_4}{1 + 2\xi T_5 p + T_5^2 p^2}, T_5 = \gamma T_1, \gamma = 5 \dots 10. \quad (5)$$

The transfer function of the slow channel controller should in this case be

$$W_{PMK} = \frac{K_5}{1 + T_6 G p}. \quad (6)$$

It is customary to represent the frequency response of systems in a logarithmic scale along both axes. The

logarithmic frequency response of the object and controller connected in series is equal to the product of their AFC, on a logarithmic graph this product is obtained by graphical summation. When summing the effects on two channels, the smallest of them can be neglected. This fact on the logarithmic graph is manifested in the fact that the frequency response of the sum looks like the envelope of the both AFC, and at the point of intersection it is 1.5 times greater than each of them.

Fig. 7 shows the desired frequency response of the slow and fast channels (W_1 and W_2), and Fig. 8 shows the frequency response of the slow and fast channel controllers.

For the separation of motions along the modulators it is sufficient that the AFC of the fast channel should exceed the frequency response of the slow channel in the high-frequency band and be less in the zone of slow frequencies. These requirements are provided by the type of regulators. The separation of motions along the modulators is achieved by providing a twofold or larger slope of the AFC of the slow channel and introducing the integrator into the regulator. In this case, the slope of the fast channel AFC is single in the region starting much earlier than its intersection with the AFC of the slow channel and ending much later than its intersection with the frequency axis. In this area, the slope of the regulator should be zero.

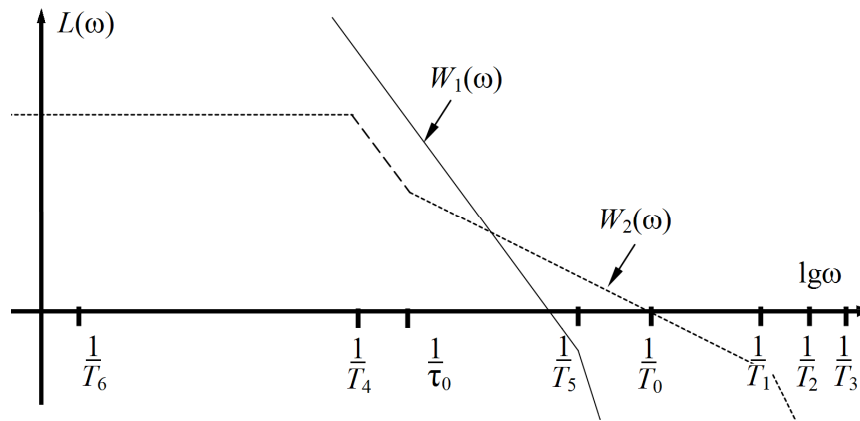


Fig. 7. The form of the frequency response of the slow (W_1) and fast (W_2) channels for effective mode separation.

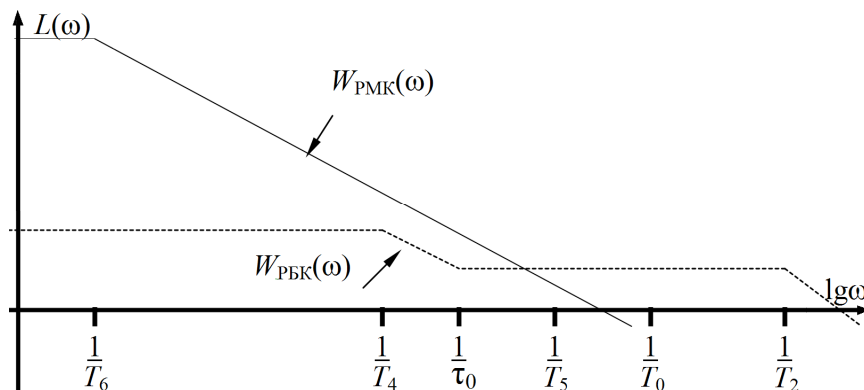


Fig. 8. The form of the frequency responses of the electronic part of the PLL slow (W_{11}) and fast (W_{21}) channels.

If the system is stable when using only a slow channel, this indicates an error setting. A properly tuned system is stable only when the fast channel is turned on. A large range of control is provided by the slow channel.

VII. HIGH-VOLTAGE AMPLIFIERS AND A NON-INTEGERSLOPE OF AFC

Usually high-voltage amplifiers are used to form high-voltage control signals for modulators. These amplifiers develop a voltage in the range of -300 V to $+300\text{ V}$ at the output. Successful separation of motions allows us to dispense with a conventional operational amplifier in a fast channel with a reasonable output, the output voltage range of which is from -12 V to $+12\text{ V}$. The high-voltage amplifier based on an operational amplifier with a high-voltage

cascade on two or more transistors. This amplifier was covered by negative feedback. The drawback of this solution was the selected version of the frequency response and the frequency characteristics of the frequency response. The large output impedance of such an amplifier in combination with a capacitive load (piezo ceramic modulator of resonator length) generated an additional aperiodic link in the model of this amplifier. This link is not properly taken into account in the mathematical model of the system, and sometimes misinterpreted. The emerging propensity to vibrations of a closed system was perceived as a manifestation of the resonant properties of the modulator. At the current level of development of electronic technology for the formation of high voltage in a slow channel, it is advisable to use an integral high-voltage operational amplifier (for example, OPA547T or more modern analogs).

Another problem of high-voltage amplifiers is the need for a correct choice (assignment) of the range of output voltages of these amplifiers. In the earliest schemes, amplifiers were used with a range of output voltages from zero to +160 V, then from zero to +300 V, after which amplifiers with an output from -300 V to +300 V began to be used. A balanced output has advantages, but there are and the disadvantages of such a solution. The advantage is that if the circuit is adjusted when the electronic part is de-energized (mechanical alignment of the laser mirrors and other settings of the optical circuit is performed), then the received settings correspond to the zero output signals of all amplifiers. In this case, in the absence of error signals at the inputs of high-voltage amplifiers, the system is in an equilibrium state, near the frequency of the radiation to which the initial tuning was performed. When using unipolar high-voltage amplifiers, the optical scheme should be set up with high-voltage amplifiers switched on, to which a signal corresponding to a zero error is fed. In this case, such amplifiers should form a signal equal to half the range of the output signals (in this case +80 V or +150 V).

The disadvantage of amplifiers with an alternating output signal is that for some types of piezo ceramic modulators only one polarity of the applied voltage is recommended, i.e., for such modulators, this mode is not recommended. The use of modulators in abnormal mode reduces their lifespan, in general, it should be noted that the use of any parts or elements in an abnormal mode might not only be undesirable, but also unacceptable.

For a long time, the use of high-voltage amplifiers with amplitude-frequency characteristic, the slope of which takes an intermediate value between -20 dB/dec and zero, has been practiced in PLL and AHF systems. Such a slope is provided by means of approximation. The use in a negative feedback of a high-voltage circuit amplifier containing several resistors, each shunted by a capacitor, provides such a "fractional" slope at a given portion of the AFC, for example, corresponding to its attenuation is inversely proportional to the root of the frequency (i.e., -10 dB/dec).

The idea of a non-slope is that when the AFC is tilted to an open loop of -40 dB/dec in the unit gain region, the system is theoretically at the stability boundary, in practice there are always additional inertia links, so the system with such slope in the region of unit gain is unstable. If in this area the slope is -20 dB/dec , the system is stable, but the stability margin is excessively large, and accordingly the slope of the amplitude-frequency characteristic in the indicated region increases with the frequency drop not fast enough. Therefore, the required accuracy of the AFC or PLL system is achieved only in the region of too low frequencies. Therefore, the idea of a multiple slope of the contour of about -30 dB/dec is to ensure stability with not too much margin, but with a sharper increase in frequency response when moving to low frequencies.

This idea did not justify itself in comparison with the method of separation of movements. The method of separation of movements (that is, providing an AFC of the type shown in Fig.7 and 8) allows simultaneously obtaining the greatest margin of stability and the sharpest increase in

the amplitude-frequency characteristic in the low-frequency region.

VIII. DISCUSSION OF RESULTS

A correctly designed system does not need manual tuning. The PLL circuit in Fig. 1 is capable of capturing the frequency as if the frequency of the leading laser is higher than the frequency of the driven laser by the FR value, and in the case that this frequency is less by this amount. This is manifested in the fact that the capture result depends on the history of the path along which the frequency of the tunable laser was approached to the frequency of the reference laser before the PLL transition into capture mode. If the frequency of the tunable laser was initially higher than the frequency of the reference laser, after capture, it will also be larger than the reference frequency by exactly the value of the frequency of the reference oscillator. If initially the frequency of the tunable laser was lower than the frequency of the reference laser, then after switching to capture mode, it will also remain below this frequency. If in such a system the sign of feedback is reversed, then nothing will change noticeably in operability, the frequency difference will remain in the same state, i.e., it will depend on the capture history, but the phase difference will reverse the sign. For example, if initially the phase difference was equal, then after the change of the feedback sign, the phase difference will be equal, and vice versa.

When using the system of Fig. 2 capture will occur only in one single case: either in a situation where the frequency of the tunable laser is greater than the frequency of the reference laser, or in the opposite situation. If the feedback sign is reversed, then the frequency difference will change its sign. This situation will in no way depend on the capture history, since capture is possible with a single combination of the magnitude and sign of the difference between the frequencies of the reference and tunable lasers.

IX. CONCLUSION

The article offers the results of a detailed development of phase-locked loop systems for two lasers. The proposed circuits are implemented and investigated, the efficiency of using frequency-phase detectors with the failure of an additional frequency loop formed on the basis of a separate frequency detector has been experimentally confirmed. Because of the introduction of such systems, their production, debugging and use were simplified. When these systems are used, it is only necessary to monitor the correct operation of the pulse shaper. The signals applied to it from the output of the photodetector must lie in amplitude in the prescribed range. If the noise level in this channel is not more than 0.05 V and the signal level is not less than 0.5 V, then the trigger threshold of the Schmitt trigger can be set, for example, at the level of 0.1 V. If, after some modifications of the optical circuit, that the noise in it increased to values of more than 0.1 V, the system will work incorrectly. In addition, if, for example, the trigger threshold is set to 0.5 V, and during the changes in the optical circuit, the signal level

will at least briefly fall below this value, the system will also work incorrectly. However, in practice, such discrepancies almost never occur, and if they do, a violation of the correct operation of the system is easily detected, after which it will be easy to find out the cause of this phenomenon and eliminate it. Problems with the operation of the proposed system are many times less than they were when using previous modifications of this system, the structural diagram of which is shown in Fig. 1.

X. ACKNOWLEDGEMENTS

The Russian Ministry of Education and Science supported this work. The Russian Scientific Foundation (Project No. 16-12-00052) has supported this work.

REFERENCES

- [1] Bagaev S.N., Belkin A.M., Dychkov A.S. et al. "Absolute frequency measurement of molecular Iodine reference line near 732 nm used for high precision spectroscopy of Muonium". Russian-German Laser Symposium. Novosibirsk, 27.06–1.07.97. Technical digest. p. P12–P13.
- [2] Bagaev S.N., Belkin A.M., Dychkov A.S. et al. "Frequency reference in the 732-nm region for precision laser spectroscopy of muonium". 2000 Quantum Electronics. 30(7), c. 641–646.
- [3] Bagayev S.N., Belkin A.M., Dychkov A.S. et al. "Absolute Frequency Measurements in Precision Laser Spectroscopy of Muonium". In collection: Proceedings of SPIE – The International Society for Optical Engineering Proceedings of the 1998 Nonlinear Optical Phenomena and Coherent Optics in Information Technologies, ICONO-98. Moscow, RUSSIA, 1999. P. 310–318.
- [4] Friederich F., Schuricht G., Deninger A., Lison F., Spickermann G., Bolívar P. H. and Roskos H. G. "Phase-locking of the beat signal of two distributed-feedback diode lasers to oscillators working in the MHz to THz range". Optic Express. 2010. Vol. 18, No. 8. P. 8621–8629. <https://www.osapublishing.org/viewmedia.cfm?uri=oe-18-8-8621&seq=0>
- [5] Marino A. M. and Stroud C. R. "Phase-locked laser system for use in atomic coherence experiments". Rev. Sci. Instrum. 2008. N79, 013104. <http://www2.optics.rochester.edu/~stroud/publications/marino081.pdf>
- [6] Hatanaka S., Sugiyama K., Mitaki M., Misono M., Slyusarev S.N., Kitano M. "Phase locking of a mode-locked titanium-sapphire laser-based optical frequency comb to a reference laser using a fast piezoelectric actuator". Applied Optics. 2017 Apr 20; 56(12). P. 3615–3621. doi: 10.1364/AO.56.003615. <https://www.ncbi.nlm.nih.gov/pubmed/28430232>
- [7] Hou D., Ning B., Zhang S., Wu J., Zhao J. "Long-term Stabilization of Fiber Laser Using Phase-locking Technique with Ultra-low Phase Noise and Phase Drift". <https://arxiv.org/pdf/1403.2569>
- [8] Zhmud V.A., Barmasov S.V., Gitel'son V.D. "An electronic system for stabilizing the frequency of the He-Ne laser to the methane absorption lines". 1999 Instruments and Experimental Techniques. 42(4). P. 551–557.
- [9] Gitel'son V.D., Voevoda A.A., Zhmud' V.A. "Phase locking of laser frequency for metrological systems". Proceedings of Second IASTED international Multi-Conference Automation, Control and Applications (ACIT-ACA). 2005. Novosibirsk. Russia. P.399–403.
- [10] Zhmud V.A., Pestriakov E.V., Trunov V.I. B.A. "Ways of the development of phase stabilization of lasers: tasks and methods. Collection of works of NSTU". 2011. 3(65). P.119 – 128. (In Russian: Puti razvitiya tekhniki fazovoy stabilizatsii lazerov: zadachi i metody resheniya // Sbornik nauchnykh trudov NGTU. Novosibirsk. 2011. N 3(65). P.119–128).
- [11] V. A. Zhmud. Possible ways of the development of the phase laser stabilization techniques: tasks and methods of the decision. // Proceedings of RFBR and DST Sponsored "The 2-nd Russian-Indian Joint Workshop on Computational Intelligence and Modern Heuristics in Automation and Robotics", 10 – 13 September, 2011, Additional volume, p.44–47.
- [12] A phase-locked loop system for the difference frequency of two lasers. Barmasov S.V., Zhmud' V.A. Instruments and Experimental Techniques. 2000. 43(3), P. 381– 83.
- [13] A.A. Voevoda, A.S. Farnosov, V.A. Zhmud'. High-speed phase-locked-loop frequency control of identical lasers. Proceedings of SPIE, Novosibirsk, 2002, vol.4900. P. 346–351.
- [14] V.A. Zhmud, O.D. Yadrishnikov, V.M. Semibalamut. Control of the objects with a single output and with two or more input channels of influence. WIT Transaction on Modelling and Simulation. Vol.59, 2015. WIT Press. www.witpress.com. P. 147–156.
- [15] Zhmud V. The providing of the power saving control of one output value with two controlling channels having different effectiveness and cost of the controlling resource. / V. Zhmud, L. Dimitrov // Trans & MOTAUTO '15 : 23 intern. sci. and techn. conf. of transport, road-building, agricultural, hosting & hauling military technics and technologies : proc., Bulgaria, Varna, 2015. – Varna : Sci.-techn. union of mechan. Engineering, 2015. – Vol. 3. – P. 118–122. ISBN 1310-3946.



Zhmud Vadim Arkadievich – Head of the Department of Automation in NSTU, Professor, Doctor of Technical Sciences.
E-mail: oao_nips@bk.ru

630073, Novosibirsk,
str. Prosp. K. Marks, h. 20



Taichenachev Aleksey Vladimirovich – corresponding member of RAS, Professor, Doctor of Physical and Mathematical Sciences, Director of Institute of Laser Physics SB RAS.
E-mail: taich.alex@gmail.com

630090, Novosibirsk, Prosp. Acad. Lavrentieva,
h.13/3



Dimitrov Lubomir Vankov – Vice-Rector of the Technical University of Sofia (Sofia, Bulgaria), Doctor of Science, Professor, Honorary Doctor of the NSTU.
E-mail: lubomir_dimitrov@tu-sofia.bg

Bul. "St. Kliment Ohridski" 8, 1756 Studentski
Complex, Sofia, Bulgaria



Semibalamut Vladimir Mikhailovich – Director of Sibirian Branch of Geo physical service SB RAS, PhD, Assistant Professor.
E-mail: wladim28@yandex.ru.

630090, Novosibirsk, Prosp. Acad. Lavrentieva,
h.13/3

Development of Methods and Procedures of the Analysis of Corporate Social Responsibility of Manufacturing Companies

Bibigul A. Amanzholova, Natalia V. Fribus, Elena V. Khomenko
Novosibirsk State Technical University, Novosibirsk, Russia

Abstract – In this article development of methodology of the analysis of corporate social responsibility on the basis of methods, procedures and analytical indicators covering all spheres of corporate social responsibility (economic, ecological and social) is proposed. At the same time authors proceeded from necessity to provide interrelation of procedures and indicators with tactical and strategic objectives of corporate activities. As a result of implementation of author's approach it is shown that the quality of conclusions is determined by volume of the initial information provided in the public reporting and also policy of the company in the sphere of disclosure of information on corporate social responsibility.

Index Terms – Corporate social responsibility, public reporting, methods and procedures of the analysis.

I. INTRODUCTION

THE CURRENT state of national economy is in many respects determined by the financial and property capacity of manufacturing companies, however the increasing attention is paid to issues of production and social infrastructure forming in interrelation with strengthening of an economic, food and ecological safety, providing of employment of the population and its increase. These things are in the sphere of social responsibility of economic units which activities are directed to satisfaction of economic and social needs of owners, personnel, consumers of goods, services and other stakeholders. The system of methods and procedures allowing objective estimation of results of business and social activity of economic units and also their contribution to social, economic and environmental problems solution is necessary for determination of level of their satisfaction.

Works of scientists A.M. Alperovich, V.G. Bochkaryov, E.M. Guttsayt, O.V. Danilova, T.V. Zyryanova, E.I. Ivanova, O.I. Kosenko, R.E. Meshalkina, Yu.N. Popov, E.N. Puzov, V.V. Rukin, O.A. Saprykina, A.N. Saunin, L.A. Simonova, B.N. Sokolov, O.E. Terekhova, S.A. Hmelev, V.A. Shakhoviy, A.A. Shulus and others are devoted to a research of the problems connected with penetration of social responsibility into the sphere of the Russian financial accounting, the reporting, the economic analysis and audit.

Researches of E.A. Ahrens, R. Dodz, M. Poukok, J. Robertson, A. Taylor, R. Holt, B. Kollas, Zh. Perar, D. Foster, D. Khan, K. Drury, R. Braly, S. Myers, E. Helfert, L. Bernstein, F. Sharp, K. Redkhed, S. Hyus, D. Middleton laid the foundation of the scientific knowledge necessary for

development of the theory and practice of accounting and analytical activities in the sphere of corporate social responsibility.

At the same time, the specificity of the analysis of corporate social responsibility, inconsistency of its development with evolution of analytical practice promoted the solution of strictly local problems of the methodical economic analysis of social activities of economic units.

The matter is that high degree of development is appropriate for the methods of the analysis of economic aspects of activities, including methods of a complex efficiency evaluation of functioning of economic units. However in modern conditions such methods aren't capable to provide an assessment of impact of variable internal and external factors on efficiency of corporate activities. It is obvious that the interpretation of efficiency significantly differs depending on the subject and an object of assessment and also a number of the essential factors which are determined by the level of economic development. So, the current idea is that any goods have the limited life cycle, and for this reason not goods, but processes of their creation are capable to bring to the company's results in the long term.

Authors agree with the point of view of E.N. Puzov that the efficiency of activities of the company implies its comparative assessment with the similar companies, but at the same time this assessment should be monetary [1]. Therefore, criteria for estimation of the company statement should be established, however it is impossible to agree that these criteria should be exclusively monetary ones. While getting the result (creation of a certain economic good) its quality characteristics can be various and depart from the parameters which are traditionally used for economic decision making. That's why it is more reasonable to pay attention to the degree of the achieved result when defining the "efficiency" term.

The analysis of literature allows us to state that the most part of theoretical and applied researches is devoted to economic aspects of determination of efficiency of the companies functioning. Such condition limits a possibility of application of these scientific research results for the analysis of corporate social responsibility of the companies taking into account the nature of their influence on a social and economic situation. Therefore, the approaches considering the economic and social parties of efficiency of activities are necessary.

Authors marked out two points of view for the dual party of efficiency. So, R.E. Meshalkina notes two aspects of efficiency: economic (comparison of the received result and costs for its achievement) and social (level of influence of particular economic result on separate social groups) [2]. L.A. Simonova considers social efficiency "from the point of view of achievement of certain socially important results from the budget services provided to the population", and cost efficiency – "from the standpoint of a ratio of services and costs for their provision" [3]. The first point of view isn't limited by the object and subject relations, and the second is applicable only in the sphere of the public and municipal authority. Researchers fairly specify complexity of determination of social effect due to objective lack of direct quantitative indicators of the social purposes achievement as, determining essence of economic efficiency, the attention is paid only to decrease of resources expenses for the result achievement, but its quality isn't taken into account.

The specifics of a subject of our research predetermined necessity of efficiency analysis from the standpoint of management of the companies that needs development of criteria, analyzing which it is possible to determine the level and quality of management, its compliance to requirements and the interests of stakeholders. So, in the theory and practice of management there are some applicable criteria of social efficiency: labor productivity level, rational job arrangement, motivation of each employee of the company to productive and high-quality work, safety and reliability of labor relations, workforce reproduction with the increasing positive result.

As a part of social aspects of activities an important role is played by ecological aspects of efficiency without which complex assessment of corporate social responsibility is impossible. Today at all levels of management social costs arise when activities of one economic unit cause the result positive or negative for another economic unit, absolutely uninvolved in these activities.

Theoretical bases of social costs are developed in the R.H. Coase's article of "A problem of social costs" (1960) [4], the Nobel Prize laureate on economy who define social costs as the highest value which production factors in case of their alternative use can bring. Article became one of the most quoted in modern economic literature and was directed against search of "market failures" and the government intervention in their overcoming. Harmful consequences or externalities were considered as one of such "failures of the market". There is incongruity between private and social costs or private and social benefits [5].

Outstanding issues of social costs accounting raise a question about the actual price of products of the companies for society. Therefore extent of impact of manufacturing company activities on the environment should be revealed in the public reporting.

To solve this problem the system of the procedures and indicators allowing to estimate qualitatively ecological effectiveness of the company, including scale and size of negative impact on the environment, amounts of the used natural resources, effectiveness of costs for environmental protection is necessary.

Thus, the lack of quantitative indicators of the social purposes achievement, weak development of methods for corporate social responsibility assessment, indefatigable emphases on economic efficiency achievement caused tasks of this research.

Authors consider that development of methods of the corporate social responsibility analysis assumes development of the system of procedures and analytical indicators which provide an opportunity:

- to form the single data base for implementation of analytical procedures, including revealing of contradictory information;
- to identify the essential parameters of corporate social responsibility;
- to assess the state, results and prospects of corporate social responsibility.

II. PROBLEM DEFINITION

As of April 17, 2018 167 companies are brought in the National Registry of non-financial reports, 826 reports, which are issued during the period since 2000 are registered. Among them: ecological reports – 73, social reports – 311, reports in the field of sustainable development – 277, the integrated reports – 141, industry reports – 26.

In distribution of non-financial reports on industry affiliation energy (21%), oil and gas (18%) and also metallurgical and mining industries (12%) dominate (Fig. 1).

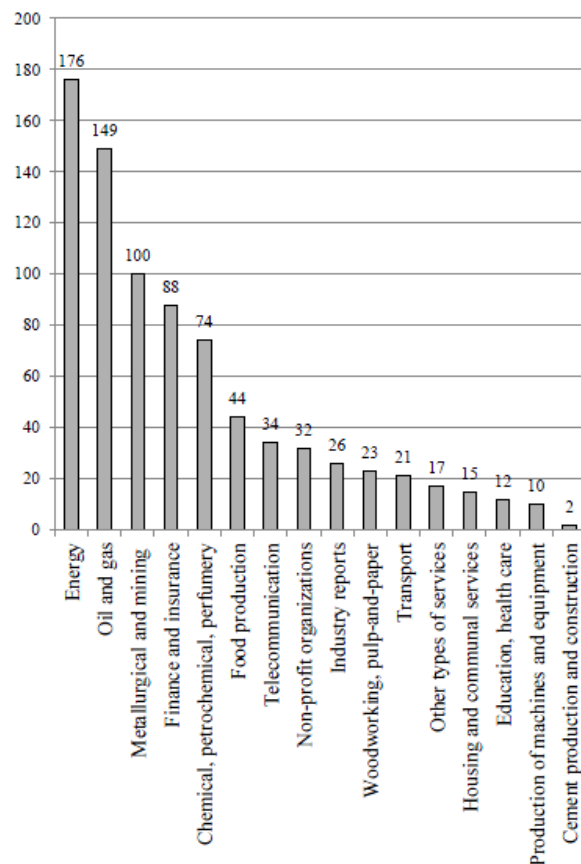


Fig. 1. Distribution of non-financial reports of the Russian companies on industry affiliation for April 17, 2018, number of reports.

As for the standards of preparation of the non-financial reporting used by the companies, according to the Russian Union of Industrialists and Entrepreneurs the Global Reporting Initiative (GRI) standards are the most popular among the Russian companies. "The number of the integrated reports in the last two years grew (mainly at the expense of the companies of nuclear sector) while social reports became singular, and ecological reports show surprising stability, statistically without changing in any way eventually" [6]. About 30 % of the companies preparing reports use two and more types of standards. At the same time, for example, the integrated reports now both on structure, and on content not too differ from reports in the field of sustainable development or annual reports. So, the fundamental idea of the Integrated Reporting Standard which is in description of the capitals changing while the creation of value added process still actually remains unrealized.

Thus, availability of numerous standards on reporting and a variety of stakeholders' informational needs resulted in considerable uncertainty concerning the choice of system of indicators in all spheres of corporate social responsibility.

Author's approach to system of indicators forming corresponds to logic of the analytical procedures implementation, i.e. estimated indicators are structured on areas of corporate social responsibility (Tab. I).

TABLE I
INDICATORS OF COMPANIES' PERFORMANCES IN DIFFERENT
SPHERES OF CORPORATE SOCIAL RESPONSIBILITY

| Economic performances | Ecological performances | Social performances |
|--|---|--|
| E1. Revenue from sales of goods, performance of works, services / Sales volume | N1. Gross energy consumption from all types of energy carriers | S1. The average staff number of the company (on age groups and gender) |
| E2. Amount of the main tax and non-tax assignments | N2. Gross consumption of source water from all types of sources | S2. The number of the dismissed employees |
| E3. Labor payment expenses and social payments | N3. Gross emissions of pollutants in the atmosphere | S3. Number of injuries for the accounting period |
| E4. Amount of actual costs on objects which will be entered into the accounting books as fixed assets (at the expense of all sources of financing) | N4. Gross amount of unused waste | S4. The number of the days of disability due to industrial traumatism |
| E5. Charitable contributions | N5. Gross amount of the taken-away waters, including amount of the sewage transferred to cleaning | S5. Total number of hours of employees training |
| E6. Sales profit | | |
| E7. Total volume of production/sales on the market | | |
| E8. Volume of production | | |

Further authors suggest the system of indicators for the analysis of corporate social responsibility which includes:

- the relative indicators characterizing efficiency in economic, social and ecological spheres;

- the indicators characterizing dynamics of absolute and relative measures on areas of corporate social responsibility;
- the integrated indicator of profitability of sales in the form of the factor model reflecting interrelation of economic and social indicators (Tab. II)

TABLE II
THE SYSTEM OF INDICATORS OF THE ANALYSIS OF
INFORMATION ON THE CORPORATE SOCIAL RESPONSIBILITY
DISCLOSED IN THE MANUFACTURING COMPANIES
REPORTING

| Indicators | Index | Calculation |
|---|--------------|-------------------------|
| Capital productivity from investments | K1 | $E1/E4$ |
| Workforce productivity | K2 | $E1/S1$ |
| Profitability of sales | K3 | $E6/E1*100\%$ |
| Turnover rate of personnel | K4 | $S2/S1$ |
| Average salary | K5 | $E3/S1$ |
| Tax burden | K6 | $E2/E1$ |
| Occurrence rate of industrial injuries | K7 | $S3*1000/S1$ |
| Severity rate of industrial injuries | K8 | $S4/S3$ |
| Relation of total number of hours of employees training to the average staff number of the company | K9 | $S5/S1$ |
| Dynamic of a gross energy consumption | $\Delta N1$ | $N1_n - N1_{n-1}$ |
| Dynamic of a gross consumption of source water | $\Delta N2$ | $N2_n - N2_{n-1}$ |
| Dynamic of gross emissions of pollutants in the atmosphere | $\Delta N3$ | $N3_n - N3_{n-1}$ |
| Dynamic of a gross amount of unused waste | $\Delta N4$ | $N4_n - N4_{n-1}$ |
| Dynamic of a gross amount of the taken-away waters | $\Delta N5$ | $N5_n - N5_{n-1}$ |
| Relation of gross amount of unused waste to volume of production | K10 | $N4/E8$ |
| Share of the Russian market on production | K11 | $E1/E7*100\%$ |
| Relation of charitable contributions to amount of the main tax and non-tax assignments | K12 | $E5/E2$ |
| Dynamic of a capital productivity from investments | $\Delta K1$ | $K1_n - K1_{n-1}$ |
| Dynamic of a workforce productivity | $\Delta K2$ | $K2_n - K2_{n-1}$ |
| Dynamic of a profitability of sales | $\Delta K3$ | $K3_n - K3_{n-1}$ |
| Dynamic of a turnover rate of personnel | $\Delta K4$ | $K4_n - K4_{n-1}$ |
| Dynamic of an average salary | $\Delta K5$ | $K5_n - K5_{n-1}$ |
| Dynamic of a tax burden | $\Delta K6$ | $K6_n - K6_{n-1}$ |
| Dynamic of an occurrence rate of industrial injuries | $\Delta K7$ | $K7_n - K7_{n-1}$ |
| Dynamic of a severity rate of industrial injuries | $\Delta K8$ | $K8_n - K8_{n-1}$ |
| Dynamic of relation of total number of hours of employees training to the average staff number of the company | $\Delta K9$ | $K9_n - K9_{n-1}$ |
| Profitability of sales (factor model) | K3 | $(E6*S1*K2)/E1^2*100\%$ |
| Dynamic of relation of gross amount of unused waste to volume of production | $\Delta K10$ | $K10_n - K10_{n-1}$ |
| Dynamic of a share of the Russian market on production | $\Delta K11$ | $K11_n - K11_{n-1}$ |
| Dynamic of relation of charitable contributions to amount of the main tax and non-tax assignments | $\Delta K12$ | $K12_n - K12_{n-1}$ |

For implementation of potential opportunities of the offered system of indicators authors proceeded from the following requirements. First, scope of all areas of corporate social responsibility is provided by indicators. Secondly, the interrelation of indicators of system and focus on the

characteristic of corporate goals achievement is provided. Thirdly, the preventing indicators and historical indicators are included in the system. There are accurate methods of their calculation and also the clear procedure of interpretation and assessment according to the level of informational content of the public reporting.

III. THEORY

The concept of corporate social responsibility has a highest importance in the modern economic theory in interpretation of externalities which influence on society and the environment. This concept is based on the idea that controlled parameters of corporate activities in modern economic conditions are not only financial ones, but also ecological and social which in total allow to characterize degree of business responsibility for results of activities and their significance for society in general.

The European Commission determines corporate social responsibility as "a concept whereby companies integrate social and environmental concerns in their business operations and in their interaction with their stakeholders on a voluntary basis" [7]. At the same time corporate social responsibility assumes doing actions by the companies over their obligations in law before society.

In researches of modern scientists and economists much attention is paid to evaluation of quality of information on the corporate social responsibility disclosed in the public reporting of the company. However single approach to such assessment is not developed. It is possible to mark two main research approaches to evaluation of quality of information on corporate social responsibility: quantitative and qualitative.

Supporters of quantitative approach suggest undertake the content analysis (Lock I., Seele P., 2016) or use a methodological basis of the Global Reporting Initiative Standards [8]. The qualitative analysis is based, as a rule, on author's methods (Daub C.-H.J. (2007); Leitonienė S., Sapkauskienė A. (2015); Habek P., Wolniak, R. (2015)) of calculation of the integrated indexes characterizing quality of disclosed information in a set of the parameters and allowing to range the companies by results of quality evaluation of reporting on corporate social responsibility.

P. Habek carries out evaluation of information quality on 17 criteria grouped for assessment of the relevance (11 criteria) and reliability (6 criteria) of information. Marks by each criterion are determined in points by a scale from 0 to 4 and further are generalized for calculation of private indexes of relevance and reliability of information and also the integrated index of the information quality [9].

L. Koep suggests to represent results of the qualitative (contextual) analysis of contents of the reporting on corporate social responsibility in three axes of coordinates: time axis (disclosure of information on events of the past or forecasts for the future); activities axis (declaring of intentions or results of their implementation); a clarity axis (the generalized or most concretized disclosure of information) [10].

In approach of J. Dyduch and J. Krasodomska it is offered to estimate quality of disclosed information taking into account such factors as the size of the company, profitability, a financial leverage, degree of an environmental impact, numerical and gender and age board, functioning in the international markets and business reputation of the company [11]. For the purposes of the analysis information provided in the annual and integrated reports is offered to be grouped according to the Directive 2014/95/EU of the European Parliament on disclosure of non-financial information [12]: business model, policy and risks in corporate social responsibility; ecological aspects; social issues and personnel; ethics issues. In the analysis the system of mark assessment from 0 to 3 is used. So, 0 points are appropriated if information isn't opened in the reporting; 1 – it is provided in a form of simple statement; 2 – information with use of Key Performance Indicators or other numerical data; 3 – simultaneous combination 1 and 2.

In the previous article [13] the research of various aspects of corporate social responsibility on the basis of a method of the morphological analysis was shown. The "morphological cube" offered by authors allowed to reveal the most significant for the analysis purposes parameters of the public reporting. The variability of parameters is caused by reporting types (financial reporting; annual report; sustainable development report), legal backgrounds (corporate obligations secured in legislation; voluntarily assumed obligations within agreements with stakeholders; pure philanthropy) and spheres of corporate social liability of the companies (economic; ecological; social). The analysis of quality of the information disclosure was carried out taking into account a mutual combination of the specified parameters on the example of the companies making essential negative impact on the environment that predetermined necessity of assessment of level of corporate social responsibility of such companies. On analysis results four possible conditions characterizing the level of the information disclosure in the reporting are outlined:

- compliance with legal requirements;
- compliance with legal requirements and requirements of the owners;
- compliance with legal requirements and requirements of the majority of stakeholders;
- compliance with legal requirements and requirements of stakeholders.

It is established that the equal level of the information disclosure on ecological activities in the reporting may be provided with various combination of factors and parameters of the reporting taking into account industry specifics of corporate activities and strategic priorities of development.

In this paper it is offered to carry out the analysis of quality of the information disclosure on the basis of the indicators characterizing results of corporate activities in various spheres of corporate social responsibility – economic, ecological and social.

The indicators given in the Tab. I are information basis for carrying out the analysis of quality of the information disclosure on corporate social responsibility in the reporting of the companies and may be provided in reports in a

different combination, with different level of specification or not provided in general. Considering the actual set of the input data provided in the reporting in each specific situation it is possible to calculate a certain set of the indicators allowing make a conclusion on quality of the information disclosure. At the same time four approaches of carrying out the analysis and interpretation of the received results are possible.

1. "Narrow and Closed Appraisal". In this case in the conditions of limitation of the data reflecting mainly economic results of corporate activities, indicators of capital productivity, a workforce productivity, and profitability of sales are calculated (Fig. 2).

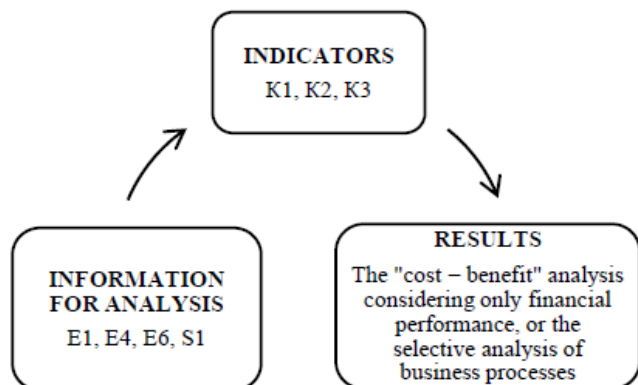


Fig. 2. The analysis of corporate social responsibility indicators in the "Narrow and Closed Appraisal" block.

2. "Broad and Closed Appraisal". In this case in a range of input data a set of the indicators characterizing social results of activities extends. So, it is possible to determine also a the turnover rate of personnel, the average salary, the tax burden, the occurrence rate of industrial injuries, the severity rate of industrial injuries and also the relation of total number of hours of employees training to the average staff number of the company (Fig. 3).

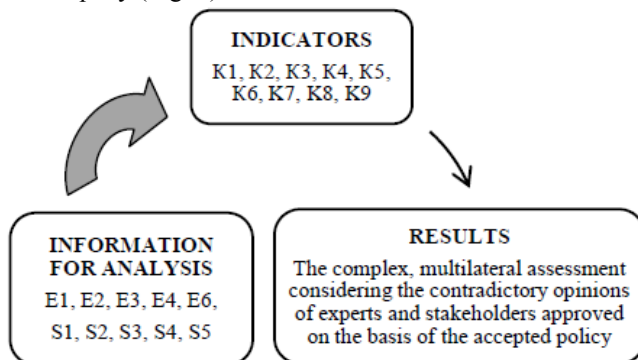


Fig. 3. The analysis of corporate social responsibility indicators in the "Broad and Closed Appraisal" block.

3. "Broad and Open Appraisal". In such situation the range of input data even more extends, including parameters of ecological effectiveness of activities that provide informational basis for the analysis of the information disclosure in all spheres of corporate social responsibility. As a part of the calculated indicators, along with received at the previous stages, indicators of dynamics of initial parameters of ecological activities (a gross energy consumption,

consumption of source water, emissions of pollutants in the atmosphere, amounts of unused waste and the taken-away waters) and also the relation of gross amount of unused waste to volume of production are determined. In the social sphere of corporate social responsibility the indicator characterizing the relation of charitable contributions to amount of the main tax and non-tax assignments is calculated. Besides, the indicators reflecting strategic priorities of the company development such as market share on production volume or sales are determined (Fig. 4).

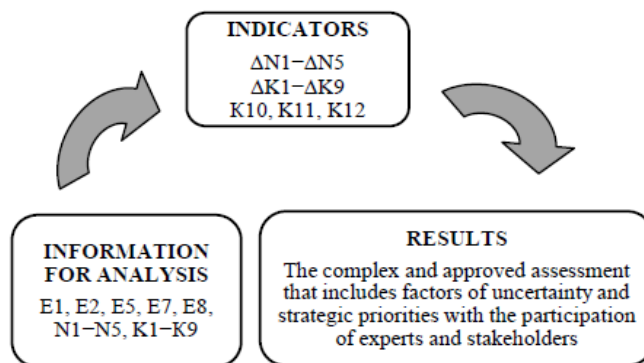


Fig. 4. The analysis of corporate social responsibility indicators in the "Broad and Open Appraisal" block.

4. "Narrow and Open Appraisal". In this case in the corporate reporting the indicators in the sphere of economic, social and ecological performances are selectively provided. So, it is possible to carry out the analysis only taking into account certain assumptions, subjective view of stakeholders on the directions and conditions of the company development and also using special analytical methods, in particular, the factorial analysis (Fig. 5).

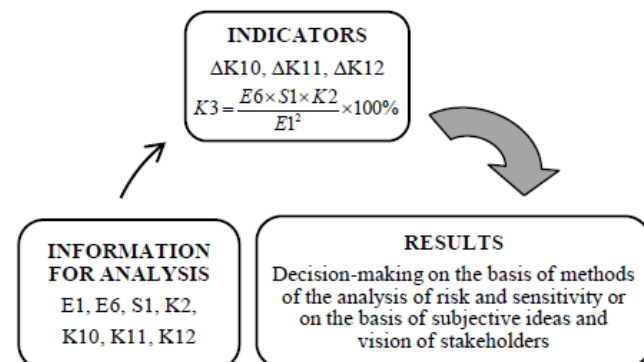


Fig. 5. The analysis of corporate social responsibility indicators in the "Narrow and Open Appraisal" block.

The variability of information provided in the public reporting of manufacturing companies provide a means of the analysis with use of various set of the recommended indicators (Tab. II) depending on the purposes of the analysis and level of disclosure of information on corporate social responsibility.

IV. EXPERIMENTAL RESULTS

The proposed method of corporate social responsibility analysis provides, on the one hand, completeness and complexity of the analysis including indicators of various spheres of corporate social responsibility, and on the other hand, promotes a fitting of system of indicators to specifics of activities and to structure of information for the analysis. Information basis for the analysis of quality of disclosure of information on corporate social responsibility is provided by data of financial reporting, the annual report for shareholders and the social report of the company. As base for an experiment the public reporting of JSC SUEK which is the largest Russian company on production and enrichment of coal is considered [14].

JSC SUEK prepares the consolidated annual financial statements according to requirements of IFRS. The individual non-financial reporting which is directly connected with information openness of the company is encouraged to compensate the shortage of information. The Company issues such reporting in a format of the social report which is prepared according to the recommendations of an international and acknowledged Global Reporting Initiative (GRI) in its latest version [15]. The report was under external audit and public assurance. The company implements social responsibility in business practice, developing an integrated approach to the solution of social and environmental problems for achievement of the long-term competition.

Results of the carried-out analysis of disclosure of information on corporate social responsibility are shown in to the Tab. III.

TABLE III
RESULTS OF THE ANALYSIS OF JSC SUEK'S CORPORATE
SOCIAL RESPONSIBILITY INDICATORS

| Indicators | 2014 | 2015 |
|--|--------|--------|
| Block 1 "Narrow and Closed Appraisal" | | |
| Capital productivity from investments (K1), million rubles | 10.19 | 11.64 |
| Workforce productivity (K2), million rubles / persons | 6.2 | 7.8 |
| Profitability of sales (K3), % | 9.7 | 10.6 |
| Block 2 "Broad and Closed Appraisal" | | |
| Capital productivity from investments (K1), million rubles | 10.19 | 11.64 |
| Workforce productivity (K2), million rubles / person | 6.2 | 7.8 |
| Profitability of sales (K3), % | 9.7 | 10.6 |
| Turnover rate of personnel (K4), persons | 17.7 | 16.4 |
| Average salary (K5), rubles | 40853 | 44082 |
| Occurrence rate of industrial injuries (K7), injuries /1000 persons | 2.52 | 2.07 |
| Severity rate of industrial injuries (K8), days/ injuries | 143.2 | 141.6 |
| Relation of total number of hours of employees training to the average staff number of the company (K9), hours/persons | 51 | 45 |
| Block 3 "Broad and Open Appraisal" | | |
| Dynamic of a gross consumption of source water (ΔN2), million m ³ | -0.198 | -0.034 |
| Dynamic of gross emissions of pollutants in the atmosphere (ΔN3), th. tonnes | 10.807 | 1.281 |
| Dynamic of a gross amount of unused waste | 54.2 | -35.6 |

| | | |
|--|------|-------|
| (ΔN4), million tonnes | | |
| Relation of gross amount of unused waste to volume of production (K10), million tonnes | 1.57 | 1.22 |
| Share of the Russian market on production (K11), % | 35.8 | 35.1 |
| Dynamic of a capital productivity from investments (ΔK1), million rubles | n/a | +1.49 |
| Dynamic of a workforce productivity (ΔK2), million rubles / person | n/a | +1.6 |
| Dynamic of a profitability of sales (ΔK3), % | n/a | +0.9 |
| Dynamic of a turnover rate of personnel (ΔK4), persons | -0.6 | -1.3 |
| Dynamic of an average salary (ΔK5), rubles | n/a | +3229 |
| Dynamic of an occurrence rate of industrial injuries (ΔK7), injuries /1000 persons | n/a | -0.52 |
| Dynamic of a severity rate of industrial injuries (ΔK8), days/ injuries | n/a | +2 |
| Dynamic of relation of total number of hours of employees training to the average staff number of the company (ΔK9), hours/persons | n/a | -6 |
| Block 4 "Narrow and Open Appraisal" | | |
| Profitability of sales (K3), % | 9.7 | 10.6 |
| Dynamic of relation of gross amount of unused waste to volume of production (ΔK10), million tonnes | 0.02 | -0.35 |
| Dynamic of a share of the Russian market on production (ΔK11), % | n/a | -0.7 |

Calculations showed that information provided in the reporting is enough for the analysis of "costs – benefit" ratio and also for the complex assessment considering expectations of owners and personnel.

So, on the indicators included in the Block 1 "Narrow and Closed Appraisal" it is possible to make a conclusion on positive dynamics of the main indicators of business activity efficiency. However it isn't possible to give an assessment of influence of social and ecological factors because indicators of economic effectiveness, except for the average staff number of the company which characterizes social aspect of activity, are generally used for calculation.

The analysis of the indicators included in the Block 2 "Broad and Closed Appraisal" supplements assessment on the first block with the factors characterizing social aspects of activities. It is possible to refer personnel policy, policy on prevention of an industrial traumatism and the system of advanced training to such aspects. At the same time assessment of the pursued social policy may be performed in interrelation with the achieved economic results. So, from calculations it is evident that profitability of sales is provided with a workforce productivity increase which rates of change (125,8 %) exceeded growth rates of the average salary (107,9 %).

Information provided in public and the audited reporting in not enough for the complex approved assessment considering economic, ecological and social spheres which would reveal factors of uncertainty and to describe options of the company development. It is proved by the fact that from 14 indicators included in the Block 3 "Broad and Open Appraisal", authors could calculate only 6 indicators.

It is important to mention that the information is not unrevealed, but in the analyzed period the comparability between volume and content of disclosed information isn't provided. The positive fact is the quality of the disclosed information on ecological aspects in the reporting for 2015. It

is possible to assume that in future periods stakeholders will be able to create complex assessment of effectiveness of the company activities.

Results of the analysis of the indicators included in the Block 4 "Narrow and Open Appraisal" prove that indicators applied to forecasting of parameters of activities on the basis of the analysis of their sensitivity of rather external factors structure should be included in the system.

V. DISCUSSION OF RESULTS

The method of analysis of the manufacturing companies' corporate social responsibility offered by authors includes the system of indicators of economic, ecological and social effectiveness. Indicators are analyzed and interpreted in interrelation, interconditionality and depending on influence of the results on stakeholders' decisions.

"Narrow and Closed Appraisal" is the first of four possible options of the analysis of information on corporate social responsibility disclosed in the reporting. In fact, it is the "costs – benefits" analysis which results allow to prove only some management decisions.

The analysis in the "Broad and Closed Appraisal" block goes out of the economic sphere of corporate social responsibility and includes, first of all, indicators of corporate social responsibility in the social sphere. However results of the analysis are interpreted on the basis of the regulations accepted in the company and policy in the field of corporate social responsibility that allows to make management decisions and to approve contradictory opinions of stakeholders, but at the same time brings certain restrictions in interpretation of the results.

The analysis "Broad and Open Appraisal" covers all spheres of corporate social responsibility of manufacturing companies and may be considered as most favorable option both from the point of view of amount of basic data, and from the point of view of the received results. Such analysis allows not only to characterize the level of corporate social liability of the company, but to reveal uncertainty factors, risks, threats of activities and to describe ways of implementation of strategic tasks of development.

At last, in the analysis "Narrow and Open Appraisal" a range of the received results is expanded by taking into account stakeholders assumptions and application of factorial models of the most significant indicators in case of limitation of input data.

At the same time it should be noted that a specific set of indicators may vary depending on industry affiliation of manufacturing companies, types of the public reporting, strategic objectives of the company development and other factors.

VI. CONCLUSION

Thus, authors offer development of methodology of the corporate social responsibility analysis on the basis of application of methods, procedures and analytical indicators which equally cover all spheres of corporate social responsibility. Authors proceeded from necessity of

providing interrelation of procedures and indicators with tactical and strategic objectives of the company development. Authors proceeded from need of ensuring interrelation of procedures and indicators with tactical and strategic objectives of activities of the companies. Experiments showed that the quality of conclusions is determined not only by volume of input information, but also by policy of the company in disclosing the essential information on various aspects of activity. In this research the ratio between the volume, structure of the analyzed information, applied methods and informational content of conclusions from the point of view stakeholders' expectation was the criterion of quality.

Authors came to conclusion that implementation of author's ideas is limited by the level of informational content of the companies public reporting. Therefore as prospect for further researches authors consider broaden of system of indicators by indicators requiring rapid response from stakeholders. Realization of these ideas requires harmonization of shareholders' expectations and potential of the financial and statistical accounting of the manufacturing companies.

REFERENCES

- [1] Puzov E.N. Evolution of concepts of management and assessment of efficiency of business // *Economic analysis: theory and practice*. 2007. No 10. C. 58-64.
- [2] Meshalkina R.E. Audit of efficiency – the objective necessity // *Finance*. 2005. No 2.
- [3] Simonova L.A. Efficiency of the state financial control // *Finance*. 2006. No 4. C. 50-52.
- [4] Coase R. H. The problem of social cost [Electronic recourse]. Mode of access: http://www.libertarium.ru/l_libfirm05 (accessed 3 May 2018).
- [5] Amanzholova B.A., Fribus N.V. Theory of social costs as the basis of environmental accounting // *Innovation processes in the context of globalization of the world economy: challenges, trends, prospects (IPEG-2015): proceedings Praha: Vědecko vydavatelské centrum Sociosféra-CZ*, 2015. pp. 9-12.
- [6] The analytical review of corporate non-financial reports of 2015-2016 of release "Responsible business practice in a reporting mirror: present and future", 2017 [Electronic resource]. Mode of access: <http://media.rsp.ru/document/1/7/4/743222fc4c6650093518c635d0e8ecdd.pdf> (accessed 30 April 2018).
- [7] European Commission, A Renewed EU Strategy 2011-14 for Corporate Social Responsibility, Brussels, 2011. [Electronic recourse]. Mode of access: <http://eurlex.europa.eu/LexUriServ/LexUriServ.do?uri=COM:2011:0681:FIN:EN:PDF> (accessed 1 May 2018).
- [8] Lock I., Seele P. The credibility of CSR reports in Europe. Evidence from a quantitative content analysis in 11 countries. *J. Clean. Prod.* 2016. pp. 186–200.
- [9] Habek P. CSR Reporting Practices in Visegrad Group Countries and the Quality of Disclosure // *Sustainability*, 2017. No 9.
- [10] Koep L. Tensions in Aspirational CSR Communication – A Longitudinal Investigation of CSR Reporting // *Sustainability*, 2017. No 9.
- [11] Dyduch J., Krasodomska J. Determinants of Corporate Social Responsibility Disclosure: An Empirical Study of Polish Listed Companies // *Sustainability*, 2017. No 9.
- [12] European Union. Directive 2014/95/EU of the European Parliament and of the Council of 22 October 2014 Amending Directive 2013/34/EU as Regards Disclosure of Non-Financial and Diversity Information by Certain Large Undertakings and Groups. 2014. [Electronic recourse]. Mode of access: <http://eurlex.europa.eu/legal-content/EN/TXT/PDF/?uri=OJ:L:2014:330:FULL&from=EN> (accessed 1 May 2018).

- [13] Amanzholova B., Fribus N., Khomenko E. Disclosure of information on ecological activity as a factor of sustainable development of manufacturing enterprises // Actual problems of electronic instrument engineering (APEIE–2016): proceedings of the 13th International Conference, Novosibirsk, 2016, 3–6 oct. Volume 1, Part 3. pp. 202-206.
- [14] JSC SUEK [Electronic resource]: official site of the company. Mode of access: <http://www.suek.ru> (accessed 20 April 2018).
- [15] Corporate social report of SUEK Group 2014-2015: creating the value [Electronic resource]. Mode of access: http://www.suek.ru/upload/files/pdf/SUEK_CSR_RUS.pdf (accessed 20 April 2018).



Bibigul A. Amanzholova, head of the Department of Audit, Accounting and Finance at NSTU, professor, Doctor of Economics, the author of more than 100 scientific publications, including 13 monographs, 2 certificates on registration of software products. Area of scientific interests: accounting, reporting, audit and internal control in management of economic entities.
E-mail: amanzholova@corp.nstu.ru



Natalia V. Fribus, senior lecturer of the Department of Audit, Accounting and Finance at NSTU, the author of 15 scientific publications. Area of scientific interests: financial accounting and reporting, ecological accounting.
E-mail: natalya_klyuh@mail.ru



Elena V. Khomenko, assistant professor of the Department of Audit, Accounting and Finance at NSTU, Candidate of Economic Sciences, the author of 46 scientific publications. Area of scientific interests: accounting, reporting, accounting and analysis of results of intellectual activity of economic entities.
E-mail: homenko_ev@mail.ru

Threats and Opportunities of Cryptocurrency Technologies

Bibigul A. Amanzholova, Pavel N. Teslya
Novosibirsk State Technical University, Novosibirsk, Russia

Abstract – The reasons for the rise of interest in cryptocurrencies are shown, the prospects for their development and possible consequences for national and international economic systems, the regulation of the circulation and use of financial and monetary authorities are evaluated.

Index Terms – Cryptocurrencies, blockchain, smart contracts, financial system.

I. INTRODUCTION

Until the beginning of 2017, the cryptocurrency markets were the object of interest of a narrow circle of pioneers of this exotic business, as well as professional financiers, and even then – mostly academic. However, already in July of this year, the wave of publications about some of these digital assets has increased dramatically. About Bitcoin, Ethereum, Ripple and other cryptocurrencies began to talk and write in popular business publications. The reason for the outbreak of interest was a fantastic rise in prices.

Statistics shows (see Fig. 1) that in 2017 the price of Bitcoin has risen from \$ 795 at the beginning of the year to 19 401 USD. for a coin in December, then Bitcoin as sharply "dived" in January 2018 to 6 852 dollars. Then Bitcoin continued his upward movement. Other cryptocurrencies made a similar rise, and their movement was well synchronized, although with some shifts, in particular, the Ethereum bubble was late relative to Bitcoin by about half a month.



Fig. 1. Bitcoin quotations (USD per unit of BTC) [1].

The increased price level and the expansion of operations immediately turned cryptocurrencies into an attractive investment object.

Worth to notice the following. Although the capitalization of cryptocurrencies reached a noticeable volume of 459 billion dollars at the end of February 2018 [2], this level is still not enough competitive with the dollar and other convertible fiat currencies. For comparison, the US M2 monetary aggregate was about \$ 14 trillion at that time. Dollar

value (capitalization) of crypto-currencies in circulation is equal to the aggregate Belgium M2, not the largest country in the Eurozone. [3].

Not all cryptocurrencies have a meaningful market liquidity. Many of them exist in latent form. It is not surprising, after all, that anyone who have appropriate qualifications was able to create cryptocurrency and launch it's circulation. At the beginning of March 2018, the portal coinmarketcap.com reports about 1523 cryptocurrencies. Of these, only 1,176 had a market quote, the rest were marked with a question mark. Among the 10 most popular cryptocurrencies, only Bitcoin, Ethereum, Ripple and Bitcoin Cash were more or less noticeable by their share in total market capitalization (see Fig.2).

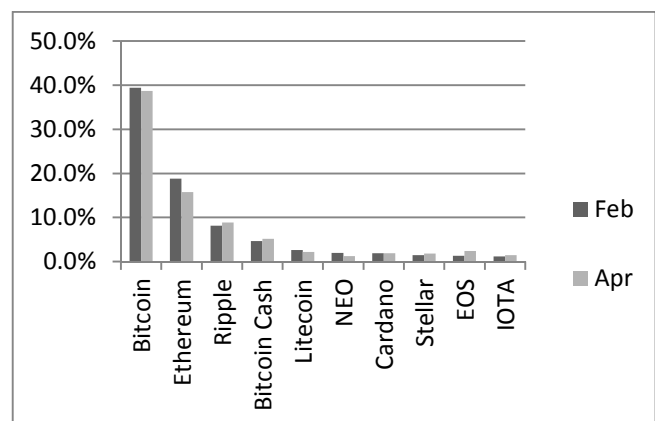


Fig. 2. Shares of individual cryptocurrencies in total market capitalization as of March 2018 (calculated by authors) [2].

The dominant position of Bitcoin had place throughout the period of existence of cryptocurrencies, that is, since 2009, but the share of Bitcoin is gradually decreasing, and along with it we now see a lot of so-called altcoins, currencies that appeared after 2013. The most notable is Ethereum.

The competition between numerous altcoins and Bitcoin does not allow the concentration of the financial potential in the segment of the cryptocurrency, which reduces the likelihood of turning some of them, into the global key currency.

One can notice that the relative weights of certain cryptocurrencies vary pretty strongly. Total capitalization also varies. In just 2 months (from February to April 2018) it decreased from \$ 459 billion to \$ 388 billion or 15.4%). Capitalization of cryptocurrencies and their specific weights of the ten cryptocurrencies with highest rating in the total "cryptomass" evolved as follows (see Tab. I).

TABLE I
CAPITALIZATION AND SPECIFIC WEIGHTS OF INDIVIDUAL
CURRENCIES IN FEBRUARY-APRIL 2018, IN BILLION US
DOLLARS AND % (CALCULATED BY [2])

| Cryptocurrency name | February 2018 | | March 2018 | |
|---------------------|---------------|------|------------|------|
| | Cap | % | Cap | % |
| Bitcoin | 181,19 | 39,5 | 150,38 | 38,7 |
| Ethereum | 86,44 | 18,8 | 61,15 | 15,7 |
| Ripple | 37,37 | 8,1 | 34,46 | 8,9 |
| Bitcoin Cash | 21,43 | 4,7 | 19,96 | 5,1 |
| Litecoin | 12,06 | 2,6 | 8,35 | 2,1 |
| NEO | 9,10 | 2,0 | 4,88 | 1,3 |
| Cardano | 8,68 | 1,9 | 7,41 | 1,9 |
| Stellar | 6,64 | 1,4 | 6,92 | 1,8 |
| EOS | 6,04 | 1,3 | 9,29 | 2,4 |
| IOTA | 5,27 | 1,1 | 5,68 | 1,5 |

The following facts are worth to note in the presented table:

- The rating of the four major currencies remained unchanged, the rest mutilated: some went down - Litecoin, NEO, and others went up - EOS, Stellar and especially EOS.
- The magnitude of change in relative positions of cryptocurrencies so great that the observer does not have a doubt, that this market does not obey the fundamental laws, in any case, at the present time.

II. PROBLEM DEFINITION

Management of transactions with cryptocurrencies is carried out on a decentralised basis. The absence of intermediaries and the underlying technology, the blockchain, which in essence – is a digital encryption (and hidden from prying eyes) of transaction records with cryptocurrencies makes the sale and other transactions involving these assets safe, anonymous, potentially cheaper and more convenient for any fairly literate person.

There are several ways to get a cryptocurrency into ownership. One of the most popular in recent years is by method of mining. This requires to create new units by computers and get bitcoin as a reward.

A lot of people in a lot of countries run computers and get coded records organized in the form of blocks connected in a chain. In cases where these newly computed blocks meet the software requirements of the designers of those cryptosystems, and receive confirmation from other participants in the network corresponding to the cryptocurrency, there are new bitcoin entering into the property of members of the network.

Along with mining there is also another way to get bitcoin, the so-called forging. Unlike mining, forging is not based on computer processing power, but rather on the possession of a particular share from the previously released amount of bitcoins. For this reason, mining is also called proof-of-work, and forging - proof-of-stake.

You can get bitcoin not only through mining and forging, but also acquire in exchange for fiat currency, goods or services, either directly from the seller, or through organized service centers, exchange offices, stock exchanges.

Bitcoin occupies a special place in the cryptocurrency system, it is used as the key currency of all cryptocurrencies world.

Cryptocurrency exchange can be carried out both through unlicensed and licensed exchange offices, the latter in Russia only three (two in Moscow and one in Yekaterinburg) [4].

There are many signs that crypto-currencies actually operate as a surrogate cash. One can find numerous reports about their use in transactions for the sale of goods and services, many of which were illegal. Finally, we can point at the practice of using Bitcoin ATMs, which clearly puts them on a par with high-power money, banknotes and coins (in September 2017, there were 1,574 ATMs in the world [5]).

III. THEORY

Cryptocurrencies have some very strong sides, which makes them an extremely attractive tool, that is used both for the purpose of hiding operation, as well as for the gaining speculative profit.

A. Anonymity and Pseudonymity

From the very beginning, a cryptocurrency was intended for anonymization or to pseudonymization participants of the transaction. (Some of the later cryptocurrencies, such as Zerocoin, are completely anonymous.) The anonymous nature of the transaction helps to gain income that is almost impossible to track to origin. Hence, it is possible to avoid tax liabilities.

B. Economizing Transaction Costs

The participants of the transaction do not need intermediaries. Their operations are completely protected from compromise. No one can make unauthorized entry into those blocks of distributed registers which reflect the transactions of the Contracting parties. At most, what they need is infrastructure services. For example, data storage services (mainly keeping cryptocurrency wallets), as well as supporting virtual platforms on which currency exchange and investment operations can be carried out. The absence of intermediaries significantly reduces credit risks and associated costs.

A powerful tool to guarantee the financial safety of transactions with cryptocurrencies is the so-called smart contract. One of the cryptocurrencies, namely Ethereum, is based on thy specific type of blockchain organization, which automatically forces the participants of the transaction to fulfill their obligations. That's a smart contract.

C. Participation in Financial Speculations and Investments

Shown in Fig. 1 the strong volatility of the price of cryptocurrencies is a serious reason for obtaining speculative benefits. Speculators can be enriched both by raising and lowering the price. It should be noted, however, that the use of fixed-term instruments in the cryptocurrency markets (such as futures, swaps or options) has not yet been reported.

Nevertheless, the emergence of such innovations is quite predictable.

Not so obvious, but have repeatedly proven the benefits of participation in IPOs amount of cryptocurrencies (ICO) showed that investors can get high returns from non-speculative operations with cryptocurrency.

However, it should be kept in mind that there exists a risk of fraud during the ICO. For this reason, many countries have established or are planning to establish restrictions on this activity.

The threats generated by crypto-currencies, have a dual nature.

D. Threats to the State, Country and Society

- Using the cryptocurrency as a mean of payment undermines national monetary sovereignty. The more transactions for goods and services is performed with the use of Bitcoin or altcoins, the narrower becomes the power domain of monetary authorities.
- Hiding of income means a criminal tax evasion. The state is deprived of its sources of income, loses the resources necessary to fulfill its obligations to citizens and the international community.
- Cryptocurrencies are actively used for the purchase and sale of illegal goods and services. There are many cases of the use of cryptocurrencies to finance illegal activities and money laundering. One of the most famous is a case of Silk Road portal.

E. Threats to Users of Cryptocurrency Networks

- The technology of the blockchain-transactions are not free from drawbacks. In particular, transactions are irreversible. If the payment is made incorrectly, it will be impossible to restore the status quo.
- Participants of the cryptocurrency transactions are vulnerable to the threats, typical for all operations with valuable information that occur through the Internet. A typical trap is the so-called phishing. People can be asked to send money to a false address. As a result, the money will be lost.
- Although the operations themselves, as reflected by means of the transaction records written in the combinations of blocks are secure, but the storage of information associated with threats of hacking of websites and stealing keys and other vital information that leads to loss of money. Threats also come from fraudsters who take malicious actions aimed at compromising the operators of cryptocurrency networks. One of the most notable examples of such threats is the bankruptcy of the Japanese cryptocurrency exchange Mt.Gox. Bankruptcy occurred as a result of its ruin. Manipulators were able to drop Bitcoin quotes, then bought up a large batch and thereby dealt a fatal blow to the exchange's finances.

In all considered cases, it will be impossible to find a fraudster due to anonymity (pseudonymity) of participants in transactions with cryptocurrencies.

IV. EXPERIMENTAL RESULTS

To combat the threats posed by crypto-currencies, or more precisely, from illegal activities and market failure, governments undertake the regulation of the markets in which cryptocurrencies are used.

The most significant issues that should be settled is, first, the interpretation of the concept of cryptocurrency, and, secondly, the definition of persons subject to selective regulation and control

A. The Interpretation of the Cryptocurrency

There is no single unified approach to the regulation of operations with cryptocurrencies in the world. Even the cryptocurrencies themselves are treated differently in different national jurisdictions. The extreme point of view is the recognition of the cryptocurrency as a means of payment. In fact, this means that the cryptocurrency acquires almost the same status as the fiat currency of the respective state. A similar approach can be found in Japan as well as in some European countries, like Germany. Note, by the way, that the Eurozone has not developed a unified approach to the issues of cryptocurrency circulation despite the use of a single Euro currency.

At the other end of the spectrum of positions in relation to cryptocurrencies is the point of view that cryptocurrency is a special kind of property. This position is held by the United States, the People's Republic of China and the Russian Federation.

B. The Approach to Building the Institutional Structure of Cryptocurrency Market Regulation

There is also no unified view on the desirable degree of liberalization of the cryptocurrency market in the world.

You can find examples of a complete ban on cryptocurrency transactions (Iceland, Bolivia, Ecuador). But the more common is a liberal point of view. It is true, also, that the "degree of liberalism" varies from country to country.

Poland can be attributed to countries with extreme liberalism. The Ministry of digital economy of Poland declared that they era intended to implement creation of a new Digital crypto-currencies PLN (dPLN), centrally issued by the National Bank of Poland.

Of countries with very strict control, one can mention the People's Republic of China. In China, financial institutions are prohibited from engaging in cryptocurrencies and using them for payment purposes. The rigidity of regulation in this area is growing. In September 2017 China's government put a complete ban on ICO. According to Coinmarketcap, the volume of the Chinese market, which previously amounted to more than 98% of the world's ICO, fell to a negligible 15% [6].

In the Russian Federation, there is still no existing legislation on cryptocurrency. However, in the autumn of 2017, the Ministry of Finance prepared a bill [7], which treats cryptocurrency as a digital financial asset (DFA). It provides for a strong tightening of the operating modes with

cryptocurrencies. In particular, there is a strict limit on the volume of transactions authorized by unskilled market participants; all transactions with the DFA are conducted only through the operators of digital financial assets exchange; procedures of ICO should be conducted in full accordance with the legislation on securities circulation, etc. One of the most important theses of the draft law is that parties to a smart contract to lose anonymity, but they instead receive protection of their rights, in the manner similar to the procedure of implementation of the protection of the rights of the parties to the agreement concluded in electronic form.

Without waiting for the adoption of the law, banks and financial companies take urgent measures to gain control over the development of distributed registers and decentralized applications. The banks are the leaders of R&D in the implementation of blockchain technology in Russia. The leaders banks are Sberbank, VTB and others. One of the most active proponents of this trend is the head of Sberbank German Gref.

For banks, the primary interest is the integration of blockchain with existing payment systems. As a result of blockchain implementation, payments will become safer, faster and cheaper. Many banking functions are still potentially vulnerable. The most vulnerable fragments of the transaction banking infrastructure would be replaced by blockchain.

Basing on blockchain, the banks plan to improve the efficiency of management, optimize the functions of the back office, and risk reduction. Smart contracts will add dynamics to the market because they will enhance the security of blockchain transactions for automated data control. Blockchain reduces the risks of working with unknown counterparties, increases the liquidity of banks and integrates the global financial system.

The Bank of Russia manages the development of new banking technologies. There was published an unprecedented document in March 2018 "Principal directions of development of financial technologies for the period 2018-2020" [8], which indicated a dozen promising platforms of financial infrastructure. One of them is a Platform based on the technology of distributed registries

V. DISCUSSION OF RESULTS

The inevitable tightening of cryptocurrency market regulation in the light of its growing scale and the threats posed by it is likely to lead a significant part of operations towards a gray or black area. The nature of the Internet is such that newly created digital technologies cannot be fully controlled by national jurisdictions. To the greatest extent, this applies to the cryptocurrency. Decentralized accounting makes it impossible to determine the national status (country of origin and country of registration) of cryptocurrency dealers, since there is no binding to any territory of the server on which the blocks of chains of the distributed registry are located [9].

However, the legalized part of the cryptocurrency market will become more secure and attractive [10]. The most important thing that should be noted is the powerful potential

of blockchain technology and smart contracts. Work on the introduction of technology of distributed registers of market transactions is actively carried out in banks of the Russian Federation – the Central Bank and commercial as well. In particular for the development of the above mentioned technologies in banks have established a special research laboratory.

The PRC is following the same path. The title of one of the articles "Zhenmin Zhibao" (February 9, 2018) reads: "China says" no "Bitcoin," Yes" blockchain technology." In the latest ranking of blockchain patent holders, almost half of the top 100 international companies are of Chinese origin [11].

Even more interesting is the question: what is the future for the financial sector after the mass introduction of blockchain and smart contracts? There is reason to believe that it is waiting for the technological revolution.

Futurists are predicting that cryptocurrency appeared to remain [12]. Thomas Frey, was invited to the Federal reserve system of the United States in September 2017 for consultation. According to his forecast, cryptocurrencies will crowd out about 25% of national currencies by 2030 [12]. The reason for this growth is that they can perform the functions of a legal tender more effectively from a technological point of view.

The potential of cryptocurrency is high not only because billions of real dollars have already been invested in them. Many think that blockchain technology underlying cryptocurrencies can be as revolutionary as the Internet. However, the future of the crypto market will be determined to a certain extent by the policy of monetary authorities. Regulators are still struggling with how to define the cryptocurrency, which is partly why there are still big holes in surveillance.

VI. CONCLUSION

The power of the potential of cryptocurrencies is determined by the peculiarities of their technological base and its dual-use. Its essence is in digital format and automated distributed registry systems. This line of development is fully consistent with the strategy focused on the digitalization of the economy.

The policy for the development of the digital economy is defined in the Address Of the President of the Russian Federation to the Federal Assembly (December 1, 2016): "...it is necessary to launch a large-scale system program for the development of the economy of the new technological generation, the so-called digital economy." After that, the following documents were adopted: the Strategy for the development of the information society in the Russian Federation for 2017-2030, approved by presidential decree of 09.05.17 №203 [13]; the program "Digital economy in the Russian Federation", approved by the order of the Government of the Russian Federation of 28.07.17 №1632-p [14].

Blockchain technology makes it almost impossible to falsify transaction records. The information recorded in the blocks is available for all interested parties and protected by

cryptographic means of the hash chain. To authenticate transactions, one has to use a pair of keys: private and public.

This mechanism of support and registration of transactions allows you to exclude intermediaries and save on the payment of their services.

The blockchain technology reliably registers any transactions with the assets, creates a record of the substantial parameters of a transaction and provides the reliability and transparency of transactions, eliminating the risk of tampering, i.e. unauthorized changes in the records and the distributed registry.

Blockchain technology is used in smart contracts. It is designed in such a way as to ensure the possibility of legally significant actions without human participation. A smart contract can be defined as a contract created on the blockchain platform, made on the basis of an electronic algorithm implemented by the built-in program, which takes into account the conditions determined by the Contracting parties. Usually a smart contract involves the use of cryptocurrency as a means of transferring value. The most notable aspect of a smart contract is that it creates a mechanism for automated control of its execution.

Smart contract automation makes up both an advantages and a disadvantages. It excludes the main subjective risk factors and violations of the terms of the contract. However, the smart contract does not allow forming of complex contracts, including consideration of the good faith, reasonable steps, reasonable timeframes, cooperation obligations, procedures, changes in contract, etc. Therefore, the conditions of the agreements are not fully can be programmed, that is why the scope of smart contracts is limited.

The use of smart contracts in economic circulation so far generates problems of a legal nature. Nevertheless, there are a lot of areas of its application, and this makes smart contract a serious tool of the future digital economy.

REFERENCES

- [1] Cryptocurrency prices [Electronic source]. – Access mode: <https://bitinfocharts.com/ru/markets/> (retrieved 04.03.18)
- [2] All Cryptocurrencies [Electronic source]. – Access mode: <https://coinmarketcap.com/all/views/all/> (retrieved 04.03.18)
- [3] Money Supply M2 [Electronic source]. – Access mode: <https://tradingeconomics.com/country-list/money-supply-m2> (retrieved 04.03.18)
- [4] <https://mir24.tv/news/16274422> (retrieved 04.03.18)
- [5] Cryptocurrency [Electronic source]. – Access mode: <http://wikipediaorg/wiki/Cryptocurrency> (retrieved 04.03.18)
- [6] China's State Media & Largest Newspaper Lauds Blockchain Technology [Electronic source]. – Access mode: <https://www.ccn.com/blockchain-technology-lauded-in-chinese-state-media/> (retrieved 04.03.18)
- [7] Federal Law (projection) «On Digital Assets» https://www.minfin.ru/ru/document/?id_4=121810
- [8] Principal directions of development of financial technologies for the period 2018-2020. – Moscow, Central Bank of Russian Federation, 2018
- [9] Voronkov N.S. International Turnover of Quasymonetarian Units: issues of legal regulation, Legal Concept. 2017. Vol. 16. No. 3, p. 128-136
- [10] Teslya P.N. Government Monetary and financial Policy / P.N.Teslya, I.V.Plotnikova. - Moscow: NIC INFRA-M, 2015.
- [11] "China says "no" to Bitcoin, "yes" to blockchain technology" <http://en.people.cn/n3/2018/0209/c90000-9425881.html> (retrieved 04.03.18)
- [12] Cryptocurrency Will Replace National Currencies By 2030, According to This Futurist <http://time.com/money/5178814/the-future-of-cryptocurrency/> (retrieved 22.04.18)
- [13] Ukaz Prezidenta RF ot 09.05.2017 №203 «O Strategii razvitiya informatsionnogo obshchestva v Rossiyskoy Federatsii na 2017 – 2030 gody» // «Sobraniye zakonodatel'stva RF», 15.05.2017, №20, st. 2901
- [14] Rasporuyazheniye Pravitel'stva RF ot 28.07.2017 №1632-r «Ob utverzhdenii programmy «Tsifrovaya ekonomika Rossiyskoy Federatsii» // «Sobraniye zakonodatel'stva RF», 07. 08. 2017, №32, st. 5138.



Bibigul A. Amanzholova, Doctor of Science in Economics, Head of Department of Audit, Accounting and Finance, Novosibirsk State Technical University, author of 100 scientific publications, including 10 monographs, 2 certificates for registration of software products. Research interests: accounting, reporting, audit and internal control in the management of economic entities.
E-mail: amanzholova@corp.nstu.ru



Pavel N. Teslya, associate Professor, candidate of economic Sciences, associate Professor of Department of Audit, Accounting and Finance, Novosibirsk State Technical University, author of 50 scientific publications, including 4 monographs. Research interests: banking, financial management, financial modeling, experimental economics.
E-mail: p.teslya@corp.nstu.ru

Innovation Strategies as a Basis for the Development of Household Care Markets in Russia

Valeria G. Badmaeva, Galina P. Litvintseva
Novosibirsk State Technical University, Novosibirsk, Russia

Abstract – The paper examines the state of the current market for household care goods in Russia and the dynamics of its development over recent years. Estimated data on its concentration are also given. The characteristic of the current market situation is presented and a forecast for its mid-term development is made. Strategies of the leading producers of household care goods are analyzed.

Index Terms – Household care market, foreign and domestic manufacturers, market concentration, detergents, environment, and company's strategy.

I. INTRODUCTION

CURRENTLY the chemical industry is a leading sector of the economy. It manufactures not only mineral fertilizers, polymers, plastic articles, paints, varnishes and lacquers but also household care goods. With new technologies being developed and the range of goods being expanded, practically any consumer can afford buying household care goods. Product lines offered by manufacturers are extremely wide beginning from low-price to superior goods made from ecologically clean and organic components.

The following segments referred to as “the household care market” are studied in the paper [2]:

1. washing substances (e.g. detergents or agents with a high chlorine content);
2. cleaning substances (e.g. water softeners for washing, glass cleaners, pipe and sink cleaners, toilet bowl cleaners, carpet cleaners, and all-purpose cleaning substances);
3. dishwashing detergents;
4. insecticide repellents.

All the above segments in total produce 100% of the household care goods on the market. The washing substances segment is the largest one. In 2016, its share amounted to 41%. Dishwashing detergents covered 9% of the market, household cleaners and air fresheners had 8.2% and 8% respectively. The share of the rest categories was 34% (Fig. 1) [4].

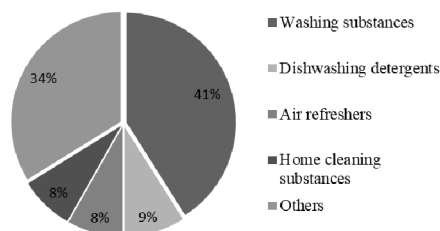


Fig. 1. Structure of the household care market in Russia in 2017 (%).

II. PROBLEM DEFINITION

Consumption of household chemical goods remains stable irrespective of the situation in the economy. The leading manufacturer of washing substances in Russia has long been the Procter & Gamble Company (USA). It once launched such brands as Myth, Tide and Ariel. Next goes the Henkel Company (Germany) with its brand Persil. The ReclittBenckise Company (Great Britain) with its Dosia washing powders is also quite popular in Russia. Among Russian companies in this segment the best results are shown by the NefisCosmetics Company, OAO (Kazan). Such Russian companies as Nevskaya Cosmetics, ZAO and the Aist Company (St. Petersburg) stand only a few position down. Let us consider shares of the main players on the household care market presented in Table I [4].

TABLE I
SHARES OF THE MAJOR MANUFACTURERS ON THE
HOUSEHOLD CARE MARKET IN 2010-2017

| Manufacturer | 2010 | 2015 | 2016 | 2017 |
|--------------------|------|-------|-------|------|
| Procter&Gamble | 0,33 | 0,282 | 0,38 | 0,44 |
| Henkel | 0,2 | 0,163 | 0,288 | 0,26 |
| ReckittBenckiser | 0,08 | 0,08 | 0,11 | 0,14 |
| NefisCosmetics | 0,09 | 0,08 | 0,072 | 0,08 |
| Aist | 0,03 | 0,025 | 0,02 | 0,02 |
| Nevskaya Cosmetica | 0,05 | 0,04 | 0,03 | 0,02 |
| Unilever | 0,03 | 0,03 | 0,03 | 0,02 |
| Other companies | 0,19 | 0,3 | 0,07 | 0,02 |

Table I shows that a high degree of prevalence of foreign manufacturers (about 85% in 2017) on the household care market in Russia is observed.

III. EXPERIMENTAL RESULTS

The authors have calculated the market concentration index based on three, four and five largest companies as well as the Herfindahl-Hirschman index (Tab. II)

TABLE II
CONCENTRATION INDICES FOR THREE, FOUR AND FIVE
COMPANIES, THE HERFINDAHL-HIRSCHMAN INDEX

| Index | 2010 | 2015 | 2016 | 2017 |
|--|------|------|------|------|
| Concentration index for three companies, % | 61 | 52 | 77 | 84 |
| Concentration index for four companies, % | 70 | 60 | 84 | 92 |

| | | | | |
|---|------|------|------|------|
| Concentration index for five companies, % | 73 | 63 | 86 | 94 |
| the Herfindahl-Hirschman index | 1833 | 2020 | 2517 | 2888 |

The analysis of the concentration indices and the Herfindahl-Hirschman index showed that the concentration on the market had changed over 6 years. In 2010, the market was moderately concentrated, namely the concentration index for 4 companies amounted to 0.7 while the Herfindahl-Hirschman index was 1833. These indices correspond to the quasi-monopoly market. In 2015, the market situation did not considerably change and the market had an average degree of concentration of 0.605 for 4 companies and the Herfindahl-Hirschman index was 2020.18. In 2016, the concentration for 4 companies increased up to 0.848 and the Herfindahl-Hirschman index was equal to 2517.3. Such indicators are characteristic of high concentration markets and of the oligopoly market. In 2017, the concentration index increased still more to 0.84 and the Herfindahl-Hirschman index was equal to 2888, which indicates that the market is approaching its monopoly.

Let us consider the dynamics of retail sales of household care goods in the period from 2010 to 2017 and estimated values for the period from 2018 to 2020 shown in Fig. 2 [7].

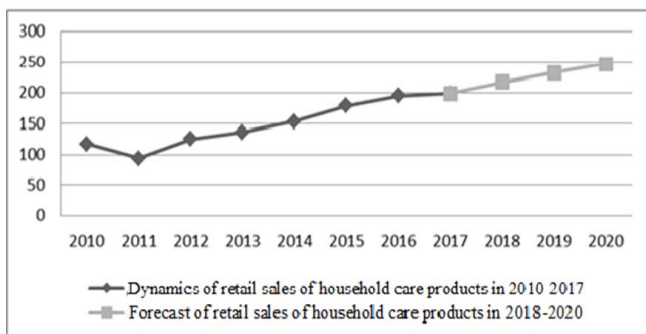


Fig. 2. Dynamics of retail sales of household care goods in 2010-2017 and the forecast for 2018-2020 (bln rubles in comparable prices).

In 2017, the volume of retail sales amounted to 198.7 bln rubles, which is 4% more than in 2016. Notice that growth rates were different in largest product line groups. Thus, as compared to the previous year the volume of sales increased in every of the major segments as follows: washing substances - by 12%, cleaning substances - by 3%, dishwashing detergents by 10% and insecticide repellents by 2%.

According to the estimated values in the period from 2018 to 2020 retail sale dynamics is expected to be positive: in 2018 sales will grow by 9%, in 2019 –by 16.5% and in 2020 by 24% compared to 2017.

Volumes of household care goods consumption grow every year, which is promoted by the wide product line, its continuous updating due to the introduction of new products as well as to a strong advertising support of their products arranged by manufacturers. In spite of a strong growth the level of consumption of household care goods in Russia is still not only lower than in Europe but it is also lower than the level recommended by the Russian sanitary standards by 1.5 times [7].

It is this fact that gives grounds to expect further sustainable growth of household care goods consumption in the nearest 3 years.

As a rule, innovation products come to Russia from foreign markets where manufacturers experiment with packaging and formulations. Their main purpose is to create a product which could be efficient and save consumers' time.

At present a trend of ecological and safe washing and cleaning substances seems to be weakly expressed on the Russian market. This is caused by a lack of attention of Russian manufacturers and consumers to environmental problems in contrast to foreign manufacturers.

Thus, the Henkel Company (Germany) is aimed at doubling the volumes of its business in parallel with decreasing the influence on the environment and increasing a positive social effect.

One of the priorities of the Company's strategy is its concern and focus on the environment. By 2020 it plans [8]:

- 1) to halve the level of greenhouse gases emission;
- 2) to reduce the volume of water consumed when using home care products by 50%;
- 3) to reduce the volume of waste products as result of the product utilization by half.

The Company's strategy includes 6 priority trends which reflect the key tasks of the sustainable development of the Company. Three trends reflect its tasks to create greater value for customers, clients, personnel, share holders and the public, namely, social development as well as efficiency, safety and health [8]. This conforms to the tasks of forming modern human capital in Russia [9]. The other three trends concern the tasks of reducing the influence on the environment: energy and climate, resources and waste products, water and waste waters.

For a long time growth and consumption of resources have inseparably been linked. Population growth and improving living standards have always meant an increase in the consumption of the Planet's resources.

This trend will continue as the world population is expected to be 9bln people by 2050. The consumption of resources will accelerate in the nearest decades because such natural resources as fossil fuels and water are consumed much quicker than the Planet can replenish them.

In the future such tendencies will become a real challenge to people. At the same time they offer great opportunities and innovations and the principle of achieving more having poorer resources will become the key factors of sustainable development.

Innovations and the principle "do more using less" will become the basis for sustainable development which does not suggest reducing the quality of life of people. The Henkel Company has divided its priority tasks into two trends –"more value" and "less influence on the environment".

By 2020, the Henkel Company plans to reduce the volume of carbon dioxide (CO₂) and waste emissions and the volume of water consumption per ton of the manufactured products by 30% (as compared to 2010). In addition, the

Company tends to improve the labor safety indicators by 40% and to increase sale volumes by 22% (Tab. III) [8].

TABLE III
SUSTAINABLE DEVELOPMENT OBJECTIVES FOR 2020
RESULTS OF 2017

| Indicators | Achieved 2017 | Objectives for 2020 |
|---|---------------|---------------------|
| Sale indicators growth | +5% | +22% |
| Labor safety enhancement | +17% | +40% |
| Reduction in energy consumption and CO ₂ emissions | -24% | -30% |
| Reduction in waste volumes | -32% | -30% |
| Reduction in water consumption | -24% | -30% |
| General efficiency | +43% | +75% |

IV. DISCUSSION OF RESULTS

The achievement of these objectives will result in general enhancement of efficiency by 75% by 2020 (as compared to 2010). The Company plans to become a leader in sales on the household care market. Let us make estimated values of shares of the main players on the household care market for the period of 2018-2020. (Fig. 3) [7].

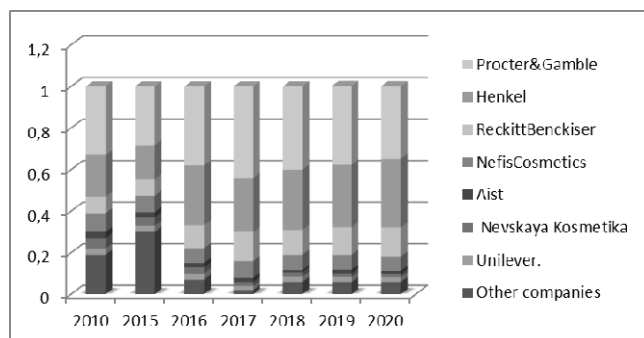


Fig. 3. Shares of the main sellers on the household care market in 2010-2017 and estimated values for 2018-2020 (%).

According to estimated values the Henkel Company will hold 33% of the household care market while the Procter & Gamble Company will hold the leading position, with its share being 35%.

The Company has achieved the objectives planned for 2010-2016 by improving the relationship between the value created by the Company and the influence on the environment by 38%. By 2017 this figure had raised to 43%. To achieve a long-term objective the Company should improve its results in these fields and it may become a leader on the household care market by 2020.

V. CONCLUSION

Thus, household care products are not only an important segment of the chemical industry (whose elements relate to an innovation economy [10]) but also affect the life quality of the population. The analysis of the household care market concentration has shown that it tends to monopolization. The Henkel Company and the Procter&Gamble Company are the

major manufacturers. By 2020, the German Company Henkel plans not only to enhance its positions of a leader on the Russian market but also to implement its innovation strategy intended to reduce a negative effect on the environment on the territory of Russia.

REFERENCES

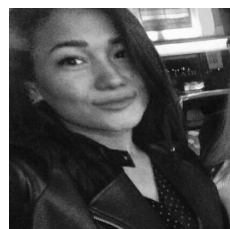
- [1] GOST P. 51696-2000 Household Care Products. General Engineering Requirements: <http://docs.cntd.ru/document/gost-r-51696-2000> (дата обращения: 21.03.2018). (in Russian)
- [2] The Economics of the Chemical Industry; textbook / I.A. Cadchikov. V.E.Somov, V.A. Balukov edited by I.A. Sadchikov. Spb Khimizdat, 2007, 446 p. (in Russian)
- [3] Knyazeva I.V. Antitrust Policy in Russia: Tutorial / I.V.Knyazeva-Moscow. – Moscow: Omega-L, 2011. – 512p. (in Russian)
- [4] Russian Industry // Federal State Statistics Service http://www.gks.ru/wps/wcm/connect/rosstat_main/rosstat/ru/statistics/publications/catalog/doc_1139918730234 (reference date: 20.03.2018).
- [5] The Statistics Portal: <https://www.statista.com/statistics/258123/distribution-of-rundd-expenditures-of-henkel-worldwide-by-sector/> (reference date: 21.03.2018).
- [6] Federal Law on “Protection of Competition” of 26.07.2006 No. 135-ФЗ (as amended and supplemented) (in Russian) http://www.consultant.ru/document/cons_doc_LAW_61763/ (reference date: 25.03.2018). (in Russian)
- [7] Euromonitor International; Russian Market for Household Care: Market Overview.: <http://www.portal.euromonitor.com> (reference date: 12.04.2018).
- [8] Henkel [<https://www.henkel.com/sustainability/strategy>] (reference date: 12.04.2018).
- [9] Litvintseva G.P., Badmaeva V.G. Evaluation of Human Capital Development in regions of the Siberian Federal District // State and municipal management.. SRAPA Bulletin. – 2017. – No. 3. – pp. 112–117. (in Russian)
- [10] Litvintseva G. P. Trends in high-technologic industries development in Russia / G. P. Litvintseva, N. A. Gakhova // 13th International Scientific-Technical Conference on Actual Problems of Electronics Instrument Engineering Proceedings (APEIE - 2016). Novosibirsk, October 3-6, 2016. In 12 Volumes / Novosibirsk State Technical University, Siberian State Research Institute of Metrology. Vol. 1, part 3. Selected Papers in English. – Novosibirsk: NSTU, 2016. – P. 256–262.



Litvintseva Galina Pavlovna, professor, D. Sc. (Econ.); head of the economic theory and applied economics department, Novosibirsk State Technical University (Russia, Novosibirsk).

Her research interests are currently focused on institutional economics and regional economics as well as the problems of inequality. She is the author of over 160 scientific and methodological publications.

E-mail: litvintseva-g@mail.ru



Badmaeva Valeria Gennadievna, a Master's degree program student at the department of economic theory and applied economics, Novosibirsk State Technical University (Russia, Novosibirsk). Her research interests include industrial development and regional economics. She has published 10 scientific papers.

E-mail: lera.badmaeva@mail.ru

On the Impact of Lending Rates on Structural Changes in the Russian Economy

Alexei A. Balabin

Institute of Economics and Industrial Engineering, the Siberian Branch of the RAS, Novosibirsk, Russia
Novosibirsk State Technical University, Novosibirsk, Russia

Abstract – To make structural changes leading to an innovative type of economic development is one of the greatest challenges faced by the Russian economy. The national banking system is expected to aid this transition. Focused on the dynamics of Russian Central Bank interest rate (key rate) and interbank lending rate (RUONIA), their impact on the loans' distribution by type of economic activity and on the share of processing industries in the banks' loan portfolio is analyzed for the period of 2007-2016. Based on correlation analysis the time lag between the movement of credit rates and changes in the structure of the Russian banks' credit portfolio was found. The lag is not less than one year. The impact of Russian Central Bank key rate is weaker than the impact of the market rate RUONIA. Also, the increase in lending rates leads to a subsequent increase in the share of processing and extractive industries, while reducing the share of trade. Conversely, the decrease in the lending rates leads (approximately at intervals of one year) to a decrease in the share of processing and extractive industries in favor of trade. The statistical study indicates that lending to the extractive and processing industries changes unidirectionally when changing the lending rates. And in parallel, the share of trade in the banks' loan portfolio is changing in the opposite direction. Thus, the hypothesis of the positive impact of lower lending rates on the progressive changes in the sectoral structure of the Russian economy is not statistically confirmed. The possible reasons of this statistical phenomenon are given.

Index Terms – Sectoral lending structure, refinancing rate, credit lag, correlation.

I. INTRODUCTION

MAKING the structural changes, reindustrialization, replacement of primitive extraction by more complete and effective processing of natural resources or by production (where appropriate) of competitive products are among the main challenges facing the Russian economy. To a certain extent, the national banking system can also contribute to this by supporting the transition of companies to modern technologies with monetary resources and by crediting those productions which determine scientific and technical progress in the country. Along with this, the specific ways of banks' enhancing participation in the industrial restructuring are seen by researchers in different ways. In general, Neoclassical theory states that in the long run the quantitative changes in money supply will not produce any effect on the level of real national product, interest rate, investment, employment. Accordingly, the changes in money supply, including changes produced through the management of interest rates, should not lead to

changes in the sectoral lending structure. In the classical example of M. Friedman, the founder of monetarism theory, "throwing money over the city from a helicopter" ultimately leads only to an increase in prices. Regarding the current situation in the financial sector of the world economy, this theoretical position is discussed in more detail in [1]. However, we must bear in mind that the theory postulates the neutrality of money only for a sufficiently long period of time, and with the perfectly uniform distribution of money among the economic agents. In real situation, the "helicopter throwing money" in different parts of the city can do it not in the same way and do it at different times. It is also possible that the helicopter pilot is acting for specific purposes, starting or stopping to scatter money in certain areas of the city.

There are numerous studies devoted to the impact of interest rates on general economic growth and to mechanisms and to extent of this impact (a review of different approaches can be found in [2]). Sometimes an author simply postulates the negative impact of higher interest rates on capital demand in medium term, which subsequently causes the decrease in output [3]. Another article [4] justify the negative impact of increasing rates on economic growth by the fact that the reduction of deposit interest rates causes the capital flow to the stock market and, ultimately, an increase in investment and output. According McKinnon [5] and Shaw [6], the increasing interest rate leads to a positive impact of the real interest rate on economic growth, both in the short and medium term. Bertola and Caballero [7] demonstrate that increasing interest rate negatively affects output due to an increase in borrowing costs on the one hand and has a positive impact on output due to an increase in investments in the current period on the other hand. In the open economy model [2] the increasing interest rate stimulates the imports of intermediate goods and leads to an increase in output, but at the same time it reduces the competitiveness of domestic goods and, accordingly, reduces their consumption and output within the country.

The diversity of theoretical hypotheses and related findings in itself suggests that the impact of interest rate on economic growth is not unequivocal. Statistics shows a negative correlation between the dynamics of interest rates and economic growth in some countries. On the other hand, there are cases of a combination of high interest rates and rapid economic growth, including in Brazil (2000-2008), Turkey (2002-2007), India (1980-2013) and Chile (1984-2013) [8]. As for the impact of interest rates on the sectoral lending

structure, the studies in this area are still at the stage of empirical analysis [9].

II. PROBLEM DEFINITION

There is the point of view, expressed by numbers of Russian scientists, businessmen and public figures, that the reduction of lending rates and, in particular, of Russian Central Bank key rate, will contribute to the accelerated growth of processing industries, making financial resources more accessible to them [10-11]. We suggest discussing this issue in more detail. Let's try to find out whether the level of lending rates affects the sectoral lending priorities. Will the lower lending rates make the manufacturing sector more attractive for lending? Or this will encourage increased lending to mining, trade and agriculture?

III. THEORY

A. Research Methodology

The correlation analysis was used to analyze the statistical relationship between lending rates and the shares of extractive and processing industries in the loan portfolio. The simplest measure of the relationship between the two random numbers is Pearson correlation coefficient, which allows to establish the presence and tightness of the relationship between the two random variables A and B . As is known, Pearson correlation coefficient can take a value in the range $[-1; +1]$. If this coefficient is $+1$, the random variables A and B are in direct linear relationship. If the correlation coefficient is -1 , the random variables A and B are in inverse linear relationship. If the correlation coefficient is zero, it means that there is no relationship between two random variables except for some special cases. Intermediate values of correlation coefficient mean more or less significant relationship between the investigated random variables. In assessing the closeness of the connection, the well-known Cheddok scale has been used. If the correlation coefficient takes a value in the interval $[0; 0.3)$, correlation is characterized as very weak, in the interval $[0.3; 0.5)$ – as weak, in the interval $[0.5; 0.7)$ – as average, in the interval $[0.7; 0.9)$ – as high, in the interval $[0.9; 1]$ – as very high.

In this case, the share of an activity (sector of industry) i in the loan portfolio of Russian banks acts as a random variable A_i , and the refinancing rate acts as a random value B . Value B may be any averaged market rate of interbank lending or Russian Central Bank key rate using as the refinancing rate.

B. Data for Studies

Russian Central Bank's information about monthly debt in credit portfolios of commercial banks on different types of activity was used as the data source for the period of 01.07.2007 - 01.01.2017. Based on given statistics, for each activity, i.e. group of industries, their monthly shares in the loan portfolio were calculated for the specified period. These data series were compared with the data of the Russian

Central Bank key rate and the data of the rates on the interbank lending market RUONIA [14].

The key rate is the auction-based minimal interest rate on repo operations performed in rubles for a period of 7 days by the Russian Central Bank from one side and commercial banks from the other side. The key rate appeared only in September 2013, but the "repo" operations themselves are used by the Russian Central Bank as a financial tool since 2003. So, this made it possible to supplement the time series of key rates with earlier dates, starting from 01.07.2007.

The rate of interbank lending RUONIA (Ruble OverNight Index Average) is the average rate of overnight loans (deposits) in ruble for standard borrowers from among three ten Russian banks having minimal credit risk. RUONIA is calculated by the Russian Central Bank since January 2010 only on the base of actual market transactions within given group of banks. RUONIA is not used for refinancing operations regulation, i.e. it is indicative in nature. There is available statistics to calculate the correlation coefficients between the industry shares and RUONIA rates just for the period of 01.01.2010 - 01.01.2017.

The terms used in the article to denote individual activities correspond to those used in Statistical Classification of Economic Activities in the European Community, Rev. 2 (2008). The terms "extraction of minerals" and "extractive industries" refer to the same as "mining" in the official classification. The designations "processing industries" and "manufacturing" are also used as equivalent.

IV. EXPERIMENTAL RESULTS

A. The Calculation of Time Lag between Changes in Lending Rates and Changes in Loan Portfolio's Industry Share

Before measuring the impact of a change in the key rate on an industry share, it is necessary to assess how long after a change in the rate this impact may occur. Indeed, a change in the key rate cannot take effect immediately.

Even assuming that commercial banks instantly rebuild their interest rate policy after the revision in the key rate, its influence will primarily touch just newly issued loans. It is also need take into account that:

- terms of lending usually are not less than several months (short-term forms of lending, as "overdraft" etc. are not considered here);

- revision of rates under existing contracts is difficult (and often impractical or impossible).

This means that the sectoral lending structure will change over time as existing loans, including credit lines, are repaid or renegotiated and new loans are issued at new interest rates.

To determine the time lag, a number of preliminary calculations of the correlation coefficient were made. In each calculation the chronological shift in a time series of industry shares in the loan portfolio was made relative to a time series of key rate values for a number of months.

For the processing industry, if we assume that the key rate is instantaneous, i.e. lag is zero, the correlation coefficient is

of +0,60. Assuming that the lag is six months, the correlation coefficient is + 0,63. For one-year lag the correlation coefficient is equal + 0,73. If the lag is one and half years, the correlation coefficient becomes significantly lower (+0,54).

The same calculation was made for the type of activity "mining". Under the assumption of a zero lag, the correlation coefficient is + 0,63. Six-months lag means the correlation coefficient + 0,72, one-year lag means + 0,74 and for one-and-half year lag the correlation coefficient equals + 0,70.

Thus, for both extractive and processing sectors, the closest statistical relationship between the share in the loan portfolio and the key rate is observed under the assumption of one-year lag.

With regard to the impact of change in the key rate on economic growth, in particular on GDP growth, the lag appears to be even longer. Thus, according to US statistics, the full impact of the new monetary policy on the amount of output may be seen only after 16-20 months after its initial change [15, p. 678].

The similar calculation of correlation between the shares of processing industries in the loan portfolio and the interbank lending rate RUONIA was made.

The correlation coefficients between RUONIA and the share of processing industries were: +0,65 (assuming no lag), +0,74 (assuming six-months lag), +0,87 (assuming one-year lag) and +0,48 (assuming one-and-half year lag).

The correlation coefficients between RUONIA and the share of extractive industry in the loan portfolio were: + 0,65 (assuming no lag), +0,73 (assuming six-months lag), +0,84 (assuming one-year lag) and + 0,78 (assuming one-and-half year lag).

For both processing and extractive sectors, a closer statistical relationship with RUONIA is observed under the assumption of one-year lag. It should also be noted that in all cases the dependence on the market rate RUONIA is stronger than the dependence on the Russian Central Bank key rate. Indeed, the surveys of banks shows that not all of them consider the Russian Central Bank key rate as a real operating lever of management [16].

B. The Calculation of Dependence of Loan Portfolio's Industry Share on Lending Rate RUONIA

Table I shows the estimated correlation coefficients between RUONIA and the shares of various activities in the total loan portfolio. Correlation coefficients are calculated on the basis of Bank of Russia data series [12-13] and the data series of the rates RUONIA [14]. The lag between changes in RUONIA and changes in shares was taken equal to one year.

TABLE I
CORRELATION BETWEEN SHARES OF ACTIVITY IN THE LOAN PORTFOLIO AND INTERBANK LENDING RATE RUONIA

| Type of activity | Size of correlation |
|--|---------------------|
| Mining | 0,84 |
| Manufacturing | 0,87 |
| Electricity, gas and water distribution | 0,15 |
| Agriculture, hunting, forestry | -0,85 |
| Construction | -0,85 |
| Transport and communications | -0,40 |
| Trade, repair of motor transport and household goods | -0,91 |
| Real estate (operations and rentals) | 0,78 |
| Other activities and final clearances | 0,33 |

From table I it is seen that for some industries like electricity, gas and water production and distribution, transport and communication, other activities, the correlation coefficients take a more close-to-zero value. This means insignificant statistical relationship between changes in these shares and lending rates. It looks quite expectable because these activities are characterized by stable markets and relative stability of cash flows. Lending to these industries, regardless of fluctuations in interest rates, leads to quite definite and predictable results. They are convenient borrowers for any bank.

The second group includes mining, manufacturing and real estate. In relation to changes of their shares, the correlation coefficients take positive values close to +1. It means that with the increase in lending rates, the share of the relevant industry in the loan portfolio is growing.

Finally, the third group consists of trade, construction and agriculture. For these types of activities, the correlation coefficients are close to -1. For this group, the growth of RUONIA leads to a decrease in their shares.

Thus, statistical relations seem paradoxical to those supporters of monetary easing, who expect the attractiveness of processing and extractive industries to grow with decreasing market interest rates. On the contrary, this decline in market interest rates, with a lag of about one year, entails a decrease in the loan portfolio's shares of extracting and processing industries in favor of trade, construction and agriculture.

Manufacturing lobbyists often point to the apparent preference that credit institutions give to their counterparts in extractive industries. However, from a statistical point of view, the shares of both activities move almost synchronously in one direction with the change in lending rates (correlation coefficient for mining +0,84, and for manufacturing +0,87). On the contrary, it is time for the merchants to take offense because their share in the loan portfolio reduces systematically (Fig.1). The graphs were constructed on the basis of the author's calculations using statistical data of the Bank of Russia [12].

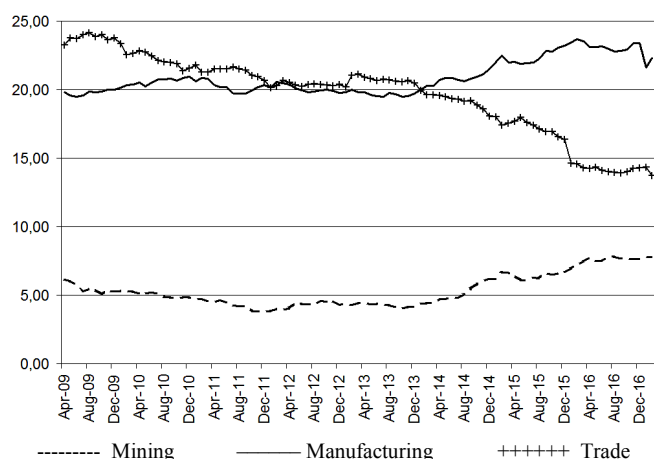


Fig.1. The share of some activities in the total loan portfolio, % .

V. DISCUSSION OF RESULTS

As revealed by the calculations, the increase in lending rates leads to a subsequent increase in the share of processing and extractive sectors, while reducing the share of trade. Conversely, the decrease in the lending rates leads (approximately at intervals of one year) to a decrease in the share of processing industry. Thus, the hypothesis of the positive impact of lower lending rates on the progressive change in the sectoral structure of the Russian economy is not statistically confirmed.

Several interpretation can be made about the statistical phenomenon found.

The first interpretation is that there were too large sectoral aggregates used in the calculation. Indeed, each of the activities includes a plurality of sectors, more or less traditional and, if I may say so, with a different degree of credit worthiness and/or relevance in a particular economic situation. Changing in lending rates causes a different reaction of the shares of these sectors in the loan portfolio. Mixing in one unit, the changes in the shares demonstrates mixed and contradictory statistical picture.

The second interpretation consists in uneven change of credit investments of banks in various activities. Liquidity reduction in the banking system manifests itself an increase in the current level of RUONIA or, to a lesser extent, the key rate. In addition to the need to maintain liquidity, this liquidity reduction causes, on the one hand, the need to limit the issuance of new loans and, on the other hand, the rapid release of funds from the loan portfolio, as far as possible. In practice, the first "victims" of this process can be trading enterprises due to their fast turnovers and relatively short terms of lending. Constructing enterprises also can be the first "victims" due to reduction/termination of lending projects. On the other hand, lending to processing industries is a much longer process, often designed for years of payback, and much more inertial. To withdraw from a lending deal with industrial enterprise ahead of schedule is very difficult task.

Conversely, the decline in lending rates opens the opportunity for a quick increase of loan portfolio by sectors, primarily trade, having the ability to quickly build

momentum and also by sectors having the temporarily "frozen" objects of unfinished construction. Thus, it may be about unequal elasticity of certain components of the loan portfolio, i.e. about relative stability in the volume of lending to certain types of activity on the one hand and, on the other hand, about large variability (depending on the availability of liquidity) in the volume of lending to other activities. Unequal elasticity ultimately leads, with some lag, to a noticeable change in the shares of highly elastic parts of the loan portfolio.

Finally, the third interpretation is the need to consider the impact of foreign policy and non-economic factors on the lending structure. First, there are anti-Russian restrictive measures in the financial sector of the economy established by a number of developed countries. These measures do not allow borrowing abroad by Russian enterprises and banks or restrain such borrowing. It is not a secret that most of these measures focus primarily on Russian major mining, energy and steel companies. For the period 2014-2017 total foreign debt on non-financial sector loans decreased from \$268.4 billion to \$181.5 billion [17]. And it forced given companies to address to domestic credit resources as far as it was possible. Secondly, a number of measures related to the accelerated development of manufacturing facilities, primarily in the military-industrial complex, have been taken in recent years [18]. Both reasons should lead to an increase in the share of extractive and processing sectors in the loan portfolio of domestic banks, regardless of changes in lending rates.

VI. CONCLUSION

The analysis of the time-lag between changes in lending rates and shares of the extractive and processing sectors in the bank's loan portfolio showed that such changes occur approximately one year after the change in rates.

The impact of the key interest rate of the Russian Central Bank is less significant than the change in the RUONIA market interbank lending rate.

A cautious conclusion can be drawn about an ambiguous effect on the share of different activities in the bank's loan portfolio causing by the change in lending rates. As it is shown by statistical study, the lending to the extractive and processing industries changes unidirectionally when lending rates change. At the same time, the share of trade in the banks' loan portfolio changes in the opposite direction.

A few hypotheses explaining the statistical dependence found are made and require further confirmation and justification. The excessive aggregation of statistical information, different speed of response of the parts of the loan portfolio, non-economic impact on lending to extracting and processing industries are among the main reasons.

REFERENCES

- [1] Growth strategy. The medium-term program of development of Russian economy till 2025 [Electronic resource] // Stolypin Institute of economic growth. Available at: <http://stolypinsky.club/strategiya-rosta-3> (accessed: 04.03.2018). (in Russian).

- [2] The transition to a moderately easy monetary policy. Appendix to the Medium-term program of social and economic development of Russia until 2025. "Growth Strategy" [Electronic resource] // Stolypin Institute of economic growth. Available at: <http://stolypinsky.club/wp-content/uploads/2017/03/6-Kolichestvennoe-smyagchenie-28.02.17-1-1.pdf> (accessed: 04.03.18). (in Russian).
- [3] Balabin A. A. The Easing Monetary Policy and Changing the Structure of the Russian Economy // ECO, 2017. №1. pp. 135-148. (in Russian).
- [4] Wickens M. Macroeconomic Theory: A Dynamic General Equilibrium Approach – Princeton University Press, 2012, 606 p.
- [5] Tobin J. Money and economic growth // Econometrica: Journal of the Econometric Society, 1965. Vol. 33. № 4. pp. 671-684.
- [6] Tobin J. A general equilibrium approach to monetary theory // Journal of Money, Credit and Banking, 1969. Vol. 1. No. 1. pp. 15-29.
- [7] McKinnon R.I. Money and capital in economic development. – Washington, D.C.: Brookings Institution Press, 2010, 184 p.
- [8] Shaw E.S. Financial deepening in economic development. – New York: Oxford University Press, 1973, 260 p.
- [9] Bertola G., Caballero R.J. Irreversibility and aggregate investment // The Review of Economic Studies. 1994. Vol. 61. № 2. pp. 223-246.
- [10] Drobyshevsky S. M., Trunin P. V., Bogachkova A. V., Sinelnikov-Murylev E. V. Effect of interest rates on economic growth // Money and credit, 2016. №9. pp. 29-40 (in Russian).
- [11] Balabin A. A. On the impact of interest rates on lending to raw and manufacturing industries // Russian Journal of Entrepreneurship, 2017. Vol. 18. № 11. pp. 1671-1680 (in Russian).
- [12] Granted Funds and Borrowings [Electronic resource] // Official site of the Central Bank of Russian Federation. Available at: <http://www.cbr.ru/statistics/?PrId=sors> (accessed: 10.08.2017).
- [13] REPO auctions minimum interest rates [Electronic resource] // Official site of the Central Bank of Russian Federation. Available at: http://www.cbr.ru/hd_base/default.aspx?prtid=repo_proc&pid=idkp_br&sid=ITM_15890 (accessed: 10.08.2017).
- [14] RUONIA: Archive [Electronic resource] // National Finance Association. Available at: <http://www.ruonia.ru/archive.html> (accessed: 10.08.2017).
- [15] Abel A., Bernanke B., Macroeconomics. – M.: Peter, 2010. – 768 p. (in Russian). See also: Abel A., Bernanke B. Macroeconomics. – 5th ed. – Pearson Education, 2005, 630 p.
- [16] Kuvshinova O. The Gods are not really listening to the bankers // Vedomosti. – 2016. – July 04 (in Russian).
- [17] External Sector Statistics [Electronic resource] // Official site of the Central Bank of Russian Federation. Available at: https://www.cbr.ru/eng/statistics/default.aspx?Prtid=svs&ch=itm_52908#CheckedItem (accessed: 10.03.2018).
- [18] Prokopenko A., Nicholas A., M. Papchenkov. Debt echo of the old scheme // Vedomosti. – 2016. – Sept. 21 (in Russian).



Balabin Alexei, associate professor of the Management department (Novosibirsk State Technical University), Senior Research Fellow (Institute of Economics and Industrial Engineering, Siberian Branch of the RAS). Ph.D. in Economics (candidate of economics sciences). The science interests and competence field are macroeconomics, government monetary policy, banking, corporate management. He is the author of 50 scientific works. Email: balabin-a-a@mail.ru

Modern Technologies in Assessing the Quality of Medical Services in the Digital Society of Russia

Tatiana G. Butova¹, Elena P. Danilina², Elizaveta A. Kanyukova³

¹Siberian Federal University, Krasnoyarsk, Russia

²Krasnoyarsk State Medical University, named after Professor V.F. Voyno-Yasenetsky, Krasnoyarsk, Russia

³N.S. Karpovich clinical hospital of ambulance, Krasnoyarsk, Russia

Abstract—The development of the information society of Russia has led to the use of modern Internet technologies in everyday life, which required the reaction of public authorities to the emerging trends and the adoption of a strategy for the development of the information society in the Russian Federation, proclaiming the use of new information technologies, such as social networks and information platforms in the implementation of projects to improve the availability and quality of medical services and goods as a strategic goal. The implementation of the identified strategies in the development of digital society in Russia, as well as an objective tendency of increase of consumer requirements to the medical services quality in the public and private health sectors, the growth of consumer dissatisfaction with quality of services require the implementation of telemedicine in addition to new technologies in all activities of medical organizations, particularly in the quality control system of medical services. The marked increase in the activity of consumers of medical services in social networks and information portals is not currently used in the practice of assessing the quality of medical services. This requires responsible researches to identify the factors hindering the introduction of new technologies in the practice of assessing the quality of medical services adapted to current trends in the activity of consumers of medical services in social networks, as well as to determine the directions of work to activate patients and medical personnel in the field of evaluation and participation in decision-making, and the formulation of the goal-setting of Internet companies to develop software products for the automation of collection and processing of consumer feedback in social networks in the medical market.

Index Terms—Information and communication technologies, telemedicine, social networks as new technologies of assessment, medical services quality.

I. INTRODUCTION

THE HISTORY of the introduction of information and communication technologies in the healthcare service of developed countries is associated with the emergence of a fundamentally new direction in the organization and provision of medical care to the population – the telemedicine. Telemedicine technologies have become widespread in the USA, Canada and Australia since the middle of the last century. In Russia, the telemedicine as a new information and communication technology began to be used only in the early 20th century. Currently, the Internet is only partially integrated into the healthcare. Meanwhile, the development of modern technologies, which led to the formation of a digital society, requires new technologies in the activities of medical

organizations to implement the strategic goal of improving the quality of life of the population. The new strategy for the development of the information society in Russia for 2017-2030 confirmed the stable trend of the Russian society – information systems, social networks have become a part of people's everyday life, which requires the introduction of modern adaptive technologies in healthcare.

II. PROBLEM DEFINITION

Telemedicine technologies solving numerous tactical problems have high efficiency, which was proved by numerous studies and implemented projects in a number of developed countries [1]. However, the integration of the telemedicine into the healthcare system is not comprehensive and systemic. The aim of the telemedicine is to provide the qualitative medical care to any person, regardless of his location and social status, which implements to a greater extent only one of the strategic objectives of the modernization of healthcare in Russia – ensuring the availability of quality medical care to the population. Meanwhile, another strategic goal – to provide the population with high-quality medical services in the implementation of the concept of quality of life cannot be solved by the telemedicine because of its functional characteristics.

Most researchers believe that the effectiveness of medical services, as a complex of medical care (which is a set of technological procedures) and services organizing medical care for consumers, is not achieved due to the fact of telemedicine technologies usage but interpretation of the results relevant to the purposes of medical care [5], as well as their application to the process of medical service delivery.

It should be noticed that the widespread use of information and communication technologies in the Russian healthcare has not led to an increase of patient satisfaction with the quality of medical services. The problem of satisfaction of the population continues to be acute alongside with the observed growth of high-tech medicine. This has led to the existing imbalance in ensuring the population's satisfaction with the quality of medical care and the introduction of new medical care technologies requires scientific understanding.

Another challenge is improvement of the practice of assessing the quality of health services through responsible research to make appropriate decisions, which requires the use of new technologies relevant to current trends in consumer behavior in the digital society.

III. THEORY

In a digital society, consumer behavior is changing which means the increase of the requirements to the quality of goods while reducing their cost. The trend is also evident in the medical services sector. Expectations for the high quality of medical services of private medical organizations have always been noted as high, and nowadays consumers have increased their requirements to the quality of medical services of budgetary organizations, which is proved by the low assessment of the quality of medical care by patients [2]. The given dissatisfaction leads to a decrease of demand for the services of medical organizations, the growth of patients practicing the self-treatment and going to the "gray" segment of the medical business- to psychics and healers- and even to religious sects. This creates serious social problems and reduces the quality of life of the population, which led to increased attention not only from the state but also public organizations to the problems of assessing the quality of health services.

The Russian society is now characterized by a new stable trend meaning that information systems and social networks are becoming a part of people's everyday life. This trend is explained by the growing effect of affiliation which is the desire to be in the society of other people, the need for communication, the implementation of emotional contacts, the manifestations of friendship and love [4]. The trend of popularity growth of social networks in discussing and solving everyday and vital problems is noted in the new strategy of the information society in Russia for 2017-2030 [8]. This process naturally stimulates the introduction of new technologies in the activities of business and public organizations, in particular in the field of medical services.

Most researchers consider the introduction of new technologies in healthcare in a broad and holistic aspect for their expansion beyond the technocratic process of medical care delivery and transformation into a complex process of medical service being the subject of assessing the quality of medical services. This explains the need to introduce new technologies not only in the process of providing medical care, but also in other medical activities, in particular, in the process of assessing the quality of medical services [2, 9].

The importance of the feedback for providing the management of medical organizations with information on quality problems, actualizes the introduction of new technologies for assessing the quality of medical services, ensuring the activity of patients in this process. One of the fundamental principles in the implementation of the task of improving the quality of health care is the active participation, awareness and literacy of patients in the practice of assessing their own health [5,3], as well as in the evaluation process.

IV. EXPERIMENTAL RESULTS

The implementation of the research objectives required the use of methods of desk and field researches. For comparative analysis of the results of the assessment of the quality of medical services of public and private organizations, the information portals and network sources of the Internet were

analyzed. In addition to the analysis of the publications, the surveys of specialists and doctors of several private medical organizations of Krasnoyarsk were conducted in the form of in-depth interviewing to identify methodological problems of assessing the quality of medical services. An initiative study in the form of a survey of patients in N.S. Karpovich ambulance hospital in Krasnoyarsk and a participant observation were conducted by a cross-functional team of teachers and students of Siberian Federal University and the Krasnoyarsk State Medical University named after Professor V. F. Voynov-Yasenetsky.

The study conducted by the authors revealed a contradiction between the strengthening of patients' requirements to the quality of medical services and their low activity in assessing the services' quality. This situation creates a problem of feedback with medical organizations, reducing the effectiveness of the developed solutions for improvement of medical services quality. In 2016, the Krasnoyarsk regional branch of the All-Russia People's Front has carried out a check of practical work on the assessment of quality of services in the ambulance hospital in Krasnoyarsk clinical hospital of ambulance and revealed that only 14 of more than 1,000 patients in the hospital answered the questions of electronic questionnaire [10]. Low activity of patients in assessing the quality of medical services confirmed the study conducted by the authors in 2018 in the clinical hospital of ambulance: in spite of a complete survey of patients the share of respondents to the questions was only 23.6%.

At the same time, the analysis of open sources showed the increase of the activity of medical services consumers both of private and budgetary organizations in social networks and information portals, which are used as technological platforms for the dialogue between consumers who assess the quality, discuss the causes of poor quality, give their opinions for medical organizations [6,7]. Within the research the authors analyzed the customers' opinions about the quality of medical services in Krasnoyarsk. Two medical organizations (a budgetary institution and a private one) were randomly selected on the service of people's reviews of companies in Krasnoyarsk -Flamp in each of the 7 districts of the city.

The analysis of the opinions showed that paid medical services have a higher rating (4 points out of 5) than the services of budget organizations, the average assessment of which was 2.5 points. 63% of patients of public organizations are dissatisfied with the long wait for the doctor, unfriendly attitude of the staff or doubt in their competence. Dissatisfied reviews of private organizations were expressed by 45% of patients, among which the largest number (73%) of negative reviews were caused by medical care – the impossibility to get through, conflicting information about the work of doctors on the site. Among the positive reviews in both types of organizations, consumers note the competence of the staff, a friendly attitude, the presence of feedback.

The analysis of 90 reviews about 16 budget medical organizations on the portal "4geo" also showed the prevalence of negative reviews – 71 %. Particular dissatisfaction was caused by violation of sanitary norms, indifference and rudeness of medical staff, incompetence of some doctors, condi-

tions of stay of patients in hospitals and polyclinics, long waiting for the doctor, material and technical conditions. An in-depth interview with consumers of medical services - users of social networks showed that activity in social networks is based on the possibility to express their point of view freely, the lack of restrictions in the answers formulated by the developers in the questionnaires, an opportunity to share their opinion.

V. DISCUSSION OF RESULTS

The current change in consumer behavior in the field of medical services, consisting in the growth of consumer expectations of obtaining of better services, is largely demonstrated in the sphere of medical care creating comfortable conditions for consumers to use medical care in the process of its providing by improvement of communication of the organization staff with patients and the material environment. This factor led to increase of the attention to the process of consumers' assessment of the quality of the entire range of medical services, not only medical care, and reducing satisfaction in the evaluation of medical care. The expectations of high quality medical care related to the issues of preservation, restoration and maintenance of health have always been high. However, due to the complexity of patient care assessment as a result of subjective perception and the high role of patients in ensuring their health, the changes to negative feedback in the assessment of medical care quality are not detected.

The revealed contradiction between the strengthening of patients' requirements to the quality of medical services and low activity in the process of quality assessment is explained by the problems of organizing of an independent assessment of the quality of medical services in the company or on the portal of the Ministry of health, the imperfection of the methodological support of the evaluation process, the lack of activity of personnel of medical organizations in the process of quality assessment and the lack of their desire to monitor the feedback continuously, preferring instead to solve the problems of complaints and claims "in the fire order" within the administrative procedures.

Meanwhile, the revealed trend of growth in the activity of consumers of medical services in social networks confirms the objective trend of the introduction of social networks as new information and communication technologies in people's lives, explained by the freedom to express their own points of view and discuss the assessment of the quality of medical services in their region. This allows us to conclude that it is in social networks that the principle of independent evaluation of the quality of medical services is implemented.

The need for introduction of new technologies in the quality assessment process has led to the fact that the organizations of the Ministry of health of Russia and a number of private companies began using information technologies in the activities of medical organizations implementing the task of improving the quality of medical services using the development of Internet questionnaires and the introduction of CRM (Customer Relationship Management)- technologies.

VI. CONCLUSION

The contradiction between the growth of consumer requirements for the quality of medical services and the decrease in activity in the practice of evaluation requires the improvement of the methods of quality assessment and the introduction of new technologies, which previously seemed unacceptable for the evaluation of the quality of medical services.

The use of social networks and information portals by consumers of medical services to assess their quality showed that an alternative tool for assessing the quality of medical services based on social networks has been formed in Russia. Consumers of health services have been more advanced in the use of new technologies, living in a new digital society than health workers. Implementation of monitoring of social networks in the process of assessing the quality of medical services and the use of the results for the development of measures to improve the quality of service in budgetary medical organizations is constrained by the lack of recommendations of the Ministry of health. This requires the necessity of development of the legislative and regulatory framework and the formation of new methodological recommendations for the assessment of the quality of medical services.

Management of private companies, free from industry-regulated guidelines, does not always realize the need for constant feedback and the introduction of social networks as a technology for assessing the quality of medical services, limited more often by CRM-systems, due to the lack of competencies of employees and the possibility of hiring specialists in this field.

The introduction of new technologies in the process of medical care will help to solve the problem of the imbalance between high-tech medical services and mass medical services available to all consumers.

New technologies will solve two problems that have not revealed their relevance for a long time. Firstly, they will change the behavior of consumers, increasing the activity and involvement in the process of assessing the quality of medical services, and secondly, they will change the attitude of the medical staff, in particular, doctors, increasing their activity and involvement in the evaluation process.

To solve the problem of the implementation of social network monitoring in the process of assessing the quality of medical services is possible through the introduction of software that will automate the process of collecting and processing patient feedback on the quality of medical services, storage of information and their implementation in the process of developing solutions to improve the quality of medical.

REFERENCES

- [1] Baranov A.A., Bishneva E.A., Namazova-Baranova L.S. *Telemeditsina - perspektivyitrudnostyeprednovymetapomrazvitiya* // *Pediatricheskayafarmakologiya*. 2013. - 10 (3). - S. 6-11.
- [2] Butova T.G., Yakovleva E.Y., Danilina E.P., Zhilnikova M.Y. *Otsenkakachestvameditsinskihuslug v usloviyahizmeneniyaotraslevogonormativnopravovogoregulirovaniya* // *Servis plus*. T. 12. 2018. № 1. S. 88-89. DOI: 10.22412/1993-7768-12-1-9

- [3] Engelbrecht R. Telemedicine – A way to better care. DeutschesForschungszentrum für Umwelt und Gesundheit Koch-Metschnikow-Forum, SektionHealth. - Berlin, Helmholtz ZentrumMünchen,2009.URL:
<http://zdrav.tomsk.ru/export/sites/ru.tomsk.zdrav/ofic/konferenz/engelbrecht.pdf>.
- [4] Karpenko L.A., Petrovskiy A.V., yaroshevskiy M.G. Kratkii psihologicheski slovar. Rostov-na-Donu: "Fenix". 1998.
- [5] Lyamina N.P., Kotelnikova E.V., Nalivaeva A.V., Karpova E.S. Informatsionno-kommunikatsionnye v meditsine: sovremennyyetrendy[Electronnyiresurs] // Sovremennyyeproblemy nauki i obrazovaniya. - 2016.- №3. URL: <http://science-education.ru/ru/article/view?id=24473> (data obrascheniya: 15.04.2018)
- [6] Informatsionnyi portal Flamp [Electronnyiresurs] //URL: <https://krasnoyarsk.flamp.ru/metarubric/kliniki?page=2> (data obrascheniya: 24.04.2018).
- [7] Informatsionnyi portal 4geo [Electronnyiresurs] //URL:<http://krasnoyarsk.4geo.ru/catalog/search/больница/responses> (data obrascheniya: 09.10.2017).
- [8] O Strategii rasvitiya informatsionnogo obshchestva v Rossiiskoi Federatsii na 2017-2030 gg: Ukaz Prezidenta RF ot 09.05.2017 N 203 [Electronic resource] // URL: <http://www.garant.ru/hotlaw/federal/1110145/> (data obrascheniya 24.03.2018).
- [9] Spiridonov A.V., Shulaev A.V. Estimating method of patient satisfaction of hospital services in the modernization of health care [Electronic resource] // Modern problems of science and education. 2013. No4. URL: <http://www.science-education.ru/ru/article/view?id=10001> (accessed: 12.09.2017).
- [10] Eksperty ONF otsenili kachestvo uslug v Krasnoyarskoi bolnitse skoroi meditsinskoj pomoschi [Electronnyiresurs] // URL: <http://onf.ru/2016/08/24/eksperty-onf-ocenili-kachestvo-uslug-v-krasnoyarskoy-bolnice-skoroy-medicinskoy-pomoshchi/> (data obrascheniya: 15.04.2018).



Personal information

Elena P. Danilina,
Apt. 245, 42 .Kapylova St.,
Krasnoyarsk, 660001, Russia.
E-mail: danjuly@rambler.ru
Tel.: +79069124104

Education

Graduated from Krasnoyarsk state medical Institute, majoring in surgery.
1991-thesis defense for the degree of Candidate of Sciences (Medicine). Subject of the study "Central and peripheral hemodynamics of patients with peritonitis treated with active detoxification" Krasnoyarsk state medical institute.

Work

1995 - Associate Professor,
Krasnoyarsk State Medical University named after Professor Voyno-Yasenetsky,



Personal information

Elizaveta A. Kanyukova,
Apt. 245, 42 .Kapylova St.,
Krasnoyarsk, 660001, Russia.
E-mail: danjuly@rambler.ru
Tel.: +79676067316

Education

2014 - graduated from Krasnoyarsk state medical university, majoring in surgery
2015-clinical internship at the Krasnoyarsk state medical university(surgery)

Work

2015 - Surgeon, N.S. Karpovich Clinical Hospital of Ambulance



Personal information

Tatiana G. Butova.,
56/9Novosibirskaya St.,
Krasnoyarsk, 660028, Russia,
E-mail: tgbutova@mail.ru
Tel: +79620832879

Education

Graduated: Krasnoyarsk State University-teacher of biology and chemistry
Leningrad Institute of Soviet trade-Economics of trade

1989 - defended the thesis for the degree of Candidate of Sciences (Economics). The theme of the research is "Planning of improvement of the organizational structure of wholesale trade management of consumer goods in the new economic conditions" Leningrad Institute of Soviet trade. Leningrad.

2005 defended the thesis for the degree of Doctor of Sciences (Economics). The theme of the study "Formation of strategies for the development of cultural organizations based on marketing technologies" RGUTiS Moscow

Work

2006 г. - Professor at the Department of Management, Siberian Federal University, Krasnoyarsk, Russia.

The Mechanism for Determining the Initial Conditions when Concluding Concession Agreements Based on the Balance of Interests of the Parties of Public-private Partnership

Sergey S. Chernov, Marina V. Rozhkova
Novosibirsk State Technical University, Novosibirsk, Russia

Abstract – The paper considers the mechanism for implementing infrastructure investment projects in the form of public-private partnership (PPPs). Particular attention is paid to the form of PPPs, such as concession agreements. The notion and types of PPPs, legislation in the sphere of PPPs, mechanisms for determining the concession fee are also considered here. Based on the determination of the balance of interests of the concessioner and the conessor, a methodology for determining the initial conditions of concession agreements was proposed for the implementation of competitive procedures for the implementation of investment projects in the form of PPPs. Approbation of the proposed methodology was carried out using the example of a boiler house reconstruction project

Index Terms – public-private partnership, concession agreement, investment project, efficiency, infrastructure, modernization, balance of interests.

I. INTRODUCTION

UNDER CURRENT conditions for the development of the Russian power industry, a number of problem areas are observed, among which the problem of outrunning aging of fixed assets (both moral and physical) is most marked in comparison with the rate of their renewal. In this context, the most acute problem is the deficit of investments required for the modernization of fixed assets in the energy sector, which in turn is due to the low commercial attractiveness of investment projects in the sector. In this regard, it becomes urgent to search for alternative tools that allow to attract investments to the industry and ensure their effectiveness. This kind of mechanism is a public-private partnership (hereinafter - PPPs), which unites the resources of business and the state for the implementation of socially significant infrastructure projects.

It should also be noted that the theoretical aspects of the economic content of PPPs in the scientific community have been given enough attention by such authors as Borshchevsky G.A., Kabashkin V.A., Mataev T.M., Mikheev V.A., Sivakova S.Yu., Varnavsky V.G., Pirogov N., Maksimov V., etc. Speaking about foreign research and publications on the issue of the State Emergency Service and its role in the implementation of infrastructure projects, it is worth paying attention to such work as "For the Good of the People : Using Public-Private Partnerships to Meet America's Essential

Needs », another work by Trefor P. Williams Associate Professor of Civil Engineering Rutgers University« Moving to Public-Private Partnerships: Learning from Experience around the World. "

Along with studying the aspects of PPPs and its role in the implementation of individual infrastructure projects, it is also important to study concession agreements, taking into account that in this form in Russia in more than 80% of cases PPPs is realized. The concession is one of the "forms of public-private partnership, which provides for a private investor to own and use state (or municipal) property for a certain period during which he must create and (or) reconstruct the received property and carry out an effective management of such property ". The concession agreement is the most common form of PPPs, which determines the urgency of assessing the effectiveness of its application

II. PROBLEM DEFINITION

To date, the role and importance of PPPs in implementing the mechanism of interaction between the state and private business is determined by the effectiveness and relevance of this type of interaction, which allows solving the most acute infrastructure problems and tasks.

It should be noted that there are many forms of implementing PPPs projects. According to [1, p.13], the most common forms of PPPs are concession agreements, as well as public-private partnership / municipal-private partnership agreements (hereinafter - PPPA / MPPA). In addition, in the Russian practice, such forms as long-term contracts with the investment component (IC), life-cycle contracts (LCC), leases with investment obligations are applied.

The objectives of the study are to reveal the nature and specific features of the application of the concession agreement in the context of PPPs and to consider its role in the implementation of infrastructure energy projects.

III. THEORY

Public-private partnership is a special form of long-term interaction between the state and business with a view to implementing socially significant investment projects aimed at developing transport, energy and social infrastructure [2, p. 79]

Public-private partnership is an effective tool for attracting investments into the public services sector. Of the variety of forms of PPPs in Russia, only two are actively used: concession agreements (CA) and public-private partnership / municipal-private partnership agreements (hereinafter - PPPA / MPPA).

The task of the study is to analyze and evaluate the CA within the framework of the industry aspect. In this regard, it is worth noting that the industry-specific feature of the CA has been reflected in the legislation: in the Federal Law "On the CA" the rules, governing agreements for heat and water supply and sanitation facilities are made in a separate chapter (Chapter 4).

IV. EXPERIMENTAL RESULTS

The possibility of modernization of the communal infrastructure through the conclusion of the CA is due to the following:

- Socio-economic importance of the industry.
- The current state of the Russian power system, characterized by a number of serious problems, namely:

1. High degree of moral and physical depreciation of fixed assets. Data on the age structure of fixed assets are presented in Figures 1 and 2.

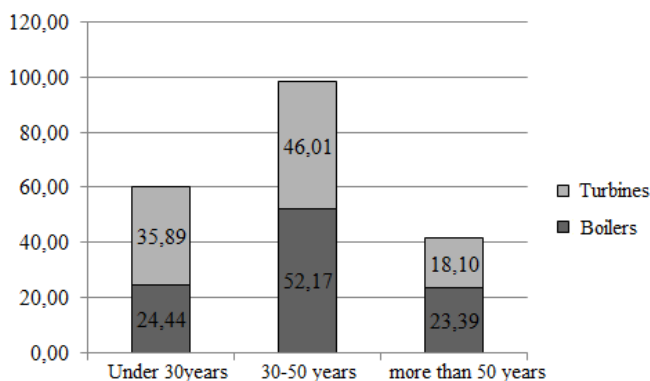


Fig. 1. Service life of heat power equipment, %.

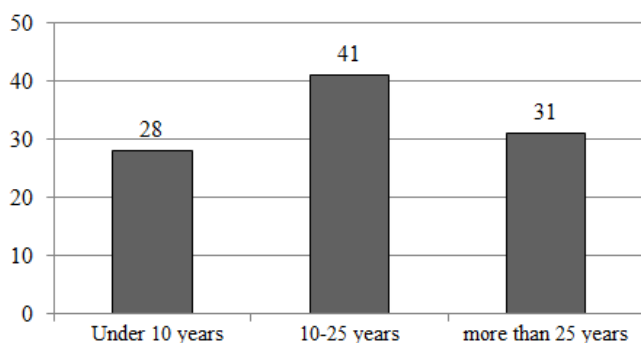


Fig. 2. Service life of heat networks, %.

According to the data presented in the graphs, only 36% of turbines and 25% of boilers have a service life of less than 30 years, and 31% of heat networks have already developed a standard service life. The following tendencies are observed [5, 6, 7]:

- The rate of replacement of heat and power equipment and heat networks is below the rate of their obsolescence, i.e. the rate of renovation of fixed assets is insufficient;

- Replacement of equipment and repair work are of a local nature, while affecting only the most emergency areas;

- Lack of innovative approach: obsolete equipment, as a rule, is replaced by a similar new one that does not meet modern standards, which aggravates the problem of obsolescence of fixed productive assets.

All this leads to such negative consequences as high level of heat losses during transport of the coolant. According to various estimates, their value reaches 40%, which in money terms is from 300 to 600 billion rubles a year [8] and the increase in accidents.

2. Low energy and economic efficiency of the industry, manifested in the following:

- specific indicators of fuel consumption and energy intensity of domestic production exceed those of developed countries by 2-3 times [6];

- non-optimal structure of generating capacities.

3. Lack of an effective long-term planning system.

4. Lack of qualified technical specialists.

5. Significant amount of cross-financing between [7]: electric and thermal energy; steam and heat; industry and population; subjects of the Russian Federation.

6. High level of accumulated non-payments (about 180 billion rubles only for large-scale generation) [7].

7. Excessive bureaucratic work in the sphere of feasibility demonstration and approval of tariffs.

8. Lack of investments in the industry due to the following reasons.

All this speaks about the need to modernize the industry, which is possible only with the joint participation of business and the state, including and within the framework of the CA. In this regard, it should be noted that the choice of a private partner for concluding the CA is based on competitive procedures provided for by law. According to the Federal Law "On the CA", consideration and evaluation of bids are carried out in the following sequence:

1. Preliminary selection of the participants of the competition (art. 29, Ch. 3). At this stage, it is checked:

- Compliance of the applicant, as well as the participant's application itself with the requirements established by the tender documentation; completeness and reliability of the materials and documents provided by the applicant;

- Compliance of the applicant with the requirements for the concessioner (Clause 2, Part 1, Chapter 1);

- Absence of decisions on liquidation, bankruptcy or opening of bankruptcy proceedings in respect of the applicant.

Based on the audit results, a decision is made to admit the applicant to participate in the tender or to refuse to admit the applicant to participate in the competition.

2. Consideration of bids for compliance with the requirements of the tender documentation (Part 1, Article 32, Chapter 3).

3. Evaluation of bids in accordance with the criteria of the competition (ch. 5-7, art.32 ch.3), for each of which are established: the initial condition in the form of a numerical

value, as well as its decrease / increase; coefficient of significance.

The criteria established by the tender documentation also include the size of the concession fee and the amount of funding from the concedent.

Possible forms of the concession fee, established by the Russian legislation, are presented in Figure 3 (Article 7 of Chapter 1 of the Federal Law "On the CA").

As can be seen in Figure 3, the concession fee may take a variety of forms: to be both a one-off and to be paid on a regular basis; expressed in absolute or relative terms; to have a property form. However, the methodology for calculating the value of the concession fee is not available, it is determined by the terms of the agreement.

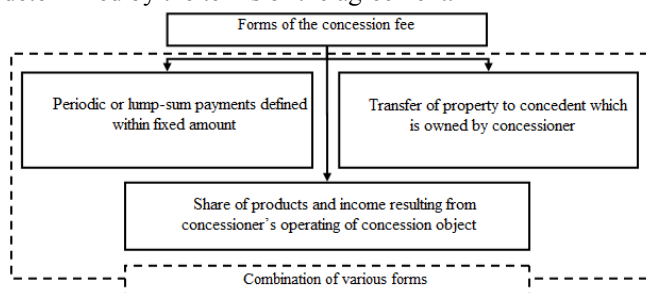


Fig. 3 Forms of the concession fee.

As noted earlier, there is no single methodology for calculating the amount of concession payments in Russian legislative practice, only their possible forms are fixed, and the rest is determined solely by the terms of the agreement. In this case, often, the value of the concession fee is one of the conditions of the concession tender, i.e. its level must satisfy the interests of both sides, because for a public partner this is a guaranteed budget revenue, and for a private partner - a significant cost that reduces the commercial attractiveness of the project.

Considering the existing methods for determining the size of the concession fee, it is worth turning to foreign practice. For example, the Law of Ukraine "On Concessions" (hereinafter referred to as the Law on Concessions) was adopted in 1999, and the methodology for calculating concession payments was approved by the Cabinet of Ministers in 2000. At the same time, it should be noted that the Russian Federal Law "On CA" and the Law of Ukraine "On concessions" are generally similar in the main issues: the content of the agreement, the object and subject composition, the rights and obligations of the parties, in this connection, we can talk about their comparability.

According to the methodology [10], the annual concession fee is determined as follows (formula 1):

$$C_{PL} = 0,07 * R_F * \frac{F_{GAL}}{F_{NG}}, \quad (1)$$

- where R_F is the market value of the concession object (determined by an independent assessment);

- F_{GAL} and F_{NG} are the average return on assets in the relevant area and the national economy as a whole (calculated by the Ministry of Economic Development on a quarterly basis on the basis of the statistical bulletin "The main performance indicators of enterprises in certain

economic sectors of Ukraine of different forms of ownership").

In addition, the following conditions are legislated:

- The C_{PL} limit is 10% of the market value of objects transferred to concession, i.e. $C_{PL} \leq 0.1 * R_F$ (item [10]);

- The amount of the concession fee may be revised as a result of the commissioning / decommissioning of a part of the agreement's objects belonging to a public partner (Article 12 of the Law of Ukraine << on Concessions>>);

- The amount of the concession fee for the relevant period is reduced by the amount of depreciation charges for the concession object for the same period, which is determined by the concession or its authorized body (Clause 3, Article 20 of the Law of Ukraine "On Concessions").

- Thus, the basis for the calculation is the market value of the concession object, which creates a number of problems, both for the state and for the private investor [11, p.335-336; 12, p.18]:

- In case of concluding a concession for the operation and / or reconstruction of an object, the market value of state assets transferred to the concessioner under the agreement at the time of its conclusion is the basis for determining the value of the concession fee

- If the concession agreement is for the purpose of creating new infrastructure objects, then the future value of the constructed object, determined by expert means, is the basis for calculation.

This approach allows us to take into account not only the industry specific features, but also the interests of both parties:

- The concessor receives a guaranteed inflow of funds to the budget due to a fixed component of the concession fee;

- The concessioner is interested in investing, even in low-profit industry (concession payment rates are directly dependent on the index of profitability of the sphere of economic activity, and inversely proportional to the size of private investment).

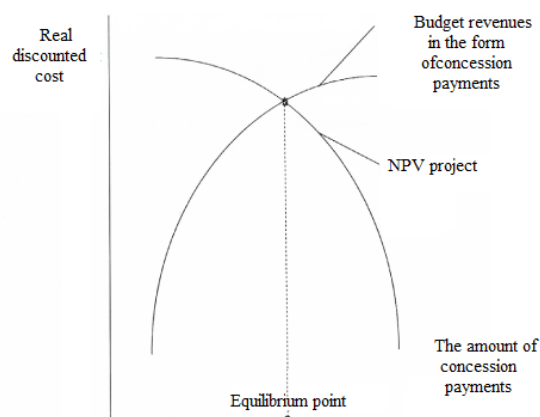


Fig. 4. Graphical interpretation of the "equilibrium point".

It can be seen from the figure that this approach helps to harmonize the economic interests of public and private partners, as it assesses the economic effectiveness of the project from the position of each of the parties of the agreement.

The author believes that such approach can be used at the stage of competitive selection in order to determine the optimal values of such essential parameters of the agreement as the value of the concession fee and tariffs for products, the amount of budgetary financing, on the basis of which applicants will be selected.

The disadvantage of the proposed methodology is that it does not take into account the amount of budgetary financing and budget revenues in the form of tax revenues. Thus, there is a need to develop a methodology for determining the optimal level of concessionary payments. This parameter has a significant impact on the project's cash flows and, as a consequence, its effectiveness for both the public and the private partner.

- The model proposed by the author of the study is based on the mechanism and specific nature of selection of bids for the purpose of concluding a concession agreement, which is carried out in several stages on the basis of a number of established qualitative and quantitative criteria. Such criteria include the size of the concession fee and the amount of budgetary financing for the project, for which initial numerical values should be established. At the same time, there is obviously a clash of state and private interests, each of which tends to satisfy its own interests, which include:

- The effectiveness of the project implementation for a public partner is determined by the indicator of budget efficiency, which is directly dependent on the value of concession payments: the higher their level, the greater the income to the budget.

- Opportunities for financing capital expenditures are limited both by the state and by the private investor, since they require a one-time diversion of significant amounts of turnover. Therefore, each partner seeks to minimize the share of its participation in the total amount of financing.

Budget efficiency and NPV of the concessioner are in inverse relationship, therefore the maximum effect for each partner will be achieved at the "point of equilibrium" [11, p.336], which meets the basic principles of PPPs: the mutually beneficial nature of cooperation, partnerships, fair distribution of rights and duties of the parties, including the costs and revenues of the project. Achieving full equilibrium is not always possible, therefore, it is necessary to strive to ensure that the difference in project efficiency for private and public partners is minimal.

The model allows to determine the initial numerical values for such criteria of the competition as the share of budget financing and the amount of concession payments. The advantage of this model is the possibility of its modification due to changes in the mathematical models for calculating the NPV of the concessioner and the budgetary efficiency compiled at the initial stage. Depending on the purpose of the study, you can change the set of variables.

The practical implementation of this model is considered using the example of a boiler house reconstruction project.

Due to the emergency condition of the boiler room No. 60, a project was developed for its technical re-equipment, which allows not only to prepare it for the heating season 2014-2015, but also to significantly improve the efficiency of its operation by transferring to a more economical type of fuel (natural gas).

Let us consider the effectiveness of this project in the form of a concession agreement. To do this, we define the main parameters of the project:

1. Terms of implementation. Reconstruction of the boiler house is carried out with a view to preparing it for the heating season 2014-2015, therefore MUE "Energia" defined the following terms:

- February 2014 - opening of the competition;
- 15.03.2014 - the conclusion of the contract, the beginning of the production of equipment;
- August 15, 2014 - construction, installation and commissioning works;
- 15.09.2014 - start of the boiler house, start of production.

If we talk about the duration of the project itself, it is equal to the useful life of the main (boiler) equipment - 15 years.

2. Selected equipment. According to the Department of Energy, Housing and Communal Services (obtained as a result of thermal calculation), the maximum total heat load for heating and hot water is 34.75 MW, while the maximum load on hot water is 4.981 MW. As a result, it was decided to install 3 boilers of the Buderus type Logano S825L (Germany) with a heat output of 12.6 MW. At the same time, the total installed capacity of the boiler house will be 37.8 MW, providing a power reserve of 3.05 MW (or 8.8% of the maximum heat load), and in summer, the heat loads for hot water will be covered by 1 boiler.

3. Production program. From the data on settlements "Developing and productive supply of thermal energy boiler house №60 in 2013 by month, thousand Gcal." Author's research shows that the annual output of the boiler room of 77.65 Gcal, leave with the collectors - 76.93 thousand Gcal, and the useful supply of thermal energy - 66.17 thousand Gcal, losses in heat networks - 10.76 thousand Gcal (or 13.9% of the annual output). At the same time, the bulk of the heat load falls on the population, which explains the unevenness of the load schedule: the winter peak (from October to April) associated with the heating of living quarters; year failure (from May to September), when the heat energy is generated only for DHW.

4. Calculation of income and expenses for the project. The basis for the calculations are: production program, technical and economic indicators of the boiler house.

1. Based on calculations made by the author of such indicators as: calculation of income and some items of costs for the project (fragment); capital expenditures; accrual of depreciation for groups of equipment with the same SPI; other operating costs of the project. A number of conclusions can be drawn, in particular:

1. Sources of project financing. It is assumed that the project is implemented in the form of a concession agreement, then its participants are a concedent in the person of the Novosibirsk Region, i.e. subject of the Russian Federation, and the concessionaire is a potential private investor. Accordingly, the project is financed from the budget, as well as from the concessionaire's own funds.

2. Concession payments for the project. Since the amount and form of payments are determined by the terms of the agreement, then we assume the following: concession

payments are paid annually by the concessionaire in a fixed amount.

The main parameters of the project were defined above, however, to apply the model developed by the author, it is also necessary to establish the following:

1. The size of the discount rate.
2. Boundaries and the step change of the optimized parameters. Within the framework of the project under consideration, we set the following values:
 - the share of budget financing varies from 0 to 100%;
 - the amount of concession payments varies in the range from 0 to 15% of the total volume of capital expenditures for the project in increments of 1%.

Having determined all the initial parameters of the model, we proceed directly to the calculations. For convenience, we will break them into several stages.

First, we determine the values of NPV (k, b) and B (k, b) for different values of the share of concession payments from capital expenditures (k) and the share of budget financing (b) using formulas 2-3.

$$NPV(c, b) = \sum_{t=1}^n [(1-\gamma) * (O_t - I_t) + \gamma * c - c] * \frac{1}{(1+E)^t} - IC * (1-b), \quad (2)$$

$$B(c, b) = \sum_{t=1}^n [\gamma * (O_t - I_t) + c - \gamma * c] * \frac{1}{(1+E)^t} - IC * b, \quad (3)$$

The results of calculations are presented in Figures 5-6.

| | | The amount of concession payment | | | | | | | | | | | | | | | |
|------------------|---------|----------------------------------|--------|--------|--------|--------|--------|--------|--------|--------|--------|--------|--------|--------|--------|--------|--------|
| | | 0 | 1 | 2 | 3 | 4 | 5 | 6 | 7 | 8 | 9 | 10 | 11 | 12 | 13 | 14 | 15 |
| budget financing | NPV | K1 | K2 | K3 | K4 | K5 | K6 | K7 | K8 | K9 | K10 | K11 | K12 | K13 | K14 | K15 | K16 |
| | 0 B1 | 36.58 | 29.13 | 21.68 | 14.23 | 6.78 | -0.67 | -8.12 | -15.57 | -23.02 | -30.46 | -37.91 | -45.36 | -52.81 | -60.26 | -67.71 | -75.16 |
| | 5 B2 | 42.40 | 34.95 | 27.50 | 20.05 | 12.60 | 5.15 | -2.30 | -9.74 | -17.19 | -24.64 | -32.09 | -39.54 | -46.99 | -54.44 | -61.89 | -69.34 |
| | 10 B3 | 48.22 | 40.77 | 33.32 | 25.87 | 18.42 | 10.97 | 3.53 | -3.92 | -11.37 | -18.82 | -26.27 | -33.72 | -41.17 | -48.62 | -56.07 | -63.51 |
| | 15 B4 | 54.04 | 46.59 | 39.14 | 31.69 | 24.25 | 16.80 | 9.35 | 1.90 | -5.55 | -13.00 | -20.45 | -27.90 | -35.35 | -42.79 | -50.24 | -57.69 |
| | 20 B5 | 59.86 | 52.41 | 44.97 | 37.52 | 30.07 | 22.62 | 15.17 | 7.72 | 0.27 | -7.18 | -14.63 | -22.07 | -29.52 | -36.97 | -44.42 | -51.87 |
| | 25 B6 | 65.69 | 58.24 | 50.79 | 43.34 | 35.89 | 28.44 | 20.99 | 13.54 | 6.09 | -1.36 | -8.80 | -16.25 | -23.70 | -31.15 | -38.60 | -46.05 |
| | 30 B7 | 71.51 | 64.06 | 56.61 | 49.16 | 41.71 | 34.26 | 26.81 | 19.36 | 11.92 | 4.47 | -2.98 | -10.43 | -17.88 | -25.33 | -32.78 | -40.23 |
| | 35 B8 | 77.33 | 69.88 | 62.43 | 54.98 | 47.53 | 40.08 | 32.64 | 25.19 | 17.74 | 10.29 | 2.84 | -4.61 | -12.06 | -19.51 | -26.96 | -34.40 |
| | 40 B9 | 83.15 | 75.70 | 68.25 | 60.80 | 53.36 | 45.91 | 38.46 | 31.01 | 23.56 | 16.11 | 8.66 | 1.21 | -6.24 | -13.69 | -21.13 | -28.58 |
| | 45 B10 | 88.97 | 81.52 | 74.08 | 66.63 | 59.18 | 51.73 | 44.28 | 36.83 | 29.38 | 21.93 | 14.48 | 7.03 | -0.41 | -7.86 | -15.31 | -22.76 |
| | 50 B11 | 94.79 | 87.35 | 79.90 | 72.45 | 65.00 | 57.55 | 50.10 | 42.65 | 35.20 | 27.75 | 20.31 | 12.86 | 5.41 | -2.04 | -9.49 | -16.94 |
| | 55 B12 | 100.62 | 93.17 | 85.72 | 78.27 | 70.82 | 63.37 | 55.92 | 48.47 | 41.03 | 33.58 | 26.13 | 18.68 | 11.23 | 3.78 | -3.67 | -11.12 |
| | 60 B13 | 106.44 | 98.99 | 91.54 | 84.09 | 76.64 | 69.19 | 61.75 | 54.30 | 46.85 | 39.40 | 31.95 | 24.50 | 17.05 | 9.60 | 2.15 | -5.30 |
| | 65 B14 | 112.26 | 104.81 | 97.36 | 89.91 | 82.46 | 75.02 | 67.57 | 60.12 | 52.67 | 45.22 | 37.77 | 30.32 | 22.87 | 15.42 | 7.98 | 0.53 |
| | 70 B15 | 118.08 | 110.63 | 103.18 | 95.74 | 88.29 | 80.84 | 73.39 | 65.94 | 58.49 | 51.04 | 43.59 | 36.14 | 28.70 | 21.25 | 13.80 | 6.35 |
| | 75 B16 | 123.90 | 116.46 | 109.01 | 101.56 | 94.11 | 86.66 | 79.21 | 71.76 | 64.31 | 56.86 | 49.42 | 41.97 | 34.52 | 27.07 | 19.62 | 12.17 |
| | 80 B17 | 129.73 | 122.28 | 114.83 | 107.38 | 99.93 | 92.48 | 85.03 | 77.58 | 70.13 | 62.69 | 55.24 | 47.79 | 40.34 | 32.89 | 25.44 | 17.99 |
| | 85 B18 | 135.55 | 128.10 | 120.65 | 113.20 | 105.75 | 98.30 | 90.85 | 83.41 | 75.96 | 68.51 | 61.06 | 53.61 | 46.16 | 38.71 | 31.26 | 23.81 |
| | 90 B19 | 141.37 | 133.92 | 126.47 | 119.02 | 111.57 | 104.13 | 96.68 | 89.23 | 81.78 | 74.33 | 66.88 | 59.43 | 51.98 | 44.53 | 37.09 | 29.64 |
| | 95 B20 | 147.19 | 139.74 | 132.29 | 124.85 | 117.40 | 109.95 | 102.50 | 95.05 | 87.60 | 80.15 | 72.70 | 65.25 | 57.80 | 50.36 | 42.91 | 35.46 |
| | 100 B21 | 153.01 | 145.57 | 138.12 | 130.67 | 123.22 | 115.77 | 108.32 | 100.87 | 93.42 | 85.97 | 78.52 | 71.08 | 63.63 | 56.18 | 48.73 | 41.28 |

Fig. 5. NPV of the concessioner, million rubles.

| Budget effectiveness | | The amount of concession payment | | | | | | | | | | | | | | | |
|----------------------|---------|----------------------------------|--------|--------|--------|--------|--------|--------|--------|--------|--------|--------|--------|--------|--------|--------|--------|
| | | 0 | 1 | 2 | 3 | 4 | 5 | 6 | 7 | 8 | 9 | 10 | 11 | 12 | 13 | 14 | 15 |
| budget financing | 0 B1 | 27.52 | 34.97 | 42.42 | 49.87 | 57.32 | 64.77 | 72.21 | 79.66 | 87.11 | 94.56 | 102.01 | 109.46 | 116.91 | 124.36 | 131.81 | 139.26 |
| | 5 B2 | 21.70 | 29.15 | 36.60 | 44.05 | 51.50 | 58.94 | 66.39 | 73.84 | 81.29 | 88.74 | 96.19 | 103.64 | 111.09 | 118.54 | 125.98 | 133.43 |
| | 10 B3 | 15.88 | 23.33 | 30.78 | 38.22 | 45.67 | 53.12 | 60.57 | 68.02 | 75.47 | 82.92 | 90.37 | 97.82 | 105.26 | 112.71 | 120.16 | 127.61 |
| | 15 B4 | 10.06 | 17.50 | 24.95 | 32.40 | 39.85 | 47.30 | 54.75 | 62.20 | 69.65 | 77.10 | 84.55 | 91.99 | 99.44 | 106.89 | 114.34 | 121.79 |
| | 20 B5 | 4.23 | 11.68 | 19.13 | 26.58 | 34.03 | 41.48 | 48.93 | 56.38 | 63.83 | 71.27 | 78.72 | 86.17 | 93.62 | 101.07 | 108.52 | 115.97 |
| | 25 B6 | -1.59 | 5.86 | 13.31 | 20.76 | 28.21 | 35.66 | 43.11 | 50.55 | 58.00 | 65.45 | 72.90 | 80.35 | 87.80 | 95.25 | 102.70 | 110.15 |
| | 30 B7 | -7.41 | 0.04 | 7.49 | 14.94 | 22.39 | 29.83 | 37.28 | 44.73 | 52.18 | 59.63 | 67.08 | 74.53 | 81.98 | 89.43 | 96.87 | 104.32 |
| | 35 B8 | -13.23 | -5.78 | 1.67 | 9.11 | 16.56 | 24.01 | 31.46 | 38.91 | 46.36 | 53.81 | 61.26 | 68.71 | 76.16 | 83.61 | 91.05 | 98.50 |
| | 40 B9 | -19.05 | -11.60 | -4.16 | 3.29 | 10.74 | 18.19 | 25.64 | 33.09 | 40.54 | 47.99 | 55.44 | 62.88 | 70.33 | 77.78 | 85.23 | 92.68 |
| | 45 B10 | -24.88 | -17.43 | -9.98 | -2.53 | 4.92 | 12.37 | 19.82 | 27.27 | 34.72 | 42.16 | 49.61 | 57.06 | 64.51 | 71.96 | 79.41 | 86.86 |
| | 50 B11 | -30.70 | -23.25 | -15.80 | -8.35 | -0.90 | 6.55 | 14.00 | 21.44 | 28.89 | 36.34 | 43.79 | 51.24 | 58.69 | 66.14 | 73.59 | 81.04 |
| | 55 B12 | -36.52 | -29.07 | -21.62 | -14.17 | -6.72 | 0.72 | 8.17 | 15.62 | 23.07 | 30.52 | 37.97 | 45.42 | 52.87 | 60.32 | 67.77 | 75.21 |
| | 60 B13 | -42.34 | -34.89 | -27.44 | -19.99 | -12.55 | -5.10 | 2.35 | 9.80 | 17.25 | 24.70 | 32.15 | 39.60 | 47.05 | 54.49 | 61.94 | 69.39 |
| | 65 B14 | -48.16 | -40.71 | -33.27 | -25.82 | -18.37 | -10.92 | -3.47 | 3.98 | 11.43 | 18.88 | 26.33 | 33.77 | 41.22 | 48.67 | 56.12 | 63.57 |
| | 70 B15 | -53.99 | -46.54 | -39.09 | -31.64 | -24.19 | -16.74 | -9.29 | -1.84 | 5.61 | 13.05 | 20.50 | 27.95 | 35.40 | 42.85 | 50.30 | 57.75 |
| | 75 B16 | -59.81 | -52.36 | -44.91 | -37.46 | -30.01 | -22.56 | -15.11 | -7.66 | -0.22 | 7.23 | 14.68 | 22.13 | 29.58 | 37.03 | 44.48 | 51.93 |
| | 80 B17 | -65.63 | -58.18 | -50.73 | -43.28 | -35.83 | -28.38 | -20.94 | -13.49 | -6.04 | 1.41 | 8.86 | 16.31 | 23.76 | 31.21 | 38.66 | 46.10 |
| | 85 B18 | -71.45 | -64.00 | -56.55 | -49.10 | -41.65 | -34.21 | -26.76 | -19.31 | -11.86 | -4.41 | 3.04 | 10.49 | 17.94 | 25.38 | 32.83 | 40.28 |
| | 90 B19 | -77.27 | -69.82 | -62.37 | -54.93 | -47.48 | -40.03 | -32.58 | -25.13 | -17.68 | -10.23 | -2.78 | 4.67 | 12.11 | 19.56 | 27.01 | 34.46 |
| | 95 B20 | -83.09 | -75.63 | -68.20 | -60.75 | -53.30 | -45.85 | -38.40 | -30.95 | -23.50 | -16.05 | -8.61 | -1.16 | 6.29 | 13.74 | 21.19 | 28.64 |
| | 100 B21 | -88.92 | -81.47 | -74.02 | -66.57 | -59.12 | -51.67 | -44.22 | -36.77 | -29.32 | -21.88 | -14.43 | -6.98 | 0.47 | 7.92 | 15.37 | 22.82 |

Fig. 6. Budgetary effectiveness, million rubles.

The presented calculations clearly demonstrate the inverse relationship between the NPV of the concessioner and the budgetary effectiveness: the concessioner receives the highest return (153.01 million rubles), provided that the project is fully financed from the budget, and there is no concession fee. In this case, the budget receives less than 88.92 million rubles. And vice versa: the maximum budgetary effectiveness is achieved with full private financing of the project and the maximum value of concession payments (15% or 19.38 million rubles).

It is also necessary to consider other extreme points:

- Full private financing and no concession fee. In this case, the NPV of the concessioner is 36.58 million rubles, and the budgetary effectiveness of 27.52 million rubles. The project is effective for both partners. However, it is necessary to take into account that the possibilities for attracting financing by a private partner are limited. In addition, this model assumes that the concessioner invests in the project own funds, and not borrowed, because the terms of lending largely depend on the amount of funds involved, the reputation of the concessioner, and so on. Full budget financing and the maximum concession fee - in this case, the concessioner's NPV is 41.28 million rubles, and the budgetary effectiveness of 22.88 million rubles. However, this option requires a one-time diversion of a large amount of funds from the budget, which is not always possible and requires agreement with the budget code.

According to the calculations, the following ratio of competitive criteria is optimal:

- The share of budget financing is 60% or 77.52 million rubles;
- The annual concession fee is 10% or 12.92 million rubles.
- Thus, the given model allows to establish initial values for competitive criteria and by that to define a range of their possible change for competitive offers of potential concessioners:
 - The maximum value of the share of budget financing is 60%, respectively, the range of this parameter varies from 0 to 60%.
 - The minimum value of concessional payments is 10%, the range of variation is from 10 to 15% (or from 12.92 million rubles to 19.38 million rubles).

In addition, the simplicity of the proposed model makes it possible to shorten the duration of competitive procedures, and also makes the process of establishing initial values of competitive criteria more transparent. The idea of dividing not only incomes, but also obligations and risks under the project, which is the basis of the model, fully complies with the principles of PPPs, involving mutually beneficial cooperation of public and private partners, and not simply the state's implementation of its social functions through private business.

V. DISCUSSION OF RESULTS

The decision to implement an investment project largely depends on the approach applied to assessing its effectiveness. As for projects implemented in the PPPs format, name-

ly in the form of concession agreements, the choice of a private partner is made on a competitive basis according to the established criteria. One of the most important criteria is the size of the annual concession fee and the amount of funding from the public partner.

However, the methodology for determining the initial conditions of competitive criteria in the form of numerical values is missing, which creates additional difficulties at the stage of compiling the tender documentation for the concessioner. In addition, in the absence of a unified methodology, the mechanism for establishing initial numerical values of competitive criteria is opaque and incomprehensible to contestants, the question arises of the validity of the magnitude of a criterion.

VI. CONCLUSION

In the course of the study, the analysis was made of the investment needs into Russia's infrastructure, including the energy sector, which is due to the current state of the industry, characterized by the following: a high degree of moral and physical depreciation of fixed assets, with insufficient investment directly for modernization and scientific development; low economic and energy efficiency of the industry. Potential sources of financing for the modernization of the energy sector were identified, including the PPPs mechanism, which is an association of public and private resources with a view to implementing socially significant infrastructure projects.

In the course of the comparative analysis, the most common form of PPPs - concession agreements was identified, which is due to the following factors: improved regulatory framework, broad subject and object composition, accounting for the specific nature of heat power facilities of the concession, more transparent and simple competitive procedures. The peculiarities of the evaluation of concession projects, various methods for calculating the value of the concession fee, and their shortcomings were discussed.

A mechanism is proposed for determining the initial conditions for concluding concession agreements on the basis of the principle of the balance of interests of the concessioner and the contender corresponding to the basic provisions of public-private partnership.

REFERENCES

- [1] Law on Public-Private Partnerships: Guidelines for Use. - Moscow: Center for the Development of Public-Private Partnership, 2015. - 40 p.
- [2] Chernov S.S., Filchenkova M.V. Public-private partnership: concept, signs, externalities // Business. Education. Right. Bulletin of the Volgograd Institute of Business. 2017. No. 3 (40). Pp. 78-82.
- [3] On public-private partnership and concessions in the municipal sphere [Electronic resource] // The site developed by the Association of Housing and Public Utilities "Development" with the assistance of the company "Housing Development". - Access mode: <http://investcomtech.ru/concess/general>. - Ver. from the screen.
- [4] Federal Law No. 115-FZ of July 21, 2005 (as amended on December 31, 2017) "On concession agreements" Electronic legal system Consultant plus // [Electronic resource] // Access mode: <http://www.consultant.ru> (the date of the last circulation on March 28, 2013)
- [5] On the main problems in power supply and heat supply [Electronic resource] // Council of energy producers. - Moscow, 2016. - Access mode: minenergo.gov.ru/system/download/2065/67244.
- [6] Problems of heat power engineering [Electronic resource] // Branch news agency "Energy news". Mode of access: <http://novostienergetiki.ru/problemny-teploenergetiki/>. - Ver. from the screen.
- [7] Current state of the heat supply industry [Electronic resource] // Ministry of Energy of the Russian Federation. - Moscow, 2016. - Access mode: minenergo.gov.ru/system/download-pdf/4759/60329
- [8] Heat flows from the regions [Electronic resource] // News portal Gazeta.Ru. - Access mode: <https://www.gazeta.ru/business/2016/02/09/8065013.shtml>. - Ver. from the screen
- [9] Optimization of the concession fee in the stochastic model of public-private partnership "[Electronic resource] // V.Arkin, A.D. Slastnikov. - Access mode: http://mathecon.cemr.rssi.ru/seminar/2016/Arkin_Slastnikov_2712.pdf.
- [10] Resolution of the Cabinet of Ministers of Ukraine No. 639 of 12.04.2000 "On Approval of the Methodology for Calculating Concessionary Payments" [Electronic Resource]: Resolution of the Cabinet of Ministers of Ukraine No. 1239 of April 12, 2000 // Continent: Information System. - M., 2012-2017. - Access mode: http://continent-online.com/Document/?doc_id=31337433. - Ver. from the screen.
- [11] Budnik V.A. Justification of the value of concession payments under construction concession contracts / V. A. Budnik // Problems of Modern Economics. - 2013. - №4. - P.334-337.
- [12] Kifak A. Concession: international experience and Ukrainian legislation // Ports of Ukraine. - 2012. - No. 09 (121). - P. 17-19
- [13] Heat supply scheme in Novosibirsk until 2030. Book 1. The current situation in the production, transmission and consumption of heat for heating purposes / Department of Power Engineering, Housing and Communal Services, 2014. - 249 p.



Sergey S. Chernov.

Was born in Komsomolsk-on-Amur in 1979. He received a Master of science degree in management in 2002, defended his thesis on speciality 08.00.05 in 2004, Candidate of economic sciences, Associate professor.

Dean of the Faculty of Power Engineering, Head of the Department of Production Management and Economics of Power Engineering of the Novosibirsk State Technical University.

The author of more than 180 scientific publications, about 50 publications of them are in journals included in the list of leading peer-reviewed scientific journals of the Higher Attestation Commission of Russia, as well as 3 publications in publications included in the international databases of SCOPUS, WOS.



Marina V. Rozhkova – South Caucasus, Azerbaidjan in 1963; Senior Lecturer of the Department of "Foreign Languages" of Novosibirsk State Technical University; Fields of interests are economics and technology as far as English is concerned; Area of expertise is English Teaching Methodology and Teaching Translation Techniques. (Address: 20, K.Marksa, Novosibirsk, 630073, Russian Federation).

Innovative Technologies in Designing New Learning Ecosystems

Evgeniya V. Dragunova, Natalia V. Pustovalova, Igor A. Valdman
Novosibirsk State Technological University, Novosibirsk, Russia

Abstract – This article discusses constructing digital model of learning system based on the interaction of biotic and abiotic components in physical or virtual space, inherent in biological ecosystems. There are identified the main actors and types of interaction between them. The priority technologies possibly applicable in the modernized learning process in the future are revealed. There are presented the results of analyzing level of digital literacy of undergraduate and graduate students, teachers in technical, socio-humanitarian and economic areas of learning with the purpose to reveal the degree of readiness of the main participants of learning process to interact in the conditions of digitalization.

Index Terms – Innovations in learning, learning ecosystem, digital literacy.

I. INTRODUCTION

ONE OF THE CONDITIONS for effective development of Russian high-tech industries, such as the electronic and radio electronic industry, the rocket and space industry, the nuclear power industry complex, etc. is the availability of specialists with necessary theoretical knowledge and practical skills, capable of inter-industry communicating, making relevant decisions in conditions of uncertainty and working in conditions of globalization and a multicultural environment, etc. Such specialists, demanded by new digital economy (companies in new markets and high-tech industries which are being aware of their shortage in competencies necessary for functioning in the digital world and striving to fill it in, can be trained only in the conditions of a new model of learning.

The sphere of modern education tends to improve the quality of services provided to learners and provide a "client-centricity". There is a "new" generation of learners. Now we can see globalizing competition in the learning system for the "learner", implementing the concepts of "universities for billions" and lifelong learning, developing areas of training of interdisciplinary and transdisciplinary specialists, changing system for evaluating learning outcomes, increasing competition between employers for "promising" graduates. At first glance, such changes can be seen as a threat to educational institutions functioning in modern conditions. However, for proactive universities, colleges, schools, there is a unique opportunity to create new services in the digital environment that could help learners acquire the necessary competencies, knowledge and abilities, and also become "providers of long-term personal educational trajectories" [1].

This article discusses constructing the Russian model of learning system, based on the interaction of biotic and abiotic

components, inherent in biological ecosystems. Ecosystem consists of all organisms living in a certain area (biotic component), as well as all inanimate physical components of the environment, with which organisms interact (abiotic component). The whole array of organisms inhabiting a particular ecosystem is called a community [2].

To construct the information field of the domain, we built a Tag Cloud using the specialized English WordItOut service (Fig. 1). In the process of constructing tag cloud there were analyzed foreign works, published in the period of 2002 – 2017, because of insignificant number of Russian-language publications (see, for example, [3]).

The cloud is based on the analysis of modern English-language publications [4-13]. Figure 1 shows that the concepts of environment, ecosystem and different types of interactions, online courses, and e-learning, content and information tools, knowledge and technology are related to the learning process. It is the consideration of these concepts that we will implement in this article.



Fig. 1. Tag Cloud.

The purpose of this article is to create a model of learning (define boundaries, describe the components, types of interaction and principles of functioning) on the basis of ecosystem concept as the most adapted one for the training of specialists being competent in new digital economy.

II. PROBLEM DEFINITION

The learning system of the future is aimed at satisfying the creation of the need for the forming a specialist who, during his studies, realizes his real potentialities (being self-determined), learns to work in a team (being positioned), receives a "primary" experience in the future practical field, and learns to develop in himself the additional abilities nec-

essary for further professional development (being self-educated).

Universities in a changing environment should focus their attention on three points: measuring the student's progress based on results, rather than on the time spent in the classroom, obtaining high-quality professionally oriented learning outcomes, providing learning opportunities throughout all life of a learner. The Russian learning system should correspond to the needs of a modern digital society, providing a wide range of learning tools adapted to the individual learning request, the ability of quick and flexible adjusting the content of the query when forming an individual trajectory. The toolkit should provide an opportunity for self-study of learning content or a joint with a mentor-consultant, an opportunity of virtual and f2f communication without age barriers, fast and friendly feedback from the instructor (or bot). The popular concept of "ecosystem", well known in the field of biology and ecology, is taken as the basis for constructing the model of the digital learning system.

To construct a model of the learning system (environment), it is necessary to determine the limits of the system, the main components (actors) and the types of interaction between them, to identify priority technologies and mechanisms that could ensure effective interaction. In addition, an important aspect is analyzing the restrictions of the Russian system, in particular, the main actors' unpreparedness to interact in conditions of digitalization (digital competencies). The necessary condition is the availability of Recommender Systems, based on Computational intelligence-based recommendation techniques, Content-based recommendation techniques and Knowledge-based recommendation techniques [14-16].

III. MODEL OF FUTURE LEARNING: TECHNOLOGY, ECOSYSTEM, BIOTIC AND ABIOTIC INTERACTIONS

The intensive use of new learning technologies of the 21st century, the transition from constructivism to connectivism, transformed the traditional trivium (teacher – student – knowledge/content) into a tetrahedron (teacher – student – knowledge/content – technology (ICT)) with separately analyzed surfaces (different types of interaction) [13]. The surface at the bottom of the tetrahedron illustrates the relations presented earlier in the trivium (lecturer/teacher – student/pupil – content). Surfaces (student – content – technology) and (teacher-content-technology) reflect the modern version of e-learning or the illustration of the "flipped classroom" approach; finally, the surface (teacher – student – technology) illustrates the possibilities of contact outside the specific subject area with the help of information and communication technologies, for example, consulting / mentoring in virtual space [17].

A. Innovative Technologies in Education

In the studies [18, 19], the main focus is on the actual principles of learning, which is based on the student's initial knowledge, combines factual knowledge and conceptual understanding of students, involves students in metacognitive

and "self-controlled" activities [17]. The teacher changes his role from "teaching to engineering of learning".

Let us consider what technologies can come to the rescue in this transition. In accordance with the curve of technology maturity in the education sector in 2018 [20, 21], built on the basis of the Gartner Hype Cycle for Emerging Technologies, there are several promising innovative triggers (Fig. 2) that can be used in forming the future and technologies that are already sufficiently well known and closely integrated into learning methods. It should be noted that the technology "Curation and Subscription Learning", not shown in Fig. 2, which in 2017 was at the Peak of Inflated Expectations, passed to the Zone of "Trough of Disillusionment" in 2018. The technologies IMS Caliper, "Data Visualization in eLearning", "Blended Learning" are disappeared. Practically does not change the position of EHR-Integrated Performance Improvement (Zone of Innovative Triggers).

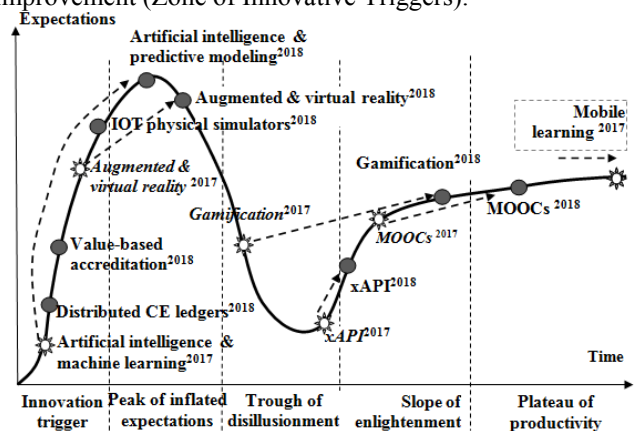


Fig. 2. The Hype Cycle for Emerging Technologies in education in 2018 (made by authors on the basis of Hype Cycles in 2017-2018).

We compared the global popularity of modern educational technologies through the Google trends tool, using the "Job and Education" filter. Technologies related to triggers (for example, CE Ledgers, Value-based accreditation) do not have yet a sufficient number of search queries, whereas MOOC, Gamification and Blended Learning have considerable popularity for several years, and the second and third one correlate with each other. The differences in the geography of search queries are interesting (Tab. I).

TABLE I
THE ANALYSIS OF SEARCH QUERIES POPULARITY

| Country | The comparative popularity of the search queries, % |
|--|---|
| Search queries: Massive Open Online Courses | |
| Taiwan | 100 |
| Philippines, Jamaica, Ecuador | 90 -78 |
| Ireland, China, Austria | 58-51 |
| Great Britain, India, Tunisia, Kenya, Hong Kong, Malaysia, Switzerland | 38-30 |
| Search queries: Gamification | |
| Singapore | 100 |
| Malaysia, the Netherlands, the Philippines, the United Arab Emirates, South Africa, Ireland, New Zealand | 59-51 |
| Slovenia, Greece, Portugal, Australia, Spain, United States, Canada | 49-35 |

| | |
|---|--------|
| Search queries: Augmented & virtual reality | |
| India | 100 |
| United Kingdom | 58 |
| Germany | 35 |
| Search queries: Blended learning | |
| Malaysia, Philippines | 100-97 |
| Singapore, Netherlands, South Africa, Ireland | 84-67 |

Table I shows that users from South-East Asia demonstrate the greatest interest in the use of information technologies in the sphere of education, which can be explained by the gradual but stable growth of their well-being, the increasing role of higher and professional education as well, as by the aiming of states of the region at the development of high technologies, including IT (India, Indonesia, Taiwan). An increasing number of citizens have access to the Internet, for example, due to urbanization and improving quality of life (China). Due to changes in the structure of the world econo-

my, the availability of higher education has become an indispensable condition for obtaining high-paying jobs, as well as an advantage in competition among job seekers for vacancies. As can be seen from Figure 2 and Table I, Massive Open Online Courses (MOOC) have reached the "Plateau of Productivity" and are one of the most popular Internet queries concerning modern education technologies. They allow to all wishing people in developed countries to gain additional competencies, in developing countries - to obtain an online education that is not available to them in their own country in the usual way.

With the help of the Google Analytics tool, we created "portraits" of the target audience of the most popular portals/platforms of the MOOC. The results are presented in Figure 3.



Fig. 3. "Portraits" of the target audience of the MOOC projects.

B. Model of Learning Ecosystem

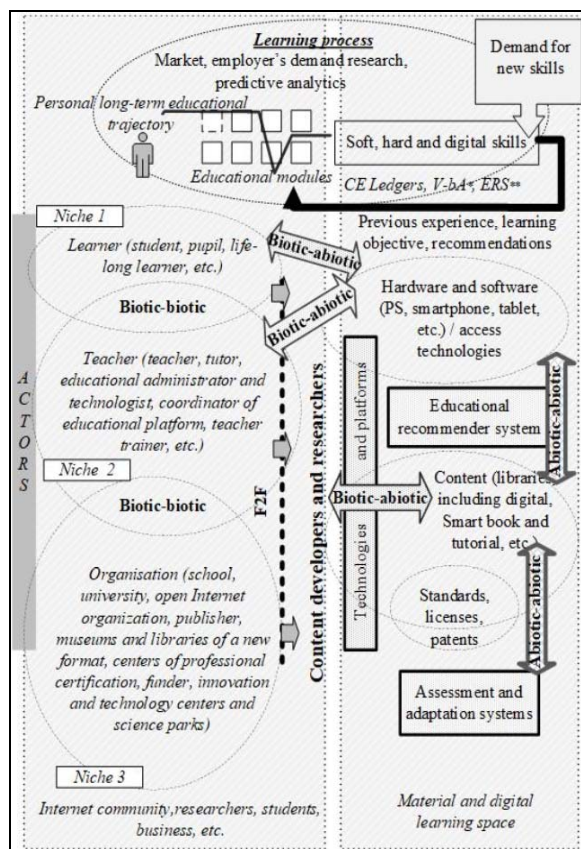
Today, we can observe the constructing of a new learning system and monitor the effectiveness of interaction between educational institutions of different types, business, state, families, social organizations, international associations and even medical institutions and research organizations. As a basis for constructing our model of learning, it is proposed to use the popular concept of forming ecosystems, successfully applied in the field of biology and ecology [2]. The learning ecosystem is understood as the set of actors (Fig. 4) existing in the educational environment (learners, teachers and organizations), and all interactions between them occurring in the physical and digital space. The modern learning ecosystem necessarily includes the digital educational ecosystem DTLE [4-6], in which not only the interaction between the main

actors, but also the properties of the digital space, are significant.

Individuals (learners and teachers) and organizations that directly participate in the educational process or carry out integration between business, the scientific community and educational centers, and control this process could be identified as biotic components of learning ecosystem. Abiotic components include hardware (tablet and personal computers, mobile devices, interactive whiteboards, 3D printers, virtual and augmented reality glasses) and software, educational platforms (online, personal development, career management, etc.), technologies (Wi-fi, 4G, WiMax), standards (developed, for example, in the field of open education by organizations: IMS GLC, IEEE LTSC, ADL) and services (Web 2.0), tools (for communication – chat rooms, e-mail, messengers, forums, for the organization of joint activities -

blogs, Wikimedia, cloud services, for assessment and adaptation of the educational ecosystem), assessing and adapting the learning ecosystem), content (including educational material resources – books, magazines, libraries, and digital educational resources – electronic libraries and specialized subscriptions, smart books and tutorial, video and audio lectures).

On the basis of biotic components and interaction between them (biotic-biotic), there are being formed the communities reflecting the interests of different actors, and facilitating the realization of interactions between them (education, business, science).



* V-bA – Value-based accreditation

**ERS – educational recommender systems

F2F– face-to-face interactions

Fig. 4 Model of learning ecosystem.

In addition, the actors such as learners and teachers are in their own niches, where actors of the same type interact with each other. The symbiotic interaction between the components provides a balance and allows the ecosystem to adapt to external influences. Modern types of interaction between components can be divided into three types: "biotic-biotic", "biotic-abiotic" and "abiotic-abiotic".

The main variant of interaction of first type is the inter-line interaction between the learner and the teacher, for example, the interaction of teachers preparing and conducting classes with students and pupils (direct interaction, eLearning, etc.). Within the framework of the "teacher" niche such relationships are possible: teacher – developer of the educational trajectories (the description of the disciplines / modules for selection, the coordination of educational trajectories), the

tutor – teacher (preparation, implementation and monitoring of the educational process), the coordinator of the educational platform – teacher (distributing resources of platform, creating and updating content, monitoring and improving the work of platforms), teacher – teacher (creating and updating the content, generating and testing new approaches and techniques, joint development and educational programs / modules).

Within the niche of the "learner", it is possible, for example, to have a student-student relationship. In this case, students exchange content, evaluate the activities of educational organizations, programs, etc. Student – pupil is one of the insufficiently mastered types of interactions, for example, consisting in joint implementing projects, informing about the peculiarities of studying in higher education in comparison with the school, preparing and conducting quests, etc. The organizations are the last group of actors. They aggregate various components of the ecosystem for its management, formalization and control of the learning process. The organizations provide hardware and software resources, facilities and platforms to other actors.

Relations of second type imply a targeted use of the abiotic components of the environment by the actors, including their creation and refinement (standards, platforms and interfaces). Thus, niche actors "teacher" use IT-interfaces and services for developing and publishing courses (edX, Moodle, Versal, Eliademy, iSpring Online, etc.), monitoring and evaluating the results of learners' activities, developing and securing educational trajectories. Such services and interfaces can be created on the basis of organizations, or online communities. Within the niche "learner" the interaction with interfaces can be directed to the joint creation and use of content. In this case, there can be both symbiotic and parasitic relationships (for example, plagiarism), depending on the contribution of each of the actors.

Relations of the third type are the most popular and promising in future field of research because of their affecting to the sphere of applying artificial intelligence technologies. In the future, "abiotic - abiotic" interaction will occur without human participation, under the guidance of Recommender Systems between hardware / software, technologies and digital content. In addition it is necessary to note the interactions of adaptive nature. They help the ecosystem as a whole to react to changes in the environment. So, profile communities (business – LinkedIn, student – community of universities in social networks, scientific and professional – Habrhabr, etc.) participate in the development of standards affecting the learning process. Developers create mashups to improve the performance of platforms. Users not only create the content, but also could define rules and procedures for its modification and use. Feedback about the work of technical services, the use of other models of monetization (subscription etc.) and the development of information technology (virtual and augmented reality) constantly changes the quality of abiotic components. Changes in the socio-economic sphere require constant changes in the biotic components. As a result, the tasks of the learning process, approaches to its organization and evaluation, and the ecosystem itself are changing.

IV. EVALUATION OF DIGITAL LITERACY OF LEARNERS AND TEACHERS: FIRST RESULTS

The present and future consumers of educational services are mostly Z Generation (Post-Millennials) and the Alfa Generation. We will take a closer look at the features of the Z Generation, which is actively studied both abroad and in Russia. For example, in the study by Sberbank, one of the aims of which was to understand how / where to interact and what to offer to the representatives of the Z Generation, such features are revealed: poor household orientation, confidence in theirs' exclusivity and the desire for self-development, setting on hedonism, the desire for rapid success, the need for ongoing social interaction, the absence of long-term trends and planning, the clip thinking, the excellent mastering of Internet technologies, the awareness that work should bring joy, love to diversity, etc. [22]. These are the peculiarities of consumers that make the issue of teachers' adaptation relevant: transition to the principles of cooperation with students, mentoring and coaching, mastering the virtual learning environment (development of online courses, the use of simulators (virtual and augmented reality), the implementation of "learning in practice on real life situations" approach, etc.

One of the restrictions of successful functioning of learning system model may be the unpreparedness of the main actors to interact under digitalization conditions.

Digital competence is a combination of knowledge, skills and attitudes, through technology, to perform tasks, solve problems, communicate, manage information, collaborate

create and share content effectively, appropriately, securely, critically, creatively, independently and ethically [23]. Digital competence has 5 levels (spheres): information and digital literacy; communication and cooperation; creation of digital content; security; problem solving [24]. The actual "hard, soft and digital" competences of students have to form as a result of efficient functioning of the learning ecosystem.

We conducted a questionnaire survey of undergraduate and graduate students as well as teachers of technical, socio-humanitarian and economic areas of learning to reveal the similarities and differences in the use of digital devices, information retrieval, usage of social networking functionality, and making financial transactions, i.e. level of digital literacy. Table II presents the summary of results of the evaluating the information literacy level of students and teachers. The survey questionnaire includes the socio-demographic data of the respondents and three parts. There were proposed to answer 23 questions. A number of questions had multiple choice. Characteristics of respondents:

- Sex: 63% of women, 37% of men;
- Category: 39% – first year students; 32% – fourth year students; 13% – graduate students; 16% – teachers;
- Average age: 18.8 years – first year students; 21.5 years – fourth year students; 22.5 years – graduate students; 46.7 years – teachers;
- Direction of learning / field of activity: technical sciences – 47.8%; economic sciences – 12.3%; humanities – 39.9%.

TABLE II
THE SUMMARY OF RESULTS OF THE EVALUATING THE DIGITAL LITERACY LEVEL OF LEARNERS AND TEACHERS*

| Evaluated parameter | First year students | Fourth year students | Postgraduate students | Teachers |
|--|--|---|--|--|
| Preferred type of digital devices | Mobile phone/ Smartphone / Laptop (42%) | Mobile phone/ Smartphone / Laptop (41%) | – Mobile phone/ Smartphone / Laptop (33%) – Personal computer (31%) | Personal computer (40%) |
| The importance of digital competencies for the future/ current profession | Pretty much necessary (71%) | Pretty much necessary (89%) | | Pretty much necessary (86%) |
| The best way to improve digital skills | Face to face learning (68%) | – Learning by doing (68%) – Face to face learning (61%) | | |
| The best way of presenting materials for learning/ teaching | – Practice activities (learning by doing) (29%) – Video (28%) | – Video (36%) – Training by game situation (28%) | – Practice activities (learning by doing) (31%) – Video (31%) | – Practice activities (learning by doing) (30%) – Training by game situation (26%) – Video (26%) |
| The most popular sources of information about new digital technologies | Social networks (37%) | Social networks (37%) | – Social networks (28%) – Blogs and Internet forums (25%) | Social networks (23%) |
| Digital skills/ frequency of using | | | | |
| • Word processing applications; • Spreadsheet applications; | Very good (37,5%) / Very frequently (46%) Good, Acceptable (30% each) / Very frequently (29%) | Very good (64%)/ Very frequently (80%) Good (39%) / Frequently (40%) | Very good (72%)/ Very frequently (67%) Good, Very good (33% each) / Very frequently (33%) | Very good (50%)/ Very frequently (90%) Acceptable (36%) / Very frequently (64%) |
| • Presentation applications; | Very good (41%) | Very good (52%) | Very good (56%) | Good (41%) |
| • Database applications; | Acceptable (32%) / Occasionally (30%) | Good (32%) / Occasionally (36%) | Acceptable (39%) / Frequently (22%) | Acceptable (23%) / Frequently (54%) |
| • Dictionary apps / Electronic dictionary | Very good (50%) / Occasionally (30%) | Acceptable (32%) / Occasionally (30%) | Acceptable (32%) / Occasionally (30%) | Acceptable (32%) / Occasionally (30%) |
| Frequency of mobile learning services usage for improve second language skills | Occasionally (23%) | Occasionally (30%) | Very rarely (33%) | Never (46%) |

*Table II presents only the most popular (frequent) responses.

Among respondents 67.1% learned how to use the equipment themselves, 24.5% were taught by a family member, 4.2% – by a teacher, 2.8% – by friends, 0.7% of respondents used books, magazines and other sources.

On average, first year students use computer technology 10.4 years, fourth year students – 12.5 years, graduate students – 13.3 years, teachers – 23.2 years. 23% of respondents believe that they know how to use specialized search tools and compose search requests, 77% of respondents in most

cases can find the information in the global network independently. It should be noted that none of the respondents have any difficulty in searching for data on the Internet. 2.8% of respondents believe that they are typing slowly, the majority of respondents – 42% rated their dialing speed as average, 38.5% – above average and 16.8% marked a high speed of typing.

The Table III shows the results of processing responses related to skills in working in a virtual environment.

TABLE III
THE RESULTS OF PROCESSING RESPONSES RELATED TO SKILLS IN WORKING IN A VIRTUAL ENVIRONMENT

| Skill | First year students | Fourth year students | Postgraduate students | Teachers |
|--|------------------------|------------------------|--|------------------------------|
| Create and update web pages | Not used (30%) | High-level skill (30%) | Acceptable level skill (33%) | High-level skill (28%) |
| Web-application development | Not used (37,5%) | Not used (39%) | Not used (50%) | Not used (77%) |
| Create and edit digital videos/ sounds | High-level skill (27%) | High-level skill (32%) | Acceptable and Poor-level skill (28% each) | Not used (31%) |
| Social network services | High-level skill (62%) | High-level skill (84%) | High-level skill (61%) | Not used (32%) |
| Use blogs | Not used (27%) | High-level skill (25%) | Not used (39%) | Not used (64%) |
| Wiki-services | High-level skill (63%) | High-level skill (43%) | High-level skill (39%) | Not used (41%) |
| Payment systems | High-level skill (45%) | High-level skill (59%) | High-level skill (44%) | Acceptable level skill (33%) |

According to the results of processing the questionnaires, there were no differences between different categories of respondents in the frequency of application of some WWW-resources. So, all categories regularly use search tools, text and voice chats, e-mail. Some differences in the frequency of using blogs ("not used" – 45% of teachers, "regularly used" – 41% of first year students), videoconferences ("regularly used" – 44% of postgraduate students and 32% of teachers), computer games ("regularly used" – 25% of first year students and 30% of fourth year students), and Wiki tools ("not used" – 40% of teachers, "regularly used" – 33% of first year and postgraduate students) have been revealed.

We should note that not all respondents have the complete understanding of what is the concept "digital competencies" consists of, assuming that this is the ability to use various digital devices, download applications and communicate in social networks. At the same time, respondents of different categories noted a different level of importance of mastering digital competencies for their professional field. Thus, 95.6% of respondents related to the field of "technical sciences" believe that a high level of digital competence is needed, and only 4.4% think that digital competencies are only needed from time to time. For the socio-humanitarian sphere, the data are respectively 52.9% and 47.1%, for the economic sector - 72.7% and 27.3%, respectively. The option "digital competencies are not important" was not chosen by any of the respondents.

V. CONCLUSION

A promising learning system must correspond to the needs of a modern digital society, maximizing innovative technol-

ogies, providing a wide range of learning tools adapted to individual learning request, the ability to quickly and flexibly adjust the content of the query in forming an individual trajectory.

Among the innovative technologies, the flipped classroom, e-learning, Life-long learning, etc., are promising for implementation. It is possible to distinguish the MOOC, the use of Internet simulators including components of virtual and augmented reality, artificial intelligence and machine learning. The analysis of popular MOOC projects showed that the main group of visitors consists of men and women from 18 to 24 years old (excluding those listed, INTUIT and Edx resources are actively used by the age group from 55 to 64 years), preferring to access to these resources from home. At the same time, the most active users are Africans, Hispanics and people of the Middle East. Unlike foreign projects, Russian MOOC-systems, including Universarium, Openedu and Lectorium, are visited more often by young women with children. At the heart of the modern learning ecosystem are the principles of effective symbiotic interaction between actors; balance between the virtual and the real components of learning environment; the possibility of flexible adaptation to changing external influences. As a result of the ecosystem functioning, the learners should acquire actual "hard, soft and digital" competencies ensuring continuous personal development and contributing a successful career.

Based on the results of the experiment, we can conclude that there is no holistic view of the content of "digital literacy" concept. Respondents perceive digital literacy as the ability to use various digital devices, skills of navigation in the Internet, downloading applications and communication in social networks. The functions of creating and developing

content (creative competence) are not perceived as a component of digital literacy.

The majority of the respondents believe that the modern Russian learning system does not fully provide the means necessary to obtain relevant digital competencies. Therefore, in the near future it is necessary to transform the learning process by incorporating modern technologies and techniques promoting digital literacy of both learners and teachers.

REFERENCES

- [1] Luksha P., Cubista J., Laszlo F., Popovich M., Ninenko I. Global Education Futures Report. Educational ecosystems for societal transformation. – Available from: <https://edu2035.org/>
- [2] Encyclopedia Britannica. Ecosystem. Encyclopedia Britannica, Inc. (Eds.) Last retrieved April 21st, 2015, <http://www.britannica.com/EBchecked/topic/178597/ecosystem>
- [3] Oleinikov B. V., Podlesnyi S. A. On the Conception of “Learning Ecosystem” and Development Directions of Education Informatization. *Znanie. Ponimanie. Umenie*. 2013. № 4. pp. 84–91.
- [4] Reyna, J. Digital Teaching and Learning Ecosystem (DTLE): A Theoretical Approach for Online Learning Environments. In *Proceedings of Ascilite 2011*. University of Tasmania, Hobart, Australia, pp. 1083–1088.
- [5] Kowch, E.G. Designing and Leading Learning Ecosystems: Challenges and Opportunities. *TechTrends*. № 62 (2), pp. 132–134.
- [6] Giannakos, M. N., Krogstie, J., & Aalberg, T. (2016). Toward a Learning Ecosystem to Support Flipped Classroom: A Conceptual Framework and Early Results. In *State-of-the-Art and Future Directions of Smart Learning*. Springer Singapore. pp. 105–114.
- [7] Põldoja H. The Structure and Components for the Open Education Ecosystem Constructive Design Research of Online Learning Tools [online] / Aalto University publication series Doctoral dissertations 175/2016. – 208 p. – Available from: <https://aaltoodoc.aalto.fi/bitstream/handle/123456789/23535/isbn9789526069937.pdf?sequence=1&isAllowed=y>
- [8] Gütl, C., & Chang, V. Ecosystem-based Theoretical Models for Learning in Environments of the 21st Century. *International Journal of Emerging Technologies in Learning (iJET)*, 2008. Vol. 3. pp. 50–60.
- [9] Chang, V. & Guetl, C. E-learning ecosystem (ELEs)-a holistic approach for the development of more effective learning environment for small-and-medium sized enterprises (SMEs). In: *Digital Ecosystems and Technologies Conference*, 2007. New York: IEEE Press. pp. 420–425.
- [10] Normak P., Pata K., Kaipainen M.: An Ecological Approach to Learning Dynamics. *Educational Technology and Society*, 2012. Vol. 15, № 3. pp. 262–274.
- [11] P. A., & Jochems, W.: The sociability of computer-supported collaborative learning environments. *Educational Technology & Society*. 2002. Vol. 5. No. 1. pp 8–25.
- [12] Uden L. The future of E-learning: E-learning ecosystem/ L. Uden, I. T. Wangsa, E. Damiani. *Proceedings of Inaugural IEEE International Conference on Digital Ecosystems and Technologies*. 2007. Cairns, Australia, 21–23 February 2007. – pp. 113–117.
- [13] Y. Z. Seghroucheni, M. Al. Achhab and B. Eddin El Mohajir Revisiting the Didactic Triangle in the Case of an Adaptive Learning System. *iJEP*. 2014. Vol. 4, № 4. pp. 27–32.
- [14] Lu Jie, Wu D., Mao M., Wang W., Zhang G. Recommender System Application Developments: A Survey. *Decis Support Syst* 74. 2015. pp. 12–32.
- [15] N. Manouselis, H. Drachsler, R. Vuorikari, H. Hummel, R. Koper, *Recommender Systems in Technology Enhanced Learning*, in *Recommender Systems Handbook*, ed by P. Kantor, F. Ricci, L. Rokach, B. Shapira (Springer, USA.), 2011 pp. 387–415.
- [16] Garcia-Martinez S. and Hamou-Lhadj A. Educational Recommender Systems: A Pedagogical-Focused Perspective, In: Tsihrantzis G., Virvou M., Jain L. (eds) *Multimedia Services in Intelligent Environments*, DOI: 10.1007/978-3-319-00375-7_8, Springer International Publishing Switzerland 2013, pp.113–124
- [17] M.Tchoshanov Engineering of Learning: Conceptualizing e-Didactics. UNESCO Institute for Information Technologies in Education. Moscow. 2013. 194 p.
- [18] How people learn. Brain, Mind, Experience, and School. Expanded edition. National academy press. Washington, D.C. – Available from: <https://www.colorado.edu/MCDB/LearningBiology/readings/How-people-learn.pdf>
- [19] Donovan, M., Bransford, J. How Students Learn: History, Mathematics, and Science in the Classroom. National Research Council Report. Washington, DC: National Academy Press. 2005. DOI: <https://doi.org/10.17226/10126>
- [20] Hicken A. 2017 eLearning Predictions: Updated Hype Curve. Web Courseworks. January 3, 2017. – Available from: <https://webcourseworks.com/2017-elearning-predictions/> (дата обращения: 01.04.2018)
- [21] Hicken A. 2018 eLearning Predictions: Updated Hype Curve. Web Courseworks. December 29, 2017. – Available from: <https://webcourseworks.com/2018-elearning-predictions-updated-hype-curve/>
- [22] 30 facts about modern youth. – Available from: https://adindex.ru/files2/news/2017_03/158487_youth_presentation.pdf
- [23] Skov A. What is digital competence? – Available from: <https://digital-competence.eu/front/what-is-digital-competence/>
- [24] DigComp 2.1: The Digital Competence Framework for Citizens with eight proficiency levels and examples of use. Luxembourg: Publications Office of the European Union, 2017. 48 p.



Eugeniya V. Dragunova, PhD, Associate Professor, Department of Economic Informatics, Novosibirsk State Technical University. Research interests – the peculiarities of ecosystems, the growth typologies, organizational changes of enterprises, development strategies of companies.



Natalya V. Pustovalova – senior lecturer, Department of Economic Informatics, Novosibirsk State Technical University. Research interests: requirements engineering, software engineering.



Igor A. Valdman, Candidate of Philosophy, Associate Professor in the Department of Sociology and Mass Communications of the Novosibirsk State Technical University. The field of scientific interests is the study of the transformation of social communications, social ontology, philosophy of education.

Overhead Power Transmission Lines Economic Efficiency Diagnostic Assessment

Yuliya V. Dronova, Boris N. Moshkin, Elena Yu. Kamysheva
Novosibirsk State Technical University, Novosibirsk, Russia

Abstract – The overhead power transmission line diagnostics is a part of a current production operation of electric grid company. The list of diagnostic types has to be developed on the basis of technical and economic factors. The solution of technical tasks is primary, and the additional diagnostic types should be used if the cost advantages are available. One of the assessment methods for overhead power transmission line diagnostics is described in the paper. The assessment technique for overhead power transmission lines economic efficiency diagnostics is considered and its cost advantages calculation is given.

Index Terms – Overhead transmission line diagnostics, economic efficiency.

I. INTRODUCTION

THERE IS no need to explain and prove the significance of applying the overhead power transmission line diagnostics. The list of activities related to diagnostics is determined by the electric grid company being responsible for power supply reliability. For instance, it could be the managing company of electric grid holding company. Diagnostics costs according to the regulatory requirements are included in service fee of the electric grid company. However, academic community representatives develop innovative diagnostic methods which make it possible to prevent the power transmission lines incidents. The process of these methods developing is rather long, but the applying process takes more time. In order to increase the interest towards new diagnostic methods it is necessary to have economic efficiency despite technical one.

II. PROBLEM DEFINITION

Conventional performance indicators for economic efficiency assessment are an integrated effect identified as Net Present Value (NPV) and Pay Back Period [1]. These indicators could be also used for economic efficiency diagnostics assessment of the overhead power transmission lines state. NPV is defined by difference between the cost advantages obtained by applying the diagnostic device for the overhead power transmission line economic efficiency assessment and the cost of new diagnostic device purchase and maintenance (Invested Capital):

$$NPV = \sum_{t=0}^T [R^{(t)} - C^{(t)}] \cdot \frac{1}{(1+e)^t} - IC, \quad (1)$$

where $R^{(t)}$ - is cost advantages obtained by applying the diagnostic device at the t^{th} calculation step, $C^{(t)}$ - is equipment maintenance costs, IC - is new diagnostic device costs (Invested Capital), T - is a performance period of diagnostic tools, t - is a calculation step, e - is a discount rate.

III. THEORY

In general, the system-based economic performance $R^{(t)}$ obtained by new device applying in power system is determined by the following factors [1]:

- company income remains unchangeable (due to reservation of overhead power transmission lines);
- the cost advantages are determined by economic costs reducing related to economic damage due to accident remediation:

$$R^{(t)} = D^{(t)} \quad (2)$$

The overhead power transmission line failures structure per components is shown in the Table I [2].

TABLE I
OVERHEAD POWER TRANSMISSION LINE FAILURES
STRUCTURE PER FOLLOWING COMPONENTS

| Overhead power transmission line components | Failure Flow in % out of the total |
|---|------------------------------------|
| Power transmission line | 13 |
| Wires and cables | 52 |
| Insulator | 31 |
| Overhead power transmission line fittings | 4 |

The overhead power transmission line failures structure per components presented in the Table I. shows that failures due to the transmission line tower destruction are the most costly and need a longer rehabilitation period. The accident remediation maintenance costs due to the failure mode need to be assessed.

To determine the losses of the company the following factors should be taken into account

- a number of overhead power transmission lines being operated by the electric grid company;

- unit economic losses caused by the costs of emergency recovery works;
- overhead power transmission lines failure flow determining the accident probability.

Then, the economic losses average annual rate is defined as:

$$D^{(t)} = \left(\sum_{k=1}^K d_i^k * n^k \right) * w, \quad (3)$$

where d_i^k - is unit economic losses due to destruction of the k-th type overhead power transmission line tower, n^k - is a number of the k-th type power transmission line towers, w - is a failure rate.

IV. EXPERIMENTAL RESULTS

The unit economic losses have been determined according to the actual statistics on economic losses.

The economic efficiency diagnostics assessment has been made on the basis of the analysis related to the emergency recovery costs of the 110 kV overhead power transmission line towers.

The electric grid company operating in the territory of Western Siberia, RF has been chosen as a subject of the research. According to the statistics related to transmission line accidents, for the last 20 years the experts have found out that the power transmission line towers falling often occurs due to wind load. To assess the overhead power transmission line state the diagnostic device has been developed, the cost of which was 12,000\$ (Invested Capital).

The accident remediation maintenance costs according to the Disturbance Investigation Report are given in the Table II [3, 4].

TABLE II
OVERHEAD TRANSMISSION LINE TOWER FALLING
CONSEQUENCES

| Overhead Power Transmission Line Type | Number of power transmission line towers, units | Accident remediation maintenance costs, in thousand US Dollars, as of 2017 costs | |
|---------------------------------------|---|--|-----------------------------------|
| | | Total | per power transmission line tower |
| OPTL-110 | 19 | 1067,9 | 56,2 |
| OPTL-110 | 3 | 88,7 | 29,6 |
| OPTL-110 | 4 | 273,7 | 68,4 |
| OPTL-110 | 2 | 295,7 | 147,8 |
| OPTL-110 | 5 | 266,0 | 53,2 |

The data given in the Table II allow to get an average value of unit economic losses [6]:

$d_i^k = 59,5$ \$ per overhead power transmission line tower according to the 2017 costs.

The overhead power transmission line failure rate depends on different factors. The major factors are a service life and operating conditions of the equipment (Fig. 1) [5].

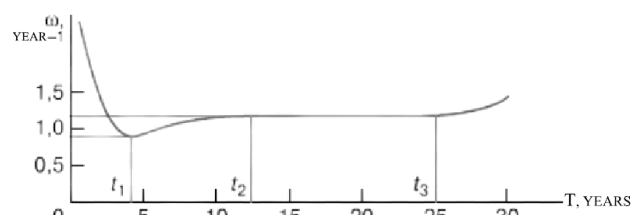


Fig. 1. Failure rate dependence on the overhead power transmission line service life.

The accidents data given in the Table III. indicate that all cases of overhead power transmission line tower falling have been noted while equipment operating for more than 20 years and wind load carrying capability.

TABLE III
TRANSMISSION LINE TOWER FALLING WHILE EQUIPMENT
OPERATING OVER 20 YEARS

| T _{case} years | Period after accident remediation (months) | Number of power transmission line towers |
|-------------------------|--|--|
| 22 | 11 | 19 |
| 32 | 13 | 5 |
| 32 | 13 | 2 |
| 34 | 12 | 3 |
| 47 | 12 | 4 |
| 41 | 12 | 3 |
| 47 | 12 | 6 |

The analyses of actual emergency cases caused by transmission line towers falling showed that all events occurred in the time period t_3 , i.e. in the period of increasing failures flow when the equipment service life exceeded more than 25 years.

Data on the overhead transmission line towers number and the failure rate depending on the period of transmission line service life are given in the Table IV.

TABLE IV
THE 110 OVERHEAD POWER TRANSMISSION LINE FAILURE
RATE

| | Period of a service life t_1 and t_2 (up to 15 years) | Period of a service life t_3 (over 15 years) | | |
|---|---|--|--------|---------|
| | | 15-25 | 25-30 | Over 30 |
| Number of the 110 OPTL | - | 1148 | 1403 | 10459 |
| Failure flow, number/year per 100 km | - | 1,2 | 1,5 | 1,7 |
| Failure flow, number/year per transmission line tower | - | 0,0027 | 0,0033 | 0,0038 |

Thus, the average annual damage for the electric grid company caused by the 110 kV overhead power transmission line tower eventual falling, service life of which is more than 30 years could run up to more than 360,000 \$ every year (Equation 3).

This damage can be avoided by using diagnostic device which allows to assess the 110 kV overhead power

transmission line towers state (annual positive cash flow $R^{(i)}$)

The Net Present Value calculation obtained by applying diagnostics device with a service life of 10 years into the Electric grid company operation has been presented in the Table V.

TABLE V
THE NPV CALCULATION RESULTS

| | | | |
|---|--------|--------|---------|
| Number of measurements per year | 1500 | 5000 | 12000 |
| Measurements cost, thousand US Dollars per year | 1514,6 | 5048,6 | 12116,7 |
| Damage, thousand US Dollars per year | 365,4 | | |
| NPV, thousand US Dollars | 2666,6 | 2640,5 | 2588,5 |

The pay back time can be calculated by the equation

$$T = \frac{IC}{CF}, \quad (4)$$

where CF - is an average annual economic viability, IC - is equipment costs.

The pay back period is less than one year.

V. CONCLUSION

The application of special overhead transmission line diagnostic device allows the electric grid company to:

- develop the overhead transmission lines tower state diagnostics assessment sheet;
- schedule overhead power transmission line maintenance service;
- reduce the costs related to power supply restoration due to overhead power transmission line towers failure.

REFERENCES

- [1] Guidelines on assessing the effectiveness and development of invest project and business plans in electric power industry (with examples): The stage of invest proposals (Part 1). The stage of Feasibility study (Part 2). Vol.1,2. Approved by the order of the Unified Energy System of Russia № 155 (dated: 31.03.2008) taking into account the RF main state expert review №24-16-1/20-113 (dated: 26.05.1999)
- [2] Company's Code 56947007-29.240.55.111-2011 Guidelines on assessing the overhead transmission lines state and overhead transmission line components residual life.
- [3] Guidelines on technical investigation and consideration of disturbances and incidents in public power supply service system, housing and utilities sector. MDK 4-01.2001/ Approved by the order of Ministry of construction industry, housing and utility sector (dated: 20.08.2001).
- [4] Manual on investigating and considering the technological disturbances in operation of power systems, electric power plants, boiler and heat systems and power grids. Approved by the Energy Deputy-Minister of the Russian Federation (29.12.2000), RD 34.20.801-2000
- [5] Handbook on designing the electrical networks / C74. edited by D.L. Faibisovitch. — Iss. 4., revised — M. ENAS, 2012. - 376 p.
- [6] Information book on prices for construction engineering. Engineering and Geodesy Surveys (base level prices given on 01.01.2001 r.). Approved by the order of Ministry of construction industry, housing and utility sector №213 (dated: 23.12.2003). Date of validity: 01.01.2004.



Yuliya V. Dronova.
630066, Russia, Novosibirsk, Pionerskaya, 32
E-mail: dronova@corp.nstu.ru
Phone: +791399009514
Novosibirsk State Technical University
1995-2001 Faculty of Power Engineering, Master's Degree in Management
2002-2005 Postgraduate study
2005 Thesis on a Candidate Degree in Economic Sciences. Research topic "Models for the energy company production risks assessment"
2005- present
Associate Professor of Production Management and Power Economics Department, Novosibirsk State Technical University



Boris N. Moschkin.
630073, Russia, Novosibirsk, Dzerzhinskij Prospect, 22-2, ap. 71
E-mail: moshkin@eco.power.nstu.ru
Phone: +79139103513
Novosibirsk State Technical University
1977-1982 Faculty of Power Engineering, Electrical Engineer
1982-1985 Postgraduate study
1985 Thesis on a Candidate Degree in Engineering. Research topic «The modes controlling of Hydro Electrical Power Plant taking into account equipment operational state»
1986- present
Associate Professor of Production Management and Power Economics Department, Novosibirsk State technical University



Elena Yu. Kamysheva.
630073, Russia, Novosibirsk, Komsomolskaya, 14, ap. 34
E-mail: kamysheva@corp.nstu.ru
Phone: +79138939515
Schadrinsk State Pegagogical University
1991-1995 – Faculty of Foreign Languages, English and German
2001-2003 Postgraduate study
2003 Thesis on a Candidate Degree in Pedagogy.
Research interest fields
Formation of the pedagogical image, Development of educational technologies
English for Specific Purposes: Economics, Power Engineering.
2014-present
Associate Professor of Foreign Languages Department, Novosibirsk State Technical University

Economic Aspects of the Sustainable Technological Development of the Oil and Gas Industry in the Context of Low Oil Prices and the Current Situation in the Energy Markets

Leontiy V. Eder^{1,2}, Irina V. Provornaya^{1,2}, Anna A. Kulik², Vasily Yu. Nemov^{1,2}

¹Trofimuk Institute of Petroleum Geology and Geophysics SB RAS, Novosibirsk, Russia

²Novosibirsk State University, Novosibirsk, Russia

Abstract – This article examines the dynamics of oil and gas companies' operating expenses as a factor of technological development. Based on the econometric model built on the basis of panel data, it was shown that with the oil prices plunging, oil and gas companies almost halved operating expenses primarily due to technological development in the field of hydrocarbons' exploration and production. It throws down a significant challenge to the Russian oil and gas industry in efficiency gains of the hard-to-recover oil and gas reserves' development and import phase-out.

Index Terms – Technological development, petroleum, unconventional resources, sustainable development, oil prices.

I. INTRODUCTION

NOWADAYS the mineral-raw base of conventional oil reserves deteriorates not only in Russia, but also in a whole world. The volume of conventional oil extraction declines and the share of hard-to-recover reserves grows, as a result, the production costs of oil and gas companies rises. Simultaneously, with the development of new production field of unconventional hydrocarbons is being underway, the total volume of energy resources extraction increases [1, 2].

The growth of unconventional and hard-to-recover hydrocarbons production leads to an increase of companies' expenditures. At high oil prices, this factor was not crucial. However, during the falling of oil prices the level and the dynamics of operating expenses become essential, because they influence on the amount of profit and determine the opportunities to involve unconventional hydrocarbons in development [3, 4].

The level and the dynamics of operating expenses have recently been determined by the quality of the raw materials source. However, low oil prices have become to a certain extent a catalyst for the technological restructuring of the world's oil and gas companies. As a result, operating expenses are essentially determined by the technological development of companies at present. The conditions of global energy markets have begun to determinate the economic aspects of the oil and gas industry's technological development. This poses significant challenges for the Russian oil and gas industry [5, 6].

The operating costs of the oil and gas majors have been reduced almost twofold over the last few years (Fig. 1). This indicator describes the efficiency of hydrocarbon production and demonstrates how many dollars were accounted for the extraction of the one ton of oil equivalent.

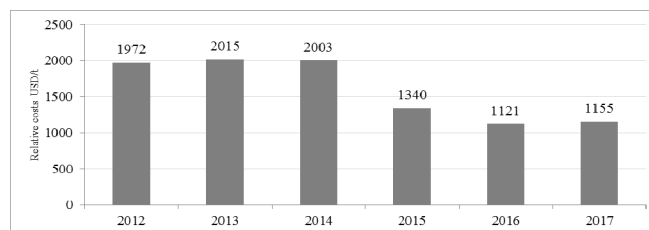


Fig. 1. The dynamics of the relative operating costs of the world's oil and gas majors, 2012 - 2017.

Looking at the similar indicator of Russian companies, it went in the opposite direction. There is a considerable upward trend in operating costs of the one ton of hydrocarbons extraction in the national currency (Fig. 2), which meant decrease in the efficiency of oil and gas production in Russia [7].

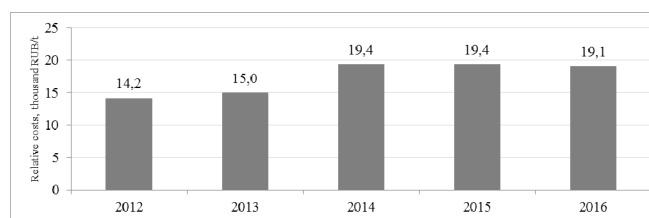


Fig. 2. The dynamics of the relative operating costs of the Russian companies, thousand rubles / t in 2012 - 2016.

In recent years, the US has dramatically increased oil production through the development of the shale oil production. As a result, in 2017 they began to export oil to other countries, although they had had to import about a half of consumed this source. Thus, to analyze how this technological breakthrough could have an influence on not only production indicators, but also financial performance of oil and gas companies is the important case.

There are well-known researchers, whose works are focused on the problems of technological development and the dynamics of expenditures. For instance, Toews, Kilian,

Kellogg, Hamilton, Ishii, Adeleye, Huntington, Fukunaga, Hirakata, Sudo, Talbi.

Toews and Naumov have studied the factors of expenses costs with a focus on its relationship with the price of oil (“The relationship between oil price and costs in the oil and gas industry”). The 25 largest oil and gas companies were considered to build two quarterly time series of the number of exploration wells drilled by these companies and the average cost of drilling. And then, a VAR-model was constructed, which illustrates the relationship between costs in oil and gas industry and real oil prices, the number of drilled wells, costs of drilling [8].

There is another article “Not all oil price shocks are alike: disentangling demand and supply shocks in the crude oil market”. Kilian, the author, has used the VAR-model to describe the crude oil market. It is proposed to decompose the real oil price into three components: crude oil demand shocks, shocks to the global demand for all industrial commodities and crude oil supply shocks [9].

According to Huntington (“Oil demand and technical progress”), the technical change can be both exogenous and induced by prices and other variables. Moreover, it has ascertained that the multiple factors that could drive energy demand may change with time, so this research provides the acceptable method to identify them. Focusing on panel data, presenting experience of different countries, the ADL-model has been used to highlight the short- and long-run oil consumption responses to prices and GDP, alongside with the technology trend and other unmeasured variables [10].

This paper proposes to take into account the economic aspects of the technological development of Russia's oil and gas industry from the perspective of the dynamics oil and gas companies' operating costs against a backdrop of world energy markets' development.

The target of research - global oil and gas majors: “ExxonMobil”, “Royal Dutch Shell”, “British Petroleum”, “Chevron Corporation”, “Total”, “China National Petroleum Corporation”, “Petrobras”.

The scope of research: the organizational/economic mechanisms of generation operating expenses.

The novelty of this paper is researching the influence of main determinants on the oil and as majors' operating expenses.

Initially, four determinants have been defined. Also, they have been separated into two groups: micro- and macroeconomics. Macroeconomics determinants are oil prices, technological factor. Microeconomics determinants are the hydrocarbons production volume.

Then, models based on panel data have been built. Finally, the qualitative model has been distinguished.

II. PROBLEM DEFINITION

The goal of research is to identify the key determinants that influence on the dynamics of the operating expenses performance as a factor of oil and gas industry's technological development, focusing on the largest global oil and gas companies' operating expenses.

The research tasks. The following tasks have been solved to achieve a target goal:

- To research the level, dynamics and structure of Russian and global oil and gas companies' operating expenses as a factor of technological development;
- To construct an econometric model based on the panel data of the influence of the main indicators on the structure and dynamics of operating costs;
- To identify the basic factors that have an influence on the structure and performance of oil and gas companies' operating expenses.

III. THEORY

In this study, factors that can influence on the level and dynamics of oil and gas companies' operating expenses are examined. To explain the effect of predictor factors on operating expenses the quarterly time series of all variables have been constructed. The ten-year period is been taken into account (2008-2017). To explain the effect of predictor factors on operating expenses the quarterly time series of all variables have been constructed, over a ten-year period between 2008 and 2017. The seven largest companies have been taken into account.

Panel data allows analyzing the several observable objects in time (combining cross-sections and time series).

In this study, three models based on panel data will be tested: the pooled regression model, the fixed-effects model, and the random-effects model.

The simplest model is the pooled regression. It is a linear regression model that looks like the following equation

$$y_{it} = x_{it}^T \beta + \alpha + \varepsilon_{it}, \quad (1)$$

where y_{it} denotes the depended variable of i-entity in t-period, x_{it}^T represents independent variables, α and β are coefficients of regression (they are the same for all observation) ε_{it} is the error term, $i = 1, \dots, n$, $t = 1, \dots, T$.

This model has the most limitations among three models, because identical behavior of all observed entities at each time is assumed. If this assumption is satisfied, the regression coefficients can be estimated by the ordinary least squares method (OLS), and these estimates will be consistent.

The assumptions for the fixed-effects models are the same instead of the entities' identity in time. This model looks like the following equation:

$$y_{it} = x_{it}^T \beta + \alpha_i + \varepsilon_{it}, \quad (2)$$

where α_i is the unknown intercept for the i-entity.

The meaning of α_i is reflection individual effects of each entity. The model is quite flexible due to the heterogeneity of the observed objects.

The random-effect model can be represented in the next equation:

$$\begin{aligned} y_{it} &= x_{it}^T \beta + u_{it}, \\ u_{it} &= \alpha_i + \varepsilon_{it}, \end{aligned} \quad (3)$$

where α_i is the unknown variable individual effect for the i -entity.

The assumption for the random-effects models is that the variation across entities is random and uncorrelated with the predictor or independent variables included in the model, so α_i remains in the errors. Also α_i as ε_{it} are assumed to have a normal probability distribution. Therefore, the structure of errors is become more complicated while the construction of a regression model is become simpler. This model is a compromise between the two previously discussed ones, because there is the less number of restrictions compared to the pooled regressions and the estimates are more significant compared to the fixed-effects model.

IV. EXPERIMENTAL RESULTS

To construct an accurately specified regression model it is necessary to analyze operating expenses for finding out internal determinants. Furthermore, it is important to study the external factors having influence on the operating activity.

To determine the structure of operating expenses by costs of account, it is sufficient to analyze the annual data, for which the year of 2017 was chosen. These data were taken from the financial statements (IFRS) of the selected companies. Operating costs consist of: production costs; costs of purchased hydrocarbons; expenses for geological prospecting; taxes (except for income tax), excises and export duties; depreciation; commercial, administrative and general expenses. A distinctive feature of these companies from Russian ones is the high share of costs for the purchase of crude oil, gas and petroleum products: more than 40%, for some companies more than 70% of total operating expenses.

The selected companies are vertically integrated, so the scope of their activities extends to the upstream sector. In addition, there has recently been the conventional resource base deterioration and development of unconventional resources' extraction. Also, it is interesting to note that there has been a considerable increase in the shale oil production. In this regard, the dynamics of oil production in the United States, the number of drilling rigs and prices for Brent crude oil have been analyzed. For this purpose, monthly data on oil production volumes have been taken from the website of the US Energy Information Agency (www.eia.gov), and data on the number of active drilling rigs have been taken from the website of the oil and gas service company "Baker Hughes" (www.bakerhughes.com) (Fig. 3). After that, the extraction efficiency of one rig has been calculated as oil production divided by the number of active rigs. The data on the level of Brent crude oil prices and drilling efficiency are shown in Figure 4.

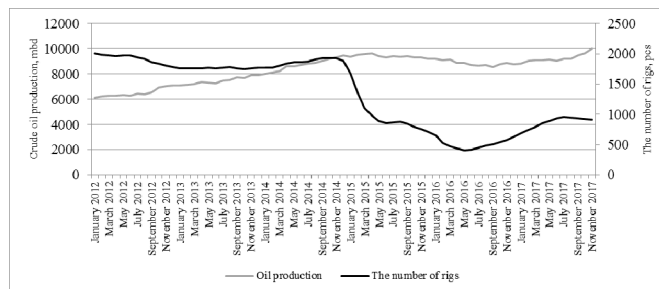


Fig. 3. The dynamics of oil production and the number of drilling rigs, 2012-2017.

The sharp decrease in the number of drilling rigs in the US occurred with the fall in oil prices in the second half of 2014. In fact, the number of drilling rigs reduced almost twofold in a few months, although there was practically no reduction in the oil production at the same time. Thus, the radical technological re-equipment, the optimization of drilling rigs' number and the withdrawal of capacities in the least profitable sectors were carrying out within six months. As a result, the ratio of the oil production per a drilling rig has almost doubled for the period December 2014 - June 2015. This ratio reflects the degree of technological efficiency of the drilling process. The peak of decline in oil prices occurred in May 2016. Further optimization of the technological activity of shale oil production has led to increase in technological efficiency. In fact, the technological efficiency index doubled in mid-2016, reaching the level of 20-22 mbd per one rig. As a result, the drilling efficiency has increased almost 7 times since the end of 2014, against the background of a decrease in oil production.

The rise in oil prices began in the second half of 2016, resulting in there was an increase in the number of drilling rigs with an asymmetric production growth rate and also there was a decrease in efficiency due to the connection to production of relatively inefficient and cost-effective shale oil reserves.

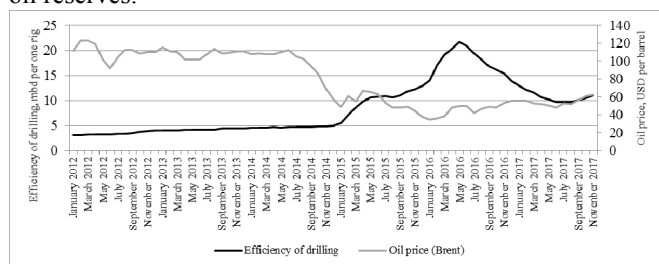


Fig. 4. The dynamics of Brent oil prices and drilling efficiency, 2012-2017.

As a result, while the oil prices were low, there were an improving of the level of oil production and falling the number of active rigs. This led to an increase of the production efficiency per one rig (production efficiency has been calculated as the oil production divided by the number of active drilling rigs).

During the construction of the regression models, financial and production indicators of the operating expenses' level and the hydrocarbon production volume of seven companies: "Exxon Mobil", "Chevron Corporation", "British Petroleum", "Royal Dutch Shell", "Total", "CNPC" and "Petrobras" will be used. The quarterly data for the last 10

years will be considered, which were collected from quarterly, interim and annual reports of these companies from 2008 to 2017. The accession rates of all variables have been taken to get rid of the time effects and to bring the series to a stationary form.

After analyzing of the economic and production indicators four hypotheses about the factors having the greatest impact on the level and dynamics of oil and gas companies' operating expenses have been put forward:

Hypothesis 1: the volume and dynamics of operating expenses are positively correlated with oil prices.

Hypothesis 2: the volume and dynamics of operating expenses are correlated with the technological factor in a

Hypothesis 3: the volume and dynamics of operating costs depend on the volume of production.

Hypothesis 4: the tax burden affects the volume and dynamics of operating costs.

In according to hypotheses put forward, four factors will be checked.

Firstly, a pooled regression model was tested. This model is a regular multivariate regression. The results are shown in the Tab. I.

TABLE I
TESTING RESULTS OF POOLED REGRESSION MODEL

| | Coefficient | Standard Error | t-statistic | P> t | [95% Conf. Interval] | |
|-------------------|-------------|----------------|-------------|-------|----------------------|--------|
| Oil Price | 0,428 | 0,033 | 13,070 | 0,000 | 0,364 | 0,493 |
| Technology factor | -0,185 | 0,029 | -6,340 | 0,000 | -0,243 | -0,127 |
| Production | -0,221 | 0,081 | -2,730 | 0,007 | -0,380 | -0,061 |
| Taxes | 0,059 | 0,013 | 4,540 | 0,000 | 0,033 | 0,084 |
| Const. | 0,011 | 0,005 | 2,210 | 0,028 | 0,001 | 0,021 |

According to the obtained results, the selected factors explain the dependent variable reasonably well. The F-statistic takes the value 76.81, which indicates the regression significance. The test significance and t-statistic show that all factors are significant. The determination coefficient takes the value 52.77%. The adjusted determination coefficient is 52.08%. The latter is more acceptable indicator of the model quality because of an adjustment to the number of degrees of freedom.

The second model is a fixed-effect, with the results being demonstrated in the Tab. II.

TABLE II
TESTING RESULTS OF MODEL WITH FIXED EFFECTS

| | Coefficient | Standard Error | t-statistic | P> t | [95% Conf. Interval] | |
|-------------------|-------------|----------------|-------------|-------|----------------------|--------|
| Oil Price | 0,427 | 0,033 | 12,960 | 0,000 | 0,359 | 0,488 |
| Technology factor | -0,183 | 0,029 | -6,290 | 0,000 | -0,240 | -0,126 |
| Production | -0,236 | 0,082 | -2,870 | 0,004 | -0,398 | -0,074 |
| Taxes | 0,065 | 0,013 | 4,940 | 0,000 | 0,039 | 0,091 |
| Const. | 0,011 | 0,005 | 2,250 | 0,025 | 0,013 | 0,021 |

According to the results, The F-statistic takes the value 78.81, which indicates the regression significance. The test significance and t-statistic show that all factors are significant. Although the determination coefficient takes the

value 52.73%, being higher than the same index of the previous model, it is not acceptable to choose this model without additional tests.

In order for OLS-estimates of a fixed-effects model to be consistent, only the uncorrelatedness of factors with errors ε_i is required. The correlation between regressors and errors u_{it} is allowed and shows the flexibility of this model. Thus, there is a marginal correlation between the individual effects and factors equaled to -0,0459.

The next step is construction of random-effects model. The results are shown in Table III.

TABLE III
TESTING RESULTS OF MODEL WITH RANDOM EFFECTS

| | Coefficient | Standard Error | t-statistic | P> t | [95% Conf. Interval] | |
|-------------------|-------------|----------------|-------------|-------|----------------------|--------|
| Oil Price | 0,427 | 0,033 | 13,070 | 0,000 | 0,364 | 0,49 |
| Technology factor | -0,184 | 0,029 | -6,340 | 0,000 | -0,242 | -0,123 |
| Production | -0,224 | 0,081 | -2,760 | 0,006 | -0,383 | -0,281 |
| Taxes | 0,060 | 0,013 | 4,640 | 0,000 | 0,035 | 0,086 |
| Const. | 0,011 | 0,006 | 1,970 | 0,049 | 0,000 | 0,024 |

With the GLS-estimates being inefficient, it is definitely essential to use Wald statistics instead of the determination coefficient to explain results. It equals to 310.90, being enough high for the regression significance. Also, Prob > chi2 = 0.0000. This is a F-test to see whether all the coefficients in the model are different than zero. If this number is less than 0.05 then the model is acceptable. Moreover, there is not correlation between differences across units and factors, so these estimates are sufficient.

After building and testing three models based on panel data, it becomes necessary to choose the best of them.

To begin with, a Wald test is needed. It compares the pooled-regression model with the fixed-effects model. This test is performed automatically in the Stata analysis package during testing a fixed-effects model. The result is shown in the last line:

F test that all $u_i=0$: F(6, 269) = 5.06 Prob > F = 0.0000

The test significance is less than 0.01, so the hypothesis about the zero equality of individual effects is rejected. It means that the fixed-effects model is better describe the dependent variable.

Next, a Broyush-Pagan test is needed to be conducted. This test compares the model of pooled regression with a random-effects model. The result is:

chi2 (1) = 50.02 Prob> chi2 = 0.0000

The test significance is less than 0.01, so it is recommended to use a model with random effects instead of a pooled regression model.

The first two tests have showed that there is a need for Hausman specification test to determine the type of individual effects.

According to the results of this test, the random-effects model describes the dependence of operating costs on the predictor factors better: the significance level is Prob> chi2 = 0.3608. The hypothesis that the factors do correlate with individual effects is rejected.

Although the companies were not selected randomly (the seven largest corporations was chosen), this conclusion is acceptable because these companies carry on business around the world and have differences in operating activities which they are focusing on. Furthermore, this model is not limited exclusively to this set of corporations, so it is better to use a model with random effects.

Thus, operating expenses of oil and gas companies are then explained according to the following model (4):

$$OpEx = 0,428 \times P_{oil} - 0,185 \times Tech - 0,224 \times Prod + 0,060 \times Tax + 0,011,$$

where P_{oil} denotes oil prices (Brent), Tech – technological factor, Prod – the volume of hydrocarbons, Tax – tax burden.

V. DISCUSSION OF RESULTS

During the period of low oil prices in the USA (2014-2018), the drilling efficiency has increased in several times. Oil and gas companies have been able to adapt to this situation and almost halve the shale oil production cost. This indicates a significant technological development in the drilling process, which reduces the costs of oil production.

Such a rapid rise in the efficiency of oil production in the United States creates significant technological difficulties for the Russian oil and gas industry, especially under sanctions dealing with the restricted access to technology innovations. While there is an increase in the efficiency of the global majors' hydrocarbon production, the same Russian companies' ratio declines, pointing at a lack in technology of Russian oil and gas industry [4-7].

The reduction of tax payments on hard-to-recover oil and gas production facilities is the main factor that helps to maintain the efficiency of Russian companies. As a result, there has recently been a trend in the transition of the Russian oil and gas industry from sector generating a significant share of the government budget to the investment sector.

VI. CONCLUSION

The decline in oil prices in 2014 triggered the processes aimed at achieving a sharp rise in efficiency of the drilling process. In fact, the costs of shale oil production have fallen almost twofold from \$70 to \$35 per barrel for a three-year period between 2014 and 2017. There are two main reasons explained this result: firstly, the increase in the technological efficiency of drilling, and secondly, the reduction in the cost of drilling.

The number of drilling rigs in the US has worsened from just under 1.9 thousand units up to about 500 pcs from 2014 till the first half of 2016. The volume of drilling has decreased negligibly at the same time. The volume of oil production in the United States has begun to grow steadily since the second half of 2016. This process accelerated in 2017.

As a result, the involvement of unconventional resources in operation clearly shows that the volume of extraction depends not so much on the availability of resource and raw

materials as on the technological development of the industry, primarily in extraction.

The profits of oil companies are determined not so much by oil prices as by technological opportunities to reduce production costs.

In the coming years, the US plans to significantly increase the volume of oil production and become one of the largest suppliers of oil to the world market. Despite the efforts of OPEC + this will make significant pressure high on the oil prices. As a result, it might be expected a deterioration in the pricing environment on the world oil market at the end of next year.

Thus, oil prices become cyclical that is confirmed by the recent fluctuations, over a ten-year period between 2008 and 2017. The improvement in the efficiency of oil production in the United States throws down significant technological challenges for the Russian oil industry.

The publication is supported by the Russian Science Foundation No. 16-18-10182, Grant of President MD-6476.2018.6.

REFERENCES

- [1] Filimonova I.V., Eder L.V., Mishenin M.V., Mamakhatov T.M. Current state and problems of integrated development of mineral resources base in Russia // В сборнике: IOP Conference Series: Earth and Environmental Science. – 2017. – С. 012011.
- [2] Eder L.V., Filimonova I.V., Provornaya I.V., Komarova A.V., Nikitenko S.M. New directions for sustainable development of oil and gas industry of Russia: innovative strategies, regional smart specializations, public-private partnership // 17th International Multidisciplinary Scientific GeoConference SGEM 2017 Vienna GREEN. 27-29 November, 2017: Conference Proceedings. - 2017. - Vol. 17, Issue 15. - P. 365-372.
- [3] Eder, L.V., Filimonova, I.V., Nemov, V.Y., Provornaya, I.V. Forecasting of energy and petroleum consumption by motor transport in the regions of the Russian Federation // Economy of Region 13(3), pp. 859-870
- [4] Eder, L.V., Filimonova, I.V., Provornaya, I.V., Nemov, V.U., Nikitenko, S.M. Regional smart specialisations in fostering innovation development of resource regions of Russia // International Multidisciplinary Scientific GeoConference Surveying Geology and Mining Ecology Management, SGEM 17(53), pp. 727-734
- [5] Eder, L.V., Filimonova, I.V., Provornaya, I.V., Nemov, V.Yu. The current state of the petroleum industry and the problems of the development of the Russian economy // IOP Conference Series: Earth and Environmental Science 84(1), 012012
- [6] Kontorovich, A.E., Eder, L.V., Filimonova, I.V., Nikitenko, S.M. Key Problems in the Development of the Power of Siberia Project // Regional Research of Russia 8(1), pp. 92-100 8(2), pp. 74-80
- [7] Eder, L.V., Filimonova, I., Nemov, V., Provornaya, I. Forecasting sustainable development of transport sectors of Russia and EU: Energy consumption and efficiency International Journal of Energy Economics and Policy 8(2), pp. 74-80
- [8] Toews, G., Naumov, A., The Relationship Between Oil Price and Costs In The Oil And Gas Industry (January 2015). OxCarre Research Paper No.152.
- [9] Kilian, L., Not All Oil Price Shocks are Alike: Disentangling Demand and Supply Shocks in the Crude Oil Market (December 2006). CEPR Discussion Paper No. 5994
- [10] Huntington, H.G., Oil Demand and Technical Progress (July 2009). Applied Economic Letters EMF OP 67.



Leontiy V. Eder – Doctor of Economics, Deputy director at Trofimuk Institute of Petroleum Geology and Geophysics SB RAS, Professor at the Department of Economics at Novosibirsk State University. Academic interests include identification of the problems of strategic development of oil and gas industry, determination of priority directions for the formation of the resource base of hydrocarbon and the conditions for its effective use, forecast of the main parameters of development of the oil and gas industry in Russia, issues of regional development of oil and gas producing areas. Author and co-author of more than 400 scientific publications.



Irina V. Provornaya – Candidate of Economics, Senior researcher at Trofimuk Institute of Petroleum Geology and Geophysics SB RAS, Associated Professor at the Department of Economics at Novosibirsk State University. Academic interests include mathematical modeling of the development of oil and gas fields, analysis of methods and directions of oil and gas supplies, analysis of the current state and forecast of the development of world hydrocarbon markets. Author and co-author of more than 90 scientific publications.



Anna A. Kulik – student of the Department of Economics at Novosibirsk State University. Academic interests include financial analysis of company's operations in oil and gas industry. Author and co-author of 5 scientific publications.



Vasily Yu. Nemov – Candidate of Economics, Senior researcher at Trofimuk Institute of Petroleum Geology and Geophysics SB RAS, Associated Professor at the Department of Economics at Novosibirsk State University. Academic interests include analysis of the current state and forecast of the development of the oil and gas markets, forecasting the development of hydrocarbon production, consumption, export and import, analysis of energy efficiency. Author and co-author of more than 40 scientific publications.

Technical, Economic and Fiscal Aspects of Increasing the Efficiency of Development of Oil and Gas Regions in the East of Russia

Irina V. Filimonova^{1,3}, Anna V. Komarova^{2,3}, Mikhail V. Mishenin^{1,3}

¹Trofimuk Institute of Petroleum Geology and Geophysics SB RAS, Novosibirsk, Russia

²Institute of Economics and Industrial Engineering SB RAS, Novosibirsk, Russia

³Novosibirsk State University, Novosibirsk, Russia

Abstract – The article is devoted to the analysis of the influence of the tax system on the development and efficiency of one of the most technologically advanced industries of the Russian economy - the oil and gas sector. It was shown that tax regulation is one of the most important tools for the short-term optimization of the costs of resource users. Calculations were carried out for the selected models in order to identify the main factors of influence on the resulting indicators. For a typical resource development project in Eastern Siberia, the maximum level of the resulting indicators, as well as revenues to regional and local budgets, corresponds to the level of oil prices of 40-45 dollars per barrel. Recommendations for changes in the existing tax system were given in order to stimulate the introduction of high-tech developments in the oil and gas sector, as well as improve the economic efficiency of investment projects.

Index Terms – Technical and economic indicators, efficiency, taxation, oil and gas sector.

I. INTRODUCTION

THE OIL and gas sector is one of the most important high-tech industries in Russia, a driver of growth in the development of high-tech products. Due to the specifics of processes at different stages of the production cycle, the industry generates a great demand for the latest technologies and equipment created in various fields - chemical, physical, geophysical, etc. Also, due to the overflow and multiplicative effects, technological development is spreading across sectors and industries of the economy. A large number of high-tech and highly paid jobs are annually created in the industry [1].

In the current conditions with unstable oil prices and restrictions on the use of foreign technologies and equipment, optimization and cost reduction, as well as the development and use of import substitution technologies at all stages of oil and gas production, are of particular importance [2, 3]. At the same time, the development, testing and introduction of new processes and equipment can take a considerable time, which is the reason for the need to reduce total costs in the short-term period due to other cost categories. One of these categories are tax payments, the regulation of which can be implemented quickly and selectively for individual projects and regions [4].

The most important territorial directions of development for the oil and gas industry in Russia are the regions of

Eastern Siberia and the Far East. In a situation of stagnant and declining production in the traditional regions of Western Siberia and the European part of Russia, which is associated with the depletion of reserves and the deterioration of the quality of the resource base, it is the eastern regions that become the new pole of growth and development not only for the fuel and energy sector but also for the country's economy in general.

However, the natural, climatic and geological characteristics, as well as the quality of recovered hydrocarbons in the region, creates additional technological difficulties, which in turn increases costs for large-scale projects and reduces their economic efficiency. Another development direction is the production of hard-to-extract and non-traditional sources of hydrocarbons in the eastern regions [5].

II. PROBLEM DEFINITION

The aim of the work was to study the impact of the tax payments on the economic effectiveness of long-term investment projects in the oil and gas sector, as well as to analyze the sensitivity of tax deductions for mineral extraction tax (MET) and export duties to changing oil prices.

The stages of the development of some of the most promising resource regions of Russia, which require the use of a large number of high-tech developments - Eastern Siberia and the Far East were analyzed. The necessity of using methods of geological and economic evaluation for the analysis of economic efficiency and ways for costs optimization was justified. Calculations were carried out for the selected models in order to identify the main factors of influence on the resulting indicators. Recommendations for changes in the existing tax system were given in order to stimulate the introduction of high-tech developments in the oil and gas sector, as well as improve the economic efficiency of investment projects.

III. THEORY

A. Stages of Development of Hydrocarbon Resources in the Regions of Eastern Siberia and the Far East

The following researchers studied the quantitative assessment of the size and structure of oil and gas resources: A.E. Kontorovich, L.M. Burstein, A.M. Brekhuntzov, A.I. Varlamov, A.S. Efimov, M.D. Belonin, V.I. Demin, N.A. Krylov, V.R. Livshits, Yu.P. Mironchev, M.S. Modilevsky, Yu.V. Podolsky, G.P. Sverchkov, V.A. Skorobogatov, V.I. Staroselsky, V.S. Staroseltsev, A.A. Trofimuk, V.I. Shpilman et al.

Currently, the regions of Eastern Siberia and the Far East are the most important territorial development area for the Russian oil and gas industry. The extraction in the traditional regions of Western Siberia and the European part of Russia is at a stagnating and falling stage, which is primarily due to the depletion of reserves and the deterioration of the quality of the mineral resource base [6].

Eastern Siberia and the Far East are characterized by significant initial resources - 20% of the total Russian oil resources and 23% of the total Russian gas resources. However, the degree of geological study of the analyzed region remains rather low - 12% for oil and 23% for gas, which indicates a high prospectivity for geological exploration.

The process of active development of energy resources in the region can be divided into two stages. The first phase began in 2008, when large (base) fields - Vankor, Verkhnechonskoye and Talakanskoye, were commissioned in three main oil production centers - Krasnoyarsk, Irkutsk and Yakutsk. The commissioning of the fields became possible after the construction and launch of a special oil port in Kozmino and the ESPO pipeline. During this period, oil production in the East of the country rose up to 13% of total oil production in the country. A distinctive feature of this period was the active decline in oil production of the traditional petroleum regions; primarily in Western Siberia (in the Khanty-Mansiysk Autonomous District), however this decline was compensated by the increase in resource production in the East of Russia.

The second stage of oil and gas resources development in Eastern Siberia and the Republic of Sakha (Yakutia) began in recent years. The period is characterized by the fact that the base fields, which were put into active development during the last 7 years, have reached the planned level of production and are expected to either stabilize or gradually reduce oil production in the coming years. Under these conditions, the main increase in oil production comes from the new oilfields which are located either next to developed petroleum centers (Suzunskoye, Srednebotuobinsky) or next to existing transport infrastructure of the oil pipeline system of the East Siberia-Pacific Ocean (Dulisminskoye, Ayanskoye, Ignyalinskoye and a number of others).

B. Geological and Economic Evaluation of Investment Projects

Geological and economic assessment of natural resources, assessment of economic efficiency of reproduction of mineral resources, assessment of investment projects in the oil and gas sector was developed in the works of the following scientists: I.Kh. Abrikosov, A.A. Arbatov, A.S. Astakhov, Yu.N. Baturin, A.A. Gert, K.G. Goffman, L.P.

Guzhnovsky, G.H. Dickenshtein, A.A. Ilyinsky, S.Ya. Kaganovich, O.S. Krasnov, M.G. Leibson, G.M. Mkrtchyan, V.D. Nalivkin, V.N. Nazarov, P.B. Nikitin, T.S. Novikova, V.P. Orlov, B.V. Robinson, V.I. Tatarenko, N.G. Feitelman, G.G. Shalmina and others.

Geological and economic assessment of the proposed site for development is one of the most important tools for making investment decisions: both the essential choice of the investment object, as well as the time-line of the project implementation, investment amounts and development scenarios. Moreover information on the structure of costs, revenues and resulting indicators helps to choose effective measures to regulate and support the implementation of projects in the key area of the country's economy [7].

The typical site of the North Tunguska region, which is part of the Leno-Tunguska oil and gas province, was chosen as the object of calculation in the study. Geological and economic assessment of the site was carried out using the software complex IPGG-Estimator, developed and adapted for Eastern Siberia at the Center for the Economy of Oil and Gas of IPGG SB RAS.

The sequence of the geological and economic assessment is determined by: the stage of geological exploration and the complexity of development of the prospective oil and gas territory; production profile simulated on the basis of analysis of the structure and quality of resources; forecast of technological indicators; forecast of costs and economic parameters and calculation of criteria of geological and economic efficiency. The planning time-frame is 30 years.

C. Reformation in the Tax System of the Oil and Gas Industry

In recent decades, the tax legislation in Russia has been actively reformed, including taxes received from the operations of the oil and gas sector which are of great importance for the country's economy. For example, the special term "oil and gas revenues" was introduced, which determines the total revenues from specific taxes in the oil and gas industry - the mineral extraction tax and export duties [8, 9].

The main directions for the reformation of the taxation of the oil and gas sector in the current period are:

- Integration and harmonization of the Russian tax system with the systems of taxes and fees of the EAEU countries as an important measure for converging and mutually integrating the economies of the partner countries. Unified export rates will reduce the likelihood of re-export of Russian hydrocarbons in the event that the EAEU countries have lower export duties. Moreover the system of export and import duties should be reorganized in accordance with the agreement on accession to the WTO.

- Reorientation of the operations of companies, primarily in the oil refining sector, from the external to the domestic market, which will increase the share of added value produced domestically and revenues for oil and gas companies, as well as the amount of tax payments and the level of technological development of the industry.

- Diversification of tax rates applied for the oil and gas sector in order to effectively regulate and stimulate the

development of promising areas characterized by complex technical, economic, geological and extraction conditions of resource use.

A significant measure for the taxation system of the oil and gas industry was the introduction of a "tax maneuver" in 2015, implying a gradual increase in mineral extraction tax rates for oil and condensate, while reducing export duties on crude oil and light oil products.

Calculation of tax deductions for mineral extraction tax for oil is based on the base rate, which changes annually, and two main factors, one of which reflects the change in world oil prices, and the second - the extraction characteristics for each facility. The complex coefficient, reflecting the characteristics of production, includes characteristics of the amount of the reserves, the degree of depletion of the site's reserves and the specific deposit, the region of extraction and properties of oil, the degree of extraction complexity.

IV. EXPERIMENTAL RESULTS

Calculation of the tax payments on the basis of the current tax rates for MET and export duties showed that as the price of oil increases, payable amounts for these taxes increase as well as formulas of their calculation suggest a direct dependence on world oil prices. At the same time, if at a price level of 30 dollars per barrel the total share of specific oil and gas taxes in the price was 48%, then with the prices rising to 100 dollars per barrel this share increased to 87%. The high level of the export duty and the MET testifies to the strong sensitivity of the resulting indicators of the implementation of investment projects to the rates of these taxes. That, in turn, justifies the importance of rates changes and the application of tax incentives as a tool to improve the efficiency of oil and gas resources development (Tab. I).

TABLE I
PRICE OF OIL CALCULATED BY NETBACK METHOD

| Indicator | Value, dollar per barrel | | | |
|--|--------------------------|-------------|-------------|-------------|
| Average price of Urals oil | 30 | 50 | 75 | 100 |
| Rate of export customs duty on crude oil | 7.1 | 17.9 | 32.3 | 44.9 |
| Network tariff for oil transportation via ESPO | 3.9 | 4.8 | 7.1 | 9.6 |
| Tariff rate for oil transshipment services in the port of Kozmino | 0.3 | 0.3 | 0.5 | 0.6 |
| Price of oil by the Netback method | 19.4 | 29.2 | 38.0 | 46.5 |
| Operating costs of oil production | 13.9 | 26.3 | 42.3 | 58.1 |
| Including MET | 7.4 | 17.2 | 29.1 | 41.9 |
| Net profit | 5.5 | 2.9 | -4.3 | -11.6 |
| Share of export customs duty and MET in the average price of Urals oil, % | 48% | 70% | 82% | 87% |
| Share of the oil price by the Netback method in average price of Urals oil, % | 65% | 58% | 51% | 47% |

* price of Urals oil corresponding to exchange rate of ruble per the US dollar for the calculation: 30 dollars per barrel - 78 rubles per dollar, 50 dollars per barrel - 65 rubles per dollar, 75 dollars per barrel - 43 rubles per dollar, 100 dollars per barrel - 32 rubles per dollar.

Analysis of the dependence from the dynamics of world prices for each tax separately showed that at \$ 30 dollars per barrel MET contributes more than the customs duty - 25% and 24% respectively. However, with an increase in the price

and an increase in the overall tax burden on the sector, the ratio of tax deposits changes. With an oil price of \$ 50 dollars per barrel the share is 34% for MET and 36% for export duty on oil, at a price of \$ 100 dollars per barrel - 42% and 45% respectively. Both taxes explicitly contain a direct dependence on world oil prices in the calculation formulas (Fig. 1).

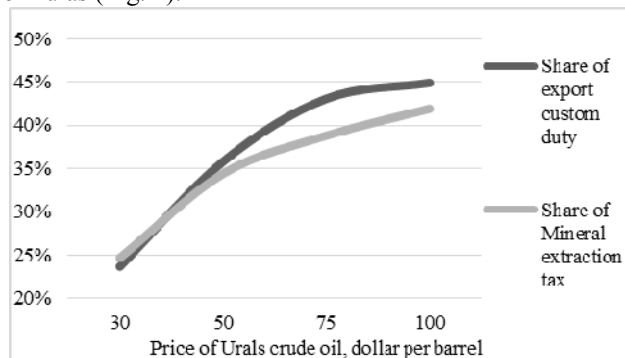


Fig. 1. The dynamics of the change in the share of the mineral extraction tax and the export duty in the price of oil in the world market.

Thus, there is a clear tendency for an accelerating increase in both the overall tax burden and the payments for individual taxes, with an increase in world oil prices. The calculations also took into account the uneven increase in the national currency rate, which follows the increase in oil prices.

To assess the impact of key indicators of the national currency rate and world oil prices on the resulting indicators for the implementation of the investment project, geological and economic modeling of the development of a typical lot of the North Tunguska oil and gas region was carried out. Changes in revenues, capital expenditures and operating costs, including tax payments by budget level, as well as net profit, cash flow (CF), net present value (NPV), internal rate of return (IRR), payback period with and without discounting were calculated. Variations of the indicators were considered depending on changes in oil prices in the range of 30-100 dollars per barrel (Tab. II).

TABLE II
MAIN TECHNICAL AND ECONOMIC
DEVELOPMENT INDICATORS OF THE OILFIELD OF THE
KRASNOYARSK REGION

| Indicator | Market price of oil, dollar per barrel | | | |
|--|--|-------------|-------------|-------------|
| | 30 | 50 | 75 | 100 |
| Oil production, billion tons | 100 | 100 | 100 | 100 |
| Revenues, billion rubles | 1213 | 1529 | 1498 | 1379 |
| Capital investments, billion rubles.. | 298 | 298 | 298 | 298 |
| Exploration | 17 | 17 | 17 | 17 |
| Drilling of the wells | 161 | 161 | 161 | 161 |
| Infrastructure | 72 | 72 | 72 | 72 |
| Transport | 48 | 48 | 48 | 48 |
| Operating costs, billion rubles. | 620 | 875 | 942 | 995 |
| Taxes, billion rubles | 464 | 728 | 779 | 798 |
| Federal budget | 276 | 520 | 605 | 632 |
| Regional budget | 46 | 49 | 44 | 43 |

| | | | | |
|--|------------|------------|------------|------------|
| Local budget | 132 | 149 | 120 | 113 |
| Extrabudgetary funds | 9,5 | 9,5 | 9,5 | 9,5 |
| Profit before income tax, billion rubles | 459 | 532 | 387 | 345 |
| Profit tax, billion rubles | 92 | 106 | 77 | 69 |
| Net profit, billion rubles | 367 | 426 | 310 | 276 |
| CF, billion rubles | 302 | 365 | 247 | 215 |
| NPV, billion rubles | 18 | 39 | 25 | 15 |
| IRR, % | 16,3 | 23,5 | 18,6 | 16 |
| Profitability index | 1,2 | 1,4 | 1,3 | 1,1 |
| Payback period from the beginning of exploration (with discounting) | 18 | 12 | 14 | 13 |
| Payback period from the beginning of development (without discounting) | 15 | 5 | 7 | 6 |

V. DISCUSSION OF RESULTS

The analysis showed that the share of specific taxes in the oil and gas sector, such as mineral extraction tax and export customs duty, can range from 47% to 86% in the average price of oil, which demonstrates the high importance of the tax system as an instrument for regulating the development of this industry.

The study showed that the project's economic efficiency is highly sensitive to changes in exchange rates and oil prices, which have a direct impact on the level of payments of oil and gas taxes. The change in oil prices at an interval of 30-75 dollars per barrel. has the highest level of impact on the resulting indicators of the investment project. At the same time, the price growth on the segment of 75-100 dollars per barrel. has less impact on the effectiveness of the project. The maximum level of net present value, the maximum level of internal rate of return and the minimum payback period corresponds to the level of oil prices of 40-45 dollars per barrel, which can be called the inflection point.

From the point of view of budgetary efficiency, direct dependence of revenues of the federal budget from the oil prices was observed. However, in the case of revenues of regional and local budgets, the picture is similar to the resulting indicators of the project, when the maximum is reached at the inflection point at the level of 40-45 dollars per barrel.

VI. CONCLUSION

In the current conditions of highly volatile oil prices and limited supplies of foreign equipment, one of the effective methods for reducing costs to support the introduction of new technologies for oil and gas production is tax regulation. An optimized tax system and application of tax incentives allows stimulating the development of both a specific industry and individual territories and regions. Moreover the active development of the oil and gas sector in the regions of Eastern Siberia and the Far East can serve as factor for the socio-economic development of the subjects of the Federation in the Siberian and Far Eastern federal districts.

The modern tax system, aimed at reducing the tax payments in conditions of low oil prices, opens up certain opportunities for resource users to improve the efficiency of

investment projects, and in some cases to pass the break-even point.

The dependence of the MET and export duty paid to the federal budget on the change in the price level for oil carries high risks of destabilizing the parameters of the country's economic development and provokes the need to take emergency decisions in the event of a change in the price situation on world markets.

Further reform of fiscal policy should include: (1) the transition to a system that reduces the impact of world oil prices and the dollar's exchange rate on the total amount of tax deductions in order to increase the stability of the financial flows of the implemented projects, and (2) the review of the parameters of the "tax maneuver" in the direction of prioritization of tax incentives for the extraction and sale of hydrocarbon resources for the domestic market.

In the direction of improving the tax legislation, it is necessary to continue the policy of stimulating oil production in the perspective regions on the basis of development and refinement of the parameters of the already existing benefits by following:

1. modification of the timeline for a zero rate for MET, which should be counted from the moment of the beginning of hydrocarbon production, and not from the moment of license granting.

2. Changes in the terms of the preferential rate for export customs duties for the fields of Eastern Siberia and the Far East, which should be applied to the entire volume of oil produced and engaged until the project reaches break-even point.

The study was carried out with the financial support of the Russian Foundation for Basic Research in the framework of the scientific project No. 18-010-01032 and the grant of the President of the Russian Federation MD-6723.2018.6.

REFERENCES

- [1] Eder L.V., Filimonova I.V., Provornaya I.V., Komarova A.V., Nikitenko S.M. New directions for sustainable development of oil and gas industry of Russia: innovative strategies, regional smart specializations, public-private partnership // 17th International Multidisciplinary Scientific GeoConference SGEM 2017 Vienna GREEN. 27-29 November, 2017: Conference Proceedings. - 2017. - Vol. 17, Issue 15. - P. 365-372.
- [2] Eder, L.V., Filimonova, I., Nemov, V., Provornaya, I. Forecasting sustainable development of transport sectors of Russia and EU: Energy consumption and efficiency International Journal of Energy Economics and Policy 8(2), pp. 74-80
- [3] Eder, L.V., Filimonova, I.V., Provornaya, I.V., Nemov, V.Yu. The current state of the petroleum industry and the problems of the development of the Russian economy // IOP Conference Series: Earth and Environmental Science 84(1), 012012
- [4] Lykova, L.N. Tax policy of Russia under the crisis conditions Zhurnal Novoi Ekonomicheskoi Associacii 1(29), pp. 186-192
- [5] Filimonova I.V., Eder L.V., Mishenin M.V., Mamakhmatov T.M. Current state and problems of integrated development of mineral resources base in Russia // В сборнике: IOP Conference Series: Earth and Environmental Science. – 2017. – С. 012011.
- [6] Kontorovich, A.E., Eder, L.V., Filimonova, I.V., Nikitenko, S.M. Key Problems in the Development of the Power of Siberia Project // Regional Research of Russia 8(1), pp. 92-100 8(2), pp. 74-80

- [7] Eder, L.V., Filimonova, I.V., Provornaya, I.V., Nemov, V.U., Nikitenko, S.M. Regional smart specialisations in fostering innovation development of resource regions of Russia // International Multidisciplinary Scientific GeoConference Surveying Geology and Mining Ecology Management, SGEM 17(53), pp. 727-734
- [8] Eder, L.V., Filimonova, I.V., Nemov, V.Y., Provornaya, I.V. Forecasting of energy and petroleum consumption by motor transport in the regions of the Russian Federation // Economy of Region 13(3), pp. 859-870
- [9] Smirnova, N.V., Rudenko, G.V. Priorities for improving taxation in oil industry in Russia Indian Journal of Science and Technology 9(19),93907



Irina V. Filimonova – Doctor of Economics, Leading researcher at the Trofimuk Institute of Petroleum Geology and Geophysics SB RAS, Professor and head of the chair at the Department of Economics at Novosibirsk State University. Academic interests include: strategic planning and development of Russia's oil and gas industry, geological and economic assessment of reserves and resources, incl. unconventional hydrocarbon resources, the reproduction of the mineral resource base and the forecast for oil and gas production, primarily in Eastern Siberia, the Far East, the Arctic, state regulation of the fuel and energy sector in Russia and the Asia-Pacific countries. Author and co-author of more than 250 scientific publications.



Anna V. Komarova – Researcher at the Institute of Economics and Industrial Engineering SB RAS, Senior lecturer at the Department of Economics at Novosibirsk State University. Academic interests include assessment of investment projects in the oil and gas sector, use of modern technologies in the oil and gas industry, institutional changes in the oil and gas industry, taxation of the fuel and energy sector, socio-economic development of resource regions. Author and co-author of more than 40 scientific publications.



Mikhail V. Mishenin – Candidate of Economic Sciences, Senior researcher at the Trofimuk Institute of Petroleum Geology and Geophysics SB RAS, Associated professor at the Department of Economics at Novosibirsk State University. Academic interests include analysis of the structure and quality of the resource base of hydrocarbon reserves and resources; analysis of licensed policy; geological and economic assessment of hydrocarbon resources and reserves, assessment of the effectiveness of the formation and development of the pipeline system for oil and products of its processing. Author and co-author of more than 50 scientific publications.

Dependence of Wages on the Duration of Training and Length of Service in the Russian Economy Sectors

Ilya N. Karelin

Novosibirsk State Technical University, Novosibirsk, Russia

Abstract – The paper studies an influence of such characteristics of human capital as the duration of training and length of service on wages of workers in the Russian economy sectors. It is shown that in 2016, industries whose development under current conditions greatly depends on the human capital of the highest level as a rule do not attract specialists as the accumulation of human capital leads to a fairly low wage growth.

Index Terms – Human capital, individual return on education, return on length of service, sectors of the economy.

I. INTRODUCTION

IN COMPLIANCE with the strategy of scientific and technological development of the Russian Federation approved by the order of President Vladimir Putin No. 642 of 1 December 2016 scientific and technological development of the Russian economy is considered one of the priorities of the state policy [1]. This strategy is aimed to ensure independence and competitiveness of the country by creating an efficient system of reproduction and by an efficient use of the intellectual potential of the nation. To implement this goal it is necessary to fulfill such tasks as to create opportunities for finding talented young people and creating conditions for them to make a successful career in the field of science, technology and innovations and to carry out research and development work corresponding to up-to-date principles of the organization of research and innovation activities. It is also necessary to increase the receptivity and readiness of the economy and society in general to accept and introduce innovations.

To monitor the implementation of this strategy a list of realization indicators including the evaluation of the influence of science and technology on the socio-economic development, on the condition and efficiency of science, technologies and innovations, on the quality of government regulation and service support of scientific, research and innovation activities is drawn up.

It is obvious that one of the important indicators relating to the implementation of the strategy is the attractiveness of economic sectors and industries whose activity greatly depends on scientific and technological progress to young specialists.

Innovation-driven development of industry aimed at providing economic growth and economic development is a

priority task for Russia. However, most industries yield quite poor results. It can be explained both by the lack of up-to-date technologies in corresponding industries and the lack of necessary skills to produce and use new technologies. An efficient use of human capital could accelerate the development of industry due to a more active introduction of innovation technologies, which could promote the development of the economy as a whole.

It is supposed that increasing the level of work force training will improve their professional skills, which in turn will have a positive effect on the development of industry and the economy as a whole.

II. PROBLEM DEFINITION

The problem of a human capital influence on both macroeconomic and microeconomic indicators, such as, for example workers' wages or incomes, is one of the most discussed problems in the economic literature on human capital. In particular, private return on education in countries, regions and professions is evaluated at the microeconomic level. The task of this paper is to test the availability of human capital and to evaluate the degree of dependence of human capital (i.e. education and the length of service) in the Russian economic sectors on workers' wages. Based on the results of calculations it will be possible to propose a classification of the Russian economy sectors according to the degree of the human capital influence on wages. This will make it possible to evaluate an economic significance of education and the degree of involvement of the personnel in these sectors in scientific and technological progress and in generating a knowledge-driven economy.

III. THEORY

Theoretical reasons for the capacity of skills and technologies to promote industrial growth were grounded in works on neoclassical models of growth. For example, according to the traditional neoclassical growth theory industrial growth is caused by one or more of the three factors which include an increase in the work force (due to the population and education growth), an increase in capital (through savings and investments) and technological improvements. According to the Solow growth model a long-term growth occurs because of the exogenous effect of

technological progress which leads to a rise in labor productivity [2]. However, endogenous growth models assume that industrial growth depends on the mechanism which includes human capital, physical capital, technological efficiency, and labor force management but not external factors [3, 4, 5].

Direct and indirect relationships between human capital and industrial development were analyzed in a number of studies. Industrialization is considered to be one of the most efficient means to achieve such objectives as improvement in well-being, provision of employment, an increase in consumer and capital goods production as well as expanding the choice for people in general. Industrial development characterized by a positive effect of the scale of production increases demand for qualified personnel, innovative methods of management, innovation technologies and other sources of increasing labor efficiency. Therefore modern economy faces an acute necessity to acquire knowledge and to increase the number of educated and skilled people having experience in various fields of activity as it plays a decisive role for a sustainable growth and social development.

Benhabib and M. Spiegel in [6] analyzed the role of human capital in economic development and the causes of cross-country differences in performance levels of labor and technologies applied in economies. They show that the role of human capital is to promote the introduction of advanced foreign technologies and the creation of domestic technologies.

J. Mayer [7] in his research “Technology Diffusion, Human Capital and Economic Growth in Developing Countries” (2001) studied the role of importing equipment in both developed and developing countries based on the experience of empirical study and development to assess the transfer of technologies to developing countries. The results of such empirical studies testify that the import of equipment combined with human capital reserves in the economy positively and statistically significantly explain differences in growth rates among countries. This empirically confirms theoretical substantiation of the role of human capital and technologies in the economic growth.

A. Ashishand S. Badge [8] studied the importance of a qualified labor force in the development of the Indian software industry in the period from 1990 to 2003. Using the panel analysis methods with fixed effects they found out that professional abilities and skills of engineers holding B Sc degrees had a significant influence on the software export. They also found out that it was private but not state colleges that had the greatest influence on improving the skills and qualification of engineers and programmers.

Guisan (2005) [9] studied the situation with human capital, population growth and industrial development in Mexico and Turkey as compared with other counties of OECD in the period from 1964 and 2004. It was shown that in comparison with the level of human capital development, growth of population, industry and trade both countries could have a higher growth of the real GDP per capita if they had a higher level of secondary education. The author considers important to note that improvements in education will have positive consequences for increasing both the productive and

nonproductive real value added cost per capita in these countries.

K. Abdul, N. Al-Huda и A. Shabbir [10] studied the human capital components and discussed their role in achieving sustainable industrial development. A model of a dynamic development of the industrial sector in Malaysia which covered the period from 1981 to 2010 was developed for the purpose of an empirical analysis. In conclusion to the paper the authors emphasized a special value of human capital as the GDP variable of the manufacturing industry has the highest elasticity in terms of variable employment. This is caused by the labor performance growth due to investments in human capital in the fields of education and public health.

An increase in the number of jobs is expected to lead to an increase in the production output to satisfy the market demand of local residents and export. In addition, increasing labor efficiency decreases production costs while investments in education and public health programs help to improve skills and knowledge as well as provide opportunities for workers in this sector.

E.A. Anikina and V.I. Chechina [11] analyze indicators which serve to evaluate the return on investments in education. The authors calculated a current norm of return on investments in education by the formula $R = (Y_n - X_0)/C_n$, where Y_n is the earnings of a person having n years of training; X_0 is earnings of a person with no training; C_n is the volume of investment during n years of training. In 2005, this indicator for higher education amounted to 0.71; in 2009, it was 0.75. When life earnings were used, this ratio amounted to 1.307 in 2005; it was 1.236 in 2009 and 1.245 in 2013. In conclusion, the authors notice a significant correlation of earnings, education and age, with the last dependence being U-like, which presupposes the availability of maximal earnings at a certain age.

IV. EXPERIMENTAL RESULTS

To test the above relationship, the method proposed by Mincer and used, for example, by A.V. Koritsky in his paper [12] will be used. In this paper an influence of human capital on various economic indicators is analyzed. An evident advantage of the methodology is its simplicity in interpreting the obtained indicators.

The logarithm of average earnings of the i^{th} person $LN(W_i)$ is a dependent variable. The constructed human capital measures such as the duration of training (H_i), length of service of a person EXP_i and its square EXP_i^2 are used as independent variables.

To take into account inter-industry differences, parameters of the regression equation will be evaluated for every sector due to which we will be able to compare the influence of human capital components in various sectors.

The Mincer equation relating the earnings logarithm to other explanatory variables will be the basic regression equation to test the hypothesis. Thus, the evaluated regression equation will have the following form:

$$LN(W_i) = \alpha + \beta H_i + \gamma EXP_i + \delta EXP_i^2 + e_i, \quad (1)$$

where $LN(W_i)$ is a natural logarithm of an average wage of the i^{th} individual for the past six months in rubles;

H_i is the duration of training of an individual in years at the moment of questioning;

EXP_i is the length of service of the i^{th} individual in years;

α is a constant having the meaning of the average earning logarithm in rubles for individuals with no education

β is the coefficient for the duration of training;

γ is the coefficient for the duration for the length of service in years;

δ is the coefficient for the length of service squared;

e_i is an error of the regression equation

The coefficients β, γ, δ are interpreted as a relative increase in % or portions of the unit of average earnings when the duration of training or the length of service are increased by 1 year.

The following results can be expected:

- 1) the coefficient β will be significant and positive;
- 2) the coefficient γ will be significant and positive;
- 3) the coefficient δ will be significant and negative.

The information base was formed as a result of the longitudinal survey of households during the Russian monitoring of the economic situation and the health of the population carried out by the National Research University of the Higher School of Economics. This survey is a series of annual nation-wide representative inquiries based on the probability stratified multi-stage territorial sample developed jointly with leading world experts in this field [13].

Quite many types of training without mentioning its duration were presented in the survey. The duration was calculated as follows: the duration of full secondary education was taken equal to 11 years, the duration of the B Sc program was taken equal to 4 years, the duration of the postgraduate program was taken equal to 5 years (together with the M Sc program – 2 years), the duration of the secondary vocational education in a technical school was taken equal to 3 years. Half of the duration of the corresponding nominal level was used as the duration of incomplete education.

The length of service was obtained as a difference between the age and the duration of training with the deduction of 6 years [12].

Calculations were made for 30 industries included in the questionnaire. It should be mentioned that the aim of the authors of the survey was not to bring the industries under study into line with the classification of the main types of economic activity.

Questionnaire data of the 25th wave of 2016 were used for calculations as to all individuals. Individuals who failed to give correct answers about their average earnings for the past six months, their educational level, the industry they work in and their length of service were excluded from calculations. As a result, 6,916 values of variables were obtained (Tab. I).

The constant α is given in the 1st column; the coefficient β (with the duration of training) is given in the 2nd column; the coefficient γ (with the length of service) is given in the 3^d column and the coefficient δ (with the length of service squared) is given in the 4th column of Table I. The determinacy coefficient (R^2) is given in the 5th column; the

number of individuals included in the final sample is given in the 6th column and the industry code is given in the 7th column. Calculations concerning religious organizations (code 22) and social organizations (code 32) in view of a very small number of observations (4 and 3 correspondingly) were not included in the Table.

TABLE I
RESULTS OF CALCULATION OF EQUATION
PARAMETERS (1)

| α | β | γ | δ | R^2 | N | industry |
|---------------------|-------------------|-------------------|-------------------|-------|------|----------|
| 1 | 2 | 3 | 4 | 5 | 6 | 7 |
| 8.70*** (0.22) | 0.08*** (0.01) | 0.02*** (0.01) | 0.00*** (0.00) | 0.10 | 438 | 1 |
| 9.33*** (0.32) | 0.04* (0.02) | 0.02** (0.01) | 0.00** (0.00) | 0.08 | 182 | 2 |
| 9.72*** (0.39) | 0.04 (0.02) | -0.01 (0.01) | 0.00 (0.00) | 0.02 | 187 | 3 |
| 9.41*** (0.34) | 0.06*** (0.02) | 0.02 (0.01) | 0.00 (0.00) | 0.05 | 227 | 4 |
| 9.31*** (0.29) | 0.05*** (0.02) | 0.01 (0.01) | 0.00 (0.00) | 0.05 | 225 | 5 |
| 9.43*** (0.20) | 0.05*** (0.01) | 0.02*** (0.01) | 0.00*** (0.00) | 0.08 | 469 | 6 |
| 9.65*** (0.21) | 0.03** (0.01) | 0.02*** (0.01) | 0.00** (0.00) | 0.04 | 607 | 7 |
| 9.25*** (0.25) | 0.03** (0.02) | 0.00 (0.01) | 0.00 (0.00) | 0.04 | 236 | 8 |
| 6.52*** (0.53) | 0.20*** (0.03) | 0.03*** (0.01) | 0.00*** (0.00) | 0.2 | 183 | 9 |
| 7.99*** (0.17) | 0.10*** (0.01) | 0.03*** (0.01) | 0.00*** (0.00) | 0.13 | 779 | 10 |
| 7.64*** (0.47) | 0.14*** (0.03) | 0.02 (0.02) | 0.00** (0.00) | 0.13 | 206 | 11 |
| 8.46*** (0.20) | 0.10*** (0.01) | 0.01 (0.01) | 0.00 (0.00*) | 0.12 | 566 | 12 |
| 8.33*** (0.29) | 0.09*** (0.02) | 0.06*** (0.01) | 0.00*** (0.00) | 0.25 | 356 | 13 |
| 8.92*** (0.14) | 0.06*** (0.01) | 0.02*** (0.01) | 0.00*** (0.00) | 0.06 | 1322 | 14 |
| 7.23*** (0.83) | 0.18*** (0.06) | 0.04* (0.02) | 0.00* (0.00) | 0.07 | 177 | 15 |
| 9.74*** (0.45) | 0.04 (0.03) | 0.00 (0.02) | 0.00 (0.00) | 0.14 | 14 | 16 |
| 9.43*** (0.28) | 0.05*** (0.02) | -0.01 (0.01) | 0.00 (0.00) | 0.10 | 249 | 17 |
| 7.82*** (1.56) | 0.15 (0.10) | 0.03 (0.05) | 0.00 (0.00) | 0.10 | 29 | 18 |
| 8.74*** (2.15) | 0.02 (0.14) | 0.02 (0.07) | 0.00 (0.00) | 0.01 | 42 | 20 |
| 10.48*** (1.61) | -0.04 (0.11) | 0.03 (0.03) | 0.00 (0.00) | 0.07 | 28 | 21 |
| 10.46*** (0.84) | -0.03 (0.06) | 0.00 (0.03) | 0.00 (0.00) | 0.13 | 35 | 23 |
| 10.12*** (0.64*) | -0.02 (0.04) | 0.01 (0.03) | 0.00 (0.00) | 0.10 | 47 | 24 |
| 8.61*** (1.07) | 0.11 (0.07) | 0.01 (0.03) | 0.00 (0.00) | 0.23 | 33 | 25 |
| 7.67*** (0.81) | 0.10** (0.05) | 0.10*** (0.03) | 0.00*** (0.00) | 0.34 | 36 | 26 |
| 11.94 (8.25) | -0.17 (0.55) | 0.10 (0.11) | 0.00*** (0.00) | 0.01 | 33 | 27 |
| 7.82 (2.86) | 0.09 (0.18) | 0.12 (0.06) | 0.00 (0.00) | 0.83 | 5 | 28 |
| 5.00** (1.63) | 0.35** (0.12) | 0.16** (0.05) | 0.00*** (0.00) | 0.87 | 8 | 29 |
| 9.67*** (1.31) | -0.02 (0.09) | 0.11*** (0.04) | 0.00*** (0.00) | 0.2 | 36 | 30 |

| | | | | | | |
|--------------------|-----------------|------------------|-------------------|------|----|----|
| 10.81*** (1.48) | -0.17 (0.13) | 0.37** (0.14) | -0.02** (0.01) | 0.45 | 14 | 31 |
|--------------------|-----------------|------------------|-------------------|------|----|----|

Notes: robust standard errors are shown in brackets. * is the significance level of 10%; ** is the significance level of 5%; *** is the significance level of 1%.

V. RESULTS AND DISCUSSION

It is seen from the Table that the estimates of the constant are significant everywhere in the range from 5 to 12 excluding industries 27 and 28. The estimates of the coefficients with a variable duration of training are significant and positive in the range from -0.17 to 0.35 in many sectors.

The coefficients with the length of service are in the range from -0.01 to 0.73 and are significant only in 12 sectors such as food processing industry, civil engineering, building, transport, government bodies, education, army, trade, finances, public services, public catering and mass media.

In general, the determinacy coefficients of the models obtained are rather low, which shows that there are unaccounted factors affecting wages of workers.

The values of coefficients with the duration of training as a whole are approximately similar to those in other studies [14], which proves the validity of the repeated calculations.

Then the table was sorted out by the coefficient β after excluding sectors with negligible coefficients and divided into 3 groups based on the range of values of this coefficient: 1) from 0.03 to 0.088; 2) from 0.088 to 0.14; 3) from 0.14 to 0.12 (Tab. II).

TABLE II
SELECTED CALCULATION DATA FROM TABLE I

| group | α | β | industry |
|-------|----------|---------|--------------------------------------|
| 1 | 9.25*** | 0.03** | agriculture |
| | 9.65*** | 0.03** | transport, communication, |
| | 9.33*** | 0.04* | civil engineering |
| | 9.31*** | 0.05*** | heavy industry |
| | 9.43*** | 0.05*** | housing and communal services |
| | 9.43*** | 0.05*** | building |
| | 9.41*** | 0.06*** | oil and gas industry |
| | 8.92*** | 0.06*** | trade, public services |
| | 8.7*** | 0.08*** | light and food processing industries |
| 2 | 8.33*** | 0.09*** | army, MIA, security bodies |
| | 7.67*** | 0.1** | services to population |
| | 8.46*** | 0.1 | public health |
| | 7.99*** | 0.1 | education |
| | 7.64*** | 0.14 | science and culture |
| 3 | 7.23*** | 0.18 | finances |
| | 6.52*** | 0.2 | government bodies |

Nine sectors were included in the first group, with many of them being in the industry scope. An increase in the duration of training by 1 year in this group is related to a fairly low growth of average wages from 3% to 8%. This group of industries can be characterized as industries with a low return

on the duration of training. It is clear that these are mainly industries of material production.

Five sectors namely army, public services, education, public health and science were included in the second group. An increase in the duration of training by 1 year in this group leads to a relatively low growth of average wages from 9% to 14%. This group of industries can be characterized as industries with an average return on the duration of training. These sectors are related to providing various services.

Two sectors, namely finances and government bodies, were included in the third group. An increase in the duration of training by 1 year in this group leads to a fairly high growth of average wages from 14% to 20%. This group of industries can be characterized as sectors with a high return on the duration of training. These sectors are related to administration and resource allocation.

Coefficients with the length of service were in the range from -0.01 to 0.73. When sectors in which this coefficient is insignificant are excluded, twelve sectors remain. The results are given in Table III.

TABLE III
INDUSTRIES WITH THE SIGNIFICANCE COEFFICIENT γ
WITH THE LENGTH OF SERVICE

| group | α | γ | industry |
|-------|----------|----------|--------------------------------------|
| 1 | 8.7 | 0.02 | light and food processing industries |
| | 9.33 | 0.02 | civil engineering |
| | 9.43 | 0.02 | building |
| | 9.65 | 0.02 | transport, communication |
| | 8.92 | 0.02 | trade |
| | 6.52 | 0.03 | government bodies |
| | 7.99 | 0.03 | education |
| 2 | 7.23 | 0.04 | finances |
| | 8.33 | 0.06 | security bodies |
| 3 | 7.67 | 0.1 | public services |
| | 9.67 | 0.11 | mass media |
| | 5 | 0.16 | public catering facilities |

These sectors can also be classified based the degree of the effect of the length of service on the level of wages.

Seven sectors with a low return on the length of service (in the range from 2% to 4% for 1 year of service record) are included in the first group of sectors.

Two sectors with an average return on the length of service are included in the second group and two sectors are included in the third group where an additional year of service record is related to an increase in average wages in the range from 11% to 16%. These groups cannot be placed in advance in any classified group but it can be noticed that several material production industries are in the upper part of the table and immaterial production industries follow them.

VI. SUMMARY AND CONCLUSIONS

The effect of both the duration of training and the length of service on average wages in the economic sectors of the

Russian Federation based on the data of the sampling survey conducted in 2016 is positive and in the majority of sectors significant. The results in the sectors poorly represented by respondents were insignificant (up to 50 values).

It can be concluded that the highest value of the human capital return is observed in the sectors of immaterial production where there is the highest degree relationship between the education level and the length of service of workers and the level of their wages. Unfortunately, the major industries of material production (mining and processing industries, building, agriculture and housing and communal services) belong to the group of sectors with the lowest degree of relationship between education and wages. In these sectors, as we can assume, there is a need to introduce new technologies and to use highly skilled labor force. These sectors do not seem professionally attractive to talented young people because of low financial benefits offered to them in these sectors.

This situation hampers the implementation of the strategy of scientific and technological development. It is clear that there is a need to develop and realize various methods of the government policy which promote the development of up-to-date science-intensive industries in Russia where highly skilled engineers and qualified scientists work.

Hence, Russian industry obviously needs further development of human capital, which is an essential prerequisite to its successful growth. It is necessary by means of a carefully developed government policy to encourage cooperation between the private sector and concerned educational institutions to improve and raise the level of human skills and abilities in the field of industrial activity, for example by means of tax concessions.

To gain competitive advantages in these industries jobs which require high skills at the level of secondary and higher professional education should be created. The need to create such jobs should be understood and comprehended by not only government bodies but also by owners and managers of these enterprises. Otherwise the Russian Federation will lose its last advantages and will be in a suspended state under conditions of certain Western sanctions.

VII. ACKNOWLEDGMENT

We are grateful to reviewers for valuable remarks and support of this research.

The results of research were received within performance of the state task of the Ministry of Education and Science of the Russian Federation, the project 26.2024.2017/4.6.

REFERENCES

- [1] <http://www.kremlin.ru/acts/bank/41449>
- [2] R. Solow, "A Contribution to the Theory of Economic Growth," *Quarterly Journal of Economics*, Vol. 70, No. 1, 1956, pp. 65-94
- [3] P. M. Romer, "Endogenous Technological Change," *Journal of Political Economy*, Vol. 98, No. 5, 1990, pp. S71- S102. <http://dx.doi.org/10.1086/261725>
- [4] R. Lucas, "On the Mechanics of Economic Development," *Journal of Monetary Economics*, Vol. 22, No. 1, 1988, pp. 3-42.
- [5] R. Barro, "Economic Growth in a Cross-Section of Countries," *Quarterly Journal of Economics*, Vol. 106, No. 11, 1991, pp. 407-443.
- [6] Benhabib and M. Spiegel, "Role of Human Capital in Economic Development: Evidence from Aggregate Cross-Country Data," *Journal of Monetary Economics*, Vol. 34, No. 2, 1994, pp. 142-173.
- [7] J. Mayer, "Technology Diffusion, Human Capital and Economic Growth in Developing Countries," *United Nations Conference on Trade and Development (UNCTAD)*, No. 154, 2001
- [8] A. Ashish and S. Badge, "Private Investment in Human Capital and Industrial Development; The Case of the Indian Software Industry," *Regional Comparative Advantage and Knowledge Based Entrepreneurship*, Working Paper, No. 55, 2008.
- [9] M. C. Guisan, "Human Capital, Population Growth and Industrial Development in Mexico and Turkey. A Comparative Analysis with Other OECD Countries, 1964-2004," *Working Paper*, No. 2, 2005
- [10] K. Abdul, N. Al-Huda and A. Shabbir, "Human Capital and the Development of Manufacturing Sector in Malaysia," *Social Science Research Network*, 2012
- [11] Otsenka effektivnosti investitsii v obrazovanie v rossii s pozitivnoi tendentsiei. Anikina E.A., Chechina V.I. V sbornike: *Ekonomika i upravlenie: problemy i perspektivy* Materialy vserossiiskoi nauchno-prakticheskoi konferentsii. 2017. S. 17-21.
- [12] Koritskii, Aleksei Vladimirovich. *Chelovecheskii kapital kak faktor ekonomicheskogo rosta regionov Rossii* [Tekst] : monografiya / A. V. Koritskii ; nauch. red. T. V. Grigorova ; Sibirskii un-t potrebitel'skoi koop. - Novosibirsk : SibUPK, 2010. - 363, [1] s. : tabl.; 20 sm.; ISBN 978-53-34-00054-4
- [13] Rossiiskii monitoring ekonomicheskogo polozheniya i zdorov'ya naseleniya NIU-VShE (RLMS-HSE)), provodimiy Natsional'nym issledovatel'skim universitetom "Vysshaya shkola ekonomiki" i OOO «Demoskop» pri uchastii Tsentra narodonaseleniya Universiteta Severnoi Karoliny v Chapel Khille i Instituta sotsiologii Federal'nogo nauchno-issledovatel'skogo sotsiologicheskogo tsentra RAN. (Saity obsledovaniya RLMS-HSE: <http://www.cpc.unc.edu/projects/rlms> i <http://www.hse.ru/rlms>)
- [14] Berndt E.R. *Praktika ekonometriki: klassika i sovremennost' + primery*. God vypuska: 2005 Izdatel'stvo: YuNITI-DANA Seriya: Zarubezhnyi uchebnik ISBN: 5-238-00859-7 Yazyk: Russkii



Karelin Ilya Nikolaevich (b.1982), assistant professor, department of economic theory and applied economics, NSTU.

His research interests are currently focused on theoretical and methodological bases of monitoring the development of economic systems of the national economy.

He is the author of 21 publications.

E-mail: karelin-iliya@yandex.ru

On the Implementation of Innovative Projects. The Effect of the Investment Leverage

Yury V. Kirillov, Evgeniya V. Dragunova, Anatoly V. Kravchenko
Novosibirsk State Technical University, Novosibirsk, Russia

Abstract – This article presents the construction of mathematical models for estimating the economic conditions in which positive effect is possible for using loan capital, for implementation of investment projects leading to the growth of net present value (NPV). The authors obtained economic and mathematical calculations that allow linking the parameters of innovation and investment projects (the norm of the investor's profitability, the cost of loan capital, the time of its entry into the financial and time frame of the project, the time of the beginning of repayment of the financial obligations, duration of project). These parameters determine the effect of NPV index growth. This effect is related to the favorable conditions for loan capital raising in comparison with financing only by own funds. The authors obtained an analytical expression that determines at which point in time the loan capital should be entered into the financial and time frame of the project implementation, in order for the NPV index to increase its value. Also, the authors found out what should be the cost of the loan capital, so that its attraction would give the effect of an increase in the NPV index. The mathematical relations and the economic conclusions drawn on their basis are backed by practical results, given in a graphic form.

Index Terms – Investments, net value, cost of capital.

I. INTRODUCTION

ONE of the important trends in economic development at the present stage is innovation. The well-known foreign economic restrictions of the last time should also contribute to a "turning" of the economy onto the rails of innovative development, which will later ensure the achievement of the goals set in the strategic program [1] in order to ensure national economic security and strengthen the competitiveness of our country in foreign markets.

From the point of view of achieving the final result, innovation activity can be viewed as the process of implementing a special investment project [2], the effectiveness of which is estimated, first of all, by the index of reduced net income [3]. The main feature for high-tech industries (undoubtedly, electronic instrument engineering may be classified as one of them) is having DDP phase in investment part of the project. In Russian Federation investment in DDP hasn't exceeded 1.1% of GDP. Improvement in the rate of investment hasn't been changing significantly for past few years, and it still hasn't reached its pre-crisis level (comparing to 2009 and 2002, when the rate was equal to 1.25% of GDP). Among BRICS countries, Russia is far below China, comparing the rate of inner investment in DDP (2.1% of GDP), but ahead of South Africa (0.7%) and India (0.6%). The rate of investment is equal to Brazil (1.2%).

As mentioned in the report "Will stronger borders weaken innovation", the rate of investment in DDP in total revenues of companies from the USA, Germany, Japan and Switzerland increased on 4.5% in 2017. The given data testify that financing of investment projects related to the development and implementation of innovative technologies should be increased. That is why, in modern conditions, along with the importance of implementing innovation and investment projects, it is equally topical to decide the issue of assessing the effectiveness of such projects.

The issues of assessing the effectiveness of innovations are examined in sufficient detail in the modern economic literature. In the Russian literature, the effectiveness of innovation is associated with an assessment of the effectiveness of investment taking into account the level of risk [2, 4], as well as estimates of the capital structure adopted in financial management [5]. In the foreign literature, these approaches are represented either by reforming organizational structure associated with the introduction of the stage of R&D [6–10], or classical assessments based on the theory of capital structure [11–16], or by determining the indicator of investment efficiency under the conditions risk management [17–20].

The common point of these approaches is that the efficiency of innovations is estimated, first of all, by the NPV, however the standard algorithm of its calculation does not take into account the structure of the investment capital of the project. In real innovative projects very often, with a lack of own funds, loan capital is attracted, which, on the one hand, makes it possible to realize the investment part of the project, but, on the other hand, reduces its revenue payments by paying off the financial obligations. That is why the assessment of the impact of borrowed capital (taking into account the cost of loan capital, the time of its entry into the financial and time frame of the project implementation) becomes particularly relevant when deciding the issue of assessing the effectiveness of innovation.

II. PROBLEM DEFINITION

It is necessary to assess the impact which is using the loan capital (LC) on the net present value of the project (NPV). To solve this problem, it is necessary to give quantitative estimates when answering the following questions:

- 1) at which point in time, the LC should be entered into the financial and time frame of the project implementation, in order for the NPV index to increase its value;
- 2) what should be the cost of the LC, so that its attraction would give the effect of an increase in the NPV index.

By analogy with the classical statement of the capital structure problem, the quantitative assessment of which is expressed by the known equation of the effect of the financial leverage [21, 22], the increase in the NPV index when introduced into the project LC can be called the **investment leverage effect (ILE)**.

III. THEORY

Obviously, the quantitative assessment of the ILE will be determined by the financial temporary chart of the project implementation, therefore we would consider the scheme of its implementation in Fig. 1 as the most frequently used in practice:

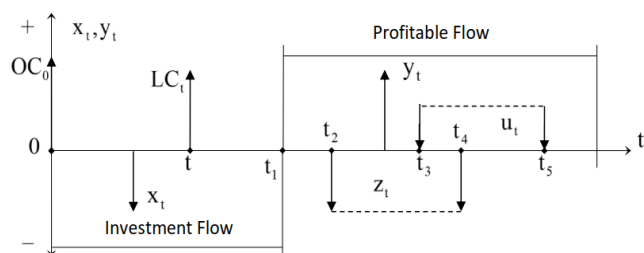


Fig. 1. Generic scheme for implementation of investment project.

In accordance with the mathematical calculations performed for such projects by the rules of financial mathematics, the NPV indicator will be determined by the present value of the corresponding project payments:

$$NPV(x_t, y_t) = P_0(y_t) + P_0(LC_t) - [P_0(x_t) + P_0(z_t) + P_0(u_t)], \quad (1)$$

where $P_0(y_t)$ and $P_0(x_t)$ – net value to the beginning of the project costs of its inflows and outflows, respectively; $P_0(LC_t)$ – net value to the beginning of the project costs at the moment t of the LC; $P_0(z_t)$ and $P_0(u_t)$ – net value to the beginning of the project costs of payments for the repayment of LC_t and payment to the owners OC_0 , respectively.

Write down (1) in the next form:

$$NPV(x_t, y_t) = [P_0(y_t) - P_0(x_t)] + [P_0(LC_t) - P_0(z_t) - P_0(u_t)],$$

then $P_0(y_t) - P_0(x_t) = NPV_0$ it can be considered as the base rates of present value calculated on the basis of the rates of inflows y_t and outflows x_t in the business plan of the project, but $P_0(LC_t) - P_0(z_t) - P_0(u_t) = \Delta NPV_t$ – as an increase in present value due to the using of the loan capital in the project LC_t with the costs of the OC_0 . As a result, equation (1) can be represented in the form:

$$NPV(x_t, y_t) = NPV_t = NPV_0 + \Delta NPV_t.$$

It is obvious that the increase in the present value of the project through the using of loan capital will be provided if $\Delta NPV_t > 0$, then the condition $\Delta NPV_t = 0$ will determine

the *limiting* or *critical* values of the project parameters under which ILE occurs.

Firstly, we consider the case of using free OC_0 , when u_t and, respectively $P_0(u_t) = 0$. If the rate of return on an investor i_0 and the cost of loan capital, for example, on a loan LC_t in the form of a rate of interest r , so

$$P_0(LC_t) = \frac{LC_t}{(1+i_0)^t}, \quad P_0(z_t) = \sum_{t_2}^{t_4} \frac{z_t}{(1+i_0)^t},$$

then the limiting condition for ILE in general for an investment project:

$$\frac{LC_t}{(1+i_0)^t} = \sum_{t_2}^{t_4} \frac{z_t}{(1+i_0)^t}, \quad (2)$$

$$\text{so that } LC_t = \sum_{t_2}^{t_4} \frac{z_t}{(1+r)^t}.$$

In practice, the flow of repayment payments, as a rule, is an annuity, and, for the overwhelming number of cases, in the form of a postnumbered rent – $Po(1,1)$ – with annual payments $z_t = z = \text{const}$ and annual accrual of interest at a rate r . Then on the base on rules of financial mathematic for $Po(1,1)$ common condition (2) for ILE can be written down in correct form:

$$\frac{LC_t}{(1+i_0)^t} = z \cdot \frac{[1 - (1+i_0)^{-(t_4-t_2)}]}{i_0} \cdot \frac{1}{(1+i_0)^{t_2}},$$

$$\text{so that } LC_t = z \cdot \frac{[1 - (1+r)^{-(t_4-t_2)}]}{r} \cdot \frac{1}{(1+r)^{(t_2-t)}}.$$

Having expressed here z through LC_t and performed simple transformations, we get the following expression:

$$\Delta NPV_t = \frac{LC_t}{(1+i_0)^t} - \frac{LC_t \cdot r \cdot (1+r)^{(t_2-t)}}{[1 - (1+r)^{-(t_4-t_2)}]} \times \frac{[1 - (1+i_0)^{-(t_4-t_2)}]}{i_0 \cdot (1+i_0)^{t_2}} \quad (3)$$

which determines the ratio of the parameters of the investment project under which the conditions for the emergence of ILE are created, if the flow of repayment payments – $Po(1,1)$.

If the right part (3) lead to a common denominator

$$\Delta NPV_t = LC_t \cdot \frac{V_1 - V_2}{V_3}, \quad (4)$$

$$\text{Where, } V_1 = [1 - (1+r)^{-(t_4-t_2)}] \cdot i_0 \cdot (1+i_0)^{t_2},$$

$$V_2 = (1+i_0)^t \cdot r \cdot (1+r)^{(t_2-t)} \cdot [1 - (1+i_0)^{-(t_4-t_2)}],$$

$$V_3 = (1+i_0)^t \cdot [1 - (1+r)^{-(t_4-t_2)}] \cdot i_0 \cdot (1+i_0)^{t_2},$$

then it is not difficult to determine that the sign of the increase in the income of the project – ΔNPV_t – will be determined by the numerator of expression (4), obviously, its denominator is always positive. Then

$$[1 - (1+r)^{-(t_4-t_2)}] \cdot i_0 \cdot (1+i_0)^{t_2} - (1+i_0)^t \cdot r \cdot (1+r)^{(t_2-t)} \cdot [1 - (1+i_0)^{-(t_4-t_2)}] = (1+i_0)^t \cdot \delta,$$

where difference

$$\delta = i_0 \cdot (1+i_0)^{t_2-t} \cdot [1 - (1+r)^{-(t_4-t_2)}] - r \cdot (1+r)^{(t_2-t)} \cdot [1 - (1+i_0)^{-(t_4-t_2)}] \quad (5)$$

will be actually determine the sign of the increase in net present value of the project ΔNPV_t .

In depends on the ratio of the rate of return i_0 and the cost of loan capital r , also the delayed start of repayment LC_t $t_2 - t = \Delta t_1$ and its duration $t_4 - t_2 = \Delta t_2$ it can be allocated the following cases of magnitude ΔNPV_t .

1. If $i_0 = r$ and $\Delta t_1 = \Delta t_2$, so, how it follows from (5), $\Delta = 0$ and $\Delta NPV_t = 0$. That result will be obviously got and in cases $\Delta t_1 > \Delta t_2$ and $\Delta t_1 < \Delta t_2$.

2. If $i_0 > r$ and $\Delta t_1 = \Delta t_2$, so, how it follows from (5), $\Delta NPV_t > 0$, if conditions are met:

$$a) \quad r \cdot \left(\frac{1+r}{1+i_0} \right)^{\Delta t} > i_0 \cdot \left(\frac{1+i_0}{1+r} \right)^{\Delta t};$$

$$b) \quad r \cdot \left(\frac{1+r}{1+i_0} \right)^{\Delta t} < i_0 \cdot \left(\frac{1+i_0}{1+r} \right)^{\Delta t} \text{ and}$$

$$i_0 \cdot (1+i_0)^{\Delta t} - r \cdot (1+r)^{\Delta t} > r \cdot \left(\frac{1+r}{1+i_0} \right)^{\Delta t} - i_0 \cdot \left(\frac{1+i_0}{1+r} \right)^{\Delta t}.$$

3. If $i_0 > r$ and $\Delta t_1 > \Delta t_2$, and also $\Delta t_1 < \Delta t_2$ so, how it follows from (5), $\Delta NPV_t > 0$, if conditions are met:

$$a) \quad r \cdot \left(\frac{1+r}{1+i_0} \right)^{\Delta t_2} > i_0 \cdot \left(\frac{1+i_0}{1+r} \right)^{\Delta t_2};$$

$$b) \quad r \cdot \left(\frac{1+r}{1+i_0} \right)^{\Delta t_2} < i_0 \cdot \left(\frac{1+i_0}{1+r} \right)^{\Delta t_2} \text{ and}$$

$$i_0 \cdot (1+i_0)^{\Delta t_1} - r \cdot (1+r)^{\Delta t_1} > r \cdot \left(\frac{1+r}{1+i_0} \right)^{\Delta t_2} - i_0 \cdot \left(\frac{1+i_0}{1+r} \right)^{\Delta t_2}.$$

4. If $i_0 < r$ and $\Delta t_1 = \Delta t_2$, so, how it follows from (5), $\Delta NPV_t > 0$, if conditions are met:

$$a) \quad r \cdot \left(\frac{1+r}{1+i_0} \right)^{\Delta t} > i_0 \cdot \left(\frac{1+i_0}{1+r} \right)^{\Delta t} \text{ and}$$

$$r \cdot \left(\frac{1+r}{1+i_0} \right)^{\Delta t} - i_0 \cdot \left(\frac{1+i_0}{1+r} \right)^{\Delta t} > i_0 \cdot (1+i_0)^{\Delta t} - r \cdot (1+r)^{\Delta t}.$$

5. If $i_0 < r$ and $\Delta t_1 > \Delta t_2$, and also $\Delta t_1 < \Delta t_2$, so how it fol-

lows from (5), $\Delta NPV_t > 0$, if conditions are met:

$$a) \quad r \cdot \left(\frac{1+r}{1+i_0} \right)^{\Delta t_2} > i_0 \cdot \left(\frac{1+i_0}{1+r} \right)^{\Delta t_2};$$

$$b) \quad r \cdot \left(\frac{1+r}{1+i_0} \right)^{\Delta t_2} > i_0 \cdot \left(\frac{1+i_0}{1+r} \right)^{\Delta t_2} \text{ and}$$

$$r \cdot \left(\frac{1+r}{1+i_0} \right)^{\Delta t_2} - i_0 \cdot \left(\frac{1+i_0}{1+r} \right)^{\Delta t_2} > i_0 \cdot (1+i_0)^{\Delta t_1} - r \cdot (1+r)^{\Delta t_1}.$$

IV. EXPERIMENT RESULTS

The influence of individual parameters on the increase in the net value of the project is clearly shown graphically on the graphs constructed on the basis of equation (4). So, with the values of the project parameters shown in Table 1,

TABLE 1
THE DATA OF PARAMETERS OF THE PROJECT

| $r, \%$ | LC_t , mln. rub. | $t_4, y.$ | $t_2, y.$ | $t, y.$ |
|---------|--------------------|-----------|-----------|---------|
| 10 | 100 | 15 | 10 | 5 |

we obtain the functional dependence $\Delta NPV_t = f(i_0)$, depicted in Fig. 2:

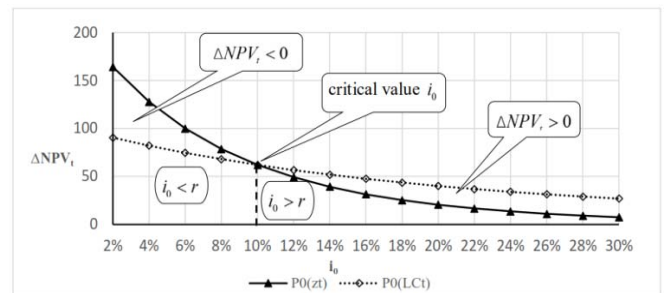


Fig. 2. The impact of the rate of return on growth ΔNPV_t .

Other things being equal, the excess of the rate of return i_0 repayment rates r leads to an increase in the net value of the project due to ILE, which corresponds to the fulfillment of condition 2 a) above.

Dependence ΔNPV_t on the time of the entry LC_t into the project implementation scheme (other things being equal, $i_0 = 10\%$) depicted in Fig. 3.

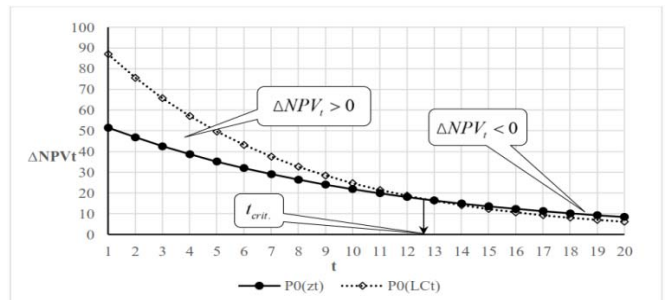


Fig. 3. The impact of the input time LC_t on increment ΔNPV_t .

Critical time for input LC_t is the moment $t_{crit.}$, which can be determined from condition:

$$\Delta NPV_t = 0 \rightarrow \frac{LC_t}{(1+i_0)^{t_{crit.}}} = \frac{LC_t \cdot r \cdot (1+r)^{(t_2-t_{crit.})}}{[1-(1+r)^{-(t_4-t_2)}]} \times$$

$$\times \frac{[1-(1+i_0)^{-(t_4-t_2)}]}{i_0 \cdot (1+i_0)^{t_2}},$$

from which using algebraic transformations,

$$\left(\frac{1+r}{1+i_0} \right)^{t_{crit.}} = \frac{[1-(1+i_0)^{-(t_4-t_2)}]}{[1-(1+r)^{-(t_4-t_2)}]} \cdot \frac{r}{i_0} \cdot \left(\frac{1+r}{1+i_0} \right)^{t_2},$$

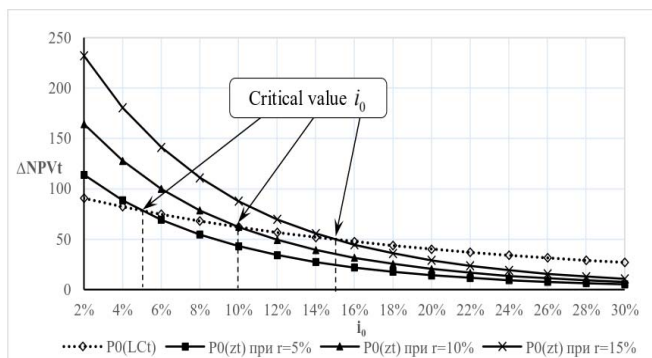
then determine the logarithm

$$t_{crit.} = \frac{Ln + \ln\left(\frac{r}{i_0}\right) + t_2 \cdot \ln\left(\frac{1+r}{1+i_0}\right)}{\ln\left(\frac{1+r}{1+i_0}\right)}, \quad (6)$$

$$\text{where, } Ln = \ln\left\{ \frac{[1-(1+i_0)^{-(t_4-t_2)}]}{[1-(1+r)^{-(t_4-t_2)}]} \right\}.$$

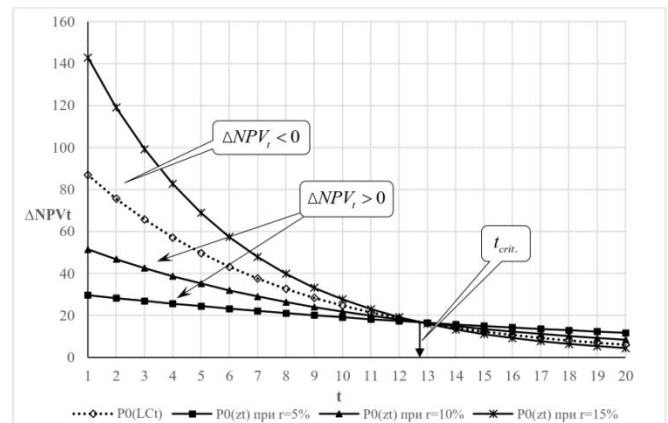
For the rates of the parameters are given in Table 1 and $i_0 = 10\%$, by the formula (6) we obtain $t_{crit.} = 12,77$, that corresponds to the schedule $\Delta NPV_t = f(t)$ on Fig. 3.

On the basis of equation (4), it is also possible to graphically display the conditions for the appearance of ILE when several parameters are changed. In Fig. 4 is a graph of the function $\Delta NPV_t = f(i_0, r)$.


Fig. 4. The impact of cost LC_t on the conditions for the occurrence ILE.

From the analysis of the graphs in Fig. 4 it becomes obvious that with an increase in the cost of loan capital, the critical value of the yield standard for the emergence of ILE is shifted to higher values, where $i_0 > r$.

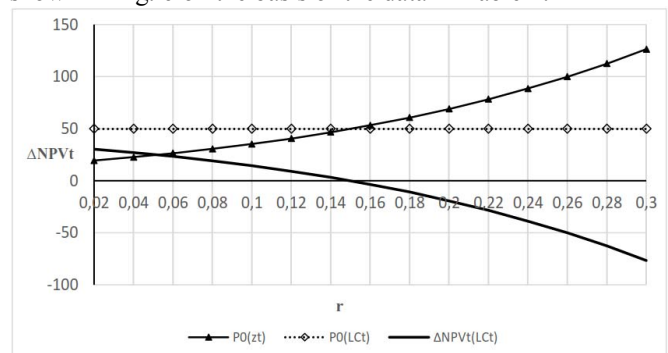
Dependence ΔNPV_t on the time of the entry LC_t and changing its costs (by other equal conditions, $i_0 = 10\%$) depicted in Fig. 5.


Fig. 5. The impact of the input time LC_t and its costs on increment ΔNPV_t .

Analysis of the graphs in Fig. 5 shows that the cost of loan capital has different effects on the ILE conditions. Thus, given the project parameters (see Tab.1) and the rate $r = 15\%$, the effect of the investment lever is generally not possible until the time $t_{crit.}$ input LC_t in the project implementation scheme, and at rates $r = 5-10\%$ ILE provides a positive value ΔNPV_t for any $t < t_{crit.}$. Rate $t_{crit.}$ can be calculated for every r by formula (6).

The considered effect besides the mathematical one has an obvious economic justification: than previously, loan capital LC_t will be put into the implementation scheme of the project, the more his positive contribution to the value NPV , but at the same time, costs also increase due to the growth of interest payments on the loan $3K_t$. The positive increment NPV will be determined by the ratio of the norm of the investor's profitability i_0 , rates of the loan r and time of its getting t due to ILE, so it is clearly shown in the graphs of the above Fig. 2 – 5.

A separate effect of the cost of loan capital on growth is shown in Fig. 6 on the basis of the data in Table 1.


Fig. 6. The impact of cost LC_t on increment ΔNPV_t .

The growth of rates r – cost LC_t – will naturally lead to an increase in repayment payments z_t and, respectively, an

increase $P_0(z_t)$, so that $P_0(LC_t)$ doesn't depend on r , so $\Delta NPV_t = P_0(LC_t) - P_0(z_t)$ will go down. Critical cost rate LC_t , at which the net present value of the project will begin to decrease in comparison with the base rate NPV_0 , will be obviously determined by condition $P_0(LC_t) = P_0(z_t)$. Then the equation for determining $r_{crit.}$, taking (3) into account, is written in the form

$$\frac{1}{(1+i_0)^t} = \frac{r_{crit.} \cdot (1+r_{crit.})^{(t_2-t)}}{[1-(1+r_{crit.})^{-(t_4-t_2)}]} \cdot \frac{[1-(1+i_0)^{-(t_4-t_2)}]}{i_0 \cdot (1+i_0)^{t_2}},$$

which can be solved by numerical methods or by means of the module "Parameter selection" MS Excel.

If you use paid OC_0 , when payment to owners $u_t \neq 0$, so, obviously, $\Delta NPV_t = P_0(LC_t) - P_0(z_t) - P_0(u_t)$, where

$$P_0(u_t) = \sum_{t_3}^{t_5} \frac{u_t}{(1+i_0)^t}$$

and

$$\Delta NPV_t = \frac{LC_t}{(1+i_0)^t} - \frac{LC_t \cdot r \cdot (1+r)^{(t_2-t)}}{[1-(1+r)^{-(t_4-t_2)}]} \times \frac{[1-(1+i_0)^{-(t_4-t_2)}]}{i_0 \cdot (1+i_0)^{t_2}} - \sum_{t_3}^{t_5} \frac{u_t}{(1+i_0)^t} \quad (7)$$

In the event that a particular type of payment stream is known u_t , equation (7) will obviously allow to determine the impact u_t on project growth NPV , as well as the critical value of the size $u_t^{crit.}$ and $LC_t^{crit.}$ at which this growth will cease.

V. FINDINGS AND CONCLUSIONS

The using of loan capital in the economy in general and in the implementation of investment projects in particular is at the same time an urgent task from the point of view of its theoretical importance and contradictory in terms of its practical implementation.

On the one hand, attracting loan capital enables investors to implement promising innovative projects in the event of a shortage (or lack of own funds). On the other hand, the need to repay debts reduces the positive effect of obtaining the net income of the project and, thereby, reduces its financial stability. The latter circumstance is especially important to take into account in the conditions of inflation and unstable conjuncture of the modern market.

The way out, in our opinion, is the construction of mathematical models of project performance indicators that will allow to accurately determine the conditions for obtaining the investment leverage effect when using loan capital in the form of mathematical relationships between individual project parameters. In this article, this was done for the NPV index – the net present value.

The obtained results clearly demonstrate the possibilities of mathematical modeling for studying the dynamics of investment processes with a view to their further application in practice.

We believe that the using of mathematical modeling to study other indicators of investment and innovation projects (such as DPI – discounted profitability index and DPP – discounted payback period) will undoubtedly expand and deepen the scope of economic analysis in solving complex but urgent tasks of innovation policy in modern stage of development of our country.

REFERENCE

- [1] Strategiya innovacionnogo razvitiya Rossijskoj Federacii na period do 2020 goda. Utverzhdena rasporyazheniem Pravitel'stva Rossijskoj Federacii ot 8 dekabrya 2011 g. № 2227-r. Oficial'nyj sajt Ministerstva obrazovaniya i nauki Rossijskoj Federacii [Elektronnyj resurs]. URL: <http://mon.gov.ru/dok/akt/9130/> (Accessed: 21.08.2017)/
- [2] Hotyasheva O.M. Innovacionnyj menedzhment: Uchebnoe posobie. 2-e izd. – SPb.: Piter, 2006. – 384 s.
- [3] The 2017 Global Innovation 1000 study. [Электронный ресурс]. URL: [https://www.strategyand.pwc.com/innovation1000/\(Дата обращения: 21.08.2017\)/](https://www.strategyand.pwc.com/innovation1000/(Дата обращения: 21.08.2017)/)
- [4] Vilenskij P.L., Livshic V.N., Smolyak S.A. Ocenka ehffektivnosti investicionnyh proektov. Teoriya i praktika – M.: Delo, 2008. – 1104 s.
- [5] Kovalev V.V. Vvedenie v finansovyj menedzhment. – M.: Finansy i statistika, 2006. – 768 s.
- [6] Richard A. Bettis. (2017). Organizationally Intractable Decision Problems and the Intellectual Virtues of Heuristics. Journal of Management. vol. 43, 8: pp. 2620-2637.
- [7] Gautam Ahuja, Elena Novelli. (2017). Activity Overinvestment: The Case of R&D. Journal of Management, vol. 43, 8: pp. 2456-2468.
- [8] Ingrid Smithey Fulmer, Robert E. Ployhart. (2016). "Our Most Important Asset" Journal of Management, vol. 40, 1: pp. 161-192.
- [9] Wei-Chuan Kao. (2017). Innovation quality of firms with the research and development tax credit. Review of Quantitative Finance and Accounting, Volume 49, Issue 3, pp 1–36.
- [10] Edmund H. Mantell. (2005). Rent seeking and the value of time. Journal of Economics and Finance, Volume 29, Issue 2, pp 221–241.
- [11] Baker M., Wurgler J. (2002). Market timing and capital structure // Journal of Finance. № 57. P. 76-89.
- [12] Faccio M., Xu J. (2015). Taxes and capital structure // Journal of Financial and Quantitative Analysis. V. 50. №. 03. P. 277-300.
- [13] Longstaff F. A., Strebulaev I. (2014). A. Corporate taxes and capital structure: A long-term historical perspective. National Bureau of Economic Research. №. w20372.
- [14] Rajan R. G., Zingales L. (1995). What do we know about capital structure? Some evidence from international data // The journal of Finance. V. 50. №. 5. P. 1421-1460.
- [15] Modigliani F., Miller M.H. (1958). The Cost of Capital, Corporation Finance and the Theory of Investment // The American Economic Review. V. 48. № 3. P. 261–297.
- [16] Modigliani F., Miller M.H. (1963). Corporate Income Taxes and The Cost of Capital // American Economic Review. P. 433-443.
- [17] Levén, P., Holmström, J., Mathiassen, L. (2014). Managing research and innovation networks: Evidence from a government sponsored cross-industry program. Research Policy, 43(1), 156-168.
- [18] Marmier, F., Gourc, D., Laarz, F. (2013). A risk oriented model to assess strategic decisions in new product development projects. Decision Support Systems, 56, 74-82.
- [19] Marxt, C., Brunner, C. (2013). Analyzing and improving the national innovation system of highly developed countries: The case of Switzerland. Technological Forecasting and Social Change, 80(6), 1035-1049.
- [20] Moutinho, R., Au-Yong-Oliveira, M., Coelho, A., Manso, J. (2015). Beyond the "innovation's black-box": Translating R&D outlays into employment and economic growth. Socio Economic Planning Sciences, 50, 45-58.



Yuri V. Kirillov, PhD, Associate Professor, Department of Economic Informatics, Novosibirsk State Technical University. Research interests – the financial mathematics, the economic and mathematical investment analysis, multicriteria optimization.



Evgeniya V. Dragunova, PhD (Economics), Associate Professor, Department of Economic Informatics, Novosibirsk State Technical University. Research interests – the peculiarities of ecosystems, the growth typologies, organizational changes of enterprises, development strategies of companies.



Anatoliy V. Kravchenko, PhD (Technical science), Associate Professor, Department of Economic Informatics, Novosibirsk State Technical University. Research interests – analysis of corporate information systems, modeling of business processes, development of investment business plans

- [21] Kirillov YU.V., Nazimko E.N. Mnogokriterial'naya model' optimizacii struktury kapitala // Ekonomicheskij analiz: teoriya i praktika. – 2011. - № 32. – S. 57 - 63.
- [22] Kirillov YU.V., Nazimko E.N. Ekonomiko-matematicheskij analiz ehffekta finansovogo rychaga // Finansovaya analitika: problemy i resheniya. – 2014. - № 34. – S. 56 - 62.

Benchmarking Models for the Regulation of Electricity Distribution Companies

Natalia A. Kolkova, Sergey S. Chernov
Novosibirsk State Technical University, Novosibirsk, Russia

Abstract – The present article deals with the efficiency assessment of electricity distribution companies considering world trends in the sphere of tariff regulation of natural monopolies. The transformation of state regulation principals goes through is a result of new a mechanism implementation. The new mechanism is to limit the tariffs growth rate using the “inflation minus” principal. Modern tariff regulation is not only aimed at costs reduction in long-term prospect. The state also creates new incentives to increase the regulated industries efficiency. One of the ways of stimulating companies is creation of a quasi-competitive environment by means of comparative analysis (benchmarking). The article demonstrates some approaches to tariff regulation of foreign electricity distribution companies, parametric and non-parametric benchmarking models and problems in their specification; gives strong and weak points of the models and shows the results of approbation of the models in Siberian electricity distribution companies. The current work presents results of the COLS model of analysis which is a part of FTS (Federal Tariff Service) project containing guidelines to determine captive expense efficiency level. The captive expense regulation model was developed based on the activity analysis of 51 electricity distribution organizations in SFD (Siberian Federal District) in years 2014 – 2016.

Index Terms – Electric power, electricity distribution companies, tariff regulation, benchmarking, X-efficiency.

I. INTRODUCTION

THE ACTIVITIES of electricity distribution companies are to provide energy transportation services from producers to consumers, to administer the energy system operation etc. Electricity distribution organizations aren't part of energy production, but the economy infrastructure objects of any state. Therefore state pricing, including tariff formation, is used to determine the cost of electricity distribution services. Under state regulation, the issue of evaluating the efficiency administration of electricity distribution facilities is on a special position, since the degree of reliability and quality of power supply to consumers depends on the efficiency of infrastructure facilities operation.

The efficiency of electricity distribution facilities is estimated based on the influence of the electricity distribution component of the cost on the total cost of energy delivered to the consumer. The cost of the services of electricity distribution companies is defined as the ratio of the gross revenue requirement (expenditures for operating and investment activities) to the volume of services provided (capacity, electric power).

In the recent time, the problem of coherent setting the tariffs for electricity distribution companies is acute since the state doesn't set the tariff figure higher than the inflation level; and electricity distribution companies face the shortage of funds for operation business.

In Russian economic science the problem of tariff regulation in the energy sector is widely discussed. In their research V.V. Bushuev, N.I. Voropai, A.M. Mastepanov concentrate on the establishing the system of organizational and economic measures in order to maintain stable financial inflow to the sector which would lead to sustainable development of the electric power industry. The questions concerning organization of efficient electricity distribution companies operation were studied in the works of A.Z. Gamma. The issue of electricity distribution companies' costs was also studied by V.M. Gornshtein.

According to the authors, the stimulation of electricity distribution companies for the efficient fund spending and services quality increase can be reached by the transparent mechanism of state regulation (regulation of natural monopolies activities). In this situation, the use of benchmarking in the regulation can be a solution for the problem. The basic feature of benchmarking is comparison of companies (in this case in electricity distribution sector) with each other in order to determine the level of their effectiveness.

Benchmarking of electricity distribution business is popular in Canada, the US, Great Britain, Germany, Norway and others.

The article Benchmarking of Electricity Distribution Companies' Tariff Regulation, 2013 by I.I. Drobysh [1] demonstrates the review of existing benchmarking models used in foreign states in the regulation of electricity distribution sector. The problems of evaluation the electricity distribution companies' efficiency were studied by M.A. Sorokina in her article Evolution of Tariff Formation Methods for Services of Natural Monopolies, 2015 [2], where the author presents a list of limitations for stimulation regulation use (in particular, benchmarking) and forms certain expectations regarding the results of natural monopolies reformation. The author Y.A. Orlova in her article Reform of Tariff Regulation in Electricity Distribution Companies in Russia: Conditions of Competition Increase in the Sector, 2014 [3] presents the basic models of tariff regulation used worldwide and prognosis of the tariff regulation effects. In the article of E.M. Sedakova Methods of Tariff Regulation in Foreign Countries, 2015 the author presents the main methods to evaluate the activities of electricity distribution companies, including DEA, TFP,

COLS and SFA. The issues of the efficiency analysis of complex systems functioning based on DEA were studied by V.E. Krivonozhko, A.I. Propoi, R.V. Sen'kov, A. Lassits and T. Babcheva as well as M.V. Tsapenko, N.V. Diligenskii and A.V. Davydov.

While analyzing publications of Russian authors dealing with applying benchmarking for REDC activities regulation we reveal that research works devoted to appliance of comparative analysis of the operational costs are very few. However the article of I.A. Dolmatov and I.V. Maskaev [4] the results of DEA, SFA and COLS in 12 Russian electricity distribution companies are presented; and the potential possibility of using benchmarking to regulate electricity distribution companies in Russia is announced.

II. PROBLEM DEFINITION

The aim of the article is to test the foreign benchmarking models for electricity distribution companies.

Main tasks:

- to study the models of benchmarking when regulating the activities of electricity distribution companies to demonstrate companies' strengths and weaknesses;
- to test the benchmarking models used abroad for electricity distribution companies in Siberian federal district (SFD);
- to draw a conclusion on the possibility of regulation the activities of Russian electricity distribution companies using benchmarking.

The subjects of research are regional electricity distribution companies in SFD.

III. THEORY

In international practice are already widely used the models benchmarking [4]:

- The Producer Price Index, PPI-analysis;
- The Data Envelopment Analysis, DEA- analysis;
- Econometric analysis;
- Stochastic Frontier Analysis, SFA-analysis.

Comparative analysis is popular in many countries of the world and is widely represented in the works of foreign authors. Some of the benchmarking methods include DEA

worked out in 1978 by Charnes, Cooper and Rhodes and based on the ideas of Farrel expressed in 1957. Among others who has dealt DEA were Weinstein and Query in 1957 and in the recent years W. Wiliam, Cooper, Lawrence, Seiford and JouZhu.

Corrected ordinary least squares (COLS) is one of the most popular parametric methods of benchmarking being used by foreign countries. It was presented for the first time as a method of evaluating the costs function in 1957 by Wisten. The justification of theoretical features of evaluation obtained using the COLS was researched in works of Gabrielden in 1975 and Greene in 1980. One more method being used all over the world is stochastic frontier analysis (SFA). Its basics were represented by Aigner, Lovell, Schmidt and Meeusen, Van den Broel in 1977.

As stated earlier, the current research plans to study theoretical basics of such methods as Producer Price Index (PPI), Data envelopment analysis (DEA), Stochastic frontier analysis (SFA). As a result of their analysis we are planning to reveal strengths and weaknesses and apply this method to regional electricity distribution companies (REDC).

IV. EXPERIMENTAL RESULTS

Let us look at the basic methods of benchmarking being used abroad.

A. Producer Price Index (PPI-analysis)

This benchmarking method belongs to the group of non-parametric methods. PPI can be defined as a ratio of resource to the product. E.g. Irish electricity distribution companies define it as a ratio of operating expenditures to the costs of deforestation (1 km).

The advantage of this model of benchmarking besides the simple calculation is the absence of special requirements to the database (e.g. minimum observation).

The example of applying this method on REDCs is described as follows. Tab. I shows figures for electricity distribution companies in SFO in 2016.

The initial data for the analysis are taken from the report on the structure and electricity and costs for distribution organizations transmission services.

TABLE I
INDICATORS OF INDUSTRIAL AND ECONOMIC ACTIVITIES OF COMPANIES FOR 2016

| № | REDC | Gross revenue (GR), mil rubles | Standard unit of electrical substation, thousand s.u. | Standard unit of power lines, thousand s.u. | Actual volume of electrical supply, mil kW p.h. | Ratio standard unit to GR | Ratio actual volume of electrical supply to GR |
|---|-----------------------------------|--------------------------------|---|---|---|---------------------------|--|
| 1 | Zarinsk Electric Networks | 117,47 | 5 656,50 | 1 871,30 | 144,84 | 64,08 | 1,23 |
| 2 | South-Siberian Energy Company | 56,41 | 2 221,60 | 893,88 | 304,29 | 55,23 | 5,39 |
| 3 | MUP Electric Networks | 137,79 | 4 874,67 | 2 016,87 | 140,92 | 50,01 | 1,02 |
| 4 | OGUEP Oblkommunenergo | 1 743,87 | 55 396,90 | 21 043,72 | 3 129,47 | 43,83 | 1,79 |
| 5 | Novosibirsk Electric Networks RES | 7 228,91 | 140 962,00 | 105 130 | 12 260,41 | 34,04 | 1,7 |
| 6 | TYVA Energy Company MRSK | 863,82 | 13 765,20 | 15 448,80 | 450,26 | 33,82 | 0,52 |
| 7 | Altay Energy Company MRSK | 5 468,84 | 84 371,24 | 87 135,28 | 7 051,85 | 31,36 | 1,29 |
| 8 | Omsk Energy Company MRSK | 5 011,60 | 92 231,29 | 64 179,73 | 7 912,68 | 31,21 | 1,58 |

| | | | | | | | |
|----|--|----------|------------|-----------|-----------|-------|------|
| 9 | Krasnoyarsk Energy Company MRSK | 7 007,78 | 115 140,00 | 75 195,00 | 12 491,96 | 27,16 | 1,78 |
| 10 | Electricity Distribution Networks of Siberia | 116,79 | 2 624,80 | 453,09 | 92,65 | 26,35 | 0,79 |
| 11 | Electricity Distribution Networks of Abakan | 322,16 | 5 327,30 | 2 889,54 | 523,68 | 25,51 | 1,63 |
| 12 | Chita Energy Company MRSK | 4 665,95 | 59 051,40 | 58 783,40 | 5 585,82 | 25,25 | 1,2 |
| 13 | Kuzbassenergo MRSK | 4 497,51 | 64 417,47 | 45 938,06 | 15 588,76 | 24,54 | 3,47 |
| 14 | Energiya-Tranzit | 101,48 | 1 870,70 | 402,42 | 82,61 | 22,4 | 0,81 |
| 15 | Buryat Energy Company MRSK | 3 985,81 | 43 653,15 | 44 826,37 | 4 101,10 | 22,2 | 1,03 |
| 16 | Yenisei Ferroalloy Plant Electricity Distribution Networks | 165,92 | 3 120,60 | 177,98 | 187,5 | 19,88 | 1,13 |
| 17 | Kusbass Electricity Distribution Company | 4 273,86 | 48 009,20 | 29 963,96 | 2 442,65 | 18,24 | 0,57 |
| 18 | Khakasia Energy Company MRSK | 3 608,00 | 23 384,40 | 17 312,38 | 11 419,87 | 11,28 | 3,17 |

Fig. 1 shows the ratio of the total number of standard units to GR volume.

According to data presented in Tab. I, the most efficient companies of the group are Zarinisk Electric Networks, South-Siberian Energy Company, MUP Electric Networks. While such companies as Kusbass Electricity Distribution Company and Buryat Energy Company MRSK and Khakasia Energy Company MRSK as well as Yenisei Ferroalloy Plant Electricity Distribution Networks are inefficient.

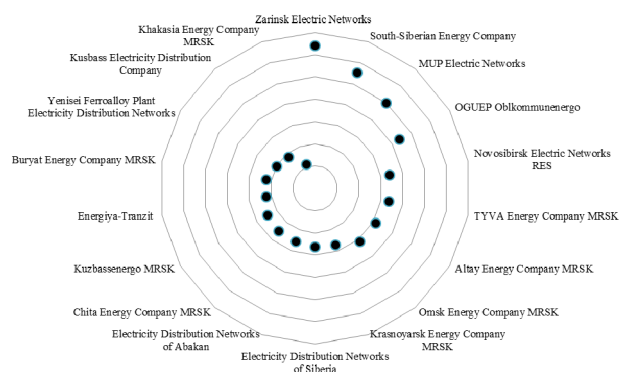


Fig. 1. Results of PPI-analysis (ratio of s.u. to GR).

Fig. 2 shows the ratio of actual volume of electricity supply to GR volume.

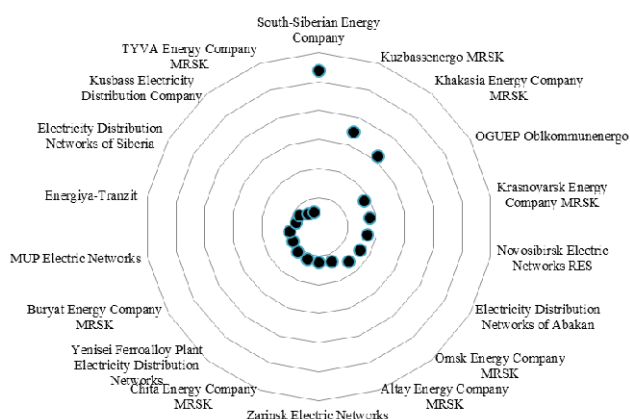


Fig. 2. Results of PPI-analysis (the ratio of the actual volume of electricity supply to GR).

The most efficient companies of the group are South-Siberian Energy Company, Kuzbassenergo MRSK and Khakasia Energy Company MRSK. Such companies as

Kusbass Electricity Distribution Company and Electricity Distribution Networks of Siberia are inefficient.

In the result of the PPI-analysis, Khakasia Energy Company MRSK demonstrates a high index value defined as ratio of actual volume of electricity supply to GR volume. However, the ratio of s.u. to GR gets the lowest value in the group of interest.

Based on this information, it is possible to identify the following drawbacks of the model:

1. evaluation of certain aspects of the company's production activities;
2. there is a linear relationship between the resource and the product (non-correspondence of reality);
3. there is no accounting system for random model errors;
4. there is no differentiation of electricity distribution companies in terms of operation of fixed production assets, etc.

PPI method isn't the only one used in Ireland. The regulatory authority also uses econometric data analysis.

Such characteristics of Russia as vast territory and low population density intensify the weaknesses of the model. Therefore, PPI method can't become the key way of calculating the efficiency index for domestic electricity distribution companies. However, this method can be used to analyze the activity of a company in order to set growth factors for the company economic efficiency.

B. Data Envelopment Analysis (DEA-analysis)

This method is based on linear programming [6] and it's mentioning in domestic scientific resources is occasional [7, 8]. This type of analysis gives an opportunity to evaluate a large number of electricity distribution companies. Data envelopment analysis implies the formation of multidimensional space input and output parameters of the company each of which corresponds to a certain point.

Let's look at the basic DEA model. The basic CCR model [9] generates cost and output function for k electricity distribution companies ($k=1, \dots, n$) using the weights v_i and u_r . The main idea of CCR model lies in the method of estimating the comparative efficiency in complex multidimensional systems [9].

$$\text{Costs} = v_1 x_{1k} + \dots + v_m x_{mk}, \quad (1)$$

$$\text{Output} = u_1 y_{1k} + \dots + u_s y_{sk}, \quad (2)$$

where x_{1k}, \dots, x_{mk} – number of factors that influence the costs;

v_1, \dots, v_m – factors' weights that influence the costs;

y_{1k}, \dots, y_{sk} – number of factors that influence the results of company's activity;

u_1, \dots, u_s – factors' weights, that influence the results of company's activity.

Target function is a ratio of output to costs that has to be maximized:

$$\theta_k = \frac{u_1 y_{1k} + \dots + u_s y_{sk}}{v_1 x_{1k} + \dots + v_m x_{mk}} \rightarrow \max \quad (3)$$

Restrictions:

$$\theta_k = \frac{u_1 y_{1k} + \dots + u_s y_{sk}}{v_1 x_{1k} + \dots + v_m x_{mk}} \leq 1 (k = 1, \dots, n) \quad (4)$$

$$v_1, \dots, v_m \geq 0 \quad (5)$$

$$u_1, \dots, u_s \geq 0 \quad (6)$$

The right-scale solution of the linear programming corresponds to (θ^*, v^*, u^*) where the maximum value of the target function is reached. An efficient electricity distribution company has a value $\theta^* = 1$ and has one more optimal solution $v^* > 0, u^* > 0$.

Let's give an example of assessment of electricity distribution companies' activity. To evaluate the efficiency of electric grid companies, the DeaFronter application is used (Microsoft Excel supplement), developed by Professor Joe Zhu of the business school in Worcester.

Model Jou Zhu has the following criteria:

- partially linear form of the production function;
- Input-oriented;
- the adoption of constant (constant returns to scale, CRS) or variable (variable returns to scale, VRS) returns of scale.

The practice of DEA-analysis of efficiency is most often used in the input-oriented model, since managing the resource variables is relatively easier than variables of the output parameter [10].

The main disadvantage of this CCR-model is the prerequisite of linear homogeneity [11], therefore for the analysis of the TCO activity efficiency the BCC-input model was used, which differs from the CCR-models by adopting a variable scale effect.

The model allows the recognition of the increasing or decreasing economies of scale for each enterprise, and, in this connection, the division of efficiency into technical efficiency and efficiency, depending on the scale effect [9].

Tab. II presents REDCs in Siberia in 2016. Resource is presented as a ratio of captive expenses to the number of interface points and a ratio of GRR to technological energy loss. Output is considered as volume electricity supplied.

TABLE II
THE VALUE OF VARIABLE "INPUT" AND "OUTPUT" BCC OF THE MODEL OF ESTIMATION OF THE COMPARATIVE EFFECTIVENESS OF REDC FOR 2016

| № | DMU | Captive expense, kRUB/ the number of interface points | GR of electric power dissipation, kRUB | Actual volume of electrical supply, million kWh |
|----|--|---|--|---|
| 1 | Altay Energy Company MRSK | 6,62 | 1084188,90 | 7051,85 |
| 2 | Buryat Energy Company MRSK | 10,40 | 608493,50 | 4101,10 |
| 3 | GAES "MRSK Sibiri" | 5,93 | 189108,44 | 449,01 |
| 4 | Krasnoyarsk Energy Company MRSK | 13,27 | 2960043,00 | 12491,96 |
| 5 | Kuzbassenergo MRSK | 16,49 | 1304770,73 | 15588,76 |
| 6 | Omsk Energy Company MRSK | 5,69 | 1144773,44 | 7912,68 |
| 7 | Khakasia Energy Company MRSK | 11,64 | 438094,00 | 11419,87 |
| 8 | Chita Energy Company MRSK | 8,67 | 1351797,00 | 5585,82 |
| 9 | Novosibirsk Electric Networks RES | 6,35 | 3658191,00 | 12260,41 |
| 10 | Electricity Distribution Networks of Siberia | 65,41 | 8193,60 | 92,65 |
| 11 | Electricity Distribution Networks of Abakan | 5,36 | 122474,10 | 523,68 |
| 12 | Kusbass Electricity Distribution Company | 10,33 | 494829,30 | 2442,65 |
| 13 | OGUEP Oblkommunenergo | 4,78 | 1327957,30 | 3129,47 |
| 14 | TYVA Energy Company MRSK | 5,58 | 219497,70 | 450,26 |
| 15 | RUSAL | 31,01 | 6231,34 | 188,33 |
| 16 | MUP Electric Networks | 2,03 | 20566,40 | 140,92 |
| 17 | South-Siberian Energy Company | 1,80 | 40159,00 | 304,29 |
| 18 | Zarinsk Electric Networks | 2,24 | 52974,00 | 144,84 |

Fig. 3 shows the companies' efficiency rating. Companies with index equal one form the efficiency boundary. Analyzing the Tab. II we note that the ratio of captive expenses to the number of interface points of South-Siberian Energy Company is minimal while that of Electricity Distribution Networks of Siberia is maximum.

Using the figures of efficiency we come up with the descriptive statistics as in Tab. III.

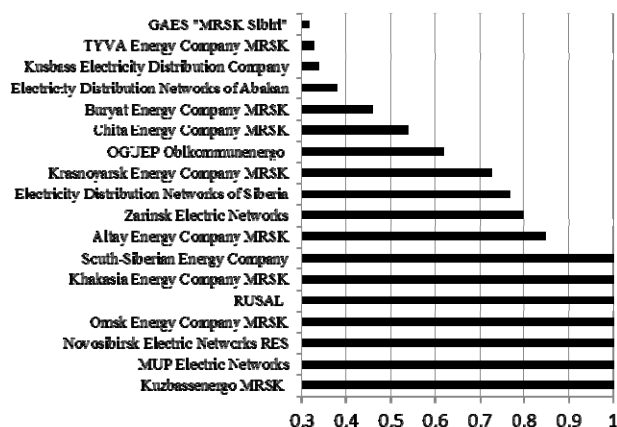


Fig. 3. Results of DEA-modeling.

TABLE III
DESCRIPTION STATISTICS

| Volume of focus group | Selected middle value | Minimum | Maximum |
|-----------------------|-----------------------|---------|---------|
| 18 | 0,73 | 0,317 | 1 |

The descriptive statistics shows that usually the level of efficiency in REDCs is satisfactory. The average quality value is 0,73. The minimum of efficiency value is 0,317 and is showed by «GAES MRSK Sibiri».

Formal estimation results let us divide all REDCs into three groups. The 1st group will have efficiency value of 0,59 (6 companies); the 2nd group will have the efficiency value of 0,59 – 0,86 (5 companies); and the 3rd group will have the value of >0,86 (7 companies).

As well as some other methods, DEA is used in New South Wales in order to study production efficiency of the companies with the operation costs, network length and transformer capacity as resource; and net electricity supply, number of consumers and peak load as a product. This benchmarking model is also used in Germany and Austria (efficiency rating and x-efficiency growth factor are to define). Operation costs value and capital costs are used as resource. The number of interface points, peak load and power line length are used as a product.

The main advantage of this method is no background concerning functional form of the model and the possibility to test statistic hypotheses. There are also some weaknesses:

- a sustainable database is required;
- random model errors aren't taken into account;
- high response to outliers in data;
- difficulty defining differences in operation conditions.

In the result of non-parametric comparative analysis methods in electricity distribution companies and it's approbation on REDCs of Siberia we reveal that DEA can help to reveal target indicators to reduce a non-reference companies' costs i.e. to conduct resource optimization. Using of this method can determine potential costs reduction of electricity distribution companies.

For DEA-analysis, many foreign software have been developed, including Excel-add-ons DEA-Frontier and the program KonSi-DEA Analysis, as well as the domestic

development of Morgunova EP-Data Envelopment Analysis Software [11].

Thus, the principal possibility of conducting an input-oriented method of DEA analysis with variable return to scale (in cases when empirical studies testify to the influence of scale on reaching the efficiency boundary) is analyzed. Using this method will determine the potential for reducing the costs of grid companies.

Method of cumulative factor productivity and data envelopment analysis are a part of non-parametric methods group. Denote the dimension of physical quantities in the paper it is allowed to use SI units. It is allowed to use off-system units only if it is the common standard of notation in some field of science.

C. Econometric Analysis

Econometric analysis is one of parametric methods (regressive costs model). Using of this method allows conducting a quantitative description of correlations between economic variables. In general the regressive costs model for benchmarking in REDCs looks as follows:

$$\ln C = f(x_1, \dots, x_n) + \varepsilon, \quad (7)$$

where C – REDCs costs;

x_1, \dots, x_n – regression factors;

ε – random variable which characterizes deviation of the real efficiency indicator value from the theoretical one that is found by means of regression equation.

Benchmarking using the econometric approach includes:

1. Selection of regression factors;

At this stage, the choice is made of variables that characterize the natural indicators of the electricity grid business (electricity supply), prices for production factors and characteristics of the functioning environment. The regression model factors must meet the following requirements:

- quantitative measurability. If it is necessary to include qualitative factors in the model, they should be given quantitative certainty (scores, ranks);
- absence of correlation of factors among themselves and functional connection.

2. Define the form of the cost function;

In determining the form of a function, the linear, translogarithmic, and Cobb-Douglas functions are usually used. For the electric grid company's cost model, the Cobb-Douglas function should be selected, since TCO costs depend on many factors (the number of conventional units of equipment, the payroll, climatic conditions, the productive supply of electricity, etc.).

The form of the cost function is determined for a particular study and justified based on it in front of others, which is the bottleneck of the parametric method of estimating costs.

3. Choosing a method for estimating the cost function

When choosing a method for estimating costs, the least-squares method, the least-squares corrected method, and the modified least-squares method are usually used.

Econometric analysis as well as DEA and TFP-analysis are used in New South Wales. The operational costs function is

presented in linear and logarithmic form and uses such variables as number of consumers, power line length, net electricity supply, peak load and type of networks (can be urban or rural) [1].

The ability to run statistic tests and determine the differences in operating conditions of electricity distribution companies are the model's definite strong points.

However the method has some weaknesses as well:

- a sustainable database is required;
- evidentiary base to choose the form of the costs function and its variables is required;
- the results depend on the model specification.

The draft "Instructions for setting the base level of operational captive expenses in regional electricity distribution companies using benchmarking to regulate electricity distribution prices" was introduced in 2013 by the Federal Tariff Service (its authority has been later given to FAS). Operating costs of REDC are composed of captive expenses ("raw and other materials", "repair of fixed assets", "labor compensation" and other) and non-captive ("rent", "taxes" and so on). With the help of benchmarking, the efficiency index of operating expenses of REDC calculated, which are indexed annually. Thus, it becomes possible to take into account the efficiency factor of the electric grid company in determining the necessary gross proceeds. In the article "Development of Captive Expense Regulation Model of the Siberian Electricity Distribution Companies" [12], it was noted that the use of this model is inappropriate for the regulation of REDC in Siberia. Let us consider in more detail the methodology for the effective level of controlled expenditures.

Captive expenses are determined in accordance with the regression model of the effective level of expenditure. The multiple regression model presented in the draft guidelines for determining the controlled costs is as follows:

$$\begin{aligned} Lu(OPEX) = & \beta_0 + \beta_1 \ln(p) + \beta_2 \ln(w) + \\ & + \beta_3 \ln(C) + \beta_4 \ln\left(\frac{C}{L}\right) + \beta_5 \ln(T) + \beta_6 \ln\left(\frac{T_{hv}}{T}\right) + \\ & + \beta_7 \ln\left(\frac{L_{hv}}{L}\right) + \beta_8 \ln(k_1) + \beta_9 \ln(k_2) + \beta_{10} \ln(k_3) + \varepsilon. \end{aligned} \quad (8)$$

To determine the effective operating costs, the least-squares method was used. To describe the cost model of the electric grid company, the Cobb-Douglas function was chosen, since various regressors were included in the model (Tab. IV).

TABLE IV
REGISTERS OF OPERATING EXPENSES MODEL OF FST

| Variable | Description | Measuring Unit |
|----------------------|---|------------------|
| <i>OPEX</i> | Captive expenses | Mil rubles |
| <i>L</i> | Length of power lines | km |
| <i>C</i> | Number of connection points | piece |
| <i>T</i> | Transformer substation capacity | MVA |
| <i>w</i> | Average remuneration | thousands rubles |
| <i>p</i> | Consumer goods basket value in the region | thousands rubles |
| <i>k₁</i> | Number of crossings through zero | days |

| | | |
|-----------------------|--|-----|
| <i>k₂</i> | Average temperature in January | C |
| <i>k₃</i> | Thickness of ground surface icing | mm |
| <i>T_{hv}</i> | Transformer substation capacity | MVA |
| <i>L_{hv}</i> | Length of power lines (high voltage power) | km |

As the result of the research work on more than 50 Siberian electricity distribution companies operation within 2014 – 2016, the calculation of captive expense efficiency level in the companies using the criteria mentioned above was called unreasonable due to the following reasons:

- GRR of most electricity distribution companies of Siberia is less than 500 million rubles (63% companies' GRR is less than 500 mil rub);
- high interconnection between some variables;
- most of electricity distribution companies have no funds to high voltage transmission (25,5%);
- more than 20% of companies with GRR higher than 500 mil rub have no funds to high voltage transmission which leads to lack of coherence of efficient companies;
- the formula for efficiency index calculation assumes experts' model adjustment which can negatively affect the transparency of tariff regulation process.

On the basis of the foreign literature studied, as well as the results of the research of domestic scientists and the result of the analysis of the draft methodological recommendations, it was possible to form a model for the effective level of controlled expenditures (on the basis of the least squares method), a detailed description of which is given in the article "Development of Captive Expense Regulation Model of the Siberian Electricity Distribution Companies" [12].

We represent the regression equation (according to data for 2014):

$$\begin{aligned} LN(OPEX) = & 1,372005 - \\ & 1,23797 * \ln(k_1) + 0,795379 * \ln(k_2) \\ & + 0,699515 * \ln(k_3). \end{aligned} \quad (9)$$

In Tab. V described the variables of the model.

TABLE V
DESCRIPTION OF VARIABLE MODELS

| № | Variable | Description | Measuring Unit |
|---|----------------------|--|------------------|
| 1 | <i>k₁</i> | Consumer goods basket cost in the region | thousands rubles |
| 2 | <i>k₂</i> | Actual volume of output | Mil kW p.h. |
| 3 | <i>k₃</i> | Energy loss level | % |

Thus, the model presented above determines the effective level of controlled expenditures for each power grid company. Companies can not influence the factor "The cost of the consumer basket in the region," that is, the effectiveness of REDC depends on the actual volume of output and the energy loss level.

D. Stochastic Frontier Analysis (*κ*SFA-analysis)

Parametric methods also include method of stochastic production frontier which is an improved version of traditional econometric analysis. The key idea of the method is to divide a random variable into noise (v_i) and inefficiencies ($u_i \geq 0$), $\varepsilon_i = v_i - u_i$.

Unlike COLS model (OLS – rests are considered as ineffectiveness) some SFA models have weakened factor that individual effect can be interpreted as company inefficiency.

When implementing the benchmarking principles for electricity distribution companies operation regulation it's important to consider that the companies of the sector operate in different conditions. There for, the question of coherence is disputable and its lack is in fact an amount sum of inefficiencies and obstacles.

SFA is used along with DEA in Australia, Finland, New South Wales and Germany. Germany uses the linear model of DEA; the scale return is also constant. Regulatory authorities of these countries can study the production efficiency, rate the efficient companies and define target indicators to reduce companies' costs.

Advantages of SFA:

- room for statistical tests conduct;
- separation of random error and inefficiency of a company;
- differences in operating conditions are considered.

The main weakness of the model is the requirement of a large amount of data to distinguish random variable between noise and inefficiency. This fact makes it impossible to use SFA in the research since the information required for noise analysis isn't available.

Benchmarking of the electricity distribution companies can be applied in different ways. Data analysis can be performed in parametric or non-parametric manner; data input and output can be presented in a functional form or can be single (PPI – analysis). The production possibility frontier can be evaluated on panel data or by means of cross-sectional analysis.

V. DISCUSSION OF RESULTS

The article demonstrates the principal possibility of applying econometric analysis to resolve problems to determine the optimal level of captive expenses of operational costs which is seen as a promising direction in Russian tariff regulation policy.

The multiple regression model (formula 9) can allow the regulatory body (e.g. FAS) to conclude about the efficiency of operational activities of any electricity distribution company.

The results reflect the real situation. Companies with high basic period efficiency have the higher captive expenses level in the current period. While regulating the activity of electricity distribution companies, benchmarking creates a quasi competitive environment. This favors the formation of financial bases for sustainable development of electricity distribution business.

VI. CONCLUSION

During the research work the author conducted the benchmarking models review which is successfully applied for electricity distribution companies abroad. Academic resource analysis indicates the lack of research on the appliance of benchmarking to evaluate efficiency of operational costs in order to regulate Russian electricity distribution companies.

Considering this, the approbation of the models by foreign countries tariff regulation was performed. The process of analyzing the potential use of benchmarking revealed that DEA – analysis favors the identification of potential costs decrease.

The article also demonstrates

- the benchmarking technology based on DEA – analysis procedures;
- the results of econometric analysis of FTS guidelines for the level of captive expense determination which reveals its unreasonableness for a number of factors.
- captive expense regulation model elaborated by foreign academic resources analysis and FTS's captive expense regulation model.

The actual state of things for companies can be determined by using benchmarking: the company with high basic period efficiency have the higher captive expenses level in the current period. While regulating the activity of electricity distribution companies, benchmarking creates a quasi competitive environment which favors the formation of financial bases for sustainable development of electricity distribution business.

Thus, the present article demonstrates the possible appliance of the input oriented method (DEA) and econometric analysis. The approbation results the conclusion that the chosen factors of the multiple regression model to independent variable (captive expense) evaluation (consumer goods basket cost, actual volume of output, energy loss level) let us form the efficient level of captive expense.

REFERENCES

- [1] Drobysh I. Benchmarking in the regulation of tariffs for electric grid companies // Proceedings of the ISA RAS. Vol. 63. 1/2013, pp. 97-106. (in Russian).
- [2] Sorokin M. Evolution of Tariffing Methods for Services of Natural Monopolies // Problems of Accounting and Finances, 2015.-№4 (20). - pp. 63-68. (in Russian).
- [3] Orlova Yu. Tariff reform of electric grid companies in Russia: conditions for increasing the competitiveness of the sector // Contemporary competition. 2014. № 4. pp. 26-48. . (in Russian).
- [4] Dolmatov I., Maskaev I. Methodological approaches to benchmarking of Russian electric grid companies / // Materials of the XIV April international scientific conference on the problems of economic development and society: in 4 books. Book 2 - 2014. - pp. 248-256. (in Russian).
- [5] Bushdt A. Electric grid companies: "boiler" tariff and the influence of the external environment // Russian Entrepreneurship, 2011 №1 (2). pp. 122-126. (in Russian).
- [6] Weinstein, M. A. Query 2: The sum of values from a normal and a truncated normal distribution // Technometrics, 6(1), 104-105. Winsten, C., 1957. «Discussion on Mr. Farrell's Paper» Journal of the Royal Statistical Society, Series A, General, 120, pp. 282-284.

- [7] Krivonozhko V., Propoi A., Senkov R., Rodchenkov I., Anokhin P. Analysis of the performance of complex systems // Design Automation. 1999.-№1. -pp. 2-7. (in Russian).
- [8] Senkov R. Parametric optimization methods in the analysis of the effectiveness of complex systems based on ASF technology: dis. Cand. fiz.-mat. Sciences: 05.13.18 / Senkov Roman Viktorovich; sci. hands. E.V. Krivonozhko-Moscow, 2002. -153 liters. (in Russian).
- [9] Tsapenko M., Diligensky N., Davydov A., Multicriteria methodology for identifying promising areas of scientific research // Bulletin of the Samara State Technical University. Series: Engineering. 2011. № 4 (32). pp. 26-33. (in Russian).
- [10] Porunov A. Assessment of the comparative effectiveness of public environmental management in the region by the DEA analysis method // Scientific Journal of Research Institute of ITMO. - 2016. №1. - pp. 104-111. (in Russian).
- [11] Morgunov E.P. Multidimensional classification based on an analytical method for assessing the effectiveness of complex systems: dis. Cand. tech. Sciences: 05.13.11 / Evgeny Pavlovich Morgunov; sci. hands. O.I. Antamoshkina, Krasnoyarsk, 2003, p. 160. (in Russian).
- [12] Chernov S., Kolkova N. Development of Captive Expense Regulation Model of the Siberian Electricity Distribution Companies // Problems of regional energy = Problems of regional energy. - 2017. - No. 3 (35). - pp. 109-120. (in Russian).



Kolkova Natalia Aleksandrovna, post-graduate student of the Department of Production Management and Economics of Power Engineering, Novosibirsk State Technical University, Russia, Novosibirsk. The total number of scientific publications is 12. The field of scientific interests is electricity supply, tariff formation in power engineering, energy economics, energy saving and energy efficiency increase.



Chernov Sergey Sergeevich, PhD Associate Professor, Dean of the Faculty of Energy, Head of Department of Production Management and Energy Economics in Novosibirsk State Technical University, Russia, Novosibirsk. The total number of scientific publications is more than 150. The field of scientific interests is strategic management and marketing in the energy sector, energy economics, energy saving and energy efficiency.

The study was supported financially by the Novosibirsk State Technical University (Project C-18, 2018).

Russian High Tech Companies: Growth Factors and Limitations

Natalya A. Kravchenko, Anton A. Goryushkin, Anastasiya I. Ivanova,
Svetlana A. Kuznetsova, Sophia R. Khalimova, Almira T. Yusupova
Institute of Economics and Industrial Engineering SB RAS, Novosibirsk State University,
Novosibirsk, Russia

Abstract – The competitiveness of modern economy is determined mainly by the high-technology business activities. Case of Russian economy is under discussion. The paper is concentrated on the revealing and estimation the factors of growth of the companies operating in knowledge-intensive services and high-tech manufacturing sector of national economy. The empirical part is based on data provided by Business Environment and Enterprise Performance Survey (BEEPS) arranged by the World Bank. Dynamics of employees' number during three years was chosen as an explaining variable. Such approach is quiet common. Internal determinants were presented by factors related to innovative capacities, human capital, resource conditions and financial limitations. Company's age and ownership structure were taken into account also. A two-step assessment procedure was applied in order to determine and estimate the factors of growth. Significant factors were selected with the help of best subsets regression and then these factors were further analyzed using OLS. Results revealed that company's age has negative influence to its growth in both analyzed sectors; another common factor which has positive influence is presented by highly educated employees' share. Share of dominating owner and credit application turned to be positively significant for knowledge intensive services. Government subsidies and equipment purchase positively influence on manufacturing companies' growth.

Index Terms – Russian high tech business, growth factors, manufacturing and knowledge intensive companies.

I. INTRODUCTION

QUESTIONS related to growing companies' identification and determination of key factors of their growth traditionally draw attention of many researchers. Performance and results demonstrated by such companies have great influence on national economy's current state and development. Several particular areas could be defined among such studies. First of all it is necessary to mention stochastic approaches based on Gibrat's law according to which company's growth rate has stochastic nature and doesn't depend on its size and other factors [1]. The second area of research includes papers proving that only selected companies are growing. They are called fast growing firms and have specific characteristics, which deserve special attention. Such companies have great influence on national economy and determine its competitiveness [2-4]. The third area concerns papers which discuss relationship between growth rates and combinations of internal and external conditions including macroeconomic, institutional, regional, cultural and other

factors. [5]. Special attention is paid on fast growing high tech companies, determinants of their growth which act differently in developed and developing economies.

II. PROBLEM DEFINITION

High tech companies play important role in Russia also; to great extent they determine possibilities and competitiveness of domestic economy. Fast growing high tech and knowledge intensive companies create new jobs under favorable external environment and could play stabilizing role in the periods of recession and crisis. They are traditionally supported and stimulated within state innovative and industrial policy.

The main goal of our research is to find out and to assess the influence of technological and strategic factors on private high tech companies' growth in the Russian transition economy. We also pay attention to the barriers and limitations of their development.

We focus our research on the analysis of microeconomic growth determinants assuming that macroeconomic factors are similar for all national companies. Some spatial heterogeneity effects are taken into consideration indirectly.

III. THEORY

Two groups of high tech companies' growth factors are usually discussed in research papers. These groups include external and internal factors.

External factors deal with demand and supply; they are related to external environment of innovative companies. Demand factors are determined by consumers' needs, their attitude to risk and existing market realities. Supply factors include availability of technological information, raw materials and financial resources. Environment factors embrace different legal norms, administrative rules, political modes etc.

Internal factors are associated with such available resources as company's innovative capacities and technical competencies, financial possibilities, human resources, system and culture of management, business model and others.

Piatier report was a pioneer research paper which focused on high tech companies' growth factors [6]. Several general factors including learning effect, bank financing availability, venture capital influence, and role of standards in new products development, were identified in this publication. Special role of technology was defined later [7].

Empirical research showed that significant factors include such indicators as personal characteristics of entrepreneur – company's founder, market orientation, access to resources, human capital, social capital, financial capital and intellectual property [5]. Most papers assume that relationship between high technologies, innovations and growth is positive. However this statement needs to be explained.

There are rather few papers which deal with microeconomic factors of high tech business growth in developing economies including Russia. This is related with short history of Russian entrepreneurship on one side, and with lack of available empirical data on the other.

Lack of entrepreneurial traditions [8], unfavorable institutional environment [9,10], high level of administrative barriers [11] and other external factors still have strong influence on the new business development in Russia [12]. Few papers discussing Russian technological companies [13] show that they act in the hostile and instable environment and therefore they have to find new ways to develop competitive business.

Summing up existing publications concerning growth factor of Russian high tech companies we could state that their results are in general ambivalent and depend on the characteristics of used data sets and assessment methods.

Our analysis of a number of Russian high tech companies' cases enabled us to identify several success factors and barriers of their development. It was revealed that company's success is based on the original innovative ideas and strong team which could implement these ideas. Financial limitations always are significant for high tech players; however possibilities to overcome them not necessary mean further successful growth. High tech business development requires creation and development of effective cooperation models. These models embracing different actors and should be based on confidence. Such cooperation is especially important at regional level.

Researchers working with companies' surveys data often meet objective instrumental difficulties. These difficulties include data omissions and non representative samples, differences in observation periods and others [14].

In most cases, researchers choose for assessment OLS, general regression models, logit and probit regression [15].

IV. EMPIRICAL BASIS OF RESEARCH

The empirical part of our research is based on the data on private companies created with the help of companies' surveys conducted by World Bank once in 4 years - Business Environment and Enterprise Performance Survey (BEEPS). The latest survey was conducted in 2012.

According to the aims of our research, we formed a set of Russian high-tech companies with number of employees from 20 to 100 according to Eurostat classification. 264 companies were included in our set.

We divided our set to two groups according to sectoral patterns of technological innovation: high-tech manufacturing sector and knowledge-intensive services.

A two-step assessment procedure was applied in order to determine and estimate the factors of growth. Significant

factors were selected with the help of best subsets regression and then these factors were further analyzed using OLS.

Some general characteristics of companies included in our sample are presented below in Table I. We consider that these aspects are relevant to the context of our research.

TABLE I
GENERAL CHARACTERISTICS OF THE SAMPLE

| Characteristic | High tech manufacturing | Knowledge intensive services |
|--|-------------------------|------------------------------|
| Number of companies | 176 | 88 |
| Average age of the company, years | 12,5 | 11,5 |
| Average percentage of the company owned by the largest owner | 68.8% | 76.2% |
| Average number of permanent, full-time individuals working in the company at the end of fiscal year | 44 | 37 |
| Average number of permanent, full-time individuals working in the company three fiscal years ago | 47 | 33 |
| Subsidies from the national, regional or local governments or European Union sources over the last three years, share of companies | 6,9% | 2,3% |
| Purchase of any fixed assets (machinery, vehicles, equipment, land or buildings) in fiscal year, share of companies | 53,1% | 52,9% |
| Application for any loans or lines of credit in the fiscal year, share of companies | 37,4% | 19,3% |
| Use of technology licensed from a foreign-owned company (excluding office software), share of companies | 15,9% | 20,5% |
| Innovative activities during the last three years, share of companies, including | | |
| Introduction of new or significantly improved products or services | 59,1% | 45,0% |
| Introduction of any new or significantly improved organizational or management practices or structures | 41,2% | 35,0% |
| Introduction of any new or significantly improved marketing methods | 37,7% | 32,1% |
| Spending on research and development activities | 40,0% | 16,7% |

High tech manufacturing group included 176 companies while high tech knowledge intensive group – 88.

Knowledge intensive companies turned out to be younger than manufacturing ones. They employed fewer high qualified employees comparing with manufacturing firms. Most representatives of both groups are characterized by highly concentrated ownership structure. However in manufacturing companies minorities often have blocking stake.

Average size of manufacturing company decreased during three years. At the same time number of growing firms remained significant.

The average size of knowledge intensive company, on the other hand, has increased, and more than half of the sample is growing, with the average growth rate exceeding one for manufacturing companies. It should be pointed out that similar results were initially obtained for developed countries [16].

We paid attention to equipment purchase, exploitation of state subsidies and bank credits as well as licensed foreign technologies.

It was found that service companies have received fewer subsidies and less often have asked for bank credits. At the same time, they have bought machines and equipment as often as high-tech manufacturing companies and have used even more foreign licensed technologies.

General analysis of innovative activities showed that on average high-tech manufacturing companies are more engaged in innovation activities and spend more money on R&D comparing to service companies.

Dynamics of employee number during three years was chosen as main growth indicator and therefore dependant variable at the stage of growth analysis. Such approach is rather popular in literature. Internal characteristics influencing company's growth included factors related to innovative capacities, human capital, resource conditions, and financial limitations. Company's age and ownership structure were also taken into account. Main attention was paid to internal (specific) growth factors which play crucial role as macro-economic and institutional factors have general character and are common for all companies. Regional conditions were also analyzed through company's location which was presented by distance from Moscow.

V. RESULTS AND THEIR INTERPRETATION

Our analysis made it possible to define different factors, which are significant for the explanation of employment dynamics in Russian small and medium size high-tech companies.

Age of the company turned to be a common growth determinant negatively related to employment increase. This means that new jobs are created mainly by young companies. Such conclusion confirms previous results obtained by other researchers [7, 17, 18].

Share of employees with a university degree is another common factor having positive influence on jobs creation. It should be noted that lack of qualified staff is considered to be the main growth barrier for Russian high tech companies. So our results confirm that growing high tech companies create qualified new jobs; this fact presents the difference between them and companies working in other sectors.

Technological characteristics of companies are reflected in differentiation of significant growth factors for high-tech manufacturing companies and knowledge-intensive companies in services. This can be possibly related to the fact that high-technology manufacturing deals with long-circle technologies, high entry costs, capital intensity and long-term production. Services, which are represented in our sample mainly by IT firms, are based on short-circle technologies with low entry barriers, quick changes and low capital intensity.

Knowledge-intensive companies in services

Employment growth of knowledge intensive service companies is negatively related to company's age and positively related to highly qualified employees. Two more factors also turned out to have positive influence. They are: "Percentage of the firm owned by the largest owner" and "Application for any loans or lines of credit in the fiscal year".

In most Russian companies, ownership is highly concentrated. One can assume that ownership consolidation helps to make quick operative decisions and to decrease agent's costs related to disperse ownership structure. Besides as entrepreneurship in Russia has rather short history usually in small and medium size businesses company's owner acts as chief executive manager (CEO).

Application for credits is a signal that managers and owners are confident of growth perspectives. Lack of financial limitations also helps to hire new employees.

High-tech manufacturing companies

In addition to the common determinants mentioned earlier employment growth in high tech manufacturing companies depends also on state subsidies and fixed assets' purchase.

We deal with private companies. However nowadays government in Russia (both federal and regional) continues to support industrial enterprises in the form of subsidies, remains a significant investor in equity and takes an active part in market transactions using state procurement system.

State subsidies are to some extent a substitution of undeveloped financial markets and serve as significant source of investments for manufacturing companies, helping to deal with financial limitations. Equipment purchase means an increase in operation scale and new jobs creation.

Negative relationship between innovations in previous three years and employment increase turned to be an unexpected result. Possible explanation could be that companies are orientated on process innovations, which are capital-intensive and labor saving and lead to jobs' cut. Such a result needs more studies and analysis.

VI. CONCLUSION

In conclusion it is necessary to point out that our analysis of performance and development indicators of Russian private high tech companies, based on the World Bank empirical data set BEEPS, showed that young companies play crucial role in the creation of new jobs in small and medium size high tech business. Specific factors are significant for different sectors (high tech knowledge intensive services and high tech manufacturing). Positive influence of human capital quality on high tech business growth was determined in both analyzed sectors. This conclusion seems to be significant not only for the development of evolutionary economics but also for state innovative and industrial policy formation. Defined determinants of high tech companies' growth could be taken into account under investment decisions making also.

ACKNOWLEDGEMENTS

The study presented here is the part of the Project № 17-02-00221 "Development of High Tech Companies in Russian Regions: Factors and Barriers of Growth", supported by Russian Humanitarian Scientific Fund.

REFERENCES

- [1] Eeckhout J. (2004) "Gibrat's law for (All) Cities", The American Economic Review, No. 94(5), pp. 1429-1451.
- [2] Acs Z., Mueller P. (2008) "Employment Effects of Business Dynamics: Mice, Gazelles and Elephants", Small Business Economics, No. 30(1), pp. 85-100.
- [3] Acs Z., Parsons W., Tracy S. (2008). High-Impact Firms: Gazelles Revisited. Washington, DC: Corporate Research Board, LLC.
- [4] Simon H. (2009) "Hidden Champions of the 21st Century. Success Strategies and Unknown World Market Leaders", Springer-Verlag, New York, XVI, pp. 402.
- [5] Audretsch D.B., Keilbach M.C., Lehmann E.E. (2006) "Entrepreneurship and economic growth", Oxford University Press, 240 pp.
- [6] Piatier A. (1984) "Barriers to innovation: a study carried out for the Commission of the European Communities", Directorate-General Information Market and Innovation, London.
- [7] Audretsch D.B. (1995) "Innovation Growth and Survival", International journal of industrial organization, No. 13(4), pp. 441-457.
- [8] Kihlgren A. (2003) "Small business in Russia – factors that slowed its development: an analysis", Communist and Post-Communist Studies, No. 36(2), pp. 193-207.
- [9] Aidis R., Estrin S., Mickiewicz T. (2008) "Institutions and entrepreneurship development in Russia: a comparative perspective", Journal of Business Venturing, No. 23(6), pp. 656-672.
- [10] Bhaumik S.K., Estrin S. (2007) "How Transition Paths Differ: Enterprise Performance in Russia and China", Journal of Development Economics, No. 82 (2), pp. 374-392.
- [11] Molz R., Tabbaa I., Totskaya N. (2009) "Institutional Realities and Constraints on Change: The Case of SME in Russia", Journal of East-West Business, No. 15(2), pp. 141-156.
- [12] Zhuplev A., Shtykho D. (2009) "Motivations and obstacles for small business entrepreneurship in Russia: fifteen years in transition", Journal of East-West Business, No. 15(1), pp. 25-49.
- [13] Shirokova G., Shatalov A. (2010) "Factors of New Venture Performance in Russia", Management Research Review, No. 33(5), pp. 484-498.
- [14] Nightingale P., Coad A. (2014) "Muppets and gazelles: Political and methodological biases in entrepreneurship research", Industrial and Corporate Change, No. 23(1), pp. 113-143.
- [15] Daunfeldt S.O., Elert N., Johansson D. (2015) "Are high-growth firms overrepresented in high-tech industries?" Industrial and Corporate Change, No. 25(1), pp. 1-21.
- [16] Henrekson M., Johansson D. (2010) "Gazelles as job creators: a survey and interpretation of the evidence", Small Business Economics, Springer, No. 35(2), pp. 227-244.
- [17] Kane T.J. (2010) "The Importance of Startups in Job Creation and Job Destruction", Hudson Institute, Kauffman Foundation Research Series: Firm Formation and Economic Growth.
- [18] Haltiwanger J., Jarmin R., Miranda J. (2013) "Who Creates Jobs? Small versus Large versus Young", Review of Economics and Statistics, No. 95(2), pp. 347-361.



Ivanova Anastasiya I. - engineer of the department of Industrial Enterprises Management at Institute of Economics and Industrial Engineering, professor assistant at NSU. Research interests deal investment attractiveness of Russian national and regional economy, innovative activities, regional economics.



Kuznetsova Svetlana A. - candidate of science, senior researcher of the department of Industrial Enterprises Management at Institute of Economics and Industrial Engineering, Head of the department of Management at NSU. Research interests deal with problems of business strategy, innovation management, innovative entrepreneurship, and companies' strategies in the digital economy.



Khalimova Sophia R. - candidate of science, researcher of the department of Industrial Enterprises Management at Institute of Economics and Industrial Engineering, associate professor at NSU. Research interests deal with development of innovative activities, national and regional innovative systems innovative entrepreneurship, regional economics



Yusupova Almira T. - doctor of science, leading researcher of the department of Industrial Enterprises Management at Institute of Economics and Industrial Engineering, professor at NSU. Research interests deal with contemporary industrial markets development, innovative entrepreneurship, lease finance of fixed assets.



Kravchenko Natalya A. – doctor of science, head of the department of Industrial Enterprises Management at Institute of Economics and Industrial Engineering, professor at NSU. Research interests deal with innovations economics, national and regional innovative systems, innovative entrepreneurship, investment and financial management, industrial and investment policy, development programs creation methodology.



Goryushkin Anton A. – researcher of the department of Industrial Enterprises Management at Institute of Economics and Industrial Engineering, professor assistant at NSU. Research interests deal with mathematical methods of industrial enterprises activities modeling, statistical methods of economic information analysis.

Financial and Economic Aspects of Diversification Formation Patterns in Strategy Development of Regional Mechanical Engineering

Larisa I. Lugacheva, Maria M. Musatova, Elena A. Solomennikova

Institute of Economics and industrial engineering SB RAS, Novosibirsk state University, Novosibirsk, Russia

Abstract – The article presents the results of the study of adaptation problems of Russian defense industry enterprises in the course of diversification. The different priorities of goals in the implementation of diversification strategy in the development of civil and military products for the defense industry organizations is shown. The mechanisms of institutional support and competitiveness of machine-building companies in the region in the transition to the production of civil and dual-use products are discussed. The existing institutions of diversification are systematized and their functions are clearly identified, both at the Federal and regional levels. The article substantiates the importance and role of regional engineering for the Russian economy and considers the range of possible alternative methods of financing diversification, providing the transition to an effective model of real technological development of civil engineering. The forms and examples of successful diversification in defense industry enterprises in Novosibirsk Oblast are analyzed. The necessity of a differentiated approach to development of the processes of diversification at defense enterprises is proven. It should take into account the specifics of military-technical products and the possibility of using unique capacities in certain groups of defense enterprises in the manufacture of civilian high-tech products. The factors affecting the prospects and dynamics of diversification of production of defense enterprises in the Novosibirsk Oblast are identified. The mechanisms of diversification are specified and the measures to ensure its implementation by the authorities are formulated and proposed.

Index Terms – Diversification, regional engineering, hi-tech, competitiveness.

I. INTRODUCTION

IN RECENT YEARS, Russia has seen a multifaceted systematic approach to the creation of real technological development. The exhaustion of the raw material model of economic growth based on high incomes from raw material exports and the imposition of sanctions by the West make a priority of the development of high-tech engineering industries without alternatives. The completion of the cycle of rearmament of the Russian army and the reduction of national defense spending, which are closely correlated with the dynamics of oil prices, require urgent measures to form a balanced economy. As further support for continuous increase in military expenditure in conditions of economic stagnation is not possible in the coming years, new prospects for the machine-building complex will be associated with import substitution, the development of digital technologies and diversification of production [1; 2].

According to the state arms development Program of the Russian Federation, the large-scale rearmament of the army and navy will be completed by 2020. Accordingly, in this

regard, the state defense order will be sharply reduced, and to maintain a stable financial position, defense enterprises need to switch to the production of civilian products at the available capacities.

The subject of the study is the institutional environment of diversification in Russia and its regions – substrate and the space of relations deformed by the state, based on the motives of the development of diversification, which the country needs in the conditions of ongoing sanctions. In the last decade in Russian regions with the most developed machine-building industry, defense industries have started to play a practically system-forming role in the regional economy. Study of the institutional configuration of processes of diversification and factors of the formation of markets for civil high-tech products in Russia is useful for the development of strategic decisions and policies to stimulate machine-building companies with a defense profile at both the Federal and regional levels. Although the implementation of the strategy of transition to the model of diversification of the economy marked a number of successes, there remain a number of problems.

The purpose of this work is to study the features in the behavior and functioning of the defense engineering industries of the Russian Federation and Novosibirsk province in the transition to the model of diversification,

The article applies the political economy approach with the use of the methodological apparatus of modern institutionalism and logical analysis. The tasks of the work are solved on the basis of a set of system methods: structural-logical and factor analysis, revealing the coherence of public policy in the processes of diversification and the existing market environment. The paper uses methods of systematization, classification, grouping and comparison. For the analysis of factors and conditions of activation of processes of diversification in regional mechanical engineering, case study methods are applied.

II. PROBLEM DEFINITION

Under the conditions of the 4th industrial revolution, the part of innovative technological solutions and breakthrough science-intensive projects is initially presented in the civil sector. In retrospect, it was the opposite: breakthrough technologies were created in the military-industrial sector and only then transferred to the civil one. An example is the degree of integration of communication, which is available in

the widespread modern smartphones, but in cosmic conditions will appear in ten or fifteen years. The diametrically changed situation with the emergence of innovative technologies, both in the world and in Russia, leads to the emergence of new forms of interaction between the defense sector and the civil sector of the economy, to the transfer of technology (in two directions). In the current economic realities in developed countries, the MIC becomes both a source of new technologies for civil segments and an active consumer [3]. At the same time, there are adaptation problems of Russian defense enterprises in the course of diversification [4].

Organization of the defense industry in implementing the strategy of diversification faces different priorities in the development of civil and military products (Fig. 1).

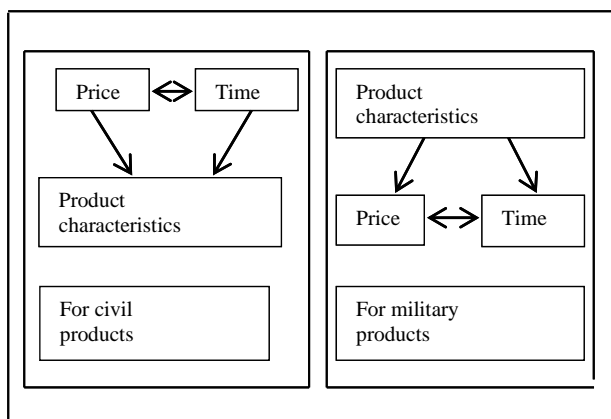


Fig. 1. Priority of goals in the production of machine-building products at defense enterprises.

In the development of military-technical products, their tactical and technical properties are the priority, whereas production time and price are of a subordinate nature. In the market for civil products, the priority is the price and timing of the product to the buyer, and the quality of consumer characteristics are set depending on these parameters. In this regard, the profitability of civilian production will be largely determined by the scale of production (mass, serial, large-scale production).

III. ADAPTATION PROBLEMS OF RUSSIAN DEFENSE ENTERPRISES IN THE COURSE OF DIVERSIFICATION

The problems and peculiarities of the Russian defense complex are that most of its enterprises were originally created exclusively for military purposes and until recently they carried out their activities isolated. Theoretically, the successful transfer of technologies from the “defense sector” to the “civil sector” provides the defense industry with significant advantages in creating competitive products. At the same time, technological maneuvers to transfer capacities during diversification are faced with the lack of equipment necessary for the production of civilian products [5]. Enterprises are often not competent enough in marketing and after-sales service of civil products, they lack the competence, capacity and personnel for their production and to assess

consumer demand for new products. As in accordance with the all-Russian concept of diversification of the defense industry, the proportion of military and civilian production will dynamically change in the direction of increasing the output of civilian goods, so the readjustment of capacities and technological equipment at the enterprises of the defense industry will require constant financial resources and institutional support (Tab. I).

While government authorities have developed substantial tools to support diversification projects, analysts and experts have expressed concerns that not all enterprises in this sector will be able to take advantage of these opportunities effectively and quickly (Tab. II) [6, 7].

In our view, the greatest difficulties in the transition to diversification of production may arise from enterprises related to the ammunition and special chemicals industry, engaged in the production of conventional weapons and other production.

At the end of 2016, Russian President Vladimir Putin set a goal to increase the share of civilian products to at least 17% of the total production of the Russian defense industry by 2020, to 30% by 2025, and to 50% by 2030. However, by the beginning of 2018 this figure was 17%, while in some regions of Russia with a very developed defense industry, in particular in Novosibirsk Oblast (NSO), the share of civil production was significantly higher – 26.6%. This was also facilitated by the growing innovation activity of enterprises of NSO, the high industrial, scientific and technical, educational and personnel potential of the region and the intensive formation of competitive advantages of the regional machine-building complex (RMC) [8].

TABLE I
INSTITUTIONAL SUPPORT FOR DIVERSIFICATION FOR ADAPTATION AT THE FEDERAL LEVEL

| Diversification institutions | Functions |
|---|---|
| NGO "Conversion" (joint structure of Rostec and Vnesheconombank) | What to produce and how to sell? Specializes in identifying the needs of the market in civilian products, finding areas and opportunities for the promotion and sale of products of defense enterprises, on the formation of their "product thinking". |
| Special program of the industrial development Fund "Diversification" (the Fund of diversification of the defense industry): for enterprises included in the register of defense organizations | How to produce? Provides participants with access to cheap and long-term money for the creation of samples and components for the civil industry: preferential loans from 200 to 700 million rubles for up to five years with an interest rate of 1% in the first three years of the loan and 5% - for the remaining period. The target value of sales of new products is not less than 50% of the loan amount per year, starting from the second year of serial production. |
| Joint program of the Ministry of industry and industry and the Ministry of education to create and develop engineering centers at universities | Who to cooperate? The creation of engineering centers, with main focus on areas that contribute to the diversification of the products of the defense industry. |
| GIS industry platform | How to provide information support? The installation of the civil defense projects of the enterprises. On the base of that, interactive catalogs of high-tech products manufactured by the defense industry (more than 2200 entries of high-tech products of civil and dual-use) are formed. |
| The main pool of projects to diversify the defense industry (more than 170 planned for implementation in the next four to five years). Formed By The Ministry Of Industry And Trade. | Elimination of duplication of projects of large corporations (Rostec, Rosatom and Roscosmos), identification of opportunities for cooperation on specific project proposals related to the production of civil products. |
| Agency for technological development | Assistance to Russian enterprises in the implementation of world-class technological solutions in order to achieve the competitiveness of domestic products. |

Compiled by authors

TABLE II
SECTORAL STRUCTURE OF RUSSIAN DEFENSE INDUSTRY
To 2016

| Industry | The share of industry in the defense industry of the Russian Federation, % |
|----------------------------------|--|
| Aviation | 14,3 |
| Radio | 11,7 |
| Shipbuilding | 9,6 |
| Electronic | 8,1 |
| Communication | 7,5 |
| Conventional weapons | 7,4 |
| Ammunition and special chemicals | 6,9 |
| Rocket and space | 6,0 |
| Other | 28,5 |
| Total | 100 |

IV. RESEARCH RESULT. ECONOMIC CHARACTERISTICS OF RMC AND PROCESSES OF DIVERSIFICATION

NSO provides 20% of the output of all machinery products in Siberia. The regional complex covers about 80 large and medium-sized machine-building companies, among which about 50 represent defense plants. The sharp activation of innovation processes in the RMC between 2014-2017 was accompanied by the implementation of the policy of import substitution and technical re-equipment of the Russian army. The new geopolitical situation strengthened provision of orders to the defense enterprises of the machine-building complex and gave an additional impetus to its innovation and technological development [9,10].

Although at the present time, the RMC is noticeably behind leading foreign manufacturers, especially with regard to the production of precision machining devices and mechanisms with high-tech software control and the degree of renewal of fixed assets in engineering, in General, the value of the RMC for the country is determined by the composition of the products. New Siberian companies producing unique science-intensive products continued progressive development even during the recession and sanctions. Their products were in demand both in domestic and foreign markets [11].

Distinctive features of the RMC in NSO are constant support from regional development institutions, a significant orientation, compared with the Russian engineering industry as a whole, to the foreign market (in the structure of commodity exports, the share of machinery, equipment and vehicles is more than 50%). As part of the strategy of import substitution over the past years, companies have been mainly engaged in the process of replacing machine-made products at an already achieved technical level and presented in foreign markets in a wide format; only in isolated cases, the production of high-tech products without analogues elsewhere in the world, was carried out.

Since 2016, NSO has had a diversification program which implies the transition of RMC to the next technological level. In recent years, within the RMC in NSO there has been an intensive formation of the economy of high-tech projects in such areas as: telemedicine, biomedicine, robotics, information technology, development of materials with desired properties for wide application in space activities, environmental management, Arctic exploration, etc. Siberian enterprises in the defense industry have produced civilian goods under the Arctic program of "Gazprom".

The authorities of the city have two important areas of joint activity with defense industry enterprises in the implementation of the "Smart City" program: the introduction of energy-saving lighting of buildings and streets, and intelligent regulation of traffic flows. On the basis of Institute research, Institute of electronic devices (NIIEP) business partners are willing to place orders for the production of civilian products. In particular, automated control and management systems for housing and communal services, LED products and dynamic navigation systems for Russian Railways, as well as a multi-functional optical-electronic control system based on thermal imaging equipment necessary to ensure the safety of high-speed highways. And at the plant "Trud", the snow-melting machine for the needs of the city. NIIEP also expressed its readiness to join this programme.

In addition to Federal state support for defense enterprises, regions can play an important role in implementation of the diversification strategy. However, as they see it, they need a

real incentive and financial leverage to act on diversification. Due to the limitation of regional budgets, it is possible that defence industry enterprises pay all taxes from the civil sector in the region where they are located and receive various kinds of support.

Institutional changes are needed not only at the Federal level but also at the regional level to diversify. It is the new institutional environment that creates the conditions for the effective implementation of innovative and technological solutions in the civil sector of RMC (Tab. III).

In recent years, enterprises of the defense industry in NSO were provided with tripartite support and assistance for diversification:

- * from the Executive - financial support measures;
- * from the Legislature - formation of the correct legislative framework for local defense enterprises;
- * from the banking sector – lending to the defense industry, including at a reduced rate.

TABLE III
INSTITUTIONAL SUPPORT FOR DIVERSIFICATION AT THE REGIONAL LEVEL

| Diversification institutions | Functions |
|---|---|
| Board of Directors of academic institutions with the participation and support of universities and the Federal Agency of scientific organizations | <ul style="list-style-type: none"> • Identification of areas and projects for the diversification of defense enterprises; • identification of prospects of scientific developments for implementation in cooperation with the defense industry |
| NSO industry development fund | <ul style="list-style-type: none"> • Provision of counselling, information and services in a "One Stop Shop" for support of subjects of industrial activity; • providing their own financing of development projects of industrial enterprises at 5% per annum in the first phase of the projects of the program of re-industrialization of the economy of the Novosibirsk region |
| The regional center of normative and technical support of innovations will be created on the basis of NSTU | Help inventors to bring projects to industrial designs and bring products to market. |
| Business Association of heads of defense enterprises "Commonwealth. Efficiency. Development" (SIR) | <ul style="list-style-type: none"> • Proposals on amendments to the state program - providing subsidies for compensation of costs for the maintenance of purchased movable property, etc.; • cooperation with the regional Parliament; operational assistance in solving issues arising in the field of industry. |
| Program "Workers for advanced technologies" | <ul style="list-style-type: none"> • Organization of work on interaction with the real sector of the economy; • carrying out activities to retain young professionals in the workplace. |

Compiled by authors

V. DISCUSSION OF RESULTS, FORMS AND EXAMPLES OF SUCCESSFUL DIVERSIFICATION IN THE DEFENCE INDUSTRY IN NSO

The strategy of diversification of defense industry enterprises does not imply the launch of a uniform universal mechanism for decision-making on the organization of civil production at existing facilities and strict bringing production share to the borders established in the program documents. With the increase in output of civilian products at defense industry enterprises, a differentiated approach and a wide range of indirect solutions are needed for them, the search for options for active cooperation between defense industry enterprises, the formation of horizontal and vertical integration ties, the establishment of partnership relations between the defense industry enterprises and regional technology parks, clusters to create truly competitive and high-tech products.

The differentiated approach should take into account the specifics of the military-technical products and the possibility of using the unique capacities in certain groups of defense enterprises in the manufacture of civilian high-tech products [7, 12].

In NSO, defense industry enterprises can be divided into the following groups with respect to diversification.

1. Enterprises already producing highly technical dual-use products and products for the civil sector, supplied to the markets (the share of civil and dual-use products is more than 20%). They are part of large corporations and state corporations, within the framework of which in the last two years, units have been established, specializing in the organization of production and promotion of such products, such as:

- United Aircraft Corporation, UAC (civil aviation aircraft);
- Almaz-Antey Concern (air traffic control systems, telecommunication equipment). Almaz-Antey Corporation has

created a department of civil products and intends to deal with medical equipment;

- Shvabe Concern (medical equipment, devices for scientific research, energy-saving lighting) [13];
- Rostec Corporation, which has many enterprises in the NSO, is actively involved in development, is ready to buy technologies and innovative companies and to participate in cooperation with the enterprises of RMC and Rostec. Rostec plans to invest 4.3 trillion rubles in the diversification of the defense industry of the Novosibirsk region by 2025;
- Roscosmos Corporation has a good foundation in its enterprises for the production of civil products, including medical equipment.

The defense industry organizations of this group are able to increase the production of high-tech products for the civil sector with minimal state support. Such enterprises of the defense industry in the NSO are the majority. A number of enterprises of the NSO defense industry from the group were able to start diversification on their own through the development of cooperative chains. Concerns and state corporations of the defense industry are the center of the ecosystem of high-tech companies: third- and fourth-level suppliers of equipment and technologies and partners in the production of civilian products.

Among them is the Novosibirsk aviation plant (NAZ) Chkalov. As part of diversification, the plant is increasing production of components for the operation of civil aircraft "Superjet", the number of which in the country's fleet requires an increase in the supply of spare parts and components within the framework of import substitution and diversification programs. Because NAZ is thoroughly equipped for the production of components for the Superjet, it is included in a conglomerate for the construction of a new aircraft MS-21 with the Irkutsk aviation plant. The enterprise will not have to - rebuild the production line for the production of parts of another model of the aircraft. However, Chkalov will make only parts for the MS-21 and supply them further along the chain of cooperative ties to other UAC plants, which are engaged in the manufacture of units. Chkalov is planning a seven-fold increase in the production of spare parts for civilian aircraft in 2018 [14, 15].

The Novosibirsk Komintern plant (a subsidiary of the Almaz-Antey Concern) is developing equipment for civil areas. It plans to launch new production for the enterprise at the turn of 2018-2019, when the state defense order is expected to be reduced. While the plant has a serious state order through the Ministry of defense and export orders within the framework of interstate agreements (50% in the portfolio structure). Diversification for production of civilian goods is conducted in four directions: airfields; robotics, which includes the development of all types of drones (air, ground, underground); development of specialized software; innovative medical technology. In 2018, the research institute of measuring instruments and the Novosibirsk Komintern plant in cooperation with the institute of oil and gas geology and geophysics SO RAN started mass production of geolocators, indispensable for the detection of underground utilities without drilling [16].

Rostec Corporation includes NSO defense industry enterprises in interregional cooperation within the framework of diversification. So in the Republic of Dagestan (Kaspiysk) assembly production of agricultural machinery is organized under the subsidiary "Sissel-mash-Spetstekhnika". Thus, its civilian products enter the markets of the Southern and North Caucasus Federal districts. Assembly of equipment will be carried out at the facilities of the Caspian defense Electromechanical plant (cemz), 25.5% of which is owned by Rostec. By the end of 2018, it is planned to localize up to 60% of the production of all components at the production base of cemz.

2. Enterprises whose products are very difficult or fundamentally do not fit into the markets of civilian products (missile systems, special ammunition, etc.). For such enterprises, it is likely that it is necessary to increase the production of high-tech military-technical products of export orientation with a very modest contribution to the civilian sector or to create a new segment undeveloped of competitors in sales of civilian products.

An example of the successful diversification of enterprises of this group for the development of a new niche in the market of civil products is JSC (Novosibirsk mechanical plant "Iskra"), which initially had a production orientation (production of gunpowder and explosives) for exclusively military purposes. By 2018, the company has mastered a wide range of detonating cords for mining and coal industry, exploration and similar works. In 2017 "Sparks" had a share of about 72-75% of the Russian market of mining industry. The company is mainly engaged in the development and manufacture of means of initiation for the mining and coal industry. The priority of further technical development of the plant is the development and production of electronic blasting systems.

3. Enterprises which traditionally have a small share of citizens' products, do not exceed 10% in the total volume of such production and sales. It is possible to diversify these enterprises, but at a high cost and with a serious reorganization. Diversification may force defense enterprises to develop individual civilian industries, using the accumulated working capital of the past years, including export contracts, as well as free production capacity.

The NSO has all the possibilities and an urgent need to create a variety of models for financing civil projects of defense enterprises of this group.

The defense enterprises of the national defense company own large areas that are not involved. In the framework of diversification of such areas with secured communications are beginning to be used as industrial parks. Small business can become the main partner of defense industry enterprises in the production of civil products. Large defense organizations, even with the support of state corporations, find it quite difficult to occupy a new niche in the market of civilian products.

Small enterprises are more flexible and mobile in making innovative and technological decisions. They respond quickly to changes in the external environment and make decisions at any stage of the project: the initial, its full launch and improvement, optimization and completion.

Regional authorities propose to place new small business enterprises in the territories of industrial parks: private and public.

In Novosibirsk, one of the few private industrial parks in the country operates on the basis of a cartridge plant. The concept of creating the Kirovsky industrial park was developed by the agency of innovative development at the city hall of Novosibirsk for implementation of the program of diversification of the "Sibelektroterm" enterprise. In the industrial Park (the territory of Sibelektroterm), it is planned to launch electrometallurgical production, production of mining equipment and agricultural machinery on a cluster basis.

On the part of the state authorities for enterprises belonging to the third group, they will require co-financing of projects, for them it is very problematic to enter the market of high-tech civilian products. Production and sale of a number of civil products is chronically unprofitable due to the discrepancy between the existing production system and the level of real effective demand.

FANO intends to create a Board of Directors of research institutes on the basis of the Novosibirsk academic city in order to coordinate innovative areas of work of defense enterprises in the field of: telemedicine, biomedicine, robotics, information technology, development of materials with specified properties that can be widely used in space activities, issues of environmental management, development of the Arctic, etc., as well as the search for projects to diversify defense enterprises [17].

VI. CONCLUSION

The analysis shows that the mechanisms of diversification, in our opinion, should include mechanisms to stimulate demand for innovation through the distribution of investment resources among consumers of innovation. Many innovative and technological developments of civil products are promoted through the scientific and technological initiative, through Federal and regional target programs. Their formation takes place mainly on the principles of public-private partnership and the availability of co-financing from the industrial partner. However, the potential consumers of high-tech products, unfortunately, are not yet ready to go for a risky, so-called venture type of co-financing.

The factors influencing the prospects and dynamics of development of diversification of production of defense enterprises in the NSO are currently:

- development of various forms of cooperation between defense enterprises, between defense enterprises and various sectors of the economy, intra-regional and inter-regional cooperation of defense enterprises of machine-building profile;
- search for options for cooperation between the Executive structures of the region with the defense industry in the format: orders of components at their capacities through contract agreements; conclusion of franchise agreements; organization of joint ventures, etc.
- establishment of the project centre of diversification of government structures in the NSO. This structure could coordinate the processes of technical re-equipment and di-

versification of enterprises of the military-industrial complex, identify drivers of regional economic growth on the basis of defense industry enterprises, taking into account the already selected areas of its development, review and take into account the already formed expensive competencies when choosing a product portfolio for civil production.

The strategy of diversification and its implementation requires changes in the legal framework and the establishment of barriers for the import of imported equipment for those Russian analogues that fully comply with foreign ones and are not more expensive than imported equipment.

The government structure can regulate public procurement and establish priorities for purchase by government agencies of domestic products, which will increase the efficiency of output of civil production in the enterprises of the defense industry. To date, for example, 40-60% of all medical equipment is imported, although about 3/4 of the medical equipment has Russian analogues, which leads to intense competition in the market of medical equipment.

In our opinion, the transition to the production of civilian products will be successful only if the state forms a state order, at least partially, and for civilian products, which should be produced by the defense industry. State structures for defense enterprises should probably form a plan of state procurement for the medium term (3-5 years), which will show the profile of high-tech equipment and its demand in the foreseeable period of time.

REFERENCES

- [1] Afontsev S.A. The exit from the crisis in the conditions of sanctions: the mission is not feasible? Questions of economy. 2015. № 4, pp. 20-36. (in Russian).
- [2] Huebener P., O'Brien S., Porter T., Stockdale L., Zhou Y.R. Exploring the Intersection of Time and Globalization // Globalizations. 2016. Vol. 13. Iss. 3. P. 243-255. doi: URL: <http://dx.doi.org/10.1080/14747731.2015.1057046>. Дата обращения 12.07.2016.
- [3] Gansler J.S. Democracy's Arsenal: Creating a Twenty First Century Defense Industry. Massachusetts, Boston: MIT Press, 2011. 432 p.
- [4] Batkovskij A.M., Fomin A.V., Leonov A.V., Pronin A.Yu. a.yu. Improving the management of the military-industrial complex: monograph. M.: OntoPrint, 2016. 472 p. (in Russian).
- [5] Hartley K. Defense Economics: Its Contribution and New Developments. Department of Politics and Economics, Royal Military College of Canada, 2003. 247 p.
- [6] Zlodeev V. Conversion 5.0. //vedomosti Assemblyman FNL 30.06.17. URL: <http://ведомостинсо.рф/Конверсия-5.0>. Date treatment 2.07.2017. (in Russian).
- [7] Biryukov A.V. Cluster policy as a factor in increasing the competitiveness of defence industries //microeco-nomics. 2009. № 5. C. 70-75. (in Russian).
- [8] Temereva Yu. How diversification PJС in Russia. Economy and business. November 8, 2017. URL: <http://tass.ru/ekonomika/4710238>. (in Russian). Date treatment 12.11.2017.
- [9] Warsaw A.E., Dubinin M. Synergy production of military and civilian products (for example, the aviation industry)//national interests: priorities and security. 2017 t. 13. No. 1. C. 20-33. URL: <https://cyberleninka.ru/article/v/sinergiya-proizvodstva-voennoy-i-grazhdanskoy-produktsii-na-primere-aviatsionnoy-promyshlennosti>. (in Russian). Date treatment 22.03.2017
- [10] Warsaw A.E. Economic growth and innovative development: national security issues//Concept. No. 2 2015. P. 3-21. (in Russian).
- [11] Sobolev L.B. Restructuring defense industry//finance and credit. 2016. No. 47. P. 47-62. URL:

- <https://cyberleninka.ru/article/v/restrukturizatsiya-oborono-promyshlennogo-kompleksa>. Date treatment 12.12.2016. (in Russian).
- [12] Falcman V.K. Prerequisites of import substitution and export high-tech products development//ECO. 2016. № 4. Pp. 56-73. (in Russian).
- [13] Schwab K. The fourth industrial revolution. Moscow: Eksmo, 2016. 475pp. (in Russian).
- [14] Shevel'ko D.A. The State program "development of the aeronautical industry to 2013-2025": basic examination results//Herald of ITS AS-SETS WORTH 13.91%. No. 2 2015. C. 214-218. (in Russian).
- [15] Epova N.R. Increased presence of Russian aircraft market: problems and perspectives/ Baikal Research Journal. 2014. № 2. C. 14. URL: <http://brj-bguenp.ru/reader/article.aspx?id=19028>. Date treatment 14.02.2015. (in Russian).
- [16] Zabolotny. P. "Daughter" Almaz-Anthea "in Novosibirsk is prepared with the year 2019 to produce civilian goods. URL: <http://tass.ru/sibir-news/3616173>. Date treatment 13.09. 2016. (in Russian).
- [17] Kotykov M. In Novosibirsk will create Council of scientific institutes to study the PJC diversification projects. Siberia. June 21, 2017. <http://tass.ru/sibir-news/4354933>. Date treatment 22.06.2017. (in Russian).



Lugacheva L. I. – Cand. Econ. Of Sciences, leading researcher of IEIE SB RAS, Associate Professor of Novosibirsk State University. Author of more than 140 publications . Research interests: problems of development and restructuring of Siberian machine building, integration processes in manufacturing, economic security of the region; formation of innovative potential of machine building; institutional components and factors of development of regional engineering.
Email: lugamus@yandex.ru



Solomennikova E. A. – kand. Econ. Sciences, leading researcher of IEIE SB RAS, Associate Professor of Novosibirsk State University. Author of more than 160 publications. Research interests: transformation of traditional enterprise management systems in the conditions of business digitalization; organizational design of high-tech business.
Email: esolom46@mail.ru.



Musatova M. M. – Cand. Econ. of Sciences, senior researcher of IEIE SB RAS, Associate Professor of Novosibirsk State University. Author of more than 110 publications. Research interests: methodological and applied problems of integration processes of Russian companies, industry and engineering. Research Maria Musatova was supported by grants of Russian Foundation for Humanities and Russian Foundation for basic research: Grant RGNF № 09-02-00418a "Econometric evaluation of integration processes of Russian companies" - project Manager. Grant of RGNF № 12-12-54003 "Priorities of post-crisis development of machine-building complex of the Novosibirsk region" - responsible executor of the project. RFBR grant № 17-02-00016 "Economic and mathematical methods of analysis of the behavior of private equity funds in the Russian market of corporate control" — the responsible executor of the project.
Email: maria.musatova@gmail.com

Resources of Developing Hi-Tech Spheres in Russia

Olga E. Malykh, Elena A. Gafarova

The Federal State-Funded Educational Institution of Higher Professional Education

Ufa State Petroleum Technological University, Ufa, Russia

Institute of socio-economic research – autonomous branch of Federal State Budgetary Research Institution of Ufa

Scientific Centre of Russian Academy of Science, Ufa, Russia

Abstract – In the article authors analyze resources of developing hi-tech spheres in Russia. On the base of Cobb-Douglas specification authors show interdependence between gross domestic product, investment in basis capital, average annual number of employees of enterprises and organizations, internal current expenses for scientific research and development, number of employees that are assigned to R&D, activity of postgraduate training programs and doctoral studies, relative share of innovational goods, works and services in gross amount of goods, works and services.

Index Terms – Resources, hi-tech spheres, scientific research and development.

I. INTRODUCTION

Economic policy of Russian government has acquired new features in the last few years. Goal of creating innovational model of economic growth has attracted attention of domestic and foreign researches. In practical aspect one can notice adjustment of an adequate mechanism of realization, part of which is state program of supporting promising spheres in Russia that is aimed at developing domestic factors of economic growth. Base of creating innovational economy is modernization and even reindustrialization of economic system of the country. Herewith requirements to resources are being significantly changed: labour is becoming more complicated at the expense of intellectual component and capital increases even more through using results of intellectual activity [1, 2]. Authors think that this hypothesis needs to be examined because spending on modernization of socio-economic system is quite significant.

On current stage of the study we will analyze quality of resources of development of hi-tech spheres and their influence on GDP through a group of criteria among these are investment in basis capital, average annual number of employees of enterprises and organizations, internal current expenses for scientific research and development, number of employees that are assigned to R&D, activity of postgraduate training programs and doctoral studies, relative share of innovational goods, works and services in gross amount of goods, works and services.

Hypothesis of this study: these factors have unequal influence on developing hi-tech and science-driven spheres of Russia.

Research objective is to define through econometric methods scope of influence of these factors (part of them) on dynamics of gross added value and on the basis of this

describe resource perspectives of hi-tech and science-driven spheres development in Russia.

Calculations were made using data of Federal Statistical Service as well as informational and statistical materials of “Statistics of science and education” by Federal State Funded Research Institution – Republican research scientific and consulting center of expertise.

II. PROBLEM DEFINITION

Today high grade of technological performance is a main element that allows companies to maintain a position in the context of global competition. Since the beginning of XXI century gross expenses on R&D has continually been growing (see Table I).

TABLE I
GLOBAL EXPENCSES ON R&D

| Year | Scope of R&D, bln. USD | Rate of growth, % |
|------|------------------------|-------------------|
| 2005 | 400 | |
| 2006 | 409 | 2,2 |
| 2007 | 447 | 9,3 |
| 2008 | 501 | 12,2 |
| 2009 | 538 | 7,3 |
| 2010 | 508 | -5,6 |
| 2011 | 560 | 10,3 |
| 2012 | 614 | 9,7 |
| 2013 | 638 | 3,8 |
| 2014 | 647 | 1,4 |
| 2015 | 680 | 5,1 |
| 2016 | 680 | 0,04 |
| 2017 | 702 | 3,2 |

Source: assembled by authors in accordance to data [3]

One can notice the way leading innovational companies of the world are presented in the top-25 list depending on their kind of activity. Thus, there are 8 pharmaceutical and biotechnological companies, 6 – automobile manufacturing, 5 – software development and service, 3 – hardware technologies. One retail trade company, one - semiconductor industry, one – in the sector of means of manufacturing and manufactured goods (see Table II).

TABLE II
TOP-25 GLOBAL COMPANIES R&D SPENDING, %

| R&D Spending by Industry | 2015 | 2016 | 2017 |
|---------------------------|------|------|------|
| Computing and Electronics | 24 | 24 | 23,1 |
| Healthcare | 21 | 22,1 | 22,7 |
| Auto | 16 | 15,4 | 15,5 |

| | | | |
|-----------------------|-----|------|------|
| Software and Internet | 11 | 12,9 | 14,5 |
| Industrials | 11 | 10,8 | 10,2 |
| Chemicals and Energy | 6 | 5,5 | 5 |
| Aerospace and Defends | 3 | 3,2 | 3,2 |
| Consumer | 3 | 3 | 2,9 |
| Telecom | 2 | 1,6 | 1,6 |
| Other | 2 | 1,6 | 1,6 |
| Total, bln. USD | 680 | 680 | 702 |

Source: assembled by authors in accordance to data [3].

Data on 2015-2017 allow noticing certain changes in the R&D structure. In all spheres of economic activities except healthcare, software and Internet spending decreased. In average spending on R&D in medicine sphere is growing by 0,85% annually, and by 1,75% in software and service sector.

Among countries we also can mark leaders on general R&D spending (top-25 by companies' affiliation) (see Table III).

TABLE III
TOP-25 COMPANIES BY COUNTRY

| Country | Number of companies | R&D spending, bln. USD |
|----------------|---------------------|------------------------|
| USA | 15 | 137,2 |
| Germany | 3 | 24,5 |
| Switzerland | 2 | 21 |
| Japan | 2 | 15,5 |
| South Korea | 1 | 12,7 |
| United Kingdom | 1 | 5,9 |
| France | 1 | 5,5 |

Source: assembled by authors in accordance to data [3].

Development of hi-tech sectors becomes the shaping factor of economic growth therefore it requires a careful attention not only from the point of view of corporations but states' governments as well. Russia is no exception even though it has constantly encountered of various kinds of limitations. For a long time there was a prohibition on technology import for USSR and Russia (Jackson-Vanik amendment). Then problems of transformational period emerged. Therefore Russia's significant underrun in hi-tech sphere has taken place.

Today we see certain positive changes that include creating a set of rules and regulations like "Strategy of scientific and technical development of the Russian Federation" in 2016. We would like to analyze what has been achieved.

But we see methodological limitations in different approaches to defining hi-tech production, hi-tech and science-driven spheres. Aforementioned strategy does not clarify the situation as it does not give any definitions. Therefore any research in the sphere cannot be comprehensive.

III. THEORY

In a decision by the government of Russian Federation on 15.04.2015 "Developing science and technologies in 2013-2020" priority spheres of R&D are: information and communication technologies and electronics; space and aviation technologies; new materials and chemical

technologies; new transport technologies; advanced weaponry; military and special technics; manufacturing technology; technologies of living systems; ecology and national environmental management; energy saving technologies.

Classification of hi-tech branches depends on a country but there is a common feature – that is an index of research intensity that has to be more than the average in the industry. In Russia list of hi-tech branches composes of: aviation and rocket-building industry; computer equipment; automotive manufacturing; arms and weaponry manufacturing; nanoelectronics; equipment for electronic calculation and offices; telecommunications and radio; medicine and pharmaceutical industry; nuclear and nanotechnologies; biotechnologies.

We can single out certain factors of hi-tech and knowledge-based branches.

Scope of influence of each factor can be described through the following criteria: public education system (postgraduates quantity and enrollment); highly qualified personnel (quantity of personnel that is employed in R&D); possibility for a wide implementation of scientific achievements (quantity of organizations that perform researches and development); large spending on R&D (main means of manufacturing); prevailing usage of hi-tech solutions in manufacturing (main means of manufacturing and development; constant renewal of manufacturing; sufficient level of investment; state support; efficient protection of intellectual property).

IV. EXPERIMENTAL RESULTS

For the study of aforementioned hypothesis we chose the following indexes in Russian Federation in 2000-2017: gross domestic product, bln. roubles; investment in basic capital by means of all finance sources (in de facto present prices), bln. roubles; annual average quantity of enterprises' and organizations' personnel; current internal expenses on R&D (by kind of activity: fundamental researches, applied researches, developments), bln. roubles; number of personnel that are employed in R&D (by categories: researchers, technics, assisting personnel, other staff), people; results of postgraduate and doctoral candidacy studies (quantity of people, acceptance and graduation rate, including thesis defenses), people; relative share of innovative goods, works and services in gross amount of goods, works and services in the goods, works and services in gross amount of goods, works and services.

Investment into basic capital were chosen as a factor that characterizes capital spending instead of fixed assets cost, because fixed assets are highly depreciated and low utilization in certain economic spheres. During the study basic data were transformed in the following way: in order to enhance veracity of study of GDP and investment dynamics under the conditions of inflation processes authors recalculated these indexes, which were estimated in current prices, into matching prices in 2000. Econometric modelling was made on the basis of specification by kind of Cobb-Douglas extended function. As the result of the study we

received cointegration correlation that characterizes long-term dependence, it is presented in Table IV with its most statistically significant coefficients.

TABLE IV
RESULTS OF ECONOMETRIC MODELLING (DEPENDENT VARIABLE: GDP LOGARITHM FOR ONE EMPLOYED IN THE ECONOMY)

| Indexes of regression | Ratio values |
|--|--------------|
| Regression factors | |
| Logarithm of annual average employment | 0.215*** |
| Logarithm of investment into basic capital for one employed in the economy | 1.068*** |
| Logarithm of innovational goods, works and services in gross amount of goods, works and services | 0.277*** |
| Logarithm of share of applied research spending in current amount of R&D internal current spending | -0.300** |
| Trend | -0.072*** |

Notes: ** – ratio values on the level of 5%;

*** – ratio values on the level of 1%.

Thus workforce productivity in Russian Federation is defined by number of employed, capital, innovation and spending on scientific researches. Indexes that characterize number of high-qualified personnel as well as results of postgraduate training programs and doctoral studies activity proofed to be statistically insignificant in regression equation and therefore were excluded from the analysis.

V. DISCUSSION OF RESULTS

Giving an interpretation of received results, authors can state that model shows that share of innovational goods, works and services in gross amount of goods, works and services and therefore development dynamics has an influence over Russia's GDP dynamics as well as dynamics of hi-tech branches development. But influence of aggregate extensive factors is more significant (number of employed and score of investment into basic capital).

Therefore we see that resources of development are underutilized for hi-tech spheres such as public education system, highly qualified personnel, possibility for a wide implementation of scientific achievements in the society, large-scale spending in R&D, prevailing usage of hi-tech solutions in manufacturing, constant renewal of manufacturing, sufficient level of investment; state support and efficient protection of intellectual property.

At large spending in R&D in Russia in current prices are growing from 111,7 bln. roubles in 2000 up to 1259 bln. roubles in 2016 (eleven-fold growth), including internal spending – in twelve-fold growth (from 76,7 up to 943,7 bln. roubles) and nine-fold external spending (from 35 up to 314,2 bln. roubles). During calculations growth of spending for a single R&D organization estimated in 25% (from 0,187 up to 0,234 bln. roubles), for a single employee employed in R&D sphere – growth estimated in 52% (from 86 up to 131 thousand roubles), and for a single researcher – growth estimated in 41% (from 180 up to 255 thousand roubles). We

can also note significant influence of inflation as well as the fact that in the 16 years structure of R&D spending has been non-optimum, because total spending are poorly linked to spending for a single entity and a single researched.

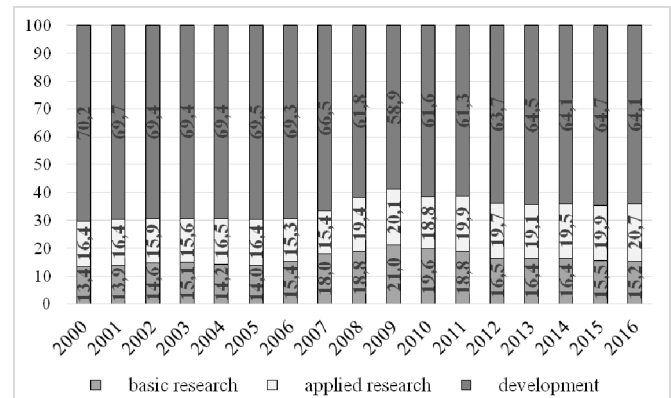


Fig. 1. Structure of current R&D spending by kind of activity in Russia (%).

Increase of share of R&D spending does not influence Russia's GDP because of ineffective structure of spending distribution, deterioration of quality characteristics of labour force, rupture of correlation between number of researches and assisting personnel.

Data on basic means of manufacturing that are used for R&D by kinds of economic activity are present only for 2014-2016. For the first time we can observe dynamics of hi-tech manufacturing. For this study authors required dynamics of used machine and equipment for the period up to 5 years. We can see that in 2014-2016 in the Russian economy this index has increased in almost 37% (from 2572,7 up to 3520,8 bln. roubles, that includes hi-tech and medium-tech of high level kinds of economic activity growth estimated in 2,5 times (from 13,4 up to 34,1 bln. roubles), in hi-tech kinds of economic activity growth estimated in 2,7 times (from 9,2 up to 24,9 bln. roubles), in medium-tech of high level kinds of economic activity growth estimated in 2,2 times (from 4,2 up to 9,3 bln. roubles) and science-driven kinds of economic activity growth estimated only in 26% (from 241,6 up to 304,3 bln. roubles).

Number of organizations in R&D sphere in 2012-2016 grew for 13% (from 3566 up to 4032), that includes hi-tech and medium-tech of high level kinds of economic activity growth estimated in 37% (from 239 up to 328), in hi-tech kinds of economic activity growth estimated in 30% (from 152 up to 193), in medium-tech of high level kinds of economic activity growth estimated in 55% (from 87 up to 135) and science-driven kinds of economic activity growth estimated only in 10% (from 3158 up to 3499).

Characteristics of labour force in R&D shows us number of people employed in the sphere and results of postgraduate activity. At large in the Russian economy number of R&D personnel in 2005-2016 decreased by 11% (from 813207 up to 722291 people).

At the same time in hi-tech and medium-tech of high level kinds of economic activity growth estimated in 97% (from 30354 up to 59868 people), in hi-tech kinds of economic activity growth estimated in 234% (from 20095 up to 47148 people), in medium-tech of high level kinds of economic

activity growth estimated in 24% (from 10259 up to 12720 people) and science-driven kinds of economic activity decrease estimated in 8% (from 685624 up to 633604 people).

Results of postgraduate activity changed in 2014 because of educational system transformation in Russia and change of statistical survey methods. Nevertheless we see a variety of trends of such indexes as number of postgraduates and acceptance to postgraduate studies. Thus in 2014-2016 total quantity of postgraduates increased from 8616 up to 23676 people. Data in graduation are still not published, so currently we cannot give a precise esteem. At the same time postgraduate enrollment decreases including priority vectors of development. From 2014 to 2016 it has decreased for 9,7% (from 8397 up to 7582 people), that includes hi-tech and medium-tech of high level kinds of economic activity where decrease estimated in 16% (from 4691 up to 3936 people), in hi-tech kinds of economic activity decrease estimated in 15,6% (from 3676 up to 3102 people), in medium-tech of high level kinds of economic activity decrease estimated in 18% (from 1015 up to 834 people) and science-driven kinds of economic activity decrease estimated in 9% (from 2858 up to 2602 people).

We must also note that state statistics has begun defining indexes of hi-tech sector development only since 2014 which hinders researches.

VI. CONCLUSION

Prevailing approach that is based on priority of demand for science by the manufacturer is dangerous for Russia because it does not stimulate development of scientific potential and, therefore, creating breakthrough technologies. Conversely it hinders development of hi-tech spheres by, first of all, deteriorating quality characteristics of labour force through creating a “qualified user” of modern technologies, but not a creator.

Growth of absolute measure of spending on R&D is taking place against the background of their non-optimal structure including shares of spending between fundamental, application researches and developments, deterioration of correlation between number of researchers and assisting staff and employee compensation plan not fulfilling its stimulation function in scientific sphere.

REFERENCES

- [1] Malikh O.E., Polyanskaya I.K., Kononova M.E., Kuzmina O.Y., Tarasyuk O.V., Osipova I.V. Implementation of the State Economic Policy in the Field of Education // *Iejme – Mathematics Education* 2016, Vol. 11, № 8, 3104 – 3113.
- [2] Malykh O.E., Polyanskaya I.K., Lebedev I.A., Sajranov V.A., Sajranova M.V., Tsaregorodtsev E.I. Resources of innovative development of region in the conditions of formation of knowledge economy // *Mediterranean Journal of Social Sciences*. 2015. T. 6. № 3. FROM. 345-350.
- [3] Strategy & Global Innovation 1000, 2017 / Mode of access: <https://www.strategyand.pwc.com/innovation1000>
- [4] Malikh O.E., Hurmatullina A.F., Kononova M.E., Kuzmina O.Y., Titova N.B. Integral Assessment of the Social and Economic Development of Megacities in Russia // *Iejme – Mathematics Education* 2016, Vol. 11, № 7, 2455 – 2469.

- [5] Malykh O.E., Polyanskaya I.K., Kayumova A.F., Shamsutdinova A.F. Assessing the level of the social-economic development of million-plus cities as the degree to which the administrative resource is realized // *Life Science Journal*. 2014. T. 11. № 10. FROM. 628-633.



Olga E. Malykh, professor, Doctor of Economics, the author of 100 scientific publications, including 7 monographs. Area of scientific interests: state economic policy, knowledge economy.
E-mail: kafedra-et@mail.ru



Elena A. Gafarova, PhD in Economics, Docent, Senior Researcher of Economic-Mathematical Modeling Sector of Institute of Social and Economic Researches of the Ufa Federal Research Center of the Russian Academy of Sciences, the author of 100 scientific publications. Area of scientific interests: regional growth modeling, econometric and simulation modeling.
E-mail: gafarovaea@mail.ru

Digital Transformation of Enterprises of Microelectronics

Valeriy I. Mamonov, Olga V. Milekhina
Novosibirsk State Technical University, Novosibirsk, Russia

Abstract – The article presents the results of a study in the field of operating mode modeling of robot technical systems of high-tech industries. It is demonstrated that the modeling of the production system functioning in the form of multiphase queuing systems makes it possible to obtain approximate analytical solutions in line with the requirements of the predictive analytics, and could become another step to a digital transformation of electronic instrument-making enterprises.

Index Terms – Digital transformation, electronic instrument-making, queuing systems.

I. INTRODUCTION

FOR A LONG TIME, the microelectronic industry used to be and still is the basis for the development of the high-technology sector of the national economy. At the same time, "...for the further growth and in order to reach a level of the global competitors, it is necessary for us to succeed on new fast growing markets, moving from iron to intellect" [1]. The development of the informatization of the society by means of the penetration of information and communication technologies into all spheres of the life of the society and a large-scale introduction of electronics allow us to consider the electronic industry as a driving force for the transition to a new techno-economic paradigm. This requires not only the development of the institutional environment on the level of the State programs [2-6], federal target programs [7], and government guarantees of their implementation [8-12], solving of system problems in the sphere of defense-industrial sector [13], but also on the level of the entities of the economy. As envisioned by the leaders of the State Corporation "Rostec", the enterprises of the electronic industry should be "... in the avant-garde of the Russian digital economy" [14], being the initiators and active changemakers in the scientific, technological, engineering, and manufacturing spheres. The analysis of the specialized publications reveals keen interest of CEOs and engineering and technical community of the enterprises to solve these problems in the full range of issues: from analytical reviews of the dynamics of scientific publications in the spheres of nanotechnologies [15], creation of the institutional environment and the development of the supporting subsystems [16-20], and the prospects of the strategies implementation [21,22], the development of serial entrepreneurship and successfulness of high-technology business [23], to aspects of engineering and technology solutions and application of new materials [24-31]. So, there is demonstrated a general commitment to the integration of vertical and horizontal value-added chains. Vertically, there

is foreseen a coherence of all operational procedures of the production of microelectronic products from the design of the products to the production, including logistics and services, when "...the data on the operational procedures, efficiency of the processes, quality management and operational planning, which are optimized for different platforms, are available on-line in the integrated network" [32]. The horizontal integration of the value-added chain makes it possible to take the manufacturing process out of the context of the performing of separate operations. It creates a basis for the coherence of interests of consumers, suppliers, and key partners on the basis of a single industrial platform of interactions between the stakeholders [33,34]. Contrary to the traditional information transfer from the source to a consumer at the automation of business processes the digitalization should lead to management decision making [35]. In this case it is important to remember that in the digital economy the main basic resources are information and human capital [33-36]. After all, the personnel of organizations, its possibilities and actions would determine whether the digitalization of the microelectronic industry is implemented and the corresponding systemic, synergetic and coordination effects of the networking interaction are obtained [37]. It is known that the decrease of the personnel resistance to the introduction of new technologies (digitalization is not an exception) is directly proportional to the level of changes in the technology of the implementation of labor chains on the workplaces, and is inversely proportional to the time of the transformations. Consequently, the early involvement of the personnel into the digital transformation and the active internal marketing of the project aimed to transfer to new technologies of the management decision-making formation on the basis of the single industrial platform of the interaction of stakeholders make it possible to increase the probability of a positive scenario of the development of enterprises of the nanoindustry. What could be taken as a benchmark for the comparison of the old and new variants of the implementation of the labor chains on the workplaces? A modeling of operating modes of robot technical systems of high-tech manufacturing industries can be considered as one of the first steps to the digital transformation. The introduction of original operations of the digital modeling to the typical technological processes of collection, analysis, processing and storage of data, which lead to the formation of management decisions, will make it possible to organize a more flexible manufacturing process, which could sufficiently impact on the yield ratio.

II. PROBLEM DEFINITION

Robot technical systems (RTS) are equipped with highly-efficient automated equipment, which should function with high shift utilization even under the accelerated amortization policy. The most important task of the efficient usage of such production equipment is to provide full machine utilization in accordance with the throughput capacity. The execution of all necessary works is achieved by means of the maintenance of the routing of items between the complexes organized according to their functions. Thus, for example, an operation on a printed circuit board is queued for the execution of the corresponding operation. In this case, the scheduling would be correlated with the sequencing of operations and functionality of the RTS elements. In order to avoid long queues for processing, it is necessary to determine the throughput capacity of the RTS elements depending on the incoming flows of items for the processing. The problem of the throughput capacity determination, load diagrams and utilization rate of the production equipment are of primary importance in the MES-systems. The attention to these problems is due to the fact that the production time in the RTS depends on its throughput capacity and the planned flow of items, which finally determines the order execution time.

III. THEORY

The knowledge of the production lead time is a key factor for the planning and observance of the lead time of the order or work items. A priori calculation of this important schedule-planning rule is very difficult due to the fact that one of the essential components of the production lead time (in-process queue) can be determined only statistically depending on the characteristics of a multitude of subjects of labor to be processed, as well as on the control parameters, which assign modes of operation of technological units of equipment in RTS. Besides, the value of the in-process queue time is very sensitive to changes in the initial data (capacity utilization rate, random disturbances, and management actions). One of the approaches to the study of production systems is to consider them as a network of queuing systems. The presentation of a technological process as a multiphase queuing system (QS), in terms of which applications are identified with works (lot of various parts, order accounting entities), and the application of this approach to the solution of the problems of the assessment of the throughput capacity of RTS depending on the incoming flow of units to be processed is of a special attention in terms of practical use.

We consider a production system constituting a set of interrelated subsystems, each in general consisting of a group of work centers. The operation of each subsystem is interpreted using the QS models. Each production subsystem processes the items flow in accordance with their routing, and when the process is completed in the system, the flow enters another production system (for assembling or for further processing).

When the process is modeled in the form of a multiphase QS, no additional constraints in the form of a strictly

sequential technological chain are imposed: the items can pass through the subsystems as many times as it is foreseen by the flow routing.

Let us consider the model description of the RTS operation. The key feature of the processes going on in the center is the randomness of the ongoing discrete events: randomness of the waiting time for processing, randomness of volumes of incoming flows, queuing situation, effects of disturbing factors at random time moments and controlling actions. It should be noted that one of the most favorable and known nowadays research tools to study such processes is the queuing theory, which makes it possible to obtain analytical dependences between technical and organizational and economic characteristics of the system and its parameters.

But the applicability of the classic models of the queuing theory to the problems of the analysis of production systems is restricted due to the fact that the model description is not adequate: the problems arising in production systems differ from that in the classical systems. This peculiar feature causes a necessity to introduce control to the operations flow in RTS.

In a production subsystem, for which the promptitude of the execution of released works is an important indicator of the operation, the control parameter is the intensity of the production of the elements of the order in RTS, which in terms of the queuing theory corresponds to the service rate.

The control strategies of the service rate in RTS can be different. For example, the dynamic change of the service rate depending on the queue length or the waiting time, switching of shift modes, different variants of the management of the work of the operators and production equipment.

That is why the queuing system with control is of a special attention of researchers, due to the fact, that when this or that control type is introduced to the order service process, the problem can be reduced to an optimization problem: under this control type with the resource management it is possible to achieve such operating modes of RTS, when the indices of effectiveness meet the required level.

Let us consider the operation of the RTS automated equipment as a multichannel queuing system with control, which is related with the dynamic change of the service rate depending on the queue length. Particularly, the control means that the service rate $\mu_0 = 1/t$, where t is the average processing time of the order, is remained the same for as long as the number of orders in the queue n is less than N_1 . When the number of orders in the queue is increased, the service rate increases abruptly in the moments, when the number of orders L , waiting to be processed, passes one of the critical (threshold) values N_i , where $i = 1, \dots, m$ is the number of switching steps. In this case the service rate remains constant and equal to μ_i within each interval. The multistep control process is shown in Fig. 1.

Let us consider another control type, which is more general in comparison with that described above: a multichannel model with cycle control.

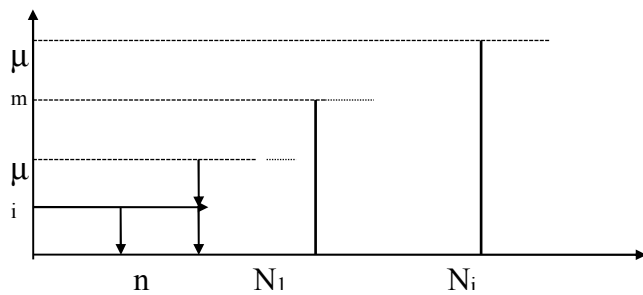


Fig. 1. The changes in the service rate in QS with the multistep service.

In this case, the subsystem functions in the following way: the processing of orders is carried out with the service rate $\mu_0 = 1/t$ for as long as the number of orders in the queue n is less than M . If the number of orders is more or equal to N , then the service rate increases to $\mu_1 = \mu_0 + \Delta\mu$ and remains equal to μ_1 for as long as the number of orders reduces to M . So, there is a direct cycle (Fig. 2) in the section from M to N and a reverse cycle in the section from N to M . Obviously, that at $N = M + 1$ the hysteretic system is transformed into a system with one-step control.

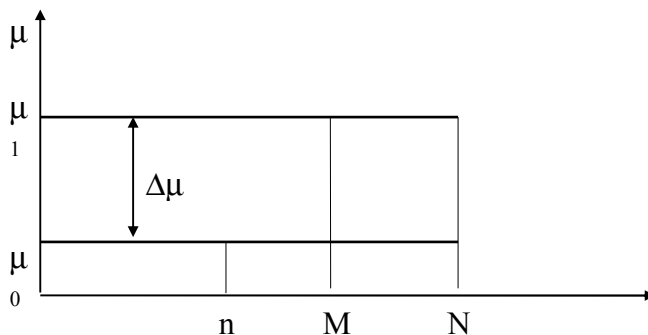


Fig. 2. The changes in the service rate at the cycle control of QS.

IV. EXPERIMENTAL RESULTS

The models corresponding to the above mentioned control types have many control parameters, in particular: vector of additional resources values and vector of switching levels. The time parameters of the order service process in the work center heavily depend on them. It is always possible to distinguish two constituents in the structure of the service process of the items lots, the first constituent is associated with the operations flow of the technological process τ_j , and the second is associated with the waiting θ_j . Both constituents directly depend on the operating mode of the subsystem and its utilization rate (characteristics of the throughput capacity of the work center). The smart control over all parameters, which are allowable by the manufacturing organization, would be that, under which the value of the efficiency criterion of the subsystem operation corresponds to a certain pair of values (τ_j, θ_j) , this value is determined in terms of the operational efficiency of the studied system as a whole $C(\tau, \theta)$.

When the components of the target function are determined, it is possible to demonstrate the efficiency of the introduction of control to the subsystem by setting

numerically input parameters. The experimental calculations were carried out with a multistep control in the QS subsystem under the following conditions. The intensity of the inflow of orders was constant, the number of switches m and the value $\Delta n = \Delta n_i = N_{i+1} - N_i$, where $i = 1, \dots, m$ were considered as variables. The analysis of the calculations shows that with a rise in the number of switches the QS subsystem functions only in some operating modes for a considerable portion of time, i.e. some probabilities are highly improbable, the others are of substantial probability. Thus, it can be concluded about the assigning of the reasonable limits in the attracted time resource. Another important conclusion means that at a fixed number of operating modes m and the increased Δn , the orders number in the queue increases; at the fixed Δn and the decision to often transfer to different forced modes, the orders in queue decreases insufficiently.

The analysis of the similar dependences for the cycle control type also shows its high efficiency. The advantage of the cycle control type in comparison with the stepped control is obvious, because with other parameters being equal (the same number of switches, the same switching moments for the forced mode) the subsystem moves out of the forced operation mode later at the cycle control.

V. DISCUSSION OF RESULTS

The obtained end formulas, which characterize the operating modes of QS and time parameters of the orders service, make it possible to give a comparative assessment of the control types of the equipment operation in RTS. We used the equation $[(C_{\min \text{ step}} - C_{\min \text{ cycl}}) 100 / C_{\min \text{ step}}] \%$ as a criterion of the efficiency of the control types. The value of the efficiency criterion was determined in the form of a loss function (losses due to the increase of the production time and the orders' queuing time). The experimental calculations carried out on the example of one RTS show that the advantage of the introduction of the cycle control in comparison with one-step control is in average 6-10 %. And the orders' queuing time reduces in the average by 8 %.

The model description of the production system by multiphase QS foresees exponential distribution of random values. In practice, the items flows in the productive process are operated on the basis of the control parameters and decision rules. That is why the application of the exponential distribution law requires additional grounds. But the application of another type of distribution of random values leads to the use of the Monte-Carlo technique in solving the mentioned problems.

VI. CONCLUSION

It should be noted that general analytical techniques for the calculation of the characteristics of the network of queuing systems require further investigations and elaborations. The review of the studies in this direction shows that there are scarce scientific publications dealing with the optimization of multiphase QS, and the solving of problems of the synthesis of the optimal dynamics of the networks causes considerable

difficulties. At the same time the modeling of the operation of the production system consisting of the technologically interrelated RTS in the form of multiphase queuing systems makes it possible to obtain approximate analytical solutions in accordance with the requirements of the predictive analytics at production site.

Nowadays, there are various opinions about the prospects of the digitalization of enterprises of the microelectronic industry. One thing is clear: the transition to the networking interaction of the enterprises of the microelectronic industry is inevitable and it would be consistently introduced on the national level. Only a mutually profitable cooperation of partner enterprises on the basis of the informational transparency in the framework of the platforms, and a new understanding of a competitive cooperation are able to construct new models of business and value-creating networks, to personalize relations with consumers and partners, and in a relatively short time to solve problems set by the government, because "...the Russian economy and the country itself have no future without digital economy. That is why this is the absolute priority problem we have to solve" [38].

REFERENCES

- [1] V. Borovko. URL: <http://digitalrostec.ru> (Accessed 05 March, 2018)
- [2] Gosudarstvennaya programma Rossiyskoi Federatsii "Razvitie elektronnoi i radioelektronnoi promyshlennosti na 2013–2025 gg." [State Program of the Russian Federation "Development of electronic and radio-electronic industry in 2013–2025"]. URL: <http://government.ru/programs/249/events/> (Accessed 15 March, 2018)
- [3] Programma "Tsifrovaya ekonomika Rossiyskoi Federatsii" [Program Digital Economy of the Russian Federation] URL: <http://digitalrostec.ru> (Accessed 15.03.2018)
- [4] Tsifrovaya ekonomika. Videnie 2025 (GK Rostec) [Digital Economy. 2025 Vision (State Corporation "Rostec")] URL: <http://digitalrostec.ru> (Accessed 5.03.2018)
- [5] Postanovlenie Pravitelstva Rossiyskoi Federatsii ot 28 avgusta 2017 g. № 1030 "O sisteme upravleniya realizatsiei programmy "Tsifrovaya ekonomika Rossiyskoi Federatsii" [RF Government Decree # 1030 dated 28 August, 2017 "On the Management System for the Implementation of the Program "Digital Economy of the Russian Federation"]
- [6] Plan meropriyatiy po napravleniyu "Formirovanie issledovatel'skikh kompetentsiy i tekhnologicheskikh zadatkov programmy "Tsifrovaya ekonomika Rossiyskoi Federatsii [The Plan of Measures for the Direction "The Formation of Research Competences and Technological Reserves" for the Program «Digital Economy of the Russian Federation»]. URL: <http://government.ru/news/30892/> (Accessed 05 March, 2018)
- [7] Federalnaya tselevaya programma "Razvitie oboronno-promyshlennogo kompleksa e Rossiyskoi Federatsii na 2011–2020 gody". Utverzhdena Postanovleniem Pravitelstva Rossiyskoi Federatsii ot 6 fevralya 2013 № 97. [Federal Target Program "Development of the Defense Industrial Complex of the Russian Federation in 2011–2020". Approved by RF Government Decree # 97 dated 6 February, 2013] URL: <http://government.ru/docs/14233/> (Accessed 05 March, 2018)
- [8] Postanovlenie Pravitelstva Rossiyskoi Federatsii ot 17 fevralya 2016 goga № 110 "Ob utverzhdenii pravil predostavleniya iz federalnogo byudzheta subsidii rossiyskim predpriyatiyam radioelektronnoy promyshlennosti na kompensatsiyu chasti zatrat na uplatu protsentov po kreditam, poluchennym v rossiyskikh kreditnykh organizatsiyakh na tseli realizatsii projektov po sozdaniyu infrastruktury otrasli, v tom chisel klasterov v sfere radioelektroniki. [RF Government Decree # 110 dated 17 February, 2016 "On the Approval of the Rules for Provision of Subsidies from the Federal Budget to the Russian Enterprises of the Radioelectronic Industry on Compensation of Part of Costs for Interest Payment on the Credits Received in the Russian Credit Institutions for the Implementation of Projects Aimed to Create the Infrastructure of the Industry, Including Clusters in the Sphere of Radioelectronics"] URL: <http://government.ru/programs/249/events/> (Accessed 05 March, 2018)
- [9] Postanovlenie Pravitelstva Rossiyskoi Federatsii ot 17 fevralya 2016 goga № 109 "Ob utverzhdenii Pravil predostavleniya iz federalnogo byudzheta subsidii rossiyskim predpriyatiyam organizatsiyam na vozmeschenie chasti zatrat na sozдание nauchno-tekhnicheskogo zadela po razrabotke bazovykh tekhnologiy proizvodstva prioritetnykh elektronnykh komponentov i radioelektronnoy apparatury" [RF Government Decree # 109 dated 17 February, 2016 "On the Approval of the Rules for Provision of Subsidies from the Federal Budget to Russian Organizations on Compensation of Part of Costs for the Creation of Scientific-and-Technological Reserves for the Elaboration of Basic Technologies for Production of priority Electronic Components and Radioelectronic equipment"] URL: <http://government.ru/programs/249/events/> (Accessed 05 March, 2018)
- [10] Rasporyazhenie Pravitelstva Rossiyskoi Federatsii ot 7 avgusta 2014 goda № 1478-p "O gosgarantiyakh na projekt rekonstruktsii i tekhnicheskogo perevooruzheniya proizvodstva elektrooborudovaniya v ramkakh FTsP "Razvitie oboronno-promyshlennogo kompleksa Rossiyskoi Federatsii na 2011–2020 gody" [RF Government Order # 1478-r dated 7 August, 2014 "On Government Guarantees the project of the Reconstruction and Technical Upgrading of Electrical Equipment Manufacturing within the Framework of the FTP "The Development of the Defense-Industrial Complex of the Russian Federation in 2011–2020"]. URL: <http://government.ru/docs/14233/> (Accessed 05 March, 2018)
- [11] Prikaz Minobrnauki Rossii ot 01.11.2012 g. № 881 "Ob utverzhdenii kriteriev otneseniya tovarov, rabot, uslug k innovatsionnoy i vysokotekhnologichnoy produktsii dlya tseley formirovaniya plana zakupki takoy produktsii" [The Order of the Ministry of Education and Science of the Russian Federation # 881 dated 1 November, 2012 "On the Approval of Criteria for Qualifying Products, Works, Services as Innovation and High-Tech Products for the Purposes of the Formation of the Procurement Plan of such Products"]
- [12] Ukaz Prezidenta Rossiyskoi Federatsii ot 07.07.2011 g. № 899 "Ob utverzhdenii prioritetnykh napravleniy razvitiya nauki, tekhnologii i tekhniki v Rossiyskoi Federatsii i perechnya kriticheskikh tekhnologiy Rossiyskoi Federatsii. [Decree of the President of the Russian Federation Decree # 899 dated 7 July 2011 "2012 "On the Approval of of Priority Directions for the Development of Science and Technology in the Russian Federation and the List of Critical Technologies of the Russian Federation"]
- [13] Sistemnye zadachi Minpromtorga Rossii v sfere oboronno-promyshlennogo kompleksa. [System Problems of the Ministry of Industry and Trade of the Russian Federation in the sphere of the Defense Industrial Complex.] URL: <http://minpromtorg.gov.ru/activities/industry/sisizadachi/oboronprom/> (Accessed 07 March, 2018)
- [14] S. Chemezov. URL: <http://digitalrostec.ru> (Accessed 06 March, 2018)
- [15] N. Murashova, A. Polyakova, E. Yurtov. Analysis of dynamics of scientific publications for areas related to nanotechnology and extraction // Nanoindustry, 2017, 3. URL: <http://www.nanoindustry.ru/journal/article/6037> (Accessed 11 March, 2018)
- [16] S. Kanev. Creating successful business for two years: experience of MPI // Nanoindustry, 2017. 2. URL: <http://www.nanoindustry.ru/journal/article/5978> (Accessed 16 March, 2018)
- [17] D. Krakhin. Creation of high-tech infrastructure as natural stage of development of startups // Nanoindustry, 2017, 3. URL: <http://www.nanoindustry.ru/journal/article/6034> (Accessed 16.03.2018)
- [18] A. Kovalev. Zelenograd Nanotechnology Center: creating technology startups and developing innovative production. // Nanoindustry, 2017. 2. URL: <http://www.nanoindustry.ru/journal/article/5972> (Accessed 15 March, 2018)
- [19] V. Uzllov. "Deadman" or "team of tomorrow", it's time to determine who you are in today's market! // Nanoindustry, 2017. 7. URL: <http://www.nanoindustry.ru/journal/article/6334> (Accessed 15 March, 2018)
- [20] V. Bespalov. MIET: integration of education, science and production // Nanoindustry, 2017. 5. URL: <http://www.nanoindustry.ru/journal/article/6185> (Accessed 11 March, 2018)
- [21] L. Ratkin. On strategy of scientific and technological development of the Russian Federation in the sphere of new technologies.

- //Nanoindustry, 2017. 8. URL: <http://www.nanoindustry.su/journal/article/6430> (Accessed 02 March, 2018)
- [22] K. Borisov, E. Gruzina et al. Implementation of program of nanotechnology industry development in the Russian federation until 2015 // Nanoindustry, 2017. 5. URL: <http://www.nanoindustry.su/journal/article/6193> (Accessed 15 March, 2018)
- [23] D. Kovalevich. Development of serial entrepreneurship in nanotechnology industry // Nanoindustry, 2017. 4. URL: <http://www.nanoindustry.su/journal/article/6134> (Accessed 07 March, 2018)
- [24] M. Kabanov. Technology is our main accent // Nanoindustry, 2017. 3. URL: <http://www.nanoindustry.su/journal/article/6030> (Accessed 15 March, 2018)
- [25] Ch. Schwind. Process solutions that are changing semiconductor and electronics industry. // Nanoindustry, 2017. 2. URL: <http://www.nanoindustry.su/journal/article/5973> (Accessed 01 March, 2018)
- [26] D. Gudilin. Quantum technologies, basis for new technological revolution // Nanoindustry, 2017. 7. URL: www.nanoindustry.su/journal/article/6337 (Accessed 5 March, 2018)
- [27] A. Zimnyakov. Nanomaterials that will change world. // Nanoindustry, 2017. 8. URL: <http://www.nanoindustry.su/journal/article/6430> (Accessed 09 March, 2018)
- [28] D. Gudilin. Minimal Fab, look into future of semiconductor industry // Nanoindustry, 2017, 5. URL: <http://www.nanoindustry.su/journal/article/6186> (Accessed 05 March, 2018)
- [29] T. Altayev. Measuring systems for “Generation Industry 4.0”// Nanoindustry, 2017. 6. URL: <http://www.nanoindustry.su/journal/article/6281> (Accessed 07 March, 2018)
- [30] A. Akhmetova, I. Yaminsky. Advanced technologies center: production and innovations // Nanoindustry, 2017. 6. URL: <http://www.nanoindustry.su/journal/article/6293> (Accessed 15 March, 2018)
- [31] Sh. Hara. Minimalist systems with maximum capabilities // Nanoindustry, 2017. 4. URL: <http://www.nanoindustry.su/journal/article/6133> (Accessed 15 March, 2018)
- [32] Yu.A. Kovalchuk, I.M. Stepnov. The Digital Economy: transformation of Industrial Enterprises // Innovations in Management, 2017. 1(11). pp.32-43
- [33] K. Schwab. The Fourth Industrial Revolution. (Translated from English). Moscow: Izd-vo “E”, 2017. 208 p.
- [34] N.N. Kulikova. Coordination of the Economic Interests of the Participants of Inter-Organizational Relationships in Formation of the Value Chain in the Electronic Industry. // The Russian Journal of Entrepreneurship, 2015. 16 (23). pp. 4229-4244.
- [35] S.A. Kuznetsova, V.D. Markova. Tsifrovaya ekonomika: novye aspekty issledovaniy i obucheniya v sfere menedzhmenta // Innovations, 2017. 6 (224). pp. 27-33 [Digital Economy: New Aspects of Studies and training in the Sphere of Management // Innovations, 2017. 6 (224). pp. 27-33].
- [36] A.V. Babkin, D.D. Burkaltseva, D.G. Kosten, Yu.N. Vorobiev. Formation of Digital Economy in Russia: Essence, Features, Technical Normalization, Development Problems. // St. Petersburg Polytechnic University Journal. Economics, 2017. V.10. 3. pp.9-25.
- [37] Yu.A. Kovalchuk, I.M. Stepnov. Formation of a Systematic, Synergic and Coordination Effects in the Network Communication of the Modernization Project / Interdisciplinarity in the Modern Humanities and Social Sciences – 2017. Academic World in Interdisciplinary Practices: Proceedings of the Second Annual All-Russian Scientific Conference (Rostov-on-Don, 22–24 June, 2017.). V. 2. Sectional Reports. – Rostov-on-Don; Taganrog: Publishing House of Southern Federal University, 2017. – Part 2. – 456 p. – pp. 219-229.
- [38] V.V. Putin. URL: <http://digitalrostec.ru> (Accessed 31 March, 2018)



Mamonov Valeriy Ivanovich, Candidate of Sciences (Economics), Head of the Chair of Computer Science in Economics, Novosibirsk State Technical University, Associate Professor. Research interests: Industry 4.0, Modeling of production systems. The author of more than 50 research papers.



Milekhina Olga Viktorovna, Candidate of Sciences (Economics), Assistant Professor of the Chair of Computer Science in Economics, Novosibirsk State Technical University, Associate Professor. Research interests: digitalization of economy, Industry 4.0, performance management of economic and social systems. The author and co-author of more than 50 research and teaching and guiding papers.

Ecosystems as Network Forms of Business Organization

Vera D. Markova, Svetlana A. Kuznetsova

Institute of Economics and Industrial Engineering of SB RAS, Novosibirsk State University,
Novosibirsk, Russia

Abstract – The article is aimed at developing methodological aspects of building and functioning of business ecosystems on the basis of digital platforms. The review of foreign experience in building business ecosystems and the analysis of 1C Company – the Russian business ecosystem – has made it possible to conclude that business ecosystems have similar basic structure including four main types of players, irrespective of a wide variety of digital platforms on which such ecosystems are built. Using the example of 1C Company, the main actors of a business ecosystem are identified, possible distribution of tasks between them are specified and the fundamental features of network ecosystem are described. It has been shown that a certain level of openness of digital platforms maximizes the capacity of independent participants to develop digital platforms and business ecosystems built on the basis of such platforms.

Index Terms–Digital platform, innovations, business ecosystem, 1C Company.

I. INTRODUCTION

DIGITAL REVOLUTION caused by rapid dissemination and penetration of digital technologies into all sectors of economic and social life has led to drastic changes in business organization and management. As pointed out by Michael Porter, we have witnessed the most significant transformation of business since the Second Industrial Revolution of the late XIX – early XX centuries [1]. In Russia, the development of digital economy is declared as a strategic objective of the development of the country, which has been a focus of a number of state documents: Strategy for the Development of Information Society for 2017 - 2030, the state program "Digital Economy of the Russian Federation" [2], etc.

The development of digital platforms and formation of digital business ecosystems seems to be the most important specific feature of digital economy in terms of business organization and management. However, despite rapid development of platform-based business models, little research has been done about methodological issues of their formation.

The analysis of literature has shown that American researchers take the lead in studying platforms and business ecosystems; they summarized the main success stories of digital businesses, as would be expected, because the USA far surpasses other countries in the number of enterprises operating on the basis of digital platforms. The articles of the Russian authors, still being few in number, focus primarily on partial or the most specialized issues of digital transformation.

The article seeks to develop methodological aspects of building and functioning of digital business ecosystems on the basis of foreign and domestic experience.

II. PROBLEM DEFINITION

A variety of successfully functioning digital platforms has evoked interest and encouraged studies aimed at identifying and describing their specific types. The best-known classification is suggested by A. Gawer and M. Cusumano [3] who distinguished between the two predominant types of platforms: internal or company specific platforms, and external or industry-wide platforms.

Internal platforms (product and/or technology) are the assets integrated into a unified structure (knowledge, design solutions, technologies, components, etc.) on the basis of which the company can effectively develop a set of related products, implementing differentiation strategy. Development of internal business platforms is specified by their potential benefits – fixed cost savings, modular approach effects, etc.

Unlike internal platforms, industry-wide platforms are the assets which provide a foundation for the development and production of complementary products, technologies and services by other, as a rule, independent companies. Industry-wide platforms form the base for the large number of companies to create complementary innovations in the form of specific products, related services or elements of technology (e.g. 1C system, Mir (payment system), digital platforms Yandex, Mail.ru, Telegram, etc.).

Another classification of digital platforms is based on the value created and approaches to monetize the value [4]. As part of this approach, four types of platform companies have been specified:

- Companies creating transaction platforms, i.e. those which facilitate transactions (exchange of value) between different types of actors, such as Uber, eBay, Russian platform Yula, Avito, and many other multi-sided platforms.
- Companies developing innovation platforms, which consist of technological building blocks, used as a foundation for a wide range of complementary services or products. Such complementary innovators can be dispersed throughout the world, but together they form an innovation ecosystem. A fundamental feature of such platforms is the possibility for the platform owners to tap into a potentially unlimited pool of external innovators. Such an approach forms a bedrock for a continual cycle of innovation and growth, with the scale of

platforms being both the outcome of initial success and the driver for the further growth. Platform owners tend to create large share of value added and innovations through collaborative development of products or services. External innovators (the developers of complementary products or services) seek for successful platforms and attempt to join them, i.e. such platforms become magnets for external partners – complementary innovators;

- Companies based on integrated platforms, i.e. those which have both transaction and innovation platforms such as Apple, which have platforms like the App Store, providing interaction between sellers and buyers and, at the same time, controlling a vast developer ecosystem that supports content creation on the platform.

- Companies based on investment platform, i.e. those which implement portfolio strategy and act as holding companies or start-up platform investors (or both). For example, SoftBank, which started as a telecom company and has diversified further into the platforms with large stakes in Yahoo!, Alibaba Group, etc. Portfolio approach makes it possible for the companies to jointly adopt best management practices and innovative business models, use them in a more efficient way, providing better opportunities for implementation of such innovations and new approaches.

In our view, the potential to build a business ecosystem can be found in a branch-wise innovative platform with a certain level of openness for external actors. Openness of the digital platform coupled with the possibility to attract assets from independent participants gives reason to characterize it as a multi-sided platform unlike the two-sided one such as Uber. It is the multi-sided nature of the digital platform which provides the foundation for building an ecosystem.

Environmental approach to business management was proposed by James F Moore. He argues that a business ecosystem as a form of business organization differs from the markets and organizational hierarchies of firms. An ecosystem provides more opportunities for creative entrepreneurs through overall incentives for education and development and sharing innovation-related risks and costs [5].

S. Muegge defines platform ecosystem as a group of actors who come bundled together around a shared business platform [6].

It is to be noted that, despite the diversity of platform business models, ecosystems built on their basis have the similar basic structure including four main types of players: the company – the owner of the platform – which, as a rule, controls IP addresses, intellectual property and decides who and in what way may join the platform; interface providers with ecosystem members; customers who buy or use the products created on the basis of the platform. However, the most important players are the developers who create complementary products and services on the basis of the platform.

In other words, a business ecosystem is an economic community of companies and individuals whose main assets are various communications between the creators of the platform and the developers of complementary products contributing to the development of intellectual property of the ecosystem, distribution partners, other companies—data providers, algorithm developers, etc. – and also between the

groups of users who can exchange the experience gained and the lessons learned from the use of products and services provided by the ecosystem.

Of course, the network effect arises within a business ecosystem due to modern digital technologies, but, above all, due to the increasing participation of external actors and their enhanced capabilities.

Thus, openness of a business platform leads to the fact that the platform oversteps the bounds of a single company, building ecosystems which represent new network forms of business organization.

III.1C-ECOSYSTEM

In the Russian market, one of the best-known business ecosystems is built by 1C Company which specializes in the development and distribution of software for automation of routine business operations, accounting and providing timely information for taking business decisions at enterprises in various sectors of economy. The main product of the company is 1C:Enterprise – an integrated platform and a series of software solutions with multiple customization capabilities and business applications for the enterprises operating in various spheres and branches which allows them to integrate hard- and software of other vendors.

1C:Enterprise consists of a digital platform (core framework) and a system of business applications (configurations) developed on its basis. 1C digital platform has a developed internal programming language which specifies functionalities of various business tasks at hand. There is a great number of business applications developed and distributed on 1C:Enterprise platform. 1C configurations *per se* are software solutions for implementing specific tasks, such as accounting, trading operations, etc. In particular, 1C provides such standard products as 1C:Enterprise Accounting, 1C:Payroll & HR Management, etc.

Like many up-to-date business platforms, 1C performs two interdependent functions: it is both an application development tool for business automation and an instrument for implementation of business solutions.

A strategically important issue of platform functioning, which in many respects predetermines the formation of a business ecosystem on the basis of this platform is the level of platform openness, as mentioned above. A platform owner through the platform openness mechanism tackles complicated tasks: on the one hand, platform integrity maintenance and retention of leadership position; on the other hand, creation of incentives for independent partners to join the platform and contribute to its further development.

1C architecture is characterized by closeness of the core framework of the digital platform and openness of its application development tools, which provides such competitive advantages as customization of business software solutions for specific needs of clients and continuous development of the system, given the changes in regulating environment and specific business needs.

A business ecosystem built on the basis of 1C platform enables a vast number of users, i.e. enterprises of various sizes operating in different spheres and branches of economy as

well as enhanced partner network which consists of more than 10 000 constant clients in 600 cities from 25 countries. The key economic actors of 1C ecosystem are presented in Figure 1.

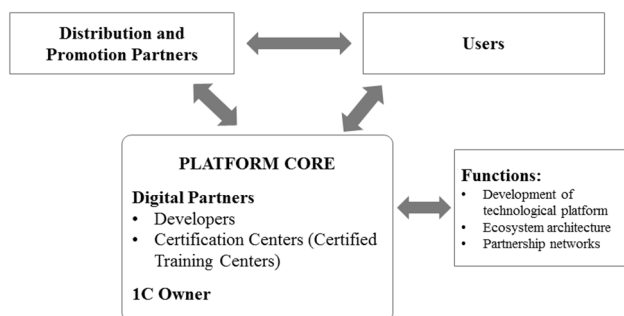


Fig. 1. 1C Business Ecosystem.

Source: compiled by the authors based on the scheme proposed in [7]

The core of the business ecosystem is 1C Company and its digital platform. 1C Company – the owner of intellectual property (platform technology) – establishes functioning/operational regulations and the architecture of 1C ecosystem, develops the conditions for collaboration with 1C partners and the system of incentives, ensures quality standards and, above all, provides continuous updating of information in the sphere of accounting and taxation.

Another group of members is independent developers, who have a special role to play in 1C ecosystem, i.e. to extend functionality of 1C digital platform, and certificate authorities who are supposed to provide general rules of functioning and standardization of operations within the ecosystem.

1C Company's partners include Certified Training Centers (CTC), partner network (partnership) for installing 1C software, consulting firms and marketing network. These partners provide distribution of 1C products, backup maintenance services, information and technological support. Today, 1C Company has a wide partner network in CIS: 5300 dealers in 570 cities. 1C Company offers to its dealers, a wide range of software products, provides high discounts as well as marketing and product support, ensures delivery, conducts training and regular seminars, etc.

1C business ecosystem also involves collaborative organizations providing counseling, automation and installment of 1C products in such specific spheres of management as document flow, budgetary accounting, etc.

One of the most efficient ways of implementing 1C platform solution is through franchising network operations. 1C Company has created an extensive franchising network – a community of 3000 organizations operating in Russia and CIS – which focus on rendering a full range of services to end-users. The franchising partnership based on 1C platform reinforces the network effects due to the increasing number of users, contribution to the development of application-oriented configurations and the formation of entry barriers with the continuously growing market share of 1C platform.

Thus, 1C digital platform has created a successfully operating business ecosystem with the participation of independent

companies varying in size, sector, etc. Successful development of 1C ecosystem has made it possible to transform the landscape of the Russian industry of management and accounting automation at enterprise and to drive the main competitors out of the market.

IV. SPECIFIC CHARACTER OF BUSINESS ECOSYSTEMS

The overview of studies related to the genesis and functioning of best-known global ecosystems built on the basis of digital platforms and the analysis of 1C digital platform and business ecosystem has revealed the following specific characteristics of business ecosystem as network structures [8]:

1. existence of a core framework within the ecosystem which is usually a digital or technology platform;

2. formation of community within the ecosystem comprising of various types of market agents;

3. formation of ecosystem architecture with its rules and regulations for distribution of gains among the actors, access to the platform resources and provision of consistency and coordination in ecosystem technological development. Platform owner establishes the rules and regulations for the operation of business ecosystem, which are aimed at further development of the ecosystem and achievement of network effect;

4. existence of management system within the business ecosystem where the platform owner plays the key role in integrating, providing, coordinating and motivating ecosystem members, encouraging innovative development of the ecosystem, and stimulating partners and consumers to join the ecosystem in order to increase its efficiency.

V. CONCLUSION

In modern economy, improvement of efficiency and risk reduction of innovative activity in many respects depends on the existence of partner network, which facilitates the exchange of ideas, new products and competences with clients, suppliers, research organizations and other parties concerned. The closeness of companies as well as the concentration only on their own fields of business activity, tends to narrow the vision of business prospects and limits the development horizons, which finally can lead to the loss of long-term competitiveness of an enterprise. Membership in a business ecosystem allows the companies to take advantage of innovative opportunities, anticipate consumer needs, benefit from innovative activity of complementary product developers and guide them in a useful direction, etc. As a result, innovations turn into the main leverage for the development of an ecosystem.

To conclude, management of ecosystems necessitates the change in priorities and management mindset: from closeness and orientation to the development of their own businesses to a search for new approaches in engaging with partners and consumers on the basis of credibility and trustworthiness, taking into account strategic interests of all ecosystem members. A fundamentally new competence for the companies should be their ability to build comparable and mutually

supportive business models not only for internal use but also for other ecosystem members.

REFERENCES

- [1] Porter Michael, Jim Heppelmann. (2014). How Smart, Connected Products are Transforming Competition.
- [2] State Program "Digital Economy of the Russian Federation – 2024" <http://static.government.ru/media/files/9gFM4FHj4PsB79I5v7yLVuPgu4bvR7M0.pdf>
- [3] Gawer A, Cusumano M. (2014). Industry Platforms and Ecosystem Innovation. *J. Prod. Innov. Management*, 31 (3): 417–433.
- [4] Evans P., Gawer A. (2016). The Rise of the Platform Enterprise. A Global Survey. Access: https://www.thecge.net/app/uploads/2016/01/PDF-WEB-Platform-Survey_01_12.pdf
- [5] Moore J. F. (2006). Business ecosystems and the view from the firm. *Antitrust Bulletin*; Spring, vol. 51, No 1: 31-75.
- [6] Muegge S. (2013). Platforms, communities and business ecosystems: Lessons learned about technology entrepreneurship in an interconnected world. *Technology innovation management review*, 2013, 3(2): 5-15.
- [7] Parker G., Alstyne M. Van, Chaudary S. Platform Revolution: How Networked Markets Are Transforming the Economy--And How to Make Them Work for You.// Harvard Business Review – Russia, Jan.-Feb.: 29-36.
- [8] Kuznetsova S.A., Markova V.D. (2018). Formation of digital business ecosystems and platforms using the case of 1C Company. *Innovations*, №2: 52-57.



Markova Vera – Doctor of Science, chief research fellow of the Institute of economics and industrial engineering SB RAS, professor of Novosibirsk State University. The field of scientific interests includes development of business strategy, marketing of innovation, innovative entrepreneurship, and digital transformation of business.



Kuznetsova Svetlana - Candidate of Science, senior research fellow of the Institute of economics and industrial engineering SB RAS, associate professor of Novosibirsk State University. The field of scientific interests includes problems of business strategy, innovation management, and companies' strategies in the digital economy.

If Development of Technologies Can Win Shadow Economy

Ekaterina N. Nevzorova¹, Anna P. Kireenko², Yulia V. Leontyeva³

¹ Baikal State University/ Department of Public administration, Irkutsk, Russia

² Baikal State University/ Department of Taxation and Customs, Irkutsk, Russia

Far Eastern Federal University / Department of Finance, Vladivostok, Russia

³ Ural Federal University named after the first President of Russia B. N. Yeltsin, Ekaterinburg, Russia

Abstract – The aim of the paper is to evaluate mutual influence of technological development and shadow economy, and answer the question if the shadow economy is reduced with the development of technologies. We are studying whether there is any link between such indicators as the shadow economy scale and the economy structure; ecological efficiency of the national economy; share of R&D expenditure in GDP; labor productivity. The World Bank data, International Standard Industrial Classification of All Economic Activities and Environmental Performance Index were used in the research. The studying sample consists of 402 observations covering the period 2010-2015 years. Studying process includes correlation analysis and cluster analysis of the data using SPSS. The main conclusion is that there is a statistical relationship among the scale of the shadow economy and the indicators of the structure of the economy; ecological efficiency of the economy; the share of R&D in GDP, and an indicator of labor productivity. The share of R&D expenditure in GDP is extremely low in the countries with a high level of shadow economy, as well as in the countries that have a significant share of resource rents in GDP. The increase in the share of R&D expenditure in GDP will be associated with both growth in labor productivity and a decrease in the size of the shadow economy.

Index Terms – Technological development, shadow economy, R&D, labor productivity.

I. INTRODUCTION

AT PRESENT the impact of high technology production on the economic development of certain countries and regions is growing. So far high technology economic sectors which have significant competitive advantages has formed in Russia, or the country is pretending to create them in the mid-term period: air- and spacecraft industry, aviation and rocket and space industry, shipbuilding, radio electronic industry, nuclear power industry complex, power engineering industry, information and communication technologies.

Certain hurdles on the way of technological development are built by the shadow economy. First, the shadow economy is closely connected with tax evasion and inadequate tax revenues reduce the state's ability to finance any expenditure. This is especially true since the federal budgets dominate in the structure of costs for scientific research and development in all fields of science. Second, due to the lack of significant benefits to fund scientific development the organizations that invest their net profit into R & D are in a less profitable

position than those who withdraw money from circulation by illegal means.

One can suggest that high technological barriers hamper the development of the shadow economy. For example, such economic activities as electricity production are less imposed to the threat of the transition into the shadow sector. And vice versa, in the conditions of low technological barriers the possibility of shadow economy development increases (e.g. retailing, household services).

II. PROBLEM DEFINITION

To evaluate mutual influence of technological development and shadow economy, and answer the question if the shadow economy is reduced with the development of technologies, we are studying whether there is any link between such indicators as the shadow economy scale and the economy structure (or “economic structure”); ecological efficiency of the national economy; share of R & D in GDP; labor productivity.

The study of the behavior of legislative norm violators, to which the participants of the shadow economy belong, is based, first of all, on G. Becker's model (1968) [1], which studies rational motives of the offender. Becker uses the traditional assumption that in criminal activity individuals rationally maximize the expected utility from the commission of a crime, and also that utility is a positive function of income. An individual will commit a crime if the expected utility from the crime is positive, and won't if it is negative. G. Becker's model was developed by Allingham M.G., Sandmo A. (1972) [2] and their followers, incl. Yitzhaki S. (1974) [3]. The later works, which analyse the factors of adherence to formal norms, consider also the socio-psychological factors. For example, the supporters of institutional economic theory argue that the decision to enforce or disobey legislation is related to the perception of the relationship between formal and informal norms in society (North D. (1990) [4], Pejovich S. (1999) [5], Helmke G., Levitsky S. (2003) [6]).

III. THEORY

Literature sources devoted to the study of the scale of the shadow economy prove that there is a statistical relationship with the following factors:

- GDP per capita (Schneider F., Buehn A., Montenegro C.E. (2010) [7, p. 8], Schneider F. (2016) [8, p. 39]);
- inflation (Maddah M., Sobhani B. (2014) [9, p. 14], Aruoba S. B. (2010) [10, p. 31])
- unemployment rate (Schneider F. (2016) [8, p. 39])
- tax and social security contribution burdens (Tanzi V. (1983) [11, p. 289], Schneider F., Williams C. (2013) [12, p. 37])
- Gini coefficient (Rosser J.B., Rosser M.V. (2001) [13, p. 47], Chong A., Gradstein M. (2007) [14, p. 176], Kar, S., Saha S. (2012) [15, p. 9])
- secondary school enrolment rate (% gross) (Schneider F., Buehn A. (2012) [16, p.11], Buehn A., Farzanegan M.R. (2013) [17])
- complexity and cost of regulatory processes for doing business (Friedman E., Johnson S., Kaufmann D., Zoido-Lobaton P. (2000) [18, p. 470], Djankov S., La Porta R., Lopez-de-Silanes F., Shleifer A. (2002) [19, p. 26], Kucera D., Roncolato L. (2008) [20, p. 340])
- assessment of corruption (Johnson S., Kaufmann D., Shleifer A. (1997) [21, p. 164])
- share of agriculture in GDP (Vuletin G. J. (2008) [22, p. 14], and also F. Schneider (2014) [23, p. 9])
- impact of certain economic sectors (agriculture, industry and services) to the scale of the shadow economy [24].

Particular attention in studying the determinants of the scale of the shadow economy deserves the role of resource rent. For example, a review by Heinrich A. (2011) [25] states that in a country experiencing a resource boom, the state cannot create an effective institution of taxation. The same problem is considered in the book [26]. A number of works are devoted to studying the relationship between the resource rent and corruption, for example [27], where corruption is seen as a factor contributing to the growth of the shadow economy.

Empirical micro-surveys of business indicate that the level of business involvement in shadow activities is influenced by the activity sector. Krstić G. and Radulović B. (2015) [28] detect in Serbia: most business entities active in the shadow economy operates in the construction sector, agriculture, catering and transportation. Similar results were revealed by Schneider F. (2013) [29]: he found that the shadow economy (27 countries of the European Union plus Croatia, Norway, Switzerland, and Turkey) are most proliferated in the construction sector, trade, hotels & restaurants, and transportation. In a similar vein the study by Putnins T. and Sauka A. (2011) [30] found that the shadow economy was predominant in the construction sector, followed by services and retail trade (on data by Baltic States).

Negative statistical relationship between the share of R&D expenditures in GDP and the scale of the shadow economy is noted in [31]. One of the existing problems in this regard, noted at the international level - is the use of tax incentives related to R & D [32].

Also, the results of resource use are reflected at the environmental conditions. It, in turn, is a component in

assessing the quality of life¹. Our early studies confirmed the hypothesis that the quality of life is negatively related to the scale of the shadow economy [33]. In studies by Elgin C., Oztunali O. [34], Biswas A. K., Farzanegan M. R., Thum M. [35] the relationship between the ecological situation and the shadow economy is analyzed.

IV. RESEARCH METHODOLOGY

To analyze the relationship between the shadow economy and the indicators of technological development we selected the following variables (Tab. 1).

TABLE I
ANALYZED VARIABLES

| Factor | Variable | Data source | Period for which data is available | Identification mark |
|---------------------------|---|--|------------------------------------|---------------------|
| Size of shadow economy | Size of the shadow economy as a percentage of GDP | Medina & Schneider (2018) [36] | 1991-2015 | SHADOW |
| Structure of economy | Agriculture, value added (% of GDP) | World Bank ² | 1990-2016 | Agriculture |
| | Industry, value added (% of GDP) | World Bank ³ | 1990-2016 | Industry |
| | Services, etc., value added (% of GDP) | World Bank ⁴ | 1990-2016 | Services |
| | Total natural resources rents (% of GDP) | World Bank ⁵ | 1970-2015 | Resources rents |
| Environmental Performance | Environmental Performance Index | Environmental Performance Index (EPI) ⁶ | 2007-2016 | EPI |
| Research and development | Research and development expenditure (% of GDP) | World Bank ⁷ | 1996-2015 | R&D |
| Labor productivity | Output per worker (GDP constant 2011 international \$ in PPP) | International Labour Organization ⁸ | 2010-2016 | Output per worker |

Data on the structure of the economy are explored following the International Standard Industrial Classification of All Economic Activities (ISIC), Rev.3.1⁹. According to this classification:

¹ http://ec.europa.eu/eurostat/statistics-explained/index.php?title=Quality_of_life_indicators

² <https://data.worldbank.org/indicator/NV.AGR.TOTL.ZS?view=chart>

³ <https://data.worldbank.org/indicator/NV.IND.TOTL.ZS?view=chart>

⁴ <https://data.worldbank.org/indicator/NV.SRV.TETC.ZS?view=chart>

⁵ <https://data.worldbank.org/indicator/NY.GDP.TOTL.RT.ZS?view=chart>

⁶ <http://sedac.ciesin.columbia.edu/data/set/eipi-environmental-performance-index-2016>

⁷ <https://data.worldbank.org/topic/science-and-technology>

⁸

<http://www.ilo.org/ilostat/faces/oracle/webcenter/portalapp/pagehierarchy/Package27.jsp>

⁹ ISIC Rev.3.1 (International Standard Industrial Classification of All Economic Activities, Rev.3.1), Detailed structure and explanatory notes

Agriculture corresponds to ISIC divisions 1-5 and includes forestry, hunting, and fishing, as well as cultivation of crops and livestock production.

Industry corresponds to ISIC divisions 10-45 and includes manufacturing (ISIC divisions 15-37). It comprises value added in mining, manufacturing (also reported as a separate subgroup), construction, electricity, water, and gas.

Services correspond to ISIC divisions 50-99 and they include value added in wholesale and retail trade (including hotels and restaurants), transport, and government, financial, professional, and personal services such as education, health care, and real estate services. Also included are imputed bank service charges, import duties, and any statistical discrepancies noted by national compilers as well as discrepancies arising from rescaling.

Resource rent is included in the results of other areas, but World Bank data allow it to be considered separately (Total natural resources rents (% of GDP)¹⁰. In the review by Heinrich A. (2011) [25] there was articulated that in a country experiencing a resource boom, the state cannot establish an effective institution of taxation.

In order to take into account the impact of the environmental situation in our work, we use the indicator “Environmental Performance Index” (EPI)¹¹ which evaluate a country's environmental performance in different policy categories relative to clearly defined targets (9 policy categories: health impacts, air quality, water and sanitation, water resources, agriculture, forests, fisheries, biodiversity and habitat, and climate and energy).

Due to the limitedness of the data, we study the period 2010-2015. The sample consists of 402 observations (if an observation has a missing value, this observation is excluded).

We implement correlation analysis and cluster analysis of the data. The calculations are performed by using SPSS. Through correlation analysis we test presence or absence of a statistical relationship between variables. For more profound analysis we perform clustering procedures (k-means algorithm). Performing the cluster analysis we pursue several goals:

- detection of a cluster structure - splitting the sample into clusters having the most different characteristics (the minimum number of clusters is optimal for this goal);
- data compression (for this purpose clustering is performed so as to ensure a high degree of similarity within each cluster);
- novelty detection (in this case, the most interesting are atypical objects allocated in the process of clustering that do not fit into any of the clusters).

Then we create the graphic representation of results.

V. EXPERIMENTAL RESULTS

Initially the data are analyzed to evaluate conformance to the normal distribution. The analysis is carried out by plotting histograms, as well as the Kolmogorov-Smirnov test.

TABLE II
STATISTICS

| | Agriculture | Industry | Services | Resources rent | EPI | SHADOW | Output per worker | R&D |
|----------------|-------------------|--------------------|--------------------|----------------|--------------------|-------------------|-------------------|---------|
| Mean | 6,35 | 29,76 | 63,89 | 4,86 | 77,65 | 23,57 | 58102 | 1,20 |
| Median | 3,79 | 28,57 | 64,75 | 1,17 | 80,02 | 22,38 | 54295 | 0,82 |
| Mode | 0,04 ^a | 10,19 ^a | 29,03 ^a | 0,00 | 72,94 ^a | 7,83 ^a | 59237 | 0,38 |
| Std. Deviation | 7,19 | 10,02 | 11,65 | 9,14 | 10,70 | 11,01 | 36420 | 1,06 |
| Variance | 51,71 | 100,46 | 135,68 | 83,48 | 114,42 | 121,16 | 1,33E+09 | 1,11 |
| Skewness | 2,46 | 1,31 | -0,54 | 3,44 | -1,53 | 0,468 | 1,10 | 1,04 |
| Kurtosis | 7,48 | 3,15 | 0,22 | 13,99 | 2,77 | -0,535 | 2,28 | 0,22 |
| Range | 44,71 | 58,90 | 58,62 | 60,83 | 56,24 | 49,910 | 205013 | 4,28 |
| Minimum | 0,04 | 10,19 | 29,03 | 0,00 | 34,50 | 6,66 | 1750 | 0,01 |
| | Singapore | Ethiopia | Azerbaijan | Malta | Madagascar | Switzerland | Burundi | Lesotho |
| Maximum | 44,74 | 69,08 | 87,65 | 60,83 | 90,74 | 56,57 | 206763 | 4,29 |
| | Ethiopia | Kuwait | Luxembourg | Kuwait | Finland | Georgia | Luxembourg | Israel |

a. Multiple modes exist. The smallest value is shown

TABLE III
ONE-SAMPLE KOLMOGOROV-SMIRNOV TEST

| | | Agriculture | Industry | Services | Resources rent | EPI | SHADOW | Output per worker | R&D |
|------------------------|----------|-------------|----------|----------|----------------|-------|--------|-------------------|-------|
| Most Extreme | Absolute | ,190 | ,095 | ,065 | ,297 | ,153 | ,093 | ,064 | ,149 |
| Positive Differences | Positive | ,181 | ,095 | ,038 | ,253 | ,111 | ,093 | ,064 | ,149 |
| Negative Differences | Negative | -,190 | -,058 | -,065 | -,297 | -,153 | -,067 | -,061 | -,131 |
| Kolmogorov-Smirnov Z | | 3,807 | 1,906 | 1,302 | 5,960 | 3,072 | 1,856 | 1,276 | 2,987 |
| Asymp. Sig. (2-tailed) | | ,000 | ,001 | ,067 | ,000 | ,000 | ,002 | ,077 | ,000 |

a. Test distribution is Normal.

The most variables don't follow a normal distribution¹². In our sample, the value $p > 0.05$ for the indicators “Services, etc., value added (% of GDP)”, and “Output per worker”, that is, the probability of error is not significant; so these variables are conform to the normal distribution, and parametric tests can be applied to these variables. In other cases, non-parametric tests should be used.

In order to bring data to a single scale, the indicators were normalized. Further we performed correlation analysis. Due to the fact that the data are not normally distributed, their correlation analysis can be performed using nonparametric indicators. Of the possible indicators we used the Kendall rank correlation coefficient. The Spearman's rank correlation coefficient was not used, because variables can have repeated data values.

TABLE IV

<https://unstats.un.org/unsd/cr/registry/regcst.asp?Cl=17&Lg=1>

¹⁰ <https://data.worldbank.org/indicator/NY.GDP.TOTL.RT.ZS?view=chart>

¹¹ <http://sedac.ciesin.columbia.edu/data/set/epi-environmental-performance-index-2016>

¹² If p-value is less than the significance level (0.05), the null-hypothesis that it is normally distributed can be rejected.

KENDALL'S TAU_B*

| Zscore | SHAD OW | Agricul ture | Indus try | Servi ces | Resources rent | EPI | Output per worker | R&D |
|----------------------|------------|-----------------|--------------|--------------|-------------------|------|-------------------------|-----|
| SHADOW | | | | | | | | |
| Agriculture | ,498 | | | | | | | |
| Industry | ,086 | ,111 | | | | | | |
| Services | -,327 | -,458 | -,654 | | | | | |
| Resources rent | ,269 | ,346 | ,384 | -,532 | | | | |
| EPI | -,404 | -,455 | -,220 | ,477 | -,365 | | | |
| Output per worker | -,545 | -,729 | -,126 | ,437 | -,369 | ,506 | | |
| R&D | -,516 | -,469 | -,162 | ,410 | -,401 | ,487 | ,532 | |

* Correlation is significant at the 0.01 level (2-tailed).

The relationship strength is qualitatively assessed based on the Chaddock scale [37]. The scale of the shadow economy has the closest correlation relationship (significant at the 0.01 level) with the following indicators:

- Output per worker (noticeable, negative);
- R & D (noticeable, negative);
- Agriculture (moderate, positive);
- EPI (moderate, negative);
- Services (moderate, negative);
- Resources rent (weak, positive).

We performed cluster analysis by using k-means technique. To improve the quality of clustering we used option “Use running means”. When choosing the number of clusters, we were guided by the following criteria:

1. F-test for variables: comparing 2-, 3-, 4-, 5-, 6- and 7-cluster models demonstrates significant results for all variables.
2. The total value of F-test for alternative models: other things being equal, the model with the maximum value of F-test is preferable.

TABLE V
F-TEST

| Variable (Zscore) | Number of clusters | | | | | |
|-------------------|--------------------|--------|--------|--------|--------|--------|
| | 2 | 3 | 4 | 5 | 6 | 7 |
| SHADOW | 348,9 | 178,0 | 112,6 | 90,0 | 74,0 | 107,5 |
| Agriculture | 220,0 | 217,8 | 381,4 | 298,7 | 239,8 | 271,1 |
| Industry | 88,9 | 176,7 | 170,3 | 129,7 | 127,9 | 100,6 |
| Services | 469,3 | 274,2 | 245,4 | 177,1 | 163,8 | 139,7 |
| Resources rent | 102,4 | 333,4 | 291,9 | 456,1 | 289,4 | 210,1 |
| EPI | 375,0 | 184,1 | 296,0 | 252,6 | 200,9 | 200,4 |
| Output per worker | 223,1 | 138,5 | 150,4 | 140,0 | 235,2 | 264,5 |
| R&D | 278,9 | 106,9 | 137,8 | 103,6 | 82,3 | 223,1 |
| Total | 2106,6 | 1609,6 | 1785,7 | 1647,9 | 1413,3 | 1517,0 |

Starting with model consisting from 7 clusters, the total F-test value decreases with increasing number of clusters. By this criterion, the 6-cluster model is clearly inferior to the rest.

3. Average distance between the cluster centers: all analyzed models have an acceptable value of the average distance between cluster centers (more than 2).
4. Compactness of clusters (the members of each cluster should be as close to each other as possible; a common measure of compactness is the variance).

TABLE VI

DISTANCE OF CASE FROM ITS CLASSIFICATION CLUSTER CENTER (VARIANCE)

| Cluster number | Number of clusters | | | | | |
|----------------|--------------------|-------|-------|-------|-------|-------|
| | 2 | 3 | 4 | 5 | 6 | 7 |
| 1 | 0,425 | 0,826 | 0,322 | 0,373 | 0,189 | 0,038 |
| 2 | 1,929 | 0,632 | 0,373 | 0,278 | 0,271 | 0,292 |
| 3 | | 0,465 | 0,462 | 0,038 | 0,003 | 0,289 |
| 4 | | | 0,438 | 0,438 | 0,320 | 0,270 |
| 5 | | | | 0,422 | 0,932 | 0,932 |
| 6 | | | | | 0,038 | 0,003 |
| 7 | | | | | | 0,189 |

Comparing the models, we elicited: the 4-cluster model has the minimum variance value (i.e. this is the most compact model from all analyzed).

5. Filling of clusters (the more equally filled clusters the better model).

TABLE VII

NUMBER OF CASES IN EACH CLUSTER

| Cluster number | Number of clusters | | | | | |
|----------------|--------------------|-----|-----|-----|-----|-----|
| | 2 | 3 | 4 | 5 | 6 | 7 |
| 1 | 231 | 118 | 168 | 15 | 14 | 7 |
| 2 | 171 | 23 | 15 | 158 | 196 | 119 |
| 3 | | 261 | 19 | 7 | 6 | 121 |
| 4 | | | 200 | 200 | 163 | 119 |
| 5 | | | | 22 | 16 | 16 |
| 6 | | | | | 7 | 6 |
| 7 | | | | | | 14 |
| Total | 402 | 402 | 402 | 402 | 402 | 402 |

Starting with the 5-cluster model, there are formed clusters which contain 1-2% of all observations of sample. However, analyzing the membership of clusters we find that these clusters can be defined as “outliers”: they contain data of countries characterized by anomalous deviation of the values of variables from the rest sample. For the 5-cluster model such “outlier” is a cluster containing 2 countries: Kuwait and Oman. (Here should be noted that one country can be member of several clusters, according to the data for different years). This cluster is also allocated when sample dividing into more clusters. For the 6-cluster model there is distinguished a cluster which contain only 1 country: Luxembourg. Among the models being compared, the 7-cluster model has the most equally filling of clusters (except the mentioned “outliers”).

As a result of the cluster analysis we draw the following conclusions:

In the 2-cluster model the most significant variables for clustering are “services (% of GDP)”, “size of the shadow economy”, EPI.

For the 3-cluster model the most significant variables for clustering are: “resources rents (% of GDP)”, “services (% of GDP)”, “agriculture (% of GDP)”. In this case, comparing with the 2-cluster model, there is formed a cluster of countries, where dominant majority are hydrocarbon exporting countries: Azerbaijan, Kazakhstan, Kuwait, Mongolia, Oman, Trinidad and Tobago, and United Arab Emirates.

For the 4-cluster model the most significant variables are: EPI, “resources rents (% of GDP)”, “agriculture (% of

GDP)". At the same time, a cluster of countries with a minimum EPI index is formed, it consists of Burundi, Cambodia, Ethiopia, Ghana, Madagascar, Mali, Mozambique, Nepal, Pakistan, Togo, Vietnam.

For the 5-cluster model the most significant variables are the same as them the 4-cluster model, but their contribution to the clustering of countries are changed – "resources rents (% of GDP)", "agriculture (% of GDP)", EPI. There is formed a cluster which consists of minimum number of countries (two countries): Kuwait and Oman. For these countries are typical the maximum "output per worker" and the minimum "R&D expenditure (% of GDP)".

For the 4-cluster model the most significant variables are: "resources rents (% of GDP)", "output per worker", EPI. There is formed a cluster which consists of one country - Luxembourg. For these countries are typical the maximum "output per worker" (for sample and the maximum "services (% of GDP)").

When the 7-cluster model is formed, the cluster having middle size of the shadow economy is divided into 2 clusters, №3 and №2: the latter has substantially higher "size of the shadow economy", higher "agriculture (% of GDP)", "industry (% of GDP)", and lower "services (% of GDP)", EPI, "output per worker" and "R&D expenditure (% of GDP)". The most significant variables for clustering are: "agriculture (% of GDP)", "output per worker" and "R&D expenditure (% of GDP)". The data of the 7-cluster model are shown in the table and in the figure (left-to-right order as the size of the shadow economy increases).

TABLE VIII
FINAL CLUSTER CENTERS

| Variable | Cluster number | | | | | | |
|-------------------------------------|----------------|--------|--------|--------|--------|--------|--------|
| | 6 | 4 | 1 | 3 | 5 | 2 | 7 |
| SHADOW | -1,188 | -0,975 | -0,390 | -0,081 | 0,793 | 0,890 | 1,224 |
| Agriculture | -0,841 | -0,643 | -0,784 | -0,328 | -0,246 | 0,652 | 3,783 |
| Industry | -1,729 | -0,262 | 3,627 | -0,303 | 2,326 | 0,265 | -1,140 |
| Services | 2,007 | 0,622 | -2,637 | 0,463 | -1,850 | -0,631 | -1,355 |
| Resources rent | -0,524 | -0,413 | 5,177 | -0,257 | 2,199 | -0,002 | 0,864 |
| EPI | 0,830 | 0,670 | -1,791 | 0,449 | -0,188 | -0,658 | -3,222 |
| Output per worker | 3,957 | 0,828 | 1,876 | -0,063 | -0,276 | -0,863 | -1,481 |
| R&D | 0,159 | 1,312 | -0,984 | -0,311 | -0,929 | -0,714 | -0,908 |
| Number of countries in each cluster | 1 | 23 | 2 | 26 | 5 | 36 | 10 |

Clusters Members:

Cluster 6 – Luxembourg.

Cluster 4 – Australia, Austria, Belgium, Canada, Czech Republic, Denmark, Estonia, Finland, France, Germany, Iceland, Ireland, Israel, Japan, Korea (Rep.), Netherlands, Norway, Singapore, Slovenia, Sweden, Switzerland, United Kingdom, United States.

Cluster 1 – Kuwait, Oman.

Cluster 3 – Argentina, Brazil, Bulgaria, Chile, Costa Rica, Croatia, Cyprus, Czech Republic, Estonia, Greece, Hungary, Italy, Latvia, Lithuania, Malta, Mauritius, Mexico, New Zealand, Poland, Portugal, Romania, Russian Federation, Slovakia, Spain, United Arab Emirates, Uruguay.

Cluster 5 – Azerbaijan, Kazakhstan, Mongolia, Trinidad and Tobago, United Arab Emirates.

Cluster 2 – Armenia, Belarus, Bosnia and Herzegovina, Botswana, China, Colombia, Egypt, El Salvador, Georgia, Guatemala, India, Indonesia, Kazakhstan, Kyrgyzstan, Lesotho, Malaysia, Mexico, Moldova, Mongolia, Morocco, Namibia, Nicaragua, Oman, Paraguay, Peru, Philippines, Romania, Senegal, Sri Lanka, Thailand, Tunisia, Turkey, Ukraine, Uruguay, Viet Nam.

Cluster 7 – Burundi, Cambodia, Ethiopia, Ghana, Madagascar, Mali, Mozambique, Nepal, Pakistan, Togo.

The results of clustering are shown in the Fig. 1 (except for clusters №6 and №1, which represented by individual countries). The units of measurement for Y-axes are percents. Right scale is used to display the values of "R&D expenditure (% of GDP)". The value "output per worker" is reflected on the left axis: the displayed value is equal to the value of the indicator divided by 1000 (units of measurement - US \$).

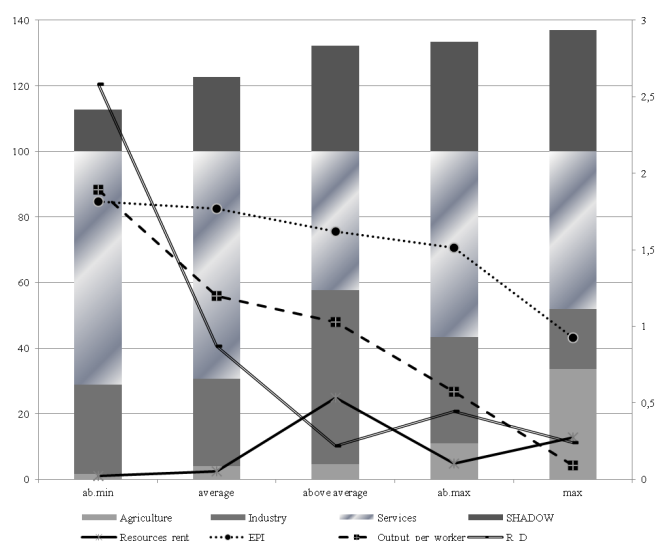


Fig. 1. Average values of variables for clusters.

V. DISCUSSION OF RESULTS

We found that the initial sample contains observations that differ significantly by value of the analyzed variables: all analyzed variables are significant. The structure of the economy is crucial when we splitting sample even into two clusters which characterized by a high and low level of shadow economy correspondingly. In this case, the consequences of economic activity on the environment are also significant. When we divide sample into a larger number of clusters, the indicator "resource rent" acquires significance. Differences in level of R & D expenditures and labor productivity are beginning to be significant for dividing countries in more clusters (more detailed analysis). For the first time, they are manifested their influence when occurs allotment of a small cluster (where objects that are most untypical for whole sample).

VI. CONCLUSION

Based on the results of the analysis conducted, we can formulate the conclusion that there is a statistical relationship among the scale of the shadow economy and the indicators of the structure of the economy; ecological efficiency of the economy; the share of R & D in GDP, and an indicator of labor productivity. According to the data used in the work, the share of R & D in GDP is extremely low in the countries with a high level of shadow economy, as well as in the countries that have a significant share of resource rents. But the results of our analysis also suggest that the transition to an innovative type of development, when the national economy will not be significantly dependent on the export of raw materials, and the corresponding increase in the share of R & D in GDP will be associated with both growth in labor productivity and a decrease in the level of the shadow economy. In turn, the efforts to withdraw economic activity from the non-observed sector will also allow increasing the funds available to the public sector, which can serve as an additional resource for the development of knowledge-intensive industries.

ACKNOWLEDGMENT

This work was funded by the RFFR grant №17-22-21001

REFERENCES

- [1] Becker G.S. Crime and Punishment: An Economic Approach //Journal of Political Economy. 1968. V. 76. No. 2. pp. 169-217.
- [2] Allingham M.G., Sandmo A. Income tax evasion: A theoretical analysis //Journal of public economics. 1972. V. 1. No. 3-4. pp. 323-338.
- [3] Yitzhaki S. Income tax evasion: A theoretical analysis //Journal of public economics. 1974. V. 3. No. 2. pp. 201-202.
- [4] North D. Institutions, Institutional Change and Economic Performance. – Cambridge: Cambridge University Press, 1990. – 152 p.
- [5] Pejovich S. The effects of the interaction of formal and informal institutions on social stability and economic development //Journal of Markets and Morality. 1999. V. 2. No. 2. pp. 164-181.
- [6] Helmke G., Levitsky S. Informal Institutions and Comparative Politics: A Research Agenda //Perspectives on Politics. 2004. No. 2(4). pp. 725-740.
- [7] Schneider F., Buehn A., Montenegro C.E. Shadow economies all over the world: new estimates for 162 countries from 1999 to 2007 //World Bank Policy Research Working Paper Series. 2010. No. 5356. – 52 p.
- [8] Schneider F. Out of the shadows: measuring informal economic activity. In: Miller T. and Kim A.B. (eds) 2016 Index of Economic Freedom. – Washington DC : The Heritage Foundation, 2016. – pp. 35-49.
- [9] Maddah M., Sobhani B. The effective factors on informal economy in developing countries (panel data model) //International Journal of Regional Development. 2014. V. 1. No. 1. pp. 12-25.
- [10] Aruoba S.B. Informal sector, government policy and institutions //2010 Meeting Papers (Society for Economic Dynamics). 2010. V. 324. – 59 p.
- [11] Tanzi V. The underground economy in the United States: annual estimates, 1930-80 //Staff Papers. 1983. V. 30. No. 2. pp. 283-305.
- [12] Schneider F., Williams C.C. The shadow economy. – London : Institute of Economic Affairs, 2013. – 184 p.
- [13] Rosser J.B., Rosser M.V. Another failure of the Washington consensus on transition countries: inequality and underground economies //Challenge. 2001. V. 44. No. 2. pp. 39-50.
- [14] Chong A., Gradstein M. Inequality and informality //Journal of Public Economics. 2007. V. 91. No. 1-2. pp. 159-179.
- [15] Kar S., Saha S. Corruption, shadow economy and income inequality: evidence from Asia //Discussion Paper Series (Forschungsinstitut zur Zukunft der Arbeit). 2012. No. 7106. – 28 p.
- [16] Schneider F., Buehn A. Shadow economies in highly developed OECD Countries: what are the driving forces? //IZA Discussion Paper. 2012. No. 6891. – 32 p.
- [17] Buehn A., Farzanegan M.R. Impact of education on the shadow economy: institutions matter //Economics Bulletin. 2013. V. 33. No. 3. pp. 2052-2063.
- [18] Friedman E., Johnson S., Kaufmann D., Zoido-Lobaton P. Dodging the grabbing hand: the determinants of unofficial activity in 69 countries //Journal of public economics. 2000. V. 76. No. 3. pp. 459-493.
- [19] Djankov S., La Porta R., Lopez-de-Silanes F., Shleifer A. The regulation of entry //The quarterly Journal of economics. 2002. V. 117. No. 1. pp. 1-37.
- [20] Kucera D., Roncolato L. Informal employment: two contested policy issues //International Labour Review. 2008. V. 147. No. 4. pp. 321-348.
- [21] Johnson S., Kaufmann D., Shleifer A., Goldman M., Weitzman M. The unofficial economy in transition //Brookings papers on economic activity. 1997. V. 1997. No. 2. pp. 159-239.
- [22] Vuletin G.J. Measuring the informal economy in Latin America and the Caribbean //IMF Working paper. 2008. No. 102. – 29 p.
- [23] Schneider F. The shadow economy: an essay. – Linz, Johannes Kepler University of Linz, Department of Economics, 2014 – 23 c.
- [24] Sabirianova Peter K. Income Tax Flattening: Does It Help to Reduce the Shadow Economy? //IZA Discussion Paper. 2009. No. 4223. – 48 p.
- [25] Heinrich A. Challenges of a Resource Boom: Review of the Literature //Research Centre for East European Studies Working Paper. 2011. No. 114. – 57 p.
- [26] Barma N.H., Kaiser K., Le T.M., Viñuela L. Rents to riches? Taxing Resource Wealth: The Political Economy of Fiscal Regimes. – Washington DC : The World Bank. 2011. – 276 p.
- [27] Ades A., Di Tella R. Rents, competition, and corruption //American economic review. 1999. V. 89. No. 4. pp. 982-993.
- [28] Krstić G., Radulović B. Shadow Economy in the Business and Entrepreneurial Sectors. In: Krstić G., Schneider F. (eds) Formalizing the Shadow Economy in Serbia. Contributions to Economics. – Springer, Cham, 2015. – pp. 77-99.
- [29] Schneider F., Kearney A. T. The shadow economy in Europe, 2013. – Linz : Johannes Kepler Universität. 2013. – 24 p.
- [30] Putniņš T. J., Sauka A. Size and determinants of shadow economies in the Baltic States //Baltic Journal of Economics. 2011. V. 11. No. 2. pp. 5-25.
- [31] Markellos R. N., Psychoyios D., Schneider F. Sovereign debt markets in light of the shadow economy //European Journal of Operational Research. 2016. V. 252. No. 1. pp. 220-231.
- [32] OECD. Tax Incentives for Research and Development: Trends and Issues. – Paris: OECD, 2003. – 37 p.
- [33] Kireenko A., Nevzorova E. Impact of shadow economy on quality of life: Indicators and model selection //Procedia Economics and Finance. 2015. V. 25. pp. 559-568.
- [34] Elgin C., Oztunali O. Pollution and informal economy //Economic Systems. 2014. V. 38. No. 3. pp. 333-349.
- [35] Biswas A. K., Farzanegan M. R., Thum M. Pollution, shadow economy and corruption: Theory and evidence //Ecological Economics. 2012. V. 75. pp. 114-125.
- [36] Medina L., Schneider F. Shadow Economies Around the World: What Did We Learn Over the Last 20 Years? // IMF Working Paper. 2018. No. 18/17. – 79 p.
- [37] Chaddock R.E. Principles and Methods of Statistics, New York, 1925. – 471 p.



Kireenko Anna Pavlovna – Doctor of Economics, professor, Head of the department of tax and customs of Baikal State University. Honored worker of science and higher education of the Irkutsk region. Research interests: tax, tax regulations, tax evasion, underground economy. Over the past five years it has published more than 50 scientific papers.



Nevzorova Ekaterina Nikolaevna – PhD in Economics, Associate Professor, Baikal State University, Department of Public Administration. Research interests: shadow economy, informal sector economics, corruption, public economics, property rights. The total number of academic articles published in recent 5 years – 15.



Yulia Vladimirovna Leontyeva – PhD in Economics, Associate Professor, Ural Federal University named after the first President of Russia B. N. Yeltsin, Department of Financial and Tax Management. Research interests: taxation, tax policy, transport taxation. More than 35 scientific papers published for the last 5 years.

Creation of Software Product Supporting the Development of High-Tech Food Production of Functional & Special Purpose

Lada N. Rozhdenstvenskaya, Olga V. Rogova
Novosibirsk State Technical University, Novosibirsk, Russia

Abstract – The paper proves the necessity of developing a software product which could provide high-tech manufacturing of functional and specialized food products. The software product proposed in the paper will allow prompt computer modeling of the composition of food products, dishes and articles of food with specified properties taking into account priority areas of research. A personalized approach to the population's nutrition based on individual food peculiarities lays down new requirements to digital technologies providing foodstuff manufacturing. The main potential consumers of the product under development are determined. The main parts of the software product performance specification are presented. Preliminary calculations of the cost of the proposed software product development are made.

Index Terms - Software product, high-tech production, functional and specialized food products.

I. INTRODUCTION

A NEED TO CREATE a technological medium that can help to implement advanced consumer standards is currently becoming obvious.

The development of an innovation reproduction type demanded new approaches to creating a new organizational and economic mechanism of its regulation based on new intelligent products.

In compliance with the RF government policy in the field of the population's nutrition, efforts of the government, producers and specialists in process manufacturing in the agricultural sector and the food processing industry have recently been concentrated on stating and implementing specified advanced programs aimed at creating and high-tech production of new generation foodstuffs, that is functional and specialized products.

These processes in the food industry due to the scarcity of the available food resources and a high market demand for food products with specified characteristics resulted in the need to solve the following problems:

- using alternative food sources [1]– [4];
- regard for individual peculiarities of consumers, first of all food intolerance (e.g. lactose and gluten intolerance, phenylketonuria, diabetes, etc.) and allergies [5] – [7];
- creating new bases of food products used as raw materials in food manufacturing which make it possible not only to evaluate nutritional and biological qualities of certain ingredients but also by using specified criteria choose raw material sources promising for creating specialized and

functional food products as well as food supplements [8] – [11].

- The relevance of these challenges is caused by the fact that under present-day conditions a need for an individual approach to nutrition is sensed more and more even on the level of public catering facilities. Therefore most ingredients in dishes cannot be replaced by mere exclusion e.g. of tomatoes from salads and increasing the volume of other vegetables. That is why an effective mechanism to improve food formulae taking into account consumers' individual wishes or medical limitations should be developed.

- A tendency of a personalized approach to nutrition is expanding. This approach helps to develop menus which take into account consumers' individual wishes and food peculiarities. As a result a need appears to develop data bases providing the creation of new functional and specialized food products (FSFP) and dishes to compose food rations based on them with regard for consumers' medical indications, metabolic peculiarities and individual preferences

- A symbiosis of scientific and empirical knowledge of food manufacturing and medicine is a world-wide tendency in developing high-tech FSFPs.

- Therefore developing high-tech FSFP is becoming a multifactor task covering knowledge of various fields of science and consisting of the following stages:

- substantiation of the choice of functional ingredients and their dosages to produce foodstuffs from the recommended raw materials based on individual or group requirements and the evaluation of their qualitative and quantitative composition;
- study of the effect of a complex use of the chosen functional ingredients on the change in the raw material state in the process of manufacturing and study of their effect on a set of indicators characterizing the quality and safety of finished FSFPs;
- development of food formulae and technologies of FSFP production as well as development and approval of normative documents for groups of FSFPs
- carrying out an expertise of the design indicators of quality and safety of the proposed FSFPs as to the conformity to the Russian and international standards; substantiation of the recommended date of consumption; evaluation of a relative biological value of the proposed FSFPs.

The efficiency of fulfilling this task can be increased by using information technologies.

At present software products (SP) which make it possible to work out individual rations for medical and preventive diets are being developed with due regard for individual peculiarities and preferences of consumers [11] – [13].

The foregoing proves the necessity to develop new SPs allowing efficient computer modeling of the composition of food products, dishes and articles of food with specified organoleptic and physico-chemical properties taking into account the priorities of science development in the field of high-tech production of FSFPs.

II. PROBLEM DEFINITION

The task of this research is to create the basis for developing a SP which can facilitate high-tech production of FSFPs. The proposed SP will allow computer modeling of the composition of food products, dishes and articles of food with specified properties taking into account the priorities of science development in the field of high-tech production of FSFPs.

III. THEORY

SPs which allow developing menus and diets with regard for individual peculiarities and preferences of customers are presented on the Novosibirsk market by two companies, namely Expert Soft Co, Ltd and 1C Co, Ltd [14, 15].

The Expert Soft Co, Ltd offers two SPs: “NASSR-Clinical Nutrition” (market price is 29,000 rubles) and “School Meals” (market price is 25,000 rubles).

The 1C Co, Ltd offers the following SPs: “1C Medicine. Dietary Nutrition” (market price is 33,600 rubles), “1C School Meals (market price is 13,000 rubles) and “1C Preschool Nutrition (market price is 13,000 rubles).

When making a comparative analysis of the “School Meals” and the “1C School Meals” in terms of a possibility to make menus with regard for individual peculiarities of consumers it has been found that both SPs make it possible to:

- make card files of dishes, a product nomenclature and typical periodic menus;
- develop formulae of dishes with rated physical and chemical indicators, with a specified nutrition and energy value as well as vitamin and mineral content;
- automatically analyze the above indicators when composing periodic menus;
- analyze daily rations (to make a comparison of planned and actual norms of the above indicators).

In addition to the above the “1C School Meals” allows calculating foodstuff consumption based on the foodstuff loading norms and taking into account losses in the process of cold cooking.

The peculiar functions of the SP “School Meals” is an automatic computation of average indicators of the dish yield based on the results of control tests and a possibility of a separate analysis of the consumption of proteins and vegetable and animal fats.

An analysis of the proposed SPs functional has shown that they are designed to work with FSFPs created by the already approved formulae.

SP data do not provide a possibility to create and analyze an effect of various kinds of cooking on foodstuffs with specified physical and chemical indicators, with a specified nutrition and energy value as well as vitamin and mineral content.

A personalized approach to nutrition and the world tendencies in the food processing industry mentioned above make it necessary to develop a SP which could help to develop new kinds of food products based on the specified indicators of a nutrition and energy value as well as vitamin and mineral content taking into account an effect of various kinds of cooking and using unconventional raw material sources on them. An example of such a task can be creating high-tech manufacturing of meat functional products with the use of hydrolyzates of hydrobionts, a complex of domestic starter cultures of microorganisms, water-alcoholic infusions and balsam syrups based on herbs, vitamin B complexes, bioavailable ferrum, etc.

This SP will also make it possible to improve dish compositions, with high organoleptic indicators and their biological value being preserved, when it is necessary to replace some ingredients potentially dangerous and causing a consumer's allergy. Another purpose of the developed SP is an offered choice of potential ingredients in computer modeling of dish formulae for people with food problems (lactose-free and gluten-free nutrition, etc.).

The proposed SP is designed to satisfy needs of a wide variety of users whose task is to develop new FSFPs such as research centers, educational institutions, and food processing enterprises manufacturing finished and semi-finished food products.

To increase the efficiency and quality of designing such a SP it is necessary to design a performance specification.

It will allow developers to clearly understand the SP goals and to minimize development efforts and it will also help them to avoid task duplication.

IV. RESULTS

To develop a SP which can provide high-tech production of FSFPs, a performance specification was designed, with requirements to the process of modeling and optimization of formulae of food products with specified characteristics and recommendations on designing the SP given in [16] – [25] taken into account.

The developed performance specification contains the following sections:

1. The SP name and application area.
2. The development purpose. The section contains the characteristic of the SP functional and operational purpose and a user's characteristic.
3. Technical requirements to the SP. The section contains requirements to functional characteristics, logical structure of databases, usability, performance, operation conditions, software compatibility, users' interfaces, hardware, software and interaction.

4. Requirements to the SP marking, packaging, transportation and storage.

5. Stages and steps of the SP development and acceptance.

After completing the performance specification design a preliminary calculation of the SP development cost was made.

At present there is not any standard document available that allows estimating an SP development cost. The calculation of the SP development cost was made based on the normative standards of labor intensity given in [26]. In calculating the following factors were taken into account:

- a degree of the SP development novelty - the first implying the development of a new SP with individual characteristics;
- the first group of complexity of the task being carried out implying the development of algorithms for solving problems of optimal planning, multifactor analysis, calculation of normative standards and forecasting;
- the second group of complexity comprising SPs having a comparatively complex logical structure characterized by a variety of forms of input and output documents or a difficulty of data acquisition;
- the problems being solved which include calculation of a nutrition and energy value, vitamins and minerals with regard for an effect of various kinds of cooking (primary processing, cold processing, marinating, boiling, poaching, stewing, frying, roasting, browning, baking, intensive cooling and shock-freezing) on each of the mentioned indicators.

Based on the normative data presented in [26] the labor intensity of the SP development was determined, namely 3097 normal hours:

- development of a database and its filling - 1760 normal hours;
- SP development – 1337 normal hours.

Taking into account the fact that a minimal hour rate in Russia is approximately 1,200 rubles, a preliminary cost of the development of the proposed SP will be 3,716,400 rubles.

V. RESULTS AND DISCUSSION

The main prospective users of the proposed SP: scientific centers, educational institutions, food industry enterprises manufacturing finished and semi-finished foodstuffs as well as other users whose task is to develop new FSFPs.

The SP performance specification has been developed to facilitate high-tech production of FSFPs. A preliminary cost of the SP development is 3,716,400 rubles.

VI. SUMMARY AND CONCLUSIONS

In conclusion it should be noticed that the development of the SP proposed in the paper will make it possible to rationalize and facilitate the development of new kinds of food products based on the specified indicators of a food and energy value, vitamins and minerals taking into account an effect of various kinds of cooking on these indicators.

In future this will allow effective computer modeling of the composition of food products, dishes and food articles with specified properties with regard for priority areas of science development in the field of high-tech FSFP production.

REFERENCES

- [1] The Protein Challenge 2040 [Electronic resource]. Access mode: <https://www.forumforthefuture.org/project/protein-challenge-2040/overview> (date of circulation: 15.04.2018).
- [2] The future of food: the investment case for a protein shake up, 2016 briefing [Electronic resource]. Access mode: <http://www.fairr.org/wp-content/uploads/FAIRR-and-ShareAction-Protein-Briefing-September-2016.pdf> (date of circulation: 15.04.2018).
- [3] Rozhdestvenskaya L.N., Bychkova E.S. Developing innovative product of high biological value for nutrition of athletes // Technology and the study of merchandise of innovative foodstuffs. 2013. Vol. 6 pp. 20-25. (in Russian).
- [4] Bychkova E.S., Rozhdestvenskaya L.N. Assessment of prospects of strategy of development of a product on the basis of creation of innovations // Technology and the study of merchandise of innovative foodstuffs. 2013. Vol. 5 pp. 108-113. (in Russian).
- [5] Dietary Guidelines Advisory Committee. Scientific Report of the 2015 Dietary Guidelines Advisory Committee (2015) [Electronic resource]. Access mode: <http://www.health.gov/dietaryguidelines/2015-scientific-report/PDFs/Scientific-Report-of-the-2015-Dietary-Guidelines-Advisory-Committee.pdf> (date of circulation: 15.04.2018).
- [6] Goals in Nutrition Science 2015–2020. [Electronic resource]. Access mode: <https://www.ncbi.nlm.nih.gov/pmc/articles/PMC4563164/> (date of circulation: 15.04.2018).
- [7] De Toro-Martin, J.; Arsenault, B.J.; Després, J.-P.; Vohl, M.-C. Precision Nutrition: A Review of Personalized Nutritional Approaches for the Prevention and Management of Metabolic Syndrome. *Nutrients*. 2017, 9, 913 [Electronic resource]. Access mode: <http://www.mdpi.com/2072-6643/9/8/913> (date of circulation: 15.04.2018).
- [8] Nutrigenomics and Personalized Diets: What Will They Mean for Food? [Electronic resource]. Access mode: <https://www.ncbi.nlm.nih.gov/pmc/articles/PMC4414021/> (date of circulation: 15.04.2018).
- [9] Rozhdestvenskaya L.N., Bychkova E.S. The substantiation of perspective directions of designing of products of a functional food // Food industry. 2012. Vol. 11 pp. 14-16. (in Russian).
- [10] Rozhdestvenskaya L.N., Bychkova E.S. Implementation of the strategy for the prevention of micronutrient deficiencies // News of higher educational institutions. Food technology. 2014. Vol. 2-3 pp. 82-85. (in Russian).
- [11] FoodTech and personalized nutrition – 1 – From marketing to genetics [Electronic resource]. Access mode: <http://parisinnovationreview.com/articles-en/foodtech-and-personalized-nutrition-from-marketing-to-genetics> (date of circulation: 15.04.2018).
- [12] Time to get personal? How to embrace digital technology in tomorrow's nutraceuticals [Electronic resource]. Access mode: <http://www.nutritioninsight.com/news/time-to-get-personal-how-to-embrace-digital-technology-in-tomorrows-nutraceuticals.html> (date of circulation: 15.04.2018).
- [13] Rozhdestvenskaya L.N., Rogova O.V. Comparative analysis of the functionality of systems of automation of business processes management of food industry enterprises // Modern Economy Success. 2017. Vol. 5 pp. 120-124. (in Russian).
- [14] Solutions for the industry: Planned food [Electronic resource]. Access mode: <https://solutions.1c.ru/plan-meal> (date of circulation: 15.04.2018).
- [15] Programs for the development of recipes [Electronic resource]. Access mode: <http://es-nsk.ru/programmi.html> (date of circulation: 15.04.2018).
- [16] Muratova EI, Tolstykh SG Design of confectionery recipes. – Tambov: Publishing House of the TSTU, 2010. – 32 p. (in Russian).
- [17] Borisenko AA, Sarycheva LA Modeling, development and optimization of products for healthy nutrition. – Stavropol: SevKaz GTU, 2012. – 197 p. (in Russian).
- [18] Muratova EI, Tolstykh SG, Dvoretzky SI, Zyuzina OV, Leonov DV Automated design of complex multi-component food products. –

- Tambov: Publishing house of FGBOU HPE "TSTU", 2011. – 80 p. (in Russian).
- [19] SL Gaptar, OV Ryavkin, ON Sorokoletov, VM Fomin, TI Dyachuk Designing products with predetermined properties. – Novosibirsk: Publishing House of NSAU, 2016. - 89 p. (in Russian).
- [20] Derkanosova NM, Zhuravlev AA, Sorokina IA Modeling and optimization of technological processes of food production: Textbook. – Voronezh: VGTA, 2011. - 195 p. (in Russian).
- [21] GOST 28806-90 The quality of software. Terms and Definitions. – M.: Publishing house of standards, 1992. 8с.(in Russian).
- [22] GOST 19.201-78 Unified system of program documentation. Technical task. Requirements for content and design. – M.: Publishing house of standards, 1990. 4 p.(in Russian).
- [23] 830-1998. IEEE Recommended Practice for Software Requirements Specifications [Electronic resource]. Access mode:<http://www.math.uaa.alaska.edu/~afkjm/cs401/IEEE830.pdf>(date of circulation: 15.04.2018).
- [24] ISO/IEC/ IEEE 29148-201 [Electronic resource]. Access mode: <http://mmf.nsu.ru/sites/default/files/iso-iec-ieee-29148-2011.pdf> (date of circulation: 15.04.2018).
- [25] GOST R ISO / IEC 9126-93. Information technology. Evaluation of software products. Characteristics of quality and guidelines for their application. – M.: Gosstandart of Russia, 2004. 13 pp.(in Russian).
- [26] OST 4.071.030. Creation of the system. Standards of labor intensity. Industry standard Automated enterprise management system. – M.: Publishing house of standards, 2001. 23 p.(in Russian).



Rozhdestvenskaya Lada Nikolaevna (b. 1971), PhD (Eng.), associate professor, head of the Department of Food Production Technology, Novosibirsk State Technical University. Her research interests are focused on food safety, food security, and traceability of food chains as well as on specialized and functional food. She is the author and co-author of 200 scientific papers. (Address: 20, K. Marx Prospekt, Novosibirsk, 630073, Russian Federation. Email: lada2006job@mail.ru).



Rogova Olga Valerieevna (b. 1986), PhD (Eng.), senior lecturer at the Department of Food Production Technology, Novosibirsk State Technical University. Her research interests include systems of automation of business process management at food industry enterprises. She is the author and co-author of 75 scientific papers. (Address: 20, K. Marx Prospekt, Novosibirsk, 630073, Russian Federation. Email: rogova@corp.nstu.ru).

Building a Quality System for an Electronic Component Base for High-Tech Industries

Ivan P. Rozhnov¹, Nadezhda T. Avramchikova¹, Galina Y. Belyakova²

¹Reshetnev Siberian State University of Science and Technology, Krasnoyarsk, Russia

²Siberian Federal University, Krasnoyarsk, Russia

Abstract – The main aspects of quality assurance for the electronic component base (ECB) installed in the flight samples of space vehicles are considered. It is shown that the homogeneity analysis of ECB batches is now becoming a vital task, especially for ECBs with a high level of integration. The economic justification for creating special batches as a way of centralizing the equipment of space vehicles on the principle of equal reliability is given.

Index Terms – Quality system, electronic component base, clustering algorithms, special batch.

I. INTRODUCTION

ENSURING successful operation and supporting and encouraging the activities of domestic high-tech enterprises for the purpose of modernizing the economy are among the main tasks of the state economic policy of Russia.

A number of sectors of the machine-building complex are commonly ascribed to high-tech and knowledge-intensive industries, including: the production of electronic computer facilities, the aviation and space-rocket industry, the production of industrial robots and means of complex industrial automation, as well as a number of subsectors of the radio-electronic industry (the production of different means of radio communication, radar-location and radio navigation, complex radio-electronic technology and instrument making).

In the rocket-manufacturing sector, equipping the spacecraft with highly-reliable electronic components is one of the main tasks [1]. First of all, it is necessary to avoid low-grade forged products not meeting requirements relating to reliability. In solving this task, it is necessary to purchase the electronic component base (ECB) from approved suppliers and also perform inspection tests, screening tests and the destructive physical analysis (DPA) of the ECB. The individual rejection of components is of particular importance [2].

The delivered ECB batches for the complete set of on-board equipment of the spacecraft (S) can be nonuniform, collected from several production batches of plates. So, for the chips (C) of quality category OS - one batch of plates is required, for VP up to 4 [3], for IS of the class V (S), one party of plates is required, and for Q (B) up to the 4 [4]. Therefore, the test data on the selection of ECB of categories of quality of VP and Q (B) need to be distributed to all the whole batch of components with the belief that the lot is produced from one party of plates or that the variation in the

parameters of crystal batches is small. This is connected to the fact that rather minor changes in production can lead to considerable changes in the characteristics of sensitivity, for example, to radiative effects.

II. PROBLEM DEFINITION

The uniformity analysis of batches of the purchased ECB is becoming a vital task, especially for ECBs with a high level of integration where fluctuations in the technological process can lead to mistakes in the evaluation test, and the size of a mistake will influence directly the operating term of the on-board equipment [5].

III. THEORETICAL ASPECTS OF THE QUALITY SYSTEM OF PRODUCTION IN HIGH-TECH INDUSTRIES

The key activities of space industry enterprises encompass the projection, development, production, purchase, test and sale of elements of spacecraft, including on-board systems, on-board devices, clusters, mechanisms, designs, radio products, materials, algorithms, software, documentation and files on their manufacture and operation.

According to the majority of theoretical approaches, the high technological effectiveness of goods, work and services is characterized by the fact that these processes are performed:

- by enterprises of knowledge-intensive branches of economy;
- using the latest processing equipment, technological processes and technologies;
- with the participation of highly-skilled, specially-trained personnel.

The spiralling cost of science and education in the structure of the production of goods is reflected in the concept of knowledge intensity of branches of the economy. Knowledge-intensive production is characterized by a number of features. First, it relates to unique, usually costly and technically complex products demanding expenditure on skilled scientific work. Secondly, it is characterized by unstable demand, more dynamic competitiveness and sensitivity to scientific and technological progress.

However, besides the concept of knowledge-intensive production, there is the concept of high-tech production. Some authors consider these concepts as synonyms, others refute these statements, and a third group support the idea of

them of them having common features. High-tech production is technically complex production involving complex technological processes. One feature of this complexity is that in high-tech industries, production is based not only on the results of applied scientific research, but also on fundamental scientific research.

Industries are divided into four groups depending on the degree to which they are knowledge-intensive: high, medium-to-high, medium-to-low and low technologies. Knowledge-intensive production includes the first two groups. Thus, it is possible to come to the conclusion that high-tech production is one of the components of knowledge-intensive production. The spheres of aerospace, computer and electronic communications and pharmaceuticals relate to high-tech production. Medium-to-high industries encompass scientific instrument manufacture, technologies connected to land and other transport, electrical equipment, engineering chemistries and also non-electrical inventory [6].

In the conditions of a market economy, competition between those involved in knowledge-intensive production escalates more and more, and buyers become more and more fastidious to the quality of this production. Therefore, the tendency directed to achieving the highest level of quality can be defined by the competitiveness of knowledge-intensive production. From this it follows that the inability of Russian producers in the knowledge-intensive sphere to compete in foreign markets with foreign producers signifies that Russian producers do not manage to adapt to the increasing requirements of consumers to the quality of knowledge-intensive production.

In order to improve the quality and competitiveness of knowledge-intensive production, various tools are used:

- improvement of methods of mass self-checking at all stages of the product life cycle;
- use of a coordinated system of predicting and scheduling for the necessary level of quality;
- multifold activation of human potential and carrying out the personnel policy adapted to the market conditions of management;
- modernization of the knowledge-intensive branches of the economy and support from the state.

Thus, the searching of ways to improve the level of quality of high-tech industries acts as an important problem, the solution to which will increase the ability of Russians engaged in knowledge-intensive production to enter competition in foreign market and is an indispensable condition for competitive production in the space industry.

IV. FEATURES OF THE USE OF ELECTRONIC COMPONENTS IN SPACECRAFT

Inhomogeneity of batches. In the space-rocket industry, the formation of the electronic component base is a defining factor in the on-board systems of the spacecraft (S). It is necessary to know how many homogeneous groups (clusters) comprise the ECB production batch. It is especially important for imported components of the quality level 'Industry' where there are no requirements for the uniformity of production, for the quality level 'Military' without a

guarantee of radiation resistance, and also for assessing the 'life cycle' (steady state life test).

If the considered set of components consists of several different groups, then to have a reasonable opinion it is necessary to carry out tests for each group, having revealed them in advance.

It is proposed to create selections for the quality assessment of ECBs using the following criteria:

- ECBs made of one crystal batch of plates - one selection;
- ECBs made not of one crystal batch of plates - determination of the number of homogeneous groups, the number of selections is equal to the number of groups.

The forming of selections has to be made from ECBs already having undergone POT and DPA as after these procedures the copies which do not meet the requirements of the equipment are eliminated, and the results of the assessment are not distorted by products with potential defects.

The clustering of ECBs is important from the point of view of ensuring reliability and, to a larger degree, radiation resistance. The ionizing radiation as a physical factor of a space environment in many respects determines the operating term of the spacecraft [7]. While assessing the radiation resistance of clusters of ECBs of the same production, it is necessary to be guided by the requirements of GOST PB 20.39.414.2.

The modern methods of cluster analysis offer a wide choice of means of identifying group parameters that are heterogeneous in their set. The most widespread among similar methods is the method to k- average (k-means) [8]. The algorithms realizing this method are algorithms of global optimization and depend on the choice of initial values (average parameters of the centres of groups – clusters). At the same time, the method of identification of various groups of products in parameters has to yield reproducible results. It is essential to increase the accuracy of the discriminatory analyses of algorithms and methods [5, 9, 10] which can become a basis of the automated system for the identification of various groups of products in parameters.

Special batches of electronic components. One of the most important stages of integrating the on-board equipment of a spacecraft is work with manufacturers. The main characteristics of quality and reliability are defined in the process of manufacture. In the course of equipping the spacecraft, it is necessary to buy ECBs of the highest quality existing in Russia, and then to perform serious work on the rejection of potentially unreliable components, so that all remaining components meet requirements. However, experience has shown that the batch production of manufacturers does not always meet the set standards, and as a result, the organization of work with manufacturers for the issue of special batches of ECBs for the space industry is of vital importance.

This special batch, therefore, has to be a prototype of components meeting the requirements for the quality of production of the space industry. The characteristics of the separate products in the special batch must differ from the products of the regular batches of ECBs of quality categories VP or OS. Furthermore, the characteristics of all sets of

products included in the special party must differ from the parameters of regular batches.

In order to compile the list of padding requirements for the ECB special batches, it is proposed to perform the comparative analysis of a sequence of tests according to the American standards [4] for chips and semiconductor devices [11] in the quality categories 'Space' (for space application) and 'Military' (for military application) and the requirements of Russian standards for quality categories VP, OS and OSD (GOST PB 20.39.411).

An important role in defining the concept of a special batch was played by the experience of international cooperation during the creation of the Sesat satellite with a 10-year operating term and a 12-year technical resource which successfully functions in orbit for more than 15 years. As a result of the performed comparative analysis of the sequence of tests, it became clear that the ECBs of quality categories 'Space' and 'Military' have two differences: the assessment of parameter drift and the monitoring of the existence of foreign particles in under-body space (PIND).

For this reason, when taking the decision to use special batches in additional tests, it is necessary to perform an assessment of parameter drift and of the monitoring of the existence of foreign particles in the under-body space. These tests are implemented in the technical test centre JSC ITTs-NPO PM as no manufacturer in Russia is able to modify the technological process according to these requirements. As a result, the special batch is a collaborative product of the manufacturer and JSC ITTs-NPO PM.

The choice of this organization is due to the fact that in Russia only JSC ITTs-NPO PM is systemically engaged in this work. It is necessary to acknowledge the experience of other organizations in attempts to use the idea of special batches as unsuccessful. At the present stage, 30 decisions directly related to the manufacture and delivery of special batches with various manufacturers have been issued. It should be noted that the idea of creating special batches began its implementation in 2002 and with some plants already exist some revisions of decisions which were specified and developed on the basis of accumulated experience.

V. CONCLUSION

The requirements of the space industry make the equipping of spacecraft with on-board electronic systems impossible without serious change to the technological process of ECB manufacture. The development of a separate technological process for the manufacture of an electronic component base for the space industry, demanding considerable investment, renders the small-scale supply of products unprofitable. Thus, the volume of ordered batches has to be greatest possible. This situation coincides with the idea of equipping all spacecraft with ECBs of an equally high level of quality according to the principle of equal reliability, providing quality of production by means of differentiation in the requirements for reliability of protection depending on the size of possible damage and the probability of its infliction.

The process of formation the requirements for implementing special batches and the corresponding regulating documentation in its current state, allows on-board systems in the space-rocket industry to be provided with quality ECBs, and the accumulated experience allows its range to be expanded.

The uniformity analysis of ECB batches is becoming a vital task, especially for ECBs with a high level of integration where fluctuations in the technological process can lead to critical mistakes in evaluation tests and in the physical characteristics of the ECB (radiation resistance). Thus, it is possible to draw a conclusion that upgrading the electronic component base in the space industry is a result of building centralized spacecraft equipment on the principle of equal reliability and the creation of special batches.

REFERENCES

- [1] Fedosov V.V. Issues of ensuring the operability of the electronic component base in spacecraft equipment. SibSAU. Krasnoyarsk. 2015
- [2] Luk'yanenko M.V., Churlyayeva N.P., Fedosov V.V. Reliability of electronic products in spacecraft equipment. SibSAU. Krasnoyarsk. 2016
- [3] OST V 11 0998-99. Microcircuits integrated. General specifications
- [4] MIL-PRF-38535 – Performance Specification: Integrated Circuits (Micricircuit) Manufacturing, General Specifications for. – 2007. – Department of Defence, United States of America
- [5] Orlov V.I., Stashkov D.V., Kazakovtsev L.A., Rozhnov I.P., Nasyrov I.R., Kazakovtseva O.B. Improved method of forming production batches of electronic components with special quality requirements // Modern high technologies, Vol. 1, 2018. - P. 37-42 (in Russian)
- [6] Proskurnin S.D. The role of high-tech products in the economic development of Russia // Basic research. Vol. 9, 2016. P. 404-410 (in Russian)
- [7] Danilin N., Belosludtsev S.. Problems of application of modern industrial electronic component base of foreign production in rocket and space technology // Modern electronics. Vol. 7. 2007. P. 8-12 (in Russian)
- [8] Arthur D., Vassilvitskii S. k-Means++: The Advantages of Careful Seeding//Proc. of the Eighteenth Annual ACM-SIAM Symp. on Discrete algorithms, ser. SODA '07. -2007, P.1027-1035
- [9] Kazakovtsev L.A., Stashkov D.V., Rozhnov I.P., Kazakovtseva O.B. Further Development of the Greedy Heuristic Method for Clustering Problems // Control Systems and Information Technology, Vol. 4(70), 2017. - P. 34-40 (in Russian)
- [10] Orlov V.I., Rozhnov I.P., Kazakovtseva O.B., Kazakovtsev L.A. Analysis of clustering algorithms and their ensembles for problem of detection of homogeneous production batches of electronic devices // Ekonomika i menedzhment system upravleniya, Vol. 4.4 (26), 2017. - P. 486-492 (in Russian)
- [11] MIL-PRF-19500 - General specification: Qualified manufacturers list of products qualified under performance specification semiconductor devices



Rozhnov Ivan Pavlovich

Graduated from the Krasnoyarsk State Academy of Precious Metals and Gold in 1995. Speciality: Enterprise Economics and Management

- 1996 – 2005 – civil servant in the administration of the Krasnoyarsk Territory
- 2005 – 2009 – civil servant at the Ministry of Economic Development and Trade of the Russian Federation
- 2009 – 2013 – branch director of insurance companies in the Krasnoyarsk Territory
- 2013 – 2017 – deputy director of Ashpyl
- 2017 - present - postgraduate, Reshetnev Siberian State University of Science and Technology

31 Krasnoyarsky Rabochy Avenue, 660037, Krasnoyarsk. Russia
e-mail: ris2005@mail.ru



Avramchikova Nadezhda Timofeevna

(Doctor of Economic Sciences)

Graduated from Saratov Economic Institute in 1971. Speciality: Economics and Accountancy in Industry

- 1971-1987 – civil servant at the Federal State Statistics Service for the Krasnoyarsk Territory
- 1987- 2004 – civil servant at the Ministry of Economics and Trade of the Krasnoyarsk Territory

- 2004 - present – professor at the Department of Finance and Credit, Reshetnev Siberian State University of Science and Technology
31 Krasnoyarsky Rabochy Avenue, 660037, Krasnoyarsk. Russia
e-mail: avr-777@yandex.ru



Belyakova Galina Yakovlevna

(Doctor of Economic Sciences)

Graduated from:

1. Leningrad Technological Institute for the Pulp and Paper Industry in 1967. Speciality: Economics and Organisation of the Wood-processing and Pulp-and-paper Industry.
2. Siberian Technological Institute in 1972. Speciality: Machinery and Apparatus in the Pulp-and-paper Industry.

- until 2003 – head of the Department of Management, Siberian Technological University
- 2003-2012 - head of the Department of International Business, Reshetnev Siberian State Aerospace University
- 2012 - present – professor at the Department of Economics and Management, Siberian Federal University
79 Svobodny Avenue, 660041, Krasnoyarsk. Russia
e-mail: belyakova.gya@mail.ru

Return on Investment Study for the Project of Energy-Saving Devices Implementation

Nataliya V. Rozumnaya, Andrei D. Egorov, Alena Y. Tutrina
Novosibirsk State Technical University, Novosibirsk, Russia

Abstract – The article consider features of enterprises investment activity in high-tech industries and research results of energy saving problem in Russia and in the world. Authors had analyzed world energy market. The actuality of investment project aims to realize energy saving on enterprise is proved. The authors consider potential methods of technical realization of investment project and propose new version of engineering solution on the basis of reactor power compensator implementation. Technic and economic basis of investment project implementation of filter compensating devices is made for “Greenhouse complex “Novosibirskiy””.

Index Terms – Investments, energy saving, efficiency, reactive power compensator.

I. INTRODUCTION

ONE OF the most significant development aspects of Russian producers in high-tech fields is their investment activity. The reasons of investments necessary are the huge expense to the research-and-development, modernization of material and technical base, buildup etc. Effective companies' activity in development and implementation of innovations and increase of its competitiveness are determined by its investment activity level.

In foreign and domestic research studies of : Alexander G., Bailey J., O.Ph. Bystrov, I.V. Grishina, Galbraith J.K. Keynes, J.M., Lipsits I., V.V. Litvinova, I.I. Roizman, Sharpe W., A.Shahnazarova investments are considering as factor of stable economic growth.. [1]-[8]

On J.M. Keynes's point of view [9], state regulation effectiveness of economic processes relies on finding the resources for state investment, total employment and drop and fixing rate of interest.

In “The Theory of Economic Development: An Inquiry into Profits, Capital, Credit, Interest, and the Business Cycle” Schumpeter emphasizes that “the credit let to refuse to initial capital accumulation and relieve access for innovators to the market for realization their ideas in practice”. [7]

The correlation between public development and investment activity shows completely in the scientific studies of Shahnazarov, Grishina, Roizman. The author's in their research results came to the conclusion that region investment activity and public development has a cause and effect relation: the first is the result attribute and second is the generalized factorial attribute. [8] Research results are proved by regression model.

Last decades in Russia makes more effects for creation of favorable investment climate. Most part of statistical data [10] confirm the activation of investment activity. The

capital investments in Russian federation are presented in the Fig. 1.

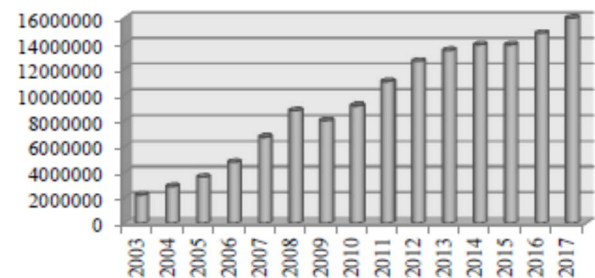


Fig. 1. Capital investment in Russian Federation, million rubles (table is based on the Rosstat data).

The main goal is the favorable economic condition for high-tech industry enterprises by regulation its amortization, financing and lending and tax policy and state support of investment activity. Various regulation investment market conceptions can be implemented as real and foreseeable economy condition requires. The main idea is the necessary of balance support between strategic goal achievement and normal parameters of current economic situation. Dimension and structure of capital investment is the significant parameter for development evaluation of domestic enterprises (table is based on the Rosstat data), Tab. I.

TABLE I
CAPITAL INVESTMENT IN KINDS OF BASIC ASSETS,
BILLIONS RUBLES [10]

| | 2010 | 2011 | 2012 | 2013 | 2014 | 2015 | 2016 |
|--------------------------------|-------|--------|--------|--------|--------|--------|--------|
| Capital investment Total | 91521 | 110357 | 125861 | 134502 | 139026 | 138972 | 146398 |
| a.o. housings | 11117 | 13956 | 15337 | 16815 | 20144 | 21728 | 22543 |
| buildings and constructions | 39628 | 47768 | 55602 | 55827 | 56653 | 50691 | 56181 |
| machines, equipment, transport | 34727 | 41856 | 47316 | 52128 | 50520 | 43751 | 44807 |
| other | 6049 | 5777 | 7606 | 9732 | 11709 | 12802 | 12867 |

Though, in absolute terms the aggregate investment volume has not satisfied requirements of Russian economic. At present basic factors that inhibit of investment activity are following:

- administrative hurdles for entrepreneurs
- insufficient legal defense of domestic investors

- high lending rate in spite of rates decrease at financial market
- lack of effective mechanisms of transformation personal savings in investments
- weak development of stock market
- high state economic position dependence on external market trends on current GDP structure.

Domestic investors consider change risks in political sphere as serious problem.

Federal service of state statistics [10] share of high-tech production in import is more 63% in 2017 and in export is 14,5%. However, need to notice that share of high-tech production in export has positive dynamic from 10% in 2010 to 14,5% in 2016.

Effective usage of investment resources in high-tech industries one of the main factors that has been defining the economic growth in the country in long-term perspective. This theme is more important for power industry so far as power saving problem is actual in all countries.

Studies of domestic researchers as A.A. Averchenkova, T. Yu. Anisimova, S.N. Bobyleva, E.E. Merker, S.V. Solovyeva, L.M. Simonova, A.S. Holodina are devoted to energy development and energy efficiency. [11]-[15] Problems of energy efficiency increase in the world are considered in the studies a lot of foreign authors as M. Bazilian, N. Jollands, E. Gacs, T. Graaf, S. Nakhooda, S.B. Pasquier. [16]-[17] Foreign countries have experience in energy efficiency increase in such foreground directions as interindustry police; transport; housing sector; communal services; business. [18]

Main feature of power saving problem solution in foreign countries is not only the initiation of laws but realization practical-oriented programs. Elaboration and implementation of specific projects can provide appreciable result.

II. PROBLEM DEFINITION

World energy market analysis demonstrates regular growth as prices and volume of sales on manufactories. Consumption of energy resources characterized by its irrational usage. A lot of researchers notice that, apparently, if mankind continues this way we will completely out of energy resources stores in nearest fifty years.

Unforeseen circumstances of failure of electrical power industry can be caused by unequal proportion on the world market as because of the demand and supply on these services. Energy economy of Russia and in the whole world aims to energy loss saving.

Electric energy consumption data per employed worker in Russia manufacture are showed in Tab. II from 2012 till 2016. These data are borrowed from the Federal statistic committee. [10]

Data from Tab. II show the growth of the energy consumption, especially, in industrial regions. Energy loss saving damage reaches from 5 to 10 million dollars a year. Nowadays contemporary enterprises use a huge amount of electrical energy and do not undertake something to improve or decrease its costs. We had analyzed statistical data and can conclude that Russia concedes effectiveness of electrical

energy usage to Japanese in six times, USA in two times and Germany in one or two times. [19]

TABLE II
ENERGY CONSUMPTION PER ONE EMPLOYED IN RUSSIA'S
MANUFACTURING

| Energy consumption per one employed in Russia's manufacturing, kilowatt hours | 2012 | 2013 | 2014 | 2015 | 2016 |
|---|--------|--------|--------|--------|--------|
| Russian Federation | 67448 | 69249 | 68498 | 69697 | 71335 |
| Central Federal District | 40292 | 42410 | 43004 | 42569 | 43079 |
| Northwestern Federal District | 67319 | 67439 | 66850 | 69738 | 72579 |
| Southern Federal District | 43418 | 42299 | 45343 | 40562 | 40916 |
| North Caucasian Federal District | 35798 | 36692 | 34391 | 33489 | 38069 |
| Privolzhsky Federal District | 47366 | 48367 | 47733 | 49166 | 51378 |
| Ural Federal District | 110402 | 114756 | 115817 | 117016 | 117186 |
| Siberian Federal District | 137170 | 135767 | 132168 | 139319 | 139857 |
| Far Eastern Federal District | 43069 | 53090 | 47853 | 50969 | 53862 |

According to domestic and foreign specialists power inputs share at enterprises has 30-40% in the production value. Thus, managers need to analyze and audit the energy consumption of its manufactures and also elaborate tools and compensator methods of reactive power. To cope with this task, the world market needs such product as reactive power compensator. This tool carries out functions of increase electrical power factor; reduce peak of electric power consumption; increase energy quality; give the guarantee of equipment long-term service; cut down power costs on 20-30%. [20]

Therefore, the energy market grows and compensator is an innovative prize for solution of energy loss saving problem. As we knew, compensator setting have not only technical advantages in use on enterprises but economic benefit. The problem of ineffective energy distribution goes to compensatory setting on every enterprise. Market trend shows the increase in demand on electric power. It will be profitably for reactive power compensator.

The goal of the article is the development and economic justification of investment project for implementation of energy-saving systems on the enterprise.

III. THEORY

The important task is to reduce nonlinear loads on supply network and improvement of electric power quality on enterprise. The implementation of multifunctional devices which provide the minimization of high-harmonic volume and compensation of reactive power is a complex decision. One of such devices is a power corection device with harmonic filtering. Power corection device with harmonic filtering can be used as rejection filter for linear and nonlinear loads separation or shunting of harmonics current.

Consider expedience advisability of power corection device with harmonic filtering implementation of different kinds. There are tee and gamma-type of low-pass filter. Therefore, specialists calculated that for effective decrease of harmonics current levels in the net and with such schemes are necessary to establish installed capacity CB that close to the feed transformer power. [21]

With connection in parallel LC-chains are calibrated to the frequency of single-harmonic realizes chain power correction device with harmonic filtering. Deficit of reactive power on substation bus can be covered completely by power correction device with harmonic filtering and established power of a capacitor uses on 80-90 %. We can conclude that power correction device with harmonic filtering most economical and simple filters. Simplified schemes are showed on Fig. 2.

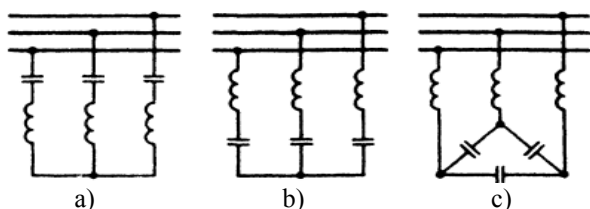


Fig. 2. Simplified scheme of power correction devices with harmonic filtering.

The most widespread scheme in Fig. 2, b.

BK have technical conditions on exploitation which provide the voltage overloading and current limiting over rating value. The capacitor type determines these conditions. Usually the voltage should be no more 10% and current should be no more 30% from rating value. Sometimes capacitors should have additional requirement which restrict its power to rating value in operating mode.

Central compensation of higher harmonics by nonsinusoidal mode in some cases can be economically attractive. The idea of centralized filtration of higher harmonics is the compact allocation on the one of the distribution substations which provide the decrease of nonsinusoidality to legitimate value in all network nodes.

Centralized correction of nonsinusoidal mode of distributing network is the most effective for current network with stable configuration and loads. In the networks 110 kw and over such approach cannot be effective because of the probabilistic nature of its amplitude versus frequency plot.

Usage of power correction device with harmonic filtering of average and low power had been defined exclusive standards to accuracy of adjustment for prevention of detached harmonic intensification in chain, correction device with harmonic filtering overload and other debilitating effects.

Increase of specific weight of nonlinear loads which have small capacity coefficient came to necessary to implement power correction device with harmonic filtering with sufficiently high power capacity. It allows to reduce requirements for power correction device with harmonic filtering accuracy of adjustment.

According to this approach, the necessary to establish a huge amount of power correction device with harmonic filtering goes out while it is enough to establish one power

correction device with harmonic filtering with certain frequency tuning. This frequency finds by solution of differential equation.

To compensate a lot number of power correction device with harmonic filtering have been using bridging connection series of power correction device with harmonic filtering. But in this case the number of reactors varieties increases, its modernization and interchangeability impedes. These shortcomings can be made up partly for complicated combined filters (two and four-frequency filters) with the same interchangeable groups of reactors.

Thus, today the usage of power correction device with harmonic filtering is one of the common way of levels high harmonics decrease. It let to solve the problem partly or completely which is related to reactive power compensation.

There is a widespread view abroad that power correction device with harmonic filtering is more cost effective decision than increase of converters pulse number [21]. Power correction devices with harmonic filtering are incorporated in fast-acting statistic compensatory devices are made for compensation of reactive power and decrease of voltage and levels of high harmonics fluctuation.

The scheme of reactive power compensator is showed in Fig. 3.

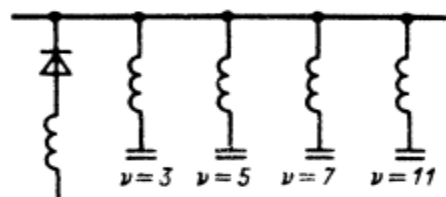


Fig. 3. The scheme of reactive power compensator.

Power correction devices with harmonic filtering are using in enterprises have capacitors with a large unit power. The nominal voltage conforms to it. When voltage over 15 kw it uses serial switching of capacitors with a lower rated voltage [21].

At some enterprises of the paper and pulp industry uses power correction devices with harmonic filtering that consist of a regulated reactor and an unregulated CB. The switching of the universal regulated reactor covers required current range.

But how it was early noted, when it is necessary to install several power correction devices with harmonic filtering, its cost and dimensions increase. That all leads to increase in cost of operations to reduce the values of higher harmonics and to reactive power compensation.

There are significant overloads of power correction devices with harmonic filtering and its damages in cases where it is impossible to exclude the appearance of high harmonics of lower order than the frequency of power correction devices with harmonic filtering. It occurs in electric-arc steel furnace chains [21]. Usage of c is ineffective in chains with a complicated character of currents and voltages amplitude spectrum that have significant levels of interharmonics.

Thus, there were intensive search for solutions which have a result that allow to avoid previously mentioned

disadvantages. To use active and hybrid filters is the most effective solution.

IV. EXPERIMENTAL RESULTS

From 4th of April 2017 till 5th of April 2107 at the industry enterprise "Greenhouse complex "Novosibirskiy"" were made measure of parameters of electricity networks quality. That was measured through professional analyzer of electricity quality Hioki PW 3198 with production serial number 140337762 and usage of clamp meter 5000A «Hioki-9669» with production serial number 140326024, 140326025, 140326026 and 140326017.

The purpose of the measurements was to determine the conformity parameters of the electrical network and its conformity with the requirements of GOST 32144-2013, for further calculation of the electrical and functional parameters of the filter compensate devices.

The measurements were carried out at three control points - transformer substation -10, transformer substation -11, energised from urban electric networks and energizing area No. 10, and central switchboard-2, energised from the reciprocating (engine) gas generator installation and energize areas No. 1 and No. 2. The choice of this control points was due to the fact that from this were energised areas where problems with the work of the "supplementary lighting" system occurred.

During the measurements, the load was about 50% from the nominal load. The system of electrical "supplementary lighting" works during with shortage of sunlight. The operating mode of the "supplementary lighting" system depends on external factors, such as the weather and the duration of daylight hours.

The system of "supplementary lightening" on the area number 1 consists of luminaires, which are grouped into groups of 20-24 luminaires per group. Each group is controlled by control switchboard. In this sector there are 20 control switchboard, which are energised from 10 cells that are connected to the common input of two parallel-operating reciprocating (engine) gas generator.

The main problem in this area was that switching on the lamps one by one in the section No. 1 and the reaching the total power of the switched luminaires in the order 600-700 kw new luminaires stopped to switch on, and then all previously switched on luminaires go out.

The first area works stably only with area number 2, which is also energized from reciprocating (engine) gas generator. Stable operation without disconnection of the first area is possible with parallel operation of the second area at the power from 300 kw. At the second area, single-phase luminaires of 64-600-001 natrium pendant lighting fixture for industrial premises with a power of 600 Watt are installed. According to the scheme in the second area, lamps with a total power of 930 kw.

Specific of this system of "supplementary lighting" of the area number 10, energised from two transformer substations transformer substation -10 and transformer substation -11 with transformers of 1250 kVA, is that each next group of luminaires must switch on with a time delay no more one

minute from the previous one. The delay depends on the luminaires starting current and its other characteristics and network requirements.

Results of the measurements showed that the voltage at the enterprise does not exceed the limit values. The maximum voltage waveform distortion factor was fixed on the reciprocating (engine) gas generator THDU = 21.73%. The The maximum voltage waveform distortion factor was THDI = 33.15% while the measurements at transformer substation -10. In general, during measurements at all three points, was revealed the excess of the permissible parameters of the voltage harmonic component in accordance with GOST 32144-2013, as well as high values of the current harmonic component.

Transformer substation -10 and transformer substation -11 are not equipped with compensators. At these points, during the measurements was fixed the power factor $\cos(\varphi) = 0.94$. It is recommended to implement filter compensating systems to improve the quality of electricity.

This solution will provide the necessary compensation of reactive power and reduce the distortion of the voltage curve, which will reduce losses, and increase the stability of the electrical network.

The implementation of installations promotes to reduce the load on the transformer and power cables, increase the voltage in the system on 1-5%, depending on the number of included stages (thereby, voltage equalization that depends on the existing load occurs.). Also, the cost of active energy will be reduced.

The problem of luminaires operating on area number 1 is the design features as the existence of an internal 6-pulse rectifier. It means that it is a source of higher harmonics in the network. If total network load increases, it will lead to increase in the power of harmonic distortion and activation the internal protection of the luminaires and its switching off. Propose to install filter compensating device to decide this problem. The cost of such equipment is shown in Tab. III.

TABLE III
COST OF EQUIPMENT, RUB.

| Title | Delta | | Star | |
|-------|------------|---------|------------|---------|
| | Condensate | Reactor | Condensate | Reactor |
| TS-10 | 69806 | 42112 | 123574 | 80288 |
| TS-11 | 41360 | 18080 | 53240 | 24096 |
| CS-2 | 34320 | 24096 | 44880 | 31712 |

From the Tab. III the better choice as mostly economically attractive is a delta scheme for transformer substation -10 because the cost difference of equipment has a significant value.

Evidently, it is economically attractive to install the power correction devices with harmonic filtering on the transformer substation -11 in the delta scheme. So far as cost difference of equipment is not so significant it will be better to use star-scheme because of its reactivity worth.

TABLE IV
PROVIDING POWER IN NETWORK POWER CORRECTION
DEVICES WITH HARMONIC FILTERING, BY VARIOUS
CONNECTIONS CB, REACTIVE VOLT-AMPERE

| | Delta | Star |
|-------|--------|--------|
| TS-10 | 218,79 | 431,04 |
| TS-11 | 67,48 | 117,4 |
| CS -2 | 114,6 | 162,24 |

Technically speaking, the installation of power correction devices with harmonic filtering on CS-2 is impossible because the power in the chain will be over but the overcompensation is impossible. On this area, apparently, to replace "supplementary lighting" system on more accomplished is economically attractive.

By power correction devices with harmonic filtering will occur reactive power compensation. As a result of this process the full capacity flows will decrease. This will reduce power losses.

Since the system of "supplementary illumination" includes only in the case of sunlight deficit, it is necessary to determine the period of its operation.

In Novosibirsk, the average light hours per year last 12 hours, from 08:00 to 20:00. As a result, suppose that the system of "supplementary illumination" will be turned on fully, so the entire nominal power of the system will be used.

The energised power was determined by the area No. 10 from transformer substation -10 as a result. The results are summarized in Tab. V.

TABLE V
POWER VALUES ARE CONSUMED FROM TS-10

| | P, kw | Q, reactive volt-ampere | S, amp. kilovolt ampere |
|---------|-------|----------------------------|-------------------------------|
| Maximum | 832 | 296 | 882 |
| Minimum | 818 | 284 | 866 |
| Average | 823.7 | 288.74 | 872.92 |

The energy losses occur by reduce of reactive power level in the chain. Thus, the economic efficiency that can be gotten by reduce of reactive power level might be count of the basis costs on energy losses.

TABLE VI
LOSS OF ENERGY FOR THE YEAR BEFORE AND AFTER
INSTALLATION POWER CORRECTION DEVICES WITH
HARMONIC FILTERING

| Loss of energy for the year before and after installation of power correction devices with harmonic filtering, kW*h | ΔW_{before} | ΔW_{after} | ΔW_{saved} |
|---|---------------------|--------------------|--------------------|
| | 184000 | 164744 | 19256 |
| Loss of energy for the year before and after installation of power correction devices with harmonic filtering, rub. | before | after | Saved energy |
| | 441600 | 395385 | 46214 |

Calculation results showed the star-scheme and its equipment is economically attractive.

Outside organization costs had to be considered. This organization will make a necessary measurement and

payment settlement and provide recommendations for solution of this problem. All of the above labors cost 50 000 rub.

Also it is necessary to take into account that delivery cost of the equipment and its setup calculates as 10% from its cost.

Thus, capital investments on transformer substation -10 are 173110 rub. and on transformer substation -11 – 135070 rub.

TABLE VII
EFFICIENCY ECONOMIC INDICATORS OF IMPLEMENTED
EQUIPMENT

| | NPV, rub. | IRR, decimal fraction | DPP, years | PI, decimal fraction |
|-------|-----------|--------------------------|------------|----------------------------|
| TS-10 | 58375 | 0,37 | 0,75 | 1,34 |
| TS-11 | 27696 | 0,3 | 0,84 | 1,21 |

Had analyzed the Tab. VII, we can conclude that project profitability is 34% and 21%. Project payback period till 10 months. This equipment economically feasible to implement.

As said above, the setup if this equipment will give some positive aspects which are difficult to express in number. For instance, if the conditions of other equipment service become better energy accounting meter will operate with high accuracy and power supply reliability will increase.

V. DISCUSSION OF RESULTS

We put for discussion the results of economic bases for investment project of equipment energy loss saving implementation. It is important to know the researchers point of view concerning various directions for solution energy saving problems in the world.

The actual theme of favorable investment climate development in Russia was considered in this article. This theme requires new scientific approaches for solution in contemporary conditions of world policy.

The problems had been considered in the article concerning increase the share of high-tech production in Russia. The modern situation in high-tech industries with Rosstat statistic showed in the Table VIII.

TABLE VIII
PRODUCTION INDEX IN HIGH-TECH
PROCESS KINDS OF ECONOMIC ACTIVITY IN RUSSIA

| Production index in high-tech process kinds of economic activity in Russia in % at previous year | 2012 | 2013 | 2014 | 2015 | 2016 |
|--|-------|-------|-------|-------|------|
| | 113,1 | 109,3 | 117,4 | 100,7 | 96,8 |

The analysis of Table VIII shows the decrease of indexes in 2015-2016. Thus, the economic growth and strong position Russia in the world are possible on the conditions of high-tech industries development. Future of our country depends on these indexes in decades.

VI. CONCLUSIONS

Proposed investment project for greenhouse complex is actual in the conditions of modern energy loss saving problem. The engineering solution is a choice of equipment for transformer substation -10 delta-scheme, for transformer substation -11 – star-scheme. The implementation of this investment project is economically attractive. The “Greenhouse complex “Novosibirskiy”” is recommended to continue investment activity for technological process improvement. It recommends to move agro-industrial complex and enterprises of other industries where energy losses are great in this direction.

It is significant to notice the importance of state policy that should promotes to realization of energy saving projects and create favorable conditions for investment activity in the country.

REFERENCES

- [1] Sharpe W., Alexander G., Bailey J. Investments. M.: INFRA-M. – 2001. – 1028 p.
- [2] Bystrov O.Ph. Investment activity administration in regions of Russian Federation: Monograph / O.Ph. Bystrov, V.Ya. Pozgnyakov. - M.: INFRA-M, 2012. – 358 p. (in Russian)
- [3] Galbraith J.K. Economics and The Public Purpose. M.: Progress. – 1976. – 406 p.
- [4] Keynes J. Tract of Monetary Reform. London. Macmillan, 1924. – 209 p.
- [5] Lipsits I.V., Kossov V.V. Economic analysis of real investments. M.: «Economist». – 2007. – P.345 (in Russian)
- [6] Litvinova V.V. Investment attraction and investment climate in region: monograph. M.: Financial university, 2013. – 116 p. (in Russian)
- [7] Schumpeter J. The Theory of Economic Development. M.: Progress. – 1982. – P. 159. (in Russian)
- [8] Shahnazarov A.G., Grishina I.V., Roizman I.I. National investment support system on the regional level / A.G. Shahnazarov, I.V. Grishina, I.I. Roizman // Investments in Russia. - 2012. - №12. - P. 6-7 (in Russian)
- [9] Keynes J.M. Selected works. M.: Economics, 1993. – 543 p.
- [10] Official site of Federal state statistics service. - [Electronic resource]. – Access mode: <http://www.gks.ru>
- [11] Energy efficiency and sustained development / Bobylev S.N., Averchenkov A.A., Soloveva S.V., Kirushin P.A. / Under edition. S.N. Bobylev. – M: TsEPiK, 2010. – 148 p. (in Russian)
- [12] Anisimova T.Yu. The method of conducting energo-economic analysis of enterprise activity in the system of energetic management. Economic analysis: theory and practice, 2014.- N2(353), P.37-44. (in Russian)
- [13] Kiryushin P.A. Ecologico-economical evaluation of reducing energy intensity in Russia // *Bulletin of the Chuvash University*. – 2011. – №1. – P. 338-391. (in Russian)
- [14] Merker, E. E. Energy saving in manufacturing and exergetic analysis of technological process. Study book / E.E. Merker. - M.: TNT, 2014. - 316 p. (in Russian)
- [15] Holodionova A.S., Simonova L.M. Evaluation program efficiency of energy-saving actions at oil and gas production enterprise // *Tyumen State University Herald. Social, Economic, and Law Research* – 2014. - №11. – P. 135-141 (in Russian)
- [16] Bazilian, M., Nakhooda, S., & Graaf, T. (2014). Energy governance and poverty. *Energy Research and Social Science*, 1(2014), 217–225.
- [17] Jollands N., GacsE., Pasquier S. B. Innovations in multi-level governance for energy / N.Jollands, E.Gacs, S.B. Pasquier // [Electronic resource] / International Energy Agency. – 2009. – Access mode – URL: https://iea.org/publications/freepublications/publication/mlg_fina_web.pdf
- [18] Energy efficiency governance [Electronic resource] // International Energy Agency.– Access mode – URL: http://iea.org/publications/freepublications/publication/gov_handbook.pdf (Accessed data 19.03.2018)
- [19] Kabyshev A.V. reactive power compensation in electrical installation of industrial enterprises: study book / A.V. Kabyshev. Томск: Publishing house Tomsk polytechnic university, 2012. – 234 p. (in Russian)
- [20] Kochkin V.I. Implementation of reactive power compensator in networks of energy system and enterprises / V.I. Kochkin, O.P. Nechaev. M.: Publishing house SC ENAS, 2002. – 248 p. (in Russian)
- [21] Zhezhenlenko I.V. Higher harmonics in electrical generating systems of industrial enterprises. – 4-e ed., rewritten and completed ed.. – M.: Energoatomizdat. 2000. – 331 p. (in Russian)



Rozumnaya Natalia Vyacheslavovna. Candidate of Science (PhD) in Economics, Associate Professor of Marketing and Service Department Novosibirsk State Technical University. Research interests are mergers and acquisitions, investment analysis, market research, statistics. More than 80 papers and manuals have been published.



Egorov, Andrey Dmitrievich. Bachelor of Energy. The master's degree in 1 year of study at Novosibirsk state technical University. Research interests are energy saving problems, evaluation of the effectiveness of investment projects.



Tyutrina Alena Yurevna. Bachelor of Sociology. The master's degree of marketing will be obtained at the Novosibirsk State Technical University in 2019. Scientific interests are marketing and sociological research, consumer behavior, internet marketing, advertising and PR.

The Application of Modified RFM-analysis to Increase the Loyalty of Consumers of Industrial Rubber Articles

Vladislav Yu. Shchekoldin, Marina Ye. Tsoy
Novosibirsk State Technical University, Novosibirsk, Russia

Abstract – In the paper the trends in the Novosibirsk market of industrial rubber articles were analyzed, the key problems of the industry were revealed. The groups of customers with homogeneous behavior were identified by a modified RFM-analysis applied to client database of the company engaged in the producing and sale of industrial rubber articles. The structure of each group was studied. Loyalty programs to meet in most effective ways the needs of the customers from the selected groups have been developed.

Index Terms – Market of industrial rubber articles, consumer loyalty, modified RFM-analysis.

I. INTRODUCTION

THE RUSSIAN market of industrial rubber articles in last few years is characterized by rather contradictory trends. On the one hand it is experiencing a very obvious and definite decline, on the other hand it could be noted that a number of domestic companies managed to increase sales of some types of products. This could be explained by the fact that the market processes are affected by both the decrease in demand for key consumer industries and their transition to cheaper substitute goods, and the ruble's devaluation, which allowed domestic companies to compete with foreign producers.

According to experts [1] the capacity of the Russian industrial rubber articles market in 2016 was more than 240 thousand tons of products sold for more than 80 billion rubles taking into account the import component and prices of Russian producers. The highly demanded products on the market of industrial rubber articles are industrial hoses, accounting for approximately 16% of all sales on the market, which corresponds to 12% of the turnover for this type of product. Next place is occupied by fabric and conveyor belts (13% and 7% respectively), as well as drilling and high pressure hoses, whose market share in tonnage is approximately 14%, which is 6% of the turnover in money terms.

It should be noted that the market of industrial rubber articles in Russia is represented by domestic and foreign manufacturers in ratio 3:2 approximately (58% and 42% in 2017) [1]. Among foreign companies there are so-called “white” and “yellow” (Asian) producers. The first of them (European manufacturers, the USA, Japan, etc.) are the most competitive in quality, but their products are more expensive than domestic ones. Asian producers (first of all, China, India,

etc.) are competitive in price, but their products often have a lower quality than other companies suggest to the market.

Among the key problems of the Russian rubber articles industry the specialists outline the following: aging of technologies and equipment and a high degree of depreciation of fixed assets (52% experts are mentioned about it), stagnation in the economy and a drop in final demand (33%), high costs and low availability of sufficient financing (6%); strengthening the influence of substitute goods (6%) [1]. It is noteworthy that among the main issues of the industry the experts did not identify the problem of insufficient client-oriented strategies of enterprises in the industrial rubber articles sector, which means that enterprises are not really interested in their customers' needs, only hoping that the goods produced by them will be acquired by somebody. Obviously such a situation does not lead to expand the market shares and increase the competitiveness of companies in general.

One of the most effective ways of attracting and retaining clients is the development and implementation of loyalty programs [2], allowing to take into account the historical features of consumers behavior and predict their future actions.

II. PROBLEM STATEMENT

When one wants to analyze the history of consumer behavior he/she could address to RFM-analysis and its various modifications, which have been developed by domestic and foreign scientists, and successfully applied in practice through last three decades. The standard approach of RFM-analysis [3] assumes that the customers are classified into five equal groups by three factors – the remoteness (R) of the last purchase for the concrete period of time, the frequency (F) of purchases for this time period, and the amount of money (M) spent by the customer for the time period.

Unfortunately the standard approach is not out of practical drawbacks. In particular there is a probability of “accidental” referring the client to the group of consumers that is not appropriate to describe his/her behavior. Such a situation could lead to inefficiency in both marketing strategy of the whole company, and marketing activities developed by the company for this certain group of customers [4].

To overcome these problems RFM-analysis technique can be improved on the basis of MRFM-approach (first “ M ” means “modified”), proposed and tested by authors in [5]. The MRFM-analysis assumes the application of cumulative

curves approach [6] using the cluster analysis to identify homogeneous groups of consumers, for each of which the development of corresponding loyalty programs is occurred [7].

III. MRFM-ANALYSIS IN PRACTICE

The MRFM-analysis method was applied to study the clients of a manufacturing company operating on the Novosibirsk market of industrial rubber articles. This company has been operating for almost 20 years, it is engaged in the production and wholesale of rubber and asbestos products. The company is the official dealer of Rubex Group – one of the largest manufacturers of industrial rubber articles in Russia, and also the official dealer of the Kursk Plant of Rubber Machinery.

The assortment of manufactured products consists of conveyor belts, flat and accessory driving belts, sleeves, rubber covers, technical plates, etc. In general the market appears to be very rich, since it employs both local manufacturers and branches of domestic and foreign companies located in various regions of the Russian Federation from Moscow region to Far East. At the same time the main competitors are domestic producers (66% of the Novosibirsk market), companies from China (26%), Germany and other European countries (8%).

The presence of various manufacturers in the market leads to a serious variety in quality and price of the products that affects customer satisfaction. As a rule, consumers of industrial rubber articles are manufacturing companies associated with different branches of industry, as well as wholesale and retail trading companies. Therefore the company faces the task of bringing business to the consumers by studying its behavior.

To analyze company's client base the authors used data on purchases made by 951 clients through ten months of 2016-2017. Due to the peculiarities of maintaining the database it was unloaded discretely with a period of 30 days. The analysis allowed distinguishing seven segments of customers:

- “loyal customers”: 6 or more deals in the last 90 days;
- “perspective customers”: 2-5 deals for the last 60 days;
- “newbies”: only one transaction for the last 30 days;
- “suspended customers”: 1-5 deals in the period 31-150 days;
- “sleeping customers”: 1-5 transactions in more than 150 days;
- “customers of the risk zone”: 6 or more transactions in 91-180 days;
- “lost customers”: 6 or more transactions in a period of more than half a year.

The client's distribution by groups and segments is presented in Table I. For the convenience of perceiving the results, the customers in the same segment are singled out in the same tone. In addition to the client's number in each segment, the amount of money spent by them during the purchase was determined. As it follows from Table I the largest share of the company's sales (83%) is accounted for by loyal and prospective customers, who make up 37% of the client base, and most often purchase the company's products.

The analysis of the client's quantities was supplemented by studying the budgets of their transactions. To do this the original database was sorted by increasing values of M -indicator, and groups of consumers coded from 1 to 5 were identified. The customer grades by codes were as follows: $M = 1$ – customers with a transaction budget of up to 10,000 rubles; $M = 2$ – customers with a budgets from 10,000 to 100, 000 rubles; $M = 3$ – customers with a budgets from 100,000 to 500,000 rubles; $M = 4$ – customers with a budgets from 500,000 to 1 million rubles; $M = 5$ – clients with the budgets over 1 million rubles.

After determining which groups the clients are in, it could be traced the amount of money they spent (Tab. II). The largest number of customers falls into categories 1 and 2 in terms of M (32% and 43% respectively). The most often they are “sleeping” and “suspended” customers (44% and 24% respectively), which confirms the necessity in developing the targeted programs to maintain their loyalty. The number of companies whose transaction budget exceeds one million rubles is only 5%, and from Table II it follows that the overwhelming majority (40 of 46) are really (true) loyal.

IV. RECOMMENDATIONS FOR THE DEVELOPMENT OF THE LOYALTY PROGRAMS

Based on the results of the MRFM-analysis homogeneous groups were identified. They give us an opportunity to offer a loyalty program package targeted at consumers of four levels, which will be available with additional possibilities and privileges. Various offers for each level client have been developed, including bonuses, incentives and personalized events [7].

BUSINESS PARTNER level is designed to activate the clients of the groups “sleeping”, “suspended” and “newbie”, i.e. for small organizations or private customers who make purchases often, but for amounts up to 10,000 rubles. For them the following additional bonuses designed to increase sales were developed:

TABLE I
MRFM-ANALYSIS OF THE CUSTOMERS BY DISTINGUISHED GROUPS AND SEGMENTS

| Number of deals | Remoteness of the last purchase, days | | | | | | | | | | | | | |
|---------------------|--|------|-----------|-----|-----------|-----|--------|-----|-------|-----|-------------|-------|------|-------|
| | 180+ | | 151-180 | | 121-150 | | 91-120 | | 61-90 | | 31-60 | | 0-30 | |
| | Number of clients / Monetary, million rubles | | | | | | | | | | | | | |
| | Lost | | Risk zone | | | | | | Loyal | | | | | |
| 10 or more | 2 | 1,3 | — | — | 1 | 0,1 | 3 | 1,6 | 5 | 2,7 | 18 | 15,2 | 102 | 106,3 |
| 6-9 | 6 | 1,3 | 2 | 0,1 | 2 | 0,2 | 5 | 1,1 | 10 | 2,8 | 30 | 6,9 | 34 | 6,6 |
| Total for a group | 8 | 2,6 | 2 | 0,1 | 3 | 0,3 | 8 | 2,7 | 15 | 5,5 | 48 | 22,1 | 136 | 112,9 |
| Total for a segment | 8 | 2,6 | 13 | | | 3,1 | | | 199 | | | 140,5 | | |
| | Sleeping | | | | Suspended | | | | | | Perspective | | | |
| 4-5 | 8 | 0,3 | 7 | 0,9 | 7 | 0,6 | 12 | 0,8 | 17 | 3,1 | 20 | 2,3 | 31 | 4,2 |
| 3 | 16 | 0,9 | 5 | 0,2 | 4 | 0,2 | 15 | 1,4 | 9 | 1,8 | 16 | 1,4 | 23 | 0,9 |
| 2 | 51 | 4,5 | 11 | 0,5 | 10 | 0,2 | 21 | 0,7 | 14 | 1,4 | 28 | 1,0 | 36 | 7,6 |
| 1 | 218 | 4,4 | 24 | 0,6 | 14 | 0,2 | 32 | 0,6 | 38 | 0,8 | — | — | — | — |
| Total for a group | 293 | 10,1 | 47 | 2,2 | 35 | 1,2 | 80 | 3,5 | 78 | 7,1 | 64 | 4,7 | 90 | 12,7 |
| Total for a segment | 340 | | 12,3 | | 193 | | 11,8 | | | | 154 | | 17,4 | |
| | | | | | | | | | | | Newbies | | | |
| | | | | | | | | | | | 44 | | 2,1 | |

TABLE II
NUMBER OF CUSTOMERS WITH INCREASING
VALUES OF MONETARY

| Monetary, thousand rubles | Number of clients in segment | | | | | | | Total number of clients |
|---------------------------------|------------------------------|-------------|---------|-----------|----------|-----------|------|----------------------------------|
| | Loyal | Perspective | Newbies | Suspended | Sleeping | Risk zone | Lost | |
| till 10 | – | 36 | 28 | 80 | 160 | – | – | 304 |
| from 10 to 100 | 51 | 90 | 14 | 91 | 154 | 6 | 2 | 408 |
| from 100 to 500 | 75 | 23 | 1 | 16 | 24 | 5 | 3 | 147 |
| from 500 to 1,000 | 33 | 3 | – | 4 | 1 | 2 | 3 | 46 |
| more than 1,000 | 40 | 2 | 1 | 2 | 1 | – | – | 46 |
| In total | 199 | 154 | 44 | 193 | 340 | 13 | 8 | 951 |

- cumulative discount system;
- provision of catalogs of products;
- promotion with gifts at the beginning and the end of the year.

SILVER PARTNER level is represented by medium-sized trade organizations, falling mainly in the category of "sleeping", with a purchase frequency of no more than 5 times per last 10 months and a total purchase amount of 10,000 to 100,000 rubles. Also this group includes "prospective" customers who have made 1-3 purchases per last month, and "suspended" clients, who bought more than a month ago and made no more than 5 transactions. For this group of customers the following options were proposed:

- cumulative discount system;
- invitations to free online and offline seminars on products and technologies with experts;
- the opportunity to participate in free trainings, conducted by the company's specialists and guest coaches.

GOLD PARTNER level includes "loyal" customers who make 6-9 deals per last three months with a total amount from 100 to 500 thousand rubles. Mostly they are trading

companies (intermediaries), selling products in the field of mechanical engineering. The companies of this group interested in flat and drive belts, sleeves, rubber coatings, technical plates, etc. So for them the following possibilities will be relevant:

- personalised discount system;
- invitations to VIP-seminars on products and technologies with invited experts and producers;
- personal manager assignment;
- bonuses based on the results of the year (return of a certain percentage depending on the volume of purchase, as well as on the degree of fulfillment of additional obligations).

PLATINUM PARTNER level is directed to the most significant customers of the company. In the majority these are large industrial enterprises, their transaction budget amounts to more than 500 thousand rubles. The main moments in co-operation with them are stability, reliability and confidence in the supplier. For such clients the following suggestions could be available:

- personal discount system;
- personal manager assignment;
- flexible system of payment for shipped products like 70/30, 50/50, 30/70, etc;
- guarantee of the arrival of goods on time, or payment of costs in the event of delivery delay;
- intermediate warehousing services and implementation of the cross-docking schemes at the client's request.

As it can be seen from the content of the submitted programs they cover most segments of the company's clients, focusing more on those that more effectively cooperate with the company.

V. CONCLUSIONS

Summarizing the conducted research it could be noted that the implementation of MRFM-analysis as a segmentation tool is an effective way for improving the interactions with client groups and, as a consequence, to increase company's sales and profits. Therefore the results obtained allowed de-

veloping loyalty programs for clients of different levels. In accordance with such programs targeted activities aimed at improving the efficiency of interaction with all type of customers were proposed. In addition, the research confirmed the universality of the MRFM-analysis method, which is expressed in obtaining correct results for the industrial rubber products market.

REFERENCES

- [1] Rubbers, tires and rubber materials-2017 - The results of the industry conference INVEN-TRA. October 10th, 2017. – URL: <http://www.creonenergy.ru/consulting/detailConf.php?ID=121358> (in Russian).
- [2] Griffin J. Customer Loyalty: How to Earn It, How to Keep It, New and Revised Edition. San Francisco, CA: Jossey-Bass. 2002. 272 p.
- [3] Hughes, A. Boosting Response with RFM. – New York: Marketing Tools, 1996. 263 p.
- [4] Miglautsch J. Thoughts on RFM Scoring // The Journal of Database Marketing. 2000. Vol. 8. p. 67-72.
- [5] Shchekoldin V., Tsoy M. RFM-analysis as a tool for segmentation of high-tech products' consumers // 13th International Scientific-Technical Conference on Actual Problems of Electronic Instrument Engineering (APEIE- 2016). 2016. T.1, Vol. 3. p. 358-363.
- [6] Shchekoldin V. Developing the risk classification based on ABC-analysis of possible damage and its probability // Proceedings of IFOST-2016, Novosibirsk. 2016. T.1, Vol.1. p. 317-319.
- [7] Tsoy M., Shchekoldin V., Lezhnina M. Building segmentation on the basis of modified RFM-analysis to increase customer loyalty // Russian Journal of Entrepreneurship. 2017. Vol.18, Iss. 21. p. 3113-3134. (in Russian)



Shchekoldin Vladislav Yurievitch,
Candidate of Science (PhD) in Computer
Science, Associate Professor of Marketing and
Service Department Novosibirsk State Tech-
nical University. Research interests are
experimental design, logistics, econometrics,
statistics, and marketing research. More than
60 papers and manuals have been published.



Tsoy Marina Yevgenienva,
Candidate of Science (PhD) in Economy Sci-
ence, Associate Professor, Head of Marketing
and Service Department Novosibirsk State
Technical University. Research interests are
consumer behavior, marketing research, and
marketing logistics. More than 60 papers and
manuals have been published.

Changes in Banking Business Models Driven by Technological Innovations

Svetlana V. Stepanova, Viktoria L. Karakchieva
Novosibirsk State Technical University, Novosibirsk, Russia

Abstract – The article presents the findings of a research on the impact of technological developments on business models in banking organizations. Technological advancements create added value for the recipients of financial services. In this context, credit risks continue unabated, while cyber and operational risks are only increasing. Innovations spur the banks to reinvent their distribution channels, key partners, resources patterns, and revenue streams. Ignoring the changing business landscape may produce customers' dissatisfaction and backlash or result in innovative risks exposures. The authors identify the factors that shape the corporate governance arrangements with banking organizations, emphasize the importance of developing a new risk management framework that could adequately meet the technological challenges and outline the key factors that are likely to shape banking technological development patterns in the nearest future.

Index Terms – Bank, business model, innovative technologies.

I. INTRODUCTION

BANKING INDUSTRY has changed drastically. Its development has been so rapid that outpaced performance standards within the industry. Many of the changes are driven by technological developments in financial sector. These developments seem to blur the conventional idea of the bank. The essence of this phenomenon is discussed in [1]. The Internet, social networks, smart phones, mobile wallet services, current accounts that are available outside the brick and mortar branch – these and other innovations are changing customers' behavior patterns and thus lead to the deterioration of vanilla banking industry. The customer no longer considers a payment as a banking service; s/he pays for a commodity, transfers money to his relatives or friends, pays fines and loans using his/her cell phone or mobile wallet. In fact, for a transaction to be completed it must pass through the system of settlements centers of The Bank of Russia (if it concerns the transactions within the Russian Federation) and be posted in the accounts of the paying and receiving banks. However, the customer will see this complicated process as a single heartbeat. Nowadays, guarantee schemes and security deposits support faster transactions (if it does not concern those within one bank), and the customer is enjoying short-term credit facilities without even knowing it.

In its Review of international best practices of implementing express payment systems and Proposals on their introduction in Russia (published in December 2017), The Bank of Russia states that there are over twenty national

express payment systems operating throughout the world, and eighteen more countries are in the path to launch such systems [2]. Despite the innovative nature of express payments, the methods of their risks mitigation are still within the traditional framework. For Faster Payments (UK) the solution is making deposits into a special separate account with The Bank of England; for BIR/Swiss (Sweden) – depositing funds to the system operator's escrow-accounts with the Riksbank. The Bank of Russia also recognizes the relevance of express payments for national financial market. It outlines the main requirements for the system: quality (usability and speed), availability (365/24/7 access, low cost), and reliability (data and transaction security, final clearances with The Bank of Russia).

It is entirely appropriate that financial organizations place particular emphasis on developing instant payment systems. From the customer's standpoint today, speed is the key value when it concerns money transfers. However, instant payments are exposed to serious risks associated with money laundering, partly because they are largely anonymous.

Customer expectations of fast transactions coupled with the need for close control over transactions as a policy measure to prevent money-laundering, result in a massive contradiction in modern banking. Historically, there are organizations and practices that can be referred to as the predecessors of modern instant payment systems, namely, the banks that struggled to attract customers with faster money transfer services. Within an ideal economic model free from money transit, fraudulent encashment and other money laundering activities, this business model would only enjoy its advantages. However, this is not the case in real life. The banks providing fast transactions turned to be very attractive for the customers involved in series transactions having no economic grounds. In their drive to satisfy customers' needs, many of those banks end up with fatal outcomes. A case in point is Bank24.ru headquartered in Ekaterinburg that lost its operating license on 16 September 2014. However, the bank was in good financial standing so that it was able to completely settle all its obligations before it was terminated [3]. Today banks subject most of their customers' payments to rigorous scrutiny in order to prevent laundering. Nevertheless, this aspect of a bank transaction is difficult to automate, which significantly slows down the operations. To cope with this shortcoming, remitting banks and The Bank of Russia are reducing their payment processing time. However, receiving banks are deliberately slow to carry out pay-in operations and likely to use the delayed funds to their own benefit. We believe that

introducing instant payment system can eliminate this problem.

Other banking activities are also affected by new technological developments. In its assessment of innovative technologies adoption throughout credit organizations in 2016, Deloitte (a company providing audit and consulting advisory), cited the leading players among the top twenty banks with the largest aggregate assets as at 1 June 2016. In the study, eleven innovations under consideration were classified into four groups: digital technologies (contactless cards, on-line wallet), security (“smart” identification), analytics (big data analysis, personal financial managers), and gamification (quests, games for clients), P2P/P2B crediting. The highest scored was Sberbank, second and third shared Alfa-Bank and Tinkoff Bank [4]. Earlier in 2018, The Council for legislative support of digital economy development in the Russian Federation nominated Sberbank as the leader to promote artificial intelligence nationwide. German Gref, the Head of the largest Russian bank, believes that as soon as in the nearest five years more than 80% of decision-making will be made by artificial intelligence. Again, the corner stone here is time economy, for both decision-makers and customers [5].

Leading players on the field of technological innovations remain the same, but a wider range of FSPs (financial services providers) are becoming more and more concerned with the implementation of innovative experiences. The main reasons for close attention to new technological solutions are as follows: (1) decreased profitability in banking sector and, consequently, search for the ways to gain extra income, provide cost reduction and acquire new customers, and (2) growing competition from non-regulated FSPs that are intruding into the realm of conventional banking and deplete its revenue pool. These players are fintechs and mobile operators that challenge banks in the monetary transfer market. Finding the best directions for the banks on this arduous journey is a priority objective of bank management.

II. PROBLEM DEFINITION

Despite the fact that Russian commercial banks show growing interest to technological development, the flagship in this process is the Central Bank of Russia. The regulator’s comprehensive approach and its commitment to this area of work is supported by a special Fintech section on The Bank of Russia’s official website. This section contains the outlines of technological development in finance industry for the period 2018 – 2020 adopted by The Bank of Russia [6]; latest news, reviews, analytics advisory reports and policy briefs. This information equips financial organizations with better understanding of where the industry is headed and thus enables them to adjust their behavior accordingly.

At the *Finopolis* – a forum, devoted to technological innovations in finance and held for the third time in 2017, Elvira Nabiullina, the Head of The Bank of Russia, pointed out that in compliance with the global trend towards technological development, national financial sector would have to build up new business models [7]. In this path, the emphasis would be not only on the conveniences and cost-

effectiveness provided by new technological solutions, but also on their associated risks.

Therefore, we need to identify the main elements in banking business model that are most sensitive to technological innovations and assess the nature of technological impact that can not only provide new opportunities but also generate threats to the sustainability of a financial organization.

III. THEORY

The first thing we should do is to clarify what we mean by business model. From the perspective of this research, we may anticipate that the most suitable will be the concept of disruptive innovations developed by Clayton Christensen, who takes value proposition as the first element of the business model [8]. In this part, the model is adequate to the technologically centered businesses. Technological innovations offer new solutions to the customer, that differ from what he knew before, they are faster and, probably, more cost-effective. However, the further unfolding of the model seems less promising from our perspective.

Therefore, within the framework of this research we shall seek guidance in the concept suggested by A. Osterwalder [9]. In his view, the business model includes nine interlinked building blocks: Customer Segments (CS), Value Proposition (VP, here he follows Christensen), Channels (CH), Customer Relationships (CR), Revenue Streams (RS), Key Resources (KR), Key Activities (KA), Key Partnerships (KP), and Cost Structure (CS).

Let us look at the business model blocks in terms of their exposure to innovative technologies.

Any bank that seeks to reinvent its business model will start from defining its customer segments. We believe that technological innovations will eventually reach all the bank customers, whatever customer group they belong. Through technological innovations, banks will deliver added value (or value proposition) such as time economy, usability and lower costs to both mass affluent and ordinary customers.

Concerning customer base, we need to emphasize the opportunities provided by CRM systems in carrying out comprehensive monitoring of customer information, services, products, transactions and their growth dynamics. CRM-systems deliver new experiences to the bank employees and significantly increase the efficiency of customer communications as banks become more responsive to customer requirements, ready to develop customized offers and drive cross sales. CRM should be seen as a modern technology to address the concerns of customer attraction and retention as well as new deposit acquisition.

We believe that the most distinct changes in customer-bank relations are in the area of distribution channels. Some of them are in intermediate position between customer communication tools such as providing aid and advice on standard questions, and sales channels for bank products. It depends on the functionality assigned to a particular tool. For example, chat bots equipped with artificial intelligence enable information gathering (Sberbank, Promsvyazbank, Raiffeisen Bank and others). Russian Standard Bank uses its

chat bots not only to provide general information about its products and services, but also to inform the clients about their balance status, credits and transactions. Moreover, the messengers of many fintechs (for example, Yandex.Money, QIWI) are able to identify the customer and thus provide access to his/her personal electronic wallet and carry out money transfers [10]. Recently Tinkoff Bank has announced the launch of the mobile messenger with instant in-chat money transfer functionality.

However, this cannot yet be referred to as full value distribution channel. Historically, most transactions were carried out in bank branches; later this pattern was changed by the ATM. Russian ATM were first introduced in the early 1990s; but nowadays they are declining as cashless payments are replacing cash-based operations: customers make payments via terminals in retail outlets and carry out miscellaneous transactions offered by online banking systems. The graphs below illustrate these changes (Fig. 1 and 2 present the authors' calculations based on the figures provided by The Bank of Russia).

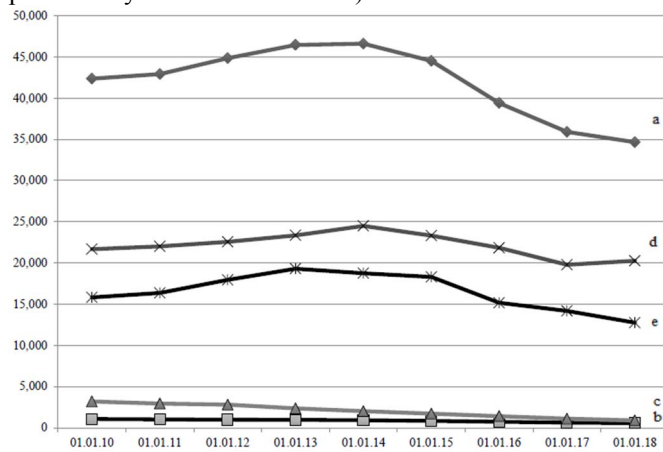


Fig. 1. Trends for financial institutions and their offices in the Russian Federation from 2009 to 2017, units.
Curve a – total number of offices; Curve b – the number of main offices;
Curve c – the number of branches; Curve d – the number of satellite offices;
Curve e – other structural units of banking institutions.

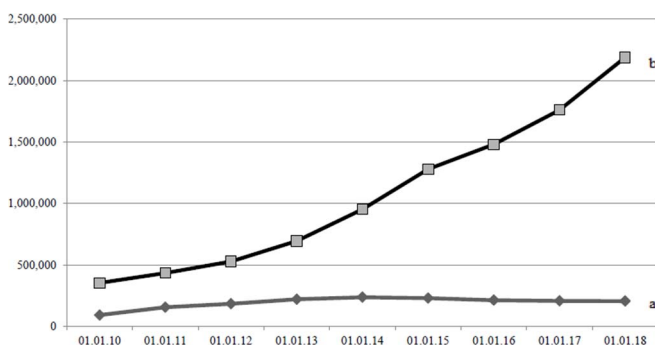


Fig. 2. Trends for ATM and electronic terminals installed in retail outlets in Russia within the period from 2009 to 2017, units.
Curve a – ATM, Curve b – electronic terminals.

Within the modern financial sector, we can see the organizations that no longer have brick and mortar branches and operate in “entirely remote” mode. In Russia, a case in the point is Tinkoff Bank. This pattern allows banks to have

leaner offices, reduce the costs to purchase or rent office space and hire operating staff.

Using digital channels to deliver banking products evidently requires new software solutions; furthermore, it calls for reinvented contractual relations. In particular, the client's conventional physical signature is likely to become irrelevant as banks offer remote access to deposits, loans and other digital financial services. These changes should be considered as an integral part of the new business model.

Currently, within the reach of remote financial services are as many as 97.6 % of legal entities and 89.8 % of individuals. Electronically transmitted payment instructions account for 95% and 69 % respectively. The trends for these indicators are shown in Fig. 3.

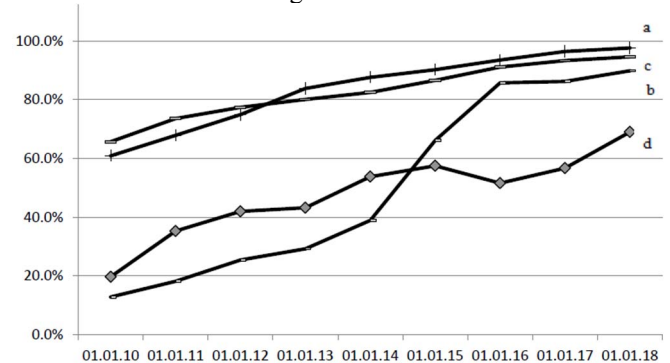


Fig. 3. Trends for on-line financial services in the Russian Federation provided within the period from 2009 to 2017.
Curve a – accounts of legal entities available via the Internet to the total number of accounts, percentage. Curve b – retail customers' accounts available via the Internet to the total number of accounts, percentage. Curve c – payment instructions from legal entities received via the Internet to the total number of payment instructions (for the year prior to the date, percentage). Curve d – payment instructions from retail customers received via the Internet to the total number of payment instructions (for the year prior to the date, percentage).

In their move to new technological landscape, banks have to pursue the strategy of permanent technological development. This will bring to the agenda the question of key partnerships in the sphere of innovation. Banks rarely disclose information about the digital technologies they utilize. They may develop their own solutions or buy standard products from external vendors and only have them maintained by the bank's software engineers, with any radical changes being introduced by the provider. Selecting the pattern to provide e-Banking solutions can be pivotal for the organization. If they choose to develop in-house IT solutions, banks will have to cope with extra costs for employing a larger team of software engineers and mitigate the risks of staff quit, i.e. if the key members of IT staff leave the company, this may cause internal disruptions and interrupt the bank's online operations. Exposed to this type of risks are mostly small and medium-sized banks, whereas larger organizations, such as *Alfa-Bank*, *Promsvyazbank*, and *VTB* are likely to develop in-house IT solutions. *Sberbank* has its software solutions developed within its spin-off *Sbertech*. Therefore, key partnerships and key resources should be viewed as interlinked elements of the business model producing a kind of U-tube effect as they are both targeted at the same goals.

A FSP *Tochka* provides an interesting example of how banks interact with fintechs. This organization is not a bank in the conventional sense: it is a high-tech multibank service working under the brand name *Tochka – the bank for entrepreneurs*. When one opens an account with *Tochka*, s/he becomes a customer of Bank Otkritie Financial Corporation (PJ-SC), General Banking License № 2209 of 24.11.2014 or QIWI Bank (JSC), Banking License № 2241 of 22.01.2015. Both banks have established branches named *Tochka*. When choosing *Tochka*, the customers' key consideration is not the service provider but the technological solution behind the service. This suggests a case of a fintech and bank nexus. We believe this trend is only going to accelerate.

The pressures of increasing crediting risks and declining interest margins force some digitally centered banks to declare their commitment to transaction business lines rather than traditionally accepted lending. The mentioned above *Tinkoff Bank* and *Tochka – the branch of Bank Otkritie Financial Corporation (PJ-SC)* and *QIWI Bank (JSC)*, have claimed to follow this model.

Some elements of banking business models are more sensitive to technologically driven changes than others are. Most prominent changes are summarized in Tab. I.

TABLE I
MAJOR CHANGES IN BANKING BUSINESS MODELS BY THE
DEPLOYMENT OF INNOVATIONS

| Business model element | Changes |
|------------------------|--|
| Value Proposition | Speed, usability, lower costs |
| Customer Relationships | CRM-systems, artificial intelligence-based tools |
| Channels | Reduction of traditional branches, increasing use of online and digital channels |
| Key Partnerships | IT solution providers, fintechs |
| Key Resources | IT-staff, technologies |
| Revenue Streams | Increasing proportion of revenue from transaction business |
| Cost Structure | Increasing costs for software and communication services, leaner branches |

IV. EXPERIMENTAL RESULTS

Reviewing financial statements of a number of banking institution, we discovered deviations of their working business models against the estimated version. For example, a comparison of the 2017 balance sheets of *Tinkoff Bank* and *VTB Bank (PJSC)* did not reveal any serious differences in their consolidate asset-liability structures, See Tab. II, [11, 12].

Let us remind that *Tinkoff Bank* is a technologically advanced, digitally centered organization with no branches, while *VTB Bank* is a conventional banking institution for high-net-worth corporate clients. Nevertheless, both banks reported the largest proportion of their assets as comprised by lending business lines. However, a deeper analysis identifies the differences inside their balance sheet patterns. In *VTB Bank*, personal loans account for 3.8% of its cumulative loan portfolio, while in *Tinkoff* this proportion is

as large as 87.6%, nearly 92% are credit card loans at call. Revenue patterns also differ drastically. In *Tinkoff* the percentage of lending-based revenue was only 1.7 times the amount of its commission revenue, while in *VTB* the excess was as much as by 17 times.

TABLE II
ASSETS ON THE BALANCE SHEETS OF VTB BANK AND
TINKOFF BANK AS OF 01.01.2018, %

| Item | VTB Bank | Tinkoff |
|---|----------|---------|
| Loans and advances to customers | 67,9 | 56,3 |
| Dealing Securities | 14,0 | 29,3 |
| Fixed assets, intangible assets and inventory | 3,4 | 2,5 |
| Other assets | 14,7 | 11,9 |
| Total | 100 | 100 |

This confirms our assumption about an increasing proportion of transaction-based income gains in digitally centered banks. Credit exposures play a substantial role in their assets pattern, which generates serious risks escalated by the non-collateral nature of the loans available by credit cards. For our theoretical explanations, we referred to the business model canvas developed by A. Osterwalder that does not give room for risk management concerns. Probably, the author left this element outside his business model because the model was developed for the organizations other than financial service providers and was primarily targeted at customer attraction and increasing sales.

Therefore, we shall add risk management as a supplementary element to the existing framework. Its importance will be growing fueled by continuous technological developments and growing operational risks in various manifestations.

V. DISCUSSION OF RESULTS

The need to reinvent banking business models is evident. The new business landscape and massive technological advances that are occurring in all banking institutions spur this need. They all have no choice but adopt these changes, while may do it at different rates. Ignoring these challenges and commitment to old business schemes carries two major threats. Technological backwardness will cause customers' dissatisfaction and backlash; the failure to understand innovation risks may result in substantial financial losses.

The losses may be due to unauthorized write-offs from the accounts that are handled online. The Central Bank is most likely to estimate and manage cyber risks such as by setting higher threshold capital adequacy ratio for troubled organizations or by implementing some other measures. A comprehensive assessment of information security is made against the two major criteria. Firstly, the organizational measures developed and implemented by a bank, such as internal standards and regulations, staff qualification, information access screening, software facilities and equipment. Secondly, performance in compliance with these measures: records of unauthorized write-offs, interruptions (and their durations) due to DDOS-attacks, failures of

automated banking systems and their parts because of cyber-risks (such as virus contaminations, etc.).

Innovative process in banking sector shows no letup in the pace of change. Within this process, we can see a two-way interaction of innovations and business models: innovations affect business models and business models are capable to affect the rate and trajectory of the technological change. The key factors to determine the innovative vector in banking are as follows: developing new customer identification instruments, mergers within the industry, partly because of recovery and resolution measures assisted by The Fund of Banking Sector Consolidation and introduction of open API (application programming interface).

VI. CONCLUSION

The technological changes that are sweeping through banking sector have seriously influenced financial services providers. Driven by innovations, they modify their distribution channels, key partners, resources patterns, and revenue streams. Innovative technologies create added value for end-users, which is the key factor that makes banks stay technologically centered. Within this context, credit risks continue unabated, while cyber and operational risks are only increasing. New business models should take all these factors into consideration.

REFERENCES

- [1] Brett K. Bank 3.0. Why Banking Is No Longer Somewhere You Go But Something You Do. – Marshall Cavendish International, 2012. – 360 p.
- [2] Obzor mirovogo opyta ispol'zovaniya sistem bystrykh platezhej i predlozheniya po vnedreniyu v Rossii. [Review of international best practices of implementing express payment systems and Proposals on their introduction in Russia]. [Electronic resource]. URL: https://www.cbr.ru/Content/Document/File/36010/rev_pay.pdf (accessed: 20.04.2018). (In Russian).
- [3] Gosteva E., Brytkova A. [Bank24.ru: Best way to die for a new life]. Bank24.ru: krasivaya smert' radi novoj zhizni. [Electronic resource]. URL: <http://www.banki.ru/news/daytheme/?id=8300352> (accessed: 20.04.2018). (In Russian).
- [4] Stognej A., Sedlov D. [Banks for advanced users]. Banki dlya prodvinytyh. [Electronic resource]. URL: <https://www.rbc.ru/newspaper/2016/08/24/57bb7ffe9a7947340fa28c1f> (accessed: 20.04.2018). (In Russian).
- [5] Sberbank – samyj tekhnologichnyj bank Rossii. [Sberbank is the most technologically advanced bank in Russia]. [Electronic resource]. URL: <https://my-sberonline.ru/sberbank-samyj-tehnologichnyj-bank-rossii.html> (accessed: 20.04.2018). (In Russian).
- [6] Osnovnye napravleniya razvitiya finansovyh tekhnologij na period 2018 – 2020 gg. [Financial technologies development guidelines for the period from 2018 to 2020]. [Electronic resource]. URL: http://www.cbr.ru/Content/Document/File/35816/ON_FinTex_2017.pdf (accessed: 23.04.2018). (In Russian).
- [7] Ferenc V. [Fintechs – it is just the present] Fintekh – ehto uzhe nastoyashchee // Bankovskoe obozrenie. – 2017. – № 11. – pp. 24 – 28. (In Russian).
- [8] Christensen C. The Innovator's Dilemma. – Collins Business, 2003. – 320 p.
- [9] Osterwalder A., Pigneur Y. Business Model Generation: A Handbook for Visionaries, Game Changers, and Challengers. – John Wiley and Sons, Ltd, 2010. – 288 p.
- [10] Pominov D. Telegram-banking. [Electronic resource]. URL: <https://bosfera.ru/bo/telegram-banking> (accessed: 23.04.2018). (In Russian).
- [11] Bank VTB (PAO) [Electronic resource]. URL: <http://www.e-disclosure.ru/portal/company.aspx?id=1210> (accessed: 27.04.2018). (In Russian).
- [12] AO «Tinkoff Bank» [JSC Tinkoff Bank]. [Electronic resource]. URL: <http://www.e-disclosure.ru/portal/company.aspx?id=2989> (accessed: 27.04.2018). (In Russian).



Stepanova Svetlana Vladimirovna, associate professor with the Department of Audit, Accounting and Finance, Novosibirsk State Technical University, Candidate of Sciences (Economics), an author of 25 publications. Area of research: bank management, money laundry prevention, remuneration.
E-mail: S.Stepanova@corp.nstu.ru



Karakchieva Viktoria Lembitovna, associate professor with the Department of Foreign Languages, Novosibirsk State Technical University, Candidate of Sciences (Philology). Area of research: business communication, thesaurus approach to business terminology.
E-mail: karakchieva@corp.nstu.ru

Ambient Intelligence for Increasing Innovation Performance of Enterprises

Lenka Štofová, Petra Szaryszová, Martin Bosák, Alexander Tarča, Zuzana Hajduová
Faculty of Business Economics of the University of Economics in Bratislava with seat in Košice,
Košice, Slovak Republic

Abstract – The new development of the changing global environment brings to the attention of ideas in the form of trends that show the future environment very differently from the current state. Technical experts are discussing the growing presence of internet of things and technologies, the involvement of all devices, and the prediction of how to create ambient intelligence. This type of intelligence refers to an electronic environment that is sensitive and responsive to the presence of users. Within these ambient systems, we can identify what the user needs and at the same time obtain it without asking for it. Ambient intelligence is a combination of neural networking, smart technologies, cloud computing, big data, websites, bearers, and user interface to services that can automate processes and make recommendations to improve the quality of users' lives. On a wider scale, there are modern high-tech possibilities to closely monitor the impact on the quality and safety of the current market environment by ambient intelligence and sensory management solutions. The aim of the paper is to highlight the selected trends of ambient intelligence system applications as an innovative paradigm to support smart innovation that will further enhance the quality of the automotive industry's technological solution in Slovak republic with advancing developments inspired by other successful companies' results acting in this sector. The reliability of their most important measures were obtained by correlation analysis and multiple linear regression.

Index Terms – Ambient intelligence, innovation, quality performance, sensory management, smart manufacturing, automotive industry.

I. INTRODUCTION

AT PRESENT, people around the world are increasingly influenced by the intensive expansion of the Internet, as a key element in the development of individuals and companies on a global scale. The development of the human community is equally important for the still accelerating growth of other new technologies and very often we are now surrounded by “smart” things. Smart usually refers to intelligent sophisticated devices that provide a high level of functionality.

Ambient intelligence technology (AmT) is an emerging discipline that brings intelligence to our life and makes those environments sensitive to us. In its essence it is a network of hidden intelligent interfaces that recognize the presence and utilize environment to human needs. For businesses and their stable position in the market, it is important to keep track of all changes and to constantly develop, because we are currently in the fourth industrial revolution and the classic

business models and the production are changing. Customer requirements are becoming increasingly demanding, and Industry 4.0 has been introduced to create a new competitive advantage based on industry change (Schmidt et al., 2015).

The rise of ubiquitous systems is sustained by the development and progressive adoption of the Internet of Things (IoT) devices and their enabling technologies. IoT has significant potential in high-risk Environment, Health, and Safety (EHS) industries, where human lives are at stake and IoT-based applications are primed to offer safe, reliable, and efficient solutions due to their ability to operate at the different level and provide rich low-level information (Thibaud et al., 2018).

The paper is focused on the smart trends in automotive industry according the summarized results of strategic research studies. Authors applied their research on Slovak enterprises acting in automotive industry, which starting to use more intelligent tools for enhancing their quality in every ways of their business success, improving productivity and accelerating innovation.

II. PROBLEM DEFINITION

In these days much is being discussed about the growing presence of IoT applications and technologies, and the prediction of how to create ambient intelligence more efficient for increasing the performance also in business sector. There are modern high-tech possibilities to narrowly monitor the impact on the quality and safety of the current market environment by ambient intelligence and sensory management solutions. Smart factory is one of the key component implementations of the Industry 4.0 concept. The combination of these trends makes possible the development of autonomous systems combining robotics and machine learning for designing similar business systems. The priority focus of the automotive industry in Slovakia is on the robotics and in-depth data analysis, which in the most important way influences their innovation performance following routing of the best practices of companies that apply successfully parts of the concept to achieving overall performance and competitiveness. Research problem is defined as the determination of the measures' role in smart manufacturing for improving productivity and accelerating innovation in Slovak automotive industry enterprises. The aim of the paper is to research the ambient intelligence system applications as an innovative paradigm to support smart innovation that will further enhance the quality of the

automotive industry technological solutions in Slovak medium-sized and large enterprises. It requires to study the association between independent (smart manufacturing) and dependent (productivity and innovation) variables as important measures. The research is centred on investigating the relationships between a set of multiple independent and multiple dependent variables with little past information of such relationships.

III. INTERNET OF THINGS STRATEGIC RESEARCH STUDIES

The Industry 4.0 is a new production model that converges and accelerates the entire value chain. Vertical and horizontal integration of IT and automated production will lead to an end-to-end solution. IT, IoT, Internet of Services (IoS) and Cyber Physical System (CPS), machines, products with people work together.

The International Energy Research Centre (IERC) brings together EU-funded projects with the aim of defining a common vision for IoT technology and addressing European research challenges. The aims of IERC are to provide information on research and innovation trends, and to present the state of the art in terms of IoT technology and societal analysis, to apply developments to IoT-funded projects and to market applications and EU policies. The final aim is to test and develop innovative and interoperable IoT solutions in areas of industrial and public interest. It is addressed as an IoT continuum of research, innovation, development, deployment, and adoption (Vermesan et al., 2017).

According to a study published at the International Symposium on Intelligent Production and Automation, which was attended by two leading Danish universities, the definition is as follows: “Smart factory is an industrial solution that offers flexible and adaptive manufacturing processes that can handle production problems in dynamically changing conditions in a world of high complexity” (Radziwon et al., 2014, p. 1187). This solution is supported by high automation, which is characterized by the merging of hardware software with mechanization. This will reduce unneeded personnel, waste resources and, ultimately, optimize. This perspective can be also seen as cooperation between different industrial and non-industrial partners and smart solutions to achieve dynamic organization.

Lasi et al. (2014) the Smart factory was one of the key component implementations of the Industry 4.0 concept, describing it as follows: “The production will be completely equipped with sensors, cameras and autonomous systems. With the use of Smart technology related to holistic digital factory models, a CPS product and a simulation, we will achieve fully autonomous factories.”

Smart factory brings a number of advantages – reduction of production costs, resource efficiency, personalized products in one-piece production batch, flexible, autonomous and adaptive production, shorter processes, product individualization for the customer, flexibility, decentralization and economy, higher productivity, customer

orientation, better service, shorter processes and continuous times.

A. *Internet of Things of Digital Transformation*

Robotic devices, drones and autonomous vehicles, block chains, augmented and virtual reality, digital assistants and machine learning (artificial intelligence or AI) are the technologies that will provide the next phase of development of IoT applications. The combination of these disciplines makes possible the development of autonomous systems combining robotics and machine learning for designing similar systems. This trend of hyper connected world offers many benefits to businesses and consumers, and the processed data produced by hyper connectivity allows stakeholders in the IoT value network ecosystems to make smarter decisions and provide to customer better experience.

The IoT is bridging the gap between the virtual, digital and physical worlds by bringing together people, processes, data and things while generating knowledge through IoT applications and platforms. IoT achieves this addressing security, privacy and trust issues across these dimensions in an era where technology, computing power, connectivity, network capacity and the number and types of smart devices are all expected to increase. “Technology research trends way people interact with the intelligent environment cyberspaces, from using appliances at home to caring for patients or elderly persons” (Vermesan et al., 2017).

The massive deployment of IoT devices creates systems that synergistically interact to form totally new and unpredictable services, providing an unprecedented economic impact that offers multiple opportunities. The potential of the IoT is underexploited, the physical and the intelligent are largely disconnected, and requiring a lot of manual effort to find integrates and uses information in a meaningful way. IoT and its advances in intelligent spaces can be categorized with the key technologies at the core of the Internet (Noor, 2015).

B. *Significant Smart Trends in the Automotive Industry*

In this section, we summarize the main trends that can have a significant impact on the further development of the automotive industry. All major finishers are already investing a significant amount in the development of electric vehicles. Grants are enough to support the purchase of more than 1.000 vehicles, but only about 300 cars have registered in the program. The number of electric vehicles in the world has almost doubled last year. More than a third of a million new electric cars were sold in China. Although in absolute terms the number of electric vehicles is rising rapidly in the total sales of all cars, they represent only a negligible share in the level of the statistical variation (0.2 %). Last year, according to data from the International Energy Agency, they traveled around two million passengers, with 95 % of them focusing on only 10 countries in the world. These are countries with generous state grants when buying an electric vehicle or a hybrid vehicle in the coming years. Development in the field of charging stations, battery production and changes in the specialization of some suppliers may be

expected. New opportunities for development and research, as well as for data processing (ICT), are emerging with the development of this segment. Slovak enterprises acting in automotive industry are also trying to support sales by selling grants.

Within the EU, several projects are planned and implemented to enable uninterrupted and efficient use of interconnected vehicles and autonomous vehicle management cross-border transport corridors in the border area. Slovakia wants to contribute to the implementation of a European strategy for deploying intelligent transport systems, which have the ambition to use all modern technologies such as big data, artificial intelligence and the internet of things for a totally new travel experience. The automotive industry has considerable overhead in related industries such as materials and mechanical engineering, power engineering, robotics and information and communication technologies where there is a great potential for smart transport opportunities in two areas:

- Autonomous ride.
- Vehicle interconnection in the communications network and data exchange.

In Fig. 1 are presented results of Pareto analysis of the most used automotive industry smart technologies of Slovak enterprises.

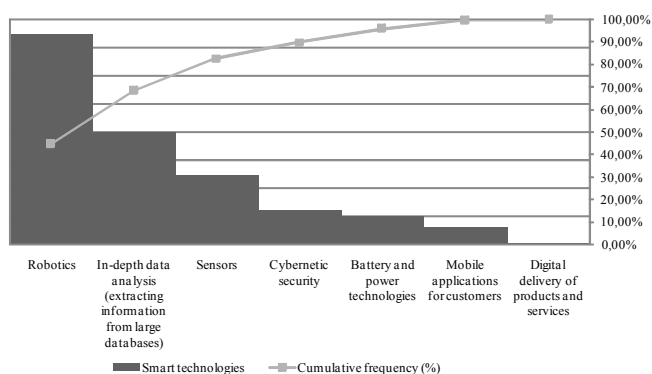


Fig. 1. Pareto analysis of the most important smart technologies for the automotive industry.

Source: Own processing

Data usage is the cornerstone of the fourth industrial revolution, but the massive flow of information from an increasing number of sensors, devices, applications and information systems is of little value without proper analytical techniques. This fact is confirmed by the trend of increasing the strategic importance of data analytics for companies in the automotive industry. As technologies that will have the greatest strategic importance for automotive organizations, respondents rated 67 % of Slovak robotics suppliers, an increase of 26 % compared to the previous year. The second biggest leap is the depth analysis area (15 % increase), before the expected trend of the sensors (8 %). Accelerating intelligent devices, many of which work autonomously, will also enhance the importance of power system and battery innovations. Based on the results of survey, Pareto analysis carried out confirms the priority focus on the robotics and in-depth data analysis of the

automotive industry in Slovakia, which in the most important way influences their performance in a positive sense.

Based on current knowledge in the area of ambient intelligence, authors have treated the overview of the best practice of companies that apply successfully sub-systems of this concept to achieving higher quality, productivity, competitiveness and overall performance (Table 1).

TABLE I
EXAMPLES OF AMBIENT INTELLIGENCE APPLICATIONS
IN INDUSTRIAL PRACTICE

| Ambient Intelligence | Company | Applications in practice |
|------------------------------|---|--|
| Smart factory | Siemens EWA German conglomerate company (Siemens - EWA, 2015) | <ul style="list-style-type: none"> – Data management - With the help of sensors are data stored on the server, monitored, analyzed and evaluated. – Intelligent Production Planning - The technical information are programmed into the automation system program. – Production control - all production is interwoven with a large number of cameras, sensors and control points to monitor quality. – Integration of products and production life cycles - systematic production co-operation with the R&D department. – Many machines, PLCs, assembly machines and semi-automatic machines, including SINEMATIC panels, had to be mounted to the Smart factory. |
| Cyber physical system | Synapticon GmbH German company. (Synapticon, 2015) | <ul style="list-style-type: none"> – Developed its own platform for creating CPS, consisting of modular systems based on compatible electronic modules that enable the creation of various types of control units, sensors and controls. – The DYNARC platform includes SOMANET R&D modules to create virtual production prototypes. It also includes SOMANET chips for custom or mass production, providing enterprise-wide communication, sensor acquisition, and component motion monitoring by manufacturing (still under development). – OBLAC Tools, a web tool that creates an environment for system configuration, software development, and maintenance of DYNARC hardware. In addition, it combines Embedded systems with Cloud. |
| RFID technology | Siemens AG Germany-based technology company (Siemens, 2015) | <ul style="list-style-type: none"> – Siemens AG uses RFID, enabling technology to be transparent throughout the production and supply chain. This means that material flows are constantly under surveillance. RFID also enables fast data acquisition. – The wide portfolio of SIMATIC RF products employs ultra-short waves, characterized by large |

| | | |
|---------------------------|--|---|
| | | ranges, fast reading and, above all, mass readings, i.e. reading several transponders at a time. |
| Internet of Things | SIGFOX French company (Sigfox, 2015) | – M2M communications through a 2G mobile network to track fleet and track remote devices. |
| Big Data | SAP AG Germany company (SAP, 2015) | <ul style="list-style-type: none"> – The SAP HANA platform has a core in a fast in-memory database. As a result, all data are stored in the memory, allowing for high performance and fast processing. – The SAP HANA cloud platform, which is used to handle large volumes of data using analytics tools. |
| Cloud computing | IBM Automotive industry American worldwide company (IBM, 2015) | <ul style="list-style-type: none"> – IBM Cloud is based on a hybrid cloud model that focuses on integrating the private Cloud with the public. – SaaS business applications - this platform offers rental around a hundred applications for an enterprise that will promote innovation, enable complex business analyzes, and bring together co-workers across the enterprise. – IaaS Infrastructure Services - this platform offers open cloud infrastructure services for IT operations. – PaaS developer platform - this platform allows you to build applications exactly to your needs. – Private / hybrid Cloud - dynamically linked private and public clouds and their organization, management and security will enable innovation to accelerate. |
| Smart product | Tesla Motors, Inc. American electric-automobile manufacturer (Tesla Motors, 2015) | <ul style="list-style-type: none"> – The S model automobile, introduced by the three P85D, 85D and 70D models, is the Smart product. This car is equipped with sensors that monitor driving characteristics, smart assistive systems and software. – The Tesla electric car connected to the Tesla network may, if necessary, repair it autonomously, for example by downloading updates or sending a buzz to the owner of the car that it is necessary to visit the service. This is referred to as the Intelligent Maintenance System, which regularly monitors the vehicle condition and responds before a fault occurs. |
| Smart sensor | Weiss Spindeltechnologie GmbH German automotive manufacturing company (Weiss, 2015) | <ul style="list-style-type: none"> – Using Smart Maintenance, specifically spindle maintenance on machines - after installing the SM124 sensor module and intelligent SINAMICS and SINUMERIC systems into the machine, the unexpected downtime will be reduced by analyzing data from the spindle. – As a result of this implementation, Smart Spindle is able to send spindle speed, spindle temperature, tool condition, |

| | | |
|---------------------|--|--|
| | | clamping status and tracking data wirelessly via Wi-Fi to the maintenance worker's computer, which monitors the production process and sends the maintenance to the machine, before a failure occurs. |
| Industry 4.0 | Volkswagen Group German multinational automotive manufacturing company (Volkswagen, 2015) | – For example Volkswagen has a tradition of interactive solutions in manufacturing known as Industry 4.0. This refers to the automation and data exchange in manufacturing technologies, using cloud computing and connecting the individual objects via the IoT. Industry 4.0 enables faster, more effective production of vehicles with higher regard for the natural environment. |

Source: Own processing

The Government of the Slovak republic sees great potential in the coming of the next industrial revolution. The Slovak republic is an industrialized country with a long tradition of industrial production and a good level of technical education and has the best conditions for developing its own concept. This is called the National Industry Initiative 4.0 and was based on the German Industrie 4.0 Concept.

IV. RESEARCH METHODOLOGY

The goal of research analysis was to provide a compact view on the automotive industry in Slovakia using the data on automobile producers and their suppliers. The analysis was prepared from the data available on www.ipdap.sk, www.okba.sk, and www.finstat.sk which also provide more detailed information. This material is not supposed to substitute official and exact statistical overviews, but rather seeks to describe overall trends in the automotive industry of the Slovak economy while using different sources including Open Data of the state.

The survey has been limited to those medium and large scale manufacturing enterprises which are in process of acquiring, developing or utilizing smart manufacturing for improving productivity and accelerating innovation. Among the 104 (100 %) respondents, 16 % were the automobile manufacturers, 48 % industries were the automobile component manufacturers, 19 % industries were consumer goods manufacturers and remaining 17 % were process industries.

The survey has been conducted to determine the role in smart manufacturing for improving productivity and accelerating innovation. The reliability of the constructs and their measures were obtained through correlation analysis and multiple linear regression, were employed to predict the results. The reliability of the identified dependent variables was obtained through the reliability analysis for finding out the value of Cronbach's alpha (Table 2) for all the measuring instruments, respectively dependent variables.

TABLE II
CRONBACH'S ALPHA FOR DEPENDENT VARIABLES

| Dependent Variable | Description | Cronbach's Alpha |
|--------------------|--------------------------------------|------------------|
| PDV | Productivity | 0.976 |
| INN | Innovation | 0.878 |
| SM | Smart Manufacturing | 0.889 |
| FMS | Flexible manufacturing system | 0.917 |
| MI | Manufacturing intelligence | 0.946 |
| SMES | Smart Manufacturing Execution System | 0.967 |

Cronbach's alpha was calculated, as recommended for empirical research in operations management. For each scale is greater than 0.85, which is considered adequate for exploratory research.

V. RESULTS AND DISCUSSIONS

Manufacturing has been evolving over the years as different needs and technologies arise. The customer of the twenty-first century, demands products and services those are fast, right, cheap and easy. The quest for lower operating costs and improved manufacturing efficiency and introduction of innovative concepts has forced a large number of manufacturing firms to embark on smart manufacturing (SM) projects of various types. SMs have been identified as new way for manufacturing companies to gain a competitive advantage. The dramatic developments in SM at various organizational levels can be attributed to numerous benefits that improve the competitive position of the adopting enterprises. SM impact not just manufacturing, but also the whole business operations, giving new challenges to an enterprise's ability to manage both manufacturing and manufacturing informatics solutions.

To empirically assess the role of smart manufacturing in improving productivity and accelerating innovation, author's key aim in data analysis is to study the association between independent and dependent variables. Since our research centered on investigating the relationships between a set of multiple independent and multiple dependent variables with little past information of such relationships, canonical correlation analysis (Table 3) followed by regression analysis are deemed to be the suitable multivariate statistical methods to use.

TABLE III
CORRELATIONS BETWEEN INDEPENDENT AND DEPENDENT VARIABLES

| | SM | FMS | MI | SMES | PDV | INN |
|------|-------|-------|-------|-------|-------|-------|
| SM | 1 | 0.624 | 0.526 | 0.623 | 0.607 | 0.541 |
| FMS | 0.624 | 1 | 0.693 | 0.702 | 0.762 | 0.776 |
| MI | 0.526 | 0.781 | 1 | 0.749 | 0.773 | 0.732 |
| SMES | 0.623 | 0.702 | 0.738 | 1 | 0.814 | 0.779 |
| PDV | 0.607 | 0.681 | 0.773 | 0.796 | 1 | 0.649 |
| INN | 0.541 | 0.776 | 0.732 | 0.779 | 0.649 | 1 |

The canonical correlation measures the bi-variate correlation between linear composites of the independent (smart manufacturing) and dependent variables (productivity and innovation). The inbuilt flexibility of canonical

correlation in accordance with types and number and of variables used, both independent and dependent, makes it a rational contender for numerous of the more difficult problems addressed with multivariate techniques. Canonical correlation analysis handles the association among composites of sets of multiple independent and dependent variables.

Realised analysis generates a number of independent canonical functions that maximize the correlation between the linear composites, which are sets of independent and dependent variables. Every canonical function is in fact based on the correlation between two canonical variates, one variate for the independent variables and one for the dependent variables. One more unique trait of canonical correlation is that the variates are imitated to maximize their correlation. Furthermore, this type of correlation never ends with the imitation of a single relationship between the sets of variables. As an alternative, many canonical functions may be imitated. The utmost number of canonical variates that can be extracted from the sets of variables matches the number of variables in the smallest data set.

Presented results of research study introduce the empirical evidence for depicting the role of smart manufacturing for improving productivity and accelerating innovation in large and medium scale enterprises of the Slovak automotive industry. The role of smart manufacturing has been explored and examined for achieving productivity and innovation in an enterprise. It has been statistically found that the different constituents of smart manufacturing have a positive impact on the achievement of productivity and innovation. It is found that there is a vast role of flexible manufacturing system, manufacturing intelligence and smart manufacturing execution system in modifying products in real time, achieving productivity and innovation. It has been found that a strong positive correlation (0.814) exists between smart manufacturing execution system and productivity and (0.752) between manufacturing intelligence and innovation of this study. A plant with smart manufacturing execution system and manufacturing intelligence will operate more efficiently and smartly to improve productivity and accelerate innovation.

VI. CONCLUSION

This research examined the role of smart manufacturing for achieving productivity and innovation in an automotive industry. Empirical evidence was offered to maintain associations between smart manufacturing, productivity and innovation. Innovation and productivity will be the key for pushing toward faster and more frequent product transitions while operating globally. The results recommend that smart manufacturing is quite important to manufacturing organizations for increasing productivity and accelerating innovation. The role of implementing the soft, intermediate and hard technologies was explored and found to be less significant when compared to the SM and leads to the connotation that a strategic shift has been witnessed towards the virtual organizations. Smart manufacturing is most

responsive in the context of performance and innovation oriented production.

The paper explained the concept of smart manufacturing and presented some information that get advantage of these innovative technological environment. This can lead to new levels of business optimization as organizations become smarter about the performance metrics and the way they collect information to measure optimal productivity. The reliability of the identified dependent variables was obtained through the reliability analysis for finding out the value of Cronbach's alpha. The pair-wise correlations between variables were examined to establish the mutual association and to avoid the problem of multi-collinearity. It has been observed that surveyed enterprises have shifted their mind focus towards the smart manufacturing for achieving productivity and innovation.

The IoT brings to manufacturing plants a higher a degree of control over the whole process and reduction of costs. Implementing the IoT to the entire manufacturing process can also lower the personnel requirements. It is more demanding on the qualified workforce that can control modern technologies and programs. Furthermore, innovation teams in several places around the Slovak republic have experience with modern technologies.

In general, the future of ambient intelligence depends on the availability of qualified personnel, the access to modern technologies, willingness of companies to innovate, as well as on the adherence to strict standards in IT security. IoT can bring improvements not only in optimization of finances, but also in the positive impact on the natural environment and the society as such.

ACKNOWLEDGEMENT

The article is written within the project of young scientists, young teachers and PhD students number I-18-109-00.

REFERENCES

- [1] IBM. Cloud computing [online]. 2015 [cit. 22. 04. 2018]. Dostupné z: <http://www.ibm.com/cloud-computing/cz/cs/>
- [2] Noor, A. 2015. The connected life: The internet of everything coming to building near you. Mechanical engineering. 2015: 137 (9): 36-41. ISSN 0025-6501
- [3] Radziwon et al. 2014. The Smart Factory: Exploring Adaptive and Flexible Manufacturing Solutions. Procedia Engineering, 2014, 69: 1184-1190. ISSN 1877-7058. DOI: 10.1016/j.proeng. 2014.03.108.
- [4] SAP. 2015. Predictive Maintenance and Service, cloud edition [online]. 2015b. Dostupné z: <http://www.sapappcenter.com/p/1004#details-section>
- [5] Schmidt, R. et al. 2015. Industry 4.0 – Potentials for creating Smart Products: Empirical research Results. Business Information Systems: Lecture Notes in the business Information processing, 2015, 208: 16-27. DOI: 10.1007/978-3-39-19027-3_2
- [6] Siemens. 2015. Electronic Works Amberg - Siemens Industry Software. In: Youtube [online]. Dostupné: [cit. 22. 04. 2018]. Dostupné z URL: <https://www.youtube.com/watch?v=eZdrwqZnLes>
- [7] Siemens. 2015. Spindel Technologie - ahead of competition [online prezentace]. Erlangen, Siemens AG, 2015 [cit. 22. 04. 2018]. Dostupné z: <http://www.weissgmbh.com/uploads/media/WEISS_SMI24_en.pdf>
- [8] Sigfox. 2015. Connected world [online]. 2015. [cit. 22. 04. 2018]. Dostupné z: <http://www.sigfox.com/en/#!/connected-world>
- [9] Synapticon. 2015. We're living in a highly virtualized world [online]. [cit. 22. 04. 2018]. Dostupné z: <https://www.synapticon.com/cyber-physical-systems/>
- [10] Tesla Motors 2015 [online]. [cit. 22. 04. 2018]. Dostupné z: <https://www.teslamotors.com/about>
- [11] Thibaud, M., Chi, H., Zhou, W., Piramuthu, S. 2018. Internet of Things (IoT) in high-risk Environment, Health and Safety (EHS) industries: A comprehensive review. Decision Support Systems.
- [12] Vermesan, O., Eisenhauer, M., Sunmaeker, H., Guillemin, P., Serrano, M., Tragos, E. Z., Bahr, R. 2017. Internet of Things Cognitive Transformation Technology Research Trends and Applications. Cognitive Hyperconnected Digital Transformation; Vermesan, O., Bacquet, J., Eds, 17-95.
- [13] Volkswagen. 2015. SEAT breaks new ground in training for Industry 4.0 [online]. 2015 [cit. 22. 04. 2018]. Dostupné z: https://www.volkswagenag.com/en/news/2017/06/seat_training_for_industry.html
- [14] Weiss. 2015. Smart Spindle. [online]. 2015 [cit. 22. 04. 2018]. Dostupné z: <https://www.weissgmbh.com/en/products/the-smart-spindle/>



Ing. Lenka Štofová, PhD.

Lenka Štofová is an assistant working at the Department of Management of the Faculty of Business Economics of the University of Economics in Bratislava with seat in Košice. At this faculty she earned her higher education and also a PhD degree (2016). In her active research activities she is the author and co-author of several scientific and professional papers published in international and national journals registered in Scopus database and conference proceedings. Her research and educational orientation is focused on the management, management systems and enterprise planning, quality, strategic business performance and efficiency mainly in the field of automotive industry. Within her PhD study and work as an assistant she participated in the preparation and realization of several research projects in Slovak republic f. e. for young scientists and other.



Ing. Petra Szaryszová, PhD.

She works as an assistant professor at the Department of Management of the Faculty of Business Economics of the University of Economics in Bratislava with seat in Košice, where she earned her higher education and later a PhD degree (2012) and currently works as a Secretary of the Department. She is a co-author of monographs and textbooks in Slovak Republic and is author and co-author of several scientific and professional articles published in international and national journals registered in Scopus database and conference proceedings. She participated actively in the preparation and implementation of several research projects in Slovak Republic. In her scientific research and educational activities, she focuses on the management, management systems, quality, innovation, certification, auditing, enterprise planning, business performance and business ethics.



Prof. h.c. Ing. Martin Bosák, PhD.

He works at the Department of Management Faculty of Business Economy University of Economics in Košice. He earned higher education and later a PhD. degree (1999) at Technical University of Kosice. In 2009 he earned prof.h.c. at Kokshetau University, Kazakhstan. He is an author or co-author of several monographs and textbooks in Slovakia and abroad. He is an author of several scientific and professional articles published in foreign and national journals and conference proceedings and he participated actively in national and international conferences. He is a team leader and participates in national and foreign projects. He devotes in his activity to areas of production management, environmental impact assessment of technologies, waste management and sustainable development.



Ing. Alexander Tarča, PhD.

He works at the Department of Information and Language Communication Faculty of Business Economy University of Economics in Košice. He earned higher education and later a PhD. degree (2010) at Technical University of Kosice. He is an author of several scientific and professional articles published in foreign and national journals and conference proceedings and he participated actively in national and international conferences. He participates in national and foreign projects. He devotes in his activity to areas of production management, environmental impact assessment of technologies, information management and project management.



doc. RNDr. Zuzana Hajduová, PhD.

She is Assistant Professor of Business Economics and Management. She is an expert on quantitative methods and mathematics, as well as their application in the field of economic policy. In her scientific endeavors she concentrates her empirical research on the quality, with the focus on Six Sigma. She participated in several research projects and scientific works for Department of Quantitative methods, Faculty of Business Economics with seat in Košice, University of Economics in Bratislava. She has published a lot of articles in various scientific journals. She has also participated in many international conferences and workshops. She is a member of many scientific committees of international and national conferences. He took part in the solution of many domestic and international projects.

Economic Evaluation of Energy Service Contract Implementation from the View of Its Participants

Anastasia A. Tupikina, Marina V. Rozhkova
Novosibirsk State Technical University, Novosibirsk, Russia

Abstract - The article considers one of the most promising tools for implementing measures to improve energy performance - the energy service contract (ESC). When considering the contract from the view of its participants, distinctive features of investment projects were revealed. The components of the cash flow generated under the contract for the customer and the energy service company (ESCO) are determined. An evaluation model of the ESC was developed, based on the net present value (NPV) criterion and taking into account the balance of interests of its participants. Approbation of the obtained model was carried out using the example of ESC, implemented at the energy company of the Siberian Federal District. Using the results obtained, recommendations were proposed to improve the performance based contract as a whole. The possibilities of using the obtained model in real conditions are determined.

Index Terms – Energy performance, energy service contract, investment project, economic efficiency, net present value.

I. INTRODUCTION

IMPROVING the energy performance of the Russian economy is a matter that has not lost its relevance for quite a long time. The demand, not only for energy performance technologies, but also for various energy performance tools, leads to the formation of new types of services in this field, including the Energy Service Contract (ESC). Although energy service in Russia can not be called an entirely new field of activity, according to experts, there are a large number of factors that impede the active development of the market for energy services [1, 2]. At the same time, the possibility of attracting an energy service company (ESCO) as a designer, executor and a source of financing activities to improve energy performance makes this type of interaction attractive for organizations that do not have sufficient experience and / or funds.

It is the possibility of transferring costs and risks in the implementation of the project to the ESCO gives explanation to the fact that the overwhelming majority of customers of ESC are represented by state and municipal institutions of various levels (in 2016 the share of commercial enterprises among customers was about 5%) [3, p. 7].

Unfortunately, it can not be said that this focus of energy services on budget organizations maximizes the energy performance of the country's economy as a whole, since the largest potential for energy saving in Russia (more than 30%) is currently concentrated in the fuel and energy sector and a quarter of the potential is in industry and housing and communal services [4].

One of the reasons for the lack of interest in ESC can be called the high risks that arise in the process of its conclusion and implementation by both the customer and the ESCO. Part of these risks is caused by the investment nature of the ESC, therefore, their reduction can be achieved through a competently constructed system for planning and forecasting various project parameters that affect the cash flows generated by it.

II. PROBLEM DEFINITION

Considering the ESCO from the positions of the ESCO and the customer, it is possible to distinguish for both sides distinctive features of the investment project:

1. The ESCO invests in the project, expecting to receive their return and additional income in the future through payments from the savings achieved.

2. The customer can also take part in the project financing. In addition, the ESC for the customer can be viewed to some extent as an installment payment for energy performance measures. As an effect, which the customer expects to receive is the saving of the energy resource in physical and monetary terms, which reduces its operating costs.

3. The ESC is concluded for a certain period, during which both the ESCO and the customer should fully pay back the costs incurred.

Thus, when deciding on the implementation of an ESC, as well as selecting its key parameters, an important role is played by the economic evaluation of the contract implementation.

It should be noted that in the process of concluding and implementing the ESC, its parties often have opposite interests regarding some of the main parameters of the project - for example, the price of the contract (the share of savings that is paid by ESCO on a regular basis), the contract term (it is more profitable for the customer to start earning all the savings wholly, the ESCO, on the contrary, should recoup the costs incurred), etc.

Thus, the performance of the project as a whole does not always mean the performance for each of the contract participants. It follows that it is necessary to develop a model for the economic evaluation of an ESC that takes into account the interests of its parties (the customer and the ESCO) and allows for the selection of the most significant project parameters.

To achieve this goal, the following main tasks must be solved:

1. Definition of the components of cash flows arising in the process of implementation of the ESC with the ESCO and the customer.

2. Construction of a model for the evaluation performance of an ESC, taking into account the balance of interests of its participants.

3. Approbation of the obtained model on the example of a real ESC.

The subject of the study is an energy service contract, implemented by one of the energy companies of the Siberian Federal District.

III. THEORY

The evaluation performance of the energy saving measures implemented within the framework of the energy service contract can be divided into 3 stages:

1. Overall evaluation performance of the energy saving project.

2. Evaluation performance of the project from the position of the ESC and the customer.

3. Selection or adjustment of the main parameters of the contract in order to maximize the cumulative effect.

The overall evaluation performance of the project is a standard evaluation of the investment project and is used, as a rule, for the feasibility study of the expediency of implementing measures to increase the performance. Thus, the evaluation performance of the project and the evaluation performance of the ESC should be divided.

As a basis for the formation of a model for the economic evaluation of ESC participants it is advisable to use the NPV as one of the most popular criteria for evaluation performance of investments.

First of all, it is necessary to determine the structure of cash flows arising in the process of implementing a contract from each of the parties and to compute formulas for calculating NPV.

Initial investments in project implementation (I_t , rub.), including costs for preliminary surveys and project preparation, project implementation, as well as transaction costs for attracting investments, can be divided between the contract parties in the ratio d_{ESCO} : $(1 - d_{ESCO})$, established by the contract.

Also important parameters of the project, common for the ESCO and the customer are: the contract term (T , years) and the discount rate (E , %).

For an ESC, the annual cash flow consists of the following components:

1. Payments from the received savings in monetary terms (PAY_t), forming the profitable part of the project. This parameter can be expressed by the formula (1):

$$PAY_t = \alpha_{ESCO} \cdot \Delta E_t \quad (1)$$

where α_{ESCO} , % – the price of the contract (the amount of money saved in the contract, transferred by the customer in favor of the ESCO);

ΔE_t , rub. – economy of the fuel and energy resource (FER) in monetary terms, taking into account the forecast prices for fuel and energy resources in the period t .

2. Project maintenance costs during the contract period (C_t , rub.), which may be represented by maintenance costs (if the contract provides for such obligation of ESCO), unforeseen expenses, interest on loans, taxes directly related to the project being implemented.

Thus, the NPV of an ESCO is determined according to formula (2):

$$NPV_{ESCO} = -\sum_{t=1}^T \frac{d_{ESCO} \cdot I_t}{(1+E)^t} + \sum_{t=1}^T \frac{PAY_t - C_t}{(1+E)^t} \quad (2)$$

As for the contract customer, the annual cash flow can be presented in the form of the following components:

1. The inflow of funds under the project is primarily represented by the share of energy savings that remains with the customer after payment of the ESCO of its share in accordance with the price of the contract:

$$E_{CUST,t} = (1 - \alpha_{ESCO}) \cdot \Delta E_t \quad (3)$$

2. The profit from the increase in output related to the increase in equipment productivity ($NP_{REAL,t}$, rub.), which is the difference between the income from sales of this product ($D_{REAL,t}$, rubles), operating costs associated with the use of new equipment ($C_{EXP,t}$, rub) and income tax ($H_{NP,t}$, rub).

3. Effects from the project implementation that arise beyond the boundaries of the object ($D_{EC,t}$, rub.), which can be either positive or negative.

4. Interest on loans (PC_t , rub.).

5. Residual value of equipment / assets that are transferred to the ownership of the customer upon completion of the contract ($K_{BAL,t}$, rub).

Then the NPV of the customer:

$$NPV_{CUST} = -\sum_{t=1}^T \frac{(1 - d_{ESCO}) \cdot I_t}{(1+E)^t} + \frac{K_{BAL}}{(1+E)^T} + \sum_{t=1}^T \frac{E_{CUST,t} + NP_{REAL,t} \pm D_{EC,t} - PC_t}{(1+E)^t} \quad (4)$$

It is obvious that the energy service contract can be concluded only on the terms of mutually beneficial cooperation. It follows that when choosing the main parameters of the contract, it is advisable to follow the principle of the maximum cumulative efficiency of contract participants. Thus, the target function of the model will look like this:

$$f = NPV_{ESCO} + NPV_{CUST} \rightarrow \max \quad (5)$$

Since the energy service contract can be presented as separate investment projects for the customer and ESCOs with interconnected cash flows, in evaluating its performance, it is also necessary to observe the condition of non-negativity of the NPV of each participant:

$$\begin{aligned} NPV_{ESCO} &\geq 0 \\ NPV_{CUST} &\geq 0 \end{aligned} \quad (6)$$

The relations presented in formula (6) are model constraints.

As the optimized parameters of the model, it is necessary to consider such parameters of the ESC, the magnitude of which has the opposite effect on the NPV of the customer and the ESCO:

1. The price of the contract, which directly affects the annual distribution of the amount of savings between the parties ($\alpha_{ESCO}, \%$).

2. Distribution of initial investments between the customer and the ESCO ($d_{ESCO}: (1 - d_{ESCO}), \%$).

3. Term of the contract (T , years). For the customer, as a rule, it is of interest to shorten the contract term in order to obtain savings in full as soon as possible. For an ESCO, on the contrary, the term of the contract should ensure the payback of the invested funds, and its increase allows increasing the cumulative efficiency of investments.

Due to the fact that optimization in three parameters is a rather laborious task, in order to simplify this procedure, it is possible to specify one of the parameters as the target and the subsequent optimization of the variants of combinations of optimized parameters that remain by the method of searching and constructing the matrix of values of the objective function.

IV. EXPERIMENTAL RESULTS

With a view to approbation of the presented model, a project implemented by one of the thermal power stations of the Siberian Federal District was considered in 2013. The project assumed the replacement of heat network insulation in order to reduce losses to the normative level. The implementation of this project is not only conditioned by technical necessity, but also economically feasible, which is confirmed by the following facts:

1. Almost at all sections of pipelines the service life of the insulation exceeds the normative one.

2. There are complaints to the administration from consumers "forced to pay losses through bare pipes".

3. According to the overall evaluation performance of the project, given in the business plan, the NPV of the project is 5.575 million rubles.

The involvement of an energy service company in the implementation of this project is due, first of all, to the limitations imposed by the existing tariff system on the possibility of including costs for modernization and repair activities of capital funds in a regulated tariff for thermal energy. A high degree of deterioration of heat networks and a lack of funds to invest in their rehabilitation is one of the main problems of heat power engineering. Thus, it is necessary to evaluate the performance of this project on the part not only of the customer, but also of the ESCO.

The main parameters of the project are given below:

The cost of replacement insulation (I_0) - 70.6 million rubles. (including overheads and estimated profit of the contractor). It is planned to finance the project by the ESC in full ($d_{ESCO} = 100\%$).

The planned term of the project (T) is 5 years.

Savings in volume terms are defined as the difference between actual losses through pipeline insulation in the base period (ΔQ_{BASE} , Gcal) and standard losses (ΔQ_{STAND} , Gcal), the levels of which are planned to be achieved during the project implementation. As a cost component, the fuel component of the cost of thermal energy (s_t^B , RUR / Gcal) is used, estimated due to the company's fuel balance and price

indexes for various types of fuel). Thus, the effect of implementing measures to replace insulation (ΔE_t , rub.) is estimated by the formula (7):

$$\Delta E_t = (\Delta Q_{BASE} - \Delta Q_{STAND}) \cdot s_t^B \quad (7)$$

The distribution of savings between the ESCO and the customer according to the initial plan is 80 / 20%.

An estimate of the savings in monetary terms and its distribution among the parties is shown in Figure 1 (the calculation was carried out for 10 years with a view to further considering the extension of the project implementation period).

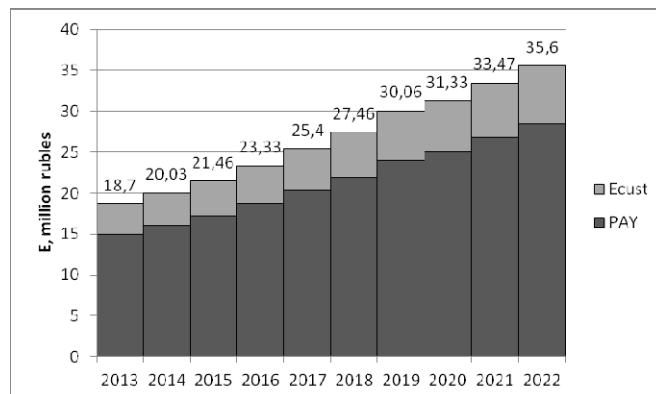


Fig. 1. The forecast of saving fuel and energy resources for the project in monetary terms.

The annual costs of the ESCO for this project consist of the following values (C_i):

1. Interest on loans, calculated on the basis of drawing up a credit schedule at an interest rate of 10%.

2. Expenses for the maintenance of the facility during the contract period, represented by the costs of conducting annual surveys, the binding nature of which is fixed by the contract. The costs are estimated on the basis of the business plan of the analogue facility (testing in another part of the heat networks of the same company). The project does not involve other costs for exploitation of the insulation by the ESCO.

For the project customer under this contract, negative cash flows are absent, which is due to the following reasons:

1. Revenues from increased productivity are not available due to limited revenue from the company's sales schedules for the heat load of consumers.

2. When concluding an energy service contract, the planned replacement of thermal insulation is a repair work and it is not supposed to be included in the investment program as a reconstruction or modernization program. Thus, this project does not generate depreciation charges, since it does not imply a change in the value of fixed assets.

3. According to cl. 14 of the Government Decision no. 1075 "when implementing the plan for energy saving measures and improving energy performance, the period of the additional organization's funds saved by the organization due to cost reduction is 2 years after the end of the payback period of the specified activities" [5]. It follows that the payment for services of an energy service company is realized from the amount of energy savings and may not be included in the cash flow of the project.

The discount rate for the project (E) is equal to the rate of return on the invested capital in the heat supply sector set by the order of the Federal Tariff Service of Russia of 16.12.2013 No. 1618-e [6] at the level of 10.96%.

With such distribution of investments and saving of fuel and energy resources, the corporate-customer essentially receives exclusively positive flows in the form of a share of savings determined by the price of the contract. The NPV of the customer for the project implementation period with the initial values of the parameters is 15.86 million rubles, which is 3 times higher than the total figure for the project.

However, with this allocation of savings and investments for 5 years of project implementation, the NPV of the ESCO is -39.78 million rubles. Thus, according to the proposed model, not only one of the constraints ($NPV_{ESCO} < 0$) is not fulfilled, but also the objective function of the model takes a negative value (-23.9 million rubles).

The redistribution of savings in favor of ESCO ($d_{ESCO} = 100\%$) does not give a positive result, since the customer in this case does not have any cash flows at all, and the NPV of the energy service company, as well as the objective function of the model, remains negative (-23.9 million rubles.). Thus, despite the positive economic efficiency of the project as a whole, the conclusion of an energy service contract on baseline conditions is impossible because of the inefficiency of this project for an energy service company. The solution to this problem can be a change in the initial parameters of the contract and their optimization using the proposed model.

V. DISCUSSION OF RESULTS

As possible solutions for increasing the cumulative efficiency of the project in question, the following methods can be proposed:

Option 1. Expansion of the contract to 10 years (the standard life of insulation) with preservation of the initial allocation of investment and savings.

Option 2. Increase the contract period to 10 years (the standard lifetime of the insulation), while preserving the initial distribution of investment and redistribution of savings.

Option 3. Redistribution of investments between the ESCO and the customer. As a source of partial financing of the project, the customer can use funds from the repair fund in the amount of 10.6 million rubles. The allocation of investments and the duration of the contract are thus optimized parameters.

The results of calculating the project performance for the options considered are presented in Table 1.

TABLE I
PROJECT PERFORMANCE IMPLEMENTATION AT VARIOUS
VALUES OF INITIAL PARAMETERS

| Option | 1 | 2 | 3.1 | 3.2 | 3.3 |
|-------------------------|-------|-------|-------|------|-------|
| T, years | 10 | 10 | 8 | 7 | 8 |
| d_{ESCO} , % | 100 | 100 | 85 | 85 | 85 |
| α_{ESCO} , % | 80 | 89 | 80 | 85 | 85 |
| NPV_{ESCO} , mln.rub | 3,14 | 16,45 | 3,38 | 1,23 | 9,48 |
| NPV_{CUST} , mln.rub. | 29,57 | 16,26 | 13,83 | 5,68 | 7,73 |
| f, mln.rub. | 32,71 | 32,71 | 17,21 | 6,91 | 17,21 |

The results obtained can be characterized as follows:

1. Extending the term of the contract by 2 times allows to achieve an increase in both the cumulative efficiency and efficiency for each of the participants (for the customer, the NPV increases almost for 2 times). However, such decision may entail difficulties in reconciling long-term heat tariffs with regulators, which should be taken into account.

2. The option of extending the period with the redistribution of savings between the customer and the ESCO can be described as the most "fair", since this option allows achieving almost equal NPV values for the customer and the ESCO while maintaining the cumulative effect. In this case, the NPV of the customer is close enough in value to the original version.

For the case of redistribution of investments between the customer and the ESCO, various combinations of the term and the price of the contract were considered. Based on the obtained NPV values, there are 3 characteristic variants:

3.1. If the contract price is kept at the level of 80%, the minimum contract term, which provides the ESCO with the return of the invested funds is 8 years.

3.2. The minimum term of the contract, at which the cumulative effect takes a positive value - 7 years. With this option, the minimum contract price should be 85%.

3.3. The option in which NPV customers and ESCOs are close to each other ("fair" option) - the contract period is 8 years with a contract price of 85%.

Thus, from the view of maximizing the cumulative effect and respecting the principles of mutually beneficial cooperation, the most preferable is the 2 variant of the combination of contract parameters. Nevertheless, using the proposed model, the customer can choose such initial parameters of the energy service contract, which are more in line with his available funding and cost constraints.

VI. CONCLUSION

Thus, the evaluation performance of measures implemented within the framework of an ESC is a complex, multi-step process, the importance of which can not be overemphasized. The investment nature of the ESC, as well as the opposite of the interests of its parties, substantially increase the risk of this type of activity. At the same time, despite possible conflicts between the customer and the ESCO, the ESC should remain a mutually beneficial type of cooperation.

The proposed model for evaluation performance of the ESC allows not only to maximize the cumulative effect, which, incidentally, may differ significantly from the project performance indicators calculated without the conditions of the energy service, but also to preserve the balance of the interests of the customer and the ESCO. In practical terms, this model can have several applications:

- determination of optimal contract parameters when concluding an ESC;
- determination of the initial parameters of the contract by the customer for the purpose of their inclusion in competitive conditions (when selecting an ESCO through a tender);
- an assessment of the feasibility of concluding an ESC for given initial parameters.

Further development of this research implies the approbation of the model obtained by the example of contracts of various sectoral direction in order to identify the need for adjustments.

REFERENCES

- [1] Tulikov A.V. Market of energy services in Russia: vague prospects or a growth tool? // Energy saving. 2015. № 3. P. 8-11. (in Russian).
- [2] Ivanov G.N. Energy service contracts - application in the Russian practice [Electronic resource] // Energosovet. 2011. № 2 (15). URL: http://www.energosovet.ru/bul_stat.php?idd=150 (reference date: 05/20/2017). (in Russian).
- [3] A Brief Overview of the Russian Energy Services Market for 2016 - Moscow: RAESKO, 2017. - 12 p. (in Russian).
- [4] Bushuev V.V. Energy Efficiency as a Factor of Sustainable Development of the RF Economy (using the example of ES-2030) / Institute of Energy Strategy; Ministry of Energy of Russia; Union of Oil and Gas Producers of Russia. - 2009 (in Russian).
- [5] Decree of the Government of the Russian Federation No. 1075 dated October 22, 2012 (as amended on 08.02.2018) "On Pricing in the Sphere of Heat Supply".
- [6] Order of the Federal Tariff Service (FTS of Russia) of December 16, 2013 N 1618-e Moscow "On approval of the minimum rate of return for calculation of tariffs in the sphere of heat supply using the method of ensuring the return on invested capital for a long-term period of regulation with the beginning of long-term regulatory period in 2014 " (in Russian).



Tupikina Anastasia Alexeevna
Novosibirsk State Technical University,
Novosibirsk, Russia
Senior lecturer of the Department "Production
Management and Economics of Energy"
Area of scientific interests: energy saving and
energy efficiency, planning at power companies
E-mail: tupikina.aa@mail.ru



Marina V. Rozhkova
South Caucasus, Azerbaidjan in 1963; Senior
Lecturer of the Department of "Foreign
Languages" of Novosibirsk State Technical
University; Fields of interests are economics and
technology as far as English is concerned; Area
of expertise is English Teaching Methodology
and Teaching Translation Techniques.
(Address: 20, K.Marksa, Novosibirsk, 630073,
Russian Federation).
Email: marina.rozhkova.63@mail.ru

THE CONTENTS

| | |
|--|----|
| KHARITONOV S.A., KHARITONOV A.S., KALUZHSKIY D.L., VOROBYEVA S.V. | 13 |
| Analytical research of electromagnetic processes in direct current starter-generator system «Synchronous generator with combined excitation – active rectifier» (generation mode), Novosibirsk, Russia | |
| ZINOVIEV G.S., UDOVICHENKO A.V. | 21 |
| Reactive power compensators based on simple AC voltage regulators), Novosibirsk, Russia | |
| DYBKO M.A., TOKAREV V.G., BROVANOV S.V., KHARITONOV S.A. | 25 |
| Performance evaluation of shunt active power filter based on parallel multilevel inverters), Novosibirsk, Russia | |
| GRISHANOV E.V., BROVANOV S.V. | 32 |
| Theoretical aspects of the common-mode leakage current suppression in a photovoltaic power generation system based on multilevel H-bridge type converters), Novosibirsk, Russia | |
| EFIMOV A.A. | 38 |
| Dynamic and energy performances of voltage active converter at its operation on elevated frequencies, Saint-Petersburg, Russia | |
| ZINOVIEV G.S. | 44 |
| Development of set of electric energy quality factors, Novosibirsk, Russia | |
| GARGANEEV A.G., KASHEUTOV A.V., KASHIN E.I. | 48 |
| Phase current curve analyzing of hysteresis-synchronous motor powered with autonomous voltage inverter, Tomsk, Russia | |
| ANTONOV A.A., SURIN I.K., PICHUGIN I.V., VASILYEV V.YU. | 52 |
| A ZVS/ZCS hybrid driver integrated circuit in 250 nm BCD technology for energy-efficient switch mode power supply units, , Novosibirsk, Russia | |
| YURKEVICH V.D., ZINOVIEV G.S. | 58 |
| Robust voltage tracking control of three-phase four- wire split DC bus inverter via time-scale separation technique, Novosibirsk, Russia | |
| MARTINOVICH M.V., BELOVA I.A., SKOLOTA V.A., ZAEV I.V. | 65 |
| Neural network load current observer for DC converter, Novosibirsk, Russia | |

| | |
|--|-----|
| FILYUSHOV YU.P., SIMAKOV G.M., PALAGUSHKIN B.V. The rule of electric drive multi criteria optimization solutions choice, Novosibirsk, Russia | 71 |
| IVANOV V.V., MYATEZH S.V., KAPUSTIN A.V., ALEKSEEVA I.K. Improvement of controllable zone-phase regulated rectifiers by structural synthesis methods means, Novosibirsk, Russia | 76 |
| VOLKOV A.G. Power generation system for wind turbines based on novel multizone converters , Novosibirsk, Russia | 81 |
| CHERNAYA M.M., OSIPOV A.V., SHINYAKOV YU.A., SUKHORUKOV M.P. Prospects in the field of energy-conversion devices design for high-voltage power systems, Tomsk, Russia | 86 |
| ZAPOLSKIY S.A., OSIPOV A.V., ZHURAVLEV I.M., KHLYSTUNOV M.E. Single-cycle LCL-T resonant converter for solar battery, Tomsk, Russia | 90 |
| MATVEYEV D.A., BALZAMOV A.YU., FEDOTOV YU.B., NESTEROV S.A. Universal control system of a semiconductor electric energy converter on programmable logic devises, Saransk, Russia | 94 |
| SIDOROV V.E., SHTEIN D.A., ZAEV I.V., KHOROSHEV M.A. Mathematical analysis of multiport converter operation modes, Novosibirsk, Russia | 102 |
| KUROCHKIN D.A., GEIST A.V., SHTEIN D.A., VOLKOV A.G. Development of boost converter mathematical model with an additional inductance (1C2-2L) , Novosibirsk, Russia | 106 |
| KHOROSHEV M.A., MAKAROV D.V., ZAEV I.V., SIDOROV V.E. Analysis of dynamic processes in the electric power generating system of variable frequency for aircrafts, Novosibirsk, Russia | 112 |
| DYMOV I.S., KOTIN D.A. Signal-adaptive current controller in the cascade system of rotor radial displacement updating, Novosibirsk, Russia | 119 |
| KABIROV V.A., SEMYONOV V.D., VINTONYAK N.P., BORODIN D.B., TYUNIN S.S. Digital pulse-width modulator with asynchronous change of compare register value and short delay time, Tomsk, Russia | 124 |

| | |
|--|-----|
| KRAMARENKO N.V. Soft capture of movable target by robot-manipulator, Novosibirsk, Russia | 130 |
| MANUSOV V.Z., KHRIPKOV V.V. Comparative analysis of mathematical models for the coefficient of conductor resistance increase due to higher harmonics, Novosibirsk, Russia | 133 |
| RYKOV A.A., ISAKOV P.Y. Motion control algorithms for points, Novosibirsk, Russia | 137 |
| RASHITOV P.A., VERSHANSKIY E.A., PETROV M.I. Influence of the topology of the distributed series compensation devices on power transformer losses, Moscow, Russia | 143 |
| OSIPOV A.V., LOPATIN A.A., LATYPOV R.A., SHEMOLIN I.S. Soft switching stacked-up boost push-pull converter, Tomsk, Russia | 148 |
| LOPATKIN N.N., LUCENKO I.S., CHERNOV YU.A. Virtual instrument for assessment of simulated signal integrated harmonics factors), Biysk, Russia | 152 |
| LOPATKIN N.N. Assessment of output voltage quality of three-phase multilevel inverter with nearest vector selecting space vector control), Biysk, Russia | 158 |
| LOPATKIN N.N. Aggregate factors of switchings and integrated voltage harmonics of three-phase multilevel voltage source inverter with nearest vector selecting space vector control), Biysk, Russia | 164 |
| ABDRAKHMANOV V.KH., SALIKHOV R.B., VAZHDAEV K.V. Development of a sound recognition system using STM32 microcontrollers for monitoring the state of biological objects, Ufa, Russia | 170 |
| BASINYA E.A., KAZARBIN S.V. Personal computer user`s activity monitoring software development for the enterprise business process optimizing, Novosibirsk, Russia | 174 |
| BASINYA E.A., RAVTOVICH YU.K. Implementation of an intrusion detection and prevention system module for corporate network traffic management, Novosibirsk, Russia | 178 |
| BOBOBEKOV K.M. A polynomial method for synthesizing a two-channel regulator stabilizing a three-mass system, Novosibirsk, Russia | 184 |

| | |
|--|-----|
| BORISOV A.P. Development of a monitoring and management system for the study of energy-intensive processes of processing agricultural raw materials, Barnaul, Russia | 190 |
| BUTYRLAGIN N.V., CHERNOV N.I., PROKOPENKO N.N., YUGAI V.YA. CMOS current logic elements: application features for processing analog and digital signals, Rostov-on-Don, Russia , Zelenograd, Russia | 196 |
| DVORNIKOV O.V., DZIATLAU V.L., TCHEKHOVSKI V.A., PROKOPENKO N.N., BUGAKOVA A.V. Basic parameters and characteristics of the Op-Amp based on the BiJFet array chip MH2XA030 intended for the design of radiation-hardened and cryogenic analog ICs, Minsk, Belarus, Zelenograd, Russia | 200 |
| FILIMONOV A.B., FILIMONOV N.B. The peculiarities of application of the potential fields method for the problems of local navigation of mobile robots, Moscow, Russia | 208 |
| FRANTSUZOVA G.A. PI2D-controllers synthesis for nonlinear non-stationary plants, Novosibirsk, Russia | 212 |
| GUNKO A.V., SEROKLINOV G.V. Features of estimation of resistance of separate grades of wheat to influence of various stress factors on change of biological potentials, Novosibirsk, Russia | 217 |
| HALINA T.M., STALNAYA M.I., IVANOV I.A., RYBALKINA T.I., RYAZANOVA E.D. Speed regulation of single-phase engines used in agriculture), Barnaul, Russia | 223 |
| IVOILOV A.YU., ZHMUD V.A., TRUBIN V.G., ROTH H. Using the numerical optimization method for tuning the regulator coefficients of the two-wheeled balancing robot, Novosibirsk, Russia, Siegen, Germany | 228 |
| KARGIN V.A., VOLGIN A.V., MOISEEV A.P. Adaptive system for automatic control of output effort of electromagnetic sausage-filler, Saratov, Russia | 237 |
| KRASNOVA S.A. Cascade synthesis of external perturbations observers based on virtual models , Moscow, Russia | 241 |

| | |
|--|-----|
| KUZNETSOV S.A., PIVTSOV V.S., SEMENKO A.V. A powerful single-mode diode laser with automated control as the source of pumping of the ytterbium laser, Novosibirsk, Russia | 247 |
| LARINA L.V., RUSLJAKOV D.V., TIKHONOVA O.B. Experimental installation for the investigation of the influence of the methods of feeding on the relative humidity of capillary-porous materials with the built-in software, Rostov-on-Don, Russia | 252 |
| MURAVYOVA E.A., SHARIPOV M.I. Intelligent control system for process parameters based on a neural network, Sterlitamak, Russia | 256 |
| VOTRINA O.A., SABLINA G.V. Development of the stabilizing algorithm for pendulum systems based on modal technique, Novosibirsk, Russia | 261 |
| SALIKHOV R.B., ZAINITDINOVA A.A. System of monitoring and remote control of microclimate in greenhouses, Ufa, Russia | 265 |
| STUKACH O.V., ERSHOV I.A., SYCHEV I.V. Towards the distributed temperature sensor with potential characteristics of accuracy, Tomsk, Russia, Novosibirsk, Russia | 268 |
| TKALICH V.L., LABKOVSKAIA R.IA., PIROZHNIKOVA O.I., KALINKINA M.E., KOZLOV A.S. Analysis of errors in micromechanical devices, St. Petersburg, Russia | 272 |
| UTKIN A.V., UTKIN V.A. Robust control algorithm for turbine – generator unit, Moscow, Russia | 277 |
| UTKIN A.V., KRASNOVA S.A. Decomposition principle in the problem of synthesis of state observers for SISO systems under the action of external disturbances, Moscow, Russia | 284 |
| VOEVODA A.A., BOBOBEKOV K.M. Reduction of the matrix polynomial decomposition of the transfer function to a coprime form using the Sylvester matrix, Novosibirsk, Russia | 290 |
| VOSKOBOINIKOV YU.E., KRYSOV D.A. A stabilized algorithm of nonparametric identification for a system with high-level noise measurement of input signal, Novosibirsk, | 295 |

| | |
|---|-----|
| Russia | |
| ZHMUD V.A., DIMITROV L.V., IVOYLOV A.YU. Additional simplification of the precision frequency synthesizer, Novosibirsk, Russia, Sofia, Bulgaria | 301 |
| ZHMUD V.A., DIMITROV L.V., IVOYLOV A.YU. Providing of smooth switching of sine signals for precision frequency synthesizer, Novosibirsk, Russia, Sofia, Bulgaria | 307 |
| ZHMUD V.A., DIMITROV L.V., TRUBIN V.G., ROTH H. Control of object in the loop with feedback using imperfect sensors of position and acceleration, Novosibirsk, Russia, Sofia, Bulgaria, Siegen, Germany | 312 |
| ZHMUD V.A., TAICHENACHEV A.V., DIMITROV L.V., SEMIBALAMUT V.M. Smart phase locking of the frequency of two identical lasers to each other, Novosibirsk, Russia, Sofia, Bulgaria | 319 |
| AMANZHOLOVA B.A., FRIBUS N.V., KHOMENKO E.V. Development of methods and procedures of the analysis of corporate social responsibility of manufacturing companies, Novosibirsk, Russia | 327 |
| AMANZHOLOVA B.A., TESLYA P.N. Threats and opportunities of cryptocurrency technologies, Novosibirsk, Russia | 335 |
| BADMAEVA V.G., LITVINTSEVA G.P. Innovation strategies as a basis for the development of household care markets in Russia, Novosibirsk, Russia | 340 |
| BALABIN A.A. On the impact of lending rates on structural changes in the Russian economy, Novosibirsk, Russia | 343 |
| BUTOVA T.G., DANILINA E.P., KANYUKOVA E.A. Modern technologies in assessing the quality of medical services in the digital society of Russia, Krasnoyarsk, Russia | 348 |
| CHERNOV S.S., ROZHKOVA M.V. The mechanism for determining the initial conditions when concluding concession agreements based on the balance of interests of the parties of public-private partnership, Novosibirsk, Russia | 352 |

| | |
|--|-----|
| DRAGUNOVA E.V., PUSTOVALOVA N.V., VALDMAN I.A. Innovative technologies in designing new learning ecosystems, Novosibirsk, Russia | 358 |
| DRONOVA YU.V., MOSHKIN B.N., KAMYSHEVA E.YU. Overhead power transmission lines economic efficiency diagnostic assessment , Novosibirsk, Russia | 365 |
| EDER L.V., PROVORNAYA I.V., KULIK A.A., NEMOV V.YU. Economic aspects of the sustainable technological development of the oil and gas industry in the context of low oil prices and the current situation in the energy markets, Novosibirsk, Russia | 368 |
| FILIMONOVA I.V., KOMAROVA A.V., MISHENIN M.V. Technical, economic and fiscal aspects of increasing the efficiency of development of oil and gas regions in the east of Russia, Novosibirsk, Russia | 374 |
| KARELIN I.N. Dependence of wages on the duration of training and length of service in the Russian economy sectors, Novosibirsk, Russia | 379 |
| KIRILLOV YU.V., DRAGUNOVA E.V., KRAVCHENKO A.V. On the implementation of innovative projects. The effect of the investment leverage, Novosibirsk, Russia | 384 |
| KOLKOVA N.A., CHERNOV S.S. Benchmarking models for the regulation of electricity distribution companies , Novosibirsk, Russia | 390 |
| KRAVCHENKO N.A., GORYUSHKIN A.A., IVANOVA A.I., KUZNETSOVA S.A., KHALIMOVA S.R., YUSUPOVA A.T. Russian high tech companies: growth factors and limitations, Novosibirsk, Russia | 398 |
| LUGACHEVA L.I., MUSATOVA M.M., SOLOMENNKOVA E.A. Financial and economic aspects of diversification formation patterns in strategy development of regional mechanical engineering, Novosibirsk, Russia | 402 |
| MALYKH O.E., GAFAROVA E.A. Resources of developing hi-tech spheres in Russia, Ufa, Russia | 409 |
| MAMONOV V.I., MILEKHINA O.V. Digital transformation of enterprises of | 413 |

| | |
|---|-----|
| microelectronics, Novosibirsk, Russia | |
| MARKOVA V.D., KUZNETSOVA S.A. Ecosystems as network forms of business organization, Novosibirsk, Russia | 418 |
| NEVZOROVA E.N., KIREENKO A.P., LEONTYEVA YU.V. If development of technologies can win shadow economy, Irkutsk, Russia, Vladivostok, Russia, , Ekaterinburg, Russia | 422 |
| ROZHDENSTVENSKAYA L.N., ROGOVA O.V. Creation of software product supporting the development of high-tech food production of functional &special purpose, Novosibirsk, Russia | 429 |
| ROZHN OV I.P., AVRAMCHIKOVA N.T., BELYAKOVA G.Y. Building a quality system for an electronic component base for high-tech industries, Krasnoyarsk, Russia | 433 |
| ROZUMNAYA N.V., EGOROV A.D., TUTRINA A.Y. Return on investment study for the project of energy-saving devices implementation, Novosibirsk, Russia | 437 |
| SHCHEKOLDIN V.YU., TSOY M.YE. The application of modified RFM-analysis to increase the loyalty of consumers of industrial rubber articles, Novosibirsk, Russia | 443 |
| STEPANOVA S.V., KARAKCHIEVA V.L. Changes in banking business models driven by technological innovations, Novosibirsk, Russia | 447 |
| ŠTOFOVÁ L., SZARYSZOVÁ P., BOSÁK M., TARČA A., HAJDUOVÁ Z. Ambient intelligence for increasing innovation performance of enterprises, Košice, Slovak Republic | 452 |
| TUPIKINA A.A., ROZHKOVA M.V. Economic evaluation of energy service contract implementation from the view of its participants, Novosibirsk, Russia | 459 |

AUTHOR INDEX

| | | | | | |
|--------------------|-------------|------------------|-----------------------------|------------------|-------------|
| Abdrakhmanov V.Kh. | 170 | Chernov S.S. | 352, 390 | Gafarova E.A. | 409 |
| Alekseeva I.K. | 76 | Chernov Yu.A. | 152 | Garganeev A.G. | 48 |
| Amanzholova B.A. | 327, 335 | Danilina E.P. | 348 | Geist A.V. | 106 |
| Antonov A.A. | 52 | Dimitrov L.V. | 301, 307, 312, 319 | Goryushkin A.A. | 398 |
| Avramchikova N.T. | 433 | Dragunova E.V. | 358, 384 | Grishanov E.V. | 32 |
| Badmaeva V.G. | 340 | Dronova Yu.V. | 365 | Gunko A.V. | 217 |
| Balabin A.A. | 343 | Dvornikov O.V. | 200 | Hajduová Z. | 452 |
| Balzamov A.Yu. | 94 | Dybko M.A. | 25 | Halina T.M. | 223 |
| Basinya E.A. | 174, 178 | Dymov I.S. | 119 | Isakov P.Y. | 137 |
| Belova I.A. | 65 | Dziatlau V.L. | 200 | Ivanov I.A. | 223 |
| Belyakova G.Y. | 433 | Eder L.V. | 368 | Ivanov V.V. | 76 |
| Bobobekov K.M. | 184, 290 | Efimov A.A. | 38 | Ivanova A.I. | 398 |
| Borisov A.P. | 190 | Egorov A.D. | 437 | Ivoilov A.Yu. | 228 |
| Borodin D.B. | 124 | Ershov I.A. | 268 | Ivoylov A.Yu. | 301, 307 |
| Bosák M. | 452 | Fedotov Yu.B. | 94 | Kabirov V.A. | 124 |
| Brovanov S.V. | 25, 32 | Filimonov A.B. | 208 | Kalinkina M.E. | 272 |
| Bugakova A.V. | 200 | Filimonov N.B. | 208 | Kaluzhskij D.L. | 13 |
| Butova T.G. | 348 | Filimonova I.V. | 374 | Kamysheva E.Yu. | 365 |
| Butyrlagin N.V. | 196 | Filyushov Yu.P. | 71 | Kanyukova E.A. | 348 |
| Chernaya M.M. | 86 | Frantsuzova G.A. | 212 | Kapustin A.V. | 76 |
| Chernov N.I. | 196 | Fribus N.V. | 327 | Karakchieva V.L. | 447 |
| | | | | Karelin I.N. | 379 |
| | | | | Kargin V.A. | 237 |

| | | | | | |
|-----------------|----------|-------------------|---------------|------------------------|-------------|
| Kasheutov A.V. | 48 | Kuznetsov S.A. | 247 | Musatova M.M. | 402 |
| Kashin E.I. | 48 | Kuznetsova S.A. | 398, 418 | Myatezh S.V. | 76 |
| Kazarbin S.V. | 174 | Labkovskaia R.Ia. | 272 | Nemov V.Yu. | 368 |
| Khalimova S.R. | 398 | Larina L.V. | 252 | Nesterov S.A. | 94 |
| Kharitonov A.S. | 13 | Latypov R.A. | 148 | Nevzorova E.N. | 422 |
| Kharitonov S.A. | 13, 25 | Leontyeva Yu.V. | 422 | Osipov A.V. | 86, 90, 148 |
| Khlystunov M.E. | 90 | Litvintseva G.P. | 340 | Palagushkin B.V. | 71 |
| Khomenko E.V. | 327 | Lopatin A.A. | 148 | Petrov M.I. | 143 |
| Khoroshev M.A. | 102, 112 | Lopatkin N.N. | 152, 158, 164 | Pichugin I.V. | 52 |
| Khripkov V.V. | 133 | Lucenko I.S. | 152 | Pirozhnikova O.I. | 272 |
| Kireenko A.P. | 422 | Lugacheva L.I. | 402 | Pivtsov V.S. | 247 |
| Kirillov Yu.V. | 384 | Makarov D.V. | 112 | Prokopenko N.N. | 196, 200 |
| Kolkova N.A. | 390 | Malykh O.E. | 409 | Provornaya I.V. | 368 |
| Komarova A.V. | 374 | Mamonov V.I. | 413 | Pustovalova N.V. | 358 |
| Kotin D.A. | 119 | Manusov V.Z. | 133 | Rashitov P.A. | 143 |
| Kozlov A.S. | 272 | Markova V.D. | 418 | Ravtovich Yu.K. | 178 |
| Kramarenko N.V. | 130 | Martinovich M.V. | 65 | Rogova O.V. | 429 |
| Krasnova S.A. | 241, 284 | Matveyev D.A. | 94 | Roth H. | 228, 312 |
| Kravchenko A.V. | 384 | Milekhina O.V. | 413 | Rozhdenstvenskaya L.N. | 429 |
| Kravchenko N.A. | 398 | Mishenin M.V. | 374 | Rozhkova M.V. | 352, 459 |
| Krysov D.A. | 295 | Moiseev A.P. | 237 | Rozhnov I.P. | 433 |
| Kulik A.A. | 368 | Moshkin B.N. | 365 | | |
| Kurochkin D.A. | 106 | Muravyova E.A. | 256 | | |

| | | | | | |
|--------------------|-------------|-------------------|-------------|---------------------|-------------------------------------|
| Rozumnaya N.V. | 437 | Stukach O.V. | 268 | Vershanskiy E.A. | 143 |
| Rusljakov D.V. | 252 | Sukhorukov M.P. | 86 | Vintonyak N.P. | 124 |
| Ryazanova E.D. | 223 | Surin I.K. | 52 | Voevoda A.A. | 290 |
| Rybalkina T.I. | 223 | Sychev I.V. | 268 | Volgin A.V. | 237 |
| Rykov A.A. | 137 | Szaryszová P. | 452 | Volkov A.G. | 81, 106 |
| Sablina G.V. | 261 | Taichenachev A.V. | 319 | Vorobyeva S.V. | 13 |
| Salikhov R.B. | 170, 265 | Tarča A. | 452 | Voskoboinikov Yu.E. | 295 |
| Semenko A.V. | 247 | Tchekhovski V.A. | 200 | Votrina O.A. | 261 |
| Semibalamut V.M. | 319 | Teslya P.N. | 335 | Yugai V.Ya. | 196 |
| Semyonov V.D. | 124 | Tikhonova O.B. | 252 | Yurkevich V.D. | 58 |
| Seroklinov G.V. | 217 | Tkalich V.L. | 272 | Yusupova A.T. | 398 |
| Sharipov M.I. | 256 | Tokarev V.G. | 25 | Zaev I.V. | 65, 102, 112 |
| Shchekoldin V.Yu. | 443 | Trubin V.G. | 228, 312 | Zainitdinova A.A. | 265 |
| Shemolin I.S. | 148 | Tsoy M.Ye. | 443 | Zapolskiy S.A. | 90 |
| Shinyakov Yu.A. | 86 | Tupikina A.A. | 459 | Zhmud V.A. | 228, 301, 307, 312, 319 |
| Shtein D.A. | 102, 106 | Tutrina A.Y. | 437 | Zhuravlev I.M. | 90 |
| Sidorov V.E. | 102, 112 | Tyunin S.S. | 124 | Zinoviev G.S. | 21, 44, 58 |
| Simakov G.M. | 71 | Utkin A.V. | 277, 284 | | |
| Skolota V.A. | 65 | Utkin V.A. | 277 | | |
| Solomennikova E.A. | 402 | Valdman I.A. | 358 | | |
| Stalnaya M.I. | 223 | Vasilyev V.Yu. | 52 | | |
| Stepanova S.V. | 447 | Vazhdaev K.V. | 170 | | |
| Štofová L. | 452 | | | | |

2018 14TH INTERNATIONAL SCIENTIFIC-TECHNICAL
CONFERENCE ON ACTUAL PROBLEMS
OF ELECTRONIC INSTRUMENT ENGINEERING
PROCEEDINGS
APEIE-2018
In 8 Volumes

МАТЕРИАЛЫ XIV МЕЖДУНАРОДНОЙ НАУЧНО-
ТЕХНИЧЕСКОЙ КОНФЕРЕНЦИИ
«АКТУАЛЬНЫЕ ПРОБЛЕМЫ ЭЛЕКТРОННОГО
ПРИБОРОСТРОЕНИЯ»
АПЭП-2018
В 8 томах

Председатель Международного программного комитета:
Батаев А.А., д.т.н., проф., ректор НГТУ.

Председатели национального комитета:
Вострецов А.Г. – д.т.н., проф., проректор по научной работе, НГТУ,
Лисицына Л.И. – д.т.н., проф., НГТУ,
Хрусталева В.А. – д.т.н., проф., декан факультета РЭФ, НГТУ.

Том 1
Часть 6
Труды на английском языке

Подписано в печать 27.09.2018. Формат 60 x 84 1/8
Бумага офсетная. Тираж 45 экз. Печ. л. 59.5 Заказ № 1256

Отпечатано в типографии
Новосибирского государственного технического университета
630073, г. Новосибирск, пр. К.Маркса, 20.